Effect of polygenic risk scores for Alzheimer's disease on brain structure, cerebrospinal fluid, and cognition

A Thesis Submitted for the Degree of Doctor of Philosophy

By

Snehal P. Pandya

Department of Psychology,

Brunel University London

2025

To my dearest Mummy,

Thank you for standing by my side in every aspect of life, and for being my pillar of strength always.

This is for you…

ABSTRACT

Background: Apolipoprotein E (APOE) is the most studied gene in relation to, and has the strongest genetic association with, sporadic Alzheimer's disease (AD). The APOE epsilon 4 (ε4) risk variant is found in approximately 14% of the general population and in approximately 37% of the AD population, globally. This indicates that the presence of ε4 is not required for the development of sporadic AD. In fact, sporadic AD is considered a polygenic disease with thousands of causative variants. Therefore, there is a need to investigate other genes and associated variants, and the concurrent effect of these on sporadic AD. Polygenic risk scores (PRSs) are ideal for this purpose as they consider multiple genetic variants/single nucleotide polymorphisms (SNPs) that have genome-wide significance, simultaneously. However, PRSs are difficult to calculate since numerous factors must be taken into consideration, and there is no optimal procedure. Nonetheless, PRSs can improve understanding of genotype-to-phenotype associations and risk predictions.

Aim: The aim of the current research is to investigate whether PRSs for AD can predict cross-sectional regional grey matter volume (Experiment One), cross-sectional cerebrospinal fluid (CSF) biomarkers (Experiment Two Part A), cross-sectional cognitive markers (Experiment Two Part B), longitudinal CSF biomarkers (Experiment Three Part A), and/or longitudinal cognition (Experiment Three Part B) across the continuum of sporadic AD.

Methodology: Participants from the Alzheimer's Disease Neuroimaging Initiative (n = 738; mean age in years: 73.94 ± 7.58) were analysed using various binomial hierarchical logistic regression models, and multiple hierarchical linear regression models, that controlled for numerous demographic and clinical variables. Participants were stratified by several variables to assess risk of AD in different groups. Three PRSs were constructed: PRSwithAPOE, PRSwithoutAPOE, and APOEonlyPRS. SNPs relating to APOE were from the entire APOE region, and three statistical thresholds were calculated for each of the three PRSs.

Results: Overall, PRSwithAPOE and APOEonlyPRS were associated consistently with outcome measures. Generally, PRSwithAPOE and APOEonlyPRS were: associated negatively with bilateral hippocampus (right (R) > left (L)), bilateral amygdala (R > L), bilateral entorhinal area, and R middle occipital gyrus; associated positively with CSF amyloid-beta 42 (Aβ42) more than they

were with CSF phosphorylated-tau181 (p-tau181), cross-sectionally; associated negatively with memory and visuospatial cognition, cross-sectionally; associated with CSF p-tau181 more than they were with CSF Aβ42, longitudinally; associated positively with longitudinal cognitive decline.

Discussion: The results highlight that stratification by amyloid positivity improves risk prediction over stratification by clinical diagnosis. The findings also concur to previous literature indicating that CSF amyloid decreases early on in AD after which it reaches a plateau, whereas changes in tau continue throughout the disease. The current research presents a novel, systematic, and thorough approach to evaluate risk of sporadic AD, including: a multi-modal approach that assesses outcome measures that are used to diagnose individuals with AD clinically (i.e., brain structure, CSF biomarkers, and symptomology); the use of both cross-sectional and longitudinal study designs; a multi-stratification approach whereby participants are divided in several ways to assess risk in different groups – for some groups, findings have been reported for the first time (to knowledge).

Conclusion: This work highlights the added value of non-ε4-APOE SNPs and non-APOE SNPs (i.e., both PRSwithAPOE and APOEonlyPRS) in detecting associations with AD-specific cross-sectional and longitudinal outcome measures. In parallel with existing literature, an ideal threshold has not been determined in the current research. However, it may be that certain thresholds identify associations better according to the outcome measure at hand. Additionally, the current research demonstrates the clinical relevance of PRSs for AD and that these may support diagnosis and prognosis of AD. It is recommended that future investigations assess PRSwithAPOE and APOEonlyPRS with longitudinal CSF biomarkers, in independent samples, and in ethnically diverse populations.

CONTENTS

LIST OF ABBREVIATIONS

List of abbreviations commonly used within this thesis:

AD	Alzheimer's disease
ADNI	Alzheimer's Disease Neuroimaging Initiative
APOE	Apolipoprotein E
Aβ	Amyloid beta
CSF	Cerebrospinal fluid
CU	Cognitively unimpaired
ε	Epsilon
FDR	False discovery rate
GWAS	Genome-wide association study
L	Left
LOAD	Late-onset Alzheimer's disease
MCI	Mild cognitive impairment
MMSE	Mini-mental state examination
MRI	Magnetic resonance imaging
MTL	Medial temporal lobe
NFT	Neurofibrillary tangle
PHS	Polygenic hazard score
PRS	Polygenic risk score
p-tau	Phosphorylated tau
R	Right
ROI	Region of interest
SNP	Single nucleotide polymorphism

LIST OF TABLES

CHAPTER 5A

CHAPTER 5B

CHAPTER 6A

CHAPTER 6B

LIST OF FIGURES

CHAPTER 5B

ACKNOWLEDGEMENTS

I am forever indebted to Prof. Annalena Venneri (primary supervisor) and Dr. Matteo De Marco (second supervisor) for supporting me to achieve this milestone. Thank you for your invaluable supervision, feedback, encouragement, and mentorship in professional development opportunities, throughout these three years. Thank you for making my PhD journey intellectually stimulating, collaborative, and enjoyable.

I am grateful to Dr. Riccardo Manca for the excellent guidance that he has provided as well.

Thank you to my parents and brother for supporting me in immeasurable ways while I worked long hours and weekends to juggle two demanding roles, (as a full-time Doctoral Researcher and a part-time Clinical Trials Manager). Thank you for cheering me up during the challenging periods.

I dedicate this PhD thesis to my incredible mother, Mrs Mangla P. Pandya.

CHAPTER 1

INTRODUCTION

1.1. HISTORY

In 1901, Alois Alzheimer, a German psychiatrist, observed a 51-year-old patient named Auguste D with progressive cognitive impairment and psychiatric symptoms. After her demise in 1906, Alzheimer conducted *post-mortem* histological analyses and documented what is now known as amyloid beta (Aβ) plaques and hyperphosphorylated tau. This disease was first described in a notable lecture, by Alzheimer himself, as "presenile dementia" and later, at the suggestion of his colleague, Emil Kraepelin, termed "Alzheimer's disease" (Maurer, Volk, and Gerbaldo, 1997; Sery et al., 2013).

1.2. THE ALZHEIMER'S DISEASE CONTINUUM

Alzheimer's disease (AD) is a progressive, irreversible, and debilitating neurodegenerative disease, and the most common form of dementia globally, accounting for 60-80% of cases (Bekris et al., 2010; DeTure and Dickson, 2019). According to the World Health Organisation, 115.4 million individuals will have AD by 2050. It, therefore, has worldwide socio-economic burden (Bekdash, 2021).

The main symptomatic feature of AD is the gradual loss of memory, which increases in severity over time, until the individual loses capacity. Initially, an individual will experience difficulties with forming and recalling recent memories. As the disease progresses, they will have impaired language, speech, decision making, reasoning, and executive function. These become apparent in work or social situations or, during daily or household activities. Visuospatial and movement decline may also come about. Changes in mood and emotional state may occur alongside memory decline. Psychiatric conditions, such as delusions and hallucinations, are not suggestive of AD, but may arise at any point on the AD continuum. Although the presence of apathy, depression, agitation, circadian sleep-wake disruptions, or psychosis can be found at any point along the AD continuum, these can increase cognitive decline rapidly (Li et al., 2014), and these symptoms are significant risk factors even in healthy ageing individuals (Ismail et al., 2016). Neurological symptoms, such as seizures, hypertonia, myoclonus, incontinence, and mutism, may also appear during late stages (Bekris et al., 2010; DeTure and Dickson, 2019; Lyketsos et al., 2011).

The AD continuum consists of three broad phases: preclinical AD (asymptomatic; healthy cognition), prodromal AD or MCI due to AD (symptomatic), and dementia due to AD (functional impairment) (Vermunt et al., 2019). AD has a long preclinical phase spanning decades (Jack Jr et al., 1999; Vickers et al., 2016), a lengthy prodromal phase, and a clinical duration of between 8 to 10 years, on average (Masters et al., 2015). However, the duration that individuals remain in each stage is subjective and is influenced by a range of factors, including genetics, brain reserve, coexisting brain diseases, medical comorbidities, and environmental factors (Aisen et al., 2017).

Preclinical AD refers to individuals that have AD-related biomarker evidence without the presence of clinical symptoms (Dubois et al., 2010; Startin et al., 2019). Some individuals with preclinical AD may pass away without any clinical symptoms. However, they would have shown symptoms, had they lived long enough (Jack Jr et al., 2010). Biomarker evidence refers to the presence of neuropathological hallmarks of AD, i.e., accumulation of extracellular Aβ plaques and intracellular tau deposits as detected by positron emission tomography (PET) brain scans. Some examples of PET tracers that may be used to identify the extent of amyloid or tau pathology include, 11 C-labelled Pittsburgh Compound-B (11C-PiB), fludeoxyglucose 18 Amyvid 45 florbetapir (18F-AV45-Florbetapir), fludeoxyglucose 18 florbetaben (18F-Florbetaben), fludeoxyglucose 18 flutemetamol (18F-Flutemetamol), and fludeoxyglucose 18 Amyvid 1251 flortaucipir (18F-AV1251-Flortaucipir). Biomarker evidence can also be obtained from assays in cerebrospinal fluid (CSF) drawn via lumbar punctures, and hyperphosphorylated tau in the form of intracellular neurofibrillary tangles (NFTs) and neuropil threads, as found via CSF and blood plasma assays (Braak and Braak, 1991; Dubois et al., 2016; Hari et al., 2022). Specifically, the key biomarkers of Aβ in the AD brain are increased levels of PET Aβ and reduced CSF Aβ42; these precede tau pathology and neurodegeneration (Aisen et al., 2017). The major biomarkers of neuronal injury in the brain are, increased CSF total tau (t-tau) and phosphorylated tau (p-tau), and reduced 18 fluorodeoxyglucose (FDG) uptake in the temporoparietal cortex measured via PET scans that detect brain metabolism (Jack Jr et al., 2011).

Interestingly, some research suggests that amyloid detected by PET or CSF in individuals with preclinical AD may be sufficient for the diagnosis of AD, whereas other work indicates that this does not predict progression to a symptomatic stage of AD. However, the presence of tau, in addition to amyloid, increases progression to clinical AD rapidly (Dubois et al., 2016). Nonetheless, the accumulation of both amyloid and tau proteins leads to progressive synaptic, neuronal, and axonal damage (Frisoni et al., 2010), and precedes structural changes in the brain,

including decline in hippocampal volume, and atrophy in medial, basal, and lateral temporal lobes, and medial parietal isocortex, and reductions in cortical glucose metabolism (Jack Jr et al., 2011).

According to the model devised by Jack Jr et al. (2010; 2011), these neuropathological and neurodegenerative changes occur before decline in memory and cognition, and precede impact on daily living and quality of life. These alterations can occur up to 30 years before symptomology (Bateman et al., 2012; Golde 2022). For example, changes in CSF Aβ42 can occur 25 years before the onset of symptoms, changes in PET Aβ deposition can occur 15 years before symptoms, increased levels of CSF tau and increased brain atrophy can occur 15 years before clinical symptoms, and cerebral hypometabolism and impaired episodic memory can occur 10 years before symptomology (Bateman et al., 2012). Therefore, the model indicates that these pathological changes do not occur suddenly or simultaneously, rather, they follow a temporal and sequential pattern, and all worsen progressively (Jack Jr et al., 2011).

Furthermore, the preclinical AD phase allows for preventative measures, prevention of clinical progression, research into novel biomarkers, and disease modifying therapies (Dubois et al., 2016). Fourteen modifiable (and preventive) risk factors have been identified; education, hearing loss, high low-density lipoprotein cholesterol, depression, traumatic brain injury, physical inactivity, diabetes, smoking, hypertension, obesity, excessive alcohol, social isolation, air pollution, and visual loss, that if addressed, collectively lower the risk of clinical dementia by approximately 45% (Livingston et al., 2024). Non-modifiable risk factors include advancing age, female sex, and genetics (Breijyeh and Karaman, 2020; Serrano-Pozo and Growdon, 2019; Zhang et al., 2021). Although AD is not part of healthy ageing, ageing is the utmost risk factor for AD (Kamboh, 2022). The prevalence of AD increases by 5.3% in individuals aged 65-74 years, increases by 13.8% in individuals aged 75-84 years, and increases by 34.6% in those aged 85 years and over (Rajan et al., 2021).

Prodromal AD, or MCI due to AD, refers to the category of patients that show both biomarker evidence and the symptomatic predementia phase of AD (Albert et al., 2011; Scharre, 2019), of which there are many subtypes. The severity of MCI varies from memory impairment only, to decline in other cognitive domains (Jack Jr et al., 2010). However, the threshold for a clinical diagnosis of dementia has not been met by these patients (Startin et al., 2019). Amnestic MCI (aMCI) refers to patients who show episodic memory impairment of the hippocampal type

(Mantzavinos and Alexiou, 2017). Multidomain MCI (mdMCI) refers to patients who have varying levels of impairment in various cognitive faculties, e.g., language, executive function, and visuospatial abilities. These may be in the presence (mdMCI+a) or absence (mdMCI-a) of memory impairment (Peterson, 2004). Cognitive deficits may be noticeable to the individuals themselves and their family and friends, but not to others. These deficits may not interfere with patients' ability to perform daily activities. However, the conversion rate from MCI or aMCI to AD is found to be between 10.2% to 33.6% over one year, 9.8% to 36.3% over two years, 33% over the course of five years, and 55.5% over 10 years (Ward et al., 2013). The transition from preclinical AD to prodromal AD is subtle, symptoms appear gradually rather than abruptly. Some individuals are aware of changes in cognitive function before these are apparent on tests of episodic memory, psychomotor speed, verbal fluency, and concept formation (Aisen et al., 2017).

The least prevalent form of MCI is where patients have impairment in one non-memory cognitive faculty, i.e., language, executive function, or visuospatial abilities. This is known as, single non-memory domain MCI. This may lead to different outcomes, such as frontotemporal lobar dementia or Lewy body dementia (Peterson, 2004).

Patients with MCI or early-AD are found to experience depression, verbal agitation, and physical agitation frequently. Additionally, MCI patients progress to AD at an increased rate if they have depression (Lyketsos et al., 2011) or other neuropsychiatric conditions (Ismail et al., 2016).

Similarly, mild behavioural impairment is found to increase likelihood of the development of AD and dementia, even in those without cognitive impairment (Taragano et al., 2009). The Mild Behavioural Impairment Checklist, devised by Ismail et al. (2016), is a diagnostic paradigm aimed at identifying individuals with increased risk of developing dementia, with or without cognitive symptoms. Mild behavioural impairment is a neurobehavioural syndrome that occurs in later life (>50 years of age) and can appear at any point across the preclinical AD continuum, from healthy ageing adults to patients with subjective cognitive decline and MCI. Individuals with mild behavioural impairment show changes in behaviour and personality, thus suggestive of neurodegeneration. For instance, decreased motivation, affective dysregulation, impulse dyscontrol, social inappropriateness or, abnormal perception or thought. These may occur during interpersonal relationships, in workplaces, or other social situations, but they maintain the ability to perform daily activities with minimal assistance. Therefore, mild behavioural

impairment and MCI are two different entities (Creese and Ismail, 2022). However, both can cooccur and increase risk of AD and dementia (Ismail et al., 2016).

Dementia due to AD refers to patients with greater levels of biomarker evidence and increased impairment in multiple cognitive and functional domains. Cognitive domains where impairments manifest include episodic memory, verbal fluency, and executive function such as, planning, problem-solving, and multi-tasking, language, visuospatial, and behaviour. Functional domains showing alterations include basic and complex activities of daily living, e.g., routine medication intake, telephone use, financial decisions, keeping appointments, and everyday technology use such as television, radio, remote controls. Cognitive decline, however, precedes functional decline. Dementia due to AD is also progressive: mild, moderate, and severe (Aisen et al., 2017; Jack Jr et al., 2010). During these latter phases, patients are likely to experience severe forms of neuropsychiatric conditions, such as delusions, hallucinations, and aggression, that affect daily function and quality of life (Lyketsos et al., 2011).

1.3. SPORADIC ALZHEIMER'S DISEASE VS. FAMILIAL ALZHEIMER'S DISEASE

AD can be split further into a sporadic form and a genetically determined familial form. The sporadic subtype, late-onset AD (LOAD), occurs after the age of 65 years. The sporadic form accounts for more than 90% of AD cases. Sporadic AD is most likely due to the complex interplay between genetic and environmental factors (Piaceri, Nacmias, and Sorbi, 2013). It is thought that in approximately 70% of sporadic AD there is a contribution of genetic factors via some so-called "risk genes" (Lane, Hardy, and Schott., 2017). Conversely, the familial subtype, early-onset AD (EOAD), occurs before the age of 65 years, and can be detected as early as age 20. This subtype accounts for 1-6% of cases (DeTure and Dickson, 2019), of whom 10-15% follow an autosomal dominant inheritance pattern (Jarmolowicz et al., 2014; Wingo et al., 2012) where mutations in at least one of the following genes, passed on from one parent, results in the AD phenotype: amyloid precursor protein (APP), presenilin 1 (PSEN1), or presenilin 2 (PSEN2). PSEN1 mutations cause AD in the majority of autosomal dominant cases (Cruts et al., 1998). The remaining ~90% of familial AD is therefore due to autosomal recessive inheritance (DeTure and Dickson, 2019; Wingo et al., 2012).

1.3.1. Sporadic Alzheimer's disease

No causative gene of sporadic AD has been identified. However, the Apolipoprotein E (APOE) gene is the most studied and some allelic forms are found to increase risk of sporadic AD (Bekris et al., 2010).

APOE is a 34 kDa glycoprotein (Li et al., 2020). Its main function is cholesterol homeostasis and lipid metabolism (Lumsden et al., 2020). In humans, APOE does not cross the blood-brain barrier. Therefore, there are two independent pools of APOE (Linton et al., 1991). Peripheral APOE is produced mainly in liver hepatocytes, and found in plasma, whereas APOE in the central nervous system is produced in astrocytes, and found in CSF (Li et al., 2020; Lumsden et al., 2020).

The APOE protein contains 299 amino acids (Rall Jr, Weisgraber, and Mahley, 1982) and is encoded by the APOE gene located on chromosome 19q13.32 (Rao et al., 2018). The APOE gene has three alleles/haplotypes: epsilon (ε)2, ε3, and ε4, corresponding to three isoforms: E2, E3, and E4. Therefore, six genotypes: ε2ε2, ε2ε3, ε3ε3, ε2ε4, ε3ε4, and ε4ε4 – in ascending order of AD risk and APOE plasma levels (Li et al., 2020). ε3 is the "standard" allele, for which the DNA sequence, TGC, results in amino acid cytosine (Cys) at position 112, and the DNA sequence, CGC, results in amino acid arginine (Arg) at position 158. However, single nucleotide polymorphisms (SNPs) at reference SNP (rs) 429358 and rs7412, in exon 4, result in DNA sequence alterations and therefore change the amino acids at codon 112 and 158. Such polymorphisms lead to the formation of either the ε4 "risk" allele or the ε2 "protective" allele (Kamboh, 2022). Refer to Table 1.1 and Table 1.2 for details. The expected fourth allele, ε1 or ε3r, Cys112: Arg158, is rarely found. Worldwide, it has only been found in three Caucasian families in Italy and one Yoruba family in Nigeria (Fernandez-Calle et al., 2022; Seripa et al., 2007). The ε3 allele is most common and thus found in ~78% of the global population, ε4 is found in ~14% of the general global population, whereas ε2 is only found in ~7% (Lumsden et al., 2020). Similarly, in the global AD population, ε3 is the most common allele and found in ~60% of patients, ε4 is prevalent in ~37% of patients, and ε2 is found in ~4% of patients (Liu et al., 2013).

Table 1.1: Three APOE alleles, the two associated codons and, their DNA sequences and amino acids.

	Codon 112		Codon 158	
Allele	**DNA Sequence**	**Amino Acid**	**DNA Sequence**	**Amino Acid**
ε3	TGC	Cytosine	CGC	Arginine
ε2	TGC	Cytosine	TGC	Cytosine
ε4	CGC	Arginine	CGC	Arginine

ε: epsilon. DNA: deoxyribonucleic acid.

Green = no change/no mutation; red = change/mutation.

Table 1.2: Six APOE genotypes and the amino acid for each allele within the genotype.

Genotype	Allele	Codon 112	Codon 158
APOE ε2ε2	ε2	Cytosine	Cytosine
	ε2	Cytosine	Cytosine
APOE ε2ε3	ε2	Cytosine	Cytosine
	ε3	Cytosine	Arginine
APOE ε2ε4	ε2	Cytosine	Cytosine
	ε4	Arginine	Arginine
APOE ε3ε3	ε3	Cytosine	Arginine
	ε3	Cytosine	Arginine
APOE ε3ε4	ε3	Cytosine	Arginine
	ε4	Arginine	Arginine
APOE ε4ε4	ε4	Arginine	Arginine
	ε4	Arginine	Arginine

APOE: apolipoprotein E. ε: epsilon.

Green = no change/no mutation; red = change/mutation. Adapted from Kamboh et al. (2022).

Interestingly, the frequency of ε4 varies by ancestry. A greater frequency of ε4 is found in Central Africa (40%), followed by Oceania (37%), and then Australia (26%). In Europe and Asia, the frequency of ε4 is between 10-25% (Belloy, Napolioni and Greicius, 2019). Previous work indicates that ε4 frequency is greatest in those of Japanese ancestry, followed by Caucasian, African American, and Hispanic ancestries (Farrer et al., 1997). However, a recent and large meta-analysis of global genetic ancestry has reported frequencies of APOE alleles as follows; ε4: 41.6% (Black), 40.6% (White), 29.9% (Hispanic), and 21.6% (East Asian, i.e., Japanese and Korean); ε3: 72.8% (East Asian), 61.3% (Hispanic), 50.6% (White), and 43.3% (Black); ε2: 19.7% (Black), 11.1% (White), 10.6% (Hispanic), and 5.6% (East Asian) (Belloy et al., 2023; Jackson, Hyman and Serrano-Pozo, 2024). These numerical figures reflect the complexity of the ε4 allele and the heterogeneity in risk of AD.

The ε2 isoform has been found to reduce risk of AD by 23% (Corder et al., 1994), whereas the ε4 isoform has been found to increase risk of AD by three-fold in heterozygous individuals (ε3ε4) and by 15-fold in homozygous individuals (Sims, Hill, and Williams, 2020). APOE ε4 can reduce age of AD onset (Meyer et al., 1998) by approximately one-two decades (Corder et al., 1993). Additionally, at the age of 85 years, the lifetime risk of AD is 51% for APOE ε4ε4 males and 60% for APOE ε4ε4 females, 23% for APOE ε3ε4 males and 30% for APOE ε3ε4 females (Genin et al., 2011). APOE ε4 can also increase the rate of cognitive decline (Craft et al., 1998). Faster rates of cognitive decline are evident in individuals that are Aβ positive without dementia and APOE ε4 carriers, as compared with non-carriers (Mormino et al., 2014; Lim et al., 2015).

About 95 other risk genes have been identified from genome-wide association studies (GWASs) and meta-analyses of GWASs, between 2009-2022 (Kamboh, 2022; see Figure 1.1). Other genes are continually being investigated to find additional risk loci associated with sporadic AD.

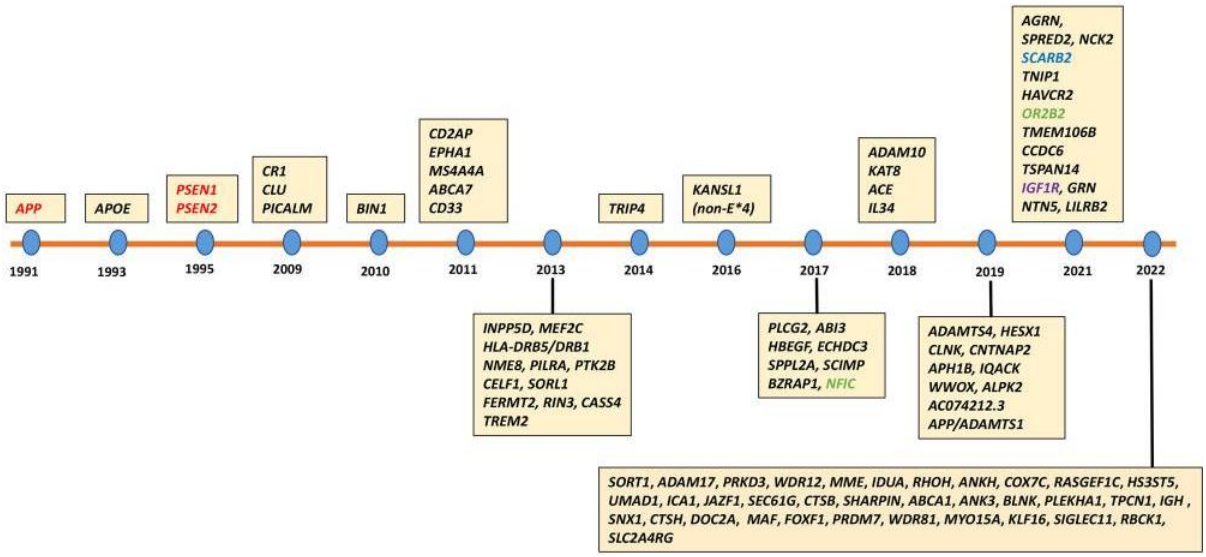

Figure 1.1: Timeline showing the discovery of AD risk genes.

Genes in red relate to early-onset AD; green refers to transethnic genes; purple relates to African Americans only; blue refers to Japanese only; **black** relate to genes discovered in Europeans/whites. (Kamboh, 2022, page 157).

1.3.2. Familial Alzheimer's disease

Three genes have a strong association with familial AD. These are, the APP gene, PSEN1 gene, and the PSEN2 gene. APP is found on chromosome 21q21.1-21q21.3, it consists of 18 exons and has a genomic region of ~290 kb. PSEN1 is located on chromosome 14q24.2, contains 13 exons and holds a genomic region of ~ 84 kb. PSEN2 is encoded on chromosome 1q42.13, consists of 12 exons and has a genomic region of ~25 kb (Cacace, Sleegers, and Van Broeckhoven, 2016).

Within the human APP protein, the γ-secretase contains four proteins: Anterior PHarynx-defective-1 (APH-1), NiCasTrin (NCT), PreSENilin (PSEN), and Presenilin ENhancer 2 (PEN2). PSEN has two isoforms, PSEN1 and PSEN2, both control catalytic activity of the γ-secretase (Zhao et al., 2019a). The majority of mutations found in APP, PSEN1, and PSEN2 genes, have been associated with Aβ, particularly Aβ40 and Aβ42, and thus with familial AD (Kamboh, 2022). Interestingly, mutations in other regions of this amino acid sequence (positions 670-723) have not been associated with familial AD, i.e., APH-1, NCT, and PEN2, which are part of the γ-secretase complex, β-site Amyloid precursor protein Cleaving Enzyme-1 (BACE1), part of β-secretase, or the A Disintegrin And Metalloprotease (ADAM) genes ADAM10 and ADAM17, part of the α-secretase complex (Kamboh, 2022).

Most APP, PSEN1, and PSEN2 mutations are autosomal dominant missense mutations. However, two mutations are autosomal recessive, p.Ala673Val (Di Fede et al., 2009) and p.Glu693Δ (Tomiyama et al., 2008). APP mutations increase total Aβ or increase Aβ42, whereas PSEN1 and PSEN2 mutations increase Aβ42 and decrease Aβ40. In either case, the Aβ42:Aβ40 ratio increases in the brain (Giri, Zhang, and Lu, 2016). This change in the ratio is associated with early age of onset and familial AD disease progression (Kamboh, 2022).

Interestingly, having a trisomy of (or part of) chromosome 21, i.e., where the APP gene is located, results in the Down syndrome phenotype (Patterson, 2009). Such individuals develop neuropathology that is similar to AD, including Aβ deposition and, the presence of NFTs and tau hyperphosphorylation (Hof et al., 1995). These findings may support the Amyloid Cascade Hypothesis (Hardy and Higgins, 1992).

Although it has long been known that mutations in APP, PSEN1, or PSEN2 genes lead to familial AD, it has recently been reported that rare variants and pathogenic mutations in these genes also increase risk of, or cause, sporadic AD. Cruchaga et al. (2012) suggest that simply dividing AD into

early-onset vs. late-onset may not be useful mechanistically, as mutations in these three genes can be found in both AD subtypes and the presence of APOE ε4 increases risk of both AD subtypes. Of note, Cruchaga et al. (2018) report that genetic variants for LOAD influence risk in both sporadic LOAD and familial LOAD, as well as in sporadic EOAD. Although LOAD variants are not associated with risk of autosomal dominant EOAD, it is possible that they may contribute to age at onset. Interestingly, 25% of families with sporadic AD have members with familial AD. This is more than expected as only a small proportion of the population have familial AD. The male:female ratio in this group of AD patients is said to be 1:1.3, compared with 1:1.8 in families with sporadic AD only. Therefore, it may be suggested that a subtype of familial AD is present (Brickell et al., 2006).

1.4. NEUROPATHOLOGY OF ALZHEIMER'S DISEASE

1.4.1. Amyloid

Aβ, a 4 kDa peptide, (DeTure and Dickson, 2019) is produced from the APP protein throughout life (Gouras, Olsson, and Hansson, 2015) by enzyme complexes β-secretase and γ-secretase. These enzymes cleave APP into various amino acid fragments: 38, 40, 42, 43, 45, 46, 48, 49, and 51 (Breijyeh and Karaman, 2020; Kamboh, 2022), thus resulting in Aβ38-51.

APP is initially cleaved by either α-secretase at amino acid site 687 that leads to the production of the transmembrane carboxyl fragment APP-C83, or it is cleaved by β-secretase at amino acid site 671 that generates the production of transmembrane carboxyl fragment APP-C99. APP-C83 is cleaved by the transmembrane aspartyl protease γ-secretase that is non-neurotoxic/cleaves normally, and produces smaller harmless peptides. APP-C99 is also cleaved by transmembrane aspartyl protease γ-secretase, but is neurotoxic/cleaves abnormally, resulting in long pathogenic peptides (Bekris et al., 2010; Kamboh, 2022). PSEN1 and PSEN2 are important for γ-secretase, and are accountable for both cleavage and release of Aβ (Chen et al., 2017). APP-C99 is then further cleaved by γ-secretase via endopeptidase (ε) activity. This results in either Aβ48 that is cleaved chronologically by γ-secretase via carboxypeptidase activity, leading to the formation of Aβ45, Aβ42, and Aβ38, or, results in Aβ49 that is again cleaved by γ-secretase and leads to Aβ46, Aβ43, and Aβ40 (Kamboh, 2022). Refer to Figure 1.2. APP plays a range of key roles, including

neuronal development, signalling, and intracellular transport (Chen et al., 2017; Simic et al., 2016).

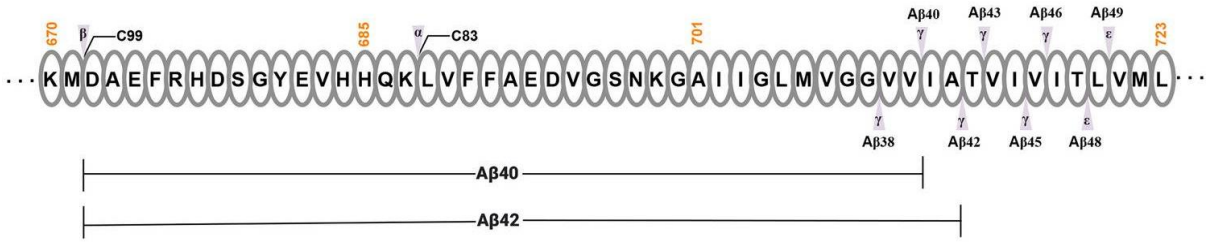

Figure 1.2: Diagram showing the amyloid precursor protein amino acid sequence from codon 670-723 and the associated amyloid peptides (Kamboh, 2022, page 154).

Reproduced under the Creative Commons Attribution 4.0 License (see Appendix A.1).

Aβ40 is the most common form of Aβ found in the human brain, followed by Aβ42 (Bekris et al., 2010). Both Aβ40 and Aβ42 are associated with AD (Simic et al., 2016), and Aβ42 plays a vital role in plaque formation (Citron et al., 1996) as it is prone to oligomerise and form fibrils (Kamboh, 2022) that accumulate into amyloid plaques (Breijyeh and Karaman, 2020).

Amyloid plaques have different morphological formations, including neuritic, diffuse, dense-core, classic, and compact plaques (Breijyeh and Karaman, 2020). The two most common forms of amyloid plaque, diffuse and neuritic plaques, can also be found in asymptomatic individuals and thus increase risk of AD. Neuritic plaque density is associated significantly with cognitive impairment, whereas a definitive association has not been found for diffuse plaques (Caselli et al., 2017).

Neuritic plaques with tau-positive neurites contain a dense amyloid core. The core has a peripheral region where dystrophic neurites and activated microglia are found; these changes are thought to steer neuronal degeneration and cognitive decline in AD (DeTure and Dickson, 2019; Dickson, 1997). Some of these dystrophic neurites contain tau filaments, i.e., paired helical filaments, and thus are difficult to differentiate from NFTs (Caselli et al., 2017; DeTure and Dickson, 2019).

The Amyloid Cascade Hypothesis, proposed by Hardy and Higgins (1992), which has since been dominating AD research (Simic et al., 2016), states that Aβ plays a central role in AD pathology

(Michalicova, Majerova, and Kovac, 2000). The overproduction of Aβ is thought to influence other pathologies, including astrocytosis, microglial activation, NFTs, synaptic loss, and neuronal death, in both familial and sporadic AD (Simic et al., 2016). This theory therefore suggests that a reduction in Aβ deposits is an effective treatment for AD (Michalicova, Majerova, and Kovac, 2000).

1.4.2. Tau

Tubulin-associated unit (tau) is a phosphoprotein distributed across the healthy brain and is encoded by the microtubule-associated protein tau (MAPT) gene, located on chromosome 17. Tau can be found in six isoforms in the adult brain and can range from 352-441 amino acids in length (Gong and Iqbal, 2008; Simic et al., 2016), i.e., resulting in fragments of 352, 381, 383, 410, 412, and 441 in length (Blennow et al., 2010). Several phosphorylation sites for amino acids threonine and serine have been identified in tau, although threonine181 (p-tau181), threonine231, and threonine217 (p-tau217) are studied commonly (Blennow et al., 2010; Palmqvist et al., 2025).

The main functions of tau are stabilising microtubules, promoting neurite outgrowth, and facilitating organelles to nerve terminals. When phosphorylated, tau regulates microtubule binding and assembly (Breijyeh and Karaman, 2020; Gong, Grundke-Iqbal, and Iqbal, 2005; Michalicova, Majerova, and Kovac, 2000; Sery et al., 2013; Simic et al., 2016). The normal level of tau phosphorylation is due to the regulation of tau kinases and tau phosphatases (Gong and Iqbal, 2008).

Tau is found seven-fold more in the AD brain than in the healthy ageing brain. This increase is in the form of hyperphosphorylated tau, which is also misfolded (Khatoon, Grundke-Iqbal, and Iqbal, 1992). Hyperphosphorylation causes tau to detach from microtubules (Sery et al., 2013; Breijyeh and Karaman, 2020) and form thick bundles of insoluble intracellular inclusions, known as NFTs, composed of paired helical filaments. These consist of two filaments twisted around each other and are made up of tau isoforms, each with 3-repeats or 4-repeats (DeTure and Dickson, 2019; Michalicova, Majerova, and Kovac, 2000). The filaments measure between 8-20 nm and can be found in every 80 nm distance (Crowther, 1991). Neuropil threads also consist of tau filaments, found in dendrites and axons; they too can appear as paired helical filaments (Mitchell et al., 2000).

Many factors contributing to the hyperphosphorylation of tau have been considered, including Aβ, dysregulation of phosphorylation/dephosphorylation, upregulation of tau kinases, downregulation of tau phosphatases, and reduction of brain glucose metabolism. Although a definitive reason for tau hyperphosphorylation has still not been found (Gong, Grundke-Iqbal, and Iqbal, 2005; Gong and Iqbal, 2008), the process contributes to dendritic, axonal, and synaptic dysfunction and impairs synaptic plasticity, causing neurodegeneration (Caselli et al., 2017). Therefore, memory deterioration in AD is associated with synaptic pathology in the hippocampus (Naseri et al., 2019), and a significant association between the presence of NFTs and AD symptomology is found (Michalicova, Majerova, and Kovac, 2000). Thus, the Tau Hypothesis indicates AD is a tauopathy, and this initiates the AD cascade (Chen et al., 2017).

1.4.3. Pathogenesis of Alzheimer's disease

In addition to the above-mentioned Amyloid Cascade Hypothesis and Tau Hypothesis, other hypotheses for AD have also been proposed. These include: the Dual-Cascade Hypothesis that suggests both Aβ and tau pathologies occur simultaneously, although via different cellular pathways, and lead to AD; the Inflammatory Hypothesis, Cholinergic Hypothesis, and Adrenergic Hypothesis (van der Kant, Goldstein and Ossenkoppele, 2020).

Cholinergic neurons are distributed widely across the brain. However, cholinergic neurons in the nucleus basalis of Meynert in the basal forebrain that project to the hippocampus, amygdala, and neocortex, play an important role in memory and learning. Cholinergic signal transduction relating to these cognitive domains relies upon acetylcholine, an excitatory neurotransmitter. Acetylcholine is also important for suppression of inflammation. However, dysregulation and deficiency of acetylcholine and cholinergic neurons lead to abnormalities in APP metabolism and tau phosphorylation. Therefore, this causes neurotoxicity, neuroinflammation and neuronal death, and results in the AD phenotype (Bekdash, 2021; Chen et al., 2022).

In addition, it is also thought that dysregulation of both the cholinergic system and the adrenergic system leads to AD pathology. Noradrenergic neurotransmission relies on norepinephrine. This neurotransmitter has a key role in memory, learning, and attention. Synthesis of norepinephrine occurs largely in the Locus Coeruleus, and neurons here project to the hippocampus, amygdala, hypothalamus, cerebellum, striatum, basal forebrain, and the cortex. Therefore, abnormalities in the Locus Coeruleus, norepinephrine, and adrenergic receptors, contribute greatly to Aβ

pathology and AD (Bekdash, 2021). Despite the existence of several theories, the precise pathogenesis of AD remains unclear (Chen et al., 2022).

1.4.4. Neuropathological Staging

Various attempts have been made to define categories to explain severity of neuropathological change. In 1985, the National Institute on Aging looked at neocortical total plaque density (Caselli et al., 2017). In 1991, the Consortium to Establish a Registry for Alzheimer's Disease (CERAD) investigated neuritic plaques (Mirra et al., 1991) and Braak and Braak (1991) focused on Aβ plaques and NFTs. See Figures 1.3, 1.4, and 1.5.

CERAD criteria state tissue samples should be taken from neocortical regions: superior and middle temporal gyri, middle frontal gyrus, and inferior parietal lobule (Mirra et al., 1991). Figure 1.3 provides examples of Sparse vs. Moderate vs. Frequent neuritic plaque formation.

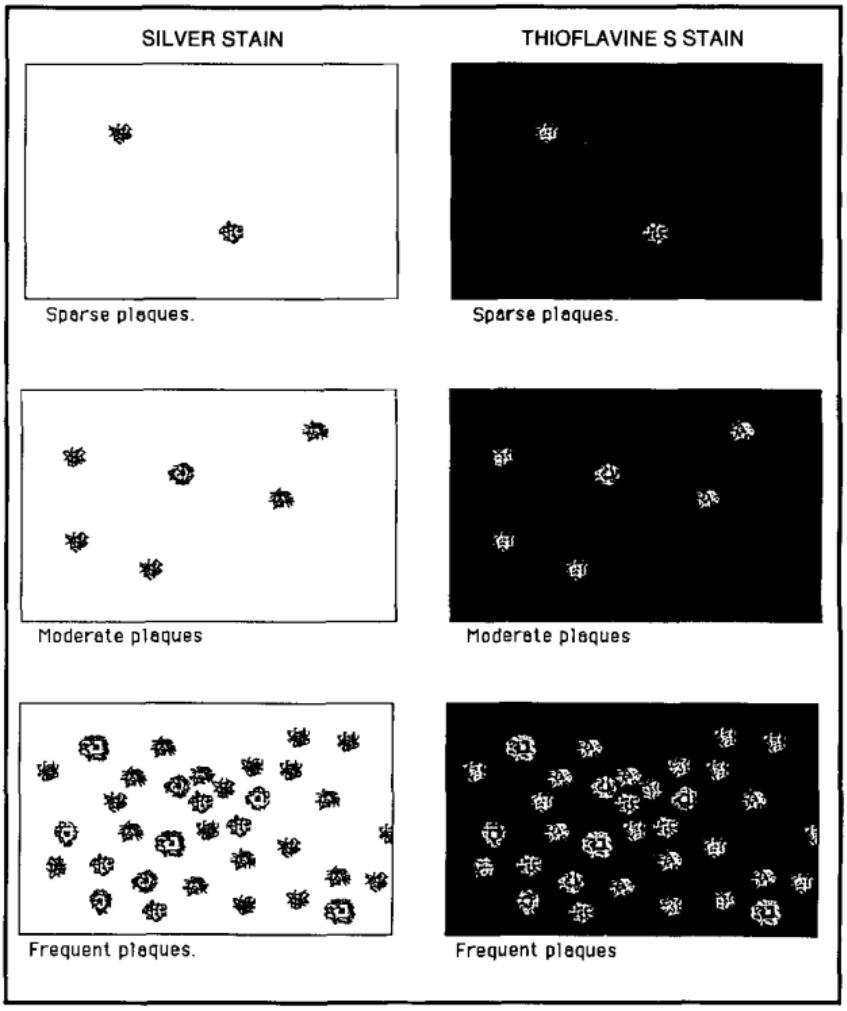

Figure 1.3: Examples of CERAD scores based on neuritic plaques per x100 microscopic field, using silver stain and thioflavine stain (Mirra et al., 1991; page 480).

See Appendix A.2 for license to reuse image.

Braak and Braak Aβ propagation:

- Stage A: Low levels of amyloid deposits are found in the basal sections of the isocortex, particularly in the frontal, temporal, and occipital lobes.
- Stage B: Medium levels are found in all isocortical regions, other than the primary sensory and primary motor areas.
- Stage C: High levels are found in all areas of the isocortex (Braak and Braak, 1991). See Figure 1.4.

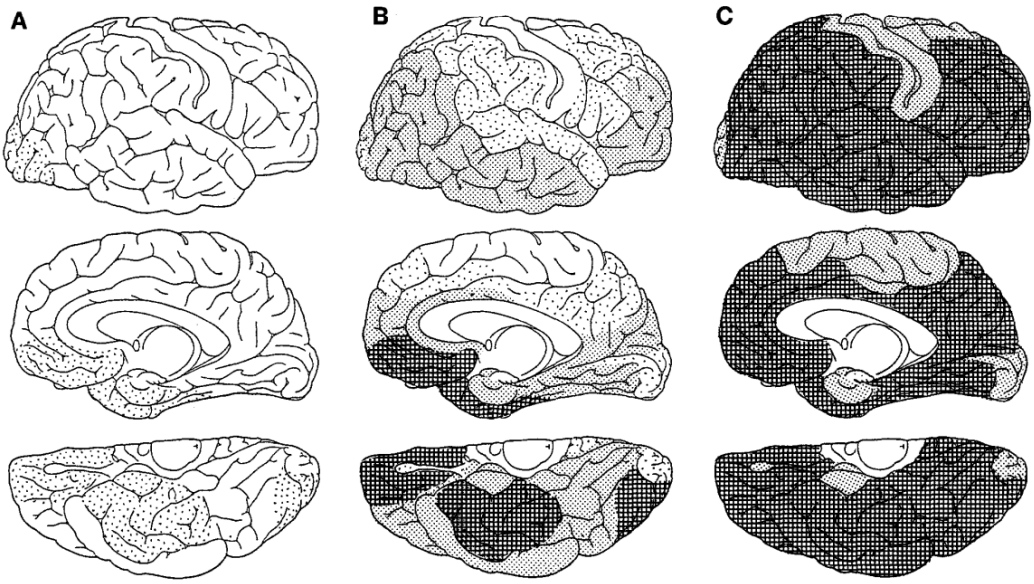

Figure 1.4: The propagation of amyloid through Braak Stages A-C (Braak and Braak, 1991; page 243).

See Appendix A.3 for license to reuse image.

Braak and Braak p-tau propagation:

- Stages I-II, transentorhinal: Moderate levels of NFTs and neuropil threads are found in the transentorhinal region, located between the entorhinal region and temporal isocortex, and mild levels found in the hippocampus.
- Stages III-IV, limbic: High levels found in the transentorhinal and entorhinal regions, with mild-to-moderate levels in the hippocampus, and low levels in the isocortex.
- Stages V-VI, isocortical: High levels in the hippocampus and extreme levels in the isocortex (Braak and Braak, 1991). Refer to Figure 1.5.

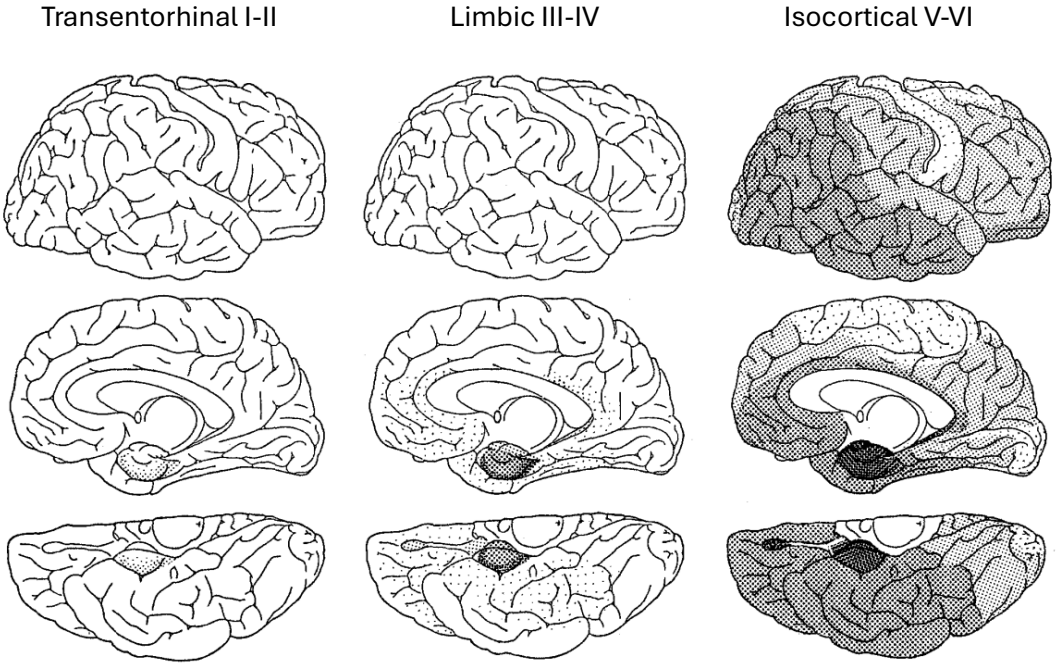

Figure 1.5: The propagation of tau through Braak Stages I-VI (Braak and Braak, 1991; page 246). See Appendix A.3 for license to reuse image.

In 1997, the National Institute on Aging and Reagan Institute Working group combined CERAD scores with Braak and Braak Aβ staging to determine the likelihood of dementia due to AD. These combined criteria were:

- Low likelihood of AD: CERAD score Sparse + Braak and Braak NFT stage I/II.
- Intermediate likelihood of AD: CERAD score Moderate + Braak and Braak NFT stage III/IV.
- High likelihood of AD: CERAD score Frequent + Braak and Braak NFT stage V/VI (Caselli et al., 2017).

In 2002, the Thal amyloid phases were established:

- Phase 1: Aβ plaques in neocortex only.
- Phase 2: Aβ plaques in the above region and allocortical regions.
- Phase 3: Aβ plaques in regions specified in Phase 1 and 2, plus diencephalic nuclei, striatum, cholinergic nuclei in basal forebrain.
- Phase 4: Aβ plaques in regions specified in Phase 1, 2, and 3, plus other brainstem nuclei – substantia nigra, red nucleus, central grey, superior and inferior collicle, inferior olivary nucleus, and intermediate reticular zone.
- Phase 5: Aβ plaques in regions specified in Phase 1, 2, 3, and 4, plus cerebellum and other brainstem nuclei – pontine nuclei, locus coeruleus, parabrachial nuclei, reticulo-tegmental nucleus, dorsal tegmental nucleus and, oral and central raphe nuclei (Thal et al., 2002). Refer to Figure 1.6.

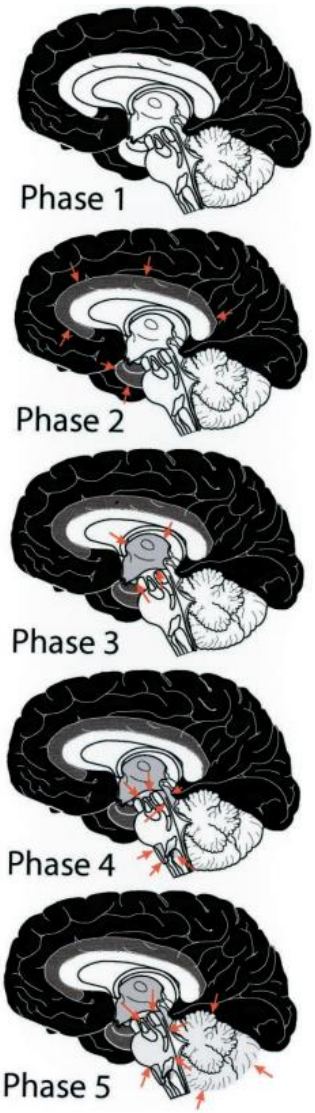

Figure 1.6: Thal phases highlighting the progression of AD, as demonstrated by **black** and grey shading, and red arrows (Thal et al., 2002; page 1795).

See Appendix A.4 for license to reuse image.

As evident, the criteria devised by CERAD, Braak and Braak, and Thal, differ. However, they all evolve around limbic, neocortical, and subcortical regions (Caselli et al., 2017).

In 2012, the National Institute on Aging–Alzheimer's Association (NIA–AA) established the ABC score to indicate the level of neuropathological change. A refers to amyloid levels, B refers to Braak and Braak NFT stages, and C refers to CERAD neuritic plaque scores; each with four levels. Refer to Table 1.3. The ABC score then corresponds to a descriptor: Not, Low, Intermediate, or High. Intermediate or High descriptors demonstrate neuropathological change that is sufficient for dementia due to AD (Hyman et al., 2012). Refer to Table 1.4.

Table 1.3: Criteria for A + B + C (ABC) score. Adapted from Hyman et al. (2012).

A: **A**β Thal plaque score	A0: No Aβ or amyloid plaques A1: Thal phase 1 or 2 A2: Thal phase 3 A3: Thal phase 4 or 5
B: **B**raak and Braak NFT score	B0: No NFTs B1: Braak and Braak NFT stage I or II B2: Braak and Braak NFT stage III or IV B3: Braak and Braak NFT stage V or VI
C: **C**ERAD neuritic plaque score	C0: No neuritic plaques C1: CERAD score Sparse C2: CERAD score Moderate C3: CERAD score Frequent

Aβ: amyloid beta. CERAD: Consortium to Establish a Registry for Alzheimer's Disease. NFT: neurofibrillary tangles.

Table 1.4: AD neuropathologic change ratings based on ABC scores. Adapted from Hyman et al. (2012).

		B: NFT score (Braak and Braak stage)		
A: Aβ plaque score (Thal phase)	**C: Neuritic plaque score (CERAD score)**	B0 or B1 (Braak & Braak: None, I or II)	B2 (Braak & Braak: III or IV)	B3 (Braak & Braak: V or VI)
A0 (Thal: 0)	C0 (CERAD: None)	AD neuropathological change level: Not	AD neuropathological change level: Not	AD neuropathological change level: Not
A1: (Thal: 1 or 2)	C0 or C1 (CERAD: None or Sparse)	AD neuropathological change level: Low	AD neuropathological change level: Low	AD neuropathological change level: Low
	C2 or C3 (CERAD: Moderate or Frequent)	AD neuropathological change level: Low	AD neuropathological change level: Intermediate	AD neuropathological change level: Intermediate
A2: (Thal: 3)	C0, C1, C2 or C3 (CERAD: None, Sparse, Moderate or Frequent)	AD neuropathological change level: Low	AD neuropathological change level: Intermediate	AD neuropathological change level: Intermediate
A3: (Thal: 4 or 5)	C0 or C1 (CERAD: None or Sparse)	AD neuropathological change level: Low	AD neuropathological change level: Intermediate	AD neuropathological change level: Intermediate
	C2 or C3 (CERAD: Moderate or Frequent)	AD neuropathological change level: Low	AD neuropathological change level: Intermediate	AD neuropathological change level: High

Aβ: amyloid beta. AD: Alzheimer's disease. CERAD: Consortium to Establish a Registry for Alzheimer's Disease. NFT: neurofibrillary tangles.

It is not possible to gauge AD prognosis definitively from an individual pathophysiological biomarker (Aisen et al., 2017). Therefore, Jack Jr et al. (2016) devised a descriptive classification system to categorise seven AD biomarkers into three groups: A/T/N. A refers to the amount of Aβ detected in amyloid PET or CSF Aβ42, T refers to the amount of tau detected in CSF p-tau, or tau PET, and N refers to the extent of neurodegeneration or neuronal injury detected in 18F-FDG PET, magnetic resonance imaging (MRI), or CSF t-tau. Each of these three groups are given a positive or negative value depending on their presence or absence. Note, this is not a diagnostic system, it is an approach to describe multiple biomarkers accurately using a standardised system, due to the lack of agreed terminology between AD researchers.

Recently, the Alzheimer's Association Workgroup (Jack Jr et al., 2024) have published revised criteria for the classification of AD biomarkers. They divide biomarkers into three categories: (1) biomarkers that indicate AD-specific neuropathology, i.e., Core 1 and Core 2; (2) biomarkers that are important in AD pathogenesis but are not AD-specific; (3) biomarkers involved commonly in non-AD co-pathologies. These are listed according to the ATXN framework, where X refers to a new biomarker category beyond ATN (Jack Jr et al., 2018), and according to the biomarker collection method, i.e., CSF, plasma, or imaging. See Figure 1.7.

Biomarker category	CSF or plasma analytes	Imaging
Core Biomarkers		
Core 1		
A (Aβ proteinopathy)	Aβ 42	Amyloid PET
T_1: (phosphorylated and secreted AD tau)	p-tau217, p-tau181, p-tau231	
Core 2		
T_2 (AD tau proteinopathy)	MTBR-tau243, other phosphorylated tau forms (e.g., p-tau205), non-phosphorylated mid-region tau fragments[a]	Tau PET
Biomarkers of non-specific processes involved in AD pathophysiology		
N (injury, dysfunction, or degeneration of neuropil)	NfL	Anatomic MRI, FDG PET
I (inflammation) Astrocytic activation	GFAP	
Biomarkers of non-AD copathology		
V vascular brain injury		Infarction on MRI or CT, WMH
S α-synuclein	αSyn-SAA[a]	

Figure 1.7: Categorisation of fluid and imaging biomarkers for AD (Jack et al., 2024; page 5146).

Aβ: Amyloid-beta. AD: Alzheimer's disease. αSyn-SAA: alpha-synuclein seed amplification assay. CSF: Cerebrospinal fluid. CT: Computed tomography. FDG: Fluorodeoxyglucose. GFAP: Glial fibrillary acidic protein. MRI: Magnetic resonance imaging. MTBR: Microtubule-binding region. NfL: Neurofilament light chain. PET: Positron emission tomography. WMH: White matter hyperintensity.

[a]Informative when measured in CSF only.

1.5. DIAGNOSIS OF ALZHEIMER'S DISEASE

The presence of Aβ plaques and NFTs alone is inadequate to diagnose AD as these can appear in non-demented individuals (Caselli, et al., 2017). Therefore, clinical diagnosis of AD is based on clinical history, neurological examination and neurological imaging, and neuropsychological assessment (Bekris et al., 2010). According to the Diagnostic and Statistical Manual of Mental Disorders, Fifth Edition, Text Revision (DSM-5-TR), a diagnosis of AD requires (1) decline in memory and learning, and a decline in at least one of the following cognitive faculties: complex attention, executive function, language, perceptual-motor, and social cognition, and (2) difficulties in activities of daily living as a result of impaired cognitive function (Yokoi, 2023). The Clinical Dementia Rating (CDR) scale is a common semi-structured interview method that is used to detect decline in memory, cognition, and function. Both the patient and informant are interviewed separately to assess level of dysfunction in (1) memory, (2) orientation, (3) judgement, (4) problem solving, (5) community affairs, and (6) home and hobbies. Each of the six categories are scored from 0 to 3: a "box score" of 0 refers to "none", 0.5 refers to "questionable", 1 relates to "mild", 2 refers to "moderate", and 3 refers to "severe". Using clinical scoring rules, the box scores are then translated to "global CDR scores" between 0 to 3 again: 0 refers to "no impairment", 0.5 relates to "questionable dementia", 1 refers to "mild dementia", 2 relates to "moderate dementia", and 3 refers to "severe dementia" (Morris et al., 1993).

Historically, AD dementia could only be conclusively diagnosed during *post-mortem* examination for Aβ and tau pathology. However, through the use of molecular neuroimaging modalities, these pathologies can be found and visualised while the patient is living (DeTure and Dickson, 2019) and, thus, initiate treatment earlier. According to the revised criteria set by the Alzheimer's Association Workgroup, a diagnosis of AD may be based on abnormality found in either, (1) amyloid PET, (2) CSF ratios of Aβ42:Aβ40, p-tau181:Aβ42, or t-tau:Aβ42, or (3) plasma p-tau217 (Jack Jr et al., 2024). Additionally, in recent times, there has been a conscious effort to integrate CSF Aβ42, t-tau, p-tau, and amyloid PET biomarkers into clinical decision making (Aisen et al., 2017). However, a definitive diagnosis of AD requires both a clinical assessment and a *post-mortem* examination (Bekris et al., 2010).

1.6. IMPACT OF APOLIPOPROTEIN E ON AMYLOID AND TAU

1.6.1. Amyloid

The effect of APOE on Aβ deposition is isoform-dependent, with APOE ε2 showing the lowest Aβ levels and plaque deposition cross-sectionally, and longitudinally (Fagan et al., 2002; Grothe et al., 2017). The association between APOE ε4 and sporadic AD was first described by Corder et al. (1993) and this association has been found consistently across the spectrum of sporadic AD (Fernandez-Calle et al., 2022). APOE ε4 carriers have 10-40% more prevalence of amyloid positivity than non-carriers (Jansen et al., 2015). Compared with APOE ε4 heterozygotes (Tiraboschi et al., 2004) and ε3 homozygotes (Rebeck et al., 1993), APOE ε4 homozygotes have increased NFTs, increased Aβ plaques, and increased density of such plaques (Schmechel et al., 1993; Tiraboschi et al., 2004). APOE genotype has also been shown to affect amyloid PET scan outcomes and CSF Aβ levels. For instance, APOE ε4 carriers, including those with normal cognition (Reiman et al., 2009), show increased amyloid Pittsburgh compound B (PIB) PET positivity and reduced CSF Aβ42. This effect is greater for APOE ε4 homozygotes than heterozygotes (Morris et al., 2010; Sunderland et al., 2004). APOE ε4 is also associated with reduced Aβ clearance (Kanekiyo, Xu, and Bu, 2014; Deane et al., 2008). However, the precise mechanisms of Aβ clearance and the role of APOE in Aβ clearance are complex, thus requiring further research in relation to AD (Fernandez-Calle et al., 2022).

The association between APOE genotype and amyloid remains when stratifying by diagnostic status. For example, amyloid PET in cognitively healthy ageing individuals that are APOE ε4 carriers, shows increased levels of amyloid deposition (Gonneaud et al., 2016), specifically, from the age of 70 years (Jack Jr et al., 2015), and amyloid deposition in frontal, temporal, and parietal lobes is associated with cognition (Kantarci et al., 2012), as compared with ε4 non-carriers. Additionally, those that are heterozygous for ε4 have significantly reduced CSF Aβ42 (Sunderland et al., 2004), and this is further reduced in individuals that are ε4 homozygous (Morris et al., 2010). Conversely, APOE ε2 is associated with increased CSF Aβ42 levels than those without an ε2 allele (Morris et al., 2010). At baseline, APOE ε4 is associated with increased likelihood of being Aβ positive. Longitudinally, ε4 carriers have greater cortical Aβ accumulation as they develop Aβ pathology from an earlier age and at a faster rate than non-carriers (Mishra et al., 2018). Of note, longitudinal accumulation of Aβ is faster in those who are both Aβ negative and APOE ε4 carriers, than those who are both Aβ positive and APOE ε3 or ε2 carriers. However, such findings are not observed in Aβ positive individuals with the various APOE genotypes (Lim and Mormino, 2017).

Therefore, the influence of APOE genotype goes beyond that of Aβ status when investigating Aβ accumulation longitudinally in healthy ageing Aβ negative individuals.

Interestingly, cognitively healthy individuals that are APOE ε4 carriers have greater mean Aβ plaque density in all cortical regions than early-MCI or late-MCI patients that are ε4 non-carriers. Early-MCI and late-MCI patients that are ε4 carriers have substantially greater mean Aβ plaque density than AD patients that are ε4 non-carriers (Murphy et al., 2013), and AD patients that are ε4 carriers have the greatest amyloid levels (Fleisher et al., 2013). Therefore, a positive ε4 carrier status seems to outweigh diagnostic status.

1.6.2. Tau

In terms of the possible impact of APOE genotype on tau, APOE ε4 is associated with the amnestic AD phenotype and tau propagation in medial and temporal regions, typical of Braak and Braak (1991) staging (Sanchez et al., 2021; Vogel et al., 2021) even after adjusting for global cortical Aβ burden (Baek et al., 2020). ε4 non-carriers have lower levels of tau in the entorhinal cortex and neocortex (Whitwell et al., 2018).

Using mass-spectrometry the concentrations of APOE isoforms have been studied in healthy ageing subjects and AD patients. Both the individual levels of APOE isoform 3 and APOE isoform 4 concentrations are associated positively with CSF t-tau and CSF p-tau concentrations. These associations are found in both healthy ageing subjects and AD patients (Martinez-Morillo et al., 2014).

In AD patients, APOE ε4 is associated with increased p-tau and t-tau, rapid cognitive deterioration (Wattmo, Blennow, and Hansson, 2020), impaired cortical plasticity, poor astrocyte survival rates, and worse disease prognosis (Koch et al., 2017), as compared with AD patients that are ε4 non-carriers. Similarly, in early-MCI patients, APOE ε4 is associated with increased CSF p-tau and t-tau (Risacher et al., 2013). Therefore, associations are present regardless of the diagnostic group when APOE ε4 is present.

In *post-mortem* brains of AD patients, compared with those with no APOE ε4 allele or ε4 heterozygotes, patients that are homozygous for ε4 have increased levels of tau in the presence of Aβ pathology (Tiraboschi et al., 2004). However, in the absence of Aβ pathology, APOE ε4 is not

associated with tau. Similarly, APOE ε2 is associated with reduced tau in the presence of Aβ but this association is not found without Aβ pathology (Farfel et al., 2016). Therefore, the effect of APOE genotype on tau is influenced by amyloid, and this is also the case for some of the above-mentioned studies that show associations between APOE and tau. For example, Sanchez et al. (2021) found that associations between APOE ε4 and neocortical regions were mediated by Aβ.

Evidently, APOE genotype has a strong impact on amyloid pathology. In contrast, although an association is found between APOE genotype and tau, the findings are difficult to interpret. This is because it is challenging to isolate a direct link between APOE genotype and tau, due to the effect of amyloid. The impact of APOE genotype on tau may be secondary to the effect of APOE genotype on amyloid (Fernandez-Calle et al., 2022). Therefore, the relevance of observed associations between APOE genotype and tau with AD risk and disease progression are unclear (Yamazaki et al., 2019).

1.7. NEURODEGENERATION IN ALZHEIMER'S DISEASE

Not only are changes evident at the microscopic level, but they are also seen at the macroscopic level. For instance, enlarged sulci in frontal and temporal cortices due to atrophy in gyri, atrophy in the precuneus and posterior cingulate gyrus, leading to enlarged frontal and temporal horns of the lateral ventricles, atrophy in limbic lobes, reduced brain weight, and loss of neuromelanin pigmentation in the locus coeruleus (Sengoku, 2019). However, some of these changes found through neuroimaging tools are not specific to AD. The healthy ageing brain may show moderate cortical atrophy, particularly in frontal lobes (Piguet et al., 2009). Although, atrophy in the amygdala and hippocampus, and enlargement of the temporal horn, are characteristic of AD (Apostolova et al., 2012), these changes are also present in other neurodegenerative diseases, such as hippocampal sclerosis. Nonetheless, together, these neurodegenerative features are highly suggestive of AD (DeTure and Dickson, 2019).

Many imaging techniques have been used to study the brain in different ways. The brain can be examined at a structural level, functional level, and at a neuromolecular level. Examples of common neuroimaging methods include, structural MRI, diffusion tensor imaging (DTI), arterial spin labelling (ASL), functional MRI (fMRI), resting state fMRI (rs-fMRI), PET, and single photon emission computed tomography (SPECT).

1.7.1. Grey Matter Changes in Hippocampus and Cortical Regions

In comparison with other modalities, images acquired from MRI offer a good level of detail and provide a strong grey matter vs. white matter contrast (Marquez and Yassa, 2019). This allows for examination of anatomical location, cortical area, thickness, and volume, and morphological characteristics, both cross-sectionally and longitudinally.

Changes in brain volume and brain weight have been found in healthy ageing individuals. For instance, after the age of 50 years, mean volume is found to reduce by approximately 2% per decade (Miller, Alston, and Corsellis, 1980) and between the ages of 45-50 years, reductions in brain weight begin, where reductions are at the most after the age of 86 years (Dekaban and Sadowsky, 1978). AD is also associated with substantial decline in brain weight (Uylings and de Brabander, 2002).

Longitudinal analysis of healthy participants over a five-year period indicates that the mean shrinkage is greatest in the caudate, cerebellum, hippocampus, and association cortices. When looking at the association with age, shrinkage increases in the hippocampus, cerebellum, and prefrontal white matter. A late-onset, age-related, increase in shrinkage of the entorhinal cortex is also found (Raz et al., 2005). Age-related longitudinal shrinkage of the entorhinal cortex, over a five-year period, is also associated with reduced memory performance (Rodrigue and Raz, 2004). In addition to this association with the entorhinal cortex, Rosen et al. (2003) found that hippocampal volume was also associated with the extent of memory decline. Specifically, the change in shape of the cornu ammonis 1 has been found to predict conversion from a CDR score of 0 to 0.5 (Csernansky et al., 2005). Therefore, the hippocampus, hippocampal subfields, and the entorhinal cortex are sensitive biomarkers of memory decline, and as age increases, regional brain shrinkage increases.

Annual rates of hippocampal volume loss reduce progressively, and more so for AD patients, followed by MCI patients, and then cognitively healthy individuals. Compared with MCI patients who remain stable over time, MCI patients who experience clinical decline over a three-year period also have greater annual hippocampal volume loss. This is the case for cognitively healthy participants as well (Jack Jr et al., 2000).

Longitudinal investigation of the hippocampus and other AD-vulnerable regions, e.g., entorhinal cortex, temporopolar cortex, lateral temporal cortex, inferior parietal cortex, inferior parietal

sulcus, posterior cingulate cortex, and inferior frontal cortex, show a sigmoidal pattern of atrophy and thinning. Rates of atrophy and thinning are accelerated during the early stages of AD, i.e., throughout the presymptomatic and aMCI stages, and then decelerated (Sabuncu et al., 2011). Interestingly, it has also been reported that the entorhinal cortex and inferior temporal gyrus predict longitudinal hippocampal volume loss in MCI and AD patients (Desikan et al., 2010). These results are comparable with those found in neuropathological studies of amyloid and tau, whereby the entorhinal cortex is impacted before the hippocampus (Braak and Braak, 1991).

In comparison with healthy ageing individuals, MCI patients have smaller cornu ammonis 1-2 transition zone volumes. In comparison with both healthy ageing subjects and MCI patients, AD patients have significantly reduced volumes of the subiculum and cornu ammonis 1, in addition to reduced volume of the cornu ammonis 1-2 transition zone (Mueller and Weiner, 2009). Comparable results have been obtained by Mueller et al. (2010). However, in addition, they also find significant reductions in the volumes of the entorhinal cortex and total hippocampus. Rather than the total hippocampal volume, the volume of the cornu ammonis 1-2 transition zone is shown to differentiate between healthy ageing adults vs. MCI patients. These patterns of volumetric loss between individuals across the AD continuum are comparable with those found with histopathological analysis of medial temporal lobe (MTL) structures and hippocampal subfields. Of note, in healthy controls and AD patients, the presence of APOE ε4 has been associated with volume loss of the cornu ammonis 3 and dentate gyrus (Mueller and Weiner, 2009).

Additionally, cortical thickness in healthy ageing participants, MCI patients, and AD patients has been studied. Differences in global mean cortical thickness is shown to be greater between MCI vs. AD than between healthy participants vs. MCI. This may be due to the severity of symptoms experienced in the latter stages of the AD continuum. When comparing healthy participants vs. MCI, changes in regional cortical thickness are found frequently in MTL regions. In contrast, widespread isocortical regions are involved when comparing changes in cortical thickness between MCI vs. AD, although significant changes are found mostly within the temporal lobes, particularly in the L hemisphere. Specifically, significant between-group differences in regional cortical thickness are found in medial and lateral L temporal lobe regions. However, regions within the primary motor, sensory, and occipital cortices are spared. In fact, changes in thickness of the MTL are observed more between healthy participants vs. MCI, whereas changes in lateral temporal lobe are found between MCI vs. AD (Singh et al., 2006).

Furthermore, the relationship between CDR scores (that reflect clinical severity) and cortical thickness has also been explored. In comparison to participants with a CDR score of 0, those with a CDR score of 0.5 show significant reductions in cortical thickness of MTL regions than in other regions. Although changes in cortical thickness between those with a CDR score of 0.5 vs. 1 are present, these are not significant. In comparison to participants with a CDR of 1, those with a CDR of 2 show significant reductions in cortical thickness of the frontal, temporal, medial occipital, and posterior cingulate regions (Im et al., 2008). Therefore, these findings are comparable to those reported by Singh et al. (2006) and indicate that MTL regions are vulnerable to AD-related changes early on, whereas widespread cortical thinning occurs as the disease progresses.

1.7.2. White Matter Changes

Although AD is considered a grey matter disease, white matter is also affected. Some research exploring white matter integrity, during healthy ageing and AD, focuses on the fornix and cingulum. The fornix is the major input/output white matter fibre bundle of the hippocampus and projects to the hypothalamus and thalamus. The fornix is crucial for cognition and episodic memory. The cingulum connects the cingulate and parahippocampal gyrus to the septal cortex. Long association fibres from the cingulate gyrus also project into frontal, parietal, and temporal cortices. Therefore, the fornix and cingulum provide major connections between the limbic system and the rest of the brain (Bennett, Huffman, and Stark, 2015; Marquez and Yassa, 2019; Senova et al., 2020). Other work indicates that AD patients have disruptions in intrahemispheric tracts, including the inferior longitudinal fasciculus, superior longitudinal fasciculus, and inferior fronto-occipital fasciculus, as well as disruptions in projection fibre tracts, including corticospinal tract, forceps minor, and forceps major (Yang et al., 2021). Similarly, in comparison with cognitively healthy individuals, MCI patients show reduced intracellular compartment metrics in several white matter locations that connect the frontal lobe with the occipital, parietal, and temporal lobes, such as, the longitudinal fasciculus and the inferior fronto-occipital fascicle (Bergamino et al., 2022). These findings support the concept of AD-related disconnection since both local and global network alterations are evident. Of note, the longitudinal fasciculus and the inferior fronto-occipital fascicle have been associated with cognition, emotion, object recognition, and visual processing, and correlate with cognitive impairment in both MCI and AD (Dou et al., 2020).

When compared with cognitively healthy ageing subjects, AD patients have reduced fractional anisotropy in intracortical projection fibre tracts, specifically in the corpus callosum, the splenium of the corpus callosum, cingulum, fornix, and frontal, temporal, and occipital lobes. Increased fractional anisotropy is observed in extracortical projection fibre tracts, such as in pyramidal, extrapyramidal, and somatosensory tracts. AD patients also have increased mean diffusivity in the corpus callosum, splenium of the corpus callosum, and frontal, temporal, and parietal lobes, as compared with healthy ageing subjects (Bozzali et al., 2002; Naggara et al., 2006; Teipel et al., 2007). These results are in line with previous findings suggesting intracortical networks are vulnerable in AD and temporal-to-frontal disconnections in AD, with relative sparing of sensorimotor pathways (Naggara et al. 2006; Teipel et al., 2007).

Similar findings have been obtained by Huang, Friedland, and Auchus (2007). In comparison with cognitively healthy ageing individuals, AD patients have lower fractional anisotropy and higher radial diffusivity in the temporal, parietal, and frontal regions. MCI patients show reduced axial diffusivity in temporal regions, reduced fractional anisotropy in parietal regions, and greater radial diffusivity in parietal regions. The greatest amount of change observed between healthy ageing individuals and MCI or AD patients was in temporal regions, followed by parietal regions, and then frontal regions. In both AD and MCI patients, fractional anisotropy and radial diffusivity in temporal regions correlated with episodic memory, fractional anisotropy and radial diffusivity in frontal regions correlated with executive function, and radial diffusivity in parietal regions correlated with visuospatial function. Therefore, alterations are observed in regions that serve higher cortical function, rather than in those that have primary functions, e.g., occipital lobes.

Choo et al. (2010) demonstrated that MCI and AD patients have reduced fractional anisotropy in the parahippocampal region. In addition to this, AD patients have reduced fractional anisotropy in cingulum fibres near the posterior cingulate. However, cingulum fibres near the middle cingulate gyrus show no reductions in either MCI or AD patients. These findings indicate that the cingulum bundle disruption commences near MTL structures and as AD progresses, from preclinical to clinical AD, the disruption is evident in the posterior cingulate cingulum. However, the middle cingulate cingulum is relatively spared during early AD.

These results have been expanded upon. Villain et al. (2008) found that hippocampal atrophy is associated with cingulum bundle disruption, and the cingulum is strongly correlated with hypometabolism in the posterior cingulate cortex, middle cingulate gyrus, thalamus, mammillary

bodies, parahippocampal gyrus, and hippocampus, i.e., the Papez circuit, and the right (R) temporoparietal cortex, in AD. Therefore, these various studies highlight the involvement of white matter tracts in the corpus callosum, fornix, temporal white matter, and the perforant path in AD, thus supporting the disconnection hypothesis.

The perforant path is essential for healthy hippocampal function. The perforant path is a large neuronal projection that arises from layers II and III of the entorhinal cortex (Hyman et al., 1986). Axons from layers II and IV project to granule cells and pyramidal cells of the dentate gyrus and cornu ammonis 3, and axons from III and IV project to pyramidal cells of cornu ammonis 1 and the subiculum (Anand and Dhikav, 2012; Mollink et al., 2019). Lesions in the perforant path cause neuronal loss in entorhinal cortex layer II (Peterson et al., 1994). This is one of the earliest pathological features of AD and is also affected in AD severely (Augustinack et al., 2010; Lenz et al., 2023). Therefore, examining changes in the perforant path is key to understanding AD pathophysiology. Since the perforant path is only a ~2-3 mm thick fibre sheet, it is challenging to study this path exclusively in humans (Marquez and Yassa, 2019). However, Yassa, Muftuler, and Stark (2010) devised an ultrahigh submillimeter resolution DTI (microstructural DTI) protocol to measure perforant path integrity. Not only did the perforant path signal reduce with age, but the signal could predict neuropsychological test performance of hippocampal function. Thus, suggesting that perforant path integrity is required for memory.

1.7.3. Altered Activation of the Hippocampus and Cortical Regions

Hippocampal hyperactivation is associated with memory function and Aβ deposition, specifically the dentate gyrus and cornu ammonis 3 subregions of the hippocampus, during ageing and aMCI (Bakker et al., 2012; Yassa et al., 2011). MCI patients also show greater MTL activation during episodic memory processing (Dickerson et al., 2005). Additionally, those with Aβ positivity exhibit hippocampal hyperactivation at baseline and longitudinally, as well as greater cognitive decline over time. This is in contrast to MCI patients who are Aβ negative. Interestingly, when amyloid and hippocampal volume is controlled for, an association between hippocampal volume and faster clinical progression is present (Huijbers et al., 2015). However, as disease progresses across the AD continuum, this hyperactivation reduces (Dickerson et al., 2005) due to hippocampal atrophy (Klink et al., 2021).

For instance, in comparison with cognitively healthy subjects, mild MCI patients show increased hippocampal activation during a fMRI memory recognition task. In contrast to cognitively healthy subjects, AD patients demonstrate reduced hippocampal and entorhinal activation during the memory recognition task. This suggests hippocampal hyperactivation during the early stages of the AD continuum and hypoactivation as the disease progresses (Dickerson et al., 2005).

Celone et al. (2006) went one step further and found that mild MCI patients not only demonstrated greater activation in the hippocampus during an associative memory task, using fMRI, but they also showed greater deactivation of medial and lateral parietal regions of the default mode network. In comparison, severe MCI and mild AD patients showed significantly reduced activation in the hippocampus and loss of deactivation in medial and lateral parietal regions that was also associated with greater activation in the neocortical attention network. These findings suggest a relationship between memory-related activation of the hippocampus and deactivation of parietal regions. Sperling (2007) suggested that this reflects a distributed memory network that includes MTL regions and, medial and lateral parietal regions, or a compensatory response to memory decline.

Interestingly, using high-resolution fMRI during a pattern separation task, Yassa et al. (2010) highlighted that the source of the hippocampal hyperactivation in aMCI is a result of changes specifically in the cornu ammonis 3 and dentate subregions. These changes may be partly due to the imbalance in the anterolateral entorhinal cortex-cornu ammonis 3-dentate network. Thus, hypoactivation in the anterolateral entorhinal cortex and hyperactivation in cornu ammonis 3 and dentate regions (Reagh et al., 2018).

Moreover, in AD, reduced regional glucose metabolism is found in the posterior cingulate, precuneus, temporoparietal, and frontal multimodal association regions. In contrast, the primary visual cortex, sensorimotor cortex, basal ganglia, and cerebellum, are comparatively unaffected (Herholz, Carter, and Jones, 2007). For example, Mosconi et al. (2008) examined cerebral glucose metabolism in healthy ageing controls, MCI, and AD patients. 98% of healthy ageing individuals did not show cortical hypometabolism, 86% of MCI patients exhibited cortical hypometabolism suggestive of neurodegenerative disease, and 99% of AD patients showed hypometabolism in parietotemporal and posterior cingulate cortex, this included both mild AD and severe AD patients. Additionally, 68% of MCI patients had reduced fluorodeoxyglucose 18F-FDG uptake across both hemispheres symmetrically, whereas 11% showed greater hypometabolism in the

left (L) hemisphere, and 10% exhibited greater hypometabolism in the R hemisphere. In comparison, 84% of AD patients showed reduced 18F-FDG uptake in both hemispheres symmetrically, 10% had greater hypometabolism in the L hemisphere, and 6% had increased hypometabolism in the R hemisphere. Therefore, some disease heterogeneity was evident. When investigating the hippocampus alone, only 4% of healthy ageing participants showed hippocampal hypometabolism, 84% of MCI patients showed hippocampal hypometabolism, and 98% of AD patients had hippocampal hypometabolism. The presence of hippocampal hypometabolism differentiated AD patients from healthy ageing controls with 98% sensitivity and 96% specificity, and differentiated AD patients from dementia with Lewy bodies and FTD patients with 98% sensitivity and 75% specificity. The differential specificity between the different dementia subtypes substantially improved when combining cortical hypometabolism with hippocampal hypometabolism. Similarly, the combination of cortical hypometabolism and hippocampal hypometabolism differentiated MCI patients from healthy ageing subjects with 98% sensitivity and 92% specificity. Therefore, the investigation of cerebral glucose metabolism is a reliable method to support clinical diagnosis of AD, and the presence of hypometabolism in the hippocampus, parietotemporal, and posterior cingulate, provides added value to the clinical diagnosis of AD (Mosconi et al., 2005). The concordance rate between visual examination of FDG PET scans and clinical diagnosis of AD has been found to be 93.4% (Tripathi et al., 2014). In most cases, reduced glucose metabolism provides greater diagnostic input than reductions in volumetric measures. For MCI and AD patients, reduced glucose metabolism exceeds volume loss (De Santi et al., 2001). These results are comparable with those found by several other researchers demonstrating that healthy ageing individuals and those at the very early stages of the AD continuum show hyperactivation, whilst those who are progressing to (late) MCI or AD, show hypoactivation (Bakker et al., 2012; Dickerson et al., 2005; Sorg et al., 2007).

Furthermore, the combined advantage of FDG PET and amyloid PET has also been investigated. Landau et al. (2012) examined this across the AD continuum. During longitudinal follow-up stages, for healthy ageing subjects, amyloid deposition was associated with cognitive decline over time. For late-MCI patients, both hypometabolism and amyloid deposition were associated with longitudinal cognitive decline, however, there was a greater association with hypometabolism. Thus, indicating that amyloid deposition is linked with the earliest stages of clinical decline and once clinical dysfunction is recognisable/a clinical diagnosis is received, hypometabolism and cognitive decline progress simultaneously. These findings are in line with the model suggested by Jack Jr et al. (2010). Amyloid deposition occurs while ageing individuals

are cognitively intact, and during the later stages, glucose hypometabolism reflects the underlying synaptic dysfunction. It is at this point where variability in cognitive decline among AD patients is noticed, where cognition is affected by other factors such as, comorbidities, lifestyle, and education (Landau et al., 2012).

1.7.4. Impaired Network Connectivity

The brain consists of many functional networks, including the default mode network, salience, sensory motor, dorsal attention, and control networks. The default mode network involves the medial prefrontal cortex, posterior cingulate cortex, precuneus, anterior cingulate cortex, parietal cortex, and the MTL (Marquez and Yassa, 2019). The default mode network is the largest, most active at rest, and comprehensively studied network. Of note, this network was the first to be identified as being altered in AD and shown to be associated with episodic memory (Brier et al., 2012; Alves et al., 2019). These findings are in line with the spatial distribution of amyloid and tau pathology within regions of the default mode network and thus indicate impact to synaptic connectivity (Marquez and Yassa, 2019).

1.7.4.1. Medial Temporal and Other Networks

Ritchey, Libby, and Ranganath (2015) proposed that there are two main networks which connect with the hippocampus and are differentially involved in episodic memory. (1) the posterior-medial network, which involves the parahippocampal cortex, retrosplenial cortex, posterior cingulate, precuneus, angular gyrus, anterior thalamus, presubiculum, mammillary bodies, and medial prefrontal cortex, and (2) the anterior-temporal network, which involves the perirhinal cortex, ventral anterior temporal cortex, lateral orbitofrontal cortex, and amygdala. Berron et al. (2021) specifically investigated progression of tau PET pathology in MTL regions and the posterior-medial network. They found, in early disease stages, tau accumulation is in the entorhinal and transentorhinal regions initially, followed by anterior and posterior hippocampus, Brodmann area 36, and parahippocampal cortex. In later stages, the medial and temporal regions, inferior parietal region, retrosplenial cortex and precuneus are affected. These patients also show that tau-related reductions in functional connectivity in the posterior-medial network correlate with memory impairment.

fMRI and rs-fMRI studies highlight that preclinical AD, i.e., individuals at risk of AD due to increased levels of amyloid burden, is associated with functional alterations of brain networks (Busche and Konnerth, 2016). Hyperactivation of the hippocampus and impaired activation of the default mode network during memory encoding tasks have been found in individuals at genetic risk of AD due to the presence of the APOE ε4 allele (Bookheimer et al., 2000; Machulda et al., 2011), those who are cognitively healthy and have a build-up of amyloid (Hedden et al., 2009; Sperling et al., 2009; Sheline et al., 2011), and patients with early AD (Bakker et al., 2012; Dickerson et al., 2005; Sorg et al., 2007).

Grady et al. (2001) examined memory for unfamiliar faces with short-delay intervals, using PET. In terms of brain activity, increasing delay intervals resulted in mild AD patients exhibiting greater activation in the R prefrontal, anterior cingulate, and L amygdala, whereas controls showed greater activation in bilateral prefrontal and parietal cortices. Increased activation in the R prefrontal cortex correlated with improved memory performance in both cohorts, and activation in the L amygdala was also associated with improved performance in patients. This unexpected activation of the L amygdala may represent compensatory behaviour or may reflect that patients process emotional content of faces to a greater extent. Based on the above findings, functional connectivity of the R prefrontal cortex and L amygdala was investigated further. In patients, activation of the R prefrontal cortex correlated positively with activation of other prefrontal regions, whereas in controls it was correlated positively with the L prefrontal cortex, bilateral extrastriate and parietal regions, and R hippocampus. In patients, activation of the L amygdala correlated with bilateral posterior parahippocampal gyri, L prefrontal regions, anterior and posterior cingulate, thalamus, and insula, whereas in controls it was associated with temporal and occipital areas mainly. These results indicate that healthy older adults utilise posterior visual regions and the prefrontal cortex, required for facial processing, and the hippocampus, for facial memory. Patients, on the contrary, show limited correlations between these regions – an anterior-posterior disconnection. Although patients may exhibit increased activation in MTL regions during cognitive tasks, the hippocampus may be functionally disconnected to the prefrontal cortex, and the amygdala may have increased functional connectivity to the prefrontal cortex (Grady et al., 2001). Therefore, significant alterations in connectivity are not only found within MTL structures, but these changes also affect connectivity with other brain areas.

Furthermore, the anterior-posterior disconnection phenomenon is not only evident during task-based studies but also during resting-state. Wang et al. (2007) examined whole-brain rs-fMRI.

Compared with healthy subjects, early AD patients have decreased positive correlations between the prefrontal and parietal lobes, and increased positive correlations within prefrontal, parietal, and occipital lobes. Thus, increased within-lobe connections show a compensatory effect for the decreased connections between lobes – a potential AD biomarker. Therefore, studying both positive and negative correlations may uncover the intrinsic organisation of brain function (Fox et al., 2005).

1.7.4.2. Intrinsic Networks

Intrinsic connectivity networks are disrupted in AD and MCI patients, and in those at high risk of AD. Atypical resting-state functional connectivity within the default mode and attention networks is thought to be associated with Aβ pathology in elderly subjects with and without cognitive symptoms (Koch et al., 2015). Other changes in the ageing population include increased resting-state connectivity between the default mode and salience networks in amyloid positive individuals with low neocortical tau, and reduced resting-state connectivity between the default mode and salience networks in amyloid positive individuals with increased tau-PET signal (Schultz et al., 2017).

Investigating patients with prodromal AD, Myers et al. (2014) looked at spatial patterns of amyloid-beta plaques using PIB PET and intrinsic connectivity using rs-fMRI. Globally, Aβ plaques and intrinsic functional connectivity patterns were positively correlated in the default mode network and, in medial and lateral heteromodal fronto-parietal attention networks. Locally, greater amyloid levels were found in network cores, than in network peripheries.

Koch et al. (2015) also examined patients with prodromal AD, using PIB PET, rs-fMRI, and task-fMRI based on an attention-demanding task with varying levels of difficulty. In contrast to Myers et al. (2014), Koch et al. (2015) found local PIB uptake correlated negatively with default mode network connectivity. Additionally, increased PIB uptake, particularly in the frontal, parietal, and temporal lobes, correlated with impaired cognition. Findings suggest atypical intrinsic network connectivity is associated with Aβ pathology and cognitive impairment.

Zhao et al. (2019b) also used rs-fMRI to demonstrate that AD patients exhibit alterations beyond the default mode network. Compared with healthy controls, AD patients show reduced functional connectivity in the default mode, executive control, and frontoparietal networks.

Additionally, in the executive control network, the L superior frontal gyrus and L thalamus show increased connectivity, while the L anterior cingulate shows decreased connectivity. In the frontoparietal network, the superior parietal gyrus and L paracentral lobule show increased connectivity, while the L supramarginal gyrus shows decreased connectivity. Between-network changes are also present, the L anterior cingulate and L inferior parietal region have reduced functional connectivity. Thus, large-scale functional network alterations are present, and may demonstrate inter-network functional connectivity is required to perform tasks, which may be impaired in AD.

1.7.5. Summary

Taking all the evidence from neuroimaging studies discussed above into consideration, it is clear that patients along the spectrum of AD are subjected to brain atrophy and shrinkage, reduction of cortical thickness, reduced brain weight and white matter integrity, impaired activation of default mode, attention, and salience networks, and hyperactivation of hippocampal and cortical regions during the early stages of the disease vs. hypoactivation in later stages. Thus, leading to impairments in memory and overall cognition.

CHAPTER 2

SYSTEMATIC REVIEW

2.1. INTRODUCTION

Sporadic AD is considered a polygenic disease. However, to date, the APOE gene is by far the most studied gene and has the strongest genetic association with sporadic AD (De Marco et al., 2020). This association, first identified by Saunders et al. (1993), is thought to influence both EOAD and LOAD (Sims, Hill, and Williams, 2020).

Importantly, APOE is neither necessary nor sufficient to cause AD (Sims, Hill, and Williams, 2020). Evidently, sporadic AD is not as straightforward as familial AD, in terms of causative genes/variants. Therefore, more research is required to understand the disease mechanisms in sporadic AD, including individuals who do not have the APOE ε4 variant.

As such, studying a candidate gene or a single genetic variant is not adequate to measure disease mechanisms or risk. The first genome-wide association study (GWAS) on LOAD was conducted by Grupe et al. (2007). However, the first most powerful GWAS on AD was conducted by Harold et al. (2009), involving 16,000 individuals, including cases and controls. The largest GWAS specifically on sporadic AD to date has been conducted by Wightman et al. (2021), with 1,126,536 individuals, consisting of 90,338 cases and 1,036,225 controls. Results from such studies show that there are 50+ risk loci associated with AD (Sims, Hill, and Williams, 2020; Sun et al., 2021) and additional variants may be discovered by further powerful GWASs. Therefore, sporadic AD is a complex polygenic disease where numerous genetic variants need to be assessed as they are individually thought to have small effects on overall disease risk. In doing so, this increases power, strengthens predictive accuracy, and provides sufficient information to identify individuals at high risk. Polygenetics combines these various genetic variants (Dezhina et al., 2019; Lewis and Vassos, 2020).

The polygenic risk score (PRS) and polygenic hazard score (PHS) are predictive models (Chatterjee, Shi, and Garcia-Closas, 2016), and expand upon the findings from GWASs. The overarching aim of these predictive models is to identify the level of risk of a given disease, using information from across the genome, aggregated into a single quantitative score (Altmann et al., 2020; Ding et al., 2021). First described by the International Schizophrenia Consortium (2009), calculations are based on a set of risk variants in a discovery (or training) sample, i.e., from a large, or the most informative, GWAS. The sum of all risk alleles, at the various variants in the replication (or target) sample, are taken and weighted by each risk allele's effect size. The effect size is estimated from the independent disease-specific GWAS. This is calculated separately for each

individual (Dunbridge, 2013; Lewis and Vassos, 2020). Thus, there are two key steps in this model: (1) determining which variants to include, and (2) estimating the weights to be added, from GWAS to the variants included in step (1) (Chatterjee, Shi, and Garcia-Closas, 2016).

The conceptual difference between PRS and PHS is in the method used to calculate effect sizes. Effect sizes for PHS are derived from Cox proportional hazard regression model and use a multivariate approach, i.e., effects for each variant are assessed in the presence of all other relevant variants. On the contrary, effect sizes for PRS are estimated using odds ratio from logistic regression and use a univariate approach. Interestingly, there are inconsistent findings in terms of which of these approaches yield robust results (Chasioti et al., 2019; Leonenko et al., 2019; Altmann et al., 2020). However, it has been reported that PRS can differentiate AD patients from controls with an area under the curve (AUC) of 75% to 90% (Sims, Hill, and Williams, 2020).

Earlier studies used unweighted PRSs as it was not considered that different variants may have different effects on disease. It should be noted that taking weights from GWASs does not acknowledge the impact of different races, study populations, and study designs, on the disease. Nonetheless, the formation of PRSs is continually being improved, for instance, by selecting appropriate variants and enhancing estimation of weights (Janssens, 2019) using GWASs with greater sample sizes and GWASs that use data from AD patients with biomarker evidence rather than those with clinical diagnosis only (Altmann et al., 2020), therefore, increasing the generalisability of findings.

Although these predictive models may be considered simplistic, they best predict the genetic architecture of complex multifactorial diseases and progressive diseases, such as AD, even whilst individuals are asymptomatic, as these scores can be determined at any point in time (Baker and Escott-Price, 2020; Lewis and Vassos, 2020). PRSs can also enable early diagnosis, aid understanding of disease prognosis and disease mechanisms, inform therapeutic intervention, and contribute to individualised treatment (Torkamani, Wineinger, and Topol, 2018). In addition, PRSs may be a viable approach to recruit individuals to clinical trials, selecting those who are at most risk vs. least risk of developing the disease, and thus increasing statistical power (Baker and Escott-Price, 2020).

The application of these predictive models is well utilised in psychiatric illnesses. GWASs have shown psychiatric disorders, such as schizophrenia and bipolar disorder, have thousands of

common variants that play a role in genetic architecture, and thus are regarded polygenic disorders (Dezhina et al., 2019). As such, the effect of PRS on brain structure and function has been studied in patients with schizophrenia, bipolar disorder (Simoes et al., 2020; Quide et al., 2022), psychosis (Ranlund et al., 2017) and major depressive disorder (Harris et al., 2019). Previous research has utilised data from healthy individuals, those at familial risk, and patients. In terms of studies specifically using patient data in their target sample, Deng et al. (2022) showed PRS in schizophrenia patients is associated with abnormalities in connectivity and negative symptoms, with negative symptoms affecting PRS-related working memory performance more than connectome topology. Walton et al. (2013) highlighted a positive correlation between PRS and L dorsolateral prefrontal inefficiency during working memory processing in such patients. Whalley et al. (2016) found a significant interaction between PRS for schizophrenia and major depressive disorder status, particularly psychological distress and neuroticism. Abe et al. (2021) showed higher PRS for schizophrenia and bipolar disorder is associated with reduced cortical thickness of the ventromedial prefrontal cortex. PRS for bipolar disorder is also correlated with functional hub strength of the ventromedial prefrontal cortex. Interestingly, Nivard et al. (2017) demonstrated PRS for schizophrenia is also associated with childhood and adolescent psychopathology. Therefore, evidently, genetic architecture influences both brain structure and function, in a range of psychiatric illnesses. Additionally, PRSs are being integrated into risk models of breast and prostate cancers to predict the development and progression of disease (Escott-Price, 2021).

Moreover, the importance and value of PRSs in AD has relatively recently received greater attention. Non-APOE variants are found to modify the disease risk and age of onset in APOE ε4 homozygous and heterozygous individuals. Thus, demonstrating non-APOE and APOE variants and gene pathways, interact (van der Lee et al., 2018; Zhang et al., 2020). Other research has shown the effect estimates from non-APOE risk loci range from an odds ratio between ~1.1 to ~2.1. Therefore, their individual contribution to sporadic AD is small (Sims, Hill, and Williams, 2020); however, their combined effect is of interest. There is also some research into the influence of AD risk variants, acquired through GWAS, on brain structure and function in asymptomatic individuals. However, the long-term impact of AD PRS on brain features remains inconclusive (Sims, Hill, and Williams, 2020). Evidently, these predictive models are underutilised in AD, and in other neurological diseases (Escott-Price, 2021).

2.1.1. Aim and Objective

The aim of Chapter 2 (Systematic Review) is to review systematically papers exploring PRS/PHS and structural neuroimaging parameters in AD, MCI, and cognitively unimpaired (CU) subjects. This in turn will increase understanding of the current level of knowledge surrounding possible associations.

2.2. METHODS

A literature search was conducted in three online databases: PubMed, Scopus, and Web of Science. The search took place between 31 January 2023 and 15 March 2023. This search was re-run on 05 March 2024 and again on 05 July 2025 to identify further papers. The search terms used were, "polygen*" in combination with "Alzheimer", "cogniti*", "dementia", "MCI", "mild cognitive impairment", "subjective cognitive complaint", or "prodromal", and in combination with "structure*", "anatomic*", "MRI", "DTI", "grey matter", "gray matter" or "white matter. The precise strings are reported in Appendix B Table B.1. No time limits were set (in relation to the date of publication).

After removal of duplicates, the titles and abstracts of the remaining papers were inspected and selected, the following exclusion criteria were applied: (1) AD PRS and brain structure in young samples, i.e., not age-matched; (2) association between AD and a non-relevant topic, e.g., brain function, brain connectivity networks, glaucoma, handgrip, herpes, or socioeconomic status; (3) various irrelevant sub-topics of AD, e.g., treatments, or pathology; (4) other types of dementia or unspecified dementia; (5) other neurological disorders; (6) brain injury; (7) neurodevelopmental disorders; (8) psychiatric disorders; (9) cognition; (10) intelligence; (11) general papers about genetics, PRSs, brain structure, or brain ageing; (12) animal studies; (13) alcohol or substance use; (14) reviews or meta-analyses not picked up by database filters; (15) methods papers, e.g., improving PRS/risk prediction; (16) other irrelevant papers, e.g., cardiovascular diseases, sleep, cells, gene expression, or handedness.

Other database filters that were implemented:

- PubMed – include papers in English, include papers on humans, exclude reviews, exclude systematic reviews, exclude meta-analyses, exclude preprints
- Scopus – include papers in English, include articles from journals that are at the final publication stage, exclude reviews
- Web of Science – include papers in English, include articles, include early access papers, exclude reviews

Papers selected for this review were assessed in line with a customised set of criteria and a points system (adapted from Manca et al., 2018) for assessment of quality. This was to not only ensure quality papers for this review and to omit possible biases, but to show the quality of papers

available in this subfield. The 11 criteria and points system (maximum 18 points) are outlined in Appendix B Table B.2.

The selected papers were reviewed by two independent assessors (AV and MDM), any discrepancies were reviewed by a third independent assessor (RM), before findings were considered for inclusion in this review.

2.3. RESULTS

The literature search in three online databases resulted in 3605 papers. Note, this number does not include papers that the databases recognised as meeting exclusion criteria (i.e., not in English, non-human subjects, reviews, systematic reviews, and meta-analyses), as explained in the previous section. Depending on the features available in the online databases, the databases were able to filter out either, all vs. some, of the above-mentioned exclusion criteria. If databases were unable to recognise papers that met exclusionary criteria, they were included in the total number of papers and duplicate number of papers given in this section. 64 papers met all eligibility criteria. These papers were published between 2010 and 2025. See Figure 2.1 for details.

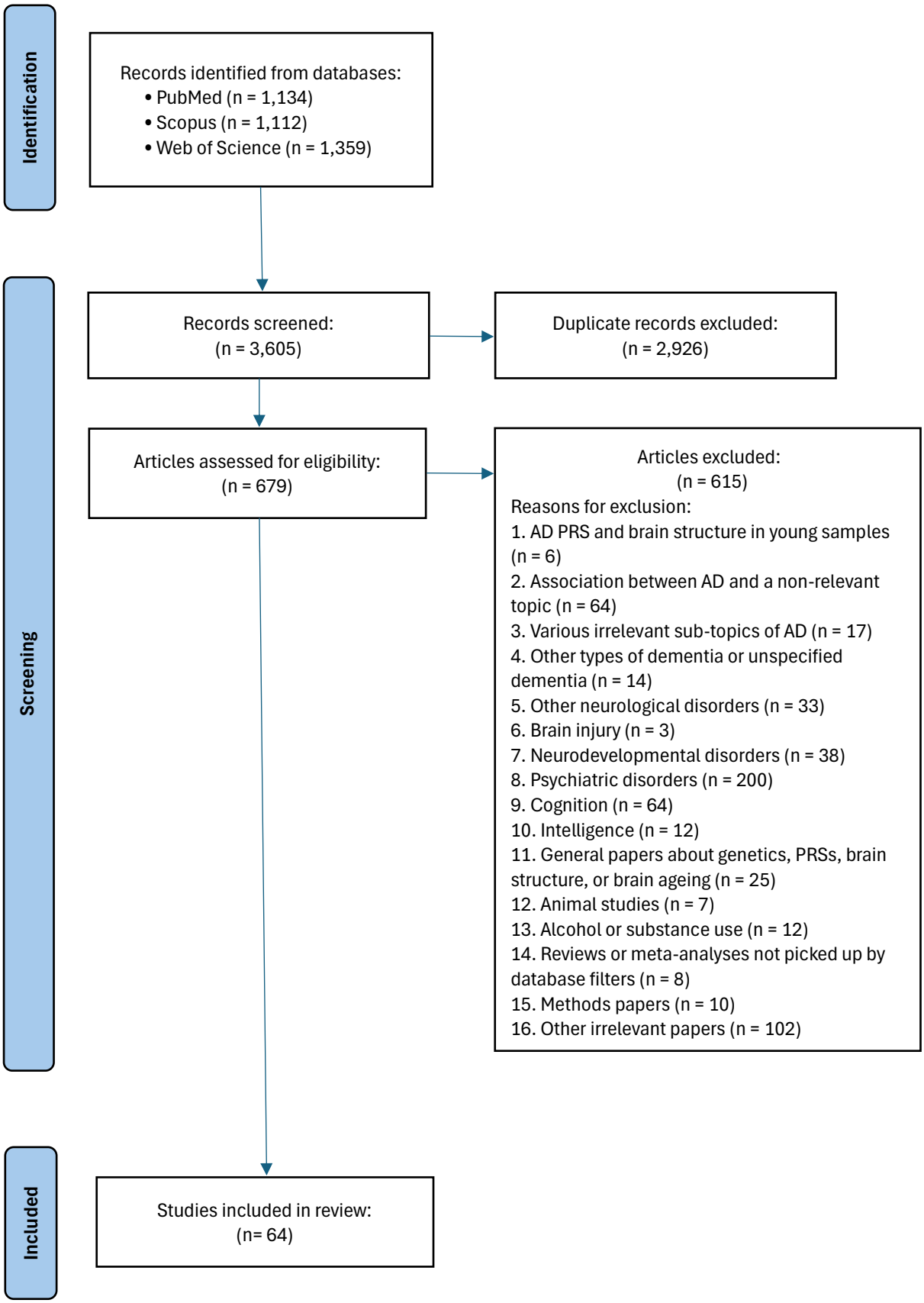

Figure 2.1: Flow diagram outlining the study selection process. Adapted from PRISMA 2020 guidelines (Page et al., 2021).

2.3.1. Characteristics of Papers

The 64 papers selected for review were on the basis that either the entire paper investigated structural parameters, or because part of the paper included structural parameters and therefore such sections were extracted for review.

Of the 64 papers, 54 papers investigated MRI measures (34 regional, 7 whole brain, 13 both regional and whole brain), 5 papers looked at DTI outcome measures (1 regional, 3 whole brain, 1 both regional and whole brain), 4 papers looked at both MRI and DTI (2 regional, 2 regional and whole brain), and 1 paper assessed MRI and diffusion-weighted imaging (DWI) using regional and whole brain measures. See Appendix B Table B.3 for details.

2.3.2. Summary of Demographic Variables

2.3.2.1. Age

Most papers recruited elderly participants from across the AD spectrum, and control participants were well age-matched (as shown in Appendix B Tables B.3). There were a few exceptions; Xiao et al. (2017) assessed participants whose age were comparatively young, mean age 31.59 (SD 9.27), and 2 papers did not comment upon participants' age (Desikan et al., 2017; Manca, Pardinas, and Venneri, 2023). There were also differences among the method in which various researchers stated participants' age, some reported mean age and standard deviation, whereas others reported the mean only. Therefore, further comparisons regarding age are not possible here.

2.3.2.2. Ancestry

Majority of discovery GWASs were conducted on non-Hispanic white participants with European ancestry. However, a few GWASs also included participants from other backgrounds. For instance, South Asian (India, Pakistan) and East Asian (China, Korea) (de Silva et al., 2022), African and Asian (Corlier et al., 2018), African, Central Asian, and East Asian (Zhao et al., 2019b), Asian and Yoruban heritage (Sabuncu et al., 2012), and African, Asian, Hispanic, and other/mixed (Sloan et al., 2010). Refer to Appendix B Table B.4 for details.

Most participants that were recruited for the studies (papers) identified for this systematic review were of European ancestry. Five papers included a small subsample of minority groups. For instance, those with Asian, African, or Hispanic ancestries (Chen et al., 2024), African, Central Asian, and East Asian ancestries (Zhao et al., 2019b). The remaining 3 papers did not specify the race, ancestry, or ethnicity of participants but stated that their participant sample included a small proportion of "other races" (Liu et al., 2021; Liu et al., 2022) or that 6.5% of their participants were non-white and from minority ethnic backgrounds (Manca, Pardinas, and Venneri, 2022). See Appendix B Table B.4 for more information.

2.3.2.3. Family History

There was a lack of transparency when it came to researchers stating whether family history had been taken into consideration, only 1 (Harrison et al., 2016) out of 64 papers had included family history, and another 3 (Ebenau et al., 2021; Lee et al., 2021; Xiao et al., 2017) out of 64 papers did not include family history. The remaining papers did not mention this point.

2.3.2.4. Sample Size

The number of participants in the various studies were significantly different, ranging from 66 to 72,004 participants (see Appendix B Table B.2).

2.3.2.5. Diagnostic Status

Of the 64 papers, 32 investigated CU participants only (Armstrong et al., 2020; Brenowitz et al., 2023; Caspers et al., 2020; Corlier et al., 2018; Chandler et al., 2025; Chen et al., 2023; Chen et al., 2024; Ebenau et al., 2021; Foo et al., 2021; Habes et al., 2016; Habes et al., 2018; Harrison et al., 2016; Harrison et al., 2023; Hayes et al., 2020; He et al., 2023; Kirchner et al., 2023; Korbmacher et al., 2024; Lancaster et al., 2019; Lancaster et al., 2023; Liu et al., 2023; Lorenzini et al., 2024; Roe et al., 2024; Rutten-Jacobs et al., 2018; Sabuncu et al., 2012; Sha et al., 2023; Soldan et al., 2024; Steventon et al., 2023; Tank et al., 2022; Vacher et al., 2022a; Williams et al., 2021; Xiao et al., 2017; Zhao et al., 2019b), 3 papers explored MCI patients only (Kauppi et al., 2018; Liu et al., 2021; Liu et al., 2022), 4 assessed both CU and MCI subjects (De Marco et al., 2020; de Silva et al., 2022; Desikan et al., 2017; Hohman et al., 2017), 1 paper examined those with subjective memory complaints, early-MCI, and late-MCI (Reas et al., 2023) 2 looked at CU,

subjective cognitive decline, and MCI subjects (Nordengen et al., 2022; Sloan et al., 2010), 3 papers investigated CU and AD subjects (Kulminski et al., 2024; Roostaei et al., 2018; Wang et al., 2019), and 19 papers assessed CU, MCI, and AD subjects (Ahmad et al., 2018; Altmann et al., 2020; Chung et al., 2023; Ge et al., 2018; Genius et al., 2025; Homann et al., 2022; Kannappan et al., 2022; Lee et al., 2021; Lorenz et al., 2025; Li et al., 2021; Lupton et al., 2016; Manca, Pardinas, and Venneri, 2023; Meda et al., 2012; Mormino et al., 2016; Prieto et al., 2020; Tan et al., 2019; Vacher et al., 2022b; Xu et al., 2022; Zhao et al., 2020). This selection, therefore, covered the AD spectrum.

2.3.2.6. Datasets

Of the 64 papers, most of the participant data that were manipulated came from the Alzheimer's Disease Neuroimaging Initiative (ADNI). For 20 of these papers, the data source was ADNI only (Altmann et al., 2020; Chung et al., 2024; De Marco et al., 2020; De Silva et al., 2022; Desikan et al., 2017; Ge et al., 2018; Hayes et al., 2020; Hohman et al., 2017; Kannappan et al., 2022; Kauppi et al., 2018; Lee et al., 2021; Li et al., 2021; Manca, Pardinas, and Venneri, 2023; Meda et al., 2012; Mormino et al., 2016; Prieto et al., 2020; Reas et al., 2023; Sabuncu et al., 2012; Wang et al., 2019; Xu et al., 2022) and for 7 papers, the participant data were from both ADNI and an additional source (Genius et al., 2025; Liu et al., 2021; Liu et al., 2022; Lorenz et al., 2025; Lupton et al., 2016; Roostaei et al., 2018; Tan et al., 2019). Fourteen papers utilised participant data from the UK Biobank (Armstrong et al., 2020; Chandler et al., 2025; Chen et al., 2023; Chen et al., 2024; Foo et al., 2021; Harrison et al., 2023; He et al., 2023; Korbmacher et al., 2024; Lancaster et al., 2019; Rutten-Jacobs et al., 2018; Sha et al., 2023; Steventon et al., 2023; Tank et al., 2022; Liu et al., 2023), and 1 paper utilised participants from ADNI, UK Biobank, and an additional source (Zhao et al., 2019b). The remaining 22 papers used various other data sources (Ahmad et al., 2018; Brenowitz et al., 2023; Caspers et al., 2020; Corlier et al., 2018; Ebenau et al., 2021; Habes et al., 2016; Habes et al., 2018; Homann et al., 2022; Kirchner et al., 2023; Kulminski et al., 2024; Lancaster et al., 2023; Lorenzini et al., 2024; Nordengen et al., 2022; Roe et al., 2024; Sloan et al., 2010; Soldan et al., 2024; Vacher et al., 2022a; Vacher et al., 2022b; Williams et al., 2021; Xiao et al., 2017; Zhao et al., 2020; Harrison et al., 2016).

2.3.3. Summary of Polygenic Scores

Of the 64 papers, 47 papers calculated PRSs, 9 papers used PHSs, 2 papers utilised both PRSs and PHSs, and 5 papers used a similar concept to polygenic scores. 1 paper did not state the type of polygenic score used distinctively, but PRS is presumed due to the methodology described.

Most papers calculated polygenic scores using SNPs found to be associated with AD by the International Genomics of Alzheimer's Project (IGAP) (Lambert et al., 2013). Other papers used alternative GWASs and meta-analyses (Becker et al., 2004; Beecham et al., 2014; Bertram et al., 2007; Bellenguez et al., 2022; de Rojas et al., 2021; Desikan et al., 2017; Ge et al., 2019; Gibson et al., 2019; Harold et al., 2009; Hibar et al., 2017; Jansen et al., 2019; Kanehisa et al., 2008; Kunkle et al., 2019; Marioni et al., 2018; Nikpay et al., 2015; Sims et al., 2017; van Meurs et al., 2013; Wightman et al., 2021) or genomic data from other studies i.e., ADNI, UK Biobank, Human Connectome Project, Paediatric Imaging, neurocognition, and genetics, and the Philadelphia neurodevelopment cohort (Zhao et al., 2019b). See Appendix B Table B.4 for details.

Interestingly, only 21 papers utilised a vast number of SNPs in their polygenic calculations, i.e., 296 SNPs (Genius et al., 2025), 365 SNPs (Zhao et al., 2019b), 834 SNPs (Sloan et al., 2010), 2,466 SNPs (Xiao et al., 2017), 8,070 SNPs (Wang et al., 2019), 12,148 SNPs (Armstrong et al., 2020), 12,361 SNPs (He et al., 2023), 16,123 SNPs (Mormino et al., 2016), 27,150 SNPs (Meda et al., 2012), 101,450 SNPs (Altmann et al., 2020), 111,843 SNPs (Harrison et al., 2023), 134,456 SNPs and 135,584 SNPs (de Silva et al., 2022), 136,598 SNPs (Lancaster et al., 2019), 354,674 SNPs (Foo et al., 2021), 1,105,067 SNPs (Sha et al., 2023), 1,312,100 SNPs (Liu et al., 2023), 6,578,321 SNPs (Tank et al., 2022), 6,739,456 SNPs (Soldan et al., 2024), 7,055,881 SNPs (Chen at al., 2022), 7,485,124 SNPs (Kannappan et al., 2022), and 13,377,200 SNPs (Nordengen at al., 2022). The remaining papers used between 4 and 85 SNPs.

Furthermore, of the 64 papers, 13 papers included APOE SNPs when calculating polygenic scores (De Marco et al., 2020; Desikan et al., 2017; Ge et al., 2018; Harrison et al., 2016; Hayes et al., 2020; Kauppi et al., 2018; Kulminski et al., 2024; Li et al., 2021; Meda et al., 2012; Prieto et al., 2020; Reas et al., 2023; Sloan et al., 2010; Vacher et al., 2022b), 25 papers did not include APOE SNPs in polygenic scores (Altmann et al., 2020; Brenowitz et al., 2023; Caspers et al., 2020; Chen et al., 2024; Chung et al., 2023; Corlier et al., 2018; de Silva et al., 2022; Ebenau et al., 2021; Habes et al., 2016; Habes et al., 2018; Hohman et al., 2017; Lancaster et al., 2019; Lancaster et al., 2023; Lee et al., 2021; Liu et al., 2021; Liu et al., 2023; Lupton et al., 2016; Nordengen et al.,

2022; Soldan et al., 2024; Tan et al., 2019; Tank et al., 2022; Vacher et al., 2022a; Xiao et al., 2017; Xu et al., 2022; Liu et al., 2022), 15 papers constructed two sets of polygenic scores, one with and one without APOE SNPs (Ahmed et al., 2018; Armstrong et al., 2020; Chandler et al., 2025; Foo et al., 2021; Genius et al., 2025; Harrison et al., 2023; He et al., 2023; Kirchner et al., 2023; Lorenz et al., 2025; Lorenzini et al., 2024; Mormino et al., 2016; Roe et al., 2024; Sabuncu et al., 2012; Sha et al., 2023; Wang et al., 2019), and 11 papers did not state whether APOE SNPs were included or excluded from polygenic scores, or whether both types of scores were constructed (Chen et al., 2023; Homann et al., 2022; Kannappan et al., 2022; Korbmacher et al., 2024; Manca, Pardinas, and Venneri, 2022; Roostai et al., 2018; Rutten-Jacobs et al., 2018; Steventon et al., 2023; Williams et al., 2021; Zhao et al., 2019b; Zhao et al., 2020).

Additionally, of the 64 papers, only 6 papers stated the medium used for polygenic information, i.e., blood (Genius et al., 2025; Harrison et al., 2016; Soldan et al., 2024), homocysteine (Roostaei et al., 2018), lymphocyte DNA (Caspers et al., 2020), or from *post-mortem* brain tissue (Chung et al., 2023).

2.3.4. Software Used to Construct Polygenic Scores

To construct polygenic scores, 23 papers out of 64 utilised the PLINK package (Armstrong et al., 2020; Brenowitz et al., 2023; Caspers et al., 2020; Chung et al., 2023; Harrison et al., 2023; Hohman et al., 2017; Homann et al., 2022; Kannappan et al., 2022; Lancaster et al., 2023; Lee et al. 2021; Lupton et al., 2016; Mormino et al., 2016; Roe et al., 2024; Roostaei et al., 2018; Rutten-Jacobs et al., 2018; Sabuncu et al., 2012; Soldan et al., 2024; Steventon et al., 2023; Vacher et al., 2022a; Williams et al., 2021; Xiao et al., 2017; Zhao et al., 2019b; Zhao et al., 2020), 14 papers used the PRSice package, found within R Statistical Software (Altmann et al., 2020; Chandler et al., 2025; Chen et al., 2023; de Silva et al., 2022; Foo et al., 2021; Ge et al., 2018; Genius et al., 2025; He et al., 2023; Korbmacher et al., 2024; Lancaster et al., 2019; Liu et al., 2021; Liu et al., 2022; Manca, Pardinas, and Venneri, 2022; Wang et al., 2019), 1 paper employed the Epitools package in R (Prieto et al., 2020), and 2 papers utilised R but did not state the specific toolbox (Ahmad et al., 2018; Sloan et al., 2010). Additionally, 1 paper used Ldpred (Tank et al., 2022), 1 utilised MatLab (Meda et al., 2012), and 3 used PRS-CS (Kirchner et al., 2023; Lorenz et al., 2025; Sha et al., 2023). The remaining 19 papers did not state clearly the software and/or package used to calculate polygenic scores (Chen et al., 2024; Corlier et al., 2018; De Marco et al., 2020; Desikan et al., 2017; Ebenau et al., 2021; Habes et al., 2016; Habes et al., 2018; Harrison et al.,

2016; Hayes et al., 2020; Kauppi et al., 2018; Kulminski et al., 2024; Li et al., 2021; Liu et al., 2023; Lorenzini et al., 2024; Nordengen et al., 2022; Reas et al., 2023; Tan et al., 2019; Vacher et al., 2022b; Xu et al., 2022).

2.3.5. Frequent Genes Identified Across Papers

A set of 23 genes were found to be used in polygenic score calculations repeatedly, i.e., used in several papers. Note that these findings were from 43 out of 64 papers only as these papers either stated the genes that were used to construct general AD polygenic scores or the authors provided this information via email communication when requested, and used summary statistics from AD-specific discovery GWASs or other AD-specific measures to construct polygenic scores. The genes relate to generic AD polygenic scores only rather than region-specific or pathway-specific PRSs. Each gene from the set of 23 genes appeared in 10 to 28 different papers, a frequency of 23.26% to 65.12% (refer to Table 2.1 for details). The remaining 226 genes were used to construct polygenic scores in between 1 to 7 papers only, a frequency of 2.33% to 16.28% (see Appendix B Table B.5). The group of 23 genes are all protein coding genes, and are involved in protein binding activities and signalling pathways.

Furthermore, a total of 38 region-specific PRSs or pathway-specific PRSs were found across the papers, namely: Activation of Immune Response PRS, Amyloid PRS, APP Metabolism PRS, Cholesterol Metabolism PRS, Cholesterol Transport PRS, Clathrin/Adaptor Protein Complex 2 PRS, Clearance PRS, Cortical Grey Matter PRS, Cortical White Matter PRS, Cytoskeleton/Axon Development PRS, Endocytosis PRS, Extrinsic Epigenetic Age Acceleration PRS, Fractional Anisotropy PRS, Hematopoietic Cell Lineage PRS, Haemostasis PRS, Hippocampal PRS, Homocysteine PRS, Immune Activation PRS, Immune Response PRS, Inflammatory PRS, Intrinsic Epigenetic Age Acceleration PRS, Mean Diffusivity PRS, Microglia PRS, Migration PRS, Module-based PRS 6 (neuritic plaque formation), Module-based PRS 9 (NFT formation), Plasma Lipoprotein Particle Assembly PRS, Protein Folding PRS, Protein Ubiquitination PRS, Protein-Lipid Complex PRS, Protein-Lipid Complex Subunit Organisation PRS, Protein-Lipid Complex Assembly PRS, Regulation of Amyloid Precursor Protein Catabolic Process PRS, Regulation of Aβ Formation PRS, Reverse Cholesterol Transport PRS, Signal Transduction PRS, Tau Protein Binding PRS, and Ventricle PRS.

Table 2.1: Names and frequencies of the top 23 genes used to construct polygenic scores in 43 (out of 64) papers.

Gene Acronym	Gene Full Name	Frequency (n | %)
HLA-DRB5	Human leukocyte antigens, major histocompatibility complex, class II, DR beta 5	10 | 23.26%
SPI1	Spi-1 proto-oncogene	10 | 23.26%
SPPL2A	Signal peptide peptidase like 2A	11 | 25.58%
CELF1	CUGBP Elav-like family member 1	12 | 27.91%
NME8	NME/NM23 family member 8	12 | 27.91%
RIN3	Ras and Rab interactor 3	12 | 27.91%
MEF2C	Myocyte enhancer factor 2C	13 | 30.23%
CD2AP	CD2 associated protein	17 | 39.53%
EPHA1	EPH receptor A1	18 | 41.86%
ZCWPW1	Zinc finger CW-type and PWWP domain containing 1	18 | 41.86%
CASS4	Cas scaffold protein family member 4	21 | 48.84%
FERMT2	FERM domain containing kindlin 2	21 | 48.84%
INPP5D	Inositol polyphosphate-5-phosphatase D	21 | 48.84%
MS4A6A	Membrane spanning 4-domains A6A	21 | 48.84%
PTK2B	Protein tyrosine kinase 2 beta	22 | 51.16%
SLC24A4	Solute carrier family 24, member 4	22 | 51.16%
BIN1	Bridging integrator 1	23 | 53.49%
PICALM	Phosphatidylinositol binding clathrin assembly protein	23 | 53.49%
SORL1	Sortilin related receptor 1	23 | 53.49%
ABCA7	ATP(adenosine triphosphate)-binding cassette, sub-family, A member 7	24 | 55.81%
CR1	Complement C3b/C4b receptor 1 (Knops blood group)	25 | 58.14%
CLU	Clusterin	26 | 60.47%
APOE	Apolipoprotein E	28 | 65.12%

(Gene Cards, 2025; The National Center for Biotechnology Information, 2025).

2.3.6. Quality Assessment Outcomes

The average quality assessment score for the papers was 9.55 points, with a range between 2 points (Rutten-Jacobs et al., 2018) to 14 points (Altmann et al., 2020; Genius et al., 2025) out of a maximum of 18 points. The score for each criterion per paper and total score per paper have been displayed in Appendix B Table B.6.

2.3.7. Regional Imaging of the Hippocampus

Much research has focused primarily on the association between polygenic scores and the hippocampus or subregions within the hippocampus. For instance, Foo et al. (2021) aimed to identify the association between PRS and hippocampus, using regional MRI. PRS, including APOE SNPs, was associated negatively with the whole L and R hippocampus. When parcellated, PRS, including APOE SNPs, was also associated inversely with L cornu ammonis 1, L cornu ammonis 4, L molecular layer, L granule cell layer of dentate gyrus, R subiculum, bilateral hippocampus-amygdala-transition-area, and bilateral hippocampal tail. Hippocampal subfields segregated into head, body, and tail were investigated also. PRS, with APOE SNPs, was associated with all three subregions and the whole hippocampus. High PRS was associated with reduced volume of the L cornu ammonis 1, L molecular layer, L granule cell layer of dentate gyrus, R hippocampal tail, and entire L hippocampus. However, when APOE SNPs were removed from PRS, none of these associations were present. Additionally, PRS effects on hippocampal subfield volume was associated with older age than younger age, demonstrating age, but not sex, impacted findings in this cohort. Although this was a cross-sectional study only, the researchers investigated a large pool of CU participants who underwent standardised MRI procedures and genetic assays.

Similarly, Kannappan et al. (2022) assessed the association between PRS and regional hippocampal atrophy, using MRI. Regardless of whether CU, MCI, and AD subjects were grouped together, or whether they were stratified according to clinical diagnosis (MCI vs. MCI+AD), PRS was associated more strongly with the 12 subfields of the L hippocampus and the entire hippocampus, than with the 12 subfields in the R hippocampus and the entire hippocampus. The 12 subfields consisted of cornu ammonis 1, cornu ammonis 3, cornu ammonis 4, hippocampal tail, hippocampal fissure, subiculum, presubiculum, parasubiculum, molecular layer, granule cells in the molecular layer of the dentate gyrus, fimbria, and the hippocampus-amygdala-transition-area. Compared with CU subjects, in MCI and MCI+AD cohorts, PRS was associated significantly with L cornu ammonis 1, cornu ammonis 4, hippocampal tail, subiculum,

presubiculum, molecular layer, granule cells in the molecular layer of the dentate gyrus, and hippocampus-amygdala-transition-area. However, PRS was associated moderately with L cornu ammonis 3, parasubiculum, and fimbria. On the other hand, the association between PRS and R parasubiculum was weaker than that found in the L parasubiculum. PRS was not associated with either the L or R hippocampal fissure in any groups. Note, the effect of PRS on hippocampal subfields was larger in the MCI+AD cohort since this included a sample of AD patients. It was not possible to assess the associations for AD patients independently due to the small sample size. Therefore, replication in a larger AD cohort is required to validate these results. Nonetheless, these findings indicate the vulnerability of the L hippocampus to AD, specifically the cornu ammonis 1, cornu ammonis 4, hippocampal tail, subiculum, presubiculum, molecular layer, granule cells in the molecular layer of the dentate gyrus and hippocampus-amygdala-transition-area, and suggest these may be potential imaging biomarkers to aid early prediction of AD.

A potential imaging biomarker has been suggested by Zhao et al. (2020). They found that PRS was associated significantly with 21 out of 33 radiomic features of the hippocampus, as measured by regional MRI, in MCI patients. This suggests, hippocampal radiomic features, including intensity, textural, shape, and wavelet features, may be useful AD-specific biomarkers, and may predict progression from MCI to AD.

Similarly, Xu et al. (2022) looked at the association between polygenic risk and regional hippocampal atrophy as assessed by MRI, however, with PHS in this instance. They observed a significant interaction between PHS and disease stage (i.e., CU, MCI, AD) with the R fimbria. No associations were found in other hippocampal subfields – cornu ammonis 1, cornu ammonis 3, cornu ammonis 4, hippocampal tail, hippocampal fissure, subiculum, presubiculum, parasubiculum, molecular layer, granule cells in the molecular layer of the dentate gyrus, and the hippocampus-amygdala-transition-area. This is a contrast to the findings of Kannappan et al. (2022) who utilised PRS over PHS and found associations with the above-mentioned hippocampal subfields, where the association was stronger with the L hemisphere than R hemisphere.

Additionally, Mormino et al. (2016) found that high PRS was associated with reduced hippocampal volume at baseline in CU and MCI subjects. Including or excluding APOE SNPs did not alter this finding; a contrast to Lancaster et al. (2019)'s results. When including APOE SNPs to PRS, the association with hippocampal volume strengthened slightly (Mormino et al., 2016).

Additionally, Hohman et al. (2017) found that PRS was not associated with hippocampal atrophy in a group of subjects with suspected non-AD pathophysiology. This is when patients show evidence of neurodegeneration in the absence of amyloid deposition. Evidently, findings from these studies are inconsistent and show the urgent need to study non-APOE genes and therefore non-lipid metabolism pathways across the AD spectrum.

Similarly, the findings by Ge et al. (2018) highlight the need to investigate other pathways. They took one step further and stratified participants into Aβ positive vs. negative. In Aβ positive participants, APOE ε4 status and PRS were correlated weakly with baseline hippocampal volume but were not associated with longitudinal hippocampal changes. In Aβ negative participants, PRS was associated significantly with longitudinal hippocampal volume changes, but was not associated with baseline hippocampal atrophy. These findings highlight PRS influence both Aβ positive and negative individuals, however, the time course varies. These results also suggest genetic risk for AD has an effect not only on the Aβ pathway, but also on other pathways, in turn, altering AD-related brain regions.

Interestingly, when Kirchner et al. (2023) studied gene variants separately, the APOE ε4 SNP, serotonin-transporter-linked promoter region (5-HTTLPR) SNP, and brain-derived neurotrophic factor (BDNF) rs6265 SNP, were associated with the entire hippocampus, and the former two variants were also associated with hippocampal subfield volumes. There were no associations between the kidney and brain expressed protein (KIBRA) rs17070145 SNP, or the catechol-o-methyltransferase (COMT) rs4680 with the hippocampus. Seventeen GWASs were then used to identify seven lead SNPs which affect hippocampal volume. Four of these SNP-related associations (rs17178139, rs1861979, rs57246240, and rs7873551) with whole hippocampal volume were replicated in the CU sample used by Kirchner et al. (2023). The rs160459 SNP was associated with the granule layer of the dentate gyrus, rs17178006 was associated with cornu ammonis 1, and rs2909443 was associated with hippocampal tail. However, when utilising the PRS, no such associations were found in either the entire hippocampus or in hippocampal subfields.

Homann et al. (2022) performed an in-house GWAS. A PRS computed using summary statistics from this GWAS was not associated with hippocampal volume. Although APOE SNPs are well studied and widely associated with AD risk, they did not reach significance levels in the GWAS performed in this study. However, the APOE ε4-related SNP, rs429358, alone, was associated with

L hippocampal volume. In contrast, when Homann et al. (2022) computed a PRS using the GWAS from Hibar et al. (2017), PRS was associated with L hippocampal volume, R hippocampal volume, and the total hippocampal volume. Again, the APOE ε4 SNP did not reach genome-wide significance in relation to hippocampal volume in this GWAS. Additionally, when Homann et al. (2022) calculated a PRS using Jansen et al. (2019)'s GWAS, the PRS was associated with white matter damage. Evidently, this field lacks in consistency and replicability of findings, highlighting the challenges encountered.

Lupton et al. (2016) investigated the association between PRS with both hippocampal and amygdala volumes, using MRI. PRS, without APOE and TREM2 SNPs, was associated with reduced hippocampal volume in CU individuals and MCI patients, but not in AD patients. This association was stronger in females. Although APOE genotype explained more of the variance in hippocampal volume than PRS, the combined effects of PRS, APOE ε4, and TREM2, explained more of this variance than APOE ε4 alone. On the other hand, no such associations were found between PRS and amygdala volume.

Furthermore, Wang et al. (2019) examined the association between PRS and Ch4 volume. The basal forebrain contains magnocellular cholinergic neurons segregated into regions Ch1 to Ch4. Ch4 relates to the nucleus basalis of Meynert of the basal forebrain and is associated with AD. Ch4 is thought to hold 90% of cholinergic neurons. In AD patients, PRS, with and without APOE SNPs, were not associated with Ch4 volume. This finding remained constant at several thresholds, i.e., p = 0.001, 0.05, 0.1, 0.2, 0.3, 0.4, and 0.5. However, in CU individuals, PRS, with and without APOE SNPs, were associated significantly with Ch4 volume. It may be that Ch4 volume was reduced significantly in the AD cohort, to such an extent that it was not measurable. This explanation may still uphold as to the reason why associations were not found in the AD group, despite information regarding AD severity in this cohort not being known.

2.3.8. Regional Imaging of Various Cortical Regions

2.3.8.1. Grey Matter

Many studies have assessed the relationship between polygenic scores with structural parameters of a range of brain regions. For instance, Corlier et al. (2018) explored the association

between PRS and cortical thickness using MRI in CU individuals. ROIs were: hippocampus, parahippocampal and entorhinal cortex, precuneus, caudal and rostral anterior cingulate, posterior cingulate cortex, isthmus of the cingulate cortex, supramarginal gyrus, caudal and rostral middle frontal gyrus. High PRS, excluding APOE SNPs, was significantly associated with increased regional cortical thinning. Interestingly, despite the PRS being calculated using inflammation-related and immune-related gene SNPs, no significant association was found between PRS and baseline serum C-reactive protein. Thus, suggesting various mechanisms need to be assessed still to understand AD risk better.

Sabuncu et al. (2012) found that PRS, with APOE, was associated significantly with average thickness across the heteromodal association cortex and MTL. Thickness of each ROI in the Desikan-Killiany atlas (Desikan et al., 2006) was then assessed. PRS, including APOE, was correlated significantly with the thickness of the isthmus of the cingulate and was associated weakly with the inferior temporal and orbitofrontal regions. However, no associations were found in other ROIs. Additionally, PRS without APOE was also associated significantly with cortical thickness in these AD-related regions and remained significant in APOE ε3 homozygotes.

Furthermore, Harrison et al. (2016) utilised a hypothesis-driven PRS, using APOE, clusterin (CLU), and phosphatidylinositol binding clathrin assembly protein (PICALM) SNPs, as these have consistently been reported to increase AD risk. Harrison et al. (2016) found that PRS was not associated with thinning of the hippocampus, or the entorhinal cortex and subiculum subregions, at baseline. However, longitudinally, PRS was associated with reduced thickness of the hippocampus, and entorhinal cortex and subiculum subregions, over a two-year period in CU individuals.

Roe et al. (2024) examined the association between PRS, with and without SNPs from the APOE region, and structural MRI ROIs based on early Braak and Braak (1991) staging. CU participants from the Center for Lifespan Changes in Brain and Cognition (discovery sample) and the Betula and Netherlands Study of Depression and Anxiety (replication samples) were studied. Findings showed that high PRS with APOE was associated with increased volume loss than expected for their age in bilateral hippocampus, bilateral amygdala, and R entorhinal cortex. A greater number of associations were found using the PRSs with APOE than PRSs without APOE. These associations were found in the replication dataset, except for the amygdala. This anomaly may have been because the length of follow-up was reduced in the replication sample. Nonetheless,

these results indicate that APOE SNPs increase the predictive power of the PRS that includes APOE, since the associations weaken or diminish with PRS that excludes APOE.

On the other hand, Hayes et al. (2020) constructed a PHS for AD from the GWAS by IGAP (Lambert et al., 2013). Hayes et al. (2020) investigated the association between PHS including APOE SNPs, regional brain volume as measured by MRI, and body mass index (BMI) (normal: 18.5 to <25; overweight: ≥25 to 30; obese: ≥30). In CU subjects with increased BMI, associations were significant and negative between PHS and volume of the entorhinal cortex, and associations were significant and negative between PHS and volume of the hippocampus. In those with reduced BMI, PHS was not associated significantly with entorhinal cortex volume. When the sample was stratified by sex, these associations remained significant in females only. Additionally, BMI, PHS, and the interaction between BMI x PHS, did not alter volume of the precentral gyrus or postcentral gyrus (motor and sensory regions that are relatively spared by AD pathology). Therefore, these results highlight that PHS and BMI influence regions that are AD-specific.

Similarly, Prieto et al. (2020) studied the association between PHS, with APOE SNPs, and regional brain volume, using MRI. In the entire cohort consisting of CU, MCI, and AD subjects, PHS was associated significantly with volume of the R entorhinal cortex. A significant association was present for both those with high PHS, and low PHS. However, such associations were not found in the L entorhinal cortex. In MCI patients specifically, PHS was associated significantly with volume of the L hippocampus. This significance was present in both those with high PHS, and low PHS. However, no such associations were found in CU or AD subjects. In the AD cohort, high PHS was associated significantly with volume of the R entorhinal cortex. Therefore, most associations were found in the L hippocampus and the R entorhinal cortex. These results are similar to those found by Desikan et al. (2017), where PHS, which included APOE SNPs, was associated with hippocampal and entorhinal cortex volumes. Additionally, using PRS in MCI patients, Liu et al. (2021) found that PRS was associated with reduced hippocampal and entorhinal cortex volumes. Ebenau et al. (2021) found that PRS without APOE in cognitively healthy subjects with complaints of subjective decline, was associated with neurodegeneration in the MTL. However, APOE ε4 on its own was not associated with neurodegeneration. Together, these findings suggest that these regions, within the MTL, may be important targets for showing polygenic risk across the AD continuum.

Steventon et al. (2023) looked at whether an AD polygenic score could predict volumes of MTL regions in healthy female participants from the UK Biobank that were post-menopausal. The ROIs were volumes of the hippocampus, parahippocampal gyrus, perirhinal cortex, entorhinal cortex, amygdala, and the temporal lobe, and subregions of the hippocampus, i.e., cornu ammonis 1, cornu ammonis 2/3, cornu ammonis 4, and the dentate gyrus. Polygenic scores were generated at four thresholds: p = 0.5, 0.1, 0.00001, and 0.0000005. However, all results indicated that polygenic scores were not associated with any of the MTL structures. Similarly, polygenic scores did not interact with menopause age (mean age in years: 50.83 ± 3.96), or with the duration of hormone replacement therapy (mean years: 6.61 ± 5.28), to impact MTL regions. Of note, compared with the majority of literature, Steventon et al. (2023) did not state explicitly whether the polygenic scores referred to PRSs, PHSs, or both. Although, it may be implied that PRSs were constructed as they stated that AD *risk* was being investigated. They also did not mention whether APOE SNPs were included or excluded from polygenic scores.

Kauppi et al. (2018) devised a brain atrophy score using the sum of weighted measures from hippocampal volume, entorhinal cortex, middle temporal gyrus, isthmus cingulate, bank of the superior temporal sulcus, superior temporal gyrus, medial and lateral orbitofrontal gyri thickness. In comparison with using the atrophy score alone, the combined PHS with APOE plus atrophy score, increased prediction of MCI progression to AD, and reached an AUC of 82%. These results indicate that the utility of PHS over and beyond APOE is advantageous, and indicate regions that are susceptible to AD-related atrophy.

Reas et al. (2023) developed a multimodal hazard score that integrated (1) age, (2) the Desikan et al. (2017) PHS that includes APOE ε2 and ε4 SNPs, (3) an imaging hazard score derived from 64 volumetric MRI ROIs, and (4) an episodic memory score using the Rey Auditory Verbal Learning Test (RAVLT). These data were obtained from ADNI participants with subjective memory complaints or patients with MCI, to predict conversion to AD dementia over a five-year period. Conversion to AD was predicted modestly by increasing (1). Adding (1) + (2) enhanced prediction of the model significantly. Conversion to AD was improved by adding (1) + (2) + (3) and increased further when including (1) + (2) + (3) + (4), i.e., the entire multimodal hazard score. Additionally, time to AD dementia onset decreased substantially as the multimodal hazard score increased. Therefore, it seems that this novel score has a greater predictive value than PHS alone.

Other studies have used a vast number of ROIs as well. For example, Chen et al. (2023) investigated 68 cortical ROIs and 41 subcortical ROIs, using MRI. They found 39 out of 51 risk factors were associated significantly with the hippocampus, entorhinal cortex, inferior temporal cortex, and middle temporal cortex. These risk factors covered a wide range, including several sociodemographic, physical, lifestyle and environmental, dietary, health conditions, medications, operations, and cognitive function variables. However, the association between PRS and brain structures was not reported upon.

Lancaster et al. (2023) assessed the association between PRS, without APOE, and regional volume and thickness, in a group of CU participants from the PROTECT study. Participants were split into groups, either low PRS (1st decile) or high PRS (10th decile), and 66 ROIs obtained from MRI were studied in total. A negative association between high PRS and reduced thickness of the cingulate cortex was found. Interestingly, PRS was not associated with hippocampal volume, and hippocampal volume was not significantly different between those with low PRS vs. high PRS. This may have been due to the small number of participants (n = 16) that were included in the study. A sub-analysis on CU UK Biobank participants showed that PRS, without APOE and major histocompatibility complex regions, was associated with thickness of the R anterior caudal cingulate cortex. Thus, these results were similar to the findings observed in the PROTECT cohort.

On the other hand, Vacher et al. (2022b) found that PHS was associated significantly with longitudinal alterations in cortical volume across most of the 33 ROIs that were studied. The associations were strongest with AD-specific regions, that is: entorhinal cortex, temporal lobe, posterior cingulate, and precuneus. Atrophy rates were fastest in those with high PHS. However, when stratifying participants according to APOE ε4 status, no associations between PHS and cortical atrophy remained significant after controlling for multiple testing in ε4 non-carriers. Similarly, Tan et al. (2019) found that PHS, without APOE, was associated with longitudinal cortical volume decline in 11 ROIs, effects were strongest in the entorhinal cortex, inferior parietal cortex, and inferior and middle temporal cortex. Compared with subjects with low PHS, those with high PHS reflected greater volume loss.

Compositional brain scores (i.e. composite scores derived by grouping together regional brain volumes) may be used to improve risk-prediction further. Genius et al. (2025) incorporated compositional brain scores in their models to study whether volumetric changes in 34 cortical and 7 subcortical ROIs were associated with higher odds of being on the AD continuum vs. CU Aβ

negative, and whether any disease stage was influenced by PRS with APOE and/or PRS without APOE. Data from CU participants from the Alzheimer's and Families study and, MCI and AD participants from ADNI, were used. Participants were divided into four groups based on Jack Jr et al. (2016)'s A/T/N framework, using A only (obtained via CSF): CU A- vs. CU A+, MCI A+, and AD A+. Volumetric changes, as assessed by MRI, were combined using compositional data analysis (compositional brain scores) to differentiate CU A- participants from disease-stage groups. When comparing CU A- low PRS (with APOE) vs. CU A+ low PRS (with APOE), the regions that contributed to the compositional brain score were similar and included the amygdala, putamen, and pallidum. When comparing CU A- low PRS (with APOE) vs. CU A+ high PRS (with APOE), middle temporal regions, temporal and frontal poles, caudal anterior cingulate, and pars orbitalis contributed to the compositional brain score and increased the odds of being in the CU A+ high PRS with APOE group. Additionally, when comparing CU A- low PRS (with APOE) vs. MCI A+ low PRS (with APOE), volumetric changes in the rostral anterior cingulate contributed significantly to the compositional brain score and increased the likelihood of being in the MCI A+ low PRS with APOE group. When comparing CU A- low PRS (with APOE) vs. MCI A+ high PRS (with APOE), volumetric changes in the entorhinal area and thalamus proper contributed greatly to the compositional brain score and increased odds of being in the MCI A+ high PRS with APOE group. In the MCI A+ group, irrespective of low PRS with APOE vs. high PRS with APOE, the putamen, parahippocampal gyrus, fusiform, pallidum, lateral occipital, and frontal pole regions contributed greatly to the compositional brain score and increased probability of being associated with the MCI A+ group. Further, when comparing CU A- low PRS (with APOE) vs. AD A+ high PRS (with APOE), volumetric changes in the amygdala and parahippocampus contributed significantly to the compositional brain score and increased the likelihood of being in the AD A+ high PRS with APOE group. In AD A+ participants, irrespective of low PRS with APOE vs. high PRS with APOE, the frontal pole, insula, and putamen contributed to the compositional brain score and was associated with higher odds of being in the AD A+ group. Results using a PRS without APOE were also reported. When comparing CU A- low PRS (without APOE) vs. CU A+ low PRS (without APOE), the regions that contributed to the compositional brain score were similar. However, in addition, the entorhinal cortex and parahippocampus contributed to the compositional brain score significantly and increased odds of being in the CU A+ low PRS without APOE group. When comparing CU A- low PRS (without APOE) vs. CU A+ high PRS (without APOE), volumetric changes in the precuneus, fusiform, inferior temporal, medial orbitofrontal, and lateral orbitofrontal regions contributed greatly to the compositional brain score and were associated with increased odds of being in the CU A+ high PRS without APOE group. In CU A+

participants, irrespective of low PRS without APOE vs. high PRS without APOE, the amygdala, supramarginal, and pallidum contributed to the compositional brain score and increased odds of being associated with the CU A+ group. Additionally, when comparing CU A- low PRS (without APOE) vs. MCI A+ high PRS (without APOE), volumetric changes in the entorhinal cortex, thalamus proper, and pallidum contributed significantly to the compositional brain score and increased the likelihood of being in the MCI A+ high PRS without APOE group. In MCI A+ participants, regardless of low PRS without APOE vs. high PRS without APOE, the frontal pole, putamen, pallidum, fusiform, and caudal anterior cingulate regions contributed to the compositional brain score and increased odds of being in the MCI A+ group. Moreover, when comparing CU A- low PRS (without APOE) vs. AD A+ high PRS (without APOE), volumetric changes in the parahippocampus, amygdala, middle temporal, and fusiform regions contributed to the compositional brain scores greatly and increased the probability of being associated with the AD A+ high PRS without APOE group. In AD A+ participants, regardless of low PRS without APOE vs. high PRS without APOE, the frontal pole, putamen, and insula contributed to the compositional brain score and increased odds of being part of the AD A+ group. Evidently, high PRS (with or without APOE) differentiates CU participants with no biomarker evidence vs. CU participants with biomarker evidence. Therefore, PRS is useful for identifying individuals at risk of AD. This study highlights that the combination of composition brain scores and PRSs may enhance prediction.

On the contrary, Kulminski et al. (2024) devised risk profiles based on three genes only. Kulminski et al. (2024) assessed the association between low genetic risk vs. high genetic risk of AD and grey matter volume/thickness across temporo-limbic regions using MRI. Participants were from the National Alzheimer's Coordinating Centre Uniform Data Set and were stratified into risk groups based on the presence of APOE ε3ε4 or ε4ε4 and major allele homozygotes of translocase of outer mitochondrial membrane 40 homolog (TOMM40) rs2075650 and apolipoprotein C1 (APOC1) rs12721046 (low risk) vs. APOE e3ε4 or ε4ε4 and minor allele heterozygotes TOMM40 or APOC1 (high risk). These risk stratification criteria were based on the finding that those that are carriers of ε4, *plus* minor alleles of TOMM40 or APOC1, are at four-fold higher risk of AD. Hence, the model being scrutinised here is similar to the PRS model, since it relates to risk prediction. However, the difference is that Kulminski et al. (2024) did not use GWAS summary statistics. The 27 ROIs also included a hippocampal occupancy score: the ratio of hippocampal volume relative to the interior lateral ventricular volume. This measure has been shown to have higher discriminative accuracy than hippocampal volume alone. The 27 ROIs were also inclusive of an AD signature volume composite, that refers to grey matter volumes of the hippocampus,

parahippocampal gyrus, entorhinal cortex, superior temporal cortices (middle, inferior, and superior). In the AD model that was unadjusted, low risk was associated with reduced volumes of the L hippocampus, R hippocampus, L entorhinal cortex, R parahippocampus, L hippocampal occupancy score, and AD signature volume composite, as well as reduced thickness of the L entorhinal cortex, L parahippocampus, L superior temporal, R entorhinal, and R parahippocampus. Whereas, high risk was associated with reduced volumes of the L hippocampus, R hippocampus, L entorhinal cortex, L middle temporal, L parahippocampus, L precuneus, R entorhinal cortex, R parahippocampus, R precuneus, L hippocampal occupancy score, R hippocampal occupancy score, and AD signature volume composite. High risk was also associated with reduced thickness of the L entorhinal cortex, L parahippocampus, L precuneus, L superior temporal, R entorhinal cortex, R parahippocampus, and R precuneus. On the other hand, in the AD model that had been adjusted for the first five principal components, sex and age, low risk was associated with reduced volumes of the L hippocampus and R hippocampus, as well as thickness of the L entorhinal cortex, R entorhinal cortex, and R parahippocampus. In contrast, high risk was associated with L hippocampal volume only. Participants were then stratified by diagnosis. In AD cases, low risk was associated with L hippocampal volume. High risk was associated with reduced volumes of the L hippocampus, L entorhinal cortex, and R entorhinal cortex, as well as reduced thickness of the L entorhinal cortex, L precuneus, and R entorhinal cortex. In CU participants, low risk was associated with reduced volumes of the L entorhinal cortex and AD signature volume composite, and reduced thickness of the R entorhinal cortex. On the contrary, high risk was associated with increased thickness of the R middle temporal region. The findings regarding low risk control subjects indicate that having APOE ε3ε4 or ε4ε4 genotypes without the presence of minor alleles of TOMM40 and APOC1 may modulate or reduce the likelihood of AD-related symptomology in the presence of structural changes.

2.3.8.2. White Matter

In terms of white matter, Habes et al. (2018) looked at the association between PRS and white matter hyperintensities in periventricular posterior regions, periventricular frontal regions, periventricular dorsal regions, and deep white matter hyperintensities, using MRI. PRS was only associated significantly with white matter hyperintensities in periventricular frontal regions in subjects aged >65 years. This result is in line with the notion that frequency of sporadic AD heightens after this age and, therefore, impacted regional white matter in this study.

Additionally, Lorenz et al. (2025) studied the associations between PRSs that included vs. excluded APOE and regional white matter microstructure of limbic tracts. Specifically, tracts in the cingulum, fornix, inferior longitudinal fasciculus, uncinate fasciculus, inferior temporal gyrus, middle temporal gyrus, and superior temporal gyrus. These were measured using standard DTI metrics, as well as an advanced bi-tensor model that accounted for free water content in each voxel. Free water metrics are thought to improve quantification of white matter as they differentiate well between extracellular (free water) vs. intracellular space. Participants from several datasets (i.e., ADNI, Biomarkers of Cognitive Decline Among Normal Individuals (BIOCARD), Baltimore Longitudinal Study of Aging (BLSA), National Alzheimer's Coordinating Center, Religious Orders Study and Rush Memory and Aging Project, Vanderbilt Memory and Aging Project, and Wisconsin Registry for Alzheimer's Prevention (WRAP)) were assessed as a whole group (CU, MCI, and AD). PRS that included SNPs from the entire APOE region was associated negatively with radial diffusivity corrected for free water in the superior temporal gyrus, middle temporal gyrus transcallosal tract, cingulum, inferior temporal gyrus transcallosal tract, fornix and uncincate fasciculus, associated negatively with mean diffusivity corrected for free water in the fornix and uncinate fasciculus, associated positively with free water in the fornix, cingulum, inferior temporal gyrus transcallosal tract and inferior longitudinal fasciculus, associated positively with fractional anisotropy corrected for free water in the cingulum and the superior temporal gyrus transcallosal tract, and associated negatively with axial diffusivity corrected for free water in the fornix. However, after correcting for multiple comparisons, the associations between PRS with APOE and mean diffusivity corrected for free water in the uncinate fasciculus, free water in the inferior temporal gyrus transcallosal tract and inferior longitudinal fasciculus, fractional anisotropy corrected for free water in the superior temporal gyrus transcallosal tract, and axial diffusivity corrected for free water in the fornix no longer remained significant. In comparison, PRS that excluded SNPs from the APOE region was associated negatively with radial diffusivity corrected for free water in the fornix, superior temporal gyrus transcallosal tract, and uncincate fasciculus, associated positively with fractional anisotropy corrected for free water in the uncinate fasciculus, associated negatively with mean diffusivity corrected for free water in the fornix and inferior longitudinal fasciculus, and associated positively with free water in the fornix. However, these associations did not survive corrections for multiple testing. Therefore, high PRS with APOE was associated with high free water, high fractional anisotropy corrected for free water, low mean diffusivity corrected for free water, and low radial diffusivity for free water in limbic white matter tracts. Although these associations were found using PRS without APOE as well, they did not retain significance.

Additionally, in cognitively impaired participants, high PRS with APOE was associated with low radial diffusivity corrected for free water, low high axial diffusivity corrected for free water, and high fractional diffusivity corrected for free water in limbic white matter tracts. However, CU participants that had low vs. high PRS with APOE did not show such effects.

2.3.8.3. Grey Matter and White Matter

Armstrong et al. (2020) found high PRS, with APOE, was associated with greater baseline volume of the hippocampus and parahippocampal gyrus. Longitudinally (mean follow-up: 4.7 years), PRS with APOE was associated with a slower rate of ventricle enlargement and atrophy in frontal and parietal white matter. These findings remained in these CU participants when removing APOE SNPs from PRS.

Additionally, Zhao et al. (2019b) investigated 101 ROIs across the brain, using MRI. PRS, constructed using UK Biobank GWAS, predicted ROI volumes in four validation datasets significantly. Specifically, for ROIs, namely, R nucleus accumbens area, L and R putamen, L and R cerebellum white matter, L and R cerebellum exterior, L hippocampus, fourth ventricle, cerebellar vermal lobules VIII-X, and total brain volume ROIs, the PRS-predicted ROI volumes were associated significantly with the true ROI volumes in ADNI (mean age in years: 62.51 ± 7.47), Human Connectome Project (mean age in years: 28.82 ± 3.68), Paediatric Imaging (mean age in years: 12.28 ± 4.99), and the Neurocognition, and Genetics, Philadelphia Neurodevelopmental Cohort (mean age in years: 21.14 ± 7.47) datasets. Additionally, PRS predicted significantly 29 ROI volumes in three datasets, 56 ROI volumes in two datasets, and 84 ROI volumes in one dataset. Note, participants' ages were lower considerably in non-ADNI datasets. Nonetheless, PRS successfully predicted widespread ROIs.

2.3.9. Regional Imaging of Various Cortical Regions using Pathway-Specific Polygenic Scores (Grey Matter)

In comparison with the level of studies investigating genome-wide polygenic scores, a relatively small number of structural imaging studies have assessed region-specific or pathway-specific polygenic scores. For instance, Vacher et al. (2022a) constructed region-specific PRSs without APOE SNPs, i.e., Hippocampal PRS, Ventricle PRS, Cortical Grey Matter PRS, and Cortical White Matter PRS, and explored the association with regional brain atrophy, measured with MRI, in CU

participants. Low PRS was defined as one standard deviation below the mean, whereas high PRS was defined as one standard deviation above the mean. They found the four region-specific PRSs were associated significantly with longitudinal volume changes. Low PRS was associated with reduced rates of volumetric change, regardless of amyloid load. High PRS was associated with increased volume alterations, particularly in the hippocampus. When subjects were stratified according to amyloid status, region-specific PRSs were similar for both groups. This may have been because the rs2075650 SNP, found on the TOMM40 gene, and known to be associated with amyloid, was included in the Hippocampal PRS. Similarly, Lancaster et al. (2019) found that the Microglia PRS, consisting of 56 genes within the microglia network, was associated with hippocampal volume.

Nordengen et al. (2022) investigated the association between PRSs, without APOE SNPs, and MTL atrophy, consisting of the entorhinal cortex and, Brodmann area 35 and 36, using MRI. Cross-sectionally, a negative association was found between Inflammation PRS and baseline MTL volume. However, no associations were found with the PRS or pathway-specific Cardiovascular PRS. In longitudinal analyses, high Inflammation PRS and high Cardiovascular PRS were associated significantly with increased MTL atrophy over time, compared with those with low pathway-specific PRSs.

Liu et al. (2022) examined PRSs without APOE and regional atrophy in MCI patients, using MRI. Intrinsic Epigenetic Age Acceleration PRS, a measure of biological age, was associated significantly with volumetric changes in the fusiform gyrus, and with the Extrinsic Epigenetic Age Acceleration PRS, a measure of functional decline of the immune system. However, the Intrinsic Epigenetic Age Acceleration PRS was not associated with volumetric alterations in the ventricles, hippocampus, or middle temporal gyrus.

Similarly, Xiao et al. (2017) found LOAD PRS, APOE PRS, and LOAD PRS + APOE PRS were not associated with volume of the hippocampus, amygdala, thalamus, caudate, putamen, accumbens area and pallidum, nor with brain-wide cortical thickness/grey matter volume. Only one association was found. However, LOAD PRS was associated negatively with the surface area of the frontal pole.

Harrison et al. (2023) explored associations between genome-wide PRSs, and nine pathway-specific PRSs, with regional thickness and volume, in CU older adults from the UK Biobank with

MRI data. The pathway-specific PRSs were: Protein-Lipid Complex Assembly PRS, Regulation of Aβ Formation PRS, Protein-Lipid Complex PRS, Regulation of Amyloid Precursor Protein Catabolic Process PRS, Tau Protein Binding PRS, Reverse Cholesterol Transport PRS, Protein-Lipid Complex Subunit Organisation PRS, Plasma Lipoprotein Particle Assembly PRS, and Activation of Immune Response PRS. All pathway-specific PRSs, other than the Immune Response PRS, were associated negatively with cortical thickness in the R inferior temporal, R middle temporal, R and L supra-marginal, R inferior parietal, R and L parahippocampal, and R temporal pole regions, and particularly in the hippocampus, when APOE was included in these pathway-specific PRSs. There was a negative association between Immune Response PRS and R posterior cingulate, again when APOE was included. When APOE was excluded from all pathway-specific PRS, none of the associations remained significant after correcting for multiple comparisons. Similarly, the genome-wide PRS with APOE was not associated significantly with regional cortical thickness after correcting for multiple testing. Regarding cortical volumes, other than the Immune Response PRS, all remaining pathway-specific PRSs with and without APOE, were associated negatively with subcortical volumes, particularly in the hippocampus. The Protein-Lipid Complex PRS, with and without APOE, was also associated negatively with L and R accumbens. The genome-wide PRS with APOE was associated with the above-mentioned regions as well. Of note, the Immune Response PRS did not include APOE at any stage and may provide some explanation as to why different results were obtained with this score.

Moreover, Meda et al. (2012) looked at the association between 27,150 genome-wide common SNPs and 94 ROIs using MRI and parallel-independent component analysis, in the ADNI dataset. They found four genetic networks/components (1: 332 SNPs from 169 genes, 2: 377 SNPs from 182 genes, 3: 482 SNPs from 267 genes, and 4: 332 SNPs from 169 genes) were associated with one structural network consisting of 40 ROIs, including both volume and cortical thickness. Regions that provided input significantly to the structural network included thickness of the entorhinal cortex and amygdala, and volume of the hippocampus. Genes that provided input significantly to the four components included APOE ε3 and ε4, solute carrier family 9 member A7 (SLC9A7), shroom family member 2 (SHROOM2), zinc finger protein 673 (ZNF673), vacuolar protein sorting 13 homolog C (VPS13C), and adenosine triphosphate synthase (ATP5G2) genes. Genetic network 2 (with 332 SNPs) contained genes involved with risk of AD. Additionally, these associations were able to differentiate significantly between baseline diagnosis groups, i.e., CU, MCI, or AD. This study has been included in this review since it uses a method similar to the

polygenic score concept, and evidently is able to distinguish variants, other than APOE, which are associated with structural imaging parameters.

Sloan et al. (2010) used the hierarchical clustering method that has been shown to distinguish patterns efficaciously (Levenstien, Yang, Ott, 2003). This method was used by the researchers to find associations between imaging genetics and brain morphology. They found, 33 genes and 78 SNPs were associated with AD and neurodegeneration pathways, grey matter density and L and R hippocampal volume. Specifically, four clusters of SNPs were apparent. Cluster 1 was associated with grey matter density, clusters 2 and 3 were associated with grey matter density and hippocampal volume, and cluster 4 was associated with L and R hippocampal volume. The genes within these clusters were found to be associated with various functions, including cleavage of amyloid proteins, Aβ production, and apoptosis. This study has been included in this review as it implements a method that is conceptually similar to pathway-specific polygenic analysis.

Chung et al. (2023) used a comparable approach. They examined associations between module-based PRSs, without APOE, and regional cortical thickness derived from MRI of ADNI participants. Module-based PRSs were constructed using co-expression network models. These define modules of genes that are highly co-expressed based on correlation analysis of gene expression values (Chung et al., 2017). Such analysis revealed 14 gene sets, i.e., modules; five of the modules related to neuritic plaque formation, and nine modules related to NFTs. Module-based PRS 6 (neuritic plaque formation) was associated significantly with cortical thickness in bilateral frontal, parietal, and temporal, lobes. Module-based PRS 6 was localised particularly to Wernicke's area. Module-based PRS 9 (NFT formation) was associated significantly with bilateral frontal lobes. Therefore, module-based PRSs are useful for revealing and explaining clinical heterogeneity in AD patients, as compared with genome-wide PRSs that predict overall AD risk.

2.3.10. Whole Brain Imaging

2.3.10.1. Grey Matter

Some work has focussed on PRS and whole brain MRI measures. For instance, Habes et al. (2016) implemented the Spatial Pattern of Atrophy for Recognition of Brain Ageing (SPARE-BA), an index that measures typical brain ageing, and the Spatial Pattern of Atrophy for Recognition of Early AD

(SPARE-AD), in their study. The latter index has demonstrated efficacy in predicting progression from healthy ageing, to MCI, to AD (Davatzikos et al., 2009; Da et al., 2013). In the Study of Health in Pomerania population sample, those aged >65 years were classified as advanced brain ageing, whereas others were grouped into the resilient to ageing cohort. Compared with the resilient to ageing cohort, subjects in the advanced brain ageing group had reduced grey matter volumes, specifically and significantly in the thalamus, insular cortex, cingulate cortex, frontal cortex, inferior parietal cortex, and lateral temporal cortex, with the most distinguished differences in the medial and inferior temporal lobe, including the hippocampus. However, when establishing associations between PRS, without APOE SNPs, and these indexes, PRS was not associated with the SPARE-BA index when the cohort was studied together, or in the advanced brain ageing cohort in group comparisons. Also, PRS was not associated with the SPARE-AD index in the entire cohort; however, a significant association was found in the advanced brain ageing group. The latter result adheres to the known finding that individuals aged ≥65 years are prone to AD. This study implemented a novel pattern analysis tool to quantify grey matter atrophy.

Similarly, Lee et al. (2021) utilised the PRS method. They investigated the association between PRS and whole brain atrophy, as measured by MRI. They found increased AD PRS was associated with reduced cortical thickness in bilateral medial temporal cortices. However, AD PRS was not associated with mean lobar cortical thickness.

Manca, Pardinas, and Venneri (2023) showed AD PRS was associated significantly and negatively with grey matter volume in the bilateral medio-temporal regions, R inferior temporal and posterior cingulate regions in the whole sample. Whereas, in group comparisons, which included AD patients with and without psychosis, AD PRS was associated with grey matter in the L medio-temporal regions of AD patients with psychosis only.

Furthermore, Caspers et al. (2020) looked at the association between PRS and cortical thickness in CU individuals. They calculated both total PRS and several pathway-specific PRSs. This was to group together all SNPs along the same biological pathway, and thus separate them from the total PRS since different pathways may work in various, or opposing, methods. Total PRS was associated with clusters in the subcentral and ventral gyrus, parietal operculum, and ventral precentral sulcus of the R hemisphere, and in medial occipital cortex, middle temporal gyrus, superior and inferior temporal sulcus, and inferior temporal gyrus of the L hemisphere. Similar associations were found when implementing the Cholesterol Metabolism PRS and APP

Metabolism PRS. However, the APP Metabolism PRS was associated additionally with the superior parietal cortex. After adjusting for APOE status, the only association which remained significant was between the APP Metabolism pathway and the superior parietal cortex. Therefore, cortical atrophy was influenced heavily by APOE in this cohort of elderly CU subjects.

Research looking into PHS and whole brain MRI volumetric measures has also been conducted. De Marco et al. (2020) found, in the MCI cohort, PHS was associated negatively with grey matter in mediotemporal regions, including the anterior hippocampus, amygdala, bilateral dorsal entorhinal cortex, and L posterior hippocampus. Stratification by APOE ε4 status yielded no significant associations. No such associations were found in the CU cohort. In all Aβ positive subjects, PHS was associated negatively with grey matter volume in the L anterior hippocampus and amygdala. Stratification by APOE genotype showed, in ε3ε3 participants, PHS was associated negatively with grey matter in sensorimotor cortex. Of note, the SNP corresponding to APOE ε4 was included in PHS calculations. This SNP had a log hazard ratio of 1.03, compared with the other 32 SNPs that had hazard ratios ranging from 0.07 to 0.30. Although this APOE SNP contributes greatly to the PHS, the other SNPs provide further genetic insights into the disease and associated volumetric changes.

Additionally, Li et al. (2021) looked at whole brain MRI and found that PHS correlated with reduced grey matter volume in the precuneus, inferior parietal lobe, and temporal lobe. PHS also correlated with greater grey matter volume in the frontal and occipital lobes. Between-group comparisons highlighted a progressive increase in this association as the disease advanced. However, due to limited sample size, particularly in the AD group, this study requires replication in a larger dataset.

2.3.10.2. White Matter

Sha et al. (2023) investigated a cohort of CU participants using whole brain DTI. They found high PRS, with and without APOE, was associated with greater white matter connectivity in 62 out of 90 ROIs. Similarly, Rutten-Jacobs et al. (2018) looked at white matter. They created white matter-specific PRSs. The White Matter Hyperintensity Volume PRS was significantly associated with AD. However, the Mean Diffusivity PRS and Fractional Anisotropy PRS, which measure white matter integrity, were not associated with AD. In contrast to many of the above studies, the strength of this research was the large participant pool obtained from the UK Biobank.

Moreover, in terms of whole brain white matter changes, Chandler et al. (2025) investigated the association between PRS for AD and white matter hyperintensity volumes in 32,114 participants from the UK Biobank. Global white matter hypersensitivity volumes were obtained using T1- and T2-weighted Fluid-Attenuated Inversion Recovery (FLAIR) MRI images. They found that PRS, without SNPs from the APOE region, was associated positively with white matter hyperintensity volumes. However, the strength of this association increased when using a PRS that included APOE SNPs, therefore showing the importance of APOE SNPs in this sample.

2.3.11. Regional and Whole Brain Imaging

2.3.11.1. Grey Matter

Some researchers have assessed polygenic scores in relation with both regional and whole brain structural measures. For example, Altmann et al. (2020) found that PHS was associated significantly with whole brain and ventricular grey matter loss. Liu et al. (2023) investigated the association between PRS for AD and regional and whole brain MRI measures in CU individuals. High PRS was associated strongly with low total cortical surface area and low intracranial volume. Additionally, PRS was associated positively with L caudate nucleus volume, and associated negatively with the L putamen volume.

In addition to investigating PRS in CU participants, Roostaei et al. (2018) also assessed AD patients. They found that the Homocysteine PRS was not associated with total grey matter volume in AD patients. High Homocysteine PRS was associated with reduced total grey matter volume in CU individuals. Additionally, in terms of regional alterations, high Homocysteine PRS was associated with increased regional grey matter atrophy in the occipital lobe of CU participants.

2.3.11.2. White Matter

Taking a regional and global white matter alterations approach, Korbmacher et al. (2024) examined the association between PRS for AD and white matter microstructural changes in CU participants from the UK Biobank, using DTI measures. Associations were studied both cross-sectionally and longitudinally. In addition, they looked at PRSs for several psychiatric disorders.

PRS for AD was associated strongly with annual rate of change in white matter microstructure of the global cerebral peduncle. Regionally, the strongest and consistent association was found between PRS for AD and white matter microstructure of the medial cerebral peduncle. The same findings were evident cross-sectionally. However, none of these associations remained significant after correcting for multiple comparisons. Nonetheless, the researchers suggested that insight from regional differences increases understanding of gene-brain associations, more than global averages. Importantly, for the construction of the AD PRS, Korbmacher et al. (2024) mentioned that summary statistics were obtained from a recent AD GWAS only, they did not mention the specific GWAS nor anything regarding APOE.

2.3.11.3. Grey Matter and White Matter

Many studies have explored various structural parameters, such as regional and/or global measures in grey matter and/or white matter. Brenowitz et al. (2023) looked at whole brain and regional MRI of CU subjects. They reported, high PRS, without APOE, was associated with white matter hyperintensity, but not with hippocampal or total brain volume. APOE ε4 was not associated with any outcome measure and there were no interactions between PRS and APOE ε4. As the mean age of participants was 55.8 (± 3.3) years, this study suggests APOE-related brain alterations may begin to show in late life only, e.g., >65 years. Nonetheless, this study highlights the contribution of PRS, and therefore various non-APOE variants, to brain changes.

Similarly, Tank et al. (2022) studied the association between PRS and, regional and whole brain MRI measures, in CU subjects. LOAD PRS, excluding APOE ε4, was associated significantly with the volume of the L hippocampus in total, and with L hippocampal body. This suggests that the L hippocampus is more susceptible to AD-related alterations than the R hippocampus. LOAD PRS was not associated with white matter hyperintensities. Additionally, there was no significant interaction between LOAD PRS and APOE ε4 SNP with any ROIs or hippocampal subfields. It should be noted, although the ε4 allele was controlled for, other SNPs in linkage disequilibrium with APOE ε4 SNPs were not removed from the PRS. This may have impacted the results.

Interestingly, Chen et al. (2024) acquired UK Biobank data to investigate associations between PRS and brain volume in 101 ROIs using MRI, as well as white matter integrity in 110 ROIs using DTI. They showed that PRS was associated with greater volume in the R inferior lateral ventricles and smaller volume in the L entorhinal cortex. PRS was also associated with average radial

diffusivity, average mean diffusivity, posterior thalamic radiation L1, and average L1. Of note, these results were found in a PRS that did not include the APOE region, therefore indicating that it is possible to observe significant findings that survive the stringent Bonferroni correction method using PRS without APOE. Additionally, the researchers used data from CU white British participants and a smaller sample of non-British participants comprising of Asian, African, and Hispanic descent. Thus, improving the generalisability of study findings.

Furthermore, He et al. (2023) examined the association between PRS with and without APOE, and 64 cortical ROIs, 14 subcortical ROIs, and 18 white matter tracts in a cohort of CU participants from the UK Biobank, using MRI and DTI data. After correcting for multiple comparisons, negative associations were present between PRS with APOE and cortical area of the superior frontal, pars orbitalis, and lateral orbitofrontal, and positive associations between PRS with APOE and cuneus and precuneus. Negative associations were also observed between PRS with APOE and cortical volumes of the pars orbitalis, lateral orbitofrontal, and rostral anterior cingulate, and positive associations between PRS with APOE and superior parietal and cuneus regions. Therefore, negative associations were apparent with the prefrontal and cingulate regions, whereas positive associations were found with the occipital lobe. Additionally, after correcting for multiple testing, PRS was associated negatively with subcortical volumes, specifically, the hippocampus, caudate, thalamus, accumbens, putamen, and amygdala. However, for both cortical area and subcortical volumes, when APOE SNPs were removed from the PRS, these associations were no longer present. For regional white matter integrity measures, there was a positive association between PRS and mean diffusivity, and a negative association between PRS and fractional anisotropy, in association fibres, commissural fibres, limbic system fibres, and projection fibres. However, again, when APOE SNPs were removed from the PRS, significant associations diminished. Thus, these findings indicate that these associations were strongly an effect of the APOE region.

Williams et al. (2021) used both regional structural MRI and whole brain DTI to develop five models that predict MCI from CU. (1) PRS + age resulted in AUC 74%. (2) A thickness/volume signature was obtained using regional structural MRI measures, specifically, hippocampus, entorhinal cortex, middle temporal gyrus, bank of superior temporal sulcus, superior temporal gyrus, isthmus cingulate, lateral orbitofrontal cortex, and medial orbitofrontal cortex. The PRS + age + thickness/volume signature resulted in an AUC of 80%, although this was not a statistically significant improvement. (3) A mean diffusivity signature was also obtained using DTI to assess

grey matter. The PRS + age + mean diffusivity signature and (4) PRS + age + thickness/volume signature + mean diffusivity signature significantly improved prediction; both provided an AUC of 83%, and both were significant statistically in comparison to (1). (5) In another model, the thickness/volume signature and mean diffusivity signature were adjusted for predicted brain age difference. This was an attempt to omit variance related to general ageing. The PRS + age + predicted brain age difference-adjusted thickness/volume and mean diffusivity signatures resulted in a similar AUC, 82%. Again, this was significant statistically in comparison to (1). Additionally, when the PRS was removed and replaced by APOE status in all models, the AUC was lower significantly for all models. This suggests PRS goes over and beyond APOE.

Similarly, Soldan et al. (2024) were interested in a range of structural parameters using a PRS without APOE. The researchers examined the association between PRS without the APOE and a range of structural measures in CU participants cross-sectionally, and longitudinally over an average of 5.3 years. Participants were from the Preclinical Alzheimer's disease Consortium that included data from various studies, (i.e., Adult Children Study; Australian Imaging, Biomarker, and Lifestyle study (AIBL study); BIOCARD; BLSA; WRAP)). Of note, participants that had a diagnosis of "impaired not MCI" were part of the CU sample tested by Soldan et al. (2024) since they did not meet criteria for MCI. The structural parameters were hippocampal volume, a composite score of ROIs vulnerable to AD (via machine learning; SPARE-AD), and a composite score of ROIs that showed advanced non-AD-related atrophy (via machine learning; SPARE-BA); all derived from MRI T1-weighted images. Global white matter hyperintensity volumes, as measured with MRI FLAIR, were also assessed. When looking at APOE genotype alone, rates of atrophy in hippocampal volume and the AD-vulnerable composite score were greatest in ε4 homozygotes, followed by ε4 heterozygotes, and then ε4 non-carriers. Cross-sectionally, PRS without the APOE region was not associated with baseline volumes of the hippocampus, AD-vulnerable composite score, AD-non-vulnerable composite score, or global white matter hyperintensity volumes. Longitudinally, high PRS without APOE alone was associated with reduced hippocampal volume, higher AD-vulnerable composite score, and higher global white matter hyperintensity volumes. Additionally, interactions between PRS without APOE, ε2, and ε4 were assessed (excluding the ε2ε4 genotype for ease). However, no interactions were observed regarding the rate of change in hippocampal volume, AD-vulnerable-ROIs composite score, or AD-non-vulnerable composite score. On the other hand, an interaction between PRS without APOE x ε4 x time was evident regarding white matter hyperintensities. Therefore, in comparison with low PRS without APOE, the presence of both a high PRS without APOE and ε4 carriership

increased the rate of white matter hyperintensity volumes. Evidently, PRS without APOE and ε4 impact structural parameters longitudinally, both independently and simultaneously.

Various pathway-specific PRSs have been studied in relation to grey matter and white matter alterations. For example, de Silva et al. (2022) investigated the effects of AD PRS and a Coronary Artery Disease PRS on whole brain and regional brain atrophy. AD PRS and Coronary Artery Disease PRS were associated with whole brain baseline grey matter atrophy in CU subjects and MCI patients. AD PRS and Coronary Artery Disease PRS were associated with white matter hyperintensities in the occipital lobe in AD patients. Longitudinally, AD PRS was associated with whole brain volume decline in CU participants at month 12 and month 24, and with whole brain volume decline in MCI patients at month 3, 6, 12, and 24. These findings suggest genetics influence disease progression over time. However, such associations were not found in AD patients.

Ahmad et al. (2018) looked at several pathway-specific PRSs and the standard genome-wide PRS in relation with regional and whole brain atrophy, using MRI data. PRS was not associated with hippocampal volume, white matter lesions, or total brain volume. The pathway-specific Immune Response PRS with APOE ε4, and Clathrin/AP2 Adaptor Complex PRS without APOE ε4, were associated with white matter lesions. However, the Clathrin/AP2 Adaptor Complex PRS with APOE ε4 was not associated with white matter lesions. The Endocytosis PRS, Cholesterol Transport PRS, Hematopoietic Cell Lineage PRS, Protein Ubiquitination PRS, Haemostasis PRS, Protein Folding PRS, or Clathrin/AP2 Adaptor Complex PRS were not associated with hippocampal volume or total brain volume.

Moreover, Lorenzini et al. (2024) studied regional grey matter volume and global white matter (hyperintensity volumes and tracts). Lorenzini et al. (2024) investigated the association between PRS without APOE ε2 and ε4, six pathway-specific PRSs without the APOE region, and hippocampal volume, measured by MRI T1-weighted images; global and lobar (frontal, parietal, temporal, and occipital) periventricular and deep white matter hyperintensity volumes, measured with MRI FLAIR; 10 white matter tracts – genu, body, and splenium of the corpus callosum (commissural fibres), cingulum and fornix (limbic fibres), superior and inferior longitudinal fasciculus and superior fronto-occipital fasciculus (associative fibres), corona radiata and internal capsule (projection fibres), using DWI. The six pathway-specific PRSs were: Immune Activation PRS, Signal Transduction PRS, Inflammatory PRS, Migration PRS, Amyloid

PRS, and Clearance PRS. Non-demented participants from the European Prevention of Alzheimer's Disease study were assessed. Several associations were reported. High Migration PRS and high Clearance PRS (both without SNPs from the APOE region) were associated with low hippocampal volumes. However, these did not survive corrections for multiple comparisons. High Clearance PRS (without the APOE region) was associated with high white matter hyperintensity volumes in most regions, although more so in the frontal, temporal periventricular, parietal deep white matter, and global white matter. Further, high PRS without APOE was associated with high white matter hyperintensity in temporal periventricular and deep white matter and parietal deep white matter. However, these associations no longer retained significance after correcting for multiple testing. High PRS without APOE was associated with high fractional anisotropy in the genu and low mean diffusivity in the splenium of the corpus callosum. Additionally, high Migration PRS (without APOE region) was associated with high fractional anisotropy in the commissural tract (genu, body, and splenium of the corpus callosum) and corona radiata. High Migration PRS (without APOE region) was associated with low mean diffusivity in the cingulum, genu, and splenium of the corpus callosum. Evidently, most of these associations were found using the Migration PRS, that is linked to cholesterol and lipid dysfunction. This study may indicate the contribution of genetics and early dysfunction of cholesterol and lipid metabolism to white matter integrity in elderly non-demented individuals.

2.4. DISCUSSION

The overall aim of this systematic review was to gather the current level of knowledge surrounding the associations between polygenic scores and structural neuroimaging parameters. In all, polygenic scores were consistently associated with regions that are vulnerable to AD. Specifically, regions within the MTL and limbic system (i.e., hippocampus, entorhinal cortex, parahippocampal cortex, parahippocampal gyrus, amygdala, thalamus, posterior cingulate gyrus, precuneus, caudal and rostral anterior cingulate, isthmus of the cingulate cortex, and supramarginal gyrus), and subregions within the hippocampus (i.e., sections: whole, left, and right; subfields: head, body, and tail; parcellations: cornu ammonis 1, cornu ammonis 3, cornu ammonis 4, hippocampal fissure, presubiculum, subiculum, parasubiculum, molecular layer, granule cell layer of dentate gyrus, hippocampus amygdala-transition-area, and fimbria). However, polygenic scores were also associated with other temporal lobe regions (i.e., middle temporal gyrus, inferior temporal cortex, superior temporal sulcus, inferior temporal sulcus, inferior temporal gyrus, and fusiform area), frontal lobe regions (i.e., orbitofrontal cortex, rostral anterior cingulate, rostral middle frontal gyrus, and middle frontal gyrus), occipital lobe regions (i.e., medial occipital cortex, and cuneus), the parietal lobe and inferior parietal lobe, and subcortical nuclei, thus, demonstrating the heterogeneity of sporadic AD. These regional associations were found in structural studies assessing grey matter (volume, atrophy, and thickness), white matter, or both tissues, across the AD spectrum.

The above-mentioned associations were observed regardless of the type of polygenic score; both PRS and PHS yield similar results. Although a few papers selected for this review use PHS to find associations with brain parameters, PHS was initially devised to assess age-specific risk of developing AD or for predicting the age of disease onset (Desikan et al., 2017). This may explain why most of the papers in this review (73.44%) implement the PRS method alone, in addition to the relative ease with which these can be constructed. Some papers identified for the current systematic review also used PRS to study specific pathways or regions. However, this does not seem to be the case for papers that implemented the PHS method.

Moreover, the association between polygenic scores and regional brain alterations highlight that numerous variants and therefore many genes, impact the AD brain. This finding is strengthened further at a functional study level as associations between genetics and task-based hippocampal function are only apparent when looking at multiple variants via PRS, rather than a single SNP (Xiao et al., 2017). This shows the urgent need to assess various genes and their

variants further, beyond APOE and non-lipid pathways (Hohman et al., 2017). Despite many studies having focussed on APOE alone, when APOE is neither required nor sufficient to cause AD (Sims, Hill, and Williams, 2020), the combined effect of these numerous other variants is of substantial interest. Additionally, polygenic scores are adjustable and therefore interaction effects between polygenic scores with APOE and without APOE can also be explored, as well as establishing the extent by which non-APOE variants affect pathological brain changes. Pathway-specific polygenic scores are possible; these also provide novel insights that studying APOE alone does not achieve. Although not all gene functions or protein functions are known and many may interact with one another in ways that are not known still, or overlap (Femminella et al., 2021; Leonenko et al., 2019), the polygenic methodology provides insights into gene functions, and genetic and biological pathways.

Although a few studies in the current review have stratified subjects by APOE genotype, APOE ε4 carriers vs. non-carriers, or according to ε4 allele dose, not all of these have reported upon the association between the effect on polygenic score and brain parameters. Vacher et al. (2022b) found that in comparison with ε4 non-carriers, an association between PHS and regional grey matter atrophy was evident in ε4 carriers. Further work is required to clarify sufficiently the different associations of PRS in ε4 carriers and non-carriers.

There are many discrepancies in terms of the type of polygenic scores that are used to find the aforementioned associations, regardless of whether the studies explore regional or whole brain structural parameters. For instance, in some studies associations were found by PRS with APOE, in others PRS without APOE, in some other cases, the associations were found regardless of whether APOE SNPs were or were not used to compute the scores. Similarly, in some studies associations were found for PHS with APOE, whereas in others PHS without APOE was associated with neuroimaging parameters. In terms of the strength of the associations found when using APOE SNPs, in some instances APOE SNPs increased the association strongly and in other cases there was a weak increase in strength only. These inconsistent findings may be because various *p* value thresholds have been implemented to construct the polygenic scores, along with a varying number of SNPs that have been used to calculate polygenic scores (Tank et al., 2022), thus, making it difficult to make comparisons between polygenic scores directly (Ebenau et al., 2021). Since there is no set number of SNPs that may be used to calculate polygenic scores, this may explain the resulting variance between studies in terms of both the association and strength of the association. In addition, although various confounding variables,

such as age and sex, and in some cases number of APOE ε4 alleles or APOE genotypes, have been controlled for, the above inconsistent findings have resulted still.

Furthermore, it is evident that far more research has been conducted on structural alterations in grey matter, and only a few studies have investigated the association between polygenic scores and white matter, although some studies have assessed white matter in combination with grey matter. Nonetheless, these studies have found associations between polygenic scores and global white matter hyperintensity volumes as well as in the cingulum, fornix, cerebellum, cerebellar peduncles, and periventricular regions, and alterations in various white matter tracts, (i.e., association fibres, commissural fibres, limbic system fibres, and projection fibres). However, more research exploring the polygenic effect on white matter changes, is necessary to understand AD disease mechanisms further.

Another issue is regarding the generalisability of findings. Most of the studies have either used a relatively small number of participants, only subjects of white race, or a combination of both. Additionally, GWAS used to obtain SNPs for polygenic scores have also been conducted on such subjects. In order to increase efficacy and validity of these findings, subjects in whom the GWAS is being conducted, and subjects for whom polygenic scores are being constructed, need to include larger samples and racially diverse populations.

To assess the association between polygenic scores and neuroimaging parameters, participants were selected from ADNI alone (31.25%), ADNI plus another dataset (10.94%), UK Biobank alone (18.75%), UK Biobank plus another dataset (3.13%), ADNI, UK Biobank and an additional dataset (1.56%) while only 34.38% of participants were recruited from other sources or independent cohorts. This shows 65.63% of the papers included data from well-known sources. There is an urgent need to explore independent cohorts. Since a large majority of papers use ADNI and/or UK Biobank data, it may be an idea to compare associations found vs. not found, between these various papers. However, as participant samples used within these datasets may differ, this is challenging.

Moreover, structural imaging parameters may indicate early disease detection and early diagnosis, whereas functional parameters could provide useful insights into future disease prognosis and progression. MRI is the most widely used method to assess neurostructural changes (Risacher and Saykin, 2013). MRI is quantitatively sensitive to structural changes that

occur in mild and preclinical AD, and can also detect structural loss preceding cognitive decline, since deterioration of tissue is thought to be a result of progressive neuronal and synaptic loss (McEvoy and Brewer, 2010). Although atrophy is not an AD-specific marker (van Oostveen and de Lange, 2021), the topographical pattern of atrophy may be considered a sensitive surrogate marker of AD diagnosis (McEvoy and Brewer, 2010), starting with the hippocampus and, entorhinal and perirhinal cortices (van Oostveen and de Lange, 2021). AD brain atrophy is presented as signal loss in MTL regions and widening of CSF spaces via MRI (Teipel et al., 2013).

MRI can also be used to differentiate between pathological atrophy vs. atrophy due to ageing, and can help to rule out other causes of dementia, such as normal-pressure hydrocephalus, intracranial mass, or vascular dementia (Petrella, Coleman, and Doraiswamy, 2003). MRI is therefore essential for early detection of AD and diagnosis (Yang and Mohammed, 2020).

Additionally, DTI measures can identify microstructural white matter changes that are not detectable with the T1-weighted structural MRI sequence. DTI signatures, such as reduced fractional anisotropy and increased mean diffusivity, add to those found by structural MRI and help to detect AD (Nir et al., 2013). Interestingly, alternations in fibre tract integrity have been found to occur independently from hippocampal volumetric changes in AD. The retrogenesis model of AD pathogenesis suggests fibre tracts that mature late during brain development, such as those found within the hippocampus, neocortical association areas, and the basal forebrain, are most vulnerable to AD (Kilimann et al., 2013).

2.5. CONCLUSION

Overall, the current systematic review has found that polygenic scores are associated with a range of structural neuroimaging parameters. This review has highlighted the challenges in constructing polygenic scores, and the difficulties of testing large samples with racially diverse populations. Of note, this limitation is challenging to address due to the lack of data available from minority racial groups and the lack of GWAS data from such groups. Additionally, there is a need to assess multiple parameters using different study designs, i.e., neuroimaging, CSF, and cognition both cross-sectionally and longitudinally, within the same cohort of participants.

CHAPTER 3

OVERVIEW OF CURRENT RESEARCH

3.1. OVERALL AIM

Taking the findings from Chapter 2 (Systematic Review) into consideration, by building upon previous methods and improving upon some of the limitations from previous work, the current research will implement the PRS method. The overall aim of the current work is to investigate whether PRSs for AD can predict structural brain biomarkers, fluid biomarkers, and cognitive markers, across the continuum of sporadic AD, using both a cross-sectional and a longitudinal approach. Specifically, associations between PRSs for AD and cross-sectional structural MRI measures (regional grey matter volume), cross-sectional and longitudinal CSF biomarkers (amyloid and tau), cross-sectional cognitive markers (memory, executive function, language, and visuospatial composite scores) and longitudinal cognitive decline will be examined using numerous stratifications to assess risk in different groups of individuals – this is the novelty of the current work; a multimodal approach, that has not been explored previously.

3.2. ETHICAL APPROVAL

The current research uses data from ADNI (a secondary data source). Institutional review boards of each ADNI site have approved the study protocol. All participants provided written informed consent and had the right to withdraw at any point without negative implications (Weber et al., 2021). For research governance, compliance with ethical standards and informed consent, and associated materials, consult the ADNI website (https://adni.loni.usc.edu/).

Before the current research began, an application for ethical review through the Brunel Research Ethics Online system was made (https://breo.brunel.ac.uk/Account/Login?returnUrl=/ActivityForm/Index). Approval to proceed without any additional extended review was granted by the College of Health, Medicine, and Life Sciences Research Ethics Committee at Brunel University (of) London on 21 December 2022; reference: 40561-NER-Dec/2022- 42767-1 (see Appendix C.1). ADNI granted access to the data on 17 December 2022 (see Appendix C.2).

3.3. PARTICIPANTS

ADNI was founded in 2004 by Dr. Michael W. Weiner. The initial project was a five-year longitudinal study (ADNI-1). This was followed by ADNI-GO, ADNI-2, ADNI-3, and ADNI-4, as further funding was obtained. There are currently 60 sites across America and Canada assessing patients with MCI and AD, and healthy individuals with and without subjective memory decline. The studies have been designed to develop a range of markers for early detection and progression of AD, such as clinical markers using physical and neurological examinations, neuropsychological markers using cognitive assessments, imaging markers using MRI, PET, rs-fMRI, DTI, and ASL, genetic markers using blood samples, and biochemical markers using CSF obtained via lumbar punctures (ADNI, 2025). ADNI-4 began in June 2023 and is ongoing; the primary outcome has been to increase inclusion of unrepresented populations to improve generalisability of results (ClinicalTrials.gov, 2024). Participants progressed from ADNI-1 through to ADNI-4, sequentially. Thus, reflecting the improved study protocols and procedures, including longitudinal brain imaging, and inclusion of other forms of memory assessment (Weber et al., 2021).

For the current research, participant inclusion criteria were based on the availability of required ADNI data, i.e., genetic, imaging, biomarker status, APOE ε4 status, Mini-Mental State Examination (MMSE) data, and detailed cognitive scores. Participants who did not have these data or had a history of chronic psychiatric diagnosis were excluded. The latter criterion was selected to ensure that the AD phenotype was truly being studied, rather than the effect of psychiatric disorders on AD risk or the effect of psychiatric disorders on the AD continuum. As the current research began in 2022, data from ADNI-4 have not been used to ensure that the same cohort of participants and their data are examined across various experiments for consistency, and to ensure that data were readily available for analyses (without delay). Hence, participants selected for the current research include those from ADNI-1 to ADNI-3.

3.4. EXPERIMENTS

To achieve the overall aim of the current research, the following experiments will be carried out:

3.4.1. Experiment One: Associations between Polygenic Risk Scores and Regional Grey Matter Volume

The aim of this experiment is to investigate associations between PRSs for AD (i.e., PRSwithAPOE, PRSwithoutAPOE, and APOEonlyPRS that will be calculated using three statistical thresholds each) and regional grey matter volume across the continuum of sporadic AD.

It is hypothesised that:

1) There will be significant associations between polygenic scores and regional grey matter volume in MTL structures. In ascending order, these associations will be strongest when using PRSwithAPOE, followed by APOEonlyPRS, and then PRSwithoutAPOE (whole group).
2) In APOE ε4 carriers, there will be significant associations between polygenic scores and regional grey matter volume in MTL structures, as compared with APOE ε4 non-carriers. In ascending order, these associations will be strongest when using PRSwithAPOE, followed by APOEonlyPRS, and then PRSwithoutAPOE (APOE ε4 status).
3) In MCI and AD dementia patients, there will be significant associations between polygenic scores and regional grey matter volume in MTL structures, as compared with CU participants. In ascending order, these associations will be strongest when using PRSwithAPOE, followed by APOEonlyPRS, and then PRSwithoutAPOE (diagnostic status).
4) In amyloid positive participants, there will be significant associations between polygenic scores and regional grey matter volume in MTL structures, as compared with amyloid negative participants. In ascending order, these associations will be strongest when using PRSwithAPOE, followed by APOEonlyPRS, and then PRSwithoutAPOE (amyloid status).

These hypotheses will be tested using multiple hierarchical linear regression models to investigate associations between the PRSs (independent/predictor variable) and 114 ROIs (dependent/outcome variable), as follows:

1) In the whole group.
2) In the whole group that is stratified by APOE ε4 status (ε4 non-carriers vs. ε4 carriers).

3) In the whole group that is stratified by diagnostic status (CU vs. MCI vs. AD dementia).
4) In the whole group that is stratified by amyloid status (amyloid negative vs. amyloid positive).

3.4.2. Experiment Two Part A: Associations between Polygenic Risk Scores and Cross-Sectional Cerebrospinal Fluid Biomarkers

The aim of this experiment is to investigate associations between PRSs for AD (i.e., PRSwithAPOE, PRSwithoutAPOE, and APOEonlyPRS at three thresholds each) and AD-specific cross-sectional CSF biomarkers (i.e., Aβ42, and p-tau181).

It is hypothesised that:

1) The association between PRS and CSF biomarkers will be strongest for PRSwithAPOE, followed by APOEonlyPRS, and then PRSwithoutAPOE (whole group).
2) In APOE ε4 carriers, the association between PRS and CSF biomarkers will be strongest for PRSwithAPOE, followed by APOEonlyPRS, and then PRSwithoutAPOE (APOE ε4 status).
3) In MCI and AD dementia patients, the association between PRS and CSF biomarkers will be strongest for PRSwithAPOE, followed by APOEonlyPRS, and then PRSwithoutAPOE, as compared with CU participants (diagnostic status).

These hypotheses will be tested using binomial hierarchical logistic regression models to assess whether PRSs (independent/predictor variable) can predict CSF Aβ42 status and/or CSF p-tau181 status (dependent/outcome variable), as follows:

1) In the whole group where p-tau181 is not controlled vs. controlled (Aβ42 models), Aβ42 is not controlled vs. controlled (p-tau181 models), and neither biomarkers are controlled (Aβ42 + p-tau181 models).
2) In the whole group that is stratified by APOE ε4 status where p-tau181 is not controlled vs. controlled (Aβ42 models), Aβ42 is not controlled vs. controlled (p-tau181 models), and neither biomarkers are controlled (Aβ42 + p-tau181 models).
3) In the whole group that is stratified by diagnostic status where p-tau181 is not controlled vs. controlled (Aβ42 models), Aβ42 is not controlled vs. controlled (p-tau181 models), and neither biomarkers are controlled (Aβ42 + p-tau181 models).

3.4.3. Experiment Two Part B: Associations between Polygenic Risk Scores and Cross-Sectional Cognitive Markers

The aim of this experiment is to examine associations between PRSs for AD (i.e., PRSwithAPOE, PRSwithoutAPOE, and APOEonlyPRS at three thresholds each) and AD-specific cross-sectional cognitive markers (i.e., memory, executive function, language, and visuospatial competency).

It is hypothesised that:

1) The association between PRS and cognitive markers will be strongest for PRSwithAPOE, followed by APOEonlyPRS, and then PRSwithoutAPOE (whole group).
2) In APOE ε4 carriers, the association between PRS and cognitive biomarkers will be strongest for PRSwithAPOE, followed by APOEonlyPRS, and then PRSwithoutAPOE (APOE ε4 status).
3) In MCI and AD dementia patients, the association between PRS and cognitive markers will be strongest for PRSwithAPOE, followed by APOEonlyPRS, and then PRSwithoutAPOE, as compared with CU participants (diagnostic status).
4) In amyloid positive participants, the association between PRS and cognitive markers will be strongest for PRSwithAPOE, followed by APOEonlyPRS, and then PRSwithoutAPOE (amyloid status).

These hypotheses will be tested using multiple hierarchical linear regression models to investigate whether there are associations between PRSs (independent/predictor variable) and memory, executive function, language, and visuospatial abilities (dependent/outcome variable), as follows:

1) In the whole group.
2) In the whole group that is stratified by APOE ε4 status.
3) In the whole group that is stratified by diagnostic status.
4) In the whole group that is stratified by amyloid status.

3.4.4. Experiment Three Part A: Associations between Polygenic Risk Scores and Longitudinal Cerebrospinal Fluid Biomarkers

The aim of this experiment is to investigate associations between PRSs for AD (i.e., PRSwithAPOE, PRSwithoutAPOE, and APOEonlyPRS at three thresholds each) and AD-specific longitudinal CSF biomarkers (i.e., Aβ42 and p-tau181).

It is hypothesised that:

1) The association between PRS and longitudinal CSF biomarkers will be strongest for PRSwithAPOE, followed by APOEonlyPRS, and then PRSwithoutAPOE (whole group).
2) In APOE ε4 carriers, the association between PRS and longitudinal CSF biomarkers will be strongest for PRSwithAPOE, followed by APOEonlyPRS, and then PRSwithoutAPOE (APOE ε4 status).
3) In MCI and AD dementia patients, the association between PRS and longitudinal CSF biomarkers will be strongest for PRSwithAPOE, followed by APOEonlyPRS, and then PRSwithoutAPOE, as compared with CU participants (diagnostic status).

These hypotheses will be tested using binomial hierarchical logistic regression models to assess whether PRSs (independent/predictor variable) can predict change in CSF Aβ42 status and/or CSF p-tau181 status (dependent/outcome variable) over 24 months, as follows:

1) In the whole group where p-tau181 is not controlled vs. controlled (Aβ42 models), and Aβ42 is not controlled vs. controlled (p-tau181 models).
2) In the whole group that is stratified by APOE ε4 status where p-tau181 is not controlled vs. controlled (Aβ42 models), and Aβ42 is not controlled vs. controlled (p-tau181 models).
3) A: In the whole group that is stratified by diagnostic status where p-tau181 is not controlled vs. controlled (Aβ42 models), and Aβ42 is not controlled vs. controlled (p-tau181 models).

   B: In the whole group that is stratified by diagnostic status and is stratified further by APOE ε4 status where p-tau181 is not controlled vs. controlled (Aβ42 models), and Aβ42 is not controlled vs. controlled (p-tau181 models).

These hypotheses will be scrutinised further using multiple hierarchical linear regression models, this time, to investigate associations between PRSs (independent/predictor variable) and

differential scores of Aβ42 status and/or CSF p-tau181 status (dependent/outcome variable) between baseline and Month 24, as follows:

1) In the whole group where p-tau181 is not controlled vs. controlled (Aβ42 models), and Aβ42 is not controlled vs. controlled (p-tau181 models).
2) In the whole group that is stratified by APOE ε4 status where p-tau181 is not controlled vs. controlled (Aβ42 models), and Aβ42 is not controlled vs. controlled (p-tau181 models).
3) A: In the whole group that is stratified by diagnostic status where p-tau181 is not controlled vs. controlled (Aβ42 models), and Aβ42 is not controlled vs. controlled (p-tau181 models).
   B: In the whole group that is stratified by diagnostic status and is stratified further by APOE ε4 status where p-tau181 is not controlled vs. controlled (Aβ42 models), and Aβ42 is not controlled vs. controlled (p-tau181 models).

3.4.5. Experiment Three Part B: Associations between Polygenic Risk Scores and Longitudinal Cognition

The aim of this experiment is to examine associations between PRSs for AD (i.e., PRSwithAPOE, PRSwithoutAPOE, and APOEonlyPRS at three thresholds each) and AD-specific longitudinal cognitive deterioration (i.e., decline in memory and any one other cognitive domain)

It is hypothesised that:

1) The association between PRS and longitudinal cognitive decline will be strongest for PRSwithAPOE, followed by APOEonlyPRS, and then PRSwithoutAPOE (whole group).
2) In APOE ε4 carriers, the association between PRS and longitudinal cognitive decline will be strongest for PRSwithAPOE, followed by APOEonlyPRS, and then PRSwithoutAPOE (APOE ε4 status).
3) In MCI and AD dementia patients, the association between PRS and longitudinal cognitive decline will be strongest for PRSwithAPOE, followed by APOEonlyPRS, and then PRSwithoutAPOE, as compared with CU participants (diagnostic status).
4) In amyloid positive participants, the association between PRS and longitudinal cognitive decline will be strongest for PRSwithAPOE, followed by APOEonlyPRS, and then PRSwithoutAPOE (amyloid status).

5) In tau positive participants, the association between PRS and longitudinal cognitive decline will be strongest for PRSwithAPOE, followed by APOEonlyPRS, and then PRSwithoutAPOE (tau status).

These hypotheses will be tested using binomial hierarchical logistic regression models to investigate whether PRSs (independent/predictor variable) can predict change in longitudinal cognition (dependent/outcome variable) over 24 months, as follows:

1) In the whole group.
2) In the whole group that is stratified by APOE ε4 status.
3) A: In the whole group that is stratified by diagnostic status.
   B: In the whole group that is stratified by diagnostic status and stratified further by APOE ε4 status.
4) A: In the whole group that is stratified by amyloid status.
   B: In the whole group that is stratified by amyloid status and stratified further by APOE ε4 status.
5) A: In the whole group that is stratified by p-tau status.
   B: In the whole group that is stratified by p-tau status and stratified further by APOE ε4 status.

3.5. OTHER INFORMATION

This will be followed by a General Discussion and a General Conclusion.

By completing this research, it is hoped that insights into AD-specific genetics and mechanisms may be improved; the understanding of associations between PRSs for AD and cross-sectional/longitudinal alterations in structural and fluid biomarkers, and symptomology, will be clearer; knowledge surrounding the potential for PRSs to be used in clinical settings to support diagnosis and prediction of disease trajectory may be enhanced. These are all important factors for a time-sensitive and debilitating disease, such as AD, where early prevention, early diagnosis, and early treatment are essential for better outcomes.

CHAPTER 4

EXPERIMENT ONE – ASSOCIATIONS BETWEEN POLYGENIC RISK SCORES AND REGIONAL GREY MATTER VOLUME

4.1. INTRODUCTION

Genetics of familial AD are well known. This is due to the discovery of pathogenic mutations in APP, PSEN1, and PSEN2, that led to the Amyloid Cascade Hypothesis (Hardy and Higgins, 1992; Lambert et al., 2023). There are currently 43 recognised pathogenic or likely pathogenic mutations in APP, 213 pathogenic or likely pathogenic mutations in PSEN1, and 11 pathogenic or likely pathogenic mutations in PSEN2 (Alz Forum, 2025).

In contrast, the genetics of sporadic AD is complex and not well understood. Sporadic AD is caused by a combination of genetic factors, environmental factors, cardiovascular comorbidities, and lifestyle choices. Genetics alone accounts for approximately 70% of sporadic AD (Lane, Hardy, and Schott, 2017). Various GWASs, whole-exome sequencing studies, and whole-genome sequencing studies, have attempted to comprehend the genetic architecture underlying sporadic AD. Such work has found that several genes, in addition to APOE, are associated with sporadic AD. Although these genes individually have low risk associated with them, together, they are thought to increase risk of sporadic AD further. Examples are: ACE (Farrer et al., 2000), ABI3 (Sims et al., 2017), ABCA7 (Reitz et al., 2013), ABCA1, ADAM10, ATP8B4, RIN3, ZCWPW1 (Holstege et al., 2022), BIN1, CLU, CR1, CD2AP, CD33, EPHA1, MS4A, PICALM (Guerreiro et al., 2013; Harold et al., 2009; Lambert et al., 2009), SORL1 (Rogaeva et al., 2007), and TREM2 (Jonsson et al., 2013). Although these findings aid our understanding of sporadic AD, these genes only explain a proportion of the total genetic variance.

It is thought that 30.62% of the genetic variance is explained by known AD SNPs (25.21% between APOE ε2 and APOE ε4 vs. 5.41% between ABCA7, BIN1, CASSA4, CD2AP, CD33, CEF1, CLU, CR1, DSG2, FERMT2, HLA-DRB5/HLA-DRB1, INPP5D, MEF2C, MS4A4E, MS4A6A, NME8, PICALM, PTK2B, SLC24A4/RIN3, SORL1, and ZCWPW1), whereas 69.38% of the genetic variance remains to be discovered (28.63% in known AD regions as listed above, plus APP, EPHA1, PSEN1, PSEN2, TREM2, and UNC5C vs. 40.74% in unknown regions). Additionally, 53.24% of the total phenotypic variance has been shown to be explained by genetics (i.e., all SNPs in the dataset examined). Of this, 16.30% of the phenotypic variance is explained by known SNPs (13.42% between APOE ε2 and ε4 vs. 2.88% between ABCA7, BIN1, CASSA4, CD2AP, CD33, CEF1, CLU, CR1, DSG2, FERMT2, HLA-DRB5/HLA-DRB1, INPP5D, MEF2C, MS4A4E, MS4A6A, NME8, PICALM, PTK2B, SLC24A4/RIN3, SORL1, and ZCWPW1) and 36.94% of the phenotypic variance is thought to be explained by undiscovered SNPs (15.24% in known AD regions, as listed above, plus APP, EPHA1, PSEN1, PSEN2, TREM2, and UNC5C vs. 21.69% in unknown regions). Of the 21.69% of SNPs

located in unknown regions, 41% of the SNPs are thought to be located adjacent to known AD regions, and the remaining 59% are in other regions or a result of gene-gene interactions (Ridge et al., 2016). In contrast, some research suggests that APOE explains only 4-6% of the variance, other known AD variants explain up to 33%, and additional risk genes are located on chromosomes 1 to 22, i.e., on every autosome (Ridge et al., 2013; Lee et al., 2013). Regardless of these discrepancies, research is still required to identify the large proportion of remaining sporadic AD risk genes and variants.

Furthermore, there is some disagreement in the scientific community regarding whether sporadic AD is an oligogenic disease that involves less than 100 causative variants (Zhang et al., 2020) or a polygenic disease that involves up to 11,000 causative variants (Lake et al., 2023; Lambert et al., 2023). As mentioned in Chapter 1 (Introduction), Kamboh (2022) identified 95 risk loci from GWAS and meta-analyses of GWAS, that are associated with sporadic AD. However, predictive models that use polygenic scores to go above and beyond GWAS results, demonstrate that substantially far more genes are associated with sporadic AD. For instance, deconstructing the polygenic scores calculated by the authors of 43 papers (out of 64 papers) reviewed in Chapter 2 (Systematic Review), has shown that 249 genes may be associated with sporadic AD, including those mentioned by Ridge et al. (2016). Of note, these are not all considered risk genes. A set of 23 genes (out of the 249 genes) are found frequently in polygenic score calculations. Apart from MS4A6A, SPI1, and SPPL2A, that were found in Chapter 2 (Systematic Review), 20 of the genes (out of the set of 23) have been reported previously (Giri, Zhang, and Lu, 2016). Nonetheless, overall, these various findings reflect the increasing heterogeneity of results, the lack of clarity regarding genes involved in sporadic AD, and the need to construct these polygenic models and statistical models systematically and objectively.

Moreover, regional structural signatures consistent with AD-vulnerability, such as the hippocampus, other medial temporal regions, and regions within the limbic system, have been highlighted in Chapter 2 (Systematic Review). The heterogeneity and regional variability of sporadic AD is further evident since polygenic scores are also associated with volumetric measures of other temporal lobe regions, regions within the frontal, parietal, and occipital lobes, and subcortical nuclei. Additionally, there are only two papers currently that have studied a large number of regional volumes, i.e., 101 ROIs (Zhao et al., 2019b; Chen et al., 2024). This shows the need for more research investigating associations between PRS and a high amount of ROIs.

4.1.1. Aims, Objectives, and Hypotheses

Taking the aforementioned points into consideration, and the inconsistencies and limitations evident in Chapter 2 (Systematic Review) and in wider research, Chapter 4 (Experiment One) is anticipated to disentangle some of these issues.

The overall aim of Chapter 4 (Experiment One) is:

- To investigate associations between PRSs for AD (i.e., PRSwithAPOE, PRSwithoutAPOE, and APOEonlyPRS) and regional grey matter volume across the spectrum of sporadic AD.

This aim will be explored using the following objectives:

- To construct PRSs in a methodical manner.
- To state clearly whether APOE SNPs have, or have not, been used in PRS calculations.
- To demonstrate whether APOE SNPs affect PRSs.
- To clarify whether PRSs are associated with regional grey matter volumes in the sporadic AD continuum.

It is hypothesised that:

1) There will be significant associations between polygenic scores and regional grey matter volume in MTL structures. In ascending order, these associations will be strongest when using PRSwithAPOE, followed by APOEonlyPRS, and then PRSwithoutAPOE (whole group).
2) In APOE ε4 carriers, there will be significant associations between polygenic scores and regional grey matter volume in MTL structures, as compared with APOE ε4 non-carriers. In ascending order, these associations will be strongest when using PRSwithAPOE, followed by APOEonlyPRS, and then PRSwithoutAPOE (APOE ε4 status).
3) In MCI and AD dementia patients, there will be significant associations between polygenic scores and regional grey matter volume in MTL structures, as compared with CU participants. In ascending order, these associations will be strongest when using PRSwithAPOE, followed by APOEonlyPRS, and then PRSwithoutAPOE (diagnostic status).
4) In amyloid positive participants, there will be significant associations between polygenic scores and regional grey matter volume in MTL structures, as compared with amyloid

negative participants. In ascending order, these associations will be strongest when using PRSwithAPOE, followed by APOEonlyPRS, and then PRSwithoutAPOE (amyloid status).

In turn, these will provide detailed and systematic insights into understanding the genetic and biological mechanisms of sporadic AD, and steadily increase the generalisability of findings to individuals with different AD-related characteristics and biomarkers. The contribution to solving the genetic architecture of this debilitating disease may lead to the development of effective therapeutic interventions.

4.2. METHODS

4.2.1. Participants

738 ADNI participants were eligible for the current research. Of these, 184 were CU (across all available longitudinal follow-up visits), 416 received a clinical diagnosis of MCI (at the time the MRI visit took place), and 138 had a clinical diagnosis of AD dementia (during the visit at which MRI had taken place).

4.2.2. Participant Characteristics

Participant demographics and other characteristics, (i.e., age, education, sex, race, APOE genotype, APOE ε4 status, amyloid status, and family history), can be found for the entire cohort in Table 4.1, and per diagnostic status in Table 4.2.

In terms of race, the participant sample consisted of individuals of white (93.63%, n = 691), minority ethnic (6.10%, n = 45), and unknown (0.27%, n = 2) races. Minority races covered Native Americans, Asians, Hawaiian/Pacific, Black, and Mixed. All available races were included in the analyses to maximise the sample size and potential generalisability of results.

For analyses that required stratification by APOE ε4 status, APOE genotypes were grouped into APOE ε4 carriers (i.e., ε2ε4, ε3ε4, and ε4ε4) vs. non-carriers (i.e., ε2ε2, ε2ε3, and ε3ε3).

Additionally, family history includes history of both AD, and unspecified dementia, in first degree relatives (i.e., mother, father, or sibling).

Table 4.1: Participant demographics and other characteristics for the entire cohort (n = 738).

ENTIRE COHORT (n = 738)		
Age		
Age range		55 – 96 years
Mean age		73.94 years
Standard deviation		7.58 years
Education		
Education range		6 – 20 years
Mean education		16.09 years
Standard deviation		2.75 years
	n	**%**
Sex		
Male	407	55.15
Female	331	44.85
Race		
Native Americans	2	0.27
Asian	10	1.36
Hawaiian/Pacific	2	0.27
Black	24	3.25
White	691	93.63
Mixed	7	0.95
Unknown	2	0.27
APOE Genotype		
ε4ε4	53	7.18
ε3ε4	238	32.25
ε3ε3	366	49.59
ε2ε4	15	2.03
ε2ε3	65	8.81
ε2ε2	1	0.14
APOE ε4 Status		
ε4 Non-Carrier	432	58.54
ε4 Carrier	306	41.46
Amyloid Status		
Negative	266	36.04
Positive	472	63.96
Family History of Alzheimer or Dementia		
Negative	34	4.61
Positive	704	95.39

APOE: apolipoprotein E. ε: epsilon.

Table 4.2: Participant demographics and other characteristics per diagnostic status.

COGNITIVELY UNIMPAIRED (n = 184)			MILD COGNITIVE IMPAIRMENT (n = 416)			ALZHEIMER'S DISEASE DEMENTIA (n = 138)		
Age			**Age**			**Age**		
Age range	60 – 89 years		Age range	55 – 96 years		Age range	56 – 95 years	
Mean age	73.71 years		Mean age	73.24 years		Mean age	76.38 years	
Standard deviation	5.83 years		Standard deviation	8.01 years		Standard deviation	7.89 years	
Education			**Education**			**Education**		
Education range	6 – 20 years		Education range	8 – 20 years		Education range	8 – 20 years	
Mean education	16.48 years		Mean education	16.00 years		Mean education	15.86 years	
Standard deviation	2.65 years		Standard deviation	2.73 years		Standard deviation	2.88 years	
	n	**%**		**n**	**%**		**n**	**%**
Sex			**Sex**			**Sex**		
Male	88	47.83	Male	243	58.41	Male	76	55.07
Female	96	52.17	Female	173	41.59	Female	62	44.93
Race			**Race**			**Race**		
Native Americans	0	0	Native Americans	2	0.48	Native Americans	0	0
Asian	1	0.54	Asian	4	0.96	Asian	5	3.62
Hawaiian/Pacific	0	0	Hawaiian/Pacific	2	0.48	Hawaiian/Pacific	0	0
Black	8	4.35	Black	14	3.37	Black	2	1.45
White	174	94.57	White	386	92.79	White	131	94.93
Mixed	1	0.54	Mixed	6	1.44	Mixed	0	0
Unknown	0	0	Unknown	2	0.48	Unknown	0	0
APOE Genotype			**APOE Genotype**			**APOE Genotype**		
ε4ε4	3	1.63	ε4ε4	23	5.53	ε4ε4	27	19.57
ε3ε4	40	21.74	ε3ε4	133	31.97	ε3ε4	65	47.10
ε3ε3	114	61.96	ε3ε3	213	51.20	ε3ε3	39	28.26
ε2ε4	1	0.54	ε2ε4	10	2.40	ε2ε4	4	2.90
ε2ε3	26	14.13	ε2ε3	36	8.65	ε2ε3	3	2.17
ε2ε2	0	0	ε2ε2	1	0.24	ε2ε2	0	0

APOE ε4 Status			**APOE ε4 Status**			**APOE ε4 Status**		
ε4 Non-Carrier	140	76.09	ε4 Non-Carrier	250	60.10	ε4 Non-Carrier	42	30.43
ε4 Carrier	44	23.91	ε4 Carrier	166	39.90	ε4 Carrier	96	69.57
Amyloid Status			**Amyloid Status**			**Amyloid Status**		
Negative	105	57.07	Negative	148	35.58	Negative	10	7.25
Positive	79	42.93	Positive	268	64.42	Positive	128	92.75
Family History of Alzheimer or Dementia			**Family History of Alzheimer or Dementia**			**Family History of Alzheimer or Dementia**		
Negative	11	5.98	Negative	18	4.33	Negative	5	3.62
Positive	173	94.02	Positive	398	95.67	Positive	133	96.38

APOE: apolipoprotein E. ε: epsilon.

4.2.3. Genetic Data

Genotyping was conducted by ADNI using an Illumina Human 610-Quad BeadChip array for ADNI-1 participants and an Illumina OmniExpress BeadChip array for ADNI-GO and ADNI-2 participants, using blood samples, in accordance with the protocol outlined by Saykin et al. (2015).

For the current research, quality controlled genetic data were made available by Manca, Pardinas, and Venneri. (2022). Genotype data were manipulated using the PLINK 2.0 software to extract common high-quality autosomal markers between individuals, as described by Chang et al. (2015). Quality control parameters were, 90% call rate, 5% minor allele frequency, and Hardy-Weinberg equilibrium mid-*p* value 10^{-6} (Manca, Pardinas, and Venneri, 2022); any SNPs that did not meet these requirements were removed to ensure uncommon SNPs, or incomplete genetic data, did not overinfluence the results (Ramanan 2022). Subsequently, 1.3 million SNPs passed quality control. With this data, genetic principal components were generated using Principal Components Analysis in Related Samples (Conomos, Miller, and Thornton, 2015) and the first x10 principal components were used as covariates in the main analysis of the current research to control for population structure/stratification (Tank et al., 2022). Robust relatedness estimates, corrected for x3 principal components, were calculated using Principal Components-Relate (Conomos et al., 2016). The Principal Components Analysis in Related Samples and Principal Components-Relate were run on GENESIS R software (Gogarten et al., 2019; Manca, Pardinas, and Venneri, 2022).

Principal components are applied to genetic data to gauge population structure in the participants being studied. The top principal components from this analysis are used as they reflect best the genetic variability in the data. However, most methods that investigate population structure often fail, either where datasets include related individuals or where relatedness is unknown, as the outputs reflect family structure/relatedness rather than population structure (Price et al., 2010). Additionally, some methods are unable to distinguish between ancestral groups vs. clusters of relatives in genetic datasets. Genetic datasets include individuals from various ancestral groups, therefore ancestral diversity must be accounted for to avoid false associations and reduced power (Thornton and Bermejo, 2014). Principal Components Analysis in Related Samples is a robust and accurate inference tool that accounts for known and unknown relatedness in datasets and therefore able to capture reliably population structure, including ancestry, rather than family structure (Conomos, Miller, and Thornton, 2015). The principal

components derived from this method are then used to adjust the population structure and ancestry of individuals in the dataset, using Principal Components-Relate, to provide reliable estimates of familial relatedness (Conomos et al., 2016).

4.2.4. Calculating Polygenic Risk Scores

PRSs were constructed using PRS-continuous shrinkage (PRS-CS) priors on SNP effect sizes, a Bayesian regression approach. This means, the amount of shrinkage applied to each SNP depends on the strength of its association with the GWAS. Further, effect sizes for each linkage disequilibrium block are updated together, rather than individually, (a computational advantage). PRS-CS requires two datasets only: GWAS summary statistics and an external linkage disequilibrium reference panel (Ge et al., 2019), and provides a superior out-of-sample prediction than other methods (Sha et al., 2023). For the current research, GWAS summary statistics data from Jansen et al. (2019) and linkage disequilibrium reference panel data from the 1000 Genomes Project (Genome.gov, 2017) European sample were used. After merging the data from these datasets, 455,027 SNPs were retained, and a Bayesian posterior effect size was calculated from each SNP. The continuous shrinkage parameter was inferred using PRS-CS-auto; this automatically learns from the data. Therefore, a validation dataset is not required. PRS-CS-auto is also shown to perform well with large training datasets (Ge et al., 2019).

PRSs were generated on PRSice v2 (Choi and O'Reilly, 2019) using posterior effect sizes without pruning, at x10 GWAS *p* value thresholds: 5×10^{-8}, 1×10^{-6}, 1×10^{-5}, 0.0001, 0.001, 0.01, 0.05, 0.1, 0.5, and 1. The number of SNPs identified at the various thresholds are displayed in Table 4.3. Raw PRS figures were standardised to *Z* scores by centring by mean and dividing by 1 standard deviation, and thus converting these figures into analysis-compatible data. These data were made available by Manca, Pardinas, and Venneri (2022).

Table 4.3: Number of SNPs identified at x10 *p* value thresholds for PRSwithAPOE, PRSwithoutAPOE, and APOEonlyPRS.

PRS Threshold	Number of SNPs at Threshold PRSwithAPOE	Number of SNPs at Threshold PRSwithoutAPOE	Number of SNPs at Threshold APOEonlyPRS
5×10^{-8} (Threshold 1)	172	121	51
1×10^{-6} (Threshold 2)	234	181	53
1×10^{-5} (Threshold 3)	353	294	59
0.0001 (Threshold 4)	660	580	80
0.001 (Threshold 5)	1,561	1,465	96
0.01 (Threshold 6)	7,376	7,238	138
0.05 (Threshold 7)	28,732	28,537	195
0.1 (Threshold 8)	53,304	53,081	223
0.5 (Threshold 9)	235,506	235,192	314
1 (Threshold 10)	455,027	454,638	389

PRS: polygenic risk score. SNPs: single nucleotide polymorphisms.

4.2.5. Polygenic Risk Scores with APOE SNPs vs. without APOE SNPs

PRSs were calculated using discovery GWAS summary statistics from Jansen et al. (2019). The target sample, i.e., ADNI participants, were not included in the above-mentioned GWAS used to calculate PRSs (Manca, Pardinas, and Venneri, 2022).

Three PRSs were calculated: (1) PRS that included APOE SNPs, "PRSwithAPOE", (2) PRS that excluded APOE SNPs, "PRSwithoutAPOE", and (3) PRS using all SNPs within the APOE region, "APOEonlyPRS". The entire APOE region on chromosome 19,44,400,000 to 46,500,000, was removed from PRSwithoutAPOE (Altmann et al., 2020). APOE genotype information for all participants was gathered from the ADNI database. Note, PRSwithAPOE and PRSwithoutAPOE were extracted from Manca, Pardinas, and Venneri (2022). However, APOEonlyPRS was newly calculated for the current research.

4.2.6. MRI Acquisition and Preprocessing

ADNI-1 to ADNI-3 participants underwent T1-weighted MRI brain scans at either 1.5 Tesla (T) or 3 T. T refers to the magnetic strength of the MRI. The higher the T, the better the image resolution and contrast, separation of grey and white matter, and quantification of cortical volume. 7 T to 9.4 T allow for improved visualisation of small anatomical structures. However, most scans are acquired at ≤1.5 T and only a small proportion are acquired at ≥ 3 T (Duyn, 2012). Although MRI scans on ADNI participants have been acquired at different strengths and across various sites, thus with a range of imaging protocols and data processing algorithms, results are still comparable (Marchewka et al., 2014). Acquisition parameters have been harmonised to ensure comparability. Pooling of MRI data has been shown previously to have only minimal effects on neuro-volumetric quantification, and therefore this method is supported by other researchers to aid increase in knowledge and understanding of complex diseases (Stonnington et al., 2008).

Of the 738 participants eligible for the current study, 197 scans had been acquired at 1.5 T and 541 scans had been acquired at 3 T. MRI data were analysed using voxel-based morphometry using MatLab (Mathworks Inc., UK) and Statistical Parametric Mapping (SPM) 12 (Wellcome Centre for Human Neuroimaging, London, UK) in line with the most updated version of the protocol outlined by Ashburner and Friston (2000). The Neuromorphometrics atlas (Neuromorphometrics, Inc., USA), part of the Computational Anatomy Toolbox 12 (Gaser et al., 2024), was used in SPM12 to segment the brain into 114 ROIs in total, across the L and R hemispheres. Images were: (1) reoriented to the bi-commissural axis, i.e., anterior commissure

and posterior commissure; (2) reoriented images were segmented into 3 tissues, i.e., grey matter vs. white matter vs. CSF; (3) grey matter maps were modulated and registered to the International Consortium of Brain Mapping template in the Montreal Neurological Institute (MNI) standard space, a stereotactic coordinate system – (x, y, z); (4) normalised images were smoothed with an 8 mm full-width at half-maximum Gaussian kernel (Manca, Pardinas, and Venneri, 2022). The global volume of each tissue map, i.e., grey matter vs. white matter vs. CSF, was quantified for each participant using SPM12. Total intracranial volume was calculated by summing the quantitative values of the three tissues for each participant.

4.2.7. Statistical Analyses

To test the stated hypotheses, analysis was divided into five stages. All statistical analyses were performed on IBM SPSS Statistics v29.0.1.0.

4.2.7.1. Stage 1 Analysis: Covariates

Covariates in addition to x10 genetic principal components, scanner strength, total intracranial volume, and MMSE score, were identified. Variables that were tested for this purpose were: Age, sex, education, and family history.

For continuous variables, i.e., age, and education, when comparing with the three diagnostic statuses, one-way between-groups analysis of variance were used, and where applicable, *post-hoc* comparisons were conducted using independent-sample t-tests, followed by the Benjamini-Hochberg false discovery rate (FDR) method (Benjamini and Hochberg, 1995) to correct the statistical outputs. For these continuous variables, i.e., age and education, when comparing with APOE ε4 status, or amyloid status, independent-sample t-tests were performed. For categorical variables, i.e., sex, and family history, when comparing with the three diagnostic statuses, 2x3 Chi-square tests were conducted, and when comparing APOE ε4 status, or amyloid status, 2x2 Chi-square analyses were completed.

4.2.7.2. Stage 2 Analysis: Selecting the Optimal Polygenic Risk Score Thresholds

Independent-sample t-tests were conducted to find the PRS threshold that was most sensitive to show significant differences in ROIs between diagnostic groups:

(A) Independent-sample t-tests were performed between CU participants with amyloid negativity (n = 106) vs. MCI and AD dementia patients with amyloid positivity (n = 394). This was to compare healthy participants with negative biomarker status vs. pathologically ageing participants with biomarker evidence.

(B) Independent-sample t-tests were conducted between CU participants with amyloid positivity (n = 78) vs. MCI and AD dementia patients with amyloid positivity (n = 394). This was to explore whether PRS thresholds were sensitive to differentiate participants with biomarker evidence and clinical diagnosis vs. no clinical diagnosis.

Stage 2 analyses (A), and (B), were completed using x10 PRSwithAPOE thresholds, x10 PRSwithoutAPOE threshold, and x10 APOEonlyPRS thresholds.

4.2.7.3. Stage 3 Analysis: Polygenic Risk Scores as Predictors of Clinical Diagnosis and/or Amyloid Status

Binomial hierarchical logistic regression analyses were performed to test whether PRS (independent / predictor variable) could predict clinical diagnosis / cognitive status, and / or, amyloid status / biomarker status (dependent / outcome variable).

(A) Diagnostic status: CU vs. MCI
• Model 1: Age, and education (covariates)
• Model 2: Age, education, and PRS

(B) Diagnostic status: CU vs. AD dementia
• Model 1: Age, and education (covariates)
• Model 2: Age, education, and PRS

(C) Diagnostic status: MCI vs. AD dementia
• Model 1: Age, and education (covariates)
• Model 2: Age, education, and PRS

(D) Amyloid status
• Model 1: Age (covariate)
• Model 2: Age, and PRS

(E) Amyloid status, repeated using additional covariates
• Model 1: Age, sex, education, family history, MMSE, and x10 genetic principal components (covariates)
• Model 2: All variables in Model 1, plus PRS

Covariates included only those that are consistently shown to affect diagnosis in AD, or amyloid status in AD. Other possible covariates were incorporated in the main analysis. For Stage 3 analyses (A), (B), (C), and (D), as above, binomial hierarchical logistic regression models were run

for x10 PRSwithAPOE thresholds separately, x10 PRSwithoutAPOE thresholds separately, and then x10 APOEonlyPRS thresholds separately.

4.2.7.4. Stage 4 Analysis: Associations between Polygenic Risk Scores and Regions of Interest

Multiple hierarchical linear regression analyses were performed to investigate whether there are associations between PRS (independent / predictor variable) and 114 ROIs (dependent / outcome variable). Based on the findings from Stages 1, 2, and 3, PRS thresholds that were selected for the main analysis were Thresholds 1 (most conservative), 5 (mid-point), and 10 (least conservative), for PRSwithAPOE, PRSwithoutAPOE, and APOEonlyPRS.

(A) Whole-group analysis

• Model 1: Age, sex, education, family history, amyloid positivity, scanner strength, total intracranial volume, x10 genetic principal components, and MMSE, (i.e., all covariates).

• Model 2: All variables in Model 1, plus PRS.

MMSE score was added as a covariate in whole-group analysis to control for the level of cognitive decline, since the group consisted of CU, MCI, and AD dementia participants. For Stage 4 (A), as above, analyses were completed using PRSwithAPOE Thresholds 1, 5, and 10, separately, followed by PRSwithoutAPOE Thresholds 1, 5, and 10, separately, and then APOEonlyPRS Thresholds 1, 5, and 10 separately.

(n = 738).

(B) Stratification by APOE ε4 status

• Model 1: Age, sex, education, family history, amyloid positivity, scanner strength, total intracranial volume, x10 genetic principal components, and MMSE (i.e., all covariates).

• Model 2: All variables in Model 1, plus PRS.

Analyses were completed using PRSwithAPOE Thresholds 1, 5, and 10, separately, followed by PRSwithoutAPOE Thresholds 1, 5, and 10, separately, and then APOEonlyPRS Thresholds 1, 5, and 10 separately.

(ε4 non-carriers, n = 432; ε4 carriers n = 306).

(C) Stratification by diagnostic status

• Model 1: Age, sex, education, family history, amyloid positivity, scanner strength, total intracranial volume, x10 genetic principal components, and MMSE (i.e., all covariates).

• Model 2: All variables in Model 1, plus PRS.

Analyses were performed using PRSwithAPOE Thresholds 1, 5, and 10, separately, followed by PRSwithoutAPOE Thresholds 1, 5, and 10, separately, and then APOEonlyPRS Thresholds 1, 5, and 10 separately.

(CU, n = 184; MCI, n = 416; AD dementia, n = 138).

(D) Stratification by amyloid status

• Model 1: Age, sex, education, family history, scanner strength, total intracranial volume, x10 genetic principal components, and MMSE.

• Model 2: All variables in Model 1, plus PRS.

Analyses were conducted using PRSwithAPOE Thresholds 1, 5, and 10, separately, followed by PRSwithoutAPOE Thresholds 1, 5, and 10, separately, and then APOEonlyPRS Thresholds 1, 5, and 10 separately. Amyloid status was not treated as a covariate as the data were stratified by amyloid status itself, and amyloid positive participants are likely to be on the AD continuum. However, all other variables in the models were kept constant, i.e., from (A) to (D) for consistency. APOE ε4 status was not treated as a covariate as this was controlled by the PRS itself, i.e., PRSwithAPOE vs. PRSwithoutAPOE.

(Amyloid negative, n = 266; amyloid positive, n = 472).

For Stage 1 to Stage 3 analyses, *p* was significant at the 0.05 level. For Stage 4 (A) to (D), a strategic decision was taken to correct for multiple comparisons and reduce the likelihood of type 1 errors by using FDR. *p* was significant at the 0.05 level after FDR correction. For consistency, *post-hoc* comparisons in Stage 1 analysis were also corrected using FDR.

4.3. RESULTS

4.3.1. Stage 1 Results: Covariates

4.3.1.1. Age

There was a significant difference in mean age between the diagnostic groups, ($F_{2, 735}$ = 9.225, p <0.001). *Post-hoc* comparisons using independent-sample t-tests and FDR were carried out to establish where the differences were. There was a significant difference between CU vs. AD dementia participants, (t(241.816) = -3.359, p = 0.000907306623669), and between MCI vs. AD dementia patients, (t(552) = -4.011, p = 0.000068743945891). However, there was no significant difference between CU and MCI participants, (t(471.381) = 0.801, p = 0.424). After FDR correction, the differences remained; a significant difference in mean age between CU vs. AD dementia participants (p = 0.000604871) and between MCI vs. AD dementia patients (p = 0.0000229146) was observed. There was no significant difference in mean age between APOE ε4 non-carriers vs. APOE ε4 carriers, (t(736) = 1.915, p = 0.056). Additionally, there was no significant difference in mean age between amyloid negative vs. amyloid positive participants, (t(736) = 1.915, p = 0.056)

4.3.1.2. Sex

There were no significant differences in sex between the diagnostic groups, (X^2(2) = 5.782, p = 0.056), between APOE ε4 non-carriers vs. APOE ε4 carriers, (X^2(1) = 0.114, p = 0.764), or between amyloid negative vs. amyloid positive participants, (X^2(1) = 1.408, p = 0.248).

4.3.1.3. Education

There was no significant difference in the mean number of years in education between the diagnostic groups, ($F_{2, 235}$ = 2.645, p = 0.072), between APOE ε4 non-carriers vs. APOE ε4 carriers, (t(736) = 1.722, p = 0.085), and between amyloid negative vs. amyloid positive participants (t(736) = 1.019, p = 0.308).

4.3.1.4. Family History

There was no significant difference in family history between the diagnostic groups, ($X^2(2) = 1.165$, $p = 0.585$). On the other hand, there was a significant difference in family history between APOE ε4 non-carriers vs. APOE ε4 carriers, ($X^2(1) = 6.399$, $p = 0.012$). However, there was no significant difference in family history between amyloid negative vs. amyloid positive participants, ($X^2(1) = 0.211$, $p = 0.717$).

For consistency, all four variables were treated as covariates in the main (Stage 4) analysis. This was because age and family history were individually significantly different at least once, i.e., either for diagnostic status or APOE ε4 status. In addition, sex, education and amyloid status were also treated as covariates in the main analysis since previous literature indicates that these variables impact AD.

4.3.2. Stage 2 Results: Selecting the Optimal Polygenic Risk Score Thresholds

4.3.2.1. (A) Differentiating between CU Amyloid Negative vs. MCI Amyloid Positive and AD dementia Amyloid Positive

All x10 PRSwithAPOE thresholds were able to differentiate statistically between CU participants that were amyloid negative vs. MCI and AD dementia patients that were amyloid positive (p <0.001). For PRSwithoutAPOE, apart from Threshold 2, all other thresholds were able to distinguish statistically between both groups. PRSwithoutAPOE Thresholds 9 and 10 were particularly significant (p <0.001). All x10 APOEonlyPRS thresholds were also able to differentiate statistically between both groups as well (p <0.001). See Table 4.4 for details.

Table 4.4: Independent-sample t-test outputs comparing CU participants with amyloid negativity and MCI vs. AD dementia patients with amyloid positivity using PRSwithAPOE, PRSwithoutAPOE, and APOEonlyPRS.

	PRSwithAPOE			PRSwithoutAPOE			APOEonlyPRS		
PRS Threshold	**t**	**df**	***p***	**t**	**df**	***p***	**t**	**df**	***p***
1	-8.489	249.309	<0.001	-1.981	145.458	0.049	-8.009	246.034	<0.001
2	-8.423	245.602	<0.001	-1.896	145.097	0.060	-7.981	245.890	<0.001
3	-8.470	244.980	<0.001	-2.035	144.236	0.044	-8.030	246.452	<0.001
4	-8.515	243.666	<0.001	-2.577	498	0.010	-8.027	245.894	<0.001
5	-8.399	238.653	<0.001	-2.571	498	0.010	-7.925	245.632	<0.001
6	-8.452	236.199	<0.001	-2.806	498	0.005	-7.889	244.141	<0.001
7	-8.587	233.124	<0.001	-3.063	498	0.002	-8.023	246.626	<0.001
8	-8.598	234.580	<0.001	-3.115	498	0.002	-8.039	247.941	<0.001
9	-8.827	229.701	<0.001	-3.560	498	<0.001	-8.099	248.291	<0.001
10	-8.879	229.135	<0.001	-3.671	498	<0.001	-8.094	247.660	<0.001

APOE: apolipoprotein E. df: degrees of freedom. PRS: polygenic risk score. t: test statistic.

4.3.2.2. (B) Differentiating between CU Amyloid Positive vs. MCI Amyloid Positive and AD dementia Amyloid Positive

All x10 PRSwithAPOE thresholds were able to distinguish statistically between CU participants that were amyloid positive vs. MCI and AD dementia patients that were amyloid positive (p <0.0001). For PRSwithoutAPOE, all x10 thresholds were able to differentiate between the two groups, particularly using Threshold 10 (p <0.001). Similarly, all x10 APOEonlyPRS thresholds were able to identify statistically between both groups of participants (p <0.001). Refer to Table 4.5 for details.

Table 4.5: Independent-sample t-test outputs comparing CU participants with amyloid positivity and MCI vs. AD dementia patients with amyloid positivity using PRSwithAPOE, PRSwithoutAPOE, and APOEonlyPRS.

	PRSwithAPOE			PRSwithoutAPOE			APOEonlyPRS		
PRS Threshold	**t**	**df**	***p***	**t**	**df**	***p***	**t**	**df**	***p***
1	-4.967	124.084	<0.001	-2.989	470	0.003	-4.203	121.364	<0.001
2	-4.951	122.254	<0.001	-3.078	470	0.002	-4.208	121.327	<0.001
3	-5.050	121.700	<0.001	-3.162	470	0.002	-4.284	121.036	<0.001
4	-5.083	122.226	<0.001	-2.990	470	0.003	-4.292	121.172	<0.001
5	-5.031	121.492	<0.001	-2.697	470	0.007	-4.253	121.675	<0.001
6	-4.613	470	<0.001	-2.536	470	0.012	-4.145	120.946	<0.001
7	-4.810	470	<0.001	-2.941	470	0.003	-4.221	121.443	<0.001
8	-4.822	470	<0.001	-3.063	470	0.002	-4.196	121.444	<0.001
9	-4.841	470	<0.001	-3.247	470	0.001	-4.074	120.859	<0.001
10	-4.869	470	<0.001	-3.367	470	<0.001	-4.037	121.503	<0.001

APOE: apolipoprotein E. df: degrees of freedom. PRS: polygenic risk score. t: test statistic.

4.3.3. Stage 3 Results: Polygenic Risk Scores as Predictors of Clinical Diagnosis and/or Amyloid Status

4.3.3.1. (A) Differentiating between CU vs. MCI

All x10 PRSwithAPOE thresholds were able to predict significantly CU individuals from clinically diagnosed MCI patients. 4.1% to 5.8% of the variation in diagnosis was explained by the model. All x10 PRSwithoutAPOE thresholds were able to predict significantly between CU vs. MCI participants. 2.5% to 4.3% of the variation in clinical diagnosis was accounted for by the model. Similarly, all x10 APOEonlyPRS thresholds were able to distinguish between both groups. 3.1% to 3.4% of the variation was explained by the model. See Table 4.6 for exact numerical figures.

Table 4.6: Model 2 to show whether PRS can predict clinical diagnosis (CU vs. MCI). Model controlled for age and education.

PRSwithAPOE

PRS Threshold	Chi-square	df	*p*	Nagelkerke R^2	Wald	df	*p*	OR	95% CI	Nagelkerke R^2 Model 1
1	17.893	3	<0.001	0.041	12.074	1	<0.001	1.430	1.169-1.751	0.012
2	18.127	3	<0.001	0.042	12.302	1	<0.001	1.435	1.173-1.756	0.012
3	18.452	3	<0.001	0.043	12.580	1	<0.001	1.443	1.178-1.767	0.012
4	18.663	3	<0.001	0.043	12.773	1	<0.001	1.448	1.182-1.775	0.012
5	18.520	3	<0.001	0.043	12.651	1	<0.001	1.445	1.180-1.770	0.012
6	19.468	3	<0.001	0.045	13.531	1	<0.001	1.465	1.195-1.795	0.012
7	21.821	3	<0.001	0.050	15.642	1	<0.001	1.511	1.231-1.854	0.012
8	21.854	3	<0.001	0.050	15.683	1	<0.001	1.511	1.232-1.854	0.012
9	24.416	3	<0.001	0.056	17.951	1	<0.001	1.561	1.270-1.918	0.012
10	24.959	3	<0.001	0.058	18.422	1	<0.001	1.571	1.278-1.931	0.012

PRSwithoutAPOE

PRS Threshold	Chi-square	df	*p*	Nagelkerke R^2	Wald	df	*p*	OR	95% CI	Nagelkerke R^2 Model 1
1	10.901	3	0.012	0.025	5.791	1	0.016	1.241	1.041-1.490	0.012
2	11.163	3	0.011	0.026	6.049	1	0.014	1.248	1.046-1.488	0.012
3	11.137	3	0.011	0.026	6.011	1	0.014	1.245	1.045-1.484	0.012
4	11.764	3	0.008	0.027	6.606	1	0.010	1.260	1.056-1.502	0.012
5	11.471	3	0.009	0.027	6.330	1	0.012	1.254	1.051-1.496	0.012
6	11.592	3	0.009	0.027	6.454	1	0.011	1.258	1.054-1.501	0.012
7	14.198	3	0.003	0.033	8.942	1	0.003	1.315	1.099-1.574	0.012
8	14.765	3	0.002	0.034	9.477	1	0.002	1.328	1.109-1.592	0.012
9	17.810	3	<0.001	0.041	12.324	1	<0.001	1.387	1.155-1.665	0.012
10	18.714	3	<0.001	0.043	13.175	1	<0.001	1.401	1.168-1.681	0.012

APOEonlyPRS

PRS Threshold	Chi-square	df	*p*	Nagelkerke R^2	Wald	df	*p*	OR	95% CI	Nagelkerke R^2 Model 1
1	13.990	3	0.003	0.033	8.517	1	0.004	1.343	1.102-1.636	0.012
2	13.885	3	0.003	0.032	8.423	1	0.004	1.340	1.100-1.633	0.012
3	14.011	3	0.003	0.033	8.530	1	0.003	1.344	1.102-1.638	0.012
4	14.082	3	0.003	0.033	8.594	1	0.003	1.345	1.103-1.641	0.012
5	13.692	3	0.003	0.032	8.238	1	0.004	1.336	1.096-1.628	0.012
6	13.375	3	0.004	0.031	7.962	1	0.005	1.328	1.090-1.616	0.012
7	14.014	3	0.003	0.033	8.542	1	0.003	1.343	1.102-1.636	0.012
8	13.938	3	0.003	0.032	8.470	1	0.004	1.341	1.101-1.634	0.012
9	14.474	3	0.002	0.034	8.966	1	0.003	1.353	1.110-1.650	0.012
10	14.339	3	0.002	0.033	8.849	1	0.003	1.350	1.108-1.645	0.012

APOE: apolipoprotein E. CI: confidence interval. df: degrees of freedom. OR: odds ratio. PRS: polygenic risk score. Model 1 without PRS.

4.3.3.2. (B) Differentiating between CU vs. AD dementia

All x10 PRSwithAPOE thresholds were able to differentiate significantly between CU individuals vs. clinically diagnosed AD dementia patients. 29.4% to 32.0% of the variation in diagnosis was explained by the model. Additionally, all x10 PRSwithoutAPOE thresholds were able to predict significantly CU participants from AD dementia patients. 9.4% to 14.2% of the variation in diagnosis was accounted for by the model. Similarly, all x10 APOEonlyPRS thresholds were able to identify between both groups of participants. The model accounted for 26.7% to 27.6% of the variability. See Table 4.7 for precise numerical figures.

Table 4.7: Model 2 to show whether PRS can predict clinical diagnosis (CU vs. AD dementia). Model controlled for age and education.

PRSwithAPOE

PRS Threshold	Chi-square	df	*p*	Nagelkerke R^2	Wald	df	*p*	OR	95% CI	Nagelkerke R^2 Model 1
1	79.657	3	<0.001	0.294	50.803	1	<0.001	2.705	2.057-3.556	0.064
2	80.197	3	<0.001	0.296	51.121	1	<0.001	2.702	2.057-3.548	0.064
3	81.775	3	<0.001	0.301	51.976	1	<0.001	2.730	2.078-3.587	0.064
4	82.622	3	<0.001	0.304	52.527	1	<0.001	2.746	2.090-3.609	0.064
5	81.681	3	<0.001	0.301	52.103	1	<0.001	2.712	2.068-3.555	0.064
6	82.203	3	<0.001	0.302	52.574	1	<0.001	2.718	2.074-3.561	0.064
7	84.257	3	<0.001	0.309	53.666	1	<0.001	2.773	2.111-3.642	0.064
8	84.174	3	<0.001	0.309	53.572	1	<0.001	2.781	2.114-3.656	0.064
9	86.578	3	<0.001	0.317	54.748	1	<0.001	2.837	2.152-3.740	0.064
10	87.636	3	<0.001	0.320	55.439	1	<0.001	2.862	2.170-3.774	0.064

PRSwithoutAPOE

PRS Threshold	Chi-square	df	*p*	Nagelkerke R^2	Wald	df	*p*	OR	95% CI	Nagelkerke R^2 Model 1
1	23.426	3	<0.001	0.094	7.387	1	0.007	1.374	1.093-1.727	0.064
2	24.301	3	<0.001	0.098	8.198	1	0.004	1.393	1.110-1.748	0.064
3	26.435	3	<0.001	0.106	10.138	1	0.001	1.458	1.156-1.839	0.064
4	27.602	3	<0.001	0.110	11.190	1	<0.001	1.492	1.180-1.885	0.064
5	26.637	3	<0.001	0.107	10.330	1	0.001	1.461	1.159-1.841	0.064
6	28.274	3	<0.001	0.113	11.778	1	<0.001	1.500	1.190-1.892	0.064
7	30.639	3	<0.001	0.122	13.863	1	<0.001	1.563	1.236-1.977	0.064
8	31.483	3	<0.001	0.125	14.612	1	<0.001	1.589	1.253-2.015	0.064
9	35.178	3	<0.001	0.139	17.707	1	<0.001	1.681	1.320-2.141	0.064
10	35.923	3	<0.001	0.142	18.339	1	<0.001	1.696	1.332-2.159	0.064

APOEonlyPRS

PRS Threshold	Chi-square	df	*p*	Nagelkerke R^2	Wald	df	*p*	OR	95% CI	Nagelkerke R^2 Model 1
1	73.058	3	<0.001	0.273	46.617	1	<0.001	2.551	1.950-3.338	0.064
2	73.324	3	<0.001	0.273	46.787	1	<0.001	2.560	1.955-3.351	0.064
3	74.186	3	<0.001	0.276	47.340	1	<0.001	2.577	1.968-3.374	0.064
4	74.220	3	<0.001	0.276	47.388	1	<0.001	2.576	1.968-3.373	0.064
5	73.024	3	<0.001	0.272	46.708	1	<0.001	2.548	1.949-3.332	0.064
6	72.044	3	<0.001	0.269	46.207	1	<0.001	2.527	1.934-3.301	0.064
7	73.016	3	<0.001	0.272	46.823	1	<0.001	2.550	1.950-3.334	0.064
8	72.990	3	<0.001	0.272	46.787	1	<0.001	2.552	1.951-3.337	0.064
9	71.386	3	<0.001	0.267	45.712	1	<0.001	2.503	1.918-3.266	0.064
10	71.778	3	<0.001	0.268	45.909	1	<0.001	2.515	1.926-3.284	0.064

APOE: apolipoprotein E. CI: confidence interval. df: degrees of freedom. OR: odds ratio. PRS: polygenic risk score. Model 1 without PRS.

4.3.3.3. (C) Differentiating between MCI vs. AD dementia

All x10 PRSwithAPOE thresholds were able to distinguish significantly between clinically diagnosed MCI patients vs. clinically diagnosed AD dementia patients. 13.6% to 14.5% of the variation in clinical diagnosis was explained by the model. None of the PRSwithoutAPOE thresholds were able to differentiate significantly between MCI vs. AD dementia patients. However, the model accounted for 4.4% to 5.0% of the variation in clinical diagnosis. On the other hand, all x10 APOEonlyPRS thresholds were able to distinguish between both groups of participants. The model accounted for 1.32% to 1.39% of the variability. See Table 4.8 for exact numerical figures.

Table 4.8: Model 2 to show whether PRS can predict clinical diagnosis (MCI vs. AD dementia). Model controlled for age and education.

PRSwithAPOE

PRS Threshold	Chi-square	df	*p*	Nagelkerke R^2	Wald	df	*p*	OR	95% CI	Nagelkerke R^2 Model 1
1	53.260	3	<0.001	0.136	35.152	1	<0.001	1.812	1.489-2.205	0.042
2	54.078	3	<0.001	0.138	35.835	1	<0.001	1.828	1.500-2.227	0.042
3	55.605	3	<0.001	0.142	37.206	1	<0.001	1.850	1.518-2.254	0.042
4	56.377	3	<0.001	0.143	37.849	1	<0.001	1.864	1.528-2.273	0.042
5	56.655	3	<0.001	0.144	38.129	1	<0.001	1.871	1.533-2.282	0.042
6	56.875	3	<0.001	0.145	38.240	1	<0.001	1.883	1.541-2.302	0.042
7	55.787	3	<0.001	0.142	37.271	1	<0.001	1.872	1.531-2.290	0.042
8	55.514	3	<0.001	0.141	36.998	1	<0.001	1.871	1.529-2.289	0.042
9	54.624	3	<0.001	0.139	36.291	1	<0.001	1.860	1.520-2.277	0.042
10	54.512	3	<0.001	0.139	36.197	1	<0.001	1.858	1.518-2.273	0.042

PRSwithoutAPOE

PRS Threshold	Chi-square	df	*p*	Nagelkerke R^2	Wald	df	*p*	OR	95% CI	Nagelkerke R^2 Model 1
1	16.728	3	<0.001	0.044	0.705	1	0.401	1.090	0.892-1.331	0.042
2	17.009	3	<0.001	0.045	0.987	1	0.320	1.108	0.905-1.357	0.042
3	17.839	3	<0.001	0.047	1.818	1	0.178	1.150	0.939-1.409	0.042
4	17.967	3	<0.001	0.047	1.946	1	0.163	1.155	0.943-1.414	0.042
5	17.766	3	<0.001	0.047	1.746	1	0.186	1.147	0.936-1.405	0.042
6	18.837	3	<0.001	0.050	2.809	1	0.094	1.192	0.971-1.463	0.042
7	18.656	3	<0.001	0.049	2.631	1	0.105	1.186	0.965-1.456	0.042
8	18.732	3	<0.001	0.049	2.705	1	0.100	1.188	0.968-1.457	0.042
9	18.916	3	<0.001	0.050	2.889	1	0.089	1.194	0.973-1.464	0.042
10	18.870	3	<0.001	0.050	2.842	1	0.092	1.193	0.972-1.464	0.042

APOEonlyPRS

PRS Threshold	Chi-square	df	*p*	Nagelkerke R^2	Wald	df	*p*	OR	95% CI	Nagelkerke R^2 Model 1
1	53.501	3	<0.001	0.136	35.387	1	<0.001	1.814	1.491-2.207	0.042
2	53.829	3	<0.001	0.137	35.660	1	<0.001	1.819	1.495-2.213	0.042
3	54.617	3	<0.001	0.139	36.364	1	<0.001	1.830	1.504-2.227	0.042
4	54.606	3	<0.001	0.139	36.364	1	<0.001	1.830	1.504-2.227	0.042
5	53.965	3	<0.001	0.138	35.829	1	<0.001	1.818	1.495-2.211	0.042
6	53.650	3	<0.001	0.137	35.515	1	<0.001	1.818	1.495-2.211	0.042
7	53.545	3	<0.001	0.137	35.437	1	<0.001	1.815	1.492-2.209	0.042
8	53.497	3	<0.001	0.136	35.404	1	<0.001	1.814	1.491-2.207	0.042
9	51.507	3	<0.001	0.132	33.695	1	<0.001	1.783	1.467-2.168	0.042
10	51.834	3	<0.001	0.132	33.968	1	<0.001	1.788	1.470-2.173	0.042

APOE: apolipoprotein E. CI: confidence interval. df: degrees of freedom. OR: odds ratio. PRS: polygenic risk score. Model 1 without PRS.

4.3.3.4. (D) Differentiating between Amyloid Negative vs. Amyloid Positive

All x10 PRSwithAPOE thresholds were able to predict significantly amyloid status. 17.4% to 18.2% of the variation in amyloid status was explained by the model. Additionally, all x10 PRSwithoutAPOE thresholds were able to differentiate between amyloid statuses. 2.9% to 3.5% of the variation in amyloid status was accounted by the model. Similarly, all x10 APOEonlyPRS thresholds were able to distinguish between both groups of participants. The model accounted for 1.69% to 1.73% of the variability. See Table 4.9 for precise numerical figures.

Table 4.9: Model 2 to show whether PRS can predict amyloid status. Model controlled for age.

PRSwithAPOE

PRS Threshold	Chi-square	df	*p*	Nagelkerke R^2	Wald	df	*p*	OR	95% CI	Nagelkerke R^2 Model 1
1	103.079	2	<0.001	0.179	73.988	1	<0.001	2.299	1.902-2.780	0.022
2	102.108	2	<0.001	0.177	73.485	1	<0.001	2.284	1.891-2.759	0.022
3	103.772	2	<0.001	0.180	74.274	1	<0.001	2.309	1.909-2.794	0.022
4	104.873	2	<0.001	0.182	75.027	1	<0.001	2.323	1.920-2.812	0.022
5	103.856	2	<0.001	0.180	74.391	1	<0.001	2.309	1.909-2.792	0.022
6	102.720	2	<0.001	0.178	74.025	1	<0.001	2.291	1.897-2.767	0.022
7	101.668	2	<0.001	0.176	73.603	1	<0.001	2.275	1.886-2.745	0.022
8	100.835	2	<0.001	0.175	73.150	1	<0.001	2.266	1.879-2.733	0.022
9	100.076	2	<0.001	0.174	72.674	1	<0.001	2.259	1.873-2.724	0.022
10	100.295	2	<0.001	0.174	72.841	1	<0.001	2.261	1.875-2.727	0.022

PRSwithoutAPOE

PRS Threshold	Chi-square	df	*p*	Nagelkerke R^2	Wald	df	*p*	OR	95% CI	Nagelkerke R^2 Model 1
1	16.584	2	<0.001	0.030	4.820	1	0.028	1.187	1.019-1.384	0.022
2	15.744	2	<0.001	0.029	3.999	1	0.046	1.169	1.003-1.363	0.022
3	16.496	2	<0.001	0.030	4.735	1	0.030	1.186	1.017-1.382	0.022
4	17.327	2	<0.001	0.032	5.542	1	0.019	1.203	1.031-1.403	0.022
5	17.026	2	<0.001	0.031	5.251	1	0.022	1.197	1.026-1.396	0.022
6	18.226	2	<0.001	0.033	6.424	1	0.011	1.221	1.046-1.425	0.022
7	18.426	2	<0.001	0.034	6.619	1	0.010	1.226	1.050-1.431	0.022
8	18.532	2	<0.001	0.034	6.722	1	0.010	1.228	1.052-1.435	0.022
9	18.960	2	<0.001	0.035	7.133	1	0.008	1.236	1.058-1.445	0.022
10	19.179	2	<0.001	0.035	7.349	1	0.007	1.240	1.061-1.449	0.022

APOEonlyPRS

PRS Threshold	Chi-square	df	*p*	Nagelkerke R^2	Wald	df	*p*	OR	95% CI	Nagelkerke R^2 Model 1
1	99.276	2	<0.001	0.173	70.716	1	<0.001	2.269	1.874-2.746	0.022
2	98.783	2	<0.001	0.172	70.415	1	<0.001	2.261	1.869-2.736	0.022
3	99.835	2	<0.001	0.173	70.929	1	<0.001	2.278	1.881-2.759	0.022
4	99.856	2	<0.001	0.173	70.927	1	<0.001	2.280	1.882-2.761	0.022
5	98.600	2	<0.001	0.171	70.036	1	<0.001	2.263	1.869-2.741	0.022
6	97.983	2	<0.001	0.170	69.948	1	<0.001	2.251	1.861-2.723	0.022
7	98.796	2	<0.001	0.172	70.411	1	<0.001	2.262	1.869-2.737	0.022
8	98.894	2	<0.001	0.172	70.447	1	<0.001	2.264	1.871-2.740	0.022
9	97.253	2	<0.001	0.169	69.387	1	<0.001	2.242	1.854-2.711	0.022
10	96.986	2	<0.001	0.169	69.247	1	<0.001	2.236	1.850-2.703	0.022

APOE: apolipoprotein E. CI: confidence interval. df: degrees of freedom. OR: odds ratio. PRS: polygenic risk score. Model 1 without PRS.

4.3.3.5. (E) Differentiating between Amyloid Negative vs. Amyloid Positive after Correcting for Several Variables

All x10 PRSwithAPOE thresholds were able to predict significantly amyloid status. 2.67% to 2.77% of the variation in amyloid status was explained by the model. However, none of the PRSwithoutAPOE thresholds were able to differentiate between amyloid statuses. Despite this, 1.86% to 1.87% of the variation in amyloid status was accounted by the model. In comparison, all x10 APOEonlyPRS thresholds were able to distinguish between both groups. The model accounted for 2.70% to 2.74% of the variability. See Table 4.10 for exact numerical figures.

Table 4.10: Model 2 to show whether PRS can predict amyloid status after controlling for additional variables – age, sex, education, family history, MMSE, and x10 genetic principal components.

PRSwithAPOE

PRS Threshold	Chi-square	df	*p*	Nagelkerke R^2	Wald	df	*p*	OR	95% CI	Nagelkerke R^2 Model 1
1	164.716	16	<0.001	0.276	50.296	1	<0.001	2.091	1.705-2.564	0.185
2	163.447	16	<0.001	0.274	49.428	1	<0.001	2.071	1.691-2.537	0.185
3	164.468	16	<0.001	0.276	50.061	1	<0.001	2.090	1.704-2.563	0.185
4	165.112	16	<0.001	0.277	50.538	1	<0.001	2.101	1.712-2.578	0.185
5	163.941	16	<0.001	0.275	49.678	1	<0.001	2.085	1.699-2.557	0.185
6	162.375	16	<0.001	0.273	48.746	1	<0.001	2.062	1.683-2.527	0.185
7	161.400	16	<0.001	0.271	48.104	1	<0.001	2.051	1.674-2.513	0.185
8	160.694	16	<0.001	0.270	47.576	1	<0.001	2.044	1.668-2.504	0.185
9	158.731	16	<0.001	0.267	46.134	1	<0.001	2.020	1.649-2.474	0.185
10	158.856	16	<0.001	0.267	46.271	1	<0.001	2.020	1.650-2.474	0.185

PRSwithoutAPOE

PRS Threshold	Chi-square	df	*p*	Nagelkerke R^2	Wald	df	*p*	OR	95% CI	Nagelkerke R^2 Model 1
1	107.336	16	<0.001	0.187	1.368	1	0.242	1.102	0.936-1.297	0.185
2	106.695	16	<0.001	0.186	0.731	1	0.393	1.074	0.912-1.264	0.185
3	106.981	16	<0.001	0.186	1.015	1	0.314	1.087	0.924-1.279	0.185
4	107.389	16	<0.001	0.187	1.420	1	0.233	1.105	0.938-1.301	0.185
5	107.229	16	<0.001	0.187	1.261	1	0.261	1.099	0.932-1.296	0.185
6	107.486	16	<0.001	0.187	1.516	1	0.218	1.110	0.940-1.310	0.185
7	107.697	16	<0.001	0.187	1.726	1	0.189	1.120	0.946-1.326	0.185
8	107.736	16	<0.001	0.187	1.764	1	0.184	1.123	0.946-1.333	0.185
9	107.369	16	<0.001	0.187	1.401	1	0.237	1.110	0.934-1.321	0.185
10	107.427	16	<0.001	0.187	1.458	1	0.227	1.113	0.936-1.323	0.185

APOEonlyPRS

PRS Threshold	Chi-square	df	*p*	Nagelkerke R^2	Wald	df	*p*	OR	95% CI	Nagelkerke R^2 Model 1
1	163.302	16	<0.001	0.274	48.994	1	<0.001	2.071	1.689-2.539	0.185
2	162.956	16	<0.001	0.273	48.742	1	<0.001	2.064	1.684-2.529	0.185
3	163.672	16	<0.001	0.274	49.211	1	<0.001	2.078	1.694-2.549	0.185
4	163.305	16	<0.001	0.274	48.915	1	<0.001	2.075	1.691-2.546	0.185
5	162.368	16	<0.001	0.273	48.175	1	<0.001	2.061	1.680-2.528	0.185
6	161.289	16	<0.001	0.271	47.573	1	<0.001	2.043	1.668-2.503	0.185
7	161.948	16	<0.001	0.272	48.014	1	<0.001	2.056	1.677-2.520	0.185
8	162.119	16	<0.001	0.272	48.114	1	<0.001	2.058	1.679-2.524	0.185
9	160.728	16	<0.001	0.270	47.106	1	<0.001	2.033	1.660-2.489	0.185
10	160.644	16	<0.001	0.270	47.088	1	<0.001	2.029	1.658-2.484	0.185

APOE: apolipoprotein E. CI: confidence interval. df: degrees of freedom. OR: odds ratio. PRS: polygenic risk score. Model 1 without PRS.

4.3.4. Stage 4 Results: Associations between Polygenic Risk Scores and Regions of Interest

A graphical representation of the ROIs that were associated with most PRSs and PRS thresholds across most stratifications is shown in Figure 4.1 (bilateral hippocampus, bilateral amygdala, bilateral entorhinal area) and Figure 4.2 (R middle occipital gyrus).

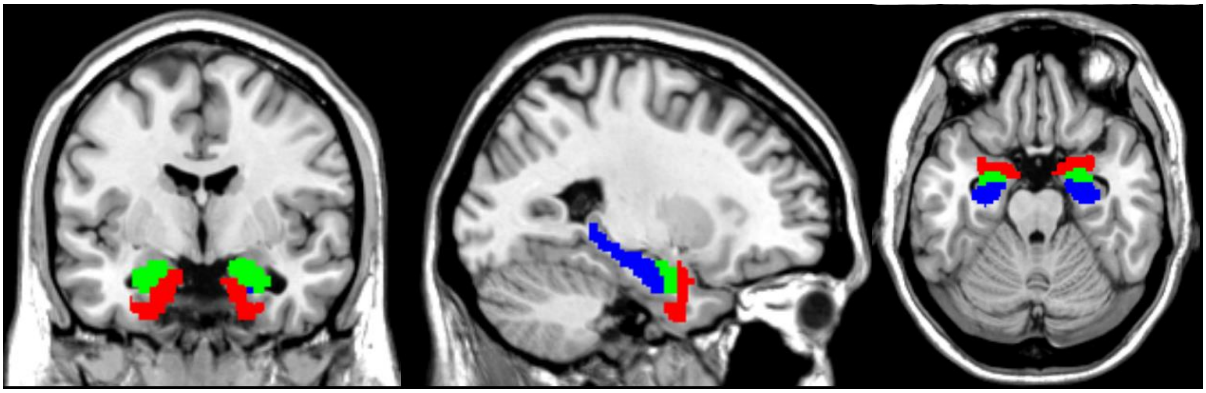

Figure 4.1: ROIs associated with different PRSs and PRS thresholds across most stratifications.

MNI coordinates: -26 -4 -22.

Blue: bilateral hippocampus. Green: bilateral amygdala. Red: bilateral entorhinal area.

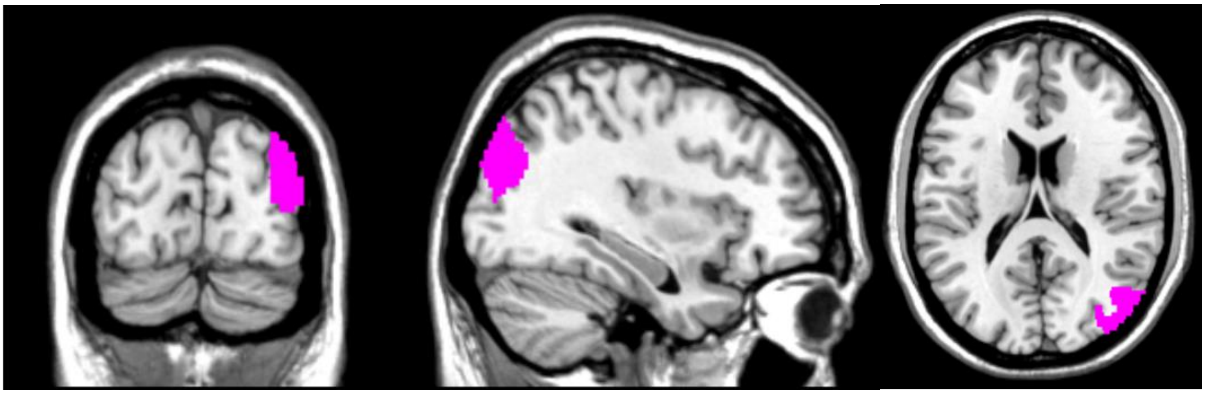

Figure 4.2: R middle occipital gyrus associated with different PRSs and PRS thresholds across most stratifications.

MNI coordinates: 34 -84 18.

Pink: R middle occipital gyrus.

4.3.4.1. (A) Whole group

PRSwithAPOE:

Whole group analysis using PRSwithAPOE Threshold 1 showed that PRSwithAPOE Threshold 1 was associated significantly with 21 ROIs. These were, in ascending order of significance: R hippocampus, R amygdala, L hippocampus, L amygdala, R middle occipital gyrus, R parahippocampal gyrus, R fusiform gyrus, R entorhinal area, R inferior temporal gyrus, L inferior temporal gyrus, R temporal gyrus, L entorhinal area, R cuneus, R inferior occipital gyrus, R posterior cingulate gyrus, L fusiform gyrus, R middle temporal gyrus, L parahippocampal gyrus, R precuneus, R occipital fusiform gyrus, and R calcarine cortex. However, after correcting for multiple comparisons using FDR, PRSwithAPOE Threshold 1 was associated significantly and negatively with five ROIs only. In ascending order, these were: R hippocampus (p = 0.00002674896), R amygdala (p = 0.000895545366711), L hippocampus (p = 0.001402658481438), L amygdala (p = 0.0077890684289835), and R middle occipital gyrus (p = 0.0228). Overall, the addition of PRSwithAPOE Threshold 1 to the model increased predictability of associations by up to 1.9%. Refer to Table 4.11, and Appendix D Table D.1 for further details.

PRSwithAPOE Threshold 5 was associated significantly with 19 ROIs. These were, in ascending order: R hippocampus, R amygdala, L hippocampus, L amygdala, R middle occipital gyrus, R parahippocampal gyrus, L entorhinal area, R entorhinal area, L inferior temporal gyrus, R inferior temporal gyrus, R temporal pole, R posterior cingulate gyrus, L parahippocampal gyrus, R fusiform gyrus, R cuneus, R calcarine cortex, R middle temporal gyrus, R inferior occipital gyrus, and L postcentral gyrus medial segment. However, after correcting for multiple comparisons, PRSwithAPOE Threshold 5 remained associated significantly and negatively with four ROIs only. In ascending order, these were: R hippocampus (p = 0.000010960758), R amygdala (p = 0.000522359597847), L hippocampus (p = 0.000364246297782), and L amygdala (p = 0.002547464345523). On the whole, adding PRSwithAPOE Threshold 5 to the model increased predictability of the associations by up to 2.1%. Refer to Table 4.11, and Appendix D Table D.2 for more information.

Additionally, PRSwithAPOE Threshold 10 was associated significantly with 19 ROIs. These were, in ascending order: R hippocampus, L hippocampus, R amygdala, L amygdala, L entorhinal area, R parahippocampal gyrus, R middle occipital gyrus, R entorhinal area, L parahippocampal gyrus, R temporal pole, L inferior temporal gyrus, R inferior temporal gyrus, R subcallosal area, R cuneus, R fusiform gyrus, R calcarine cortex, R frontal pole, R thalamus proper, and R posterior

cingulate gyrus. However, after implementing FDR corrective methods, PRSwithAPOE Threshold 10 remained associated significantly and negatively with four ROIs only. In ascending order, these were: R hippocampus (p = 0.000005830416), L hippocampus (p = 0.000266085514839), R amygdala (p = 0.000343368110162), and L amygdala (p = 0.0017303133714945). Adding PRSwithAPOE Threshold 10 to the model increased predictability of the associations by up to 2.1%. Refer to Table 4.11, and Appendix D Table D.3 for further information.

PRSwithoutAPOE:

Whole group analysis using PRSwithoutAPOE Threshold 1 demonstrated that PRSwithoutAPOE Threshold 1 was associated significantly with four ROIs. These were, in ascending order: L superior frontal gyrus, R hippocampus, L hippocampus, and R basal forebrain. PRSwithoutAPOE Threshold 5 was associated significantly with five ROIs. In ascending order, these were: R supramarginal gyrus, L hippocampus, L frontal pole, R hippocampus, and R occipital fusiform gyrus. Additionally, PRSwithoutAPOE Threshold 10 was associated significantly with 6 ROIs. These were, in ascending order: L hippocampus, R hippocampus, R supramarginal gyrus, L frontal pole, L amygdala, and R frontal pole. However, none of these associations remained significant after correcting for multiple comparisons. Additionally, adding PRSwithoutAPOE Threshold 1 to the model increased predictability of the associations by up to 0.4%, adding PRSwithoutAPOE Threshold 5 to the model increased predictability of the associations by up to 0.6%, and adding PRSwithoutAPOE Threshold 10 to the model increased predictability of the associations by up to 0.8%. Refer to Appendix D Table D.4 (PRSwithoutAPOE Threshold 1), Table D.5 (PRSwithoutAPOE Threshold 5), and Table D.6 (PRSwithoutAPOE Threshold 10) for more details.

APOEonlyPRS:

Whole group analysis using APOEonlyPRS Threshold 1 revealed that APOEonlyPRS Threshold 1 was associated significantly with 25 ROIs. In ascending order of significance, these were: R hippocampus, R amygdala, L hippocampus, R middle occipital gyrus, L amygdala, R parahippocampal gyrus, R fusiform gyrus, R inferior occipital gyrus, L postcentral gyrus medial segment, R occipital fusiform gyrus, L fusiform gyrus, R inferior temporal gyrus, R entorhinal area, L entorhinal area, R middle temporal gyrus, R temporal gyrus, R cuneus, L parahippocampal gyrus, R posterior cingulate gyrus, R precuneus, R superior parietal lobule, R lingual gyrus, R precentral gyrus medial segment, L inferior temporal gyrus, and L inferior occipital gyrus. However, implementing FDR corrective methods, APOEonlyPRS Threshold 1 remained

associated significantly and negatively with five ROIs only. In ascending order, these were: R hippocampus (p = 0.000249017495772), R amygdala (p = 0.002239319878449), L hippocampus (p = 0.011662596067996), L amygdala (p = 0.0153078257065644), and R middle occipital gyrus (p = 0.018422944712178). Generally, APOEonlyPRS Threshold 1 increased predictability of the associations by up to 1.3%. Refer to Table 4.12, and Appendix D Table D.7 for further details.

APOEonlyPRS Threshold 5 was associated significantly with 25 ROIs. In ascending order, these were: R hippocampus, R amygdala, L hippocampus, R middle occipital gyrus, L amygdala, R parahippocampal gyrus, R fusiform gyrus, R inferior occipital gyrus, L postcentral gyrus medial segment, R inferior temporal gyrus, R occipital fusiform gyrus, L fusiform gyrus, R middle occipital gyrus, R entorhinal area, L entorhinal area, R temporal pole, L parahippocampal gyrus, R cuneus, R posterior cingulate gyrus, R precuneus, L inferior temporal gyrus, R superior parietal lobule, R angular gyrus, R lingual gyrus, and L inferior occipital gyrus. After applying FDR corrective measures, APOEonlyPRS Threshold 5 was associated significantly and negatively with five ROIs only. In ascending order, these were: R hippocampus (p = 0.00032841568704), R amygdala (p = 0.002481703846062), L hippocampus (p = 0.01396102784404), R middle occipital gyrus (p = 0.0184792111345185), and L amygdala (p = 0.01980123335616). On the whole, APOEonlyPRS Threshold 1 increased predictability of the associations by up to 1.2%. Refer to Table 4.12, and Appendix D Table D.8 for more information.

Additionally, APOEonlyPRS Threshold 10 was associated significantly with 25 ROIs. In ascending order of significance, these were: R hippocampus, R amygdala, L hippocampus, R middle occipital gyrus, L amygdala, R parahippocampal gyrus, R inferior occipital gyrus, R fusiform gyrus, L postcentral gyrus medial segment, L fusiform gyrus, L parahippocampal gyrus, R inferior temporal gyrus, L entorhinal area, R entorhinal area, R posterior cingulate gyrus, R middle temporal gyrus, R occipital fusiform gyrus, R cuneus, R temporal pole, L inferior temporal gyrus, L inferior occipital gyrus, R lingual gyrus, L opercular part of the inferior frontal gyrus, R precuneus, and R angular gyrus. However, after FDR correction, APOEonlyPRS Threshold 10 was associated significantly and negatively with five ROIs, and these were: R hippocampus (p = 0.000511996810374), R amygdala (p = 0.004295979251736), L hippocampus (p = 0.021105099796812), L amygdala (p = 0.029754), and R middle occipital gyrus (p = 0.03591). Overall, the addition of APOEonlyPRS Threshold 10 increased predictability of associations by up to 1.2%. Refer to Table 4.12, and Appendix D Table D.9 for further information.

Table 4.11: Associations between PRSwithAPOE thresholds and ROIs found in the whole group that survived FDR correction.

	R Square (Model 1)	R Square (Model 2)	R Square Change	Sig. F Change (Model 2)	FDR Corrected value	Standardised beta of PRS
PRSwithAPOE Threshold 1						
Amygdala L	0.417	0.428	0.011	0.000273300646631	0.0078	-0.114
Amygdala R	0.464	0.478	0.014	0.000015711322223	0.0009	-0.129
Hippocampus L	0.449	0.462	0.013	0.000036912065301	0.0014	-0.125
Hippocampus R	0.476	0.496	0.019	0.00000023464	0.0000	-0.152
Middle occipital gyrus R	0.347	0.357	0.010	0.001	0.0228	-0.109
PRSwithAPOE Threshold 5						
Amygdala L	0.417	0.430	0.012	0.000089384713878	0.0025	-0.123
Amygdala R	0.464	0.478	0.015	0.000009164203471	0.0005	-0.133
Hippocampus L	0.449	0.464	0.015	0.000009585428889	0.0004	-0.134
Hippocampus R	0.476	0.497	0.021	0.000000096147	0.0000	-0.157
PRSwithAPOE Threshold 10						
Amygdala L	0.417	0.430	0.013	0.000060712749877	0.0017	-0.126
Amygdala R	0.464	0.478	0.015	0.000009036002899	0.0003	-0.134
Hippocampus L	0.449	0.465	0.016	0.000004668166927	0.0003	-0.140
Hippocampus R	0.476	0.498	0.021	0.000000051144	0.0000	-0.161

APOE: apolipoprotein E. FDR: false discovery rate. L: left. PRS: polygenic risk score. R: right.

Table 4.12: Associations between APOEonlyPRS thresholds and ROIs found in the whole group that survived FDR correction.

	R Square (Model 1)	R Square (Model 2)	R Square Change	Sig. F Change (Model 2)	FDR Corrected value	Standardised beta of PRS
APOEonlyPRS Threshold 1						
Amygdala L	0.417	0.427	0.009	0.000671395864323	0.0153	-0.106
Amygdala R	0.464	0.476	0.013	0.000039286313657	0.0022	-0.123
Hippocampus L	0.449	0.459	0.010	0.000306910422842	0.0117	-0.109
Hippocampus R	0.476	0.493	0.016	0.000002184363998	0.0002	-0.139
Middle occipital gyrus R	0.347	0.358	0.011	0.000646419112708	0.0184	-0.112
APOEonlyPRS Threshold 5						
Amygdala L	0.417	0.426	0.009	0.0008684751472	0.0198	-0.104
Amygdala R	0.464	0.476	0.012	0.000043538663966	0.0025	-0.122
Hippocampus L	0.449	0.458	0.010	0.00036739546958	0.0140	-0.108
Hippocampus R	0.476	0.492	0.016	0.00000288083936	0.0003	-0.138
Middle occipital gyrus R	0.347	0.358	0.011	0.000648393373141	0.0185	-0.112
APOEonlyPRS Threshold 10						
Amygdala L	0.417	0.426	0.008	0.001305	0.0298	-0.100
Amygdala R	0.464	0.475	0.012	0.000075368057048	0.0043	-0.118
Hippocampus L	0.449	0.458	0.009	0.000555397363074	0.0211	-0.104
Hippocampus R	0.476	0.492	0.015	0.000004491200091	0.0005	-0.135
Middle occipital gyrus R	0.347	0.357	0.009	0.001260	0.0359	-0.106

APOE: apolipoprotein E. FDR: false discovery rate. L: left. PRS: polygenic risk score. R: right.

4.3.4.2. (B) Whole group stratified by APOE ε4 status

PRSwithAPOE:

Whole group stratification by APOE ε4 status indicated that for APOE ε4 non-carriers, PRSwithAPOE Threshold 1 was associated significantly with six ROIs. In order of the strength of the associations, these were: L putamen, L opercular part of the inferior frontal gyrus, R putamen, R basal forebrain, R inferior temporal gyrus, and L basal forebrain. For APOE ε4 carriers, PRSwithAPOE Threshold 1 was associated significantly with five ROIs. These were, in ascending order: R accumbens area, L precentral gyrus, R superior frontal gyrus, L posterior insula, and R posterior insula. However, for both APOE ε4 non-carriers and carriers, none of the above associations remained significant after correcting for multiple comparisons. Overall, the addition of PRSwithAPOE Threshold 1 increased predictability of the associations by up to 1.4% for ε4 non-carriers and by up to 1.3% for ε4 carriers. Refer to Appendix D Table D.10 (ε4 non-carriers) and Table D.11 (ε4 carriers) for more details.

For APOE ε4 non-carriers, PRSwithAPOE Threshold 5 was associated significantly with six ROIs. In ascending order, these were: L putamen, L opercular part of the inferior frontal gyrus, R putamen, L hippocampus, L superior occipital gyrus, and R hippocampus. For APOE ε4 carriers, PRSwithAPOE Threshold 5 was associated significantly with six ROIs. These were, in ascending order: R accumbens area, R superior frontal gyrus, R posterior insula, L precentral gyrus, L posterior insula, and R calcarine cortex. However, for both APOE ε4 non-carriers and carriers, the above associations did not survive FDR correction. Adding PRSwithAPOE Threshold 5 to the model increased predictability by up to 1.4% for APOE ε4 non-carriers and up to 1.2% for ε4 carriers. Refer to Appendix D Table D.12 (ε4 non-carriers) and Table D.13 (ε4 carriers) for further details.

Furthermore, for APOE ε4 non-carriers, PRSwithAPOE Threshold 10 was associated significantly with six ROIs. In ascending order, these were: L basal forebrain, L opercular part of the inferior frontal gyrus, L putamen, L hippocampus, L planum temporale, and R basal forebrain. For APOE ε4 carriers, PRSwithAPOE Threshold 10 was associated significantly with seven ROIs. These were, in ascending order: R superior frontal gyrus, R posterior insula, L precentral gyrus, R basal forebrain, R accumbens area, R anterior insula, and L posterior insula. However, again for both APOE ε4 non-carriers and carriers, the above associations did not remain significant after FDR correction. Despite this, PRSwithAPOE Threshold 10 increased predictability of the associations

by up to 1.0% for ε4 non-carriers and up to 1.4% for ε4 carriers. Refer to Appendix D Table D.14 (ε4 non-carriers) and Table D.15 (ε4 carriers) for more information.

PRSwithoutAPOE:

Whole group stratification by APOE ε4 status highlighted that for APOE ε4 non-carriers, PRSwithoutAPOE Threshold 1 was associated significantly with two ROIs. In chronological order of the significance of associations, these were: L frontal pole, and L hippocampus. For APOE ε4 carriers, PRSwithoutAPOE Threshold 1 was associated significantly with two ROIs as well. These were, in ascending order: L opercular part of the inferior frontal gyrus, and R opercular part of the inferior frontal gyrus. However, for both APOE ε4 non-carriers and carriers, these associations did not survive FDR correction. Despite this, adding PRSwithoutAPOE Threshold 1 to the model increased predictability of the associations by up to 1.0% for ε4 non-carriers and up to 1.2% for ε4 carriers. Refer to Appendix D Table D.16 (ε4 non-carriers) and Table D.17 (ε4 carriers) for further information.

For APOE ε4 non-carriers, PRSwithoutAPOE Threshold 5 was associated significantly with eight ROIs. In ascending order, these were: L frontal pole, L hippocampus, R supramarginal gyrus, R occipital fusiform gyrus, L supramarginal gyrus, R inferior occipital gyrus, R hippocampus, and L superior occipital gyrus. For APOE ε4 carriers, PRSwithoutAPOE Threshold 5 was associated significantly with L opercular part of the inferior frontal gyrus only. However, for both APOE ε4 non-carriers and carriers, these associations did not remain significant after correcting for multiple comparisons. Nonetheless, the addition of PRSwithoutAPOE Threshold 5 increased predictability of the associations by up to 1.5% for ε4 non-carriers and by up to 1.1% for ε4 carriers. Refer to Appendix D Table D.18 (ε4 non-carriers)and Table D.19 (ε4 carriers) for more details.

Moreover, for APOE ε4 non-carriers, PRSwithoutAPOE Threshold 10 was associated significantly with six ROIs. In ascending order, these were: L frontal pole, R supramarginal gyrus, L hippocampus, L supramarginal gyrus, R occipital fusiform gyrus, and L planum temporale. For APOE ε4 carriers, PRSwithoutAPOE Threshold 10 was associated significantly with R hippocampus only. Again, for both APOE ε4 non-carriers and carriers, none of these associations survived corrective methods for multiple comparisons. Of note, adding PRSwithoutAPOE Threshold 10 to the model increased predictability by up 1.3% in ε4 non-carriers and up to 0.9%

in ε4 carriers. Refer to Appendix D Table D.20 (ε4 non-carriers) and Table D.21 (ε4 carriers) for further details.

APOEonlyPRS:

Whole group stratification by APOE ε4 status showed that for APOE ε4 non-carriers, APOEonlyPRS Threshold 1 was associated significantly with six ROIs. In order of the significance of the associations, these were: L putamen, R thalamus proper, R parahippocampal gyrus, R putamen, L pallidum, and L accumbens area. For APOE ε4 carriers, APOEonlyPRS Threshold 1 was associated significantly with seven ROIs. These were, in ascending order: R accumbens area, R superior frontal gyrus, L precentral gyrus, R basal forebrain, L accumbens area, R precentral gyrus, and R anterior insula. For both APOE ε4 non-carriers and carriers, none of these associations remained significant after correcting for multiple comparisons. Overall, APOEonlyPRS Threshold 1 increased predictability of the associations by up to 1.2% for ε4 non-carriers and up to 1.8% for ε4 carriers. Refer to Appendix D Table D.22 (ε4 non-carriers) and Table D.23 (ε4 carriers) for more information.

For APOE ε4 non-carriers, APOEonlyPRS Threshold 5 was associated significantly with four ROIs. In ascending order, these were: L putamen, R thalamus proper, R putamen, and R parahippocampal gyrus. For APOE ε4 carriers, APOEonlyPRS Threshold 5 was associated significantly with 10 ROIs. These were, in ascending order: R accumbens area, R superior frontal gyrus, L precentral gyrus, R basal forebrain, L accumbens area, L posterior insula, R precentral gyrus, R anterior insula, R posterior insula, and R putamen. For both APOE ε4 non-carriers and carriers, the above associations did not survive FDR correction. Adding APOEonlyPRS Threshold 5 to the model increased predictability by up to 1.4% for APOE ε4 non-carriers and up to 1.8% for ε4 carriers. Refer to Appendix D Table D.24 (ε4 non-carriers) and Table D.25 (ε4 carriers) for further information.

Additionally, for APOE ε4 non-carriers, APOEonlyPRS Threshold 10 was associated significantly with five ROIs. In ascending order, these were: R thalamus proper, L putamen, L basal forebrain, R basal forebrain, and R putamen. For APOE ε4 carriers, APOEonlyPRS Threshold 10 was associated significantly with nine ROIs. These were, in ascending order: R accumbens area, R superior frontal gyrus, L precentral gyrus, R basal forebrain, R precentral gyrus, R anterior insula, L accumbens area, R posterior insula, and L posterior insula. Once again, for both APOE ε4 non-carriers and carriers, these associations did not remain significant after FDR correction. Despite

this, the addition of APOEonlyPRS Threshold 10 increased predictability of the associations by up to 1.2% for ε4 non-carriers and by up to 1.9% for ε4 carriers. Refer to Appendix D Table D.26 (ε4 non-carriers) and Table D.27 (ε4 carriers) for more details.

4.3.4.3. (C) Whole group stratified by diagnostic status

PRSwithAPOE:

Whole group stratification by diagnostic status demonstrated that for CU participants, PRSwithAPOE Threshold 1 was associated significantly with 23 ROIs. In ascending order of significance, these were: R hippocampus, R posterior orbital gyrus, L posterior orbital gyrus, R parahippocampal gyrus, R superior parietal lobule, L supplementary motor cortex, R calcarine cortex, R amygdala, R precuneus, L parahippocampal gyrus, L hippocampus, R thalamus proper, R inferior temporal gyrus, L precentral gyrus, L putamen, L amygdala, L orbital part of the inferior frontal gyrus, R fusiform gyrus, R frontal operculum, L thalamus proper, L inferior temporal gyrus, R triangular part of the inferior frontal gyrus, and R middle cingulate gyrus. After correcting for multiple comparisons using FDR, PRSwithAPOE Threshold 1 was associated significantly and negatively with R hippocampus (p = 0.043464052883946) only. Refer to Table 4.13 for details. For MCI patients, PRSwithAPOE Threshold 1 was associated significantly with five ROIs. In ascending order, these were: R subcallosal area, L central operculum, L opercular part of the inferior frontal gyrus, L orbital part of the inferior frontal gyrus, and L posterior orbital gyrus. However, after FDR correction, no ROIs survived. For AD dementia patients, PRSwithAPOE Threshold 1 was associated significantly with six ROIs. These were, in ascending order: L entorhinal area, L amygdala, L hippocampus, R amygdala, R frontal operculum, and L parahippocampal gyrus. However, again, no ROIs survived FDR correction. Interestingly, adding PRSwithAPOE Threshold 1 to the model increased predictability of the associations by up to 4.6% for CU participants, up to 2.5% for MCI patients, and up to 5.7% for AD dementia patients. Refer Appendix D Table D.28 (CU), Table D.29 (MCI), and Table D.30 (AD dementia) for further details.

For CU participants, PRSwithAPOE Threshold 5 was associated significantly with 21 ROIs. In ascending order, these regions were: R hippocampus, R posterior orbital gyrus, L posterior orbital gyrus, R parahippocampal gyrus, R calcarine cortex, R superior parietal lobule, R precuneus, L supplementary motor cortex, R amygdala, R inferior temporal gyrus, L parahippocampal gyrus, R frontal operculum, R thalamus proper, L amygdala, L hippocampus, L precentral gyrus, L orbital part of the inferior frontal gyrus, L putamen, L inferior temporal gyrus, R triangular part of the

inferior frontal gyrus, and L thalamus proper. For MCI patients, PRSwithAPOE Threshold 5 was associated significantly with six ROIs. These were, in ascending order: R subcallosal area, L central operculum, L opercular part of the inferior frontal gyrus, L orbital part of the inferior frontal gyrus, L posterior orbital gyrus, and L triangular part of the inferior frontal gyrus. For AD dementia patients, PRSwithAPOE Threshold 5 was associated significantly with six ROIs. In ascending order, these regions were: L entorhinal area, L amygdala, L hippocampus, R frontal operculum, R amygdala, and L parahippocampal gyrus. However, none of these associations survived corrections for multiple comparisons. Nevertheless, overall, adding PRSwithAPOE Threshold 5 to the model increased predictability by up to 4.4% for CU participants, up to 1.4% for MCI patients, and up to 5.9% for AD dementia patients. Refer to Appendix D Table D.31 (CU), Table D.32 (MCI) and Table D.33 (AD dementia) for more information.

Furthermore, for CU participants, PRSwithAPOE Threshold 10 was associated significantly with 23 ROIs. In order of the strength of the associations, these were: R hippocampus, R parahippocampal gyrus, R frontal operculum, L posterior orbital gyrus, R posterior orbital gyrus, L parahippocampal gyrus, L hippocampus, R calcarine cortex, L amygdala, R amygdala, L orbital part of the inferior frontal gyrus, R superior parietal lobule, L putamen, R triangular part of the inferior frontal gyrus, R precuneus, R thalamus proper, R inferior temporal gyrus, L supplementary motor cortex, R lateral orbital gyrus, L inferior temporal gyrus, R posterior cingulate gyrus, L thalamus proper, and L calcarine cortex. After FDR correction, PRSwithAPOE Threshold 10 was associated significantly and negatively with two ROIs only, these were: R hippocampus (p = 0.029863646323128) and R parahippocampal gyrus (p = 0.048753588842109). See Table 4.13 for more information. For MCI patients, PRSwithAPOE Threshold 10 was associated significantly with six ROIs. These regions were, in ascending order: R subcallosal area, L central operculum, L opercular part of the inferior frontal gyrus, L orbital part of the inferior frontal gyrus, L posterior orbital gyrus, and L frontal operculum. After FDR correction, PRSwithAPOE Threshold 10 was associated significantly and positively with R subcallosal area (p = 0.048156063797526) only. Refer to Table 4.13 for more details. For AD dementia patients, PRSwithAPOE Threshold 10 was associated significantly with seven ROIs. In ascending order, these were: L entorhinal area, L amygdala, R frontal operculum, L hippocampus, L parahippocampal gyrus, R amygdala, and R posterior insula. However, no ROIs survived FDR correction. Nonetheless, adding PRSwithAPOE Threshold 10 to the model increased overall predictability by up to 4.9% for CU participants, up to 1.9% for MCI patients, and up to 4.6% for AD dementia patients. Refer to Appendix D Table D.34 (CU), Table D.35 (MCI) and Table D.36 (AD dementia) for further information.

PRSwithoutAPOE:

Whole group stratification by diagnostic status revealed that for CU participants, PRSwithoutAPOE Threshold 1 was associated significantly with two ROIs and these were: L occipital fusiform gyrus, and R middle temporal gyrus. For MCI patients, PRSwithoutAPOE Threshold 1 was associated significantly with two ROIs also: R hippocampus, and L hippocampus. In comparison, for AD dementia patients, PRSwithoutAPOE Threshold 1 was associated significantly with nine ROIs. In ascending order, these were: R basal forebrain, L subcallosal area, L medial frontal cortex, R subcallosal area, R lateral orbital gyrus, R orbital part of the inferior frontal gyrus, L medial orbital gyrus, R gyrus rectus, and R medial orbital gyrus. However, for all three diagnostic statuses, none of the above-mentioned associations remained significant after correcting for multiple comparisons. Despite this, the addition of PRSwithoutAPOE Threshold 1 improved predictability of the associations by up to 1.6% for CU participants, up to 0.7% for MCI patients, and up to 3.6% for AD dementia patients. Refer to Appendix D Table D.37 (CU), Table D.38 (MCI), and Table D.39 (AD dementia) for more details.

For CU participants, PRSwithoutAPOE Threshold 5 was associated significantly with two ROIs: L occipital fusiform gyrus, and R supramarginal gyrus. For MCI patients, PRSwithoutAPOE Threshold 5 was associated significantly with three ROIs: R hippocampus, followed by L frontal pole, and then L hippocampus. In contrast, for AD dementia patients, PRSwithoutAPOE Threshold 5 was associated significantly with nine ROIs. These were, in ascending order: R basal forebrain, L superior frontal gyrus medial segment, L accumbens area, L subcallosal area, L anterior cingulate gyrus, L medial orbital gyrus, R lateral orbital gyrus, L temporal pole, and R orbital part of the inferior frontal gyrus. However, for all diagnostic statuses, none of these associations survived FDR correction. Interestingly, adding PRSwithoutAPOE Threshold 5 to the model increased overall predictability by up to 1.4% in CU participants, up to 0.7% in MCI patients, and up to 4.6% for AD dementia patients. Refer to Appendix D Table D.40 (CU), Table D.41 (MCI) and Table D.42 (AD dementia) for further details.

Additionally, for CU participants, PRSwithoutAPOE Threshold 10 was associated significantly with two ROIs: R postcentral gyrus, followed by R frontal operculum. For MCI patients, PRSwithoutAPOE Threshold 10 was associated significantly with the R hippocampus only. For AD dementia patients, PRSwithoutAPOE Threshold 10 was associated significantly with three ROIs. In ascending order, these were: R superior parietal lobule, R precuneus, and R basal forebrain. Once again, these associations did not survive FDR corrective measures. Nonetheless, the

addition of PRSwithoutAPOE Threshold 10 increased predictability of the associations by up to 1.9% in CU participants, up to 0.6% in MCI patients, and up to 2.5% in AD dementia patients. Refer to Appendix D Table D.43 (CU), Table D.44 (MCI), and Table D.45 (AD dementia) for more information.

APOEonlyPRS:

Whole group stratification by diagnostic status indicated that for CU participants, APOEonlyPRS Threshold 1 was associated significantly with 30 ROIs. In order of the level of significance of these associations, these were: R hippocampus, R parahippocampal gyrus, L posterior orbital gyrus, R posterior orbital gyrus, R fusiform gyrus, L parahippocampal gyrus, L hippocampus, R calcarine cortex, L orbital part of the inferior frontal gyrus, L putamen, R superior parietal lobule, L fusiform gyrus, R lingual gyrus, R inferior temporal gyrus, R precuneus, L amygdala, L lingual gyrus, L supplementary motor cortex, R anterior orbital gyrus, R amygdala, L postcentral gyrus medial segment, R postcentral gyrus, L thalamus proper, R putamen, L medial orbital gyrus, R frontal operculum, R thalamus proper, R lateral orbital gyrus, L inferior temporal gyrus, and R middle temporal gyrus. After correcting for multiple comparisons using FDR, APOEonlyPRS Threshold 1 was associated significantly and negatively with two ROIs: L posterior orbital gyrus (p = 0.034667769315274), and then R parahippocampal gyrus (p = 0.040092237908388) only. See Table 4.14 for further details. For MCI patients, APOEonlyPRS Threshold 1 was associated significantly with five ROIs. In ascending order, these were: R subcallosal area, L central operculum, L opercular part of the inferior frontal gyrus, L orbital part of the inferior frontal gyrus, and L posterior orbital gyrus. No ROIs survived FDR correction. For AD dementia patients, APOEonlyPRS Threshold 1 was associated significantly with nine ROIs. These were, in ascending order: L entorhinal area, L amygdala, R frontal operculum, R amygdala, L hippocampus, L anterior cingulate gyrus, L parahippocampal gyrus, R subcallosal area, and L triangular part of the inferior frontal gyrus. However, again, no ROIs survived FDR correction. Interestingly, adding APOEonlyPRS Threshold 1 to the model increased predictability by up to 4.5% for CU participants, up to 1.6% for MCI patients, and up to 5.4% for AD dementia patients. Refer to Appendix D Table D.46 (CU), Table D.47 (MCI) and Table D.48 (AD dementia) for further information.

For CU participants, APOEonlyPRS Threshold 5 was associated significantly with 26 ROIs. In ascending order, these regions were: R hippocampus, L posterior orbital gyrus, R parahippocampal gyrus, R posterior orbital gyrus, L parahippocampal gyrus, R calcarine cortex,

L orbital part of the inferior frontal gyrus, L hippocampus, R fusiform gyrus, L putamen, R superior parietal lobule, L fusiform gyrus, R lingual gyrus, R precuneus, L lingual gyrus, L amygdala, R anterior orbital gyrus, R inferior temporal gyrus, R postcentral gyrus, L thalamus proper, R amygdala, L postcentral gyrus medial segment, L supplementary motor cortex, R putamen, L medial orbital gyrus, and R middle temporal gyrus. For MCI patients, APOEonlyPRS Threshold 5 was associated significantly with six ROIs. These were, in ascending order: R subcallosal area, L central operculum, L opercular part of the inferior frontal gyrus, L orbital part of the inferior frontal gyrus, L posterior orbital gyrus, and R middle occipital gyrus. For AD dementia patients, APOEonlyPRS Threshold 5 was associated significantly with nine ROIs. In ascending order, these regions were: L entorhinal area, L amygdala, R frontal operculum, R amygdala, L hippocampus, L anterior cingulate gyrus, R subcallosal area, L parahippocampal gyrus, and L triangular part of the inferior frontal gyrus. However, for all three diagnostic statuses, none of these associations survived corrections for multiple comparisons. Nonetheless, generally, adding APOEonlyPRS Threshold 5 to the model increased predictability of the associations by up to 4.0% for CU participants, up to 2.5% for MCI patients, and up to 5.2% for AD dementia patients. Refer to Appendix D Table D.49 (CU), Table D.50 (MCI), and Table D.51 (AD dementia) for more details.

Additionally, for CU participants, APOEonlyPRS Threshold 10 was associated significantly with 22 ROIs. In ascending order of significance, these were: R hippocampus, R parahippocampal gyrus, L parahippocampal gyrus, R calcarine cortex, L putamen, L posterior orbital gyrus, L hippocampus, L lingual gyrus, R precuneus, R amygdala, R superior parietal lobule, L fusiform gyrus, R fusiform gyrus, R posterior orbital gyrus, R anterior orbital gyrus, R putamen, R thalamus proper, L amygdala, R lingual gyrus, R postcentral gyrus, L supplementary motor cortex, and R inferior temporal gyrus. In comparison, for MCI patients, APOEonlyPRS Threshold 10 was associated with four ROIs. These regions were: R subcallosal area, L opercular part of the inferior frontal gyrus, L central operculum, and then L orbital part of the inferior frontal gyrus. For AD dementia patients, APOEonlyPRS Threshold 10 was associated significantly with nine ROIs. In ascending order, these were: L entorhinal area, L amygdala, R frontal operculum, L hippocampus, R amygdala, L anterior cingulate gyrus, L triangular part of the inferior frontal gyrus, L parahippocampal gyrus, and R subcallosal area. Again, for all diagnostic statuses, no ROIs survived FDR corrective measures. Overall, adding APOEonlyPRS Threshold 10 to the model increased overall predictability by up to 4.1% for CU participants, up to 1.3% for MCI patients, and up to 4.7% for AD dementia patients. Refer to Appendix D Table D.52 (CU), Table D.53 (MCI) and Table D.54 (AD dementia) for all further details.

Table 4.13: Associations between PRSwithAPOE thresholds and ROIs found in CU and MCI participants that survived FDR correction.

	R Square (Model 1)	R Square (Model 2)	R Square Change	Sig. F Change (Model 2)	FDR Corrected value	Standardised beta of PRS
PRSwithAPOE Threshold 1						
CU						
Hippocampus R	0.380	0.426	0.046	0.000381263621789	0.0435	-0.225
PRSwithAPOE Threshold 10						
CU						
Hippocampus R	0.380	0.428	0.049	0.000261961809852	0.0298	-0.233
Parahippocampal gyrus R	0.508	0.540	0.032	0.000855326120037	0.0488	-0.190
MCI						
Subcallosal area R	0.380	0.399	0.019	0.000422421612259	0.0482	0.153

APOE: apolipoprotein E. CU: cognitively unimpaired. FDR: false discovery rate. MCI: mild cognitive impairment. PRS: polygenic risk score. R: right.

Table 4.14: Associations between APOEonlyPRS thresholds and ROIs found in CU participants that survived FDR correction.

	R Square (Model 1)	R Square (Model 2)	R Square Change	Sig. F Change (Model 2)	FDR Corrected value	Standardised beta of PRS
APOEonlyPRS Threshold 1						
CU						
Parahippocampal gyrus R	0.508	0.541	0.033	0.000703372594884	0.0401	-0.189
Posterior orbital gyrus L	0.382	0.422	0.040	0.000912309718823	0.0347	-0.208

APOE: apolipoprotein E. CU: cognitively unimpaired. FDR: false discovery rate. L: left. PRS: polygenic risk score. R: right.

4.3.4.4. (D) Whole group stratified by amyloid status

PRSwithAPOE:

Whole group stratification by amyloid status highlighted that for amyloid negative participants, PRSwithAPOE Threshold 1 was associated significantly with L frontal operculum only. However, this did not survive FDR corrective measures. In comparison, for amyloid positive participants, PRSwithAPOE Threshold 1 was associated significantly with 20 ROIs. In chronological order of significance, these regions were: R hippocampus, R amygdala, L hippocampus, R middle occipital gyrus, L amygdala, L entorhinal area, R entorhinal area, R parahippocampal gyrus, R middle temporal gyrus, R inferior occipital gyrus, R posterior cingulate gyrus, L parahippocampal gyrus, R anterior orbital gyrus, L inferior temporal gyrus, R temporal pole, L cuneus, R cuneus, R fusiform gyrus, L postcentral gyrus medial segment, and R inferior temporal gyrus. After correcting for multiple comparisons, PRSwithAPOE Threshold 1 remained to be associated significantly and negatively with seven ROIs. In ascending order, these were: R hippocampus (p = 0.000295485967722), L hippocampus (p = 0.00161943751137), R amygdala (p = 0.002147297916333), R middle occipital gyrus (p = 0.010572238320048), L amygdala (p = 0.0107807111348304), R entorhinal area (p = 0.0454208571428571), and L entorhinal area (p = 0.049723). See Table 4.15 for further information. Of note, PRSwithAPOE Threshold 1 increased overall predictability by up to 1.2% for amyloid negative participants and up to 2.7% for amyloid positive participants. Refer to Appendix D Table D.55 (amyloid negative) and Table D.56 (amyloid positive) for more information.

For amyloid negative participants, PRSwithAPOE Threshold 5 was associated significantly with R subcallosal area only. However, this did not survive FDR correction. On the contrary, for amyloid positive participants, PRSwithAPOE Threshold 5 was associated significantly with 16 ROIs. These were, in ascending order: R hippocampus, L hippocampus, R amygdala, L amygdala, R middle occipital gyrus, L entorhinal area, R entorhinal area, R parahippocampal gyrus, R middle temporal gyrus, L parahippocampal gyrus, L inferior temporal gyrus, R posterior cingulate gyrus, R temporal pole, R inferior occipital gyrus, L postcentral gyrus medial segment, and L middle temporal gyrus. However, after FDR correction, PRSwithAPOE Threshold 5 was associated significantly and negatively with seven ROIs only. In ascending order, these were: R hippocampus (p = 0.000167255473008), L hippocampus (p = 0.000939623794632), R amygdala (p = 0.001073440140348), L amygdala (p = 0.0073985139990555), R middle occipital gyrus (p = 0.016301006479626), L entorhinal area (p = 0.038), and R entorhinal area (p = 0.0488571428571429). See Table 4.15 for more information. Additionally, adding PRSwithAPOE

Threshold 5 to the model increased predictability by up to 1.0% in amyloid negative participants and up to 2.8% in amyloid positive participants. Refer to Appendix D Table D.57 (amyloid negative) and Table D.58 (amyloid positive) for further information.

Moreover, for amyloid negative participants, PRSwithAPOE Threshold 10 was associated significantly with two ROIs: L occipital pole, followed by R cuneus. However, neither survived FDR correction. For amyloid positive participants, PRSwithAPOE Threshold 10 was associated significantly with 12 ROIs. In ascending order, these were: R hippocampus, L hippocampus, R amygdala, L amygdala, L entorhinal area, R middle occipital gyrus, R entorhinal area, R parahippocampal gyrus, L parahippocampal gyrus, R temporal pole, R middle temporal gyrus, and L inferior temporal gyrus. After correcting for multiple comparisons, PRSwithAPOE Threshold 10 remained to be associated significantly and negatively with four ROIs: R hippocampus (p = 0.00012458515023), L hippocampus (p = 0.001276444398489), R amygdala (p = 0.003422779000762), followed by L amygdala (p = 0.0194206838629455). See Table 4.15 for additional information. Overall, PRSwithAPOE Threshold 10 increased predictability of the associations by up to 1.5% in amyloid negative participants and by up to 2.9% in amyloid positive participants. Refer to Appendix D Table D.59 (amyloid negative) and Table D.60 (amyloid positive) for more details.

PRSwithoutAPOE:

Whole group stratification by amyloid status showed that for amyloid negative participants, PRSwithoutAPOE Threshold 1 was associated significantly with two ROIs: L thalamus proper, and R hippocampus. For amyloid positive participants, PRSwithoutAPOE Threshold 1 was associated significantly with three ROIs: R caudate, L caudate, and then R frontal pole. However, for both amyloid negative and amyloid positive participants, these associations did not remain significant after correcting for multiple comparisons. Despite this, adding PRSwithoutAPOE Threshold 1 to the model increased overall predictability by up to 1.5% amyloid negative participants and by up to 1.0% in amyloid positive participants. Refer to Appendix D Table D.61 (amyloid negative) and Table D.62 (amyloid positive) for further details.

For amyloid negative participants, PRSwithoutAPOE Threshold 5 was associated significantly with three ROIs. In order of the level of significance, these regions were: R hippocampus, L hippocampus, and R amygdala. For amyloid positive participants, PRSwithoutAPOE Threshold 5 was associated significantly with six ROIs. In ascending order, these were: L frontal pole, R frontal

pole, R caudate, R superior occipital gyrus, L fusiform gyrus, and R supramarginal gyrus. Again, for both amyloid negative and amyloid positive participants, none of these associations remained significant after FDR correction. However, the addition of PRSwithoutAPOE Threshold 5 increased predictability by up to 1.4% in amyloid negative individuals and by up to 0.9% in amyloid positive individuals. Refer to Appendix D Table D.63 (amyloid negative) and Table D.64 (amyloid positive) for more information.

Additionally, for amyloid negative participants, PRSwithoutAPOE Threshold 10 was associated significantly with eight ROIs. These were, in ascending order: L hippocampus, L basal forebrain, L planum polare, L amygdala, R amygdala, R hippocampus, R posterior orbital gyrus, and R basal forebrain. However, none of these associations remained significant after correcting for multiple comparisons. For amyloid positive participants, PRSwithoutAPOE Threshold 10 was associated significantly with five ROIs. In ascending order, these were: L frontal pole, R frontal pole, R supramarginal gyrus, R inferior occipital gyrus, and R middle cingulate gyrus. After FDR correction, PRSwithAPOE Threshold 10 was associated significantly and positively with L frontal pole (p = 0.036082899815586) only. See Table 4.16 for more details. Overall, adding PRSwithoutAPOE Threshold 10 to the model increased predictability of the associations by up to 2.2% in amyloid negative participants and by up to 1.5% in amyloid positive participants. Refer to Appendix D Table D.65 (amyloid negative) and Table D.66 (amyloid positive) for further information.

APOEonlyPRS:

Whole group stratification by amyloid status demonstrated that for amyloid negative participants, APOEonlyPRS Threshold 1 was not associated with any ROIs. In contrast, for amyloid positive participants, APOEonlyPRS Threshold 1 was associated significantly with 21 ROIs. In ascending order of significance, these were: R hippocampus, R amygdala, R middle occipital gyrus, L hippocampus, L amygdala, R entorhinal area, L entorhinal area, R parahippocampal gyrus, R inferior occipital gyrus, L cuneus, L parahippocampal gyrus, R anterior orbital gyrus, R middle temporal gyrus, L postcentral gyrus medial segment, R temporal pole, R fusiform gyrus, R posterior cingulate gyrus, R cuneus, R inferior temporal gyrus, R occipital fusiform gyrus, L middle occipital gyrus, and L inferior temporal gyrus. However, after correcting for multiple comparisons, APOEonlyPRS was associated significantly and negatively with six ROIs only. In ascending order, these were: R hippocampus (p = 0.000948664103274), R amygdala (p = 0.00144519432879), L hippocampus (p =0.0041949890536305), R middle occipital gyrus (p = 0.004473817029838), L

amygdala (p = 0.0167152844259936), and L entorhinal area (p = 0.0478637142857143). See Table 4.17 for additional information. Generally, adding APOEonlyPRS Threshold 1 to the model increased predictability by up to 1.1% for amyloid negative participants and by up to 2.4% for amyloid positive participants. Refer to Appendix D Table D.67 (amyloid negative) and Table D.68 (amyloid positive) for more details.

For amyloid negative participants, APOEonlyPRS Threshold 5 was not associated with any ROIs. On the other hand, for amyloid positive participants, APOEonlyPRS Threshold 5 was associated significantly with 21 ROIs. In ascending order of significance, these were: R hippocampus, R amygdala, R middle occipital gyrus, L hippocampus, L amygdala, R entorhinal area, L entorhinal area, R parahippocampal gyrus, R inferior occipital gyrus, L parahippocampal gyrus, R middle temporal gyrus, L cuneus, R anterior orbital gyrus, L postcentral gyrus medial segment, R fusiform gyrus, R posterior cingulate gyrus, R temporal pole, R cuneus, R inferior temporal gyrus, L middle occipital gyrus, and L inferior temporal gyrus. However, after FDR corrective measures, APOEonlyPRS Threshold 5 was associated significantly and negatively with five ROIs only: R hippocampus (p = 0.001005023794344), R amygdala (p = 0.00141291473745), R middle occipital gyrus (p = 0.004593284591172), L hippocampus (p = 0.0049616370728805), and then L amygdala (p = 0.0212922357304128). See Table 4.17 for more information. Overall, adding APOEonlyPRS Threshold 5 to the model increased predictability by up to 1.1% for amyloid negative participants and by up to 2.4% for amyloid positive participants. Refer to Appendix D Table D.69 (amyloid negative) and Table D.70 (amyloid positive) for further details.

Furthermore, for amyloid negative participants, APOEonlyPRS Threshold 10 was associated significantly with eight ROIs. In ascending order, these were: L opercular part of the inferior frontal gyrus, L frontal operculum, L lateral orbital gyrus, L occipital pole, L transverse temporal gyrus, R opercular part of the inferior frontal gyrus, R lingual gyrus, and R subcallosal area. However, these ROIs did not survive FDR-corrective measures. For amyloid positive participants, APOEonlyPRS Threshold 10 was associated significantly with 19 ROIs. In ascending order of significance, these were: R hippocampus, R amygdala, R middle occipital gyrus, L hippocampus, L amygdala, L entorhinal area, R entorhinal area, R inferior occipital gyrus, R parahippocampal gyrus, L parahippocampal gyrus, L cuneus, L postcentral gyrus medial segment, R anterior orbital gyrus, R middle temporal gyrus, R fusiform gyrus, R posterior cingulate gyrus, L inferior temporal gyrus, L middle occipital gyrus, and L fusiform gyrus. After correcting for multiple comparisons, APOEonlyPRS Threshold 10 was associated significantly and negatively with five ROIs only: R

hippocampus (p = 0.001779452841642), R amygdala (p = 0.003777790296237), L hippocampus (p = 0.005982226219089), R middle occipital gyrus (p = 0.00673688018223), followed by L amygdala (p = 0.0228). See Table 4.17 for more details. The addition of APOEonlyPRS Threshold 10 improved predictability of the associations by up to 1.6% for amyloid negative participants and by up to 2.3% for amyloid positive participants. Refer to Appendix D Table D.71 (amyloid negative) and Table D.72 (amyloid positive) for more information.

Table 4.15: Associations between PRSwithAPOE thresholds and ROIs found in amyloid positive participants that survived FDR correction.

	R Square (Model 1)	R Square (Model 2)	R Square Change	Sig. F Change (Model 2)	FDR Corrected value	Standardised beta of PRS
PRSwithAPOE Threshold 1						
Amygdala L	0.383	0.400	0.017	0.000472838207668	0.0108	-0.137
Amygdala R	0.444	0.465	0.021	0.000037671893269	0.0021	-0.153
Entorhinal area L	0.397	0.409	0.012	0.002617	0.0497	-0.117
Entorhinal area R	0.452	0.463	0.011	0.002789	0.0454	-0.110
Hippocampus L	0.422	0.443	0.021	0.000042616776615	0.0016	-0.155
Hippocampus R	0.442	0.469	0.027	0.000002591982173	0.0003	-0.174
Middle occipital gyrus R	0.354	0.372	0.018	0.000370955730528	0.0106	-0.142
PRSwithAPOE Threshold 5						
Amygdala L	0.383	0.401	0.018	0.000259596982423	0.0074	-0.143
Amygdala R	0.444	0.466	0.021	0.000028248424746	0.0011	-0.155
Entorhinal area L	0.397	0.410	0.013	0.002	0.0380	-0.122
Entorhinal area R	0.452	0.463	0.010	0.003	0.0489	-0.109
Hippocampus L	0.422	0.445	0.023	0.000016484627976	0.0009	-0.163
Hippocampus R	0.442	0.470	0.028	0.000001467153272	0.0002	-0.178
Middle occipital gyrus R	0.354	0.370	0.016	0.000714956424545	0.0163	-0.136
PRSwithAPOE Threshold 10						
Amygdala L	0.383	0.399	0.016	0.000681427503963	0.0194	-0.134
Amygdala R	0.444	0.463	0.019	0.000090073131599	0.0034	-0.146
Hippocampus L	0.422	0.445	0.023	0.000022393761377	0.0013	-0.161
Hippocampus R	0.442	0.471	0.029	0.000001092852195	0.0001	-0.181

APOE: apolipoprotein E. FDR: false discovery rate. L: left. PRS: polygenic risk score. R: right.

Table 4.16: Associations between PRSwithoutAPOE and ROIs found in amyloid positive participants that survived FDR correction.

	R Square (Model 1)	R Square (Model 2)	R Square Change	Sig. F Change (Model 2)	FDR Corrected value	Standardised beta of PRS
PRSwithoutAPOE Threshold 10						
Frontal pole L	0.469	0.484	0.015	0.000316516665049	0.0361	0.131

APOE: apolipoprotein E. FDR: false discovery rate. L: left. PRS: polygenic risk score.

Table 4.17: Associations between APOEonlyPRS thresholds and ROIs found in amyloid positive participants that survived FDR correction.

	R Square (Model 1)	R Square (Model 2)	R Square Change	Sig. F Change (Model 2)	FDR Corrected value	Standardised beta of PRS
APOEonlyPRS Threshold 1						
Amygdala L	0.383	0.399	0.016	0.000733126509912	0.0167	-0.132
Amygdala R	0.444	0.466	0.022	0.00002535428647	0.0014	-0.156
Entorhinal area L	0.397	0.409	0.012	0.002939	0.0479	-0.115
Hippocampus L	0.422	0.440	0.018	0.000147192598373	0.0042	-0.144
Hippocampus R	0.442	0.467	0.024	0.000008321614941	0.0009	-0.165
Middle occipital gyrus R	0.354	0.375	0.021	0.000117732027101	0.0045	-0.154
APOEonlyPRS Threshold 5						
Amygdala L	0.383	0.398	0.015	0.000933869988176	0.0213	-0.130
Amygdala R	0.444	0.466	0.022	0.00002478797785	0.0014	-0.156
Hippocampus L	0.422	0.440	0.018	0.000174092528873	0.0050	-0.142
Hippocampus R	0.442	0.466	0.024	0.000008815998196	0.0010	-0.165
Middle occipital gyrus R	0.354	0.375	0.021	0.000120875910294	0.0046	-0.154
APOEonlyPRS Threshold 10						
Amygdala L	0.383	0.397	0.014	0.001	0.0228	-0.126
Amygdala R	0.444	0.464	0.019	0.000066277022741	0.0038	-0.148
Hippocampus L	0.422	0.439	0.017	0.000209902674354	0.0060	-0.140
Hippocampus R	0.442	0.465	0.023	0.000015609235453	0.0018	-0.160
Middle occipital gyrus R	0.354	0.374	0.020	0.000177286320585	0.0067	-0.150

APOE: apolipoprotein E. FDR: false discovery rate. L: left. PRS: polygenic risk score. R: right.

4.4. DISCUSSION

Associations between PRS for AD and cross-sectional grey matter volumes of 114 regions were investigated in 738 participants from ADNI. These associations were investigated using three PRSs (i.e., PRSwithAPOE, PRSwithoutAPOE, and APOEonlyPRS) at three thresholds each (i.e., Threshold 1: $p = 5 \times 10^{-8}$, Threshold 5: $p < 0.001$, and Threshold 10 $p < 1$). First, the participant cohort was studied as a whole group, controlled by MMSE score among other variables. Then, the whole group was stratified by APOE ε4 status, followed by diagnostic status, and then the whole group was stratified by amyloid status. All hypotheses can be accepted partly.

For whole group analysis using PRSwithAPOE, Threshold 1 was associated negatively with grey matter volume in five regions – R hippocampus, R amygdala, L hippocampus, L amygdala, and R middle occipital gyrus (in ascending order); Threshold 5 was associated negatively with grey matter volume in four regions – R hippocampus, R amygdala, L hippocampus, and L amygdala; Threshold 10 was associated negatively with grey matter volume in four regions – R hippocampus, L hippocampus, R amygdala, and L amygdala. For whole group analysis using APOEonlyPRS, Threshold 1 was associated negatively with R hippocampus, R amygdala, L hippocampus, L amygdala, and R middle occipital gyrus (in ascending order); Threshold 5 was associated negatively with R hippocampus, R amygdala, L hippocampus, R middle occipital gyrus, and L amygdala; Threshold 10 was associated negatively with R hippocampus, R amygdala, L hippocampus, L amygdala, and R middle occipital gyrus. Therefore, high PRS was associated with increased grey matter loss in these regions. The level of significance of these associations was greater when PRSwithAPOE thresholds were used, in comparison to when APOEonlyPRS thresholds. This highlights the superiority of non-APOE SNPs in identifying associations with grey matter volume. No other associations were able to withstand corrections for multiple comparisons, and PRSwithoutAPOE thresholds were not associated with any ROIs.

When the whole group was stratified by APOE ε4 status, i.e., APOE ε4 non-carriers vs. carriers, associations found using PRSwithAPOE, PRSwithoutAPOE, and APOEonlyPRS did not survive FDR corrective measures.

When the whole group was stratified by diagnostic status, PRSwithAPOE Threshold 1 was associated negatively with grey matter volume of the R hippocampus in CU participants; PRSwithAPOE Threshold 10 was associated negatively with grey matter volume of the R hippocampus and R parahippocampal gyrus in CU participants and was associated positively

with the R subcallosal area in MCI patients. In comparison, APOEonlyPRS Threshold 1 was associated negatively with grey matter volume of the L posterior orbital gyrus and the R parahippocampal gyrus in CU participants. No other associations survived corrections for multiple comparisons, and PRSwithoutAPOE thresholds were not associated with any regions.

When the whole group was stratified by amyloid status, i.e., amyloid negative vs. amyloid positive, associations between PRS and regional grey matter volume were found in amyloid positive participants only. When using PRSwithAPOE, Threshold 1 was associated negatively with grey matter volume in seven regions – R hippocampus, L hippocampus, R amygdala, R middle occipital gyrus, L amygdala, R entorhinal area, and L entorhinal area (in ascending order); Threshold 5 was associated negatively with grey matter volume in the same seven regions but in a different order – R hippocampus, L hippocampus, R amygdala, L amygdala, R middle occipital gyrus, L entorhinal area, and R entorhinal area; Threshold 10 was associated negatively with four regions – R hippocampus, L hippocampus, R amygdala, and L amygdala. When using PRSwithoutAPOE, Threshold 10 was associated positively with grey matter volume of the L frontal pole only. Additionally, when APOEonlyPRS was used, Threshold 1 was associated negatively with grey matter volume in six regions – R hippocampus, R amygdala, L hippocampus, R middle occipital gyrus, L amygdala, and L entorhinal area (in ascending order); Threshold 5 was associated negatively with grey matter volume in five regions – R hippocampus, R amygdala, R middle occipital gyrus, L hippocampus, and L amygdala; Threshold 10 was associated negatively with grey matter volume in the same five regions, although in a different order of significance – R hippocampus, R amygdala, L hippocampus, R middle occipital gyrus, and L amygdala. Generally, high PRS was associated with increased regional grey matter loss and the level of significance of these associations was greater when PRSwithAPOE thresholds were used and therefore indicating the importance of non-APOE SNPs in risk prediction. No other associations remained after correcting for multiple comparisons. Generally, these associations reflect the effect of PRSwithAPOE and APOEonlyPRS on grey matter volume of global MTL structures related to early AD pathology.

Although in some cases, the addition of PRSs to the models did not improve predictability, in most cases, PRSs increased predictability of the associations between PRSs and regional grey matter volume in various between-group comparisons, as follows:

Whole group PRSwithAPOE:

Up to 1.9% (Threshold 1); up to 2.1% (Threshold 5); up to 2.1% (Threshold 10).

Whole group PRSwithoutAPOE:

Up to 0.4% (Threshold 1); up to 0.6% (Threshold 5); up to 0.8% (Threshold 10).

Whole group APOEonlyPRS:

Up to 1.3% (Threshold 1); up to 1.2% (Threshold 5); up to 1.2% (Threshold 10).

APOE ε4 non-carriers PRSwithAPOE:

Up to 1.4% (Threshold 1); up to 1.4% (Threshold 5); up to 1.0% (Threshold 10).

APOE ε4 non-carriers PRSwithoutAPOE:

Up to 1.0% (Threshold 1); up to 1.5% (Threshold 5); up to 1.3% (Threshold 10).

APOE ε4 non-carriers APOEonlyPRS:

Up to 1.2% (Threshold 1); up to 1.4% (Threshold 5); up to 1.2% (Threshold 10).

APOE ε4 carriers PRSwithAPOE:

Up to 1.3% (Threshold 1); up to 1.2% (Threshold 5); up to 1.4% (Threshold 10).

APOE ε4 carriers PRSwithoutAPOE:

Up to 1.2% (Threshold 1); up to 1.1% (Threshold 5); up to 0.9% (Threshold 10).

APOE ε4 carriers APOEonlyPRS:

Up to 1.8% (Threshold 1); up to 1.8% (Threshold 5); up to 1.9% (Threshold 10).

CU PRSwithAPOE:

Up to 4.6% (Threshold 1); up to 4.4% (Threshold 5); up to 4.9% (Threshold 10).

CU PRSwithoutAPOE:

Up to 1.6% (Threshold 1); up to 1.4% (Threshold 5); up to 1.9% (Threshold 10).

CU APOEonlyPRS:

Up to 4.5% (Threshold 1); up to 4.0% (Threshold 5); up to 4.1% (Threshold 10).

MCI PRSwithAPOE:

Up to 2.5% (Threshold 1); up to 1.4% (Threshold 5); up to 1.9% (Threshold 10).

MCI PRSwithoutAPOE:

Up to 0.7% (Threshold 1); up to 0.7% (Threshold 5); up to 0.6% (Threshold 10).

MCI APOEonlyPRS:

Up to 1.6% (Threshold 1); up to 2.5% (Threshold 5); up to 1.3% (Threshold 10).

AD PRSwithAPOE:

Up to 5.7% (Threshold 1); up to 5.9% (Threshold 5); up to 4.6% (Threshold 10).

AD PRSwithoutAPOE:

Up to 3.6% (Threshold 1); up to 4.6% (Threshold 5); up to 2.5% (Threshold 10).

AD APOEonlyPRS:

Up to 5.4% (Threshold 1); up to 5.2% (Threshold 5); up to 4.7% (Threshold 10).

Amyloid negative PRSwithAPOE:

Up to 1.2% (Threshold 1); up to 1.0% (Threshold 5); up to 1.5% (Threshold 10).

Amyloid negative PRSwithoutAPOE:

Up to 1.5% (Threshold 1); up to 1.4% (Threshold 5); up to 2.2% (Threshold 10).

Amyloid negative APOEonlyPRS:

Up to 1.1% (Threshold 1); up to 1.1% (Threshold 5); up to 1.6% (Threshold 10).

Amyloid positive PRSwithAPOE:

Up to 2.7% (Threshold 1); up to 2.8% (Threshold 5); up to 2.9% (Threshold 10).

Amyloid positive PRSwithoutAPOE:

Up to 1.0% (Threshold 1); up to 0.9% (Threshold 5); up to 1.5% (Threshold 10).

Amyloid positive APOEonlyPRS:

Up to 2.4% (Threshold 1); up to 2.4% (Threshold 5); up to 2.3% (Threshold 10).

Overall, associations between PRS and hippocampal grey matter volume were present. This was irrespective of whether PRSwithAPOE thresholds or APOEonlyPRS thresholds were used, and regardless of whether the cohort was investigated as a whole group or whether the whole group was stratified according to diagnostic status or amyloid status. In the whole group, and in amyloid positive participants alone, PRSwithAPOE and APOEonlyPRS were both associated with the bilateral hippocampus. However, when the whole group was stratified by diagnostic status, PRSwithAPOE was associated with the R hippocampus only, rather than the bilateral hippocampus. Additionally, regardless of whether PRSwithAPOE or APOEonlyPRS thresholds were used, associations with the bilateral amygdala appeared constantly in the whole group and in amyloid positive participants. Importantly, PRSwithAPOE and APOEonlyPRS thresholds were associated with R hippocampus more than L hippocampus and were associated with R amygdala more than L amygdala. Clearly, hemispheric asymmetry was evident in these participants.

Other regions that were observed to be associated significantly with PRSs, although occasionally, were R entorhinal area (in amyloid positive participants using PRSwithAPOE Threshold 1 and 5), L entorhinal area (amyloid positive PRSwithAPOE Threshold 1; amyloid positive APOEonlyPRS

Threshold 1), and R parahippocampal gyrus (in CU participants using APOEonlyPRS Threshold 1; CU PRSwithAPOE Threshold 10) that are within the MTL, as well as the R middle occipital gyrus (in the whole group using PRSwithAPOE Threshold 1; whole group APOEonlyPRS Threshold 1, 5, and 10; amyloid positive PRSwithAPOE Threshold 1 and 10; amyloid positive APOEonlyPRS Threshold 1, 5, and 10). In one instance each, the L posterior orbital gyrus (CU APOEonlyPRS Threshold 1), R subcallosal area (MCI PRSwithAPOE Threshold 10), and L frontal pole (amyloid positive PRSwithoutAPOE Threshold 10) also appeared.

The addition of PRS increased predictability of the associations across the various comparisons, ranging from a maximum of 1.2% to 5.7% for PRSwithAPOE Threshold 1, 0.4% to 3.6% for PRSwithoutAPOE Threshold 1 and 1.1% to 5.4% for APOEonlyPRS Threshold 1, between a maximum of 1.0% to 5.9% for PRSwithAPOE Threshold 5, 0.6% to 4.6% for PRSwithoutAPOE Threshold 5 and 1.1% to 5.2% for APOEonlyPRS Threshold 5, and ranging from a maximum of 1.0% to 4.9% for PRSwithAPOE Threshold 10, 0.6% to 2.5% for PRSwithoutAPOE Threshold 10 and 1.2% to 4.7% for APOEonlyPRS Threshold 10.

4.4.1 Interpretation

Grey matter volume and other neuroanatomical measures are highly heritable. Therefore, these measures are appropriate for studying genetic imaging analysis, both regionally and globally (Foley et al., 2017; Winkler et al., 2009). Complementary to the research reviewed in Chapter 2 (Systematic Review), in the current research, PRSwithAPOE and APOEonlyPRS thresholds were associated negatively with grey matter volume in the hippocampus consistently. This was evident across the bilateral hippocampus, R more than L. Similarly, a meta-analysis showed bilateral hippocampal atrophy in MCI and AD patients (Shi et al., 2009). In healthy ageing women, i.e., the sex that is most at risk of AD, APOE ε4 carriers showed greater hippocampal volume loss over a two-year period than ε4 non-carriers (Cohen et al., 2001). Shi et al. (2009) found specifically that the R hippocampus was subjected to atrophy more than the L hippocampus across all diagnostic statuses, although to different extents. Additionally, in healthy ageing participants that were APOE ε4 carriers, a smaller bilateral hippocampal area was apparent when compared with ε4 non-carriers, and the R hippocampal area was significantly smaller (Tohgi et al., 1997). This may provide an additional reason to explain asymmetry in hippocampal volume, greater volume loss in R hippocampus, and increased associations with PRSs. Likewise, Lind et al. (2006) showed greater volume loss in the R hippocampus of APOE ε4 carriers than in non-carriers, again in

healthy ageing adults. They also found that APOE ε4 carriers had substantially higher false-alarm rates in a recognition-memory task than ε4 non-carriers and that these rates correlated significantly with R hippocampal volume. Therefore, asymmetry in hippocampal deterioration, (i.e., increased volume loss in R hippocampus), may be a structural biomarker that indicates the onset of the AD continuum, and increased associations between this region and PRSwithAPOE/APOEonlyPRS may highlight a genetic biomarker. To this extent, Foley et al. (2017) demonstrated that genetic risk for AD was accelerated by neuroanatomical alterations, mainly hippocampal changes. Boutet et al. (2014) indicated that hippocampal atrophy was not only present at the global hippocampal level, but it was observable at subregional and cellular levels as well. The researchers found bilateral volume loss in the stratum radiatum, stratum, and stratum moleculare of the cornu ammonis, and stratum pyramidal of the subiculum. Again, these studies indicate that hippocampal volumetric changes are a key biomarker for detecting AD risk early, and that findings from the current research are in line with previous work.

Furthermore, PRSwithAPOE and APOEonlyPRS thresholds were associated negatively with the amygdala. This association was evident across the bilateral amygdala, and more so in the R amygdala. This hemispheric preference was seen with R hippocampal volume too. Previous studies have shown the association between polygenic scores and both the hippocampus and amygdala (Murray, Chandler, and Lancaster, 2021). Lehtovirta et al., (1995) showed that AD patients that were APOE ε4 homozygotes had smaller hippocampus and amygdala volumes than ε3ε4 carriers and ε4 non-carriers, particularly the R hippocampus and R amygdala. Lupton et al. (2016) found that APOE ε4 alone was associated with reduced hippocampal and amygdala volume, in MCI and AD patients. Again, findings from the current research are representative of previous literature since PRSs that included SNPs from the entire APOE region were associated with both the hippocampus and amygdala.

Additionally, the hemispheric asymmetry found in the current research (R > L) provides evidence in support of the Right Hemi-Ageing model. This model suggests that the R hemisphere is subjected to greater age-related cognitive decline that the L (Dolcos, Rice, and Cabeza, 2002). Although the results do not support the Hemispheric Asymmetry Reduction in Older Adults model that proposes reduced lateralisation of the prefrontal cortex, the findings from the current research may indicate that reduced lateralisation due to changes in neural mechanisms, or compensatory changes in cognition, impact the R hemisphere to a greater extent (Cabeza et al., 2002; Mizrak et al., 2024).

Interestingly, the ongoing debate about a third protein, in addition to amyloid and tau, that may contribute to AD neurodegeneration, may also partially explain why PRSwithAPOE and APOEonlyPRS were associated with bilateral amygdala. The TAR DNA-binding protein 43 (TDP-43) found in frontotemporal dementia and amyotrophic lateral sclerosis, seems to spread in the AD brain as well and in a specific pattern (Josephs et al., 2017). Josephs et al. (2016) reported that TDP-43 is found first in the amygdala (stage 1), and then spreads to the entorhinal cortex and the subiculum (stage 2), the dentate gyrus in the hippocampus, and the occipito-temporal cortex (stage 3), then the insular cortex, ventral striatum, basal forebrain, and inferior temporal cortex (stage 4), followed by the substantia nigra, inferior olive, and midbrain tectum (stage 5) before spreading to the basal ganglia and middle frontal lobe (stage 6). Although the propagation of TDP-43 is similar to the NFT staging described by Braak and Braak (1991), the involvement of the amygdala differs. For instance, in Braak and Braak (1991) staging, early on in AD, NFTs are found in the amygdala minimally. Comparatively, in TDP-43 staging, the protein is deposited moderately-to-severely earlier on. Additionally, the presence of APOE ε4 may increase risk of TDP-43 pathology in AD (Yamazaki et al., 2019) both independently, and mediated by, amyloid and tau pathology in the brains of AD patients (Wennberg et al., 2018).

Moreover, Braak and Braak (1991) highlighted that amyloid plaques are deposited in the basal sections of the isocortex, particularly in the frontal, temporal, and occipital lobes. Higher levels of tau are deposited in the entorhinal cortex before such amounts are found in the hippocampus (Braak and Braak, 1991). Anatomical and histological studies of the AD brain have indicated that neurodegeneration occurs in the second layer of the entorhinal cortex and then propagates into the hippocampus, temporal cortex, frontoparietal cortex, and subcortical nuclei (Rao et al., 2022).

Therefore, the explanations relating to amyloid, tau, and TDP-43 provide reasons to support the associations found between PRSwithAPOE and APOEonlyPRS with regions that are characteristic of AD, i.e., hippocampus and entorhinal area, and regions within close proximity, i.e., amygdala, and parahippocampal gyrus. The propagation of these three proteins may also explain why associations were found with atypical regions, i.e., middle occipital gyrus, frontal pole, subcallosal area, and posterior orbital gyrus. These findings also reflect the usefulness of PRSs in identifying other regions that are vulnerable to change in the participant sample used for the current research.

Notably, the PRSwithAPOE and PRSwithoutAPOE were constructed using many genes, thousands of SNPs, and therefore involving several biological pathways (Lancaster et al., 2019). It is unlikely that the biological pathways that underlie all the genes are known. Thus, it would not be correct to merely presume that these associations are all due to the amyloid, tau, or TDP-43 pathways as several biological and genetic pathways have been tested.

4.4.2. Limitations and Strengths

Although the current research used a large participant pool, participants that fulfil certain characteristics or biomarkers were limited. For instance, participants were divided into ε4 non-carriers vs. carriers rather than according to the six APOE genotypes, and a separate analysis on minority racial groups was not possible due to insufficient sample sizes. However, this is an ongoing issue in research that cannot be resolved immediately due to limited availability of data in races different from white. Additionally, it was not feasible to list all the genes that were linked to the SNPs used in the polygenic scores. This was because many of the SNPs are not associated consistently with the same genes as they exist on "cut-off" regions or are found in non-coding regions (Freedman et al., 2011).

On the contrary, the current research was completed successfully and in line with the stated objectives. Polygenic scores were constructed in a methodical manner and stated clearly whether APOE SNPs were included; this was in an attempt to reduce ambiguity and increase reliable interpretation of findings. The current research mentioned whether APOE SNPs affect PRSs, and whether associations with grey matter volumes were present. Further, in comparison with previous literature, a high number of regions were examined (114 ROIs). Also, participants were stratified in many ways and various statistical models were devised to make comparisons. These models were controlled for appropriate covariates, including the use of total intracranial volume to control for individual differences in brain size, that is reported to be a sound measure (Shi et al., 2009). Most importantly, the current research highlighted that associations between PRSs and grey matter volume in AD-vulnerable regions are present. It demonstrated that stratification by amyloid status improved identification of associations between PRSs and regional grey matter volume in comparison to stratification by diagnostic status. The latter relies heavily upon the expertise of clinicians. Previous work has highlighted poor diagnostic accuracy of AD in those that are ε4 non-carriers and that *post-mortem* follow-ups have shown diagnostic inaccuracies of up to 25% of cases (Escott-Price et al., 2018).

4.4.3. Future Directions

It would be useful to examine whether associations between PRSs and fluid biomarkers, as well as cognitive markers, can be identified. A clinical diagnosis of MCI and AD dementia may incorporate findings from MRI, fluid biomarkers, and cognitive assessments. However, due to the aforementioned diagnostic inaccuracies, it would be beneficial to see whether PRSs can predict associations with these other markers of AD and support the clinical diagnosis of this debilitating disease.

4.5. CONCLUSION

Associations between PRSs and regional grey matter volumes are present. Specifically, the most consistent results were that PRSwithAPOE and APOEonlyPRS thresholds were associated with volumes of the bilateral hippocampus and bilateral amygdala (R > L). In terms of the top thresholds per PRS, PRSwithAPOE Thresholds 5 and 10 were best, and APOEonlyPRS Thresholds 1 and 5 were best. Generally, PRSwithAPOE thresholds outperformed APOEonlyPRS thresholds. These findings highlight that these PRSs can be advantageous in clinical settings.

CHAPTER 5A

EXPERIMENT TWO PART A – ASSOCIATIONS BETWEEN POLYGENIC RISK SCORES AND CROSS-SECTIONAL CEREBROSPINAL FLUID BIOMARKERS

5A.1 INTRODUCTION

The preclinical and prodromal stages of AD are key windows for treatment intervention and disease modification (Aisen et al., 2022). The hallmark pathological biomarkers of AD, i.e., Aβ, t-tau, and p-tau are measured commonly via PET imaging, CSF, and more recently also in blood, in both research and clinical settings as they are shown to reflect underlying pathology best (Voyle et al., 2016). These biomarkers indicate current pathological load. Although numerous SNPs have been identified from AD GWAS, little is known about the mechanisms by which these risk loci impact AD pathology (Martiskainen et al., 2015). Therefore, combining (CSF) biomarkers with PRS increases predictability and sensitivity of identifying individuals with future AD risk, and those who may benefit from targeted intervention (Wang et al., 2024).

CSF is in close proximity to the extracellular space of the brain and therefore, as AD pathology occurs in the brain, biochemical changes in the brain may be reflected best in CSF. In comparison with plasma, CSF is affected less by peripheral factors (Wang et al., 2025). CSF Aβ42 reduces in AD. Based on studies conducted between 1998 to 2002 in the European Union, United States of America (USA), and Japan, the mean sensitivity of Aβ42 to distinguish AD from healthy ageing is 86.1%, and the mean specificity of Aβ42 to differentiate AD from other neurodegenerative diseases that can cause dementia is 90.8%. In contrast, CSF p-tau181 increases in AD. Based on research conducted between 1995 to 2022 in the European Union, USA, Japan, and China, the mean sensitivity of p-tau is 73.7%. This is lower than the mean sensitivity of t-tau, at 81.6%, and Aβ42. However, the mean specificity of p-tau is 92.4%, and for p-tau181 in particular, it is 92.5% (Andreasen, Sjogren, and Blennow, 2003). The high specificity of p-tau may not be surprising since it is thought to reflect the formation of NFTs (Blennow et al., 2010). Whereas for t-tau, the mean specificity is 88.4% and is less than that of p-tau or Aβ42 (Andreasen, Sjogren, and Blennow, 2003). Additionally, Aβ42 and p-tau181 are established CSF biomarkers of AD (Wang et al., 2025), whereas t-tau is considered a marker of general neurodegeneration (Wattmo, Blennow, and Hansson, 2020) that reflects the level of neuronal and axonal degeneration (Blennow et al., 2010). Therefore, the combination of CSF Aβ42 and p-tau181 is relevant and specific to AD both pathologically and clinically to identify the disease earlier, and in line with the A/T(/N) framework (Jack et al., 2016).

Associations between PRS with or without APOE, and CSF Aβ42, Aβ42:Aβ40 ratio, p-tau or p-tau181, and t-tau have been examined in individuals across the AD continuum. For instance, Skoog et al. (2021) investigated the association between PRS for AD without APOE, APOE ε4

alone, and CSF Aβ42, t-tau, and p-tau in a cohort of cognitively healthy 70-year-olds from the general population, via H70 Gothenburg Birth Cohort Studies. APOE ε4 was found to be associated with Aβ42, t-tau, and p-tau individually, and all associations survived Bonferroni correction. However, the association between PRS and Aβ42 did not survive correction. After stratifying by APOE ε4 status, PRS without APOE was associated with Aβ42 in ε4 carriers only. No interactions were found between PRS (or APOE ε4) and Aβ42 status in relation to t-tau or p-tau.

In a sample of CU, MCI, and AD participants that were studied as a whole cohort, from the Swedish Biomarkers For Identifying Neurodegenerative Disorders Early and Reliably (BioFINDER) study, PRS2 that included 1742 SNPs without APOE was found to be associated significantly with high CSF p-tau181 and t-tau. This association remained significant after adjusting for the CSF Aβ42:Aβ40 ratio. Although the association weakened after adjusting for Aβ status, it remained significant. Mediation analysis showed that the association between PRS and p-tau181 was mediated by Aβ positivity, by 37%. Additionally, the association between PRS4 that included 63 SNPs without APOE, and p-tau181, was mediated by Aβ positivity as well, by 40%. Therefore, the accumulation of p-tau181 is dependent upon Aβ in part. Conversely, when testing this in a validation dataset consisting of ADNI participants, PRS2 was not associated with p-tau181. Although PRS4 was associated with level of p-tau181, it was not mediated by Aβ positivity. Therefore, the association was tau-specific and independent of Aβ. These discrepancies between the two cohorts may be to the differing number of SNPs that met the statistical thresholds: PRS2 included 1742 SNPs (BioFINDER) vs. 2185 SNPs (ADNI), and PRS4 had 63 SNPs (BioFINDER) vs. 80 SNPs (ADNI). Therefore, genetic diversity introduced variability in the findings (Kumar et al., 2022).

Associations between PRS and CSF biomarkers have been examined in MCI patients alone. For example, Louwersheimer et al. (2016) used data from MCI patients from the Amsterdam Dementia Cohort, and the Dementia Competence Network and found positive associations between PRS without APOE and tau, and between PRS without APOE and p-tau. However, no association was found with Aβ. When looking at APOE ε4 in isolation, ε4 was associated with all CSF biomarkers individually, i.e., Aβ, tau, and p-tau. After stratifying participants by APOE ε4 status, the effect of PRS without APOE on CSF biomarkers was stronger in ε4 non-carriers than in carriers. However, in comparison with PRS that included APOE, associations were stronger when using APOE ε4 alone. Although this study shows that ε4 predicts CSF biomarkers better than a PRS that does not include APOE, it also highlights that PRS without APOE may be essential for

finding MCI-specific vulnerability in ε4 non-carriers as well as general neurodegeneration in such individuals.

Furthermore, Schultz et al. (2017) looked at data from a sample of participants, with a mean age of 61.2 years, from the Wisconsin Registry for Alzheimer's Prevention study. Participants in this study were recruited from the community or were adult children of patients with AD. Associations between a Cholesterol PRS using APOE ε4, CLU, and ABCA7 SNPs, and CSF biomarkers were investigated. In comparison with those with low PRS, high PRS was associated negatively with Aβ42:Aβ40, high PRS was associated positively with t-tau:Aβ42, and high PRS was associated positively with p-tau:Aβ42. However, PRS was not associated with either t-tau or p-tau on its own. PRS without APOE ε4 was not associated with any CSF biomarkers. Additionally, APOE ε4 alone was associated with Aβ42:Aβ40, t-tau:Aβ42, and p-tau:Aβ42. Nested likelihood models indicated that the model with APOE ε4 fits better than the model without APOE ε4 for Aβ42:Aβ40 and t-tau:Aβ42, but not for p-tau:Aβ42. When adding CLU SNPs to these models, the associations strengthened. These findings suggest that APOE ε4 has a major role in cholesterol metabolism, adding CLU increases the significance of associations, and variants from both APOE and CLU genes impact amyloid more than tau.

In a cohort of AD patients from Kuopio on whom CSF biomarker analysis had been conducted, APOE ε4 carriers had reduced Aβ42. The APOE risk score was associated with Aβ42 and t-tau, but not p-tau. PRS without APOE was associated with Aβ42 only. Interestingly, 10.8% of the variance in Aβ42 was explained by a model that incorporated APOE risk score, age, and sex. This went up to 12.6% when adding PRS without APOE to the model. Therefore, 1.8% of the variation in Aβ42 was explained by non-APOE variants. Although adding PRS without APOE to the t-tau and p-tau models increased the variance in t-tau (by 0.6%) and p-tau (by 0.1%), neither were significant statistically. In a sub-study of confirmed neuropathological AD cases from Kuopio University Hospital, PRS without APOE was correlated positively with γ-secretase activity in *post-mortem* temporal cortex tissue. Interestingly, no such results were found using the PRS with APOE. This indicates that γ-secretase activity within the APP protein may be independent of APOE, and such activity heightens with increasing the number of risk variants. These findings suggest that when APOE is included in the CSF Aβ42 model, non-APOE variants improve the model moderately. Nevertheless, non-APOE variants provide interesting insights regarding their involvement with γ-secretase activity and amyloid (Martiskainen et al., 2015).

Moreover, associations between PRS and CSF biomarkers in Chinese participants have also been explored. For instance, Li et al. (2020) studied AD patients from Chongqing Daping Hospital. Negative associations were found between PRS with APOE and Aβ42, and between PRS with APOE and Aβ42:Aβ40 ratio, whereas positive associations were found between PRS with APOE and t-tau, and between PRS with APOE and p-tau. These associations remained after adjusting for age, sex, and APOE genotype. Additionally, PRS with APOE was used to differentiate participants with the highest (third tertile) and lowest (first tertile) levels of Aβ42. PRS with APOE predicted Aβ42 levels with an AUC of 61%. This increased to 69% after taking age and sex into consideration. Of note, these findings were from patients with probable AD as they received a clinical diagnosis only, using the National Institute of Neurological and Communicative Disorders and Stroke (NINCDS) and the Alzheimer's Disease and Related Disorders Association (ADRDA) NINCDS-ADRDA criteria. Further, although these findings are from Chinese patients, the discovery GWAS that was utilised to construct the PRS (with APOE), used non-Chinese participants. Thus, for accurate prediction, large-scale GWASs conducted on ethnic minorities are essential to build PRS models that are applicable widely.

Therefore, Li et al. (2024) used discovery and validation datasets from Chinese populations. Both datasets included patients with AD, and CU individuals that were 60-years old or above and without a family history of AD. Diagnosis of AD was based on the clinical NINCDS-ADRDA criteria. Associations between PRS and CSF biomarkers were explored again. However, on this occasion, the PRS excluded APOE. PRS without APOE and the Aβ42:Aβ40 ratio were associated negatively, and remained significant after controlling for age, sex, and APOE genotype. PRS without APOE and Aβ42 were associated negatively, PRS without APOE and t-tau were associated positively as was PRS without APOE and p-tau181. However, after controlling for age, sex, and APOE genotype, these associations weakened. Although the sample size used was relatively small, the findings suggest that the PRS without APOE method can be used in Chinese populations to predict CSF-related AD pathology. This indicates that the PRS model may be generalisable to non-European samples. This is important particularly since the prevalence of AD and the distribution of APOE genotypes differs in ethnic minorities. For instance, the prevalence of AD (and dementia) is higher significantly in rural areas than in urban areas of China (Jia et al., 2014).

Evidently, there are discrepancies in whether associations are found between PRS and CSF biomarkers and in the direction of the associations. For instance, some studies find associations between PRS without APOE and t-tau, p-tau, or p-tau181 specifically, in mixed cohorts with CU,

MCI, and AD (Kumar et al., 2022) or in MCI patients alone (Louwersheimer et al., 2016). Whereas other studies do not find such associations in AD (Schultz et al., 2017) nor any associations between PRS without APOE and Aβ in MCI patients (Louwersheimer et al., 2016), and there are inconsistencies in whether associations between PRS and p-tau181 are mediated by Aβ positivity (Kumar et al., 2012). Additionally, some work suggests PRS with APOE is associated with Aβ42 in AD (Martiskainen et al., 2015; Schultz et al., 2017), negative associations are present in AD (Li et al., 2020; Li et al., 2024), or negative associations with the Aβ42:Aβ40 ratio are present in AD (Schultz et al., 2017; Li et al., 2020; Li et al., 2024). Other work indicates positive associations between PRS with APOE and p-tau or t-tau in AD (Li et al., 2020; Li et al., 2024), whereas some studies indicate that these associations are present only when investigated in combination with Aβ42, i.e., p-tau:Aβ42 ratio or t-tau:Aβ42 ratio, not when p-tau or t-tau are studied in isolation (Schultz et al., 2017).

5A.1.1. Aims, Objectives, and Hypotheses

Associations between PRSs and CSF biomarkers must be examined carefully. Although the accumulation of Aβ and p-tau are central to AD pathology, it is not clear how these processes are related to the genetic risk of sporadic AD (Kumar et al., 2022).

The overall aim of Chapter 5A (Experiment Two Part A) is:

- To investigate whether PRSs for AD can predict AD-specific CSF biomarkers, cross-sectionally.

This aim will be explored using the following objective:

- To examine the association between PRSs (i.e., PRSwithAPOE, PRSwithoutAPOE, and APOEonlyPRS) and cross-sectional CSF biomarkers (i.e., Aβ42, and p-tau181), systematically.

It is hypothesised that:

1) The association between PRS and CSF biomarkers will be strongest for PRSwithAPOE, followed by APOEonlyPRS, and then PRSwithoutAPOE (whole group).
2) In APOE ε4 carriers, the association between PRS and CSF biomarkers will be strongest for PRSwithAPOE, followed by APOEonlyPRS, and then PRSwithoutAPOE (APOE ε4 status).
3) In MCI and AD dementia patients, the association between PRS and CSF biomarkers will be strongest for PRSwithAPOE, followed by APOEonlyPRS, and then PRSwithoutAPOE, as compared with CU participants (diagnostic status).

Hence, this research will provide a comprehensive and systematic investigation of polygenic influences on AD-specific CSF biomarkers. In turn, this will highlight the impact of genetic risk on pathology across the continuum of sporadic AD.

5A.2. METHODS

5A.2.1. Participants (Stage 1: Amyloid Study | Stage 2: Tau Study)

Data from 524 ADNI participants were used for each study, i.e., Amyloid Study vs. Tau Study. The demographics and characteristics of these participants are shown in Table 5A.1.

In terms of race, the participant sample consisted of white (93.32%, n = 489), minority (6.30%, n = 33), and unknown (0.38%, n = 2) races. Minority races of this sample were Native Americans, Asians, Hawaiian/Pacific, Black, and Mixed. All available races were included in the analysis to maximise the sample size, and generalisability of the results.

As with Chapter 4 (Experiment One), where analysis required stratification by APOE ε4 status, APOE genotypes were grouped into APOE ε4 non-carriers (i.e., ε2ε2, ε2ε3, and ε3ε3) vs. carriers (i.e., ε2ε4, ε3ε4, and ε4ε4).

Family history included history of AD and/or unspecified dementia, in first degree relatives.

Table 5A.1: Participant demographics and characteristics of the entire cohort (n = 524) used for Stage 1 (Amyloid Study) and Stage 2 (Tau Study).

ENTIRE COHORT (n = 524)		
Age		
Age range		55 – 96 years
Mean age		73.85 years
Standard deviation		7.54 years
Education		
Education range		6 – 20 years
Mean education		16.01 years
Standard deviation		2.73 years
	n	**%**
Sex		
Male	297	56.68
Female	227	43.32
Race		
Native Americans	2	0.38
Asian	7	1.34
Hawaiian/Pacific	2	0.38
Black	16	3.05
White	489	93.32
Mixed	6	1.15
Unknown	2	0.38
APOE Genotype		
ε4ε4	48	9.16
ε3ε4	163	31.11
ε3ε3	254	48.47
ε2ε4	8	1.53
ε2ε3	50	9.54
ε2ε2	1	0.19
APOE ε4 Status		
ε4 Non-carrier	305	58.21
ε4 Carrier	219	41.79
Amyloid Status		
Negative	212	40.46
Positive	312	59.54
Tau Status		
Negative	329	62.79
Positive	195	37.21
Family History of Alzheimer's or Dementia		
Negative	23	4.39
Positive	501	95.61

APOE: apolipoprotein E. ε: epsilon.

5A.2.2. Participants (Stage 3: Amyloid and Tau Study)

Data from 345 ADNI participants were used in this study. The demographics and characteristics of these participants are shown in Table 5A.2.

In terms of race, the participant sample consisted of individuals with white (92.75%, n = 320) and minority ethnic (7.25%, n = 25) backgrounds. Minority ethnic backgrounds of this sample were Native Americans, Asians, Hawaiian/Pacific, and Black. All available ethnicities were included in the analysis to maximise the sample size, and generalisability of the results.

As with Chapter 4 (Experiment One), where analysis required stratification by APOE ε4 status, APOE genotypes were grouped into APOE ε4 non-carriers vs. carriers.

Family history included history of AD and/or unspecified dementia, in first degree relatives.

Table 5A.2: Participant demographics and characteristics of the entire cohort (n = 345) used for Stage 3 (Amyloid and Tau Study).

ENTIRE COHORT (n = 345)		
Age		
Age range	55 – 95 years	
Mean age	73.52 years	
Standard deviation	7.60 years	
Education		
Education range	8 – 20 years	
Mean education	15.90 years	
Standard deviation	2.65 years	
	n	**%**
Sex		
Male	184	53.33
Female	161	46.67
Race		
Native Americans	1	0.29
Asian	6	1.74
Hawaiian/Pacific	1	0.29
Black	13	3.77
White	320	92.75
Mixed	4	1.16
Unknown	0	0
APOE Genotype		
ε4ε4	28	8.12
ε3ε4	103	29.86
ε3ε3	172	49.86
ε2ε4	3	0.87
ε2ε3	39	11.3
ε2ε2	0	0
APOE ε4 Status		
ε4 Non-carrier	211	61.16
ε4 Carrier	134	38.84
Amyloid Status		
Negative	181	52.46
Positive	164	47.54
Tau Status		
Negative	181	52.46
Positive	164	47.54
Family History of Alzheimer's or Dementia		
Negative	17	4.93
Positive	328	95.07

APOE: apolipoprotein E. ε: epsilon.

5A.2.3. Genetic Data, Calculation of Polygenic Risk Scores, and Polygenic Risk Score Thresholds

The steps described in Chapter 4 (Experiment One) were applied to Chapter 5A (Experiment Two Part A) for consistency. All three PRSs were used (i.e., PRSwithAPOE, PRSwithoutAPOE, and APOEonlyPRS) with all three thresholds (i.e., Threshold 1 $p = 5 \times 10^{-8}$, Threshold 5 $p < 0.001$, and Threshold 10 $p < 1$).

5A.2.4. Cerebrospinal Fluid Biomarkers

Clinical fluid biomarkers, specifically CSF Aβ42 and CSF p-tau181 measurements, were obtained from "UPPENBIOMK9". These measurements were found in the file titled "UPENNBIOMK_ROCHE_ELECSYS_METHODS_20231109" that was downloaded directly from ADNI on 11 December 2024. To ensure consistency for each participant across Experiments, measurements of CSF Aβ42 and CSF p-tau181 were taken from the date that was closest to the MRI visit that had been used in Chapter 4 (Experiment One). This formed participants' "baseline" for the current work. UPPENBIOMK9 was used as it was the first (2017 batch) and largest dataset available from the University of Pennsylvania Biomarkers group and the most relevant, with published thresholds.

CSF Aβ42 measurements were stratified into negative vs. positive cases based on the threshold of 977 pg/mL, i.e., > 977 pg/mL = negative vs. ≤ 977 pg/mL = positive. This threshold was used because of the high concordance between CSF amyloid vs. PET amyloid that has been validated in ADNI samples, with an AUC of 92.1% (Hansson et al., 2018).

To determine the optimal threshold for concordance, thresholds are tested on: (1) performance, i.e., Positive Percentage Agreement (PPA) that indicates sensitivity and Negative Percentage Agreement (NPA) that shows specificity, and (2) robustness, that indicates the stability of PPA and NPA at the chosen threshold when changing it slightly. The Overall Percentage Agreement (OPA) highlights the proportion of patients that receive the same classification by CSF vs. PET. This model was validated in ADNI participants: the concordance between CSF amyloid vs. visual read-based PET amyloid was PPA = 83.6%, NPA = 85.3%, OPA = 84.4%, and AUC = 92.1%; the concordance between CSF amyloid vs. SUVR-based PET was PPA = 79.2%, NPA = 84.3%, and OPA = 81.4%; the concordance between visual read-based PET vs. SUVR-based PET was PPA = 95.1%, NPA = 88.0%, and OPA = 91.8% (Hansson et al., 2018).

The CSF p-tau181 measurements were stratified into negative vs. positive cases based on the threshold of 26.64 pg/mL, i.e., < 26.64 pg/mL = negative vs. ≥ 26.64 pg/mL = positive. This threshold was used as it has been validated for ADNI samples (Meyer et al., 2020) and the UPPENBIOMK9 2017 cohort specifically (Bucci et al., 2021).

5A.2.5. Statistical Analysis

Analyses were divided into three stages. All statistical analyses were conducted on IBM SPSS Statistics v29.0.1.0.

5A.2.5.1. Stage 1 Analysis: Amyloid

Binomial hierarchical logistic regression analyses were performed to test whether PRS (independent / predictor variable) could predict CSF Aβ42 status (dependent / outcome variable). *P* was significant at the 0.05 level.

(A) Whole-group analysis, not controlled for p-tau181 status

• Model 1: Age, sex, education, family history, MMSE, x10 genetic principal components.

• Model 2: All variables in Model 1, plus PRS.

Analyses were completed using PRSwithAPOE Thresholds 1, 5, and 10, separately, followed by PRSwithoutAPOE Thresholds 1, 5, and 10, separately, and then APOEonlyPRS Thresholds 1, 5, and 10 separately.

(n = 524).

(B) Whole-group analysis, controlled for p-tau181 status (*post-hoc*)

• Model 1: Age, sex, education, family history, MMSE, x10 genetic principal components, CSF p-tau181.

• Model 2: All variables in Model 1, plus PRS.

Analyses were completed using PRSwithAPOE Thresholds 1, 5, and 10, separately, followed by PRSwithoutAPOE Thresholds 1, 5, and 10, separately, and then APOEonlyPRS Thresholds 1, 5, and 10 separately.

(n = 524).

(C) Stratification by APOE ε4 status, not controlled for p-tau181 status

• Model 1: Age, sex, education, family history, MMSE, x10 genetic principal components.

• Model 2: All variables in Model 1, plus PRS.

Analyses were completed using PRSwithAPOE Thresholds 1, 5, and 10, separately, followed by PRSwithoutAPOE Thresholds 1, 5, and 10, separately, and then APOEonlyPRS Thresholds 1, 5, and 10 separately.

(ε4 non-carrier, n = 305; ε4 carriers, n = 219).

(D) Stratification by APOE ε4 status, controlled for p-tau181 status (*post-hoc*)

• Model 1: Age, sex, education, family history, MMSE, x10 genetic principal components, CSF p-tau181.

• Model 2: All variables in Model 1, plus PRS.

Analyses were completed using PRSwithAPOE Thresholds 1, 5, and 10, separately, followed by PRSwithoutAPOE Thresholds 1, 5, and 10, separately, and then APOEonlyPRS Thresholds 1, 5, and 10 separately.

(ε4 non-carrier, n = 305; ε4 carriers, n = 219).

(E) Stratification by diagnostic status, not controlled for p-tau181 status

• Model 1: Age, sex, education, family history, MMSE, x10 genetic principal components.

• Model 2: All variables in Model 1, plus PRS.

Analyses were completed using PRSwithAPOE Thresholds 1, 5, and 10, separately, followed by PRSwithoutAPOE Thresholds 1, 5, and 10, separately, and then APOEonlyPRS Thresholds 1, 5, and 10 separately.

(CU, n = 118; MCI, n = 301; AD dementia, n = 105).

(F) Stratification by diagnostic status, controlled for p-tau181 status (*post-hoc*)

• Model 1: Age, sex, education, family history, MMSE, x10 genetic principal components, CSF p-tau181.

• Model 2: All variables in Model 1, plus PRS.

Analyses were completed using PRSwithAPOE Thresholds 1, 5, and 10, separately, followed by PRSwithoutAPOE Thresholds 1, 5, and 10, separately, and then APOEonlyPRS Thresholds 1, 5, and 10 separately.

(CU, n = 118; MCI, n = 301; AD dementia, n = 105).

5A.2.5.2. Stage 2 Analysis: Tau

Binomial hierarchical logistic regression analyses were performed to test whether PRS (independent / predictor variable) could predict CSF p-tau181 status (dependent / outcome variable). *P* was significant at the 0.05 level.

(A) Whole-group analysis, not controlled for Aβ42 status

• Model 1: Age, sex, education, family history, MMSE, x10 genetic principal components.

• Model 2: All variables in Model 1, plus PRS.

Analyses were completed using PRSwithAPOE Thresholds 1, 5, and 10, separately, followed by PRSwithoutAPOE Thresholds 1, 5, and 10, separately, and then APOEonlyPRS Thresholds 1, 5, and 10 separately.

(n = 524).

(B) Whole-group analysis, controlled for Aβ42 status (*post-hoc*)

• Model 1: Age, sex, education, family history, MMSE, x10 genetic principal components, CSF Aβ42.

• Model 2: All variables in Model 1, plus PRS.

Analyses were completed using PRSwithAPOE Thresholds 1, 5, and 10, separately, followed by PRSwithoutAPOE Thresholds 1, 5, and 10, separately, and then APOEonlyPRS Thresholds 1, 5, and 10 separately.

(n = 524).

(C) Stratification by APOE ε4 status, not controlled for Aβ42 status

• Model 1: Age, sex, education, family history, MMSE, x10 genetic principal components.

• Model 2: All variables in Model 1, plus PRS.

Analyses were completed using PRSwithAPOE Thresholds 1, 5, and 10, separately, followed by PRSwithoutAPOE Thresholds 1, 5, and 10, separately, and then APOEonlyPRS Thresholds 1, 5, and 10 separately.

(ε4 non-carrier, n = 305; ε4 carriers, n = 219).

(D) Stratification by APOE ε4 status, controlled for Aβ42 status (*post-hoc*)

• Model 1: Age, sex, education, family history, MMSE, x10 genetic principal components, CSF Aβ42.

• Model 2: All variables in Model 1, plus PRS.

Analyses were completed using PRSwithAPOE Thresholds 1, 5, and 10, separately, followed by PRSwithoutAPOE Thresholds 1, 5, and 10, separately, and then APOEonlyPRS Thresholds 1, 5, and 10 separately.

(ε4 non-carrier, n = 305; ε4 carriers, n = 219).

(E) Stratification by diagnostic status, not controlled for Aβ42 status

• Model 1: Age, sex, education, family history, MMSE, x10 genetic principal components.

• Model 2: All variables in Model 1, plus PRS.

Analyses were completed using PRSwithAPOE Thresholds 1, 5, and 10, separately, followed by PRSwithoutAPOE Thresholds 1, 5, and 10, separately, and then APOEonlyPRS Thresholds 1, 5, and 10 separately.

(CU, n = 118; MCI, n = 301; AD dementia, n = 105).

(F) Stratification by diagnostic status, controlled for Aβ42 status (*post-hoc*)

• Model 1: Age, sex, education, family history, MMSE, x10 genetic principal components, CSF Aβ42.

• Model 2: All variables in Model 1, plus PRS.

Analyses were completed using PRSwithAPOE Thresholds 1, 5, and 10, separately, followed by PRSwithoutAPOE Thresholds 1, 5, and 10, separately, and then APOEonlyPRS Thresholds 1, 5, and 10 separately.

(CU, n = 118; MCI, n = 301; AD dementia, n = 105).

5A.2.5.3. Stage 3 Analysis: Amyloid and Tau

Binomial hierarchical logistic regression analyses were carried out to test whether PRS (independent / predictor variable) could predict CSF Aβ42 and p-tau181 statuses (dependent / outcome variables). Participants with the same status for each CSF biomarker were selected for this analysis, and therefore this was examined as a binary variable, i.e., either negative for both CSF Aβ42 and p-tau181 or positive for both CSF Aβ42 and p-tau181. *P* was significant at the 0.05 level.

(A) Whole-group analysis

• Model 1: Age, sex, education, family history, MMSE, x10 genetic principal components.

• Model 2: All variables in Model 1, plus PRS.

Analyses were completed using PRSwithAPOE Thresholds 1, 5, and 10, separately, followed by PRSwithoutAPOE Thresholds 1, 5, and 10, separately, and then APOEonlyPRS Thresholds 1, 5, and 10 separately.

(n = 345).

(B) Stratification by APOE ε4 status

• Model 1: Age, sex, education, family history, MMSE, x10 genetic principal components.

• Model 2: All variables in Model 1, plus PRS.

Analyses were completed using PRSwithAPOE Thresholds 1, 5, and 10, separately, followed by PRSwithoutAPOE Thresholds 1, 5, and 10, separately, and then APOEonlyPRS Thresholds 1, 5, and 10 separately.

(ε4 non-carriers, n = 211; ε4 carriers, n = 134).

(C) Stratification by diagnostic status

• Model 1: Age, sex, education, family history, MMSE, x10 genetic principal components.

• Model 2: All variables in Model 1, plus PRS.

Analyses were completed using PRSwithAPOE Thresholds 1, 5, and 10, separately, followed by PRSwithoutAPOE Thresholds 1, 5, and 10, separately, and then APOEonlyPRS Thresholds 1, 5, and 10 separately.

(CU, n = 74; MCI, n = 193; AD dementia, n = 78).

For all cross-sectional CSF studies, FDR correction was not required as there was only one dependent / outcome variable (with two levels each) being tested at any one time, i.e., Amyloid Study – negative vs. positive, Tau Study – negative vs. positive, or Amyloid and Tau Study – negative on both biomarkers vs. positive on both biomarkers. FDR is crucial to use when multiple dependent / outcome variables are being tested simultaneously, which was not the case here.

5A.3. RESULTS

5A.3.1. Stage 1 Results: Amyloid Study

5A.3.1.1. (A) Whole group, not controlled for p-tau181 status

PRSwithAPOE:

PRSwithAPOE thresholds were associated significantly with CSF Aβ42 when CSF p-tau181 was not controlled for. The significance was strongest when Threshold 1 was used (p = 0.000000000000307), followed by Threshold 5 (p = 0.0000000000005017), and then Threshold 10 (p = 0.0000000000028955). These were all associated positively, i.e., high PRS, positive CSF Aβ42. See Table 5A.3, Figure 5A.1, (and Appendix E1 Table E1.1).

APOEonlyPRS:

APOEonlyPRS thresholds were associated significantly with Aβ42 when p-tau181 was not controlled for. In ascending order of significance; Threshold 5 (p = 0.00000000000029938), followed by Threshold 1 (p = 0.00000000000031273), and then Threshold 10 (p = 0.00000000000097476). These were all associated positively, i.e., high PRS, positive CSF Aβ42. See Table 5A.3, Figure 5A.2, (and Appendix E1 Table E1.1).

5A.3.1.2. (B) Whole group, controlled for p-tau181 status (post-hoc)

PRSwithAPOE:

PRSwithAPOE thresholds were associated significantly with CSF Aβ42 when controlled for CSF p-tau181. The significance was greatest for Threshold 1 (p = 0.000000000010753), Threshold 5 (p = 0.000000000027988), then Threshold 10 (p = 0.00000000013452). These were all associated positively, i.e., high PRS, positive CSF Aβ42. See Table 5A.3, Figure 5A.1, (and Appendix E1 Table E1.2).

APOEonlyPRS:

APOEonlyPRS thresholds were associated significantly with Aβ42 when controlled for p-tau181. In ascending order of significance; Threshold 1 (p = 0.000000000013243), followed by Threshold

5 (p = 0.000000000013862), and then Threshold 10 (p = 0.00000000005105). These were all associated positively, i.e., high PRS, positive CSF Aβ42. Refer to Table 5A.3, Figure 5A.2, (and Appendix E1 Table E1.2).

Table 5A.3: Associations between PRSs and cross-sectional CSF Aβ42 status in the whole group when CSF p-tau181 status was not controlled for vs. was controlled for.

Not controlled for p-tau181 status

PRS & Threshold	Chi-square	df	*p*	Nagelkerke R^2	Wald	df	*p*	OR	95% CI	Nagelkerke R^2 Model 1
PRSwithAPOE										
1	176.411	16	<0.001	0.389	53.163	1	0.000000000000307	2.567	1.993-3.308	0.256
5	174.969	16	<0.001	0.386	52.198	1	0.0000000000005017	2.550	1.978-3.288	0.256
10	168.462	16	<0.001	0.374	48.758	1	0.0000000000028955	2.441	1.900-3.135	0.256
APOEonlyPRS										
1	176.835	16	<0.001	0.390	53.127	1	0.00000000000031273	2.579	1.999-3.328	0.256
5	177.310	16	<0.001	0.391	53.212	1	0.00000000000029938	2.606	2.015-3.370	0.256
10	173.077	16	<0.001	0.383	50.894	1	0.00000000000097476	2.501	1.944-3.217	0.256

Controlled for p-tau181 status

PRS & Threshold	Chi-square	df	*p*	Nagelkerke R^2	Wald	df	*p*	OR	95% CI	Nagelkerke R^2 Model 1
PRSwithAPOE										
1	207.758	17	<0.001	0.445	46.186	1	0.000000000010753	2.459	1.897-3.187	0.341
5	204.922	17	<0.001	0.440	44.313	1	0.000000000027988	2.411	1.861-3.124	0.341
10	199.591	17	<0.001	0.431	41.242	1	0.00000000013452	2.313	1.790-2.987	0.341
APOEonlyPRS										
1	207.456	17	<0.001	0.445	45.778	1	0.000000000013243	2.459	1.895-3.191	0.341
5	207.568	17	<0.001	0.445	45.689	1	0.000000000013862	2.477	1.904-3.223	0.341
10	203.268	17	<0.001	0.437	43.137	1	0.00000000005105	2.367	1.831-3.062	0.341

APOE: apolipoprotein E. CI: confidence interval. df: degrees of freedom. OR: odds ratio. PRS: polygenic risk score. P-tau: phosphorylated tau.

Not controlled for p-tau181 status (whole group)

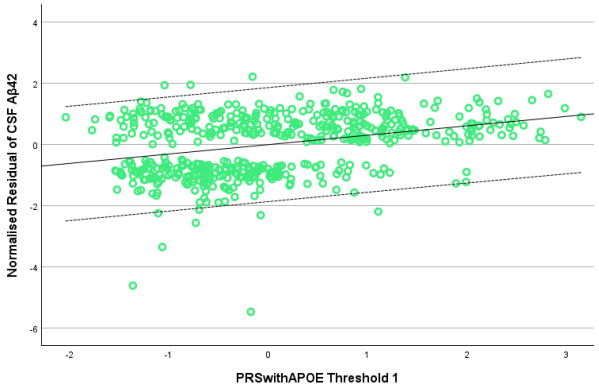

R^2 = 0.106.
CSF Aβ42 = -3.96E – 3 + 0.31 * PRSwithAPOE T1.

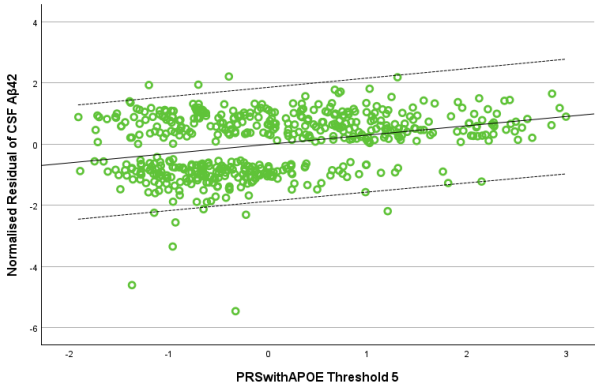

R^2 = 0.103.
CSF Aβ42 = -3.15E – 3 + 0.30 * PRSwithAPOE T5.

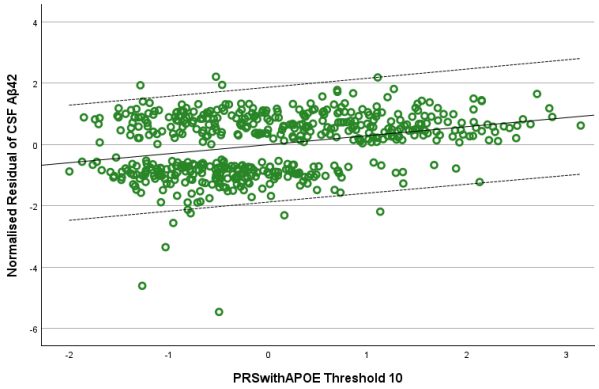

R^2 = 0.094.
CSF Aβ42 = -3.28E – 3 + 0.29 * PRSwithAPOE T10.

Controlled for p-tau181 status (whole group)

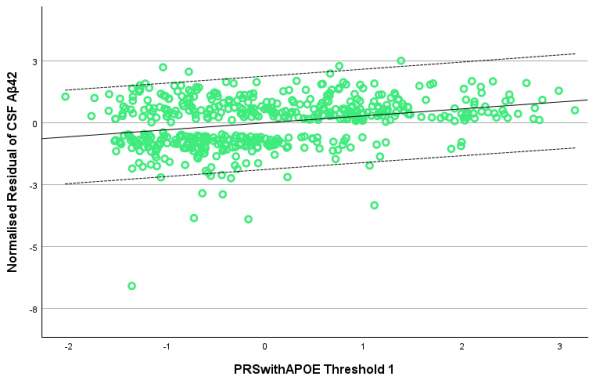

R^2 = 0.088.
CSF Aβ42 = -4.09E – 3 + 0.28 * PRSwithAPOE T1.

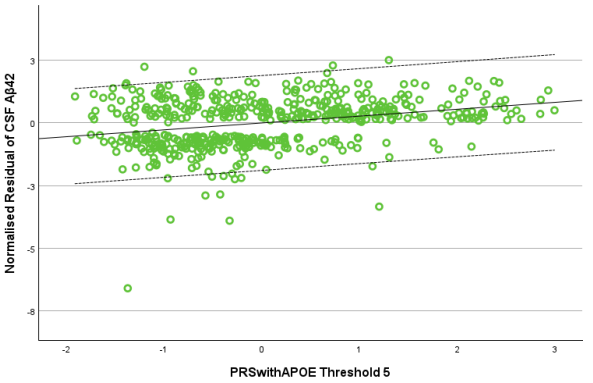

R^2 = 0.084.
CSF Aβ42 = -3.25E – 3 + 0.27 * PRSwithAPOE T5.

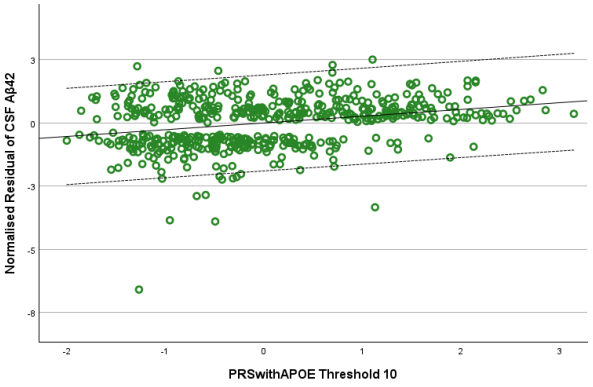

R^2 = 0.077.
CSF Aβ42 = -3.41E – 3 + 0.27 * PRSwithAPOE T10.

(T: threshold).

Figure 5A.1: Scatterplots to visualise associations between PRSwithAPOE thresholds and cross-sectional CSF Aβ42 in the whole group when CSF p-tau181 status was not controlled for vs. was controlled for.

Note, the scatterplots are for visualisation purposes only. The scatterplots show the residualised variable (i.e., CSF Aβ42 positivity) modelled as a function of PRS using linear regression. The R^2 in the scatterplots differs from the Nagelkerke (pseudo) R^2 as the two coefficients are calculated in different ways as part of different types of inferential models. The X axis shows the PRS of interest, and the Y axis indicates the normalised residual of CSF Aβ42 where all covariates have been regressed out.

Not controlled for p-tau181 status (whole group)

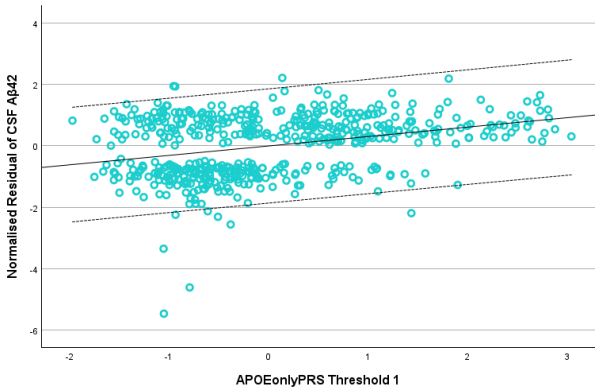

R^2 = 0.107.
CSF Aβ42 = -2.09E – 3 + 0.31 * APOEonlyPRS T1.

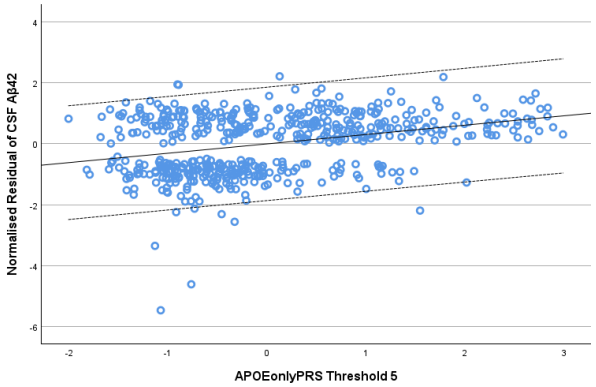

R^2 = 0.107.
CSF Aβ42 = -1.69E – 3 + 0.31 * APOEonlyPRS T5.

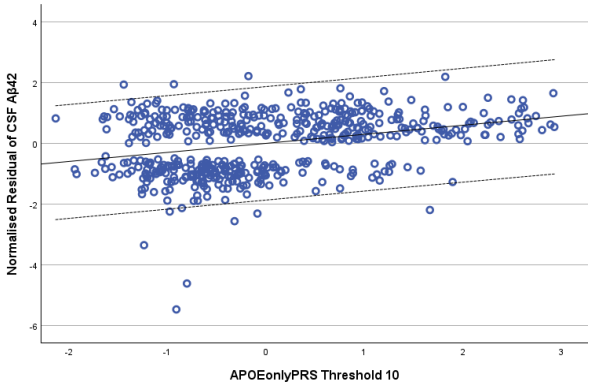

R^2 = 0.100.
CSF Aβ42 = 1.85E – 3 + 0.30 * APOEonlyPRS T10.

Controlled for p-tau181 status (whole group)

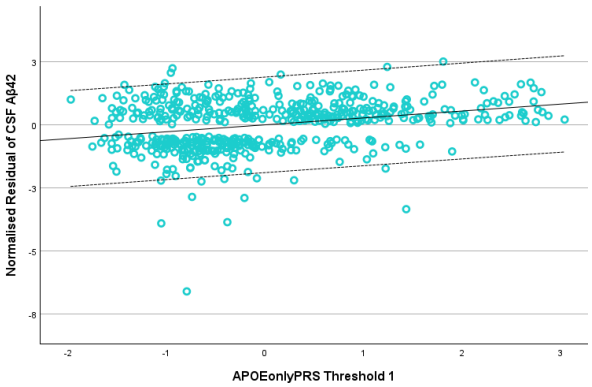

R^2 = 0.084.
CSF Aβ42 = -2.22E – 3 + 0.27 * APOEonlyPRS T1.

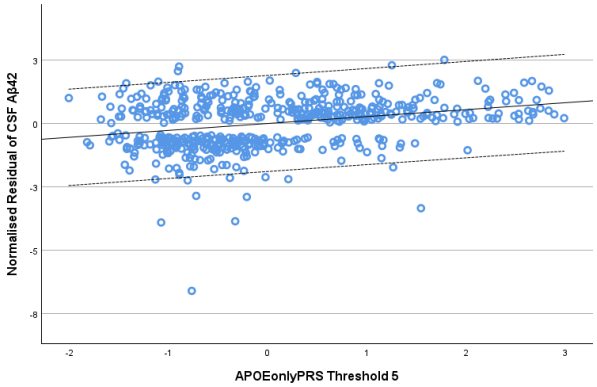

R^2 = 0.083.
CSF Aβ42 = -1.84E – 3 + 0.27 * APOEonlyPRS T5.

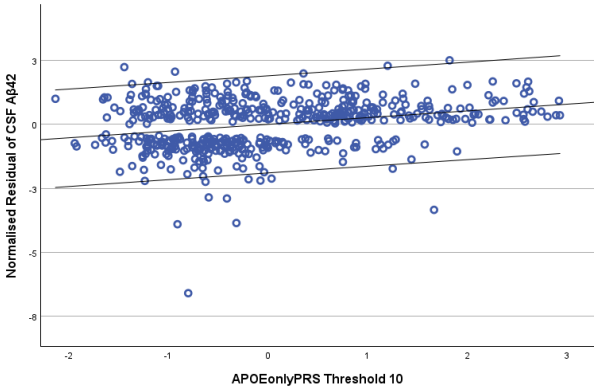

R^2 = 0.077.
CSF Aβ42 = 1.32E – 3 + 0.26 * APOEonlyPRS T10.

(T: threshold).

Figure 5A.2: Scatterplots to visualise associations between APOEonlyPRS thresholds and cross-sectional CSF Aβ42 in the whole group when CSF p-tau181 status was not controlled for vs. was controlled for.

Note, the scatterplots are for visualisation purposes only. The scatterplots show the residualised variable (i.e., CSF Aβ42 positivity) modelled as a function of PRS using linear regression. The R^2 in the scatterplots differs from the Nagelkerke (pseudo) R^2 as the two coefficients are calculated in different ways as part of different types of inferential models. The X axis shows the PRS of interest, and the Y axis indicates the normalised residual of CSF Aβ42 where all covariates have been regressed out.

5A.3.1.3. (C) Stratification by APOE ε4 status, not controlled for p-tau181 status

PRSwithAPOE:

In APOE ε4 carriers, PRSwithAPOE thresholds were associated significantly with Aβ42 when p-tau181 was not controlled for, (p = 0.002 for all thresholds). These were all associated positively, i.e., high PRS, positive CSF Aβ42. Refer to Table 5A.4, Figure 5A.3, (and Appendix E1 Table E1.3). No associations were found in ε4 non-carriers (Appendix E1 Table E1.4).

PRSwithoutAPOE:

For ε4 carriers, PRSwithAPOE thresholds were associated significantly with Aβ42 when p-tau181 was not controlled for. In ascending order; Threshold 1 (p = 0.016), then Threshold 5 (p = 0.032). These were associated positively, i.e., high PRS, positive CSF Aβ42. See Table 5A.4, Figure 5A.4, (and Appendix E1 Table E1.3). No associations were observed in ε4 non-carriers (Appendix E1 Table E1.4).

APOEonlyPRS:

In ε4 carriers, APOEonlyPRS thresholds were associated significantly with Aβ42 when p-tau181 was not controlled for. In ascending order of significance; Threshold 1 (p = 0.012), Threshold 5 (p = 0.016), then Threshold 10 (p = 0.023). These were all associated positively, i.e., high PRS, positive CSF Aβ42. See Table 5A.4, Figure 5A.5, (and Appendix E1 Table E1.3). No associations were found in ε4 non-carriers (Appendix E1 Table E1.4).

5A.3.1.4. (D) Stratification by APOE ε4, controlled for p-tau181 status (post-hoc)

PRSwithAPOE:

In APOE ε4 carriers, PRSwithAPOE thresholds were associated significantly with Aβ42 when controlled for p-tau181, (p = 0.002 for all thresholds). These were all associated positively, i.e., high PRS, positive CSF Aβ42. Refer to Table 5A.4, Figure 5A.3, (and Appendix E1 Table E1.5). No associations were found in ε4 non-carriers (Appendix E1 Table E1.6).

PRSwithoutAPOE:

For ε4 carriers, PRSwithAPOE thresholds were associated significantly with Aβ42 when controlled for p-tau181. In ascending order; Threshold 1 (p = 0.015), then Threshold 5 (p = 0.040).

These were associated positively, i.e., high PRS, positive CSF Aβ42. See Table 5A.4, Figure 5A.4, and Appendix E1 Table E1.5. No associations were observed in ε4 non-carriers (Appendix E1 Table E1.6).

APOEonlyPRS:

In ε4 carriers, APOEonlyPRS thresholds were associated significantly with Aβ42 when controlled for p-tau181. In ascending order of significance; Threshold 1 (p = 0.010), Threshold 5 (p = 0.013), then Threshold 10 (p = 0.020). These were all associated positively, i.e., high PRS, positive CSF Aβ42. Refer to Table 5A.4, Figure 5A.5, (and Appendix E1 Table E1.5). No associations were found in ε4 non-carriers (Appendix E1 Table E1.6).

Table 5A.4: Associations between PRSs and cross-sectional CSF Aβ42 status in ε4 carriers when CSF p-tau181 status was not controlled for vs. was controlled for.

Not controlled for p-tau181 status

PRS & Threshold	Chi-square	df	*p*	Nagelkerke R^2	Wald	df	*p*	OR	95% CI	Nagelkerke R^2 Model 1
PRSwithAPOE										
1	50.299	16	<0.001	0.371	9.351	1	0.002	2.888	1.464-5.700	0.292
5	50.459	16	<0.001	0.372	9.649	1	0.002	2.815	1.465-5.410	0.292
10	50.106	16	<0.001	0.370	9.550	1	0.002	2.737	1.445-5.184	0.292
PRSwithoutAPOE										
1	44.973	16	<0.001	0.336	5.780	1	0.016	1.821	1.117-2.969	0.292
5	43.674	16	<0.001	0.327	4.589	1	0.032	1.761	1.049-2.954	0.292
APOEonlyPRS										
1	45.909	16	<0.001	0.342	6.279	1	0.012	2.290	1.198-4.380	0.292
5	45.297	16	<0.001	0.338	5.812	1	0.016	2.212	1.160-4.217	0.292
10	44.388	16	<0.001	0.332	5.197	1	0.023	2.061	1.107-3.838	0.292

Controlled for p-tau181 status

PRS & Threshold	Chi-square	df	*p*	Nagelkerke R^2	Wald	df	*p*	OR	95% CI	Nagelkerke R^2 Model 1
PRSwithAPOE										
1	55.208	17	<0.001	0.403	10.006	1	0.002	3.128	1.543-6.341	0.319
5	54.855	17	<0.001	0.401	10.010	1	0.002	2.947	1.509-5.757	0.319
10	54.321	17	<0.001	0.397	9.800	1	0.002	2.845	1.478-5.476	0.319
PRSwithoutAPOE										
1	49.217	17	<0.001	0.364	5.958	1	0.015	1.878	1.132-3.115	0.319
5	47.296	17	<0.001	0.352	4.228	1	0.040	1.746	1.026-2.970	0.319
APOEonlyPRS										
1	50.405	17	<0.001	0.372	6.645	1	0.010	2.411	1.235-4.706	0.319
5	49.761	17	<0.001	0.368	6.163	1	0.013	2.328	1.195-4.535	0.319
10	48.642	17	<0.001	0.360	5.420	1	0.020	2.132	2.132-1.127	0.319

APOE: apolipoprotein E. CI: confidence interval. df: degrees of freedom. OR: odds ratio. PRS: polygenic risk score. P-tau: phosphorylated tau.

Not controlled for p-tau181 status (ε4 carriers)

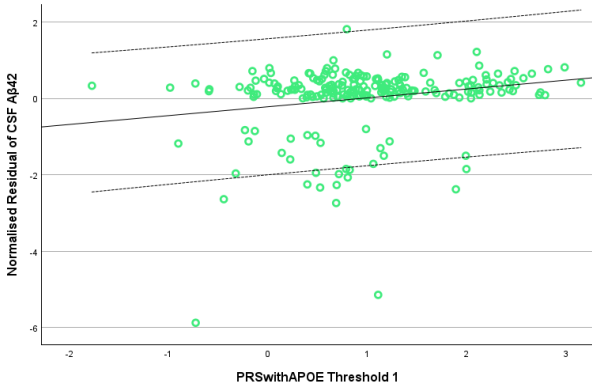

R^2 = 0.044.
CSF Aβ42 = -0.22 + 0.23 * PRSwithAPOE T1.

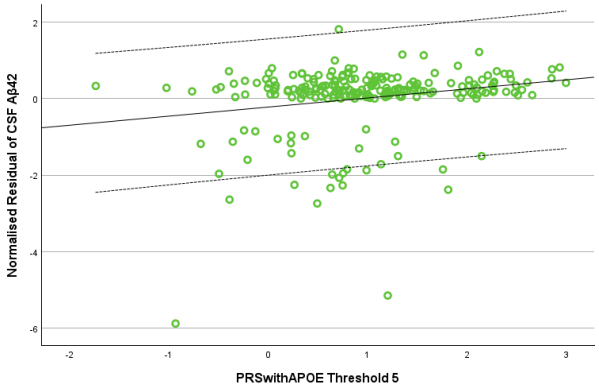

R^2 = 0.047.
CSF Aβ42 = -0.22 + 0.24 * PRSwithAPOE T5.

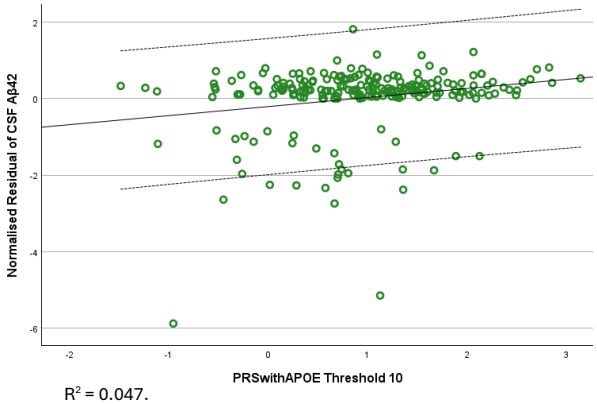

R^2 = 0.047.
CSF Aβ42 = -0.21 + 0.24 * PRSwithAPOE T10.

Controlled for p-tau181 status (ε4 carriers)

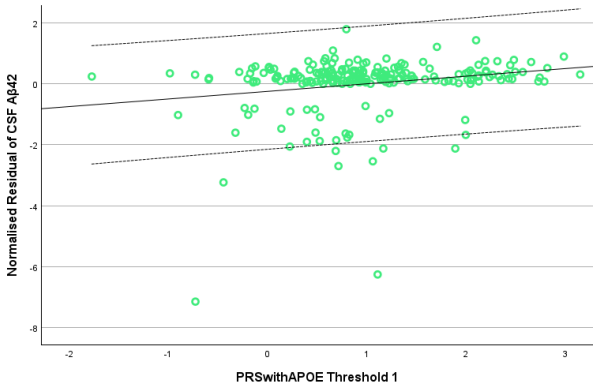

R^2 = 0.045.
CSF Aβ42 = -0.25 + 0.25 * PRSwithAPOE T1.

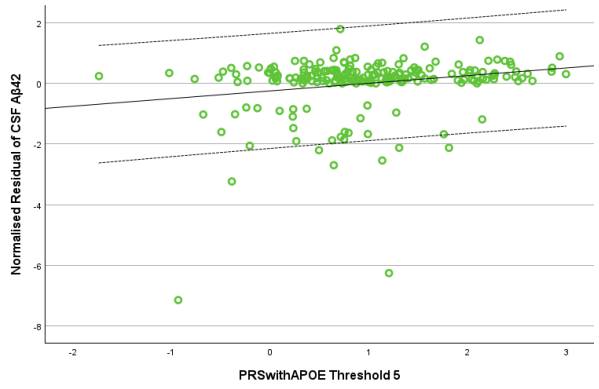

R^2 = 0.047.
CSF Aβ42 = -0.25 + 0.25 * PRSwithAPOE T5.

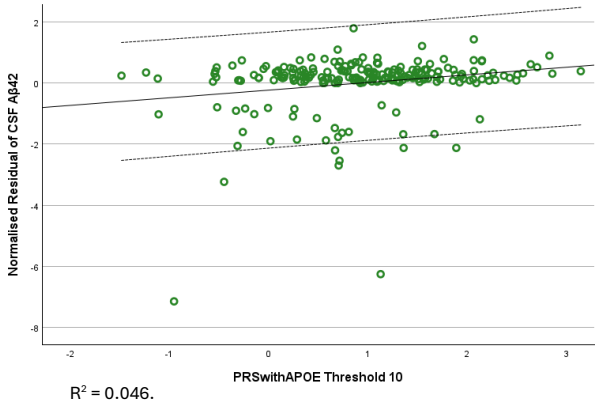

R^2 = 0.046.
CSF Aβ42 = -0.23 + 0.25 * PRSwithAPOE T10.

(T: threshold).

Figure 5A.3: Scatterplots to visualise associations between PRSwithAPOE thresholds and cross-sectional CSF Aβ42 in ε4 carriers when CSF p-tau181 status was not controlled for vs. was controlled for.

Note, the scatterplots are for visualisation purposes only. The scatterplots show the residualised variable (i.e., CSF Aβ42 positivity) modelled as a function of PRS using linear regression. The R^2 in the scatterplots differs from the Nagelkerke (pseudo) R^2 as the two coefficients are calculated in different ways as part of different types of inferential models. The X axis shows the PRS of interest, and the Y axis indicates the normalised residual of CSF Aβ42 where all covariates have been regressed out.

Not controlled for p-tau181 status (ε4 carriers)

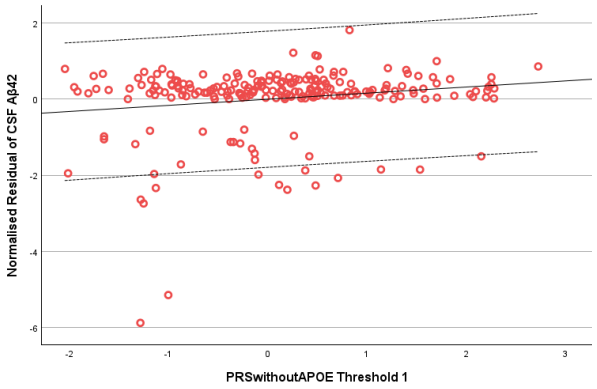

R^2 = 0.032.
CSF Aβ42 = -5.17E – 3 + 0.16 * PRSwithoutAPOE T1.

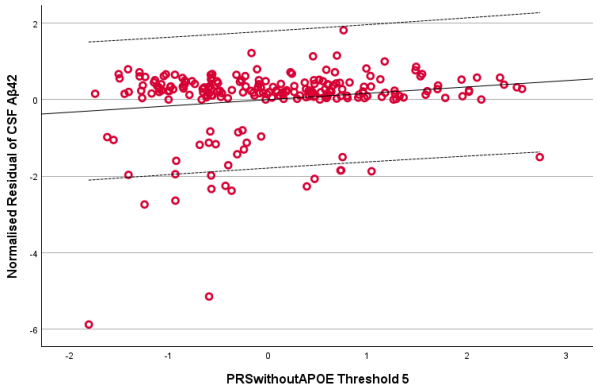

R^2 = 0.030.
CSF Aβ42 = -1.62E – 3 + 0.17 * PRSwithoutAPOE T5.

Controlled for p-tau181 status (ε4 carriers)

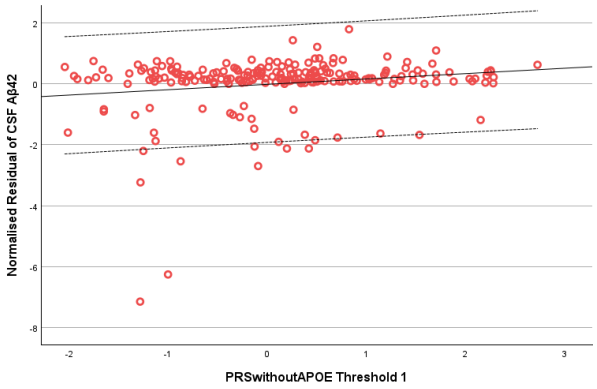

R^2 = 0.033.
CSF Aβ42 = -0.02 + 0.18 * PRSwithoutAPOE T1.

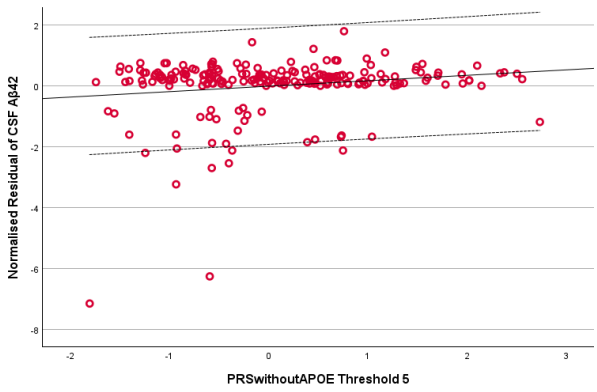

R^2 = 0.031.
CSF Aβ42 = -0.01 + 0.18 * PRSwithoutAPOE T5.

(T: threshold).

Figure 5A.4: Scatterplots to visualise associations between PRSwithoutAPOE thresholds and cross-sectional CSF Aβ42 in ε4 carriers when CSF p-tau181 status was not controlled for vs. was controlled for.

Note, the scatterplots are for visualisation purposes only. The scatterplots show the residualised variable (i.e., CSF Aβ42 positivity) modelled as a function of PRS using linear regression. The R^2 in the scatterplots differs from the Nagelkerke (pseudo) R^2 as the two coefficients are calculated in different ways as part of different types of inferential models. The X axis shows the PRS of interest, and the Y axis indicates the normalised residual of CSF Aβ42 where all covariates have been regressed out.

Not controlled for p-tau181 status (ε4 carriers)

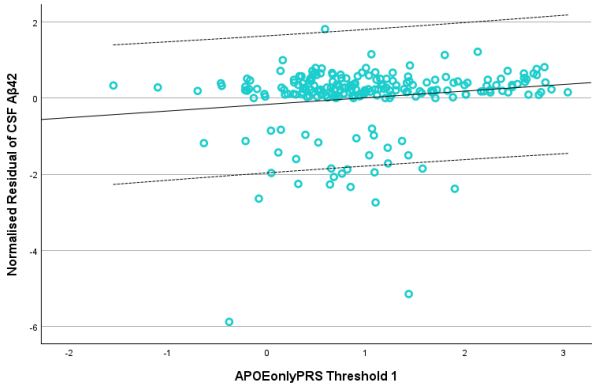

R^2 = 0.025.
CSF Aβ42 = -0.17 + 0.17 * APOEonlyPRS T1.

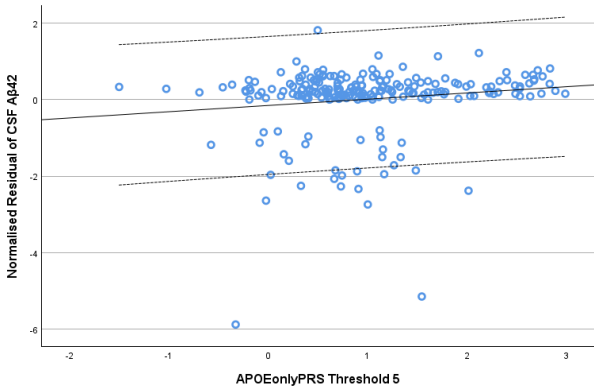

R^2 = 0.022.
CSF Aβ42 = -0.15 + 0.16 * APOEonlyPRS T5.

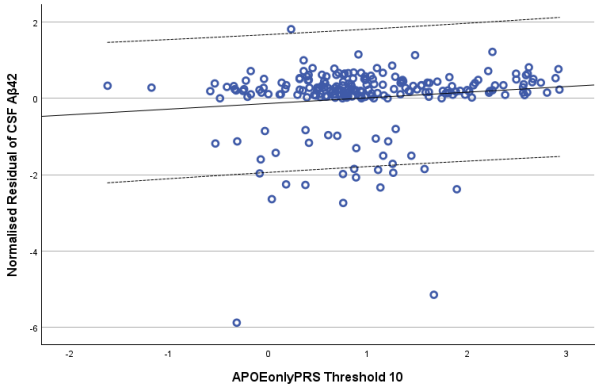

R^2 = 0.018.
CSF Aβ42 = -0.14 + 0.15 * APOEonlyPRS T10.

Controlled for p-tau181 status (ε4 carriers)

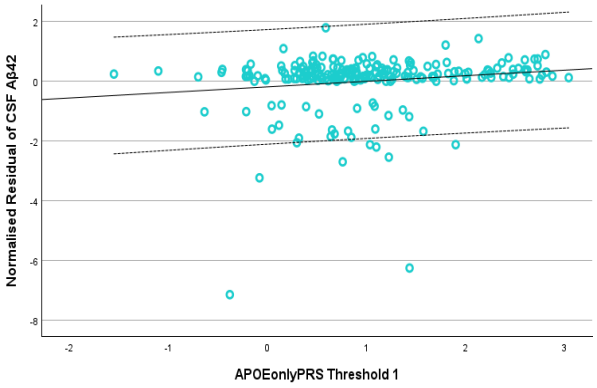

R^2 = 0.025.
CSF Aβ42 = -0.19 + 0.19 * APOEonlyPRS T1.

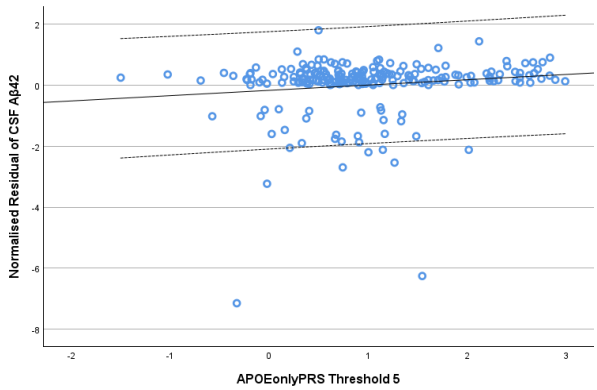

R^2 = 0.022.
CSF Aβ42 = -0.17 + 0.17 * APOEonlyPRS T5.

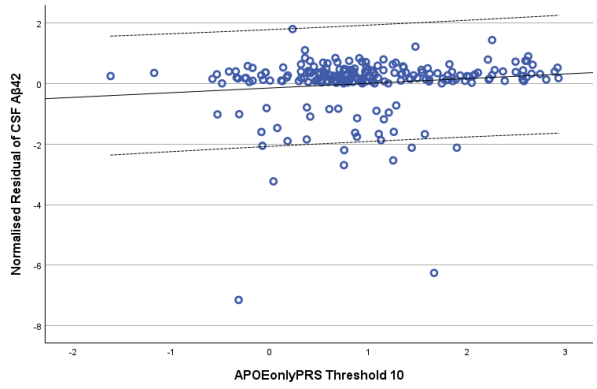

R^2 = 0.018.
CSF Aβ42 = -0.15 + 0.15 * APOEonlyPRS T10.

(T: threshold).

Figure 5A.5: Scatterplots to visualise associations between APOEonlyPRS thresholds and cross-sectional CSF Aβ42 in ε4 carriers when CSF p-tau181 status was not controlled for vs. was controlled for.

Note, the scatterplots are for visualisation purposes only. The scatterplots show the residualised variable (i.e., CSF Aβ42 positivity) modelled as a function of PRS using linear regression. The R^2 in the scatterplots differs from the Nagelkerke (pseudo) R^2 as the two coefficients are calculated in different ways as part of different types of inferential models. The X axis shows the PRS of interest, and the Y axis indicates the normalised residual of CSF Aβ42 where all covariates have been regressed out.

5A.3.1.5. (E) Stratification by diagnostic status, not controlled for p-tau181 status

PRSwithAPOE:

In MCI patients, PRSwithAPOE thresholds were associated significantly with Aβ42 when p-tau181 was not controlled for. The significance was most for Threshold 5 (p = 0.00000000045464), followed by Threshold 1 (p = 0.00000000057928), then Threshold 10 (p = 0.0000000017625). These were all associated positively, i.e., high PRS, positive CSF Aβ42. See Table 5A.5, Figure 5A.6, (and Appendix E1 Table E1.7). No associations were found in the CU participants (Appendix E1 Table E1.8) or AD dementia patients (Appendix E1 Table E1.9).

PRSwithoutAPOE:

For AD dementia patients, PRSwithoutAPOE thresholds were associated significantly with Aβ42 when p-tau181 was not controlled for. In ascending order; Threshold 1 (p = 0.023), then Threshold 5 (p = 0.040). These were associated positively, i.e., high PRS, positive CSF Aβ42. Refer to Table 5A.5, Figure 5A.7, and Appendix E1 Table E1.9. No associations were found in CU (Appendix E1 Table E1.8) or MCI (Appendix E1 Table E1.7).

APOEonlyPRS:

In the CU group, APOEonlyPRS thresholds were associated significantly with Aβ42 when p-tau181 was not controlled for. The significance was greater when Threshold 5 (p = 0.040) was used, followed by Threshold 10 (p = 0.042), and then Threshold 1 (p = 0.044). These were associated positively, i.e., high PRS, positive CSF Aβ42. See Table 5A.5, Figure 5A.8 (and Appendix E1 Table E1.8).

For MCI patients, APOEonlyPRS thresholds were associated significantly with Aβ42 when p-tau181 was not controlled for. In order of significance; Threshold 5 (p = 0.0000000013), Threshold 1 (p = 0.0000000013227), then Threshold 10 (p = 0.0000000023045). Again, these were associated positively, i.e., high PRS, positive CSF Aβ42. See Table 5A.5, Figure 5A.9 (and Appendix E1 Table E1.7). No associations were found in AD dementia patients (Appendix E1 Table E1.9).

5A.3.1.6. (F) Stratification by diagnostic status, controlled for p-tau181 status (post-hoc)

PRSwithAPOE:

In MCI patients, PRSwithAPOE thresholds were associated significantly with Aβ42 when controlled for p-tau181. The significance was strongest for Threshold 1 (p = 0.0000000069589), followed by Threshold 5 (p = 0.000000008378), then Threshold 10 (p = 0.000000029695). These were all associated positively, i.e., high PRS, positive CSF Aβ42. Refer to Table 5A.5, Figure 5A.6, (and Appendix E1 Table E1.10). No associations were found in CU (Appendix E1 Table E1.11) or AD dementia cohorts (Appendix E1 Table E1.12).

PRSwithoutAPOE:

For AD dementia patients, PRSwithoutAPOE thresholds were associated significantly with Aβ42 when controlled for p-tau181. In ascending order; Threshold 5 (p = 0.030), then Threshold 1 (p = 0.032). These were associated positively, i.e., high PRS, positive CSF Aβ42. See Table 5A.5, Figure 5A.7, and Appendix E1 Table E1.12. No associations were found in CU (Appendix E1 Table E1.11) or MCI groups (Appendix E1 Table E1.10).

APOEonlyPRS:

In CU, APOEonlyPRS thresholds were associated significantly with Aβ42 when controlled for p-tau181. In ascending order of significance; Threshold 5 (p = 0.044), Threshold 1 (p = 0.049), then Threshold 10 (p = 0.050). These were associated positively, i.e., high PRS, positive CSF Aβ42. Refer to Table 5A.5, Figure 5A.8, (and Appendix E1 Table E1.11).

For MCI patients, APOEonlyPRS thresholds were associated significantly with Aβ42 when controlled for p-tau181. In order of significance; Threshold 1 (p = 0.000000018362), Threshold 5 (p = 0.000000020127), then Threshold 10 (p = 0.000000037266). Again, these were associated positively, i.e., high PRS, positive CSF Aβ42. See Table 5A.5, Figure 5A.9, (and Appendix E1 Table E1.10). No associations were found in AD dementia patients (Appendix E1 Table E1.12).

Table 5A.5: Associations between PRSs and cross-sectional CSF Aβ42 status according to diagnostic status when CSF p-tau181 status was not controlled for vs. was controlled for.

Not controlled for p-tau181 status

PRS & Threshold	Chi-square	df	*p*	Nagelkerke R^2	Wald	df	*p*	OR	95% CI	Nagelkerke R^2 Model 1
PRSwithAPOE in MCI										
1	98.443	16	<0.001	0.377	38.390	1	0.00000000057928	3.050	2.143-4.340	0.189
5	99.708	16	<0.001	0.381	38.863	1	0.00000000045464	3.176	2.209-4.568	0.189
10	93.025	16	<0.001	0.359	36.220	1	0.0000000017625	2.962	2.080-4.219	0.189
PRSwithoutAPOE in AD dementia										
1	23.571	16	0.099	0.524	5.153	1	0.023	6.898	1.302-36.544	0.349
5	21.258	16	0.169	0.478	4.206	1	0.040	4.825	1.072-21.710	0.349
APOEonlyPRS										
CU										
1	16.854	16	0.395	0.183	4.038	1	0.044	1.723	1.013-2.930	0.138
5	17.056	16	0.382	0.185	4.214	1	0.040	1.755	1.026-3.001	0.138
10	16.952	16	0.389	0.184	4.131	1	0.042	1.753	1.020-3.011	0.138
MCI										
1	95.633	16	<0.001	0.368	36.780	1	0.0000000013227	2.956	2.083-4.197	0.189
5	96.066	16	<0.001	0.369	36.813	1	0.0000000013	2.995	2.101-4.269	0.189
10	93.180	16	<0.001	0.360	35.698	1	0.0000000023045	2.835	2.014-3.990	0.189

Controlled for p-tau181 status

PRS & Threshold	Chi-square	df	*p*	Nagelkerke R^2	Wald	df	*p*	OR	95% CI	Nagelkerke R^2 Model 1
PRSwithAPOE in MCI										
1	121.956	17	<0.001	0.450	33.546	1	0.0000000069589	2.933	2.038-4.220	0.304
5	121.347	17	<0.001	0.448	33.185	1	0.000000008378	2.981	2.056-4.322	0.304
10	115.784	17	<0.001	0.431	30.727	1	0.000000029695	2.796	1.944-4.023	0.304
PRSwithoutAPOE in AD dementia										
1	28.985	17	0.035	0.629	4.578	1	0.032	13.085	1.241-137.944	0.401

5	25.159	17	0.091	0.555	4.704	1	0.030	5.470	1.178-25.404	0.401
APOEonlyPRS										
CU										
1	17.596	17	0.415	0.190	3.883	1	0.049	1.709	1..003-2.913	0.148
5	17.775	17	0.403	0.192	4.038	1	0.044	1.739	1.014-2.984	0.148
10	17.549	17	0.418	0.190	3.846	1	0.050	1.723	1.000-2.968	0.148
MCI										
1	118.643	17	<0.001	0.440	31.660	1	0.000000018362	2.794	1.953-3.995	0.304
5	118.612	17	<0.001	0.440	31.482	1	0.000000020127	2.813	1.960-4.038	0.304
10	115.876	17	<0.001	0.431	30.287	1	0.000000037266	2.671	1.883-3.791	0.304

AD: Alzheimer's disease. APOE: apolipoprotein E. CI: confidence interval. CU: cognitively unimpaired. df: degrees of freedom. MCI: mild cognitive impairment. OR: odds ratio. PRS: polygenic risk score. P-tau: phosphorylated tau.

Not controlled for p-tau181 status (MCI)

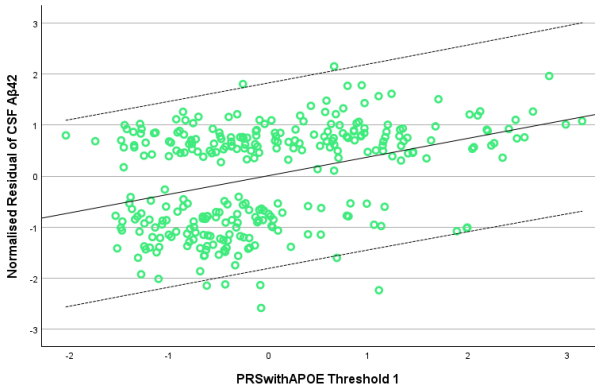

R^2 = 0.143.
CSF Aβ42 = 9.56E – 3 + 0.36 * PRSwithAPOE T1.

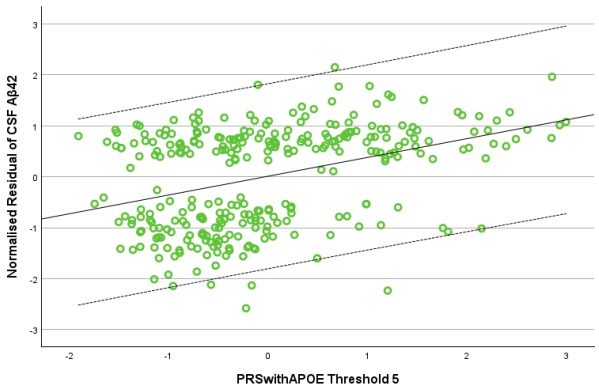

R^2 = 0.144.
CSF Aβ42 = 0.01 + 0.37 * PRSwithAPOE T5.

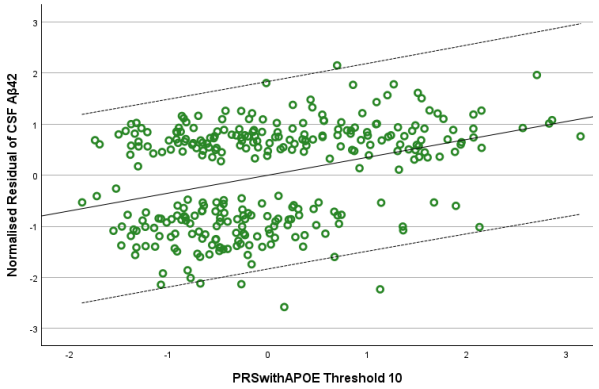

R^2 = 0.125.
CSF Aβ42 = 7.06E – 5 + 0.35 * PRSwithAPOE T10.

Controlled for p-tau181 status (MCI)

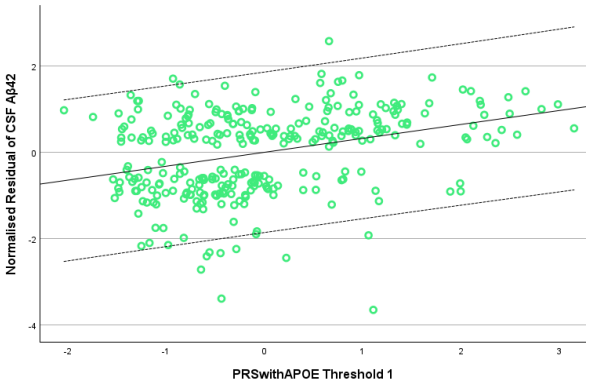

R^2 = 0.111.
CSF Aβ42 = 4.74E – 4 + 0.32 * PRSwithAPOE T1.

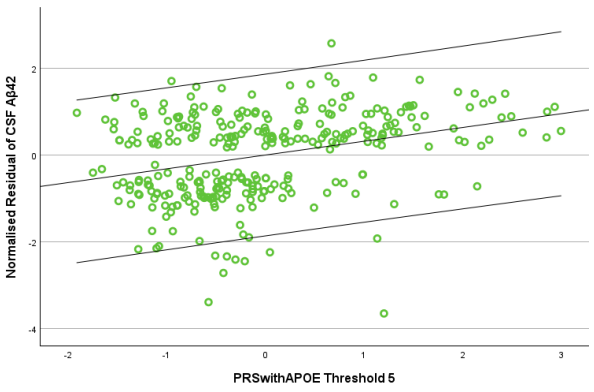

R^2 = 0.106.
CSF Aβ42 = 1.45E – 3 + 0.32 * PRSwithAPOE T5.

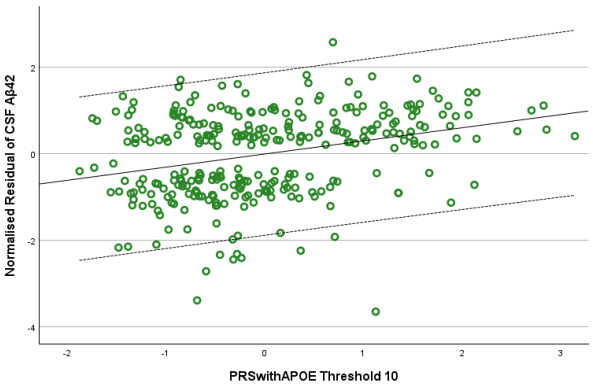

R^2 = 0.093.
CSF Aβ42 = -7.88E – 3 + 0.30 * PRSwithAPOE T10.

(T: threshold).

Figure 5A.6: Scatterplots to visualise associations between PRSwithAPOE thresholds and cross-sectional CSF Aβ42 in MCI patients when CSF p-tau181 status was not controlled for vs. was controlled for.

Note, the scatterplots are for visualisation purposes only. The scatterplots show the residualised variable (i.e., CSF Aβ42 positivity) modelled as a function of PRS using linear regression. The R^2 in the scatterplots differs from the Nagelkerke (pseudo) R^2 as the two coefficients are calculated in different ways as part of different types of inferential models. The X axis shows the PRS of interest, and the Y axis indicates the normalised residual of CSF Aβ42 where all covariates have been regressed out.

Not controlled for p-tau181 status (AD dementia)

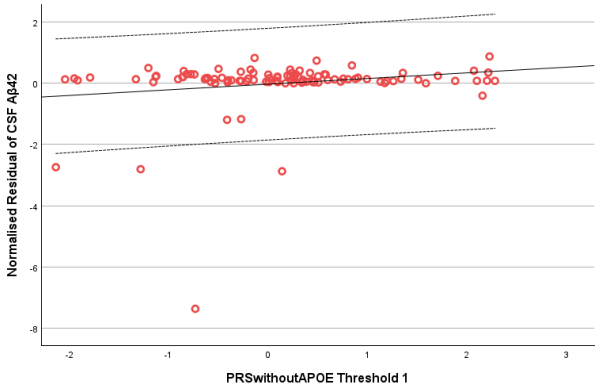

R^2 = 0.038.
CSF Aβ42 = -0.03 + 0.18 * PRSwithoutAPOE T1.

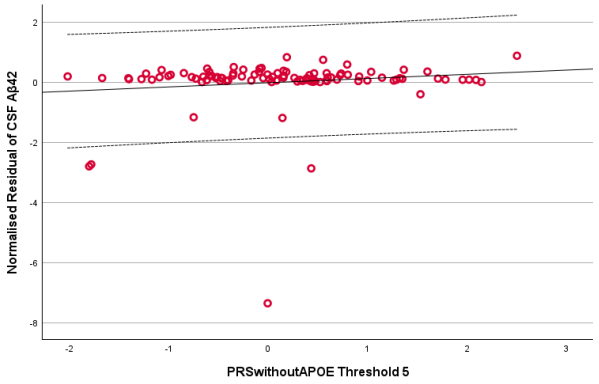

R^2 = 0.020.
CSF Aβ42 = -0.02 + 0.14 * PRSwithoutAPOE T5.

Controlled for p-tau181 status (AD dementia)

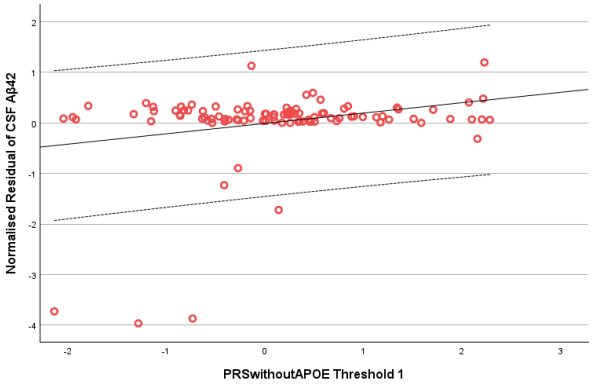

R^2 = 0.073.
CSF Aβ42 = -0.01 + 0.21 * PRSwithoutAPOE T1.

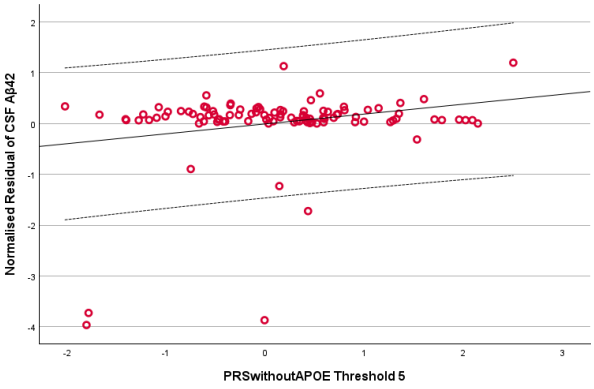

R^2 = 0.058.
CSF Aβ42 = -8.63E – 3 + 0.19 * PRSwithoutAPOE T5.

(T: threshold).

Figure 5A.7: Scatterplots to visualise associations between PRSwithoutAPOE thresholds and cross-sectional CSF Aβ42 in AD dementia patients when CSF p-tau181 status was not controlled for vs. was controlled for.

Note, the scatterplots are for visualisation purposes only. The scatterplots show the residualised variable (i.e., CSF Aβ42 positivity) modelled as a function of PRS using linear regression. The R^2 in the scatterplots differs from the Nagelkerke (pseudo) R^2 as the two coefficients are calculated in different ways as part of different types of inferential models. The X axis shows the PRS of interest, and the Y axis indicates the normalised residual of CSF Aβ42 where all covariates have been regressed out.

Not controlled for p-tau181 status (CU)

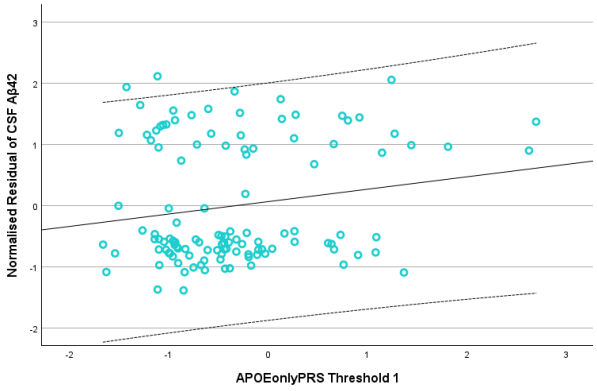

R^2 = 0.030.
CSF Aβ42 = 0.07 + 0.20 * APOEonlyPRS T1.

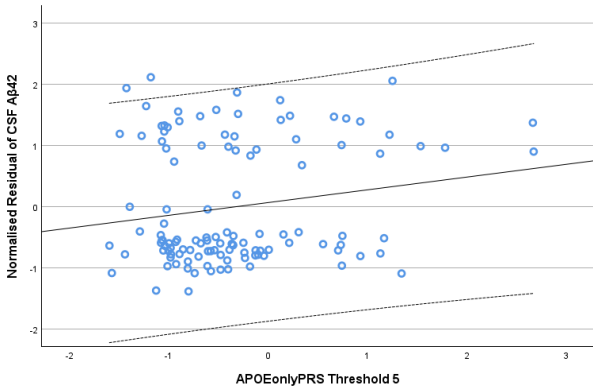

R^2 = 0.031.
CSF Aβ42 = 0.07 + 0.21 * APOEonlyPRS T5.

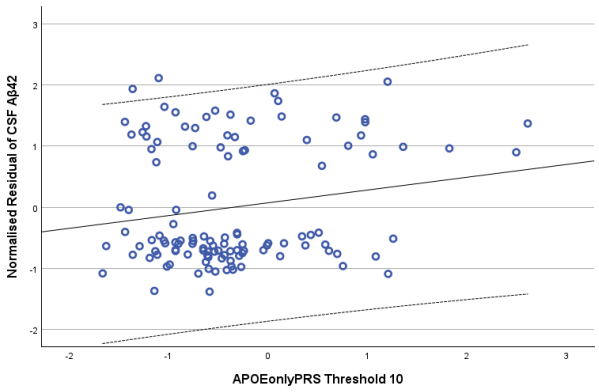

R^2 = 0.031.
CSF Aβ42 = 0.07 + 0.21 * APOEonlyPRS T10.

Controlled for p-tau181 status (CU)

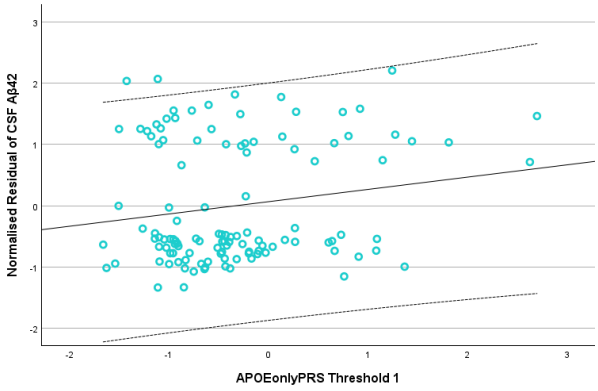

R^2 = 0.030.
CSF Aβ42 = 0.07 + 0.20 * APOEonlyPRS T1.

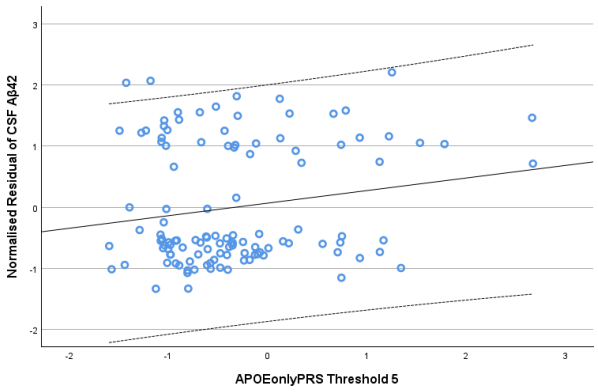

R^2 = 0.031.
CSF Aβ42 = 0.07 + 0.21 * APOEonlyPRS T5.

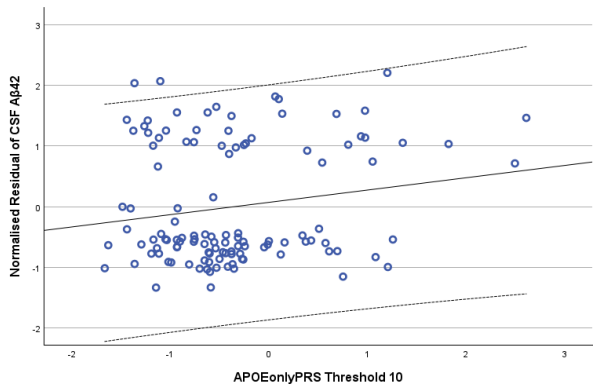

R^2 = 0.029.
CSF Aβ42 = 0.07 + 0.20 * APOEonlyPRS T10.

(T: threshold).

Figure 5A.8: Scatterplots to visualise associations between APOEonlyPRS thresholds and cross-sectional CSF Aβ42 in CU participants when CSF p-tau181 status was not controlled for vs. was controlled for.

Note, the scatterplots are for visualisation purposes only. The scatterplots show the residualised variable (i.e., CSF Aβ42 positivity) modelled as a function of PRS using linear regression. The R^2 in the scatterplots differs from the Nagelkerke (pseudo) R^2 as the two coefficients are calculated in different ways as part of different types of inferential models. The X axis shows the PRS of interest, and the Y axis indicates the normalised residual of CSF Aβ42 where all covariates have been regressed out.

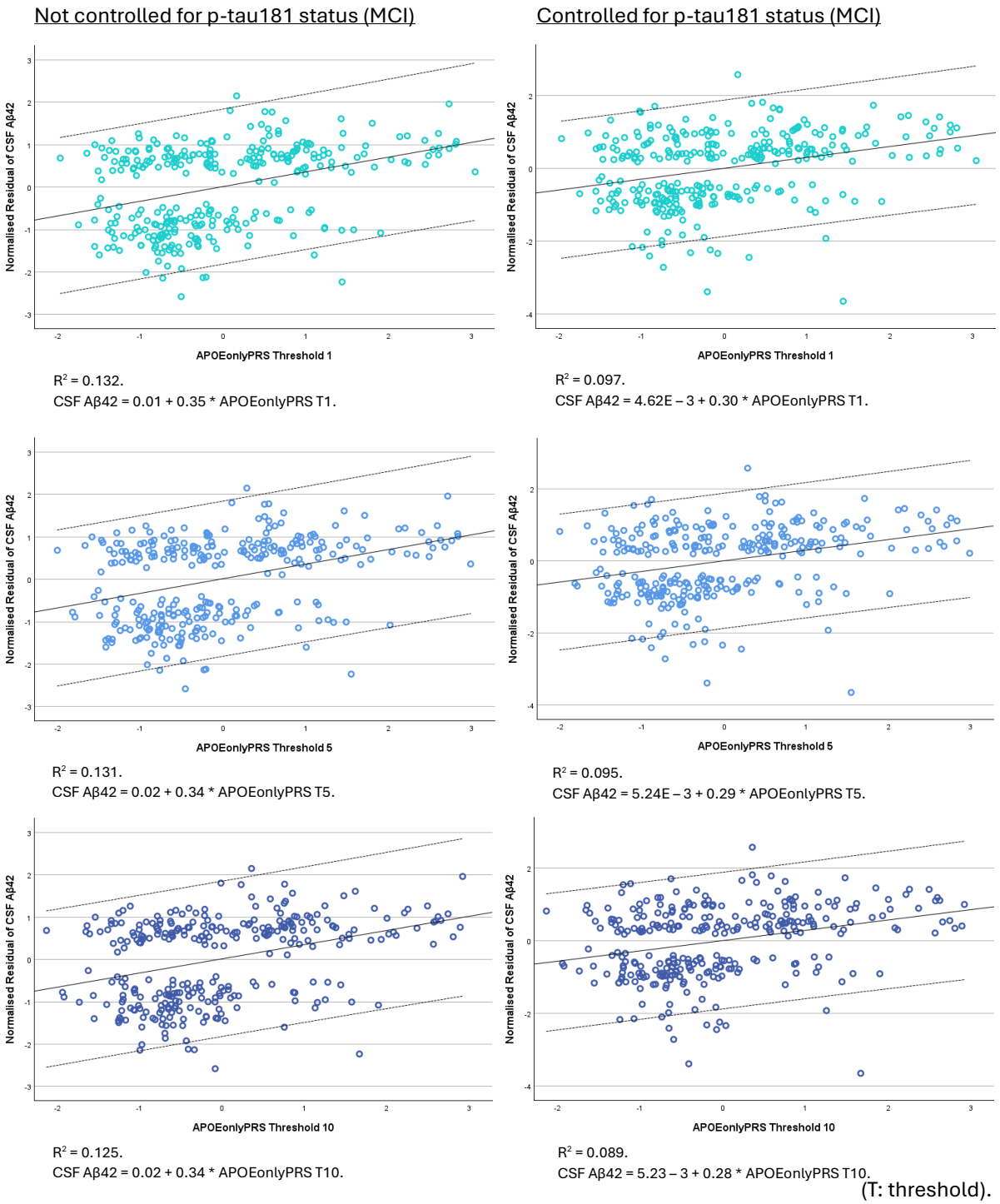

(T: threshold).

Figure 5A.9: Scatterplots to visualise associations between APOEonlyPRS thresholds and cross-sectional CSF Aβ42 in MCI patients when CSF p-tau181 status was not controlled for vs. was controlled for.

Note, the scatterplots are for visualisation purposes only. The scatterplots show the residualised variable (i.e., CSF Aβ42 positivity) modelled as a function of PRS using linear regression. The R^2 in the scatterplots differs from the Nagelkerke (pseudo) R^2 as the two coefficients are calculated in different ways as part of different types of inferential models. The X axis shows the PRS of interest, and the Y axis indicates the normalised residual of CSF Aβ42 where all covariates have been regressed out.

5A.3.1.7. Other related findings

In the whole group, not controlling vs. controlling for p-tau181 status did not generate different results when PRSwithoutAPOE Thresholds 1, 5, or 10 were used. In both instances, no associations were found between PRSwithoutAPOE and cross-sectional Aβ42. See Appendix E1 Table E1.1 (not controlled for p-tau181) and Table E1.2 (controlled for p-tau181).

5A.3.2. Stage 2 Results: Tau Study

5A.3.2.1. (A) Whole group, not controlled for Aβ42 status

PRSwithAPOE:

PRSwithAPOE thresholds were associated significantly with CSF p-tau181 when CSF Aβ42 was not controlled for. The significance was greatest when Threshold 5 was used (p = 0.000062017805674), followed by Threshold 10 (p = 0.000141043200499), and then Threshold 1 (p = 0.000254054306593). These were all associated positively, i.e., high PRS, positive CSF p-tau181. See Table 5A.6, Figure 5A.10, (and Appendix E1 Table E1.13).

APOEonlyPRS:

APOEonlyPRS thresholds were associated significantly with p-tau181 when Aβ42 was not controlled for. In ascending order of significance; Threshold 5 (p = 0.000055199027228), Threshold 10 (p = 0.000069975440667), then Threshold 1 (p = 0.000070064027593). These were all associated positively, i.e., high PRS, positive CSF p-tau181. See Table 5A.6, Figure 5A.10, (and Appendix E1 Table E1.13).

5A.3.2.2. (B) Whole group, controlled for Aβ42 status (post-hoc)

PRSwithAPOE and APOEonlyPRS:

PRSwithAPOE thresholds and APOEonlyPRS thresholds were not associated with p-tau181 when controlled for Aβ42 (Appendix E1 Table E1.14).

Table 5A.6: Associations between PRSs and cross-sectional CSF p-tau181 status in the whole group when Aβ42 status was not controlled for vs. was controlled for.

Not controlled for Aβ42 status

PRS & Threshold	Chi-square	df	*p*	Nagelkerke R^2	Wald	df	*p*	OR	95% CI	Nagelkerke R^2 Model 1
PRSwithAPOE										
1	91.222	16	<0.001	0.220	13.382	1	0.000254054306593	1.437	1.183-1.745	0.190
5	94.018	16	<0.001	0.226	16.010	1	0.000062017805674	1.492	1.227-1.814	0.190
10	92.401	16	<0.001	0.223	14.488	1	0.000141043200499	1.476	1.208-1.803	0.190
APOEonlyPRS										
1	93.828	16	<0.001	0.226	15.809	1	0.000070064027593	1.481	1.220-1.798	0.190
5	94.315	16	<0.001	0.227	16.261	1	0.000055199027228	1.491	1.228-1.811	0.190
10	93.853	16	<0.001	0.226	15.812	1	0.000069975440667	1.485	1.222-1.805	0.190

Aβ: amyloid beta. APOE: apolipoprotein E. CI: confidence interval. df: degrees of freedom. OR: odds ratio. PRS: polygenic risk score.

Not controlled for Aβ42 status (whole group; PRSwithAPOE)

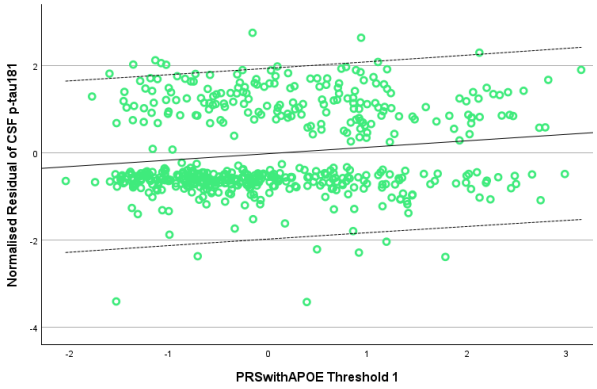

R^2 = 0.024.
CSF p-tau181 = -0.02 + 0.15 * PRSwithAPOE T1.

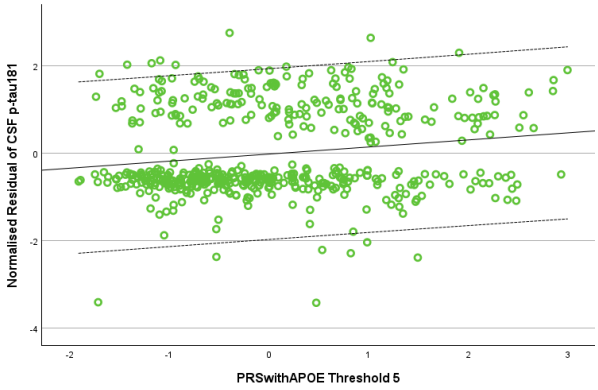

R^2 = 0.029.
CSF p-tau181 = -0.02 + 0.16 * PRSwithAPOE T5.

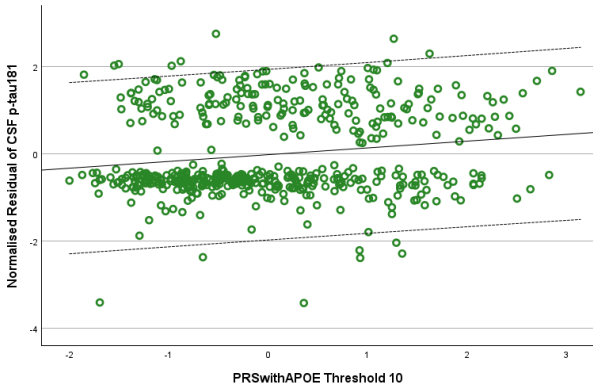

R^2 = 0.026.
CSF p-tau181 = -0.02 + 0.15 * PRSwithAPOE T10.

Not controlled for Aβ42 status (whole group; APOEonlyPRS)

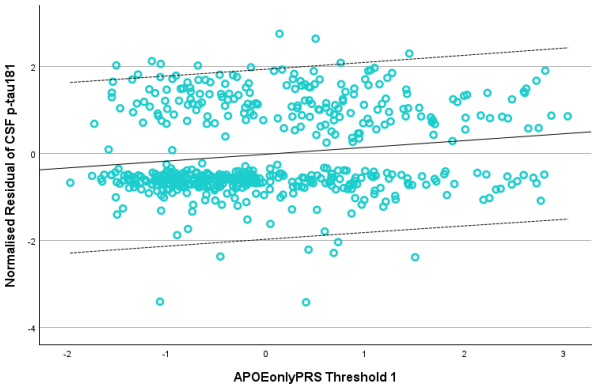

R^2 = 0.028.
CSF p-tau181 = -0.02 + 0.16 * APOEonlyPRS T1.

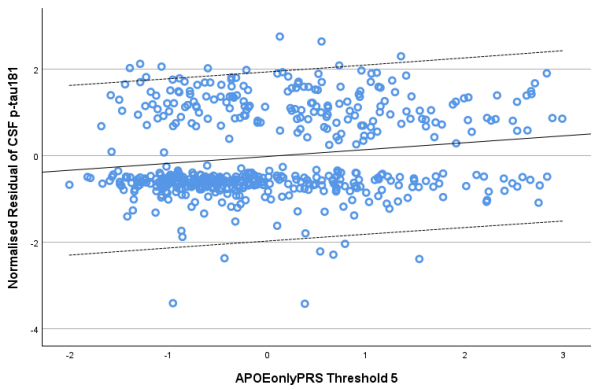

R^2 = 0.028.
CSF p-tau181 = -0.02 + 0.16 * APOEonlyPRS T5.

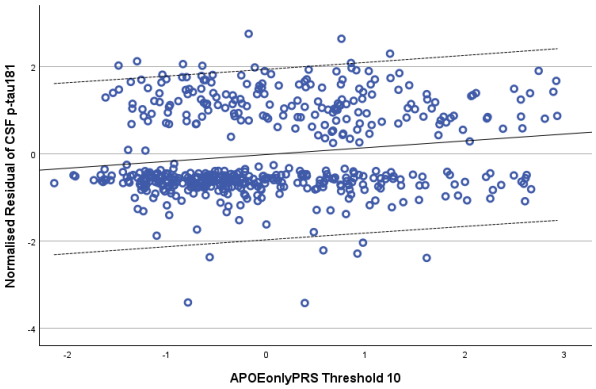

R^2 = 0.027.
CSF p-tau181 = -0.02 + 0.16 * APOEonlyPRS T10.

(T: threshold).

Figure 5A.10: Scatterplots to visualise associations between PRSwithAPOE thresholds, APOEonlyPRS thresholds, and CSF p-tau181 in the whole group when CSF Aβ42 status was not controlled for.

Note, the scatterplots are for visualisation purposes only. The scatterplots show the residualised variable (i.e., CSF p-tau181 positivity) modelled as a function of PRS using linear regression. The R^2 in the scatterplots differs from the Nagelkerke (pseudo) R^2 as the two coefficients are calculated in different ways as part of different types of inferential models. The X axis shows the PRS of interest, and the Y axis indicates the normalised residual of CSF p-tau181 where all covariates have been regressed out.

5A.3.2.3. (E) Stratification by diagnostic status, not controlled for Aβ42 status

PRSwithAPOE:

In MCI patients, PRSwithAPOE thresholds were associated significantly with p-tau181 when Aβ42 was not controlled for. The significance was highest for Threshold 5 (p = 0.002), followed by Threshold 10 (p = 0.003), then Threshold 1 (p = 0.006). These were all associated positively, i.e., high PRS, positive CSF p-tau181. Refer to Table 5A.7, Figure 5A.11, (and Appendix E1 Table E1.15). No associations were found in CU individuals (Appendix E1 Table E1.16) or AD dementia patients (Appendix E1 Table E1.17).

APOEonlyPRS:

For MCI patients, APOEonlyPRS thresholds were associated significantly with p-tau181 when Aβ42 was not controlled for. In ascending order of significance; Threshold 5 and 10 (p = 0.003), then Threshold 1 (p = 0.004). These were all associated positively, i.e., high PRS, positive CSF p-tau181. Refer to Table 5A.7, Figure 5A.11, (and Appendix E1 Table E1.15).

In AD dementia patients, APOEonlyPRS thresholds were associated significantly with p-tau181 when Aβ42 was not controlled for. The significance was strongest when using Threshold 5 (p = 0.026), followed by Threshold 1 (p = 0.029), and then Threshold 10 (p = 0.050). Again, these were all associated positively, i.e., high PRS, positive CSF p-tau181. See Table 5A.7, Figure 5A.12, (and Appendix E1 Table E1.17). No associations were found in CU individuals (Appendix E1 Table E1.16).

Table 5A.7: Associations between PRSs and cross-sectional CSF p-tau181 status according to diagnostic status when CSF Aβ42 status was not controlled for.

Not controlled for Aβ42 status

PRS & Threshold	Chi-square	df	*p*	Nagelkerke R^2	Wald	df	*p*	OR	95% CI	Nagelkerke R^2 Model 1
PRSwithAPOE										
MCI										
1	41.796	16	<0.001	0.181	7.704	1	0.006	1.449	1.115-1.883	0.150
5	44.289	16	<0.001	0.191	10.066	1	0.002	1.537	1.178-2.004	0.150
10	42.761	16	<0.001	0.185	8.599	1	0.003	1.505	1.145-1.977	0.150
APOEonlyPRS										
MCI										
1	42.555	16	<0.001	0.184	8.396	1	0.004	1.466	1.132-1.900	0.150
5	43.060	16	<0.001	0.187	8.864	1	0.003	1.483	1.144-1.923	0.150
10	42.934	16	<0.001	0.186	8.713	1	0.003	1.480	1.141-1.920	0.150
AD dementia										
1	27.882	16	0.033	0.341	4.792	1	0.029	1.758	1.061-2.913	0.284
5	28.081	16	0.031	0.343	4.947	1	0.026	1.789	1.072-2.987	0.284
10	26.811	16	0.044	0.329	3.835	1	0.050	1.655	1.000-2.742	0.284

AD: Alzheimer's disease. APOE: apolipoprotein E. CI: confidence interval. df: degrees of freedom. MCI: mild cognitive impairment. OR: odds ratio. PRS: polygenic risk score.

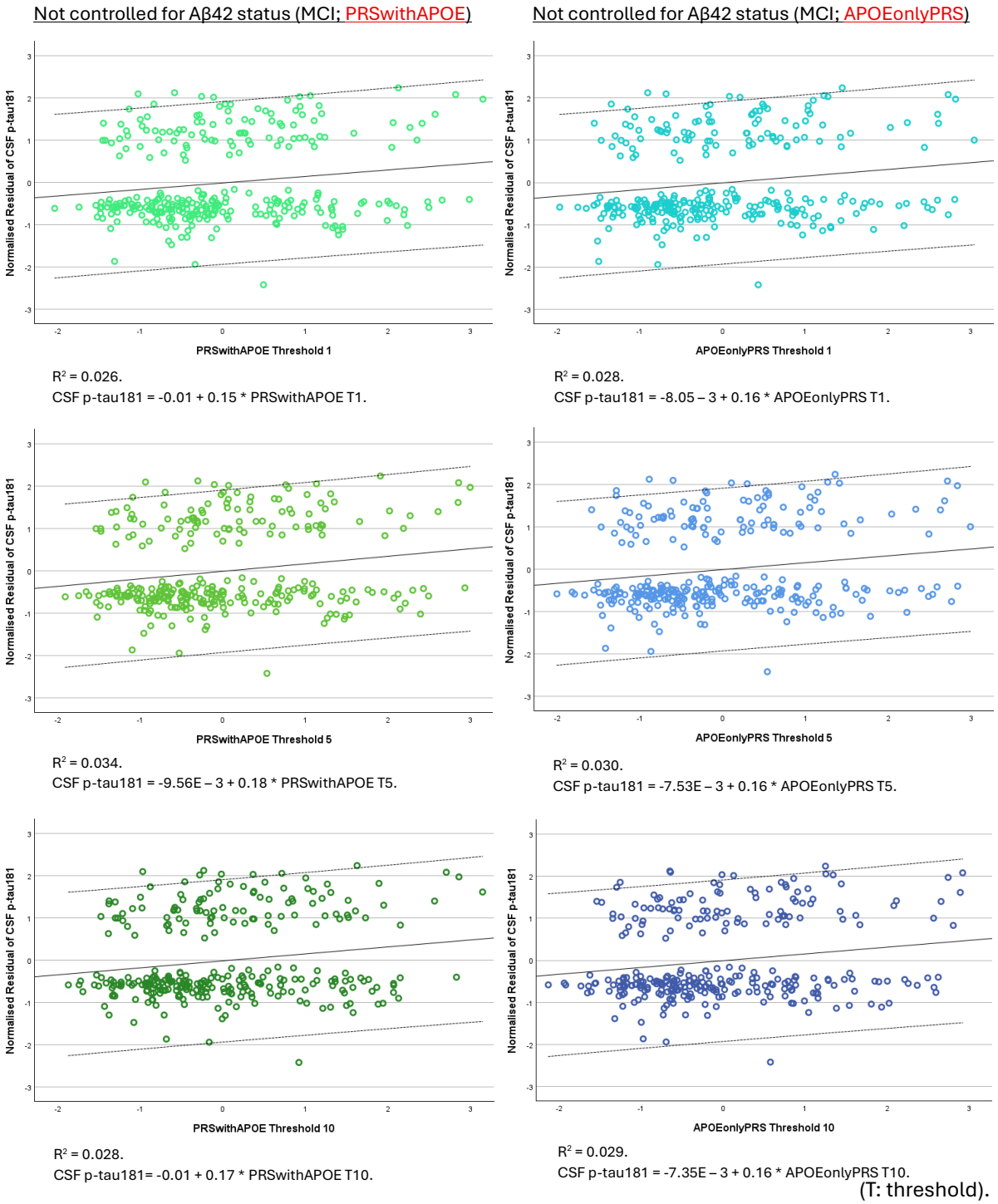

Figure 5A.11: Scatterplots to visualise associations between PRSwithAPOE thresholds, APOEonlyPRS thresholds, and CSF p-tau181 in MCI patients when Aβ42 was not controlled for.

Note, the scatterplots are for visualisation purposes only. The scatterplots show the residualised variable (i.e., CSF p-tau181 positivity) modelled as a function of PRS using linear regression. The R^2 in the scatterplots differs from the Nagelkerke (pseudo) R^2 as the two coefficients are calculated in different ways as part of different types of inferential models. The X axis shows the PRS of interest, and the Y axis indicates the normalised residual of CSF p-tau181 where all covariates have been regressed out.

Not controlled for Aβ42 status (AD dementia)

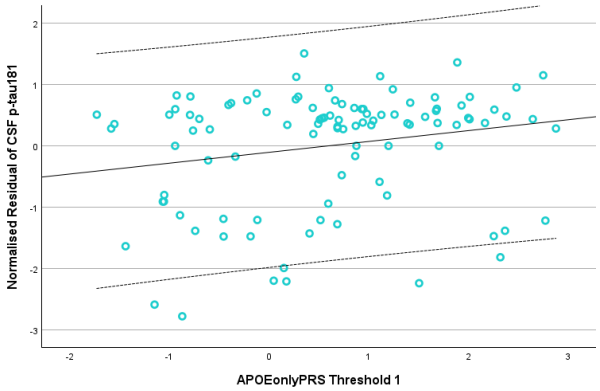

R^2 = 0.044.
CSF p-tau181 = -0.10 + 0.18 * APOEonlyPRS T1.

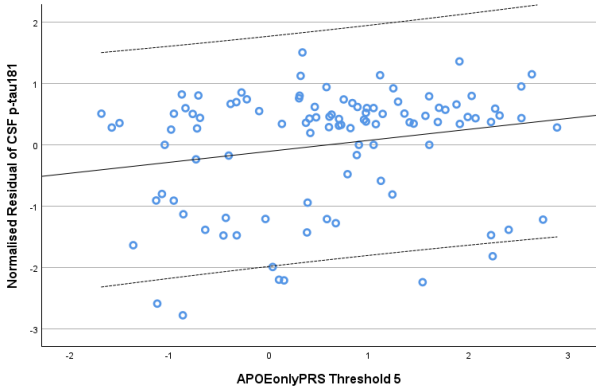

R^2 = 0.045.
CSF p-tau181 = -0.11 + 0.18 * APOEonlyPRS T5.

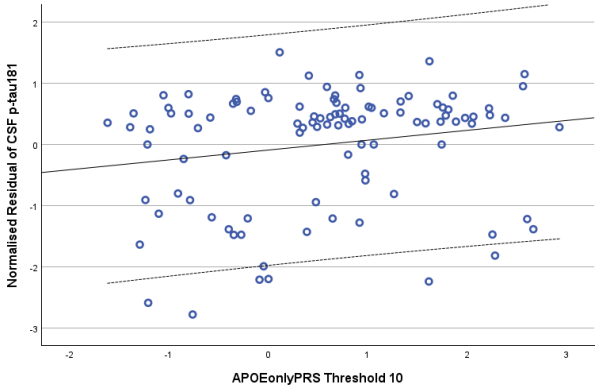

R^2 = 0.036.
CSF p-tau181 = -0.09 + 0.16 * APOEonlyPRS T10.

(T: threshold).

Figure 5A.12: Scatterplots to visualise associations between APOEonlyPRS thresholds and CSF p-tau181 in AD dementia patients when Aβ42 was not controlled for.

Note, the scatterplots are for visualisation purposes only. The scatterplots show the residualised variable (i.e., CSF p-tau181 positivity) modelled as a function of PRS using linear regression. The R^2 in the scatterplots differs from the Nagelkerke (pseudo) R^2 as the two coefficients are calculated in different ways as part of different types of inferential models. The X axis shows the PRS of interest, and the Y axis indicates the normalised residual of CSF p-tau181 where all covariates have been regressed out.

5A.3.2.4. (F) Stratification by diagnostic status, controlled for Aβ42 status (post-hoc)

PRSwithAPOE and APOEonlyPRS:

PRSwithAPOE thresholds and APOEonlyPRS thresholds were not associated with p-tau181 when controlled for Aβ42. See Appendix E1 Table E1.18 (CU), Table E1.19 (MCI), and Table E1.20 (AD dementia) for details.

5A.3.2.5. Other related findings

In the whole group, and when the whole group was stratified by diagnosis, not controlling vs. controlling for Aβ42 status did not lead to different results when PRSwithoutAPOE thresholds were used. In all four cases, no associations were found between PRSwithoutAPOE and cross-sectional p-tau181. Refer to Appendix E1 Table E1.13 (whole group not controlled for Aβ42), Table E1.14 (whole group controlled for Aβ42), Table E1.15 (MCI not controlled for Aβ42), Table E1.16 (CU not controlled for Aβ42), Table E1.17 (AD dementia not controlled for Aβ42), Table E1.18 (CU controlled for Aβ42), Table E1.19 (MCI controlled for Aβ42), and Table E1.20 (AD dementia controlled for Aβ42).

When the whole group was stratified by APOE ε4 status, not controlling vs. controlling for Aβ42 status did not generate different results. In both instances, no associations were found between p-tau181 and PRSwithAPOE thresholds, PRSwithoutAPOE thresholds, or APOEonlyPRS thresholds. Consult Appendix E1 Table E1.21 (ε4 non-carriers not controlled for Aβ42), Table E1.22 (ε4 carriers not controlled for Aβ42), Table E1.23 (ε4 non-carriers controlled for Aβ42), and Table E1.24 (ε4 carriers controlled for Aβ42).

5A.3.3. Stage 3 Results: Amyloid and Tau Study

5A.3.3.1. (A) Whole group

PRSwithAPOE:

PRSwithAPOE thresholds were associated significantly with CSF biomarker positivity. The level of significance was highest when Threshold 5 was used (p = 0.0000000010463), followed by Threshold 1 (p = 0.0000000018512), and then Threshold 10 (p = 0.0000000041875). These were all positive associations, i.e., high PRS, positive on both CSF Aβ42 and p-tau181. Refer to Table 5A.8, Figure 5A.13, (and Appendix E1 Table E1.25).

PRSwithoutAPOE:

PRSwithoutAPOE thresholds were not associated with CSF biomarker statuses (Appendix E1 Table E1.25).

APOEonlyPRS:

APOEonlyPRS thresholds were associated significantly with CSF biomarker positivity. In ascending order of significance; Threshold 5 (p = 0.00000000051275), Threshold 1 (p = 0.00000000054241), and then Threshold 10 (p = 0.00000000081276). These were all positive associations, i.e., high PRS, positive on both CSF Aβ42 and p-tau181. See Table 5A.8, Figure 5A.13, (and Appendix E1 Table E1.25).

Table 5A.8: Associations between PRSs and cross-sectional CSF biomarker status of both Aβ42 and p-tau181 in the whole group.

PRS & Threshold	Chi-square	df	*p*	Nagelkerke R^2	Wald	df	*p*	OR	95% CI	Nagelkerke R^2 Model 1
PRSwithAPOE										
1	183.381	16	<0.001	0.554	36.124	1	0.0000000018512	3.020	2.106-4.330	0.440
5	185.368	16	<0.001	0.559	37.237	1	0.0000000010463	3.111	2.161-4.479	0.440
10	180.150	16	<0.001	0.547	34.535	1	0.0000000041875	2.963	2.062-4.256	0.440
APOEonlyPRS										
1	187.522	16	<0.001	0.563	38.518	1	0.00000000054241	3.214	2.223-4.646	0.440
5	188.052	16	<0.001	0.565	38.628	1	0.00000000051275	3.254	2.243-4.721	0.440
10	186.338	16	<0.001	0.561	37.729	1	0.00000000081276	3.158	2.188-4.558	0.440

APOE: apolipoprotein E. CI: confidence interval. df: degrees of freedom. OR: odds ratio. PRS: polygenic risk score.

CSF Aβ42 and p-tau181 positivity (whole group; PRSwithAPOE)

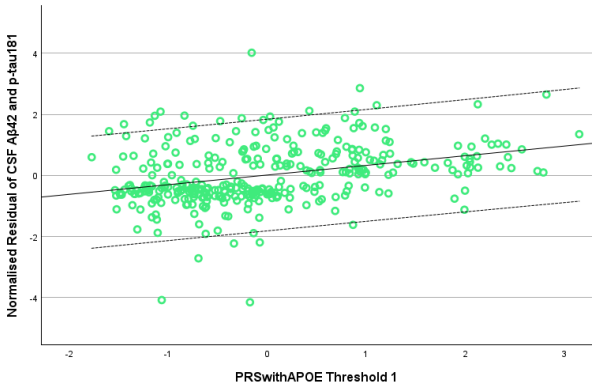

R^2 = 0.109.
CSF Aβ42 & p-tau181 = 7.33E – 3 + 0.32 * PRSwithAPOE T1.

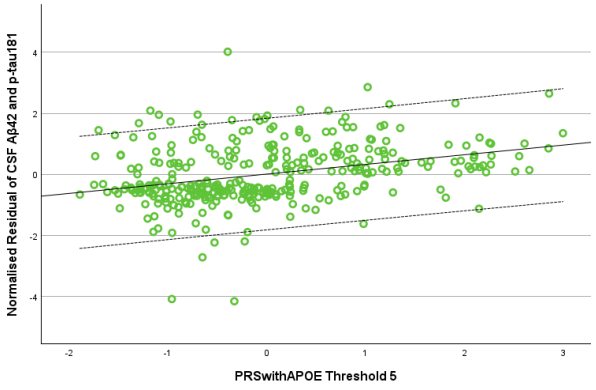

R^2 = 0.111.
CSF Aβ42 & p-tau181 = 5.65E – 3 + 0.32 * PRSwithAPOE T5.

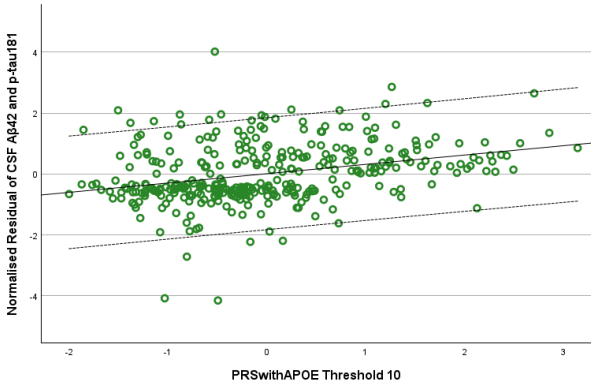

R^2 = 0.100.
CSF Aβ42 & p-tau181 = 3.92E – 3 + 0.31 * PRSwithAPOE T10.

CSF Aβ42 and p-tau181 positivity (whole group; APOEonlyPRS)

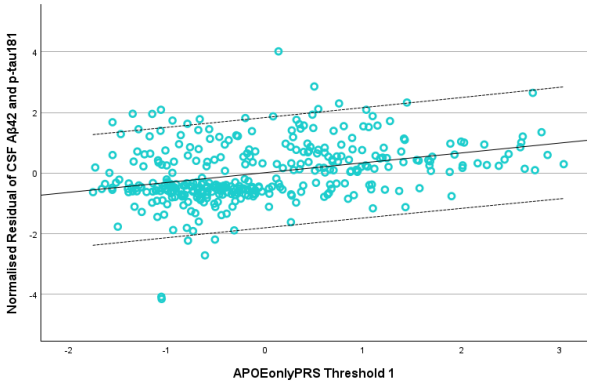

R^2 = 0.118.
CSF Aβ42 & p-tau181 = 8.79E – 3 + 0.33 * APOEonlyPRS T1.

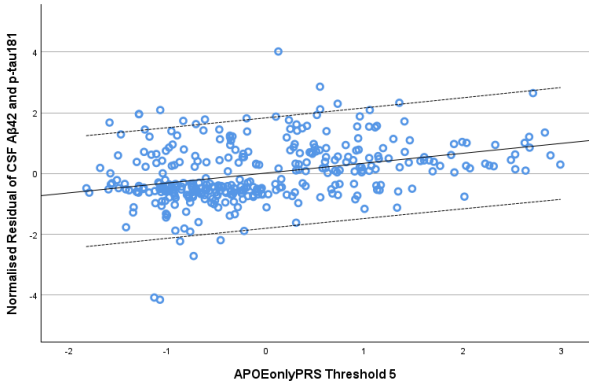

R^2 = 0.119.
CSF Aβ42 & p-tau181 = 9.7E – 3 + 0.33 * APOEonlyPRS T5.

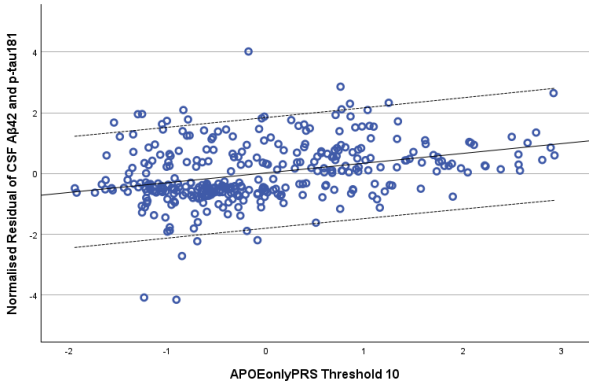

R^2 = 0.116.
CSF Aβ42 & p-tau181 = 0.01 + 0.32 * APOEonlyPRS T10.

(T: threshold).

Figure 5A.13: Scatterplots to visualise associations between PRSwithAPOE thresholds, APOEonlyPRS thresholds, and CSF biomarker status of both Aβ42 and p-tau181 in the whole group.

Note, the scatterplots are for visualisation purposes only. The scatterplots show the residualised variable (i.e., CSF Aβ42 positivity + CSF p-tau181 positivity) modelled as a function of PRS using linear regression. The R^2 in the scatterplots differs from the Nagelkerke (pseudo) R^2 as the two coefficients are calculated in different ways as part of different types of inferential models. The X axis shows the PRS of interest, and the Y axis indicates the normalised residual of CSF Aβ42 and CSF p-tau181 where all covariates have been regressed out.

5A.3.3.2. (B) Stratification by APOE ε4

PRSwithAPOE, PRSwithoutAPOE and APOEonlyPRS:

No associations were found between any of the PRS thresholds and CSF biomarker statuses. See Appendix E1 Table E1.26 (ε4 non-carriers) and Appendix E1 Table E1.27 (ε4 carriers).

5A.3.3.3. (C) Stratification by diagnostic status

PRSwithAPOE:

In MCI patients, PRSwithAPOE thresholds were associated significantly with CSF biomarker positivity. The significance was strongest when using Threshold 5 (p = 0.00000011616), followed by Threshold 1 (p = 0.0000002634), and then Threshold 10 (p = 0.00000036757). These were all positive associations, i.e., high PRS, positive on both CSF Aβ42 and p-tau181. Refer to Table 5A.9, Figure 5A.14, (and Appendix E1 Table E1.28). No associations were found in CU individuals (Appendix E1 Table E1.29) or AD dementia patients (Appendix E1 Table E1.30).

PRSwithoutAPOE:

PRSwithoutAPOE thresholds were not associated with CSF biomarker statuses. Refer to Appendix E1 Table E1.28 (MCI), Table E1.29 (CU), and Table E1.30 (AD dementia).

APOEonlyPRS:

For CU participants, APOEonlyPRS thresholds were associated significantly with CSF biomarker positivity. In order of significance; Threshold 10 (p = 0.030), Threshold 5 (p = 0.044), and then Threshold 1 (p = 0.048). These were all positive associations, i.e., high PRS, positive on both CSF Aβ42 and p-tau181. See Table 5A.9, Figure 5A.15, (and Appendix E1 Table E1.29).

In MCI patients, APOEonlyPRS thresholds were associated significantly with CSF biomarker positivity. In ascending order of the level of significance; Threshold 5 (p = 0.00000025582), Threshold 1 (p = 0.00000025935), and then Threshold 10 (p = 0.00000040088). These were all positive associations, i.e., high PRS, positive on both CSF Aβ42 and p-tau181. Refer to Table 5A.9, Figure 5A.14, (and Appendix E1 Table E1.28). No associations were found in AD dementia patients (Appendix E1 Table E1.30).

Table 5A.9: Associations between PRSs and cross-sectional CSF biomarker status of both Aβ42 and p-tau181 according to diagnostic status.

PRS & Threshold	Chi-square	df	*p*	Nagelkerke R^2	Wald	df	*p*	OR	95% CI	Nagelkerke R^2 Model 1
PRSwithAPOE in MCI										
1	83.839	16	<0.001	0.473	26.501	1	0.0000002634	3.442	2.150-5.510	0.295
5	87.649	16	<0.001	0.490	28.084	1	0.00000011616	3.812	2.324-6.252	0.295
10	82.771	16	<0.001	0.469	25.857	1	0.00000036757	3.575	2.188-5.843	0.295
APOEonlyPRS										
CU										
1	21.908	16	0.146	0.490	3.900	1	0.048	4.698	1.012-21.818	0.386
5	22.145	16	0.139	0.494	4.075	1	0.044	4.837	1.047-22.353	0.386
10	23.566	16	0.099	0.521	4.703	1	0.030	6.668	1.200-37.044	0.386
MCI										
1	84.634	16	<0.001	0.477	26.531	1	0.00000025935	3.589	2.207-5.835	0.295
5	85.260	16	<0.001	0.480	26.557	1	0.00000025582	3.678	2.241-6.036	0.295
10	83.549	16	<0.001	0.472	25.690	1	0.00000040088	3.468	2.144-5.610	0.295

APOE: apolipoprotein E. CI: confidence interval. CU: cognitively unimpaired. df: degrees of freedom. MCI: mild cognitive impairment. OR: odds ratio. PRS: polygenic risk score.

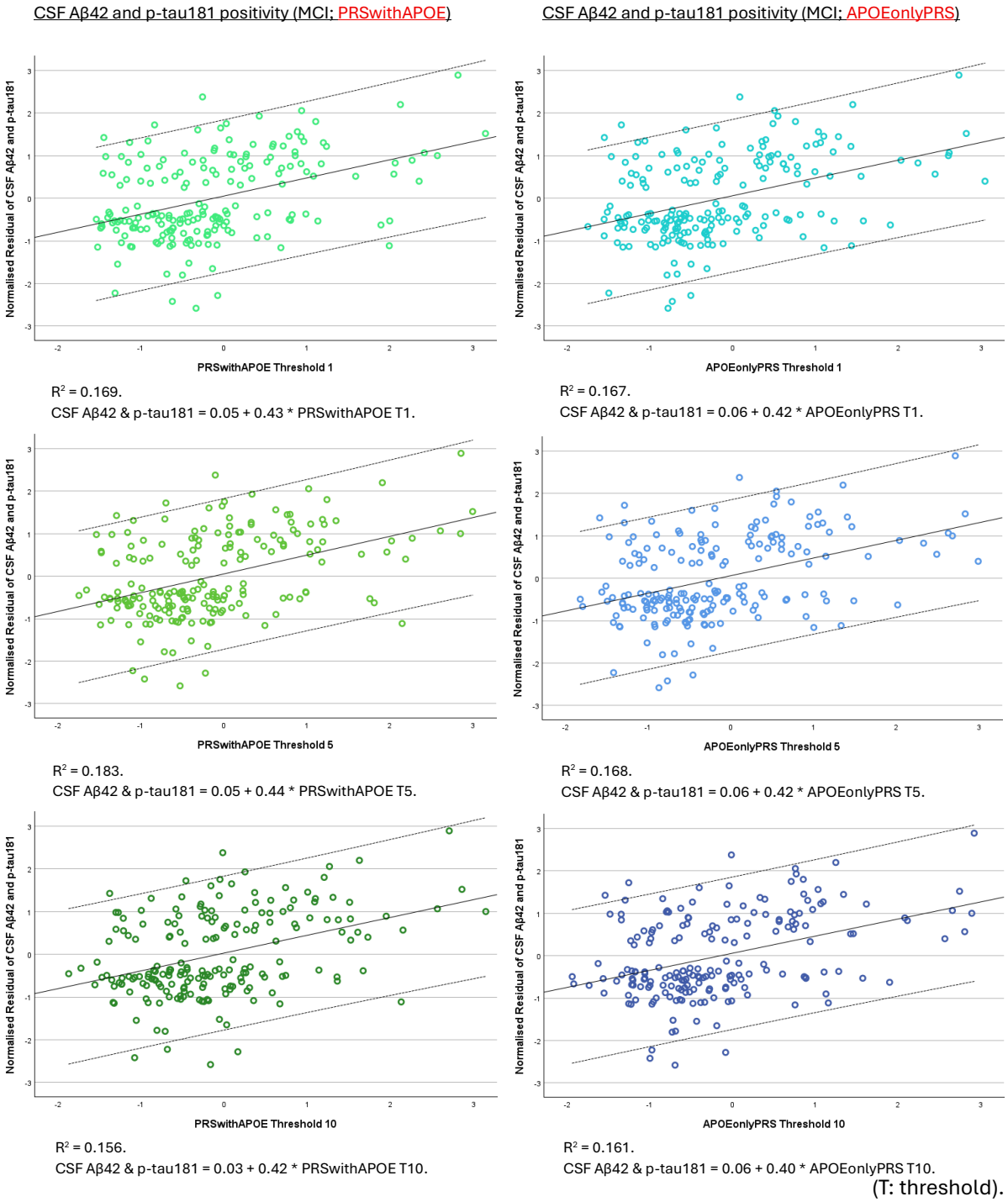

(T: threshold).

Figure 5A.14: Scatterplots to visualise associations between PRSwithAPOE thresholds, APOEonlyPRS thresholds, and CSF biomarker status of both Aβ42 and p-tau181 in MCI patients.

Note, the scatterplots are for visualisation purposes only. The scatterplots show the residualised variable (i.e., CSF Aβ42 positivity + CSF p-tau181 positivity) modelled as a function of PRS using linear regression. The R^2 in the scatterplots differs from the Nagelkerke (pseudo) R^2 as the two coefficients are calculated in different ways as part of different types of inferential models. The X axis shows the PRS of interest, and the Y axis indicates the normalised residual of CSF Aβ42 and CSF p-tau181 where all covariates have been regressed out.

CSF Aβ42 and p-tau181 positivity (CU)

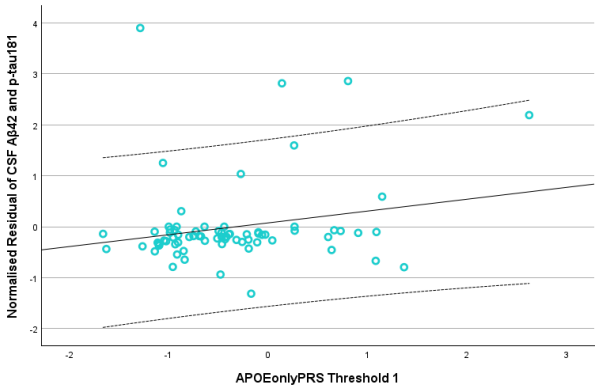

R^2 = 0.046.
CSF Aβ42 & p-tau181 = 0.07 + 0.23 * APOEonlyPRS T1.

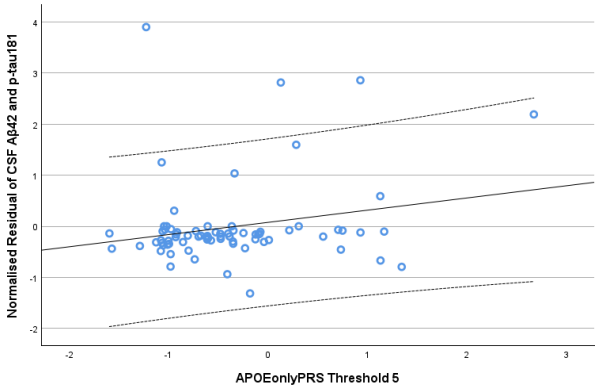

R^2 = 0.049.
CSF Aβ42 & p-tau181 = 0.08 + 0.24 * APOEonlyPRS T5.

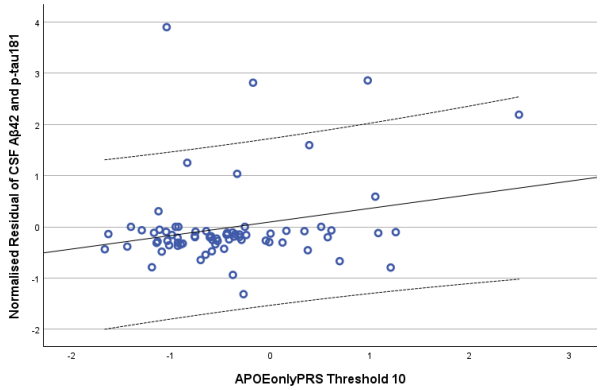

R^2 = 0.058.
CSF Aβ42 & p-tau181 = 0.10 + 0.27 * APOEonlyPRS T10.
(T: threshold).

Figure 5A.15: Scatterplots to visualise associations between APOEonlyPRS thresholds and CSF biomarker status of both Aβ42 and p-tau181 in the CU participants.

Note, the scatterplots are for visualisation purposes only. The scatterplots show the residualised variable (i.e., CSF Aβ42 positivity and CSF p-tau181 positivity) modelled as a function of PRS using linear regression. The R^2 in the scatterplots differs from the Nagelkerke (pseudo) R^2 as the two coefficients are calculated in different ways as part of different types of inferential models. The X axis shows the PRS of interest, and the Y axis indicates the normalised residual of CSF Aβ42 and CSF p-tau181 where all covariates have been regressed out.

5A.4. DISCUSSION

Associations between PRSs for AD and CSF biomarkers were examined, specifically Aβ42 and p-tau181. The three PRSs were: PRSwithAPOE, PRSwithoutAPOE, and an APOEonlyPRS, and the three thresholds per PRS were: Threshold 1 ($p = 5 \times 10^{-8}$), Threshold 5 ($p < 0.001$), and Threshold 10 ($p < 1$). In the Amyloid Study, associations between all PRSs at all thresholds and CSF Aβ42 were investigated without controlling for p-tau181 status. Then, associations between PRSs and Aβ42 controlled for CSF p-tau181 status were examined. In the Tau Study, associations between PRSs and p-tau181 that was not controlled for Aβ42 status were assessed. Then, associations between PRSs and p-tau181 were investigated after controlling for Aβ42 status. In the Amyloid and Tau Study, associations between PRSs and biomarker positive participants vs. biomarker negative participants were assessed, i.e., Aβ42 and p-tau181 negative vs. Aβ42 and p-tau181 positive. For all three CSF studies, the data were studied at a whole-group level that was controlled for MMSE, then the whole group was stratified by APOE ε4 status, and lastly, the whole group was stratified by diagnosis. All hypotheses can be accepted partly.

5A.4.1. Amyloid Study

For whole group analysis, all PRSwithAPOE and APOEonlyPRS thresholds were associated significantly and positively with Aβ42 when p-tau181 was not controlled for. Therefore, high PRS was associated with Aβ42 positivity. There were small differences in the level of significance found when using PRSwithAPOE vs. APOEonlyPRS. For instance, when using Threshold 1, PRSwithAPOE improved the prediction of associations with Aβ42 than APOEonlyPRS; when using Threshold 5, APOEonlyPRS was better than PRSwithAPOE; when using Threshold 10, APOEonlyPRS was better than PRSwithAPOE. The top thresholds per PRS were PRSwithAPOE Threshold 1 and APOEonlyPRS Threshold 5. Additionally, the models explained 3.89% (PRSwithAPOE Threshold 1) and 3.90% (APOEonlyPRS Threshold 5) of the variance in Aβ42. Overall, PRSwithAPOE Threshold 1 predicted the associations the best.

When the whole group analysis was not controlled for p-tau181, all PRSwithAPOE and APOEonlyPRS thresholds were associated significantly with Aβ42. These were associated positively; high PRS was associated with Aβ42 positivity. However, the level of significance reduced for all PRSs at all thresholds when p-tau181 was controlled. Again, there were small differences in the level of significance found when using PRSwithAPOE vs. APOEonlyPRS. The same pattern was observed, i.e., when using Threshold 1, PRSwithAPOE was better than

APOEonlyPRS at predicting associations with Aβ42; when using Threshold 5, APOEonlyPRS was superior to PRSwithAPOE; when using Threshold 10, APOEonlyPRS was better than PRSwithAPOE. The top thresholds per PRS were PRSwithAPOE Threshold 1 and APOEonlyPRS Threshold 1. Additionally, the models explained 4.45% and 4.45% of the variation in Aβ42. Overall PRSwithAPOE Threshold 1 predicted the associations the most.

The whole group was then stratified by APOE ε4 status. In ε4 carriers, with the exception of PRSwithoutAPOE Threshold 10, all other PRSs and thresholds were associated significantly and positively with Aβ42 positivity when p-tau181 was not adjusted for. Therefore, high PRS was associated with Aβ42 positivity. For all thresholds, PRSwithAPOE improved the prediction of associations with Aβ42 the most, followed by APOEonlyPRS, and then PRSwithoutAPOE. In terms of the best thresholds per PRS, APOEonlyPRS Threshold 1 and PRSwithoutAPOE Threshold 1 were superior. The models explained 3.42% and 3.36% of the variation in Aβ42. Overall, all PRSwithAPOE thresholds were better than other PRSs, and no differences in the level of significance was found when using either of the three PRSwithAPOE thresholds. These models explained between 3.70% to 3.72% of the variance in Aβ42.

Then p-tau181 was controlled. In ε4 carriers, again excluding PRSwithoutAPOE Threshold 10, all other PRSs and thresholds were associated significantly with Aβ42. These were associated positively; high PRS was associated with Aβ42 positivity. The same pattern was observed, PRSwithAPOE was superior at identifying associations with Aβ42, followed by APOEonlyPRS, and then PRSwithoutAPOE. When PRSwithAPOE was used, the significance of the associations remained the same regardless of whether p-tau181 had or had not been controlled. When PRSwithoutAPOE Threshold 1 was used, the significance of the associations increased slightly when p-tau181 was controlled, whereas it reduced when PRSwithoutAPOE Threshold 5 was used. Similarly, when APOEonlyPRS thresholds were used, the significance of the associations increased slightly when p-tau181 was adjusted for. The top thresholds per PRS when controlling for p-tau181 were again APOEonlyPRS Threshold 1, PRSwithoutAPOE Threshold 1, and all three PRSwithAPOE thresholds. The models explained 4.03% and 3.42%, and between 3.97% to 4.03% of the variance in Aβ42. Again, more than when p-tau181 was not controlled.

Furthermore, the whole group was stratified by diagnosis. For CU participants, APOEonlyPRS thresholds were associated significantly and positively with Aβ42 when p-tau181 was not controlled. Thus, high PRS was associated with Aβ42 positivity. APOEonlyPRS Threshold 5 was

superior at predicting the associations and the model explained 1.85% of the Aβ42 variance, then Threshold 10, followed by Threshold 1. The same pattern was evident when p-tau181 had been controlled. However, adjusting for p-tau181 reduced the associations slightly, although they remained significant and positive, and the model improved by 0.05% and explained 1.90% of the variation in Aβ42.

For MCI patients, all PRSwithAPOE thresholds and APOEonlyPRS thresholds were associated significantly with Aβ42 when p-tau181 was not controlled. High PRS was associated with Aβ42 positivity and thus associated positively. For all thresholds, PRSwithAPOE improved the prediction of the associations with Aβ42 more than APOEonlyPRS. The top thresholds per PRS were, PRSwithAPOE Threshold 10 and APOEonlyPRS Threshold 5. Additionally, the models explained 3.59% and 3.69% of the variance. Overall, PRSwithAPOE Threshold 10 was superior at identifying associations. When p-tau181 was controlled, for MCI patients, all PRSwithAPOE thresholds and APOEonlyPRS thresholds remained associated significantly and positively with Aβ42. Again, at all thresholds, the level of significance of the associations was better when PRSwithAPOE was used rather than APOEonlyPRS. In this case, the best thresholds per PRS were PRSwithAPOE Threshold 1 and APOEonlyPRS Threshold 1. The models explained 4.50% and 3.68% of the variance in Aβ42. Overall, PRSwithAPOE Threshold 1 was better. Although, controlling for p-tau181 reduced the level of significance of these associations.

In AD dementia patients, only PRSwithoutAPOE Thresholds 1 and 5 were associated significantly and positively with Aβ42 when p-tau181 had not been controlled. PRSwithoutAPOE Threshold 1 identified associations more than Threshold 5, and the model explained 5.24% of the variance. However, when p-tau181 was adjusted for, the level of significance reduced when PRSwithoutAPOE Threshold 1 was used but increased when PRSwithoutAPOE Threshold 5 was used. In this instance, PRSwithoutAPOE Threshold 5 improved predictability of associations the most, and the model accounted for 5.55% of the variance in Aβ42.

5A.4.2. Tau Study

For whole group analysis, all PRSwithAPOE and APOEonlyPRS thresholds were associated significantly and positively with CSF p-tau181 when Aβ42 was not controlled. Therefore, high PRS was associated with p-tau181 positivity. There were small differences in the level of significance found when using PRSwithAPOE vs. APOEonlyPRS. APOEonlyPRS Threshold 1 was better than

PRSwithAPOE Threshold 1 at predicting the associations with p-tau181; APOEonlyPRS Threshold 5 was superior to PRSwithAPOE Threshold 5; APOEonlyPRS Threshold 10 was better than PRSwithAPOE Threshold 10 at identifying the associations. The best thresholds per PRS were PRSwithAPOE Threshold 10 and APOEonlyPRS Threshold 5. Additionally, the models explained 2.23% and 2.27% of the variance in p-tau181. Overall, APOEonlyPRS Threshold 5 was better slightly at identifying the associations. When the whole group analysis controlled for Aβ42, none of the above-mentioned associations remained significant. However, the models accounted for 2.96% of the variance in p-tau181 when PRSwithAPOE Threshold 10 was used and 2.97% when APOEonlyPRS Threshold 5 was used. Therefore, controlling for Aβ42 improved the models' ability to explain variation in p-tau181, although they did not lead to significant associations.

When the whole group was stratified by ε4 status, PRSs were not associated significantly with biomarker statuses.

Moreover, the whole group was stratified by diagnosis. In MCI patients, all PRSwithAPOE and APOEonlyPRS thresholds were associated significantly and positively with p-tau181 when Aβ42 had not been controlled. APOEonlyPRS Threshold 1 was superior to PRSwithAPOE Threshold 1 and PRSwithAPOE Threshold 5 was better than APOEonlyPRS Threshold 5. Whereas the level of significance obtained was the same regardless of whether PRSwithAPOE Threshold 10 or APOEonlyPRS Threshold 10 was used. The top thresholds per PRS were PRSwithAPOE Threshold 5 and, APOEonlyPRS Thresholds 5 and 10. The models explained 1.91%, 1.87%, and 1.86% of the variance in p-tau181. Overall, PRSwithAPOE Threshold 5 was best. However, when Aβ42 was controlled, these associations no longer retained any significance. Nonetheless, the models accounted for 2.85% of the variance in p-tau181 when PRSwithAPOE Threshold 5 was used, 2.84% when APOEonlyPRS Threshold 5 was used, and 2.84% when APOEonlyPRS Threshold 10 was used. Although controlling for Aβ42 diminished associations, it increased the models' capability of accounting for variation in p-tau181.

For AD dementia patients, all APOEonlyPRS thresholds were associated significantly and positively with p-tau181 when Aβ42 was not adjusted for. APOEonlyPRS Threshold 1 was best, and the model explained 3.41% of the variance in p-tau181; followed by Threshold 5, and then Threshold 10. However, these associations were no longer evident when controlling for Aβ42. Regardless, APOEonlyPRS Threshold 1 explained 3.58% of the variance in p-tau181 still, and,

therefore improved upon the variance accounted for, in comparison to APOEonlyPRS Threshold 1 where Aβ42 was not controlled.

5A.4.3. Amyloid and Tau Study

For whole group analysis, all PRSwithAPOE and APOEonlyPRS thresholds were associated significantly with CSF Aβ42 and p-tau181. Thus, high PRS was associated positively with both Aβ42 and p-tau181 positivity. Again, there were small differences between the levels of associations when PRSwithAPOE vs. APOEonlyPRS were used. APOEonlyPRS Threshold 1 was superior to PRSwithAPOE Threshold 1, APOEonlyPRS Threshold 5 was better than PRSwithAPOE Threshold 5, and APOEonlyPRS Threshold 10 was superior at finding the associations than PRSwithAPOE Threshold 10. The top thresholds per PRS were PRSwithAPOE Threshold 5 and APOEonlyPRS Threshold 5, and these explained 5.59% and 5.65% of the variance in Aβ42 and p-tau181. Overall, it was APOEonlyPRS Threshold 5.

When the whole group was stratified by ε4 status, PRSs were not associated significantly with p-tau181. This was regardless of whether Aβ42 had or had not been controlled for.

Moreover, the whole group was then stratified by diagnosis. In CU participants, all APOEonlyPRS thresholds were associated significantly and positively with biomarker positivity. Therefore, high PRS was associated with both Aβ42 and p-tau181 positivity. APOEonlyPRS Threshold 10 was associated the most and explained 5.21% of the Aβ42 and p-tau181 variance.

For MCI patients, all PRSwithAPOE and APOEonlyPRS thresholds were associated significantly and positively with biomarker positivity. Thus, high PRS was associated with Aβ42 and p-tau181 positivity. APOEonlyPRS Threshold 1 was better than PRSwithAPOE Threshold 1, whereas with Thresholds 5 and 10, PRSwithAPOE was superior to APOEonlyPRS. In terms of the top threshold per PRS, Threshold 5 for both PRSwithAPOE and APOEonlyPRS was best, and the models explained 4.90% and 4.80% of the variation in Aβ42 and p-tau181. Overall, PRSwithAPOE Threshold 5 identified associations the most.

5A.4.4. Interpretation

In the whole group, PRSwithAPOE and APOEonlyPRS were associated more with Aβ42 than with p-tau181. The difference observed when using PRSwithAPOE vs. APOEonlyPRS was small. However, the level of the significance was higher when associations were found using APOEonlyPRS than PRSwithAPOE. When p-tau181 was controlled, the association between PRSwithAPOE and Aβ42, and between APOEonlyPRS and Aβ42 reduced but remained significant. In contrast, when Aβ42 was controlled, the association between PRSwithAPOE and p-tau181 and between APOEonlyPRS and p-tau181 disappeared. These findings suggest that an interaction effect was present, whereby the effect of amyloid was stronger in comparison to p-tau181, and as suggested by Kumar et al. (2022), accumulation of p-tau181 was dependent upon Aβ. Similarly, in participants that were negative vs. positive in both biomarkers, there were small differences when using PRSwithAPOE vs. APOEonlyPRS. However, APOEonlyPRS was superior at predicting the associations. Nonetheless, these findings indicate that non-APOE SNPs are important too as they have small but significant effects on associations. It may be suggested that non-APOE SNPs reduce the likelihood of inflating results or decrease the chance of false-positive findings, that may be found when using APOE ε4 only.

In ε4 carriers, all three PRSs were associated more with Aβ42 than p-tau181. In fact, none of the PRSs were associated with p-tau181 whether Aβ42 was or was not controlled for. When p-tau181 was controlled for, the level of significance of the associations between PRS and Aβ42 remained constant when using PRSwithAPOE but increased when using APOEonlyPRS. Therefore, PRS had a greater effect on ε4 carriers; to the extent that adjusting for p-tau181 either did not impact the results, or they increased the level of significance. However, when using PRSwithoutAPOE, the association changed depending on the threshold used when p-tau181 was controlled for, i.e., the level of significance increased when PRSwithoutAPOE Threshold 1 was used, decreased with PRSwithoutAPOE Threshold 5, but remained unchanged when PRSwithoutAPOE Threshold 10 was used. This highlights that PRSwithoutAPOE is not reliable to study associations between PRS and amyloid. If researchers conduct similar analysis but use one PRSwithoutAPOE threshold only, they must select the threshold cautiously. Moreover, regardless of whether p-tau181 was or was not controlled for, the level of significance of the associations was greatest when using PRSwithAPOE, followed by APOEonlyPRS, and then PRSwithoutAPOE. Therefore, in comparison with using APOE SNPs alone, the combination of APOE-only SNPs plus non-APOE SNPs improved the predictability further. As no associations were found between PRSs and either Aβ42 or p-tau181 in ε4 non-carriers, this shows the extent to which ε4 carriership affects CSF biomarkers.

However, ε4 status does not seem to influence associations between PRSs and being negative vs. positive on both biomarkers.

In terms of diagnosis, for CU participants, APOEonlyPRS was associated with Aβ42. The level of the significance reduced when the model was adjusted for p-tau181, however, it remained significant. No associations were found with p-tau181. When participants were either negative on both biomarkers or positive on both biomarkers, associations were only found using APOEonlyPRS. Therefore, even in CU participants that are matched well with MCI and AD dementia patients in terms of age and education, APOE SNPs play an important role in Aβ42 status.

In MCI, PRSwithAPOE and APOEonlyPRS were associated more with Aβ42 than with p-tau181. When p-tau181 was controlled, the significance of the associations between PRSwithAPOE and Aβ42, and APOEonlyPRS and Aβ42, reduced slightly. Regardless of whether p-tau181 was or was not controlled for, the associations that were evident between PRS and Aβ42 improved significantly when PRSwithAPOE was used instead of APOEonlyPRS. Comparatively, when assessing p-tau181, the associations were almost the same whether PRSwithAPOE or APOEonlyPRS were used. However, controlling for Aβ42 resulted in these associations no longer being significant. Therefore, both biomarkers appear to be mediated by each other, i.e., Aβ42 is mediated by p-tau181 and vice versa. However, the effect of Aβ42 outweighs and diminishes any association that is found in p-tau181. Similarly, APOE SNPs plus non-APOE SNPs have an important role in individuals being either negative in both biomarkers or positive in both biomarkers, in comparison with using only APOE SNPs.

The majority of findings in the current work highlight that PRSwithAPOE and APOEonlyPRS are associated with Aβ42 more than p-tau181. This indicates that APOE SNPs plus non-APOE SNPs, and SNPs within the APOE region alone, influence CSF biomarkers. Therefore, APOE SNPs other than the known ε4 and ε2, effect AD pathology at large.

The APOE protein impacts accumulation of amyloid. This is thought to be due to processes involved in the production, fibrillisation, and clearance of amyloid, as well as the interaction between APOE, amyloid, tau, neuroinflammation and, neuronal structure and function. For instance, dysfunction of amyloid causes an increase in amyloid aggregation/plaques and reduces clearance of amyloid in the brain. Consequently, this results in a reduction of amyloid in

CSF (Liu et al., 2016; Young et al., 2023). In fact, Aβ42 is considered the least soluble Aβ peptide that is produced from APP (Shaw et al., 2009).

ε4 is associated with a greater prevalence of Aβ positivity and Aβ burden in the elderly (Lopresti et al., 2020). ε4 carriers reach the threshold for amyloid positivity 10-15 years before ε3ε3 carriers, whereas ε3ε3 carriers reach the threshold four years before ε2 carriers (Young et al., 2023). This evidence supports the results of the current research further. At the time point these data were collected cross-sectionally from ε4 carriers and non-carriers, ε4 carriers were most likely amyloid positive. Therefore, when stratifying the sample by ε4 status, PRSwithAPOE and APOEonlyPRS were associated with Aβ42 in ε4 carriers only. Of note, the damaging effect of ε4 on amyloid burden outweighs the protective effect of ε2. This is because ε4 influences the abovementioned mechanistic pathways more than ε2 (Young et al., 2023).

Specifically, ε4 dosage is found to be associated with increased cerebral amyloid deposition and reduced levels of CSF Aβ42, i.e., Aβ positivity, across the AD continuum (Liu et al., 2016). Thus, an inverse association is present between CSF Aβ42 levels and total Aβ in the brain (Vemuri et al., 2010). This suggests that these individuals may be close to, or have met, the threshold for CSF Aβ42 positivity, (i.e., reduced Aβ42 in the CSF). In the current research, where participants were categorised as amyloid negative vs. amyloid positive, PRSwithAPOE and APOEonlyPRS were associated positively with Aβ42 positivity (i.e., reduced Aβ42 in the CSF) when assessed as a whole cohort and individually as ε4 carriers vs. CU participants vs. MCI patients vs. AD dementia patients. Additionally, the level of CSF Aβ42 reduces in an ε4 dose-dependent manner, whereby ε4 homozygotes have lower Aβ42 than heterozygotes and ε4 non-carriers (Shaw et al., 2009).

Similarly, ε4 dosage is shown to increase CSF p-tau and tau in early-MCI and late-MCI (Liu et al., 2016). This may indicate that these patients may be close to, or have met, the threshold for CSF p-tau positivity. If this is the case, this is further evidence in support of the findings in the current research as PRS *with APOE* and *APOE only PRS* were associated positively with p-tau181 positivity when Aβ42 was not adjusted for in the whole group, in MCI, and in AD dementia patients. Comparatively, Tiraboschi et al. (2004) and Farfel et al. (2016) found that APOE was associated with tau levels in the presence of Aβ but not in the absence of Aβ.

However, Aβ and tau pathologies can co-exist (Busche and Hyman, 2020). The Amyloid Cascade Hypothesis highlights that Aβ triggers tau pathology, neuronal degeneration and death, and

eventually dementia (Hardy and Higgins, 1991; Blennow et al., 2010; Gulisano et al., 2018). Therefore, if Aβ causes tauopathy, then the finding that controlling for Aβ42 reduced or removed associations between PRS and p-tau181 in the current research makes sense logically, i.e., Aβ is the dominating protein.

Contrastingly, some researchers indicate that Aβ and tau pathologies work collaboratively. This may suggest that clinical trials that focus on tau only, need to be reconsidered. However, the literature on the synergistic effect of Aβ and tau is in its infancy and requires investigating further (Busche and Hyman, 2020). Of note, this may explain why associations between PRS and Aβ42 reduced slightly when adjusting for p-tau181, i.e., the interaction effect between both proteinopathies.

Although Aβ and tau are the hallmarks of AD pathology, other processes such as glial activation, and other proteins such as TDP-43 and α-synuclein need to be explored. Together, these may explain AD pathology better (Busche and Hyman, 2020). In due course, the Amyloid Cascade Hypothesis may require an update to include how other processes and other proteins influence amyloid and tau, the disease (Herrup, 2015), therapies, and genetic/phenotypic variation.

5A.4.5. Limitations and Strengths

The associations found between PRSs and CSF biomarkers should be interpreted with caution as the cut-offs, although in line with previous work, are arbitrary. This is an ongoing issue, hence, there are inconsistencies between published papers (Wang et al., 2024). However, associations (or lack of associations) provide useful insights into the heterogeneity of AD disease mechanisms and the challenges of *in vitro* analysis. Additionally, models were not adjusted for race due to the small number of non-white participants. Nevertheless, models were adjusted for ancestry using the top 10 genetic principal components. Where adequate numbers of non-white populations are available, researchers should control for race. Although ancestry influences disease processes and adds to the heterogeneity of sporadic AD further, the true impact in minority ancestries is not well known.

This research investigates many outcome measures that are central to the pathology of sporadic AD, i.e., Aβ42 and p-tau181, that are hallmarks of AD proteinopathy, whilst adjusting vs. not adjusting for the alternate biomarker. Of note, these are all in addition to the several PRSs and

thresholds, numerous variables that have been controlled for, and the various stratifications that have been conducted (as explained in detail in Chapter 4 (Experiment One)).

5A.4.6. Future Directions

A longitudinal study that investigates the prognostic value of PRSs directly on the continuum of sporadic AD. This would be the most suitable approach to understand the meaning of the associations observed, clearly. This will demonstrate whether PRSs can be used to predict longitudinal changes and disease progression using CSF biomarkers that form part of the clinical diagnosis of AD while patients are living.

5A.5. CONCLUSION

Generally, PRS is associated with Aβ42 more than p-tau181. The PRS thresholds that performed well consistently are, PRSwithAPOE Threshold 1 and APOEonlyPRS Threshold 5. Both PRSwithAPOE and APOEonlyPRS are associated significantly and positively with Aβ42. However, the level of significance reduces when the models are adjusted for p-tau181, although they remain significant. On the contrary, where associations are found using PRSwithAPOE and APOEonlyPRS, controlling for p-tau181 removes any significance. Additionally, the association between PRSs and biomarker-negative vs. biomarker-positive on both Aβ42 and p-tau181 appears to vary according to the stratification used. Similarly, PRSwithoutAPOE seems to be unreliable since the level of significance between the thresholds vary (i.e., increases, decreases, or remains the same) when Aβ42 models are adjusted for p-tau181 in comparison with models that are not controlled for p-tau181, particularly when examining ε4 carriers or AD dementia patients. Evidently, any associations that are significant and positive reliably are obtained using PRSwithAPOE and APOEonlyPRS in the current research, and both perform similarly. Overall, this research provides further evidence in support of the Amyloid Cascade Hypothesis since Aβ42 is found to have a crucial role in the AD continuum.

CHAPTER 5B

EXPERIMENT TWO PART B – ASSOCIATIONS BETWEEN POLYGENIC RISK SCORES AND CROSS-SECTIONAL COGNITIVE MARKERS

5B.1. INTRODUCTION

Cognition is considered to be highly polygenic (Habtewold et al., 2020). 11,600 SNPs from 709 genes, from 148 loci, are associated with general cognitive function (Davies et al., 2018). Specifically, 29 SNPs have been found to be associated with verbal memory (Arpawong et al., 2017), and 428 SNPs from 112 loci have been found to be associated with executive function (Hatoum et al., 2022). Therefore, using PRSs to study associations between genetics and cognition is valid.

The association between psychotic disorders and cognition has sparked interest in whether this is due to the polygenetic mechanism (Liebers et al., 2016). The association between PRSs and psychotic disorders, particularly schizophrenia, have been studied well. The consensus is that PRS for schizophrenia is associated with general cognition (Lencz et al., 2014; Habtewold et al., 2020; Trampush et al., 2017). Some patients with schizophrenia experience cognitive impairment specifically in the domains of memory, attention, and executive function (van Os and Kapur, 2009). In healthy older adults, PRS for schizophrenia has been found to be associated with decreased total cognition and is driven by decreased performance in attention and language domains, with small effects on the verbal memory domain (Liebers et al., 2016). Habtewold et al. (2020) assessed patients with schizophrenia. They found that PRS for schizophrenia was associated significantly with subtests from the Weschler Adult Intelligence Scale (WAIS-III), i.e., low digit-symbol substitution, information, calculation, and block design, with high Continuous Performance Test-variability, and with general cognitive function. However, PRS for schizophrenia was not associated with subtests from the Word Learning Task, i.e., immediate recall and delayed recall in patients. Thus, in schizophrenia, general cognitive function as well as the domains of attention, language, and executive function are impacted to a greater level than memory.

Of note, psychiatric disorders share a high degree of genetic correlation. Whereas, the genetic aetiology of neurodegenerative diseases, such as AD, are distinct from other neurological diseases or psychiatric disorders (The Brainstorm Consortium et al., 2018). Therefore, when utilising the PRS method, although numerous SNPs are being investigated simultaneously, the effect of individual SNPs are disease-specific as well. Highlighting this increases confidence scientifically that the disease at hand, i.e., AD, is truly being investigated, rather than other diseases that may have overlapping genetic architecture. However, the APOE gene specifically may be considered pleiotropic as it is found to influence AD as well as other neurodegenerative

diseases, such as dementia with Lewy bodies, Parkinson's disease, amyotrophic lateral sclerosis and multiple sclerosis (Fernandez-Calle et al., 2022).

A known non-modifiable risk factor for AD is increasing age. Age is found to influence the effect of APOE on AD risk, and the impact of polygenic architecture on AD risk. Therefore, age, APOE, and polygenetics all increase the heterogeneity of AD further. In individuals aged 60 to 79 years, heritability of AD explained by variants on chromosome 19 vs. other chromosomes is 9.6% vs. 12.2%. Whereas, in individuals aged ≥80 years, it is 0.7% vs. 23.4%. Therefore, chromosome 19 (that includes APOE) has a greater effect on younger older adults, whereas other chromosomes have a greater impact on the elderly (Lo et al., 2019). In relation to cognition, APOE ε4 is associated significantly with reduced total cognition, and PRS for AD is associated modestly with lower total cognition. Thus, the association was driven by a single variant in this study (Liebers et al., 2016).

Verbal memory decline is the earliest symptom in the AD continuum (Howieson et al., 1997). Association between autobiographical memory, as assessed via the Survey of Autobiographical Memory self-report measure, and PRS for AD has been studied in a sample of the PROTECT study participants aged 50+ years without diagnosis of dementia. In comparison with those with low PRS, high PRS was associated significantly with reduced autobiographical memory total score. This was driven by the semantic memory domain, i.e., high PRS was associated with low semantic memory (Lancaster et al., 2023). Similarly, PRS for AD, and the APOE ε4 SNP alone, have also been found to be associated strongly with verbal memory. Liebers et al. (2016). Eissman et al. (2023) showed that PRS for AD with APOE SNPs was associated with a memory composite score. However, when APOE SNPs were removed from the PRS, the association was no longer significant. Therefore, in this cohort of unimpaired and MCI patients aged 60+ years, APOE has a stronger effect on memory. Moreover, Elman et al. (2020) used data from participants that fulfilled ADNI criteria for aMCI (i.e., Weschler Logical Memory Story A delayed recall score of ≥1.5 SDs below the education-adjusted mean, subjective memory complaint, CDR score of 0.5, and MMSE score of ≥24), and had RAVLT data available. Elman et al. (2020) stratified aMCI patients by their performance on the RAVLT delayed recall task, i.e., RAVLT-normal (scoring ≥8) vs. RAVLT-impaired (scoring ≤7). Findings indicated that aMCI patients in the RAVLT-impaired group had higher PRSs than those in the RAVLT-normal group. Further, PRS excluding the APOE region was associated significantly with RAVLT groups even after controlling for APOE ε4 status. In line with previous work (Logue et al., 2018), here too, PRS excluding APOE provides information above and beyond

APOE variants. However, this is contrary to the results found by Eissman et al. (2023) and that may be due to the participant sample being tested (i.e., unimpaired and MCI vs. aMCI), and/or the memory test being used (i.e., specific vs. composite score). Of note, the additional criterion relating to memory impairment as detected by the RAVLT reduces false positives, increases diagnostic accuracy, and increases confidence that patients with true cognitive impairments are being investigated (Elman et al., 2020).

Additionally, associations between Digitised Clock Drawing Task performance and PRS with APOE ε4 have been examined using the Framingham Heart Study dataset. Thompson et al. (2023) gauged performance based on total scores and composite scores (i.e., command clock: drawing efficiency vs. simple motor vs. information processing vs. spatial reasoning; copy clock: drawing efficiency vs. simple motor vs. information processing vs. spatial reasoning). High PRS was found to be associated significantly with low Digitised Clock Drawing Task total score. High PRS was also associated strongly with low composite scores, specifically, drawing efficiency of the command clock, and poor information processing speed in the command and copy clock conditions. When repeating the analysis after removal of AD patients, the association between high PRS and low composite scores of drawing efficiency and information processing remained in the command condition only.

Moreover, hearing impairment is considered a major modifiable risk factor for AD. Using hearing aids is a protective factor. Ray, Popli, and Fell (2018) observed that hearing loss was associated with cognitive decline if left untreated, as it results in reduced cognitive stimulation (Livingston et al., 2020). Wang et al. (2022) found associations between PRS for hearing impairment and cognitive function, specifically in the domains of fluid intelligence, numeric memory, prospective memory, reaction time, and the pairs matching tests in the UK Biobank sample, and with the Montreal Cognitive Assessment (MoCA) in the Chinese Alzheimer's Biomarker and Lifestyle study sample.

Overall, there is a lack of clarity on whether PRSs can predict cognitive domains, and whether associations are due to PRSs with APOE, PRSs without APOE, SNPs on chromosome 19, or APOE ε4 only. There are also contradictions regarding the diagnostic group(s) the associations are found in.

5B.1.1. Aims, Objectives, and Hypotheses

Evidently, associations between PRS and cognitive markers need to be explored thoroughly, particularly due to the inconsistencies amongst previous literature.

The overall aim of Chapter 5B (Experiment Two Part B) is:

- To investigate whether PRSs for AD can predict AD-specific cognitive markers, cross-sectionally.

This aim will be explored using the following objective:

- To examine the associations between PRSs (i.e., PRSwithAPOE, PRSwithoutAPOE, and APOEonlyPRS) and cross-sectional cognitive markers (i.e., memory, executive function, language, and visuospatial competency), systematically.

It is hypothesised that:

1) The association between PRS and cognitive markers will be strongest for PRSwithAPOE, followed by APOEonlyPRS, and then PRSwithoutAPOE (whole group).
2) In APOE ε4 carriers, the association between PRS and cognitive biomarkers will be strongest for PRSwithAPOE, followed by APOEonlyPRS, and then PRSwithoutAPOE (APOE ε4 status).
3) In MCI and AD dementia patients, the association between PRS and cognitive markers will be strongest for PRSwithAPOE, followed by APOEonlyPRS, and then PRSwithoutAPOE, as compared with CU participants (diagnostic status).
4) In amyloid positive participants, the association between PRS and cognitive markers will be strongest for PRSwithAPOE, followed by APOEonlyPRS, and then PRSwithoutAPOE (amyloid status).

Therefore, this research will present a comprehensive and systematic examination of AD-specific cognitive markers. This will reflect the impact of genetic risk on symptomology across the continuum of sporadic AD.

5B.2. METHODS

5B.2.1. Participants

All 738 participants whose data were used in Chapter 4 (Experiment One) were used in the current research as well. The demographics and characteristics of these participants are shown in Table 5B.1.

Table 5B.1: Participant demographics and characteristics of the entire cohort (n = 738).

ENTIRE COHORT (n = 738)		
Age		
Age range	55 – 96 years	
Mean age	73.94 years	
Standard deviation	7.58 years	
Education		
Education range	6 – 20 years	
Mean education	16.09 years	
Standard deviation	2.75 years	
Cognitive Composite Scores		
Memory z-score range	-7.195322059 – 4.771449796	
Memory z-score mean	-1.292616035	
Memory z-score standard deviation	1.584914972	
Executive function z-score range	-6.236781562 – 2.751685996	
Executive function z-score mean	-0.902696668	
Executive function z-score standard deviation	1.497383029	
Language z-score range	-6.611175067 – 2.966976576	
Language z-score mean	-0.892687667	
Language z-score standard deviation	1.352509033	
Visuospatial z-score range	-6.489123576 – 0.776811447	
Visuospatial z-score mean	-0.462240831	
Visuospatial z-score standard deviation	1.391413636	
	n	**%**
Sex		
Male	407	55.15
Female	331	44.85
Race		
Native Americans	2	0.27
Asian	10	1.36
Hawaiian/Pacific	2	0.27
Black	24	3.25
White	691	93.63

Mixed	7	0.95
Unknown	2	0.27
APOE Genotype		
ε4ε4	53	7.18
ε3ε4	238	32.25
ε3ε3	366	49.59
ε2ε4	15	2.03
ε2ε3	65	8.81
ε2ε2	1	0.14
APOE ε4 Status		
ε4 Non-Carrier	432	58.54
ε4 Carrier	306	41.46
Amyloid Status		
Negative	266	36.04
Positive	472	63.96
Family History of Alzheimer's or Dementia		
Negative	34	4.61
Positive	704	95.39

APOE: apolipoprotein E. ε: epsilon.

5B.2.2. Genetic data and, Calculation of Polygenic Risk Scores and Polygenic Risk Score Thresholds

The steps described in Chapter 4 (Experiment One) were applied to the current Chapter for consistency. All three PRSs were used (i.e., PRSwithAPOE, PRSwithoutAPOE, and APOEonlyPRS) with all three thresholds (i.e., Thresholds 1, 5, and 10).

5B.2.3. Cognitive Markers

Four cognitive markers of AD were examined as composite scores – memory, executive function, language, and visuospatial abilities. These scores were found in the file titled "UW - Neuropsych Summary Scores [ADNI1,GO,2,3]" version "December 01, 2023" that was downloaded directly from ADNI on 19 August 2024. The four cognitive composite scores were labelled as "ADNI-MEM" (memory), "ADNI_EF2" (executive function), "ADNI-LAN" (language), and "ADNI-VS" (visuospatial) in the file. Note that the "Executive function composite score (2)" was used as the original Executive Function composite score overlapped with the Language composite score, i.e., both had Category Fluency (animals and vegetables). To ensure consistency for each participant across Experiments, the cognitive composite scores were taken from the date that was closest to the MRI visit that was used in Chapter 4 (Experiment One). This formed participants' "baseline" for the current work.

ADNI calculated the cognitive composite scores after carrying out statistical modelling using the Single Factor Model. These models accounted for different versions of the cognitive tests and for missing items. The criteria for an excellent fit were: Confirmatory Fit Index (CFI) > 0.95, Tucker Lewis Index (TLI) > 0.95, and Root Mean Squared Error of Approximation (RMSEA) < 0.05, and were used by ADNI. Where these findings were stated clearly by ADNI, the model fit the data well – model for Language using ADNI-1 data: TLI = 0.96, CFI = 0.97, and RMSEA = 0.039; model for Language using ADNI-2 and ADNI-GO data: TLI = 0.94, CFI = 0.93, and RMSEA = 0.028; model for Visuospatial: TLI = 0.97, CFI = 0.96, and RMSEA = 0.026 (ADNI, 2023).

The following assessments were used to calculate cognitive composite scores:

Memory composite score

- RAVLT: x5 trials, interference, immediate recall, 30-minute delay, and recognition
- Alzheimer's Disease Assessment Scale-Cognitive Subscale (ADAS-Cog): Word list learning (x3 trials), recall, and recognition
- Logical Memory: Immediate, and delayed
- MMSE: Object recall (ball; flag; tree)

Executive function composite score

- Wechsler Adult Intelligence Scale-Revision (WAIS-R): Digit symbol
- Digit Span: Forwards
- Digit Span: Backwards
- Trails: A
- Trails: B
- Clock Drawing
- ADAS: Number cancellation
- Montreal Cognitive Assessment (MoCA): Alternate trail making
- MoCA: Digit span forward
- MoCA: Digit span backward
- MoCA: Letters
- MoCA: Serial 7s
- MoCA: Abstraction (2 items)

Language composite score

- Category Fluency: Animals
- Category Fluency: Vegetables
- Boston Naming: Total
- ADAS-Cog: Following commands
- ADAS-Cog: Object naming
- ADAS-Cog: Ideation practice
- MMSE: Object naming (watch; pencil)
- MMSE: Repeating a sentence
- MMSE: Reading a sentence
- MMSE: Writing a sentence

- MMSE: Following a series of instructions
- MoCA: Letter F fluency
- MoCA: Animal naming (lion; camel; rhino)
- MoCA: Sentence repetition (2 tasks)

Visuospatial composite score

- Clock Copy: Circle
- Clock Copy: Symmetry
- Clock Copy: Numbers
- Clock Copy: Hands
- Clock Copy: Time
- ADAS-Cog: Constructional praxis
- MMSE: Copy design

The WAIS-R was developed by Wechsler in 1981 to test intellectual functioning and cognitive abilities in adults using 11 subsets: six verbal tests and five performance tests. Scores from these subsets are used to calculate a verbal intelligence quotient, performance intelligence quotient, and an overall intelligence quotient (Crawford et al., 1989).

The MMSE was devised by Folstein, Folstein, and McHugh (1975). The 30-point scale measures severity of cognitive impairment. It tests global cognition: memory, attention, orientation, language, and visuospatial abilities. The MMSE is useful for examining cognitive change over time and measuring the effect of treatment intervention on cognition (Bernard and Goldman, 2010; Ferhadieh et al., 2024).

MoCA was developed by Nasreddine in 2005. The 30-point scale assesses short-term memory recall, visuospatial abilities, executive function, attention, working memory, language, and orientation. It has high sensitivity and specificity at identifying individuals that are CU, and those with MCI or mild AD dementia. The MoCA is sensitive particularly to detecting MCI, more so than the MMSE (Nasreddine et al., 2005).

The BNT was devised by Kaplan, Goodglass, and Weintraub (1983). The 60-item battery examines visual naming ability. It was originally developed to assess aphasia. However, it is used widely to

measure anomic aphasia in dementia and related diseases, and to evaluate progression over time (Nebreda et al., 2010; Pedraza et al., 2009).

ADAS was developed by Rosen, Mohs, and Davis (1984) to test for severe cognitive impairment in dementia and consists of a 150-point scale. However, the ADAS-Cog subscale was extended for use in pre-dementia, particularly MCI. ADAS-Cog has a 70-point scale to examine memory, language, and praxis, and the efficacy of treatment interventions (Kueper, Speechley, and Montero-Odasso, 2018; Farhadieh et al., 2024).

The RAVLT was devised by Rey (1964) for testing episodic memory in dementia and pre-dementia. It is used commonly as an early marker of AD in those with memory complaints and is useful at differentiating AD from psychiatric disorders as well (Moradi et al., 2017).

Logical Memory is a subtest of the Wechsler Memory Scale that was developed by Wechsler (1945). Logical Memory assesses verbal episodic memory: immediate recall, delayed recall, and delayed recognition. The narrative that individuals learn during this task is sensitive to measure cognitive decline. It is not only useful for use in AD patients, but also detects change in MCI, can distinguish aMCI from healthy ageing, can predict AD from MCI, and can differentiate AD from dementia with Lewy bodies and vascular dementia (Ahn et al., 2019).

5B.2.4. Statistical Analysis

For the current research, all cognitive composite scores were z-transformed for interpretability before being analysed. Data were analysed on IBM SPSS Statistics v29.0.1.0.

All variables that were used as covariates in Chapter 4 (Experiment One), other than those relating to neuroimaging features (i.e., scanner strength, and total intracranial volume), were used as covariates in the current research for consistency, i.e., age, sex, education, family history, amyloid status, x10 genetic principal components, and MMSE.

Multiple hierarchical linear regression analyses were performed to investigate whether there are associations between PRS (independent / predictor variable) and cognition (dependent / outcome variable), i.e., memory, executive function, language, and visuospatial abilities. *P* was significant at the 0.05 level.

(A) Whole-group analysis, for each cognitive domain separately

• Model 1: Age, sex, education, family history, amyloid status, x10 genetic principal components, and MMSE.

• Model 2: All variables in Model 1, plus PRS.

Analyses were completed using PRSwithAPOE Thresholds 1, 5, and 10 separately, APOEonlyPRS Thresholds 1, 5, and 10 separately, and then PRSwithoutAPOE Thresholds 1, 5, and 10 separately.

(n = 738).

(B) Stratification by APOE ε4 status, for each cognitive domain separately

• Model 1: Age, sex, education, family history, amyloid status, x10 genetic principal components, and MMSE.

• Model 2: All variables in Model 1, plus PRS.

Analyses were completed using PRSwithAPOE Thresholds 1, 5, and 10 separately, APOEonlyPRS Thresholds 1, 5, and 10 separately, and then PRSwithoutAPOE Thresholds 1, 5, and 10 separately.

(ε4 non-carriers, n = 432; ε4 carriers, n = 306).

(C) Stratification by diagnostic status, for each cognitive domain separately

• Model 1: Age, sex, education, family history, amyloid status, x10 genetic principal components, and MMSE.

• Model 2: All variables in Model 1, plus PRS.

Analyses were completed using PRSwithAPOE Thresholds 1, 5, and 10 separately, APOEonlyPRS Thresholds 1, 5, and 10 separately, and then PRSwithoutAPOE Thresholds 1, 5, and 10 separately.

(CU, n = 184; MCI, n = 416; AD dementia, n = 138).

(D) Stratification by amyloid status, for each cognitive domain separately

• Model 1: Age, sex, education, family history, x10 genetic principal components, and MMSE (covariates).

• Model 2: All variables in Model 1, plus PRS.

Analyses were completed using PRSwithAPOE Thresholds 1, 5, and 10 separately, APOEonlyPRS Thresholds 1, 5, and 10 separately, and then PRSwithoutAPOE Thresholds 1, 5, and 10 separately.

(Amyloid positive, n = 266; amyloid negative, n = 472).

FDR correction was applied where associations between PRS and at least one cognitive composite score was significant. *P* was significant at the 0.05 FDR-corrected level.

5B.3. RESULTS

5B.3.1. (A) Whole group

PRSwithAPOE:

Whole group analysis using PRSwithAPOE showed that Threshold 1 was associated significantly with the memory composite score (p = 0.003) and the visuospatial composite score (p = 0.029); Thresholds 5 and 10 were associated significantly with the memory composite score only (p = 0.003 and p = 0.006, respectively). These were all associated negatively, i.e., high PRS, low cognitive composite score. Associations between PRSwithAPOE and memory retained significance after FDR correction, (PRSwithAPOE Thresholds 1 and 5: p = 0.012; PRSwithAPOE Threshold 10: p = 0.024). No other associations were observed. See Table 5B.2, Figure 5B.1, Figure 5B.2, and Appendix E2 Table E2.1.

PRSwithoutAPOE:

PRSwithoutAPOE thresholds were not associated with any of the cognitive composite scores (Appendix E2 Table E2.1).

APOEonlyPRS:

Whole group analysis using APOEonlyPRS indicated that Thresholds 1, 5, and 10 were associated significantly with the memory composite score, (p = 0.003, p = 0.002, and p = 0.006, respectively), and retained significance after FDR correction, (p = 0.012, p = 0.008, and p = 0.024, respectively). These were all associated inversely. No other associations were found. See Table 5B.2, Figure 5B.1, and Appendix E2 Table E2.1.

Table 5B.2: Associations between PRSs and cross-sectional cognitive composite scores in the whole group.

PRS & Threshold	R Square (Model 1)	R Square (Model 2)	R Square Change	Sig. F Change (Model 2)	Standardised beta of PRS
Memory composite score					
PRSwithAPOE					
1	0.566	0.571	0.005	0.003*	-0.080
5	0.566	0.571	0.005	0.003*	-0.080
10	0.566	0.571	0.005	0.006**	-0.074
APOEonlyPRS					
1	0.566	0.572	0.005	0.003*	-0.080
5	0.566	0.572	0.006	0.002***	-0.081
10	0.566	0.571	0.005	0.006**	-0.074
Visuospatial composite score					
PRSwithAPOE					
1	0.242	0.247	0.005	0.029	-0.078

APOE: apolipoprotein E. PRS: polygenic risk score.

Asterisks indicate associations that withstood corrective measures (false discovery rate) at the 0.05 level: *0.012; **0.024; ***0.008.

Memory (whole group; PRSwithAPOE)

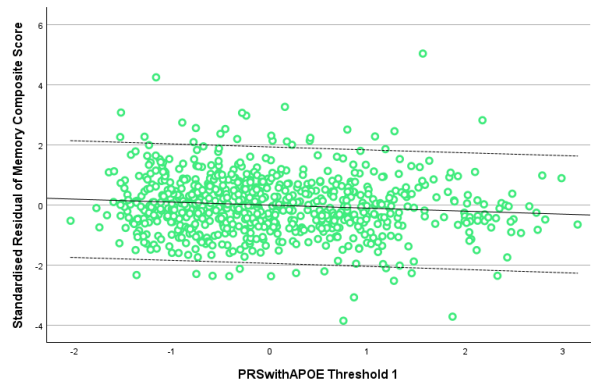

R^2 = 0.010.
Memory composite score = 3.67E – 4 – 0.10 * PRSwithAPOE T1.

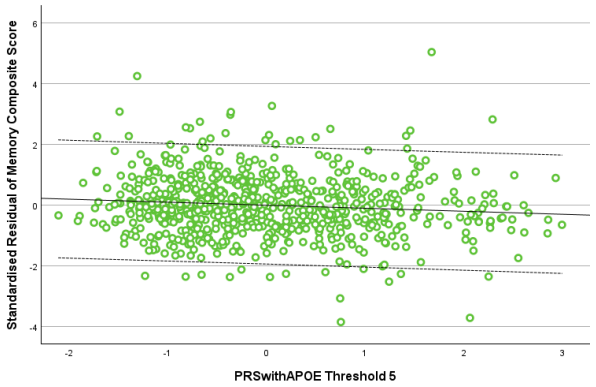

R^2 = 0.010.
Memory composite score = 1.22E – 4 – 0.10 * PRSwithAPOE T5.

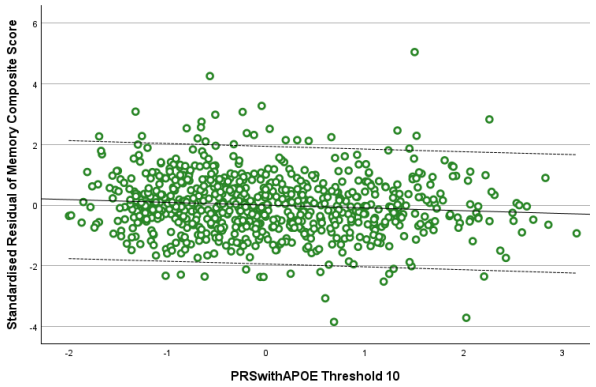

R^2 = 0.009.
Memory composite score = 9.54E – 5 – 0.09 * PRSwithAPOE T10.

Memory (whole group; APOEonlyPRS)

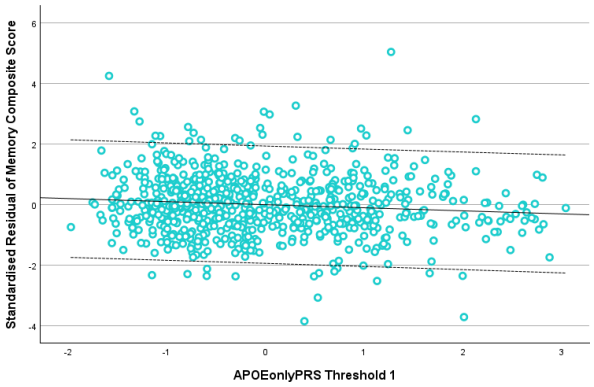

R^2 = 0.011.
Memory composite score = 4.79E – 4 – 0.10 * APOEonlyPRS T1.

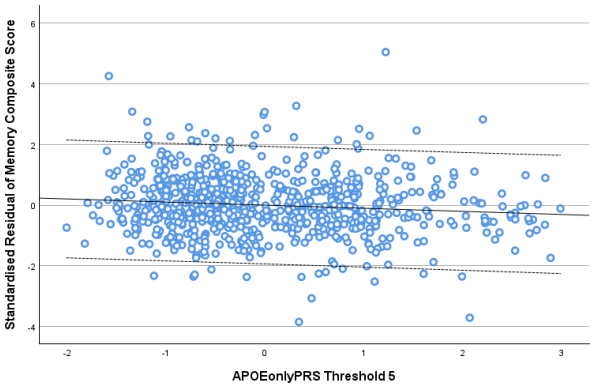

R^2 = 0.011.
Memory composite score = 4.5E – 4 – 0.10 * APOEonlyPRS T5.

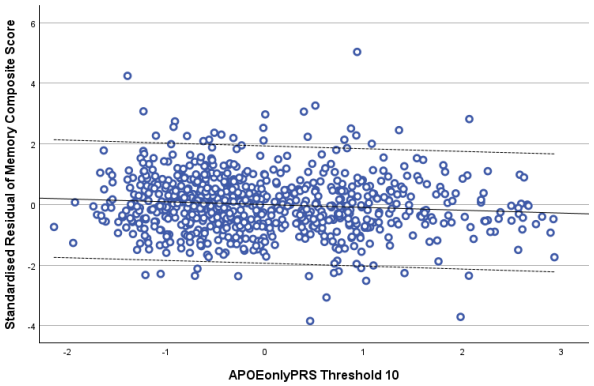

R^2 = 0.009.
Memory composite score = 2.63E – 4 – 0.09 * APOEonlyPRS T10.

(T: threshold).

Figure 5B.1: Scatterplots to visualise the associations between PRSwithAPOE thresholds, APOEonlyPRS thresholds, and memory composite scores in the whole group.

Note, the scatterplots are for visualisation purposes only. The scatterplots show the residualised variable (i.e., memory composite score) modelled as a function of PRS using linear regression. The X axis shows the PRS of interest and the Y axis represents the standardised residual of the memory composite score after all covariates have been regressed out.

Visuospatial (whole group; PRSwithAPOE)

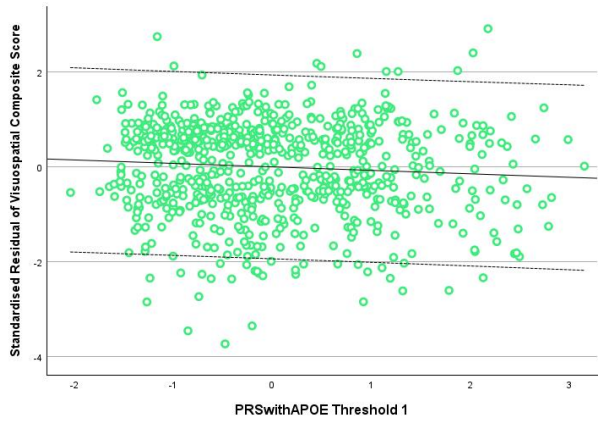

R^2 = 0.006.
Visuospatial composite score = 2.69E – 4 – 0.07 * PRSwithAPOE T1.

Figure 5B.2: Scatterplot to visualise the association between PRSwithAPOE Threshold 1 and visuospatial composite scores in the whole group.

Note, the scatterplots are for visualisation purposes only. The scatterplots show the residualised variable (i.e., visuospatial composite score) modelled as a function of PRS using linear regression. The X axis shows the PRS of interest and the Y axis represents the standardised residual of the visuospatial composite score after all covariates have been regressed out.

5B.3.2. (B) Stratification by APOE ε4 status

PRSwithAPOE:

In ε4 carriers, PRSwithAPOE Threshold 1 and 5 were associated significantly with the visuospatial composite score, (p = 0.010 and p = 0.027, respectively). Both were associated negatively. However, only PRSwithAPOE Threshold 1 remained significant after FDR correction, (p = 0.040). No other associations were evident. See Table 5B.3, Figure 5B.3, and Appendix E2 Table E2.2. No associations were observed in ε4 non-carriers (Appendix E2 Table E2.3).

PRSwithoutAPOE:

PRSwithoutAPOE thresholds were not associated with any cognitive composite score. See Appendix E2 Table E2.2 (ε4 carriers) and Appendix E2 Table E2.3 (ε4 non-carriers).

APOEonlyPRS:

In ε4 carriers, APOEonlyPRS Thresholds 1, 5, and 10 were associated significantly with the visuospatial score, (p = 0.028, p = 0.031, and p = 0.026, respectively). Again, these were all associated inversely. However, these did not survive FDR corrective measures. No other associations were apparent. See Table 5B.3, Figure 5B.3, and Appendix E2 Table E2.2. No associations were evident in ε4 non-carriers (Appendix E2 Table E2.3).

Table 5B.3: Associations between PRSs and cross-sectional visuospatial composite scores in ε4 carriers.

PRS & Threshold	R Square (Model 1)	R Square (Model 2)	R Square Change	Sig. F Change (Model 2)	Standardised beta of PRS
Visuospatial composite score					
PRSwithAPOE					
1	0.317	0.333	0.016	0.010*	-0.135
5	0.317	0.329	0.012	0.027	-0.116
APOEonlyPRS					
1	0.317	0.329	0.012	0.028	-0.113
5	0.317	0.329	0.011	0.031	-0.110
10	0.317	0.329	0.012	0.026	-0.114

APOE: apolipoprotein E. PRS: polygenic risk score.

*Association withstood corrective measures (false discovery rate) at the 0.05 level: 0.040.

Visuospatial (ε4 carriers; PRSwithAPOE)

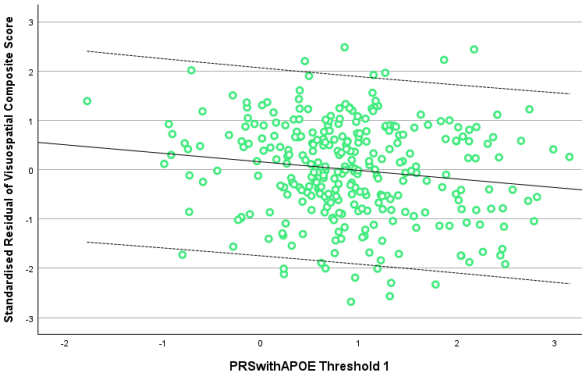

R^2 = 0.021.
Visuospatial composite score = 0.16 – 0.17 * PRSwithAPOE T1.

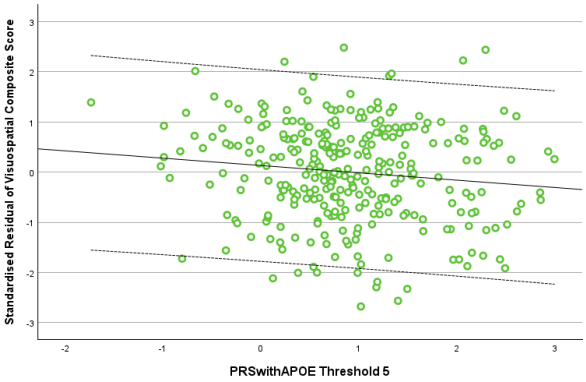

R^2 = 0.015.
Visuospatial composite score = 0.13 – 0.15 * PRSwithAPOE T5.

Visuospatial (ε4 carriers; APOEonlyPRS)

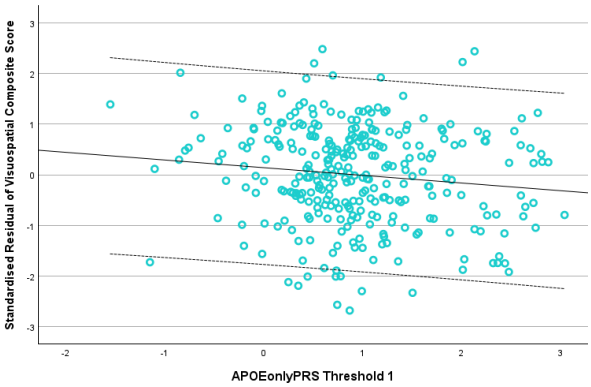

R^2 = 0.015.
Visuospatial composite score = 0.14 – 0.15 * APOEonlyPRS T1.

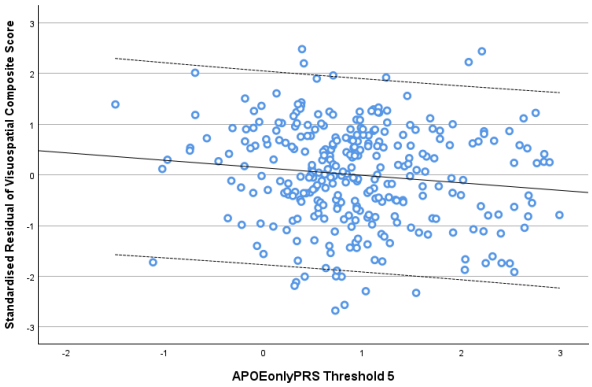

R^2 = 0.015.
Visuospatial composite score = 0.14 – 0.15 * APOEonlyPRS T5.

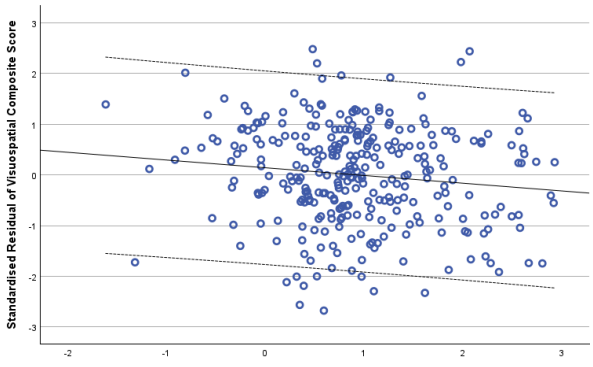

R^2 = 0.016.
Visuospatial composite score = 0.14 – 0.15 * APOEonlyPRS T10.

(T: threshold).

Figure 5B.3: Scatterplots to visualise the associations between PRSwithAPOE thresholds, APOEonlyPRS thresholds, and visuospatial composite scores in ε4 carriers.

Note, the scatterplots are for visualisation purposes only. The scatterplots show the residualised variable (i.e., visuospatial composite score) modelled as a function of PRS using linear regression. The X axis shows the PRS of interest and the Y axis represents the standardised residual of the visuospatial composite score after all covariates have been regressed out.

5B.3.3. (C) Stratification by diagnostic status

PRSwithAPOE:

In the AD dementia group, PRSwithAPOE Thresholds 1, 5, and 10 were associated significantly with the executive function composite score, (p = 0.029, p = 0.020, and p = 0.008, respectively). These were all associated positively, i.e., high PRS, high executive function composite score. However, only PRSwithAPOE Threshold 10 survived FDR correction, (p = 0.032). See Table 5B.4, Figure 5B.4, and Appendix E2 Table E2.4. No associations were observed in CU (Appendix E2 Table E2.5) or MCI groups (Appendix E2 Table E2.6).

Exploratory analyses were conducted to examine whether these associations were driven by ε4 carriers. Stratifying AD dementia patients by ε4 status (AD ε4 non-carriers, n = 42; AD ε4 carriers, n = 96) did not yield any associations between PRSwithAPOE and executive function. Rather, in AD dementia patients that were ε4 carriers, PRSwithAPOE Thresholds 1, 5, and 10 were associated significantly and negatively with the visuospatial score (p = 0.008, p = 0.010, and p = 0.015, respectively). However, only PRSwithAPOE Threshold 1 (p = 0.032) and Threshold 5 (p = 0.040) remained significant after FDR corrections. See Appendix E2 Table E2.7 (AD dementia ε4 non-carriers) and Table E2.8 (AD dementia ε4 carriers).

PRSwithoutAPOE:

In MCI patients, PRSwithoutAPOE Threshold 10 was associated significantly with the executive function composite score (p = 0.046). This association was positive. However, after FDR correction, this association was no longer significant. No other associations were found. Consult Table 5B.4, Figure 5B.5, and Appendix E2 Table E2.6

Exploratory analysis where MCI patients were stratified by ε4 status (MCI ε4 non-carriers, n = 250; MCI ε4 carriers, n = 166) did not result in any associations being significant. See Appendix E2 Table E2.9 (MCI ε4 non-carriers) and Table E2.10 (MCI ε4 carriers)

APOEonlyPRS:

In AD dementia patients, APOEonlyPRS Thresholds 1, 5, and 10 were associated significantly with the executive function composite score (p = 0.018, p = 0.019, and p = 0.029, respectively). These were associated positively. However, they did not survive corrections for multiple comparisons

using FDR. No other associations were evident. Refer to Table 5B.4, Figure 5B.4, and Appendix E2 Table E2.4.

Further analyses were conducted to examine whether these associations were driven by ε4 carriers. No associations were found with executive function when diagnostic statuses were stratified by ε4 status. In fact, in AD dementia patients that were ε4 carriers, APOEonlyPRS Thresholds 1, 5, and 10 were associated significantly and inversely with the language composite score ($p = 0.034$, $p = 0.043$, and $p = 0.042$, respectively). See Appendix E2 Table E2.7 (AD dementia ε4 non-carriers) and Table E2.8 (AD dementia ε4 carriers). Therefore, an additional analysis was carried out to investigate whether this association may be explained by tau positivity. However, stratification by tau status did not shed further light on this. The above-mentioned further analyses did not survive FDR corrective measures.

Additionally, in AD dementia patients that were ε4 carriers, APOEonlyPRS Thresholds 1, 5, and 10 were associated significantly with the visuospatial score ($p = 0.022$, $p = 0.022$, and $p = 0.016$, respectively). These were associated negatively. However, they did not survive FDR correction. See Appendix E2 Table E2.7 (AD dementia ε4 non-carriers) and Table E2.8 (AD dementia ε4 carriers).

Table 5B.4: Associations between PRSs and cross-sectional executive function composite scores according to diagnostic status.

PRS & Threshold	R Square (Model 1)	R Square (Model 2)	R Square Change	Sig. F Change (Model 2)	Standardised beta of PRS
Executive function composite score					
PRSwithAPOE in AD dementia					
1	0.405	0.429	0.024	0.029	0.178
5	0.405	0.433	0.027	0.020	0.191
10	0.405	0.441	0.035	0.008*	0.215
APOEonlyPRS in AD dementia					
1	0.405	0.434	0.028	0.018	0.194
5	0.405	0.433	0.028	0.019	0.192
10	0.405	0.430	0.024	0.029	0.179
PRSwithoutAPOE in MCI					
10	0.353	0.360	0.007	0.046	0.087

APOE: apolipoprotein E. PRS: polygenic risk score.

*Association withstood corrective measures (false discovery rate) at the 0.05 level: 0.032.

Executive function (AD dementia; PRSwithAPOE)

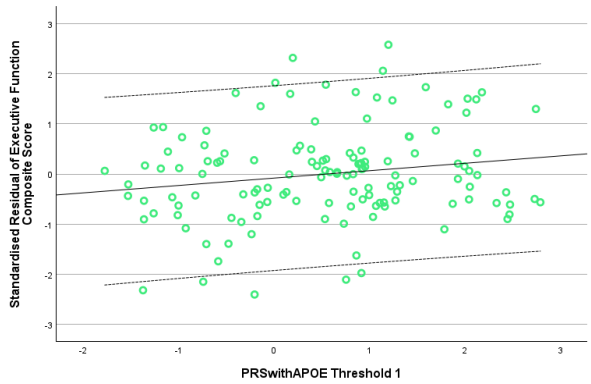

R^2 = 0.031.
Executive function composite score = -0.08 + 0.15 * PRSwithAPOE T1.

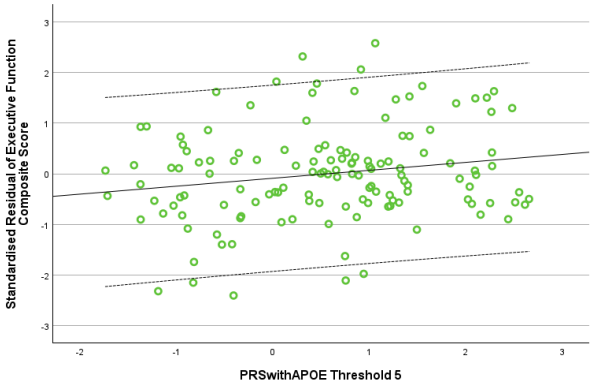

R^2 = 0.035.
Executive function composite score = -0.09 + 0.16 * PRSwithAPOE T5.

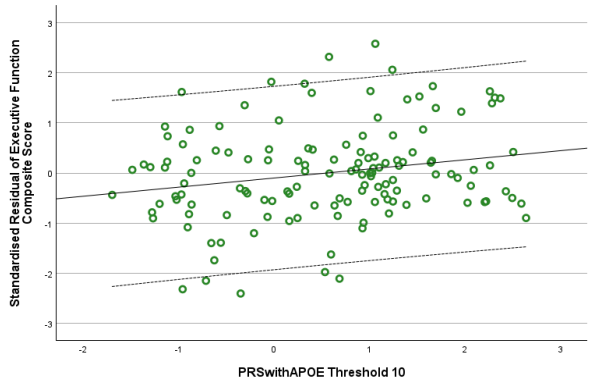

R^2 = 0.045.
Executive function composite score = -0.10 + 0.18 * PRSwithAPOE T10.

Executive function (AD dementia; APOEonlyPRS)

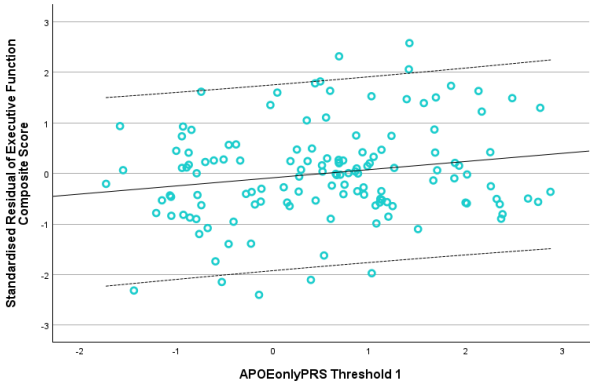

R^2 = 0.035.
Executive function composite score = -0.09 + 0.16 * APOEonlyPRS T1.

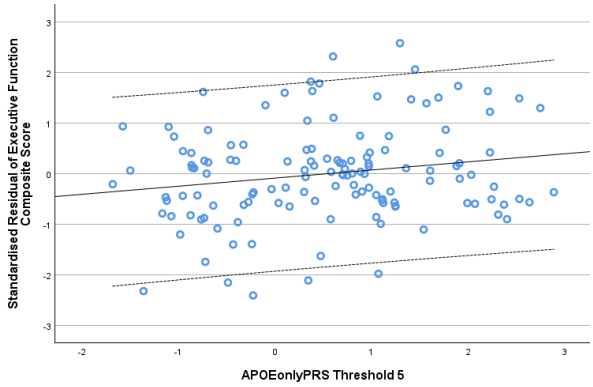

R^2 = 0.035.
Executive function composite score = -0.09 + 0.16 * APOEonlyPRS T5.

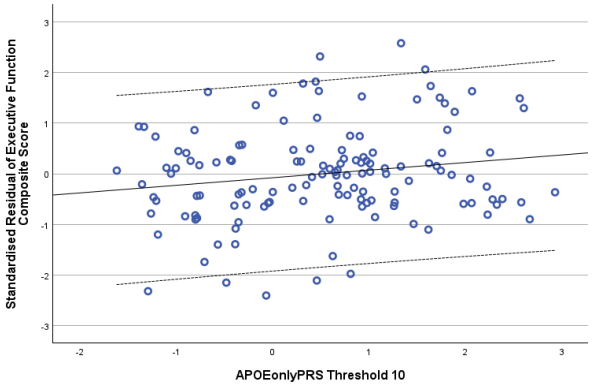

R^2 = 0.030.
Executive function composite score = -0.08 + 0.15 * APOEonlyPRS T10.

(T: threshold).

Figure 5B.4: Scatterplots to visualise the associations between PRSwithAPOE thresholds, APOEonlyPRS thresholds, and executive function composite scores in AD dementia patients.

Note, the scatterplots are for visualisation purposes only. The scatterplots show the residualised variable (i.e., executive function composite score) modelled as a function of PRS using linear regression. The X axis shows the PRS of interest and the Y axis represents the standardised residual of the executive function composite score after all covariates have been regressed out.

Executive function (MCI; PRSwithoutAPOE)

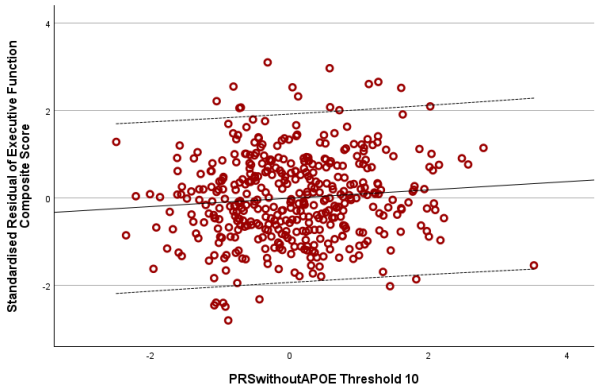

R^2 = 0.009.

Executive function composite score = -5.01E – 3 + 0.09 * PRSwithoutAPOE T10.

(T: threshold).

Figure 5B.5: Scatterplot to visualise the association between PRSwithoutAPOE Threshold 10 and executive function composite scores in MCI patients.

Note, the scatterplots are for visualisation purposes only. The scatterplots show the residualised variable (i.e., executive function composite score) modelled as a function of PRS using linear regression. The X axis shows the PRS of interest and the Y axis represents the standardised residual of the executive function composite score after all covariates have been regressed out.

5B.3.4. (D) Stratification by amyloid status

PRSwithAPOE:

In amyloid positive participants, PRSwithAPOE Thresholds 1, 5, and 10 were associated significantly with the memory composite score, (p = 0.005, p = 0.004, and p = 0.010, respectively) and survived FDR corrective methods, (p = 0.020, p = 0.016, and p = 0.040, respectively). See Table 5B.5, Figure 5B.6, and Appendix E2 Table E2.11. In amyloid negative participants, PRSwithAPOE Threshold 5 was associated significantly with the visuospatial composite score, (p = 0.034), however, this did not survive FDR correction. These were all associated negatively. No other associations were apparent. See Table 5B.6, Figure 5B.7, and Appendix E2 Table E2.12.

Exploratory analyses were conducted to examine whether the above associations were driven by ε4 carriers, (amyloid positive ε4 non-carriers, n = 212; amyloid positive ε4 carriers, n = 260; amyloid negative ε4 non-carriers, n = 220; amyloid negative ε4 carriers, n = 46). This was the case indeed for amyloid negative participants where PRSwithAPOE Threshold 1 was used (p = 0.050); the association was both significant and related inversely. See Appendix E2 Table E2.13 (amyloid negative ε4 carriers) and Table E2.14 (amyloid negative ε4 non-carriers). However, in amyloid positive participants, stratifying amyloid status by ε4 status did not result in associations with memory. Rather, in amyloid positive participants that were ε4 carriers, PRSwithAPOE Thresholds 1 and 5 were associated significantly and negatively with the visuospatial composite score (p = 0.018 and p = 0.045). However, these did not withstand FDR corrective measures. See Appendix E2 Table E2.15 (amyloid positive ε4 carriers) and Table E2.16 (amyloid positive ε4 non-carriers).

PRSwithoutAPOE:

PRSwithoutAPOE was not associated with any of the cognitive composite scores. Consult Appendix E2 Table E2.11 (amyloid positive) and Appendix E2 Table E2.12 (amyloid negative).

APOEonlyPRS:

In amyloid positive participants, APOEonlyPRS Thresholds 1, 5, and 10 were associated significantly with the memory composite score, (p = 0.005, p = 0.005, and p = 0.010, respectively), and survived FDR corrections, (p = 0.020, p = 0.020, and p = 0.040, respectively). These were associated inversely, see Table 5B.5 and Figure 5B.6. No other associations were found in amyloid positive participants (Appendix E2 Table E2.11) and no associations were evident in amyloid negative participants (Appendix E2 Table E2.12).

Additional exploratory analyses showed that this association was no longer significant when stratifying amyloid status further by ε4 status. In fact, in amyloid positive participants that were ε4 carriers, APOEonlyPRS Thresholds 1, 5, and 10 were associated significantly with visuospatial scores ($p = 0.039$, $p = 0.047$, and $p = 0.040$, respectively). These were again associated negatively (Appendix E2 Table E2.15), however, they did not retain significance after FDR corrections. No associations were observed in amyloid positive ε4 non-carriers (Appendix E2 Table E2.16).

Table 5B.5: Associations between PRSs and cross-sectional memory composite scores in amyloid positive participants.

PRS & Threshold	R Square (Model 1)	R Square (Model 2)	R Square Change	Sig. F Change (Model 2)	Standardised beta of PRS
Memory composite scores					
PRSwithAPOE					
1	0.572	0.580	0.007	0.005*	-0.091
5	0.572	0.580	0.008	0.004**	-0.093
10	0.572	0.578	0.006	0.010***	-0.084
APOEonlyPRS					
1	0.572	0.579	0.007	0.005*	-0.091
5	0.572	0.580	0.008	0.005*	-0.092
10	0.572	0.578	0.006	0.010***	-0.083

APOE: apolipoprotein E. PRS: polygenic risk score.

Asterisks indicate associations that withstood corrective measures (false discovery rate) at the 0.05 level: *0.020; **0.016; ***0.040.

Table 5B.6: Associations between PRSwithAPOE Threshold 5 and cross-sectional visuospatial composite scores in amyloid negative participants.

PRS & Threshold	R Square (Model 1)	R Square (Model 2)	R Square Change	Sig. F Change (Model 2)	Standardised beta of PRS
Visuospatial composite scores					
PRSwithAPOE					
5	0.184	0.499	0.015	0.034	-0.123

PRS: polygenic risk score.

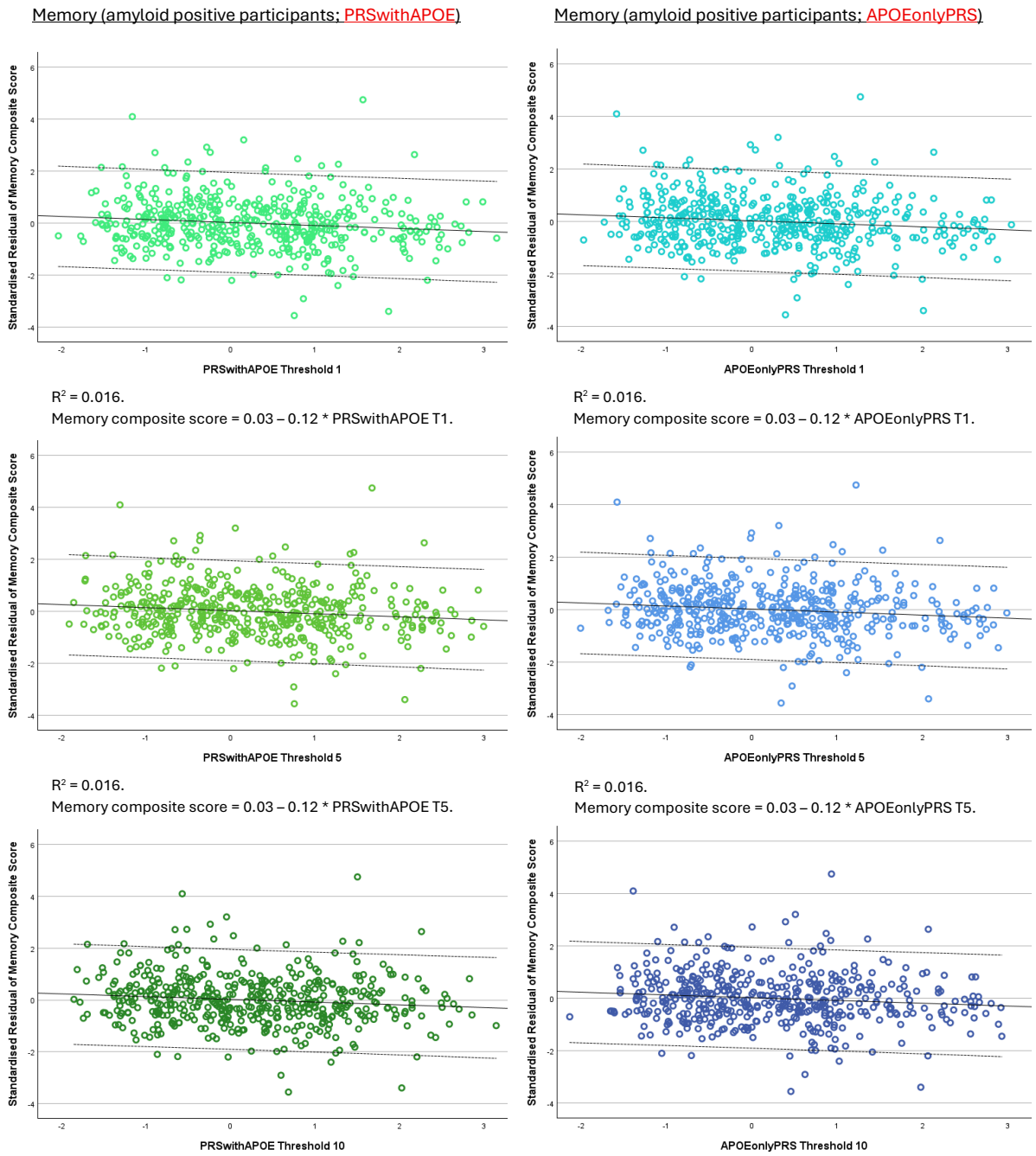

Figure 5B.6: Scatterplots to visualise the associations between PRSwithAPOE thresholds, APOEonlyPRS thresholds, and memory composite score in amyloid positive participants.

Note, the scatterplots are for visualisation purposes only. The scatterplots show the residualised variable (i.e., memory composite score) modelled as a function of PRS using linear regression. The X axis shows the PRS of interest and the Y axis represents the standardised residual of the memory composite score after all covariates have been regressed out.

Visuospatial (amyloid negative; PRSwithAPOE)

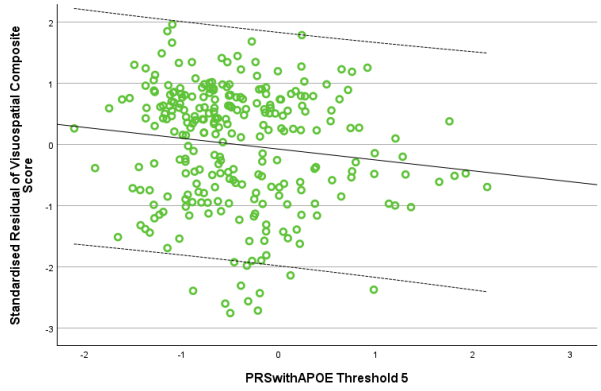

R^2 = 0.017.

Visuospatial composite score = 0.08 – 0.18 * PRSwithAPOE T5.

(T: threshold).

Figure 5B.7: Scatterplot to visualise the association between PRSwithAPOE Threshold 5 and visuospatial composite scores in amyloid negative participants.

Note, the scatterplots are for visualisation purposes only. The scatterplots show the residualised variable (i.e., visuospatial composite score) modelled as a function of PRS using linear regression. The X axis shows the PRS of interest and the Y axis represents the standardised residual of the visuospatial composite score after all covariates have been regressed out.

5B.4. DISCUSSION

Associations between PRS for AD and cognitive composite scores were studied, specifically a memory composite score, executive function composite score, language composite score, and a visuospatial composite score. The three PRSs were: PRSwithAPOE, PRSwithoutAPOE, and APOEonlyPRS, and the three thresholds for the PRSs were: Threshold 1 ($p = 5 \times 10^{-8}$), Threshold 5 ($p < 0.001$), and Threshold 10 ($p < 1$). Associations between all PRSs at all thresholds and all composite scores were examined. These associations were studied as a whole group that was controlled for MMSE, then the whole group was stratified by APOE ε4 status, the whole group was stratified by diagnosis, and lastly, the whole group was stratified by amyloid status. All hypotheses can be accepted partly.

For whole group analysis, all PRSwithAPOE thresholds and APOEonlyPRS thresholds were associated significantly with the memory composite score. There were no differences between the significance of these associations when using PRSwithAPOE Threshold 1 or APOEonlyPRS Threshold 1, and when using PRSwithAPOE Threshold 10 or APOEonlyPRS Threshold 10. However, there was a small difference in the associations when using PRSwithAPOE Threshold 5 vs. APOEonlyPRS Threshold 5, whereby the level of significance was greater with APOEonlyPRS. Therefore, overall, when it came to using a PRSwithAPOE score vs. an APOE-only score, neither improved the predictability of the associations with memory. Nonetheless, both types of scores showed associations that were negative: high PRS was associated with poor memory performance, and all withstood FDR corrective measures. On the other hand, PRSwithAPOE Threshold 1 was associated significantly with the visuospatial composite score, whereas none of the APOEonlyPRS thresholds found such an association. Therefore, the combination of several risk variants, plus APOE variants, added value and went beyond APOE variants alone in finding associations with visuospatial abilities. This association was negative also: high PRS was associated with poor visuospatial skills. However, this did not withstand FDR correction. Adding PRS to the model increased the predictability of the associations by up to 0.6% and this was significant statistically. Overall, Threshold 1 and Threshold 5 identified associations between PRS (i.e., PRSwithAPOE and APOEonlyPRS) and memory, and visuospatial competence, the best.

When the whole group was stratified by APOE ε4 status, in ε4 carriers, PRSwithAPOE Thresholds 1 and 5 were associated negatively and significantly with the visuospatial composite score. Therefore, high PRSwithAPOE was associated with poor visuospatial abilities. The association was stronger when using Threshold 1 than Threshold 5. Also, all APOEonlyPRS thresholds were

associated significantly and inversely with the visuospatial composite score. Thus, high APOEonlyPRS was associated with poor visuospatial skills. This association had a greater level of significance when using Threshold 10, followed by Threshold 1, and then Threshold 5. The level of significance of the associations were higher using PRSwithAPOE Thresholds 1 and 5 than when using APOEonlyPRS Thresholds 1 and 5. Therefore, as with whole-group analysis, here too in ε4 carriers, PRS added value compared with using APOE SNPs alone. Additionally, adding PRS to the model increased the predictability of the associations by up to 1.6% in ε4 carriers and this was significant statistically. Overall, PRSwithAPOE Threshold 1 and APOEonlyPRS Threshold 10 identified associations between PRS and visuospatial proficiency the most, where PRSwithAPOE Threshold 1 exceeded APOEonlyPRS Threshold 10. However, only the association between PRSwithAPOE Threshold 1 and visuospatial cognition remained significant after FDR corrective measures.

Furthermore, when the whole group was stratified by diagnosis, in AD dementia, all PRSwithAPOE thresholds were associated positively and significantly with the executive function composite score. Therefore, high PRS was associated with better executive function. The level of significance was highest when using Threshold 10, followed by Threshold 5, and then Threshold 1. Additionally, adding PRSwithAPOE to the model improved the predictability of the associations by up to 3.5% in AD dementia patients. In MCI, PRSwithoutAPOE Threshold 10 was associated significantly and positively with the executive function composite score. Adding PRSwithoutAPOE to the model increased predictability of the associations by 0.7% in MCI and this was significant statistically. In AD dementia, all APOEonlyPRS thresholds were associated positively and significantly with the executive function composite score. The level of significance was greater when using Threshold 1, followed by Threshold 5, and then Threshold 10. Adding APOEonlyPRS to the model improved the predictability of the associations by up to 2.8% for AD dementia patients. Overall, the thresholds that were best at identifying these associations were, PRSwithAPOE Threshold 10 for AD dementia, PRSwithoutAPOE Threshold 10 for MCI, and APOEonlyPRS Threshold 1 for AD dementia. Interestingly, for PRSwithAPOE, the addition of more variants led to a greater level of significance, i.e., PRSwithAPOE Threshold 10, whereas, for APOEonlyPRS, a conservative number of variants increased the level of significance, i.e., APOEonlyPRS Threshold 1. However, after correcting for multiple comparisons, only the association between PRSwithAPOE Threshold 10 and executive function in AD dementia patients retained significance. As per the rationale for this research, and comparable with the findings in Chapter 4 (Experiment One), the combined effect of many variants is of key interest in sporadic

AD and PRSwithAPOE Threshold 10 reflects this in the current work, whereas, when the APOE region was investigated in isolation, the variants that may be near ε2 and ε4 variants may be associated better with cognition, i.e., APOEonlyPRS Threshold 1.

Moreover, when the whole group was stratified by amyloid status, in amyloid positive participants, all PRSwithAPOE thresholds and all APOEonlyPRS thresholds were associated with the memory composite score. There were no differences between the level of significance when using PRSwithAPOE Threshold 1 or APOEonlyPRS Threshold 1, and when using PRSwithAPOE Threshold 10 and APOEonlyPRS Threshold 10. However, there was a small difference in the association when using PRSwithAPOE Threshold 5 and APOEonlyPRS Threshold 5; thus, indicating PRSwithAPOE Threshold 5 is better slightly than APOEonlyPRS Threshold 5. These were all associated negatively, i.e., high PRS was associated with poor memory performance and remained significant after FDR correction. Adding PRSwithAPOE or APOEonlyPRS to the model increased the predictability of these associations by up to 0.8% and this was significant statistically. Additionally, in amyloid negative participants, PRSwithAPOE Threshold 5 was associated negatively with the visuospatial composite score but did not retain significance after FDR corrective measures. Adding the PRSwithAPOE here improved the predictability of the association by 1.5%. Overall, Threshold 1 and Threshold 5 identified associations between PRS (i.e., PRSwithAPOE and APOEonlyPRS) and memory, and visuospatial performance better.

5B.4.1. Interpretation

The majority of associations found between PRSs and the cognitive domains investigated, were obtained in the presence of APOE SNPs. The APOE protein is responsible for transporting cholesterol and phospholipids to dendritic spines and synapses for maintenance and growth. This is vital for synapse formation and function, and these are essential for learning, memory (Dias et al., 2025), and other cognitive processes. In support of this, the current research showed that both PRSwithAPOE and APOEonlyPRS were associated with cross-sectional memory, executive function, and visuospatial performance.

Both PRSwithAPOE and APOEonlyPRS were associated negatively with memory. Wang et al. (2025) devised two models to study associations between PRS for AD without APOE SNPs and cognition. Model 1 was adjusted for age, sex, education, smoking status (past and current), BMI, and x10 principal components, whereas Model 2 controlled for all variables that were included in

Model 1 plus ε4 allele dosage. In CU, when using Model 1, PRS was associated negatively with the memory composite score only. However, when Model 2 was used, no associations were found. In MCI, when using Model 1, PRS was associated negatively with the memory, executive function, and visuospatial composite scores. However, when Model 2 was used, these associations no longer remained. These findings indicate that ε4 dosage had a significant effect on associations. Although these models are not the same as those used in the current research, the results gathered using Model 1 by Wang et al. (2025) highlight the importance of controlling for cognitive variability in the sample. For instance, the current research controlled for MMSE (in addition to age, sex, education, family history, and x10 genetic principal components), and therefore reduced the likelihood of false-positive findings or inflation of the results. Thus, PRSwithoutAPOE was not observed to be associated with memory. In fact, PRSwithoutAPOE Threshold 10 was the only PRS that was associated minimally with the visuospatial composite score in MCI patients. Similarly, Eissman et al. (2023) found that when APOE SNPs were removed from the PRS, it was no longer associated with the memory composite score. Therefore, the current research confirms further that the APOE protein and associated gene variants, as well as non-APOE variants that are of low effect size, have an essential role in memory processes and associated biological pathways, and mechanisms.

The finding that PRSwithAPOE and APOEonlyPRS were associated negatively with memory remained when stratifying the whole sample by amyloid status, i.e., in amyloid positive participants. As these participants consisted of CU, MCI, and AD dementia participants, MMSE score was controlled for again. Previous research has shown consistently that aMCI patients that are amyloid positive present prominent episodic memory deficits than aMCI patients that are amyloid negative. For instance, aMCI amyloid positive participants have lower scores on various memory tests, i.e., Word Total Recall, Logical Memory Immediate Free Recall, Logical Memory Delayed Free Recall, and Verbal Paired Associate Learning tasks. These findings remained significant even after controlling for MMSE (Alves et al., 2021). Additionally, APOE ε4 increases amyloid pathology (Jansen et al., 2015; Tachibana et al., 2019). Therefore, high PRS in the presence of amyloid positivity may increase cognitive decline further (Ge et al., 2018), particularly when the PRS includes ε4 and other APOE SNPs or when an APOE-only risk score is used.

The current research also highlights that PRSwithAPOE was associated negatively with visuospatial cognition. This is similar to the results obtained by Thompson et al. (2023). This

finding remained when stratifying the sample by amyloid status, i.e., in amyloid negative participants. It is possible that some participants that were stratified into amyloid negative group may have some accumulation of amyloid pathology. However, due to the relatively high cut-off, these participants may have been categorised as amyloid negative rather than amyloid positive (Bilgel and Resnick, 2020). Elman et al. (2020) controlled for subthreshold amyloid, i.e., amyloid that was below the cut-off, and found that this reduced cognitive performance. Therefore, subthreshold amyloid may be of clinical relevance as well. In the current research, those who were under the amyloid threshold may have driven the association in part. Therefore, in amyloid negative participants, high PRSwithAPOE was associated with reduced visuospatial performance. Alternatively, in amyloid negative participants, PRS may play a key role in visuospatial performance. Of the 738 participants that were examined in the current research, 524 participants had CSF p-tau181 data available. These data highlighted that 63% were tau negative, whereas 37% were tau positive. Therefore, this strengthens the notion that in those who do not have high levels of AD-related proteinopathies, the genetic architecture may be responsible for the deterioration in visuospatial cognition, specifically the combination of APOE SNPs plus PRS, although these findings did not survive FDR corrective measures. The observation that PRSwithAPOE, in addition to APOEonlyPRS, was associated negatively with visuospatial abilities remained when stratifying the sample by ε4 status, i.e., in ε4 carriers. Again, this provides evidence that ε4 carriers are likely to have increased amyloid pathology and are therefore vulnerable to impaired cognition, specifically visuospatial decline.

Furthermore, when stratifying the sample by clinical diagnosis, in AD dementia patients, PRSwithAPOE and APOEonlyPRS were associated positively with executive function. In MCI patients, PRSwithoutAPOE was associated positively with executive function. These findings may be regarded as spurious. However, the extent to which AD affects executive function is unclear. The current research is comparable with previous work that indicates executive function is preserved during the early stages of AD as compared with other cognitive domains. Whereas other literature suggests that executive function is impaired to the same extent or worse than other cognitive faculties during AD (Karantzoulis and Galvin, 2011). This discrepancy is also evident in Alves et al. (2021)'s research. They explored associations between various tests of executive function in aMCI amyloid negative vs. aMCI amyloid positive participants. aMCI patients that were amyloid positive performed worse on the Trail Making Test B. However, no such differences were found in other tests of executive function or attention, i.e., Digit Span Backward, Trail Making Test A, Verbal Semantic Fluency, or Cancellation Task. The researchers suggest that

reduced performance on Trail Making Test B in aMCI amyloid positive patients may be due to impaired visuospatial abilities. However, previous research with aMCI that are stratified by amyloid status does not show consistent findings in relation to performance in tasks of attention and executive function. Another example of this inconsistency is demonstrated by Zhao et al. (2023) who found that PRS for AD without APOE ε2 and ε4 was associated with visuospatial abilities, in addition to executive function, memory, and language/fluency. Of note, the discovery sample consisted of a European GWAS that was used to devise PRSs in a South Asian population, i.e., the Diagnostic Assessment of Dementia for the Longitudinal Aging Study in India. The findings should be interpreted with caution as this population is genetically, racially, ethnically, and geographically diverse. Nonetheless, the inconsistencies reported may be applicable to the current research as PRSs appear to be associated positively with executive function, and that is unexpected. Moreover, in Chapter 4 (Experiment One), stratification by amyloid status improved the predictability of associations between PRS and grey matter volume. Similarly, here too, stratifying participants by amyloid status, rather than clinical diagnosis, leads to reliable findings.

5B.4.2. Limitations and Strengths

It was not possible to adjust the models for race due to the small number of non-white participants. Nonetheless, models were adjusted for ancestry using the top 10 genetic principal components.

This research investigates many outcome measures that are central to the symptomology of sporadic AD. For instance, the cognitive faculties of memory, executive function, language, and visuospatial domains that are vulnerable to AD. Of note, these are all in addition to the several PRSs and thresholds, numerous variables that have been controlled for, and the various stratifications that have been conducted in Chapter 5A (Experiment Two Part A) and in Chapter 4 (Experiment One).

5B.4.3. Future Directions

A longitudinal study that investigates the prognostic value of PRSs directly on the continuum of sporadic AD is needed. This will demonstrate whether PRS can be used to predict longitudinal changes and disease progression using cognitive test scores. Cognitive decline that has been captured by neuropsychological assessments is a vital part of diagnosing AD clinically while patients are living.

5B.5. CONCLUSION

Overall, PRS can be used to predict cognitive outcome measures in individuals along the AD continuum. The PRS thresholds that performed well consistently are, PRSwithAPOE Threshold 1 and APOEonlyPRS Threshold 1. PRSwithAPOE and APOEonlyPRS are useful at discovering associations with memory and visuospatial cognition, and these are both associated inversely and significantly. Both PRSwithAPOE and APOEonlyPRS perform at the same level when assessing memory in the whole cohort or in amyloid positive participants. Additionally, in the whole group, PRSwithAPOE outperforms APOEonlyPRS since PRSwithAPOE is associated with visuospatial cognition as well. Similarly, in amyloid negative participants, PRSwithAPOE surpasses APOEonlyPRS since PRSwithAPOE is associated significantly more with visuospatial skills. Of note, if stratification measures are used, amyloid status is reliable in comparison to clinical diagnosis as the latter is dependent upon the expertise of clinicians. Therefore, the current research provides evidence in support of the notion that there is a need for the PRS technique in clinical settings as it can help with, and improve, the diagnosis of AD and in potentially assessing the progression along the continuum of sporadic AD.

CHAPTER 6A

EXPERIMENT THREE PART A – ASSOCIATIONS BETWEEN POLYGENIC RISK SCORES AND LONGITUDINAL CEREBROSPINAL FLUID BIOMARKERS

6A.1. INTRODUCTION

PRS is a valid technique to predict change over time. PRS can be useful at different timepoints along the disease to gauge prognosis and outcome. This tool has been shown to be relevant clinically in cardiovascular diseases and cancer, although in AD it is in the research discovery stage (Lewis and Vassos, 2020).

A limited amount of research has been conducted on the association between PRS and longitudinal amyloid and tau. Although this work has received attention recently only, some reports indicate that PRS with APOE is associated with such biomarkers (Luckett et al., 2022) whereas others suggest PRS without APOE is associated with these biomarkers (Li et al., 2023; Liu, Lutz, and Luo, 2021; Pettigrew 2025). Of note, measures of amyloid and tau in such work have been obtained via CSF, PET, or blood-plasma. Further research, with consistent findings, is required for PRS to be used in clinical trials of AD and then clinical settings, potentially (Lewis and Vassos, 2020).

Liu, Lutz, and Luo (2021) investigated the association between PRS that included 40 non-APOE SNPs and longitudinal CSF tau, and p-tau. Data from 767 MCI participants from ADNI were used. PRS was associated with increased levels of CSF tau and p-tau over time.

In comparison, Li et al. (2023) used a PRS with six non-APOE SNPs only to assess the association with longitudinal changes in CSF biomarkers. 767 ADNI participants with a diagnosis of MCI, at baseline or follow-up, were used. Of these, 294 were diagnosed with AD during follow-up. PRS was associated with increased CSF tau and p-tau181, and reduced CSF Aβ.

Moreover, blood-based biomarkers are minimally invasive and cost-effective for both research and clinical settings. Pettigrew et al. (2025) were the first to examine associations between PRS without SNPs from the APOE region, longitudinal Aβ42:Aβ40 ratio and p-tau181, in plasma. 177 cognitively healthy individuals from the BIOCARD Study, USA, with a mean age of 57.7 years were followed up for an average of 15.8 years. APOE ε4 carriers had lower Aβ42:Aβ40 ratios and higher p-tau181 over time than ε4 non-carriers. In ε4 non-carriers, PRS without APOE was associated with greater Aβ42:Aβ40 decline over time. In comparison with those who remained cognitively intact over time, those that developed MCI or dementia had reduced levels of Aβ42:Aβ40 at baseline and increased levels of p-tau181 over time. These findings suggest that blood-based

biomarkers may be useful for predicting brain amyloid positivity and dementia onset, as well as differentiating between diagnostic statuses.

Luckett et al. (2022) investigated the association between PRS, including and excluding APOE, and amyloid accumulation over 6.1 years using PET. Data from 90 participants from the Flemish Prevent AD Cohort KU Leuven, with a mean age of 67.8 years, were used. Participants were deemed cognitively healthy at baseline and this status was based on an MMSE score of ≥27 and a CDR score of 0. PRS with APOE, that was calculated at the 0.00000005 level, was associated positively with amyloid accumulation. However, PRSs at the 0.00001 and 0.1 levels were not associated with amyloid. APOE ε2 + APOE ε4 was also associated positively with amyloid accumulation, although not associated as significantly as the PRS stated above. These results may indicate that stringent PRS thresholds, and therefore thresholds that are closer to genome-wide significance, are useful for identifying associations in cognitively intact individuals and reduce noise, whereas liberal thresholds are suited better for predicting AD cases from controls.

6A.1.1. Aims, Objectives, and Hypotheses

Evidently, associations between only PRSs without APOE (using limited numbers of SNPs) and longitudinal CSF biomarkers have been assessed previously. Thus, more research that investigates associations between various PRSs, several PRS thresholds, and longitudinal CSF biomarkers is required. In particular, data must be scrutinised further to understand the continuum of sporadic AD better.

The overall aim of Chapter 6A (Experiment Three Part A) is:

- To investigate whether PRSs for AD can predict AD-specific longitudinal CSF biomarkers.

This aim will be explored using the following objective:

- To examine the associations between PRSs (i.e., PRSwithAPOE, PRSwithoutAPOE, and APOEonlyPRS) and longitudinal CSF biomarkers (i.e., Aβ42 and p-tau181), systematically.

It is hypothesised that:

1) The association between PRS and longitudinal CSF biomarkers will be strongest for PRSwithAPOE, followed by APOEonlyPRS, and then PRSwithoutAPOE (whole group).
2) In APOE ε4 carriers, the association between PRS and longitudinal CSF biomarkers will be strongest for PRSwithAPOE, followed by APOEonlyPRS, and then PRSwithoutAPOE (APOE ε4 status).
3) In MCI and AD dementia patients, the association between PRS and longitudinal CSF biomarkers will be strongest for PRSwithAPOE, followed by APOEonlyPRS, and then PRSwithoutAPOE, as compared with CU participants (diagnostic status).

Overall, this research will provide a thorough and systematic presentation of AD-specific and longitudinal CSF biomarkers and address the shortcomings of previous literature.

6A.2. METHODS

6A.2.1. Participants

Data from 171 ADNI participants were used in this study. Participants' demographics and characteristics are shown in Table 6A.1.

In terms of race, the participant sample consisted of individuals of white (94.15%, n = 161) and minority (5.85%, n = 10) races. Minority races of this sample were Asians, Black, and Mixed. All available races were included in the analysis to maximise the sample size and generalisability of the results.

As with the previous chapters, where analysis required stratification by APOE ε4 status, APOE genotypes were grouped into APOE ε4 non-carriers vs. carriers.

Family history included history of AD and/or unspecified dementia, in first degree relatives.

Table 6A.1: Participant demographics and characteristics of 171 participants.

ENTIRE COHORT (n = 171)		
Age		
Age range		55 – 90 years
Mean age		73.13 years
Standard deviation		7.09 years
Education		
Education range		6 – 20 years
Mean education		16.30 years
Standard deviation		2.85 years
	n	**%**
Sex		
Male	99	57.89
Female	72	42.11
Race		
Native Americans	0	0
Asian	2	1.17
Hawaiian/Pacific	0	0
Black	4	2.34
White	161	94.15
Mixed	4	2.34
Unknown	0	0
APOE Genotype		
ε4ε4	16	9.36
ε3ε4	56	32.75
ε3ε3	76	44.44
ε2ε4	2	1.17
ε2ε3	21	12.28
ε2ε2	0	0
APOE ε4 Status		
ε4 Non-carrier	97	56.73
ε4 Carrier	74	43.27
Amyloid Status		
Negative	70	40.94
Positive	101	59.06
Tau Status		
Negative	111	64.91
Positive	60	35.09
Family History of Alzheimer's or Dementia		
Negative	6	3.51
Positive	165	96.49
CSF Change at 24 months		
Aβ42 improved	72	42.11
Aβ42 worsened	99	57.89

p-tau181 improved	56	32.75
p-tau181 worsened	115	67.25
CSF Differential Scores		
Aβ42 range	-2.702249546 – 3.441438820	
Aβ42 mean	0.046558334	
Aβ42 standard deviation	0.620613553	
p-tau181 range	-8.855570391 – 8.386109753	
p-tau181 mean	0.215896774	
p-tau181 standard deviation	1.923967254	

Aβ: amyloid beta. APOE: apolipoprotein E. CSF: cerebrospinal fluid. ε: epsilon. P-tau: phosphorylated tau.

6A.2.2. Genetic data and, Calculation of Polygenic Risk Scores and Polygenic Risk Score Thresholds

The steps described in Chapter 4 (Experiment One) were applied to Chapter 6A (Experiment Three Part A) for consistency. All three PRSs were used (i.e., PRSwithAPOE, PRSwithoutAPOE, and APOEonlyPRS) with all three thresholds (i.e., Thresholds 1, 5, and 10).

6A.2.3. Cerebrospinal Fluid Biomarkers

For continuity, longitudinal CSF Aβ42 and p-tau181 measurements were assessed at 24 months after the point at which these measurements were taken for the cross-sectional work in Chapter 5A (Experiment Two Part A) that formed the "baseline" observation. The "UPPENBIOMK9" assay was used, and these data were found in the same "UPENNBIOMK_ROCHE_ELECSYS_METHODS_20231109" file that was downloaded from ADNI on 11 December 2024 for Chapter 5A (Experiment Two Part A).

6A.2.4. Statistical Analyses

Analyses were divided into four stages. All statistical analyses were completed on IBM SPSS Statistics v29.0.1.0.

First, participants' measurements of Aβ42 and p-tau181 at 24 months were compared with the measurements that were used in Chapter 5A (Experiment Two Part A) (baseline). Based on these comparisons, participants were categorised as having either worsened or improved over 24 months.

Second, differential scores were calculated for Aβ42 and p-tau181 individually. Differential scores = Measurement at 24 months minus Measurement used in Chapter 5A (Experiment Two Part A) (baseline). The difference between these raw measurements was z-transformed, where averages and standard deviations were based on CU participants, before being analysed.

In contrast to Chapter 5A (Experiment Two Part A), the current research did not examine participants that were negative on both biomarkers or positive on both biomarkers. Although 114 out of the 171 participants met these criteria, adequate changes in biomarker status over 24 months was observed in nine participants. Therefore, only nine participants changed from not having the same biomarker status on both Aβ42 and p-tau181 (i.e., negative/positive or positive/negative) to having the same biomarker status on both biomarkers (i.e., negative/negative or positive/positive). This was not sufficient for statistical analysis. 105 out of the 114 participants' biomarker status was unchanged; 57 participants remained negative on both biomarkers and 48 participants remained positive on both biomarkers.

6A.2.4.1. Stage 1 Analysis: Logistic Regression – Amyloid Study

> 977 = Aβ42 negative (Hansson et al., 2018)

- More negative (Higher values / numerical figures further away from 977) at 24 months in comparison with baseline = Improved
- Less negative (Lower values / numerical figures closer to 977) at 24 months in comparison with baseline = Worsened

≤ 977 = Aβ42 positive (Hansson et al., 2018)

- Less positive (Higher values / numerical figures closer to 977) at 24 months in comparison with baseline = Improved
- More positive (Lower values / numerical figures further away from and smaller than 977) at 24 months in comparison with baseline = Worsened

Binomial hierarchical logistic regression analyses were carried out to test whether PRS (independent / predictor variable) could predict change in CSF Aβ42 over 24 months i.e., improvement or worsening (dependent / outcome variable). *P* was significant at the 0.05 level.

(A) Whole-group analysis, not controlled for p-tau181 status

• Model 1: Age, sex, education, family history, MMSE, and x10 genetic principal components.

• Model 2: All variables in Model 1, plus PRS.

Analyses were completed using PRSwithAPOE Thresholds 1, 5, and 10 separately, PRSwithoutAPOE Thresholds 1, 5, and 10 separately, and APOEonlyPRS Thresholds 1, 5, and 10 separately.

(n = 171).

(B) Whole-group analysis, controlled for p-tau181 status (*post-hoc*)

• Model 1: Age, sex, education, family history, MMSE, x10 genetic principal components, and CSF p-tau181.

• Model 2: All variables in Model 1, plus PRS.

Analyses were completed using PRSwithAPOE Thresholds 1, 5, and 10 separately, PRSwithoutAPOE Thresholds 1, 5, and 10 separately, and APOEonlyPRS Thresholds 1, 5, and 10 separately.

(n = 171).

(C) Whole group stratified by APOE ε4 status, not controlled for p-tau181 status

• Model 1: Age, sex, education, family history, MMSE, and x10 genetic principal components.

• Model 2: All variables in Model 1, plus PRS.

Analyses were completed using PRSwithAPOE Thresholds 1, 5, and 10 separately, PRSwithoutAPOE Thresholds 1, 5, and 10 separately, and APOEonlyPRS Thresholds 1, 5, and 10 separately.

(ε4 non-carriers, n = 97; ε4 carriers, n = 74).

(D) Whole group stratified by APOE ε4 status, controlled for p-tau181 status (*post-hoc*)

• Model 1: Age, sex, education, family history, MMSE, x10 genetic principal components, and CSF p-tau181.

• Model 2: All variables in Model 1, plus PRS.

Analyses were completed using PRSwithAPOE Thresholds 1, 5, and 10 separately, PRSwithoutAPOE Thresholds 1, 5, and 10 separately, and APOEonlyPRS Thresholds 1, 5, and 10 separately.

(ε4 non-carriers, n = 97; ε4 carriers, n = 74).

(E) Whole group stratified by diagnostic status, not controlled for p-tau181 status

• Model 1: Age, sex, education, family history, MMSE, and x10 genetic principal components.

• Model 2: All variables in Model 1, plus PRS.

Analyses were completed using PRSwithAPOE Thresholds 1, 5, and 10 separately, PRSwithoutAPOE Thresholds 1, 5, and 10 separately, and APOEonlyPRS Thresholds 1, 5, and 10 separately.

A sufficient number of AD dementia patients was not available for this stratification in comparison to the number of variables (x15 vs. x16) being studied in the models. Therefore, this analysis was not conducted for the AD dementia group. Analyses were completed for CU and MCI participants only.

(CU, n = 39; MCI, n = 108; AD dementia, n = 24).

(F) Whole group stratified by diagnostic status, controlled for p-tau181 status (*post-hoc*)

• Model 1: Age, sex, education, family history, MMSE, x10 genetic principal components, and CSF p-tau181.

• Model 2: All variables in Model 1, plus PRS.

Analyses were completed using PRSwithAPOE Thresholds 1, 5, and 10 separately, PRSwithoutAPOE Thresholds 1, 5, and 10 separately, and APOEonlyPRS Thresholds 1, 5, and 10 separately.

An adequate number of AD dementia patients was not available for this stratification in comparison with the number of variables (x16 vs. x17) being studied in the models. Therefore, this analysis was not conducted for the AD dementia group. Analyses were completed for CU and MCI participants only.

(CU, n = 39; MCI, n = 108; AD dementia, n = 24).

(G) For exploratory analysis, diagnostic status was stratified further by APOE ε4 (not controlled for p-tau181 status)

• Model 1: Age, sex, education, family history*, MMSE, and x10 genetic principal components.

• Model 2: All variables in Model 1, plus PRS.

Analyses were completed using PRSwithAPOE Thresholds 1, 5, and 10 separately, PRSwithoutAPOE Thresholds 1, 5, and 10 separately, and APOEonlyPRS Thresholds 1, 5, and 10 separately.

A sufficient number of CU ε4 carriers, AD dementia ε4 non-carriers, and AD dementia ε4 carriers was not available for this stratification, particularly when taking into consideration the number of variables (x15 vs. x16) being studied in the models. Therefore, this analysis was not conducted for these three participant groups. Analyses were completed for CU ε4 non-carriers, MCI ε4 non-carriers, and MCI ε4 carriers only.

*Additionally, for CU ε4 non-carriers and MCI ε4 carriers, family history was not added to the models as it was a constant variable, i.e., positive family history for all participants in these two groups. Family history was added to the models for the MCI ε4 carriers' group only.

(CU ε4 non-carriers, n = 29; CU ε4 carriers, n = 10; MCI ε4 non-carriers, n = 61; MCI ε4 carriers, n = 47; AD dementia ε4 non-carriers, n = 7; AD dementia ε4 carriers, n = 17).

(H) For exploratory analysis, diagnostic status was stratified further by APOE ε4 (controlled for p-tau181status – *post-hoc*)

• Model 1: Age, sex, education, family history*, MMSE, x10 genetic principal components, and CSF p-tau181.

• Model 2: All variables in Model 1, plus PRS.

Analyses were completed using PRSwithAPOE Thresholds 1, 5, and 10 separately, PRSwithoutAPOE Thresholds 1, 5, and 10 separately, and APOEonlyPRS Thresholds 1, 5, and 10 separately.

An adequate number of CU ε4 carriers, AD dementia ε4 non-carriers, and AD dementia ε4 carriers was not available for this stratification, particularly when taking into consideration the number of variables (x16 vs. x17) being studied in the models. Therefore, this analysis was not conducted for these three participant groups. Analyses were completed for CU ε4 non-carriers, MCI ε4 non-carriers, and MCI ε4 carriers only.

*Additionally, for CU ε4 non-carriers and MCI ε4 carriers, family history was not added to the models as it was a constant variable, i.e., positive family history for all participants in these two groups. Family history was added to the models for the MCI ε4 carriers' group only.

(CU ε4 non-carriers, n = 29; CU ε4 carriers, n = 10; MCI ε4 non-carriers, n = 61; MCI ε4 carriers, n = 47; AD dementia ε4 non-carriers, n = 7; AD dementia ε4 carriers, n = 17).

6A.2.4.2. Stage 2 Analysis: Logistic Regression – Tau Study

< *26.64 = P-tau181 negative* (Bucci et al., 2021; Meyer et al., 2020)

- Less negative (Lower values / numerical figures closer to 0) at 24 months as compared with baseline = Improved
- More negative (Higher values / numerical figures closer to 26.64) at 24 months as compared with baseline = Worsened

≥ *26.64 = P-tau181 positive* (Bucci et al., 2021; Meyer et al., 2020)

- Less positive (Lower values / numerical figures closer to 0) at 24 months as compared with baseline = Improved
- More positive (Higher values / numerical figures larger and further away from 26.64) at 24 months as compared with baseline = Worsened

Binomial hierarchical logistic regression analyses were carried out to test whether PRS (independent / predictor variable) could predict change in CSF p-tau181 over 24 months i.e., improvement vs. worsening (dependent / outcome variable). *P* was significant at the 0.05 level.

(A) Whole-group analysis, not controlled for Aβ42 status

• Model 1: Age, sex, education, family history, MMSE, and x10 genetic principal components.

• Model 2: All variables in Model 1, plus PRS.

Analyses were completed using PRSwithAPOE Thresholds 1, 5, and 10 separately, PRSwithoutAPOE Thresholds 1, 5, and 10 separately, and APOEonlyPRS Thresholds 1, 5, and 10 separately.

(n = 171).

(B) Whole-group analysis, controlled for Aβ42 status (*post-hoc*)

• Model 1: Age, sex, education, family history, MMSE, x10 genetic principal components, and CSF Aβ42.

• Model 2: All variables in Model 1, plus PRS.

Analyses were completed using PRSwithAPOE Thresholds 1, 5, and 10 separately, PRSwithoutAPOE Thresholds 1, 5, and 10 separately, and APOEonlyPRS Thresholds 1, 5, and 10 separately.

(n = 171).

(C) Whole group stratified by APOE ε4 status, not controlled for Aβ42 status

• Model 1: Age, sex, education, family history, MMSE, and x10 genetic principal components.

• Model 2: All variables in Model 1, plus PRS.

Analyses were completed using PRSwithAPOE Thresholds 1, 5, and 10 separately, PRSwithoutAPOE Thresholds 1, 5, and 10 separately, and APOEonlyPRS Thresholds 1, 5, and 10 separately.

(ε4 non-carriers, n = 97; ε4 carriers, n = 74).

(D) Whole group stratified by APOE ε4 status, controlled for Aβ42 status (*post-hoc*)

• Model 1: Age, sex, education, family history, MMSE, x10 genetic principal components, and CSF Aβ42.

• Model 2: All variables in Model 1, plus PRS.

Analyses were completed using PRSwithAPOE Thresholds 1, 5, and 10 separately, PRSwithoutAPOE Thresholds 1, 5, and 10 separately, and APOEonlyPRS Thresholds 1, 5, and 10 separately.

(ε4 non-carriers, n = 97; ε4 carriers, n = 74).

(E) Whole group stratified by diagnostic status, not controlled for Aβ42 status

• Model 1: Age, sex, education, family history, MMSE, and x10 genetic principal components.

• Model 2: All variables in Model 1, plus PRS.

Analyses were completed using PRSwithAPOE Thresholds 1, 5, and 10 separately, PRSwithoutAPOE Thresholds 1, 5, and 10 separately, and APOEonlyPRS Thresholds 1, 5, and 10 separately.

A sufficient number of AD dementia patients was not available for this stratification in comparison with the number of variables (x15 vs. x16) being studied in the models. Therefore, this analysis was not conducted for the AD dementia group. Analyses were completed for CU and MCI participants only.

(CU, n = 39; MCI, n = 108; AD dementia, n = 24).

(F) Whole group stratified by diagnostic status, controlled for Aβ42 status (*post-hoc*)

• Model 1: Age, sex, education, family history, MMSE, x10 genetic principal components, and CSF Aβ42.

• Model 2: All variables in Model 1, plus PRS.

Analyses were completed using PRSwithAPOE Thresholds 1, 5, and 10 separately, PRSwithoutAPOE Thresholds 1, 5, and 10 separately, and APOEonlyPRS Thresholds 1, 5, and 10 separately.

An adequate number of AD dementia patients was not available for this stratification in comparison to the number of variables (x16 vs. x17) being studied in the models. Therefore, this analysis was not conducted for the AD dementia group. Analyses were completed for CU and MCI participants only.

(CU, n = 39; MCI, n = 108; AD dementia, n = 24).

(G) For exploratory analysis, diagnostic status was stratified further by APOE ε4 (not controlled for Aβ42 status)

• Model 1: Age, sex, education, family history*, MMSE, and x10 genetic principal components.

• Model 2: All variables in Model 1, plus PRS.

Analyses were completed using PRSwithAPOE Thresholds 1, 5, and 10 separately, PRSwithoutAPOE Thresholds 1, 5, and 10 separately, and APOEonlyPRS Thresholds 1, 5, and 10 separately.

A sufficient number of CU ε4 carriers, AD dementia ε4 non-carriers, and AD dementia ε4 carriers was not available for this stratification, particularly when taking into consideration the number of variables (x15 vs. x16) being studied in the models. Therefore, this analysis was not conducted for these three participant groups. Analyses were completed for CU ε4 non-carriers, MCI ε4 non-carriers, and MCI ε4 carriers only.

*Additionally, for CU ε4 non-carriers and MCI ε4 carriers, family history was not added to the models as it was a constant variable, i.e., positive family history for all participants in these two groups. Family history was added to the models for the MCI ε4 carriers' group only.

(CU ε4 non-carriers, n = 29; CU ε4 carriers, n = 10; MCI ε4 non-carriers, n = 61; MCI ε4 carriers, n = 47; AD dementia ε4 non-carriers, n = 7; AD dementia ε4 carriers, n = 17).

(H) For exploratory analysis, diagnostic status was stratified further by APOE ε4 (controlled for Aβ42 status – *post-hoc*)

• Model 1: Age, sex, education, family history*, MMSE, x10 genetic principal components, and CSF Aβ42.

• Model 2: All variables in Model 1, plus PRS.

Analyses were completed using PRSwithAPOE Thresholds 1, 5, and 10 separately, PRSwithoutAPOE Thresholds 1, 5, and 10 separately, and APOEonlyPRS Thresholds 1, 5, and 10 separately.

An adequate number of CU ε4 carriers, AD dementia ε4 non-carriers, and AD dementia ε4 carriers was not available for this stratification, particularly when taking into consideration the number of variables (x16 vs. x17) being studied in the models. Therefore, this analysis was not conducted for these three participant groups. Analyses were completed for CU ε4 non-carriers, MCI ε4 non-carriers, and MCI ε4 carriers only.

*Additionally, for CU ε4 non-carriers and MCI ε4 carriers, family history was not added to the models as it was a constant variable, i.e., positive family history for all participants in these two groups. Family history was added to the models for the MCI ε4 carriers' group only.

(CU ε4 non-carriers, n = 29; CU ε4 carriers, n = 10; MCI ε4 non-carriers, n = 61; MCI ε4 carriers, n = 47; AD dementia ε4 non-carriers, n = 7; AD dementia ε4 carriers, n = 17).

For Stages 1 and 2, FDR correction was not necessary as there was only one dependent / outcome variable (with two levels each) being tested at any one time, i.e., amyloid – negative vs. positive, or tau – negative vs. positive.

6A.2.4.3. Stage 3 Analysis: Linear Regression – Amyloid Study

Multiple hierarchical linear regression analyses were conducted to investigate associations between PRS (independent / predictor variable) and differential scores of CSF Aβ42 (dependent / outcome variable) between baseline and month 24. *P* was significant at the 0.05 level.

(A) Whole-group analysis, not controlled for p-tau181 status

• Model 1: Age, sex, education, family history, MMSE, and x10 genetic principal components.

• Model 2: All variables in Model 1, plus PRS.

Analyses were completed using PRSwithAPOE Thresholds 1, 5, and 10 separately, PRSwithoutAPOE Thresholds 1, 5, and 10 separately, and APOEonlyPRS Thresholds 1, 5, and 10 separately.

(n = 171).

(B) Whole-group analysis, controlled for p-tau181 status (post-hoc)

• Model 1: Age, sex, education, family history, MMSE, x10 genetic principal components, and CSF p-tau181.

• Model 2: All variables in Model 1, plus PRS.

Analyses were completed using PRSwithAPOE Thresholds 1, 5, and 10 separately, PRSwithoutAPOE Thresholds 1, 5, and 10 separately, and APOEonlyPRS Thresholds 1, 5, and 10 separately.

(n = 171).

(C) Whole group stratified by APOE ε4 status, not controlled for p-tau181 status

• Model 1: Age, sex, education, family history, MMSE, and x10 genetic principal components.

• Model 2: All variables in Model 1, plus PRS.

Analyses were completed using PRSwithAPOE Thresholds 1, 5, and 10 separately, PRSwithoutAPOE Thresholds 1, 5, and 10 separately, and APOEonlyPRS Thresholds 1, 5, and 10 separately.

(ε4 non-carriers, n = 97; ε4 carriers, n = 74).

(D) Whole group stratified by APOE ε4 status, controlled for p-tau181 status (*post-hoc*)

• Model 1: Age, sex, education, family history, MMSE, x10 genetic principal components, and CSF p-tau181.

• Model 2: All variables in Model 1, plus PRS.

Analyses were completed using PRSwithAPOE Thresholds 1, 5, and 10 separately, PRSwithoutAPOE Thresholds 1, 5, and 10 separately, and APOEonlyPRS Thresholds 1, 5, and 10 separately.

(ε4 non-carriers, n = 97; ε4 carriers, n = 74).

(E) Whole group stratified by diagnostic status, not controlled for p-tau181 status

• Model 1: Age, sex, education, family history, MMSE, and x10 genetic principal components.

• Model 2: All variables in Model 1, plus PRS.

Analyses were completed using PRSwithAPOE Thresholds 1, 5, and 10 separately, PRSwithoutAPOE Thresholds 1, 5, and 10 separately, and APOEonlyPRS Thresholds 1, 5, and 10 separately.

A sufficient number of AD dementia patients was not available for this stratification in comparison with the number of variables (x15 vs. x16) being studied in the models. Therefore, this analysis was not conducted for the AD dementia group. Analyses were completed for CU and MCI participants only.

(CU, n = 39; MCI, n = 108; AD dementia, n = 24).

(F) Whole group stratified by diagnostic status, controlled for p-tau181 status (*post-hoc*)

• Model 1: Age, sex, education, family history, MMSE, x10 genetic principal components, and CSF p-tau181.

• Model 2: All variables in Model 1, plus PRS.

Analyses were completed using PRSwithAPOE Thresholds 1, 5, and 10 separately, PRSwithoutAPOE Thresholds 1, 5, and 10 separately, and APOEonlyPRS Thresholds 1, 5, and 10 separately.

An adequate number of AD dementia patients was not available for this stratification in comparison to the number of variables (x16 vs. x17) being studied in the models. Therefore, this analysis was not conducted for the AD dementia group. Analyses were completed for CU and MCI participants only.

(CU, n = 39; MCI, n = 108; AD dementia, n = 24).

(G) For exploratory analysis, diagnostic status was stratified further by APOE ε4 (not controlled for p-tau181 status)

• Model 1: Age, sex, education, family history*, MMSE, and x10 genetic principal components.

• Model 2: All variables in Model 1, plus PRS.

Analyses were completed using PRSwithAPOE Thresholds 1, 5, and 10 separately, PRSwithoutAPOE Thresholds 1, 5, and 10 separately, and APOEonlyPRS Thresholds 1, 5, and 10 separately.

An insufficient number of CU ε4 carriers, AD dementia ε4 non-carriers, and AD dementia ε4 carriers was available for this stratification in comparison with the number of variables (x15 vs. x16) used in the models. Therefore, analyses were not conducted for these three groups. Analyses were completed for CU ε4 non-carriers, MCI ε4 non-carriers, and MCI ε4 carriers only.

*Additionally, CU ε4 non-carriers and MCI ε4 carriers, family history was not added to the models as this was a constant variable, i.e., positive family history for all participants in these two groups. Family history was added to the models for the MCI ε4 carriers' group only.

(CU ε4 non-carriers, n = 29; CU ε4 carriers, n = 10; MCI ε4 non-carriers, n = 61; MCI ε4 carriers, n = 47; AD dementia ε4 non-carriers, n = 7; AD dementia ε4 carriers, n = 17).

(H) For exploratory analysis, diagnostic status was stratified further by APOE ε4 (controlled for p-tau181 status – *post-hoc*)

• Model 1: Age, sex, education, family history*, MMSE, x10 genetic principal components, and CSF p-tau181.

• Model 2: All variables in Model 1, plus PRS.

Analyses were completed using PRSwithAPOE Thresholds 1, 5, and 10 separately, PRSwithoutAPOE Thresholds 1, 5, and 10 separately, and APOEonlyPRS Thresholds 1, 5, and 10 separately.

An insufficient number of CU ε4 carriers, AD dementia ε4 non-carriers, and AD dementia ε4 carriers was available for this stratification in comparison with the number of variables (x16 vs. x17) used in the models. Therefore, analyses were not conducted for these three groups. Analyses were completed for CU ε4 non-carriers, MCI ε4 non-carriers, and MCI ε4 carriers only.

*For CU ε4 non-carriers and MCI ε4 carriers, family history was not added to the models as this was a constant variable, i.e., positive family history for all participants in these two groups. Family history was added to the models for the MCI ε4 carriers' group only.

(CU ε4 non-carriers, n = 29; CU ε4 carriers, n = 10; MCI ε4 non-carriers, n = 61; MCI ε4 carriers, n = 47; AD dementia ε4 non-carriers, n = 7; AD dementia ε4 carriers, n = 17).

6A.2.4.4. Stage 4 Analysis: Linear Regression – Tau Study

Multiple hierarchical linear regression analyses were conducted to investigate associations between PRS (independent / predictor variable) and differential scores of CSF p-tau181 (dependent / outcome variable) between baseline and month 24. *P* was significant at the 0.05 level.

(A) Whole-group analysis, not controlled for Aβ42 status

• Model 1: Age, sex, education, family history, MMSE, and x10 genetic principal components.

• Model 2: All variables in Model 1, plus PRS.

Analyses were completed using PRSwithAPOE Thresholds 1, 5, and 10 separately, PRSwithoutAPOE Thresholds 1, 5, and 10 separately, and APOEonlyPRS Thresholds 1, 5, and 10 separately.

(n = 171).

(B) Whole-group analysis, controlled for Aβ42 status (*post-hoc*)

• Model 1: Age, sex, education, family history, MMSE, x10 genetic principal components, and CSF Aβ42.

• Model 2: All variables in Model 1, plus PRS.

Analyses were completed using PRSwithAPOE Thresholds 1, 5, and 10 separately, PRSwithoutAPOE Thresholds 1, 5, and 10 separately, and APOEonlyPRS Thresholds 1, 5, and 10 separately.

(n = 171).

(C) Whole group stratified by APOE ε4 status, not controlled for Aβ42 status

• Model 1: Age, sex, education, family history, MMSE, and x10 genetic principal components.

• Model 2: All variables in Model 1, plus PRS.

Analyses were completed using PRSwithAPOE Thresholds 1, 5, and 10 separately, PRSwithoutAPOE Thresholds 1, 5, and 10 separately, and APOEonlyPRS Thresholds 1, 5, and 10 separately.

(ε4 non-carriers, n = 97; ε4 carriers, n = 74).

(D) Whole group stratified by APOE ε4 status, controlled for Aβ42 status (*post-hoc*)

• Model 1: Age, sex, education, family history, MMSE, x10 genetic principal components, and CSF Aβ42.

• Model 2: All variables in Model 1, plus PRS.

Analyses were completed using PRSwithAPOE Thresholds 1, 5, and 10 separately, PRSwithoutAPOE Thresholds 1, 5, and 10 separately, and APOEonlyPRS Thresholds 1, 5, and 10 separately.

(ε4 non-carriers, n = 97; ε4 carriers, n = 74).

(E) Whole group stratified by diagnostic status, not controlled for Aβ42 status

• Model 1: Age, sex, education, family history, MMSE, and x10 genetic principal components

• Model 2: All variables in Model 1, plus PRS

Analyses were completed using PRSwithAPOE Thresholds 1, 5, and 10 separately, PRSwithoutAPOE Thresholds 1, 5, and 10 separately, and APOEonlyPRS Thresholds 1, 5, and 10 separately.

A sufficient number of AD dementia patients was not available for this stratification in comparison with the number of variables (x15 vs. x16) being studied in the models. Therefore, this analysis was not conducted for the AD dementia group. Analyses were completed for CU and MCI participants only.

(CU, n = 39; MCI, n = 108; AD dementia, n = 24).

(F) Whole group stratified by diagnostic status, controlled for p-tau181 status (*post-hoc*)

• Model 1: Age, sex, education, family history, MMSE, x10 genetic principal components, and CSF p-tau181.

• Model 2: All variables in Model 1, plus PRS.

Analyses were completed using PRSwithAPOE Thresholds 1, 5, and 10 separately, PRSwithoutAPOE Thresholds 1, 5, and 10 separately, and APOEonlyPRS Thresholds 1, 5, and 10 separately.

An adequate number of AD dementia patients was not available for this stratification in comparison to the number of variables (x16 vs. x17) being studied in the models. Therefore, this analysis was not conducted for the AD dementia group. Analyses were completed for CU and MCI participants only.

(CU, n = 39; MCI, n = 108; AD dementia, n = 24).

(G) For exploratory analysis, diagnostic status was stratified further by APOE ε4 (not controlled for p-tau181 status)

• Model 1: Age, sex, education, family history*, MMSE, and x10 genetic principal components

• Model 2: All variables in Model 1, plus PRS

Analyses were completed using PRSwithAPOE Thresholds 1, 5, and 10 separately, PRSwithoutAPOE Thresholds 1, 5, and 10 separately, and APOEonlyPRS Thresholds 1, 5, and 10 separately.

An insufficient number of CU ε4 carriers, AD dementia ε4 non-carriers, and AD dementia ε4 carriers was available for this stratification in comparison with the number of variables (x15 vs. x16) used in the models. Therefore, analyses were not conducted for these three groups. Analyses were completed for CU ε4 non-carriers, MCI ε4 non-carriers, and MCI ε4 carriers only.

*Additionally, CU ε4 non-carriers and MCI ε4 carriers, family history was not added to the models as this was a constant variable, i.e., positive family history for all participants in these two groups. Family history was added to the models for the MCI ε4 carriers' group only.

(CU ε4 non-carriers, n = 29; CU ε4 carriers, n = 10; MCI ε4 non-carriers, n = 61; MCI ε4 carriers, n = 47; AD dementia ε4 non-carriers, n = 7; AD dementia ε4 carriers, n = 17).

(H) For exploratory analysis, diagnostic status was stratified further by APOE ε4 (controlled for p-tau181 status – *post-hoc*)

• Model 1: Age, sex, education, family history*, MMSE, x10 genetic principal components, and CSF p-tau181

• Model 2: All variables in Model 1, plus PRS

Analyses were completed using PRSwithAPOE Thresholds 1, 5, and 10 separately, PRSwithoutAPOE Thresholds 1, 5, and 10 separately, and APOEonlyPRS Thresholds 1, 5, and 10 separately.

An insufficient number of CU ε4 carriers, AD dementia ε4 non-carriers, and AD dementia ε4 carriers was available for this stratification in comparison with the number of variables (x16 vs. x17) used in the models. Therefore, analyses were not conducted for these three groups. Analyses were completed for CU ε4 non-carriers, MCI ε4 non-carriers, and MCI ε4 carriers only.

*For CU ε4 non-carriers and MCI ε4 carriers, family history was not added to the models as this was a constant variable, i.e., positive family history for all participants in these two groups. Family history was added to the models for the MCI ε4 carriers' group only.

(CU ε4 non-carriers, n = 29; CU ε4 carriers, n = 10; MCI ε4 non-carriers, n = 61; MCI ε4 carriers, n = 47; AD dementia ε4 non-carriers, n = 7; AD dementia ε4 carriers, n = 17).

For the Stages 3 and 4, FDR correction was not required as there was only one dependent / outcome variable being tested at any one time, i.e., amyloid, or tau.

6A.3. RESULTS

6A.3.1. Stage 1 Results: Logistic Regression – Amyloid Study

6A.3.1.1. (A) Whole group, not controlled for p-tau181 status

PRSwithoutAPOE:

No associations (Appendix F1 Table F1.1).

6A.3.1.2. (B) Whole group, controlled for p-tau181 status (post-hoc)

PRSwithoutAPOE:

PRSwithoutAPOE Threshold 1 was associated significantly with CSF Aβ42 when p-tau181 was controlled for ($p = 0.043$). This was a negative association, i.e., high PRS, CSF Aβ42 did not worsen at 24 months. Refer to Table 6A.2 and Figure 6A.1. No other associations were found (Appendix Appendix F1 Table F1.2).

Table 6A.2: Association between PRSwithoutAPOE Threshold 1 and longitudinal change in CSF Aβ42 measurement in the whole group when CSF p-tau181 status was controlled for.

PRS & Threshold	Chi-square	df	*p*	Nagelkerke R^2	Wald	df	*p*	OR	95% CI	Nagelkerke R^2 Model 1
PRSwithoutAPOE Threshold 1	26.965	17	0.059	0.196	4.098	1	0.043	0.684	0.474-0.988	0.167

APOE: apolipoprotein E. CI: confidence interval. df: degrees of freedom. OR: odds ratio. PRS: polygenic risk score.

Controlled for p-tau181 status (whole group)

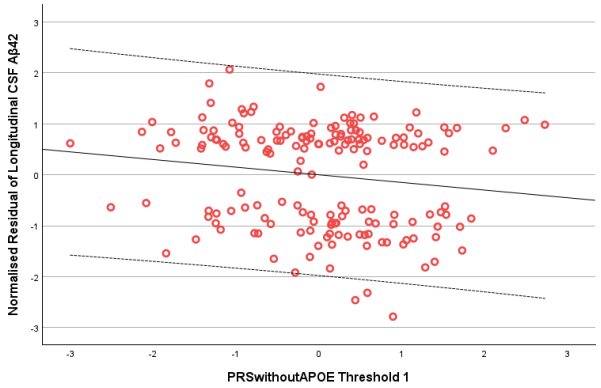

R^2 = 0.023.
Longitudinal CSF Aβ42 = -1.23E – 3 – 0.15 * PRSwithoutAPOE T1.
(T: threshold).

Figure 6A.1: Scatterplot to visualise the association between PRSwithoutAPOE Threshold 1 and longitudinal change in CSF Aβ42 measurement in the whole group when p-tau181 status was controlled for.

Note, the scatterplots are for visualisation purposes only. The scatterplots show the residualised variable (i.e., longitudinal change in CSF Aβ42) modelled as a function of PRS using linear regression. The R^2 in the scatterplots differs from the Nagelkerke (pseudo) R^2 as the two coefficients are calculated in different ways as part of different types of inferential models. The X axis shows the PRS of interest, and the Y axis indicates the normalised residual of CSF Aβ42 where all covariates have been regressed out.

6A.3.1.3. (C) Whole group stratified by APOE ε4 status, not controlled for p-tau181 status

PRSwithAPOE:

In APOE ε4 carriers, PRSwithAPOE Thresholds 5 and 10 were associated significantly with CSF Aβ42 when CSF p-tau181 was not controlled for. In ascending order of significance, Threshold 10 (p = 0.012), then Threshold 5 (p = 0.019). These were positive associations, i.e., high PRS, CSF Aβ42 worsened at 24 months. See Table 6A.3, Figure 6A.2, and Appendix F1 Table F1.3. No associations were observed in ε4 non-carriers (Appendix F1 Table F1.4).

APOEonlyPRS:

In ε4 carriers, APOEonlyPRS Threshold 5 (p = 0.030) and Threshold 1 (p = 0.031) were associated significantly and positively with CSF Aβ42 when CSF p-tau181 was not controlled for, i.e., high PRS, CSF Aβ42 worsened at 24 months. Refer to Table 6A.3, Figure 6A.3, and Appendix F1 Table F1.3. No associations were found in ε4 non-carriers (Appendix F1 Table F1.4).

6A.3.1.4. (D) Whole group stratified by APOE ε4 status, controlled for p-tau181 status (post-hoc)

PRSwithAPOE:

In APOE ε4 carriers, PRSwithAPOE Thresholds 5 and 10 were associated significantly with CSF Aβ42 when CSF p-tau181 was controlled for. In ascending order of significance, Threshold 10 (p = 0.015), then Threshold 5 (p = 0.026). These were both positive associations, i.e., high PRS, CSF Aβ42 worsened at 24 months. See Table 6A.3, Figure 6A.2, and Appendix F1 Table F1.5. No associations were detected in ε4 non-carriers (Appendix F1 Table F1.6).

APOEonlyPRS:

In ε4 carriers, APOEonlyPRS Thresholds 1 and 5 were associated significantly and positively with CSF Aβ42 when CSF p-tau181 was controlled for, (p = 0.034 for both thresholds). Therefore, high PRS, CSF Aβ42 worsened at 24 months. Refer to Table 6A.3, Figure 6A.3, and Appendix F1 Table F1.5. No associations were evident in ε4 non-carriers (Appendix F1 Table F1.6).

Table 6A.3: Associations between PRSs and longitudinal change in CSF Aβ42 measurement in ε4 carriers when CSF p-tau181 status was not controlled for vs. was controlled for.

Not controlled for p-tau181 status

PRS & Threshold	Chi-square	df	*p*	Nagelkerke R^2	Wald	df	*p*	OR	95% CI	Nagelkerke R^2 Model 1
PRSwithAPOE										
5	24.988	16	0.070	0.388	5.488	1	0.019	3.092	1.203-7.951	0.303
10	26.114	16	0.052	0.403	6.281	1	0.012	3.615	1.323-9.876	0.303
APOEonlyPRS										
1	23.867	16	0.092	0.374	4.649	1	0.031	2.612	1.091-6.253	0.303
5	23.885	16	0.092	0.374	4.682	1	0.030	2.622	1.095-6.279	0.303

Controlled for p-tau181 status

PRS & Threshold	Chi-square	df	*p*	Nagelkerke R^2	Wald	df	*p*	OR	95% CI	Nagelkerke R^2 Model 1
PRSwithAPOE										
5	25.891	17	0.076	0.400	4.985	1	0.026	2.948	1.141-7.615	0.325
10	27.085	17	0.057	0.415	5.843	1	0.016	3.457	1.264-9.450	0.325
APOEonlyPRS										
1	25.196	17	0.090	0.391	4.492	1	0.034	2.610	1.075-6.339	0.325
5	25.154	17	0.091	0.391	4.480	1	0.034	2.602	1.073-6.307	0.325

APOE: apolipoprotein E. CI: confidence interval. df: degrees of freedom. OR: odds ratio. PRS: polygenic risk score. P-tau: phosphorylated tau.

Not controlled for p-tau181 status (ε4 carriers)

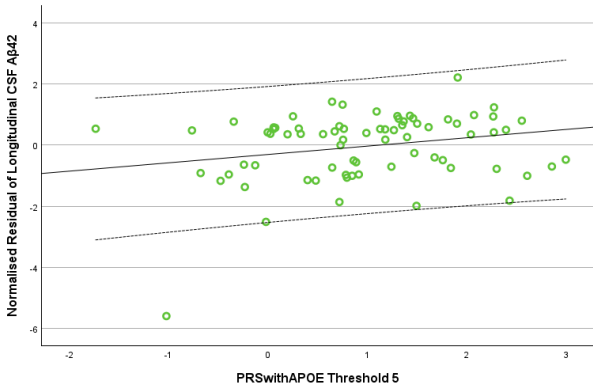

R^2 = 0.056.
Longitudinal CSF Aβ42 = -0.30 + 0.27 * PRSwithAPOE T5.

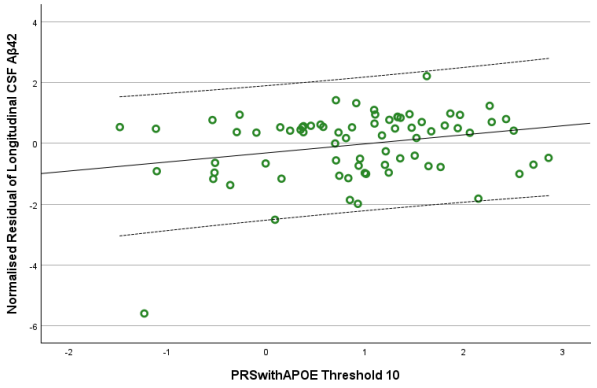

R^2 = 0.065.
Longitudinal CSF Aβ42 = -0.31 + 0.30 * PRSwithAPOE T10.

Controlled for p-tau181 status (ε4 carriers)

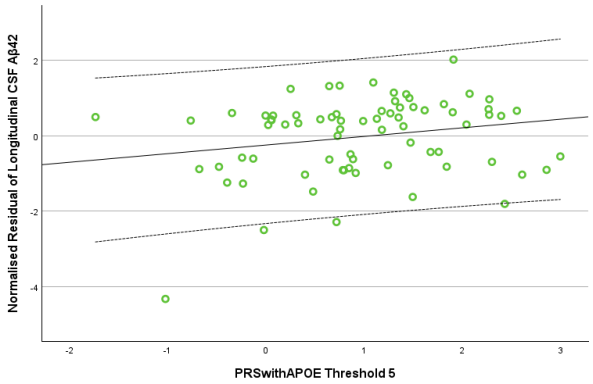

R^2 = 0.045.
Longitudinal CSF Aβ42 = -0.24 + 0.23 * PRSwithAPOE T5.

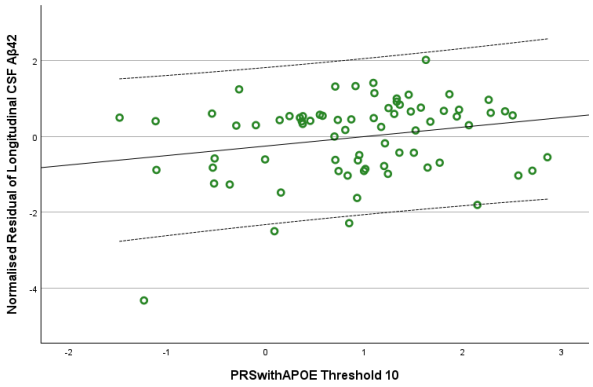

R^2 = 0.053.
Longitudinal CSF Aβ42 = -0.25 + 0.25 * PRSwithAPOE T10.

(T: threshold).

Figure 6A.2: Scatterplots to visualise associations between PRSwithAPOE thresholds and longitudinal change in CSF Aβ42 measurement in ε4 carriers when CSF p-tau181 status was not controlled for vs. was controlled for.

Note, the scatterplots are for visualisation purposes only. The scatterplots show the residualised variable (i.e., longitudinal change in CSF Aβ42) modelled as a function of PRS using linear regression. The R^2 in the scatterplots differs from the Nagelkerke (pseudo) R^2 as the two coefficients are calculated in different ways as part of different types of inferential models. The X axis shows the PRS of interest, and the Y axis indicates the normalised residual of CSF Aβ42 where all covariates have been regressed out.

Not controlled for p-tau181 status (ε4 carriers)

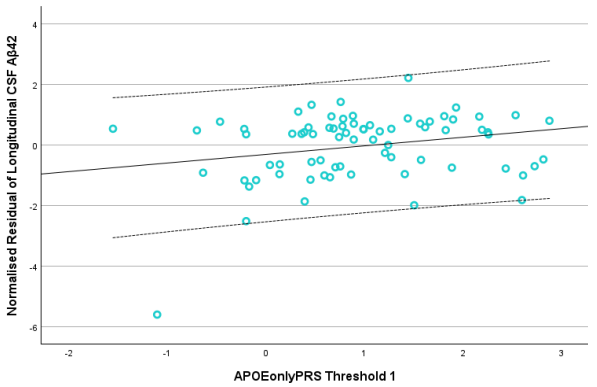

R^2 = 0.057.
Longitudinal CSF Aβ42 = -0.31 + 0.28 * APOEonlyPRS T1.

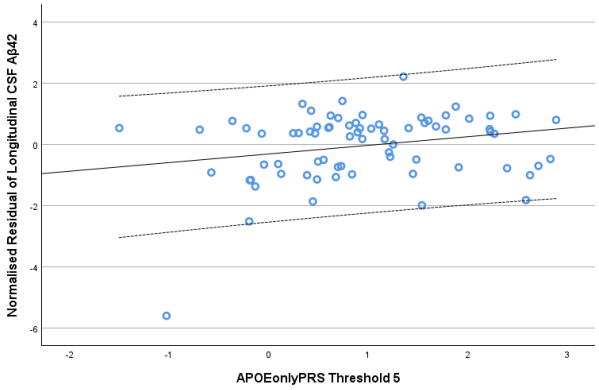

R^2 = 0.056.
Longitudinal CSF Aβ42 = -0.31 + 0.28 * APOEonlyPRS T5.

Controlled for p-tau181 status (ε4 carriers)

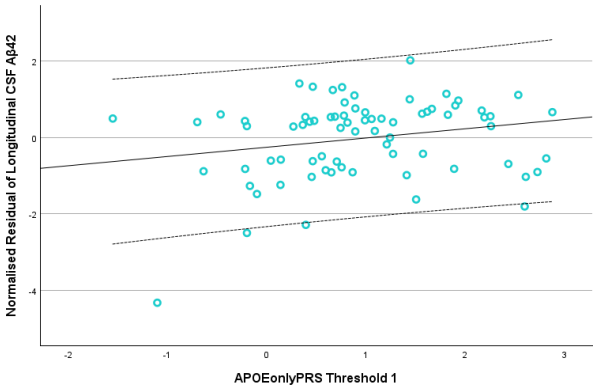

R^2 = 0.048.
Longitudinal CSF Aβ42 = -0.25 + 0.24 * APOEonlyPRS T1.

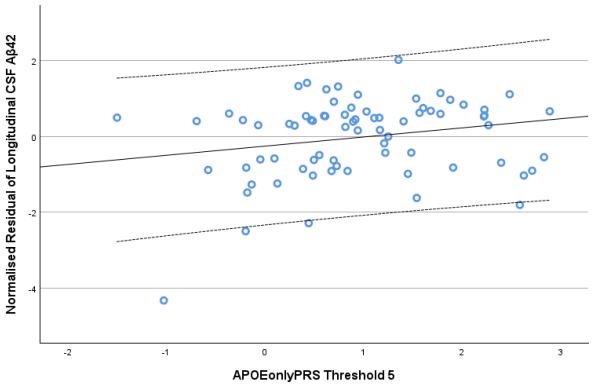

R^2 = 0.047.
Longitudinal CSF Aβ42 = -0.25 + 0.24 * APOEonlyPRS T5.

(T: threshold).

Figure 6A.3: Scatterplots to visualise associations between APOEonlyPRS thresholds and longitudinal change in CSF Aβ42 measurement in ε4 carriers when CSF p-tau181 status was not controlled for vs. was controlled for.

Note, the scatterplots are for visualisation purposes only. The scatterplots show the residualised variable (i.e., longitudinal change in CSF Aβ42) modelled as a function of PRS using linear regression. The R^2 in the scatterplots differs from the Nagelkerke (pseudo) R^2 as the two coefficients are calculated in different ways as part of different types of inferential models. The X axis shows the PRS of interest, and the Y axis indicates the normalised residual of CSF Aβ42 where all covariates have been regressed out.

6A.3.1.5. (E) Whole group stratified by diagnostic status, not controlled for p-tau181 status – CU and MCI only

PRSwithAPOE:

For CU participants, PRSwithAPOE thresholds were not associated with CSF Aβ42 when CSF p-tau181 was not controlled for. This was also the case for MCI patients. See Appendix F1 Table F1.7 (CU) and Table F1.8 (MCI).

APOEonlyPRS:

In CU participants, APOEonlyPRS Threshold 10 (p = 0.047) was associated significantly and positively with CSF Aβ42 when CSF p-tau181 was not controlled for. Therefore, high PRS was associated with worsening of CSF Aβ42 measurement at 24 months. Refer to Table 6A.4 and Figure 6A.4. No other associations were evident (Appendix F1 Table F1.7 and Table F1.8).

6A.3.1.6. (F) Whole group stratified by diagnostic status, controlled for p-tau181 status (post-hoc) – CU and MCI only

PRSwithAPOE:

For CU participants, PRSwithAPOE Threshold 5 was associated significantly and positively with CSF Aβ42 when CSF p-tau181 was controlled for (p = 0.044). Therefore, high PRS was associated with worsening of CSF Aβ42 measurement at 24 months. See Table 6A.4, Figure 6A.4, and Appendix F1 Table F1.9. No associations were observed in MCI (Appendix F1 Table F1.10).

APOEonlyPRS:

For CU participants, APOEonlyPRS was associated significantly and positively with CSF Aβ42 when CSF p-tau181 was controlled for. In ascending order of significance, Threshold 10 (p = 0.046), then Threshold 5 (p = 0.048). Therefore, high PRS was associated with worsening of CSF Aβ42 measurement at 24 months. Refer to Table 6A.4 and Figure 6A.4. No other associations were found in CU (Appendix F1 Table F1.9) or MCI (Appendix F1 Table F1.10).

Table 6A.4: Associations between PRSs and longitudinal change in CSF Aβ42 measurement in CU participants when CSF p-tau181 status was not controlled for vs. was controlled for.

Not controlled for p-tau181 status

PRS & Threshold	Chi-square	df	*p*	Nagelkerke R^2	Wald	df	*p*	OR	95% CI	Nagelkerke R^2 Model 1
APOEonlyPRS										
10	26.684	16	0.045	0.673	3.943	1	0.047	73.733	1.057-5142.963	0.429

Controlled for p-tau181 status

PRS & Threshold	Chi-square	df	*p*	Nagelkerke R^2	Wald	df	*p*	OR	95% CI	Nagelkerke R^2 Model 1
PRSwithAPOE										
5	24.307	17	0.111	0.630	4.067	1	0.044	19.577	1.087-352.529	0.444
APOEonlyPRS										
5	25.013	17	0.094	0.643	3.911	1	0.048	23.596	1.029-541.193	0.444
10	27.134	17	0.056	0.681	3.995	1	0.046	55.052	1.081-2804.252	0.444

APOE: apolipoprotein E. CI: confidence interval. df: degrees of freedom. OR: odds ratio. PRS: polygenic risk score. P-tau: phosphorylated tau.

Controlled for p-tau181 status (CU; PRSwithAPOE)

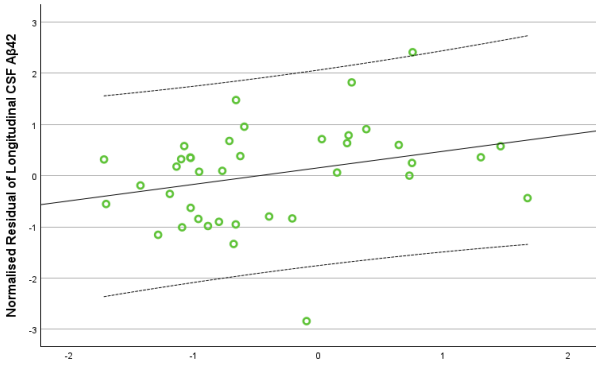

R^2 = 0.086.
Longitudinal CSF Aβ42 = 0.15 + 0.32 * PRSwithAPOE T5.

Not controlled for p-tau181 status (CU; APOEonlyPRS)

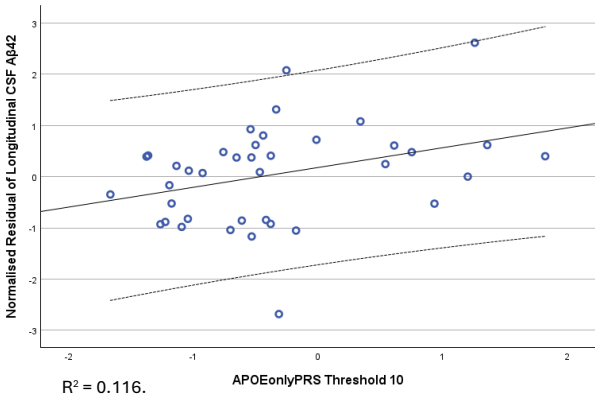

R^2 = 0.116.
Longitudinal CSF Aβ42 = 0.18 + 0.39 * APOEonlyPRS T10.

Controlled for p-tau181 status (CU; APOEonlyPRS)

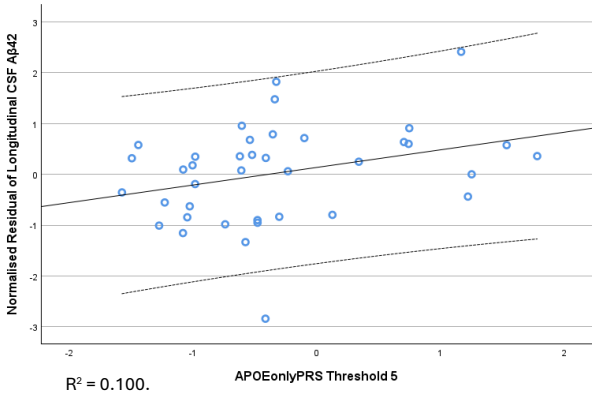

R^2 = 0.100.
Longitudinal CSF Aβ42 = 0.14 + 0.35 * APOEonlyPRS T5.

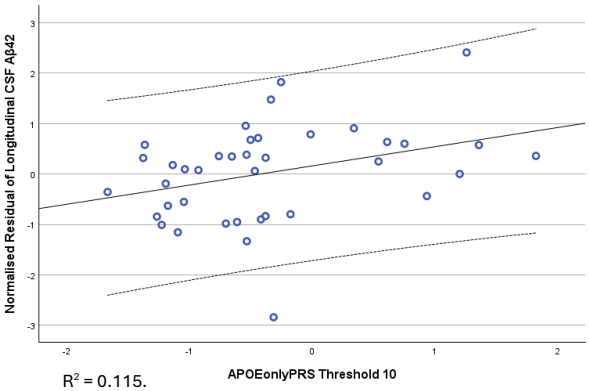

R^2 = 0.115.
Longitudinal CSF Aβ42 = 0.16 + 0.38 * APOEonlyPRS T10.

(T: threshold).

Figure 6A.4: Scatterplots to visualise associations between PRSwithAPOE Threshold 5, APOEonlyPRS thresholds, and longitudinal change in CSF Aβ42 measurement in CU participants when CSF p-tau181 status was not controlled for vs. was controlled for.

Note, the scatterplots are for visualisation purposes only. The scatterplots show the residualised variable (i.e., longitudinal change in CSF Aβ42) modelled as a function of PRS using linear regression. The R^2 in the scatterplots differs from the Nagelkerke (pseudo) R^2 as the two coefficients are calculated in different ways as part of different types of inferential models. The X axis shows the PRS of interest, and the Y axis indicates the normalised residual of CSF Aβ42 where all covariates have been regressed out.

6A.3.1.7. Other related findings

In the whole group, not controlling vs. controlling for p-tau181 status did not lead to different results when using PRSwithAPOE thresholds or APOEonlyPRS thresholds. In both cases, no associations were found between PRSwithAPOE and APOEonlyPRS with longitudinal Aβ42. See Appendix F1 Table F1.1 (whole group not controlled for p-tau181) and Appendix F1 Table F1.2 (whole group controlled for p-tau181).

When the whole group was stratified by APOE ε4 status and when the whole group was stratified by diagnosis (CU vs. MCI only), not controlling vs. controlling for p-tau181 status did not change the findings when PRSwithoutAPOE thresholds were used. In all four cases, no associations were found between PRSwithoutAPOE and longitudinal Aβ42. See Appendix F1 Table F1.3 (ε4 carriers not controlled for p-tau181), Table F1.4 (ε4 non-carriers not controlled for p-tau181), Table F1.5 (ε4 carriers controlled for p-tau181), Table F1.6 (ε4 non-carriers controlled for p-tau181), Table F1.7 (CU not controlled for p-tau181), Table F1.8 (MCI not controlled for p-tau181), Table F1.9 (CU controlled for p-tau181), and Table F1.10 (MCI controlled for p-tau181).

Additionally, when the diagnostic status (CU vs. MCI only) was stratified further by ε4 status (CU ε4 non-carriers vs. MCI ε4 non-carriers vs. MCI ε4 carriers), not controlling vs. controlling for p-tau181 status did not generate different results. In both instances, PRSwithAPOE thresholds, PRSwithoutAPOE thresholds and APOEonlyPRS thresholds were not associated with longitudinal Aβ42. See Appendix F1 Table F1.11 (CU ε4 non-carriers not controlled for p-tau181), Table F1.12 (MCI ε4 non-carriers not controlled for p-tau181), Table F1.13 (MCI ε4 carriers not controlled for p-tau181), Table F1.14 (CU ε4 non-carriers controlled for p-tau181), Table F1.15 (MCI ε4 non-carriers controlled for p-tau181), and Table F1.16 (MCI ε4 carriers controlled for p-tau181).

6A.3.2. Stage 2 Results: Logistic Regression – Tau Study

6A.3.2.1. (C) Whole group stratified by APOE ε4 status, not controlled for Aβ42 status

PRSwithAPOE:

For APOE ε4 non-carriers, PRSwithAPOE thresholds were associated significantly with CSF p-tau181 when Aβ42 was not controlled for. In ascending order of significance, Threshold 5 (p = 0.005), followed by Threshold 1 (p = 0.006), and then Threshold 10 (p = 0.037). These were all associated negatively, i.e., high PRS, CSF p-tau181 did not worsen at 24 months. Refer to Table 6A.5, Figure 6A.5, and Appendix F1 Table F1.17. No associations were found in ε4 carriers (Appendix F1 Table F1.18).

APOEonlyPRS:

In APOE ε4 non-carriers, APOEonlyPRS thresholds were associated significantly and negatively with CSF p-tau181 when Aβ42 was not controlled for. Thresholds 1 and 5 (p = 0.002) were significant the most, followed by Threshold 10 (p = 0.007). Therefore, high PRS was associated with a lack of worsening of the CSF p-tau181 measurement at 24 months. See Table 6A.5, Figure 6A.6, and Appendix F1 Table F1.17. No associations were evident in ε4 carriers (Appendix F1 Table F1.18).

6A.3.2.2. (D) Whole group stratified by APOE ε4 status, controlled for Aβ42 status (post-hoc)

PRSwithAPOE:

In APOE ε4 non-carriers, PRSwithAPOE thresholds were associated significantly and negatively with CSF p-tau181 when Aβ42 was controlled for. In ascending order of significance, Thresholds 1 and 5 (p = 0.005), followed by Threshold 10 (p = 0.037). Therefore, high PRS was associated with a lack of worsening of the CSF p-tau181 measurement at 24 months. Refer to Table 6A.5, Figure 6A.5, and Appendix F1 Table F1.19. No associations were observed in ε4 carriers (Appendix F1 Table F1.20).

APOEonlyPRS:

In APOE ε4 non-carriers, APOEonlyPRS thresholds were associated significantly and negatively with CSF p-tau181 when Aβ42 was controlled for. Thresholds 1 and 5 ($p = 0.002$) were significant the most, followed by Threshold 10 ($p = 0.007$). Therefore, high PRS was associated with a lack of worsening of the CSF p-tau181 measurement at 24 months. See Table 6A.5, Figure 6A.6, and Appendix F1 Table F1.19. No associations were found in ε4 carriers (Appendix F1 Table F1.20).

Table 6A.5: Associations between PRSs and longitudinal change in CSF p-tau181 measurement in ε4 non-carriers when CSF Aβ42 status was not controlled for vs. was controlled for.

Not controlled for Aβ42 status

PRS & Threshold	Chi-square	df	*p*	Nagelkerke R^2	Wald	df	*p*	OR	95% CI	Nagelkerke R^2 Model 1
PRSwithAPOE										
1	26.141	16	0.052	0.321	7.598	1	0.006	0.242	0.088-0.664	0.224
5	26.391	16	0.049	0.324	7.803	1	0.005	0.249	0.094-0.660	0.224
10	22.090	16	0.140	0.277	4.333	1	0.037	0.394	0.164-0.947	0.224
APOEonlyPRS										
1	28.939	16	0.024	0.351	9.573	1	0.002	0.185	0.064-0.539	0.224
5	29.113	16	0.023	0.353	9.728	1	0.002	0.180	0.061-0.528	0.224
10	25.746	16	0.058	0.317	7.300	1	0.007	0.235	0.082-0.672	0.224

Controlled for Aβ42 status

PRS & Threshold	Chi-square	df	*p*	Nagelkerke R^2	Wald	df	*p*	OR	95% CI	Nagelkerke R^2 Model 1
PRSwithAPOE										
1	26.348	17	0.068	0.323	7.723	1	0.005	0.234	0.084-0.652	0.224
5	26.463	17	0.066	0.325	7.838	1	0.005	0.246	0.092-0.657	0.224
10	22.090	17	0.181	0.277	4.332	1	0.037	0.394	0.164-0.947	0.224
APOEonlyPRS										
1	29.030	17	0.034	0.352	9.598	1	0.002	0.183	0.062-0.535	0.224
5	29.170	17	0.033	0.353	9.755	1	0.002	0.178	0.060-0.526	0.224
10	25.749	17	0.079	0.317	7.300	1	0.007	0.235	0.082-0.672	0.224

Aβ: amyloid beta. APOE: apolipoprotein E. CI: confidence interval. df: degrees of freedom. OR: odds ratio. PRS: polygenic risk score.

Not controlled for Aβ42 status (ε4 non-carriers)

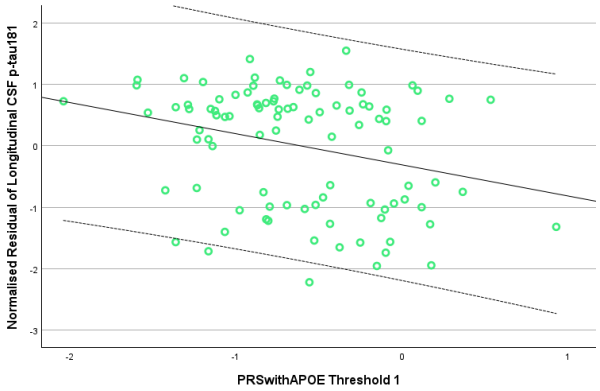

R^2 = 0.078.
Longitudinal CSF p-tau181 = -0.31 – 0.51 * PRSwithAPOE T1.

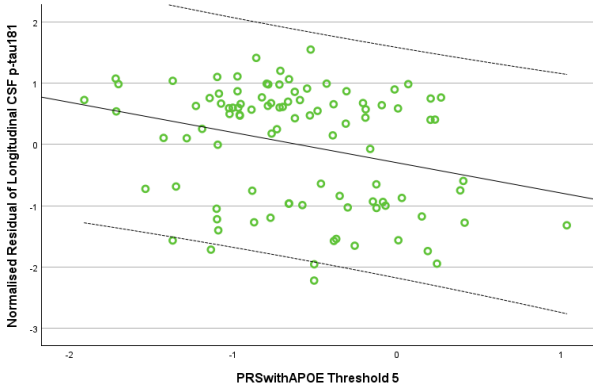

R^2 = 0.079.
Longitudinal CSF p-tau181 = -0.30 – 0.49 * PRSwithAPOE T5.

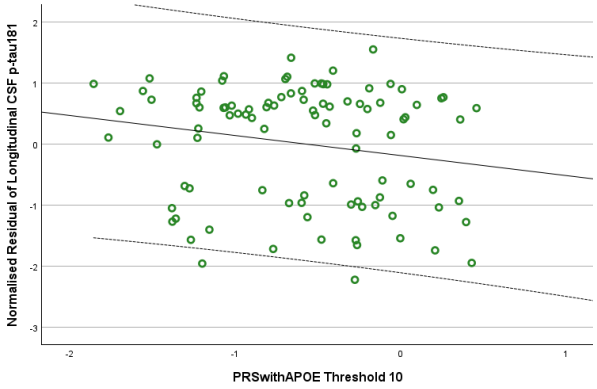

R^2 = 0.040.
Longitudinal CSF p-tau181 = -0.19 – 0.33 * PRSwithAPOE T10.

Controlled for Aβ42 status (ε4 non-carriers)

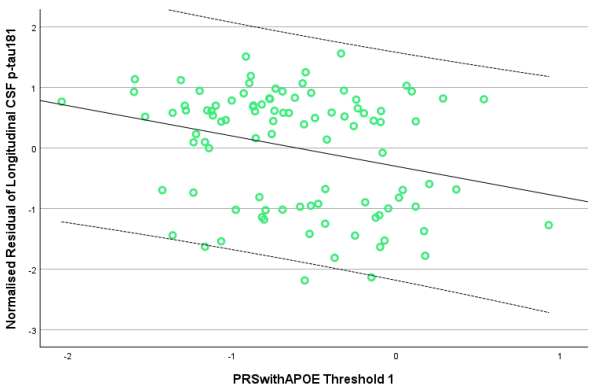

R^2 = 0.076.
Longitudinal CSF p-tau181 = -0.30 – 0.50 * PRSwithAPOE T1.

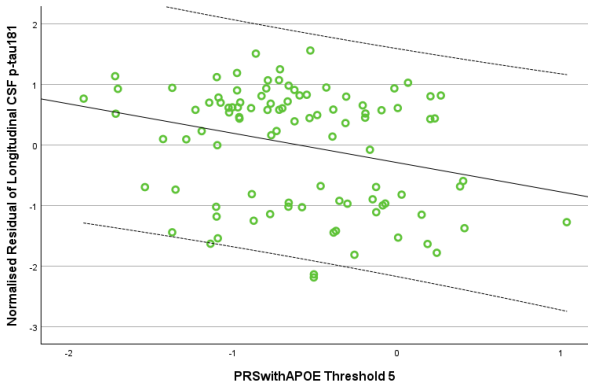

R^2 = 0.076.
Longitudinal CSF p-tau181 = -0.29 – 0.48 * PRSwithAPOE T5.

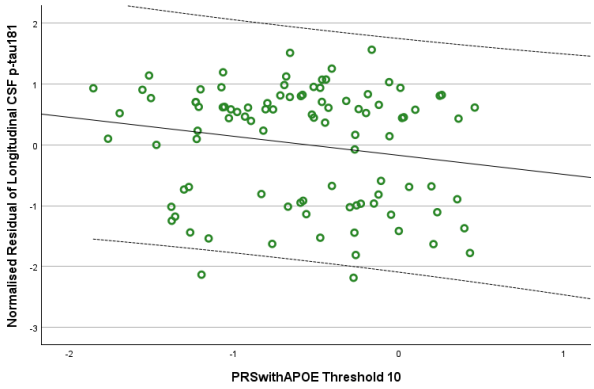

R^2 = 0.036.
Longitudinal CSF p-tau181 = -0.17 – 0.31 * PRSwithAPOE T10.

(T: threshold).

Figure 6A.5: Scatterplots to visualise associations between PRSwithAPOE thresholds and longitudinal change in CSF p-tau181 measurement in ε4 non-carriers when CSF Aβ42 status was not controlled for vs. was controlled for.

Note, the scatterplots are for visualisation purposes only. The scatterplots show the residualised variable (i.e., longitudinal change in CSF p-tau181) modelled as a function of PRS using linear regression. The R^2 in the scatterplots differs from the Nagelkerke (pseudo) R^2 as the two coefficients are calculated in different ways as part of different types of inferential models. The X axis shows the PRS of interest, and the Y axis indicates the normalised residual of CSF p-tau181 where all covariates have been regressed out.

Not controlled for Aβ42 status (ε4 non-carriers)

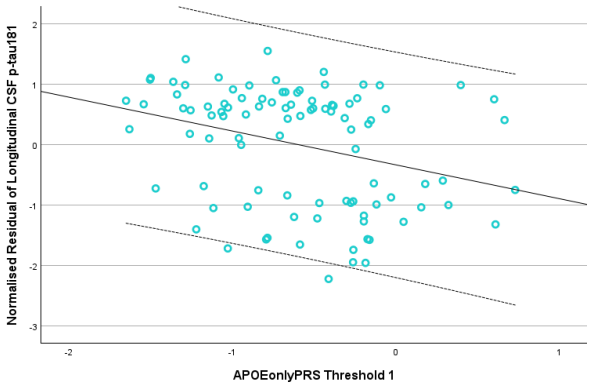

R^2 = 0.096.
Longitudinal CSF p-tau181 = -0.33 – 0.56 * APOEonlyPRS T1.

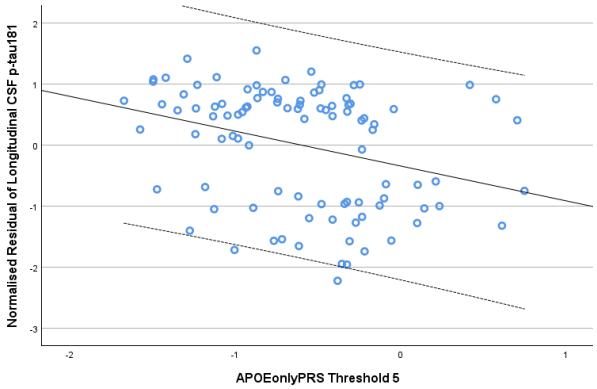

R^2 = 0.097.
Longitudinal CSF p-tau181 = -0.34 – 0.57 * APOEonlyPRS T5.

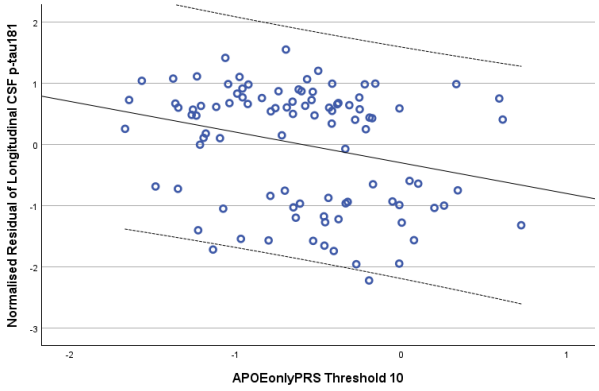

R^2 = 0.071.
Longitudinal CSF p-tau181 = -0.30 – 0.50 * APOEonlyPRS T10.

Controlled for Aβ42 status (ε4 non-carriers)

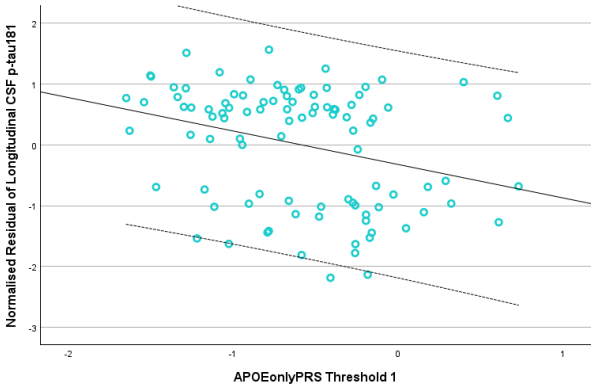

R^2 = 0.093.
Longitudinal CSF p-tau181 = -0.32 – 0.55 * APOEonlyPRS T1.

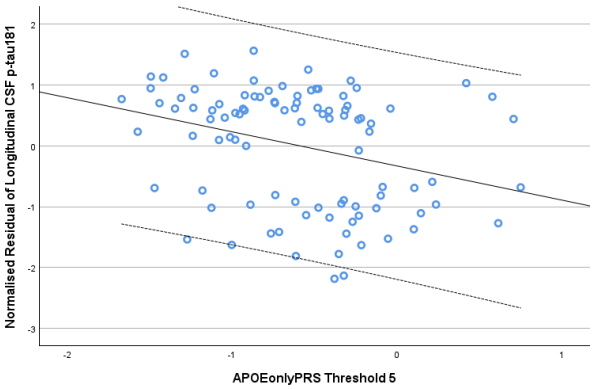

R^2 = 0.094.
Longitudinal CSF p-tau181 = -0.33 – 0.56 * APOEonlyPRS T5.

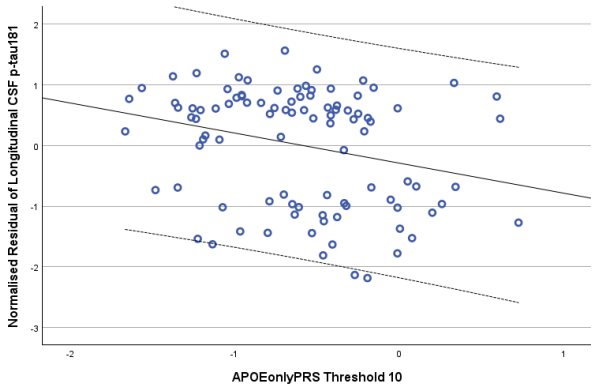

R^2 = 0.070.
Longitudinal CSF p-tau181 = -0.29 – 0.50 * APOEonlyPRS T10.

(T: threshold).

Figure 6A.6: Scatterplots to visualise associations between APOEonlyPRS thresholds and longitudinal change in CSF p-tau181 measurement in ε4 non-carriers when CSF Aβ42 status was not controlled for vs. was controlled for.

Note, the scatterplots are for visualisation purposes only. The scatterplots show the residualised variable (i.e., longitudinal change in CSF p-tau181) modelled as a function of PRS using linear regression. The R^2 in the scatterplots differs from the Nagelkerke (pseudo) R^2 as the two coefficients are calculated in different ways as part of different types of inferential models. The X axis shows the PRS of interest, and the Y axis indicates the normalised residual of CSF p-tau181 where all covariates have been regressed out.

6A.3.2.3. (G) Diagnostic status stratified further by APOE ε4 status, not controlled for Aβ42 status – CU ε4 non-carriers, MCI ε4 non-carriers, and MCI ε4 carriers only

PRSwithAPOE:

In MCI ε4 non-carriers, PRSwithAPOE Threshold 1 (p = 0.035) and Threshold 5 (p = 0.038) were associated significantly with CSF p-tau181 when Aβ42 had been controlled for. Both were negative associations, therefore, high PRS was associated with a lack of worsening of the CSF p-tau181 measurement at 24 months. See Figure 6A.6, Figure 6A.7, and Appendix F1 Table F1.21. No associations were found in CU ε4 non-carriers (Appendix F1 Table F1.22) or in MCI ε4 carriers (Appendix F1 Table F1.23).

APOEonlyPRS:

For MCI ε4 non-carriers, APOEonlyPRS thresholds were associated significantly with CSF p-tau181 when Aβ42 was not controlled for. In ascending order of significance; Threshold 5 (p = 0.019), followed by Threshold 1 (p = 0.020), and then Threshold 10 (p = 0.039). These were all negative associations, i.e., high PRS was associated with a lack of worsening of the CSF p-tau181 measurement at 24 months. See Figure 6A.6, Figure 6A.8, and Appendix F1 Table F1.21. No associations were evident in CU ε4 non-carriers (Appendix F1 Table F1.22) or in MCI ε4 carriers (Appendix F1 Table F1.23).

6A.3.2.4. (H) Diagnostic status stratified further by APOE ε4 status, controlled for Aβ42 status (post-hoc) – CU ε4 non-carriers, MCI ε4 non-carriers, and MCI ε4 carriers only

PRSwithAPOE:

For MCI ε4 non-carriers, PRSwithAPOE Threshold 5 (p = 0.046) and Threshold 1 (p = 0.049) were associated significantly with CSF p-tau181 when Aβ42 was controlled for. Both were associated negatively, i.e., high PRS was associated with a lack of worsening of the CSF p-tau181 measurement at 24 months. See Figure 6A.6, Figure 6A.7, and Appendix F1 Table F1.24. No associations were observed in CU ε4 non-carriers (Appendix F1 Table F1.25) or in MCI ε4 carriers (Appendix F1 Table F1.26).

APOEonlyPRS:

For MCI ε4 non-carriers, APOEonlyPRS thresholds were associated significantly and negatively with CSF p-tau181 when Aβ42 was controlled for. In ascending order of significance; Threshold 5 (p = 0.024), followed by Threshold 1 (p = 0.026) and then Threshold 10 (p = 0.041). Therefore, high PRS was associated with a lack of worsening of the CSF p-tau181 measurement at 24 months. See Figure 6A.6, Figure 6A.8, and Appendix F1 Table F1.24. No other associations were apparent in CU ε4 non-carriers (Appendix F1 Table F1.25) or in MCI ε4 carriers (Appendix F1 Table F1.26).

Table 6A.6: Associations between PRSs and longitudinal change in CSF p-tau181 measurement in MCI ε4 non-carriers when CSF Aβ42 status was not controlled for vs. was controlled for.

Not controlled for Aβ42 status

PRS & Threshold	Chi-square	df	*p*	Nagelkerke R^2	Wald	df	*p*	OR	95% CI	Nagelkerke R^2 Model 1
PRSwithAPOE										
1	23.382	16	0.104	0.431	4.468	1	0.035	0.165	0.031-0.877	0.347
5	23.120	16	0.111	0.427	4.325	1	0.038	0.174	0.034-0.904	0.347
APOEonlyPRS										
1	25.039	16	0.069	0.456	5.417	1	0.020	0.122	0.021-0.718	0.347
5	25.384	16	0.063	0.461	5.515	1	0.019	0.103	0.015-0.687	0.347
10	23.248	16	0.107	0.429	4.276	1	0.039	0.166	0.030-0.911	0.347

Controlled for Aβ42 status

PRS & Threshold	Chi-square	df	*p*	Nagelkerke R^2	Wald	df	*p*	OR	95% CI	Nagelkerke R^2 Model 1
PRSwithAPOE										
1	23.605	17	0.131	0.435	3.871	1	0.049	0.180	0.033-0.993	0.363
5	23.656	17	0.129	0.435	3.964	1	0.046	0.187	0.036-0.974	0.363
APOEonlyPRS										
1	25.357	17	0.087	0.461	4.961	1	0.026	0.132	0.022-0.784	0.363
5	25.760	17	0.079	0.467	5.084	1	0.024	0.110	0.016-0.750	0.363
10	24.153	17	0.115	0.443	4.176	1	0.041	0.168	0.030-0.929	0.363

Aβ: amyloid beta. APOE: apolipoprotein E. CI: confidence interval. df: degrees of freedom. OR: odds ratio. PRS: polygenic risk score.

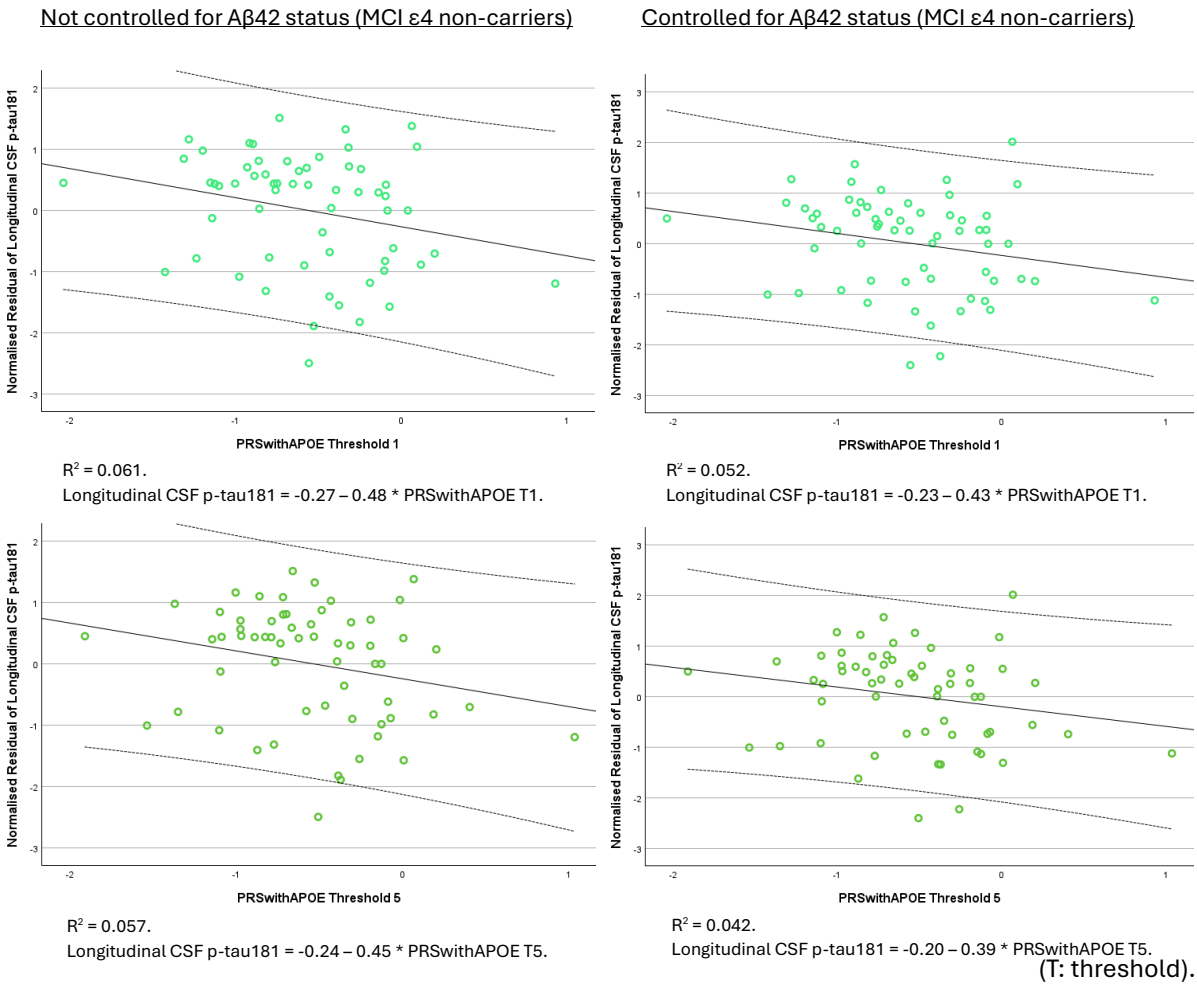

(T: threshold).

Figure 6A.7: Scatterplots to visualise associations between PRSwithAPOE thresholds and longitudinal change in CSF p-tau181 measurement in MCI ε4 non-carriers when CSF Aβ42 status was not controlled for vs. was controlled for.

Note, the scatterplots are for visualisation purposes only. The scatterplots show the residualised variable (i.e., longitudinal change in CSF p-tau181) modelled as a function of PRS using linear regression. The R^2 in the scatterplots differs from the Nagelkerke (pseudo) R^2 as the two coefficients are calculated in different ways as part of different types of inferential models. The X axis shows the PRS of interest, and the Y axis indicates the normalised residual of CSF p-tau181 where all covariates have been regressed out.

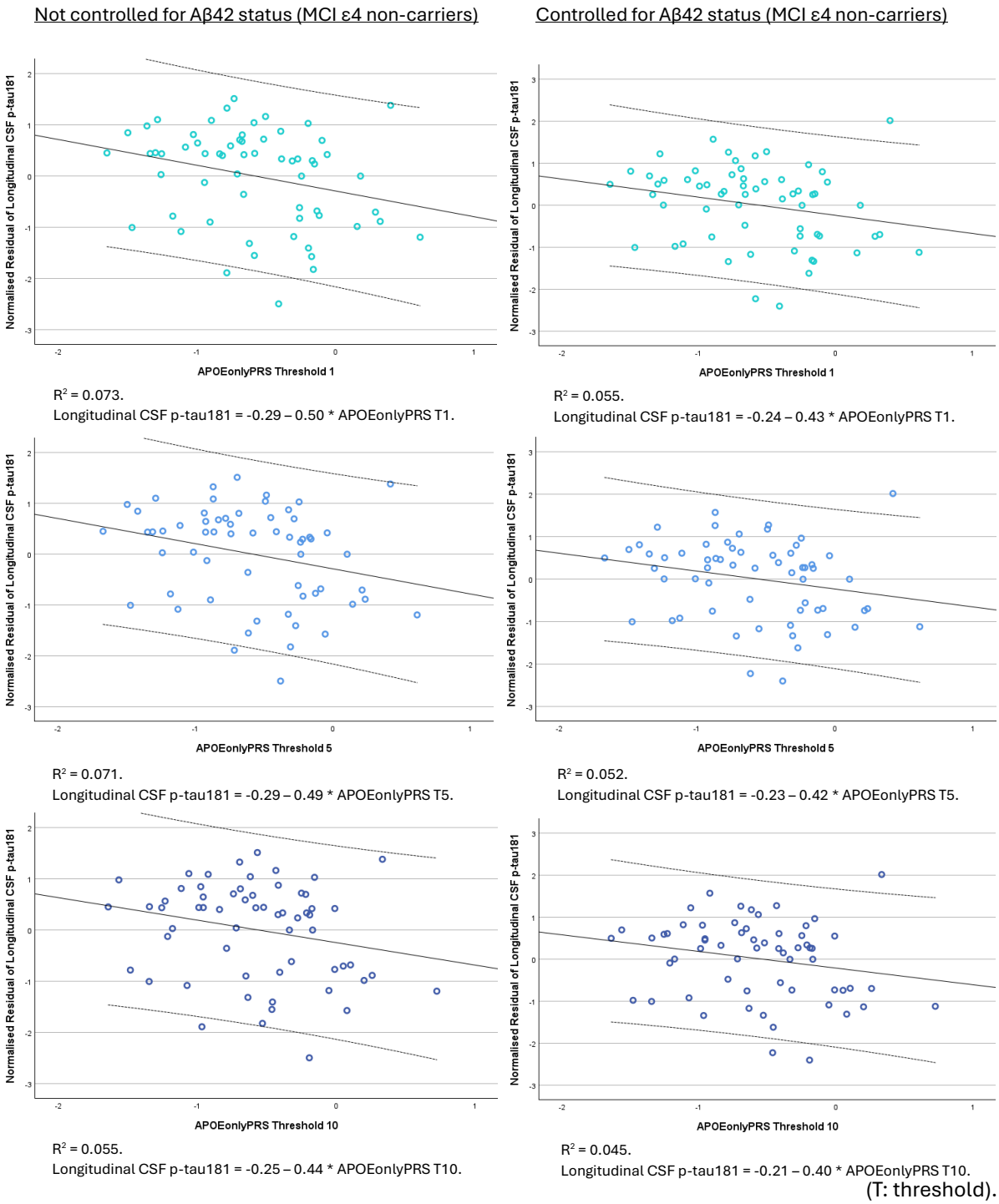

Figure 6A.8: Scatterplots to visualise associations between APOEonlyPRS thresholds and longitudinal change in CSF p-tau181 measurement in MCI ε4 non-carriers when CSF Aβ42 status was not controlled for vs. was controlled for.

Note, the scatterplots are for visualisation purposes only. The scatterplots show the residualised variable (i.e., longitudinal change in CSF p-tau181) modelled as a function of PRS using linear regression. The R^2 in the scatterplots differs from the Nagelkerke (pseudo) R^2 as the two coefficients are calculated in different ways as part of different types of inferential models. The X axis shows the PRS of interest, and the Y axis indicates the normalised residual of CSF p-tau181 where all covariates have been regressed out.

6A.3.2.5. Other related findings

In the whole group, and when the whole group was stratified by diagnosis (CU vs. MCI only), not controlling vs. controlling for Aβ42 status did not lead to different results. On all 4 occasions, PRSwithAPOE thresholds, PRSwithoutAPOE thresholds and APOEonlyPRS thresholds were not associated with longitudinal p-tau181. See Appendix F1 Table F1.27 (whole group not controlled for Aβ42), Table F1.28 (whole group controlled for Aβ42), Table F1.29 (CU not controlled for Aβ42), Table F1.30 (MCI not controlled for Aβ42), Table F1.31 (CU controlled for Aβ42), and Table F1.32 (MCI controlled for Aβ42).

When the whole group was stratified by APOE ε4 status, not controlling vs. controlling for Aβ42 status did not alter the findings when PRSwithoutAPOE thresholds were used. In both cases, no associations were found between PRSwithoutAPOE and longitudinal p-tau181. Refer to Appendix F1 Table F1.17 (ε4 non-carriers not controlled for Aβ42), Table F1.18 (ε4 carriers not controlled for Aβ42), Table F1.19 (ε4 non-carriers controlled for Aβ42), and Table F1.20 (ε4 carriers controlled for Aβ42).

Moreover, when the diagnostic status (CU vs. MCI only) was stratified further by ε4 status (CU ε4 non-carriers vs. MCI ε4 non-carriers vs. MCI ε4 carriers), again, not controlling vs. controlling for Aβ42 status did not generate different results when PRSwithoutAPOE thresholds were used. In both instances, no associations were found between PRSwithoutAPOE and longitudinal p-tau181. Consult Appendix F1 Table F1.21 (MCI ε4 non-carriers not controlled for Aβ42), Table F1.22 (CU ε4 non-carriers not controlled for Aβ42), Table F1.23 (MCI ε4 carriers not controlled for Aβ42), Table F1.24 (MCI ε4 non-carriers controlled for Aβ42), Table F1.25 (CU ε4 non-carriers controlled for Aβ42), and Table F1.26 (MCI ε4 carriers controlled for Aβ42).

6A.3.3. Stage 3 Results: Linear Regression – Amyloid Study

In the whole group, when the whole group was stratified by APOE ε4 status or diagnosis (CU vs. MCI only) and when diagnostic status (CU vs. MCI only) was stratified further by ε4 status (CU ε4 non-carriers vs. MCI ε4 non-carriers vs. MCI ε4 carriers), not controlling vs. controlling for p-tau181 status did not generate different findings. On all occasions, PRSwithAPOE thresholds, PRSwithoutAPOE thresholds and APOEonlyPRS thresholds were not associated with longitudinal CSF Aβ42.

For details, see Appendix F1 Table F1.33 (whole group not controlled for p-tau181), Table F1.34 (whole group controlled for p-tau181), Table F1.35 (ε4 non-carriers not controlled for p-tau181), Table F1.36 (ε4 carriers not controlled for p-tau181), Table F1.37 (ε4 non-carriers controlled for p-tau181), Table F1.38 (ε4 carriers controlled for p-tau181), Table F1.39 (CU not controlled for p-tau181), Table F1.40 (MCI not controlled for p-tau181), Table F1.41 (CU controlled for p-tau181), Table F1.42 (MCI controlled for p-tau181), Table F1.43 (CU ε4 non-carriers not controlled for p-tau181), Table F1.44 (MCI ε4 non-carriers not controlled for p-tau181), Table F1.45 (MCI ε4 carriers not controlled for p-tau181), Table F1.46 (CU ε4 non-carriers controlled for p-tau181), Table F1.47 (MCI ε4 non-carriers controlled for p-tau181), and Table F1.48 (MCI ε4 carriers controlled for p-tau181).

6A.3.4. Stage 4 Results: Linear Regression – Tau Study

6A.3.4.1. (E) Whole group stratified by diagnostic status, not controlled for Aβ42 status – CU and MCI only

PRSwithAPOE:

For CU participants, PRSwithAPOE was associated significantly with the differential scores of CSF p-tau181 when CSF Aβ42 was not controlled for. In ascending order of significance; Threshold 10 (p = 0.012), Threshold 1 (p = 0.021), and then Threshold 5 (p = 0.028). These were all associated negatively, i.e., high PRS, lower CSF p-tau181 differential scores. See Table 6A.7, Figure 6A.9 (and Appendix F1 Table F1.49). No associations were observed in MCI (Appendix F1 Table F1.50).

PRSwithoutAPOE:

In MCI, PRSwithoutAPOE Threshold 1 (p = 0.038) was associated significantly and positively with differential scores of CSF p-tau181 when CSF Aβ42 was not controlled for. Therefore, high PRS was linked to higher CSF p-tau181 differential scores. Refer to Table 6A.7, Figure 6A.11, and Appendix F1 Table F1.50). No associations were found in CU (Appendix F1 Table F1.49).

APOEonlyPRS:

For CU, APOEonlyPRS was associated significantly with differential scores of CSF p-tau181 when CSF Aβ42 was not controlled for. In ascending order of significance; Thresholds 1 and 10 (p = 0.016) followed by Threshold 5 (p = 0.017). These were all associated negatively, i.e., high PRS, lower differential scores of CSF p-tau181. See Table 6A.7, Figure 6A.10 (and Appendix F1 Table F1.49). No associations were apparent in MCI (Appendix F1 Table F1.50).

6A.3.4.2. (F) Whole group stratified by diagnostic status, controlled for Aβ42 status (post-hoc) – CU and MCI only

PRSwithAPOE:

In CU participants, PRSwithAPOE thresholds were associated significantly with differential scores of CSF p-tau181 when CSF Aβ42 was controlled for. In ascending order of significance;

Thresholds 1 and 10 (p = 0.002), followed by Threshold 5 (p = 0.003). These were all associated negatively, i.e., high PRS, lower CSF p-tau181 differential scores. See Table 6A.7, Figure 6A.9, and Appendix F1 Table F1.51. No associations were evident in MCI patients (Appendix F1 Table F1.52).

PRSwithoutAPOE:

For MCI patients, PRSwithoutAPOE Threshold 1 (p = 0.050) was associated significantly and positively with differential scores of CSF p-tau181 when CSF Aβ42 was controlled, i.e., high PRS, higher CSF p-tau181 differential scores. Refer to Table 6A.7, Figure 6A.11, and Appendix F1 Table F1.52. No associations were found in CU (Appendix F1 Table F1.51).

APOEonlyPRS:

For CU, APOEonlyPRS thresholds were associated significantly with differential scores of CSF p-tau181 when CSF Aβ42 was controlled for. In ascending order of significance; Threshold 1 (p = 0.003), followed by Threshold 5 (p = 0.004), and then Threshold 10 (p = 0.005). These were all associated negatively, i.e., high PRS, lower CSF p-tau181 differential scores. See Table 6A.7, Figure 6A.10 (and Appendix F1 Table F1.51). No associations were observed in MCI patients (Appendix F1 Table F1.52).

Table 6A.7: Associations between PRSs and differential scores of longitudinal CSF p-tau181 measurements by diagnostic status when CSF Aβ42 status was not controlled for vs. was controlled for.

Not controlled for Aβ42 status

PRS & Thresholds	R Square (Model 1)	R Square (Model 2)	R Square Change	Sig. F Change (Model 2)	Standardised beta of PRS
PRSwithAPOE in CU					
1	0.303	0.455	0.152	0.021	-0.495
5	0.303	0.442	0.140	0.028	-0.476
10	0.303	0.479	0.176	0.012	-0.520
APOEonlyPRS in CU					
1	0.303	0.469	0.166	0.016	-0.550
5	0.303	0.465	0.162	0.017	-0.549
10	0.303	0.468	0.165	0.016	-0.554
PRSwithoutAPOE in MCI					
1	0.065	0.108	0.043	0.038	0.228

Controlled for Aβ42 status

PRS & Thresholds	R Square (Model 1)	R Square (Model 2)	R Square Change	Sig. F Change (Model 2)	Standardised beta of PRS
PRSwithAPOE in CU					
1	0.381	0.621	0.240	0.002	-0.648
5	0.381	0.594	0.213	0.003	-0.608
10	0.381	0.619	0.238	0.002	-0.617
APOEonlyPRS in CU					
1	0.381	0.595	0.214	0.003	-0.634
5	0.381	0.589	0.208	0.004	-0.631
10	0.381	0.582	0.201	0.005	-0.617
PRSwithoutAPOE in MCI					
1	0.072	0.111	0.039	0.050	0.219

Aβ: amyloid beta. APOE: apolipoprotein E. CU: cognitively unimpaired. MCI: mild cognitive impairment. PRS: polygenic risk score.

Not controlled for Aβ42 status (CU)

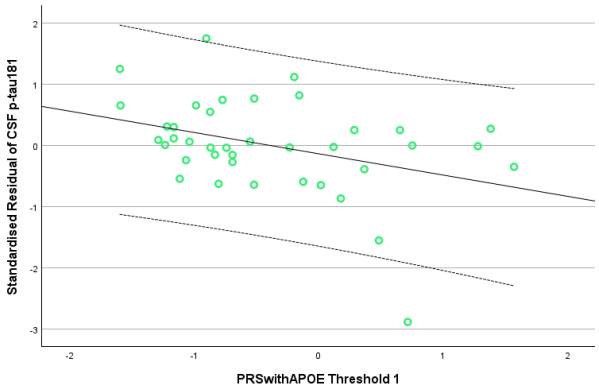

R^2 = 0.135.
Longitudinal CSF p-tau181 = -0.14 – 0.35 * PRSwithAPOE T1.

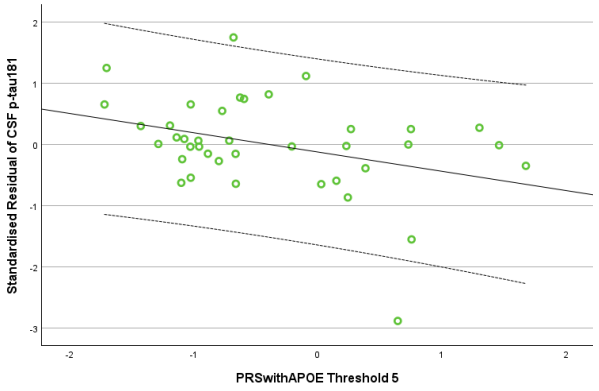

R^2 = 0.124.
Longitudinal CSF p-tau181 = -0.12 – 0.31 * PRSwithAPOE T5.

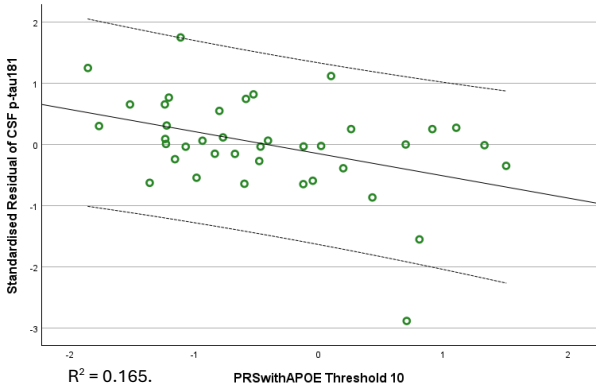

R^2 = 0.165.
Longitudinal CSF p-tau181 = -0.15 – 0.36 * PRSwithAPOE T10.

Controlled for Aβ42 status (CU)

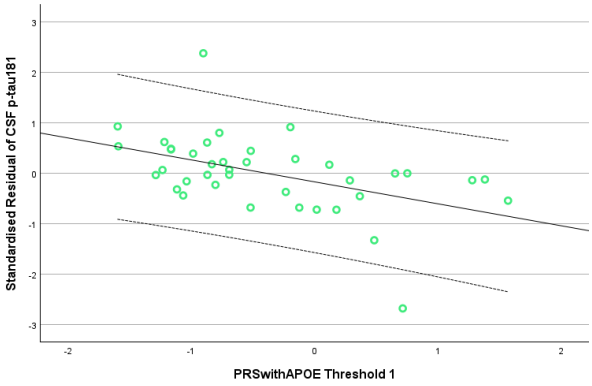

R^2 = 0.221.
Longitudinal CSF p-tau181 = -0.17 – 0.43 * PRSwithAPOE T1.

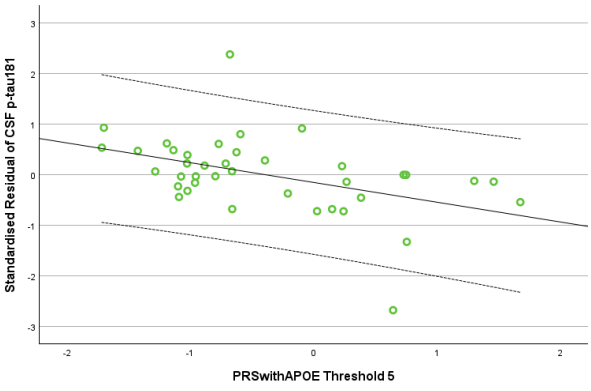

R^2 = 0.199.
Longitudinal CSF p-tau181 = -0.15 – 0.39 * PRSwithAPOE T5.

(T: threshold).

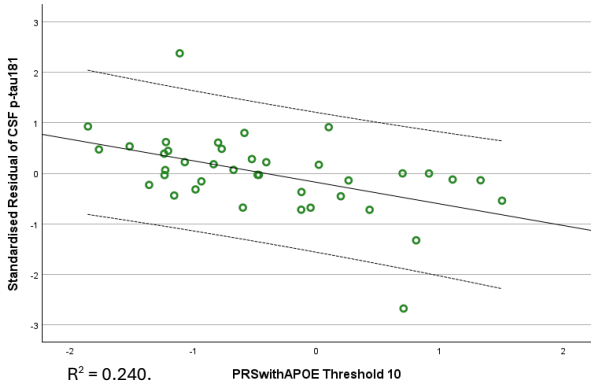

R^2 = 0.240.
Longitudinal CSF p-tau181 = -0.18 – 0.43 * PRSwithAPOE T10.

Figure 6A.9: Scatterplots to visualise associations between PRSwithAPOE thresholds and differential scores of longitudinal CSF p-tau181 measurements in CU participants when CSF Aβ42 status was not controlled for vs. was controlled for.

Note, the scatterplots are for visualisation purposes only. The scatterplots show the residualised variable (i.e., differential scores of longitudinal CSF p-tau181) modelled as a function of PRS using linear regression. The X axis shows the PRS of interest and the Y axis represents the standardised residual of differential scores of longitudinal CSF p-tau181 after all covariates have been regressed out.

Not controlled for Aβ42 status (CU)

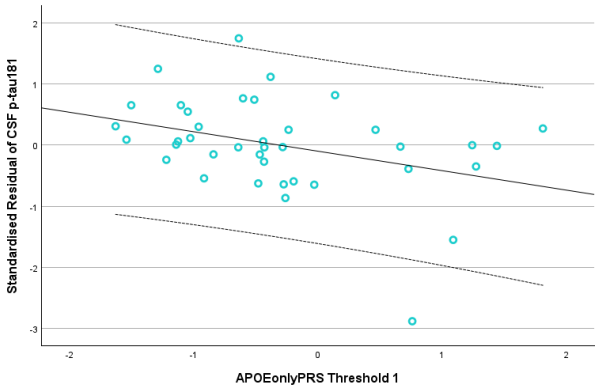

R^2 = 0.130.
Longitudinal CSF p-tau181 = -0.10 – 0.32 * APOEonlyPRS T1.

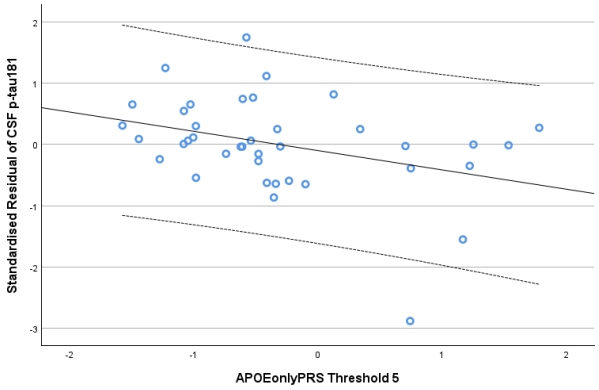

R^2 = 0.125.
Longitudinal CSF p-tau181 = -0.10 – 0.32 * APOEonlyPRS T5.

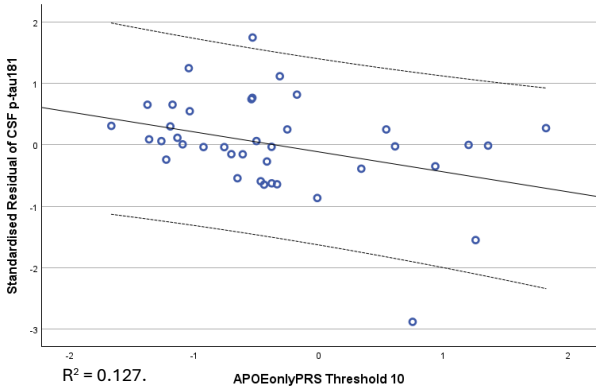

R^2 = 0.127.
Longitudinal CSF p-tau181 = -0.11 – 0.33 * APOEonlyPRS T10.

Controlled for Aβ42 status (CU)

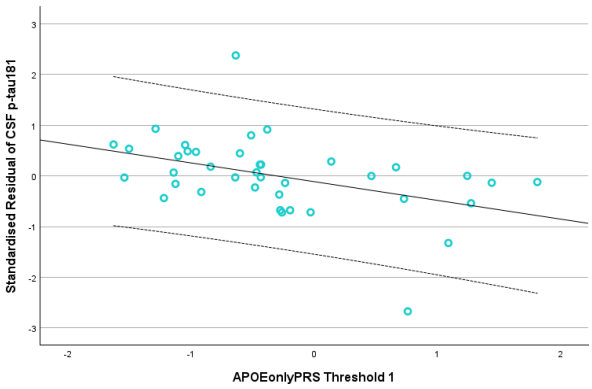

R^2 = 0.183.
Longitudinal CSF p-tau181 = -0.11 – 0.37 * APOEonlyPRS T1.

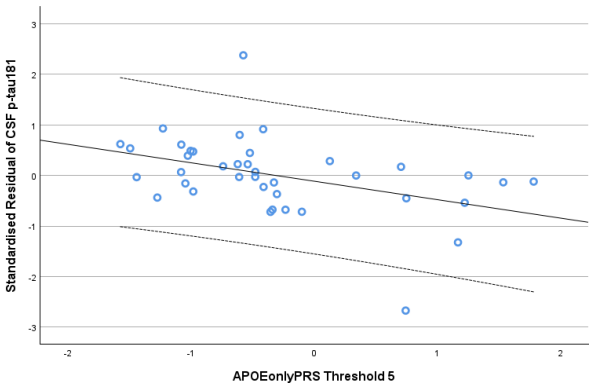

R^2 = 0.176.
Longitudinal CSF p-tau181 = -0.11 – 0.37 * APOEonlyPRS T5.

(T: threshold).

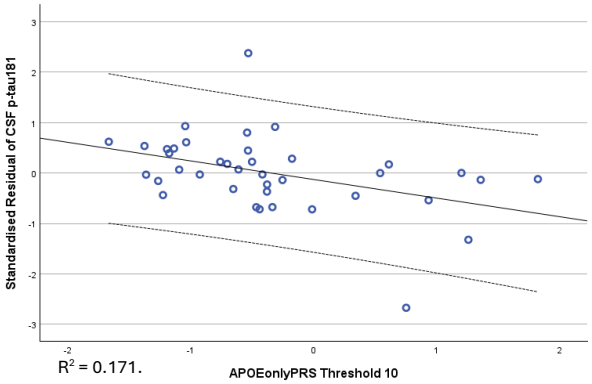

R^2 = 0.171.
Longitudinal CSF p-tau181 = -0.13 – 0.37 * APOEonlyPRS T10.

Figure 6A.10: Scatterplots to visualise associations between APOEonlyPRS thresholds and differential scores of longitudinal CSF p-tau181 measurements in CU participants when CSF Aβ42 status was not controlled for vs. was controlled for.

Note, the scatterplots are for visualisation purposes only. The scatterplots show the residualised variable (i.e., differential scores of longitudinal CSF p-tau181) modelled as a function of PRS using linear regression. The X axis shows the PRS of interest and the Y axis represents the standardised residual of differential scores of longitudinal CSF p-tau181 after all covariates have been regressed out.

Not controlled for Aβ42 status (MCI)

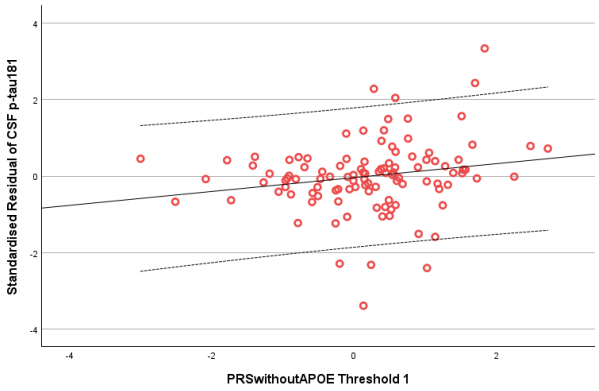

R^2 = 0.039.
Longitudinal CSF p-tau181 = -0.04 + 0.18 * PRSwithoutAPOE T1.

Controlled for Aβ42 status (MCI)

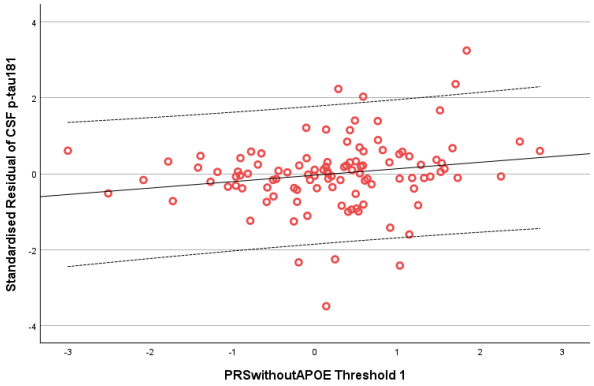

R^2 = 0.034.
Longitudinal CSF p-tau181 = -0.04 + 0.17 * PRSwithoutAPOE T1.
(T: threshold).

Figure 6A.11: Scatterplots to visualise associations between PRSwithoutAPOE Threshold 1 and differential scores of longitudinal CSF p-tau181 measurements in MCI patients when CSF Aβ42 status was not controlled for vs. was controlled for.

Note, the scatterplots are for visualisation purposes only. The scatterplots show the residualised variable (i.e., differential scores of longitudinal CSF p-tau181) modelled as a function of PRS using linear regression. The X axis shows the PRS of interest and the Y axis represents the standardised residual of differential scores of longitudinal CSF p-tau181 after all covariates have been regressed out.

6A.3.4.3. (G) Diagnostic status stratified further by APOE ε4 status, not controlled for Aβ42 status – CU ε4 non-carriers, MCI ε4 non-carriers, and MCI ε4 carriers only

PRSwithAPOE:

In CU ε4 non-carriers, PRSwithAPOE Threshold 10 (p = 0.030) was associated significantly and negatively with differential scores of CSF p-tau181 when CSF Aβ42 was not controlled for, i.e., high PRS, lower CSF p-tau181 differential scores. See Table 6A.8, Figure 6A.12, and Appendix F1 Table F1.53. No associations were apparent in MCI ε4 non-carriers (Appendix F1 Table F1.54) or MCI ε4 carriers (Appendix F1 Table F1.55).

6A.3.4.4. (H) Diagnostic status stratified further by APOE ε4 status, controlled for Aβ42 status (post-hoc) – CU ε4 non-carriers, MCI ε4 non-carriers, and MCI ε4 carriers only

PRSwithAPOE:

For CU ε4 non-carriers, PRSwithAPOE thresholds were associated significantly with CSF p-tau181 when CSF Aβ42 was controlled. In ascending order of significance; Threshold 10 (p = 0.012), Threshold 5 (p = 0.017), and then Threshold 1 (p = 0.024). These were all associated negatively, i.e., high PRS, lower CSF p-tau181 differential scores. Refer to Table 6A.8, Figure 6A.12 (and Appendix F1 Table F1.56). No associations were evident in MCI ε4 non-carriers (Appendix F1 Table F1.57) or MCI ε4 carriers (Appendix F1 Table F1.58).

Table 6A.8: Associations between PRSs and differential scores of longitudinal CSF p-tau181 measurements in CU ε4 non-carriers when CSF Aβ42 status was not controlled for vs. was controlled for.

Not controlled for Aβ42 status

PRS & Thresholds	R Square (Model 1)	R Square (Model 2)	R Square Change	Sig. F Change (Model 2)	Standardised beta of PRS
PRSwithAPOE					
10	0.461	0.629	0.168	0.030	-0.549

Controlled for Aβ42 status

PRS & Thresholds	R Square (Model 1)	R Square (Model 2)	R Square Change	Sig. F Change (Model 2)	Standardised beta of PRS
PRSwithAPOE					
1	0.549	0.711	0.162	0.024	-0.510
5	0.549	0.725	0.176	0.017	-0.551
10	0.549	0.738	0.189	0.012	-0.585

Aβ: amyloid beta. APOE: apolipoprotein E. PRS: polygenic risk score.

Not controlled for Aβ42 status (CU ε4 non-carriers)

Controlled for Aβ42 status (CU ε4 non-carriers)

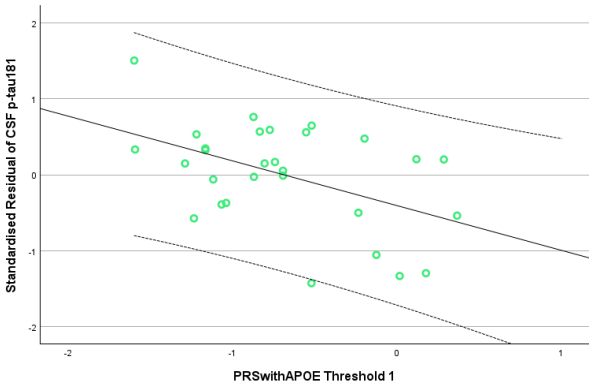

R^2 = 0.224.
Longitudinal CSF p-tau181 = -0.41 – 0.59 * PRSwithAPOE T1.

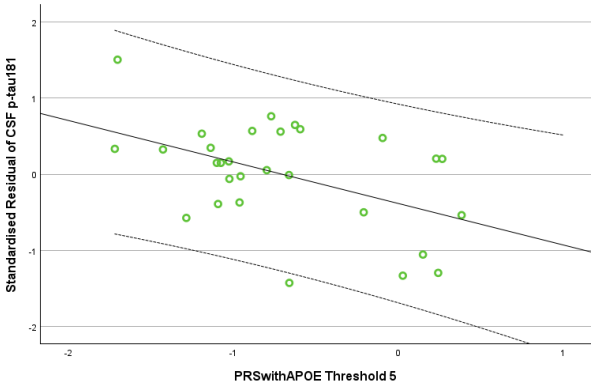

R^2 = 0.227.
Longitudinal CSF p-tau181 = -0.38 – 0.55 * PRSwithAPOE T5.

(T: threshold).

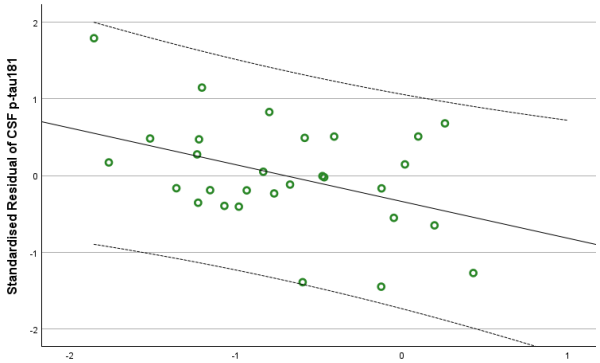

R^2 = 0.174.
Longitudinal CSF p-tau181 = -0.34 – 0.48 * PRSwithAPOE T10.

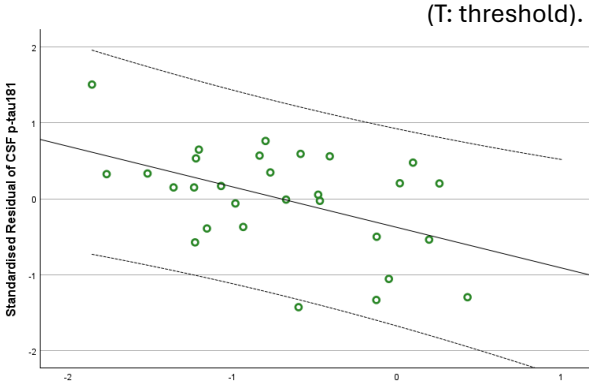

R^2 = 0.232.
Longitudinal CSF p-tau181 = -0.38 – 0.53 * PRSwithAPOE T10.

Figure 6A.12: Scatterplots to visualise associations between PRSwithAPOE thresholds and differential scores of longitudinal CSF p-tau181 measurements in CU ε4 non-carriers when CSF Aβ42 status was not controlled for vs. was controlled for.

Note, the scatterplots are for visualisation purposes only. . The scatterplots show the residualised variable (i.e., differential scores of longitudinal CSF p-tau181) modelled as a function of PRS using linear regression. The X axis shows the PRS of interest and the Y axis represents the standardised residual of differential scores of longitudinal CSF p-tau181 after all covariates have been regressed out.

6A.3.4.5. Other related findings

In the whole group and when the whole group was stratified by APOE ε4 status, not controlling vs. controlling for Aβ42 status did not alter the findings. In all four instances, PRSwithAPOE thresholds, PRSwithoutAPOE thresholds and APOEonlyPRS thresholds were not associated with longitudinal p-tau181. See Appendix F1 Table F1.59 (whole group not controlled for Aβ42), Table F1.60 (whole group controlled for Aβ42), Table F1.61 (ε4 non-carriers not controlled for Aβ42), Table F1.62 (ε4 carriers not controlled for Aβ42), Table F1.63 (ε4 non-carriers controlled for Aβ42), and Table F1.64 (ε4 carriers controlled for Aβ42).

Additionally, when the diagnostic status (CU vs. MCI only) was stratified further by ε4 status (CU ε4 non-carriers vs. MCI ε4 non-carriers vs. MCI ε4 carriers), not controlling vs. controlling for Aβ42 status did not change the results when PRSwithAPOE thresholds or APOEonlyPRS thresholds were used. In all cases, PRSwithAPOE and APOEonlyPRS were not associated with longitudinal p-tau181. Refer to Appendix F1 Table F1.53 (CU ε4 non-carriers not controlled for Aβ42), Table F1.54 (MCI ε4 non-carriers not controlled for Aβ42), Table F1.55 (MCI ε4 carriers not controlled for Aβ42), Table F1.56 (CU ε4 non-carriers controlled for Aβ42), Table F1.57 (MCI ε4 non-carriers controlled for Aβ42), and Table F1.57 (MCI ε4 carriers controlled for Aβ42).

6A.4. DISCUSSION

Associations between PRSs for AD and longitudinal changes in CSF Aβ42 and CSF p-tau181 were assessed in 171 participants. Three PRSs (i.e., PRSwithAPOE, PRSwithoutAPOE and APOEonlyPRS) at three thresholds (i.e., Threshold 1: $p = 5 \times 10^{-8}$, Threshold 5: $p < 0.001$, and Threshold 10: $p < 1$) were used. Associations were examined using two methods: first, the measurements of CSF biomarkers were assessed and categorised as having worsened (Aβ42: n = 99; p-tau181: n = 115) or improved (Aβ42: n = 72; p-tau181: n = 56) over 24 months via logistic regression models; second, differential scores of each CSF biomarker between baseline and month 24 were used and linear regression models were constructed. Analyses were performed in two ways to gauge whether manipulation of data using two methods would yield insights further. For the Logistic Regression – Amyloid Study, and the Linear Regression – Amyloid Study, associations between all PRSs at all thresholds and CSF Aβ42 were examined without controlling for CSF p-tau181 status. Then, associations between PRSs and Aβ42 controlled for p-tau181 status were investigated. For the Logistic Regression – Tau Study, and Linear Regression – Tau Study, associations between all PRSs at all thresholds and CSF p-tau181 were examined without controlling for CSF Aβ42 status. Then, associations between PRSs and p-tau181 controlled for Aβ42 status were assessed. For all four studies, the data were studied at a whole-group level that was controlled for MMSE score (among other variables), then the whole group was stratified by APOE ε4 status, the whole group was stratified by diagnostic status, and lastly, the diagnostic status was stratified further by APOE ε4 status. The hypotheses can be accepted partly.

6A.4.1. Amyloid Studies

In the Logistic Regression – Amyloid Study, for whole group analysis that had been controlled for p-tau181, PRSwithoutAPOE Threshold 1 was associated negatively with Aβ42. Therefore, high PRSwithoutAPOE scores were associated with a lack of worsening of the Aβ42 measurement over 24 months. This model explained 1.96% of the variance in Aβ42.

When the whole group was stratified by APOE ε4 status and was not controlled for p-tau181, in ε4 carriers, PRSwithAPOE Thresholds 5 and 10 were associated positively with change in Aβ42 over 24 months. These models explained 3.88% and 4.03% of the variance in Aβ42. The level of significance obtained using Threshold 10 exceeded Threshold 5 slightly. In ε4 carriers, APOEonlyPRS Thresholds 1 and 5 were associated positively with Aβ42. These models explained 3.74% and 3.74% of the variation in Aβ42. The level of significance obtained using Threshold 5

was minimally improved in comparison with Threshold 1. Both PRSwithAPOE thresholds surpassed both APOEonlyPRS thresholds, and this therefore highlights that non-APOE SNPs are important for predicting associations with Aβ42. High PRS was associated with worsening of Aβ42 over 24 months.

When the whole group was stratified by APOE ε4 status and was controlled for p-tau181, in ε4 carriers, PRSwithAPOE Thresholds 5 and 10 were associated positively with longitudinal change in Aβ42 again. The models explained 4.00% and 4.15% of the variance in Aβ42. The level of significance observed using PRSwithAPOE Threshold 10 surpassed that found with PRSwithAPOE Threshold 5, again. However, in comparison with the level of significance evident when p-tau181 was not controlled, controlling for p-tau181 reduced the significance levels. Similarly, controlling for p-tau181 when APOEonlyPRS Thresholds 1 and 5 were used, also reduced the level of significance as compared with when p-tau181 was not controlled for, although associations remained positive. These models explained 3.91% and 3.91% of the variation in Aβ42. Of note, significance of the associations found using PRSwithAPOE exceeded those found using APOEonlyPRS. Once more, this demonstrates the added value of non-APOE SNPs in risk prediction. Thus, high PRS was associated with worsening of Aβ42 over two years.

Moreover, when the whole group was stratified by diagnostic status but p-tau181 had not been controlled for, in CU individuals, APOEonlyPRS Threshold 10 was associated positively with Aβ42 at 24 months. The model explained 6.73% of the variance in Aβ42. When p-tau181 was controlled, in CU participants, the level of association found using APOEonlyPRS Threshold 10 improved minimally in comparison with when p-tau181 was not controlled. This model explained 6.81% of the variation in Aβ42. In addition, associations were found significantly and positively with APOEonlyPRS Threshold 5, although APOEonlyPRS Threshold 10 was best. Overall, PRSwithAPOE Threshold 5 surpassed all, even the associations that were found when p-tau181 was not controlled. This model explained 6.30% of the variation in Aβ42. These findings indicate the associations between PRS and Aβ42 are mediated by p-tau181, and high PRS is associated with worsening of longitudinal Aβ42 levels.

Contrastingly, the Linear Regression – Amyloid Study that used differential scores did not yield any associations.

6A.4.2. Tau Studies

In the Logistic Regression – Tau Study, when the whole group was stratified by APOE ε4 status but Aβ42 had not been controlled for, in ε4 non-carriers, PRSwithAPOE thresholds were associated negatively with change in p-tau181 over 24 months. PRSwithAPOE Thresholds 1 and 5 were similar, and surpassed PRSwithAPOE Threshold 10. These models explained 3.21%, 3.24%, and 2.77% of the variance in p-tau181. In ε4 non-carriers, APOEonlyPRS thresholds were associated positively with p-tau181. APOEonlyPRS Thresholds 1 and 5 were similar and exceeded the level of significance obtained using APOEonlyPRS Threshold 10. All APOEonlyPRS thresholds were better at identifying associations than PRSwithAPOE thresholds. Overall, APOEonlyPRS Threshold 1 and 5 were best. These models explained 3.51% and 3.53% of the variance in p-tau181. High PRS was associated with worsening of p-tau181 levels over 24 months. These findings suggest that in ε4 non-carriers, non-ε4 APOE SNPs are important in comparison with non-APOE SNPs and account more for longitudinal change in p-tau181 levels.

When the whole group was split by APOE ε4 status and Aβ42 had been controlled for, the findings above remained (unchanged). For PRSwithAPOE Thresholds 1, 5, and 10, the models explained 3.23%, 3.25%, and 2.77% of the variation in p-tau181, whereas, for APOEonlyPRS Thresholds 1, 5, and 10, the models explained 3.52%, 3.53%, and 3.17% of the variance in p-tau181. High PRS was associated with worsening of p-tau181 levels over 24 months regardless of Aβ42. These results indicate that in ε4 non-carriers, Aβ42 status has no effect on p-tau181 levels.

Furthermore, when CU and MCI groups were stratified further by APOE ε4 status (i.e., CU ε4 non-carriers, MCI ε4 non-carriers, and MCI ε4 carriers only) but Aβ42 was not controlled for, in MCI ε4 non-carriers, PRSwithAPOE Thresholds 1 and 5 were associated negatively with change in p-tau181 levels over two years. These models explained 4.31% and 4.27% of the variance in p-tau181. The level of significance was greater when PRSwithAPOE Threshold 1 was used. However, the level of significance obtained using all APOEonlyPRS thresholds were higher than those gained when PRSwithAPOE thresholds were used. APOEonlyPRS Thresholds 1 and 5 explained 4.56% and 4.61% of the variance in p-tau181. High PRS was associated with a lack of worsening of the p-tau181 levels over a two-year period. Overall, APOEonlyPRS Threshold 5 was best. Since the level of significance increased with APOEonlyPRS thresholds, this highlights that non-ε4 APOE SNPs influence p-tau181 levels in MCI ε4 non-carriers more than non-APOE SNPs.

When Aβ42 was controlled for in the aforementioned groups, in MCI ε4 non-carriers, the same PRSwithAPOE Thresholds 1 and 5 were associated negatively with change in p-tau181 over 24 months. These models explained 4.35% and 4.35% of the variance in p-tau181. However, the level of significance reduced. Similarly, all APOEonlyPRS thresholds were associated negatively with change in p-tau181 again. These models explained 4.61%, 4.67%, and 4.43% of the variance in p-tau181. However, once more, the level of significance reduced in comparison with when Aβ42 had not been controlled. Nevertheless, APOEonlyPRS Threshold 1 surpassed other APOEonlyPRS thresholds and all PRSwithAPOE thresholds. High PRS was associated with a lack of worsening of p-tau181 over time. These findings suggest that in MCI ε4 non-carriers, the influence of non-ε4 APOE SNPs on p-tau181 is modulated by Aβ42 slightly.

Implementing an additional model led to further insights that were not captured by the logistic model. In the Linear Regression – Tau Study, when the whole group was stratified by diagnosis but Aβ42 was not controlled for, in CU, PRSwithAPOE thresholds were associated negatively with differential scores of p-tau181 at 24 months. PRSwithAPOE Threshold 10 identified these associations best. However, all APOEonlyPRS thresholds surpassed PRSwithAPOE thresholds, and APOEonlyPRS Thresholds 1 and 10 had the highest level of significance. Adding these PRS thresholds to the model improved predictability of the associations by 1.66% and 1.65%. Thus, high PRS was associated with smaller changes in p-tau181 levels over 24 months. In MCI, PRSwithoutAPOE Threshold 1 was associated positively with differential scores of p-tau181 at 24 months. Adding this PRS specifically to the model increased predictability of the associations by 0.43%. High PRS was associated with larger changes in p-tau181 levels over time.

When the whole group was stratified by diagnosis and had been controlled by Aβ42, in CU, PRSwithAPOE thresholds were associated negatively with differential scores of p-tau181. Overall, PRSwithAPOE Threshold 1 and 10 were best followed by APOEonlyPRS Threshold 1. Adding these PRS thresholds to the model improved identification of the associations by 2.40%, 2.38%, and 2.14%. It should be noted that the level of significance improved minimally with PRSwithAPOE thresholds. Nonetheless, the level of significance for all PRSs increased in comparison with when Aβ42 had not been controlled. In MCI, when Aβ42 was controlled for, PRSwithoutAPOE Threshold 1 was associated positively with differential scores of p-tau181. Adding this PRS specifically to the model increased the identification of associations by 0.39%. However, the level of significance reduced in comparison with when Aβ42 was not controlled.

Additionally, when the CU and MCI groups were stratified further by APOE ε4 status (i.e., CU ε4 non-carriers, MCI ε4 non-carriers, and MCI ε4 carriers only) but not controlled for Aβ42, in CU ε4 non-carriers, PRSwithAPOE Threshold 10 was associated negatively with differential scores of p-tau181. Adding this PRS threshold to the model improved predictability of the associations by 1.68%. However, when Aβ42 was controlled for, all PRSwithAPOE thresholds were associated negatively with p-tau181. The level of significance found using PRSwithAPOE Threshold 10 was best again and was higher compared with when Aβ42 had not been controlled. Adding this PRS threshold to the model increased predictability of the associations by 1.89%. High PRS was associated with smaller changes in p-tau181 over two years.

6A.4.3. Interpretation

6A.4.3.1. Amyloid

Most of the associations found between PRSwithAPOE/APOEonlyPRS and Aβ42 were positive, i.e., high PRS predicted longitudinal worsening of the measurement of Aβ42. These associations were found in CU participants, and in ε4 carriers. In some cases, p-tau181 mediated the associations by decreasing (ε4 carriers) or increasing (CU) the level of significance. The associations that are adjusted by p-tau181 in ε4 carriers may be explained by two pathways that are thought to impact tau; APOE influences NFTs due to Aβ accumulation or APOE effects NFTs directly (Hannon et al., 2020). Additionally, Luckett et al. (2022) also found the direction of associations to be positive in CU participants using a PRS with APOE SNPs, although longitudinal Aβ accumulation was assessed using amyloid-PET.

Associations found in the CU participants (when compared to MCI and AD dementia patients) may suggest that PRSwithAPOE/APOEonlyPRS are useful in identifying those that are at risk of developing clinical symptoms of AD in the future, if they live long enough. Using PiB PET, Villemagne et al. (2011) showed that Aβ burden increased at a slow rate over time. However, for non-demented individuals that had high Aβ present at baseline, the rate of accumulation was greater. This may explain the results in the current research as it is possible that CU individuals had high Aβ burden at baseline and accumulated Aβ at a faster rate, and this was therefore captured within the two-year timeframe. The lack of associations between PRS and Aβ42 in MCI and AD dementia patients may also be explained by previous literature that indicates Aβ burden

does not change, or may change minimally, during prodromal or clinical AD since Aβ deposition reaches a maximum early on and thus the rate of change is constant. Whereas NFT accumulation, synaptic loss and gliosis continue across the disease continuum (Ingelsson et al., 2004; Jack Jr et al., 2009; Villemagne et al., 2011; Lim et al., 2017).

Furthermore, as associations were found in ε4 carriers, this conforms to existing literature that states ε4 carriers are at risk most, and PRSwithAPOE/APOEonlyPRS are useful clinically to support identification of such associations. Mishra et al. (2018) assessed participants that were cognitively heathy at baseline. With the use of PiB PET, they demonstrated that ε4 carriers had greater longitudinal Aβ accumulation throughout the cortex in comparison with ε4 non-carriers. Aβ deposition occurred earlier in life and the rate of Aβ accumulation was faster. Specifically, Grimmer et al. (2010) showed that in patients with a clinical diagnosis of probable AD, the number of ε4 alleles correlated with the rate of change in PiB uptake over 24 months, i.e., 0 = 3%, 1 = 10%, and 2 = 22%. Thus, the presence of ε4 influences and boosts disease progression.

6A.4.3.2. Tau

In comparison with the number of associations found between PRSs and longitudinal Aβ42, twice as many associations were found between PRSs and longitudinal p-tau181. This may be because, in comparison with Aβ, p-tau levels change throughout the disease (Villemagne et al., 2011) and p-tau is associated closely with neuroinflammation (Chen and Yu, 2023), microglial activation (van der Kant, Goldstein, and Ossenkoppele, 2020) neuronal integrity/loss (Giannakopoulos et al., 2003), neurodegeneration (Laccarino et al., 2017) such as grey matter volume loss (Whitwell et al., 2008), and decline in episodic memory, semantic memory, executive function, language, and visuospatial abilities (Benjanin et al., 2017).

In the current research, a positive association was found between PRSwithoutAPOE T10 and p-tau181, i.e., high PRS predicted worsening of longitudinal p-tau181. This was found in MCI patients. Similarly, Liu, Lutz, and Luo (2021) and Li et al. (2023) retrieved such findings using non-APOE PRSs in MCI patients as well. Interestingly, Aβ42 seems to modulate the associations in MCI patients by reducing the level of significance of the associations. In comparison with Chapter 5A (Experiment Two Part A), where controlling for cross-sectional Aβ42 removed any associations between PRS and p-tau181, here, Aβ42 does not have such an influence on longitudinal p-tau181 since amyloid is associated weakly with longitudinal change.

In contrast, the majority of associations found between PRSwithAPOE/APOEonlyPRS and p-tau181 were negative, i.e., high PRS predicted a lack of longitudinal worsening of the p-tau181. These were found in CU participants, ε4 non-carriers, CU ε4 non-carriers, and in MCI ε4 non-carriers. To knowledge, such findings have not been reported previously using these methodological combinations. In some instances, Aβ42 modulated the associations by decreasing (MCI ε4 non-carriers) or increasing (CU, and CU ε4 non-carriers) the level of significance of the associations. In contrast to Chapter 5A (Experiment Two Part A), where controlling for cross-sectional Aβ42 eliminated any associations between PRS and p-tau181, in the current research, Aβ42 does not have impact on longitudinal p-tau181 to such an extent.

The associations that were negative indicate that the influence of genetics on longitudinal changes in p-tau181 may be limited, (or that a two-year timeframe is not long enough to find associations in the expected direction in these groups). Other factors may be important in these groups. For instance, cardiovascular comorbidities such as high low-density lipoprotein cholesterol, hypertension, heart disease, stroke, diabetes, or obesity (Arora et al., 2023; Livingston et al., 2024), or other comorbidities such as hearing loss, depression, or traumatic brain injury in mid-life, or social isolation or visual loss in late life. Lifestyle factors such as smoking, excessive alcohol use, or physical inactivity in mid-life (Livingston et al., 2024), sleep duration, BMI (Sampatakakis et al., 2025) or diet (Mertas and Bosgelmez, 2025). Of note, adherence to a Mediterranean diet is found to be associated with lower PRS for AD (Mamalaki et al., 2024). Additionally, environmental factors such as air pollution in late life may also play a role. These factors are thought to influence mechanisms relating to vascular damage, neuropathology, inflammation, stress, cognitive reserve, and brain reserve (Livingston et al., 2024).

6A.4.4. Limitations and Strengths

Due to the small sample size, these studies require replication in a large participant pool. Despite this constraint, several associations were found that improve understanding of disease progression in different groups, that is otherwise limited in this sub-field.

6A.4.5. Future Directions

Since PRSs for AD predict changes in p-tau181 better than Aβ42, this may be improved further with an endophenotype-specific PRS. For instance, Ramanan et al. (2022) constructed a Tau PRS to predict tau accumulation in a population sample of older adults, aged ≥50 years, from the Mayo Clinic Study of Aging, USA. The PRS was based on tau-PET. Tau PRS was associated with tau-PET accumulation significantly. In independent samples from this population-based dataset, Tau PRS was associated with CSF p-tau, Braak stage NFTs in *post-mortem* tissue, and with longitudinal cognition as well. On the other hand, ε4 dosage or non-APOE-PRS for AD were not associated with tau-PET accumulation. It remains to be seen whether Tau PRS can be used in participants along the AD continuum, and how Tau PRS compares with PRSwithAPOE that contains SNPs from the entire APOE region.

6A.5. CONCLUSION

A greater number of associations were found between PRSs and longitudinal changes in p-tau181, in comparison with Aβ42. In both cases, most of the associations were found using PRSwithAPOE thresholds and APOEonlyPRS thresholds, and therefore indicate the importance of SNPs within the entire APOE region rather than the ε4 SNP alone. Due to the methodology, i.e., the extent of the stratifications used, some associations were reported for the first time, to knowledge. These novel findings provide further insight into AD mechanisms and highlight the complexity of the disease, and the challenges of studying PRSs for AD.

CHAPTER 6B

EXPERIMENT THREE PART B – ASSOCIATIONS BETWEEN POLYGENIC RISK SCORES AND LONGITUDINAL COGNITION

6B.1. INTRODUCTION

Genetics are responsible partly for the interindividual variability that is evident during cognitive decline (Andrews et al., 2016). Common SNPs have been shown to be associated with 40-50% of the variability in cognition during old age (Davies et al., 2011) and 24% of the variability in cognition observed across a lifetime (Deary et al., 2012). It is essential to differentiate individuals that are likely to decline cognitively at a faster rate in order to develop interventions and treatments that maintain cognitive health or slow down the rate of decline (Andrews et al., 2016).

Associations between PRS for AD and longitudinal cognition have been investigated previously. However, inconsistencies are observed. Some literature suggests that associations between PRS with APOE and longitudinal cognition are present (Andrews et al., 2016; Ge et al., 2018; Kauppi et al., 2020; Porter et al., 2018) whereas other work suggests that no such associations are present (Euesden et al., 2025). Some research indicates that associations are apparent when using PRS without APOE (Hayden et al., 2015; Saptoka and Dixon, 2018; Tomassen et al., 2022; Liu, Lutz, and Luo, 2021; Najar et al., 2023) and some literature suggests that associations are not present when using PRS without APOE (Porter et al., 2018; Riaz et al., 2021). In other instances, it is not clear whether APOE has or has not been used to construct PRSs (Daunt et al., 2021; Harris et al., 2014; Ritchie et al., 2019). For the most part, PRSs that include and exclude APOE have not been investigated in the same sample. Therefore, the influence of APOE SNPs on PRS in not well known. However, this is essential for understanding the true impact of APOE on both PRS and cognition longitudinally.

Andrews et al. (2016) examined the association between PRS with APOE and longitudinal cognition in 1,689 participants aged 60+ years from the Personality and Total Health Through Life Project, a non-demented community sample from Australia. Cognitive performance was measured using the California Verbal Learning Test (episodic memory), Wechsler Memory Scale (working memory), Spot-the-Word Test (vocabulary), and Symbol Digit Modalities Test (perceptual speed) over eight years, i.e., at baseline, year 4, and year 8. PRS was associated with a steeper rate of decline in episodic memory.

Similarly, Kauppi et al. (2020) investigated the association between PRS with APOE and longitudinal cognitive decline in non-demented participants, this time from the Betula study in Sweden (n = 1,870). Participants that were aged 35 to 80 years at inclusion and remained non-demented throughout the 25-year follow-up, i.e., baseline and then five time points that were five

years apart, were included. The non-demented status was based on DSM-IV criteria, along with any other information available from medical records relating to medical history, and reports from clinicians and radiologists. Cognitive decline was assessed using a cognitive composite score that comprised of results from tests of episodic memory recall, vocabulary, verbal fluency, and visuospatial ability. Results highlighted that PRS was associated with longitudinal cognitive decline. Further, when APOE ε4 was examined on its own, adding PRS improved the model significantly. Therefore, the effect of PRS was stronger than the effect of APOE ε4 alone. This may indicate that in healthy ageing, PRS is a more sensitive predictor of cognitive decline than ε4.

Ge et al. (2018) examined associations between PRS with APOE and longitudinal cognition using composite scores of memory and executive function. Data from 702 participants from ADNI that were CU, MCI or AD patients were used. When looking at the whole group, in Aβ+ participants, high PRS was associated with decline in memory and executive function. This was true even after controlling for APOE ε4. However, no such associations were found in Aβ- participants. These findings remained similar when restricting analysis to the combined cohort of CU and MCI.

On the other hand, some work indicates no association between PRS with APOE and longitudinal cognition at all. For instance, Euesden et al. (2025) used data from 5,399 participants from four cohorts. Participants from two clinical trials by GlaxoSmithKline with a mean age of 73.7 years were followed up for a mean of 48 weeks, participants from Knight Alzheimer's Disease Research Centre with a mean age of 83.77 years were followed up for 262 weeks on average, participants from ADNI with a mean age of 78.61 years were followed up for 216 weeks on average, and participants from the National Alzheimer's Coordinating Centre with a mean age of 80.41 years were followed up for 242 weeks. Thus, the follow-up period differed considerably between cohorts. These participants had a CDR score of >0. The researchers considered all such participants to be patients with cognitive decline due to an AD aetiology. Overall, PRS with APOE was not associated with cognitive decline over time. The ADNI sample was explored further. The rate of change in CDR-Sum of Boxes (CDR-SB) was not higher significantly between those with high PRS and those with a PRS at the median quantile, nor was it lower significantly in participants with low PRS than those with a PRS at the median quantile. Therefore, when PRS that included APOE was stratified in quantiles, it was not able to differentiate reliably between slow and fast AD progressors using CDR-SB over ~4.15 years.

PHS has been investigated in this context as well. Tan et al. (2018) assessed whether PHS with APOE and 31 non-APOE SNPs, CSF and PET amyloid, and CSF total tau could be used to predict cognitive and clinical decline over time. Data from 347 CU older adults and 599 MCI patients from ADNI were used. The cognitive domains that were tested were executive function and memory, and clinical decline was assessed using CDR-SB. In the combined cohort of CU + MCI patients, individuals with high PHS, amyloid pathology, and total tau pathology had steeper cognitive and clinical decline longitudinally. In comparison with using amyloid and total tau pathology alone to predict longitudinal decline, adding PHS improved predictability further and vice versa, i.e., adding amyloid and total tau to the model improved predictability rather than using PHS alone. Similar findings were observed when the CU and MCI cohorts were investigated separately. Additionally, these findings were present in APOE ε4 non-carriers as well. Further, using PHS, amyloid status and total tau status improved the prediction of time to AD rather than using PHS alone. These reports indicate that the combination of a polygenic score plus biomarker statuses improve prediction of longitudinal decline.

One of the few studies that uses both PRS with APOE and PRS without APOE in the same sample is by Marden et al. (2016). They assessed whether these PRSs were associated with longitudinal memory decline. Data from 8,253 participants, with an average baseline age of 62 years that identified as non-Hispanic white or non-Hispanic black from the Health and Retirement Study (USA), were used. Memory decline was measured using memory composite scores. Results indicated that PRS that included APOE predicted memory decline in both races. However, PRS that excluded APOE predicted memory decline in non-Hispanic whites only. Of note, as SNPs used in the PRS of black individuals was based on a GWAS that was primarily conducted on white individuals, these findings must be interpreted with caution as SNPs may have been weighted incorrectly in participants that were black. If this is true, PRS may not be predictive of memory decline in non-white samples.

Porter et al. (2018) also examined the association between PRS, that included and excluded APOE, and longitudinal cognition. 247 CU participants from the AIBL Study of Ageing, that had high amyloid burden as detected by PET and a mean age of 72.44 years, were investigated. Cognition was assessed using three cognitive composite scores of global cognition, verbal episodic memory, and the Preclinical Alzheimer's Cognitive Composite (PACC) test over a 7.5-year period. PRS that included APOE was associated with all three cognitive scores. Those that were in the highest PRS quartile showed increased rates of decline in the global composite score,

verbal episodic memory, and PACC longitudinally. However, no such associations were present when using the PRS that excluded APOE SNPs.

The predictive value of using only PRS without APOE on longitudinal cognition has also been investigated. Najar et al. (2023) looked at the association between PRS that excluded APOE and global cognitive composite scores of 965 participants from the population-based Gothenburg H70 Birth Cohort Studies in Sweden. Participants were assessed at age 70, 75, 79, and 85 years, and excluded those with a diagnosis of dementia based on DSM-III-R criteria. The global cognitive composite score was based on tests that looked at recognition memory, immediate and delayed recall, word fluency, spatial ability, and figure identification. PRS without APOE at the 0.00000005 significance level predicted global cognitive decline. However, the less stringent PRSs did not predict cognitive decline. When each cognitive assessment was investigated in isolation, PRS without APOE predicted decline in word fluency only.

Sapkota and Dixon (2018) investigated the association between PRS for AD excluding APOE and PRS for cognitive ageing with longitudinal decline in executive function. Data from 634 CU older adults, with a mean age of 70.58 years from the Victoria Longitudinal Study, were used. The PRS for AD included CLU, CR1 and PICALM, whereas the PRS for cognitive ageing included COMT and BDNF. All risk variants have been associated with cognitive decline previously. Executive function was assessed using the Hayling sentence completion, Stroop, Brixton spatial anticipation, and colour trails tests. In APOE ε4 carriers with high PRS for AD, a steeper decline in executive function was present over nine years with increasing PRS for cognitive ageing. No such associations were found in APOE ε4 carriers with low PRS for AD, APOE ε4 non-carriers with low PRS for AD, or in APOE ε4 non-carriers with high PRS for AD. Of note, Mormino et al. (2016) reported that PRS without APOE explained 1.4% of the variance in longitudinal executive function.

Tomassen et al. (2022) investigated the association between PRS with 83 non-APOE SNPs, PET-Aβ pathology, and longitudinal memory composite scores. CU older adults from the European Medical Information Framework for AD (EMIF-AD) PreclinAD cohort were examined (n = 226). In comparison with individuals that had low PRS, high PRS was associated with steeper decline in memory over time. In comparison with those that had normal Aβ, abnormal Aβ was associated with steeper decline in longitudinal memory. Additionally, when modelled together, an interaction was found whereby high PRS and abnormal Aβ were associated with steeper memory decline. These findings indicate that genes beyond APOE contribute to Aβ pathology. Interestingly,

Mormino et al. (2016) observed that PRS without APOE explained 3.2% of the variance in longitudinal memory.

Furthermore, Hayden et al. (2015) assessed the association between PRS without APOE and longitudinal cognition. Data from 7,451 participants over the age of 65 years from the Health and Retirement Study were used. Cognition was measured using the Telephone Interview for Cognitive Status-modified test. Individuals with a high PRS with either one or two APOE ε4 alleles had greater cognitive decline over time than those who were either only APOE ε4 carriers or those with a high PRS alone. Interestingly, individuals who were heterozygous or homozygous for APOE ε4 and were simultaneously heterozygous or homozygous for the CD33 C risk allele, showed even further cognitive decline. However, this association was no longer present after correcting for multiple comparisons and therefore requires further testing.

In contrast, there are some reports of no associations at all between PRS without APOE and longitudinal cognitive decline. Riaz et al. (2021) looked at associations between PRS with 23 SNPs, that excluded APOE, and cognition in 12,978 CU older adults from the Aspirin in Reducing Events in the Elderly study. Cognition was assessed using tests of episodic memory, language, executive function, and psychomotor speed. PRS was not associated with cognitive decline over time. However, APOE ε4 was associated with cognitive decline. These findings suggest that APOE not only had a strong effect on AD, but it also impacted cognition heavily. Of note, this observation differs from that found by Kauppi et al. (2020) since their findings indicated that PRS with APOE improved prediction of cognitive decline when compared with APOE ε4 alone.

Interestingly, comparisons between whether PRS vs. CSF biomarkers could be used to identify individuals that are at risk of cognitive decline over a four-year period have also been inspected. Daunt et al. (2021) used data from 290 MCI patients with a mean age of 72.3 years from ADNI, that had CSF p-tau, CSF Aβ42, and CDR-SB data available were used in the study. The genetic risk score based on the full model consisted of PRS + APOE + Age + Sex. A risk score threshold of 0.6 was selected as it provided a balance between sensitivity and specificity best. Results indicated a significant difference in progression, as defined by CDR-SB, between those that were categorised as low risk due to a score of <0.6 and those that were categorised as high risk due to a score of >0.6. On average, high-risk patients progressed by 1 point on the CDR-SB over 24 months and by 2 points over 48 months, whereas, on average, low risk patients progressed by 0.2 points on CDR-SB over 24 months and by 0.4 points over 48 months. Additionally, there was a

significant difference in CSF p-tau:Aβ42 ratio and Aβ42 alone between those that were biomarker positive vs. negative. The threshold for p-tau:Aβ42 ratio was 0.02818, and the threshold for Aβ42 was 880 pm/mL. On average, p-tau:Aβ42 ratio positive patients progressed by 1.1 points over 24 months and by 2.9 points over 48 months. In contrast, on average, p-tau:Aβ42 ratio negative patients progressed by 0.1 points over 24 months and by 0.2 points over 48 months. When using Aβ42 levels only, on average, amyloid positive patients progressed by 1 point over 24 months and by 2.6 points over 48 months. On the other hand, on average, Aβ42 negative participants progressed by only 0.3 points over 48 months. These findings indicate that identifying MCI patients that are at most vs. least risk of cognitive decline over a two-year or four-year period, using PRS or CSF measures, results in similar findings and neither of these methods surpass the other significantly. However, as Tan et al. (2018)'s work suggests, the combination of a polygenic score plus biomarkers may improve predictability of cognition over time, although this was reported in CU individuals only.

Similarly, Liu, Lutz, and Luo (2021) investigated MCI patients (n = 767). PRS with 40 non-APOE SNPs was associated with reduced performance on ADAS-Cog11, ADAS-Cog13, ADASQ4 and MOCA over time.

Moreover, Harris et al. (2014) examined the association between PRS and general cognitive decline. Data from 3,511 non-demented older participants from the Cognitive Ageing Genetics England and Scotland Consortium, that consisted of five cohorts, were used. The cognitive tests assessed for general cognitive ability, logical memory, declarative memory, verbal fluency, vocabulary, and processing speed. PRS was not associated with longitudinal cognition. Note that the five cohorts did not undergo the same tests to assess their cognitive abilities. It is possible that this may have impacted the results. However, it is not clear whether APOE SNPs were or were not included in this PRS.

Similarly, it is not certain whether the PRS used in Ritchie et al. (2019)'s work included or excluded APOE. Ritchie et al. (2019) looked at the association between PRS for AD and longitudinal cognitive decline in healthy individuals from the Lothian Birth Cohort 1936 study, based in Scotland (UK). They also assessed the association between 13 other PRSs and longitudinal cognitive decline, (namely, PRSs for educational attainment, neuroticism, conscientiousness, schizophrenia, major depressive disorder, coronary artery disease, stroke, type 2 diabetes, smoking, height, BMI, forced expiratory volume of lungs, and grip strength). These other PRSs

were studied as each phenotype of concern has previously been shown to be associated with cognition, and GWASs on these phenotypes exist. Cognition was measured during ages 70 to 79 years using tests of verbal memory, vocabulary, processing speed, and visuospatial ability. Of note, none of the PRSs were associated with cognitive change, including PRS for AD. It is not surprising that the PRS for educational attainment was not associated with cognitive decline, since many factors that influence this may not have been considered, e.g., economic, geographical and social factors. However, APOE ε4 was associated with rate of cognitive decline. Thus, the effect of ε4 on cognition was stronger than PRSs. This is comparable to the findings reported by Riaz et al. (2021), although a contrast to the results obtained by Kauppi et al. (2020).

Evidently, the literature reports inconsistent findings. Several studies have demonstrated that CU individuals that are ε4 carriers show faster cognitive decline over time than ε4 non-carriers. However, these findings are inconsistent, and some work indicates either minimal effect of ε4 status or no such effect (Albrecht et al., 2015). Rather, it shows that PRS predicts longitudinal cognition stronger than ε4 (Wisdom, Callahan, and Hawkins, 2011) or that the impact of non-APOE SNPs in the PRS may be stronger in older adults as the variability in cognitive performance between older adults is greater (Najar et al., 2023). But again, such reports are inconsistent (Wisdom, Callahan, and Hawkins, 2011). It is important to consider that where associations are found in CU individuals, in some cases, this may be driven by the inadvertent inclusion of participants whose clinical status changes from CU to MCI during the timeframe of the longitudinal study (Foster et al., 2013).

6B.1.1. Aims, Objectives, and Hypotheses

Previous literature has focussed on CU individuals at large, and most of the PRSs include APOE SNPs. Therefore, associations between PRS and cognition over time must be assessed in patient groups as well. This is important particularly due to the clinical heterogeneity of AD that makes it challenging to identify symptomatic individuals who are at risk of declining faster and identifying asymptomatic individuals that are at risk of faster cognitive decline (Wang et al., 2024). Additionally, using different types of PRSs and stratifying the data with various variables, all within the same sample, may help to understand associations better and examine whether further insights can be gained.

The overall aim of Chapter 6B (Experiment Three Part B) is:

- To investigate whether PRSs for AD can predict AD-specific longitudinal cognitive decline.

This aim will be explored using the following objective:

- To examine the associations between PRSs (i.e., PRSwithAPOE, PRSwithoutAPOE, and APOEonlyPRS) and AD-specific longitudinal cognitive decline (i.e., memory and any one other cognitive domain), systematically.

It is hypothesised that:

1) The association between PRS and longitudinal cognitive decline will be strongest for PRSwithAPOE, followed by APOEonlyPRS, and then PRSwithoutAPOE (whole group).
2) In APOE ε4 carriers, the association between PRS and longitudinal cognitive decline will be strongest for PRSwithAPOE, followed by APOEonlyPRS, and then PRSwithoutAPOE (APOE ε4 status).
3) In MCI and AD dementia patients, the association between PRS and longitudinal cognitive decline will be strongest for PRSwithAPOE, followed by APOEonlyPRS, and then PRSwithoutAPOE, as compared with CU participants (diagnostic status).
4) In amyloid positive participants, the association between PRS and longitudinal cognitive decline will be strongest for PRSwithAPOE, followed by APOEonlyPRS, and then PRSwithoutAPOE (amyloid status).

5) In tau positive participants, the association between PRS and longitudinal cognitive decline will be strongest for PRSwithAPOE, followed by APOEonlyPRS, and then PRSwithoutAPOE (tau status).

This research will present a thorough and systematic examination of longitudinal cognitive decline across the continuum of sporadic AD, that is not well understood currently (Mahedy et al., 2024).

6B.2. METHODS

6B.2.1. Participants

Data from 501 ADNI participants were used in this study. The demographics and other characteristics of these participants are shown in Table 6B.1.

In terms of race, the participant sample consisted of individuals of white (93.21%, n = 467), minority (6.59%, n = 33) and unknown (0.20%, n = 1) races. Minority races of this sample were Native Americans, Asians, Hawaiian/Pacific, and Black. All available races were included in the analysis to maximise the sample size and generalisability of the results.

As with the previous chapters, where analysis required stratification by APOE ε4 status, APOE genotypes were grouped into APOE ε4 non-carriers vs. carriers.

Family history included history of AD and/or unspecified dementia, in first degree relatives.

Table 6B.1: Participant demographics and characteristics of 501 participants.

ENTIRE COHORT (n = 501)		
Age		
Age range		55 – 96 years
Mean age		73.48 years
Standard deviation		7.52 years
Education		
Education range		6 – 20 years
Mean education		16.16 years
Standard deviation		2.69 years
	n	**%**
Sex		
Male	278	55.49
Female	223	44.51
Race		
Native Americans	2	0.40
Asian	8	1.60
Hawaiian/Pacific	2	0.40
Black	14	2.79
White	467	93.21
Mixed	7	1.40
Unknown	1	0.20
APOE Genotype		
ε4ε4	28	5.59
ε3ε4	153	30.54
ε3ε3	260	51.90
ε2ε4	12	2.40
ε2ε3	48	9.58
ε2ε2	0	0
APOE ε4 Status		
ε4 Non-carrier	308	61.48
ε4 Carrier	193	38.52
Amyloid Status		
Negative	201	40.12
Positive	300	59.88
Tau Status (n = 410)		
Negative	269	65.61
Positive	141	34.39
Family History of Alzheimer's or Dementia		
Negative	26	5.19
Positive	475	94.81
AD-specific cognitive decline after 24 months		
Non-progressors	261	52.10
Progressors	240	47.90

Aβ: amyloid beta. AD: Alzheimer's disease. APOE: apolipoprotein E. ε: epsilon. P-tau: phosphorylated tau.

6B.2.2. Genetic data and, Calculation of Polygenic Risk Scores and Polygenic Risk Score Thresholds

The steps described in Chapter 4 (Experiment One) were applied to Chapter 6B (Experiment Three Part B) for consistency. All three PRSs were used (i.e., PRSwithAPOE, PRSwithoutAPOE, and APOEonlyPRS) with all three thresholds (i.e., Thresholds 1, 5, and 10).

6B.2.3. Cognitive Markers

Cognitive progression was assessed using composite scores that were obtained 24 months after the scores selected for the cross-sectional study in Chapter 5B (Experiment Two Part B), "baseline". The longitudinal scores were found in the same "UW - Neuropsych Summary Scores [ADNI1,GO,2,3]" file, version "December 01, 2023", that was downloaded from ADNI on 19 August 2024 for Chapter 5B (Experiment Two Part B) – refer to Chapter 5B for full details.

To ensure that AD-specific cognitive decline was being investigated, worsening of memory composite scores along with worsening of one other cognitive domain was required, i.e., executive function, language, or visuospatial abilities. These participants were categorised as progressors, whereas those that did not meet these requirements were classed as non-progressors. Composite scores were used as they were, rather than transforming them to z-scores as this was not required for categorisation purposes.

6B.2.4. Statistical Analyses

All variables that were used as covariates in all previous chapters, other than those relating to neuroimaging features, were used as covariates in the current research i.e., age, sex, education, family history, amyloid status, x10 genetic principal components, and MMSE.

Binomial hierarchical logistic regression analyses were performed to examine associations between PRS (independent / predictor variable) and AD-specific longitudinal cognition (dependent / outcome variable). *P* was significant at the 0.05 level.

(A) Whole-group analysis

• Model 1: Age, sex, education, family history, amyloid status, x10 genetic principal components, and MMSE.

• Model 2: All variables in Model 1, plus PRS.

Analyses were completed using PRSwithAPOE Thresholds 1, 5, and 10 separately, PRSwithoutAPOE Thresholds 1, 5, and 10 separately, and then APOEonlyPRS Thresholds 1, 5, and 10 separately.

(n = 501).

(B) Whole group stratified by APOE ε4 status

• Model 1: Age, sex, education, family history, amyloid status, x10 genetic principal components, and MMSE.

• Model 2: All variables in Model 1, plus PRS.

Analyses were completed using PRSwithAPOE Thresholds 1, 5, and 10 separately, PRSwithoutAPOE Thresholds 1, 5, and 10 separately, and then APOEonlyPRS Thresholds 1, 5, and 10 separately.

(ε4 non-carriers, n = 308; ε4 carriers, n = 193).

(C) Whole group stratified by diagnostic status

• Model 1: Age, sex, education, family history, amyloid status, x10 genetic principal components, and MMSE.

• Model 2: All variables in Model 1, plus PRS.

Analyses were completed using PRSwithAPOE Thresholds 1, 5, and 10 separately, PRSwithoutAPOE Thresholds 1, 5, and 10 separately, and then APOEonlyPRS Thresholds 1, 5, and 10 separately.

(CU, n = 155; MCI, n = 283; AD dementia, n = 63).

(D) For exploratory analysis, the diagnostic status was stratified further by APOE ε4 status

• Model 1: Age, sex, education, family history, amyloid status, x10 genetic principal components, and MMSE.

• Model 2: All variables in Model 1, plus PRS.

Analyses were completed using PRSwithAPOE Thresholds 1, 5, and 10 separately, PRSwithoutAPOE Thresholds 1, 5, and 10 separately, and then APOEonlyPRS Thresholds 1, 5, and 10 separately.

However, analyses were not completed for CU ε4 carriers and AD ε4 non-carriers due to inadequate participant numbers, particularly since there were x17 variables between both Model 1 and Model 2.

(CU ε4 non-carriers, n = 119; CU ε4 carriers, n = 36; MCI ε4 non-carriers, n = 172; MCI ε4 carriers, n = 111; AD dementia ε4 non-carriers, n = 17; AD dementia ε4 carriers, n = 46).

(E) Whole group stratified by amyloid status

• Model 1: Age, sex, education, family history, x10 genetic principal components, and MMSE.

• Model 2: All variables in Model 1, plus PRS.

Analyses were completed using PRSwithAPOE Thresholds 1, 5, and 10 separately, PRSwithoutAPOE Thresholds 1, 5, and 10 separately, and then APOEonlyPRS Thresholds 1, 5, and 10 separately.

(Amyloid negative, n = 201; amyloid positive, n = 300).

(F) For exploratory analysis, amyloid status was stratified further by APOE ε4 status

• Model 1: Age, sex, education, family history, x10 genetic principal components, and MMSE.

• Model 2: All variables in Model 1, plus PRS.

Analyses were completed using PRSwithAPOE Thresholds 1, 5, and 10 separately, PRSwithoutAPOE Thresholds 1, 5, and 10 separately, and then APOEonlyPRS Thresholds 1, 5, and 10 separately.

(Amyloid negative ε4 non-carriers, n = 165; amyloid negative ε4 carriers, n = 36; amyloid positive ε4 non-carriers, n = 143; amyloid positive ε4 carriers, n = 157).

(G) Whole group stratified by p-tau181 status (n = 410)

• Model 1: Age, sex, education, family history, x10 genetic principal components, and MMSE.

• Model 2: All variables in Model 1, plus PRS.

Analyses were completed using PRSwithAPOE Thresholds 1, 5, and 10 separately, PRSwithoutAPOE Thresholds 1, 5, and 10 separately, and then APOEonlyPRS Thresholds 1, 5, and 10 separately.

(p-tau181 negative, n = 269; p-tau181 positive, n = 141).

(H) For exploratory analysis, p-tau181 status was stratified further by APOE ε4 status (n = 410)

• Model 1: Age, sex, education, family history, x10 genetic principal components, and MMSE

• Model 2: All variables in Model 1, plus PRS

Analyses were completed using PRSwithAPOE Thresholds 1, 5, and 10 separately, PRSwithoutAPOE Thresholds 1, 5, and 10 separately, and then APOEonlyPRS Thresholds 1, 5, and 10 separately.

(p-tau181 negative ε4 non-carriers, n = 190; p-tau181 negative ε4 carriers, n = 79; p-tau181 positive ε4 non-carriers, n = 70; p-tau181 positive ε4 carriers, n = 71).

FDR correction was not required as there was only one dependent / outcome variable (with two levels each) being tested, i.e., longitudinal cognition – progressors vs. non-progressors.

6B.3. RESULTS

6B.3.1. (A) Whole group

PRSwithAPOE, PRSwithoutAPOE and APOEonlyPRS:

PRSwithAPOE thresholds, PRSwithoutAPOE thresholds and APOEonlyPRS thresholds were not associated significantly with longitudinal cognitive decline (Appendix F2 Table F2.1).

6B.3.2. (B) Whole group stratified by APOE ε4 status

PRSwithAPOE, PRSwithoutAPOE and APOEonlyPRS:

For whole group stratification by ε4 status, the above-mentioned PRSs (each with three thresholds) were not associated significantly with longitudinal cognitive decline. See Appendix F2 Table F2.2 (ε4 non-carriers) and Table F2.3 (ε4 carriers).

6B.3.3. (C) Whole group stratified by diagnostic status

PRSwithAPOE, PRSwithoutAPOE and APOEonlyPRS:

No associations. Refer to Appendix F2 Table F2.4 (CU), Table F2.5 (MCI), and Table F2.6 (AD dementia).

6B.3.4. (D) Diagnostic status stratified further by APOE ε4 status – CU ε4 non-carriers, MCI ε4 non-carriers, MCI ε4 carriers, and AD dementia ε4 carriers only

PRSwithAPOE, PRSwithoutAPOE and APOEonlyPRS:

No associations. Consult Appendix F2 Table F2.7 (CU ε4 non-carriers), Table F2.8 (MCI ε4 non-carriers), Table F2.9 (MCI ε4 carriers), and Table F2.10 (AD dementia ε4 carriers).

6B.3.5. (E) Whole group stratified by amyloid status

PRSwithAPOE, PRSwithoutAPOE and APOEonlyPRS:

No associations. See Appendix F2 Table F2.11 (amyloid negative) and Table F2.12 (amyloid positive).

6B.3.6. (F) Amyloid status stratified further by APOE ε4 status

PRSwithAPOE, PRSwithoutAPOE and APOEonlyPRS:

No associations. Refer to Appendix F2 Table F2.13 (amyloid negative ε4 non-carriers), Table F2.14 (amyloid negative ε4 carriers), Table F2.15 (amyloid positive ε4 non-carriers), and Table F2.16 (amyloid positive ε4 carriers).

6B.3.7. (G) Whole group stratified by p-tau181 status (n = 410)

PRSwithAPOE, PRSwithoutAPOE and APOEonlyPRS:

No associations. Consult Appendix F2 Table F2.17 (tau negative) and Table F2.18 (tau positive).

6B.3.8. (H) P-tau181 status stratified further by APOE ε4 status (n = 410)

PRSwithAPOE:

In p-tau181 positive ε4 non-carriers, PRSwithAPOE thresholds were associated significantly with longitudinal cognitive decline. The significance was greatest when Threshold 10 was used (p = 0.030), followed by Threshold 1 (p = 0.048), and then Threshold 5 (p = 0.049). These were all associated positively, i.e., high PRS, progressed in decline of memory and one other cognitive domain over 24 months. No other associations were observed. Refer to Table 6B.2, Figure 6B.1, and Appendix F2 Table F2.19. No associations were observed in p-tau181 positive ε4 carriers (Appendix F2 Table F2.20), p-tau181 negative ε4 non-carriers (Appendix F2 Table F2.21) or p-tau181 negative ε4 carriers (Appendix F2 Table F2.22).

PRSwithoutAPOE:

No associations. Consult Appendix F2 Tables F2.19 to F2.22.

APOEonlyPRS:

In p-tau181 positive ε4 non-carriers, PRSwithAPOE thresholds were associated significantly with longitudinal cognitive decline. In ascending order of significance; Threshold 1 (p = 0.012), Threshold 5 (p = 0.021), then Threshold 10 (p = 0.029). Again, these were all associated positively, i.e., high PRS, progressed AD-specific cognitive decline over 24 months. Refer to Table 6B.2, Figure 6B.1, and Appendix F2 Table F2.19. No other associations were found (see Appendix F2 Tables F2.20 to F2.22).

Table 6B.2: Associations between PRSs and longitudinal cognitive decline in p-tau181 positive ε4 non-carriers.

PRS & Threshold	Chi-square	df	*p*	Nagelkerke R^2	Wald	df	*p*	OR	95% CI	Nagelkerke R^2 Model 1
PRSwithAPOE										
1	19.112	16	0.263	0.327	3.900	1	0.048	3.668	1.010-13.327	0.260
5	19.095	16	0.264	0.326	3.870	1	0.049	3.592	1.005-12.845	0.260
10	20.114	16	0.215	0.341	4.722	1	0.030	3.536	1.132-11.047	0.260
APOEonlyPRS										
1	22.141	16	0.139	0.370	6.311	1	0.012	6.305	1.499-26.520	0.260
5	20.759	16	0.188	0.351	5.325	1	0.021	5.322	1.286-22.021	0.260
10	20.094	16	0.216	0.341	4.792	1	0.029	4.808	1.179-19.615	0.260

APOE: apolipoprotein E. CI: confidence interval. df: degrees of freedom. OR: odds ratio. PRS: polygenic risk score.

p-tau181 positive ε4 non-carriers (PRSwithAPOE)

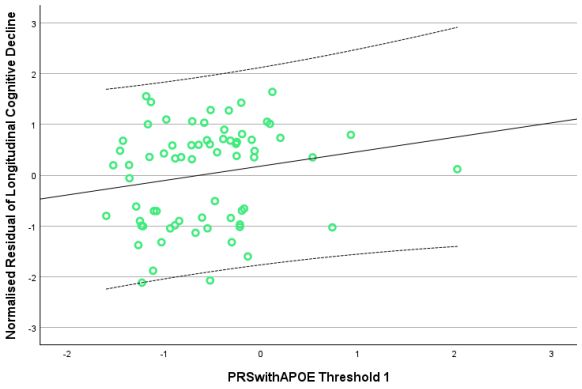

R^2 = 0.034.
Longitudinal cognitive decline = 0.18 + 0.28 * PRSwithAPOE T1.

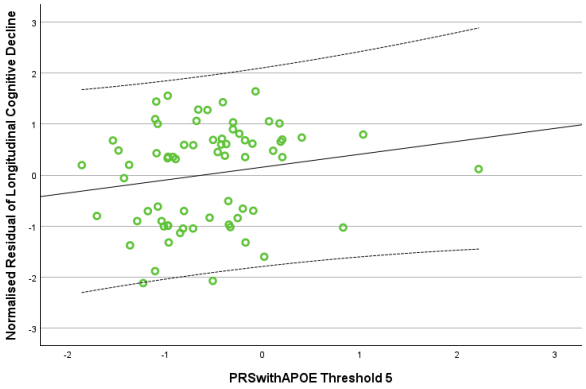

R^2 = 0.030.
Longitudinal cognitive decline = 0.16 + 0.25 * PRSwithAPOE T5.

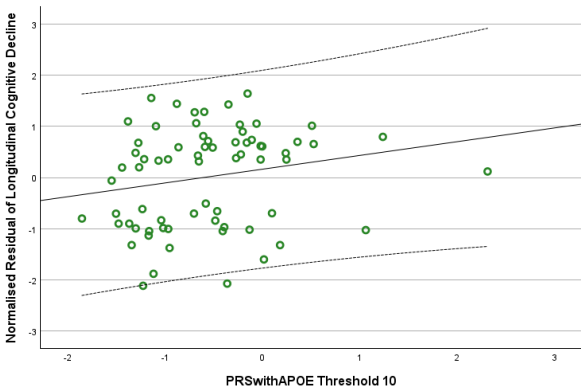

R^2 = 0.041.
Longitudinal cognitive decline = 0.16 + 0.27 * PRSwithAPOE T10.

p-tau181 positive ε4 non-carriers (APOEonlyPRS)

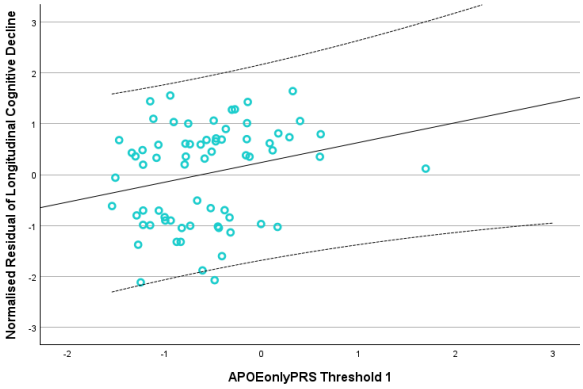

R^2 = 0.057.
Longitudinal cognitive decline = 0.24 + 0.39 * APOEonlyPRS T1.

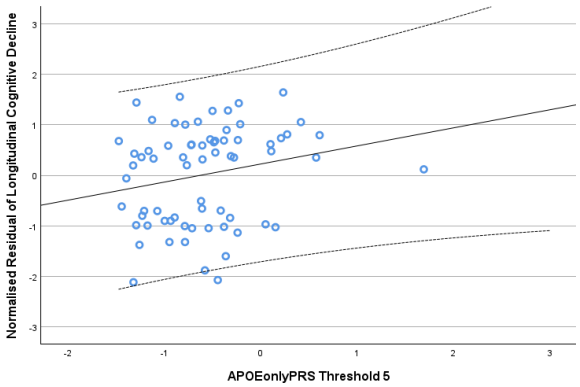

R^2 = 0.046.
Longitudinal cognitive decline = 0.22 + 0.36 * APOEonlyPRS T5.

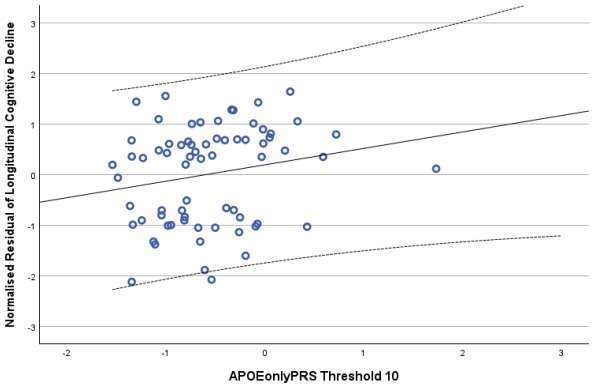

R^2 = 0.039.
Longitudinal cognitive decline = 0.20 + 0.32 * APOEonlyPRS T10.

(T: threshold).

Figure 6B.1: Scatterplots to visualise associations between PRSwithAPOE thresholds, APOEonlyPRS thresholds, and longitudinal cognitive decline in p-tau181 positive ε4 non-carriers.

Note, the scatterplots are for visualisation purposes only. The scatterplots show the residualised variable (i.e., longitudinal cognitive decline) modelled as a function of PRS using linear regression. The R^2 in the scatterplots differs from the Nagelkerke (pseudo) R^2 as the two coefficients are calculated in different ways as part of different types of inferential models. The X axis shows the PRS of interest, and the Y axis indicates the normalised residual of longitudinal cognitive decline where all covariates have been regressed out.

6B.4. DISCUSSION

Associations between PRSs for AD and AD-specific longitudinal cognition were studied. Three PRSs were used: PRSwithAPOE, PRSwithoutAPOE, and APOEonlyPRS, each with three thresholds: Threshold 1 ($p = 5 \times 10^{-8}$), Threshold 5 ($p < 0.001$), and Threshold 10 ($p < 1$). Longitudinal cognition was assessed using composite scores of memory, executive function, language, and visuospatial abilities. Progression was based on worsening of the memory composite score and one other composite score that covered another cognitive domain over 24 months. Associations were examined as a whole group that was controlled for MMSE (n = 501), then the whole group was stratified by APOE ε4 status, the whole group was stratified by diagnostic status, diagnostic status was further stratified by ε4 status, the whole group was stratified by amyloid status, and amyloid status was further stratified by ε4 status. On a sub-set of participants from the main participant pool for whom these data were available (n = 410), participants were stratified by p-tau181 status, and p-tau181 was further stratified by ε4 status. Hypotheses were met in part only.

When p-tau181 status was stratified by APOE ε4 status, two main findings were evident. First, for p-tau181 positive ε4 non-carriers, all PRSwithAPOE thresholds were associated significantly and positively with longitudinal cognitive decline. PRSwithAPOE Threshold 10 predicted associations the best. Second, for p-tau181 positive ε4 non-carriers, all APOEonlyPRS thresholds were associated significantly and positively with longitudinal cognitive decline. APOEonlyPRS Threshold 1 was superior at identifying associations. Overall, APOEonlyPRS Threshold 1 predicted associations better. Generally, the levels of significance obtained using APOEonlyPRS thresholds surpassed those attained using PRSwithAPOE thresholds. No other associations were evident.

6B.4.1. Interpretation

The results reported in the current research are parallel to previous findings. Although Aβ plaques and NFTs are both hallmarks of AD pathology, amyloid is found to be associated closely with disease pathogenesis, whereas tau is associated with severity of cognitive impairment (Nelson et al., 2012; Ramanan et al., 2022). This has been shown in both PET (Hanseeuw et al., 2019; Boccalini et al., 2023) and CSF (Clark et al., 2018) studies. Of note, rate of change in CSF t-tau and p-tau181 have been shown to be associated with rate of cognitive decline but not with cross-sectional cognition (Xiong et al., 2016). High CSF t-tau and p-tau have been associated with faster

progression to dementia (van Rossum et al., 2012). Therefore, amyloid positivity may support early detection prior to symptomology (cross-sectionally), whereas changes in tau are useful to monitor trajectory and prognosis of AD (longitudinally).

Andersson et al. (2008) investigated longitudinal changes in CSF t-tau, p-tau, and Aβ42 in 39 female participants from memory clinics who had a mean age of 61.3 years. Based on baseline RAVLT episodic memory scores, participants were split into three groups: severely impaired (n = 12), moderately impaired (n = 15) or not impaired (n = 12). AD was defined according to the NINCDS-ADRDA clinical criteria. During the three-year follow-up, p-tau increased significantly in those that were severely impaired and 80% of participants in this group converted to AD dementia. P-tau did not change in the other groups, and these participants remained non-demented mostly. T-tau or Aβ42 did not change in any of the three groups. These results support the notion that p-tau is a valid biomarker of cognitive decline, disease progression, and conversion to AD dementia. Although participant numbers were limited in this study, participants were characterised well, and results provide evidence in support of the findings in the current research as associations between PRS and cognitive decline were found in participants that were p-tau181 positive.

Moreover, evidence from tau-PET studies indicate that tau may be associated with domain-specific cognition. Scholl et al. (2016) assessed the association between uptake of a tau-PET tracer (i.e., fludeoxyglucose 18 Amyvid 1451 flortaucipir) and longitudinal memory scores in 33 CU older adults with a mean age of 78.6 years. The researchers found that tracer uptake in Braak I-II ROI predicted longitudinal decline in episodic memory that was independent of cortical amyloid pathology. Additionally, associations between tau pathology and episodic memory impairment are found to be independent of grey matter volume loss (Benjanin et al., 2017). Therefore, these results are similar to those found in the current research using CSF p-tau181 as longitudinal change in cognition was considered in the presence of decline in memory (plus one other domain) and associations were found in p-tau181 positive participants.

It has been indicated that tau levels are influenced by genetic factors. For example, Cruchaga et al. (2013) conducted a GWAS of CSF tau and CSF p-tau levels and found that SNPs within the 9p24.2 locus were associated with CSF tau levels, and SNPs within the 3q28 locus were associated with risk for AD, NFTs and global memory decline. Whereas other loci were associated with lower CSF tau and p-tau levels, lower NFTs, and slower memory decline. SNPs within the

GLIS Family Zinc Finger 2 gene locus are known to be associated with diabetes. Cruchaga et al. (2013) found a further association between this locus and CSF tau and p-tau levels, thus indicating that these SNPs increase risk of both diabetes and AD. Similarly, Deming et al. (2017) conducted a GWAS of CSF p-tau181 and found that SNPs within the INPP5D locus may influence p-tau181 levels. Ramanan et al. (2020) conducted a GWAS of tau-PET and found that SNPs within the Protein Phosphatase 2 Regulatory Subunit B and Insulin-Like Growth Factor 2 mRNA Binding Protein 3 genes were associated with higher tau deposition. Therefore, these papers may suggest that studying associations between many SNPs concurrently via PRS, cognition, and p-tau181 status, are convincing and reflect impact of genetics on cognition over time.

Furthermore, Deming et al. (2017) conducted a GWAS of CSF p-tau181 and CSF Aβ42. They reported that CSF p-tau181 levels were associated with APOE even after controlling for CSF Aβ42 levels. Therefore, the influence of APOE on p-tau181 was independent of Aβ42. Despite most of the association being driven by APOE ε4, followed by ε2 and ε3, additional signal from other SNPs within the APOE region was evident and thus may have influenced biomarker levels. These findings can be used to support the results obtained in the current research. For instance, associations between PRSwithAPOE and longitudinal cognitive decline, and APOEonlyPRS and longitudinal cognitive decline, were found in participants that were both p-tau181 positive and ε4 non-carriers. Therefore, signals from the ε2 SNP, ε3, other non-ε4 SNPs within the APOE region, plus non-APOE SNPs were powerful sufficiently to be associated with AD-specific longitudinal cognitive decline. However, as higher levels of significance were obtained using APOEonlyPRS thresholds than PRSwithAPOE thresholds, this highlights that the influence of APOE SNPs was stronger than non-APOE SNPs on longitudinal cognition in this sample.

6B.4.2. Limitations and Strengths

The current research assessed 501 participants, of which 240 showed AD-specific cognitive decline and had data available on various variables that were required for analyses. However, a larger number of participants are required, particularly when assessing cognition (Howieson, 2019). Various studies have at least 1,000+ participants, (e.g., Harris et al., 2014; Hayden et al., 2015; Andrews et al., 2016; Marden et al., 2016; Tan et al., 2018; Kauppi et al., 2020; Riaz et al., 2021; Euesden et al., 2025). Additionally, as the cognitive tests used were in English only, it limits the generalisability of findings as culturally diverse populations in non-Western countries cannot be examined. This requires urgent attention (Howieson, 2019). Despite the small sample size and

the lack of generalisable findings, the results from the current research conform to the notion that PRS and p-tau181 are useful for predicting longitudinal cognition and for tracking disease progression in AD.

Although previous literature indicates that PRS with APOE is associated with longitudinal cognition (Andrews et al., 2016; Ge et al., 2018; Kauppi et al., 2020; Porter et al., 2018) and PRS without APOE is not associated with longitudinal cognition (Porter et al., 2018; Riaz et al., 2021), these studies have not stratified their participants to the extent that the current research has nor have they stratified by p-tau status alone. In comparison, the current research has stratified participants in numerous ways, and this has not been done previously within the same sample.

6B.4.3. Future Directions

It is vital for future work to include a large number of participants and stratify them using several variables, such as those in the current research. It is crucial for these analyses to be conducted within the same participant pool in order to understand fully the different types of PRSs, biomarkers, cognitive outcomes, disease mechanisms, and disease progression.

6B.5. CONCLUSION

In participants that are both p-tau181 positive and ε4 non-carriers, PRSwithAPOE and APOEonlyPRS are associated significantly and positively with longitudinal AD-specific cognitive decline. The best threshold per PRS were PRSwithAPOE Threshold 10 and APOEonlyPRS Threshold 1. Overall, the levels of significance gained using APOEonlyPRS thresholds exceed those found using PRSwithAPOE thresholds, and APOEonlyPRS Threshold 1 was best at identifying associations. Additionally, the findings also adhere to the notion that p-tau is useful for monitoring disease progression, whereas Aβ supports early detection of AD.

CHAPTER 7

GENERAL DISCUSSION

7.1. Main Findings and Explanations

Sporadic AD accounts for >90% of AD cases, of which 70% are thought to be due to a combination of several risk genes (Lane, Hardy and Schott, 2017). Despite this, APOE is the most studied gene in sporadic AD. Given that the ε4 risk variant is found in only ~14% of the general population (Lumsden et al., 2020) and ~37% of the AD population globally (Liu et al., 2013), this indicates that ε4 is neither necessary nor sufficient to cause AD on its own. There is, therefore, a need to study other genes and associated variants (Pandya, Venneri, and De Marco, 2025), as well as the contribution of non-ε4-APOE SNPs, to understand risk of sporadic AD in ε4 non-carriers and carriers better. To examine this, the current research used the PRS method, a predictive model that examines several thousands of SNPs simultaneously, to gain insights into the concurrent effect of multiple genes/SNPs and their contribution to AD-related changes in brain structure, CSF biomarkers, and cognition. Three PRSs were constructed using three statistical thresholds each. Namely, these were: PRSwithAPOE Threshold 1 ($p = 5 \times 10^{-8}$) with 172 SNPs, Threshold 5 ($p < 0.001$) with 1,561 SNPs, and Threshold 10 ($p < 1$ after passing quality control parameters and merging of datasets) with 455,027 SNPs; PRSwithoutAPOE Threshold 1 with 121 SNPs, Threshold 5 with 1,465 SNPs, and Threshold 10 with 454,638 SNPs; APOEonlyPRS Threshold 1 with 51 SNPs, Threshold 5 with 96 SNPs, and Threshold 10 with 389 SNPs.

In Chapter 4 (Experiment One), associations between all PRSs and cross-sectional regional grey matter volume were investigated in 738 ADNI participants. The core findings were that PRSwithAPOE and APOEonlyPRS thresholds were associated negatively with grey matter volume in the bilateral hippocampus and amygdala (R > L) consistently, at both a whole-group level and in amyloid positive participants; these observations survived corrections for multiple comparisons. Therefore, high PRS predicted greater regional grey matter volume loss. Other findings that were less consistent but survived FDR corrective measures included, PRSwithAPOE and APOEonlyPRS were associated negatively with grey matter volume in the bilateral entorhinal cortex and R middle occipital gyrus at both a whole-group level and in amyloid positive participants. The level of significance obtained using PRSwithAPOE surpassed that found using APOEonlyPRS and therefore highlighted the added value of non-APOE SNPs at identifying associations with regional grey matter volume. Stratification by amyloid status revealed associations better than stratification by diagnostic status and therefore indicated the importance of biomarker evidence over dependence on clinical expertise.

In Chapter 5A (Experiment Two Part A), associations between all PRSs and cross-sectional CSF Aβ42 and CSF p-tau181 were examined. There were three studies in Part A: (1) an Amyloid Study where participants were divided into Aβ42 negative vs. positive, n = 524; (2) a Tau Study where participants were split into p-tau181 negative vs. positive, n = 524; (3) an Amyloid and Tau Study where participants were divided into those that were both Aβ42 and p-tau181 negative vs. both Aβ42 and p-tau181 positive, n = 345. These participants were sub-samples from the main cohort of 738 ADNI participants. Generally, PRSwithAPOE and APOEonlyPRS thresholds were associated positively with CSF Aβ42 more than they were associated with CSF p-tau181. In Aβ42 models (1), controlling for p-tau181 status reduced the level of significance of the associations slightly. PRSwithAPOE was best at predicting associations at the whole-group level, in ε4 carriers, and in MCI patients. APOEonlyPRS was best at identifying associations in CU participants. However, in p-tau181 models (2), controlling for Aβ42 status removed any significance altogether. In the Amyloid and Tau Study (3), PRSwithAPOE and APOEonlyPRS were associated positively with biomarker positivity of both Aβ42 and p-tau181. PRSwithAPOE was superior at predicting associations in MCI patients again, whereas APOEonlyPRS was best at identifying associations in CU participants once more. However, APOEonlyPRS was better slightly at detecting associations at the whole-group level. Overall, high PRS was associated with Aβ42 positivity regardless of whether models were controlled/not controlled for p-tau181 status and, high PRSs predicted positivity of both Aβ42 and p-tau181 simultaneously.

In Chapter 5B (Experiment Two Part B), associations between all PRSs and cross-sectional composite scores of memory, executive function, language and visuospatial cognitive composite scores were studied in all 738 ADNI participants. The main findings were that PRSwithAPOE and APOEonlyPRS were associated negatively with memory at the whole-group level and in amyloid positive participants, PRSwithAPOE was associated negatively with visuospatial cognition in the whole group and in amyloid negative participants, (although these did not survive FDR corrective measures), and PRSwithAPOE and APOEonlyPRS were associated negatively with visuospatial abilities in ε4 carriers. Therefore, high PRSs predicted reduced memory and visuospatial capabilities. Overall, PRSwithAPOE thresholds surpassed APOEonlyPRS thresholds since they identified a higher number of associations and detected associations with a greater level of significance across different stratifications. Again, these findings demonstrated that stratification by amyloid status improved identification of associations in comparison with diagnostic status.

Furthermore, in Chapter 6A (Experiment Three Part A), associations between all PRSs and longitudinal worsening of CSF Aβ42 and CSF p-tau181 were investigated in a sub-cohort of 171 ADNI participants. The key findings were that PRSwithAPOE and APOEonlyPRS were associated positively with worsening of Aβ42 over 24 months in CU participants, and in ε4 carriers. Additionally, twice as many associations were found with p-tau181. PRSwithoutAPOE was associated positively with worsening of p-tau181 over 24 months in MCI patients. However, most associations between PRSwithAPOE and APOEonlyPRS with p-tau181 were negative, i.e., high PRSs predicted a lack of worsening of p-tau181 longitudinally. Such associations were found in CU participants, ε4 non-carriers, CU ε4 non-carriers, and in MCI ε4 non-carriers. These outcomes have not been reported previously but are crucial in highlighting that genetics may have a limited influence on p-tau181 changes (or that a two-year timeframe is not long enough to find associations in the expected direction) in these groups. Of note, PRSwithAPOE and APOEonlyPRS performed similarly.

In Chapter 6B (Experiment Three Part B), associations between all PRSs and longitudinal cognitive decline in composite scores of memory, plus decline in one other cognitive domain, were examined in a sub-sample of 501 ADNI participants. The main findings were that PRSwithAPOE and APOEonlyPRS were associated positively with cognitive decline over 24 months in participants that were p-tau181-positive ε4-non-carriers. APOEonlyPRS was superior in comparison with PRSwithAPOE.

Moreover, some inconsistent and spurious findings were reported in Chapter 4 Experiment One (cross-sectional regional grey matter), Chapter 5B Experiment Two Part B (cross-sectional cognition), and in Chapter 6A Experiment Three Part A (longitudinal p-tau181). These may be explained in several additional ways. First, GWASs identify common disease-associated variants at a given locus and such findings are extended upon to construct PRSs. However, several common risk variants are likely to exist at the same loci (Koch et al., 2023). Singleton and Hardy (2011) suggested that genetics of complex diseases, like sporadic AD, are likely a combination of two hypotheses. (1) The Common-Disease-Common-Variant Hypothesis whereby common variants found in the population studied, each with low effect sizes, contribute to disease risk; (2) the Multiple Rare Variant Hypothesis whereby low-frequency variants found in the population studied, each with large effect sizes and high penetrance (i.e., from genotype to phenotype), contribute to disease. The coexistence of common variants and rare variants within the same loci is referred to as Pleomorphic Risk Loci Hypothesis, and this may increase or decrease disease

risk (Ridge et al., 2013). The Pleomorphic Risk Loci Hypothesis may explain some of the inconsistent findings in the current research, particularly those relating to Chapter 6A (Experiment Three Part A) where PRSwithAPOE and APOEonlyPRS were associated negatively with longitudinal p-tau181. This may be because rare variants are not accounted for by PRSs overall. Third, twin studies have shown that sporadic AD is 58-79% heritable (Gatz et al., 2006). Therefore, lifestyle and environmental factors (Koch et al., 2023), as well as comorbidities, may be incorporated into PRS models to improve risk prediction further. For instance, Li, Lian and Vardhanabhuti (2025) devised a model that included MRI, PRS, and lifestyle data to predict risk of neurodegenerative disease with an AUC of 81.9%. Removal of one of these variables reduced the AUC to 68.8% (without MRI), 75.8% (without PRS), and 75.9% (without lifestyle data). These models investigated neurodegenerative diseases in general rather than comparing group differences between AD, Parkinson's disease, and dementia patients.

Although the inclusion of the aforementioned (other) factors was beyond the scope of the current research, Lewis and Vassos (2020) have reported that the genetic risk of a disease is dynamic. Meaning, it is dependent upon factors that change over time, such as age and the additional factors as stated above. Therefore, although PRSs can be calculated at any point in time, and that is crucial for a time-sensitive disease like AD where early prevention, early diagnosis, and early intervention result in better outcomes, rather than calculating PRSs at any age/a younger age, it would be appropriate to devise AD PRS models when participants are at an age where risk of sporadic AD begins to increase (i.e., 65 years) and when other age-related comorbidities are likely to appear. Or, when exposure to certain lifestyle, diet, and environmental factors is likely to have been experienced to a greater extent. Thus, another plus point of the current research is the use of participants of a characteristic age.

Furthermore, PRSs can be constructed in several ways and with numerous thresholds. There are disagreements in existing literature regarding the optimal threshold for SNP selection, the top method for calculating PRS, the optimal threshold for construction of PRS, and how best to incorporate the effect of APOE (Leonenko et al., 2021). PRSs also use different discovery datasets and different replication datasets. For these reasons, it is difficult to compare PRSs and associated findings between existing literature. However, Leonenko et al. (2021) suggested that raw PRSs may be z-transformed according to the population mean instead of the sample mean to improve the comparability of findings between studies.

Importantly, although individuals of European ancestry account for ~16% of the global population, they represent ~80% of GWAS participants (Genetics for all, 2019). The current research used GWAS summary statistics from Jansen et al. (2019) for several reasons. First, this GWAS was used since it was independent from the ADNI sample that was tested in the current research. Second, if a recent LOAD GWAS with a greater number of cases had been used (e.g., Wightman et al. (2021)), there might have been an overlap between participants in the GWAS vs. participants in the current research. Third, after removal of by-proxy cases from a recent GWAS, the participant numbers from that GWAS might have been similar to those found in the GWAS by Jansen et al. (2019) that was used to calculate effect sizes for the current research. Fourth, despite the large number of cases in recent GWASs, it is challenging to identify dementia of the AD-type vs. others (and difficult to recruit age-matched controls) (Euesden et al., 2025). Fifth, Stocker et al. (2023) found that a PRS with 55 SNPs (without SNPs from the APOE region) that was generated using summary statistics from Kunkle et al. (2019) predicted AD diagnosis accurately, in comparison with a PRS with 105 SNPs (without SNPs from the APOE) that was calculated using summary statistics from Bellenguez et al. (2022). This was also found when restricting the analysis to ε4 carriers only. This may have been because the GWAS by Kunkle et al. (2019) used clinically diagnosed cases of AD, whereas Bellenguez et al. (2022) used both clinical and by-proxy cases of AD. Hence, the use of recent/large GWASs is not beneficial always, and the selection must be made appropriately. GWASs on pathologically confirmed AD cases are ideal, however, such cases are limited by far (Hardy and Escott-Price, 2025).

7.2. Limitations

Some of the limitations identified in Chapter 2 (Systematic Review) remain unaddressed in the current research, i.e., the examination of independent cohorts, and racially minoritised groups. This was due to the lack of available data. The limited racial diversity of participants is an ongoing issue in research generally, including GWASs. However, for research into sporadic AD, the requirement to examine participants that are both racially diverse and elderly adds a further caveat, as elderly individuals from racial minorities appear to be reluctant to partake in research. Importantly, language is a barrier in many cases, particularly for informed consent procedures and cognitive test batteries that are not available in multiple languages and do not consider cultural differences in stimuli used.

7.3. Contribution to the Field and Impact of Findings

Of note, PRSs for cardiovascular diseases and breast cancer have progressed gradually from research discovery studies to clinical trials to implementation in clinical settings, due to the evident clinical utility of PRSs in these diseases. However, in comparison, PRSs for AD are in their infancy due to the complexity of the disease and related multifactorial risk factors (Lewis and Vassos, 2020). However, the current research highlights several points. First, PRSwithAPOE and APOEonlyPRS may be useful in clinical settings, and in clinical trials to differentiate those who are at high vs. low risk (Baker and Escott-Price, 2020). Second, PRSwithAPOE and APOEonlyPRS may support the diagnosis of sporadic AD as well as providing insights into disease trajectory. Third, non-ε4-APOE SNPs and non-APOE SNPs provide valuable information. Fourth, there are other SNPs beyond ε4 that are useful for risk prediction. Fifth, a thorough and systematic approach for testing PRSs for AD has not been applied previously but has been fulfilled in the current work, and this may improve risk prediction further.

Moreover, in countries where Lecanemab has been approved for use, APOE genotyping in AD patients has been recommended to inform discussions and safety concerns (Cummings et al., 2023). The current research indicates that APOE SNPs beyond the ε4 variant (and non-APOE SNPs) are important. Hence, it may be suggested that the entire APOE region is investigated before decisions regarding the use of pharmacological vs. non-pharmacological treatments are made (Fujita et al., 2025). The current research may provide (one of) the first efforts, and evidence, towards this direction.

However, in the UK, testing for APOE ε4 is available to those with private healthcare but not to those on the National Health Service (NHS). For APOE testing to be made available on the NHS, further research is required to understand how the various isoforms of APOE and APOE genotypes, other genes, and polygenic risk, may influence onset and progression of AD. Although PRS has potential to guide treatment selection and predict side effects of treatments, there is a need to assess how individual SNPs, and how increased PRS load, may interact with AD and with disease-modifying treatments in the short-term and long-term.

The current research also investigates associations between PRSs and grey matter volume in the largest number of ROIs (to knowledge), i.e., 114 ROIs. In comparison, previous work has looked at 101 ROIs (Zhao et al., 2019b; Chen et al., 2024). Further, there is a limited amount of research on longitudinal changes in (CSF) p-tau/p-tau181. Hence, there are only a handful of studies

looking at the association between PRSs and longitudinal p-tau/p-tau181. The current research enhances upon this sub-field as well. Although there are more cross-sectional and longitudinal cognitive studies in the literature, data have not been scrutinised similarly to that in the current work.

Crucially, the current research shows that cross-sectionally, associations between PRSwithAPOE and APOEonlyPRS with CSF Aβ42 are stronger than associations with CSF p-tau181, and to the extent that any associations between PRSwithAPOE and APOEonlyPRS with p-tau181 are diminished after controlling for Aβ42 status. Longitudinally, associations between PRSwithAPOE and APOEonlyPRS with p-tau181 are stronger than associations between PRSwithAPOE and APOEonlyPRS with Aβ42. In comparison to the cross-sectional CSF studies, longitudinally, Aβ42 status does not have a detrimental effect on the associations with p-tau181. Additionally, p-tau181 is associated with AD-specific cognitive decline (of memory and any one other cognitive domain). Furthermore, where significant associations are found between the same PRS/PRS threshold and the same outcome variable in the same subgroup of participants, the variance in the outcome variable explained by the model is better longitudinally than cross-sectionally. Therefore, findings from the current research indicate that the prognostic value of PRSwithAPOE/APOEonlyPRS may be greater than the diagnostic value when examining Aβ42 in CU participants and in ε4 carriers, regardless of whether p-tau181 is or is not controlled for.

Subsequently, the current research provides further evidence to show that increased amyloid deposition occurs early in the continuum of AD, after which it reaches a plateau (Jack Jr et al., 2009). Hence, associations between PRSs and cross-sectional amyloid are stronger, whereas p-tau changes throughout the disease (Villemagne et al., 2011). Therefore, associations between PRSs and longitudinal p-tau are stronger. Consequently, the methodology applied to the current research has led to novel findings (to knowledge) in relation to the associations between PRSwithAPOE and APOEonlyPRS with longitudinal p-tau181 in CU participants, ε4 non-carriers, CU ε4 non-carriers, and MCI ε4 non-carriers, and the impact of p-tau181 on cognitive decline over time in p-tau181-positive ε4-non-carriers.

Additionally, the models constructed throughout the current research reflect the associations between various confounding variables with outcome measures vs. associations between various confounding variables, plus PRS, with outcome measures. These models help to distinguish the extent of the contribution of polygenetics to regional grey matter volume, CSF

biomarkers, and cognition, and therefore increase understanding of AD mechanisms. Overall, the examination of these various measures using numerous stratifications contributes to the novelty of the current work and helps to explain AD risk in different groups of participants. For consistency and interpretability of findings, for cross-sectional investigations, all variables and outcome measures were extracted from the date that was closest to the MRI data used. Similarly, for longitudinal investigations, "baseline" data were taken from the date closest to the MRI visit. Also, to improve upon previous literature, PRSs have been labelled and referred to distinctly throughout, as well as the relevant thresholds, and the directions of the associations have been stated clearly throughout to reduce ambiguity.

7.4. Recommendations for Future Research

In terms of recommendations for future investigations, research on the associations between PRSwithAPOE, PRSwithoutAPOE, and APOEonlyPRS at various thresholds with longitudinal CSF p-tau181 along with CSF Aβ42 are required. Additionally, associations between these PRSs and thresholds with regional grey matter volume, CSF biomarkers, and cognitive markers that have been assessed in the current research must be tested in independent samples, as well as in racially diverse populations. Of note, plasma p-tau217 is emerging as the top blood-based biomarker for detecting pathology in symptomatic patients; that is a less invasive, but cost-effective, alternative to CSF and PET measures (Palmqvist et al., 2025). Therefore, the investigation of the above-mentioned PRSs and several thresholds with plasma p-tau217 is also suggested. A multimodal score may also be developed to examine PRS + structural MRI measures + CSF biomarkers (and/or Plasma biomarkers) + Cognitive domains, simultaneously, to support AD diagnosis and disease trajectory further. It is essential to investigate these various outcome measures both cross-sectionally and longitudinally, and within the same cohort, to understand disease-specific genetics, mechanisms, pathways, and prognosis with the methodological approaches as applied in the current research.

CHAPTER 8

GENERAL CONCLUSION

Overall, the current research highlights that PRSwithAPOE and APOEonlyPRS are useful in clinical settings, whereas PRSwithoutAPOE are less consistent or unreliable. If stratification methods are used, stratification by amyloid status is reliable in comparison to clinical diagnosis. Associations found using PRSwithAPOE and APOEonlyPRS can be used to improve the prediction of cross-sectional regional grey matter volume loss, cross-sectional CSF biomarkers and cognition, as well as longitudinal worsening of CSF biomarkers and cognitive decline that are characteristic of AD-related changes. Although there does not seem to be an ideal threshold for detecting associations generally, it may be possible for certain thresholds to identify associations better depending on the modality/outcome measure tested. In the current research, for example: PRSwithAPOE Thresholds 5 and 10, and APOEonlyPRS Thresholds 1 and 5 for regional grey matter volume; PRSwithAPOE Threshold 1 and APOEonlyPRS Threshold 5 for cross-sectional CSF biomarkers; PRSwithAPOE Threshold 1 and APOEonlyPRS Threshold 1 for cross-sectional cognition; both PRSwithAPOE thresholds and APOEonlyPRS thresholds for longitudinal CSF biomarkers; PRSwithAPOE Threshold 10 and APOEonlyPRS Threshold 1 for longitudinal cognitive decline. This indicates the difficulty of constructing PRSs and concurs to related points reported by previous researchers.

CHAPTER 9

LIST OF REFERENCES

Abe, C., Petrovic, P., Ossler, W., Thompson, W.H., Liberg, B., Song, J., Bergen, S.E., Sellgren, C.M., Fransson, P., Ingvar, M., & Landen, M. (2021). Genetic risk for bipolar disorder and schizophrenia predicts structure and function of the ventromedial prefrontal cortex. *Journal of Psychiatry and Neuroscience, 46*(4), E441-E450. DOI: 10.1503/jpn.200165.

ADNI (2023). *Explanation of the factor scores in UWNPSYCHSUM.CSV*. https://ida.loni.usc.edu/explore/jsp/search/search.jsp?project=ADNI#studyFiles (Accessed: 30 October 2024)

ADNI (2025). *Alzheimer's Disease Neuroimaging Initiative*. Available at: https://adni.loni.usc.edu/ (Accessed: September 2025).

Ahmad, S., Bannister, C., van der Lee, S., Vojinovic, D., Adams, H.H.H., Ramirez, A., Escott-Price, V., Sims, R., Baker, E., Williams, J., Holmans, P., Vernooij, M.W., Ikram, M.A., Amin, N., van Duijn, C.M. (2018). Disentangling the biological pathways involved in early features of Alzheimer's disease in the Rotterdam study. *Alzheimer's & Dementia, 14*(7), 848-857. DOI: 10.1016/j.jalz.2018.01.005.

Ahn, Y.D., Yi, D., Joung, H., Seo, E.H., Lee, Y.H., Byun, M.S., Lee, J.H., Jeon, S.Y., Lee, J.Y., Sohn, B.K., & Lee, D.Y. (2019). Normative data for the logical memory subtest of the Wechsler memory scale-IV in middle-aged and elderly Korean people. *Psychiatry Investigation, 16*(11), 793-799. DOI: 10.30773/pi.2019.0061.

Aisen, P.S., Cumming, J., Jack Jr, C.R., Morris, J.C., Sperling, R., Frolich, L., Jones, R.W., Dowsett, S.A., Matthews, B.R., Raskin, J., Scheltens, P., & Dubois, B. (2017). On the path to 2025: understanding the Alzheimer's disease continuum. *Alzheimer's Research & Therapy, 9*(1), 60. DOI: 10.1186/s13195-017-0283-5.

Aisen, P.S., Jimenez-Maggiora, G.A., Rafii, M.S., Walter, S., & Raman, R. (2022). Early-stage Alzheimer disease: getting trial-ready. *Nature Reviews Neurology, 18*(7), 389-399. DOI: 10.1038/s41582-022-00645-6.

Albert, M.S., DeKosky, S.T., Dickson, D., Dubois, B., Feldman, H.H., Fox, N.C., Gamst, A., Holtzman, D.M., Jagust, W.J., Petersen, R.C., Snyder, P.J., Carrillo, M.C., Thies, B., & Phelps, C.H. (2011). The diagnosis of mild cognitive impairment due to Alzheimer's disease: from the National

Institute of Aging-Alzheimer's Association workgroups on diagnostic guidelines for Alzheimer's disease. *Alzheimer's & Dementia, 7*(3), 270-279. DOI: 10.1016/j.jalz.2011.03.008.

Albrecht, M.A., Szoeke, C., Maruff, P., Savage, G., Lautenschlager, N.T., Ellis, K.A., Taddei, K., Martins, R., Masters, C.L., Ames, D., Foster, J.K., & AIBL Research Group (2015). Longitudinal cognitive decline in the AIBL cohort: The role of APOE ε4 status. *Neuropsychologia, 75*, 411-419. DOI: 10.1016/j.neuropsychologia.2015.06.008.

Altmann, A., Scelsi, M.A., Shoai, M., de Silva, E., Aksman, L.M., Cash, D.M., Hardy, J., Schott, J.M., & ADNI (2020). A comprehensive analysis of methods for assessing polygenic burden on Alzheimer's disease pathology and risk beyond APOE. *Brain Communications, 2*(1), fcz047. DOI: 10.1093/braincomms/fcz047.

Alves, L., Cardoso, S., Silva, D., Mendes, T., Marôco, J., Nogueira, J., Lima, M., Tábuas-Pereira, M., Baldeiras, I., Santana, I., de Mendonça, A., & Guerreiro, M. (2021). Neuropsychological profile of amyloid-positive versus amyloid-negative amnestic mild cognitive impairment. *Journal of Neuropsychology, 15*(Suppl 1), 41-52. DOI: 10.1111/jnp.12218.

Alves, P.N., Foulon, C., Karolis, V., Bzdok, D., Margulies, D.S., Volle, E., & de Scotten, M.T. (2019). An improved neuroanatomical model of the default-mode network reconciles previous neuroimaging and neuropathological findings. *Communications Biology, 2*(370). DOI: 10.1038/s42003-019-0611-3.

Alz Forum (2025). *Mutations*. Available at: https://www.alzforum.org/mutations (Accessed: 23 July 2025).

Anand, K.S., & Dhikav, V. (2012). Hippocampus in health and disease: An overview. Annals of *Academy of Neurology, 15*(4), 239-246. DOI: 10.4103/0972-2327.104323.

Andersson, C., Blennow, K., Almkvist, O., Andreasen, N., Engfeldt, P., Johansson, S.E., Lindau, M., & Eriksdotter-Jönhagen, M. (2008). Increasing CSF phospho-tau levels during cognitive decline and progression to dementia. *Neurobiology of Aging, 29*(10), 1466-1473. DOI: 10.1016/j.neurobiolaging.2007.03.027.

Andreasen, N., Sjögren, M., & Blennow, K. (2003). CSF markers for Alzheimer's disease: total tau, phospho-tau and abeta42. *World Journal of Biological Psychiatry, 4*(4), 147-155. DOI: 10.1080/15622970310029912.

Andrews, S.J., Das, D., Cherbuin, N., Anstey, K.J., & Easteal, S. (2016). Association of genetic risk factors with cognitive decline: the PATH through life project. *Neurobiology of Aging*, *41*, 150-158. DOI: 10.1016/j.neurobiolaging.2016.02.016.

Apostolova, L.G., Green, A.E., Babakchanian, S., Hwang, K.S., Chou, Y-Y., Toga, A.W., & Thompson, P.M. (2012). Hippocampal atrophy and ventricular enlargement in normal aging, mild cognitive impairment and Alzheimer's disease. *Alzheimer Disease & Associated Disorders, 26*(1), 17-27. DOI: 10.1097/WAD.0b013e3182163b62.

Armstrong, N.M., Dumitrescu, L., Huang, C-W., An, Y., Tanaka, T., Hernandez, D., Doshi, J., Erus, G., Davatzikos, C., Ferrucci, L., Resnick, S.M., & Hohman, T.J. (2020). Association of hippocampal volume polygenic predictor score with baseline and change in brain volumes and cognition among cognitively healthy older adults. *Neurobiology of Aging, 94*, 81-88. DOI: 10.1016/j.neurobiolaging.2020.05.007.

Arora, S., Santiago, J.A., Bernstein, M., & Potashkin, J.A. (2023). Diet and lifestyle impact the development and progression of Alzheimer's dementia. *Frontiers in Nutrition, 10*:1213223. DOI: 10.3389/fnut.2023.1213223.

Arpawong, T.E., Pendleton, N., Mekli, K., McArdle, J.J., Gatz, M., Armoskus, C., Knowles, J.A., & Prescott, C.A. (2017). Genetic variants specific to aging-related verbal memory: Insights from GWASs in a population-based cohort. *PLoS One, 12*(8), e0182448. DOI: 10.1371/journal.pone.0182448.

Ashburner, J. and Friston, K. J. (2000). Voxel-based morphometry – the methods. *NeuroImage*, *11*(6 Pt 1), 805-821. DOI: 10.1006/nimg.2000.0582.

Augustinack, J. C., Helmer, K., Huber, K. E., Kakunoori, S., Zollei, L., & Fischl, B. (2010). Direct visualisation of the perforant pathway in the human brain with ex vivo diffusion tensor imaging. *Frontiers in Human Neuroscience, 4*, 42. DOI: 10.3389/fnhum.2010.00042.

Baek, M.S., Cho, H., Lee, H.S., Lee, J.H., Ryu, Y.H., & Lyoo, C.H. (2020). Effect of APOE ε4 genotype on amyloid-β and tau accumulation in Alzheimer's disease. *Alzheimer's Research & Therapy, 12*(1), 140. DOI: 10.1186/s13195-020-00710-6.

Baker, E., & Escott-Price, V. (2020). Polygenic risk scores in Alzheimer's disease: current applications and future directions. *Frontiers in Digital Health, 2*(14). DOI: 10.3389/fdgth.2020.00014.

Bakker, A., Krauss, G.L., Albert, M.S., Speck, C.L., Jones, L.R., Stark, C.E., Yassa, M.A., Bassett, S.S., Shelton, A.L., & Gallagher, M. (2012). Reduction of hippocampal hyperactivity improves cognition in amnestic mild cognitive impairment. *Neuron, 74*(3), 467-474. DOI: 10.1016/j.neuron.2012.03.023.

Bateman, R.J., Xiong, C., Benzinger, T.L.S., Fagan, A.M., Goate, A., Fox, N.C., Maruc, D.S., Cairns, N.J., Xie, X., Blazey, T.M., Holtzman, D.M., Santacruz, A., Buckles, V., Oliver, A., Moulder, K., Aisen, P.S., Ghetti, B., Klunk, W.E., McDade, E., ... Morris, J.C. (2012). Clinical and biomarker changes in dominantly inherited Alzheimer's disease. *New England Journal of Medicine, 367*(9), 795-804. DOI: 10.1056/NEJMoa1202753.

Becker, K.G., Barnes, K.C., Bright, T.J., & Wang, A.A. (2004). The genetic association database. *Nature, 36*(5), 431-432. DOI: 10.1038/ng0504-431.

Beecham, G.W., Hamilton, K., Naj, A.C., Martin, E.R., Huentelman, M., Myers, A.J., Corneveaux, J.J., Hardy, J., Vonsattel, J-P., Younkin, S.G., Bennett, D.A., De Jager, P.L., Larson, E.B., Crane, P.K., Kanmob, M.I., Kofler, J.K., Mash, D.C., Dugue, L., Gilbert, J.R., ... Montine, T.J. (2014). Genome-wide association meta-analysis of neuropathologic features of Alzheimer's disease and related dementias. *PLoS Genetics, 10*(9), e1004606. DOI: 10.1371/journal.pgen.1004606.

Bejanin, A., Schonhaut, D.R., La Joie, R., Kramer, J.H., Baker, S.L., Sosa, N., Ayakta, N., Cantwell, A., Janabi, M., Lauriola, M., O'Neil, J.P., Gorno-Tempini, M.L., Miller, Z.A., Rosen, H.J., Miller, B.L., Jagust, W.J., & Rabinovici, G.D. (2017). Tau pathology and neurodegeneration contribute to cognitive impairment in Alzheimer's disease. *Brain, 140*(12), 3286-3300. DOI: 10.1093/brain/awx243.

Bekdash, R.A. (2021). The cholinergic system, the adrenergic system and the neuropathology of Alzheimer's disease. *International Journal of Molecular Science, 22*(3), 1273. DOI: 10.3390/ijms22031273.

Bekris, L.M., Yu, C-E., Bird, T.D., & Tsuang, D.W. (2010). Review Article: Genetics of Alzheimer disease. *Journal of Geriatric Psychiatry and Neurology, 23*(4), 213-227. DOI: 10.1177/0891988710383571.

Bellenguez, C., Kucukali, F., Jansen, I.E., Kleineidam, L., Moreno-Grau, S., Amin, N., Naj, A.C., Campos-Martin, R., Grenier-Boley, B., Andrade, V., Holmans, P.A., Boland, A., Damotte, V., van der Lee, S., Costa, M.R., Kuulasmaa, T., Yang, Q., de Roajs, Bis, J.C., ... Lambert, J-C. (2022). New insights into the genetic etiology of Alzheimer's disease and related dementias. *Nature Genetics, 54*(4), 412-436. DOI: 10.1038/s41588-022-01024-z.

Belloy, M.E., Andrews, S.J., Le Guen, Y., Cuccaro, M., Farrer, L.A., Napolioni, V., & Greicius, M.D. (2023). APOE genotype and Alzheimer disease risk across age, sex, and population ancestry. *JAMA Neurology, 80*(12), 1284-1294. DOI: 10.1001/jamaneurol.2023.3599.

Belloy, M.E., Napolioni, V., & Greicius, M.D. (2019). A quarter century of APOE and Alzheimer's disease: Progress to date and the path forward. *Neuron, 101*(5), 820-838. DOI: 10.1016/j.neuron.2019.01.056.

Benard, B.A., & Goldman, J.G. (2010). MMSE - mini-mental state examination. Encyclopedia of *Movement Disorders*, 187-189. DOI: 10.1016/B978-0-12-374105-9.00186-6.

Benjamini, Y., & Hochberg, Y. (1995). Controlling the false discovery rate: A practical and powerful approach to multiple testing. *Journal of the Royal Statistical Society, Series B (Methodological), 57*(1), 289-300. DOI: 10.1111/j.2517-6161.1995.tb02031.x.

Bennett, I.J., Huffman, D.J., & Stark, C.E.L. (2015). Limbic tract integrity contributes to pattern separation performance across the lifespan. *Cerebral Cortex, 25*(9), 2988-2999. DOI: 10.1093/cercor/bhu093.

Bergamino, M., Schiavi, S., Daducci, A., Walsh, R.R. & Stokes, A.M. (2022). Analysis of brain structural connectivity networks and white matter integrity in patients with mild cognitive impairment. *Frontiers in Aging Neuroscience, 14*, 793991. DOI: 10.3389/fnagi.2022.793991.

Berron, D., Vogel, J.W., Insel, P.S., Pereira, J.A., Xie, L., Wisse, L.E.M., Yushkevich, P.A., Palmqvist, S., Mattsson-Carlgren, N., Stomrud, E., Smith, R., Standberg, O., & Hansson, O. (2021). Early stages of tau pathology and its associations with functional connectivity, atrophy and memory. *Brain, 144*(9), 2771-2783. DOI: 10.1093/brain/awab114.

Bertram, L., McQueen, M.B., Mullin, K., Blacker, D., & Tanzi, R.E. (2007). Systematic meta-analyses of Alzheimer disease genetic association studies: The AlzGene database. *Nature Genetics, 39*(1), 17-23. DOI: 10.1038/ng1934.

Bilgel, M., & Resnick, S.M. (2020). Amyloid positivity as a risk factor for memory decline and lower memory performance as an indicator of conversion to amyloid positivity: Chicken and egg. *Biological Psychiatry, 87*(9), 782-784. DOI: 10.1016/j.biopsych.2020.02.006.

Blennow, K., Hampel, H., Weiner, M., & Zetterberg, H. (2010). Cerebrospinal fluid and plasma biomarkers in Alzheimer disease. Nature Reviews Neurology, 6(3), 131-144. DOI: 10.1038/nrneurol.2010.4.

Boccalini, C., Ribaldi, F., Hristovska, I., Arnone, A., Peretti, D.E., Mu, L., Scheffler, M., Perani, D., Frisoni, G.B., & Garibotto, V. (2023). The impact of tau deposition and hypometabolism on cognitive impairment and longitudinal cognitive decline. *Alzheimer's & Dementia, 20*(1), 221-233. DOI: 10.1002/alz.13355.

Bookheimer, S.Y., Strojwas, M.H., Cohen, M.A., Saunders, A.M., Pericak-Vance, M.A., Mazziotta, J.C., & Small, G.W. (2000). Patterns of brain activation in people at risk for Alzheimer's disease. *New England Journal of Medicine, 343*(7), 450-456. DOI: 10.1056/NEJM200008173430701.

Boutet, C., Chupin, M., Lehericy, S., Marrakchi-Kacem, L., Epelbaum, S., Poupon, C., Wiggins, C., Vignaud, A., Hasboun, D., Defontaines, B., Hanon, O., Dubois, B., Sarazin, M., Hert-Pannier, L., & Colliot, O. (2014). Detection of volume loss in hippocampal layers in Alzheimer's disease using 7 T MRI: A feasibility study. *NeuroImage Clinical, 5*, 341-348. DOI: 10.1016/j.nicl.2014.07.011.

Bozzali, M., Falini, A., Franceschi, M., Cercignani, M., Zuffi, M., Scotti, G., Comi, G., & Filippi, M. (2002). White matter damage in Alzheimer's disease assessed in vivo using diffusion tensor magnetic resonance imaging. *Journal of Neurology, Neurosurgery, and Psychiatry, 72*(6), 742-746. DOI: 10.1136/jnnp.72.6.742.

Braak, H., & Braak, E. (1991). Neuropathological staging of Alzheimer-related changes. *Acta Neuropathologica, 82*(4), 239-259. DOI: 10.1007/BF00308809.

Breijyeh, Z., & Karaman, R. (2020). Comprehensive review on Alzheimer's disease: causes and treatment. *Molecule, 25*(24), 5789. DOI: 10.3390/molecules25245789.

Brenowitz, W.D., Fornage, M., Launer, L.J., Habes, M., Davatzikos, C., & Yaffe, K. (2023). Alzheimer's disease genetic risk, cognition, and brain aging in midlife. *Annals of Neurology, 93*(3), 629-634. DOI: 10.1002/ana.26569.

Brickell, K.L., Steinbart, E.J., Rumbaugh, M., Payami, H., Schellenberg, G.D., Van Derrlin, V., Yuan, W., & Bird, T. (2006). Early-onset Alzheimer disease in families with late-onset Alzheimer disease. *JAMA Neurology, 63*(9), 1307-1311. DOI: 10.1001/archneur.63.9.1307.

Brier, M.R., Thomas, J.B., Snyder, A.Z., Benzinger, T.L., Zhang, D., Raichle, M.E., Holtzman, D.M., Morris, J.C., & Ances, B.M. (2012). Loss of intranetwork and internetwork resting state functional connections with Alzheimer's disease progression. *Journal of Neuroscience, 32*(26), 8890-8899. DOI: 10.1523/JNEUROSCI.5698-11.2012.

Bucci, M., Chiotis, K., Nordberg, A. & Alzheimer's Disease Neuroimaging Initiative (2021). Alzheimer's disease profiled by fluid and imaging markers: tau PET best predicts cognitive decline. *Molecular Psychiatry, 26*(10), 5888-5898. DOI: 10.1038/s41380-021-01263-2.

Busche, M.A., & Hyman, B.T. (2020). Synergy between amyloid-β and tau in Alzheimer's disease. *Nature Neuroscience, 23*(10), 1183-1193. DOI: 10.1038/s41593-020-0687-6.

Busche, M.A., & Konnerth, A. (2016). Impairments of neural circuit function in Alzheimer's disease. *Philos Trans R Soc Lond B Biol Sci, 371*(1700), 20150429. DOI: 10.1098/rstb.2015.0429.

Cabeza, R., Anderson, N. D., Locantore, J.K., & McIntosh, A.R. (2002). Aging gracefully: compensatory brain activity in high-performing older adults. *NeuroImage, 17*, 1394-1402. DOI: 10.1006/nimg.2002.1280.

Cacace, R., Sleegers, K., & Van Broeckhoven, C. (2016). Molecular genetics of early-onset Alzheimer's disease revisited. *Alzheimer's & Dementia, 12*(6), 733-748. DOI: 10.1016/j.jalz.2016.01.012.

Caselli, R. J., Beach, T. G., Knopman, D. S., & Graff-Radford, N. R. (2017). Alzheimer's disease: Scientific breakthroughs and translational challenges. *Mayo Clinic Proceedings, 92*(6), 978-994. DOI: 10.1016/j.mayocp.2017.02.011.

Caspers, S., Rockner, M.A., Jockwitz, C., Bittner, N., Teumer, A., Herms, S., Hoffman, P., Nothen, M.N., Moebus, S., Amunts, K., Cichon, S., & Muhleisen, T.W. (2020). Pathway-specific genetic risk for Alzheimer's disease differentiates regional patterns of cortical atrophy in older adults. *Cerebral Cortex, 30*(2), 801-811. DOI: 10.1093/cercor/bhz127.

Celone, K.A., Calhoun, V.A., Dickerson, B.C., Atri, A., Chua, E.F., Miller, S.L., DePeau, K., Rentz, D.M., Selkoe, D.J., Blacker, D., Albert, M.S., & Sperling, R.A. (2006). Alterations in memory networks in mild cognitive impairment and Alzheimer's disease: An independent component analysis. *Journal of Neuroscience, 26*(40), 10222-10231. DOI: 10.1523/JNEUROSCI.2250-06.2006.

Chandler, H.L., Wheeler, J., Escott-Price, V., Murphy, K., & Lancaster, T.M. (2020). Non-APOE variants predominately expressed in smooth muscle cells contribute to the influence of Alzheimer's disease genetic risk on white matter hyperintensities. *Alzheimer's & Dementia, 21*(2), e14455. DOI: 10.1002/alz.14455.

Chang, C.A., Chow, C.A., Tellier, L.C.A.M., Vattikuti, S., Purcell, S.M., & Lee, J.J. (2015). Second-generation PLINK: Rising to the challenge of larger and richer datasets. *GigaScience, 4*, 7. DOI: 10.1186/s13742-015-0047-8.

Chasioti, D., Yan, J., Nho, K., & Saykin, A.J. (2019). Progress in polygenic composite scores in Alzheimer's and other complex diseases. *Trends in Genetics, 35*(5), 371-382. DOI: 10.1016/j.tig.2019.02.005.

Chatterjee, N., Shi, J., & Garcia-Closas, M. (2016). Developing and evaluating polygenic risk prediction models for stratified disease prevention. *Nature Reviews Genetics, 17*(7), 392-406. DOI: 10.1038/nrg.2016.27.

Chen, G-F., Xu, T-H., Yan, Y., Zhou, Y-R., Jiang, Y., Melcher, K., & Xu, H.E. (2017). Amyloid beta: structure, biology and structure-based therapeutic development. *Acta Pharmacologica Sinica, 38*(9), 1205-1235. DOI: 10.1038/aps.2017.28.

Chen, J., Li, T., Zhao, B., Chen, H., Yuan, C., Garden, G.A., Wu, G., & Zhu, H. (2024). The interaction effects of age, APOE, and common environmental risk factors on human brain structure. *Cerebral Cortex, 34*(1), bhad472. DOI: 10.1093/cercor/bhad472.

Chen, S-D., Zhang, W., Li, Y-Z., Yang, L., Huang, Y-Y., Deng, Y-T., Wu, B-S., Suckling, J., Rolls, E.T., Feng, J-F., Cheng, W., Dong, Q., & Yu, J-T. (2023). A phenome-wide association and mendelian randomization study for Alzheimer's disease: A prospective cohort study of 502493 participants from the UK Biobank. *Biological Psychiatry, 93*(9), 790-801. DOI: 10.1016/j.biopsych.2022.08.002.

Chen, Y., & Yu, Y. (2023). Tau and neuroinflammation in Alzheimer's disease: interplay mechanisms and clinical translation. *Journal of Neuroinflammation, 20*(1), 165. DOI: 10.1186/s12974-023-02853-3.

Chen, Z.R., Huang, J.B., Yang, S.L., & Hong, F.F. (2022). Role of cholinergic signaling in Alzheimer's disease. *Molecules, 27*(6), 1816. DOI: 10.3390/molecules27061816.

Choi, S.W., & O'Reilly, P.F. (2019). PRSice-2: Polygenic risk score software for biobank-scale data. *GigaScience, 8*(7), giz082. DOI: 10.1093/gigascience/giz082.

Choo, I.H., Lee, D.Y., Oh, J.S., Lee, J.S., Lee, D.S., Song, I.C., Youn, J.C., Kim, S.G., Kim, K.W., Jhoo, J.H., & Woo, J.I. (2010). Posterior cingulate cortex atrophy and regional cingulum disruption in mild cognitive impairment and Alzheimer's disease. *Neurobiology of Aging, 31*(5), 772-779. DOI: 10.1016/j.neurobiolaging.2008.06.015.

Chung, J., Wang, X., Maruyama, T., Ma, Y., Zhang, X., Mez, J., Sherva, R., Takeyama, H., Alzheimer's Disease Neuroimaging Initiative., Lunetta, K. L., Farrer, L. A., & Jun, G. R. (2017). Genome-wide association study of Alzheimer's disease endophenotypes at prediagnosis stages. *Alzheimer's & Dementia, 14*(5), 623-633. DOI: 10.1016/j.jalz.2017.11.006.

Chung, J., Sahelijo, N., Maruyama, T., Hu, J., Panitch, R., Xia, W., Mez, J., Stein, T.D., Saykin, A.J., Takeyama, H., Farrer, L.A., Crane, P.K., Nho, K., & Jun, G R. (2023). Alzheimer's disease heterogeneity explained by polygenic risk scores derived from brain transcriptomic profiles. *Alzheimer's & Dementia, 19*(11), 5173-5184. DOI: 10.1002/alz.13069.

Citron, M., Diehl, T.S., Gordon, G., Biere, A.L., Seubert, P., & Selkoe, D.J. (1996). Evidence that the 42- and 40-amino acid forms of amyloid β protein are generated from the β-amyloid precursor protein by different protease activities. *Proceedings of the National Academy of Sciences of the United States of America, 93*(23), 13170-13175. DOI: 10.1073/pnas.93.23.13170.

Clark, L.R., Berman, S.E., Norton, D., Koscik, R.L., Jonaitis, E., Blennow, K., Bendlin, B.B., Asthana, S., Johnson, S.C., Zetterberg, H., & Carlsson, C.M. (2018). Age-accelerated cognitive decline in asymptomatic adults with CSF β-amyloid. *Neurology, 90*(15), e1306-e1315. DOI: 10.1212/WNL.0000000000005291.

ClinicalTrials.gov (2024). Alzheimer's Disease Neuroimaging Initiative 4 (ADNI4). Available at https://classic.clinicaltrials.gov/ct2/show/NCT05617014 (Accessed: 29 March 2024).

Cohen, R.M., Small, C., Lalonde, F., Friz, J., & Sunderland, T. (2001). Effect of apolipoprotein E genotype on hippocampal volume loss in aging healthy women. *Neurology, 57*(12), 2223-2228. DOI: 10.1212/WNL.57.12.2223.

Conomos, M.P., Miller, M., & Thornton, T. (2015). Robust inference of population structure for ancestry prediction and correction of stratification in the presence of relatedness. *Genetic Epidemiology, 39*(4), 276-293. DOI: 10.1002/gepi.21896.

Conomos, M.P., Reiner, A.P., Weir, B.S., & Thornton, T.A. (2016). Model-free estimation of recent genetic relatedness. *American Journal of Human Genetics, 98*(1), 127-148. DOI: 10.1016/j.ajhg.2015.11.022.

Corder, E.H., Saunders, A.M., Risch, N.J., Strittmatter, D.E., Schmechel, D.E., Gaskell, Jr, P.C., Rimmler, J.B., Locke, P.A., Conneally, P.M., Schmader, K.E., Small, G.W., Roses, A.D., Haines, J.L. & Pericak-Vance, M.A. (1994). Protective effect of apolipoprotein E type 2 allele for late onset Alzheimer disease. *Nature Genetics, 7*, 180-184. DOI: 10.1038/ng0694-180.

Corder, E.H., Saunders, A.M., Strittmatter, W.J., Schmechel, D.E., Gaskell, P.C., Small, G.W., Roses, A.D., Haines, J.L., & Pericak-Vance, M.A. (1993). Gene dose of apolipoprotein E type 4 allele and the risk of Alzheimer's disease in late onset families. *Science, 261*(5123), 921-923. DOI: 10.1126/science.8346443.

Corlier, F., Hafzalla, G., Faskowitz, J., Kuller, L.H., Becker, J.T., Lopez, O.L., Thompson, P.M., & Braskie, M.N. (2018). Systemic inflammation as a predictor of brain aging: Contributions of physical activity, metabolic risk, and genetic risk. *NeuroImage, 172*, 118-129. DOI: 10.1016/j.neuroimage.2017.12.027.

Craft, S., Teri, L., Edland, S.D., Kukull, W.A., Schellenberg, G., McCormick, W.C., Bowen, J.D., & Larson, E.B. (1998). Accelerated decline in apolipoprotein E-epsilon4 homozygotes with Alzheimer's disease. *Neurology, 51*(1), 149-153. DOI: 10.1212/WNL.51.1.149.

Crawford, J. R., Allan, K.M., Stephen, D.W., Parker, D.M., & Besson, J.A.O. (1989). The Wechsler adult intelligence scale-revised (WAIS-R): factor structure in a U.K. sample. *Personality and Individual Differences, 10*(11), 1209-1212. DOI: 10.1016/0191-8869(89)90091-3

Creese, B., & Ismail, Z. (2022). Mild behavioural impairment: Measurement and clinical correlated of a novel marker of preclinical Alzheimer's disease. *Alzheimer's Research & Therapy, 14*(1), 2. DOI: 10.1186/s13195-021-00949-7.

Crowther, R. A. (1991). Straight and paired helical filaments in Alzheimer disease have a common structural unit. *Proceedings of the National Academy of Sciences of the United States of America, 88*(6), 2288-2292. DOI: 10.1073/pnas.88.6.2288.

Cruchaga, C., Chakraverty, S., Mayo, K., Vallania, F.L.M., Mitra, R.D., Faber, K., Williamson, J., Bird, T., Diaz-Arrastia, R., Foroud, T.M., Boeve, B.F., Graff-Radford, N.R., St. Jean, P., Lawson, M., Ehm, M.G., Mayeux, R., & Goate, A.M. (2012). Rare variants in APP, PSEN1 and PSEN2 increase risk for AD in late-onset Alzheimer's disease families. *PLoS One, 7*(2), e31309. DOI: 10.1371/journal.pone.0031039.

Cruchaga, C., Del-Aguila, J.L., Saef, B., Black, K., Fernandez, M.V., Budde, J., Ibanez, L., Deming, Y., Kapoor, M., Tosto, G., Mayeux, R.P., Holtzman, D.M., Fagan, A.M., Morris, J.C., Bateman, R.J., Goate, A.M., Dominantly Inherited Alzheimer Network (DIAN), Disease Neuroimaging Initiative (ADNI), NIA-LOAD family study, & Harari, O. (2018). Polygenic risk score of sporadic late-onset Alzheimer's disease reveals a shared architecture with the familial and early-onset forms. *Alzheimer's & Dementia, 14*(2), 205-214. DOI: 10.1016/j.jalz.2017.08.013.

Cruchaga, C., Kauwe, J.S., Harari, O., Jin, S.C., Cai, Y., Karch, C.M., Benitez, B.A., Jeng, A.T., Skorupa, T., Carrell, D., Bertelsen, S., Bailey, M., McKean, D., Shulman, J.M., De Jager, P.L.,

Chibnik, L., Bennett, D.A., Arnold, S.E., Harold, D., ... Goate, A.M. (2013). GWAS of cerebrospinal fluid tau levels identifies risk variants for Alzheimer's disease. *Neuron, 78*(2), 256-268. DOI: 10.1016/j.neuron.2013.02.026.

Cruts, M., van Duijn, C.M., Backhovens, H., van den Broeck, M., Wehnert, A., Serneels, S., Sherrington, R., Hutton, M., Hardy, J., St George-Hyslop, P.H., Hofman, A., & van Broeckhoven, C. (1998). Estimation of the genetic contribution of presenilin-1 and -2 mutations in a population-based study of presenile Alzheimer disease. *Human Molecular Genetics, 7*(1), 43-51. DOI: 10.1093/hmg/7.1.43.

Csernansky, J.G., Wang, L., Swank, J., Miller, J.P., Gado, M., McKeel, D., Miller, M.I., & Morris, J.C. (2005). Preclinical detection of Alzheimer's disease: Hippocampal shape and volume predict dementia onset in the elderly. *NeuroImage, 25*(3), 783-792. DOI: 10.1016/j.neuroimage.2004.12.036.

Cummings, J., Apostolova, L., Rabinovici, G.D., Atri, A., Aisen, P., Greenberg, S., Hendrix, S., Selkoe, D., Weiner, M., Petersen, R.C., & Salloway, S. (2023). Lecanemab: Appropriate use recommendations. *Journal of Prevention of Alzheimer's Disease, 10*(3), 362-377. DOI: 10.14283/jpad.2023.30.

Da, X., Toledo, J. B., Zee, J., Wolk, D. A., Xie, S. X., Ou, Y., Shacklett, A., Parmpi, P., Shaw, L., Trojanowski, J. Q., Davatzikos, C., & Alzheimer’s Disease Neuroimaging Initiative. (2013). Integration and relative value of biomarkers for prediction of MCI and AD progression: Spatial patterns of brain atrophy, cognitive scores, APOE genotype and CSF biomarkers. *NeuroImage: Clinical, 4*, 164-173. DOI: 10.1016/j.nicl.2013.11.010.

Daunt, P., Ballard, C.G., Creese, B., Davidson, G., Hardy, J., Oshota, O., Pither, R.J., & Gibson, A.M. (2021). Polygenic risk scoring is an effective approach to predict those individuals most likely to decline cognitively due to Alzheimer's disease. *Journal of Prevention of Alzheimer's Disease, 8*(1), 78-83. DOI: 10.14283/jpad.2020.64.

Davatzikos, C., Xu, F., Fan, Y., & Resnick, S. M. (2009). Longitudinal progression of Alzheimer's-like patterns of atrophy in normal older adults: the SPARE-AD index. *Brain, 132*(8), 2026-2035. DOI: 10.1093/brain/awp091.

Davies, G., Lam, M., Harris, S.E., Trampush, J.W., Luciano, M., Hill, W.D., Hagenaars, S.P., Ritchie, S.J., Marioni, R.E., Fawns-Ritchie, C., Liewald, D.C.M., Okely, J.A., Ahola-Olli, A.V., Barnes, C.L.K., Bertram, L., Bis, J.C., Burdick, K.E., Christoforou, A., DeRosse, P., ... & Deary, I.J. (2018). Study of 300,486 individuals identifies 148 independent genetic loci influencing general cognitive function. *Nature Communications, 9*(1), 2098. DOI: 10.1038/s41467-018-04362-x.

Davies, G., Tenesa, A., Payton, A., Yang, J., Harris, S.E., Liewald, D., Ke, X., Le Hellard, S., Christoforou, A., Luciano, M., McGhee, K., Lopez, L., Gow, A.J., Corley, J., Redmond, P., Fox, H.C., Haggarty, P., Whalley, L.J., McNeill, G., ... Deary, I.J. (2011). Genome-wide association studies establish that human intelligence is highly heritable and polygenic. *Molecular Psychiatry, 16*(10), 996-1005. DOI: 10.1038/mp.2011.85.

De Marco, M., Manca, R., Kirby, J., Hautbergue, G.M., Blackburn, D.J., Wharton, S.B., & Venneri, A. (2020). The association between polygenic hazard and markers of Alzheimer's disease following stratification for APOE genotype. *Current Alzheimer Research, 17*(7), 667-679. DOI: 10.2174/1567205017666201006161800.

de Rojas, I., Moreno-Grau, S., Teso, N., Grenier-Boley, B., Andrade, V., Jansen, I.E., Pedersen, N.L., Stringa, N., Zettergren, A., Hernandez, I., Montrreal, L., Antunez, C., Antonell, A., Tankard, R.M., Bis, J.C., Sims, R., Bellenguez, C., Quintela, I., Gonzalez-Perez, A., ... Ruiz, A. (2021). Common variants in Alzheimer's disease and risk stratification by polygenic risk scores. *Nature Communications, 21*(1), 3417. DOI: 10.1038/s41467-021-22491-8.

De Santi, S., De Leon, M.J., Rusinek, H., Convit, A., Tarshish, C.Y., Roche, A., Tsui, W.H., Kandil, E., Boppana, M., Daisley, K., Wang, G.J., Schyer, D., & Fowler, J. (2001). Hippocampal formation glucose metabolism and volume losses in MCI and AD. *Neurobiology of Aging, 22*(4), 529-539. DOI: 10.1016/S0197-4580(01)00230-5.

de Silva, E., Sudre, C. H., Barnes, J., Scelsi, M. A., & Altmann, A. (2022). Polygenic coronary artery disease association with brain atrophy in the cognitively impaired. *Brain Communications, 4*(6), fcac314. DOI: 10.1093/braincomms/fcac314.

Deane, R., Sagare, A., Hamm, K., Parisi, M., Lane, S., Finn, M.B., Holtzman, D.M., & Zlokovic, B.V. (2008). apoE isoform-specific disruption of amyloid β peptide clearance from mouse brain. *Journal of Clinical Investigation, 118*(12), 4002-4013. DOI: 10.1172/JCI36663.

Deary, I.J., Yang, J., Davies, G., Harris, S.E., Tenesa, A., Liewald, D., Luciano, M., Lopez, L.M., Gow, A.J., Corley, J., Redmond, P., Fox, H.C., Rowe, S.J., Haggarty, P., McNeill, G., Goddard, M.E., Porteous, D.J., Whalley, L.J., Starr, J.M., & Visscher, P.M. (2012). Genetic contributions to stability and change in intelligence from childhood to old age. *Nature, 482*(7384), 212-215. DOI: 10.1038/nature10781.

Dekaban, A.S., & Sadowsky, D. (1978). Changes in brain weights during the span of human life: Relation of brain weights to body heights and body weights. *Annals of Neurology, 4*(4), 345-356. DOI: 10.1002/ana.410040410.

Deming, Y., Li, Z., Kapoor, M., Harari, O., Del-Aguila, J.L., Black, K., Carrell, D., Cai, Y., Fernandez, M.V., Budde, J., Ma, S., Saef, B., Howells, B., Huang, K.L., Bertelsen, S., Fagan, A.M., Holtzman, D.M., Morris, J.C., Kim, S., ... Cruchaga, C. (2017). Genome-wide association study identifies four novel loci associated with Alzheimer's endophenotypes and disease modifiers. *Acta Neuropathologica, 133*(5), 839-856. DOI: 10.1007/s00401-017-1685-y.

Deng, M., Liu, Z., Zhang, W., Wu, Z., Cao, H., Yang, J., & Palaniyappan, L. (2022). Associations between polygenic risk, negative symptoms, and functional connectome topology during a working memory task in early-onset schizophrenia. *Schizophrenia, 8*(1), 54. DOI: 10.1038/s41537-022-00260-w.

Desikan, R.S., Fan, C.C., Wang, Y, Schork, A.J., Cabral, H.J., Cupples, L.A., Thompson, W.K., Besser, L., Kukull, W.A., Holland, D., Chen, C-H., Brewer, L., Karow, D.S., Kauppi, K., Witoelar, A., Karch, C.M., Bonham, L.W., Yokoyama, J.S., Rosen, H.J., ... Dale, A.M. (2017). Genetic assessment of age-associated Alzheimer disease risk: Development and validation of a polygenic hazard score. *PLoS Medicine, 14*(3), e1002258. DOI: 10.1371/journal.pmed.1002258.

Desikan, R.S., Sabuncu, M.R., Schmansky, N.J., Reuter, M., Cabral, H.J., Hess, C.P., Weiner, M.W., Biffi, A., Anderson, C.D., Rosand, J., Salat, D.H., Kemper, T.L., Dale, A.M., Sperling, R.A., & Fischl, B. (2010). Selective disruption of the cerebral neocortex in Alzheimer's disease. *PLoS ONE, 5*(9), e12853. DOI: 10.1371/journal.pone.0012853.

Desikan, R.S., Segonne, F., Fischl, B., Quinn, B.T., Dickerson, B.C., Blacker, D., Buckner, R.L., Dale, A.M., Maguire, R.P., Hyman , B.T., Albert, M.S., & Killiany, R.J. (2006). An automated labelling system for subdividing the human cerebral cortex on MRI scans into gyral based regions of interest. *NeuroImage, 31*(3), 968-980. DOI: 10.1016/j.neuroimage.2006.01.021.

DeTure, M.A. & Dickson, D.W. (2019). The neuropathological diagnosis of Alzheimer's disease. *Molecular Degeneration, 14*(1), 32. DOI: 10.1186/s13024-019-0333-5.

Dezhina, Z., Ranlund, S., Kyriakopoulou, M., Williams, S.C.R., & Dima, D. (2019). A systematic review of associations between functional MRI activity and polygenic risk for schizophrenia and bipolar disorder. *Brain Imaging and Behaviour, 13*(3), 862-877. DOI: 10.1007/s11682-018-9879-z.

Di Fede, G., Catania, M., Morbin, M., Rossi, G., Suardi, S., Mazzoleni, G., Merlin, M., Giovagnoli, A.R., Prioni, S., Erbetta, A., Falcone, C., Gobbi, M., Colombo, L., Bastone, A., Beeg, M., Manzoni, C., Francescucci, B., Spagnoli, A., Cantu, L., ... Tagliavini, F. (2009). A recessive mutation in the APP gene with dominant-negative effect on amyloidogenesis. *Science, 323*(5920), 1473-1477. DOI: 10.1126/science.1168979.

Dias, D., Portugal, C.C., Relvas, J., & Socodato, R. (2025). From genetics to neuroinflammation: The impact of ApoE4 on microglial function in Alzheimer's disease. *Cells, 14*(4), 243. DOI: 10.3390/cells14040243.

Dickerson, B.C., Salat, D.H., Greve, D.N., Chua, E.F., Rand-Giovannetti, E., Rentz, D.M., Bertram, L., Mullin, K., Tanzi, R.E., Blacker, D., Albert, M.S., & Sperling, R.A. (2005). Increased hippocampal activation in mild cognitive impairment compared to normal aging and AD. *Neurology, 65*(3), 404-411. DOI: 10.1212/01.wnl.0000171450.97464.49.

Dickson, D.W. (1997). Neuropathological diagnosis of Alzheimer's disease: A perspective from longitudinal clinicopathological studies. *Neurobiology of Aging, 18*(4 Suppl), S21-26. DOI: 10.1016/s0197-4580(97)00065-1.

Ding, Y., Zhao, K., Che, T., Du, K., Sun, H., Liu, S., Zheng, Y., Li, S., Liu, B., & Liu, Y. (2021). Quantitative radiomic features as new biomarkers for Alzheimer's disease: An amyloid PET study. *Cerebral Cortex, 31*(8), 3950-3961. DOI: 10.1093/cercor/bhab061.

Dolcos, F., Rice, H.J., & Cabeza, R. (2002). Hemispheric asymmetry and aging: right hemisphere decline or asymmetry reduction. *Neuroscience & Biobehavioral Reviews, 26*(7), 819-825. DOI: 10.1016/s0149-7634(02)00068-4.

Dou, X., Yao, H., Feng, F., Wang, P., Zhou, B., Jin, D., Yang, Z., Li, J., Zhao, C., Wang, L., An, N., Liu, B., Zhang, X., & Liu, Y. (2020). Characterizing white matter connectivity in Alzheimer's

disease and mild cognitive impairment: An automated fiber quantification analysis with two independent datasets. *Cortex, 129*, 390-405. DOI: 10.1016/j.cortex.2020.03.032.

Dubois, B., Felman, H.H., Jacova, C., Cummings, J.L., DeKosky, S.T., Barberger-Gateau, P., Delacourte, A., Frisoni, G., Fox, N.C., Galasko, D., Gauthier, S., Hampel, H., Jicha, G.A., Meguro, K., O'Brien, J., Pasquier, F., Robert. P., Rossor, M., Salloway, S., Sarazin, M., de Souza, L.C., Stern, Y., Visser, P.J., & Schelterns, P. (2010). Revising the definition of Alzheimer's disease: a new lexicon. *Lancet Neurology, 9*(11), 1118-1127. DOI: 10.1016/S1474-4422(10)70223-4.

Dubois, B., Hampel, H., Feldman, H.H., Scheltens, P., Aisen, P., Andrieu, S., Bakardjian, H., Benali, H., Bertram, L., Blennow, K., Broich, K., Cavedo, E., Crutch, S., Dartigues, J-F., Duyckaerts, C., Epelbaum, S., Frisoni, G.B., Gauthier, S., Genthon, R., ... Jack Jr, C.R. (2016). Preclinical Alzheimer's disease: Definition, natural history, and diagnostic criteria. *Alzheimer's & Dementia, 12*(3), 292-323. DOI: 10.1016/j.jalz.2016.02.002.

Dunbridge, F. (2013). Power and predictive accuracy of polygenic risk scores. *PLoS Genetics, 9*(3), e1003348. DOI: 10.1371/journal.pgen.1003348.

Duyn, J. H. (2012). The future of ultra-high field MRI and fMRI for study of the human brain. *NeuroImage, 62*(2), 1241-1248. DOI: 10.1016/j.neuroimage.2011.10.065.

Ebenau, J.L., van der Lee, S.J., Hulsman, M., Tesi, N., Jansen, I.E., Verberk, M.W., van Leeuwenstijn, M., Teunissen, C.E., Barkhof, F., Prins, N.D., Scheltens, P., Holstege, H., van Berckel, B.N.M., van der Flier, W.M. (2021). Risk of dementia in APOE ε4 carriers is mitigated by a polygenic risk score. *Alzheimer's & Dementia: Diagnosis, Assessment & Disease Monitoring, 13*(1), e12229. DOI: 10.1002/dad2.12229.

Eissman, J.M., Wells, G., Khan, O.A., Liu, D., Petyuk, V.A., Gifford, K.A., Dumitrescu, L., Jefferson, A.L., & Hohman, T.J. (2023). Polygenic resilience score may be sensitive to preclinical Alzheimer's disease changes. *Pacific Symposium on Biocomputing, 28*, 449-460.

Elman, J.A., Panizzon, M.S., Gustavson, D.E., Franz, C.E., Sanderson-Cimino, M.E., Lyons, M.J., Kremen, W.S. & Alzheimer's Disease Neuroimaging Initiative (2020). Amyloid-β positivity predicts cognitive decline but cognition predicts progression to amyloid-β positivity. *Biological Psychiatry, 87*(9), 819-828. DOI: 10.1016/j.biopsych.2019.12.021.

Escott-Price, V. (2021). Genetics: genome-wide data processing for polygenic risk scores. *Basic Science and Pathogenesis, 17*(S3), e054946. DOI: 10.1002/alz.054946.

Escott-Price, V., Myers, A., Huentelman, M., Shoai, M., & Hardy, J. (2018). Polygenic risk score analysis of Alzheimer's disease in cases without APOE4 or APOE2 alleles. *Journal of Prevention of Alzheimer's Disease, 6*(1), 16-19. DOI: 10.14283/jpad.2018.46.

Euesden, J., Ali, M., Robins, C., Surendran, P., Gormley, P., Alzheimer's Disease Neuroimaging Initiative, Pulford, D., & Cruchaga, C. (2025). Patient stratification by genetic risk in Alzheimer's disease is only effective in the presence of phenotypic heterogeneity. *PLoS One, 20*(1), e0310977. DOI: 10.1371/journal.pone.0310977.

Fagan, A.M., Watson, M., Parsadanian, M., Bales, K.R., Paul, S.M., & Holtzman, D.M. (2002). Human and murine ApoE markedly alters A beta metabolism before and after plaque formation in a mouse model of Alzheimer's disease. *Neurobiology of Disease, 9*(3), 305-318. DOI: 10.1006/nbdi.2002.0483.

Farfel, J.M., Yu, L., De Jager, P.L., Schneider, J.A., & Bennett, D.A. (2016). Association of APOE with tau-tangle pathology with and without β-amyloid. *Neurobiology of Aging, 37*, 19-25. DOI: 10.1016/j.neurobiolaging.2015.09.011.

Farhadieh, M.E., Mozafar, M., Sanaaee, S., Sodeifi, P., Kousha, K., Zare, Y., Zare, S., Rad, N.M., Jamshidi-Goharrizi, F., Allahverdloo, M., Rahimi, A., Sadeghi, M., Shafie, M., Mayeli, M., & Alzheimer's Disease Neuroimaging Initiative (2024). Polygenic hazard score predicts synaptic and axonal degeneration and cognitive decline in Alzheimer's disease continuum. *Archives of Gerontology and Geriatrics, 127*, 105576. DOI: 10.1016/j.archger.2024.105576.

Farrer, L.A., Cupples, A., Haines, J.L., Hyman, B., Kukull, W.A., Mayeux, R., Myers, R.H., Pericak-Vance, M.A., Risch, N., & van Duijn, C.M. (1997). Effects of age, sex, and ethnicity on the association between apolipoprotein E genotype and Alzheimer disease: A meta-analysis. *JAMA, 278*(16), 1349-1356. DOI: 10.1001/jama.1997.03550160069041.

Farrer, L.A., Sherbatich, T., Keryanov, S.A., Korovaitseva, G.I., Rogaeva, E.A., Petruk, S., Premkumar, S., Moliaka, Y., Song, Y. Q., Pei, Y., Sato, C., Selezneva, N.A., Voskresenskaya, S., Golimbet, V., Sorbi, S., Duara, R., Gavrilova, S., St. George-Hyslop, P.H., & Rogaev, E.I. (2000).

Association between angiotensin-converting enzyme and Alzheimer disease. *Archives of Neurology, 57*(2), 210-214. DOI: 10.1001/archneur.57.2.210.

Femminella, G.D., Harold, D., Scott, J., Williams, J., & Edison, P. (2021). The differential influence of immune, endocytotic, and lipid metabolism genes on amyloid deposition and neurodegeneration in subjects at risk of Alzheimer's disease. *Journal of Alzheimer's Disease, 79*(1), 127-139. DOI: 10.3233/JAD-200578.

Fernandez-Calle, R., Konings, S.C., Frontinan-Rubio, J., Garcia-Revilla, J., Camprubi-Ferrer, L., Svensson, M., Martinson, I., Boza-Serrano, A., Venero, J.L., Nielson, H.M., Gouras, G.K., & Deierborg, T. (2022). APOE in the bullseye of neurodegenerative diseases: Impact of the APOE genotype in Alzheimer's disease pathology and brain diseases. *Molecular Neurodegeneration, 17*(1), 62. DOI: 10.1186/s13024-022-00566-4.

Fleisher, A.S., Chen, K., Liu, X., Ayutanont, N., Roontiva, A., Thiyyagura, P., Protas, H., Joshi, A.D., Sabbagh, M., Sadowshy, C.H., Sperling, R.A., Clark, C.M., Mintun, M.A., Pontecorvo, M.J., Coleman, R. E., Doraiswamu, P.M., Johnson, K.A., Carpenter, A.P., Skovronsky, D.M., & Reiman, E.M. (2013). Apolipoprotein E ε4 and age effects on florbetapir positron emission tomography in healthy aging and Alzheimer disease. *Neurobiology of Aging, 34*(1), 1-12. DOI: 10.1016/j.neurobiolaging.2012.04.017.

Foley, S.F., Tansey, K.E., Caseras, X., Lancaster, T., Bracht, T., Parker, G., Hall, J., Williams, J., & Linden, D.E.J. (2017). Multimodal brain imaging reveals structural differences in Alzheimer's disease polygenic risk carriers: A study in healthy young adults. *Biological Psychiatry, 81*(2), 154-161. DOI: 10.1016/j.biopsych.2016.02.033.

Folstein, M.F., Folstein, S.E., & McHugh, P.R. (1975). "Mini-mental state". A practical method for grading the cognitive state of patients for the clinician. *Journal of Psychiatric Research, 12*(3), 189-198. DOI: 10.1016/0022-3956(75)90026-6.

Foo, H., Thalamuthu, A., Jiang, J., Koch, F., Mather, K.A., Wen, W., & Sachdev, P.S. (2021). Associations between Alzheimer's disease polygenic risk scores and hippocampal subfield volumes in 17,161 UK Biobank participants. *Neurobiology of Aging, 98*, 108-115. DOI: 10.1016/j.neurobiolaging.2020.11.002.

Foster, J.K., Albrecht, M.A., Savage, G., Lautenschlager, N.T., Ellis, K.A., Maruff, P., Szoeke, C., Taddei, K., Martins, R., Masters, C.L., Ames, D., & AIBL Research Group (2013). Lack of reliable evidence for a distinctive ε4-related cognitive phenotype that is independent from clinical diagnostic status: findings from the Australian imaging, biomarkers and lifestyle study. *Brain, 136*(Pt 7), 2201-2216. DOI: 10.1093/brain/awt127.

Fox, M.D., Snyder, A.Z., Vincent, J.L., Corbetta, M., Van Essen, D.C., & Raichle, M.E. (2005). The human brain is intrinsically organized into dynamic, anticorrelated functional networks. *Proceedings of the National Academy of Sciences of the United States of America, 102*(27), 9673-9678. DOI: 10.1073/pnas.0504136102.

Freedman, M.L., Monteiro, A.N.A., Gayther, S.A., Coetzee, G.A., Risch, A., Plass, C., Casey, G., De Biasi, M., Carlson, C., Duggan, D., James, M., Liu, P., Tichelaar, J.W., Vikis, H.G., You, M., & Mills, I.G. (2011). Principles for the post-GWAS functional characterization of cancer risk loci. *Nature Genetics, 43*(6), 513-518. DOI: 10.1038/ng.840.

Frisoni, G.B., Fox, N.C., Jack Jr, C.R., Scheltens, P., & Thompson, P.M. (2010). The clinical use of structural MRI in Alzheimer disease. *Nature Reviews Neurology, 6*(2), 67-77. DOI: 10.1038/nrneurol.2009.215.

Fujita, K., Kimura, T., Yamakawa, A., Niida, S., Ozaki, K., Sakurai, T., Arai, H., Shigemizu, D. & J-MINT study group (2025). Genetic background and multidomain interventions in mild cognitive impairment. *Alzheimer's Research & Therapy, 17*(1), 130. DOI: 10.1186/s13195-025-01764-0.

Gaser, C., Dahnke, R., Thompson, P.M., Kurth, F., Luders, E., & Alzheimer's Disease Neuroimaging Initiative (2024). CAT: a Computational anatomy toolbox for the analysis of structural MRI data. *GigaScience, 13*, giae049. DOI: 10.1093/gigascience/giae049.

Gatz, M., Reynolds, C.A., Fratiglioni, L., Johansson, B., Mortimer, J.A., Berg, S., Fiske, A., & Pedersen, N.L. (2006). Role of genes and environments for explaining Alzheimer disease. *Archives of General Psychiatry, 63*(2), 168-174. DOI: 10.1001/archpsyc.63.2.168.

Ge, T., Chen, C-Y., Ni, Y., Feng, Y-C.A., & Smoller, J.W. (2019). Polygenic prediction via Bayesian regression and continuous shrinkage priors. *Nature Communications, 10*(1), 1776. DOI: 10.1038/s41467-019-09718-5.

Ge, T., Sabuncu, M.R., Smoller, J.W., Sperling, R.A., & Mormino, E.C. (2018). Dissociable influences of APOE e4 and polygenic risk of AD dementia on amyloid and cognition. *Neurology, 90*(18), e1605-1612. DOI: 10.1212/WNL.0000000000005415.

Gene Cards (2025). *GeneCards: The human gene database.* Available at https://www.genecards.org/ (Accessed: August 2025).

Genetics for all. (2019). *Nature Genetics, 51*, 579. DOI: 10.1038/s41588-019-0394-y.

Genin, E., Hannequin, D., Wallon, D., Sleegers, K., Hiltunen, M., Combarros, O., Bullido, M. J., Engelborghs, S., De Deyn, P., Berr, C., Pasquir, F., Dubois, B., Tognoni, G., Fievet, N., Brouwers, N., Bettens, K., Arosio, B., Coto, E., Del Zompo, D., ... Campion, D. (2011). APOE and Alzheimer disease: A major gene with semi-dominant inheritance. *Molecular Psychiatry, 16*, 903-907. DOI: 10.1038/mp.2011.52.

Genius, P., Calle, M.L., Rodríguez-Fernández, B., Minguillon, C., Cacciaglia, R., Garrido-Martin, D., Esteller, M., Navarro, A., Gispert, J.D., Vilor-Tejedor, N., Alzheimer's Disease Neuroimaging Initiative, & ALFA study. (2025). Compositional brain scores capture Alzheimer's disease-specific structural brain patterns along the disease continuum. *Alzheimer's & Dementia, 21*(2), e14490. DOI: 10.1002/alz.14490.

Genome.gov (2017). *1000 Genomes Project.* Available at https://www.genome.gov/27528684/1000-genomes-project (Accessed: 2024).

Giannakopoulos, P., Herrmann, F.R., Bussière, T., Bouras, C., Kövari, E., Perl, D.P., Morrison, J.H., Gold, G., & Hof, P.R. (2003). Tangle and neuron numbers, but not amyloid load, predict cognitive status in Alzheimer's disease. *Neurology, 60*(9), 1495-500. DOI: 10.1212/01.wnl.0000063311.58879.01.

Gibson, J., Clarke, T., McIntosh, A.M., & Marioni, R. (2019). GWAS summary stats for meta-analysis of epigenetic age acceleration. University of Edinburgh. *Centre for Clinical Brain Sciences*. DOI: 10.7488/ds/2631.

Giri, M., Zhang, M., & Lu, Yang. (2016). Genes associated with Alzheimer's disease: An overview and current status. *Clinical Interventions in Aging, 11*, 665-681. DOI: 10.2147/CIA.S105769.

Gogarten, S.M., Sofer, T., Chen, H., Yu, C., Brody, J.A., Thornton, T.A., Rice, K.M., Conomos, M.P. (2019). Genetic association testing using the GENESIS R/Bioconductor package. *Bioinformatics, 35*(24), 5346-5348. DOI: 10.1093/bioinformatics/btz567.

Golde, T.E. (2022). Alzheimer's disease - the journey of a healthy brain into organ failure. *Molecular Neurodegeneration, 17*(1), 18. DOI: 10.1186/s13024-022-00523-1.

Gong, C.X., & Iqbal, K. (2008). Hyperphosphorylation of microtubule-associated protein tau: A promising therapeutic target for Alzheimer disease. *Current Medicinal Chemistry, 15*(23), 2321-2328. DOI: 10.2174/092986708785909111.

Gong, C.X., Liu, F., Grundke-Iqbal, I., & Iqbal, K. (2005). Post-translational modifications of tau protein in Alzheimer's disease. *Journal of Neural Transmission, 112*(6), 813-838. DOI: 10.1007/s00702-004-0221-0.

Gonneaud, J., Arenaza-Urquijo, E.M., Fouquet, M., Perrotin, A., Fradin, S., de La Sayette, V., Eustache, F., & Chetelat, G. (2016). Relative effect of APOE ε4 on neuroimaging biomarker changes across the lifespan. *Neurology, 87*(16), 1696-1703. DOI: 10.1212/WNL.0000000000003234.

Gouras, G.K., Olsson, T.T., and Hansson, O. (2015). β-amyloid peptides and amyloid plaques in Alzheimer's disease. *Neurotherapeutics, 12*(1), 3-11. DOI: 10.1007/s13311-014-0313-y.

Grady, C.L., Furey, M.L., Pietrini, P., Horwitz, B., & Rapoport, S.I. (2001). Altered brain functional connectivity and impaired short-term memory in Alzheimer's disease. *Brain, 124*(4), 739-756. DOI: 10.1093/brain/124.4.739.

Grimmer, T., Tholen, S., Yousefi, B.H., Alexopoulos, P., Förschler, A., Förstl, H., Henriksen, G., Klunk, W.E., Mathis, C.A., Perneczky, R., Sorg, C., Kurz, A., & Drzezga, A. (2010). Progression of cerebral amyloid load is associated with the apolipoprotein E ε4 genotype in Alzheimer's disease. *Biological Psychiatry, 68*(10), 879-884. DOI: 10.1016/j.biopsych.2010.05.013.

Grothe, M.J., Villeneuve, S., Dyrba, M., Bartres-Faz, D., & Wirth, M. (2017). Multimodal characterization of older APOE2 carriers reveals selective reduction of amyloid load. *Neurology, 88*(6), 569-576. DOI: 10.1212/WNL.0000000000003585.

Grupe, A., Abraham, R., Li, Yonghong, Rowland, C., Hollingworth, P., Morgan, A., Jehu L., Segurado, R., Stone, D., Schadt, E., Karnoub, M., Nowotny, P., Tacey, K., Catanese, J., Sninsky, J., Brayne, C., Rubinsztein, D., Gill, M., Lawlor, K., ... Willliams, J. (2007). Evidence for novel susceptibility genes for late-onset Alzheimer's disease from a genome-wide association study of putative functional variants. *Human Molecular Genetics, 16*(8), 865-873. DOI: 10.1093/hmg/ddm031.

Guerreiro, R., Wojtas, A., Bras, J., Carrasquillo, M., Rogaeva, E., Majounie, E., Cruchaga, C., Sassi, C., Kauwe, J.S.K., Younkin, S., Hazrati, L., Collinge, J., Pocock, J., Lashley, T., Williams, J., Lambert, J-C., Amouyel, P., Goate, A., Rademakers, R., ... Singleton, A. (2013). TREM2 variants in Alzheimer's disease. *New England Journal of Medicine, 368*(2), 117-127. DOI: 10.1056/NEJMoa1211851.

Gulisano, W., Maugeri, D., Baltrons, M.A., Fà, M., Amato, A., Palmeri, A., D'Adamio, L., Grassi, C., Devanand, D.P., Honig, L.S., Puzzo, D., & Arancio, O. (2018). Role of amyloid-β and tau proteins in Alzheimer's disease: Confuting the amyloid cascade. *Journal of Alzheimer's Disease, 64*(s1), S611-S631. DOI: 10.3233/JAD-179935.

Habes, M., Janowitz, D., Erus, G., Toledo, J.B., Resnick, S.M., Doshi, J., Van der Auwera, S., Wittfield, K., Hegenscheid, K., Hosten, N., Biffar, R., Homuth, G., Volzke, H., Grabe, H.J., Hoffman, W., & Davatzikos, C. (2016). Advanced brain aging: Relationship with epidemiologic and genetic risk factors, and overlap with Alzheimer disease atrophy patterns. *Translational Psychiatry, 6*(4), e775. DOI: 10.1038/tp.2016.39.

Habes, M., Sotiras, A., Erus, G., Toledo, J.B., Janowitz, D., Wolk, D.A., Shou, H., Bryan, N.R., Doshi, J., Volzke, H., Schminke, U., Hoffmann, W., Resnick, S.M., Grabe, H.J., & Davatzikos, C. (2018). White matter lesions: Spatial heterogeneity, links to risk factors, cognition, genetics, and atrophy. *Neurology, 91*(10), e964-975. DOI: 10.1212/WNL.0000000000006116.

Habtewold, T.D., Liemburg, E.J., Islam, M.A., de Zwarte, S.M.C., Boezen, H.M., GROUP Investigators, Bruggeman, R., & Alizadeh, B.Z. (2020). Association of schizophrenia polygenic risk score with data-driven cognitive subtypes: A six-year longitudinal study in patients, siblings and controls. *Schizophrenia Research, 223*, 135-147. DOI: 10.1016/j.schres.2020.05.020.

Hannon, E., Shireby, G.L., Brookes, K., Attems, J., Sims, R., Cairns, N.J., Love, S., Thomas, A.J., Morgan, K., Francis, P.T., & Mill, J. (2020). Genetic risk for Alzheimer's disease influences

neuropathology via multiple biological pathways. *Brain Communications, 2*(2), fcaa167. DOI: 10.1093/braincomms/fcaa167.

Hanseeuw, B.J., Betensky, R.A., Jacobs, H.I.L., Schultz, A.P., Sepulcre, J., Becker, J.A., Cosio, D.M.O., Farrell, M., Quiroz, Y.T., Mormino, E.C., Buckley, R.F., Papp, K.V., Amariglio, R.A., Dewachter, I., Ivanoiu, A., Huijbers, W., Hedden, T., Marshall, G.A., Chhatwal, J.P., … Johnson, K. (2019). Association of amyloid and tau with cognition in preclinical Alzheimer disease: A longitudinal study. *JAMA Neurology, 76*(8), 915-924. DOI: 10.1001/jamaneurol.2019.1424.

Hansson, O., Seibyl, J., Stomrud, E., Zetterberg, H., Trojanowski, J.Q., Bittner, T., Lifke, V., Corradini, V., Eichenlaub, U., Batrla. R., Buck, K., Zink, K., Rabe, C., Blennow, K., Shaw, L.M.,& Alzheimer's Disease Neuroimaging Initiative (2018). CSF biomarkers of Alzheimer's disease concord with amyloid-β PET and predict clinical progression: A study of fully automated immunoassays in BioFINDER and ADNI cohorts. *Alzheimer's & Dementia, 14*(11), 1470-1481. DOI: 10.1016/j.jalz.2018.01.010.

Hardy, J., & Escott-Price, V. (2025). The genetics of neurodegenerative diseases is the genetics of age-related damage clearance failure. *Molecular Psychiatry, 30*(6), 2748-2753. DOI: 10.1038/s41380-025-02911-7.

Hardy, J.A., & Higgins, G.A. (1992). Alzheimer’s disease: The amyloid cascade hypothesis. *Science, 256*(5054), 184-185. DOI: 10.1126/science.1566067.

Hari, R., Kurt, E., Bayram, A., Kizilates-Evin, G., Aca, B., Demiralp, R., & Gurvit, H. (2022). Volumetric changes within hippocampal subfields in Alzheimer’s disease continuum. *Neurological Sciences, 43*(7), 4175-4183. DOI: 10.1007/s10072-022-05890-7.

Harold, D., Abraham, R., Hollingworth, P., Sims, R., Gerrisj, A., Hamshere, M.L., Pahwa, J.S., Moskvina, V., Dowzell, K., Williams, A., Jones, N., Thomas, C., Stretton, A., Morgan, A.R., Lovestone, S., Powell, J., Proitsi, P., Lupton, M.K., Brayne, C., … Williams, J. (2009). Genome-wide association study identifies variants at CLU and PICALM associated with Alzheimer’s disease. *Nature Genetics, 41*(10), 1088-1093. DOI: 10.1038/ng.440.

Harris, M.A., Shen, X., Cox, S.R., Gibson, J., Adams, M.J., Clarke, T-K., Deary, I.J., Lawrie, S.M., McIntosh, A.M., & Whalley, H.C. (2019). Stratifying major depressive disorder by polygenic risk

for schizophrenia in relation to structural brain measures. *Psychological Medicine, 50*(10), 1653-1662. DOI: 10.1017/s003329171900165x.

Harris, S.E., Davies, G., Luciano, M., Payton, A., Fox, H.C., Haggarty, P., Ollier, W., Horan, M., Porteous, D.J., Starr, J.M., Whalley, L.J., Pendleton, N., & Deary, I.J. (2014). Polygenic risk for Alzheimer's disease is not associated with cognitive ability or cognitive aging in non-demented older people. *Journal of Alzheimer's Disease, 39*(3), 565-574. DOI: 10.3233/JAD-131058.

Harrison, J.R., Foley, S.F., Baker, E., Bracher-Smith, M., Holmans, P., Stergiakouli, E., Linden, D.E., Caseras, X., Jones, D.K., & Escott-Price, V. (2023). Pathway-specific polygenic scores for Alzheimer's disease are associated with changes in brain structure in younger and older adults. *Brain Communications, 5*(5), fcad229. DOI: 10.1093/braincomms/fcad229.

Harrison, T.M., Mahmood, Z., Lau, E.P., Karacozoff, A.M., Burggren, A.C., Small, G.W., & Bookheimer, S.Y. (2016). An Alzheimer's disease genetic risk score predicts longitudinal thinning of hippocampal complex subregions in healthy older adults. *eNeuro, 3*(3), ENEURO.0098-16.2016. DOI: 10.1523/ENEURO.0098-16.2016.

Hatoum, A.S., Morrison, C.L., Mitchell, E.C., Lam, M., Benca-Bachman, C.E., Reineberg, A.E., Palmer, R.H.C., Evans, L.M., Keller, M.C., & Friedman, N.P. (2022). Genome-wide association study shows that executive functioning is influenced by GABAergic processes and is a neurocognitive genetic correlate of psychiatric disorders. *Biological Psychiatry, 93*(1), 59-70. DOI: 10.1016/j.biopsych.

Hayden, K.M., Lutz, M.W., Kuchibhatla, M., Germain, C., & Plassman, B.L. (2015). Effect of APOE and CD33 on cognitive decline. *PLoS One, 10*(6), e0130419. DOI: 10.1371/journal.pone.0130419.

Hayes, J.P., Moody, J.N., Roca, J.G., & Hayes, S.M. (2020). Body mass index is associated with smaller medial temporal lobe volume in those at risk for Alzheimer's disease. *NeuroImage Clinical, 25*, 102156. DOI: 10.1016/j.nicl.2019.102156.

He, X-Y., Wu, B-S., Kuo, K., Zhang, W., Ma, Q., Xiang, S-T., Li, Y-Z., Wang, Z-Y., Dong, Q., Feng, J-F., Cheng, W., & Yu, J-T. (2023). Association between polygenic risk for Alzheimer's disease and brain structure in children and adults. *Alzheimer's Research & Therapy, 15*(109). DOI: 10.1186/s13195-023-01256-z.

Herholz, K., Carter, S.F., & Jones, M. (2007). Positron emission tomography imaging in dementia. British Journal of Radiology, 80(2), S160-S167. DOI: 10.1259/bjr/97295129.

Herrup, K. (2015). The case for rejecting the amyloid cascade hypothesis. *Nature Neuroscience, 18*, 794-799. DOI: 10.1038/nn.4017.

Hibar, D.P., Adams, H.H.H., Jahanshad, N., Chauhan, G., Stein, J.L., Hofer, E., Renteria, M.E., Bis, J.C., Arias-Vasquez, A., Ikram, M.K., Desrivieres, S., Vernooij, M.W., Abramovic, L., Alhusaini, S., Amin, N., Andersson, M., Arfanakis, K., Aribisala, B.S., Armstrong, N.J., … Ikram, M.A. (2017). Novel genetic loci associated with hippocampal volume. *Nature Communications, 8*, 13624. DOI: 10.1038/ncomms13624.

Hof, P.R., Bouras, C., Perl, D.P., Sparks, D.L., Mehta, N., & Morrison, J.H. (1995). Age-related distribution of neuropathologic changes in the cerebral cortex of patients with Down's syndrome, quantitative regional analysis and comparison with Alzheimer's disease. *Archives of Neurology, 52*(4), 379-391. DOI: 10.1001/archneur.1995.00540280065020.

Hohman, T. J., Dumitrescu, L., Oksol, A., Wagener, M., Gifford, K.A., & Jefferson, A.L. (2017). APOE allele frequencies in suspected non-amyloid pathophysiology (SNAP) and the prodromal stages of Alzheimer's disease. *PLoS One, 12*(11), e0188501. DOI: 10.1371/journal.pone.0188501.

Holstege, H., Hulsman, M., Charbonnier, C., Grenier-Boley, B., Quenez, O., Grozeva, D., van Rooji, J.G.J., Sims, R., Ahmad, S., Amin, N., Norsworthy, P.J., Dols-Icardo, O., Hummerich, H., Kawalia, A., Amouyel, P., Beecham, G.W., Berr, C., Bis, J.C, Boland, A., … Lambert, J-C. (2022). Exome sequencing identifies rare damaging variants in ATP8B4 and ABCA1 as risk factors for Alzheimer's disease. *Nature Genetics, 54*(12), 1786-1794. DOI: 10.1038/s41588-022-01208-7.

Homann, J., Osburg, T., Ohlei, O., Dobrici, V., Deecke, L., Bos, I., Vandenberghe, R., Gabel, S., Scheltens, P., Teunissen, C.E., Engelborghs, S., Frisoni, G., Blin, O., Richardson, J.C., Bordet, R., Lleo, A., Alcolea, D., Popp, J., Clark, C., … Bertram, L. (2022). Genome-wide association study of Alzheimer's disease brain imaging biomarkers and neuropsychological phenotypes in the European medical information framework for Alzheimer's disease multimodal biomarker discovery dataset. *Frontiers in Aging Neuroscience, 14*, 840651. DOI: 10.3389/fnagi.2022.840651.

Howieson, D. (2019). Current limitations of neuropsychological tests and assessment procedures. *Clinical Neuropsychologist, 33*(2), 200-208. DOI: 10.1080/13854046.2018.1552762.

Howieson, D.B., Dame, A., Camicioli, R., Sexton, G., Payami, H. & Kaye, J.A. (1997). Cognitive markers preceding Alzheimer's dementia in the healthy oldest old. *Journal of the American Geriatrics Society, 45*, 584-589. DOI: 10.1111/j.1532-5415.1997.tb03091.x

Huang, J., Friedland, R.P., & Auchus, A.P. (2007). Diffusion tensor imaging of normal-appearing white matter in mild cognitive impairment and early Alzheimer disease: Preliminary evidence of axonal degeneration in the temporal lobe. *American Journal of Neuroradiology, 28*(10), 1943-1948. DOI: 10.3174/ajnr.A0700.

Huijbers, H., Mormino, E.C., Schultz, A.P., Wigman, S., Ward, A.M., Larvie, M., Amariglio, R.E., Marshall, G.A., Rentz, D.M., Johnson, K.A., & Sperling, R.A. (2015). Amyloid-β deposition in mild cognitive impairment is associated with increased hippocampal activity, atrophy and clinical progression. *Brain, 138*(4), 1023-1035. DOI: 10.1093/brain/awv007.

Hyman, B.T., Phelps, C.H., Beach, T.G., Bigio, E.H., Cairns, N.J., Carrillo, M.C., Dickson, D.W., Duyckaerts, C., Frosch, M.P., Masliah, E., Mirra, S.S., Nelson, P.T., Schneider, J.A., Thai, D.R., Thies, B., Trojanowski, J.Q., Vinters, H.V., & Montine, T.J. (2012). National institute on aging-Alzheimer's association guidelines for the neuropathologic assessment of Alzheimer's disease. *Alzheimer's & Dementia, 8*(1), 1-13. DOI: 10.1016/j.jalz.2011.10.007.

Hyman, B.T., Van Hoesen, G.W., Kromer, L.J., & Damasio, A.R. (1986). Perforant pathway changes and the memory impairment of Alzheimer's disease. *Annals of Neurology, 20*(4), 472-481. DOI: 10.1002/ana.410200406.

Im, K., Lee, J-M., Seo, S. W., Yoon, U., Kim, S. T., Kim, Y-H., Kim, S. I., & Na, D. K. (2008). Variations in cortical thickness with dementia severity in Alzheimer's disease. *Neuroscience Letters, 436*(2), 227-231. DOI: 10.1016/j.neulet.2008.03.032

Ingelsson, M., Fukumoto, H., Newell, K.L., Growdon, J.H., Hedley-Whyte, E.T., Frosch, M.P., Albert, M.S., Hyman, B.T., & Irizarry, M.C. (2004). Early Abeta accumulation and progressive synaptic loss, gliosis, and tangle formation in AD brain. *Neurology, 62*(6), 925-931. DOI: 10.1212/01.wnl.0000115115.98960.37.

International Schizophrenia Consortium (2009). Common polygenic variation contributes to risk of schizophrenia that overlaps with bipolar disorder. *Nature, 460*(7256), 748-752. DOI: 10.1038/nature08185.

Ismail, Z., Smith, E.E., Geda, Y., Sultzer, D., Brodaty, H., Smith, G., Aguera-Ortiz, L., Sweet, R., Miller, D., & Lyketsos, C.G. (2016). Neuropsychiatric symptoms as early manifestations of emergent dementia: Provisional diagnostic criteria for mild behavioural impairment. *Alzheimer's & Dementia, 12*(2), 195-202. DOI: 10.1016/j.jalz.2015.05.017.

Jack Jr, C.R., Andrews, J.S., Beach, T.G., Buracchio, T., Dunn, B., Graf, A., Hansson, O., Ho, C., Jagust, W., McDade, E., Molinuevo, J.L., Okonkwo, O.C., Pani, L., Rafii, M.S., Scheltens, P., Siemers, E., Snyder, H.M., Sperling, R., Teunissen, C.E., & Carrillo, M.C. (2024). Revised criteria for diagnosis and staging of Alzheimer's disease: Alzheimer's association workgroup. *Alzheimer's & Dementia, 20*(8), 5143-5169. DOI: 10.1002/alz.13859.

Jack Jr, C.R., Bennett, D.A., Blennow, K., Carrillo, M.C., Dunn, B., Haeberlein, S.B., Holtzman, D.M., Jagust, W., Jessen, F., Karlawish, J., Liu, E., Molinuevo, J.L., Montine, T., Phelps, C., Rankin, K.P., Rowe, C.C., Scheltens, P., Siemers, E., Snyder, H.M., & Sperling, R. (2018). NIA-AA research framework: Toward a biological definition of Alzheimer's disease. *Alzheimer's & Dementia, 14*(4), 535-562. DOI: 10.1016/j.jalz.2018.02.018.

Jack Jr, C.R., Bennett, D.A., Blennow, K., Carrillo, M.C., Feldman, H.H., Frisoni, G.B., Hampel, H., Jagust, W.J., Johnson, K.A., Knopman, D.S., Petersen, R.C., Scheltens, P., Sperling, R.A., & Dubois, B. (2016). A/T/N: An unbiased descriptive classification scheme for Alzheimer disease biomarkers. *Neurology, 87*(5), 539-547. DOI: 10.1212/WNL.0000000000002923.

Jack Jr, C.R., Knopman, D.S., Jagust, W.J., Shaw, L.M., Aisen, P.S., Weiner, M.W., Peterson, R.C., & Trojanowski, J.Q. (2010). Hypothetical model of dynamic biomarkers of the Alzheimer's pathological cascade. *Lancet Neurology, 9*(1), 119. DOI: 10.1016/S1474-4422(09)70299-6.

Jack Jr, C.R., Lowe, V.J., Weigand, S.D., Wiste, H.J., Senjem, M.L., Knopman, D.S., Shiung, M.M., Gunter, J.L., Boeve, B.F., Kemp, B.J., Weiner, M., Petersen, R.C., & Alzheimer's Disease Neuroimaging Initiative (2009). Serial PIB and MRI in normal, mild cognitive impairment and Alzheimer's disease: implications for sequence of pathological events in Alzheimer's disease. *Brain, 132*(Pt 5), 1355-1365. DOI: 10.1093/brain/awp062.

Jack Jr, C.R., Peterson, R.C., Xu, Y., O'Brien, P.C., Smith, G.E., Ivnik, R.J., Boeve, B.F., Tangalos, E.G., & Kokmen, E. (2000). Rates of hippocampal atrophy correlate with change in clinical status in aging and AD. *Neurology, 55*(4), 484-489. DOI: 10.1212/WNL.55.4.484.

Jack Jr, C.R., Vemuri, P., Wiste, H.J., Weigand, S.D., Aisen, P.S., Trojanowski, J.W., Shaw, L.M., Bernstein, M.A., Peterson, R.C., Weiner, M.W., & Knopman, D.S. (2011). Evidence for ordering of Alzheimer's disease biomarkers. *Archives of Neurology, 68*(12), 1526-1535. DOI: 10.1001/archneurol.2011.183.

Jack Jr, C.R., Wiste, H.J., Weigand, S.D., Knopman, D.S., Vemuri, P., Mielke, M.M., Lowe, V., Senjem, M.L., Gunter, J.L., Machulda, M.M., Gregg, B.E., Pankratz, S., Rocca, W.A., & Peterson, R.C. (2015). Age, sex, and APOE ε4 effects on memory, brain structure, and β-amyloid across the adult life span. *JAMA Neurology, 72*(5), 511-519. DOI: 10.1001/jamaneurol.2014.4821.

Jackson, R.J., Hyman, B.T., & Serrano-Pozo, A. (2024). Multifaceted roles of APOE in Alzheimer disease. *Nature Reviews Neurology, 20*(8), 457-474. DOI: 10.1038/s41582-024-00988-2.

Jansen, I.E., Savage, J.E., Watanabe, K., Bryois, J., Williams, D.M., Steinberg, S., Sealock, J., Karlsson, I. K., Hagg, S., Athanasiu, L., Voyle, N., Proisi, P., Witoelar, A., Stringer, S., Aarsland, D., Almdahl, I.S., Andersen, F., Bergh, S., Bettella, F., … Posthuma, D. (2019). Genome-wide meta-analysis identifies new loci and functional pathways influencing Alzheimer's disease risk. *Nature Genetics, 51*(3), 404-413. DOI: 10.1038/s41588-018-0311-9.

Jansen, W.L., Ossenkoppele, R., Knol, D.L., Tijms, B.M., Scheltens, P., Verhey, F.R.J., & Visser, P.J. (2015). Prevalence of cerebral amyloid pathology in persons without dementia, a meta-analysis. *JAMA, 313*(19), 1924-1938. DOI: 10.1001/jama.2015.4668.

Janssens, A.C.J.W. (2019). Validity of polygenic risk scores: Are we measuring what we think we are? *Human Molecular Genetics, 28*(R2), R143-R150. DOI: 10.1093/hmg/ddz205.

Jarmolowicz, A. I., HealthSci, B., Chen, H-Y., and Panegyres, P. K. (2014). The patterns of inheritance in early-onset dementia: Alzheimer's disease and frontotemporal dementia. *American Journal of Alzheimer's Disease & Other Dementias, 30*(3), 299-306. DOI: 10.1177/1533317514545825.

Jia, J., Wang, F., Wei, C., Zhou, A., Jia, X., Li, F., Tang, M., Chu, L., Zhou, Y., Zhou, C., Cui, Y., Wang, Q., Wang, W., Yin, P., Hu, N., Zuo, X., Song, H., Qin, W., Wu, L., ... Dong, X. (2014). The prevalence of dementia in urban and rural areas of China. *Alzheimer's & Dementia, 10*(1), 1-9. DOI: 10.1016/j.jalz.2013.01.012.

Jonsson, T., Stefansson, H., Steinberg, S., Jonsdottir, I., Jonsson, P.V., Snaedal, J., Bjornsson, S., Huttenlocher, J., Levey, A.I., Lah, J.J., Rujesca, D., Hampel, H., Giegling, I., Andreassen, O.A., Engedal, K., Ulstein, I., Djurovic, S., Ibrahim-Verbaad, C., Hofman, A., ... Stefansson, K. (2013). Variant of TREM2 associated with the risk of Alzheimer's disease. *New England Journal of Medicine, 368*(2), 107-116. DOI: 10.1056/NEJMoa1211103.

Josephs, K.A., Dickson, D.W., Tosakulwong, N., Weigand, S.D., Murray, M.E., Petrucelli, L., Liesinger, A.M., Senjem, M.L., Spychalla, A.J., Knopman, D.S., Parisi, J.E., Petersen, R.C., Jack Jr, C.R., & Whitwell, J.L. (2017). Rates of hippocampal atrophy and post-mortem TDP-43 in Alzheimer's disease: A longitudinal retrospective study. *Lancet Neurology, 16*(11), 917-924. DOI: 10.1016/S1474-4422(17)30284-3.

Josephs, K.A., Murray, M.E., Whitwell, J.L., Tosakulwong, N., Weigand, S.D., Petrucelli, L., Liesinger, A.M., Petersen, R.C., Parisi, J.E., & Dickson, D.W. (2016). Updated TDP-43 in Alzheimer's disease staging scheme. *Acta Neuropathologica, 131*(4), 571-585. DOI: 10.1007/s00401-016-1537-1.

Kamboh, M.I. (2022). Genomics and functional genomics of Alzheimer’s disease. *Neurotherapeutics, 19*(1), 152-172. DOI: 10.1007/s13311-021-01152-0.

Kanehisa, M., Araki, M., Goto, S., Hattori, M., Hirakawa, M., Itoh, M., Katayama, T., Kawashima, S., Okuda, S., Tokimatsu, T., Yamanishi, Y. (2008). KEGG for linking genomes to life and the environment. *Nucleic Acids Research, 36*(Database issue), D480-484. DOI: 10.1093/nar/gkm882.

Kanekiyo, T., Xu, H., & Bu, G. (2014). ApoE and Aβ in Alzheimer's disease: Accidental encounters or partners? *Neuron, 81*(4), 740-754. DOI: 10.1016/j.neuron.2014.01.045.

Kannappan, B., Gunasekaran, T.I., Te Nijenhuis, J., Gopal, M., Velusami, D., Kothandan, G., & Lee, K. H. (2022). Polygenic score for Alzheimer’s disease identifies differential atrophy in

hippocampal subfield volumes. *PLoS One, 17*(7), e0270795. DOI: 10.1371/journal.pone.0270795.

Kantarci, K., Lowe, V., Przybelski, S.A., Weigand, S.D., Senjem, M.L., Ivnik, R.J., Preboske, G.M., Roberts, R., Dega, Y.E., Boeve, B.F., Knopman, D.S., Peterson, R.C., & Jack Jr, C.R. (2012). APOE modifies the association between Aβ load and cognition in cognitively normal older adults. *Neurology, 78*(4), 232-240. DOI: 10.1212/WNL.0b013e31824365ab.

Kaplan, E., Goodglass, H., & Weintraub, S. (1983). The Boston naming test. *Philadelphia: Lea & Febiger*.

Karantzoulis, S., & Galvin, J.E. (2011). Distinguishing Alzheimer's disease from other major forms of dementia. *Expert Review of Neurotherapeutics, 11*(11), 1579-1591. DOI: 10.1586/ern.11.155.

Kauppi, K., Fan, C.C., McEvoy, L.K., Holland, D., Tan, C.H., Chen, C-H., Andreassen, O.A., Desikan, R., Dale, A.M., & Alzheimer's Disease Neuroimaging Initiative (2018). Combining polygenic hazard score with volumetric MRI and cognitive measures improves prediction of progression from mild cognitive impairment to Alzheimer's disease. *Frontiers in Neuroscience, 12*, 260. DOI: 10.3389/fnins.2018.00260.

Kauppi, K., Rönnlund, M., Adolfsson, A.N., Pudas, S., & Adolfsson, R. (2020). Effects of polygenic risk for Alzheimer's disease on rate of cognitive decline in normal aging. *Translation Psychiatry, 10*(1), 250. DOI: 10.1038/s41398-020-00934-y.

Khatoon, S., Grundke-Iqbal, I., & Iqbal, K. (1992). Brain levels of microtubule-associated protein tau are elevated in Alzheimer's disease: A radioimmuno-slot-blot assay for nanograms of the protein. *Journal of Neurochemistry, 59*(2), 750-753. DOI: 10.1111/j.1471-4159.1992.tb09432.x.

Kilimann, I., Likitjaroen, Y., Hampel, H. & Teipel, S. (2013). Diffusion tensor imaging to determine effects of antidementive treatment on cerebral structural connectivity in Alzheimer's disease. *Current Pharmaceutical Design, 19*(36), 6416-6425. DOI: 10.2174/1381612811319360003.

Kirchner, K., Garvet, L., Wittfield, K., Ameling, S., Bulow, R., Zu Schwabedissen, H.M., Nauck, M., Volzke, H., Grabe, H.J., & van der Auwera, S. (2023). Deciphering the effect of different genetic variants on hippocampal subfield volumes in the general population. *International Journal of Molecular Sciences, 24*(2), 1120. DOI: 10.3390/ijms24021120.

Klink, K., Jaun, U., Federspiel, A., Wunderlin, M., Teunissen, C.W., Kiefer, C., Wiest, R., Scharnowski, F., Sladky, R., Haugg, A., Hellrung, L., & Peter, J. (2021). Targeting hippocampal activity with real-time fMRI neurofeedback: protocol of a single-bling randomized controlled trial in mld cognitive impairment. *BMC Psychiatry, 21*(21). DOI: 10.1186/s12888-021-03091-8.

Koch, G., Di Lorenzo, F., Loizzo, S., Motta, C., Travaglione, S., Baiula, M., Rimondini, R., Pnzo, V., Bonni, S., Toniolo, S., Sallustio, F., Bozzali, M., Caltagirone, C., Campana, G., & Martorana, A. (2017). CSF tau is associated with impaired cortical plasticity, cognitive decline and astrocyte survival only in APOE4-positive Alzheimer's disease. *Scientific Reports, 7*(1), 13728. DOI: 10.1038/s41598-017-14204-3.

Koch, K., Myers, N. E., Gottler, J., Pasquini, L., Grimmer, T., Forster, S., Manoliu, A., Neitzel, J., Kurz, A., Forstl, H., Riedl, V., Wohlschlager, A. M., Drzezga, A., & Sorg, C. (2015). Disrupted intrinsic networks link amyloid-β pathology and impaired cognition in prodromal Alzheimer's disease. *Cerebral Cortex, 25*(12), 4678-4688. DOI: 10.1093/cercor/bhu151.

Koch, S., Schmidtke, J., Krawczak, M., & Caliebe, A. (2023). Clinical utility of polygenic risk scores: a critical 2023 appraisal. *Journal of Community Genetics, 14*(5), 471-487. DOI: 10.1007/s12687-023-00645-z.

Korbmacher, M., van der Meer, D., Beck, D., Askeland-Gjerde, D.E., Eikefjord, E., Lundervold, A., Andreassen, O.A., Westlye, L.T., & Maximov, I.I. (2024). Distinct longitudinal brain white matter microstructure changes and associated polygenic risk of common psychiatric disorders and Alzheimer's disease in the UK Biobank. *Biological Psychiatry Global Open Science, 4*(4), 100323. DOI: 10.1016/j.bpsgos.2024.100323.

Kueper, J.K., Speechley, M., & Montero-Odasso, M. (2018). The Alzheimer's disease assessment scale-cognitive subscale (ADAS-Cog): Modifications and responsiveness in pre-dementia populations. A narrative review. *Journal of Alzheimer's Disease, 63*(2), 423-444. DOI: 10.3233/JAD-170991.

Kulminski, A.M., Jain-Washburn, E., Nazarian, A., Wilkins, H.M., Veatch, O., Swerdlow, R.H., & Honea, R.A. (2024). Association of APOE alleles and polygenic profiles comprising APOE-TOMM40-APOC1 variants with Alzheimer's disease neuroimaging markers. *Alzheimer's & Dementia, 21*(2), e14445. DOI: 10.1002/alz.14445.

Kumar, A., Janelidze, S., Stomrud, E., Palmqvist, S., Hansson, O., Mattsson-Carlgren, N., & Alzheimer's Disease Neuroimaging Initiative. (2022). β-amyloid-dependent and -independent genetic pathways regulating CSF tau biomarkers in Alzheimer disease. *Neurology, 99*(5), e476-e487. DOI: 10.1212/WNL.0000000000200605.

Kunkle, B.W., Grenier-Boley, B., Sims, R., Bis, J.C., Damotte, V., Naj, A.C., Boland, A., Vronskaya, M., van der Lee, S.J., Amlie-Wolf, A., Bellenguez, C., Frizatti, A., Chouraki, V., Martin, E.R., Sleegers, K., Badarinarayan, N., Jakobsdottir, J., Hamilton-Nelson, K.L., Moreno-Grau, S., ... Pericak-Vance, M.A. (2019). Genetic meta-analysis of diagnosed Alzheimer's disease identifies new risk loci and implicated AB, tau, immunity, and lipid processing. *Nature Genetics, 51*(3), 414-430. DOI: 10.1038/s41588-019-0358-2.

Laccarino, L., Tammewar, G., Ayakta, N., Baker, S.L., Bejanin, A., Boxer, A.L., Gorno-Tempini, M.L., Janabi, M., Kramer, J.H., Lazaris, A., Lockhart, S.N., Miller, B.L., Miller, Z.A., O'Neil, J.P., Ossenkoppele, R., Rosen, H.J., Schonhaut, D.R., Jagust, W.J., & Rabinovici, G.D. (2017). Local and distant relationships between amyloid, tau and neurodegeneration in Alzheimer's Disease. *NeuroImage Clinical, 17*, 452-464. DOI: 10.1016/j.nicl.2017.09.016.

Lake, J., Solsberg, C.W., Kim, J.J., Acosta-Uribe, J., Makarious, M.B., Li, Z., Levine, K., Heutink, P., Alvarado, C.X., Vitale, D., Kang, S., Gim, J., Lee, K.H., Pina-Escudero, S.D., Ferrucci, L., Singleton, A.B., Blauwendraat, C., Nalls, M.A., Yokoyama, J.S., & Leonard, H.L. (2023). Multi-ancestry meta-analysis and fine-mapping in Alzheimer's disease. *Molecular Psychiatry, 28*(7), 3121-3132. DOI: 10.1038/s41380-023-02089-w.

Lambert, J-C., Heath, S., Even, G., Campion, D., Sleegers, K., Hiltunen, M., Combarros, O., Zelenika, D., Bullido, M.J., Tavernier, B., Letenneur, L., Bettens, K., Berr, C., Pasquier, F., Fievet, N., Barberger-Gateau, P., Engelborghs, S., De Deyn, P., Mateo, I., ... Amouyel, P. (2009). Genome-wide association study identifies variants at CLU and CR1 associated with Alzheimer's disease. *Nature Genetics, 41*(10), 1094-1099. DOI: 10.1038/ng.439.

Lambert, J-C., Ibrahim-Verbaas, C.A., Harold, D., Naj, A.C., Sims, R., Bellenguez, C., Jun, G., DeStefano, A.L., Bis, J.C., Beecham, G.W., Grenier-Boley, B., Russo, G., Thornton-Wells, T.A., Jones, N., Smith, A. V., Chouraki, V., Thomas, C., Ikram, M.A., Zelenika, D., ... Amouyel, P. (2013). Meta-analysis of 74,046 individuals identifies 11 new susceptibility loci for Alzheimer's disease. *Nature Genetics, 45*(12), 1452-1458. DOI: 10.1038/ng.2802.

Lambert, J-C., Ramirez, Grenier-Boley, B., & Bellenguez, C. (2023). Step by step: Towards a better understanding of the genetic architecture of Alzheimer's disease. *Molecular Psychiatry, 28*(7), 2716-2727. DOI: 10.1038/s41380-023-02076-1.

Lancaster, T., Creese, B., Escott-Price, V., Driver, I., Menzies, G., Khan, Z., Corbett, A., Ballard, C., Williams, J., Murphy, K., & Chandler, H. (2023). Proof-of-concept recall-by-genotype study of extremely low and high Alzheimer's polygenic risk reveals autobiographical deficits and cingulate cortex correlates. *Alzheimer's Research & Therapy, 15*(1), 213. DOI: 10.1186/s13195-023-01362-y.

Lancaster, T.M., Hill, M.J., Sims, R., & Williams, J. (2019). Microglia - mediated immunity partly contributes to the genetic association between Alzheimer's disease and hippocampal volume. *Brain Behavior and Immunity, 79*, 267-273. DOI: 10.1016/j.bbi.2019.02.011.

Landau, S.M., Mintun, M.A., Joshi, A.D., Koeppe, R.A., Peterson, R.C., Aisen, P.S., Weiner, M.W., Jagust, W.J., & Alzheimer's Disease Neuroimaging Initiative (2012). Amyloid deposition, hypometabolism, and longitudinal cognitive decline. *Annals of Neurology, 72*(4), 578-586. DOI: 10.1002/ana.23650.

Lane, C.A., Hardy, J., & Schott J.M. (2017). Alzheimer's disease. *European Journal of Neurology, 25*(1), 59-70. DOI: 10.1111/ene.13439.

Levenstien, M.A., Yang, Y., & Ott, J. (2003). Statistical significance for hierarchical clustering in genetic association and microarray expression studies. *BMC Bioinformatics 4*(62). DOI: 10.1186/1471-2105-4-62.

Lee, S.H., Harold, D., Nyholt, D.R., ANZGene Consortium, International Endogene Consortium, Genetic and Environmental Risk for Alzheimer's disease Consortium, Goddard, M.E., Zondervan, K.T., Williams, J., Montgomery, G.W., Wray, N.R., & Visscher, P.M. (2013). Estimation and partitioning of polygenic variation captured by common SNPs for Alzheimer's disease, multiple sclerosis and endometriosis. *Human Molecular Genetics, 22*(4), 832-841. DOI: 10.1093/hmg/dds491.

Lee, Y-G., Jeon, S., Kang, S.W., Park, M., Baik, K., Yoo, H.S., Chung, S.J., Jeong, S.H., Jung, J.H., Lee, P.H., Sohn, Y.H., Evans, A.C., Ye, B.S., & Alzheimer's Disease Neuroimaging Initiative (2021).

Interaction of CSF a-synuclein and amyloid beta in cognition and cortical atrophy. *Alzheimer's & Dementia (Amst), 13*(1), e12177. DOI: 10.1002/dad2.12177.

Lehtovirta, M., Laakso, M.P., Soininen, H., Helisalmi, S., Mannermaa, A., Helkala, E-L., Partanen, K., Ryyanen, M., Vainio, P., Hartikainen, P., & Riekkinen Sr, P.J. (1995). Volumes of hippocampus, amygdala and frontal lobe in Alzheimer patients with different apolipoprotein E genotypes. *Neuroscience, 67*(1), 65-72. DOI: 10.1016/0306-4522(95)00014-A.

Lencz, T., Knowles, E., Davies, G., Guha, S., Liewald, D.C., Starr, J.M., Djurovic, S., Melle, I., Sundet, K., Christoforou, A., Reinvang, I., Mukherjee, S., DeRosse, P., Lundervold, A., Steen, V.M., John, M., Espeseth, T., Räikkönen, K., Widen, E., ... Malhotra, A.K. Molecular genetic evidence for overlap between general cognitive ability and risk for schizophrenia: a report from the Cognitive Genomics consorTium (COGENT). *Molecular Psychiatry, 19*(2), 168-174. DOI: 10.1038/mp.2013.166.

Lenz, M., Eicher, A., Kruse, P., Galanis, C., Kleindonas, D., Andrieux, G., Boerries, M., Jedlicka, P., Muller, U., Deller, T., & Vlachos, A. (2023). The amyloid precursor protein regulates synaptic transmission at medial perforant path synapses. *Journal of Neuroscience, 43*(29), 5290-5304. DOI: 10.1523/JNEUROSCI.1824-22.2023.

Leonenko, G., Baker, E., Stevenson-Hoare, J., Sierksma, A., Fiers, M., Williams, J., de Strooper. B., & Escott-Price, V. (2021). Identifying individuals with high risk of Alzheimer's disease using polygenic risk scores. *Nature Communications, 12*(1), 4506. DOI: 10.1038/s41467-021-24082-z.

Leonenko, G., Sims, R., Shoai, M., Frizzati, A., Bossu, P., Spalleta, G., Fox, N.C., Williams, J., GERAD consortium, Hardy, J., & Escott-Price, V. (2019). Polygenic risk and hazard scores for Alzheimer's disease prediction. *Annals of Clinical and Translational Neurology, 6*(3), 456-465. DOI: 10.1002/acn3.716.

Lewis, C.M., & Vassos, E. (2020). Polygenic risk scores: from research tools to clinical instruments. *Genome Medicine, 12*(1), 44. DOI: 10.1186/s13073-020-00742-5.

Li, A., Lian, J., & Vardhanabhuti, V. (2025). Multi-modal machine learning approach for early detection of neurodegenerative diseases leveraging brain MRI and wearable sensor data. *PLoS Digit Health, 4*(4), e0000795. DOI: 10.1371/journal.pdig.0000795.

Li, F., Xie, S., Cui, J., Li, Y., Li, T., Wang, Y., & Jia, J. (2024). Polygenic risk score reveals genetic heterogeneity of Alzheimer's disease between the Chinese and European populations. *Journal of Prevention of Alzheimer's Disease, 11*(3), 701-709. DOI: 10.14283/jpad.2024.29.

Li, H., Liu, H., Lutz, M.W., Luo, S., & Alzheimer's Disease Neuroimaging Initiative (2023). Novel genetic variants in TP37, PIK3R1, CALM1, and PLCG2 of the neurotrophin signaling pathway are associated with the progression from mild cognitive impairment to Alzheimer's disease. *Journal of Alzheimer's Disease, 91*(3), 977-987. DOI: 10.3233/JAD-220680.

Li, K., Fu, Z., Qi, S., Luo, X., Zeng, Q., Xu, X., Huang, P., Zhang, M., Calhoun, V. D., & Alzheimer's Disease Neuroimaging Initiative (2021). Polygenic hazard score associated multimodal brain networks along the Alzheimer's disease continuum. *Frontiers in Aging Neuroscience, 13*, 725246. DOI: 10.3389/fnagi.2021.725246.

Li, W.W., Wang, Z., Fan, D.Y., Shen, Y.Y., Chen, D.W., Li, H.Y., Li, L., Yang, H., Liu, Y.H., Bu, X.L., Jin, W.S., Zeng, F., Xu, Z.Q., Yu, J.T., Chen, L.Y., & Wang, Y.J. (2020). Association of polygenic risk score with age at onset and cerebrospinal fluid biomarkers of Alzheimer's disease in a Chinese cohort. *Neuroscience Bulletin, 36*(7), 696-704. DOI: 10.1007/s12264-020-00469-8.

Li, X-L., Hu, N., Tan, M-S., Yu, J-T., & Tan, L. (2014). Behavioural and psychological symptoms in Alzheimer's disease. *BioMed Research International, 2014*(1), 927804. DOI: 10.1155/2014/927804.

Li, Z., Shue, F., Zhao, N., Shinohara, M., & Bu, Guojun. (2020). APOE2: Protective mechanism and therapeutic implications for Alzheimer's disease. *Molecular Neurodegeneration, 15*(1), 63. DOI: 10.1186/s13024-020-00413-4.

Liebers, D.T., Pirooznia, M., Seiffudin, F., Musliner, K.L., Zandi, P.P., & Goes, F.S. (2016). Polygenic risk of schizophrenia and cognition in a population-based survey of older adults. *Schizophrenia Bulletin, 42*(4), 984-991. DOI: 10.1093/schbul/sbw001.

Lim, Y.Y., Mormino, E.C., & Alzheimer's Disease Neuroimaging Initiative (2017). APOE genotype and early β-amyloid accumulation in older adults without dementia. *Neurology, 89*(10), 1028-1034. DOI: 10.1212/WNL.0000000000004336.

Lim, Y.Y., Villemagne, V.L., Pietrzak, R.H., Ames, D., Ellis, K.A., Harrington, K., Snyder, P.J., Martins, R. N., Masters, C.L., Rowe, C.C., & Maruff, P. (2015). APOE ε4 moderates amyloid-related memory decline in preclinical Alzheimer's disease. *Neurobiology of Aging, 36*(3), 1239-1244. DOI: 10.1016/j.neurobiolaging.2014.12.008.

Lind, J., Larsson, A., Persson, J., Ingvar, M., Nilsson, L-G., Backman, L., Adolfsson, R., Cruts, M., Sleegers, K., Van Broeckhoven, C., & Nyberg, L. (2006). Reduced hippocampal volume in non-demented carriers of the apolipoprotein E ε4: Relation to chronological age and recognition memory. *Neuroscience Letters, 396*(1), 23-27. DOI: 10.1016/j.neulet.2005.11.070.

Linton, M.F., Gish, R., Hubi, S.T., Butler, E., Esquivel, C., Bry, W.I., Boyles, J.K., Wardell, M.R., & Young, S.G. (1991). Phenotypes of apolipoprotein B and apolipoprotein E after liver transplantation. *Journal of Clinical Investigation, 88*(1), 270-281. DOI: 10.1172/JCI115288.

Liu, C-C., Kanekiyo, T., Xu, H., & Bu, G. (2013). Apolipoprotein E and Alzheimer disease: Risk, mechanisms, and therapy. *Nature Reviews Neurology, 9*(2), 106-118. DOI: 10.1038/nrneurol.2012.263.

Liu, H., Lutz, M., & Luo, S. (2022). Genetic association between epigenetic aging-acceleration and the progression of mild cognitive impairment to Alzheimer's disease. *Journal of Gerontology, Series A, 77*(9), 1734-1742. DOI: 10.1093/gerona/glac138.

Liu, H., Lutz, M., Luo, S., & Alzheimer's Disease Neuroimaging Initiative (2021). Association between polygenic risk score and the progression from mild cognitive impairment to Alzheimer's disease. *Journal of Alzheimer's Disease, 84*(3), 1323-1335. DOI: 10.3233/JAD-210700.

Liu, S., Smit, D.J.A., Abdellaoui, A., van Wingen, G.A., & Verweij, K.J.H. (2023). Brain structure and function show distinct relations with genetic predispositions to mental health and cognition. *Biological Psychiatry: Cognitive Neuroscience and Neuroimaging, 8*(3), 300-310. DOI: 10.1016/j.bpsc.2022.08.003.

Liu, Y., Tan, L., Wang, H.F., Liu, Y., Hao, X.K., Tan, C.C., Jiang, T., Liu, B., Zhang, D.Q., Yu, J.T., & Alzheimer's Disease Neuroimaging Initiative (2016). Multiple effect of APOE genotype on clinical and neuroimaging biomarkers across Alzheimer's disease spectrum. *Molecular Neurobiology, 53*(7), 4539-4547. DOI: 10.1007/s12035-015-9388-7.

Livingston, G., Huntley, J., Liu, K.Y., Costafreda, S.G., Selbæk, G., Alladi, S., Ames, D., Banerjee, S., Burns, A., Brayne, C., Fox, N.C., Ferri, C.P., Gitlin, L.N., Howard, R., Kales, H.C., Kivimäki, M., Larson, E.B., Nakasujja, N., Rockwood, K., ... Mukadam, N. (2024). Dementia prevention, intervention, and care: 2024 report of the Lancet standing Commission. *Lancet, 404*(10452), 572-628. DOI: 10.1016/S0140-6736(24)01296-0.

Livingston, G., Huntley, J., Sommerlad, A., Ames, D., Ballard, C., Banerjee, S., Brayne, C., Burns, A., Cohen-Mansfield, J., Cooper, C., Costafreda, S.G., Dias, A., Fox, N., Gitlin, L.N., Howard, R., Kales, H.C., Kivimäki, M., Larson, E.B., Ogunniyi, A., ... Mukadam, N. (2020). Dementia prevention, intervention, and care: 2020 report of the Lancet Commission. *Lancet, 396*(10248), 413-446. DOI: 10.1016/S0140-6736(20)30367-6.

Lo, M.T, Kauppi, K., Fan, C.C., Sanyal, N., Reas, E.T., Sundar, V.S., Lee, W.C., Desikan, R.S., McEvoy, L.K., Chen, C.H. & Alzheimer's Disease Genetics Consortium (2019). Identification of genetic heterogeneity of Alzheimer's disease across age. *Neurobiology of Aging, 84*, 243e1-243.e9. DOI: 10.1016/j.neurobiolaging.2019.02.022.

Logue M.W,, Panizzon, M.S., Elman, J.A., Gillespie, N.A., Hatton, S.N., Gustavson, D.E., Andreassen, O.A., Dale, A.M., Franz, C.E., Lyons, M.J., Neale, M.C., Reynolds, C.A., Tu, X., & Kremen, W.S. (2018). Use of an Alzheimer's disease polygenic risk score to identify mild cognitive impairment in adults in their 50s. *Molecular Psychiatry, 24*(3), 421-430. DOI: 10.1038/s41380-018-0030-8

Lopresti, B.J., Campbell, E.M., Yu, Z., Anderson, S.J., Cohen, A.D., Minhas, D.S., Snitz, B.E., Royse, S.K., Becker, C.R., Aizenstein, H.J., Mathis, C.A., Lopez, O.L., Klunk, W.E., & Tudorascu, D.L. (2020). Influence of apolipoprotein-E genotype on brain amyloid load and longitudinal trajectories. *Neurobiology of Aging, 94*, 111-120. DOI: 10.1016/j.neurobiolaging.2020.05.012.

Lorenz, A., Sathe, A., Zaras, D., Yang, Y., Durant, A., Kim, M.E., Gao, C., Newlin, N.R., Ramadass, K., Kanakaraj, P., Khairi, N.M., Li, Z., Yao, T., Huo, Y., Dumitrescu, L., Shashikumar, N., Pechman, K.R., Jackson, T.B., Workmeister, A.W., ... Archer, D.B. (2025). The effect of Alzheimer's disease genetic factors on limbic white matter microstructure. *Alzheimer's & Dementia, 21*(4), e70130. DOI: 10.1002/alz.70130.

Lorenzini, L., Collij, L.E., Tesi, N., Vilor-Tejedor, N., Ingala, S., Blennow, K., Foley, C., Frisoni, G.B., Haller, S., Holstege, H., van der van der Lee, S., Martinez-Lage, P., Marioni, R.E.,

McCartney, D.L., O' Brien, J., Oliveira, T.G., Payoux, P., Reinders, M., Ritchie, C., ... Barkhof, F. (2024). Alzheimer's disease genetic pathways impact cerebrospinal fluid biomarkers and imaging endophenotypes in non-demented individuals. *Alzheimer's & Dementia, 20*(9), 6146-6160. DOI: 10.1002/alz.14096.

Louwersheimer, E., Wolfsgruber, S., Espinosa, A., Lacour, A., Heilmann-Heimbach, S., Alegret, M., Hernández, I., Rosende-Roca, M., Tárraga, L., Boada, M., Kornhuber, J., Peters, O., Frölich, L., Hüll, M., Rüther, E., Wiltfang, J., Scherer, M., Riedel-Heller, S., Jessen, F., ... Ramirez, A. (2016). Alzheimer's disease risk variants modulate endophenotypes in mild cognitive impairment. *Alzheimer's & Dementia, 12*(8), 872-881. DOI: 10.1016/j.jalz.2016.01.006.

Luckett, E.S., Abakkouy, Y., Reinartz, M., Adamczuk, K., Schaeverbeke, J., Verstockt, S., De Meyer, S., Van Laere, K., Dupont, P., Cleynen, I., & Vandenberghe, R. (2022). Association of Alzheimer's disease polygenic risk scores with amyloid accumulation in cognitively intact older adults. *Alzheimer's Research & Therapy, 14*(1), 138. DOI: 10.1186/s13195-022-01079-4.

Lumsden, A.L., Mulugeta, A., Zhou, A., & Hypponen, E. (2020). Apolipoprotein E (APOE) genotype-associated disease risks: A phenome-wide, registry-based, case-control study utilising the UK Biobank. *eBioMedicine, 56*, 102954. DOI: 10.1016/j.ebiom.2020.102954.

Lupton, M.K., Strike, L., Hansell, N.K., Wen, W., Mather, K.A., Armstrong, N.J., Thalamuthu, A., McMahon, K.L., de Zubicaray, G.I., Assareh, A.A., Simmons, A., Proitisi, P., Powell, J.F., Montgomery, G.W., Hibar, D.P., Westman, E., Tsoolaki, M., Kloszewska, I., Soininen, H., ... Wright, M.J. (2016). The effect of increased genetic risk for Alzheimer's disease on hippocampal and amygdala volume. *Neurobiology of Aging, 40*, 68-77.
DOI: 10.1016/j.neurobiolaging.2015.12.023.

Lyketsos, C.G., Carrillo, M.C., Ryan, J.M., Khachaturian, A.S., Trzepacz, P., Amatniek, J., Cederbaum, J., Brashear, R., & Miller, D.S. (2011). Neuropsychiatric symptoms in Alzheimer's disease. *Alzheimer's & Dementia, 7*(5), 532-539. DOI: 10.1016/j.jalz.2011.05.2410.

Machulda, M.M., Jones, D.T., Vemuri, P., McDade, E., Avula, R., Przybelski, S., Boeve, B.F., Knopman, D.S., Petersen, R.C., & Jack Jr, C.R. (2011). Effect of APOE ε4 status on intrinsic network connectivity in cognitively normal elderly. *Archives of Neurology, 68*(9), 1131-1136. DOI: 10.1001/archneurol.2011.108.

Mahedy, L., Anderson, E.L., Tilling, K., Thornton, Z.A., Elmore, A.R., Szalma, S., Simen, A., Culp, M., Zicha, S., Harel, B.T., Smith, G.D., Smith, E.N., & Paternoster, L. (2024). Investigation of genetic determinants of cognitive change in later life. *Translational Psychiatry, 14*(1), 31. DOI: 10.1038/s41398-023-02726-6.

Mamalaki, E., Charisis, S., Mourtzi, N., Hatzimanolis, A., Ntanasi, E., Kosmidis, M.H., Constantinides, V.C., Pantes, G., Kolovou, D., Dardiotis, E., Hadjigeorgiou, G., Sakka, P., Gu, Y., Yannakoulia, M., & Scarmeas, N. (2024). Genetic risk for Alzheimer's disease and adherence to the Mediterranean diet: results from the HELIAD study. *Nutritional Neuroscience, 27*(3), 289-299. DOI: 10.1080/1028415X.2023.2187952.

Manca, R., Pardinas, A.F., & Venneri, A. (2023). The neural signatures of psychoses in Alzheimer's disease: a neuroimaging genetics approach. *European Archives of Psychiatry and Clinical Neuroscience, 273*(1), 253-267. DOI: 10.1007/s00406-022-01432-6.

Manca, R., Sharrack, B., Paling, D, Wilkinson, I.D., & Venneri, A. (2018). Brain connectivity and cognitive processing in multiple sclerosis: A systematic review. *Journal of the Neurological Sciences, 388*, 115-127. DOI: 10.1016/j.jns.2018.03.003.

Mantzavinos, V., & Alexiou, A. (2017). Biomarkers for Alzheimer's disease diagnosis. *Current Alzheimer Research, 14*(11), 1149-1154. DOI: 10.2174/1567205014666170203125942.

Marchewka, A., Kherif, F., Krueger, G., Grabowska, A., Frackowiak, R., & Draganski, B. (2014). Influence of magnetic field strength and image registration strategy on voxel-based morphometry in a study pf Alzheimer's disease. *Human Brain Mapping, 35*(5), 1865-1874. DOI: 10.1002/hbm.22297.

Marden, J.R., Mayeda, E.R., Walter, S., Vivot, A., Tchetgen, E.J.T., Kawachi, I., & Glymour, M.M. (2016). Using an Alzheimer disease polygenic risk score to predict memory decline in black and white Americans over 14 years of follow-up. *Alzheimer Disease & Associated Disorders, 30*(3), 195-202. DOI: 10.1097/WAD.0000000000000137.

Marioni, R.E., Harris, S.E., Zhang, Q., McRae, A.F., Hagenaars, S.P., Hill, W.D., Davies, G., Ritchie, C.W., Gale, C.R., Starr, J.M., Goate, A.M., Porteous, D.J., Yang, J., Evans, K.L., Deary, I.J., Wray, N.R., & Visscher, P.M. (2018). GWAS on family history of Alzheimer's disease. *Translational Psychiatry, 8*(1), 99. DOI: 10.1038/s41398-018-0150-6.

Marquez, F., & Yassa, M.A. (2019). Neuroimaging biomarkers for Alzheimer's disease. *Molecular Neurodegeneration, 14*(1), 21. DOI: 10.1186/s13024-019-0325-5.

Martinez-Morillo, E., Hansson, O., Atagi, Y., Bu, G., Minthon, L., Diamandis, E.P., & Nielsen, H.M. (2014). Total apolipoprotein E levels and specific isoform composition in cerebrospinal fluid and plasma from Alzheimer's disease patients and controls. *Acta Neuropathologica, 127*(5), 633-643. DOI: 10.1007/s00401-014-1266-2.

Martiskainen, H., Helisalmi, S., Viswanathan, J., Kurki, M., Hall, A., Herukka, S.K., Sarajärvi, T., Natunen, T., Kurkinen, K.M., Huovinen, J., Mäkinen, P., Laitinen, M., Koivisto, A.M., Mattila, K.M., Lehtimäki, T., Remes, A.M., Leinonen, V., Haapasalo, A., Soininen, H., & Hiltunen, M. (2015). Effects of Alzheimer's disease-associated risk loci on cerebrospinal fluid biomarkers and disease progression: a polygenic risk score approach. *Journal of Alzheimer's Disease, 43*(2), 565-573. DOI: 10.3233/JAD-140777.

Masters, C.L., Bateman, R., Blennow, K., Rowe, C.C., Sperling, R.A. & Cummings, J.L. (2015). Alzheimer's disease. *Nature Reviews Disease Primers, 1*, 15056. DOI: 10.1038/nrdp.2015.56.

Maurer, K., Volk, S., & Gerbaldo, H. (1997). Auguste D and Alzheimer's disease. *Department of Medical History, 349*(9064), P1546-1549. DOI: 10.1016/S0140-6736(96)10203-8.

McEvoy, L.K. & Brewer, J.B. (2010). Quantitative structural MRI for early detection of Alzheimer's disease. *Expert Review of Neurotherapeutics, 10*(11), 1675-1688. DOI: 10.1586/ern.10.162.

Meda, S.A., Narayanan, B., Liu, J., Perrone-Bizzozero, N.I., Stevems, M.C., Calhoun, V.D., Glahn, D.C., Shen, L., Risacher, S.L., Saykin, A.J., & Pearlson, G.D. (2012). A large scale multivariate parallel ICA method reveals novel imaging-genetic relationships for Alzheimer's disease in the ADNI cohort. *NeuroImage, 60*(3), 1608-1621. DOI: 10.1016/j.neuroimage.2011.12.076.

Mertaş, B., & Boşgelmez, I.I. (2025). The role of genetic, environmental, and dietary factors in Alzheimer's disease: A narrative review. *International Journal of Molecular Sciences, 26*(3), 1222. DOI: 10.3390/ijms26031222.

Meyer, M.R., Tschanz, J.T., Norton, M.C., Welsh-Bohmer, K.A., Steffens, D.C., Wyse, B.W., & Breitner, J.C.S. (1998). APOE genotype predicts when – and whether – one is predisposed to develop Alzheimer disease. *Nature Genetics, 19*(4), 321-322. DOI: 10.1038/1206.

Meyer, P.F., Binette A.P., Gonneaud, J., Breitner, J.C.S., & Villeneuve, S. (2020). Characterization of Alzheimer disease biomarker discrepancies using cerebrospinal fluid phosphorylated tau and AV1451 positron emission tomography. *JAMA Neurology, 77*(4), 508-516. DOI: 10.1001/jamaneurol.2019.4749.

Michalicova, A., Majerova, P., & Kovac, A. (2020). Tau protein and its role in blood-brain barrier dysfunction. *Frontiers in Molecular Neuroscience, 13*, 570045. DOI: 10.3389/fnmol.2020.570045.

Miller, A.K.H., Alston, R.L. & Corsellis, J.A.N. (1980). Variation with age in the volumes of grey and white matter in the cerebral hemispheres of man: Measurements with an image analyser. *Neuropathology and Applied Neurobiology, 6*(2), 119-132. DOI: 10.1111/j.1365-2990.1980.tb00283.x.

Mirra, S.S., Heyman, A., McKeel, D., Sumi, S.M., Crain, B.J., Brownlee, L.M., Vogel, F.S., Hughes, J.P., van Belle, G., & Berg, L. (1991). The consortium of establish a registry for Alzheimer's disease (CERAD). Part II Standardization of the neuropathologic assessment of Alzheimer's disease. *Neurology, 41*(4), 479-486. DOI: 10.1212/wnl.41.4.479.

Mishra, S., Blazey, T.M., Holtzman, D.M., Cruchaga, C., Su, Y., Morris, J.C., Benzinger, T.L.S., & Gordon, B.A. (2018). Longitudinal brain imaging in preclinical Alzheimer disease: impact of APOE ε4 genotype. *Brain, 141*(6), 1828-1839. DOI: 10.1093/brain/awy103.

Mitchell, T.W., Nissanov, J., Han, Li-Ying, Mufson, E.J., Schneider, J.A., Cochran, E.J., Bennet, D.A., Lee, V.M-Y., Trojanowski, J.Q., & Arnold, S.E. (2000). Novel method to quantify neuropil threads in brains from elders with or without cognitive impairment. *Journal of Histochemistry & Cytochemistry, 48*(12), 1627-1638. DOI: 10.1177/002215540004801206.

Mizrak, H.G., Dikmen, M., Hanoğlu, L., & Şakul, B.U. (2024). Investigation of hemispheric asymmetry in Alzheimer's disease patients during resting state revealed by fNIRS. *Scientific Reports, 14*(1), 13454. DOI: 10.1038/s41598-024-62281-y.

Mollink, J., Hiemstra, M., Miller, K.L., Huszar, I.N., Jenkinson, M., Raaphorst, J., Wiesmann, M., Ansorge, O., Pallebage-Gamarallage, M., & van Cappellen van Walsum, A.M. (2019). White matter changes in the perforant path area in patients with amyotrophic lateral sclerosis. *Neuropathology and Applied Neurobiology, 45*(6), 570-585. DOI: 10.1111/nan.12555.

Moradi, E., Hallikainen, I., Hänninen, T., Tohka, J., & Alzheimer's Disease Neuroimaging Initiative (2017). Rey's auditory verbal learning test scores can be predicted from whole brain MRI in Alzheimer's disease. *NeuroImage Clinical, 13*, 415-427. DOI: 10.1016/j.nicl.2016.12.011.

Mormino, E.C., Betensky, R.A., Hedden, T., Schultz, A.P., Ward, A., Huijbers, W., Rentz, D.M., Johnson, K.A., Sperling, R.A., Alzheimer's Disease Neuroimaging Initiative, Australian Imaging Biomarkers and Lifestyle Flagship Study of Ageing & Harvard Aging Brain Study (2014). Amyloid and APOE ε4 interact to influence short-term decline in preclinical Alzheimer disease. *Neurology, 82*(20), 1760-1767. DOI: 10.1212/WNL.0000000000000431.

Mormino, E.C., Sperling, R.A., Homes, A.J., Buckner, R.L., De Jager, P.L., Smoller, J.W., & Sabuncu, M.R. (2016). Polygenic risk of Alzheimer disease is associated with early- and late-life processes. *Neurology, 87*(5), 481-488. DOI: 10.1212/WNL.0000000000002922.

Morris, J. C. (1993). The clinical dementia rating (CDR): Current version and scoring rules. *Neurology, 43*(11), 2412-2414. DOI: 10.1212/wnl.43.11.2412-a.

Morris, J.C., Roe, C.M., Xiong, C., Fagan, A.M., Goate, A.M., Holtzman, D.M. & Mintun, M.A. (2010). APOE predicts amyloid-beta but not tau Alzheimer pathology in cognitively normal aging. *Annals of Neurology, 67*(1), 122-131. DOI: 10.1002/ana.21843.

Mosconi, L. (2005). Brain glucose metabolism in the early and specific diagnosis of Alzheimer's disease. *European Journal of Nuclear Medicine and Molecular Imaging, 32*(4), 486-510. DOI: 10.1007/s00259-005-1762-7.

Mosconi, L., Tsui, W.H., Herholz, K., Pupi, A., Drzezga, A., Lucignani, G., Reiman, E.M., Holthoff, V., Kalbe, E., Sorbi, S., Diehl-Schmid, J., Perneczky, R., Clerici, F., Caselli, R., Beuthien-Baumann, B., Kurz, A., Minoshima, S. & de Leon, M. J. (2008). Multicenter standardizes 18F-FDG PET diagnosis of mild cognitive impairment, Alzheimer's disease, and other dementias. *Journal of Nuclear Medicine, 49*(3), 390-398. DOI: 10.2967/jnumed.107.045385.

Mueller, S.G., & Weiner, M.W. (2009). Selective effect of age, apo e4, and Alzheimer's disease on hippocampal subfields. *Hippocampus, 19*(6), 558-564. DOI: 10.1002/hipo.20614.

Mueller, S.G., Schuff, N., Yaffe, K., Madison, C., Miller, B., & Weiner, M.W. (2010). Hippocampal atrophy patterns in mild cognitive impairment and Alzheimer's disease. *Human Brain Mapping, 31*(9), 1339-1347. DOI: 10.1002/hbm.20934.

Murphy, K.R., Landau, S.M., Choudhury, K.R., Hostage, C.A., Shpanskaya, K.S., Sair, H.I., Petrella, J.R., Wong, T.Z., Doraiswamy, P.M., & Alzheimer's Disease Neuroimaging Initiative (2013). Mapping the effects of ApoE4, age and cognitive status on 18F-florbetapir PET measured regional cortical patterns of beta-amyloid density and growth. *NeuroImage, 78*, 474-480. DOI: 10.1016/j.neuroimage.2013.04.048.

Murray, A.N., Chandler, H.L., & Lancaster, T.M. (2021). Multimodal hippocampal and amygdala subfield volumetry in polygenic risk for Alzheimer's disease. *Neurobiology of Aging, 98*, 33-41. DOI: 10.1016/j.neurobiolaging.2020.08.022.

Myers, N., Paquini, L., Gottler, J., Grimmer, T., Koch, K., Ortner, M., Neitzel, J., Muhlau, M., Forster, S., Kurz, A., Forstl, H., Zimmer, C., Wohlschlager, A.M., Reidl, V., Drzezga, A., & Sorg, C. (2014). Within-patient correspondence of amyloid-β and intrinsic network connectivity in Alzheimer's disease. *Brain, 137*(7), 2052-2064. DOI: 10.1093/brain/awu103.

Naggara, O., Oppenheim, C., Rieu, D., Raoux, N., Rodrigo, S., Barba, G.D., & Meder, J-F. (2006). Diffusion tensor imaging in early Alzheimer's disease. *Psychiatry Research: Neuroimaging, 146*(3), 243-249. DOI: 10.1016/j.pscychresns.2006.01.005.

Najar, J., Thorvaldsson, V., Kern, S., Skoog, J., Waern, M., Zetterberg, H., Blennow, K., Skoog, I., & Zettergren, A. (2023). Polygenic risk scores for Alzheimer's disease in relation to cognitive change: A representative sample from the general population followed over 16 years. *Neurobiology of Disease, 189*, 106357. DOI: 10.1016/j.nbd.2023.106357.

Naseri, N.N., Wang, H., Guo, J., Sharma, M., & Luo, W. (2019). The complexity of tau in Alzheimer's disease. *Neuroscience Letters, 705*, 183-194. DOI: 10.1016/j.neulet.2019.04.022.

Nasreddine, Z.S., Phillips, N.A., Bédirian, V., Charbonneau, S., Whitehead, V., Collin, I., Cummings, J.L., & Chertkow, H. (2005). The Montreal cognitive assessment, MoCA: a brief screening tool for mild cognitive impairment. *Journal of the American Geriatrics Society, 53*(4), 695-699. DOI: 10.1111/j.1532-5415.2005.53221.x.

Nebreda, M.C., Garcia-Caballero, A., Asensio, E., Revilla, P., Rodriguez-Girondo, M. & Mateos, R. (2010). A short-form version of the Boston naming test for language screening in dementia in a bilingual rural community in Galicia (Spain). *International Psychogeriatrics, 23*(3), 435-441. DOI: 10.1017/S1041610210001481

Nelson, P.T., Alafuzoff, I., Bigio, E.H., Bouras, C., Braak, H., Cairns, N.J., Castellani, R.J., Crain, B.J., Davies, P., Del Tredici, K., Duyckaerts, C., Frosch, M.P., Haroutunian, V., Hof, P.R., Hulette, C.M., Hyman, B.T., Iwatsubo, T., Jellinger, K.A., Jicha, G.A., ... Beach, T.G. Correlation of Alzheimer disease neuropathologic changes with cognitive status: a review of the literature. *Journal of Neuropathology & Experimental Neurology, 71*(5), 362-381. DOI: 10.1097/NEN.0b013e31825018f7.

Nikpay, M., Goel, A., Won, H-H., Hall, L. M., Willenborg, C., Kanoni, S., Saleheen, D., Kyriakou, T., Nelson, C.P., Hopewell, J.C., Webb, T.R., Zeng, L., Dehghan, A., Alver, M., Armasu, S.M., Auro, K., Bjonnes, A., Chasman, D.I., Chen, S., ... Farrall, M. (2015). A comprehensive 1,000 genomes-based genome-wide association meta-analysis of coronary artery disease. *Nature Genetics, 47*(10), 1121-1130. DOI: 10.1038/ng.3396.

Nir, T.M., Jahanshad, N., Villalon-Reina, J.E., Toga, A.W., Jack, C.R., Weiner, M.W., Thompson, P.M., & Alzheimer's Disease Neuroimaging Initiative (2013). Effectiveness of regional DTI measures in distinguishing Alzheimer's disease, MCI, and normal aging. *NeuroImage, 3*, 180-195. DOI: 10.1016/j.nicl.2013.07.006.

Nivard, M.G., Gage, S.H., Hottenga, J.J., van Beijsterveldt, C.E.M., Abdellaoui, A., Bartels, M., Baselmans, B.M.L., Ligthart, L., St Pourcain, B., Boomsma, D.I., Munafo, M.R., & Middeldorp, C.M. (2017). Genetic overlap between schizophrenia and developmental psychopathology: Longitudinal and multivariate polygenic risk prediction of common psychiatric traits during development. *Schizophrenia Bulletin, 43*(6), 1197-1207. DOI: 10.1093/schbul/sbx031.

Nordengen, K., Palhaugen, L., Bettella, F., Bahrami, S., Selnes, P., Jarholm, J., Athanasiu, L., Shadrin, A., Andreassen, O.A., Fladby, T. (2022). Phenotype-informed polygenic risk scores are associated with worse outcome in individuals at risk of Alzheimer's disease. *Alzheimer's & Dementia: Diagnosis, Assessment & Disease Monitoring, 14*(1), e12350. DOI: 10.1002/dad2.12350.

Page, M.J., McKenzie, J.E., Bossuyt, P.M., Boutron, I., Hoffmann, T.C., Mulrow, C.D., Shamseer, L., Tetzlaff, J.M., Akl, E.A., Brennan, S.E., Chou, R., Glanville, J., Grimshaw, J.M., Hróbjartsson, A., Lalu, M.M., Li, T., Loder, E.W., Mayo-Wilson, E., McDonald, S., ... Moher, D. (2021). The PRISMA 2020 statement: an updated guideline for reporting systematic reviews. *Systematic Reviews, 10*(1), 89. DOI: 10.1186/s13643-021-01626-4.

Palmqvist, S., Warmenhoven, N., Anastasi, F., Pilotto, A., Janelidze, S., Tideman, P., Stomrud, E., Mattsson-Carlgren, N., Smith, R., Ossenkoppele, R., Tan, K., Dittrich, A., Skoog, I., Zetterberg, H., Quaresima, V., Tolassi, C., Höglund, K., Brugnoni, D., Puig-Pijoan, A., ... Hansson, O. (2025). Plasma phospho-tau217 for Alzheimer's disease diagnosis in primary and secondary care using a fully automated platform. *Nature Medicine, 31*(6), 2036-2043. DOI: 10.1038/s41591-025-03622-w.

Pandya, S., Venneri, A., & De Marco, M. (2025). Exploring polygenic risk and neuroimaging parameters across the Alzheimer's disease spectrum. *Alzheimer's & Dementia, 20*(Suppl 2), e084291. DOI: 10.1002/alz.084291. [poster abstract].

Patterson, D. (2009). Molecular genetic analysis of Down syndrome. *Human Genetics, 126*(1), 195-214. DOI: 10.1007/s00439-009-0696-8.

Pedraza, O., Graff-Radford, N.R., Smith, G.E., Ivnik, R.J., Willis, F.B., Petersen, R.C., & Lucas, J.A (2009). Differential item functioning of the Boston naming test in cognitively normal African American and Caucasian older adults. *Journal of the International Neuropsychological Society, 15*(5), 758-768. DOI: 10.1017/S1355617709990361.

Peterson, D.A., Lucidi-Phillipi, C.A., Eagle, K.L., & Gage, F.H. (1994). Perforant path damage results in progressive neuronal death and somal atrophy in layer II of entorhinal cortex and functional impairment with increasing postdamage age. *Journal of Neuroscience, 14*(11 Pt 2), 6872-6885. DOI: 10.1523/JNEUROSCI.14-11-06872.1994.

Peterson, R.C. (2004). Mild cognitive impairment as a diagnostic entity. *Journal of Internal Medicine, 256*(3), 183-194. DOI: 10.1111/j.1365-2796.2004.01388.x.

Petrella, J.R., Coleman, R.E., & Doraiswamy, P.M. (2003). Neuroimaging and early diagnosis of Alzheimer disease: A look to the future. *Radiology, 226*(2), 315-336. DOI: 10.1148/radiol.2262011600.

Pettigrew, C., Soldan, A., Wang, J., Hohman, T., Dumitrescu, L., Albert, M., Blennow, K., Bittner, T., Moghekar, A., & BIOCARD Study Team (2025). Plasma biomarker trajectories: Impact of AD genetic risk and clinical progression. *Alzheimer's & Dementia (Amst), 17*(1), e70081. DOI: 10.1002/dad2.70081.

Piaceri, I., Nacmias, B., & Sorbi, S. (2013). Genetics of familial and sporadic Alzheimer's disease. *Frontiers in Bioscience (Elite Edition), 5*(1), 167-177. DOI: 10.2741/e605.

Piguet, O., Double, K.L., Kril, J.J., Harasty, J., Macdonald, V., McRitchie, D.A., & Halliday, G.M. (2009). White matter loss in healthy ageing: A postmortem analysis. *Neurobiology of Aging, 30*(8), 1288-1295. DOI: 10.1016/j.neurobiolaging.2007.10.015.

Porter, T., Burnham, S.C., Milicic, L., Savage, G., Maruff, P., Lim, Y.Y., Li, Q-X., Ames, D., Masters, C.L., Rainey-Smith, S., Rowe, C.C., Salvado, O., Groth, D., Verdile, G., Villemagne, V.L., & Laws, S.M. (2018). Utility of an Alzheimer's disease risk-weighted polygenic risk score for predicting rates of cognitive decline in preclinical Alzheimer's disease: A prospective longitudinal study. *Journal of Alzheimer's Disease, 66*(3), 1193-1211. DOI: 10.3233/JAD-180713.

Price, A.L., Zaitlen, N.A., Reich, D., & Patterson, N. (2010). New approaches to population stratification in genome-wide association studies. *Nature Reviews Genetics, 11*(7), 459-463. DOI: 10.1038/nrg2813.

Prieto, S., Valerio, K.E., Moody, J.N., Hayes, S.M., Hayes, J.P., & Alzheimer's Disease Neuroimaging Initiative (2020). Genetic risk for Alzheimer's disease moderates the association between medial temporal lobe volume and episodic memory performance among older adults. *Journal of Alzheimer's Disease, 76*(2), 591-600. DOI: 10.3233/JAD-191312.

Quide, Y., Watkeys, O.J., Girshkin, L., Kaur, M., Carr, V.J., Cairns, M.J., & Green, M.J. (2022). Interactive effects of polygenic risk and cognitive subtype on brain morphology in schizophrenia spectrum and bipolar disorder. *European Archives of Psychiatry and Clinical Neuroscience, 272(7)*, 1205-1218. DOI: 10.1007/s00406-022-01450-4.

Rajan, K.B., Weuve, J., Barnes, L.L., McAninch, E.A., Wilson, R.S., & Evans, D.A. (2021). Population estimate of people with clinical AD and mild cognitive impairment in the United States (2020-2060). *Alzheimer's & Dementia, 17*(12), 1966-1975. DOI: 10.1002/alz.12362.

Rall Jr, S.C., Weisgraber, K.H., & Mahley, R.W. (1982). Human apolipoprotein E, the complete amino acid sequence. *Journal of Biological Chemistry, 257*(8), 4171-4178.

Ramanan, V.K., Heckman, M.G., Lesnick, T.G., Przybelski, S.A., Cahn, E.J., Kosel, M.L., Murray, M.E., Mielke, M.M., Botha, H., Graff-Radford, J., Jones, D.T., Loew, V.J., Machulda, M.M., Jack Jr, C.R., Knopman, D.S., Peterson, R.C., Ross, O.A., & Vemuri, P. (2022). Tau polygenic risk scoring: A cost-effective aid for prognostic counselling in Alzheimer's disease. *Acta Neuropathologica, 143*(5), 571-583. DOI: 10.1007/s00401-022-02419-2.

Ramanan, V.K., Wang, X., Przybelski, S.A., Raghavan, S., Heckman, M.G., Batzler, A., Kosel, M.L., Hohman, T.J., Knopman, D.S., Graff-Radford, J., Lowe, V.J., Mielke, M.M., Jack Jr, C.R., Petersen, R.C., Ross, O.A., & Vemuri, P. (2020). Variants in PPP2R2B and IGF2BP3 are associated with higher tau deposition. *Brain Communications, 2*(2), fcaa159.
DOI: 10.1093/braincomms/fcaa159.

Ranlund, S., Calafato, S., Thygesen, J.H., Lin, K., Cahn, W., Crespo-Facorro, B., de Zwarte, S.M.C., Diez, A., Di Forti, M., GROUP, Iyegbe, C., Jablensky, A., Jones, R., Hall, M-H., Kahn, R., Kalaydjieva, L., Kravariti, E., McDonald, C., McIntosh, A.M., ... Bramon, E. (2017). A polygenic risk score analysis of psychosis endophenotypes across brain functional, structural, and cognitive domains. *American Journal of Medical Genetics Part B: Neuropsychiatric Genetics, 177*(1), 21-34. DOI: 10.1002/ajmg.b.32581.

Rao, S., Ghani, M., Guo, Z., Deming, Y., Wang, K., Sims, R., Mao, C., Yao, Y., Cruchaga, C., Stephan, D.A., & Rogaeva, E. (2018). An APOE-independent cis-eSNP on chromosome 19q13.32 influences tau levels and late-onset Alzheimer's disease risk. *Neurobiology of Aging, 66*, 178.e1-178.e8. DOI: 10.1016/j.neurobiolaging.2017.12.027.

Rao, Y.L., Ganaraja, B., Murlimanju, B.V., Joy, T., Krishnamurthy, A., & Agrawal, A. (2022). Hippocampus and its involvement in Alzheimer's disease: A review. *3 Biotech, 12*(2), 55.
DOI: 10.1007/s13205-022-03123-4.

Ray, J., Popli, G., & Fell, G. Association of cognition and age-related hearing impairment in the English Longitudinal Study of Ageing. *JAMA Otolaryngology Head & Neck Surgery, 144*(10), 876-882. DOI: 10.1001/jamaoto.2018.1656.

Raz, N., Lindenberger, U., Rodrigue, K.M., Kennedy, K.M., Head, D., Williamson, A., Dahle, C., Gerstorf, D., & Acker, J. D. (2005). Regional brain changes in aging healthy adults: General trends, individual differences and modifiers. *Cerebral Cortex, 15*(11), 1676-1689. DOI: 10.1093/cercor/bhi044.

Reagh, Z.M., Noche, J.A., Tustison, N.J., Delisle, D., Murray, E.A., & Yassa, M.A. (2018). Functional imbalance of anterolateral entorhinal cortex and hippocampal dentate/CA3 underlies age-related object pattern separation deficits. *Neuron, 97*(5), 1187-1198.e4. DOI: 10.1016/j.neuron.2018.01.039.

Reas, E.T., Shadrin, A., Frei, O., Motazedi, E., McEvoy, L., Bahrami, S., van der Meer, D., Makowski, C., Loughnan, R., Wang, X., Broce, I., Banks, S.J., Fominykh, V., Cheng, W., Holland, D., Smeland, O.B., Seibert, T., Selbaek, G., Fan, C.C., Andreassen, O.A., & Dale, A.M. (2023). Improved multimodal prediction from MCI to Alzheimer's disease combining genetics with quantitative brain MRI and cognitive measures. *Alzheimer's & Dementia, 19*(11), 5151-5158. DOI: 10.1002/alz.13112.

Rebeck, G.W., Reiter, J.S., Strickland, D.K., & Hyman, B.T. (1993). Apolipoprotein E in sporadic Alzheimer's disease: Allelic variation and receptor interactions. *Neuron, 11*(4), 575-580. DOI: 10.1016/0896-6273(93)90070-8.

Reiman, E.M., Chen, K., Liu, X., Bandy, D., Yu, M., Lee, W., Ayutyanont, N., Keppler, J., Reeder, S.A., Langbaum, J.B.S., Alexander, G.E., Klunk, W.E., Mathis, C.A., Price, J.C., Aizenstein, H.J., DeKosky, S.T., & Caselli, R.J. (2009). Fibrillar amyloid-β in cognitively normal people at 3 levels of genetic risk for Alzheimer's disease. *Proceedings of the National Academy of Sciences of the United States of America, 106*(16), 6820-6825. DOI: 10.1073/pnas.0900345106.

Reitz, C., Jun, G., Naj, A., Rajbhandary, R., Vardarajan, B.N., Wang, L-S., Valladares, O., Lin, C-F., Larson, E.B., Graff-Radford, N.R., Evans, D., De Jager, P.L., Crane, P.K., Buxbaum, J.D., Murell, J.R., Raj, T., Ertekin-Taner, N., Logue, M., Baldwin, C.T., … Mayeux, R. (2013). Variants in the ATP-binding cassette transporter (ABCA7), apolipoprotein E ε4, and the risk of late-onset Alzheimer disease in African Americans. *JAMA, 309*(14), 1483-1492. DOI: 10.1001/jama.2013.2973.

Rey, A. (1964). L'examen clinique en psychologie [the clinical psychological examination]. *Paris: Presses Universitaires de France*.

Riaz, M., Huq, A., Ryan, J., Orchard, S.G., Tiller, J., Lockery, J., Woods, R.L., Wolfe, R., Renton, A.E., Goate, A.M., Sebra, R., Schadt, E., Brodtmann, A., Shah, R.C., Storey, E., Murray, A.M., McNeil, J.J., & Lacaze, P. (2021). Effect of APOE and a polygenic risk score on incident dementia and cognitive decline in a healthy older population. *Aging Cell*, 20(6), e13384. DOI: 10.1111/acel.13384.

Ridge, P.G., Hoyt, K.B., Boehme, K., Mukherjee, S., Crane, P.K., Haines, J.L., Mayeux, R., Farrer, L.D., Pericak-Vance, M.A., Schellenberg, G.D., & Kauwe, J.S.K. (2016). Assessment of the genetic variance of late-onset Alzheimer's disease. *Neurobiology of Aging, 41*, 200.e13-200.e20. DOI: 10.1016/j.neurobiolaging.2016.02.024.

Ridge, P.G., Mukherjee, S., Crane, P.K., Kauwe, J.S., & Alzheimer's Disease Genetics Consortium (2013). Alzheimer's disease: analyzing the missing heritability. *PLoS One, 8*(11), e79771. DOI: 10.1371/journal.pone.0079771.

Risacher, S.L. & Saykin, A.J. (2013). Neuroimaging biomarkers of neurodegenerative diseases and dementia. *Seminars in Neurology, 33*(4), 386-416. DOI: 10.1055/s-0033-1359312.

Risacher, S.L., Kim, S., Shen, L., Nho, K., Foroud, T., Green, R.C., Petersen, R.C., Jack Jr, C.R., Aisen, P.A., Koeppe, R.A., Jagust, W.J., Shaw, L.M., Trojanowski, J.Q., Weiner, M.W., & Saykin, A.J. (2013). The role of apolipoprotein E (APOE) genotype in early mild cognitive impairment (E-MCI). *Frontiers in Aging Neuroscience, 5*, 11. DOI: 10.3389/fnagi.2013.00011.

Ritchey, M., Libby, L.A., & Ranganath, C. (2015). Chapter 3 - cortico-hippocampal systems involved in memory and cognition: The PMAT framework. *Progress in Brain Research, 219*, 45-64. DOI: 10.1016/bs.pbr.2015.04.001.

Ritchie, S.J., Hill, W.D., Marioni, R.E., Davies, G., Hagenaars, S.P., Harris, S.E., Cox, S.R., Taylor, A.M., Corley, J., Pattie, A., Redmond, P., Starr, J.M., & Deary, I.J. (2019). Polygenic predictors of age-related decline in cognitive ability. *Molecular Psychiatry, 25*(10), 2584-2598. DOI: 10.1038/s41380-019-0372-x.

Rodrigue, K.M. & Raz, N. (2004). Shrinkage of the entorhinal cortex over five years predicts memory performance in healthy adults. *Journal of Neuroscience, 24*(4), 956-963. DOI: 0.1523/JNEUROSCI.4166-03.2004.

Roe, J.M., Vidal-Piñeiro, D., Sørensen, Ø., Grydeland, H., Leonardsen, E.H., Lakunchykova, O., Pan, M., Mowinckel, A., Strømstad, M., Nawijn, L., Milaneschi, Y., Andersson, M., Pudas, S., Bråthen, A.C.S., Kransberg, J., Falch, E.S., Øverbye, K., Kievit, R.A., Ebmeier, K.P., ... Wang, Y. (2024). Brain change trajectories in healthy adults correlate with Alzheimer's related genetic variation and memory decline across life. *Nature Communications, 15*(1), 10651. DOI: 10.1038/s41467-024-53548-z.

Rogaeva, E., Meng, Y., Lee, J.H., Gu, Y., Kawarai, T., Zou, F., Katayama, T., Baldwin, C.T., Cheng, R., Hasegawa, H., Chen, F., Shibata, N., Lunetta, K.L., Pardossi-Piguard R., Bohm, C., Wakutani, Y., Cupples, L.A., Cuenco, K.T., Green, R.C., ... George-Hyslop, P. (2007). The neuronal sortilin-related receptor SORL1 is genetically associated with Alzheimer's disease. *Nature Genetics, 39*(2), 168-177. DOI: 10.1038/ng1943.

Roostaei, T., Felsky, D., Nazeri, A., De Lager, P.L., Schneider, J.A., Bennett, D.A., & Voineskos, A.N. (2018). Genetic influence of plasma homocysteine on Alzheimer's disease. *Neurobiology of Aging, 62,* 243.e7-243.e14. DOI: 10.1016/j.neurobiolaging.2017.09.033.

Rosen, A.C., Prull, M.W., Gabrieli, J.D.E., Stoub, T., O'Hara, R., Friedman, L., Yesavage, J.A., deToledo-Morrell, L. (2003). Differential associations between entorhinal and hippocampal volumes and memory performance in older adults. *Behavioural Neuroscience, 117*(6), 1150-1160. DOI: 10.1037/0735-7044.117.6.1150.

Rosen, W.G., Mohs, R.C., & Davis, K.L. (1984). A new rating scale for Alzheimer's disease. *American Journal of Psychiatry, 141*(11), 1356-1364. DOI: 10.1176/ajp.141.11.1356.

Rutten-Jacobs, L.C.A., Tozer, D.J., Duering, M., Malik, R., Dichgans, M., Markus, H.S., & Traylor, M. (2018). Genetic study of white matter integrity in UK Biobank (N=8448) and the overlap with stroke, depression, and dementia. *Stroke, 49*(6), 1340-1347. DOI: 10.1161/STROKEAHA.118.020811.

Sabuncu, M.R., Buckner, R.L., Smoller, J.W., Lee, P.H., Fischl, B., Sperling, R.A., & Alzheimer's Disease Neuroimaging Initiative (2012). The association between a polygenic Alzheimer score and cortical thickness in clinically normal subjects. *Cerebral Cortex, 22*(11), 2653-2661. DOI: 10.1093/cercor/bhr348.

Sabuncu, M.R., Desikan, R.S., Sepulcre, J., Yeo, B.T.T., Liu, H., Schmansky, N.J., Reuter, M., Weiner, M.W., Buckner, R.L., Sperling, R.A., Fischl, B., & Alzheimer's Disease Neuroimaging Initiative (2011). The dynamics of cortical and hippocampal atrophy in Alzheimer disease. *Archives of Neurology, 68*(8), 1040-1048. DOI: 10.1001/archneurol.2011.167.

Sampatakakis, S.N., Mourtzi, N., Hatzimanolis, A., & Scarmeas, N. (2025). Advances in genetic risk scores for Alzheimer's disease and dementia: A systematic review. *Neurology International, 17*(7), 99. DOI: 10.3390/neurolint17070099.

Sanchez, J.S., Becker, J.A., Jacobs, H.I.L., Hanseeuw, B.J., Jiang, S., Schultz, A.P., Properzi, M.J., Katz, S.R., Beiser, A., Satizabal, C.L., O'Donnell, A., DeCarli, C., Killiany, R., El Fakhri, G., Normandin, M.D., Gomez-Isla, T., Quiroz, Y.T., Rentz, D.M., Sperling, R.A., ... Johnson, K.A. (2021). The cortical origin and initial spread of medial temporal tauopathy in Alzheimer's disease assessed with positron emission tomography. *Science Translational Medicine, 13*(577), eabc0655. DOI: 10.1126/scitranslmed.abc0655.

Sapkota, S., & Dixon, R.A. (2018). A network of genetic effects on non-demented cognitive aging: Alzheimer's genetic risk (CLU + CR1 + PICALM) intensifies cognitive aging genetic risk (COMT + BDNF) selectively for APOEε4 carriers. *Journal of Alzheimer's Disease, 62*(2), 887-900. DOI: 10.3233/JAD-170909.

Saunders, A.M., Strittmatter, W.J., Schmechel, D., St. George-Hyslop, P.H., Pericak-Vance, M.A., Joo, S.H., Rosi, B,L., Gusella, J.F., Crapper-MacLachlan, D.R., Alberts, M.J., Hulette, C., Crain, B., Goldgaber, D., & Roses, A.D. (1993). Association of apolipoprotein E allele epsilon 4 with late-onset familial and sporadic Alzheimer's disease. *Neurology, 43*(8), 1467-1472. DOI: 10.1212/wnl.43.8.1467.

Saykin, A.J., Shen, L., Yao, X., Kim, S., Nho, K., Risacher, S.L., Ramanan, V.K., Foroud, T.M., Faber, K.M., Sarwar, N., Munsie, L.M., Hu, X., Soared, H.D., Potkin, S.G., Thompson, P.A., Kauwe, J.S.K., Kaddurah-Daouk, R., Green, R.C., Toga, A.W., Weiner, M.W., & Alzheimer's Disease Neuroimaging Initiative (2015). Genetic studies of quantitative MCI and AD phenotypes in ADNI: Progress, opportunities, and plans. *Alzheimer's & Dementia, 11*(7), 792-814. DOI: 10.1016/j.jalz.2015.05.009.

Scharre, D.W., (2019). *Practical Neurology.* Preclinical, prodromal, and dementia stages of Alzheimer's disease. Available at: https://practicalneurology.com/articles/2019-

june/preclinical-prodromal-and-dementia-stages-ofalzheimers-disease (Accessed: December 2022).

Schmechel, D.E., Saunders, A.M., Strittmatter, W.J., Crain, B.J., Hulette, C.M., Joo, S.H., Pericak-Vance, M.A., Goldgaber, D., & Roses, A.D. (1993). Increased amyloid β-peptide deposition in cerebral cortex as a consequence of apolipoprotein E genotype in late-onset Alzheimer disease. *Proceeding of the National Academy of Sciences of the United States of America, 90(2)*, 9649-9653. DOI: 10.1073/pnas.90.20.9649.

Scholl, M., Lockhart, S.N., Schonhaut, D.R., O'Neil, J.P., Janabi, M., Ossenkoppele, R., Baker, S.L., Vogel, J.W., Faria, J., Schwimmer, H.D., Rabinovici, G.D., & Jagust, W.J. (2016). PET Imaging of tau deposition in the aging human brain. *Neuron, 89*(5), 971-982. DOI: 10.1016/j.neuron.2016.01.028.

Schultz, A.P., Chhatwal, J.P., Hedden, T., Mormino, E.C., Hanseeuw, B.J., Sepulcre, J., Huijbers, E., LaPoint, M., Buckley, R.F., Johnson, K.A., & Sperling, R.A. (2017). Phases of hyperconnectivity and hypoconnectivity in the default mode and salience networks track with amyloid and tau in clinically normal individuals. *The Journal of Neuroscience, 37*(16), 4323-4331. DOI: 10.1523/JNEUROSCI.3263-16.2017.

Schultz, S.A., Boots, E.A., Darst, B.F., Zetterberg, H., Blennow, K., Edwards, D.F., Koscik, R.L., Carlsson, C.M., Gallagher, C.L., Bendlin, B.B., Asthana, S., Sager, M.A., Hogan, K.J., Hermann, B.P., Cook, D.B., Johnson, S.C., Engelman, C.D., & Okonkwo, O.C. (2017). Cardiorespiratory fitness alters the influence of a polygenic risk score on biomarkers of AD. *Neurology, 88*(17), 1650-1658. DOI: 10.1212/WNL.0000000000003862.

Sengoku, R. (2019). Aging and Alzheimer's disease pathology. *Neuropathology, 40*(1), 22-29. DOI: 10.1111/neup.12626.

Senova, S., Fomenko, A., Gondard, E., & Lozano, A.M. (2020). Anatomy and function of the fornix in the context of its potential as a therapeutic target. *Journal of Neurology Neurosurgery and Psychiatry, 91*(5), 547-559. DOI: 10.1136/jnnp-2019-322375.

Seripa, D., Matera, M.G., Daniele, A., Bizzaro, A., Rinaldi, M., Gravina, C., Bisceglia, L., Corbo, R.M., Panza, F., Solfrizzi, V., Fazio, V.M., Dal Forno, G., Masullo, C., Dallapiccola, B., & Pilotto, A.

(2007). The missing APOE allele. *Annals of Human Genetics*, 71(Pt 4), 496-500. DOI: 10.1111/j.1469-1809.2006.00344.x

Serrano-Pozo, A., & Growdon, J.H. (2019). Is Alzheimer's disease risk modifiable? *Journal of Alzheimer's Disease, 67*(3), 795-819. DOI: 10.3233/JAD181028.

Sery, O., Povova, J., Misek, I., Pesak, L., & Janout, V. (2013). Molecular mechanisms of neuropathological changes in Alzheimer's disease: a review. *Folia Neuropathologica, 51*(1), 1-9. DOI: 10.5114/fn.2013.34190.

Sha, Z., Schijven, D., Fisher, S.E., Francks, C. (2023). Genetic architecture of the white matter connectome of the human brain. *Science Advances, 9*(7), eadd2870. DOI: 10.1126/sciadv.add2870.

Shaw, L.M., Vanderstichele, H., Knapik-Czajka, M., Clark, C.M., Aisen, P.S., Petersen, R.C., Blennow, K., Soares, H., Simon, A., Lewczuk, P., Dean, R., Siemers, E., Potter, W., Lee, V.M., Trojanowski, J.Q., & Alzheimer's Disease Neuroimaging Initiative (2009). Cerebrospinal fluid biomarker signature in Alzheimer's disease neuroimaging initiative subjects. *Annals of Neurology, 65*(4), 403-413. DOI: 10.1002/ana.21610.

Sheline, Y.I., & Raichle, M.E. (2013). Resting state functional connectivity in preclinical Alzheimer's disease: A review. *Biological Psychiatry, 74*(5), 340-347. DOI. 10.1016/j.biopsych.2012.11.028.

Shi, F., Liu, B., Zhou, Y., Yu, C., & Jiang, T. (2009). Hippocampal volume and asymmetry in mild cognitive impairment and Alzheimer's disease: Meta-analyses of MRI studies. *Hippocampus, 19*(11), 1055-1064. DOI: 10.1002/hipo.20573.

Simic, G., Leko, M.B., Wray, S., Harrington, C., Delalle, I., Jovanov-Milosevis, N., Bazadona, D., Buee, L., de Silva, R., Di Giovanni, G., Wischik, C., & Hof, P.R. (2016). Tau protein hyperphosphorylation and aggregation in Alzheimer's disease and other tauopathies, and possible neuroprotective strategies. *Biomolecules, 6*(1), 6. DOI: 10.3390/biom6010006.

Simoes, B., Vassos, E., Shergill, S., McDonald, C., Toulopoulou, T., Kalidindi, S., Kane, F., Murray, R., Bramon, E., Ferreira, H., & Prata, D. (2020). Schizophrenia polygenic risk score influence on

white matter microstructure. *Journal of Psychiatric Research, 121*, 62-67. DOI: 10.1016/j.jpsychires.2019.11.011.

Sims, R., Hill, M., & Williams, J. (2020). The multiplex model of the genetics of Alzheimer's disease. *Nature Neuroscience, 23*(3), 311-322. DOI: 10.1038/s41593-020-0599-5.

Sims, R., van der Lee, S., Naj, A. C., Bellenguez, C., Badarinarayan, Jakobsdottir, J., Kunkle, B. W., Boland, A., Raybould, R., Bis, J.C., Martin, E.R., Grenier-Boley, B., Heilmann-Heimbach, S., Chouraki, V., Kuzma, A.B., Sleegers, K., Vronskaya, M., Ruiz, A., Graham, R.R., ... Schellenberg, G.D. (2017). Rare coding variants in PLCG2, ABI3, and TREM2 implicate microglial-mediated innate immunity in Alzheimer's disease. *Nature Genetics, 49(9)*, 1373-1384. DOI: 10.1038/ng.3916.

Singh, V., Chertkow, H., Lerch, J.P., Evans, A.C., Dorr, A.E., & Kabani, N.J. (2006). Spatial patterns of cortical thinning in mild cognitive impairment and Alzheimer's disease. *Brain, 129*(Pt 11), 2885-2893. DOI: 10.1093/brain/awl256.

Singleton, A., & Hardy, J. (2011). A generalizable hypothesis for the genetic architecture of disease: pleomorphic risk loci. *Human Molecular Genetics, 20*(R2), R158-162. DOI: 10.1093/hmg/ddr358.

Skoog, I., Kern, S., Najar, J., Guerreiro, R., Bras, J., Waern, M., Zetterberg, H., Blennow, K., & Zettergren, A. (2021). A non-APOE polygenic risk score for Alzheimer's disease is associated with cerebrospinal fluid neurofilament light in a representative sample of cognitively unimpaired 70-year olds. *Journals of Gerontology: Series A, 76*(6), 983-990. DOI: 10.1093/gerona/glab030.

Sloan, C.D., Shen, L., West, J.D., Wishart, H.A., Flashman, L.A., Rabin, L.A., Santulli, R.B., Geurin, S.J., Rhodes, C.H., Tsongalis, G.J., McAllister, T.W., Ahles, T.A., Lee, S.L., Moore, J.H., & Saykin, A.J. (2010). Genetic pathway-based hierarchical clustering analysis of older adults with cognitive complaints and amnestic mild cognitive impairment using clinical and neuroimaging phenotypes. *American Journal of Medical Genetics Part B: Neuropsychiatry Genetics, 153B*(5), 1060-1069. DOI: 10.1002/ajmg.b.31078.

Soldan, A., Wang, J., Pettigrew, C., Davatzikos, C., Erus, G., Hohman, T.J., Dumitrescu, L., Bilgel, M., Resnick, S.M., Rivera-Rivera, L.A., Langhough, R., Johnson, S.C., Benzinger, T., Morris, J.C., Laws, S.M., Fripp, J., Masters, C.L., & Albert, M.S. (2024). Alzheimer's disease genetic risk and

changes in brain atrophy and white matter hyperintensities in cognitively unimpaired adults. *Brain Communications, 6*(5), fcae276. DOI: 10.1093/braincomms/fcae276.

Sorg, C., Riedl, V., Muhlau, M., Calhoun, V.D., Eichele, T., Lae, L., Drzezga, A., Forstl, H., Kurz, A., Zimmer, C., & Wohlschlager, A.M. (2007). Selective changes of resting-state networks in individuals at rish for Alzheimer's disease. *Proceedings of the National Academy of Sciences of the United States of America, 104*(47), 18760-18765. DOI: 10.1073/pnas.0708803104.

Sperling, R. (2007). Functional MRI studies of associative encoding in normal aging, mild cognitive impairment, and Alzheimer's disease. *Annals of the New York Academy of Sciences, 1097*(1), 146-155. DOI: 10.1196/annals.1379.009.

Sperling, R.A., LaViolette, P.S., O'Keefe, K., O'Brien, J., Rentz, D.M., Pihlajamaki, M., Marshall, G., Hyman, B.T., Selkoe, D.J., Hedden, T., Buckner, R.L., Becker, J.A., & Johnson, K.A. (2009). Amyloid deposition is associated with impaired default network function in older persons without dementia. *Neuron, 63*(2), 178-188. DOI: 10.1016/j.neuron.2009.07.003.

Startin, C.M., Hamburg, S., Hithersay, R., Al-Janabi, T., Mok, K.Y., Hardy, J., & Strydom, A. (2019). Cognitive markers of preclinical and prodromal Alzheimer's disease in Down syndrome. *Alzheimer's & Dementia, 15*(2), 245-257. DOI: 10.1016/j.jalz.2018.08.009.

Steventon, J.J., Lancaster, T.M., Baker, E.S., Bracher-Smith, M., Escott-Price, V., Ruth, K.S., Davies, W., Caseras, X., & Murphy, K. (2023). Menopause age, reproductive span and hormone therapy duration predict the volume of medial temporal lobe brain structures in postmenopausal women. *Psychoneuroendocrinology, 158*, 106393. DOI: 10.1016/j.psyneuen.2023.106393.

Stocker, H., Trares, K., Beyer, L., Perna, L., Rujescu, D., Holleczek, B., Beyreuther, K., Gerwert, K., Schöttker, B., & Brenner, H. (2023). Alzheimer's polygenic risk scores, APOE, Alzheimer's disease risk, and dementia-related blood biomarker levels in a population-based cohort study followed over 17 years. Alzheimer's Research & Therapy, 15(1), 129. DOI: 10.1186/s13195-023-01277-8.

Stonnington, C.M., Tan, G., Kloppel, S., Chu, C., Draganski, B., Jack Jr, C.R., Chen, K., Ashburner, J., & Frackowiak, R.S.J. (2008). Interpreting scan data acquired from multiple scanners: A study with Alzheimer's disease. *NeuroImage, 39*(3), 1180-1185.
DOI: 10.1016/j.neuroimage.2007.09.066.

Sun, Y., Zhu, J., Zhou, D., Canchi, S., Wu, C., Cox, N. J., Rissman, R. A., Gamazon, E. R., & Wu, L. (2021). A transcriptome-wide association study of Alzheimer's disease using prediction models of relevant tissues identifies novel candidate susceptibility genes. *Genome Medicine, 13*(141). DOI: 10.1186/s13073-021-00959-y.

Sunderland, T., Mirza, N., Putnam, K.T., Linker, G., Bhupali, D., Durham, R., Soares, H., Kimmel, L., Friedman, D., Bergeson, J., Csako, G., Levy, J.A., Bartko, J.J., & Cohen, R.M. (2004). Cerebrospinal fluid beta-amyloid1-42 and tau in control subjects at risk for Alzheimer's disease: The effect of APOE epsilon4 allele. *Biological Psychiatry, 56*(9), 670-676. DOI: 10.1016/j.biopsych.2004.07.021.

Tachibana, M., Holm, M.L., Liu, C.C., Shinohara, M., Aikawa, T., Oue, H., Yamazaki, Y., Martens, Y.A., Murray, M.E., Sullivan, P.M., Weyer, K., Glerup, S., Dickson, D.W., Bu, G., & Kanekiyo, T. (2019). APOE4-mediated amyloid-β pathology depends on its neuronal receptor LRP1. *Journal of Clinical Investigation, 129*(3), 1272-1277. DOI: 10.1172/JCI124853.

Tan, C.H., Bonham, L.W., Fan, C.C., Mormino, E.C., Sugrue, L.P., Broce, I.J., Hess, C.P., Yokoyama, J.S., Rabinovici, G.D., Miller, B.L., Yaffe, K., Schellenberg, G.D., Kauppi, K., Holland, D., McEvoy, L.K., Kukull, W.A., Tosun, D., Weiner, M.W., Sperling, R.A., ... Alzheimer's Disease Neuroimaging Initiative. (2019). Polygenic hazard score, amyloid deposition and Alzheimer's neurodegeneration. *Brain, 142*(2), 460-470. DOI: 10.1093/brain/awy327.

Tan, C.H., Fan, C.C., Mormino, E.C., Sugrue, L.P., Broce, I.J., Hess, C.P., Dillon, W.P., Bonham, L.W., Yokoyama, J.S., Karch, C.M., Brewer, J.B., Rabinovici, G.D., Miller, B.L., Schellenberg, G.D., Kauppi, K., Feldman, H.A., Holland, D., McEvoy, L.K., Hyman, B.T., Bennett, D.A., Andreassem, O.A., Dale, A.M., & Desikan, R.S. (2018). Polygenic hazard score: An enrichment marker for Alzheimer's associated amyloid and tau deposition. *Acta Neuropathologica, 135*(1), 85-93. DOI: 10.1007/s00401-017-1789-4.

Tank, R., Ward, J., Flegal, K.E., Smith, D.J., Bailey, M.E.S., Cavanagh, J., & Lyall, D.M. (2022). Association between polygenic risk for Alzheimer's disease, brain structure and cognitive abilities in UK Biobank. *Neuropsychopharmacology, 47*(2), 564-569. DOI: 10.1038/s41386-021-01190-4.

Taragano, F.E., Allegri, R.F., Krupitzki, H., Sarasola, D., Serrano, C.M., Lon, L., & Lyketsos, C.G. (2009). Mild behavioral impairment and risk of dementia: a prospective cohort study of 358 patients. *Journal of Clinical Psychiatry, 70*(4), 584-592. DOI: 10.4088/jcp.08m04181.

Teipel, S.J., Grothe, M., Lista, S., Toschi, N., Garaci, F.G., & Hampel, H. (2013). Relevance of magnetic resonance imaging for early detection and diagnosis of Alzheimer disease. *Medical Clinics of North America, 97(3)*, 399-424. DOI: 10.1016/j.mcna.2012.12.013.

Teipel, S.J., Stahl, R., Dietrich, O., Schoenberg, S.O., Perneczky, R., Bokde, A.L.W., Reiser, M.F., Moller, H-J., & Hampel, H. (2007). Multivariate network analysis of fiber tract integrity in Alzheimer's disease. *NeuroImage, 34*(3), 985-995. DOI: 10.1016/j.neuroimage.2006.07.047.

Thal, D.R., Rub, U., Orantes, M., & Braak, H. (2002). Phases of Aβ-deposition in the human brain and its relevance for the development of AD. *Neurology, 58(12)*, 1791-1800. DOI: 10.1212/wnl.58.12.1791.

The Brainstorm Consortium, Anttila, V., Bulik-Sulliva, B., Finucane, H.K., Walters, R.K., Bras, J., Duncan, L., Escott-Price, V., Falcone, G.J., Gormley, P., Malik, R., Patsopoulos, N.A., Ripke, S., Wei, Z., Yu, D., Lee, P.H., Turley, P., Grenier-Boley, B., Chouraki, V., ... Murray, R. (2018). Analysis of shared heritability in common disorders of the brain. *Science, 360*(6395), eaap8757. DOI: 10.1126/science.aap8757

The National Center for Biotechnology Information (2025). *Gene*. Available at: https://www.ncbi.nlm.nih.gov/gene/ (Accessed: August 2025).

Thompson, L.I., Cummings, M., Emrani, S., Libon, D.J., Ang, A., Karjadi, C., Au, R., & Liu, C. (2023). Digital clock drawing as an Alzheimer's disease susceptibility biomarker: Associations with genetic risk score and APOE in older adults. *Journal of Prevention of Alzheimer's Disease, 11*(1), 79-87. DOI: 10.14283/jpad.2023.48.

Thornton, T.A., & Bermejo, J.L. (2014). Local and global ancestry inference, and applications to genetic association analysis for admixed populations. *Genetic Epidemiology, 38 Suppl 1* (01), S5-S12. DOI: 10.1002/gepi.21819.

Tiraboschi, P., Hansen, L.A., Masliah, E., Alford, M., Thal, L.J., & Corey-Bloom, J. (2004). Impact of APOE genotype on neuropathologic and neurochemical markers of Alzheimer disease. *Neurology, 62*(11), 1977-1983. DOI: 10.1212/01.wnl.0000128091.92139.0f.

Tohgi, H., Takahashi, S., Kato, E., Homma, A., Niina, R., Sasaki, K., Yonezawa, H., & Sasaki, M. (1997). Reduced size of right hippocampus in 39- to 80-year-old mornal subjects carrying the apolipoprotein E ε4 allele. *Neuroscience Letters, 236*(1), 21-24. DOI: 10.1016/S0304-3940(97)00743-X.

Tomassen, J., den Braber, A., van der Lee, S.J., Reus, L.M., Konijnenberg, E., Carter, S.F., Yaqub, M., van Berckel, B.N.M., Collij, L.E., Boomsma, D.I., de Geus, E.J.C., Scheltens, P., Herholz, K., Tijms, B.M., & Visser, P.J. (2022). Amyloid-β and APOE genotype predict memory decline in cognitively unimpaired older individuals independently of Alzheimer's disease polygenic risk score. *BMC Neurology, 22*(1), 484. DOI: 10.1186/s12883-022-02925-6.

Tomiyama, T., Nagata, T., Shimada, H., Teraoka, R., Fukushima, A., Kanemitsu, H., Takuma, H., Kuwano, R., Imagawa, M., Ataka, S., Wada, Y., Yoshioka, E., Nishizaki, T., Watanbe, Y., & Mori, H. (2008). A new amyloid B variant favoring oligomerization in Alzheimer's-type dementia. *Annals of Neurology*, 63(3), 377-387. DOI: 10.1002/ana.21321.

Torkamani, A., Wineinger, N.E., & Topol, E.J. (2018). The personal and clinical utility of polygenic risk scores. *Nature Reviews Genetics, 19(9)*, 581-590. DOI: 10.1038/s41576-018-0018-x.

Trampush, J.W., Yang, M.L., Yu, J., Knowles, E., Davies, G., Liewald, D.C., Starr, J.M., Djurovic, S., Melle, I., Sundet, K., Christoforou, A., Reinvang, I., DeRosse, P., Lundervold, A.J., Steen, V.M., Espeseth, T., Räikkönen, K., Widen, E., Palotie, A., ... Lencz, T. (2017). GWAS meta-analysis reveals novel loci and genetic correlates for general cognitive function: a report from the COGENT consortium. *Molecular Psychiatry, 22*(3), 336-345. DOI: 10.1038/mp.2016.244.

Tripathi, M., Tripathi, M., Damle, N., Kushwaha, S., Jaimini, A., D'Souza, M.M., Sharma, R., Saw, S., & Mondal, A. (2014). Differential diagnosis of neurodegenerative dementias using metabolic phenotypes on F-18 FDG PET/CT. *The Neuroradiology Journal, 27*(1), 13-21. DOI: 10.15274/NRJ-2014-10002.

Uylings, H.B.M., & de Brabander, J.M. (2002). Neuronal changes in normal human aging and Alzheimer's disease. *Brain and Cognition, 49*(3), 268-276. DOI: 10.1006/brcg.2001.1500.

Vacher, M., Dore, V., Porter, T., Milicic, L., Villemagne, V.L., Bourgeat, P., Burnham, S.C., Cox, T., Masters, C.L., Rowe, C.C., Fripp, J., Doecke, J.D., & Laws, S.M. (2022b). Assessment of a polygenic hazard score for the onset of pre-clinical Alzheimer's disease. *BMC Genomics, 23*(1), 401. DOI: 10.1186/s12864-022-08617-2.

Vacher, M., Porter, T., Milicic, L., Bourgeat, P., Dore, V., Villemagne, V.L., Laws, S.M., & Doecke, J.D. (2022a). A targeted association study of blood-brain barrier gene SNPs and brain atrophy. *Journal of Alzheimer's Disease, 86*(4), 1817-1829. DOI: 10.3233/JAD-210644.

van der Kant, R., Goldstein, L.S.B., & Ossenkoppele, R. (2020). Amyloid-β-independent regulators of tau pathology in Alzheimer disease. *Nature Reviews Neuroscience, 21*(1), 21-35. DOI: 10.1038/s41583-019-0240-3.

van der Lee, S., Wolters, F.J., Ikram, M.K., Hofman, A., Ikram, A.A., Amin, N., & van Duijn, C.M. (2018). The effect of APOE and other common genetic variants on the onset of Alzheimer's disease and dementia: A community-based cohort study. *Lancet Neurology, 17*(5), 434-444. DOI: 10.1016/S1474-4422(18)30053-X.

van Meurs, J.B., Pare, G., Schwartz, S.M., Hazra, A., Tanaka, T., Vermeulen, S.H., Cotlarciuc, I., Yuan, X., Mälarstig, A., Bandinelli, S., Bis, J.C., Blom, H., Brown, M.J., Chen, C., Chen, Y.D., Clarke, R.J., Dehghan, A., Erdmann, J., Ferrucci, L., ... Ahmadi KR. (2013). Common genetic loci influencing plasma homocysteine concentrations and their effect on risk of coronary artery disease. *American Journal of Clinical Nutrition, 98*(3), 668-676. DOI: 10.3945/ajcn.112.044545.

van Oostveen, W.M. & de Lange, E.C.M. (2021). Imaging techniques in Alzheimer's disease: A review of applications in early diagnosis and longitudinal monitoring. *International Journal of Molecular Sciences, 22*(4), 2110. DOI: 10.3390/ijms22042110.

van Os, J., & Kapur, S. (2009). Schizophrenia. *Lancet, 374*(9690), 635-645. DOI: 10.1016/S0140-6736(09)60995-8.

van Rossum, I.A., Visser, P.J., Knol, D.L., van der Flier, W.M., Teunissen, C.E., Barkhof, F., Blankenstein, M.A., & Scheltens, P. (2012). Injury markers but not amyloid markers are associated with rapid progression from mild cognitive impairment to dementia in Alzheimer's disease. *Journal of Alzheimer's Disease, 29*(2), 319-327. DOI: 10.3233/JAD-2011-111694.

Vemuri, P., Wiste, H.J., Weigand, S.D., Knopman, D.S., Shaw, L.M., Trojanowski, J.Q., Aisen, P.S., Weiner, M., Petersen, R.C., Jack, C.R. Jr., & Alzheimer's Disease Neuroimaging Initiative (2010). Effect of apolipoprotein E on biomarkers of amyloid load and neuronal pathology in Alzheimer disease. *Annals of Neurology, 67*(3), 308-16. DOI: 10.1002/ana.21953.

Vermunt, L., Sikkes, S.A.M., van den Hout, A., Handels, R., Bos, I., van der Flier, W.M., Kern, S., Ousset, P-J., Maruff, P., Skoog, I., Verhey, F.R.J., Freud-Levi, Y., Tsolaki, M., Wallin, A.K., Rikkert, M.O., Soininen, H., Spiru, L., Zetterberg, H., Blennow, K., ... ICTUS/DSA study groups (2019). Duration of preclinical, prodromal, and dementia stages of Alzheimer's disease in relation to age, sex, and APOE genotype. *Alzheimer's & Dementia, 15*(7), 888-898. DOI: 10.1016/j.jalz.2019.04.001.

Vickers, J.C., Mitew, S., Woodhouse, A., Fernandez-Martos, C.M., Kirkcaldie, M.T., Canty, A.J., McCormack, G.H., & Kind, A.E. (2016). Defining the earliest pathological changes of Alzheimer's disease. *Current Alzheimer Research, 13*(3), 281-287. DOI: 10.2174/1567205013666151218150322.

Villain, N., Desgranges, B., Viader, F., de la Sayette, V., Mezenge, F., Landeau, B., Baron, J-C., Eustache, F., & Chetelat, G. (2008). Relationships between hippocampal atrophy, white matter disruption, and gray matter hypometabolism in Alzheimer's disease. *Journal of Neuroscience, 28*(24), 6174-6181. DOI: 10.1523/JNEUROSCI.1392-08.2008.

Villemagne, V.L., Pike, K.E., Chételat, G., Ellis, K.A., Mulligan, R.S., Bourgeat, P., Ackermann, U., Jones, G., Szoeke, C., Salvado, O., Martins, R., O'Keefe, G., Mathis, C.A., Klunk, W.E., Ames, D., Masters, C.L., & Rowe, C.C. (2011). Longitudinal assessment of Aβ and cognition in aging and Alzheimer disease. *Annals of Neurology, 69*(1), 181-192. DOI: 10.1002/ana.22248.

Vogel, J.W., Young, A.L., Oxtoby, N.P., Smith, R., Ossenkoppele, R., Strandberg, O.T., La Joie, R., Aksman, L.M., Grothe, M.J., Iturria-Medina, Y., Pontecorvo, M.J., Devous, M.D., Rabinovici, G.D., Alexander, D.C., Lyoo, C.H., Evans, A.C. & Hansson, O. (2021). Four distinct trajectories of tau deposition identified in Alzheimer's disease. *Nature Medicine, 27*(5), 871-881. DOI: 10.1038/s41591-021-01309-6.

Voyle, N., Patel, H., Folarin, A., Newhouse, S., Johnston, C., Visser, P.J., Dobson, R.J., Kiddle, S.J., EDAR and DESCRIPA study groups, & Alzheimer's Disease Neuroimaging Initiative (2016).

Genetic risk as a marker of amyloid-β and tau burden in cerebrospinal fluid. *Journal of Alzheimer's Disease, 55*(4), 1417-1427. DOI: 10.3233/JAD-160707.

Walton, E., Turner, J., Gollub, R.L., Manoach, D.S., Yendiki, A., Ho, B-C., Sponheim, S.R., Calhoun, V.D., & Ehrlich, S. (2013). Cumulative genetic risk and prefrontal activity in patients with schizophrenia. *Schizophrenia Bulletin, 39*(3), 703-711. DOI: 10.1093/schbul/sbr190.

Wang, H.F., Zhang, W., Rolls, E.T., Li, Y., Wang, L., Ma, Y.H., Kang, J., Feng, J., Yu, J.T., & Cheng, W. (2022). Hearing impairment is associated with cognitive decline, brain atrophy and tau pathology. *EBioMedicine, 86*, 104336. DOI: 10.1016/j.ebiom.2022.

Wang, K., Liang, M., Wang, L., Tian, L., Zhang, X., Li, K., & Jiang, T. (2007). Altered functional connectivity in early Alzheimer's disease: A resting-state fMRI study. *Human Brain Mapping, 28(10)*, 967-978. DOI: 10.1002/hbm.20324.

Wang, T., Han, Z., Yang, Y., Tian, R., Zhou, W., Ren, P., Wang, P., Zong, J., Hu, Y., & Jiang, Q. (2019). Polygenic risk score for Alzheimer's disease is associated with Ch4 volume in normal subjects. *Frontiers in Genetics, 10*, 519. DOI: 10.3389/fgene.2019.00519.

Wang, X., Wang, X., Edland, S.D., Broce, I.J., Dale, A.M., Banks, S.J. & Alzheimer's Disease Neuroimaging Initiative (2024). Enrichment for clinical trials of early AD: Combining genetic risk factors and plasma p-tau as screening instruments. *Alzheimer's & Dementia, 20*(12), 8484-8502. DOI: 10.1002/alz.14284.

Wang, Z., Chen, Y., Gong, K., Zhao, B., Ning, Y., Chen, M., Li, Y., Ali, M., Timsina, J., Liu, M., Cruchaga, C., & Jia, J. (2025). Cerebrospinal fluid proteomics identification of biomarkers for amyloid and tau PET stages. *Cell Reports Medicine, 6*(4), 102031. DOI: 10.1016/j.xcrm.2025.102031.

Ward, A., Tardiff, S., Dye, C., & Arrighi, H.M. (2013). Rate of conversion from prodromal Alzheimer's disease to Alzheimer's dementia: A systematic review of the literature. *Dementia and Geriatric Cognitive Disorders Extra, 3*(1), 320-332. DOI: 10.1159/000354370.

Wattmo, C., Blennow, K., & Hansson, O. (2020). Cerebro-spinal fluid biomarker levels: Phosphorylated tau (T) and total tau (N) as markers for rate of progression in Alzheimer's disease. *BMC Neurology, 20*(1), 10. DOI: 10.1186/s12883-019-1591-0.

Weber, C.J., Carrillo, M.C., Jagust, W., Jack Jr, C.R., Shaw, L.M., Trojanowski, J.Q., Saykin, A.J., Beckett, L.A., Sur, C., Rao, N.P., Mendez, P.C., Black, S.E., Li, K., Iwatsubo, T., Chang, C-C., Sosa, A.L., Rowe, C.C., Perrin, R.J., Morris, J.C., Healan, A.M.B., Hall, S.E., & Weiner, M.W. (2021). The worldwide Alzheimer's disease neuroimaging initiative: ADNI-3 updates and global perspectives. *Alzheimer's & Dementia: Translational Research & Clinical Interventions, 7*(1), e12226. DOI: 10.1002/trc2.12226.

Wechsler, D. (1945). A standardized memory scale for clinical use. *Journal of Psychology: Interdisciplinary and Applied, 19*, 87–95. DOI: 10.1080/00223980.1945.9917223

Wennberg, A.M., Tosakulwong, N., Lesnick, T.G., Murray, M.W., Whitwell, J.L., Liesinger, A.M., Petrucelli, L., Boeve, B.F., Parisi, J.E., Knopman, D.S., Petersen, R.C., Dickson, D.W., & Josephs, K.A. (2018). Association of apolipoprotein E ε4 (11), with transactive response DNA-binding protein 43. *JAMA Neurology, 75*(11), 1347-1354. DOI: 10.1001/jamaneurol.2018.3139.

Whalley, H.C., Adam, M.J., Hall, L.S., Clarke, T-K., Fernandez-Pujals, A.M., Gibson, J., Wigmore, E., Hafferty, J., Hagenaars, S.P., Davies, G., Campbell, A., Hayward, C., Lawrie, S.M., Porteous, D.J., Deary, I.J., & McIntosh, A.M. (2016). Dissection of major depressive disorder using polygenic risk scores for schizophrenia in two independent cohorts. *Translational Psychiatry, 6*(11), e938. DOI: 10.1038/tp.2016.207.

Whitwell, J.L., Graff-Radford, J., Tosakulwong, N., Weigand, S.D., Machulda, M., Senjem, M.L., Schwarz, C.G., Spychalla, A.J., Jones, D.T., Drubach, D.A., Knopman, D.S., Boeye, B.F., Ertekin-Taner, N., Petersen, R.C., Lowe, V.J., Jack Jr, C.R., & Josephs, K.A. (2018). [18F]AV-1451 clustering of entorhinal and cortical uptake in Alzheimer's disease. *Annals of Neurology, 83*(2), 248-257. DOI: 10.1002/ana.25142.

Whitwell, J.L., Josephs, K.A., Murray, M.E., Kantarci, K., Przybelski, S.A., Weigand, S.D., Vemuri, P., Senjem, M.L., Parisi, J.E., Knopman, D.S., Boeve, B.F., Petersen, R.C., Dickson, D.W., & Jack Jr, C.R. (2008). MRI correlates of neurofibrillary tangle pathology at autopsy: a voxel-based morphometry study. *Neurology, 71*(10), 743-749. DOI: 10.1212/01.wnl.0000324924.91351.7d.

Wightman, D.P., Jansen, I.E., Savage, J.E., Shadrin, A.A., Bahrami, S., Holland, D., Rongve, A., Borte, S., Winsvold, B.S., Drange, O.K., Martinsen, A.E., Skogholt, A.H., Willer, C., Brathen, G., Bosnes, I., Nielsen, J.B., Fritsche, L.G., Thomas, L.F., Pedersen, L.M., ... Posthuma, D. (2021). A

genome-wide association study with 1, 126, 563 individuals identifies new risk loci for Alzheimer's disease. *Nature Genetics, 53*(9), 1276-1282. DOI: 10.1038/s41588-021-00921-z.

Williams, M.E., Elman, J.A., McEvoy, L.K., Andreassen , O.A., Dale, A.M., Eglit, G.M.L., Eyler, L.T., Fennema-Notestine, C., Franz, C.E., Gilliespie, N.A., Hagler, D.J., Hatton, S.N., Hauger, R.L., Jak, A.J., Logue, M.W., Lyons, M.J., McKenzie, R.E., Neale, M.C., Panizzon, M.S., ... Kremen, W.S. (2021). 12-year prediction of mild cognitive impairment aided by Alzheimer's brain signatures at mean age 56. *Brain Communications, 3*(3), fcab167. DOI: 10.1093/braincomms/fcab167.

Wingo, T.S., Lah, J.J., Levey, A.I., & Cutler, D.J. (2012). Autosomal recessive causes likely in early-onset Alzheimer disease. *Archives of Neurology, 69*(1), 56-64.
DOI: 10.1093/braincomms/fcab167.

Winkler, A.M., Kochunov, P., Fox, P.T., Duggirala, R., Almasy, L., Blangero, J., & Glahn, D.C. (2009). Heritability of volume, surface area and thickness for anatomically defined cortical brain regions estimated in a large extended pedigree. *NeuroImage, 47*(Suppl 1), S162.
DOI: 10.1016/S1053-8119(09)71713-6.

Wisdom, N.M., Callahan, J.L., & Hawkins, K.A. (2011). The effects of apolipoprotein E on non-impaired cognitive functioning: a meta-analysis. *Neurobiology of Aging, 32*(1), 63-74.
DOI: 10.1016/j.neurobiolaging.2009.02.003.

Xiao, E., Chen, Q., Goldman, A.L., Tan, H.Y., Healy, K., Zoltick, B., Das, S., Kolachana, B., Callicott, J.H., Dickinson, D., Berman, K.F., Weinberger, D.R. & Mattay, V.S. (2017). Late-onset Alzheimer's disease polygenic risk profile score predicts hippocampal function. *Biological Psychiatry: Cognitive Neuroscience and Neuroimaging, 2*(8), 673-679.
DOI: 10.1016/j.bpsc.2017.08.004.

Xiong, C., Jasielec, M.S., Weng, H., Fagan, A.M., Benzinger, T.L., Head, D., Hassenstab, J., Grant, E., Sutphen, C.L., Buckles, V., Moulder, K.L., & Morris, J.C. (2016). Longitudinal relationships among biomarkers for Alzheimer disease in the adult children study. *Neurology, 86*(16), 1499-506. DOI: 10.1212/WNL.0000000000002593.

Xu, J., Guan, X., Wen, J., Zhang, M., & Xu, X. (2022). Polygenic hazard score modified the relationship between hippocampal subfield atrophy and episodic memory in older adults. *Frontiers in Aging Neuroscience, 14*, 943702. DOI: 10.3389/fnagi.2022.943702.

Yamazaki, Y., Zhao, N., Caulfield, T.R., Liu, C-C., & Bu, G. (2019). Apolipoprotein E and Alzheimer disease: Pathobiology and targeting strategies. *Nature Reviews Neurology, 15(9),* 501-518. DOI: 10.1038/s41582-019-0228-7.

Yang, F.P.G., Bal, S.S., Lee, J-F., & Chen, C-C. (2021). White matter differences in networks in elders with mild cognitive impairment and Alzheimer's disease. *Brain Connectivity, 11*(7), 180-188. DOI: 10.1089/brain.2020.0767.

Yang, K. & Mohammed, E.A. (2020). A review of artificial intelligence technologies for early prediction of Alzheimer's disease. *arXiv*:2101.01781. DOI: 10.48550/arXiv.2101.01781.

Yassa, M.A., Mattfeld, A.T., Stark, S.M., & Stark, C.E.L. (2011). Age-related memory deficits linked to circuit-specific disruptions in the hippocampus. *Proceedings of the National Academy of Sciences of the United States of America, 108*(21), 8873-8878. DOI: 10.1073/pnas.1101567108.

Yassa, M.A., Muftuler, L.T., & Stark, C.E. (2010). Ultrahigh-resolution microstructural diffusion tensor imaging reveals perforant path degradation in aged humans in vivo. *Proceedings of the National Academy of Sciences of the United States of America, 107*(28), 12687-12691. DOI: 10.1073/pnas.1002113107.

Yassa, M.A., Stark, S.M., Bakker, A., Albert, M.S., Gallagher, M., & Stark, C.E.L. (2010). High-resolution structural and functional MRI of hippocampal CA3 and dentate gyrus in patients with amnestic mild cognitive impairment. *Neuroimage, 51*(3), 1242-1252. DOI: 10.1016/j.neuroimage.2010.03.040.

Yokoi, T. (2023). Alzheimer's disease is a disorder of consciousness. *Gerontology and Geriatric Medicine, 9*, DOI: 10.1177/23337214231159759.

Young, C.B., Johns, E., Kennedy, G., Belloy, M.E., Insel, P.S., Greicius, M.D., Sperling, R.A., Johnson, K.A., Poston, K.L., Mormino, E.C., Alzheimer's Disease Neuroimaging Initiative & A4 Study Team. (2023). APOE effects on regional tau in preclinical Alzheimer's disease. *Molecular Neurodegeneration, 18*(1), 1. DOI: 10.1186/s13024-022-00590-4.

Zhang, Q., Sidorenko, J., Couvy-Duchesne, B., Marioni, R.E., Wright, M.J., Goate, A.M., Marcora, E., Huang, K.L., Porter, T., Laws, S.M., Australian Imaging Biomarkers and Lifestyle (AIBL) Study, Sachdev, P.S., Mather, K.A., Armstrong, N.J., Thalamuthu, A., Brodaty, H., Yengo, L., Yang, J.,

Wray, N.R., McRae, A.F., & Visscher, P.M. (2020). Risk prediction of late-onset Alzheimer's disease implies an oligogenic architecture. *Nature Communications, 11*(1), 4799. DOI: 10.1038/s41467-020-18534-1.

Zhang, X.X., Tian, Y., Wang, Z.T., Ma, Y.H., Tan, L., & Yu, J.T. (2021). The epidemiology of Alzheimer's disease modifiable risk factors and prevention. *Journal of Prevention of Alzheimer's Disease, 8*(3), 313-321. DOI: 10.14283/jpad.2021.15.

Zhao, B., Luo, T., Li, T., Li, Y., Zhang, J., Shan, Y., Wang, X., Yang, L., Zhou, F., Zhu Z., Alzheimer's Disease Neuroimaging Initiative, Pediatric Imaging Neurocognition and Genetics, & Zhu, H. (2019b). Genome-wide association analysis of 19,629 individuals identifies variants influencing regional brain volumes and refines their genetic co-architecture with cognitive and mental health traits. *Nature Genetics, 51*(11), 1637-1644. DOI: 10.1038/s41588-019-0516-6.

Zhao, K., Ding, Y., Han, Y., Fan, Y., Alexander-Bloch, A.F., Han, T., Jin, D., Liu, B., Lu, J., Song, C., Wang, P., Wang, D., Wang, Q., Xu, K., Yang, H., Yao, H., Zheng, Y., Yu, C., Zhou, B., ... Multi-Centre Alzheimer Disease Imaging Consortium. (2020). Independent and reproducible hippocampal radiomic biomarkers for multisite Alzheimer's disease: Diagnosis, longitudinal progress and biological basis. *Science Bulletin, 65*(13), 1103-1113. DOI: 10.1016/j.scib.2020.04.003.

Zhao, Q., Sang, X., Metmer, H., Swati, Z.N.N.K., & Lu, J. (2019a). Functional segregation of executive control network and frontoparietal network in Alzheimer's disease. *Cortex, 120*, 36-48. DOI: 10.1016/j.cortex.2019.04.026.

Zhao, W., Smith, J.A., Wang, Y.Z., Chintalapati, M., Ammous, F., Yu, M., Moorjani, P., Ganna, A., Gross, A., Dey, S., Benerjee, J., Chatterjee, P., Dey, A.B., Lee, J., & Kardia, S.L.R. (2023). Polygenic risk scores for Alzheimer's disease and general cognitive function are associated with measures of cognition in older South Asians. *Journals of Gerontology Series A: Biological Sciences and Medical Sciences, 78*(5), 743-752. DOI: 10.1093/gerona/glad057.

CHAPTER 10

APPENDICES

APPENDIX A (Chapter 1: Introduction)

Appendix A.1: Creative Commons Attribution 4.0 License

CC BY 4.0

Attribution 4.0 International

Legal Code

Canonical URL : https://creativecommons.org/licenses/by/4.0/

Other formats : Plain Text RDF/XML

See the deed

Version 4.0 • See the errata page for any corrections and the date of change

About the license and Creative Commons

Creative Commons Corporation ("Creative Commons") is not a law firm and does not provide legal services or legal advice. Distribution of Creative Commons public licenses does not create a lawyer-client or other relationship. Creative Commons makes its licenses and related information available on an "as-is" basis. Creative Commons gives no warranties regarding its licenses, any material licensed under their terms and conditions, or any related information. Creative Commons disclaims all liability for damages resulting from their use to the fullest extent possible.

Using Creative Commons Public Licenses

Creative Commons public licenses provide a standard set of terms and conditions that creators and other rights holders may use to share original works of authorship and other material subject to copyright and certain other rights specified in the public license below. The following considerations are for informational purposes only, are not exhaustive, and do not form part of our licenses.

Considerations for licensors

Our public licenses are intended for use by those authorized to give the public permission to use material in ways otherwise restricted by copyright and certain other rights. Our licenses are irrevocable. Licensors should read and understand the terms and conditions of the license they choose before applying it. Licensors should also secure all rights necessary before applying our licenses so that the public can reuse the material as expected. Licensors should clearly mark any material not subject to the license. This includes other CC-licensed material, or material used under an exception or limitation to copyright. More considerations for licensors.

Considerations for the public

By using one of our public licenses, a licensor grants the public permission to use the licensed material under specified terms and conditions. If the licensor's permission is not necessary for any reason–for example, because of any applicable exception or limitation to copyright–then that use is not regulated by the license. Our licenses grant only permissions under copyright and certain other rights that a licensor has authority to grant. Use of the licensed material may still be restricted for

other reasons, including because others have copyright or other rights in the material. A licensor may make special requests, such as asking that all changes be marked or described. Although not required by our licenses, you are encouraged to respect those requests where reasonable. More considerations for the public.

Attribution 4.0 International

By exercising the Licensed Rights (defined below), You accept and agree to be bound by the terms and conditions of this Creative Commons Attribution 4.0 International Public License ("Public License"). To the extent this Public License may be interpreted as a contract, You are granted the Licensed Rights in consideration of Your acceptance of these terms and conditions, and the Licensor grants You such rights in consideration of benefits the Licensor receives from making the Licensed Material available under these terms and conditions.

Section 1 – Definitions.

a. Adapted Material means material subject to Copyright and Similar Rights that is derived from or based upon the Licensed Material and in which the Licensed Material is translated, altered, arranged, transformed, or otherwise modified in a manner requiring permission under the Copyright and Similar Rights held by the Licensor. For purposes of this Public License, where the Licensed Material is a musical work, performance, or sound recording, Adapted Material is always produced where the Licensed Material is synched in timed relation with a moving image.

b. Adapter's License means the license You apply to Your Copyright and Similar Rights in Your contributions to Adapted Material in accordance with the terms and conditions of this Public License.

c. Copyright and Similar Rights means copyright and/or similar rights closely related to copyright including, without limitation, performance, broadcast, sound recording, and Sui Generis Database Rights, without regard to how the rights are labeled or categorized. For purposes of this Public License, the rights specified in Section 2(b)(1)-(2) are not Copyright and Similar Rights.

d. Effective Technological Measures means those measures that, in the absence of proper authority, may not be circumvented under laws fulfilling obligations under Article 11 of the WIPO Copyright Treaty adopted on December 20, 1996, and/or similar international agreements.

e. Exceptions and Limitations means fair use, fair dealing, and/or any other exception or limitation to Copyright and Similar Rights that applies to Your use of the Licensed Material.

f. Licensed Material means the artistic or literary work, database, or other material to which the Licensor applied this Public License.

g. Licensed Rights means the rights granted to You subject to the terms and conditions of this Public License, which are limited to all Copyright and Similar Rights that apply to Your use of the Licensed Material and that the Licensor has authority to license.

h. Licensor means the individual(s) or entity(ies) granting rights under this Public License.

i. Share means to provide material to the public by any means or process that requires permission under the Licensed Rights, such as reproduction, public display, public performance, distribution, dissemination, communication, or importation, and to make material available to the public including in ways that members of the public may access the material from a place and at a time individually chosen by them.

j. Sui Generis Database Rights means rights other than copyright resulting from Directive 96/9/EC of the European Parliament and of the Council of 11 March 1996 on the legal protection of databases, as amended and/or succeeded, as well as other essentially equivalent rights anywhere in the world.

k. You means the individual or entity exercising the Licensed Rights under this Public License. **Your** has a corresponding meaning.

Section 2 – Scope.

a. **License grant** .

1. Subject to the terms and conditions of this Public License, the Licensor hereby grants You a worldwide, royalty-free, non-sublicensable, non-exclusive, irrevocable license to exercise the Licensed Rights in the Licensed Material to:

A. reproduce and Share the Licensed Material, in whole or in part; and

B. produce, reproduce, and Share Adapted Material.

2. **Exceptions and Limitations** . For the avoidance of doubt, where Exceptions and Limitations apply to Your use, this Public License

does not apply, and You do not need to comply with its terms and conditions.

3. **Term** . The term of this Public License is specified in Section 6(a) .

4. **Media and formats; technical modifications allowed** . The Licensor authorizes You to exercise the Licensed Rights in all media and formats whether now known or hereafter created, and to make technical modifications necessary to do so. The Licensor waives and/or agrees not to assert any right or authority to forbid You from making technical modifications necessary to exercise the Licensed Rights, including technical modifications necessary to circumvent Effective Technological Measures. For purposes of this Public License, simply making modifications authorized by this Section 2(a)(4) never produces Adapted Material.

5. Downstream recipients .

   A. Offer from the Licensor – Licensed Material . Every recipient of the Licensed Material automatically receives an offer from the Licensor to exercise the Licensed Rights under the terms and conditions of this Public License.

   B. No downstream restrictions . You may not offer or impose any additional or different terms or conditions on, or apply any Effective Technological Measures to, the Licensed Material if doing so restricts exercise of the Licensed Rights by any recipient of the Licensed Material.

6. No endorsement . Nothing in this Public License constitutes or may be construed as permission to assert or imply that You are, or that Your use of the Licensed Material is, connected with, or sponsored, endorsed, or granted official status by, the Licensor or

others designated to receive attribution as provided in Section 3(a)(1)(A)(i) .

b. **Other rights** .

1. Moral rights, such as the right of integrity, are not licensed under this Public License, nor are publicity, privacy, and/or other similar personality rights; however, to the extent possible, the Licensor waives and/or agrees not to assert any such rights held by the Licensor to the limited extent necessary to allow You to exercise the Licensed Rights, but not otherwise.

2. Patent and trademark rights are not licensed under this Public License.

3. To the extent possible, the Licensor waives any right to collect royalties from You for the exercise of the Licensed Rights, whether directly or through a collecting society under any voluntary or waivable statutory or compulsory licensing scheme. In all other cases the Licensor expressly reserves any right to collect such royalties.

Section 3 – License Conditions.

Your exercise of the Licensed Rights is expressly made subject to the following conditions.

a. **Attribution** .

1. If You Share the Licensed Material (including in modified form), You must:

A. retain the following if it is supplied by the Licensor with the Licensed Material:

i. identification of the creator(s) of the Licensed Material and any others designated to receive attribution, in any reasonable manner requested by the Licensor (including by pseudonym if designated);

ii. a copyright notice;

iii. a notice that refers to this Public License;

iv. a notice that refers to the disclaimer of warranties;

v. a URI or hyperlink to the Licensed Material to the extent reasonably practicable;

B. indicate if You modified the Licensed Material and retain an indication of any previous modifications; and

C. indicate the Licensed Material is licensed under this Public License, and include the text of, or the URI or hyperlink to, this Public License.

2. You may satisfy the conditions in Section 3(a)(1) in any reasonable manner based on the medium, means, and context in which You Share the Licensed Material. For example, it may be reasonable to satisfy the conditions by providing a URI or hyperlink to a resource that includes the required information.

3. If requested by the Licensor, You must remove any of the information required by Section 3(a)(1)(A) to the extent reasonably practicable.

4. If You Share Adapted Material You produce, the Adapter's License You apply must not prevent recipients of the Adapted Material from complying with this Public License.

Section 4 – Sui Generis Database Rights.

Where the Licensed Rights include Sui Generis Database Rights that apply to Your use of the Licensed Material:

a. for the avoidance of doubt, Section 2(a)(1) grants You the right to extract, reuse, reproduce, and Share all or a substantial portion of the contents of the database;

b. if You include all or a substantial portion of the database contents in a database in which You have Sui Generis Database Rights, then the database in which You have Sui Generis Database Rights (but not its individual contents) is Adapted Material; and

c. You must comply with the conditions in Section 3(a) if You Share all or a substantial portion of the contents of the database.

For the avoidance of doubt, this Section 4 supplements and does not replace Your obligations under this Public License where the Licensed Rights include other Copyright and Similar Rights.

Section 5 – Disclaimer of Warranties and Limitation of Liability.

a. Unless otherwise separately undertaken by the Licensor, to the extent possible, the Licensor offers the Licensed Material as-is and as-available, and makes no representations or warranties of any kind concerning the Licensed Material, whether express, implied, statutory, or other. This includes, without limitation, warranties of title, merchantability, fitness for a particular purpose, non-

infringement, absence of latent or other defects, accuracy, or the presence or absence of errors, whether or not known or discoverable. Where disclaimers of warranties are not allowed in full or in part, this disclaimer may not apply to You.

b. To the extent possible, in no event will the Licensor be liable to You on any legal theory (including, without limitation, negligence) or otherwise for any direct, special, indirect, incidental, consequential, punitive, exemplary, or other losses, costs, expenses, or damages arising out of this Public License or use of the Licensed Material, even if the Licensor has been advised of the possibility of such losses, costs, expenses, or damages. Where a limitation of liability is not allowed in full or in part, this limitation may not apply to You.

c. The disclaimer of warranties and limitation of liability provided above shall be interpreted in a manner that, to the extent possible, most closely approximates an absolute disclaimer and waiver of all liability.

Section 6 – Term and Termination.

a. This Public License applies for the term of the Copyright and Similar Rights licensed here. However, if You fail to comply with this Public License, then Your rights under this Public License terminate automatically.

b. Where Your right to use the Licensed Material has terminated under Section 6(a), it reinstates:

1. automatically as of the date the violation is cured, provided it is cured within 30 days of Your discovery of the violation; or

2. upon express reinstatement by the Licensor.

For the avoidance of doubt, this Section 6(b) does not affect any right the Licensor may have to seek remedies for Your violations of this Public License.

c. For the avoidance of doubt, the Licensor may also offer the Licensed Material under separate terms or conditions or stop distributing the Licensed Material at any time; however, doing so will not terminate this Public License.

d. Sections 1 , 5 , 6 , 7 , and 8 survive termination of this Public License.

Section 7 – Other Terms and Conditions.

a. The Licensor shall not be bound by any additional or different terms or conditions communicated by You unless expressly agreed.

b. Any arrangements, understandings, or agreements regarding the Licensed Material not stated herein are separate from and independent of the terms and conditions of this Public License.

Section 8 – Interpretation.

a. For the avoidance of doubt, this Public License does not, and shall not be interpreted to, reduce, limit, restrict, or impose conditions on any use of the Licensed Material that could lawfully be made without permission under this Public License.

b. To the extent possible, if any provision of this Public License is deemed unenforceable, it shall be automatically reformed to the minimum extent necessary to make it enforceable. If the provision cannot be reformed, it shall be severed from this Public License without affecting the enforceability of the remaining terms and conditions.

c. No term or condition of this Public License will be waived and no failure to comply consented to unless expressly agreed to by the Licensor.

d. Nothing in this Public License constitutes or may be interpreted as a limitation upon, or waiver of, any privileges and immunities that apply to the Licensor or You, including from the legal processes of any jurisdiction or authority.

About Creative Commons

Creative Commons is not a party to its public licenses. Notwithstanding, Creative Commons may elect to apply one of its public licenses to material it publishes and in those instances will be considered the "Licensor." The text of the Creative Commons public licenses is dedicated to the public domain under the CC0 Public Domain Dedication . Except for the limited purpose of indicating that material is shared under a Creative Commons public license or as otherwise permitted by the Creative Commons policies published at creativecommons.org/policies , Creative Commons does not authorize the use of the trademark "Creative Commons" or any other trademark or logo of Creative Commons without its prior written consent including, without limitation, in connection with any unauthorized modifications to any of its public licenses or any other arrangements, understandings, or agreements concerning use of licensed material. For the avoidance of doubt, this paragraph does not form part of the public licenses.

Creative Commons may be contacted at creativecommons.org .

Creative Commons is the nonprofit behind the open licenses and other legal tools that allow creators to share their work. Our legal tools are free to use.

- Learn more about our work
- **Learn more about CC Licensing**
- Support our work
- Use the license for your own material.
- Licenses List
- Public Domain List

Appendix A.2: License to reuse image from Mirra et al. (1991).

WOLTERS KLUWER HEALTH, INC. LICENSE
TERMS AND CONDITIONS

Aug 04, 2025

This Agreement between Snehal Pandya / Brunel University of London ("You") and Wolters Kluwer Health, Inc. ("Wolters Kluwer Health, Inc.") consists of your license details and the terms and conditions provided by Wolters Kluwer Health, Inc. and Copyright Clearance Center.

The publisher has provided special terms related to this request that can be found at the end of the Publisher's Terms and Conditions.

License Number	6082000888845
License date	Aug 04, 2025
Licensed Content Publisher	Wolters Kluwer Health, Inc.
Licensed Content Publication	Neurology
Licensed Content Title	The Consortium to Establish a Registry for Alzheimer's Disease (CERAD): Part II. Standardization of the neuropathologic assessment of Alzheimer's disease
Licensed Content Author	S. S. Mirra, A. Heyman, D. McKeel, S. M. Sumi, et al.
Licensed Content Date	Apr 1, 1991
Licensed Content Volume	41
Licensed Content Issue	4
Type of Use	Dissertation/Thesis
Requestor type	University/College

Sponsorship	No Sponsorship
Format	Electronic
Will this be posted online?	Yes, on a secure website
Portion	Figures/tables/illustrations
Number of figures/tables/illustrations	1
Author of this Wolters Kluwer article	No
Will you be translating?	No
Intend to modify/change the content	No
Title of new work	PhD thesis
Institution name	Brunel University of London
Expected presentation date	Sep 2025
Portions	Figure 2.
The Requesting Person / Organization to Appear on the License	Snehal Pandya / Brunel University of London
Requestor Location	Miss. Snehal Pandya Brunel University of London London, UB8 3PH United Kingdom
Publisher Tax ID	13-2932696
Billing Type	Invoice

Billing Address	Miss. Snehal Pandya Brunel University of London London, United Kingdom UB8 3PH
Total	0.00 GBP

Terms and Conditions

Wolters Kluwer Health Inc. Terms and Conditions

1. **Duration of License:** Permission is granted for a one time use only. Rights herein do not apply to future reproductions, editions, revisions, or other derivative works. This permission shall be effective as of the date of execution by the parties for the maximum period of 12 months and should be renewed after the term expires.
    i. When content is to be republished in a book or journal the validity of this agreement should be the life of the book edition or journal issue.
    ii. When content is licensed for use on a website, internet, intranet, or any publicly accessible site (not including a journal or book), you agree to remove the material from such site after 12 months, or request to renew your permission license
2. **Credit Line:** A credit line must be prominently placed and include: For book content: the author(s), title of book, edition, copyright holder, year of publication; For journal content: the author(s), titles of article, title of journal, volume number, issue number, inclusive pages and website URL to the journal page; If a journal is published by a learned society the credit line must include the details of that society.
3. **Warranties:** The requestor warrants that the material shall not be used in any manner which may be considered derogatory to the title, content, authors of the material, or to Wolters Kluwer Health, Inc.
4. **Indemnity:** You hereby indemnify and hold harmless Wolters Kluwer Health, Inc. and its respective officers, directors, employees and agents, from and against any and all claims, costs, proceeding or demands arising out of your unauthorized use of the Licensed Material
5. **Geographical Scope:** Permission granted is non-exclusive and is valid throughout the world in the English language and the languages specified in the license.
6. **Copy of Content:** Wolters Kluwer Health, Inc. cannot supply the requestor with the original artwork, high-resolution images, electronic files or a clean copy of content.
7. **Validity:** Permission is valid if the borrowed material is original to a Wolters Kluwer Health, Inc. imprint (J.B Lippincott, Lippincott-Raven Publishers, Williams & Wilkins, Lea & Febiger, Harwal, Rapid Science, Little Brown & Company, Harper & Row Medical, American Journal of Nursing Co, and Urban & Schwarzenberg - English Language, Raven Press, Paul Hoeber, Springhouse, Ovid), and the Anatomical Chart Company
8. **Third Party Material:** This permission does not apply to content that is credited to publications other than Wolters Kluwer Health, Inc. or its Societies. For images credited to non-Wolters Kluwer Health, Inc. books or journals, you must obtain permission from the source referenced in the figure or table legend or credit line before making any use of the image(s), table(s) or other content.
9. **Adaptations:** Adaptations are protected by copyright. For images that have been adapted, permission must be sought from the rightsholder of the original material and the rightsholder of the adapted material.

10. **Modifications:** Wolters Kluwer Health, Inc. material is not permitted to be modified or adapted without written approval from Wolters Kluwer Health, Inc. with the exception of text size or color. The adaptation should be credited as follows: Adapted with permission from Wolters Kluwer Health, Inc.: [the author(s), title of book, edition, copyright holder, year of publication] or [the author(s), titles of article, title of journal, volume number, issue number, inclusive pages and website URL to the journal page].
11. **Full Text Articles:** Republication of full articles in English is prohibited.
12. **Branding and Marketing:** No drug name, trade name, drug logo, or trade logo can be included on the same page as material borrowed from *Diseases of the Colon & Rectum, Plastic Reconstructive Surgery, Obstetrics & Gynecology (The Green Journal), Critical Care Medicine, Pediatric Critical Care Medicine, the American Heart Association publications and the American Academy of Neurology publications.*
13. **Open Access:** Unless you are publishing content under the same Creative Commons license, the following statement must be added when reprinting material in Open Access journals: "The Creative Commons license does not apply to this content. Use of the material in any format is prohibited without written permission from the publisher, Wolters Kluwer Health, Inc. Please contact permissions@lww.com for further information."
14. **Translations:** The following disclaimer must appear on all translated copies: Wolters Kluwer Health, Inc. and its Societies take no responsibility for the accuracy of the translation from the published English original and are not liable for any errors which may occur.
15. **Published Ahead of Print (PAP):** Articles in the PAP stage of publication can be cited using the online publication date and the unique DOI number.
    i. Disclaimer: Articles appearing in the PAP section have been peer-reviewed and accepted for publication in the relevant journal and posted online before print publication. Articles appearing as PAP may contain statements, opinions, and information that have errors in facts, figures, or interpretation. Any final changes in manuscripts will be made at the time of print publication and will be reflected in the final electronic version of the issue. Accordingly, Wolters Kluwer Health, Inc., the editors, authors and their respective employees are not responsible or liable for the use of any such inaccurate or misleading data, opinion or information contained in the articles in this section.
16. **Termination of Contract:** Wolters Kluwer Health, Inc. must be notified within 90 days of the original license date if you opt not to use the requested material.
17. **Waived Permission Fee:** Permission fees that have been waived are not subject to future waivers, including similar requests or renewing a license.
18. **Contingent on payment:** You may exercise these rights licensed immediately upon issuance of the license, however until full payment is received either by the publisher or our authorized vendor, this license is not valid. If full payment is not received on a timely basis, then any license preliminarily granted shall be deemed automatically revoked and shall be void as if never granted. Further, in the event that you breach any of these terms and conditions or any of Wolters Kluwer Health, Inc.'s other billing and payment terms and conditions, the license is automatically revoked and shall be void as if never granted. Use of materials as described in a revoked license, as well as any use of the materials beyond the scope of an unrevoked license, may constitute copyright infringement and publisher reserves the right to take any and all action to protect its copyright in the materials.
19. **STM Signatories Only:** Any permission granted for a particular edition will apply to subsequent editions and for editions in other languages, provided such editions are for the work as a whole in situ and do not involve the separate exploitation of the permitted illustrations or excerpts. Please view: STM Permissions Guidelines
20. **Warranties and Obligations:** LICENSOR further represents and warrants that, to the best of its knowledge and belief, LICENSEE's contemplated use of the Content as represented to LICENSOR does not infringe any valid rights to any third party.

21. **Breach:** If LICENSEE fails to comply with any provisions of this agreement, LICENSOR may serve written notice of breach of LICENSEE and, unless such breach is fully cured within fifteen (15) days from the receipt of notice by LICENSEE, LICENSOR may thereupon, at its option, serve notice of cancellation on LICENSEE, whereupon this Agreement shall immediately terminate.
22. **Assignment:** License conveyed hereunder by the LICENSOR shall not be assigned or granted in any manner conveyed to any third party by the LICENSEE without the consent in writing to the LICENSOR.
23. **Governing Law:** The laws of The State of New York shall govern interpretation of this Agreement and all rights and liabilities arising hereunder.
24. **Unlawful:** If any provision of this Agreement shall be found unlawful or otherwise legally unenforceable, all other conditions and provisions of this Agreement shall remain in full force and effect.

For Copyright Clearance Center / RightsLink Only:

1. **Service Description for Content Services:** Subject to these terms of use, any terms set forth on the particular order, and payment of the applicable fee, you may make the following uses of the ordered materials:
    i. **Content Rental:** You may access and view a single electronic copy of the materials ordered for the time period designated at the time the order is placed. Access to the materials will be provided through a dedicated content viewer or other portal, and access will be discontinued upon expiration of the designated time period. An order for Content Rental does not include any rights to print, download, save, create additional copies, to distribute or to reuse in any way the full text or parts of the materials.
    ii. **Content Purchase:** You may access and download a single electronic copy of the materials ordered. Copies will be provided by email or by such other means as publisher may make available from time to time. An order for Content Purchase does not include any rights to create additional copies or to distribute copies of the materials

Other Terms and Conditions:

v1.18

Questions? customercare@copyright.com.

Appendix A.3: License to reuse images from Braak and Braak (1991).

SPRINGER NATURE LICENSE
TERMS AND CONDITIONS

Aug 03, 2025

This Agreement between Snehal Pandya / Brunel University of London ("You") and Springer Nature ("Springer Nature") consists of your license details and the terms and conditions provided by Springer Nature and Copyright Clearance Center.

License Number	6081411467284
License date	Aug 03, 2025
Licensed Content Publisher	Springer Nature
Licensed Content Publication	Acta Neuropathologica
Licensed Content Title	Neuropathological stageing of Alzheimer-related changes
Licensed Content Author	H. Braak et al
Licensed Content Date	Jan 1, 1991
Type of Use	Thesis/Dissertation
Requestor type	academic/university or research institute
Format	electronic
Portion	figures/tables/illustrations
Number of figures/tables/illustrations	2
Will you be translating?	no
Circulation/distribution	1 - 29

Author of this Springer Nature content	no
Title of new work	PhD thesis
Institution name	Brunel University of London
Expected presentation date	Sep 2025
Portions	Figure 1. Figure 4.
The Requesting Person / Organization to Appear on the License	Snehal Pandya / Brunel University of London
Requestor Location	Snehal Pandya Brunel University of London London, UB8 3PH United Kingdom
Billing Type	Invoice
Billing Address	Miss. Snehal Pandya Brunel University of London London, United Kingdom UB8 3PH
Total	0.00 GBP

Terms and Conditions

Springer Nature Customer Service Centre GmbH Terms and Conditions

The following terms and conditions ("Terms and Conditions") together with the terms specified in your [RightsLink] constitute the License ("License") between you as Licensee and Springer Nature Customer Service Centre GmbH as Licensor. By clicking 'accept' and completing the transaction for your use of the material ("Licensed Material"), you confirm your acceptance of and obligation to be bound by these Terms and Conditions.

1. Grant and Scope of License

1. 1. The Licensor grants you a personal, non-exclusive, non-transferable, non-sublicensable, revocable, world-wide License to reproduce, distribute, communicate to the public, make available, broadcast, electronically transmit or create derivative

works using the Licensed Material for the purpose(s) specified in your RightsLink Licence Details only. Licenses are granted for the specific use requested in the order and for no other use, subject to these Terms and Conditions. You acknowledge and agree that the rights granted to you under this License do not include the right to modify, edit, translate, include in collective works, or create derivative works of the Licensed Material in whole or in part unless expressly stated in your RightsLink Licence Details. You may use the Licensed Material only as permitted under this Agreement and will not reproduce, distribute, display, perform, or otherwise use or exploit any Licensed Material in any way, in whole or in part, except as expressly permitted by this License.

1. 2. You may only use the Licensed Content in the manner and to the extent permitted by these Terms and Conditions, by your RightsLink Licence Details and by any applicable laws.

1. 3. A separate license may be required for any additional use of the Licensed Material, e.g. where a license has been purchased for print use only, separate permission must be obtained for electronic re-use. Similarly, a License is only valid in the language selected and does not apply for editions in other languages unless additional translation rights have been granted separately in the License.

1. 4. Any content within the Licensed Material that is owned by third parties is expressly excluded from the License.

1. 5. Rights for additional reuses such as custom editions, computer/mobile applications, film or TV reuses and/or any other derivative rights requests require additional permission and may be subject to an additional fee. Please apply to journalpermissions@springernature.com or bookpermissions@springernature.com for these rights.

2. Reservation of Rights

Licensor reserves all rights not expressly granted to you under this License. You acknowledge and agree that nothing in this License limits or restricts Licensor's rights in or use of the Licensed Material in any way. Neither this License, nor any act, omission, or statement by Licensor or you, conveys any ownership right to you in any Licensed Material, or to any element or portion thereof. As between Licensor and you, Licensor owns and retains all right, title, and interest in and to the Licensed Material subject to the license granted in Section 1.1. Your permission to use the Licensed Material is expressly conditioned on you not impairing Licensor's or the applicable copyright owner's rights in the Licensed Material in any way.

3. Restrictions on use

3. 1. Minor editing privileges are allowed for adaptations for stylistic purposes or formatting purposes provided such alterations do not alter the original meaning or intention of the Licensed Material and the new figure(s) are still accurate and representative of the Licensed Material. Any other changes including but not limited to, cropping, adapting, and/or omitting material that affect the meaning, intention or moral rights of the author(s) are strictly prohibited.

3. 2. You must not use any Licensed Material as part of any design or trademark.

3. 3. Licensed Material may be used in Open Access Publications (OAP), but any such reuse must include a clear acknowledgment of this permission visible at the same time as the figures/tables/illustration or abstract and which must indicate that the Licensed Material is not part of the governing OA license but has been reproduced with permission. This may be indicated according to any standard

referencing system but must include at a minimum 'Book/Journal title, Author, Journal Name (if applicable), Volume (if applicable), Publisher, Year, reproduced with permission from SNCSC'.

4. STM Permission Guidelines

4. 1. An alternative scope of license may apply to signatories of the STM Permissions Guidelines ("STM PG") as amended from time to time and made available at https://www.stm-assoc.org/intellectual-property/permissions/permissions-guidelines/.

4. 2. For content reuse requests that qualify for permission under the STM PG, and which may be updated from time to time, the STM PG supersede the terms and conditions contained in this License.

4. 3. If a License has been granted under the STM PG, but the STM PG no longer apply at the time of publication, further permission must be sought from the Rightsholder. Contact journalpermissions@springernature.com or bookpermissions@springernature.com for these rights.

5. Duration of License

5. 1. Unless otherwise indicated on your License, a License is valid from the date of purchase ("License Date") until the end of the relevant period in the below table:

Reuse in a medical communications project	Reuse up to distribution or time period indicated in License
Reuse in a dissertation/thesis	Lifetime of thesis
Reuse in a journal/magazine	Lifetime of journal/magazine
Reuse in a book/textbook	Lifetime of edition
Reuse on a website	1 year unless otherwise specified in the License. If you wish to reuse the content on your website for longer than 1 year, please make this clear in the 'additional information' field and the License will include a 'Special Term' to reflect your duration choice.
Reuse in a presentation/slide kit/poster	Lifetime of presentation/slide kit/poster. Note: publication whether electronic or in print of presentation/slide kit/poster may require further permission.
Reuse in conference proceedings	Lifetime of conference proceedings
Reuse in an annual report	Lifetime of annual report
Reuse in training/CME materials	Reuse up to distribution or time period indicated in License
Reuse in newsmedia	Lifetime of newsmedia
Reuse in coursepack/classroom materials	Reuse up to distribution and/or time period indicated in license

6. Acknowledgement

6. 1. The Licensor's permission must be acknowledged next to the Licensed Material in print. In electronic form, this acknowledgement must be visible at the same time as the figures/tables/illustrations or abstract and must be hyperlinked to the journal/book's homepage.

6. 2. Acknowledgement may be provided according to any standard referencing system and at a minimum should include "Author, Article/Book Title, Journal name/Book imprint, volume, page number, year, Springer Nature".

7. Reuse in a dissertation or thesis

7. 1. Where 'reuse in a dissertation/thesis' has been selected, the following terms apply: Print rights of the Version of Record are provided for; electronic rights for use only on institutional repository as defined by the Sherpa guideline (www.sherpa.ac.uk/romeo/) and only up to what is required by the awarding institution.

7. 2. For theses published under an ISBN or ISSN, separate permission is required. Please contact journalpermissions@springernature.com or bookpermissions@springernature.com for these rights.

7. 3. Authors must properly cite the published manuscript in their thesis according to current citation standards and include the following acknowledgement: '*Reproduced with permission from Springer Nature*'.

8. License Fee

You must pay the fee set forth in the License Agreement (the "License Fees"). All amounts payable by you under this License are exclusive of any sales, use, withholding, value added or similar taxes, government fees or levies or other assessments. Collection and/or remittance of such taxes to the relevant tax authority shall be the responsibility of the party who has the legal obligation to do so.

9. Warranty

9. 1. The Licensor warrants that it has, to the best of its knowledge, the rights to license reuse of the Licensed Material. **You are solely responsible for ensuring that the material you wish to license is original to the Licensor and does not carry the copyright of another entity or third party (as credited in the published version).** If the credit line on any part of the Licensed Material indicates that it was reprinted or adapted with permission from another source, then you should seek additional permission from that source to reuse the material.

9. 2. EXCEPT FOR THE EXPRESS WARRANTY STATED HEREIN AND TO THE EXTENT PERMITTED BY APPLICABLE LAW, LICENSOR PROVIDES THE LICENSED MATERIAL "AS IS" AND MAKES NO OTHER REPRESENTATION OR WARRANTY. LICENSOR EXPRESSLY DISCLAIMS ANY LIABILITY FOR ANY CLAIM ARISING FROM OR OUT OF THE CONTENT, INCLUDING BUT NOT LIMITED TO ANY ERRORS, INACCURACIES, OMISSIONS, OR DEFECTS CONTAINED THEREIN, AND ANY IMPLIED OR EXPRESS WARRANTY AS TO MERCHANTABILITY OR FITNESS FOR A PARTICULAR PURPOSE. IN NO EVENT SHALL LICENSOR BE LIABLE TO YOU OR ANY OTHER PARTY OR ANY OTHER PERSON OR FOR ANY SPECIAL, CONSEQUENTIAL, INCIDENTAL, INDIRECT, PUNITIVE, OR EXEMPLARY DAMAGES, HOWEVER CAUSED, ARISING OUT OF OR IN CONNECTION WITH THE DOWNLOADING, VIEWING OR USE OF THE LICENSED MATERIAL REGARDLESS OF THE FORM OF ACTION, WHETHER FOR BREACH OF CONTRACT, BREACH OF

WARRANTY, TORT, NEGLIGENCE, INFRINGEMENT OR OTHERWISE (INCLUDING, WITHOUT LIMITATION, DAMAGES BASED ON LOSS OF PROFITS, DATA, FILES, USE, BUSINESS OPPORTUNITY OR CLAIMS OF THIRD PARTIES), AND WHETHER OR NOT THE PARTY HAS BEEN ADVISED OF THE POSSIBILITY OF SUCH DAMAGES. THIS LIMITATION APPLIES NOTWITHSTANDING ANY FAILURE OF ESSENTIAL PURPOSE OF ANY LIMITED REMEDY PROVIDED HEREIN.

10. Termination and Cancellation

10. 1. The License and all rights granted hereunder will continue until the end of the applicable period shown in Clause 5.1 above. Thereafter, this license will be terminated and all rights granted hereunder will cease.

10. 2. Licensor reserves the right to terminate the License in the event that payment is not received in full or if you breach the terms of this License.

11. General

11. 1. The License and the rights and obligations of the parties hereto shall be construed, interpreted and determined in accordance with the laws of the Federal Republic of Germany without reference to the stipulations of the CISG (United Nations Convention on Contracts for the International Sale of Goods) or to Germany's choice-of-law principle.

11. 2. The parties acknowledge and agree that any controversies and disputes arising out of this License shall be decided exclusively by the courts of or having jurisdiction for Heidelberg, Germany, as far as legally permissible.

11. 3. This License is solely for Licensor's and Licensee's benefit. It is not for the benefit of any other person or entity.

Questions? For questions on Copyright Clearance Center accounts or website issues please contact springernaturesupport@copyright.com or +1-855-239-3415 (toll free in the US) or +1-978-646-2777. For questions on Springer Nature licensing please visit https://www.springernature.com/gp/partners/rights-permissions-third-party-distribution

Other Conditions:

Version 1.5 - June 2025

Questions? customercare@copyright.com.

Appendix A.4: License to reuse image from Thal et al. (2002).

WOLTERS KLUWER HEALTH, INC. LICENSE
TERMS AND CONDITIONS

Aug 04, 2025

This Agreement between Snehal Pandya / Brunel University of London ("You") and Wolters Kluwer Health, Inc. ("Wolters Kluwer Health, Inc.") consists of your license details and the terms and conditions provided by Wolters Kluwer Health, Inc. and Copyright Clearance Center.

The publisher has provided special terms related to this request that can be found at the end of the Publisher's Terms and Conditions.

License Number	6082020710516
License date	Aug 04, 2025
Licensed Content Publisher	Wolters Kluwer Health, Inc.
Licensed Content Publication	Neurology
Licensed Content Title	Phases of Aβ-deposition in the human brain and its relevance for the development of AD
Licensed Content Author	Dietmar R. Thal, Udo Rüb, Mario Orantes, Heiko Braak
Licensed Content Date	Jun 25, 2002
Licensed Content Volume	58
Licensed Content Issue	12
Type of Use	Dissertation/Thesis
Requestor type	University/College
Sponsorship	No Sponsorship

Format	Electronic
Will this be posted online?	Yes, on a secure website
Portion	Figures/tables/illustrations
Number of figures/tables/illustrations	1
Author of this Wolters Kluwer article	No
Will you be translating?	No
Intend to modify/change the content	No
Title of new work	PhD thesis
Institution name	Brunel University of London
Expected presentation date	Sep 2025
Portions	Figure 4.
The Requesting Person / Organization to Appear on the License	Snehal Pandya / Brunel University of London
Requestor Location	Snehal Pandya Brunel University of London London, UB8 3PH United Kingdom
Publisher Tax ID	13-2932696
Billing Type	Invoice
Billing Address	Miss. Snehal Pandya Brunel University of London London, United Kingdom UB8 3PH

Total 0.00 GBP

Terms and Conditions

Wolters Kluwer Health Inc. Terms and Conditions

1. **Duration of License:** Permission is granted for a one time use only. Rights herein do not apply to future reproductions, editions, revisions, or other derivative works. This permission shall be effective as of the date of execution by the parties for the maximum period of 12 months and should be renewed after the term expires.
    i. When content is to be republished in a book or journal the validity of this agreement should be the life of the book edition or journal issue.
    ii. When content is licensed for use on a website, internet, intranet, or any publicly accessible site (not including a journal or book), you agree to remove the material from such site after 12 months, or request to renew your permission license
2. **Credit Line:** A credit line must be prominently placed and include: For book content: the author(s), title of book, edition, copyright holder, year of publication; For journal content: the author(s), titles of article, title of journal, volume number, issue number, inclusive pages and website URL to the journal page; If a journal is published by a learned society the credit line must include the details of that society.
3. **Warranties:** The requestor warrants that the material shall not be used in any manner which may be considered derogatory to the title, content, authors of the material, or to Wolters Kluwer Health, Inc.
4. **Indemnity:** You hereby indemnify and hold harmless Wolters Kluwer Health, Inc. and its respective officers, directors, employees and agents, from and against any and all claims, costs, proceeding or demands arising out of your unauthorized use of the Licensed Material
5. **Geographical Scope:** Permission granted is non-exclusive and is valid throughout the world in the English language and the languages specified in the license.
6. **Copy of Content:** Wolters Kluwer Health, Inc. cannot supply the requestor with the original artwork, high-resolution images, electronic files or a clean copy of content.
7. **Validity:** Permission is valid if the borrowed material is original to a Wolters Kluwer Health, Inc. imprint (J.B Lippincott, Lippincott-Raven Publishers, Williams & Wilkins, Lea & Febiger, Harwal, Rapid Science, Little Brown & Company, Harper & Row Medical, American Journal of Nursing Co, and Urban & Schwarzenberg - English Language, Raven Press, Paul Hoeber, Springhouse, Ovid), and the Anatomical Chart Company
8. **Third Party Material:** This permission does not apply to content that is credited to publications other than Wolters Kluwer Health, Inc. or its Societies. For images credited to non-Wolters Kluwer Health, Inc. books or journals, you must obtain permission from the source referenced in the figure or table legend or credit line before making any use of the image(s), table(s) or other content.
9. **Adaptations:** Adaptations are protected by copyright. For images that have been adapted, permission must be sought from the rightsholder of the original material and the rightsholder of the adapted material.
10. **Modifications:** Wolters Kluwer Health, Inc. material is not permitted to be modified or adapted without written approval from Wolters Kluwer Health, Inc. with the exception of text size or color. The adaptation should be credited as follows: Adapted with permission from Wolters Kluwer Health, Inc.: [the author(s), title of book, edition, copyright holder, year of publication] or [the author(s), titles of article, title of journal, volume number, issue number, inclusive pages and website URL to the journal page].

11. **Full Text Articles:** Republication of full articles in English is prohibited.
12. **Branding and Marketing:** No drug name, trade name, drug logo, or trade logo can be included on the same page as material borrowed from *Diseases of the Colon & Rectum, Plastic Reconstructive Surgery, Obstetrics & Gynecology (The Green Journal), Critical Care Medicine, Pediatric Critical Care Medicine, the American Heart Association publications and the American Academy of Neurology publications.*
13. **Open Access:** Unless you are publishing content under the same Creative Commons license, the following statement must be added when reprinting material in Open Access journals: "The Creative Commons license does not apply to this content. Use of the material in any format is prohibited without written permission from the publisher, Wolters Kluwer Health, Inc. Please contact permissions@lww.com for further information."
14. **Translations:** The following disclaimer must appear on all translated copies: Wolters Kluwer Health, Inc. and its Societies take no responsibility for the accuracy of the translation from the published English original and are not liable for any errors which may occur.
15. **Published Ahead of Print (PAP):** Articles in the PAP stage of publication can be cited using the online publication date and the unique DOI number.
    i. Disclaimer: Articles appearing in the PAP section have been peer-reviewed and accepted for publication in the relevant journal and posted online before print publication. Articles appearing as PAP may contain statements, opinions, and information that have errors in facts, figures, or interpretation. Any final changes in manuscripts will be made at the time of print publication and will be reflected in the final electronic version of the issue. Accordingly, Wolters Kluwer Health, Inc., the editors, authors and their respective employees are not responsible or liable for the use of any such inaccurate or misleading data, opinion or information contained in the articles in this section.
16. **Termination of Contract:** Wolters Kluwer Health, Inc. must be notified within 90 days of the original license date if you opt not to use the requested material.
17. **Waived Permission Fee:** Permission fees that have been waived are not subject to future waivers, including similar requests or renewing a license.
18. **Contingent on payment:** You may exercise these rights licensed immediately upon issuance of the license, however until full payment is received either by the publisher or our authorized vendor, this license is not valid. If full payment is not received on a timely basis, then any license preliminarily granted shall be deemed automatically revoked and shall be void as if never granted. Further, in the event that you breach any of these terms and conditions or any of Wolters Kluwer Health, Inc.'s other billing and payment terms and conditions, the license is automatically revoked and shall be void as if never granted. Use of materials as described in a revoked license, as well as any use of the materials beyond the scope of an unrevoked license, may constitute copyright infringement and publisher reserves the right to take any and all action to protect its copyright in the materials.
19. **STM Signatories Only:** Any permission granted for a particular edition will apply to subsequent editions and for editions in other languages, provided such editions are for the work as a whole in situ and do not involve the separate exploitation of the permitted illustrations or excerpts. Please view: STM Permissions Guidelines
20. **Warranties and Obligations:** LICENSOR further represents and warrants that, to the best of its knowledge and belief, LICENSEE's contemplated use of the Content as represented to LICENSOR does not infringe any valid rights to any third party.
21. **Breach:** If LICENSEE fails to comply with any provisions of this agreement, LICENSOR may serve written notice of breach of LICENSEE and, unless such breach is fully cured within fifteen (15) days from the receipt of notice by LICENSEE, LICENSOR may thereupon, at its option, serve notice of cancellation on LICENSEE, whereupon this Agreement shall immediately terminate.
22. **Assignment:** License conveyed hereunder by the LICENSOR shall not be assigned or granted in any manner conveyed to any third party by the LICENSEE without

the consent in writing to the LICENSOR.

23. **Governing Law:** The laws of The State of New York shall govern interpretation of this Agreement and all rights and liabilities arising hereunder.
24. **Unlawful:** If any provision of this Agreement shall be found unlawful or otherwise legally unenforceable, all other conditions and provisions of this Agreement shall remain in full force and effect.

For Copyright Clearance Center / RightsLink Only:

1. **Service Description for Content Services:** Subject to these terms of use, any terms set forth on the particular order, and payment of the applicable fee, you may make the following uses of the ordered materials:
   i. **Content Rental:** You may access and view a single electronic copy of the materials ordered for the time period designated at the time the order is placed. Access to the materials will be provided through a dedicated content viewer or other portal, and access will be discontinued upon expiration of the designated time period. An order for Content Rental does not include any rights to print, download, save, create additional copies, to distribute or to reuse in any way the full text or parts of the materials.
   ii. **Content Purchase:** You may access and download a single electronic copy of the materials ordered. Copies will be provided by email or by such other means as publisher may make available from time to time. An order for Content Purchase does not include any rights to create additional copies or to distribute copies of the materials

Other Terms and Conditions:

Posting of our content to third party-owned repositories or commercial/social media websites, such as ProQuest, YouTube, ResearchGate, Facebook is strictly prohibited. take no responsibility for the accuracy of the translation from the published English original and are not liable for any errors which may occur. No drug brand/ trade name or logo can be included in the same page as the material reused. Opinions expressed by the authors and advertisers are not necessarily those of the American Academy of Neurology, its affiliates, or of the Publisher. The American Academy of Neurology, its affiliates, and the Publisher disclaim any liability to any party for the accuracy, completeness, efficacy, or availability of the material contained in this publication (including drug dosages) or for any damages arising out of the use or non-use of any of the material contained in this publication.

v1.18

Questions? customercare@copyright.com.

APPENDIX B (Chapter 2: Systematic Review)

Table B.1: Strings of search terms used to identify papers for systematic review.

[polygen*] AND [Alzheimer*] AND [structur*]
[polygen*] AND [Alzheimer*] AND [anatomic*]
[polygen*] AND [Alzheimer*] AND [MRI]
[polygen*] AND [Alzheimer*] AND [DTI]
[polygen*] AND [Alzheimer*] AND [grey matter]
[polygen*] AND [Alzheimer*] AND [gray matter]
[polygen*] AND [Alzheimer*] AND [white matter]
[polygen*] AND [cogniti*] AND [structur*]
[polygen*] AND [cogniti*] AND [anatomic*]
[polygen*] AND [cogniti*] AND [MRI]
[polygen*] AND [cogniti*] AND [DTI]
[polygen*] AND [cogniti*] AND [grey matter]
[polygen*] AND [cogniti*] AND [gray matter]
[polygen*] AND [cogniti*] AND [white matter]
[polygen*] AND [dementia] AND [structur*]
[polygen*] AND [dementia] AND [anatomic*]
[polygen*] AND [dementia] AND [MRI]
[polygen*] AND [dementia] AND [DTI]
[polygen*] AND [dementia] AND [grey matter]
[polygen*] AND [dementia] AND [gray matter]
[polygen*] AND [dementia] AND [white matter]
[polygen*] AND [MCI] AND [structur*]
[polygen*] AND [MCI] AND [anatomic*]
[polygen*] AND [MCI] AND [MRI]
[polygen*] AND [MCI] AND [DTI]
[polygen*] AND [MCI] AND [grey matter]
[polygen*] AND [MCI] AND [gray matter]
[polygen*] AND [MCI] AND [white matter]
[polygen*] AND [mild cognitive impairment] AND [structur*]
[polygen*] AND [mild cognitive impairment] AND [anatomic*]
[polygen*] AND [mild cognitive impairment] AND [MRI]
[polygen*] AND [mild cognitive impairment] AND [DTI]
[polygen*] AND [mild cognitive impairment] AND [grey matter]
[polygen*] AND [mild cognitive impairment] AND [gray matter]
[polygen*] AND [mild cognitive impairment] AND [white matter]
[polygen*] AND [subjective cognitive complaint] AND [structur*]
[polygen*] AND [subjective cognitive complaint] AND [anatomic*]
[polygen*] AND [subjective cognitive complaint] AND [MRI]
[polygen*] AND [subjective cognitive complaint] AND [DTI]
[polygen*] AND [subjective cognitive complaint] AND [grey matter]
[polygen*] AND [subjective cognitive complaint] AND [gray matter]
[polygen*] AND [subjective cognitive complaint] AND [white matter]
[polygen*] AND [prodromal] AND [structur*]
[polygen*] AND [prodromal] AND [anatomic*]

[polygen*] AND [prodromal] AND [MRI]
[polygen*] AND [prodromal] AND [DTI]
[polygen*] AND [prodromal] AND [grey matter]
[polygen*] AND [prodromal] AND [gray matter]
[polygen*] AND [prodromal] AND [white matter]

Table B.2: Quality assessment scale criteria and points system.

Area	Question	Values
Methodology	1. Were *a priori* hypotheses stated clearly?	• no = 0 • yes = 1
	2. How large was the sample size?	• <1000 = 0 • >1000 = 1
	3. How many sexes were studied?	• one = 0 • two (or more if genders studied) = 1
	4. Did the study assess a population of interest?	• no (CU only) = 0 • yes (AD **or** MCI, with or without CU) = 1 • yes (AD **and** MCI, with or without CU) = 2
	5. Was APOE accounted for adequately?	• not mentioned = 0 • stratified generally (carriers vs. non-carriers, or homozygous vs. heterozygous) = 1 • various genotypes or number of alleles specified = 2
	6. Did PRS/PHS calculations include APOE SNPs?	• yes = 0 • no = 1 • both = 2
	7. Where were the SNPs used in the PRS/PHS calculations derived from?	• SNPs not derived from GWAS = 0 • number of SNPs from GWAS were limited = 1 • number of SNPs from GWAS were large = 2
Clinical characteristics	8. How was the population defined?	• not specified = 0 • defined clinically (phenotypes) = 1 • defined biologically (biomarkers) = 2
	9. Was family history of the population considered?	• no = 0 • yes = 1
	10. Were demographic and clinical information for participants specified clearly?	• no = 0 • yes (demographic only) = 1 • yes (clinical only) = 2 • yes (both demographic and clinical) = 3
Discussion	11. Were limitations of the research stated clearly?	• no = 0 • yes = 1

Table B.3: Results for all papers selected for systematic review.

Authors	Quality Assessment Score	Total sample size (n)	Participant type	Age	PRS or PHS	PRS or PHS method	PRS or PHS Software	Medium used for PRS or PHS	Area of interest	Whole-brain or regional	Global, regional, or voxel-based maps	Specific feature of interest	Main findings
Ahmad et al. (2018)	11	22,868	Rotterdam study - AD dataset: 7,623 CU, 1,270 AD. MCI dataset - 3,245 CU, 360 MCI. Additional 10,370 CU.	AD dataset-CU age: 79.53 (8.2). AD age of onset: 84.30 (6.8). MCI dataset-age 71.9 (7.2).	PRS (for AD, & PRS for disease-specific pathways)	PRS1 calculated in two ways, (1) 20 SNPs from IGAP, including APOE ε4 SNP, (2) calculated without the APOE ε4 SNP. PRS2 calculated as pathway-specific PRS using 20 SNPs from IGAP, in two ways (a) with APOE ε4, (b) without APOE ε4.	R software. Precise package within R not stated.	UNKNOWN	Structural (MRI).	Regional: hippocampus. Whole-brain.	Global hippocampus. Global cortex.	Imaging phenotypes, white matter lesions, hippocampal volume, brain volume. Progression to AD.	• PRS2 was not associated with hippocampal volume and total brain volume. • PRS2 for immune response pathway and PRS for clathrin/AP 2 adaptor complex pathway, excluding APOE ε4, were associated with white matter lesions. • PRS2 for clathrin/AP 2 adaptor complex pathway, including APOE ε4, was not associated with white

													matter lesions.
Altmann et al. (2020)	14	1,404	ADNI: 417 CU, 712 MCI, 275 AD.	CU: 74.5 (5.6), MCI 73.1 (7.5), 75.1 (7.7).	PRS and PHS (for AD)	PRS1 calculated using 55 SNPs, and PRS2 calculated using 101,450 SNPs, from Kunkle et al. (2019). Both excluding APOE regions. PRS-CS calculated using posterior effect size estimates from Ge et al. (2019). PHS calculated using SNPs from Desikan et al. (2017).	PRSice v2.1.9.	UNKNOWN	Structural (MRI).	Whole-brain, ventricles, left and right hippocampus.	Global brain, ventricles, left and right hippocampus.	Grey matter volume loss.	• Polygenic scores were associated, to a minor degree, with progressive atrophy.
Armstrong et al. (2020)	11	508	BLSA: 508 (CU).	72.3 (9.2).	PRS (for hippocampal volume)	PRS for hippocampal volume calculated using 12,148 SNPs, with and without APOE SNPs, from GWAS (Hibar et al., 2017).	PLINK	UNKNOWN	Structural (MRI).	Whole-brain: total brain, grey matter, white matter, ventricles and, lobar grey matter and white matter. Regional: hippocampus,	Global: total brain, grey/white matter, lobar grey/white matter, hippocampus, entorhinal cortex, parahippocampal gyrus.	Volume loss.	• PRS was associated with hippocampal atrophy, and frontal and parietal white matter.

										entorhinal cortex, parahippocampal gyrus.			
Brenowitz et al. (2023)	10	311	CARDIA: 311 (CU).	55.8 (3.3).	PRS (for AD)	PRS for AD calculated using 25 SNPs from GWAS IGAP, without APOE SNPs.	PLINK	UNKNOWN	Structural (MRI).	Whole-brain: total brain volume, total white matter hyperintensity. Regional: hippocampal volume.	Global hippocampal volume, brain volume, white matter hyperintensity.	White matter hyperintensity volume, total brain volume, hippocampal volume.	• High PRS was associated with increased white matter hyperintensity, not with total brain volume or hippocampal volume. • APOE ε4 was not associated with any of the above outcome measures.
Caspers et al. (2020)	7	544	1000 BRAINS: 544 (CU).	67.3 (6.7)	PRS (for AD)	PRSs calculated using SNPs from GWAS IGAP (Lambert et al., 2013), excluding APOE SNPs. Total PRS calculated using all 20 SNPs. Six pathway-specific PRSs: cholesterol metabolism (4 SNPs),	PLINK	Lymphocyte DNA.	Structural (MRI).	Whole-brain atrophy.	JuBrain atlas. FreeSurfer software. SPM.	Cortical atrophy.	• Higher PRS was associated with greater grey matter decline, influenced by APOE ε4.

						APP metabolism (6 SNPs), MAPT metabolism (3 SNPs), cytoskeleton/axon development (4 SNPs), immune response (8 SNPs), endocytosis (7 SNPs).						
Chandler et al. (2025)	8	32,114	UK Biobank: 32,114	64 (45-81)	PRS (for AD)	PRS calculated using SNPs from Kunkle et al. (2019), with and without APOE region.	PRSice v1.25	UNKNOWN	Structural (MRI T1 and T2 FLAIR)	Whole brain	Global, image-derived phenotype processing from T1-weighted and T2-weighted FLAIR images. BIANCA tool.	White matter hyperintensity volumes	• PRS without APOE associated positively with white matter hyperintensity volumes. The association increased when using PRS with APOE.
Chen et al. (2023)	7	39,983	UK Biobank: 39,983	38-73	PRS (for AD) and PheWAS	PRS calculated using 7,055,881 SNPs identified from Lambert et al. (2013)'s meta-analysis of GWASs.	PRSice	UNKNOWN	Structural (MRI).	Regional: 68 cortical regions, 41 subcortical regions.	Global. FreeSurfer.	Hippocampus, entorhinal cortex, inferior temporal cortex, middle temporal cortex. Cortical and subcortical regions. Risk factors	• No results related to PRS and imaging parameters were reported upon.

												associated with PRS and AD.	
Chen et al. (2024)	10	72,004	UK Biobank: MRI study – 36,969; DTI study – 35,035.	44-81	PRS (for AD)	PRS calculated using SNPs from Kunkle et al. (2019), without APOE region.	UNKNOWN	UNKNOWN	Structural (MRI and DTI).	Regional: 101 ROIs (MRI) and 110 ROIs (DTI).	Global 101 ROIs (MRI) and 110 ROIs (DTI).	Volume, and white matter integrity.	• PRS was associated with greater right inferior lateral ventricular volumes. • PRS was associated with average radial diffusivity, average mean diffusivity, posterior thalamic radiation L1, and average L1.
Chung et al. (2023)	12	1,076	ADNI1: 679. ADNI-GO/2: 397.	74.6 (7.5)	Similar concept to PRS. Module-based (for neuritic plaques, and neurofibrillary tangles).	Module-based PRS calculated from Beecham et al. (2014) GWAS, without APOE	PLINK	Unknown, and AD autopsy brains from the following studies: FHS, BUADRC, ROSMAP, and MCSA.	Structural (MRI)	Regional: Dorsolateral prefrontal cortex and temporal cortex.	Global dorsolateral prefrontal cortex and temporal cortex.	Cortical thickness	• Module-based PRS 6 associated with bilateral frontal, parietal, and temporal, lobed. • Module-based PRS 9 associated with bilateral frontal lobes.

Corlier et al. (2018)	10	561	CHS: 335 + 226 (CU).	77.3 (3.4).	PRS (for AD)	PRS calculated using 9 SNPs, excluding APOE SNPs, identified amongst the top 20 SNPs from GWAS Alzgene database (Bertram et al., 2007).	UNKNOWN	UNKNOWN	Structural (MRI).	Regional: hippocampus, caudal and rostral anterior cingulate, posterior cingulate cortex, isthmus of the cingulate cortex, precuneus, patahippocampal, entorhinal cortex, supramarginal gyrus, caudal and rostral middle frontal gyri.	Global hippocampus, caudal and rostral anterior cingulate, posterior cingulate cortex, isthmus of the cingulate cortex, precuneus, patahippocampal, entorhinal cortex, supramarginal gyrus, caudal and rostral middle frontal gyri.	Regional cortical thickness.	• High PRS was associated with greater regional thinning.
De Marco et al. (2020)	12	784	ADNI: 270 CU (ε3ε3 185, ε4ε3 85). 514 MCI (ε3ε3 241, ε4ε3 212, ε4ε4 61).	CU ε3ε3: 74.85 (5.67). CU ε4ε3: 72.86 (5.98). MCI ε3ε3: 73.37. MCI ε4ε3: 71.87 (7.22). MCI ε4ε4: 69.84 (6.82).	PHS (for AD)	PHS calculated on 33 AD-related SNPs, including two APOE SNPs, from IGAP.	UNKNOWN	UNKNOWN	Structural (MRI).	Whole-brain.	Voxel-based morphometry. MatLab / SPM.	MRI. Grey matter atrophy.	• In MCI patients, PHSs were negatively associated with grey matter in medio-temporal regions. When MCI patients were stratified by APOEε4 status, no significant results were found. • In Aβ, PHSs were

													negatively associated with grey matter volumes in the left anterior hippocampus and amygdala. • In ε3ε3 Aβ+, PHS predicted volume in sensorimotor regions.
De Silva et al. (2022)	11	730	ADNI: 218 (CU), 390 (MCI), 122 (AD).	CU: 73.4 (5.9). MCI: 71.5 (7.5). AD: 74.8 (8.0).	PRS (for AD) and PRS (for coronary artery disease)	PRS for AD calculated using 134,456 SNPs from GWAS (Kunkle et al., 2019). PRS for coronary artery disease using 135,584 SNPs from GWAS (Nikpay et al., 2015).	PRSice v2.1.9	UNKNOWN	Structural (MRI).	Whole-brain volume, total white matter hyperintensities. Regional white matter hyperintensities.	Global: whole-brain and lobar.	Atrophy, white matter hyperintensities.	• Both PRSs were associated with whole-brain volume decline longitudinally. • AD PRS was associated with white matter volume in the occipital lobe.
Desikan et al. (2017)	5	692	ADNI: 692 CU and MCI	Unknown	PHS (for AD)	PHS calculated using 33 SNPs from IGAP/ADGC, including 2 APOE SNPs.	UNKNOWN	UNKNOWN	Structural (MRI).	Regional: hippocampus, entorhinal cortex.	Global hippocampus, entorhinal cortex.	Volume loss.	• PHS was associated with volume loss within the entorhinal cortex, and hippocampus.

Ebenau et al. (2021)	7	703	ADC + SCIENCe: 703 (CU).	Unknown. Age for entire cohort of 829: 59.6 (8.8).	PRS (for AD)	PRS for AD calculated using 39 SNPs from GWAS (Kunkle et al., 2019; Sims et al., 2017; de Rojas et al., 2021), without APOE.	UNKNOWN	UNKNOWN	Structural (MRI).	Regional: medial temporal lobe.	Global medial temporal lobe.	Neurodegeneration/atrophy.	• PRS was associated with neurodegeneration.
Foo et al. (2021)	7	17,161	UK Biobank: 17161 (CU).	44-80.	PRS (for AD)	PRS calculated using SNPs from GWAS by Lambert et al. (2013), with and without APOE SNPs. ••354,674 SNPs.	PRSice2	UNKNOWN	Structural (MRI).	Regional: hippocampus.	Regional: hippocampus- head, body, tail. FreeSurfer software.	Hippocampal subfield volumes: CA1, CA2-3, CA4, subiculum, presubiculum, parasubiculum, hippocampal tail, hippocampal tissue, hippocampus-amygdala-transition-area, molecular layer, granule cell layer of dentate gyrus, fimbria, whole hippocampus.	• Age, not sex, influences the association between PRS and hippocampal subfield volumes. • In elderly participants, high PRS was associated with reduced volumes in left cornu ammonis 1, right hippocampal tail, and bilateral hippocampus-amygdala-transition-area. • When removing APOE SNPs

													from PRS calculation, PRS was not associated with any hippocampal subfields.
Ge et al. (2018)	7	702	ADNIGO/ADNI2: 221 CU, 367 MCI, 114 AD.	55.1-91.5	PRS (for AD)	PRS calculated using SNPs identified from IGAP, including APOE SNPs.	PRSice	UNKNOWN	Structural (MRI).	Regional: hippocampus.	Global hippocampus. FreeSurfer software.	Hippocampal volume.	• In Aβ+ cohort, PRS was weakly associated with baseline hippocampal volume but not associated with longitudinal hippocampal changes • In the Aβ- cohort, PRS was strongly associated with longitudinal changes in hippocampal volume but not baseline hippocampal atrophy.
Genius et al. (2025)	14	668	ALFA CU Aβ-: 220. ALFA CU Aβ+: 118. ADNI MCI Aβ-: 230. ADNI AD Aβ+: 100.	ALFA CU Aβ-: 56 (median). ALFA CU Aβ+: 58 (median). ADNI MCI Aβ-: 72.85 (median).	PRS for AD	PRS calculated using Wightman et al. (2021) GWAS. 296 SNPs. PRSs calculated with and	PRSice v2.0	Blood (for ALFA)	Structural (MRI T1 and T2)	Regional: 41 ROIs (34 cortical and 7 subcortical)	Global. Desikan-Killiany atlas. FreeSurfer.	Volumes.	• Compositional brain scores based on volumetric ROIs and PRS with APOE were

				ADNI AD Aβ+: 75.60 (median).		without APOE.							associated with increased likelihood of being part of disease-stage groups, rather than in the CU group. • Such findings were observed when using the PRS without APOE, although different regions contributed to the compositional brain score.
Habes et al. (2016)	9	2,705	SHIP: 2,705 (CU).	20-90.	PRS (for AD)	PRS calculated using 19 SNPs from GWAS (Lambert et al., 2013), without APOE SNPs.	UNKNOWN	UNKNOWN	Structural (MRI).	Whole-brain.	Global. MASS software. RAVENS maps. Voxel-wise analysis.	Atrophy.	• PRS was associated with spatial atrophy patterns in those aged >65 years.
Habes et al. (2018)	7	985	SHIP: 985.	Healthy: 52.2 (13.16).	PRS (for AD)	PRS calculated using 19 SNPs from IGAP GWAS, excluding APOE.	UNKNOWN	UNKNOWN	Structural (MRI).	Regional	Global regions.	MRI. White matter hyperintensities.	• AD PRS was associated with white matter hyperintensities in the dorsal

													periventricular regions, in participants aged 65+ years.
Harrison et al. (2016)	10	66	UCLA: 66 (CU).	63.0 (10.4).	PRS (for AD)	PRS calculated using SNPs from APOE, CLU, PICALM, CR1, and first-degree family history of AD. Two PRSs calculated, (1) unweighted, (2) weighted. Weights calculated from Jun et al. (2010).	UNKNOWN	Blood.	Structural (MRI).	Regional: hippocampus.	Global hippocampus. Regional hippocampus: parahippocampal cortex, CA1, CA2-3 and dentate gyrus, perirhinal cortex, fusiform, entorhinal cortex, subiculum.	Hippocampal thickness.	• No association between PRS and baseline hippocampal subregions. • Weighted and unweighted PRS were associated with the percentage change in thickness across the whole hippocampus.
Harrison et al. (2023)	11	18,172	UK Biobank: 18,172	64.2 (7.75)	PRS (for AD)	PRS calculated using SNPs from Kunkle et al. (2019), with and without APOE.	PLINK	UNKNOWN	Structural (MRI)	Regional: 26 cortical ROIs and 16 sub-cortical ROIs.	Global. Desikan-Killiany atlas. FreeSurfer.	Volume and thickness.	• Genome-wide PRS and pathway-specific PRSs were associated with cortical thickness and volume, more so when APOE SNPs were included in the scores.

Hayes et al. (2020)	7	126	ADNI: 126 (CU).	74.0 (5.9)	PHS (for AD)	PHS for AD calculated using 31 SNPs identified in GWAS IGAP, plus two APOE SNPs.	UNKNOWN	UNKNOWN	Structural (MRI).	Regional: entorhinal cortex, hippocampus.	Global entorhinal cortex, hippocampus. Desikan-Killany atlas. FreeSurfer software.	Cortical volume.	• High PHS + high BMI was associated with reduced volume in the entorhinal cortex and hippocampus.
He et al. (2023)	9	23,000	UK Biobank: 23,000 approximately	64.52 (7.50)	PRS (for AD)	PRS calculated using SNPs, with and without APOE, from Kunkle et al. (2019) GWAS at 8 thresholds.	PRSice 2	UNKNOWN	Structural (MRI and DTI)	Regional: (1) area, thickness, and volume of 32 bilateral ROIs, (2) volume of 7 bilateral subcortical segmentations, (3) fractional anisotropy and mean diffusivity of 9 bilateral white matter tracts.	Global. Desikan-Killiany atlas. FreeSurfer.	Area, thickness, volume, and white matter integrity.	• PRS with APOE was negatively associated with cortical area of the superior frontal, pars orbitalis, and lateral orbitofrontal. • PRS with APOE was positively associated with cuneus and precuneus. • PRS with APOE was negatively associated with volumes of the pars orbitalis, lateral orbitofrontal, and rostral anterior

													cingulate. • PRS with APOE was positively associated with volume in the superior parietal and cuneus regions. • PRS with APOE was positively associated with mean diffusivity. • PRS with APOE was negatively associated with fractional anisotropy in association fibres, commissural fibres, limbic system fibres, and projection fibres.
Hohman et al. (2017)	13	786	ADNI: 305 CU, 481 MCI.	CU: 73 (6). MCI: 72 (7).	PRS (for AD)	PRS calculated using 21 SNPs from Lambert et al. (2013) meta-analysis.	PLINK v1.9	UNKNOWN	Structural (MRI).	Regional: hippocampus	Global hippocampus. FreeSurfer.	MRI. Left hippocampal, right hippocampal, and intracranial, volumes.	• PRS was not associated with hippocampal volume loss.

Homann et al. (2022)	9	1,221	EMIF-AD MBD: CU, MCI, AD.	67.9 (8.3)	PRS (for AD, & PRS for AD-related imaging phenotypes: hippocampus, cortical thickness, white matter lesions)	PRS calculated using SNPs from GWAS by Jansen et al. (2019) and Hibar et al. (2017).	PLINK2	UNKNOWN	Structural (MRI).	Regional: hippocampus. Whole-brain: cortical thickness, white matter lesions.	Global hippocampus, cortical thickness, and white matter lesions.	Five MRI traits, hippocampal volume, whole-brain cortical thickness, white matter lesions.	• PRSs showed strong associations with hippocampal volume, in line with Hibar et al. (2017)'s findings. • PRSs using SNPs for AD risk, found by Jansen et al. (2019), did not show significant associations in the EMIF-AD MBD sample.
Kannappan et al. (2022)	10	1,086	ADNI: 319 CU, 591 MCI, 176 AD	CU: 75.21 (5.27). MCI: 73.43 (7.43). AD: 75.40 (7.76).	PRS (for AD hippocampal atrophy)	PRS calculated using IGAP/Lambert et al. (2013) GWAS, 7,485,124 SNPs	PLINK	UNKNOWN	Structural (MRI)	Regional: hippocampus	Regional hippocampal subfields. FreeSurfer.	MRI. Hippocampal subfield atrophy.	• CA1, CA4, hippocampal tail, subiculum, presubiculum, molecular layer, GC-ML-DG, and HATA showed stronger PRS associations in the MCI+AD than in the CU. • CA3, parasubiculum, and

													fimbria showed moderate AD PRS associations in the MCI+AD than CU. • No AD PRS association for the hippocampal fissure between groups.
Kauppi et al. (2018)	9	336	ADNI: 336 MCI	MCI: 55-89	PHS (for AD)	PHS calculated using 31 AD-associated SNPs, including APOE, from IGAP GWAS/ADGC.	UNKNOWN	UNKNOWN	Structural (MRI).	Regional: hippocampus, entorhinal cortex, middle temporal gyrus, bank of the superior temporal sulcus, isthmus cingulate, superior temporal gyrus, medial and lateral orbitofrontal gyri.	Global hippocampus, entorhinal cortex, middle temporal gyrus, bank of the superior temporal sulcus, isthmus cingulate, superior temporal gyrus, medial and lateral orbitofrontal gyri. FreeSurfer software.	MRI. Brain atrophy score (volume and thickness).	• PHS predicted time to progression, from MCI to AD. • Combining PHS with brain atrophy score improved prediction, and AUC 82%.
Kirchner et al. (2023)	9	1,806	SHIP-TREND-0: 1,806 (CU).	Female: 50.6 (13.5). Male: 50.4 (14.3).	PRS (for AD)	PRS for AD calculated using all SNPs that reached	PRS-CS	UNKNOWN	Structural (MRI).	Regional: total hippocampus volume, hippocamp	Regional hippocampus.	Regional hippocampal volume.	• PRS was not associated with hippocamp

						genome-wide significance from GWAS by Kunkle et al. (2019).				al subfield volume comprising of cornu ammonis, presubiculum, subiculum, parasubiculum, dentate gyrus, hippocampal fissure, fimbria, tail, hippocampus-amygdala transition area.			al subfield volume.
Korbmacher et al. (2024)	8	33,385	UK Biobank cross-sectional: 31,056. UK Biobank longitudinal: 2,329.	Age at baseline: 62.26 ± 7.19 (46.12-80.30). Age at follow-up: 64.70 ± 7.07 (49.33-82.59)	PRS (for AD)	PRS (GWAS not stated)	PRSice v2.0	UNKNOWN	Structural (DTI)	Global. Regional: 30 ROIs.	Global and regional. John Hopkins University atlas.	White matter microstructure.	• AD PRS was associated with cerebral peduncle. However, this did not survive corrections for multiple testing.
Kulminski et al. (2024)	10	676	NACC UDS CU: 449. NACC UDS AD: 227.	NACC UDS CU: 73.7. NACC UDS AD: 77.2.	Similar concept to PRS (no GWAS).	Similar concept to PRS (no GWAS). PRS with APOE, TOMM40 and APOC1.	Not applicable - similar concept to PRS.	UNKNOWN	Structural (MRI)	Regional: 27 ROIs in temporo-limbic regions.	Global.	Volume and thickness of 27 temporo-limbic regions.	• High risk and low risk participants had reduced volumes and reduced thickness in various ROIs across the temporo-

Lancaster et al. (2019)	6	9,707	UK Biobank: 9,707. ENIGMA: 13,163	Not stated (40-69, as per UK Biobank website)	PRS (for AD)	Whole-genome PRS calculated using SNPs from IGAP (Lambert et al., 2013). Microglia PRS calculated using 56 SNPs also from IGAP GWAS, excluding MHC and APOE regions. AD PRS included SNPs at various thresholds – ENIGMA sample: 117,446, 70,810, 45,698, 5,159, 1,479 SNPs; UK Biobank sample: 136,598, 81,407, 52,308, 9,755, 5,723, 1,598 SNPs.	PRSice v1.25	UNKNOWN	GWAS for hippocampal volume.	Regional: hippocampus.	Global hippocampus.	Hippocampal volume.	limbic regions. • Whole genome AD-RPS and microglia AD-PRS were associated with hippocampal volume.
Lancaster et al. (2023)	12	31,982	PROTECT: 16. UK Biobank: 31,966.	PROTECT: 67.4 (6.50). UK Biobank: 44-81.	PRS (for AD)	PRS for PROTECT participants calculated	PLINK v1.9	UNKNOWN	Structural (MRI)	Regional: 66 ROIs.	Global. Desikan-Killiany atlas.	Grey matter volume and thickness.	• High PRS, without APOE, was associated

						using SNPs from IGAP GWAS, excluding APOE region. PRS for UK Biobank participants calculated using SNPs from Kunkle et al. (2019), excluding APOE and MHC regions.					FreeSurfer v7.1.1		with thickness of the cingulate cortex.
Lee et al. (2021)	9	108	Breakdown of ADNI cohort of 187: 55 (CU), 87 (MCI), 45 (AD).	Unknown. Breakdown of ADNI cohort of 187 according to age -CU: 75.8 (4.9), MCI: 73.8 (7.4), AD 74.6 (8.8).	PRS (for AD)	PRS for AD calculated using 31 SNPs from GWAS (Desikan et al., 2017).	PLINK	UNKNOWN	Structural (MRI).	Whole-brain.	Global.	Cortical thickness. SurfStat toolbox for vertex-wise analyses.	• High AD PRS was associated with reduced cortical thickness in bilateral medial temporal cortex. • AD PRS was not associated with mean lobar cortical thickness.
Li et al. (2021)	11	187	ADNI: 88 CU, 77 MCI, 22 AD	CU: 77.40 (6.13). MCI: 77.13 (8.14). AD: 80.70 (7.83).	PHS (for AD)	PHS calculated using 31 SNPs, including APOE ε2 and APOE ε4	UNKNOWN	UNKNOWN	Structural (MRI).	Whole-brain.	Voxel-based morphometry	Grey matter volume.	• PHS was associated with reduced grey matter volume in the precuneus,

						genotype, from IGAP/ADGC.							inferior parietal lobule, posterior cingulate cortex, and temporal regions. • PHS was associated with increased grey matter volume in the frontal and occipital regions.
Liu et al. (2021)	13	2,140	ADNI: 767 MCI. NACC: 1,373 MCI.	ADNI: 73.4 (7.40). NACC: 77.2 (8.21)	PRS and PHS (for AD)	PRS calculated using 40 SNPs from four AD GWASs (Lambert et al., 2013; Marioni et al., 2018; Kunkle et al., 2019; Jansen et al., 2019), excluding APOE SNPs. PHS calculated using 25 SNPs from Desikan et al. (2017), i.e., IGAP/ADGC, excluding APOE SNPs.	PRSice2	UNKNOWN	Structural (MRI).	Regional: ventricles, hippocampus, entorhinal cortex, fusiform gyrus, middle temporal gyrus.	Global ventricles, hippocampus, entorhinal cortex, fusiform gyrus, middle temporal gyrus.	Regional volume.	• PRS was associated with decreased hippocampal and entorhinal cortex volumes.

Liu et al. (2022)	11	2,140	ADNI: 767 (MCI). NACC: 1,373 (MCI).	ADNI: 73.4 (7.40). NACC: 77.2 (8.21).	PRS (for AD)	PRS for extrinsic-epigenetic-age-acceleration (EEAA) calculated using 16 SNPs from GWAS IGAP (Lambert et al., 2013). PRS for intrinsic-epigenetic-age-acceleration (IEAA) calculated using 22 SNPs from GWAS (Gibson et al., 2019). Both without APOE SNPs.	PRSice3	UNKNOWN	Structural (MRI).	Regional: ventricles, hippocampus, entorhinal, fusiform gyrus, middle temporal gyrus.	Global ventricles, hippocampus, entorhinal, fusiform gyrus, middle temporal gyrus.	Volume loss.	• IEAA PRS and EEAA PRS were associated with reduced fusiform volume. No signification associations were found for other structural measures.
Liu et al. (2023)	3	36,799	UK Biobank: 36,799 (CU).	54.90 (7.43).	PRS (for AD)	PRS calculated using SNPs identified in GWAS by Lambert et al. (2013); 1,312,100 SNPs.	UNKNOWN	UNKNOWN	Structural (MRI).	Whole-brain. Regional: 14 subcortical regions and 66 surface area regions.	Global. Desikan-Killiany atlas.	Total cortical surface area, intracranial volume, average cortical thickness.	• High PRS for AD was associated with low total cortical surface area and low intracranial volume. • PRS for AD was negatively associated with the volume of

													the left putamen.
Lorenz et al. (2025)	13	2,614	CU, MCI, and AD from - ADNI: 491. BIOCARD: 104. BLSA: 399. NACC: 659. ROSMAP: 496. VMAP: 247. WRAP: 218.	ADNI: 74.7 (7.6). BIOCARD: 73.4 (6.8). BLSA: 73.2 (9.7). NACC: 71.3 (10.5). ROSMAP: 81.1 (7.2). VMAP: 73.7 (7.1). WRAP: 62.4 (6.1).	PRS (for AD)	PRS calculated using Marioni et al. (2018) GWAS, with and without SNPs from the APOE region.	PRS-CS	UNKNOWN	Structural (DTI)	Regional: Limbic white matter tracts - cingulum, fornix, inferior longitudinal fasciculus, uncinate fasciculus, inferior temporal gyrus, middle temporal gyrus, and superior temporal gyrus.	Global.	White matter microstructure.	• High PRS with APOE was associated with high free water, high fractional anisotropy corrected for free water, low mean diffusivity corrected for free water, and low radial diffusivity for free water. • In cognitively impaired participants, high PRS with APOE was associated with low radial diffusivity corrected for free water, low high axial diffusivity corrected for free water, and high fractional diffusivity

													corrected for free water.
Lorenzini et al. (2024)	12	1,738	EPAD: 1,738.	65.72 (7.31)	PRS (for AD and six pathway-specific PRSs; Immune Activation PRS, Signal Transduction PRS, Inflammatory PRS, Migration PRS, Amyloid PRS, and Clearance PRS).	PRS calculated using Bellenguez et al. (2022) GWAS, 85 SNPs. PRS with APOE ε2 and ε4, PRS without APOE ε2 and ε4, and six pathway-specific PRSs (Immune Activation PRS, Signal Transduction PRS, Inflammatory PRS, Migration PRS, Amyloid PRS, and Clearance PRS).	UNKNOWN	UNKNOWN	Structural (MRI; FLAIR; DWI)	Regional MRI: Hippocampus. MRI FLAIR: Global and regional (frontal, parietal, temporal, and occipital lobes). DWI: Regional (commissural, limbic, associative, and projection fibers).	Global hippocampus. Global frontal, parietal, temporal, and occipital lobes. Global commissural, limbic, associative, and projection fibers.	Hippocampal volume. White matter hyperintensity volumes. White matter tracts.	• PRS without APOE and pathway-specific PRSs were associated with hippocampal volume and a number of regional white matter hyperintensity volumes, and white matter tracts.
Lupton et al. (2016)	10	1,674	ADNI, AddNeuroMed, Sydney MAS, OATS: 746 CU, 648 MCI, 75.5 AD.	CU: 75.3 (5.9) 53-90. MCI 75.8 (6.7) 55-88. AD: 75.5 (7.1) 55-91.	PRS (for AD)	PRS calculated using 19 genome-wide significant AD risk variants from IGAP, excluding APOE and TREM2.	PLINK	UNKNOWN	Structural (MRI).	Regional: hippocampus, amygdala. Whole-brain: intracranial volume.	Global hippocampus, amygdala, and intracranial volume. FreeSurfer.	MRI. Hippocampal, amygdala, and intracranial volumes.	• AD PRS are associated with reduced hippocampal volume in CU and MCI individuals.

Manca, Pardinas, and Venneri (2023)	6	800	ADNI: 203 (CU), 121 (AD with psychosis, of which 383 MCI and 83 dementia), 476 (AD without psychosis, of which 49 MCI and 72 dementia)	Unknown.	PRS (for AD)	PRS for AD calculated using SNPs from Jansen et al. (2019).	PRSice v2	UNKNOWN	Structural (MRI).	Whole brain.	Global. Automated Anatomical Labelling atlas 2. Voxel-based morphometry. MatLab, SPM.	Grey matter volume.	• AD PRS was negatively associated with grey matter volume in bilateral medio-temporal and right inferior temporal and posterior cingulate regions across samples. • AD PRS was negatively associated with left medio-temporal regions in the AD with psychosis group.
Meda et al. (2012)	9	757	ADNI: 209 (CU), 367 (MCI), 181 (AD).	CU: 76.05 (4.94). MCI: 74.95 (7.37). AD: 75.57 (7.48).	Not PRS or PHS. Similar concept used.	27,150 SNPs. GWAS-type analysis.	MatLab 7.0. Not PRS/PHS, but a similar concept.	UNKNOWN	Structural (MRI).	Regional: 94 ROI.	Global: 94 ROI. FreeSurfer software.	Brain volume and cortical thickness.	• Four genetic networks were associated with one structural brain network consisting of 40 ROIs.
Mormino et al. (2016)	12	692	ADNI1: 194 CU, 332	ADNI1: CU + MCI 75.3	PRS (for AD)	PRS calculated using	PLINK v1.9	UNKNOWN	Structural (MRI).	Regional: hippocampus.	Global hippocampal volume.	Hippocampal volume.	• PRS was associated with smaller

			MCI, 166 AD.	(6.5). AD 75.8 (7.4).		16,123 SNPs below the IGAP GWAS-level significance. Another PRS calculated using 18 SNPs from IGAP GWAS-level significance. With and without APOE SNPs.					FreeSurfer software.		hippocampal volume.
Nordengen et al. (2022)	10	394	DDI: 93 normal controls, 43 normal controls with abnormal cognitive staging, 133 SCD, 101 MCI, 24 missing diagnosis.	63.9 (9.34)	PRS (for AD)	PRS calculated using 13,377,200 SNPs from GWAS Jansen et al. (2019), excluding APOE and MHC SNPs. Two types of PRS, (1) standard P-value based PRS, (2) phenotype-informed PRS (PRSinflammation and PRScardiovascular, informed by inflammatory disorder, and cardiovascular disease	UNKNOWN	UNKNOWN	Structural (MRI).	Regional: entorhinal cortex, BA35, BA36.	Global entorhinal cortex, BA35, BA36. ASHS-PMC-T1 atlas.	MRI. Medial temporal cortex.	• Inflammation PRS was associated with medial temporal lobe atrophy cross-sectionally and longitudinally. • Cardiovascular PRS was associated with medial temporal lobe atrophy longitudinally.

						risk factors/ disease, respectively).							
Prieto et al. (2020)	10	686	ADNI: CU, MCI, AD	55-91	PHS (for AD)	PHS calculated using 31 AD-associated SNPs, plus APOE SNPs using IGAP.	Epitools (package in R software)	UNKNOWN	Structural (MRI)	Regional: hippocampus, entorhinal cortex	Global hippocampus and entorhinal cortex. FreeSurfer. Desikan-Killiany atlas.	MRI. Medial temporal lobe.	• MCI cohort showed an association between left hippocampal volume and genetic risk. • AD cohort showed an association between right entorhinal cortex volume and genetic risk for AD.
Reas et al. (2023)	9	849	ADNI: Subjective memory complaint: 90, Early MCI: 276, Late MCI: 483.	Subjective memory complaint: 72.3 (5.8). Early MCI: 71.5 (7.3). Late MCI: 74.0 (7.5).	MHS (for AD). Similar concept to PRS/PHS.	Desikan et al. (2019) PHS used directly. 33 SNPs including APOE ε2 and ε4 SNPs.	UNKNOWN	UNKNOWN	Structural (MRI).	Regional: 64 ROIs.	Global. FreeSurfer v5.0.	Brain atrophy.	• Multimodal hazard score substantially predicted conversion from subjective memory complaints or MCI to AD dementia. • Higher the multimodal hazard score, time to AD dementia

													onset significantly reduced.
Roe et al. (2024)	8	522	LCBC: 229. Betula: 175. NESDA: 118. (CU)	LCBC: 63.7 (14.4). Betula: 64.3 (11.9) . NESDA: 118 45.1 (7.9).	PRS (for AD)	PRS calculated using Lambert et al., (2013), Kunkle et al. (2019), Jansen et al. (2019), and Wightman et al. (2021). X4 PRSs with SNPs from APOE region. X4 PRSs without SNPs from APOE region.	PLINK	UNKNOWN	Structural (MRI)	Regional: entorhinal, hippocampus, amygdala, and composite cortical ROI of parahippocampal, fusiform, lingual.	Global entorhinal, hippocampus, amygdala, parahippocampal, fusiform, and lingual. FreeSurfer. Desikan-Killiany atlas.	Volumes.	• High PRS was associated with increased volume loss (in hippocampus, entorhinal and amygdala) than expected considering age. Therefore, faster than expected atrophy. • More associations found using PRS with APOE than PRS without APOE.
Roostaei et al. (2018)	12	1,773	ADNI1: 190 CU, 146 AD. ADNIGO/2: 222 CU, 93 AD. MAP1: 306 CU, 160 AD. MAP2: 126 CU, 43 AD. ROS1: 264 CU, 151 AD. ROS2: 50 CU, 22 AD.	ADNI1 - CU: 76.1 (4.6). AD: 77.3 (5.7). ADNIGO/2 - CU: 73.8 (5.7). AD: 77.4 (5.9). MAP1 - CU: 86.5 (6.8). AD: 90.9 (5.3). MAP2 - CU: 84.0	PRS (for homocysteine)	PRS calculated using 13 SNPs from van Meurs et al. (2013) meta-analysis of GWAS studies on homocysteine.	PLINK v1.9	Homocysteine	Structural (MRI).	Regional. Whole-brain.	Regional voxel-based morphometry. Global map.	Grey matter atrophy.	• No association between Homocysteine-PRS and total grey matter volume in AD. • Association between Homocystei

				(7.1). AD: 91.0 (5.6). ROS1 - CU: 84.2 (6.3). AD: 89.6 (6.2). ROS2 - CU: 81.4 (7.0). AD: 87.5 (7.9).									ne-PRS and total grey matter volume in CU. • Higher Homocysteine-PRS was associated with greater regional grey matter atrophy in the occipital cortex of CU.
Rutten-Jacobs et al. (2018)	2	8,448	UK Biobank: 8448	62.2 (7.4)	PRS (for microstructural integrity)	PRS calculated using SNPs from Lambert et al. (2013).	PLINK v1.9	UNKNOWN	Structural (DTI).	Whole-brain.	Voxel-based maps.	DTI. Microstructural integrity of white matter and AD.	• White matter hyperintensity volume PRS was associated with AD, other PRSs were not.
Sabuncu et al. (2012)	11	104	ADNI: 104 (CU).	75.9 (5.1).	PRS (for AD)	PRS calculated using 26 SNPs, with and without APOE SNPs, identified from GWAS (Harold et al., 2009).	PLINK	UNKNOWN	Structural (MRI).	Regional: entorhinal cortex, temporopolar cortex, lateral temporal cortex, inferior parietal cortex, inferior parietal sulcus, posterior cingulate cortex, inferior	Global entorhinal cortex, temporopolar cortex, lateral temporal cortex, inferior parietal cortex, inferior parietal sulcus, posterior cingulate cortex, inferior	Cortical thickness.	• PRS, with and without APOE, was associated with AD-related ROIs.

										frontal cortex.	frontal cortex. FreeSurfer software.		
Sha et al. (2023)	9	30,810	UK Biobank: 30,810 (CU).	63.84.	PRS (for AD)	PRS calculated using 1,105,067 SNPs from GWAS (Kunkle et al., 2019), with and without APOE SNPs.	PRS-CS	UNKNOWN	Structural (DTI).	Regional: 90 ROI.	Global 90 ROI of the Automated Anatomical Labelling atlas.	White matter structural connectivity /tractography.	• Higher AD PRS was associated with increased white matter connectivity in 62 out of 90 regions.
Sloan et al. (2010)	7	132	DMAS: 47 (CU), 85 (MCI or cognitive complaints) .	CU: female 73.70 (6.51), male 73.1 (5.74). MCI or cognitive complaints: female 70.88 (4.92), male 71.79 (5.63).	Not PRS or PHS. Similar concept used.	834 SNPs from GWASs - KEGG Alzheimer's disease pathway (Kanehisa et al., 2008), genetic association database (Becker et al., 2004), and AlzGene database (Bertram et al., 2007).	R software. Not PRS/PHS, but a similar concept.	UNKNOWN	Structural (MRI).	Regional: hippocampus.	Global hippocampus. Voxel-based morphometry.	Volume, grey matter density.	• SNPs were associated with hippocampal volume and grey matter density, but rarely associated with verbal memory score and cognitive complaints.
Soldan et al. (2024)	11	1,093	PAC (from ACS, AIBL, BIOCARD, BLSA, and WRAP) CU: 1,093.	PAC (from ACS, ABIL, BIOCARD, BLSA, and WRAP) CU baseline: 66 (9.6).	PRS (for AD)	PRS calculated using SNPs from Kunkle et al. (2019) without APOE region.	PLINK	Blood	Structural (MRI T1; MRI FLAIR)	Regional and global: Hippocampal volume, AD-vulnerable-ROIs composite	Global hippocampal volume, AD-vulnerable-ROIs composite score, AD-	Volumes. White matter hyperintensities.	• High PRS without APOE was associated with reduced hippocampal volume,

						6,739,456 SNPs.				score, AD-non-vulnerable-ROIs composite score (all MRI T1); global white matter hyperintensities (MRI FLAIR).	non-vulnerable-ROIs composite score, and white matter hyperintensities.		higher AD-vulnerable composite score, and higher global white matter hyperintensity volumes. • An interaction between, high PRS without APOE x ε4 x time, was evident regarding white matter hyperintensities.
Steventon et al. (2023)	8	10,924	UK Biobank: 10,924	63.41 (6.65)	Polygenic score (for AD)	Polygenic score calculated using SNPs from Kunkle et al. (2019) GWAS.	PLINK	UNKNOWN	Structural (MRI)	Regional: hippocampus, parahippocampal gyrus, perirhinal cortex, entorhinal cortex, amygdala, and the temporal lobe. Subregional hippocampus: CA1, CA 2/3, CA4, and the dentate gyrus.	Global and regional. FreeSurfer v6.0.0.	Volume.	• Polygenic scores were not associated with medial temporal regions, and did not interact with menopause age to impact these structures.

Tan et al. (2019)	8	607	ADNI1: 177 CU, 297 MCI, 133 AD.	Age at baseline: CU 76.10 (4.95), MCI 75.17 (7.17), AD 75.37 (7.82).	PHS (for AD)	PHS calculated using 31 SNPs identified from IGAP GWAS (31 SNPs as written in Desikan et al., 2017, no APOE SNPs included).	UNKNOWN	UNKNOWN	Structural (MRI).	Regional: 33 ROI.	Global. Desikan-Killiany atlas. FreeSurfer.	Atrophy.	• PHS was associated with cortical volumes in 11 ROI, across the disease continuum.
Tank et al. (2022)	12	32,790	UK Biobank: 32,790 (CU).	47-80.	PRS (for AD)	PRS calculated using 6,578,321 SNPs from GWAS (Kunkle et al., 2019), without APOEε4 SNPs.	UNKNOWN	UNKNOWN	Structural (MRI).	Regional: hippocampus. Whole-brain.	Global hippocampus. Global.	12 MRI volumes, including total grey matter, white matter, white matter hyperintensity, whole brain, left hippocampus, right hippocampus. Hippocampal subdivisions - head, tail, body.	• In the fully adjusted model, PRS was associated with the volume of the left hippocampus, and left hippocampal body region. • In the fully adjusted model, there were no associations between PRS interaction with APOE and any structural volumes or any hippocampal subdivision volumes.

Vacher et al. (2022a)	8	721	AIBL: 721 (CU).	Amyloid positive: 75.48 (6.59). Amyloid negative: 72.15 (6.16).	PRS (for hippocampus, ventricles, grey matter, white matter)	PRS for hippocampus calculated using 16 SNPs. PRS for ventricles calculated using 19 SNPs. PRS for grey matter calculated using 18 SNPs. PRS for white matter calculated using 12 SNPs. No APOE SNPs.	PLINK v2.0	UNKNOWN	Structural (MRI).	Regional: ventricles, hippocampus. Whole-brain: cortical grey matter, cortical white matter.	Global ventricles, hippocampus, grey matter, white matter.	Atrophy.	• Regional PRS was associated with longitudinal changes in volume of hippocampus, ventricles, grey matter, and white matter. • High PRS was associated with accelerated volume change than those with low PRS.
Vacher et al. (2022b)	10	780	AIBL: 573 CU, 124 MCI, 83 AD.	CU: 72.9 (6.12). MCI: 75.6 (7.13). AD: 75.0 (7.85).	PHS (for AD)	PHS calculated using 31 SNPs identified from IGAP, plus two APOE SNPs.	UNKNOWN	UNKNOWN	Structural (MRI).	Regional: 33 ROIs.	Global atrophy. Desikan-Killiany atlas. FreeSurfer software.	Atrophy/longitudinal volume change.	• PHS was associated with faster regional brain atrophy.
Wang et al. (2019)	11	286	ADNI: 180 CU, 106 AD.	CU: 76.90 (6.6234). AD: 77.81 (7.2507).	PRS (for PRS)	PRS calculated using 8,070 SNPs from IGAP, with and without APOE SNPs.	PRSice v1.25	UNKNOWN	Structural (MRI).	Regional: Ch4	Regional. Ch4 probabilistic map. SPM.	Ch4 volume.	• In AD patients, PRS is not associated with Ch4 volume, whether including or excluding the APOE region.

													• In CU subjects, PRS, is associated with Ch4 volume, whether including or excluding APOE.
Williams et al. (2021)	6	564	VETSA: CU.	61.68 (5.36)	PRS (for AD)	PRS calculated using SNPs from Lambert et al. (2013) meta-analysis.	PLINK v1.9	UNKNOWN	Structural (MRI and DTI).	Regional. Whole-brain.	Global. Desikan-Killiany atlas. FreeSurfer.	Cortical thickness, hippocampal volume, grey matter diffusivity.	• The PRS + age + mean diffusivity signature and PRS + age + thickness/volume signature + mean diffusivity signature, significantly improved prediction from CU to MCI. Both provided an AUC of 83%.
Xiao et al. (2017)	11	280	Recruited by researchers : 280 (CU).	31.59 (9.27)	PRS (for AD) and PRS (for APOE)	PRS for AD calculated using SNPs identified in IGAP GWAS, excluding APOE SNPs, at various thresholds. (1) 2,466 SNPs, (2) 355 SNPs, (3) 89	PLINK	UNKNOWN	Structural (MRI).	Whole-brain: cortical thickness, surface area, grey matter volume. Regional: volume of hippocampus, amygdala, thalamus,	Global and regional. FreeSurfer software.	Global and regional volume.	• Almost no association between AD PRS with morphometric measures.

						SNPs, (4) 29 SNPs, (5) 22 SNPs, (6) 15 SNPs. PRS for APOE SNPs only.				caudate, putamen, accumbens area, pallidum.			
Xu et al. (2022)	11	163	ADNI: CU 51, 69 MCI, 43 AD	CU: 73.71 (5.88). MCI: 73.32 (7.40). AD: 75.00 (8.13),	PHS (for AD)	PHS calculated using 31 AD-associated SNPs, excluding APOE, from Desikan et al. (2017). .	UNKNOWN	UNKNOWN	Structural (MRI).	Regional: hippocampal subfields.	Regional hippocampus. Computational atlas of hippocampal formation. Hippocampal subfield-to-entire-ipsilateral-hippocampus volume ratio. FreeSurfer.	MRI. Hippocampal subfield volumes.	• Association between PHS and disease status with the right fimbria.
Zhao et al. (2019b)	5	21,821	UK Biobank: 19,629. 2,192 from ADNI (860), HCP (334), PING (461), PNC (537).	UK Biobank: 62.51 (7.47). ADNI: 62.51 (7.47). HCP: 28.82 (3.68). PING: 12.28 (4.99). PNC: 21.14 (3.71).	PRS (for predicting brain volumetric phenotypes)	PRS calculated using 365 SNPs from five GWASs (UK Biobank, ADNI, HCP, PING, PNC).	PLINK	UNKNOWN	Structural (MRI).	Regional: 101 regional brain volume phenotypes.	Global.	101 brain volumetric phenotypes (including total brain volume, grey matter, white matter)	• 11 brain volumetric ROIs from UK Biobank were associated with ROI volume in four validation datasets. • 29 ROIs were associated with at least three datasets. • 56 ROIs were associated

													with at least two datasets. • 84 ROIs were associated with at least one dataset.
Zhao et al. (2020)	9	1,720	Researchers' cohort: 231 CU, 223 MCI, 261 AD. ADNI: 356 CU, 550 MCI, 322 AD.	Researchers' cohort mean age range (SD range) in various subcohorts: 65.4-75.1 (6.2-10.0). ADNI: CU 73.9 (5.9), MCI 73.3 (7.5), AD 74.8 (7.4).	PRS (for AD)	PRS calculated using SNPs from GWAS Jansen et al. (2019).	PLINK	UNKNOWN	Structural (MRI).	Regional: hippocampus.	Global hippocampus. Multi-atlas-based label learning.	Hippocampal radiomic features as MRI marker for AD.	• In MCI patients, 21 out of 33 radiomic features were significantly associated with PRS.

Aβ: amyloid beta. AD: Alzheimer's disease. ADC: Amsterdam dementia cohort. ADGC: Alzheimer's Disease Genetics Consortium. ADNI: Alzheimer's Disease Neuroimaging Initiative. AIBL: Australian Imaging Biomarkers and Lifestyle study of ageing. ALFA: Alzheimer's and Families study. APOC1: apolipoprotein C1. APOE: apolipoprotein E. APP: amyloid precursor protein. AUC: area under the curve. BA: Brodmann area. BIANCA: Brain Intensity AbNormality Classification Algorithm. BIOCARD: Biomarkers of Cognitive Decline Among Normal Individuals. BLSA: Baltimore Longitudinal Study of Aging. BMI: body mass index. BUADRC: Boston University Alzheimer's Disease Research Centre. CA1: cornu ammonis 1. CA2: cornu ammonis 2. CA3: cornu ammonis 3. CA4: cornu ammonis 4. CARDIA: Coronary Artery Risk Development in Young Adults. CHS: Cardiovascular Health Study. CLU: Clusterin. CR1: Complement C3b/C4b receptor 1. CU: cognitively unimpaired. DMAS: Dartmouth Memory and Aging Study. DNA: deoxyribonucleic acid. DTI: diffusion tensor imaging. DWI: diffusion weighted imaging. EMIF-AD MBD: European Medical Information Framework for Alzheimer's Disease Multimodal Biomarker Discovery. EMIF-AD PreclinAD: European Medical Information Framework for AD, preclinical AD study. ENIGMA: Enhancing Neuroimaging Genetics through Meta-Analysis. EPAD: European Prevention of Alzheimer's Dementia. FHS: Framingham Heart Study. FLAIR: Fluid-Attenuated Inversion Recovery. GC-ML-DG: granule cells in the molecular layer of the dentate gyrus. GWAS: genome-wide association study. HATA: hippocampus-amygdala-transition-area. HCP: Human Connectome Project. IGAP: International Genomics of Alzheimer's Project. KEGG: Kyoto encyclopedia of genes and genomes. LCBC: Center for Lifespan Changes in Brain and Cognition. MAP: Rush Memory and Aging Project. MAPT: microtubule-associated protein tau. MASS: Multi-atlas skull striping. MCSA: Mayo Clinic Study of Aging. MCI: mild cognitive impairment. MRI: magnetic resonance imaging. MHS: multimodal hazard score. NACC: National Alzheimer's Coordinating Center. NACC UDS: National Alzheimer's Coordinating Centre Uniform Data Set. NESDA: Netherlands Study of Depression and Anxiety. OATS: Older Australian Twins Study. PheWAS: phenome-wide association study. PHS: polygenic hazard score. PICALM: Phosphatidylinositol binding clathrin assembly protein. PING: Pediatric Imaging, Neurocognition, and Genetics. PNC: Philadelphia

Neurodevelopmental Cohort. ROI: region of interest. ROS: Religious Orders Study. PRS: polygenic risk score. PRS-CS: polygenic risk score-continuous shrinkage. RAVENS: regional analysis of volumes examined in normalised space. ROSMAP: Religious Orders Study and Rush Memory and Aging Project. SCD: subjective cognitive decline. SCIENCe: Subjective Cognitive Impairment Cohort. SD: standard deviation. SHIP: Study of Health in Pomerania. SHIP-TREND-0: baseline sample between 2008 2012 from the Study of Health in Pomerania. SNP: single nucleotide polymorphism. SPM: statistical parametric mapping. Sydney MAS: Sydney Memory and Ageing Study. TOMM40: translocase of outer mitochondrial membrane 40 homolog. TREM2: triggering receptor expressed on myeloid cells 2. UCLA: University of California, Los Angeles. 1000 BRAINS: cohort of general population from West Germany. VETSA: Vietnam Era Twin Study of Aging. VMAP: Vanderbilt Memory and Aging Project. WRAP: Wisconsin Registry for Alzheimer Prevention.

•• Not stated in paper. However, author(s) responded to email communication and provided information.

Table B.4: GWASs and races of participants used in the discovery datasets and target datasets, as well as genes and SNPs used to construct polygenic scores in target datasets.

Paper Selected for Systematic Review	Discovery GWAS used	Genes and SNPs used to construct Polygenic Scores in Target Dataset	APOE included/excluded/both in Polygenic Scores	Race/Ancestry/Ethnicity of Participants in Discovery GWAS	Race/Ancestry/Ethnicity of Participants in Target Dataset
Ahmad et al. (2018)	Lambert et al. (2013)	PRS: APOE ε4 rs429358, CR1 rs6656401, BIN1 rs6733839, INPP5D rs35349669, MEF2C rs190982, TREM2 rs75932628, CD2AP rs10948363, ZCWPW1 rs1476679, EPHA1 rs11771145, NME8 rs2718058, PTK2B rs28834970, CLU rs9331896, SORL1 rs11218343, CELF1 rs10838725, MS4A6A rs983392, PICALM rs10792832, FERMT2 rs17125944, SLC24A4-RIN3 rs10498633, ABCA7 rs4147929, CASS4 rs7274581.	APOE included and excluded	European ancestry	Rotterdam
Altmann et al. (2020)	Desikan et al. (2017), Kunkle et al. (2019), and Ge et al. (2019).	PHS & PRS-CS: Genes/SNPs not listed. PRS: Genes/101450 vs. 55 SNPs not listed. Genes used in PRS p-value threshold 1.0e-8: CR1 rs679515, BIN1 rs6710467, BIN1 rs6733839, PTK2B rs73223431, PTK2B rs73223431, CLU rs867230, SPI1 rs3740688, MTCH2 rs10838738, PTPRJ rs34467936, MS4A4A rs1582763, PICALM rs3851179, SLC24A4 rs12590654, ABCA7 rs4147910, ABCA7 rs12151021.	APOE excluded	European ancestry	Central European ancestry and self-reported white non-Hispanic ethnicity
Armstrong et al. (2020)	Hibar et al. (2017)	PRS: Genes/12148 SNPs not listed.	APOE included and excluded	European ancestry	Caucasian
Brenowitz et al. (2023)	IGAP	PRS: CR1 rs4844610, BIN1 rs6733839, INPP5D rs10933431, HLA-DRB1 rs9271058, TREM2 rs75932628, CD2AP rs9473117, OARD1 rs114812713, NYAP1 rs12539172, EPHA1 rs10808026, PTK2B rs73223431, CLU rs9331896, ECHDC3 rs7920721, SPI1 rs3740688, MS4A2 rs7933202, PICALM rs3851179, SORL1 rs11218343, FERMT2 rs17125924, SLC24A4 rs12881735, ADAM10 rs593742, IQCK rs7185636, WWOX rs62039712, ACE rs138190086, ABCA7 rs3752246, CASS4 rs6024870, ADAMTS1 rs2830500.	APOE excluded	European ancestry	European ancestry; white
Caspers et al. (2020)	Lambert et al. (2013)	PRS: TOMM40 rs2075650, BIN1 rs6733839, CR1 rs6656401, ABCA7 rs4147929, FERMT2 rs17125944, HLA-DRB5, HLA-DRB1 rs9271192, PTK2B rs28834970, CD2AP rs10948363, INPP5D rs35349669, CELF1 rs10838725, MEF2C rs190982, NME8 rs2718058, ZCWPW1 rs1476679, SLC24A4/RIN3 rs10498633, MS4A6A rs983392, EPHA1 rs11771145, CASS4 rs7274581, PICALM rs10792832, CLU rs9331896, SORL1 rs11218343.	APOE excluded	European ancestry	Germany
Chandler et al. (2025)	Kunkle et al. (2019)	PRS: Genes/SNPs not listed. MHC excluded.	APOE included and excluded	Non-Hispanic white	British or Irish descent / European ancestry
Chen et al. (2023)	Lambert et al.(2013)	PRS: Genes/7055881 SNPs not listed.	UNKNOWN	European ancestry	British ancestry

Chen et al. (2024)	Kunkle et al. (2019)	PRS: Genes/SNPs used from Kunkle et al. (2019) not listed.	APOE excluded.	Non-Hispanic white	White British predominantly | Subsample of consisting of Asian, African, and Hispanic descent
Chung et al. (2023)	Beecham et al.(2019)	PRS: pathway-specific genes provided.	APOE excluded	European ancestry	European ancestry
Corlier et al. (2018)	Bertram et al.(2007)	PRS: MS4A4E rs670139, MS4A6A rs610932, IL1A rs1800587, IL1B rs1143634, CR1 rs6701713, EPHA1 rs11767557, CLU rs11136000, ABCA7 rs3764650, CD33 rs3865444.	APOE excluded	African origin, Asian, Caucasian, Hispanic, other/mixed.	White
De Marco et al. (2020)	IGAP	PHS: 33 SNPs from 25 genes - CR1, BIN1, INPP5D, HLA-DRB5, GPR115, BC043356, ZCWPW1, AL833583, PTK2B, CHRNA2, CLU, CR595071, SPI1, MS4A6A, PICALM, SORL1, FERMT2, SLC24A4, abParts, TRIP4, BZRAP1, C19orf6, APOE, ABCA7, CASS4. SNPs not listed.	APOE included	European ancestry	White
de Silva et al. (2022)	Kunkle et al. (2019), and Nikpay et al. (2015).	PRS: Genes/134456 vs. 135584 SNPs not listed.	APOE excluded	European ancestry, non-Hispanic white. European ancestry, South Asian (India, Pakistan) ancestry, and East Asian (China, Korea) ancestry.	Central-European ancestry
Desikan et al. (2017)	IGAP	PHS: APOE ε2, APOE ε4, CR1 rs4266886, CR1 rs4266886, BIN1 rs6733839, INPP5D rs10202748, HLA-DRB5 rs115124923, HLA-DQB1 rs115675626, GPR115 rs1109581, BC043356 rs17265593, BC043356 rs2597283, ZCWPW1 rs1476679, AL833583 rs78571833, PTK2B rs12679874, CHRNA2 rs2741342, CLU rs7831810, CLU rs1532277, CLU rs9331888, CR595071 rs7920721, SPI1 rs3740688, MS4A6A rs7116190, PICALM rs526904, PICALM rs543293, SORL1 rs11218343, FERMT2 rs6572869, SLC24A4 rs12590273, abParts rs7145100, TRIP4 rs74615166, BZRAP1 rs2526378, C19orf6 rs117481827, ABCA7 rs7408475, ABCA7 rs3752246, CASS4 rs7274581.	APOE included	European ancestry	American ancestry; white
Ebenau et al. (2021)	Kunkle et al. (2019), Sims et al. (2017), and de Rojas et al. (2021)	PRS: CR1 rs4844610, PRKD3 rs876461, LOC105373605 rs6733839, INPP5D rs10933431, rs4351014, rs9275152 , TREM2 rs143332484, TREM2 rs75932628, LOC107986595 rs9381040, CD2AP rs9381564, PILRA rs1859788, EPHA1 / EPHA1-AS1 rs56402156, PTK2B rs73223431, CLU rs9331896, SHARPIN rs34674752, SHARPIN / MAF1 rs34173062, LOC105376412 / LOC105376413 rs7920721, SPI1 rs3740688, rs1582763, rs3851179, SORL1 rs11218343, FERMT2 / LOC105370500 rs17125924, SLC24A4 rs11623019, rs593742, APH1B rs117618017, IQCK rs7185636, IL34 rs4985556, rs12444183, PLCG2 rs3935877, PLCG2 rs72824905, C17orf107 / CHRNE rs72835061, ZNF594-DT / SCIMP rs75511804, LRRC37A / ARL17B / LOC124904014 rs2732703, AB13 rs616338, ACE rs4311, ABCA7 rs3752231, CD33 / LOC107985327 rs12459419, CASS4 rs6024870, APP rs2154481.	APOE excluded	European ancestry	European ancestry

Foo et al. (2021)	Lambert et al. (2013)	PRS: 354674 SNPs.	APOE included and excluded	European ancestry	European descent
Ge et al. (2018)	IGAP	PRS: Genes/SNPs not listed.	APOE included	European ancestry	European ancestry
Genius et al. (2025)	Wightman et al. (2021)	PRS: Genes/296 SNPs not listed.	APOE included and excluded	Caucasian	European ancestry
Habes et al. (2016)	Lambert et al.(2013)	PRS: CR1 rs6656401, BIN1 rs6733839, CD2AP rs10948363, EPHA1 rs11771145, CLU rs9331896, MS4A6A rs983392, PICALM rs10792832, ABCA7 rs4147929, HLA-DRB5 / HLA-DRB1 rs9271192, PTK2B rs28834970, SORL1 rs11218343, SLC24A4 / RIN3 rs10498633, INPP5D rs35349669, MEF2C rs190982, NME8 rs2718058, ZCWPW1 rs1476679, CELF1 rs10838725, FERMT2 rs17125944, CASS4 rs7274581.	APOE excluded	European ancestry	Germany
Habes et al. (2018)	Lambert et al.(2013)	PRS: ABCA7 rs4147929, BIN1 rs6733839, CASS4 rs7274581, CD2AP rs10948363, CELF1 rs10838725, CLU rs9331896, CR1 rs6656401, EPHA1 rs11771145, FERMT2 rs17125944, HLA rs9271192, INPP5D rs35349669, MEF2C rs190982, MS4A6A rs983392, NME8 rs2718058, PICALM rs10792832, PTK2B rs28834970, SLC24A4/RIN3 rs10498633, SORL1 rs11218343, ZCWPW1 rs1476679.	APOE excluded	European ancestry	Germany
Harrison et al. (2016)	Lambert et al. (2013)	PRS: APOE, CLU rs11136000, PICALM rs3851179, CR1 rs3818361.	APOE included	European ancestry	USA
Harrison et al. (2023)	Kunkle et al.(2019)	PRS: Genes/SNPs used from Kunkle et al. (2019) not listed.	APOE included and excluded	Non-Hispanic white	White British or Irish decent
Hayes et al. (2020)	IGAP	PHS: APOE ε2, APOE ε4, CR1 rs4266886, CR1 rs61822977, BIN1 rs6733839, INPP5D rs10202748, HLA-DRB5 rs115124923, HLA-DQB1 rs115675626, GPR115 rs1109581, BC043356 rs17265593, BC043356 rs2597283, ZCWPW1 rs1476679, AL833583 rs78571833, PTK2B rs12679874, CHRNA2 rs2741342, CLU rs7831810, CLU rs1532277, CLU rs9331888, CR595071 rs7920721, SPI1 rs3740688, MS4A6A rs7116190, PICALM rs526904, PICALM rs543293, SORL1 rs11218343, FERMT2 rs6572869, SLC24A4 rs12590273, abParts rs7145100, TRIP4 rs74615166, BZRAP1 rs2526378, C19orf6 rs117481827, ABCA7 rs7408475, ABCA7 rs3752246, CASS4 rs7274581.	APOE included	European ancestry	White, non-Hispanic/Latino
He et al. (2023)	Kunkle et al. (2019)	PRS: Genes/SNPs used from Kunkle et al. (2019) not listed. Used 8 thresholds, with and without APOE. 5e-08: 58 SNPs with APOE and 17 without APOE. 1e-06: 76 SNPs with APOE and 30 without APOE. 5e-06: 96 SNPs with APOE and 44 without APOE. 1e-05: 120 with APOE and 65 with APOE. 5e-05: 232 SNPs with APOE and 170 without APOE. 0.0001: 346 SNPs with APOE and 281 without APOE. 0.001: 1855 with APOE and 1770 without APOE. 0.01: 12361 with APOE and 12244 without APOE.	APOE included and excluded	Non-Hispanic white	European
Hohman et al. (2017)	Lambert et al. (2013)	PRS: CR1 rs6656401, BIN1 rs6733839, CD2AP rs10948363, EPHA1 rs11771145, CLU rs9331896, MS4A6A rs983392, PICALM rs10792832, ABCA7 rs4147929, CD33 rs3865444g, HLA-DRB5/HLA-DRB1 rs9271192, PTK2B rs28834970, SORL1 rs11218343, SLC24A4/RIN3	APOE excluded	European ancestry	Caucasian European American ancestry

		rs10498633, DSG2 rs8093731g, INPP5D rs35349669, MEF2C rs190982, NME8 rs2718058, ZCWPW1 rs1476679, CELF1 rs10838725, FERMT2 rs17125944, CASS4 rs7274581			
Homann et al. (2022)	Jansen et al. (2019), and Hibar et al. (2017)	PRS: Genes/SNPs not listed.	UNKNOWN	European ancestry	European ancestry
Kannappan et al. (2022)	IGAP/Lambert et al. (2013)	PRS: Genes/7485124 SNPs not listed.	UNKNOWN	European ancestry	Non-Hispanic white
Kauppi et al. (2018)	Desikan et al.(2017)	PHS: APOE ε2, APOE ε4, ABCA7 rs4147929, BIN1 rs6733839, CASS4 rs7274581, CD2AP rs10948363, CELF1 rs10838725, CLU rs9331896, CR1 rs6656401, EPHA1 rs11771145, FERMT2 rs17125944, HLA rs9271192, INPP5D rs35349669, MEF2C rs190982, MS4A6A rs983392, NME8 rs2718058, PICALM rs10792832, PTK2B rs28834970, SLC24A4/RIN3 rs10498633, SORL1 rs11218343, ZCWPW1 rs1476679.	APOE included	European ancestry	Caucasian European American ancestry
Kirchner et al. (2023)	Kunkle et al.(2019)	PRS: All SNPs that reached genome-wide significance.	APOE included and excluded	Non-Hispanic white	European ancestry
Korbmacher et al. (2024)	UNKNOWN	PRS: Genes/SNPs not listed.	UNKNOWN	UNKNOWN	British or Irish descent / European ancestry
Kulminski et al. (2024)	Not applicable as no GWAS (concept similar to PRS but no GWAS).	Concept similar to PRS, using APOE rs429358, TOMM40 rs2075650, and APOC1 rs12721046.	APOE included	Not applicable as no GWAS (concept similar to PRS but no GWAS).	European ancestry
Lancaster et al. (2019)	IGAP/Lambert et al. (2013)	PRS: Genes/SNPs not listed here as this was a microglia PRS. SNPs at various thresholds in ENIGMA sample: 117446, 70810, 45698, 5159, 1479. SNPs at various thresholds in UK Biobank sample: 136598, 81407, 52308, 9755, 5723, 1598.	APOE excluded	European ancestry	Majority white European | Caucasian European American ancestry
Lancaster et al. (2023)	IGAP/Kunkle et al. (2019)	PRS: Genes/SNPs used from IGAP and Kunkle et al. (2019) not listed.	APOE excluded	European ancestry and non-Hispanic white	European ancestry
Lee et al. (2021)	Desikan et al. (2017)	PRS: ABCA7 rs4147929, BIN1 rs6733839, CASS4 rs7274581, CD2AP rs10948363, CELF1 rs10838725, CLU rs9331896, CR1 rs6656401, EPHA1 rs11771145, FERMT2 rs17125944, HLA rs9271192, INPP5D rs35349669, MEF2C rs190982, MS4A6A rs983392, NME8 rs2718058, PICALM rs10792832, PTK2B rs28834970, SLC24A4/RIN3 rs10498633, SORL1 rs11218343, ZCWPW1 rs1476679.	APOE excluded	European ancestry	Caucasian European American ancestry
Li et al. (2021)	Desikan et al. (2017)	PHS: APOE ε2, APOE ε4, ABCA7 rs4147929, BIN1 rs6733839, CASS4 rs7274581, CD2AP rs10948363, CELF1 rs10838725, CLU rs9331896, CR1 rs6656401, EPHA1 rs11771145, FERMT2 rs17125944, HLA rs9271192, INPP5D rs35349669, MEF2C rs190982, MS4A6A	APOE included	European ancestry	Caucasian European American ancestry

		rs983392, NME8 rs2718058, PICALM rs10792832, PTK2B rs28834970, SLC24A4/RIN3 rs10498633, SORL1 rs11218343, ZCWPW1 rs1476679.			
Liu et al. (2021)	Jansen et al. (2019), Lambert et al. (2013), Kunkle et al. (2019), Marioni et al. (2018), and Desikan et al. (2017)	PRS & PHS. PRS: CR1 rs6656401, ECHDC3 rs7920721, SORL1 rs11218343, SPI1 rs3740688, MS4A6A rs7933202, PICALM rs10792832, FERMT2 rs17125924, SLC24A4 rs12590654, SPPL2A rs59685680, ADAM10 rs593742, APH1B rs117618017, IQCK rs7185636, KAT8 rs59735493, IL34 rs4985556, WWOX rs62039712, PLCG2 rs12444183, RP11-81K2.1 rs28394864, SCIMP rs7225151, BZRAP1 rs2526380, CYB561 rs138190086, ALPK2 rs76726049, ABCA7 rs3752231, ABCA7 rs3752246, CD33 rs12459419, BIN1 rs6733839, INPP5D rs35349669, CSTF1 rs6069736, ADAMTS1 rs2830500, HESX1 rs184384746, CLNK rs6448453, MEF2C rs190982, HLA-DRB1 rs34855541, HLA-DQA1 rs9271192, UNC5CL rs187370608, CD2AP rs9381563, ZCWPW1 rs1476679, EPHA1 rs10808026, CNTNAP2 rs114360492, GPR141 rs2718058, CLU rs4236673. PHS: BIN1 rs6733839, ABCA7 rs3752246, CLU rs1532277, HLA-DRB5 rs115124923, BZRAP1 rs2526378, ZCWPW1 rs1476679, BC043356 rs2597283, PICALM rs543293, PTK2B rs12679874, MS4A6A rs7116190, AL833583 rs78571833, SLC24A4 rs12590273, HLA-DQB1 rs115675626, TRIP4 rs74615166, FERMT2 rs6572869, CR595071 rs7920721, CHRNA2 rs2741342, CR1 rs61822977, SORL1 rs11218343, SPI1 rs3740688, GPR115 rs1109581, C19orf6 rs117481827, INPP5D rs10202748, CASS4 rs7274581, abParts rs7145100.	APOE excluded	PRS & PHS: European ancestry	Predominantly non-Hispanic white vs. other races. No clarification found regarding the other races in paper.
Liu et al. (2022)	Gibson et al.(2019), and Lambert et al.(2013)	PRS: Genes/SNPs not listed here as a non-AD-specific discovery GWAS was used.	APOE excluded	IEAA PRS & EEAA PRS: European ancestry.	Predominantly non-Hispanic white vs. other races. No clarification found regarding the other races in paper.
Liu et al. (2023)	Lambert et al.(2013)	PRS: Genes/1312100 SNPs not listed.	APOE excluded	European ancestry	European ancestry
Lorenz et al. (2025)	Marioni et al. (2018)	PRS: Genes/ SNPs not listed.	APOE included and excluded	British. European ancestry.	Non-Hispanic white participants
Lorenzini et al. (2024)	Bellenguez et al. (2022)	PRS: ABCA1 rs1800978, ABCA7 rs12151021, ABI3 rs616338, ACE rs4277405, ADAM17 rs72777026, ADAMTS1 rs2830489, ANK3 rs7068231, ANKH rs112403360, APH1B rs117618017, APOE rs429358, APOE rs7412, APP rs2154481, BCKDK rs889555, BIN1 rs6733839, BLNK rs6584063, CASS4 rs6014724, CD2AP rs7767350, CLNK rs6846529, CLU rs11787077, COX7C rs62374257, CR1 rs679515, CTSB rs1065712, CTSH rs12592898, DOC2A rs1140239, EED rs3851179, EPDR1 rs6966331, EPHA1 rs11771145, FERMT2 rs17125924, FOXF1 rs16941239, GRN rs5848, HLA-DQA1 rs6605556, HS3ST5 rs785129, ICA1 rs10952097, IDUA rs3822030, IGH gene cluster rs10131280, IGH gene cluster rs7157106, IL34 rs4985556, INPP5D rs10933431, JAZF1 rs1160871, KLF16 rs149080927, LILRB2 rs587709, MAF rs450674, MINDY2 rs602602, MME rs16824536, MME rs61762319, MS4A4A rs1582763, MYO15A rs2242595, NCK2 rs143080277, PLCG2 rs12446759, PLCG2 rs72824905, PLEKHA1 rs7908662, PRDM7 rs56407236, PRKD3 rs17020490, PTK2B rs73223431, RASGEF1C rs113706587, RBCK1 rs1358782, RHOH rs2245466, SCIMP rs7225151, SEC61G rs76928645, SHARPIN rs34173062, SIGLEC11 rs9304690, SLC24A4 rs12590654, SLC24A4 rs7401792, SLC2A4RG rs6742, SNX1 rs3848143, SORL1 rs11218343, SORL1 rs74685827, SORT1 rs141749679, SPDYE3 rs7384878,	APOE included and excluded	European ancestry	European ancestry

		SPI1 rs10437655, SPPL2A rs8025980, TMEM106B rs13237518, TNIP1 rs871269, TPCN1 rs6489896, TREM2 rs143332484, TREM2 rs75932628, TREML2 rs60755019, TSPAN14 rs6586028, TSPOAP1 rs2526377, UMAD1 rs6943429, UNC5CL rs10947943, USP6NL rs7912495, WDR12 rs139643391, WDR81 rs35048651, WNT3 rs199515.			
Lupton et al. (2016)	Lambert et al.(2013)	PRS: SORL1 rs11218343, BIN1 rs6733839, CR1 rs6656401, CLU rs9331896, PICALM rs10792832, ABCA7 rs4147929, CASS4 rs7274581, FERMT2 rs17125944, EPHA1 rs11771145, MS4A6A rs983392, HLA-DRB5/HLA-DRB1 rs9271192, SLC24A4/RIN3 rs10498633, ZCWPW1 rs1476679, CD2AP rs10948363, PTK2B rs28834970, MEF2C rs190982, NME8 rs2718058, CELF1 rs10838725, INPP5D rs35349669.	APOE excluded	European ancestry	European | Australia
Manca, Pardinas, and Venneri (2022)	Jansen et al. (2019)	PHS: Genes/SNPs not listed.	UNKNOWN	European ancestry	White, plus 6.5% non-white/from minority ethnic background
Meda et al. (2012)	N/A as GWAS-type analysis, not polygenic scores.	GWAS-type analysis: Genes/27150 SNPs not listed.	APOE included	UNKNOWN	Caucasian European American ancestry
Mormino et al. (2016)	IGAP	PRS: Genes/16123 vs. 18 SNPs not listed.	APOE included and excluded	European ancestry	Caucasian European American ancestry
Nordengen et al. (2022)	Jansen et al.(2019)	PRS: Genes/1312100 SNPs not listed.	APOE excluded	European ancestry	Norway.
Prieto et al. (2020)	Desikan et al. (2017)	PHS: APOE ε2, APOE ε4, CR1 rs4266886, CR1 rs61822977, BIN1 rs6733839, INPP5D rs10202748, HLA-DRB5 rs115124923, HLA-DQB1 rs115675626, GPR115 rs1109581, BC043356 rs17265593, BC043356 rs2597283, ZCWPW1 rs1476679, AL833583 rs78571833, PTK2B rs12679874, CHRNA2 rs2741342, CLU rs7831810, CLU rs1532277, CLU rs9331888, CR595071 rs7920721, SPI1 rs3740688, MS4A6A rs7116190, PICALM rs526904, PICALM rs543293, SORL1 rs11218343, FERMT2 rs6572869, SLC24A4 rs12590273, abParts rs7145100, TRIP4 rs74615166, BZRAP1 rs2526378, C19orf6 rs117481827, ABCA7 rs7408475, ABCA7 rs3752246, CASS4 rs7274581.	APOE included	European ancestry	Non-Hispanic white
Reas et al. (2023)	Desikan et al.(2017)	Multimodal PHS: APOE ε2, APOE ε4, ABCA7 rs4147929, BIN1 rs6733839, CASS4 rs7274581, CD2AP rs10948363, CELF1 rs10838725, CLU rs9331896, CR1 rs6656401, EPHA1 rs11771145, FERMT2 rs17125944, HLA rs9271192, INPP5D rs35349669, MEF2C rs190982, MS4A6A rs983392, NME8 rs2718058, PICALM rs10792832, PTK2B rs28834970, SLC24A4/RIN3 rs10498633, SORL1 rs11218343, ZCWPW1 rs1476679.	APOE included	European ancestry	Caucasian European American ancestry
Roe et al. (2024)	Lambert et al., (2013), Kunkle et al. (2019), Jansen et al. (2019), and	PRS: Genes/SNPs not listed.	APOE included and excluded	European ancestry or Caucasian	European ancestry

	Wightman et al. (2021).				
Roostaei et al. (2018)	van Meurs et al.(2013)	PRS: Genes/SNPs not listed here as from a non-AD-specific discovery GWAS.	UNKNOWN	European descent	European ancestry
Rutten-Jacobs et al. (2018)	Lambert et al.(2013)	PRS: Genes/SNPs not listed.	UNKNOWN	European ancestry	White, European descent
Sabuncu et al. (2012)	Harold et al. (2009)	PRS: DAB1 rs1539053, CR1 rs1408077, BIN1 rs7561528, SSB rs11894266, C6orf155 rs9446432, ARID1B rs9384428, CLU rs11136000, CLU rs2582367, KCNU1 rs1157242, MS4A6A rs610932, C11orf30 rs11827375, PICALM rs3851179, CNTN5 rs10501927, BCL3 rs2965101, BCL3 rs2927438, PVRL2 rs10402271, PVRL2 rs1871047, PVRL2 rs377702, PVRL2 rs12610605, PVRL2 rs6859, TOMM40 rs157580, TOMM40 rs2075650, TOMM40 rs8106922, APOE rs439401, APOC4 rs5167, APOE rs1048699.	APOE included and excluded	European, Asian, Yoruban	Caucasian European American ancestry
Sha et al. (2023)	Kunkle et al. (2019)	PRS: Genes/1105067 SNPs not listed.	APOE included and excluded	Non-Hispanic white	White British ancestry
Sloan et al. (2010)	Becker et al.(2004), Kanehisa et al.(2008), and Bertram et al.(2007)	PRS: A2M rs1805657, A2M rs12427063, A2M rs226379, A2M rs10842789, A2M rs11613746, A2M rs7976808, A2M rs669, A2M rs226380, A2M rs4883213, ABCA1 rs1800977, ABCA1 rs4149339, ABCA1 rs4149313, ABCA1 rs2230808, ABCA1 rs363717, ABCA1 rs2230806, ABCA1 rs4149338, ABCA1 rs2066718, ABCB1 rs10267099, ABCB1 rs10280623, ABCB1 rs9282564, ABCB1 rs10225473, ABCB1 rs10264990, ABCB1 rs12720067, ABCB1 rs13233308, ABCB1 rs1202184, ABCB1 rs2188526, ABCB1 rs4728700, ABCB1 rs1055302, ABCB1 rs10259849, ABCB1 rs1202186, ABCB1 rs2520464, ABCB1 rs17327624, ABCB1 rs4148733, ABCB1 rs4148737, ABCB1 rs4437575, ABCB1 rs2235033, ABCB1 rs2214102, ABCB1 rs1202172, ABCB1 rs6950978, BAD rs671976, BAD rs477895, BCHE rs3806650, BCHE rs1803274, BCHE rs9838443, BCL2 rs1944423, BCL2 rs4987853, BCL2 rs7243091, BCL2 rs4987792, BCL2 rs4987721, BCL2 rs8083946, BCL2 rs12970840, BCL2 rs12961672, BCL2 rs2850760, BCL2 rs2046136, BCL2 rs4941185, BCL2 rs17759659, BCL2 rs7236090, BCL2 rs2551402, BCL2 rs8089538, BCL2 rs8084922, BCL2 rs4940574, BCL2 rs17756266, BCL2 rs9955190, BCL2 rs4987825, BCL2 rs6567328, BCL2 rs1381548, BCL2 rs6567326, BCL2 rs720321, BCL2 rs4987855, BCL2 rs7242542, BCL2 rs3927911, BCL2 rs954954, BCL2 rs8092560, BCL2 rs4456611, BCL2 rs4987828, BCL2 rs8094315, BCL2 rs1481031, BCL2 rs7232082, EP300 rs20551, ESR1 rs9397486, ESR1 rs2813563, ESR1 rs12681, ESR1 rs3798577, ESR1 rs2747655, ESR1 rs2459111, ESR1 rs725467, ESR1 rs1801132, FAS rs1051070, FAS rs3758483, FAS rs2234978, FBXW7 rs2203644, FBXW7 rs1516822, FBXW7 rs2714805, FBXW7 rs2255137, GABRG2 rs418210, GABRG2 rs424740, GFAP rs3760379, GFAP rs8067254, GFAP rs2070935, GFAP rs1042329, GRB2 rs4789188, GRB2 rs9302990, GRB2 rs16967789, GRB2 rs4542691, GRB2 rs4789172, GRB2 rs2891714, GRB2 rs4789182, GRB2 rs9901434, GRB2 rs4789189, GRB2 rs7219, GSK3B rs12630592, GSK3B rs11919783, GSK3B rs11921360, GSK3B rs6774210, GSK3B rs2037547, GSK3B rs6438552, GSK3B rs13320980, MTHFR rs4846049, MTHFR rs9651118, MTHFR rs17421511, MTHFR rs17367504, MTHFR rs4846056, MTHFR rs4846054, MTHFR rs1801133, MTHFR rs3737964, NAT1 rs6586712, NAT1 rs4986993, NAT1 rs10888150, NAT1 rs7845127, NAT1 rs11203942, NAT2 rs4646246, NAT2 rs1799930, NAT2 rs1801280,	APOE included	UNKNOWN | African origin, Asian, Caucasian, Hispanic, other/mixed**	USA

NAT2 rs1208, NCSTN rs12239747, NCSTN rs7540865, NCSTN rs2147471, NCSTN rs10752637, NCSTN rs12239946, NCSTN rs4656256, NCSTN rs2274185, NCSTN rs7528638, NCSTN rs17370539, NEFH rs174650, NEFH rs165734, NEFH rs165649, NEFH rs165821, NEFH rs165602, NEFH rs3815335, NGFR rs3785930, NGFR rs741073, NGFR rs603769, NGFR rs565042, NOS1 rs2682826, NOS1 rs9658570, NOS2A rs2779248, ACE rs4295, ACE rs4459610, ACE rs4344, ACE rs1800764, ACE rs4311, ADAM10 rs653765, ADAM10 rs12913383, ADAM10 rs514049, ADH1B rs1229982, ADH1B rs6810842, ADH1B rs1159918, AGT rs7079, AGT rs5050, ALS2 rs6760385, ALS2 rs2110739, ALS2 rs1981725, ALS2 rs3731702, ALS2 rs8179725, ALS2 rs16838147, ALS2 rs970595, ALS2 rs3219153, ALS2 rs2302610, ALS2 rs888012, ALS2 rs2349733, ALS2 rs7572898, ALS2 rs3731707, ALS2 rs3219169, ALS2 rs2882231, ALS2 rs3820966, ALS2 rs2276615, ALS2 rs3219156, ALS2 rs6435105, APBA1 rs11139519, APBA1 rs2309481, APBA1 rs7039417, APBA1 rs7025896, APBA1 rs975645, APBA1 rs7870154, APBA1 rs2781541, APBA1 rs7021184, APBA1 rs10867877, APBA1 rs7861901, APBA1 rs10481753, BCL2 rs8085707, BCL2 rs17676949, BCL2 rs2551397, BCL2 rs6567334, BCL2 rs12457893, BCL2 rs12457700, BCL2L1 rs6087771, BCL2L1 rs6119651, BCL2L1 rs6088997, BCL2L1 rs6060563, BCL2L1 rs3181073, BCL2L1 rs7272062, BDNF rs908867, BDNF rs12273363, BDNF rs11030123, BDNF rs7103411, BDNF rs11030101, BDNF rs7124442, BDNF rs11030102, BDNF rs6265, BDNF rs11030107, BDNF rs11030104, BDNF rs7127507, BLMH rs1050565, CASP1 rs1792766, CASP1 rs1785882, CASP1 rs530537, CASP1 rs568910, CASP1 rs11226613, CASP1 rs488992, CASP1 rs557905, CASP1 rs1785884, CASP1 rs11821722, CASP1 rs562441, CASP1 rs1623342, CASP1 rs1503399, CASP3 rs2696057, CASP3 rs6948, CASP3 rs2019978, CASP3 rs2705881, CASP3 rs1049253, CASP3 rs9685847, CASP3 rs4647603, GSK3B rs6770314, GSK3B rs9873477, GSK3B rs6771023, GSK3B rs3732361, GSK3B rs334558, GSK3B rs17811013, GSK3B rs13312998, GSK3B rs3755557, GSK3B rs1381841, GSTO1 rs4925, GSTO2 rs156697, HFE rs1800702, HFE rs1799945, HFE rs2006736, HFE rs1045537, HMOX1 rs2071746, HSPA5 rs391957, HSPA5 rs12009, HTR2A rs6314, HTR2A rs2296973, HTR2A rs9526245, HTR2A rs2224721, HTR2A rs6561335, HTR2A rs9534493, HTR2A rs9534511, HTR2A rs9316233, HTR2A rs6313, HTR2A rs621494, HTR2A rs4142900, HTR2A rs9534505, HTR2A rs9567739, HTR2A rs9526240, HTR2A rs7997012, HTR2A rs594242, HTR2A rs7984966, HTR2A rs7330636, HTR2A rs9567735, HTR2A rs927544, HTR2A rs2770293, HTR2A rs17289394, HTR2A rs1328684, HTR2A rs1410657, HTR2A rs7333412, NOS2A rs2297518, NOTCH4 rs9267845, NOTCH4 rs3096702, NQO1 rs10517, NQO1 rs1800566, NR4A2 rs12803, NTF3 rs10744685, NTF3 rs10849277, NTF3 rs4074967, NTF3 rs7484401, OLR1 rs1050283, OLR1 rs10505755, OLR1 rs1050286, OLR1 rs2742110, OPRM1 rs1799971, OPRM1 rs9479767, OPRM1 rs17277929, OPRM1 rs2236258, OPRM1 rs2236259, OPRM1 rs9322448, OPRM1 rs2236256, OPRM1 rs660756, OPRM1 rs540825, OPRM1 rs2236257, PARK2 rs7770788, PARK2 rs7752854, PARK2 rs16892792, PARK2 rs9356053, PARK2 rs6912641, PARK2 rs4596453, PARK2 rs13212608, PARK2 rs9364599, PARK2 rs9347562, PARK2 rs9456797, PARK2 rs2803062, PARK2 rs7763400, PARK2 rs9458536, PARK2 rs2023006, PARK2 rs9365393, PARK2 rs2846488, PARK2 rs2849527, PARK2 rs12525451, PARK2 rs12527638, APBA1 rs7851858, APBA1 rs12378157, APBA1 rs7036436, APBA1 rs1977552, APBA1 rs10867620, APBA1 rs11139605, APBA1 rs1217339, APBA1 rs1576507, APBA1 rs12376278, APBA1 rs7864493, APBA1 rs2777863, APBA1 rs1556211, APBA1 rs7869375, APBA1 rs987653, APBA1 rs1757957, APBA1 rs2150878, APBA1 rs7033141, APBA1 rs870695, APBA1 rs7030393, APBA1 rs1105307, APBA1 rs869150, APBA1 rs11138902, APBA1 rs959613, APBA1 rs2781535, APBA1 rs11139300, APBA1 rs10867879, APBB1 rs2723664,

[redacted]

APBB1 rs8164, APBB1 rs3763824, APOC1 rs1261088, APOC2 rs5167, APOC2 rs5127, APOC2 rs2288912, APOE rs405509, APP rs3787639, APP rs2242682, APP rs2830101, APP rs442901, APP rs2830036, APP rs2830090, APP rs2070652, APP rs2830066, APP rs9976453, CASP3 rs2720378, CASP6 rs5030535, CASP6 rs1541373, CASP6 rs1800627, CASP6 rs5030539, CASP6 rs3181191, CASP6 rs5030606, CASP7 rs7907519, CASP7 rs10787498, CASP7 rs6421366, CASP7 rs11196418, CASP7 rs4595501, CASP7 rs6585241, CASP7 rs11196422, CASP7 rs4353229, CASP7 rs7099033, CASP7 rs1127687, CASP7 rs12415607, CASP7 rs4457708, CASP7 rs12416109, CASP8 rs3769821, CASP8 rs7608692, CASP8 rs1035140, CASP8 rs700636, CASP8 rs3769827, CASP8 rs3769823, CASP8 rs6747918, CASP8 rs12693932, CAT rs564250, CAT rs769214, CETP rs1800775, CETP rs4783961, CETP rs5882, CETP rs1801706, CETP rs12447839, CETP rs17368435, CHAT rs7091005, CHAT rs10857520, CHAT rs10857529, CHAT rs17775704, CHAT rs867687, CHAT rs1917818, CHAT rs10776586, HTR2A rs977003, HTR2A rs4941573, HTR2A rs9567737, HTR2A rs9567746, HTR2A rs1328685, HTR2A rs2770302, HTR2A rs985934, HTR2A rs3125, HTR2A rs17289304, HTR2A rs2770298, HTR2A rs12584920, IDE rs7078413, IDE rs4304670, IDE rs7910977, IDE rs7908111, IDE rs2421943, IDE rs12415807, IDE rs1832197, IDE rs7100623, IDE rs2149632, IDE rs2251101, IDE rs11187060, IDE rs10509645, IDE rs11187064, IL10 rs3024498, IL10 rs1800896, IL10 rs1800872, IL10 rs1800893, IL10 rs3024496, IL10 rs1800871, IL1A rs1878320, IL1A rs1800587, IL1A rs1878321, IL1A rs17561, IL1A rs3783521, IL1A rs2856836, IL1A rs3783516, IL1A rs1800794, IL1A rs1878319, IL1A rs2071373, IL1B rs1143623, IL1B rs1143643, IL1B rs1143627, PARK2 rs6902370, PARK2 rs9365352, PARK2 rs7745115, PARK2 rs6455842, PARK2 rs7775868, PARK2 rs9346917, PARK2 rs4235937, PARK2 rs2803118, PARK2 rs6927018, PARK2 rs13206130, PARK2 rs9365417, PARK2 rs4709578, PARK2 rs4636000, PARK2 rs12210160, PARK2 rs9355977, PARK2 rs9355362, PDYN rs3830064, PDYN rs910080, PDYN rs1997794, PDYN rs10485703, PDYN rs2235749, PINK1 rs1043424, PINK1 rs686658, PINK1 s3131713, PLAU rs2227551, PLAU rs2227564, PLAU rs4065, PON1 rs13236941, PON1 rs705382, PON1 rs854573, PON1 rs854551, PON1 rs757158, PON1 rs854552, PON1 rs854572, PON1 rs854571, PON2 rs11545941, PON2 rs12704796, PON2 rs6954345, PRNP rs1799990, PRNP rs2756271, PSEN1 rs165935, PSEN1 rs3025780, PSEN1 rs362340, APP rs2234984, APP rs2830051, APP rs2026225, APP rs2830002, APP rs440666, APP rs8127927, APP rs1783016, APP rs9636777, APP rs438031, APP rs1981369, APP rs2830025, APP rs380417, APP rs2829973, APP rs2830046, APP rs6516727, APP rs1787439, APP rs466448, APP rs2829997, APP rs2830088, APP rs455465, APP rs2829970, APP rs2211771, APP rs216762, APP rs1782978, APP rs2070653, APP rs2830044, APP rs2830033, APP rs768039, APP rs466609, APPBP1 rs461943, APPBP1 rs422945, BACE1 rs525493, BACE1 rs656083, BACE1 rs638405, BACE1 rs522843, BACE1 rs7083, BACE1 rs535860, BACE1 rs609332, BACE1 rs687740, BACE1 rs490460, BACE1 rs11601511, BACE2 rs3787938, BACE2 rs914180, CHAT rs6537546, CHAT rs2103082, CHAT rs7903612, CHAT rs868750, CHAT rs11101191, CHAT rs12359885, CHAT rs1917810, CHAT rs12217567, CHAT rs3793791, CHAT rs7903496, CHAT rs7094248, CHAT rs10857528, CHRNB2 rs9427092, COMT rs9332377, COMT rs1544325, COMT rs12172430, COMT rs2239393, COMT rs11705619, COMT rs769224, COMT rs933271, COMT rs4633, CREBBP rs3789033, CREBBP rs2530890, CREBBP rs129968, CREBBP rs130021, CREBBP rs130005, CREBBP rs9392, CREBBP rs17199030, CREBBP rs886528, CST3 rs6114208, CST3 rs6515375, CST3 rs2424577, CST3 rs3827143, CTSD rs2292963, CYP1A1 rs2470893, CYP2D6 rs9607879, CYP2D6 rs764481, CYP2D6 rs742086, CYP2D6 rs5751231, CYP2D6 rs6002626, DRD2 rs6275, DRD2 rs4460839, DRD2 rs12364283, IL1B rs1143634, IL4 rs2070874, IL6

rs2069840, IL6 rs10242595, IL6 rs1800797, IL6 rs2069827, LDLR rs1433099, LDLR rs2738464, LDLR rs2738465, LPL rs13702, LPL rs1059611, LPL rs4922115, LPL rs256, LPL rs3735964, LPL rs13266204, LPL rs285, LPL rs328, LPL rs11570892, LPL rs10099160, LPL rs264, LPL rs3916027, LPL rs253, LPL rs17410577, LPL rs1534649, LRP1 rs1466535, LRP1 rs4074308, LRP1 rs1800168, LRP1 rs4759044, LRP1 rs1799986, LRP1 rs10876966, MAOA rs3027407, MAPT rs8079215, MAPT rs2435211, MAPT rs1052587, MAPT rs17571809, MAPT rs1800547, MAPT rs9468, MAPT rs2435200, MAPT rs16940758, MAPT rs754593, MAPT rs2258689, MAPT rs2435203, MAPT rs16940797, PSEN1 rs214260, PSEN1 rs165933, PSEN1 rs1800844, PSEN1 rs177415, PSEN2 rs1295645, PSEN2 rs1046240, PSEN2 rs2802268, PSEN2 rs1150895, PSEN2 rs2073489, SERPINA3 rs8005845, SERPINA3 rs17826535, SERPINA3 rs17826465, SERPINA3 rs11623487, SERPINA3 rs1884082, SERPINA3 rs2402482, SERPINA3 rs8007632, SERPINA3 rs11160196, SERPINA3 rs17826482, SLC6A3 rs11564758, SLC6A3 rs458860, SLC6A3 rs6347, SLC6A3 rs2963238, SLC6A3 rs40184, SLC6A3 rs463379, SLC6A3 rs3756450, SLC6A3 rs1809939, SLC6A3 rs6413429, SLC6A3 rs4975646, SLC6A3 rs458334, SLC6A3 rs10040882, SLC6A3 rs27072, SLC6A4 rs6354, SLC6A4 rs2054847, SLC6A4 rs1042173, SLC6A4 rs4583306, SLC6A4 rs4251417, SLC6A4 rs2020942, SLC6A4 rs12150214, SNCA rs356188, SNCA rs10005233, SNCA rs1812923, SNCA rs2301135, SNCA rs2619364, BACE2 rs914183, BACE2 rs726980, BACE2 rs2252576, BACE2 rs6517659, BACE2 rs13052926, BACE2 rs2837967, BACE2 rs2837971, BACE2 rs2837998, BACE2 rs2837993, BACE2 rs746063, BACE2 rs4818227, BACE2 rs6517655, BACE2 rs7280091, BACE2 rs12149, BACE2 rs2837981, BACE2 rs2837977, BACE2 rs960231, BACE2 rs4816713, BACE2 rs11702001, BACE2 rs9976426, BACE2 rs4818226, BACE2 rs746064, BACE2 rs914186, BACE2 rs8130833, BACE2 rs2410415, BACE2 rs9305731, BACE2 rs2837992, BACE2 rs2838000, BACE2 rs1046210, BACE2 rs8133778, BACE2 rs9981547, BACE2 rs2837983, BACE2 rs734757, BACE2 rs914185, BACE2 rs766850, BACE2 rs914181, BACE2 rs8134992, BACE2 rs1467756, BACE2 rs2837982, BAD rs3815362, BAD rs876064, DRD2 rs1079597, DRD2 rs6279, DRD2 rs2234689, DRD2 rs4630328, DRD2 rs2242592, DRD2 rs7131056, DRD2 rs6278, DRD2 rs1800498, DRD2 rs7131440, DRD2 rs4245148, DRD2 rs6277, DRD2 rs4587762, DRD2 rs7122454, DRD2 rs17529477, DRD2 rs2471851, DRD2 rs1076560, DRD2 rs4586205, DRD2 rs4245147, DRD2 rs1799978, DRD2 rs4938019, DRD3 rs1587756, DRD3 rs6280, DRD3 rs324026, DRD3 rs9817063, DRD3 rs7638876, DRD3 rs324030, DRD3 rs3732790, DRD3 rs324035, DRD3 rs963468, DRD3 rs1800828, DRD3 rs9880168, DRD3 rs324036, DRD3 rs9825563, DRD3 rs2134655, DRD3 rs4646996, DRD4 rs3758653, DRD4 rs936465, DRD4 rs4331145, DRD5 rs10033951, EP300 rs4822002, MAPT rs17571857, MAPT rs1052553, MAPT rs7521, MAPT rs17650901, MAPT rs17650771, MAPT rs2435206, MAPT rs17652121, MAPT rs2435212, MME rs4273336, MME rs3773876, MME rs1816558, MME rs6665, MME rs12696022, MME rs989692, MME rs3773885, MME rs17449556, MME rs1807004, MME rs9853221, MME rs2118073, MME rs9864287, MME rs16846960, MME rs10513470, MME rs968628, MME rs9881879, MME rs1370031, MME rs12765, MME rs9834487, MME rs701109, MME rs9867821, MME rs3796268, MME rs10513469, MME rs1025192, MPO rs2243828, MPZ rs7551761, MPZ rs4657015, MPZ rs4131826, MPZ rs7532602, MTHFR rs6541003, MTHFR rs17037396, MTHFR rs17037425, SNCA rs2737029, SNCA rs2301134, SNCA rs7684318, SOD1 rs10432782, SORL1 rs4935774, SYN1 rs2239456, TCN2 rs5753231, TCN2 rs9606756, TCN2 rs1801198, TCN2 rs5749131, TF rs1049296, TF rs8177178, TF rs8177181, TF rs8177179, TF rs1130459, TF rs4481157, TF rs8177184, TFAM rs4390300, TFAM rs12247015, TFAM rs2279340, TFAM rs1049432, TFAM rs11006128, TH rs10770141, TH rs10770140, TNF rs361525, TP53 rs2287498, TP53

		rs1042522, TP53 rs2287497, TTR rs3764478, UCHL1 rs10517002, UCHL1 rs930758, UCHL1 rs3775260, UCHL1 rs6847225, UCHL1 rs7693827, VLDLR rs8210, VLDLR rs1454626, VLDLR rs11789583, VLDLR rs6145, WT1 rs5030320, WT1 rs2301250, WT1 rs5030317.			
Soldan et al. (2024)	Kunkle et al. (2019)	PRS: Genes/6,739,456 SNPs not listed.	APOE excluded	European ancestry	European ancestry
Steventon et al. (2023)	Kunkle et al.(2019)	PRS: Genes/SNPs used from Kunkle et al. (2019) not listed.	UNKNOWN	Non-Hispanic white	British/Irish ancestry
Tan et al. (2019)	Desikan et al.(2017)	PHS: ABCA7 rs4147929, BIN1 rs6733839, CASS4 rs7274581, CD2AP rs10948363, CELF1 rs10838725, CLU rs9331896, CR1 rs6656401, EPHA1 rs11771145, FERMT2 rs17125944, HLA rs9271192, INPP5D rs35349669, MEF2C rs190982, MS4A6A rs983392, NME8 rs2718058, PICALM rs10792832, PTK2B rs28834970, SLC24A4/RIN3 rs10498633, SORL1 rs11218343, ZCWPW1 rs1476679.	APOE excluded	European ancestry	Caucasian European American ancestry
Tank et al. (2022)	Kunkle et al (2019)	PRS: Genes/6578321 SNPs not listed.	APOE excluded	Non-Hispanic white	White, European ancestry
Vacher et al. (2022a)	UNKNOWN	PRS: Genes/SNPs not listed as it is not clear whether an AD-specific discovery GWAS was used or where else the summary statistics may be from.	APOE excluded	UNKNOWN	Australia
Vacher et al. (2022b)	IGAP	PHS: Genes/31 SNPs not listed; 2 APOE SNPs included in PHS.	APOE included	European ancestry	Australia
Wang et al. (2019)	IGAP	PRS: Genes/8070 SNPs not listed.	APOE included and excluded	European ancestry	Caucasian European American ancestry
Williams et al. (2021)	Lambert et al.(2013)	PRS: ABCA7 rs4147929, APOE ε4, BIN1 rs6733839, CASS4 rs7274581, CD2AP rs10948363, CELF1 rs10838725, CLU rs9331896, CR1 rs6656401, EPHA1 rs11771145, FERMT2 rs17125944, HLA rs9271192, INPP5D rs35349669, MEF2C rs190982, MS4A6A rs983392, NME8 rs2718058, PICALM rs10792832, PTK2B rs28834970, SLC24A4/RIN3 rs10498633, SORL1 rs11218343, ZCWPW1 rs1476679.	UNKNOWN	European ancestry	Non-Hispanic white, European descent
Xiao et al. (2017)	IGAP	PRS: Genes/2466 vs. 355 vs. 89 vs. 22 vs. 15 SNPs not listed. 29 SNPs listed: MCFD2 rs6715234, BIN1 rs745717, CD2AP rs7745848, EPHA1-AS1 rs11771145, CLU rs7831810, CLU rs9331908, TSPYL5 rs12545667, ECHDC3 rs12358692, MS4A6A rs617135, PICALM rs9787874, SORL1 rs11218343, ABCA7 rs3752231, IGSF23 rs60570899, BCL3 rs2965169, BCAM rs6509172, PVRL2 rs2972564, PVRL2 rs41290100, PVRL2 rs393584, PVRL2 rs11665676, PVRL2 rs283811, TOMM40 rs116881820, APOC1 rs138235833, APOC1 rs59325138, CLPTM1 rs3760628, CLPTM1 rs73558188, RELB rs116518981, GEMIN7 rs2060250, BLOC1S3 rs620807, EXOC3L2 rs346763.	APOE excluded	European ancestry	Caucasian
Xu et al. (2022)	IGAP	PHS: CR1 rs4266886, CR1 rs61822977, BIN1 rs6733839, INPP5D rs10202748, HLA-DRB5 rs115124923, HLA-DQB1 rs115675626, GPR115 rs1109581, C043356 rs17265593, BC043356 rs2597283, ZCWPW1 rs1476679, AL833583 rs78571833, PTK2B rs12679874, CHRNA2	APOE excluded	European ancestry	Caucasian European American ancestry

		rs2741342, CLU rs7831810, CLU rs1532277, CLU rs9331888, CR595071 rs7920721, SPI1 rs3740688, MS4A6A rs7116190, PICALM rs526904, PICALM rs543293, SORL1 rs11218343, FERMT2 rs6572869, SLC24A4 rs12590273, abParts rs7145100, TRIP4 rs74615166, BZRAP1 rs2526378, C19orf6 rs117481827, ABCA7 rs7408475, ABCA7 rs3752246, CASS4 rs7274581.			
Zhao et al. (2019b)	UK Biobank; ADNI; Human Connectome Project; Pediatric Imaging, Neurocognition, and Genetics; Phipadelphia Neurodevelopmental Cohort.	PRS: Genes/365 SNPs not listed.	UNKNOWN	British ancestry | white European mainly | California | African, central Asian, east Asian, European, native American, Oceanic | Philadelphia.	A combined GWAS on the five previous GWASs - British | white European mainly | California | African, central Asian, east Asian, European, native American, Oceanic | Philadelphia.
Zhao et al. (2020)	Jansen et al. (2019)	PRS: Genes/SNPs not listed.	UNKNOWN	European ancestry	China | Caucasian European American ancestry

Table B.5: Genes used to construct polygenic scores in 43 out of 64 papers selected for systematic review.

Gene Acronym	Gene Name	Frequency (n)
A2M	Apha-2-macroglobulin	1
ABCB1	ATP(adenosine triphosphate)-binding cassette, sub-family B, member 1	1
ADAM17	ADAM (a disintegrin and metalloproteinase) metallopeptidase domain 17	1
AGT	Angiotensinogen	1
ALPK2	Alpha kinase 2	1
ALS2	Alsin rho guanine nucleotide exchange factor ALS2	1
ANK3	Ankyrin 3	1
ANKH	ANKH inorganic pyrophosphate transport regulator	1
APBA1	Amyloid beta precursor protein binding family A member 1	1
APBB1	Amyloid beta precursor protein binding family B member 1	1
APOC2	Apolipoprotein C-II	1
APOC4	Apolipoprotein C-IV	1
APPBP1	Amyloid precursor protein-binding protein 1	1
ARID1B	AT-rich interaction domain 1B	1
ARL17B	ARF like GTPase 17B	1
AS1	Antisense RNA 1	1
BACE1	Beta-secretase 1	1
BACE2	Beta-secretase 2	1
BAD	BCL2 (B-cell lymphoma 2) associated agonist of cell death	1
BCAM	Basal cell adhesion molecule (Lutheran blood group)	1
BCHE	Butyrylcholinesterase	1
BCKDK	Branched chain keto acid dehydrogenase kinase	1
BCL2	BCL2 (B-cell lymphoma 2) apoptosis regulator	1
BCL2L1	BCL2 (B-cell lymphoma 2) like 1	1
BDNF	Brain derived neurotrophic factor	1
BLMH	Bleomycin hydrolase	1
BLNK	B cell linker	1
BLOC1S3	Biogenesis of lysosomal organelles complex 1 subunit 3	1

C043356	UNKNOWN	1
C11orf30	Chromosome 11 open reading frame 30	1
C17orf107	Chromosome 17 open reading frame 107	1
C6orf155	Chromosome 6 open reading frame 155	1
CASP1	Caspase 1	1
CASP3	Caspase 3	1
CASP6	Caspase 6	1
CASP7	Caspase 7	1
CASP8	Caspase 8	1
CAT	Catalase	1
CETP	Cholesteryl ester transfer protein	1
CHAT	Choline O-acetyltransferase	1
CHRNE	Cholinergic receptor nicotinic epsilon subunit	1
CLPTM1	CLPTM1 regulator of GABA type A receptor forward trafficking	1
CNTN5	Contactin 5	1
CNTNAP2	Contactin associated protein 2	1
COMT	Catechol-O-methyltransferase	1
COX7C	Cytochrome c oxidase subunit 7C	1
CREBBP	CREB binding protein	1
CST3	Cystatin C	1
CSTF1	Cleavage stimulation factor subunit 1	1
CTSB	Cathepsin B	1
CTSD	Cathepsin D	1
CTSH	Cathepsin H	1
CYB561	Cytochrome b561	1
CYP1A1	Cytochrome P450 family 1, subfamily A, member 1	1
CYP2D6	Cytochrome P450 family 2, subfamily D, member 6	1
DAB1	DAB adaptor protein 1	1
DOC2A	Double C2 domain alpha	1
DRD2	Dopamine receptor D2	1
DRD3	Dopamine receptor D3	1
DRD4	Dopamine receptor D4	1

DRD5	Dopamine receptor D5	1
DSG2	Desmoglein 2	1
EED	Embryonic ectoderm development	1
EP300	E1A binding protein p300	1
EPDR1	Ependymin related 1	1
ESR1	Estrogen receptor 1	1
EXOC3L2	Exocyst complex component 3 like 2	1
FAS	Fas cell surface death receptor	1
FBXW7	F-box and WD repeat domain containing 7	1
FOXF1	Forkhead box F1	1
GABRG2	Gamma-aminobutyric acid type A receptor subunit gamma2	1
GEMIN7	Gem nuclear organelle associated protein 7	1
GFAP	Glial fibrillary acidic protein	1
GPR141	G-protein coupled receptor 141	1
GRB2	Growth factor receptor bound protein 2	1
GRN	Granulin precursor	1
GSK3B	Glycogen synthase kinase 3 beta	1
GSTO1	Glutathione S-transferase omega 1	1
GSTO2	Glutathione S-transferase omega 2	1
HESX1	HESX homeobox 1	1
HFE	Homeostatic iron regulator	1
HMOX1	Heme oxygenase 1	1
HS3ST5	Heparan sulfate-glucosamine 3-sulfotransferase 5	1
HSPA5	Heat shock protein family A (Hsp70) member 5	1
HTR2A	5-hydroxytryptamine receptor 2A	1
ICA1	Islet cell autoantigen 1	1
IDE	Insulin degrading enzyme	1
IDUA	Alpha-L-iduronidase	1
IGH cluster	Immunoglobulin heavy locus cluster	1
IGSF23	Immunoglobin superfamily member 23	1
IL10	Interleukin 10	1
IL4	Interleukin 4	1

IL6	Interleukin 6	1
JAZF1	JAZF zinc finger 1	1
KAT8	Lysine acetyltransferase 8	1
KCNU1	Potassium calcium-activated channel subfamily U member 1	1
KLF16	KLF transcription factor 16	1
LDLR	Low density lipoprotein receptor	1
LILRB2	Leukocyte immunoglobulin like receptor B2	1
LPL	Lipoprotein lipase	1
LRP1	LDL receptor related protein 1	1
LRRC37A	Leucine rich repeat containing 37A	1
MAF	MAF bZIP transcription factor	1
MAF1	MAF1 negative regulator of RNA polymerase III	1
MAOA	Monoamine oxidase A	1
MAPT	Microtubule associated protein tau	1
MCFD2	Multiple coagulation factor deficiency 2, ER cargo receptor complex subunit	1
MINDY2	MINDY lysine 48 deubiquitinase 2	1
MPO	Myeloperoxidase	1
MPZ	Myelin protein zero	1
MS4A2	Membrane spanning 4-domains A2	1
MS4A4E	Membrane spanning 4-domains A4E	1
MTCH2	Mitochondrial carrier 2	1
MTHFR	Methylenetetrahydrofolate reductase	1
MYO15A	Myosin XVA	1
NAT1	N-acetyltransferase 1	1
NAT2	N-acetyltransferase 2	1
NCK2	NCK adaptor protein 2	1
NCSTN	Nicastrin	1
NEFH	Neurofilament heavy chain	1
NGFR	Nerve growth factor receptor	1
NOS1	Nitric oxide synthase 1	1
NOS2A	Nitric oxide synthase 2a	1
NOTCH4	Notch receptor 4	1

NQO1	NAD(P)H quinone dehydrogenase 1	1
NR4A2	Nuclear receptor subfamily 4 group A member 2	1
NTF3	Neurotrophin 3	1
NYAP1	Neuronal tyrosine phosphorylated phosphoinositide-3-kinase adaptor 1	1
OARD1	O-acyl-ADP-ribose deacylase 1	1
OLR1	Oxidized low density lipoprotein receptor 1	1
OPRM1	Opioid receptor mu 1	1
PARK2	Parkin RBR E3 ubiquitin protein ligase	1
PDYN	Prodynorphin	1
PILRA	Paired immunoglobin like type 2 receptor alpha	1
PINK1	PTEN induced kinase 1	1
PLAU	Plasminogen activator, urokinase	1
PLEKHA1	Pleckstrin homology domain containing A1	1
PON1	Paraoxonase 1	1
PON2	Paraoxonase 2	1
PRDM7	PR/SET domain 7	1
PRNP	Prion protein (Kanno blood group)	1
PSEN1	Presenilin 1	1
PSEN2	Presenilin 2	1
PTPRJ	Protein tyrosine phosphatase receptor type J	1
RASGEF1C	RasGEF domain family member 1C	1
RBCK1	RANBP2-type and C3HC4-type zinc finger containing 1	1
RELB	RELB proto-oncogene, NF-kB subunit	1
RHOH	Ras homolog family member H	1
RP11-81K2.1	UNKNOWN	1
SEC61G	SEC61 translocon subunit gamma	1
SERPINA3	Serpin family A member 3	1
SIGLEC11	Sialic acid binding Ig like lectin 11	1
SLC2A4RG	SLC2A4 regulator	1
SLC6A3	Solute carrier family 6 member 3	1
SLC6A4	Solute carrier family 6 member 4	1
SNCA	Synuclein alpha	1

SNX1	Sorting nexin 1	1
SOD1	Superoxide dismutase 1	1
SORT1	Sortilin 1	1
SPDYE3	Speedy/RINGO cell cycle regulator family member E3	1
SSB	Small RNA binding exonuclease protection factor La	1
SYN1	Synapsin I	1
TCN2	Transcobalamin 2	1
TF	Transferrin	1
TFAM	Transcription factor A, mitochondrial	1
TH	Tyrosine hydroxylase	1
TMEM106B	Transmembrane protein 106B	1
TNF	Tumor necrosis factor	1
TNIP1	TNFAIP3 interacting protein 1	1
TP53	Tumor protein p53	1
TPCN1	Two pore segment channel 1	1
TREML2	Triggering receptor expressed on myeloid cells like 2	1
TSPAN14	Tetraspanin 14	1
TSPOAP1	TSPO associated protein 1	1
TSPYL5	Testis specific protein Y like 5	1
TTR	Transthyretin	1
UCHL1	Ubiquitin C-terminal hydrolase L1	1
UMAD1	UBAP1-MVB12-associated (UMA) domain containing 1	1
USP6NL	USP6 N-terminal like	1
VLDLR	Very low density lipoprotein receptor	1
WDR12	WD repeat domain 12	1
WDR81	WD repeat domain 81	1
WNT3	WNT family member 3	1
WT1	WT1 transcription factor	1
ZNF594-DT	ZNF594 divergent transcript	1
ABCA1	ATP(adenosine triphosphate)-binding cassette, sub-family A, member 1	2
ABI3	Abelson interacting protein, family member 3	2
ADH1B	Alcohol dehydrogenase 1B (class I) beta polypeptide	2

APH1B	APH1B (aph-1 homolog B gamma-secretase subunit) gamma secretase subunit	2
BCL3	B-cell lymphoma 3-encoded protein transcription coactivator	2
CLNK	Cytokine dependent hematopoietic cell linker	2
HLA-DQA1	Human leukocyte antigens, major histocompatibility complex, class II, DQ alpha 1	2
IL1A	Interleukin 1 alpha	2
IL1B	Interleukin 1 beta	2
MME	Membrane metalloendopeptidase	2
MS4A4A	Membrane spanning 4-domains A4A	2
PRKD3	Protein kinase D3	2
PVRL2	Poliovirus receptor-related 2	2
SHARPIN	SHANK associated RH domain interactor	2
UNC5CL	UNC-5 family C-terminal like	2
WWOX	WW domain containing oxidoreductase	2
ADAM10	ADAM (a disintegrin and metalloproteinase) metallopeptidase domain 10	3
ADAMTS1	ADAM (a disintegrin and metalloproteinase) metallopeptidase with thrombospondin type 1 motif 1	3
APOC1	Apolipoprotein C-I	3
APP	Amyloid beta precursor protein	3
ECHDC3	Enoyl-CoA hydratase domain containing 3	3
IL34	Interleukin 34	3
IQCK	IQ motif containing K	3
PLCG2	Phospholipase C gamma 2	3
SCIMP	SLP adaptor and CSK interacting membrane protein	3
ACE	Angiotensin I converting enzyme	4
CD33	CD33 molecule	4
TOMM40	Translocase of outer mitochondrial membrane 40	4
TREM2	Triggering receptor expressed on myeloid cells 2	4
HLA-DQB1	Human leukocyte antigens, major histocompatibility complex, class II, DQ beta 1	5
abParts	UNKNOWN	6
AL833583	UNKNOWN	6
BC043356	UNKNOWN	6
BZRAP1	Benzodiazepine receptor (peripheral) associated protein 1	6

C19orf6	Chromosome 19 open reading frame 67	6
CR595071	UNKNOWN	6
GPR115	G-protein coupled receptor 115	6
HLA-DRB1	Human leukocyte antigens, major histocompatibility complex, class II, DR beta 1	6
TRIP4	Thyroid hormone receptor interactor 4	6
CHRNA2	Cholinergic receptor nicotinic alpha 2 subunit	7
HLA	Human leukocyte antigens, major histocompatibility complex	7
HLA-DRB5	Human leukocyte antigens, major histocompatibility complex, class II, DR beta 5	10
SPI1	Spi-1 proto-oncogene	10
SPPL2A	Signal peptide peptidase like 2A	11
CELF1	CUGBP Elav-like family member 1	12
NME8	NME/NM23 family member 8	12
RIN3	Ras and Rab interactor 3	12
MEF2C	Myocyte enhancer factor 2C	13
CD2AP	CD2 associated protein	17
EPHA1	EPH receptor A1	18
ZCWPW1	Zinc finger CW-type and PWWP domain containing 1	18
CASS4	Cas scaffold protein family member 4	21
FERMT2	FERM domain containing kindlin 2	21
INPP5D	Inositol polyphosphate-5-phosphatase D	21
MS4A6A	Membrane spanning 4-domains A6A	21
PTK2B	Protein tyrosine kinase 2 beta	22
SLC24A4	Solute carrier family 24 member 4	22
BIN1	Bridging integrator 1	23
PICALM	Phosphatidylinositol binding clathrin assembly protein	23
SORL1	Sortilin related receptor 1	23
ABCA7	ATP(adenosine triphosphate)-binding cassette, sub-family, A member 7	24
CR1	Complement C3b/C4b receptor 1 (Knops blood group)	25
CLU	Clusterin	26
APOE	Apolipoprotein E	28

Table B.6: Quality assessment scores for all papers selected for systematic review.

Authors	Q1	Q2	Q3	Q4	Q5	Q6	Q7	Q8	Q9	Q10	Q11	TOTAL
Ahmad et al. (2018)	1	1	1	2	0	2	1	1	Not stated	1	1	**11**
Altmann et al. (2020)	1	1	1	2	2	1	2	Not stated **	Not stated	3	1	**14**
Armstrong et al. (2020)	1	0	1	0	0	2	2	1	Not stated	3	1	**11**
Brenowitz et al. (2023)	0	0	1	0	2	1	1	1	Not stated	3	1	**10**
Caspers et al. (2020)	0	0	1	0	1	1	1	1	Not stated	1	1	**7**
Chandler et al. (2025)	0	1	1	Not stated ****	0	2	1	Not stated *****	0	1	1	**8**
Chen et al. (2023)	0	1	1	0	1	Not stated	2	0	Not stated	3	1	**9**
Chen et al. (2024)	0	1	1	0	1	1	2	Not stated ****	Not stated	3	1	**10**
Chung et al. (2023)	1	1	1	2	0	1	1	1	Not stated	3	1	**12**
Corlier et al. (2018)	0	0	1	0	2	1	1	1	Not stated	3	1	**10**
De Marco et al. (2020)	1	0	1	1	2	0	1	2	Not stated	3	1	**12**
de Silva et al. (2022)	0	0	1	2	2	1	2	1	Not stated	1	1	**11**

Desikan et al. (2017)	0	0	Not stated ***	1	1	0	1	1	Not stated	0	1	**5**
Ebenau et al. (2021)	0	0	1	0	1	1	1	1	0	1	1	**7**
Foo et al. (2021)	1	1	1	0	0	2	Not stated •(2)	0	Not stated	1	1	**7**
Ge et al. (2018)	0	0	1	2	1	0	Not stated	1	Not stated	1	1	**7**
Genius et al. (2025)	0	0	1	2	1	2	2	2	0	3	1	**14**
Habes et al. (2016)	1	1	1	0	0	1	1	0	Not stated	3	1	**9**
Habes et al. (2018)	1	0	1	0	0	1	1	0	Not stated	3	1	**8**
Harrison et al. (2016)	1	0	1	0	2	0	0	1	1	3	1	**10**
Harrison et al. (2023)	1	1	1	0	1	2	2	1	Not stated	1	1	**11**
Hayes et al. (2020)	0	0	1	0	0	0	1	1	Not stated	3	1	**7**
He et al. (2023)	0	1	1	0	1	2	2	Not stated ****	Not stated	1	1	**9**
Hohman et al. (2017)	1	0	1	1	2	1	1	2	Not stated	3	1	**13**
Homann et al. (2022)	0	1	1	2	0	Not stated	Not stated	1	Not stated	3	1	**9**
Kannappan et al. (2022)	1	1	1	2	0	Not stated	2	1	Not stated	3	1	**12**
Kauppi et al. (2018)	0	0	1	1	1	0	1	1	Not stated	3	1	**9**

Kirchner et al. (2023)	0	1	1	0	1	Not stated	2	1	Not stated	3	1	**10**
Korbmacher et al. (2024)	1	1	2	0	0	Not stated	1	1	0	1	1	**8**
Kulminski et al. (2024)	0	0	1	1	2	0	0	2	0	3	1	**10**
Lancaster et al. (2019)	1	1	Not stated*	0	1	1	2	0	Not stated	0	1	**7**
Lancaster et al. (2023)	1	1	1	0	1	1	2	1	Not stated	3	1	**12**
Lee et al. (2021)	0	0	1	2	0	Not stated	1	1	0	3	1	**9**
Li et al. (2021)	1	0	1	2	1	0	1	1	Not stated	3	1	**11**
Liu et al. (2021)	0	1	1	1	2	1	1	2	Not stated	3	1	**13**
Liu et al. (2022)	1	1	1	1	2	1	1	1	Not stated	1	1	**11**
Liu et al. (2023)	0	1	1	Not stated ****	0	Not stated	2	0	Not stated	1	0	**5**
Lorenz et al. (2025)	0	1	1	2	1	2	1	1	0	3	1	**13**
Lorenzini et al. (2024)	1	1	1	0	1	2	1	1	0	3	1	**12**
Lupton et al. (2016)	0	1	1	2	1	1	1	1	Not stated	1	1	**10**
Manca, Pardinas, and Venneri (2023)	1	0	Not stated ***	2	1	Not stated	Not stated	1	Not stated	0	1	**6**

Meda et al. (2012)	1	0	1	2	0	0	2	1	Not stated	1	1	**9**
Mormino et al. (2016)	0	0	1	2	0	2	2	1	Not stated	3	1	**12**
Nordengen et al. (2022)	0	0	1	1	2	1	2	1	Not stated	3	1	**12**
Prieto et al. (2020)	1	0	1	2	0	0	1	1	Not stated	3	1	**10**
Reas et al. (2023)	0	0	1	1	1	0	1	1	Not stated	3	1	**9**
Roe et al. (2024)	1	0	1	0	0	2	1	1	0	1	1	**8**
Roostaei et al. (2018)	0	1	1	2	2	Not stated	1	1	Not stated	3	1	**12**
Rutten-Jacobs et al. (2018)	0	1	Not stated*	0	0	Not stated	Not stated	0	Not stated	0	1	**2**
Sabuncu et al. (2012)	1	0	1	0	1	2	1	1	Not stated	3	1	**11**
Sha et al. (2023)	1	1	1	0	0	2	2	0	Not stated	1	1	**9**
Sloan et al. (2010)	0	0	1	1	1	0	2	1	Not stated	1	0	**7**
Soldan et al. (2024)	0	1	1	0	1	1	2	1	0	3	1	**11**
Steventon et al. (2023)	0	1	0	0	0	Not stated	2	1	Not stated	3	1	**8**
Tan et al. (2019)	0	0	1	2	1	1	1	1	Not stated	1	0	**8**

Tank et al. (2022)	1	1	1	0	2	1	2	0	Not stated	3	1	**12**
Vacher et al. (2022a)	0	0	1	0	2	1	Not stated	0	Not stated	3	1	**8**
Vacher et al. (2022b)	0	0	1	2	2	0	1	1	Not stated	3	0	**10**
Wang et al. (2019)	0	0	1	1	2	2	2	1	Not stated	1	1	**11**
Williams et al. (2021)	1	0	0	0	1	Not stated	1	1	Not stated	1	1	**6**
Xiao et al. (2017)	1	0	1	0	2	1	2	0	0	3	1	**11**
Xu et al. (2022)	1	0	1	2	1	1	1	1	Not stated	3	1	**12**
Zhao et al. (2019b)	0	1	1	Not stated	0	Not stated	2	0	Not stated	1	0	**5**
Zhao et al. (2020)	1	1	1	2	1	Not stated	Not stated	1	Not stated	1	1	**9**

Q: question.

*Not stated so no score given. However, hypothetically would have scored "1" as UK Biobank include two or more genders.

**Not stated so no score given. However, hypothetically would have scored "1" as ADNI sample is clinically defined.

***Not stated so no score given. However, hypothetically would have scored "1" as ADNI include two or more genders.

****Not stated so no score given. However, hypothetically would have scored "0" as UK Biobank participants are a relatively healthy population.

*****Not stated so no score given. However, hypothetically would have scores "1" as UK Biobank participants are clinically defined.

• Not stated in paper. However, author(s) responded to email communication and provided information. Based on this, a score has been given in (brackets); this has not been included in the Total score as this information was not stated in the paper itself.

APPENDIX C (Chapter 3: Overview of Thesis)

Appendix C.1: Ethical approval granted by the College of Health, Medicine, and Life Sciences Research Ethics Committee at Brunel University (of) London.

College of Health, Medicine and Life Sciences Research Ethics Committee (DLS)
Brunel University London
Kingston Lane
Uxbridge
UB8 3PH
United Kingdom

www.brunel.ac.uk

21 December 2022

LETTER OF CONFIRMATION

Applicant: Miss Snehal Pandya

Project Title: Exploring the Contribution of Polymorphisms, in addition to Apolipoprotein E, to Brain Parameters in the Alzheimer's disease Spectrum

Reference: 40561-NER-Dec/2022- 42767-1

Dear Miss Snehal Pandya

The Research Ethics Committee has considered the above application recently submitted by you.

The Chair, acting under delegated authority has confirmed that, according to the information provided in your application, your project does not require ethical review.

Please note that:

- **You are not permitted to conduct research involving human participants, their tissue and/or their data. If you wish to conduct such research, you must contact the Research Ethics Committee to seek approval prior to engaging with any participants or working with data for which you do not have approval.**
- The Research Ethics Committee reserves the right to sample and review documentation relevant to the study.
- If during the course of the study, you would like to carry out research activities that concern a human participant, their tissue and/or their data, you must inform the Committee by submitting an appropriate Research Ethics Application. Research activity includes the recruitment of participants, undertaking consent procedures and collection of data. Breach of this requirement constitutes research misconduct and is a disciplinary offence.

Good luck with your research!

Kind regards,

Professor Louise Mansfield

Chair of the College of Health, Medicine and Life Sciences Research Ethics Committee (DLS)

Brunel University London

Page 1 of 1

Appendix C.2: Approval of access to the Alzheimer's Disease Neuroimaging Initiative database.

Outlook

Database Access Request

From dba@loni.usc.edu <dba@loni.usc.edu>
Date Sat 17/12/2022 02:37
To Snehal Pandya (Doctoral Researcher) <Snehal.Pandya@brunel.ac.uk>

Congratulations. Your request for access to the Alzheimer's Disease Neuroimaging Initiative (ADNI) Data has been approved. If you already had a LONI user account your permissions have been updated to provide you access to ADNI data. If you did not yet have an account, an account will be created for you and an e-mail with your account information will be sent to you shortly.

Login page: https://ida.loni.usc.edu/login.jsp?project=ADNI&page=HOME

APPENDIX D (Chapter 4: Experiment One)

Table D.1: Associations between PRSwithAPOE Threshold 1 and 114 regions of interest in the whole group

Region of Interest	R Square (Model 1)	R Square (Model 2)	R Square Change	Sig. F Change (Model 2)	FDR Corrected value	Standardised beta of PRS
Accumbens area L	0.393	0.394	0.001	0.331	0.571727272727273	-0.031
Accumbens area R	0.391	0.391	0.000	0.809	0.895398058252427	-0.008
Amygdala L	0.417	0.428	0.011	0.000273300646631	0.0077890684289835	-0.114
Amygdala R	0.464	0.478	0.014	0.000015711322223	0.000895545366711	-0.129
Angular gyrus L	0.401	0.404	0.003	0.077	0.3135	-0.056
Angular gyrus R	0.417	0.419	0.002	0.090	0.330967741935484	-0.053
Anterior cingulate gyrus L	0.410	0.410	0.000	0.992	0.992	0.000
Anterior cingulate gyrus R	0.241	0.222	0.002	0.226	0.452	-0.043
Anterior insula L	0.374	0.374	0.000	0.584	0.765241379310345	0.018
Anterior insula R	0.385	0.385	0.000	0.872	0.955846153846154	0.005
Anterior orbital gyrus L	0.399	0.402	0.002	0.093	0.3313125	-0.053
Anterior orbital gyrus R	0.358	0.360	0.003	0.094451	0.316688647058823	-0.055
Basal forebrain L	0.284	0.285	0.001	0.271	0.523627118644068	0.002
Basal forebrain R	0.344	0.345	0.001	0.298	0.547935483870968	0.002
Calcarine cortex L	0.363	0.364	0.001	0.350	0.586764705882353	-0.031
Calcarine cortex R	0.371	0.374	0.003	0.050	0.271428571428571	-0.064
Caudate L	0.195	0.196	0.001	0.364	0.601391304347826	-0.033
Caudate R	0.190	0.191	0.001	0.306	0.553714285714286	-0.038
Central operculum L	0.369	0.371	0.002	0.157	0.365265306122449	0.046
Central operculum R	0.373	0.373	0.000	0.933	0.966927272727273	-0.003
Cuneus L	0.393	0.395	0.002	0.120	0.325714285714286	-0.050
Cuneus R	0.412	0.416	0.004	0.020	0.175384615384615	-0.073
Entorhinal area L	0.409	0.414	0.005	0.019	0.1805	-0.074
Entorhinal area R	0.457	0.462	0.005	0.012024	0.171342	-0.076
Frontal operculum L	0.358	0.360	0.002	0.183007	0.409074470588235	0.044
Frontal operculum R	0.323	0.323	0.000	0.940	0.965405405405405	0.003

Frontal pole L	0.426	0.427	0.000	0.492	0.7011	0.021
Frontal pole R	0.409	0.412	0.002	0.098	0.3192	0.052
Fusiform gyrus L	0.509	0.512	0.003	0.035	0.249375	-0.061
Fusiform gyrus R	0.529	0.533	0.004	0.012019	0.195738	-0.071
Gyrus rectus L	0.431	0.431	0.000	0.896	0.954616822429906	0.004
Gyrus rectus R	0.441	0.441	0.001	0.315	0.56109375	0.031
Hippocampus L	0.449	0.462	0.013	0.000036912065301	0.001402658481438	-0.125
Hippocampus R	0.476	0.496	0.019	0.00000023464	0.00002674896	-0.152
Inferior occipital gyrus L	0.410	0.412	0.003	0.073	0.320076923076923	-0.057
Inferior occipital gyrus R	0.459	0.463	0.004	0.028	0.228	-0.066
Inferior temporal gyrus L	0.505	0.509	0.004	0.014	0.1596	-0.070
Inferior temporal gyrus R	0.543	0.547	0.004	0.012386	0.156889333	-0.069
Lateral orbital gyrus L	0.410	0.410	0.000	0.7782158	0.905271441	-0.009
Lateral orbital gyrus R	0.358	0.358	0.000	0.705	0.855	-0.012
Lingual gyrus L	0.499	0.499	0.000	0.520	0.714216867	-0.019
Lingual gyrus R	0.515	0.517	0.002	0.115	0.345	-0.045
Medial frontal cortex L	0.358	0.359	0.001	0.206	0.426981818	-0.042
Medial frontal cortex R	0.363	0.363	0.000	0.985	0.993716814	-0.001
Medial orbital gyrus L	0.472	0.473	0.000	0.413	0.636243243	-0.024
Medial orbital gyrus R	0.433	0.433	0.000	0.928	0.970568807	0.003
Middle cingulate gyrus L	0.380	0.380	0.000	0.540	0.732857143	-0.020
Middle cingulate gyrus R	0.333	0.334	0.002	0.205	0.432777778	-0.042
Middle frontal gyrus L	0.470	0.470	0.000	0.773	0.9179375	-0.009
Middle frontal gyrus R	0.465	0.465	0.000	0.484	0.69843038	-0.021
Middle occipital gyrus L	0.356	0.358	0.002	0.118	0.328097561	-0.052
Middle occipital gyrus R	0.347	0.357	0.010	0.001	0.0228	-0.109
Middle temporal gyrus L	0.500	0.502	0.002	0.074	0.241411765	-0.052
Middle temporal gyrus R	0.525	0.528	0.003	0.036	0.312444444	-0.059
Occipital fusiform gyrus L	0.467	0.467	0.000	0.804	0.907485149	-0.007
Occipital fusiform gyrus R	0.504	0.506	0.003	0.047	0.2679	-0.057

Occipital pole L	0.319	0.319	0.001	0.463	0.68548051948052	-0.025
Occipital pole R	0.361	0.362	0.001	0.378	0.606929577464789	-0.029
Opercular part of the inferior frontal gyrus L	0.258	0.261	0.003	0.094108	0.325100363636364	0.059
Opercular part of the inferior frontal gyrus R	0.263	0.264	0.001	0.430	0.645	0.028
Orbital part of the inferior frontal gyrus L	0.271	0.271	0.000	0.786	0.905090909090909	0.010
Orbital part of the inferior frontal gyrus R	0.256	0.257	0.001	0.297	0.555049180327869	-0.037
Pallidum L	0.141	0.143	0.002	0.183192	0.401613230769231	-0.051
Pallidum R	0.117	0.121	0.003	0.113	0.357833333333333	-0.061
Parahippocampal gyrus L	0.490	0.493	0.003	0.037	0.234333333333333	-0.061
Parahippocampal gyrus R	0.516	0.520	0.004	0.011	0.209	-0.072
Parietal operculum L	0.319	0.319	0.000	0.698	0.855612903225806	0.013
Parietal operculum R	0.273	0.274	0.000	0.889	0.9652	0.005
Planum polare L	0.431	0.432	0.000	0.514	0.723407407407407	-0.020
Planum polare R	0.456	0.458	0.001	0.179	0.40812	-0.041
Planum temporale L	0.333	0.333	0.000	0.921	0.972166666666667	-0.003
Planum temporale R	0.350	0.350	0.000	0.975	0.992410714285714	0.001
Postcentral gyrus L	0.378	0.379	0.000	0.478	0.698615384615385	-0.023
Postcentral gyrus R	0.380	0.382	0.002	0.129994	0.336802636363636	-0.049
Postcentral gyrus medial segment L	0.192	0.196	0.004	0.057	0.282521739130435	-0.070
Postcentral gyrus medial segment R	0.205	0.208	0.003	0.131	0.331866666666667	-0.055
Posterior cingulate gyrus L	0.533	0.535	0.002	0.086	0.3268	-0.048
Posterior cingulate gyrus R	0.495	0.498	0.003	0.031	0.2356	-0.063
Posterior insula L	0.384	0.385	0.000	0.587	0.760431818181818	0.018
Posterior insula R	0.412	0.412	0.000	0.807	0.901941176470588	0.008
Posterior orbital gyrus L	0.356	0.357	0.000	0.563	0.755082352941176	-0.019
Posterior orbital gyrus R	0.372	0.374	0.002	0.117	0.33345	-0.051
Precentral gyrus L	0.499	0.499	0.000	0.895	0.962547169811321	0.004
Precentral gyrus R	0.431	0.431	0.000	0.7782150	0.914603195876289	-0.009
Precentral gyrus medial segment L	0.284	0.287	0.002	0.138	0.342	-0.052
Precentral gyrus medial segment R	0.321	0.324	0.003	0.071	0.32376	-0.061

Precuneus L	0.474	0.477	0.003	0.055	0.285	-0.057
Precuneus R	0.478	0.481	0.003	0.039	0.234	-0.061
Putamen L	0.268	0.269	0.002	0.214	0.435642857142857	-0.044
Putamen R	0.276	0.278	0.003	0.116	0.339076923076923	-0.055
Subcallosal area L	0.471	0.471	0.000	0.582	0.771488372093023	0.016
Subcallosal area R	0.455	0.447	0.002	0.129778	0.344062604651163	0.046
Superior frontal gyrus L	0.453	0.454	0.002	0.146	0.354127659574468	-0.044
Superior frontal gyrus R	0.473	0.474	0.000	0.791	0.90174	0.008
Superior frontal gyrus medial segment L	0.410	0.411	0.001	0.233	0.457965517241379	-0.038
Superior frontal gyrus medial segment R	0.398	0.398	0.001	0.372	0.605828571428571	0.028
Superior occipital gyrus L	0.309	0.311	0.001	0.283	0.5377	-0.037
Superior occipital gyrus R	0.321	0.322	0.001	0.333	0.566597014925373	-0.033
Superior parietal lobule L	0.376	0.377	0.002	0.190	0.408679245283019	-0.042
Superior parietal lobule R	0.369	0.372	0.003	0.059	0.28025	-0.062
Superior temporal gyrus L	0.415	0.415	0.000	0.666	0.83432967032967	-0.014
Superior temporal gyrus R	0.395	0.395	0.001	0.422	0.64144	-0.026
Supplementary motor cortex L	0.351	0.353	0.002	0.114	0.351243243243243	-0.052
Supplementary motor cortex R	0.362	0.362	0.000	0.648	0.8208	-0.015
Supramarginal gyrus L	0.346	0.346	0.000	0.611	0.782629213483146	-0.017
Supramarginal gyrus R	0.345	0.345	0.000	0.519	0.721536585365854	0.021
Temporal pole L	0.397	0.399	0.002	0.150	0.35625	-0.046
Temporal pole R	0.403	0.408	0.005	0.015	0.155454545454545	-0.077
Thalamus proper L	0.229	0.230	0.001	0.383	0.606416666666667	-0.031
Thalamus proper R	0.256	0.259	0.003	0.085	0.334137931034483	-0.061
Transverse temporal gyrus L	0.254	0.255	0.001	0.389	0.607479452054795	0.031
Transverse temporal gyrus R	0.321	0.322	0.000	0.725	0.87	-0.012
Triangular part of the inferior frontal gyrus L	0.303	0.304	0.001	0.328	0.575261538461538	0.034
Triangular part of the inferior frontal gyrus R	0.286	0.286	0.000	0.687	0.851282608695652	-0.014

FDR: false discovery rate. L: left. PRS: polygenic risk score. R: right.

Table D.2: Associations between PRSwithAPOE Threshold 5 and 114 regions of interest in the whole group

Region of Interest	R Square (Model 1)	R Square (Model 2)	R Square Change	Sig. F Change (Model 2)	FDR Corrected value	Standardised beta of PRS
Accumbens area L	0.393	0.394	0.001	0.361	0.64303125	-0.029
Accumbens area R	0.391	0.391	0.000	0.893	0.933963302752294	-0.004
Amygdala L	0.417	0.430	0.012	0.000089384713878	0.002547464345523	-0.123
Amygdala R	0.464	0.478	0.015	0.000009164203471	0.000522359597847	-0.133
Angular gyrus L	0.401	0.403	0.002	0.087	0.342	-0.054
Angular gyrus R	0.417	0.419	0.002	0.117	0.381085714285714	-0.049
Anterior cingulate gyrus L	0.410	0.410	0.000	0.884	0.941831775700934	0.005
Anterior cingulate gyrus R	0.241	0.242	0.001	0.374	0.636358208955224	-0.032
Anterior insula L	0.374	0.374	0.000	0.634	0.794241758241758	0.016
Anterior insula R	0.385	0.385	0.000	0.897	0.929618181818182	0.004
Anterior orbital gyrus L	0.399	0.401	0.002	0.137	0.39045	-0.047
Anterior orbital gyrus R	0.358	0.360	0.002	0.143	0.397609756097561	-0.048
Basal forebrain L	0.284	0.285	0.001	0.278	0.565928571428571	-0.038
Basal forebrain R	0.344	0.345	0.001	0.410	0.631621621621622	-0.027
Calcarine cortex L	0.363	0.364	0.001	0.251	0.53988679245283	-0.038
Calcarine cortex R	0.371	0.375	0.004	0.036	0.2565	-0.068
Caudate L	0.195	0.195	0.001	0.441	0.6615	-0.028
Caudate R	0.190	0.191	0.001	0.343	0.620666666666667	-0.035
Central operculum L	0.369	0.371	0.002	0.106	0.355411764705882	0.053
Central operculum R	0.373	0.373	0.000	0.926	0.934194690265487	0.003
Cuneus L	0.393	0.394	0.002	0.176	0.426893617021277	-0.043
Cuneus R	0.412	0.415	0.004	0.035	0.266	-0.066
Entorhinal area L	0.409	0.415	0.005	0.011	0.179142857142857	-0.080
Entorhinal area R	0.457	0.461	0.005	0.012	0.171	-0.075
Frontal operculum L	0.358	0.360	0.002	0.175	0.433695652173913	0.045
Frontal operculum R	0.323	0.323	0.000	0.886	0.935222222222222	0.005

Frontal pole L	0.426	0.427	0.001	0.329	0.614852459016394	0.030
Frontal pole R	0.409	0.412	0.003	0.072	0.342	0.057
Fusiform gyrus L	0.509	0.511	0.002	0.075256	0.34316736	-0.051
Fusiform gyrus R	0.529	0.532	0.003	0.027	0.219857142857143	-0.062
Gyrus rectus L	0.431	0.431	0.000	0.777	0.877009900990099	0.009
Gyrus rectus R	0.441	0.441	0.001	0.289	0.578	0.033
Hippocampus L	0.449	0.464	0.015	0.000009585428889	0.000364246297782	-0.134
Hippocampus R	0.476	0.497	0.021	0.000000096147	0.000010960758	-0.157
Inferior occipital gyrus L	0.410	0.412	0.003	0.076	0.320888888888889	-0.056
Inferior occipital gyrus R	0.459	0.463	0.003	0.0417	0.2641	-0.062
Inferior temporal gyrus L	0.505	0.509	0.004	0.013	0.164666666666667	-0.072
Inferior temporal gyrus R	0.543	0.547	0.004	0.016	0.1824	-0.067
Lateral orbital gyrus L	0.410	0.410	0.000	0.991	0.991	0.000
Lateral orbital gyrus R	0.358	0.358	0.000	0.872	0.937811320754717	-0.005
Lingual gyrus L	0.499	0.499	0.000	0.576	0.76353488372093	-0.016
Lingual gyrus R	0.515	0.516	0.001	0.154926	0.3924792	-0.041
Medial frontal cortex L	0.358	0.358	0.001	0.324	0.6156	-0.033
Medial frontal cortex R	0.363	0.363	0.000	0.691	0.8292	0.013
Medial orbital gyrus L	0.472	0.473	0.000	0.534	0.73344578313253	-0.019
Medial orbital gyrus R	0.433	0.433	0.000	0.776	0.88464	0.009
Middle cingulate gyrus L	0.380	0.380	0.000	0.609	0.780067415730337	-0.017
Middle cingulate gyrus R	0.333	0.333	0.001	0.369	0.637363636363636	-0.030
Middle frontal gyrus L	0.470	0.470	0.000	0.765	0.889897959183673	-0.009
Middle frontal gyrus R	0.465	0.465	0.000	0.539	0.7315	-0.019
Middle occipital gyrus L	0.356	0.357	0.002	0.195	0.463125	-0.043
Middle occipital gyrus R	0.347	0.355	0.008	0.003	0.0684	-0.099
Middle temporal gyrus L	0.500	0.502	0.003	0.058	0.278294117647059	-0.055
Middle temporal gyrus R	0.525	0.527	0.003	0.0415	0.314857142857143	-0.058
Occipital fusiform gyrus L	0.467	0.467	0.000	0.869	0.943485714285714	-0.005
Occipital fusiform gyrus R	0.504	0.506	0.002	0.089	0.3382	-0.049

Occipital pole L	0.319	0.319	0.001	0.443	0.65587012987013	-0.026
Occipital pole R	0.316	0.316	0.000	0.496	0.7068	-0.022
Opercular part of the inferior frontal gyrus L	0.258	0.260	0.003	0.097	0.3455625	0.059
Opercular part of the inferior frontal gyrus R	0.263	0.264	0.001	0.403753	0.639275583333333	0.030
Orbital part of the inferior frontal gyrus L	0.271	0.271	0.000	0.744	0.87439175257732	0.011
Orbital part of the inferior frontal gyrus R	0.256	0.257	0.001	0.341	0.627	-0.034
Pallidum L	0.141	0.142	0.002	0.241	0.538705882352941	-0.045
Pallidum R	0.117	0.120	0.003	0.145350	0.394521428571429	-0.056
Parahippocampal gyrus L	0.490	0.494	0.004	0.026	0.228	-0.065
Parahippocampal gyrus R	0.516	0.520	0.004	0.010	0.19	-0.074
Parietal operculum L	0.319	0.319	0.000	0.481	0.703	0.024
Parietal operculum R	0.273	0.274	0.000	0.681	0.843847826086957	0.014
Planum polare L	0.431	0.432	0.001	0.391	0.646	-0.027
Planum polare R	0.456	0.458	0.001	0.204	0.474612244897959	-0.039
Planum temporale L	0.333	0.333	0.000	0.797	0.882116504854369	-0.009
Planum temporale R	0.350	0.350	0.000	0.924	0.948972972972973	-0.003
Postcentral gyrus L	0.378	0.379	0.001	0.376	0.630352941176471	-0.029
Postcentral gyrus R	0.380	0.381	0.002	0.134	0.391692307692308	-0.049
Postcentral gyrus medial segment L	0.192	0.196	0.005	0.045	0.27	-0.074
Postcentral gyrus medial segment R	0.205	0.207	0.001	0.300	0.589655172413793	-0.038
Posterior cingulate gyrus L	0.533	0.535	0.002	0.090	0.330967741935484	-0.048
Posterior cingulate gyrus R	0.495	0.498	0.004	0.024	0.228	-0.066
Posterior insula L	0.384	0.385	0.000	0.486	0.701316455696202	0.023
Posterior insula R	0.412	0.412	0.000	0.604	0.782454545454545	0.016
Posterior orbital gyrus L	0.356	0.357	0.000	0.690	0.836808510638298	-0.013
Posterior orbital gyrus R	0.372	0.374	0.002	0.129224	0.387672	-0.050
Precentral gyrus L	0.449	0.449	0.000	0.775	0.892424242424243	0.009
Precentral gyrus R	0.431	0.431	0.000	0.925	0.941517857142857	-0.003
Precentral gyrus medial segment L	0.284	0.286	0.002	0.154898	0.401326636363636	-0.050
Precentral gyrus medial segment R	0.321	0.323	0.003	0.102	0.352363636363636	-0.055

Precuneus L	0.474	0.477	0.002	0.085	0.346071428571429	-0.051
Precuneus R	0.478	0.481	0.003	0.059	0.305727272727273	-0.056
Putamen L	0.268	0.269	0.002	0.219	0.49932	-0.043
Putamen R	0.276	0.278	0.002	0.125	0.395833333333333	-0.054
Subcallosal area L	0.471	0.472	0.001	0.395	0.643285714285714	0.025
Subcallosal area R	0.445	0.448	0.003	0.056	0.3192	0.059
Superior frontal gyrus L	0.453	0.454	0.001	0.258	0.544666666666667	-0.034
Superior frontal gyrus R	0.473	0.474	0.000	0.627	0.7942	0.015
Superior frontal gyrus medial segment L	0.410	0.411	0.001	0.243	0.532730769230769	-0.037
Superior frontal gyrus medial segment R	0.398	0.398	0.001	0.416	0.63232	0.026
Superior occipital gyrus L	0.309	0.310	0.000	0.520	0.722926829268293	-0.022
Superior occipital gyrus R	0.321	0.322	0.000	0.546	0.732282352941176	-0.020
Superior parietal lobule L	0.376	0.377	0.001	0.277	0.574145454545455	-0.035
Superior parietal lobule R	0.369	0.372	0.003	0.075435	0.330753461538462	-0.058
Superior temporal gyrus L	0.415	0.415	0.000	0.599	0.784896551724138	-0.017
Superior temporal gyrus R	0.395	0.395	0.001	0.404038	0.630963452054795	-0.027
Supplementary motor cortex L	0.351	0.353	0.002	0.145410	0.385505581395349	-0.048
Supplementary motor cortex R	0.362	0.362	0.000	0.689	0.84458064516129	-0.013
Supramarginal gyrus L	0.346	0.346	0.000	0.736	0.874	-0.011
Supramarginal gyrus R	0.345	0.345	0.001	0.367	0.643661538461538	0.030
Temporal pole L	0.397	0.399	0.002	0.128843	0.39697572972973	-0.049
Temporal pole R	0.403	0.408	0.005	0.017	0.176181818181818	-0.076
Thalamus proper L	0.229	0.230	0.001	0.398	0.639042253521127	-0.031
Thalamus proper R	0.256	0.259	0.004	0.066	0.327130434782609	-0.065
Transverse temporal gyrus L	0.254	0.255	0.000	0.501	0.705111111111111	0.024
Transverse temporal gyrus R	0.321	0.322	0.000	0.800	0.876923076923077	-0.009
Triangular part of the inferior frontal gyrus L	0.303	0.304	0.001	0.303	0.585457627118644	0.035
Triangular part of the inferior frontal gyrus R	0.286	0.286	0.000	0.792	0.885176470588235	-0.009

FDR: false discovery rate. L: left. PRS: polygenic risk score. R: right.

Table D.3: Associations between PRSwithAPOE Threshold 10 and 114 regions of interest in the whole group

Region of Interest	R Square (Model 1)	R Square (Model 2)	R Square Change	Sig. F Change (Model 2)	FDR Corrected value	Standardised beta of PRS
Accumbens area L	0.393	0.394	0.001	0.244	0.545411764705882	-0.038
Accumbens area R	0.391	0.391	0.000	0.731	0.8680625	-0.011
Amygdala L	0.417	0.430	0.013	0.000060712749877	0.0017303133714945	-0.126
Amygdala R	0.464	0.478	0.015	0.000009036002899	0.000343368110162	-0.134
Angular gyrus L	0.401	0.402	0.001	0.249	0.525666666666667	-0.037
Angular gyrus R	0.417	0.419	0.002	0.165	0.447857142857143	-0.044
Anterior cingulate gyrus L	0.410	0.410	0.000	0.931	0.991906542056075	0.003
Anterior cingulate gyrus R	0.241	0.241	0.000	0.542	0.762814814814815	-0.022
Anterior insula L	0.374	0.374	0.000	0.721	0.8652	0.012
Anterior insula R	0.385	0.385	0.000	0.924	0.993735849056604	0.003
Anterior orbital gyrus L	0.399	0.401	0.002	0.157	0.458923076923077	-0.045
Anterior orbital gyrus R	0.358	0.359	0.002	0.178	0.471906976744186	-0.045
Basal forebrain L	0.284	0.285	0.002	0.206	0.533727272727273	-0.044
Basal forebrain R	0.344	0.345	0.001	0.450	0.649367088607595	-0.025
Calcarine cortex L	0.363	0.365	0.002	0.160844	0.447224780487805	-0.046
Calcarine cortex R	0.371	0.375	0.004	0.035	0.249375	-0.069
Caudate L	0.195	0.195	0.001	0.421	0.63992	-0.030
Caudate R	0.190	0.191	0.001	0.342	0.56504347826087	-0.035
Central operculum L	0.369	0.371	0.002	0.121	0.4598	0.051
Central operculum R	0.373	0.373	0.000	0.956	0.990763636363636	0.002
Cuneus L	0.393	0.395	0.002	0.125	0.431818181818182	-0.049
Cuneus R	0.412	0.416	0.004	0.023913	0.194720142857143	-0.072
Entorhinal area L	0.409	0.416	0.007	0.004610	0.105108	-0.090
Entorhinal area R	0.457	0.462	0.006	0.006454	0.0919695	-0.083
Frontal operculum L	0.358	0.360	0.002	0.144	0.443675675675676	0.048
Frontal operculum R	0.323	0.323	0.000	0.981	1	-0.001

Frontal pole L	0.426	0.428	0.002	0.128	0.429176470588235	0.048
Frontal pole R	0.409	0.413	0.003	0.043671	0.292852588235294	0.064
Fusiform gyrus L	0.509	0.511	0.002	0.085	0.440454545454545	-0.050
Fusiform gyrus R	0.529	0.532	0.003	0.025	0.19	-0.063
Gyrus rectus L	0.431	0.431	0.000	0.896	0.982153846153846	0.004
Gyrus rectus R	0.411	0.411	0.001	0.331	0.580523076923077	0.030
Hippocampus L	0.449	0.465	0.016	0.000004668166927	0.000266085514839	-0.140
Hippocampus R	0.476	0.498	0.021	0.000000051144	0.000005830416	-0.161
Inferior occipital gyrus L	0.410	0.412	0.002	0.123	0.452322580645161	-0.049
Inferior occipital gyrus R	0.459	0.462	0.002	0.072	0.4104	-0.055
Inferior temporal gyrus L	0.505	0.509	0.004	0.013	0.134727272727273	-0.072
Inferior temporal gyrus R	0.543	0.546	0.004	0.019	0.1805	-0.065
Lateral orbital gyrus L	0.410	0.410	0.000	0.794	0.89619801980198	0.008
Lateral orbital gyrus R	0.358	0.358	0.000	0.577	0.792506024096385	-0.018
Lingual gyrus L	0.499	0.500	0.001	0.359	0.568416666666667	-0.027
Lingual gyrus R	0.515	0.156	0.001	0.261	0.531321428571429	-0.032
Medial frontal cortex L	0.358	0.359	0.001	0.223	0.552652173913043	-0.040
Medial frontal cortex R	0.363	0.363	0.000	0.743	0.86430612244898	0.011
Medial orbital gyrus L	0.472	0.473	0.000	0.580	0.787142857142857	-0.017
Medial orbital gyrus R	0.433	0.433	0.000	0.990	0.99	0.000
Middle cingulate gyrus L	0.380	0.380	0.000	0.894	0.98947572815534	-0.004
Middle cingulate gyrus R	0.333	0.333	0.000	0.639	0.837310344827586	-0.016
Middle frontal gyrus L	0.470	0.470	0.000	0.983	1	0.001
Middle frontal gyrus R	0.465	0.465	0.000	0.714	0.875225806451613	-0.011
Middle occipital gyrus L	0.356	0.357	0.001	0.314	0.586819672131148	-0.033
Middle occipital gyrus R	0.347	0.354	0.007	0.005997	0.0976654285714286	-0.092
Middle temporal gyrus L	0.500	0.502	0.002	0.100	0.418	-0.048
Middle temporal gyrus R	0.525	0.527	0.002	0.088	0.422222222222222	-0.049
Occipital fusiform gyrus L	0.467	0.467	0.000	0.903	0.9804	-0.004
Occipital fusiform gyrus R	0.504	0.505	0.002	0.114	0.448137931034483	-0.046

Occipital pole L	0.319	0.319	0.001	0.357	0.573211267605634	-0.031
Occipital pole R	0.361	0.361	0.001	0.449	0.656230769230769	-0.025
Opercular part of the inferior frontal gyrus L	0.258	0.260	0.002	0.124	0.44175	0.055
Opercular part of the inferior frontal gyrus R	0.263	0.263	0.000	0.611	0.809930232558139	0.018
Orbital part of the inferior frontal gyrus L	0.271	0.271	0.000	0.939	0.991166666666667	0.003
Orbital part of the inferior frontal gyrus R	0.256	0.257	0.001	0.332	0.573454545454545	-0.035
Pallidum L	0.141	0.142	0.001	0.321	0.57178125	-0.038
Pallidum R	0.117	0.119	0.002	0.251	0.520254545454545	-0.045
Parahippocampal gyrus L	0.490	0.495	0.005	0.011	0.139333333333333	-0.075
Parahippocampal gyrus R	0.516	0.521	0.005	0.004659	0.088521	-0.081
Parietal operculum L	0.319	0.320	0.001	0.372	0.580931506849315	0.030
Parietal operculum R	0.273	0.274	0.000	0.765	0.880909090909091	0.011
Planum polare L	0.431	0.433	0.001	0.208	0.526933333333333	-0.039
Planum polare R	0.456	0.458	0.002	0.096	0.420923076923077	-0.051
Planum temporale L	0.333	0.333	0.000	0.823	0.919823529411765	-0.008
Planum temporale R	0.350	0.350	0.000	0.732	0.860288659793814	-0.011
Postcentral gyrus L	0.378	0.379	0.001	0.283582	0.567164	-0.035
Postcentral gyrus R	0.380	0.371	0.001	0.229	0.555446808510638	-0.039
Postcentral gyrus medial segment L	0.192	0.194	0.003	0.131	0.426685714285714	-0.056
Postcentral gyrus medial segment R	0.205	0.206	0.000	0.691	0.865648351648352	-0.015
Posterior cingulate gyrus L	0.533	0.534	0.001	0.160740	0.458109	-0.040
Posterior cingulate gyrus R	0.495	0.497	0.003	0.047	0.282	-0.058
Posterior insula L	0.384	0.384	0.000	0.665	0.851797752808989	0.014
Posterior insula R	0.412	0.412	0.000	0.704	0.872347826086956	0.012
Posterior orbital gyrus L	0.356	0.357	0.000	0.530	0.75525	-0.021
Posterior orbital gyrus R	0.372	0.374	0.003	0.077	0.418	-0.058
Precentral gyrus L	0.449	0.449	0.000	0.667	0.844866666666667	0.013
Precentral gyrus R	0.431	0.431	0.000	0.953	0.996715596330275	0.002
Precentral gyrus medial segment L	0.284	0.286	0.001	0.245652	0.538544769230769	-0.041
Precentral gyrus medial segment R	0.321	0.322	0.001	0.242	0.55176	-0.040

Precuneus L	0.474	0.475	0.001	0.234	0.55575	-0.036
Precuneus R	0.478	0.480	0.002	0.143	0.452833333333333	-0.044
Putamen L	0.268	0.269	0.001	0.236	0.549061224489796	-0.042
Putamen R	0.276	0.278	0.002	0.156	0.468	-0.050
Subcallosal area L	0.471	0.472	0.001	0.284495	0.559179827586207	0.032
Subcallosal area R	0.445	0.449	0.004	0.023752	0.208286769230769	0.070
Superior frontal gyrus L	0.453	0.453	0.001	0.315439	0.570794380952381	-0.031
Superior frontal gyrus R	0.473	0.474	0.001	0.304398	0.5783562	0.031
Superior frontal gyrus medial segment L	0.410	0.411	0.001	0.315361	0.579857322580645	-0.032
Superior frontal gyrus medial segment R	0.398	0.398	0.000	0.443	0.65587012987013	0.025
Superior occipital gyrus L	0.309	0.310	0.001	0.355	0.578142857142857	-0.032
Superior occipital gyrus R	0.321	0.322	0.001	0.338	0.56664705882353	-0.033
Superior parietal lobule L	0.376	0.376	0.001	0.426	0.639	-0.026
Superior parietal lobule R	0.369	0.371	0.002	0.104	0.423428571428571	-0.053
Superior temporal gyrus L	0.415	0.415	0.000	0.547	0.760463414634146	-0.019
Superior temporal gyrus R	0.395	0.395	0.001	0.401	0.617756756756757	-0.027
Supplementary motor cortex L	0.351	0.354	0.003	0.087	0.431217391304348	-0.057
Supplementary motor cortex R	0.362	0.362	0.000	0.791	0.90174	-0.009
Supramarginal gyrus L	0.346	0.346	0.000	0.986	0.994725663716814	0.001
Supramarginal gyrus R	0.345	0.346	0.001	0.245659	0.528398603773585	0.039
Temporal pole L	0.397	0.400	0.002	0.095	0.4332	-0.054
Temporal pole R	0.403	0.408	0.005	0.012	0.1368	-0.081
Thalamus proper L	0.229	0.230	0.001	0.303720	0.586848813559322	-0.037
Thalamus proper R	0.256	0.260	0.004	0.044457	0.281561	-0.072
Transverse temporal gyrus L	0.254	0.254	0.000	0.644	0.834272727272727	0.017
Transverse temporal gyrus R	0.321	0.322	0.000	0.596	0.799341176470588	-0.018
Triangular part of the inferior frontal gyrus L	0.303	0.304	0.001	0.337	0.573402985074627	0.033
Triangular part of the inferior frontal gyrus R	0.286	0.286	0.000	0.715	0.867127659574468	-0.013

FDR: false discovery rate. L: left. PRS: polygenic risk score. R: right.

Table D.4: Associations between PRSwithoutAPOE Threshold 1 and 114 regions of interest in the whole group

Region of Interest	R Square (Model 1)	R Square (Model 2)	R Square Change	Sig. F Change (Model 2)	FDR Corrected value	Standardised beta of PRS
Accumbens area L	0.393	0.393	0.000	0.550	1	-0.018
Accumbens area R	0.391	0.392	0.001	0.326	1	-0.029
Amygdala L	0.417	0.418	0.001	0.344	1	-0.028
Amygdala R	0.464	0.465	0.001	0.250	1	-0.032
Angular gyrus L	0.401	0.401	0.000	0.882	1	-0.004
Angular gyrus R	0.417	0.417	0.000	0.492514	1	0.020
Anterior cingulate gyrus L	0.410	0.410	0.000	0.601	1	0.015
Anterior cingulate gyrus R	0.241	0.242	0.002	0.223	1	-0.041
Anterior insula L	0.374	0.374	0.000	0.962	1	0.001
Anterior insula R	0.385	0.386	0.000	0.554	1	-0.018
Anterior orbital gyrus L	0.399	0.399	0.000	0.927	1	-0.003
Anterior orbital gyrus R	0.358	0.358	0.001	0.445	1	0.023
Basal forebrain L	0.284	0.285	0.001	0.292	1	-0.034
Basal forebrain R	0.344	0.348	0.004	0.048	1	-0.061
Calcarine cortex L	0.363	0.364	0.000	0.485	1	0.021
Calcarine cortex R	0.371	0.371	0.000	0.981	1	-0.001
Caudate L	0.195	0.197	0.002	0.195	1	-0.045
Caudate R	0.190	0.194	0.004	0.065	1	-0.064
Central operculum L	0.369	0.369	0.001	0.397	1	0.026
Central operculum R	0.373	0.374	0.000	0.453007	1	0.023
Cuneus L	0.393	0.394	0.002	0.183	1	0.040
Cuneus R	0.412	0.412	0.000	0.618	1	-0.015
Entorhinal area L	0.409	0.409	0.000	0.872	1	-0.005
Entorhinal area R	0.457	0.457	0.000	0.453096	1	-0.021
Frontal operculum L	0.358	0.359	0.000	0.537303	1	0.019
Frontal operculum R	0.323	0.323	0.000	0.810	1	-0.008

Frontal pole L	0.426	0.429	0.002	0.085	1	0.050
Frontal pole R	0.409	0.411	0.001	0.217	1	0.036
Fusiform gyrus L	0.509	0.509	0.001	0.338	1	0.026
Fusiform gyrus R	0.529	0.529	0.000	0.555	1	0.016
Gyrus rectus L	0.431	0.432	0.001	0.387	1	0.025
Gyrus rectus R	0.441	0.441	0.000	0.829	1	0.006
Hippocampus L	0.449	0.452	0.003	0.045	1	-0.057
Hippocampus R	0.476	0.480	0.003	0.033	1	-0.059
Inferior occipital gyrus L	0.410	0.410	0.000	0.448	1	0.022
Inferior occipital gyrus R	0.459	0.460	0.001	0.274	1	0.031
Inferior temporal gyrus L	0.505	0.506	0.001	0.149	1	-0.039
Inferior temporal gyrus R	0.543	0.543	0.000	0.596	1	-0.014
Lateral orbital gyrus L	0.410	0.410	0.000	0.862291	1	0.005
Lateral orbital gyrus R	0.358	0.359	0.000	0.513938	1	-0.020
Lingual gyrus L	0.499	0.501	0.001	0.148	1	0.039
Lingual gyrus R	0.515	0.516	0.001	0.162	1	0.037
Medial frontal cortex L	0.358	0.358	0.000	0.734	1	-0.010
Medial frontal cortex R	0.363	0.364	0.001	0.339	1	0.029
Medial orbital gyrus L	0.472	0.472	0.000	0.759	1	0.009
Medial orbital gyrus R	0.419	0.418	0.000	0.552	1	0.017
Middle cingulate gyrus L	0.380	0.380	0.000	0.663	1	0.013
Middle cingulate gyrus R	0.333	0.333	0.000	0.867830	1	-0.005
Middle frontal gyrus L	0.470	0.471	0.001	0.169	1	0.038
Middle frontal gyrus R	0.465	0.465	0.000	0.790	1	0.007
Middle occipital gyrus L	0.356	0.356	0.000	0.780	1	-0.009
Middle occipital gyrus R	0.347	0.347	0.000	0.676	1	-0.013
Middle temporal gyrus L	0.500	0.500	0.000	0.670	1	-0.012
Middle temporal gyrus R	0.525	0.525	0.000	0.581	1	-0.015
Occipital fusiform gyrus L	0.467	0.469	0.002	0.130	1	0.042
Occipital fusiform gyrus R	0.504	0.505	0.001	0.158	1	0.038

Occipital pole L	0.319	0.319	0.001	0.408575	1	0.026
Occipital pole R	0.361	0.362	0.001	0.361	1	0.028
Opercular part of the inferior frontal gyrus L	0.258	0.258	0.000	0.985	0.993716814159292	0.001
Opercular part of the inferior frontal gyrus R	0.263	0.263	0.000	0.925	1	-0.003
Orbital part of the inferior frontal gyrus L	0.271	0.271	0.000	0.917	1	-0.003
Orbital part of the inferior frontal gyrus R	0.256	0.258	0.002	0.221	1	-0.040
Pallidum L	0.141	0.141	0.000	0.910	1	-0.004
Pallidum R	0.117	0.118	0.001	0.516	1	-0.023
Parahippocampal gyrus L	0.490	0.490	0.000	0.626	1	0.013
Parahippocampal gyrus R	0.516	0.516	0.000	0.513749	1	0.017
Parietal operculum L	0.319	0.319	0.000	0.949	1	-0.002
Parietal operculum R	0.273	0.274	0.000	0.765	1	-0.010
Planum polare L	0.413	0.432	0.000	0.684	1	-0.012
Planum polare R	0.456	0.457	0.000	0.517	1	-0.018
Planum temporale L	0.333	0.333	0.000	0.804	1	-0.008
Planum temporale R	0.350	0.350	0.000	0.849	1	0.006
Postcentral gyrus L	0.378	0.378	0.000	0.954	1	0.002
Postcentral gyrus R	0.380	0.380	0.001	0.417	1	0.025
Postcentral gyrus medial segment L	0.192	0.193	0.001	0.340	1	0.033
Postcentral gyrus medial segment R	0.205	0.206	0.000	0.543	1	-0.021
Posterior cingulate gyrus L	0.533	0.534	0.001	0.216	1	-0.032
Posterior cingulate gyrus R	0.495	0.495	0.000	0.677	1	-0.011
Posterior insula L	0.384	0.385	0.000	0.536668	1	0.019
Posterior insula R	0.412	0.412	0.001	0.353	1	0.027
Posterior orbital gyrus L	0.356	0.357	0.000	0.837	1	0.006
Posterior orbital gyrus R	0.372	0.373	0.001	0.307	1	-0.031
Precentral gyrus L	0.449	0.449	0.000	0.792	1	0.008
Precentral gyrus R	0.431	0.431	0.000	0.929	1	0.003
Precentral gyrus medial segment L	0.284	0.284	0.000	0.890	1	-0.005
Precentral gyrus medial segment R	0.321	0.321	0.000	0.988	0.988	0.000

Precuneus L	0.474	0.474	0.000	0.862088	1	-0.005
Precuneus R	0.478	0.478	0.000	0.964	0.999054545454545	0.001
Putamen L	0.268	0.268	0.001	0.409188	1	-0.027
Putamen R	0.276	0.277	0.002	0.188	1	-0.043
Subcallosal area L	0.471	0.471	0.000	0.561	0.99928125	-0.016
Subcallosal area R	0.445	0.445	0.000	0.984	1	-0.001
Superior frontal gyrus L	0.453	0.456	0.004	0.027	1	-0.063
Superior frontal gyrus R	0.473	0.474	0.000	0.718	1	-0.010
Superior frontal gyrus medial segment L	0.410	0.411	0.001	0.193	1	-0.038
Superior frontal gyrus medial segment R	0.398	0.398	0.000	0.918	1	0.003
Superior occipital gyrus L	0.309	0.310	0.000	0.493054	1	0.022
Superior occipital gyrus R	0.321	0.322	0.000	0.587	1	0.017
Superior parietal lobule L	0.376	0.376	0.000	0.533	1	0.019
Superior parietal lobule R	0.369	0.369	0.000	0.667	1	0.013
Superior temporal gyrus L	0.415	0.415	0.000	0.757	1	-0.009
Superior temporal gyrus R	0.395	0.395	0.000	0.476	1	0.021
Supplementary motor cortex L	0.351	0.353	0.002	0.199	1	-0.040
Supplementary motor cortex R	0.362	0.363	0.001	0.415	1	-0.025
Supramarginal gyrus L	0.346	0.347	0.001	0.222	1	0.038
Supramarginal gyrus R	0.345	0.348	0.003	0.069	1	0.056
Temporal pole L	0.397	0.399	0.001	0.190	1	-0.039
Temporal pole R	0.403	0.404	0.001	0.347	1	-0.028
Thalamus proper L	0.229	0.229	0.000	0.802	1	0.008
Thalamus proper R	0.256	0.256	0.000	0.490	1	-0.023
Transverse temporal gyrus L	0.254	0.254	0.000	0.867980	1	-0.006
Transverse temporal gyrus R	0.321	0.322	0.000	0.694	1	-0.012
Triangular part of the inferior frontal gyrus L	0.303	0.303	0.000	0.956	1	-0.002
Triangular part of the inferior frontal gyrus R	0.286	0.286	0.000	0.784	1	-0.009

FDR: false discovery rate. L: left. PRS: polygenic risk score. R: right.

Table D.5: Associations between PRSwithoutAPOE Threshold 5 and 114 regions of interest in the whole group

Region of Interest	R Square (Model 1)	R Square (Model 2)	R Square Change	Sig. F Change (Model 2)	FDR Corrected value	Standardised beta of PRS
Accumbens area L	0.393	0.393	0.000	0.695	1	-0.012
Accumbens area R	0.391	0.391	0.000	0.578	1	-0.017
Amygdala L	0.417	0.419	0.002	0.154	1	-0.042
Amygdala R	0.464	0.465	0.001	0.230	1	-0.034
Angular gyrus L	0.401	0.401	0.000	0.864	0.98496	0.005
Angular gyrus R	0.417	0.418	0.001	0.359870	1	0.027
Anterior cingulate gyrus L	0.410	0.410	0.000	0.722	1	0.011
Anterior cingulate gyrus R	0.241	0.241	0.000	0.640	1	-0.016
Anterior insula L	0.374	0.374	0.000	0.998125	1	0.000
Anterior insula R	0.385	0.386	0.001	0.371	1	-0.027
Anterior orbital gyrus L	0.399	0.399	0.000	0.732	0.981741176470588	0.010
Anterior orbital gyrus R	0.358	0.359	0.001	0.225	1	0.038
Basal forebrain L	0.284	0.284	0.000	0.487	1	-0.023
Basal forebrain R	0.344	0.345	0.001	0.245	0.9975	-0.036
Calcarine cortex L	0.363	0.363	0.000	0.937	1	-0.002
Calcarine cortex R	0.371	0.317	0.000	0.570	1	-0.017
Caudate L	0.195	0.196	0.001	0.386	1	-0.030
Caudate R	0.190	0.192	0.003	0.128	1	-0.053
Central operculum L	0.369	0.370	0.002	0.183993	1	0.041
Central operculum R	0.373	0.374	0.001	0.300	1	0.032
Cuneus L	0.393	0.394	0.001	0.212	1	0.038
Cuneus R	0.412	0.412	0.000	0.933	1	0.002
Entorhinal area L	0.409	0.409	0.000	0.645	1	-0.014
Entorhinal area R	0.457	0.457	0.000	0.620	1	-0.014
Frontal operculum L	0.358	0.359	0.001	0.430454	1	0.024
Frontal operculum R	0.323	0.323	0.000	0.798	0.988826086956522	0.008

Frontal pole L	0.426	0.431	0.005	0.016	0.608	0.070
Frontal pole R	0.409	0.412	0.002	0.085	1	0.051
Fusiform gyrus L	0.509	0.511	0.002	0.084	1	0.047
Fusiform gyrus R	0.529	0.530	0.001	0.183131	1	0.035
Gyrus rectus L	0.431	0.431	0.001	0.424	1	0.023
Gyrus rectus R	0.441	0.441	0.000	0.941	1	-0.002
Hippocampus L	0.449	0.454	0.005	0.012	0.684	-0.072
Hippocampus R	0.476	0.480	0.004	0.019	0.5415	-0.065
Inferior occipital gyrus L	0.410	0.410	0.000	0.579	1	0.016
Inferior occipital gyrus R	0.459	0.461	0.002	0.129156	1	0.043
Inferior temporal gyrus L	0.505	0.506	0.001	0.326	1	-0.027
Inferior temporal gyrus R	0.543	0.543	0.000	0.845	0.982959183673469	-0.005
Lateral orbital gyrus L	0.410	0.410	0.001	0.430164	1	0.023
Lateral orbital gyrus R	0.358	0.358	0.000	0.904	1	0.004
Lingual gyrus L	0.499	0.500	0.001	0.183980	1	0.036
Lingual gyrus R	0.515	0.516	0.001	0.233	1	0.032
Medial frontal cortex L	0.358	0.358	0.000	0.837	0.9939375	0.006
Medial frontal cortex R	0.363	0.365	0.002	0.129255	1	0.047
Medial orbital gyrus L	0.472	0.473	0.001	0.347	1	0.026
Medial orbital gyrus R	0.433	0.434	0.001	0.323	1	0.029
Middle cingulate gyrus L	0.380	0.380	0.000	0.605	1	0.016
Middle cingulate gyrus R	0.333	0.333	0.000	0.797	0.998439560439561	0.008
Middle frontal gyrus L	0.470	0.471	0.001	0.249	0.978827586206896	0.032
Middle frontal gyrus R	0.465	0.465	0.000	0.960	1	0.001
Middle occipital gyrus L	0.356	0.356	0.000	0.703	1	0.012
Middle occipital gyrus R	0.347	0.347	0.000	0.524	0.9956	0.020
Middle temporal gyrus L	0.500	0.500	0.000	0.538	1	-0.017
Middle temporal gyrus R	0.525	0.525	0.000	0.452	1	0.020
Occipital fusiform gyrus L	0.467	0.470	0.002	0.070	1	0.051
Occipital fusiform gyrus R	0.504	0.507	0.003	0.041	0.9348	0.056

Occipital pole L	0.319	0.319	0.000	0.501	1	0.021
Occipital pole R	0.361	0.362	0.001	0.229	1	0.037
Opercular part of the inferior frontal gyrus L	0.258	0.258	0.000	0.972	1	0.001
Opercular part of the inferior frontal gyrus R	0.263	0.263	0.000	0.655	1	0.015
Orbital part of the inferior frontal gyrus L	0.271	0.271	0.000	0.844	0.991917525773196	0.007
Orbital part of the inferior frontal gyrus R	0.256	0.257	0.000	0.522	1	-0.021
Pallidum L	0.141	0.141	0.000	0.998660	1	0.000
Pallidum R	0.117	0.118	0.000	0.663	1	-0.016
Parahippocampal gyrus L	0.490	0.490	0.000	0.998967	0.998967	0.000
Parahippocampal gyrus R	0.516	0.516	0.000	0.696	1	0.011
Parietal operculum L	0.319	0.320	0.001	0.398	1	0.027
Parietal operculum R	0.273	0.275	0.001	0.263	0.967161290322581	0.037
Planum polare L	0.431	0.432	0.001	0.360391	1	-0.027
Planum polare R	0.456	0.457	0.000	0.560	1	-0.017
Planum temporale L	0.333	0.333	0.000	0.726	0.997156626506024	-0.011
Planum temporale R	0.350	0.350	0.000	0.978	1	-0.001
Postcentral gyrus L	0.378	0.379	0.000	0.481	1	-0.022
Postcentral gyrus R	0.380	0.380	0.000	0.847	0.975333333333333	0.006
Postcentral gyrus medial segment L	0.192	0.192	0.000	0.748	0.99153488372093	0.011
Postcentral gyrus medial segment R	0.205	0.205	0.000	0.903	1	0.004
Posterior cingulate gyrus L	0.533	0.534	0.001	0.238	1	-0.031
Posterior cingulate gyrus R	0.495	0.495	0.001	0.373	1	-0.024
Posterior insula L	0.384	0.385	0.001	0.283	1	0.033
Posterior insula R	0.412	0.141	0.002	0.105	1	0.048
Posterior orbital gyrus L	0.356	0.357	0.001	0.395	1	0.026
Posterior orbital gyrus R	0.372	0.372	0.000	0.460	1	-0.023
Precentral gyrus L	0.449	0.449	0.000	0.881	0.99439603960396	0.004
Precentral gyrus R	0.431	0.431	0.000	0.605997	1	0.015
Precentral gyrus medial segment L	0.284	0.284	0.000	0.761	0.997172413793103	-0.010
Precentral gyrus medial segment R	0.321	0.321	0.000	0.910	0.9975	0.004

Precuneus L	0.474	0.474	0.000	0.810	0.982340425531915	0.007
Precuneus R	0.478	0.478	0.000	0.788	0.998133333333333	0.008
Putamen L	0.268	0.268	0.000	0.606097	1	-0.017
Putamen R	0.276	0.276	0.001	0.454	1	-0.025
Subcallosal area L	0.471	0.471	0.000	0.706	0.99362962962963	0.011
Subcallosal area R	0.445	0.445	0.001	0.359866	1	0.026
Superior frontal gyrus L	0.453	0.453	0.001	0.408	1	-0.024
Superior frontal gyrus R	0.473	0.474	0.000	0.494	1	0.019
Superior frontal gyrus medial segment L	0.410	0.411	0.001	0.208	1	-0.037
Superior frontal gyrus medial segment R	0.398	0.398	0.000	0.831	0.9972	-0.006
Superior occipital gyrus L	0.309	0.311	0.002	0.183988	1	0.043
Superior occipital gyrus R	0.321	0.322	0.001	0.464	0.998037735849057	0.023
Superior parietal lobule L	0.376	0.377	0.001	0.239	1	0.036
Superior parietal lobule R	0.369	0.369	0.000	0.692	1	0.012
Superior temporal gyrus L	0.415	0.415	0.000	0.674	1	-0.012
Superior temporal gyrus R	0.395	0.395	0.000	0.767	0.993613636363636	0.009
Supplementary motor cortex L	0.351	0.352	0.001	0.244	1	-0.036
Supplementary motor cortex R	0.362	0.362	0.000	0.635	1	-0.015
Supramarginal gyrus L	0.346	0.348	0.002	0.101	1	0.051
Supramarginal gyrus R	0.345	0.351	0.006	0.009	1	0.081
Temporal pole L	0.397	0.398	0.001	0.258	0.9804	-0.034
Temporal pole R	0.403	0.403	0.000	0.513	1	-0.020
Thalamus proper L	0.229	0.229	0.000	0.805	0.986774193548387	0.008
Thalamus proper R	0.256	0.257	0.001	0.337	1	-0.032
Transverse temporal gyrus L	0.254	0.254	0.000	0.625	1	-0.016
Transverse temporal gyrus R	0.321	0.322	0.000	0.784	1	-0.009
Triangular part of the inferior frontal gyrus L	0.303	0.303	0.000	0.997536	1	0.000
Triangular part of the inferior frontal gyrus R	0.286	0.286	0.000	0.731	0.992071428571429	0.011

FDR: false discovery rate. L: left. PRS: polygenic risk score. R: right.

Table D.6: Associations between PRSwithoutAPOE Threshold 10 and 114 regions of interest in the whole group

Region of Interest	R Square (Model 1)	R Square (Model 2)	R Square Change	Sig. F Change (Model 2)	FDR Corrected value	Standardised beta of PRS
Accumbens area L	0.393	0.394	0.002	0.159	0.954	-0.044
Accumbens area R	0.391	0.392	0.001	0.308	0.900307692307692	-0.032
Amygdala L	0.417	0.421	0.004	0.027	0.6156	-0.068
Amygdala R	0.464	0.466	0.003	0.068	1	-0.054
Angular gyrus L	0.401	0.402	0.001	0.338	0.896093023255814	0.030
Angular gyrus R	0.417	0.418	0.001	0.190	0.984545454545455	0.040
Anterior cingulate gyrus L	0.410	0.410	0.000	0.865	0.939142857142857	0.005
Anterior cingulate gyrus R	0.241	0.241	0.000	0.759	0.9013125	0.011
Anterior insula L	0.374	0.374	0.000	0.659	0.894357142857143	-0.014
Anterior insula R	0.385	0.386	0.001	0.326	0.906439024390244	-0.031
Anterior orbital gyrus L	0.399	0.399	0.000	0.795	0.915454545454546	0.008
Anterior orbital gyrus R	0.358	0.359	0.001	0.282	0.945529411764706	0.034
Basal forebrain L	0.284	0.285	0.001	0.302	0.906	-0.035
Basal forebrain R	0.344	0.345	0.001	0.343	0.868933333333333	-0.031
Calcarine cortex L	0.363	0.364	0.000	0.504	0.883938461538462	-0.021
Calcarine cortex R	0.371	0.371	0.000	0.693	0.89775	-0.013
Caudate L	0.195	0.196	0.001	0.276	1	-0.039
Caudate R	0.190	0.192	0.002	0.169	0.917428571428571	-0.050
Central operculum L	0.369	0.370	0.001	0.269	1	0.035
Central operculum R	0.373	0.374	0.001	0.355	0.825918367346939	0.029
Cuneus L	0.393	0.393	0.000	0.480	0.897049180327869	0.022
Cuneus R	0.412	0.412	0.000	0.940	0.992222222222222	-0.002
Entorhinal area L	0.409	0.411	0.002	0.153	1	-0.044
Entorhinal area R	0.457	0.458	0.002	0.148068	1	-0.043
Frontal operculum L	0.358	0.359	0.000	0.489	0.899129032258065	0.022
Frontal operculum R	0.323	0.323	0.000	0.758370	0.910044	-0.010

Frontal pole L	0.426	0.432	0.006	0.008	0.228	0.080
Frontal pole R	0.409	0.413	0.004	0.028	0.532	0.068
Fusiform gyrus L	0.509	0.510	0.001	0.167	0.9519	0.039
Fusiform gyrus R	0.529	0.529	0.001	0.357	0.81396	0.025
Gyrus rectus L	0.431	0.431	0.000	0.992604	1	0.000
Gyrus rectus R	0.441	0.441	0.000	0.959	1	-0.002
Hippocampus L	0.449	0.457	0.008	0.001	0.114	-0.095
Hippocampus R	0.476	0.482	0.006	0.006088	0.347016	-0.079
Inferior occipital gyrus L	0.410	0.410	0.000	0.604	0.91808	0.016
Inferior occipital gyrus R	0.459	0.462	0.002	0.082	1	0.051
Inferior temporal gyrus L	0.505	0.506	0.001	0.344	0.852521739130435	-0.027
Inferior temporal gyrus R	0.543	0.543	0.000	0.806	0.900823529411765	-0.007
Lateral orbital gyrus L	0.410	0.411	0.001	0.261	1	0.035
Lateral orbital gyrus R	0.358	0.359	0.000	0.586129	0.902955486486486	-0.017
Lingual gyrus L	0.499	0.499	0.000	0.691	0.905448275862069	0.011
Lingual gyrus R	0.515	0.517	0.002	0.113	1	0.044
Medial frontal cortex L	0.358	0.358	0.000	0.470	0.893	-0.023
Medial frontal cortex R	0.363	0.364	0.001	0.413	0.871888888888889	0.026
Medial orbital gyrus L	0.472	0.473	0.000	0.509	0.879181818181818	0.019
Medial orbital gyrus R	0.433	0.433	0.000	0.585897	0.914962438356164	0.016
Middle cingulate gyrus L	0.380	0.381	0.001	0.342	0.886090909090909	0.030
Middle cingulate gyrus R	0.333	0.334	0.001	0.284	0.899333333333333	0.035
Middle frontal gyrus L	0.470	0.471	0.001	0.277	0.9868125	0.032
Middle frontal gyrus R	0.465	0.465	0.000	0.986	1	0.000
Middle occipital gyrus L	0.356	0.356	0.000	0.658	0.903759036144578	0.014
Middle occipital gyrus R	0.347	0.347	0.000	0.669	0.886813953488372	0.014
Middle temporal gyrus L	0.500	0.500	0.000	0.621	0.874	-0.014
Middle temporal gyrus R	0.525	0.525	0.000	0.437	0.9315	0.021
Occipital fusiform gyrus L	0.467	0.476	0.001	0.278	0.960363636363636	0.032
Occipital fusiform gyrus R	0.504	0.505	0.002	0.108	1	0.045

Occipital pole L	0.319	0.319	0.000	0.993225	0.993225	0.000
Occipital pole R	0.361	0.361	0.000	0.564	0.918514285714286	0.018
Opercular part of the inferior frontal gyrus L	0.258	0.258	0.000	0.808	0.894291262135922	-0.008
Opercular part of the inferior frontal gyrus R	0.263	0.263	0.000	0.668	0.895905882352941	-0.015
Orbital part of the inferior frontal gyrus L	0.271	0.271	0.000	0.769	0.903773195876289	-0.010
Orbital part of the inferior frontal gyrus R	0.256	0.257	0.000	0.632	0.935688311688312	-0.017
Pallidum L	0.141	0.141	0.000	0.643326	0.91673955	0.017
Pallidum R	0.117	0.118	0.000	0.640	0.935384615384615	0.018
Parahippocampal gyrus L	0.490	0.491	0.000	0.418	0.850928571428571	0.023
Parahippocampal gyrus R	0.516	0.516	0.000	0.567	0.910394366197183	-0.016
Parietal operculum L	0.319	0.319	0.000	0.523	0.864086956521739	0.021
Parietal operculum R	0.273	0.274	0.000	0.494	0.8799375	0.023
Planum polare L	0.431	0.433	0.002	0.107	1	-0.049
Planum polare R	0.456	0.457	0.001	0.398	0.856075471698113	-0.025
Planum temporale L	0.333	0.334	0.001	0.255	1	-0.037
Planum temporale R	0.350	0.350	0.000	0.790	0.918979591836735	-0.009
Postcentral gyrus L	0.378	0.379	0.001	0.353	0.838375	-0.029
Postcentral gyrus R	0.380	0.380	0.001	0.391	0.857192307692308	0.027
Postcentral gyrus medial segment L	0.192	0.193	0.002	0.243	1	0.042
Postcentral gyrus medial segment R	0.205	0.207	0.001	0.296	0.912	0.037
Posterior cingulate gyrus L	0.533	0.533	0.000	0.415	0.860181818181818	-0.022
Posterior cingulate gyrus R	0.495	0.495	0.000	0.970	1	-0.001
Posterior insula L	0.384	0.384	0.000	0.977	1	0.001
Posterior insula R	0.412	0.413	0.001	0.236	1	0.036
Posterior orbital gyrus L	0.356	0.357	0.000	0.642	0.926430379746835	0.015
Posterior orbital gyrus R	0.372	0.372	0.000	0.646	0.89809756097561	-0.015
Precentral gyrus L	0.449	0.449	0.000	0.746	0.924391304347826	0.010
Precentral gyrus R	0.431	0.431	0.000	0.819	0.89775	0.007
Precentral gyrus medial segment L	0.284	0.285	0.001	0.466	0.900406779661017	0.025
Precentral gyrus medial segment R	0.321	0.321	0.001	0.458	0.900206896551724	0.024

Precuneus L	0.474	0.475	0.001	0.283	0.921771428571428	0.031
Precuneus R	0.478	0.479	0.001	0.350	0.848936170212766	0.027
Putamen L	0.268	0.268	0.000	0.798	0.900712871287129	-0.009
Putamen R	0.276	0.276	0.000	0.577	0.913583333333333	-0.019
Subcallosal area L	0.471	0.471	0.000	0.643411	0.905541407407407	0.013
Subcallosal area R	0.445	0.446	0.002	0.148347	1	0.043
Superior frontal gyrus L	0.453	0.454	0.001	0.241	1	-0.035
Superior frontal gyrus R	0.473	0.475	0.001	0.234	1	0.035
Superior frontal gyrus medial segment L	0.410	0.411	0.001	0.324	0.9234	-0.030
Superior frontal gyrus medial segment R	0.398	0.398	0.000	0.796	0.90744	-0.008
Superior occipital gyrus L	0.309	0.310	0.000	0.751	0.92058064516129	0.011
Superior occipital gyrus R	0.321	0.321	0.000	0.913	0.981905660377358	0.004
Superior parietal lobule L	0.376	0.378	0.002	0.118	0.960857142857143	0.049
Superior parietal lobule R	0.369	0.369	0.000	0.698	0.884133333333333	0.012
Superior temporal gyrus L	0.415	0.416	0.001	0.368	0.822588235294118	-0.028
Superior temporal gyrus R	0.395	0.395	0.000	0.491	0.88847619047619	0.021
Supplementary motor cortex L	0.351	0.353	0.002	0.156	0.988	-0.046
Supplementary motor cortex R	0.362	0.362	0.000	0.918	0.978056074766355	-0.003
Supramarginal gyrus L	0.346	0.349	0.003	0.070	0.9975	0.059
Supramarginal gyrus R	0.345	0.351	0.007	0.006339	0.240882	0.088
Temporal pole L	0.397	0.399	0.002	0.117	1	-0.049
Temporal pole R	0.403	0.404	0.001	0.265	1	-0.034
Thalamus proper L	0.229	0.229	0.000	0.710	0.889450549450549	-0.013
Thalamus proper R	0.256	0.257	0.001	0.329	0.893	-0.034
Transverse temporal gyrus L	0.254	0.254	0.000	0.522	0.875117647058824	-0.022
Transverse temporal gyrus R	0.321	0.322	0.000	0.697	0.892786516853933	-0.013
Triangular part of the inferior frontal gyrus L	0.303	0.303	0.000	0.511	0.869462686567164	-0.022
Triangular part of the inferior frontal gyrus R	0.286	0.286	0.000	0.758036	0.919320255319149	0.010

FDR: false discovery rate. L: left. PRS: polygenic risk score. R: right.

Table D.7: Associations between APOEonlyPRS Threshold 1 and 114 regions of interest in the whole group

Region of Interest	R Square (Model 1)	R Square (Model 2)	R Square Change	Sig. F Change (Model 2)	FDR Corrected value	Standardised beta of PRS
Accumbens area L	0.393	0.394	0.001	0.360931	0.614121402985075	-0.029
Accumbens area R	0.391	0.391	0.000	0.944	0.996444444444444	0.002
Amygdala L	0.417	0.427	0.009	0.000671395864323	0.0153078257065644	-0.106
Amygdala R	0.464	0.476	0.013	0.000039286313657	0.002239319878449	-0.123
Angular gyrus L	0.401	0.404	0.003	0.071	0.2529375	-0.057
Angular gyrus R	0.417	0.420	0.003	0.054572	0.230415111111111	-0.060
Anterior cingulate gyrus L	0.410	0.410	0.000	0.962	1	-0.001
Anterior cingulate gyrus R	0.241	0.241	0.001	0.376	0.603718309859155	-0.032
Anterior insula L	0.374	0.374	0.000	0.580	0.777882352941176	0.018
Anterior insula R	0.385	0.385	0.000	0.729	0.8656875	0.011
Anterior orbital gyrus L	0.399	0.401	0.002	0.110924	0.351259333333333	-0.051
Anterior orbital gyrus R	0.358	0.361	0.003	0.056462	0.221954068965517	-0.062
Basal forebrain L	0.284	0.284	0.001	0.414939	0.639230351351351	-0.028
Basal forebrain R	0.344	0.344	0.000	0.690	0.874	-0.013
Calcarine cortex L	0.363	0.364	0.001	0.333	0.612290322580645	-0.032
Calcarine cortex R	0.371	0.374	0.003	0.057	0.2166	-0.062
Caudate L	0.195	0.195	0.000	0.574	0.779	-0.021
Caudate R	0.190	0.190	0.000	0.608	0.796689655172414	-0.019
Central operculum L	0.369	0.370	0.001	0.213	0.48564	0.040
Central operculum R	0.373	0.373	0.000	0.837	0.917480769230769	-0.007
Cuneus L	0.393	0.396	0.003	0.053	0.232384615384615	-0.062
Cuneus R	0.412	0.416	0.004	0.024	0.160941176470588	-0.071
Entorhinal area L	0.409	0.414	0.004	0.020	0.162857142857143	-0.073
Entorhinal area R	0.457	0.461	0.004	0.018	0.157846153846154	-0.071
Frontal operculum L	0.358	0.360	0.001	0.227	0.497653846153846	0.040
Frontal operculum R	0.323	0.323	0.000	0.760	0.875151515151515	0.010

Frontal pole L	0.426	0.426	0.000	0.883	0.940766355140187	0.005
Frontal pole R	0.409	0.411	0.002	0.174	0.431217391304348	0.403
Fusiform gyrus L	0.509	0.513	0.004	0.014624	0.151557818181818	-0.070
Fusiform gyrus R	0.529	0.534	0.005	0.006	0.0977142857142857	-0.078
Gyrus rectus L	0.431	0.431	0.000	0.838	0.909828571428571	-0.006
Gyrus rectus R	0.441	0.441	0.001	0.359603	0.630688338461538	0.028
Hippocampus L	0.449	0.459	0.010	0.000306910422842	0.011662596067996	-0.109
Hippocampus R	0.476	0.493	0.016	0.000002184363998	0.000249017495772	-0.139
Inferior occipital gyrus L	0.410	0.413	0.003	0.044	0.20064	-0.063
Inferior occipital gyrus R	0.459	0.465	0.005	0.009	0.12825	-0.078
Inferior temporal gyrus L	0.505	0.508	0.003	0.041	0.19475	-0.059
Inferior temporal gyrus R	0.543	0.547	0.004	0.015049	0.1429655	-0.067
Lateral orbital gyrus L	0.410	0.410	0.000	0.724	0.878042553191489	-0.011
Lateral orbital gyrus R	0.358	0.358	0.000	0.854	0.918452830188679	-0.006
Lingual gyrus L	0.499	0.500	0.001	0.324	0.605508196721312	-0.029
Lingual gyrus R	0.515	0.518	0.003	0.036	0.186545454545455	-0.060
Medial frontal cortex L	0.358	0.359	0.001	0.209	0.486244897959184	-0.041
Medial frontal cortex R	0.363	0.363	0.000	0.773	0.88122	-0.009
Medial orbital gyrus L	0.472	0.473	0.001	0.372	0.605828571428571	-0.027
Medial orbital gyrus R	0.433	0.433	0.000	0.972952	0.990326142857143	0.001
Middle cingulate gyrus L	0.380	0.380	0.001	0.415040	0.6308608	-0.026
Middle cingulate gyrus R	0.333	0.334	0.001	0.230	0.494716981132075	-0.040
Middle frontal gyrus L	0.470	0.470	0.000	0.506	0.694987951807229	-0.020
Middle frontal gyrus R	0.465	0.465	0.000	0.441	0.652909090909091	-0.023
Middle occipital gyrus L	0.356	0.358	0.002	0.126	0.368307692307692	-0.050
Middle occipital gyrus R	0.347	0.358	0.011	0.000646419112708	0.018422944712178	-0.112
Middle temporal gyrus L	0.500	0.502	0.002	0.087	0.1672	-0.050
Middle temporal gyrus R	0.525	0.528	0.004	0.022	0.291705882352941	-0.065
Occipital fusiform gyrus L	0.467	0.468	0.000	0.486	0.684	-0.021
Occipital fusiform gyrus R	0.504	0.508	0.004	0.013846	0.1578444	-0.071

Occipital pole L	0.319	0.319	0.001	0.403	0.629342465753425	-0.028
Occipital pole R	0.361	0.362	0.001	0.236	0.498222222222222	-0.039
Opercular part of the inferior frontal gyrus L	0.258	0.261	0.003	0.073	0.252181818181818	0.063
Opercular part of the inferior frontal gyrus R	0.263	0.264	0.001	0.361206	0.605551235294118	0.032
Orbital part of the inferior frontal gyrus L	0.271	0.271	0.000	0.835	0.924174757281553	0.007
Orbital part of the inferior frontal gyrus R	0.256	0.257	0.001	0.445	0.650384615384615	-0.027
Pallidum L	0.141	0.143	0.003	0.149	0.395023255813953	-0.055
Pallidum R	0.117	0.120	0.003	0.135	0.366428571428571	-0.057
Parahippocampal gyrus L	0.490	0.494	0.004	0.027	0.171	-0.065
Parahippocampal gyrus R	0.516	0.521	0.006	0.004	0.076	-0.081
Parietal operculum L	0.319	0.319	0.000	0.597	0.791372093023256	0.018
Parietal operculum R	0.273	0.274	0.000	0.737	0.857326530612245	0.012
Planum polare L	0.431	0.432	0.000	0.623	0.807068181818182	-0.015
Planum polare R	0.456	0.457	0.001	0.261	0.522	-0.034
Planum temporale L	0.333	0.333	0.000	0.993	0.993	0.000
Planum temporale R	0.350	0.350	0.000	0.964	0.999054545454545	0.001
Postcentral gyrus L	0.378	0.379	0.000	0.478	0.68115	-0.023
Postcentral gyrus R	0.380	0.382	0.003	0.068	0.250064516129032	-0.059
Postcentral gyrus medial segment L	0.192	0.199	0.007	0.013565	0.171823333333333	-0.091
Postcentral gyrus medial segment R	0.205	0.208	0.003	0.124	0.372	-0.056
Posterior cingulate gyrus L	0.533	0.534	0.001	0.173	0.438266666666667	-0.038
Posterior cingulate gyrus R	0.495	0.498	0.003	0.032977	0.197862	-0.062
Posterior insula L	0.384	0.384	0.000	0.692	0.866901098901099	0.013
Posterior insula R	0.412	0.412	0.000	0.972557	0.998842324324324	-0.001
Posterior orbital gyrus L	0.356	0.357	0.000	0.505	0.702073170731707	-0.022
Posterior orbital gyrus R	0.372	0.373	0.001	0.201	0.477375	-0.041
Precentral gyrus L	0.449	0.449	0.000	0.990	0.998761061946903	0.000
Precentral gyrus R	0.431	0.431	0.000	0.735	0.863814432989691	-0.010
Precentral gyrus medial segment L	0.284	0.287	0.003	0.100	0.325714285714286	-0.057
Precentral gyrus medial segment R	0.321	0.325	0.004	0.039	0.193304347826087	-0.070

Precuneus L	0.474	0.477	0.003	0.055984	0.227934857142857	-0.057
Precuneus R	0.478	0.481	0.003	0.033635	0.1917195	-0.063
Putamen L	0.268	0.269	0.001	0.270	0.530689655172414	-0.039
Putamen R	0.276	0.277	0.002	0.199	0.48268085106383	-0.045
Subcallosal area L	0.471	0.471	0.000	0.471	0.679670886075949	0.021
Subcallosal area R	0.445	0.447	0.002	0.111102	0.34231427027027	0.049
Superior frontal gyrus L	0.453	0.453	0.000	0.421	0.6315	-0.024
Superior frontal gyrus R	0.473	0.474	0.000	0.709	0.87854347826087	0.011
Superior frontal gyrus medial segment L	0.410	0.411	0.001	0.378	0.5985	-0.028
Superior frontal gyrus medial segment R	0.398	0.398	0.001	0.359804	0.621479636363636	0.029
Superior occipital gyrus L	0.309	0.311	0.001	0.214	0.478352941176471	-0.042
Superior occipital gyrus R	0.321	0.323	0.001	0.237	0.491236363636364	-0.040
Superior parietal lobule L	0.376	0.378	0.002	0.130	0.361463414634146	-0.049
Superior parietal lobule R	0.369	0.373	0.004	0.033970	0.184408571428571	-0.069
Superior temporal gyrus L	0.415	0.415	0.000	0.680	0.871011235955056	-0.013
Superior temporal gyrus R	0.395	0.396	0.001	0.278	0.537152542372881	-0.035
Supplementary motor cortex L	0.351	0.353	0.002	0.164	0.424909090909091	-0.046
Supplementary motor cortex R	0.362	0.362	0.000	0.725	0.87	-0.011
Supramarginal gyrus L	0.346	0.346	0.001	0.364	0.601391304347826	-0.030
Supramarginal gyrus R	0.345	0.345	0.000	0.792	0.893940594059406	0.009
Temporal pole L	0.397	0.398	0.001	0.257	0.523178571428571	-0.036
Temporal pole R	0.403	0.407	0.004	0.023	0.163875	-0.072
Thalamus proper L	0.229	0.230	0.001	0.340	0.605625	-0.034
Thalamus proper R	0.256	0.258	0.002	0.127	0.36195	-0.054
Transverse temporal gyrus L	0.254	0.255	0.001	0.314	0.5966	0.036
Transverse temporal gyrus R	0.321	0.322	0.000	0.815	0.910882352941176	-0.008
Triangular part of the inferior frontal gyrus L	0.303	0.304	0.001	0.336	0.608	0.033
Triangular part of the inferior frontal gyrus R	0.286	0.286	0.000	0.722	0.885032258064516	-0.012

FDR: false discovery rate. L: left. PRS: polygenic risk score. R: right.

Table D.8: Associations between APOEonlyPRS Threshold 5 and 114 regions of interest in the whole group

Region of Interest	R Square (Model 1)	R Square (Model 2)	R Square Change	Sig. F Change (Model 2)	FDR Corrected value	Standardised beta of PRS
Accumbens area L	0.393	0.393	0.001	0.405	0.659571428571429	-0.027
Accumbens area R	0.391	0.391	0.000	0.916	0.958018348623853	0.003
Amygdala L	0.417	0.426	0.009	0.0008684751472	0.01980123335616	-0.104
Amygdala R	0.464	0.476	0.012	0.000043538663966	0.002481703846062	-0.122
Angular gyrus L	0.401	0.404	0.003	0.065	0.239032258064516	-0.058
Angular gyrus R	0.417	0.420	0.003	0.044	0.218086956521739	-0.063
Anterior cingulate gyrus L	0.410	0.410	0.000	0.953	0.970017857142857	0.002
Anterior cingulate gyrus R	0.241	0.241	0.001	0.473	0.691307692307692	-0.026
Anterior insula L	0.374	0.374	0.000	0.608	0.815435294117647	0.017
Anterior insula R	0.385	0.385	0.000	0.691	0.875266666666667	0.013
Anterior orbital gyrus L	0.399	0.401	0.002	0.134	0.3819	-0.048
Anterior orbital gyrus R	0.358	0.361	0.003	0.054	0.236769230769231	-0.063
Basal forebrain L	0.284	0.284	0.001	0.416	0.658666666666667	-0.028
Basal forebrain R	0.344	0.344	0.000	0.728	0.8736	-0.012
Calcarine cortex L	0.363	0.364	0.001	0.333	0.59315625	-0.032
Calcarine cortex R	0.371	0.374	0.003	0.062	0.2356	-0.061
Caudate L	0.195	0.195	0.000	0.600	0.814285714285714	-0.019
Caudate R	0.190	0.190	0.000	0.628	0.822896551724138	-0.018
Central operculum L	0.369	0.370	0.001	0.203	0.492382978723404	0.041
Central operculum R	0.373	0.373	0.000	0.879	0.945339622641509	-0.005
Cuneus L	0.393	0.396	0.003	0.060	0.235862068965517	-0.060
Cuneus R	0.412	0.415	0.004	0.031	0.196333333333333	-0.068
Entorhinal area L	0.409	0.413	0.004	0.024	0.1824	-0.071
Entorhinal area R	0.457	0.461	0.004	0.023	0.187285714285714	-0.069
Frontal operculum L	0.358	0.360	0.001	0.229	0.532775510204082	0.039
Frontal operculum R	0.323	0.323	0.000	0.740	0.869690721649485	0.011

Frontal pole L	0.426	0.426	0.000	0.889	0.947158878504673	0.004
Frontal pole R	0.409	0.411	0.001	0.216	0.513	0.039
Fusiform gyrus L	0.509	0.513	0.004	0.017575	0.1669625	-0.068
Fusiform gyrus R	0.529	0.534	0.005	0.007	0.114	-0.076
Gyrus rectus L	0.431	0.431	0.000	0.951	0.976702702702703	-0.002
Gyrus rectus R	0.441	0.441	0.001	0.359	0.601852941176471	0.028
Hippocampus L	0.449	0.458	0.010	0.00036739546958	0.01396102784404	-0.108
Hippocampus R	0.476	0.492	0.016	0.00000288083936	0.00032841568704	-0.138
Inferior occipital gyrus L	0.410	0.413	0.003	0.048	0.21888	-0.062
Inferior occipital gyrus R	0.459	0.464	0.005	0.011	0.15675	-0.077
Inferior temporal gyrus L	0.505	0.508	0.003	0.037	0.200857142857143	-0.060
Inferior temporal gyrus R	0.543	0.547	0.004	0.016810	0.191634	-0.066
Lateral orbital gyrus L	0.410	0.410	0.000	0.803	0.906356435643564	-0.008
Lateral orbital gyrus R	0.358	0.358	0.000	0.853	0.944097087378641	-0.006
Lingual gyrus L	0.499	0.500	0.001	0.344	0.594181818181818	-0.027
Lingual gyrus R	0.515	0.518	0.003	0.047	0.22325	-0.057
Medial frontal cortex L	0.358	0.359	0.001	0.260	0.581176470588235	-0.037
Medial frontal cortex R	0.363	0.363	0.000	0.841	0.939941176470588	-0.007
Medial orbital gyrus L	0.472	0.473	0.001	0.393	0.649304347826087	-0.025
Medial orbital gyrus R	0.433	0.433	0.000	0.969	0.977575221238938	0.001
Middle cingulate gyrus L	0.380	0.380	0.000	0.455219	0.673960597402597	-0.024
Middle cingulate gyrus R	0.333	0.334	0.001	0.290	0.612222222222222	-0.035
Middle frontal gyrus L	0.470	0.470	0.000	0.523	0.736074074074074	-0.019
Middle frontal gyrus R	0.465	0.465	0.000	0.520	0.741	-0.019
Middle occipital gyrus L	0.356	0.358	0.002	0.123	0.369	-0.051
Middle occipital gyrus R	0.347	0.358	0.011	0.000648393373141	0.0184792111345185	-0.112
Middle temporal gyrus L	0.500	0.502	0.002	0.084	0.160371692307692	-0.050
Middle temporal gyrus R	0.525	0.528	0.004	0.018288	0.281647058823529	-0.067
Occipital fusiform gyrus L	0.467	0.468	0.000	0.553	0.768804878048781	-0.018
Occipital fusiform gyrus R	0.504	0.508	0.004	0.017195	0.178202727272727	-0.069

Occipital pole L	0.319	0.319	0.001	0.454614	0.681921	-0.025
Occipital pole R	0.361	0.362	0.001	0.312756	0.60430820338983	-0.033
Opercular part of the inferior frontal gyrus L	0.258	0.261	0.004	0.066	0.235125	0.065
Opercular part of the inferior frontal gyrus R	0.263	0.264	0.001	0.301	0.602	0.036
Orbital part of the inferior frontal gyrus L	0.271	0.271	0.000	0.788	0.90739393939394	0.009
Orbital part of the inferior frontal gyrus R	0.256	0.257	0.001	0.445	0.685540540540541	0.445
Pallidum L	0.141	0.143	0.002	0.180	0.466363636363636	-0.051
Pallidum R	0.117	0.120	0.003	0.154	0.418	-0.055
Parahippocampal gyrus L	0.490	0.494	0.003	0.028	0.187764705882353	-0.064
Parahippocampal gyrus R	0.516	0.521	0.005	0.004	0.076	-0.081
Parietal operculum L	0.319	0.319	0.000	0.616	0.816558139534884	0.017
Parietal operculum R	0.273	0.274	0.000	0.703	0.880681318681319	0.013
Planum polare L	0.431	0.432	0.000	0.635	0.813370786516854	-0.015
Planum polare R	0.456	0.457	0.001	0.294	0.5985	-0.032
Planum temporale L	0.333	0.333	0.000	0.999	0.999	0.000
Planum temporale R	0.350	0.350	0.000	0.904	0.954222222222222	0.004
Postcentral gyrus L	0.378	0.379	0.000	0.502	0.724405063291139	-0.022
Postcentral gyrus R	0.380	0.382	0.003	0.067	0.231454545454545	-0.059
Postcentral gyrus medial segment L	0.192	0.199	0.007	0.012	0.152	-0.092
Postcentral gyrus medial segment R	0.205	0.207	0.002	0.174	0.461302325581395	-0.050
Posterior cingulate gyrus L	0.533	0.534	0.001	0.200070	0.495825652173913	-0.036
Posterior cingulate gyrus R	0.495	0.498	0.003	0.032	0.192	-0.062
Posterior insula L	0.384	0.384	0.000	0.632	0.818727272727273	0.015
Posterior insula R	0.412	0.412	0.000	0.949	0.983509090909091	0.002
Posterior orbital gyrus L	0.356	0.357	0.000	0.576	0.791132530120482	-0.018
Posterior orbital gyrus R	0.372	0.373	0.001	0.246	0.56088	-0.038
Precentral gyrus L	0.449	0.449	0.000	0.873	0.947828571428571	0.005
Precentral gyrus R	0.431	0.431	0.000	0.733	0.8704375	-0.011
Precentral gyrus medial segment L	0.284	0.287	0.002	0.121	0.372810810810811	-0.054
Precentral gyrus medial segment R	0.321	0.324	0.003	0.058	0.244888888888889	-0.064

Precuneus L	0.474	0.477	0.003	0.059	0.240214285714286	-0.056
Precuneus R	0.478	0.481	0.003	0.033	0.1881	-0.063
Putamen L	0.268	0.269	0.001	0.289	0.621622641509434	-0.037
Putamen R	0.276	0.277	0.002	0.129	0.377076923076923	-0.045
Subcallosal area L	0.471	0.472	0.000	0.414	0.664732394366197	0.024
Subcallosal area R	0.445	0.447	0.002	0.089	0.289885714285714	0.052
Superior frontal gyrus L	0.453	0.453	0.000	0.443	0.691808219178082	-0.023
Superior frontal gyrus R	0.473	0.474	0.000	0.722	0.875617021276596	0.011
Superior frontal gyrus medial segment L	0.410	0.410	0.000	0.446	0.67792	-0.024
Superior frontal gyrus medial segment R	0.398	0.398	0.001	0.335	0.587538461538462	0.031
Superior occipital gyrus L	0.309	0.311	0.001	0.284	0.622615384615385	-0.036
Superior occipital gyrus R	0.321	0.322	0.001	0.350	0.595522388059701	-0.032
Superior parietal lobule L	0.376	0.378	0.002	0.151	0.419853658536585	-0.046
Superior parietal lobule R	0.369	0.373	0.004	0.038	0.196909090909091	-0.067
Superior temporal gyrus L	0.415	0.415	0.000	0.715	0.876451612903226	-0.011
Superior temporal gyrus R	0.395	0.396	0.001	0.313246	0.5951674	-0.032
Supplementary motor cortex L	0.351	0.353	0.001	0.199735	0.505995333333333	-0.042
Supplementary motor cortex R	0.362	0.362	0.000	0.768	0.893387755102041	-0.010
Supramarginal gyrus L	0.346	0.347	0.001	0.310	0.609310344827586	-0.034
Supramarginal gyrus R	0.345	0.345	0.000	0.795	0.9063	0.009
Temporal pole L	0.397	0.398	0.001	0.293	0.607309090909091	-0.033
Temporal pole R	0.403	0.407	0.004	0.027	0.192375	-0.070
Thalamus proper L	0.229	0.230	0.001	0.321	0.599901639344262	-0.036
Thalamus proper R	0.256	0.258	0.003	0.115	0.364166666666667	-0.056
Transverse temporal gyrus L	0.254	0.255	0.001	0.327	0.591714285714286	0.035
Transverse temporal gyrus R	0.321	0.321	0.000	0.872	0.955846153846154	-0.005
Triangular part of the inferior frontal gyrus L	0.303	0.304	0.001	0.323	0.593903225806452	0.034
Triangular part of the inferior frontal gyrus R	0.286	0.286	0.000	0.711	0.881021739130435	-0.013

FDR: false discovery rate. L: left. PRS: polygenic risk score. R: right.

Table D.9: Associations between APOEonlyPRS Threshold 10 and 114 regions of interest in the whole group

Region of Interest	R Square (Model 1)	R Square (Model 2)	R Square Change	Sig. F Change (Model 2)	FDR Corrected value	Standardised beta of PRS
Accumbens area L	0.393	0.393	0.000	0.540	0.81	-0.020
Accumbens area R	0.391	0.391	0.000	0.820	0.916470588235294	0.007
Amygdala L	0.417	0.426	0.008	0.001305	0.029754	-0.100
Amygdala R	0.464	0.475	0.012	0.000075368057048	0.004295979251736	-0.118
Angular gyrus L	0.401	0.404	0.003	0.069	0.2622	-0.057
Angular gyrus R	0.417	0.420	0.003	0.050	0.228	-0.061
Anterior cingulate gyrus L	0.410	0.410	0.000	0.912	0.953834862385321	0.003
Anterior cingulate gyrus R	0.241	0.241	0.000	0.566658	0.828192461538461	-0.020
Anterior insula L	0.374	0.374	0.000	0.583	0.830775	0.018
Anterior insula R	0.385	0.386	0.000	0.527	0.80104	0.020
Anterior orbital gyrus L	0.399	0.401	0.002	0.137	0.411	-0.047
Anterior orbital gyrus R	0.358	0.361	0.003	0.067	0.263379310344828	-0.060
Basal forebrain L	0.284	0.285	0.001	0.345	0.595909090909091	-0.033
Basal forebrain R	0.344	0.344	0.000	0.727	0.8633125	-0.012
Calcarine cortex L	0.363	0.365	0.001	0.210813	0.48065364	-0.041
Calcarine cortex R	0.371	0.374	0.003	0.053436	0.217560857142857	-0.063
Caudate L	0.195	0.195	0.000	0.564	0.835012987012987	-0.021
Caudate R	0.190	0.190	0.000	0.604	0.819714285714286	-0.019
Central operculum L	0.369	0.371	0.002	0.146	0.4161	0.047
Central operculum R	0.373	0.373	0.000	0.959	0.984918918918919	-0.002
Cuneus L	0.393	0.396	0.003	0.052865	0.223207777777778	-0.062
Cuneus R	0.412	0.415	0.004	0.030	0.19	-0.068
Entorhinal area L	0.409	0.413	0.004	0.023	0.201692307692308	-0.071
Entorhinal area R	0.457	0.461	0.004	0.025	0.203571428571429	-0.067
Frontal operculum L	0.358	0.360	0.002	0.160	0.424186046511628	0.046
Frontal operculum R	0.323	0.324	0.000	0.598	0.821349397590361	0.018

Frontal pole L	0.426	0.426	0.000	0.652	0.844636363636364	0.014
Frontal pole R	0.409	0.411	0.001	0.204	0.494808510638298	0.040
Fusiform gyrus L	0.509	0.513	0.004	0.016233	0.1850562	-0.069
Fusiform gyrus R	0.529	0.533	0.005	0.009	0.12825	-0.073
Gyrus rectus L	0.431	0.431	0.000	0.816	0.921029702970297	0.007
Gyrus rectus R	0.441	0.441	0.001	0.285	0.560172413793103	0.033
Hippocampus L	0.449	0.458	0.009	0.000555397363074	0.021105099796812	-0.104
Hippocampus R	0.476	0.492	0.015	0.000004491200091	0.000511996810374	-0.135
Inferior occipital gyrus L	0.410	0.413	0.004	0.039	0.211714285714286	-0.065
Inferior occipital gyrus R	0.459	0.465	0.005	0.007	0.114	-0.080
Inferior temporal gyrus L	0.505	0.508	0.003	0.032	0.1824	-0.062
Inferior temporal gyrus R	0.543	0.546	0.003	0.022	0.209	-0.063
Lateral orbital gyrus L	0.410	0.410	0.000	0.963838	0.981049392857143	0.001
Lateral orbital gyrus R	0.358	0.358	0.000	0.873	0.947828571428571	-0.005
Lingual gyrus L	0.499	0.500	0.001	0.190	0.481333333333333	-0.038
Lingual gyrus R	0.515	0.518	0.003	0.045	0.233181818181818	-0.057
Medial frontal cortex L	0.358	0.358	0.001	0.374	0.617913043478261	-0.029
Medial frontal cortex R	0.363	0.363	0.000	0.994	0.994	0.000
Medial orbital gyrus L	0.472	0.473	0.000	0.567359	0.818720582278481	-0.017
Medial orbital gyrus R	0.433	0.433	0.000	0.893	0.951420560747663	0.004
Middle cingulate gyrus L	0.380	0.380	0.000	0.636	0.833379310344828	-0.015
Middle cingulate gyrus R	0.333	0.333	0.001	0.389	0.633514285714286	-0.029
Middle frontal gyrus L	0.470	0.470	0.000	0.701	0.8412	-0.011
Middle frontal gyrus R	0.465	0.465	0.000	0.850	0.940776699029126	-0.006
Middle occipital gyrus L	0.356	0.358	0.002	0.147	0.408731707317073	-0.048
Middle occipital gyrus R	0.347	0.357	0.009	0.001260	0.03591	-0.106
Middle temporal gyrus L	0.500	0.502	0.002	0.111	0.204915	-0.046
Middle temporal gyrus R	0.525	0.528	0.003	0.028760	0.3515	-0.062
Occipital fusiform gyrus L	0.467	0.468	0.000	0.693	0.868153846153846	-0.012
Occipital fusiform gyrus R	0.504	0.507	0.003	0.029373	0.196971882352941	-0.063

Occipital pole L	0.319	0.320	0.001	0.314	0.586819672131148	-0.034
Occipital pole R	0.361	0.362	0.001	0.307	0.5833	-0.033
Opercular part of the inferior frontal gyrus L	0.258	0.262	0.004	0.047	0.23295652173913	0.070
Opercular part of the inferior frontal gyrus R	0.263	0.265	0.001	0.236	0.517384615384615	0.042
Orbital part of the inferior frontal gyrus L	0.271	0.271	0.001	0.454	0.708986301369863	0.026
Orbital part of the inferior frontal gyrus R	0.256	0.256	0.000	0.664	0.850516853932584	-0.015
Pallidum L	0.141	0.143	0.002	0.156	0.423428571428571	-0.054
Pallidum R	0.117	0.120	0.003	0.141	0.412153846153846	-0.056
Parahippocampal gyrus L	0.490	0.494	0.004	0.019	0.196909090909091	-0.068
Parahippocampal gyrus R	0.516	0.521	0.005	0.005	0.095	-0.079
Parietal operculum L	0.319	0.320	0.001	0.434	0.687166666666667	0.026
Parietal operculum R	0.273	0.274	0.000	0.594	0.82580487804878	0.019
Planum polare L	0.431	0.432	0.000	0.699	0.847723404255319	-0.012
Planum polare R	0.456	0.457	0.001	0.259952	0.548787555555556	-0.034
Planum temporale L	0.333	0.333	0.000	0.682	0.863866666666667	0.014
Planum temporale R	0.350	0.350	0.000	0.766	0.882060606060606	0.010
Postcentral gyrus L	0.378	0.379	0.000	0.588	0.827555555555555	-0.017
Postcentral gyrus R	0.380	0.382	0.003	0.078	0.277875	-0.057
Postcentral gyrus medial segment L	0.192	0.198	0.007	0.016203	0.205238	-0.088
Postcentral gyrus medial segment R	0.205	0.205	0.001	0.331	0.58959375	-0.035
Posterior cingulate gyrus L	0.533	0.533	0.001	0.318	0.584709677419355	-0.028
Posterior cingulate gyrus R	0.495	0.498	0.003	0.028472	0.2163872	-0.064
Posterior insula L	0.384	0.384	0.000	0.619	0.82053488372093	0.016
Posterior insula R	0.412	0.412	0.000	0.897	0.946833333333333	0.004
Posterior orbital gyrus L	0.356	0.357	0.000	0.741	0.870865979381443	-0.011
Posterior orbital gyrus R	0.372	0.373	0.001	0.210550	0.489851020408163	-0.041
Precentral gyrus L	0.449	0.449	0.000	0.697	0.854387096774194	0.012
Precentral gyrus R	0.431	0.431	0.000	0.924	0.9576	0.003
Precentral gyrus medial segment L	0.284	0.287	0.002	0.135	0.415945945945946	-0.052
Precentral gyrus medial segment R	0.321	0.324	0.003	0.089	0.298411764705882	-0.057

Precuneus L	0.474	0.476	0.002	0.103	0.335485714285714	-0.048
Precuneus R	0.478	0.481	0.003	0.049	0.23275	-0.058
Putamen L	0.268	0.269	0.001	0.269	0.547607142857143	-0.039
Putamen R	0.276	0.277	0.002	0.209	0.496375	-0.044
Subcallosal area L	0.471	0.472	0.001	0.260274	0.539477018181818	0.033
Subcallosal area R	0.445	0.448	0.003	0.051	0.223615384615385	0.060
Superior frontal gyrus L	0.453	0.453	0.000	0.605	0.811411764705882	-0.016
Superior frontal gyrus R	0.473	0.474	0.001	0.407	0.653492957746479	0.025
Superior frontal gyrus medial segment L	0.410	0.410	0.000	0.694	0.85995652173913	-0.012
Superior frontal gyrus medial segment R	0.398	0.399	0.001	0.271	0.542	0.035
Superior occipital gyrus L	0.309	0.310	0.001	0.354	0.602328358208955	-0.031
Superior occipital gyrus R	0.321	0.322	0.000	0.495	0.762567567567568	-0.023
Superior parietal lobule L	0.376	0.377	0.002	0.183	0.474136363636364	-0.043
Superior parietal lobule R	0.369	0.372	0.003	0.072	0.264774193548387	-0.058
Superior temporal gyrus L	0.415	0.415	0.000	0.881	0.947490566037736	-0.005
Superior temporal gyrus R	0.395	0.396	0.001	0.288	0.556474576271186	-0.034
Supplementary motor cortex L	0.351	0.352	0.001	0.254	0.546339622641509	-0.038
Supplementary motor cortex R	0.362	0.362	0.000	0.786	0.89604	-0.009
Supramarginal gyrus L	0.346	0.346	0.001	0.372	0.623647058823529	-0.030
Supramarginal gyrus R	0.345	0.345	0.000	0.753	0.875938775510204	0.010
Temporal pole L	0.397	0.398	0.001	0.334	0.585784615384615	-0.031
Temporal pole R	0.403	0.407	0.004	0.031	0.186	-0.068
Thalamus proper L	0.229	0.230	0.001	0.322	0.582666666666667	-0.036
Thalamus proper R	0.256	0.259	0.003	0.085	0.293636363636364	-0.061
Transverse temporal gyrus L	0.254	0.256	0.002	0.221	0.494	0.043
Transverse temporal gyrus R	0.321	0.321	0.000	0.964138	0.972670194690265	-0.002
Triangular part of the inferior frontal gyrus L	0.303	0.304	0.002	0.203	0.503086956521739	0.043
Triangular part of the inferior frontal gyrus R	0.286	0.286	0.000	0.857	0.939403846153846	-0.006

FDR: false discovery rate. L: left. PRS: polygenic risk score. R: right.

Table D.10: Associations between PRSwithAPOE Threshold 1 and 114 regions of interest in APOE ε4 non-carriers

Region of Interest	R Square (Model 1)	R Square (Model 2)	R Square Change	Sig. F Change (Model 2)	FDR Corrected value	Standardised beta of PRS
Accumbens area L	0.350	0.354	0.005	0.092	0.806769230769231	-0.069
Accumbens area R	0.363	0.366	0.003	0.164	0.692444444444445	-0.056
Amygdala L	0.349	0.354	0.004	0.108	0.7695	-0.066
Amygdala R	0.400	0.405	0.005	0.073143	1	-0.070
Angular gyrus L	0.369	0.369	0.000	0.570	1	-0.023
Angular gyrus R	0.378	0.378	0.000	0.861	1	0.007
Anterior cingulate gyrus L	0.397	0.397	0.000	0.963	0.989027027027027	0.002
Anterior cingulate gyrus R	0.205	0.210	0.005	0.105	0.798	-0.073
Anterior insula L	0.330	0.332	0.002	0.256	0.858352941176471	-0.047
Anterior insula R	0.363	0.367	0.003	0.146	0.6935	-0.059
Anterior orbital gyrus L	0.399	0.403	0.004	0.115	0.6555	-0.062
Anterior orbital gyrus R	0.346	0.346	0.000	0.944	1	-0.003
Basal forebrain L	0.261	0.268	0.007	0.047	0.893	-0.086
Basal forebrain R	0.328	0.336	0.009	0.022	0.627	-0.095
Calcarine cortex L	0.354	0.355	0.001	0.526	1	0.026
Calcarine cortex R	0.360	0.362	0.002	0.225	0.8015625	0.049
Caudate L	0.184	0.185	0.001	0.616082	1	-0.023
Caudate R	0.180	0.181	0.000	0.682	1	-0.019
Central operculum L	0.352	0.352	0.000	0.955	1	0.002
Central operculum R	0.360	0.361	0.001	0.547	1	0.024
Cuneus L	0.379	0.379	0.000	0.615	1	0.020
Cuneus R	0.422	0.424	0.002	0.287	0.88427027027027	-0.041
Entorhinal area L	0.351	0.351	0.000	0.843	1	-0.008
Entorhinal area R	0.395	0.395	0.001	0.532	1	-0.025
Frontal operculum L	0.347	0.352	0.005	0.074	0.8436	0.073
Frontal operculum R	0.320	0.322	0.001	0.371	0.919434782608696	-0.037

Frontal pole L	0.399	0.400	0.001	0.396	0.885176470588235	0.033
Frontal pole R	0.382	0.382	0.000	0.596	1	0.021
Fusiform gyrus L	0.459	0.459	0.000	0.960	0.994909090909091	-0.002
Fusiform gyrus R	0.458	0.461	0.002	0.191	0.750827586206896	-0.049
Gyrus rectus L	0.390	0.390	0.000	0.862	1	0.007
Gyrus rectus R	0.391	0.391	0.000	0.615824	1	-0.020
Hippocampus L	0.349	0.354	0.005	0.076550	0.793336363636364	-0.072
Hippocampus R	0.402	0.407	0.005	0.071	1	-0.071
Inferior occipital gyrus L	0.371	0.373	0.002	0.290	0.87	-0.042
Inferior occipital gyrus R	0.418	0.418	0.000	0.994	0.994	0.000
Inferior temporal gyrus L	0.480	0.483	0.004	0.093	0.757285714285714	-0.061
Inferior temporal gyrus R	0.518	0.523	0.005	0.031	0.7068	-0.076
Lateral orbital gyrus L	0.394	0.395	0.002	0.313	0.849571428571429	-0.040
Lateral orbital gyrus R	0.325	0.352	0.001	0.539	1	-0.026
Lingual gyrus L	0.516	0.517	0.000	0.599	1	0.019
Lingual gyrus R	0.518	0.518	0.000	0.831	1	0.008
Medial frontal cortex L	0.346	0.346	0.000	0.992736	1	0.000
Medial frontal cortex R	0.354	0.354	0.000	0.935	1	0.003
Medial orbital gyrus L	0.470	0.470	0.000	0.890	1	-0.005
Medial orbital gyrus R	0.407	0.408	0.001	0.386	0.88008	0.034
Middle cingulate gyrus L	0.396	0.398	0.002	0.298895	0.873693076923077	-0.041
Middle cingulate gyrus R	0.336	0.340	0.003	0.161	0.73416	-0.058
Middle frontal gyrus L	0.467	0.468	0.001	0.372	0.902297872340426	-0.033
Middle frontal gyrus R	0.468	0.468	0.000	0.711	1	-0.014
Middle occipital gyrus L	0.295	0.295	0.000	0.634	1	0.020
Middle occipital gyrus R	0.327	0.327	0.000	0.723	1	-0.015
Middle temporal gyrus L	0.498	0.498	0.000	0.851	1	-0.007
Middle temporal gyrus R	0.509	0.509	0.000	0.881	1	-0.005
Occipital fusiform gyrus L	0.460	0.460	0.000	0.720	1	0.013
Occipital fusiform gyrus R	0.457	0.457	0.000	0.889	1	0.005

Occipital pole L	0.333	0.333	0.000	0.933	1	-0.003
Occipital pole R	0.367	0.367	0.000	0.578	1	0.022
Opercular part of the inferior frontal gyrus L	0.222	0.234	0.011	0.013721	0.782097	0.110
Opercular part of the inferior frontal gyrus R	0.236	0.236	0.000	0.814	1	0.010
Orbital part of the inferior frontal gyrus L	0.261	0.261	0.000	0.959312	1	-0.002
Orbital part of the inferior frontal gyrus R	0.255	0.255	0.000	0.811	1	-0.010
Pallidum L	0.183	0.189	0.006	0.076829	0.7298755	-0.081
Pallidum R	0.160	0.165	0.005	0.113	0.715666666666667	-0.074
Parahippocampal gyrus L	0.427	0.429	0.002	0.299165	0.85262025	-0.040
Parahippocampal gyrus R	0.458	0.462	0.003	0.110	0.737647058823529	-0.059
Parietal operculum L	0.338	0.338	0.000	0.730726	1	0.014
Parietal operculum R	0.276	0.276	0.000	0.771	1	-0.013
Planum polare L	0.401	0.402	0.002	0.301	0.836926829268293	-0.041
Planum polare R	0.442	0.444	0.001	0.375	0.890625	-0.034
Planum temporale L	0.321	0.325	0.004	0.127	0.658090909090909	-0.064
Planum temporale R	0.315	0.315	0.000	0.918	1	0.004
Postcentral gyrus L	0.371	0.371	0.000	0.945	1	0.003
Postcentral gyrus R	0.361	0.361	0.000	0.884	1	0.006
Postcentral gyrus medial segment L	0.208	0.208	0.000	0.807	1	0.011
Postcentral gyrus medial segment R	0.198	0.198	0.000	0.719	1	0.016
Posterior cingulate gyrus L	0.517	0.519	0.002	0.193	0.7334	-0.046
Posterior cingulate gyrus R	0.485	0.485	0.000	0.756	1	-0.011
Posterior insula L	0.383	0.387	0.004	0.119	0.646	-0.062
Posterior insula R	0.403	0.405	0.002	0.217	0.798	-0.048
Posterior orbital gyrus L	0.317	0.319	0.002	0.245	0.846363636363636	-0.049
Posterior orbital gyrus R	0.321	0.324	0.003	0.163	0.714692307692308	-0.058
Precentral gyrus L	0.446	0.446	0.000	0.946	1	-0.003
Precentral gyrus R	0.415	0.416	0.001	0.513	1	0.025
Precentral gyrus medial segment L	0.258	0.258	0.000	0.958974	1	0.002
Precentral gyrus medial segment R	0.304	0.305	0.000	0.716	1	-0.015

Precuneus L	0.478	0.478	0.000	0.874	1	0.006
Precuneus R	0.491	0.491	0.000	0.958883	1	-0.002
Putamen L	0.227	0.241	0.014	0.007	0.798	-0.119
Putamen R	0.229	0.241	0.011	0.014375	0.54625	-0.108
Subcallosal area L	0.428	0.428	0.000	0.731354	1	0.013
Subcallosal area R	0.370	0.370	0.000	0.857	1	0.007
Superior frontal gyrus L	0.446	0.447	0.001	0.354	0.917181818181818	-0.035
Superior frontal gyrus R	0.460	0.460	0.000	0.659	1	-0.016
Superior frontal gyrus medial segment L	0.407	0.409	0.002	0.263	0.856628571428571	-0.044
Superior frontal gyrus medial segment R	0.406	0.406	0.000	0.993339	1	0.000
Superior occipital gyrus L	0.287	0.291	0.003	0.170	0.692142857142857	0.059
Superior occipital gyrus R	0.268	0.268	0.000	0.775	1	-0.012
Superior parietal lobule L	0.353	0.353	0.000	0.655	1	0.018
Superior parietal lobule R	0.374	0.375	0.001	0.413	0.905423076923077	-0.033
Superior temporal gyrus L	0.373	0.373	0.000	0.952	1	0.002
Superior temporal gyrus R	0.348	0.350	0.002	0.273	0.8645	0.045
Supplementary motor cortex L	0.356	0.357	0.000	0.579	1	-0.023
Supplementary motor cortex R	0.371	0.371	0.000	0.879	1	0.006
Supramarginal gyrus L	0.287	0.287	0.000	0.696	1	0.017
Supramarginal gyrus R	0.335	0.355	0.000	0.633	1	-0.020
Temporal pole L	0.328	0.332	0.003	0.145	0.718695652173913	-0.060
Temporal pole R	0.358	0.362	0.004	0.114	0.684	-0.064
Thalamus proper L	0.200	0.202	0.002	0.342	0.906697674418605	-0.043
Thalamus proper R	0.221	0.227	0.006	0.073322	0.928745333333333	-0.080
Transverse temporal gyrus L	0.237	0.237	0.000	0.700	1	0.017
Transverse temporal gyrus R	0.292	0.292	0.000	0.833	1	0.009
Triangular part of the inferior frontal gyrus L	0.274	0.276	0.001	0.368	0.932266666666667	0.039
Triangular part of the inferior frontal gyrus R	0.253	0.254	0.001	0.379	0.881755102040816	-0.039

FDR: false discovery rate. L: left. PRS: polygenic risk score. R: right.

Table D.11: Associations between PRSwithAPOE Threshold 1 and 114 regions of interest in APOE ε4 carriers

Region of Interest	R Square (Model 1)	R Square (Model 2)	R Square Change	Sig. F Change (Model 2)	FDR Corrected value	Standardised beta of PRS
Accumbens area L	0.479	0.785	0.006	0.081	1	0.08
Accumbens area R	0.444	0.457	0.013	0.011	1	0.120
Amygdala L	0.496	0.496	0.000	0.942	1	0.003
Amygdala R	0.544	0.544	0.000	0.746	1	-0.014
Angular gyrus L	0.465	0.468	0.003	0.200323	1	-0.060
Angular gyrus R	0.479	0.479	0.000	0.798011	1	0.012
Anterior cingulate gyrus L	0.445	0.445	0.000	0.941	1	0.003
Anterior cingulate gyrus R	0.312	0.314	0.002	0.329	1	0.051
Anterior insula L	0.445	0.448	0.003	0.240	1	0.056
Anterior insula R	0.431	0.436	0.005	0.110	1	0.077
Anterior orbital gyrus L	0.420	0.421	0.001	0.564	1	0.115
Anterior orbital gyrus R	0.387	0.392	0.005	0.132	1	-0.075
Basal forebrain L	0.375	0.376	0.002	0.389	1	0.043
Basal forebrain R	0.393	0.400	0.006	0.089	1	0.084
Calcarine cortex L	0.417	0.418	0.001	0.468	1	-0.035
Calcarine cortex R	0.424	0.432	0.008	0.054	1	-0.093
Caudate L	0.245	0.245	0.000	0.932	1	0.005
Caudate R	0.238	0.238	0.000	0.817	1	-0.013
Central operculum L	0.432	0.432	0.000	0.883	1	-0.007
Central operculum R	0.425	0.426	0.001	0.448	1	-0.037
Cuneus L	0.445	0.447	0.003	0.250	1	-0.054
Cuneus R	0.444	0.445	0.001	0.601	0.99295652173913	-0.025
Entorhinal area L	0.483	0.483	0.000	0.964159	0.990217351351351	0.002
Entorhinal area R	0.536	0.536	0.001	0.541	1	0.027
Frontal operculum L	0.412	0.412	0.000	0.874	1	0.008
Frontal operculum R	0.366	0.367	0.001	0.631	1	0.024

Frontal pole L	0.490	0.491	0.001	0.368	1	-0.041
Frontal pole R	0.461	0.463	0.001	0.396	1	0.040
Fusiform gyrus L	0.571	0.572	0.000	0.585	1	0.023
Fusiform gyrus R	0.614	0.615	0.001	0.381	1	0.035
Gyrus rectus L	0.506	0.507	0.001	0.400	1	-0.038
Gyrus rectus R	0.530	0.530	0.000	0.702	1	-0.017
Hippocampus L	0.567	0.567	0.000	0.719460	1	-0.015
Hippocampus R	0.560	0.561	0.001	0.367	1	-0.038
Inferior occipital gyrus L	0.466	0.467	0.001	0.560	1	-0.027
Inferior occipital gyrus R	0.528	0.529	0.001	0.376	1	-0.039
Inferior temporal gyrus L	0.553	0.553	0.001	0.565	1	0.025
Inferior temporal gyrus R	0.584	0.587	0.003	0.155	1	0.058
Lateral orbital gyrus L	0.450	0.450	0.000	0.898	1	-0.006
Lateral orbital gyrus R	0.420	0.424	0.003	0.214	1	-0.060
Lingual gyrus L	0.515	0.515	0.000	0.844	1	0.009
Lingual gyrus R	0.537	0.537	0.000	0.737	1	-0.015
Medial frontal cortex L	0.399	0.402	0.003	0.260	1	-0.056
Medial frontal cortex R	0.416	0.416	0.000	0.973030	0.981640884955752	0.002
Medial orbital gyrus L	0.495	0.497	0.002	0.291	1	-0.048
Medial orbital gyrus R	0.484	0.486	0.001	0.375	1	-0.041
Middle cingulate gyrus L	0.382	0.385	0.003	0.221	1	0.061
Middle cingulate gyrus R	0.366	0.367	0.001	0.602	0.9804	0.026
Middle frontal gyrus L	0.489	0.491	0.002	0.305	1	0.047
Middle frontal gyrus R	0.477	0.478	0.001	0.377	1	0.041
Middle occipital gyrus L	0.446	0.450	0.003	0.200034	1	-0.061
Middle occipital gyrus R	0.410	0.414	0.004	0.185	1	-0.065
Middle temporal gyrus L	0.512	0.512	0.000	0.757	1	-0.014
Middle temporal gyrus R	0.565	0.565	0.000	0.734870	1	0.014
Occipital fusiform gyrus L	0.495	0.497	0.002	0.271	1	0.050
Occipital fusiform gyrus R	0.583	0.583	0.000	0.681	1	0.017

Occipital pole L	0.368	0.368	0.000	0.666	1	-0.022
Occipital pole R	0.387	0.387	0.000	0.854	1	0.009
Opercular part of the inferior frontal gyrus L	0.323	0.323	0.000	0.914	1	0.006
Opercular part of the inferior frontal gyrus R	0.338	0.338	0.000	0.799	1	-0.013
Orbital part of the inferior frontal gyrus L	0.311	0.311	0.001	0.566	1	-0.030
Orbital part of the inferior frontal gyrus R	0.288	0.291	0.002	0.338	1	-0.051
Pallidum L	0.158	0.162	0.004	0.262	1	-0.065
Pallidum R	0.135	0.143	0.008	0.111	1	-0.094
Parahippocampal gyrus L	0.559	0.560	0.000	0.588	1	0.023
Parahippocampal gyrus R	0.598	0.598	0.000	0.938	1	0.003
Parietal operculum L	0.357	0.357	0.000	0.945	0.988348623853211	0.004
Parietal operculum R	0.340	0.344	0.004	0.211	1	0.065
Planum polare L	0.517	0.517	0.000	0.929	1	0.004
Planum polare R	0.542	0.542	0.000	0.597468	1	-0.023
Planum temporale L	0.413	0.414	0.001	0.482	1	0.034
Planum temporale R	0.448	0.448	0.000	0.719231	1	-0.017
Postcentral gyrus L	0.424	0.424	0.000	0.876	1	0.008
Postcentral gyrus R	0.427	0.427	0.000	0.944	0.996444444444444	-0.003
Postcentral gyrus medial segment L	0.206	0.210	0.004	0.247	1	-0.066
Postcentral gyrus medial segment R	0.260	0.261	0.001	0.488	1	-0.038
Posterior cingulate gyrus L	0.582	0.582	0.000	0.787	1	0.011
Posterior cingulate gyrus R	0.540	0.542	0.001	0.360170	1	-0.039
Posterior insula L	0.422	0.430	0.008	0.041	1	0.098
Posterior insula R	0.455	0.463	0.008	0.042	0.9576	0.095
Posterior orbital gyrus L	0.435	0.435	0.000	0.909	1	-0.005
Posterior orbital gyrus R	0.452	0.452	0.000	0.797872	1	-0.012
Precentral gyrus L	0.476	0.486	0.010	0.017	0.969	0.109
Precentral gyrus R	0.467	0.472	0.005	0.097	1	0.077
Precentral gyrus medial segment L	0.350	0351	0.002	0.395	1	-0.044
Precentral gyrus medial segment R	0.375	0.376	0.001	0.485	1	-0.035

Precuneus L	0.507	0.507	0.000	0.848	1	0.009
Precuneus R	0.500	0.501	0.000	0.597357	1	-0.024
Putamen L	0.348	0.353	0.005	0.151	1	0.074
Putamen R	0.375	0.381	0.006	0.114	1	0.079
Subcallosal area L	0.544	0.544	0.000	0.825	1	0.010
Subcallosal area R	0.558	0.558	0.001	0.496	1	0.029
Superior frontal gyrus L	0.475	0.475	0.000	0.723	1	0.016
Superior frontal gyrus R	0.509	0.518	0.010	0.019	0.722	0.104
Superior frontal gyrus medial segment L	0.440	0.440	0.000	0.963797	0.998844163636364	-0.002
Superior frontal gyrus medial segment R	0.422	0.424	0.001	0.445	1	0.037
Superior occipital gyrus L	0.369	0.369	0.000	0.869	1	-0.008
Superior occipital gyrus R	0.434	0.434	0.000	0.873	1	0.008
Superior parietal lobule L	0.442	0.443	0.001	0.544	1	-0.029
Superior parietal lobule R	0.408	0.408	0.000	0.721	1	-0.018
Superior temporal gyrus L	0.507	0.508	0.001	0.487	1	-0.031
Superior temporal gyrus R	0.485	0.486	0.001	0.579	1	-0.025
Supplementary motor cortex L	0.379	0.379	0.000	0.993	0.993	0.000
Supplementary motor cortex R	0.396	0.397	0.001	0.522	1	0.032
Supramarginal gyrus L	0.438	0.439	0.001	0.452	1	-0.036
Supramarginal gyrus R	0.407	0.408	0.001	0.437	1	0.038
Temporal pole L	0.491	0.491	0.001	0.535	1	0.028
Temporal pole R	0.484	0.485	0.002	0.360188	1	0.042
Thalamus proper L	0.273	0.274	0.001	0.526	1	0.034
Thalamus proper R	0.326	0.327	0.001	0.453	1	0.039
Transverse temporal gyrus L	0.334	0.334	0.000	0.972942	0.990315964285714	-0.002
Transverse temporal gyrus R	0.437	0.438	0.000	0.735425	1	-0.016
Triangular part of the inferior frontal gyrus L	0.384	0.384	0.000	0.741	1	0.017
Triangular part of the inferior frontal gyrus R	0.356	0.357	0.000	0.655	1	-0.023

FDR: false discovery rate. L: left. PRS: polygenic risk score. R: right.

Table D.12: Associations between PRSwithAPOE Threshold 5 and 114 regions of interest in APOE ε4 non-carriers

Region of Interest	R Square (Model 1)	R Square (Model 2)	R Square Change	Sig. F Change (Model 2)	FDR Corrected value	Standardised beta of PRS
Accumbens area L	0.350	0.353	0.003	0.155	0.8835	-0.058
Accumbens area R	0.363	0.364	0.002	0.308963	0.951940054054054	-0.041
Amygdala L	0.349	0.355	0.005	0.067	0.7638	-0.074
Amygdala R	0.400	0.406	0.005	0.056	0.912	-0.074
Angular gyrus L	0.369	0.369	0.000	0.713	0.979301204819277	-0.015
Angular gyrus R	0.378	0.378	0.000	0.700	0.985185185185185	0.015
Anterior cingulate gyrus L	0.397	0.397	0.000	0.879	0.972873786407767	0.006
Anterior cingulate gyrus R	0.205	0.207	0.002	0.282	0.974181818181818	-0.048
Anterior insula L	0.330	0.333	0.003	0.176	0.872347826086956	-0.056
Anterior insula R	0.363	0.367	0.004	0.116	0.777882352941177	-0.063
Anterior orbital gyrus L	0.399	0.401	0.002	0.265	0.9440625	-0.043
Anterior orbital gyrus R	0.346	0.346	0.000	0.791	0.9393125	0.011
Basal forebrain L	0.261	0.267	0.006	0.059	0.84075	-0.082
Basal forebrain R	0.328	0.333	0.005	0.074	0.703	-0.074
Calcarine cortex L	0.354	0.354	0.000	0.779	0.944744680851064	0.011
Calcarine cortex R	0.360	0.361	0.002	0.314	0.942	0.041
Caudate L	0.184	0.485	0.000	0.760	0.931612903225806	-0.014
Caudate R	0.180	0.180	0.000	0.794	0.933154639175258	-0.012
Central operculum L	0.352	0.353	0.000	0.750	0.960674157303371	0.013
Central operculum R	0.360	0.361	0.001	0.507	0.947508196721311	0.027
Cuneus L	0.379	0.380	0.001	0.392	0.971478260869565	0.034
Cuneus R	0.422	0.423	0.001	0.488	0.9272	-0.027
Entorhinal area L	0.351	0.351	0.001	0.538	0.9583125	-0.025
Entorhinal area R	0.395	0.395	0.001	0.458	0.916	-0.029
Frontal operculum L	0.347	0.350	0.004	0.135	0.855	0.061
Frontal operculum R	0.320	0.322	0.001	0.398	0.94525	-0.035

Frontal pole L	0.399	0.403	0.004	0.112	0.798	0.062
Frontal pole R	0.382	0.383	0.001	0.395	0.958085106382979	0.034
Fusiform gyrus L	0.459	0.459	0.000	0.782	0.9384	0.010
Fusiform gyrus R	0.458	0.459	0.001	0.384	0.994909090909091	-0.032
Gyrus rectus L	0.390	0.390	0.000	0.692	0.998582278481013	0.016
Gyrus rectus R	0.391	0.391	0.000	0.839	0.95646	-0.008
Hippocampus L	0.349	0.356	0.007	0.032	0.912	-0.087
Hippocampus R	0.402	0.408	0.006	0.041	0.779	-0.079
Inferior occipital gyrus L	0.371	0.373	0.001	0.330	0.964615384615385	-0.039
Inferior occipital gyrus R	0.418	0.419	0.000	0.606	0.986914285714286	0.020
Inferior temporal gyrus L	0.480	0.483	0.003	0.104	0.7904	-0.059
Inferior temporal gyrus R	0.518	0.521	0.004	0.070	0.725454545454545	-0.063
Lateral orbital gyrus L	0.394	0.394	0.000	0.616	0.989070422535211	-0.020
Lateral orbital gyrus R	0.325	0.325	0.000	0.904422	0.972680264150943	-0.005
Lingual gyrus L	0.516	0.517	0.000	0.630	0.9975	0.017
Lingual gyrus R	0.518	0.518	0.000	0.698	0.99465	0.014
Medial frontal cortex L	0.346	0.347	0.000	0.725	0.983928571428571	0.014
Medial frontal cortex R	0.354	0.355	0.001	0.464615	0.913208793103448	0.030
Medial orbital gyrus L	0.470	0.470	0.000	0.868	0.970117647058824	0.006
Medial orbital gyrus R	0.407	0.409	0.002	0.252	0.926709677419355	0.044
Middle cingulate gyrus L	0.396	0.398	0.001	0.348	0.922604651162791	-0.037
Middle cingulate gyrus R	0.336	0.337	0.001	0.549	0.948272727272727	-0.025
Middle frontal gyrus L	0.467	0.468	0.001	0.442	0.933111111111111	-0.028
Middle frontal gyrus R	0.468	0.468	0.000	0.795	0.924795918367347	-0.010
Middle occipital gyrus L	0.295	0.296	0.001	0.433	0.949269230769231	0.033
Middle occipital gyrus R	0.327	0.327	0.000	0.746	0.97751724137931	0.013
Middle temporal gyrus L	0.498	0.498	0.000	0.758	0.965339449541284	-0.011
Middle temporal gyrus R	0.509	0.509	0.000	0.923	0.939260869565217	0.003
Occipital fusiform gyrus L	0.460	0.460	0.000	0.711	0.988463414634146	0.014
Occipital fusiform gyrus R	0.457	0.458	0.001	0.465183	0.898828169491525	0.027

Occipital pole L	0.333	0.333	0.000	0.917	0.976990654205607	-0.004
Occipital pole R	0.367	0.369	0.002	0.296	0.964114285714286	0.042
Opercular part of the inferior frontal gyrus L	0.222	0.34	0.012	0.013	0.741	0.110
Opercular part of the inferior frontal gyrus R	0.236	0.237	0.001	0.533	0.96447619047619	0.027
Orbital part of the inferior frontal gyrus L	0.261	0.261	0.000	0.919	0.970055555555556	0.004
Orbital part of the inferior frontal gyrus R	0.255	0.255	0.000	0.956	0.981837837837838	-0.002
Pallidum L	0.183	0.187	0.004	0.175	0.906818181818182	-0.062
Pallidum R	0.160	0.163	0.003	0.207	0.874	-0.058
Parahippocampal gyrus L	0.427	0.429	0.002	0.203	0.890076923076923	-0.048
Parahippocampal gyrus R	0.458	0.462	0.004	0.083	0.727846153846154	-0.064
Parietal operculum L	0.338	0.338	0.001	0.554	0.942626865671642	0.024
Parietal operculum R	0.276	0.276	0.000	0.753	0.9538	0.013
Planum polare L	0.401	0.403	0.002	0.230	0.936428571428571	-0.047
Planum polare R	0.442	0.443	0.001	0.448	0.928581818181818	-0.029
Planum temporale L	0.321	0.326	0.005	0.089	0.724714285714286	-0.070
Planum temporale R	0.315	0.315	0.000	0.904203	0.981706114285714	0.005
Postcentral gyrus L	0.371	0.371	0.000	0.726	0.973694117647059	0.014
Postcentral gyrus R	0.361	0.361	0.001	0.563	0.943852941176471	0.023
Postcentral gyrus medial segment L	0.208	0.208	0.000	0.800	0.921212121212121	0.011
Postcentral gyrus medial segment R	0.198	0.200	0.002	0.308602	0.977239666666667	0.046
Posterior cingulate gyrus L	0.517	0.518	0.001	0.286	0.958941176470588	-0.037
Posterior cingulate gyrus R	0.485	0.485	0.000	0.686823	1	-0.015
Posterior insula L	0.383	0.386	0.003	0.178	0.8455	-0.053
Posterior insula R	0.403	0.404	0.001	0.404	0.92112	-0.032
Posterior orbital gyrus L	0.317	0.318	0.001	0.402	0.935265306122449	-0.035
Posterior orbital gyrus R	0.321	0.324	0.003	0.202	0.92112	-0.053
Precentral gyrus L	0.446	0.446	0.000	0.604	0.997913043478261	0.019
Precentral gyrus R	0.415	0.417	0.002	0.251	0.9538	0.044
Precentral gyrus medial segment L	0.258	0.258	0.000	0.676	1	0.018
Precentral gyrus medial segment R	0.304	0.304	0.000	0.959	0.976125	-0.002

Precuneus L	0.478	0.479	0.001	0.525	0.965322580645161	0.023
Precuneus R	0.491	0.491	0.000	0.636	0.993205479452055	0.017
Putamen L	0.227	0.241	0.014	0.007	0.798	-0.119
Putamen R	0.229	0.240	0.010	0.020	0.76	-0.103
Subcallosal area L	0.428	0.429	0.001	0.435	0.935660377358491	0.030
Subcallosal area R	0.370	0.371	0.001	0.421	0.941058823529412	0.032
Superior frontal gyrus L	0.446	0.446	0.000	0.649	0.999810810810811	-0.017
Superior frontal gyrus R	0.460	0.460	0.000	0.994	0.994	0.000
Superior frontal gyrus medial segment L	0.407	0.408	0.001	0.345750	0.938464285714286	-0.037
Superior frontal gyrus medial segment R	0.406	0.406	0.000	0.944	0.978327272727273	-0.003
Superior occipital gyrus L	0.287	0.295	0.008	0.036	0.8208	0.089
Superior occipital gyrus R	0.268	0.269	0.001	0.548	0.961107692307692	0.026
Superior parietal lobule L	0.353	0.354	0.001	0.342	0.9747	0.038
Superior parietal lobule R	0.374	0.374	0.000	0.740	0.980930232558139	-0.013
Superior temporal gyrus L	0.373	0.373	0.000	0.754	0.944571428571429	0.012
Superior temporal gyrus R	0.348	0.350	0.002	0.248	0.974896551724138	0.047
Supplementary motor cortex L	0.356	0.3560	0.000	0.992	1	0.000
Supplementary motor cortex R	0.371	0.372	0.000	0.747	0.967704545454545	0.013
Supramarginal gyrus L	0.287	0.288	0.001	0.455	0.92625	0.032
Supramarginal gyrus R	0.335	0.335	0.000	0.900	0.986538461538462	0.005
Temporal pole L	0.328	0.331	0.003	0.159	0.863142857142857	-0.058
Temporal pole R	0.358	0.361	0.003	0.152	0.912	-0.058
Thalamus proper L	0.200	0.201	0.001	0.390	0.988	-0.039
Thalamus proper R	0.221	0.228	0.007	0.061	0.772666666666667	-0.083
Transverse temporal gyrus L	0.237	0.237	0.000	0.844	0.952633663366336	0.009
Transverse temporal gyrus R	0.292	0.292	0.000	0.683	1	0.017
Triangular part of the inferior frontal gyrus L	0.274	0.276	0.002	0.345721	0.961273024390244	0.040
Triangular part of the inferior frontal gyrus R	0.253	0.253	0.000	0.686976	1	-0.018

FDR: false discovery rate. L: left. PRS: polygenic risk score. R: right.

Table D.13: Associations between PRSwithAPOE Threshold 5 and 114 regions of interest in APOE ε4 carriers

Region of Interest	R Square (Model 1)	R Square (Model 2)	R Square Change	Sig. F Change (Model 2)	FDR Corrected value	Standardised beta of PRS
Accumbens area L	0.479	0.484	0.005	0.092	1	0.077
Accumbens area R	0.444	0.456	0.012	0.014	1	0.116
Amygdala L	0.496	0496	0.000	0.778	0.974637362637363	-0.013
Amygdala R	0.544	0.544	0.000	0.627	0.99275	-0.021
Angular gyrus L	0.465	0.468	0.003	0.181293	1	-0.062
Angular gyrus R	0.479	0.479	0.000	0.832	0.988	0.010
Anterior cingulate gyrus L	0.445	0.445	0.000	0.815	0.978	0.011
Anterior cingulate gyrus R	0.312	0.315	0.004	0.230	1	0.064
Anterior insula L	0.445	0.448	0.003	0.193	1	0.062
Anterior insula R	0.431	0.437	0.006	0.087	1	0.082
Anterior orbital gyrus L	0.420	0.421	0.001	0.534	1	-0.030
Anterior orbital gyrus R	0.387	0.392	0.005	0.148	1	-0.072
Basal forebrain L	0.375	0.376	0.002	0.391	1	0.043
Basal forebrain R	0.393	0.400	0.007	0.077	1	0.088
Calcarine cortex L	0.417	0.418	0.002	0.346	1	-0.046
Calcarine cortex R	0.424	0.433	0.009	0.034	0.646	-0.103
Caudate L	0.245	0.245	0.000	0.846	0.96444	0.011
Caudate R	0.238	0.238	0.000	0.836	0.982515463917526	-0.012
Central operculum L	0.432	0.432	0.000	0.931	0.982722222222222	0.004
Central operculum R	0.425	0.425	0.000	0.660	0.9405	-0.021
Cuneus L	0.445	0.447	0.003	0.251	1	-0.055
Cuneus R	0.444	0.445	0.000	0.634	0.96368	-0.023
Entorhinal area L	0.483	0.483	0.000	0.938	0.98102752293578	-0.004
Entorhinal area R	0.536	0.537	0.001	0.506	1	0.029
Frontal operculum L	0.412	0.412	0.000	0.693	0.929435294117647	0.019
Frontal operculum R	0.366	0.367	0.001	0.537	0.987387096774194	0.031

Frontal pole L	0.490	0.492	0.002	0.334978	1	-0.044
Frontal pole R	0.461	0.463	0.001	0.384	1	0.041
Fusiform gyrus L	0.571	0.572	0.001	0.409	1	0.035
Fusiform gyrus R	0.614	0.616	0.001	0.295032	1	0.042
Gyrus rectus L	0.506	0.507	0.001	0.490	1	-0.031
Gyrus rectus R	0.530	0.531	0.000	0.692	0.939142857142857	-0.017
Hippocampus L	0.567	0.568	0.001	0.519	1	-0.027
Hippocampus R	0.560	0.562	0.002	0.278	1	-0.046
Inferior occipital gyrus L	0.466	0.467	0.001	0.535	0.999836065573771	-0.029
Inferior occipital gyrus R	0.528	0.530	0.002	0.282	1	-0.047
Inferior temporal gyrus L	0.553	0.553	0.000	0.624	1	0.021
Inferior temporal gyrus R	0.584	0.587	0.003	0.190	1	0.054
Lateral orbital gyrus L	0.450	0.450	0.000	0.978	0.995464285714286	0.001
Lateral orbital gyrus R	0.420	0.423	0.003	0.240	1	-0.057
Lingual gyrus L	0.515	0.515	0.000	0.800	0.970212765957447	0.011
Lingual gyrus R	0.537	0.537	0.000	0.759	0.972202247191011	-0.013
Medial frontal cortex L	0.399	0.401	0.002	0.375	1	-0.044
Medial frontal cortex R	0.416	0.416	0.000	0.760	0.962666666666667	0.015
Medial orbital gyrus L	0.495	0.497	0.002	0.326	1	-0.045
Medial orbital gyrus R	0.484	0.485	0.001	0.443	1	-0.035
Middle cingulate gyrus L	0.382	0.385	0.004	0.201	1	0.064
Middle cingulate gyrus R	0.366	0.367	0.001	0.542	0.980761904761905	0.031
Middle frontal gyrus L	0.489	0.491	0.002	0.348	1	0.043
Middle frontal gyrus R	0.477	0.478	0.002	0.356	1	0.043
Middle occipital gyrus L	0.446	0.449	0.002	0.260388	1	-0.053
Middle occipital gyrus R	0.410	0.414	0.004	0.180801	1	-0.066
Middle temporal gyrus L	0.512	0.512	0.000	0.663	0.970693069306931	-0.019
Middle temporal gyrus R	0.565	0.565	0.000	0.860	0.933111111111111	0.007
Occipital fusiform gyrus L	0.495	0.497	0.002	0.260168	1	0.051
Occipital fusiform gyrus R	0.583	0.583	0.000	0.723	0.947379310344827	0.015

Occipital pole L	0.368	0.368	0.001	0.557	0.976892307692308	-0.030
Occipital pole R	0.387	0.387	0.000	0.914	1	0.005
Opercular part of the inferior frontal gyrus L	0.323	0.323	0.000	0.986	0.994725663716814	0.001
Opercular part of the inferior frontal gyrus R	0.338	0.339	0.000	0.718	0.951767441860465	-0.019
Orbital part of the inferior frontal gyrus L	0.311	0.311	0.001	0.585	0.980735294117647	-0.029
Orbital part of the inferior frontal gyrus R	0.288	0.290	0.002	0.371	1	-0.048
Pallidum L	0.158	0.161	0.004	0.273	1	-0.064
Pallidum R	0.135	0.142	0.007	0.120	1	-0.092
Parahippocampal gyrus L	0.559	0.560	0.000	0.651	0.951461538461538	0.019
Parahippocampal gyrus R	0.598	0.598	0.000	0.924	0.993735849056604	0.004
Parietal operculum L	0.357	0.357	0.000	0.683	0.949536585365854	0.021
Parietal operculum R	0.340	0.343	0.003	0.225	1	0.063
Planum polare L	0.517	0.517	0.000	0.922	1	-0.004
Planum polare R	0.542	0.542	0.000	0.653	0.942303797468354	-0.019
Planum temporale L	0.413	0.414	0.001	0.516	1	0.032
Planum temporale R	0.448	0.448	0.001	0.558	0.963818181818182	-0.028
Postcentral gyrus L	0.424	0.425	0.000	0.686	0.94221686746988	-0.020
Postcentral gyrus R	0.427	0.428	0.000	0.645	0.9675	-0.022
Postcentral gyrus medial segment L	0.206	0.212	0.005	0.163	1	-0.079
Postcentral gyrus medial segment R	0.260	0.260	0.001	0.631	0.972081081081081	-0.026
Posterior cingulate gyrus L	0.582	0.582	0.000	0.925	0.985514018691589	0.004
Posterior cingulate gyrus R	0.540	0.542	0.002	0.285	1	-0.046
Posterior insula L	0.422	0.432	0.010	0.027	0.6156	0.107
Posterior insula R	0.455	0.465	0.010	0.025	0.95	0.105
Posterior orbital gyrus L	0.435	0.435	0.000	0.995	0.995	0.000
Posterior orbital gyrus R	0.452	0.452	0.000	0.842277	0.969894727272727	-0.009
Precentral gyrus L	0.476	0.485	0.009	0.026	0.741	0.103
Precentral gyrus R	0.467	0.472	0.004	0.123	1	0.072
Precentral gyrus medial segment L	0.350	0.352	0.003	0.294784	1	-0.054
Precentral gyrus medial segment R	0.375	0.376	0.001	0.480	1	-0.036

Precuneus L	0.507	0.507	0.000	0.946	0.9804	0.003
Precuneus R	0.500	0.501	0.001	0.491	1	-0.031
Putamen L	0.348	0.354	0.006	0.111	1	0.082
Putamen R	0.375	0.381	0.006	0.097	1	0.083
Subcallosal area L	0.544	0.545	0.000	0.650	0.962337662337662	0.020
Subcallosal area R	0.558	0.559	0.001	0.335212	1	0.041
Superior frontal gyrus L	0.475	0.476	0.001	0.565	0.961343283582089	0.027
Superior frontal gyrus R	0.509	0.518	0.010	0.017	0.969	0.106
Superior frontal gyrus medial segment L	0.440	0.440	0.000	0.892	0.996941176470588	-0.006
Superior frontal gyrus medial segment R	0.422	0.423	0.001	0.517	1	0.031
Superior occipital gyrus L	0.369	0.369	0.000	0.900	0.996116504854369	-0.006
Superior occipital gyrus R	0.434	0.434	0.000	0.969	0.995189189189189	0.002
Superior parietal lobule L	0.442	0.443	0.001	0.474	1	-0.034
Superior parietal lobule R	0.408	0.409	0.001	0.530	1	-0.031
Superior temporal gyrus L	0.507	0.509	0.002	0.307	1	-0.046
Superior temporal gyrus R	0.485	0.486	0.001	0.471	1	-0.033
Supplementary motor cortex L	0.379	0.379	0.000	0.790	0.968387096774194	-0.013
Supplementary motor cortex R	0.396	0.397	0.001	0.617	1	0.025
Supramarginal gyrus L	0.438	0.439	0.001	0.445	1	-0.037
Supramarginal gyrus R	0.407	0.408	0.001	0.456	1	0.037
Temporal pole L	0.491	0.491	0.000	0.626	1	0.022
Temporal pole R	0.484	0.485	0.001	0.395	1	0.039
Thalamus proper L	0.2733	0.274	0.001	0.529	1	0.034
Thalamus proper R	0.326	0.327	0.001	0.552	0.98325	0.031
Transverse temporal gyrus L	0.334	0.334	0.000	0.842204	0.979706693877551	-0.010
Transverse temporal gyrus R	0.437	0.438	0.000	0.779	0.965282608695652	-0.013
Triangular part of the inferior frontal gyrus L	0.384	0.384	0.000	0.746	0.966409090909091	0.016
Triangular part of the inferior frontal gyrus R	0.356	0.357	0.001	0.628	0.980712328767123	-0.025

FDR: false discovery rate. L: left. PRS: polygenic risk score. R: right.

Table D.14: Associations between PRSwithAPOE Threshold 10 and 114 regions of interest in APOE ε4 non-carriers

Region of Interest	R Square (Model 1)	R Square (Model 2)	R Square Change	Sig. F Change (Model 2)	FDR Corrected value	Standardised beta of PRS
Accumbens area L	0.350	0.353	0.003	0.153	0.830571428571429	-0.059
Accumbens area R	0.363	0.364	0.002	0.313	0.964378378378378	-0.041
Amygdala L	0.349	0.355	0.005	0.069	0.7866	-0.075
Amygdala R	0.400	0.405	0.004	0.086	0.700285714285714	-0.068
Angular gyrus L	0.369	0.369	0.000	0.763	0.9060625	0.012
Angular gyrus R	0.378	0.378	0.000	0.818	0.941939393939394	0.009
Anterior cingulate gyrus L	0.397	0.397	0.000	0.756	0.926709677419355	0.012
Anterior cingulate gyrus R	0.205	0.206	0.001	0.496	0.926950819672131	-0.031
Anterior insula L	0.330	0.335	0.005	0.078	0.684	-0.073
Anterior insula R	0.363	0.369	0.006	0.052	0.846857142857143	-0.079
Anterior orbital gyrus L	0.399	0.400	0.001	0.410	0.953877551020408	-0.033
Anterior orbital gyrus R	0.346	0.346	0.000	0.844	0.96216	0.008
Basal forebrain L	0.261	0.271	0.010	0.017	1	-0.104
Basal forebrain R	0.328	0.334	0.007	0.042	0.798	-0.085
Calcarine cortex L	0.354	0.354	0.000	0.729	0.933775280898876	-0.014
Calcarine cortex R	0.360	0.360	0.000	0.627	0.99275	0.020
Caudate L	0.184	0.185	0.000	0.721	0.966988235294118	-0.016
Caudate R	0.180	0.180	0.000	0.808	0.939918367346939	-0.011
Central operculum L	0.352	0.353	0.000	0.758	0.919276595744681	0.013
Central operculum R	0.360	0.360	0.000	0.921	0.981252336448598	0.004
Cuneus L	0.379	0.379	0.000	0.879	0.982411764705882	0.006
Cuneus R	0.422	0.425	0.002	0.187	0.819923076923077	-0.051
Entorhinal area L	0.351	0.352	0.001	0.395	0.938125	-0.035
Entorhinal area R	0.395	0.395	0.001	0.440	0.912	-0.031
Frontal operculum L	0.347	0.350	0.003	0.171	0.81225	0.056
Frontal operculum R	0.320	0.322	0.002	0.277	0.956909090909091	-0.046

Frontal pole L	0.399	0.403	0.004	0.107	0.762375	0.064
Frontal pole R	0.382	0.383	0.001	0.432	0.912	0.031
Fusiform gyrus L	0.459	0.459	0.000	0.728026	0.943124590909091	0.013
Fusiform gyrus R	0.458	0.459	0.000	0.582	0.990268656716418	-0.021
Gyrus rectus L	0.390	0.390	0.000	0.950	1	0.002
Gyrus rectus R	0.391	0.391	0.000	0.719	0.975785714285714	-0.014
Hippocampus L	0.349	0.357	0.008	0.029111	0.8296635	-0.089
Hippocampus R	0.402	0.407	0.005	0.059	0.747333333333333	-0.074
Inferior occipital gyrus L	0.371	0.372	0.001	0.429	0.922754716981132	-0.032
Inferior occipital gyrus R	0.418	0.418	0.000	0.691	0.984675	0.015
Inferior temporal gyrus L	0.480	0.482	0.002	0.172	0.78432	-0.050
Inferior temporal gyrus R	0.518	0.520	0.002	0.148	0.8436	-0.051
Lateral orbital gyrus L	0.394	0.394	0.000	0.977	1	0.001
Lateral orbital gyrus R	0.325	0.326	0.002	0.325	0.903658536585366	-0.041
Lingual gyrus L	0.516	0.516	0.000	0.995	0.995	0.000
Lingual gyrus R	0.518	0.518	0.000	0.602	0.9804	0.018
Medial frontal cortex L	0.346	0.346	0.000	0.979	0.987663716814159	-0.001
Medial frontal cortex R	0.354	0.355	0.000	0.737	0.933533333333333	0.014
Medial orbital gyrus L	0.470	0.470	0.000	0.727973	0.953895655172414	0.013
Medial orbital gyrus R	0.407	0.408	0.001	0.452	0.904	0.030
Middle cingulate gyrus L	0.396	0.396	0.000	0.742	0.919434782608696	-0.013
Middle cingulate gyrus R	0.336	0.336	0.000	0.868	0.979722772277228	-0.007
Middle frontal gyrus L	0.467	0.468	0.001	0.370	0.937333333333333	-0.033
Middle frontal gyrus R	0.468	0.468	0.000	0.554	0.956909090909091	-0.022
Middle occipital gyrus L	0.295	0.297	0.002	0.323081	0.92078085	0.042
Middle occipital gyrus R	0.327	0.327	0.000	0.920	0.989433962264151	0.004
Middle temporal gyrus L	0.498	0.498	0.000	0.972	0.973130434782609	0.001
Middle temporal gyrus R	0.509	0.509	0.000	0.589	1	0.019
Occipital fusiform gyrus L	0.460	0.460	0.000	0.653	0.99256	0.017
Occipital fusiform gyrus R	0.457	0.458	0.001	0.362	0.937909090909091	0.034

Occipital pole L	0.333	0.334	0.000	0.781	0.917876288659794	-0.012
Occipital pole R	0.367	0.368	0.001	0.539	0.96009375	0.025
Opercular part of the inferior frontal gyrus L	0.222	0.232	0.010	0.022	1	0.102
Opercular part of the inferior frontal gyrus R	0.236	0.236	0.000	0.659	0.975662337662338	0.020
Orbital part of the inferior frontal gyrus L	0.261	0.261	0.000	0.914917	1	-0.005
Orbital part of the inferior frontal gyrus R	0.255	0.255	0.000	0.665	0.971923076923077	-0.019
Pallidum L	0.183	0.185	0.002	0.323050	0.9443	-0.046
Pallidum R	0.160	0.161	0.001	0.455	0.894310344827586	-0.035
Parahippocampal gyrus L	0.427	0.429	0.002	0.212	0.863142857142857	-0.048
Parahippocampal gyrus R	0.458	0.461	0.003	0.126	0.798	-0.057
Parietal operculum L	0.338	0.338	0.000	0.620	0.995492957746479	0.021
Parietal operculum R	0.276	0.276	0.000	0.978	0.995464285714286	-0.001
Planum polare L	0.401	0.404	0.004	0.118	0.791294117647059	-0.062
Planum polare R	0.442	0.444	0.002	0.240	0.88258064516129	-0.045
Planum temporale L	0.321	0.328	0.007	0.040	0.912	-0.086
Planum temporale R	0.315	0.316	0.000	0.716697	0.996383634146341	-0.015
Postcentral gyrus L	0.371	0.371	0.000	0.962	1	-0.002
Postcentral gyrus R	0.361	0.363	0.002	0.280	0.912	0.044
Postcentral gyrus medial segment L	0.208	0.209	0.001	0.380001	0.941741608695652	0.040
Postcentral gyrus medial segment R	0.198	0.204	0.006	0.072	0.746181818181818	0.082
Posterior cingulate gyrus L	0.517	0.517	0.001	0.468	0.8892	-0.026
Posterior cingulate gyrus R	0.485	0.485	0.000	0.583	0.977382352941176	-0.020
Posterior insula L	0.383	0.386	0.003	0.154	0.798	-0.057
Posterior insula R	0.403	0.405	0.002	0.224	0.8512	-0.048
Posterior orbital gyrus L	0.317	0.319	0.002	0.333	0.903857142857143	-0.041
Posterior orbital gyrus R	0.321	0.324	0.003	0.194	0.819111111111111	-0.054
Precentral gyrus L	0.446	0.446	0.000	0.649	0.999810810810811	0.017
Precentral gyrus R	0.415	0.416	0.001	0.421	0.922961538461538	0.031
Precentral gyrus medial segment L	0.258	0.259	0.001	0.411	0.93708	0.036
Precentral gyrus medial segment R	0.304	0.305	0.000	0.739	0.92578021978022	0.014

Precuneus L	0.478	0.479	0.001	0.461	0.890745762711864	0.027
Precuneus R	0.491	0.491	0.000	0.723	0.958395348837209	0.013
Putamen L	0.227	0.236	0.009	0.028825	1	-0.098
Putamen R	0.229	0.236	0.007	0.057	0.81225	-0.085
Subcallosal area L	0.428	0.430	0.001	0.318	0.954	0.038
Subcallosal area R	0.370	0.371	0.001	0.340	0.901395348837209	0.039
Superior frontal gyrus L	0.446	0.447	0.001	0.542	0.950584615384615	-0.023
Superior frontal gyrus R	0.460	0.460	0.000	0.685	0.988481012658228	0.015
Superior frontal gyrus medial segment L	0.407	0.409	0.002	0.259	0.9226875	-0.044
Superior frontal gyrus medial segment R	0.406	0.406	0.000	0.759	0.9108	-0.012
Superior occipital gyrus L	0.287	0.292	0.005	0.092	0.6992	0.072
Superior occipital gyrus R	0.268	0.268	0.000	0.915494	0.993964914285714	0.005
Superior parietal lobule L	0.353	0.354	0.002	0.294	0.931	0.043
Superior parietal lobule R	0.374	0.375	0.001	0.504	0.926709677419355	-0.027
Superior temporal gyrus L	0.373	0.373	0.000	0.881	0.975087378640777	0.006
Superior temporal gyrus R	0.348	0.350	0.002	0.278	0.932117647058824	0.045
Supplementary motor cortex L	0.356	0.357	0.000	0.657	0.9855	-0.018
Supplementary motor cortex R	0.371	0.372	0.000	0.635	0.991643835616438	0.019
Supramarginal gyrus L	0.287	0.291	0.003	0.156	0.773217391304348	0.061
Supramarginal gyrus R	0.335	0.336	0.001	0.418	0.934352941176471	0.034
Temporal pole L	0.328	0.332	0.003	0.145	0.87	-0.061
Temporal pole R	0.358	0.360	0.002	0.215	0.845172413793103	-0.051
Thalamus proper L	0.200	0.201	0.002	0.380331	0.922504978723404	-0.040
Thalamus proper R	0.221	0.227	0.006	0.077	0.7315	-0.079
Transverse temporal gyrus L	0.237	0.237	0.000	0.717040	0.984850120481928	-0.016
Transverse temporal gyrus R	0.292	0.292	0.000	0.714	1	-0.016
Triangular part of the inferior frontal gyrus L	0.274	0.275	0.001	0.532	0.962666666666667	0.027
Triangular part of the inferior frontal gyrus R	0.253	0.254	0.001	0.447	0.909964285714286	-0.033

FDR: false discovery rate. L: left. PRS: polygenic risk score. R: right.

Table D.15: Associations between PRSwithAPOE Threshold 10 and 114 regions of interest in APOE ε4 carriers

Region of Interest	R Square (Model 1)	R Square (Model 2)	R Square Change	Sig. F Change (Model 2)	FDR Corrected value	Standardised beta of PRS
Accumbens area L	0.479	0.482	0.003	0.209	1	0.058
Accumbens area R	0.444	0.453	0.008	0.039	0.8892	0.098
Amygdala L	0.496	0.496	0.001	0.587	0.998776119402985	-0.025
Amygdala R	0.544	0.545	0.001	0.437	1	-0.034
Angular gyrus L	0.465	0.466	0.001	0.410	1	-0.038
Angular gyrus R	0.479	0.479	0.000	0.616	0.989070422535211	0.023
Anterior cingulate gyrus L	0.445	0.445	0.000	0.905	0.982571428571429	0.006
Anterior cingulate gyrus R	0.312	0.316	0.004	0.188	1	0.070
Anterior insula L	0.445	0.450	0.005	0.111	1	0.076
Anterior insula R	0.431	0.439	0.008	0.044	0.836	0.097
Anterior orbital gyrus L	0.420	0.421	0.001	0.481	1	-0.034
Anterior orbital gyrus R	0.387	0.390	0.003	0.217	1	-0.062
Basal forebrain L	0.375	0.378	0.003	0.252	1	0.058
Basal forebrain R	0.393	0.403	0.009	0.038	1	0.103
Calcarine cortex L	0.417	0.418	0.002	0.390	1	-0.042
Calcarine cortex R	0.424	0.431	0.006	0.074	0.937333333333333	-0.086
Caudate L	0.245	0.245	0.000	0.835	1	0.012
Caudate R	0.238	0.238	0.000	0.846	0.994268041237113	-0.011
Central operculum L	0.432	0.432	0.000	0.944	0.978327272727273	0.003
Central operculum R	0.425	0.425	0.000	0.987	0.987	-0.001
Cuneus L	0.445	0.446	0.002	0.368	1	-0.043
Cuneus R	0.444	0.444	0.000	0.778	1	-0.013
Entorhinal area L	0.483	0.483	0.000	0.631	0.985397260273973	-0.022
Entorhinal area R	0.536	0.536	0.000	0.876	0.988752475247525	0.007
Frontal operculum L	0.412	0.413	0.001	0.471815	1	0.035
Frontal operculum R	0.366	0.367	0.001	0.510	1	0.034

Frontal pole L	0.490	0.490	0.000	0.915	0.95697247706422	-0.005
Frontal pole R	0.461	0.465	0.003	0.183	1	0.062
Fusiform gyrus L	0.571	0.572	0.001	0.495	1	0.029
Fusiform gyrus R	0.614	0.615	0.001	0.545	1	0.024
Gyrus rectus L	0.506	0.507	0.001	0.559	1	-0.026
Gyrus rectus R	0.530	0.530	0.000	0.810	1	-0.011
Hippocampus L	0.567	0.569	0.001	0.333	1	-0.041
Hippocampus R	0.560	0.564	0.004	0.114	1	-0.067
Inferior occipital gyrus L	0.466	0.466	0.000	0.738	1	-0.016
Inferior occipital gyrus R	0.528	0.529	0.001	0.506	1	-0.029
Inferior temporal gyrus L	0.553	0.553	0.000	0.841	1	0.009
Inferior temporal gyrus R	0.584	0.585	0.001	0.330	1	0.040
Lateral orbital gyrus L	0.450	0.450	0.000	0.860	0.9804	0.008
Lateral orbital gyrus R	0.420	0.423	0.002	0.291	1	-0.051
Lingual gyrus L	0.515	0.515	0.000	0.980	0.9975	-0.001
Lingual gyrus R	0.537	0.537	0.000	0.983	0.991699115044248	0.001
Medial frontal cortex L	0.399	0.401	0.002	0.342	1	-0.047
Medial frontal cortex R	0.416	0.417	0.001	0.586	1	0.027
Medial orbital gyrus L	0.495	0.496	0.001	0.376	1	-0.040
Medial orbital gyrus R	0.484	0.486	0.001	0.367	1	-0.041
Middle cingulate gyrus L	0.382	0.386	0.005	0.142	1	0.074
Middle cingulate gyrus R	0.366	0.369	0.003	0.287	1	0.054
Middle frontal gyrus L	0.489	0.494	0.004	0.117	1	0.072
Middle frontal gyrus R	0.477	0.481	0.004	0.121	1	0.071
Middle occipital gyrus L	0.446	0.448	0.001	0.382	1	-0.042
Middle occipital gyrus R	0.410	0.412	0.002	0.341	1	-0.047
Middle temporal gyrus L	0.512	0.512	0.000	0.700	1	-0.017
Middle temporal gyrus R	0.565	0.565	0.000	0.838	1	0.009
Occipital fusiform gyrus L	0.495	0.497	0.002	0.309	1	0.046
Occipital fusiform gyrus R	0.583	0.583	0.000	0.880	0.983529411764706	0.006

Occipital pole L	0.368	0.369	0.001	0.471666	1	-0.037
Occipital pole R	0.387	0.387	0.000	0.859	0.989151515151515	0.009
Opercular part of the inferior frontal gyrus L	0.323	0.323	0.000	0.910	0.969532710280374	-0.006
Opercular part of the inferior frontal gyrus R	0.338	0.339	0.001	0.469	1	-0.038
Orbital part of the inferior frontal gyrus L	0.311	0.312	0.001	0.515	0.995084745762712	-0.035
Orbital part of the inferior frontal gyrus R	0.288	0.289	0.001	0.585	1	-0.029
Pallidum L	0.158	0.161	0.003	0.336	1	-0.056
Pallidum R	0.135	0.140	0.005	0.189	1	-0.078
Parahippocampal gyrus L	0.559	0.559	0.000	0.858	0.998081632653061	-0.008
Parahippocampal gyrus R	0.598	0.598	0.000	0.640	0.9728	-0.019
Parietal operculum L	0.357	0.358	0.002	0.379	1	0.045
Parietal operculum R	0.340	0.344	0.004	0.215	1	0.064
Planum polare L	0.517	0.517	0.000	0.721	1	-0.016
Planum polare R	0.542	0.543	0.001	0.435	1	-0.034
Planum temporale L	0.413	0.416	0.003	0.224	1	0.060
Planum temporale R	0.448	0.448	0.000	0.627	0.99275	-0.023
Postcentral gyrus L	0.424	0.425	0.000	0.636	0.979783783783784	-0.023
Postcentral gyrus R	0.427	0.428	0.001	0.613254	1	-0.024
Postcentral gyrus medial segment L	0.206	0.210	0.004	0.245	1	-0.066
Postcentral gyrus medial segment R	0.260	0.260	0.000	0.842	1	-0.011
Posterior cingulate gyrus L	0.582	0.582	0.000	0.724	1	0.015
Posterior cingulate gyrus R	0.540	0.541	0.000	0.660	0.99	-0.019
Posterior insula L	0.422	0.430	0.008	0.048	0.781714285714286	0.096
Posterior insula R	0.455	0.467	0.012	0.014	0.798	0.115
Posterior orbital gyrus L	0..435	0.435	0.000	0.904	0.990923076923077	-0.006
Posterior orbital gyrus R	0.452	0.453	0.001	0.551	1	-0.028
Precentral gyrus L	0.476	0.485	0.010	0.021	0.798	0.106
Precentral gyrus R	0.467	0.474	0.006	0.066	0.9405	0.085
Precentral gyrus medial segment L	0.350	0.352	0.002	0.302	1	-0.053
Precentral gyrus medial segment R	0.375	0.375	0.000	0.749	1	-0.016

Precuneus L	0.507	0.508	0.001	0.460	1	0.033
Precuneus R	0.500	0.500	0.000	0.906	0.974377358490566	0.005
Putamen L	0.348	0.352	0.004	0.201	1	0.066
Putamen R	0.375	0.380	0.005	0.137	1	0.075
Subcallosal area L	0.544	0.545	0.001	0.476	1	0.031
Subcallosal area R	0.558	0.561	0.004	0.125	1	0.065
Superior frontal gyrus L	0.475	0.476	0.001	0.403	1	0.039
Superior frontal gyrus R	0.509	0.522	0.014	0.005	0.57	0.125
Superior frontal gyrus medial segment L	0.440	0.441	0.000	0.732	1	0.016
Superior frontal gyrus medial segment R	0.422	0.424	0.002	0.362	1	0.044
Superior occipital gyrus L	0.369	0.370	0.001	0.598	1	-0.027
Superior occipital gyrus R	0.434	0.434	0.000	0.843	1	-0.010
Superior parietal lobule L	0.442	0.443	0.000	0.694	1	-0.019
Superior parietal lobule R	0.408	0.408	0.000	0.890	0.98504854368932	-0.007
Superior temporal gyrus L	0.507	0.509	0.002	0.326	1	-0.044
Superior temporal gyrus R	0.485	0.486	0.001	0.441	1	-0.035
Supplementary motor cortex L	0.379	0.379	0.000	0.701	1	-0.019
Supplementary motor cortex R	0.396	0.397	0.001	0.568	1	0.028
Supramarginal gyrus L	0.438	0.439	0.001	0.513	1	-0.031
Supramarginal gyrus R	0.407	0.408	0.001	0.539	1	0.030
Temporal pole L	0.491	0.491	0.000	0.779	0.997820224719101	0.013
Temporal pole R	0.484	0.484	0.000	0.725	1	0.016
Thalamus proper L	0.273	0.273	0.000	0.756	1	0.017
Thalamus proper R	0.326	0.326	0.000	0.830	1	0.011
Transverse temporal gyrus L	0.334	0.334	0.000	0.913	0.963722222222222	0.006
Transverse temporal gyrus R	0.437	0.437	0.000	0.958	0.983891891891892	-0.003
Triangular part of the inferior frontal gyrus L	0.384	0.385	0.001	0.613413	0.998986885714286	0.025
Triangular part of the inferior frontal gyrus R	0.356	0.357	0.000	0.769	1	-0.015

FDR: false discovery rate. L: left. PRS: polygenic risk score. R: right.

Table D.16: Associations between PRSwithoutAPOE Threshold 1 and 114 regions of interest in APOE ε4 non-carriers

Region of Interest	R Square (Model 1)	R Square (Model 2)	R Square Change	Sig. F Change (Model 2)	FDR Corrected value	Standardised beta of PRS
Accumbens area L	0.350	0.350	0.000	0.966	1	0.002
Accumbens area R	0.363	0.363	0.001	0.502	0.9538	-0.027
Amygdala L	0.349	0.351	0.001	0.338	0.988	-0.039
Amygdala R	0.400	0.402	0.002	0.273	0.8892	-0.043
Angular gyrus L	0.369	0.369	0.000	0.856917	1	0.007
Angular gyrus R	0.378	0.380	0.001	0.348	0.9918	0.037
Anterior cingulate gyrus L	0.397	0.402	0.005	0.069	1	0.071
Anterior cingulate gyrus R	0.205	0.207	0.002	0.263	0.908545454545455	-0.050
Anterior insula L	0.330	0.330	0.000	0.924	0.993735849056604	0.004
Anterior insula R	0.363	0.363	0.000	0.946	0.989394495412844	-0.003
Anterior orbital gyrus L	0.399	0.399	0.000	0.793	0.982630434782609	0.010
Anterior orbital gyrus R	0.346	0.347	0.001	0.372	0.986232558139535	0.036
Basal forebrain L	0.261	0.263	0.002	0.314	0.942	-0.044
Basal forebrain R	0.328	0.331	0.004	0.131	0.9956	-0.062
Calcarine cortex L	0.354	0.354	0.000	0.853	1	0.008
Calcarine cortex R	0.360	0.361	0.001	0.395	1	0.034
Caudate L	0.184	0.1850	0.001	0.591951	1	-0.024
Caudate R	0.180	0.183	0.003	0.208	0.94848	-0.057
Central operculum L	0.352	0.355	0.002	0.227	0.958444444444445	0.049
Central operculum R	0.360	0.363	0.002	0.210	0.920769230769231	0.050
Cuneus L	0.379	0.382	0.004	0.118	1	0.062
Cuneus R	0.422	0.422	0.000	0.980089	0.997590589285714	-0.001
Entorhinal area L	0.351	0.351	0.000	0.890	1	0.006
Entorhinal area R	0.395	0.395	0.000	0.748	1	-0.013
Frontal operculum L	0.347	0.350	0.003	0.159	1	0.057
Frontal operculum R	0.320	0.321	0.000	0.792	0.992175824175824	0.011

Frontal pole L	0.399	0.409	0.010	0.008	0.912	0.103
Frontal pole R	0.382	0.384	0.002	0.249	0.8870625	0.046
Fusiform gyrus L	0.459	0.459	0.000	0.724410	1	0.013
Fusiform gyrus R	0.458	0.459	0.000	0.622	0.998704225352113	0.018
Gyrus rectus L	0.390	0.395	0.005	0.059	1	0.074
Gyrus rectus R	0.391	0.391	0.000	0.893	0.998058823529412	0.005
Hippocampus L	0.349	0.357	0.008	0.024	1	-0.091
Hippocampus R	0.402	0.406	0.004	0.102	1	-0.064
Inferior occipital gyrus L	0.371	0.371	0.000	0.873	1	0.006
Inferior occipital gyrus R	0.418	0.421	0.003	0.172	0.933714285714286	0.052
Inferior temporal gyrus L	0.480	0.483	0.003	0.111	1	-0.058
Inferior temporal gyrus R	0.518	0.519	0.001	0.295	0.934166666666667	-0.037
Lateral orbital gyrus L	0.394	0.394	0.001	0.498	0.962237288135593	0.027
Lateral orbital gyrus R	0.325	0.325	0.000	0.729	1	0.014
Lingual gyrus L	0.516	0.517	0.000	0.580	1	0.019
Lingual gyrus R	0.518	0.521	0.003	0.091	1	0.059
Medial frontal cortex L	0.346	0.348	0.002	0.296	0.912	0.043
Medial frontal cortex R	0.354	0.355	0.001	0.439	1	0.031
Medial orbital gyrus L	0.470	0.473	0.002	0.175	0.906818181818182	0.050
Medial orbital gyrus R	0.407	0.409	0.002	0.237	0.964928571428571	0.046
Middle cingulate gyrus L	0.396	0.397	0.001	0.497	0.976862068965517	0.027
Middle cingulate gyrus R	0.336	0.336	0.000	0.916	0.994514285714286	0.004
Middle frontal gyrus L	0.467	0.470	0.003	0.140	0.938823529411765	0.054
Middle frontal gyrus R	0.468	0.468	0.001	0.407	1	0.030
Middle occipital gyrus L	0.295	0.295	0.000	0.925	0.985514018691589	0.004
Middle occipital gyrus R	0.327	0.327	0.000	0.870	1	0.007
Middle temporal gyrus L	0.498	0.498	0.000	0.763	0.888529411764706	-0.011
Middle temporal gyrus R	0.509	0.511	0.001	0.265	1	0.039
Occipital fusiform gyrus L	0.460	0.460	0.000	0.568	1	0.021
Occipital fusiform gyrus R	0.457	0.461	0.004	0.090	1	0.063

Occipital pole L	0.333	0.334	0.001	0.434	1	0.030
Occipital pole R	0.367	0.370	0.003	0.189	0.936782608695652	0.053
Opercular part of the inferior frontal gyrus L	0.222	0.228	0.006	0.087	1	0.076
Opercular part of the inferior frontal gyrus R	0.236	0.240	0.004	0.123	1	0.068
Orbital part of the inferior frontal gyrus L	0.261	0.261	0.000	0.820	1	0.010
Orbital part of the inferior frontal gyrus R	0.255	0.255	0.000	0.724488	1	-0.015
Pallidum L	0.183	0.183	0.000	0.770	1	-0.013
Pallidum R	0.160	0.160	0.000	0.624	0.988	-0.023
Parahippocampal gyrus L	0.427	0.428	0.000	0.570	1	-0.022
Parahippocampal gyrus R	0.458	0.458	0.000	0.709	1	0.014
Parietal operculum L	0.338	0.338	0.000	0.790	1	0.011
Parietal operculum R	0.276	0.276	0.000	0.775	0.992696629213483	0.012
Planum polare L	0.401	0.402	0.001	0.366	0.993428571428571	-0.035
Planum polare R	0.442	0.443	0.000	0.730	1	-0.013
Planum temporale L	0.321	0.321	0.000	0.610	1	-0.021
Planum temporale R	0.315	0.316	0.000	0.591705	1	0.022
Postcentral gyrus L	0.371	0.373	0.003	0.191	0.90725	0.052
Postcentral gyrus R	0.361	0.361	0.000	0.619	1	0.020
Postcentral gyrus medial segment L	0.208	0.209	0.001	0.487137111	1	0.031
Postcentral gyrus medial segment R	0.198	0.198	0.000	0.910	1	0.005
Posterior cingulate gyrus L	0.517	0.519	0.002	0.160	0.96	-0.049
Posterior cingulate gyrus R	0.485	0.485	0.000	0.934	0.985888888888889	-0.003
Posterior insula L	0.383	0.383	0.000	0.765	1	0.012
Posterior insula R	0.403	0.403	0.000	0.586	1	0.021
Posterior orbital gyrus L	0.317	0.317	0.000	0.911	0.998596153846154	-0.005
Posterior orbital gyrus R	0.321	0.322	0.001	0.487137147	1	-0.029
Precentral gyrus L	0.446	0.446	0.000	0.727	1	0.013
Precentral gyrus R	0.415	0.416	0.001	0.494359	1	0.026
Precentral gyrus medial segment L	0.258	0.258	0.000	0.990	0.99	0.001
Precentral gyrus medial segment R	0.304	0.304	0.000	0.884	1	0.006

Precuneus L	0.478	0.478	0.000	0.833	1	-0.008
Precuneus R	0.491	0.491	0.000	0.746	1	-0.012
Putamen L	0.227	0.230	0.003	0.238	0.935586206896552	-0.052
Putamen R	0.229	0.233	0.004	0.168	0.9576	-0.061
Subcallosal area L	0.428	0.428	0.000	0.771	0.998795454545454	0.011
Subcallosal area R	0.370	0.370	0.000	0.760	1	0.012
Superior frontal gyrus L	0.446	0.449	0.003	0.124	1	-0.058
Superior frontal gyrus R	0.460	0.460	0.000	0.980371	0.989046849557522	0.001
Superior frontal gyrus medial segment L	0.407	0.408	0.000	0.757	1	-0.022
Superior frontal gyrus medial segment R	0.406	0.407	0.001	0.479	1	0.028
Superior occipital gyrus L	0.287	0.291	0.004	0.136	0.969	0.063
Superior occipital gyrus R	0.268	0.269	0.001	0.489	1	0.030
Superior parietal lobule L	0.353	0.353	0.001	0.494846	0.989692	0.028
Superior parietal lobule R	0.374	0.374	0.000	0.857107	1	0.007
Superior temporal gyrus L	0.373	0.373	0.000	0.657	1	0.018
Superior temporal gyrus R	0.348	0.350	0.002	0.244	0.897290322580645	0.047
Supplementary motor cortex L	0.356	0.357	0.001	0.423	1	-0.032
Supplementary motor cortex R	0.371	0.372	0.000	0.597	1	-0.021
Supramarginal gyrus L	0.287	0.292	0.005	0.085	1	0.073
Supramarginal gyrus R	0.335	0.340	0.005	0.070	1	0.074
Temporal pole L	0.328	0.330	0.002	0.242	0.9196	-0.048
Temporal pole R	0.358	0.358	0.001	0.463	1	-0.030
Thalamus proper L	0.200	0.202	0.002	0.354	0.984292682926829	0.042
Thalamus proper R	0.221	0.221	0.000	0.738	1	0.015
Transverse temporal gyrus L	0.237	0.238	0.001	0.459	1	-0.033
Transverse temporal gyrus R	0.292	0.292	0.000	0.969	0.995189189189189	-0.002
Triangular part of the inferior frontal gyrus L	0.274	0.275	0.001	0.514	0.960590163934426	0.028
Triangular part of the inferior frontal gyrus R	0.253	0.254	0.001	0.460	1	0.032

FDR: false discovery rate. L: left. PRS: polygenic risk score. R: right.

Table D.17: Associations between PRSwithoutAPOE Threshold 1 and 114 regions of interest in APOE ε4 carriers

Region of Interest	R Square (Model 1)	R Square (Model 2)	R Square Change	Sig. F Change (Model 2)	FDR Corrected value	Standardised beta of PRS
Accumbens area L	0.479	0.482	0.002	0.245	1	-0.053
Accumbens area R	0.444	0.446	0.001	0.418	1	-0.038
Amygdala L	0.496	0.496	0.000	0.790	1	0.012
Amygdala R	0.544	0.544	0.000	0.822	1	0.010
Angular gyrus L	0.465	0.465	0.000	0.752	1	-0.015
Angular gyrus R	0.479	0.479	0.000	0.893	0.978865384615385	0.006
Anterior cingulate gyrus L	0.445	0.451	0.006	0.077	1	-0.083
Anterior cingulate gyrus R	0.312	0.312	0.000	0.870	1	-0.009
Anterior insula L	0.445	0.445	0.000	0.717	1	-0.017
Anterior insula R	0.431	0.432	0.001	0.398	1	-0.040
Anterior orbital gyrus L	0.420	0.421	0.000	0.715	1	-0.017
Anterior orbital gyrus R	0.387	0.387	0.000	0.778	1	0.014
Basal forebrain L	0.375	0.375	0.000	0.920	0.971111111111111	-0.005
Basal forebrain R	0.393	0.395	0.002	0.328	1	-0.048
Calcarine cortex L	0.417	0.419	0.002	0.309	1	0.049
Calcarine cortex R	0.424	0.425	0.001	0.498	1	-0.032
Caudate L	0.245	0.252	0.008	0.093	1	-0.092
Caudate R	0.238	0.244	0.006	0.126	1	-0.084
Central operculum L	0.432	0.432	0.000	0.635	1	-0.022
Central operculum R	0.425	0.425	0.001	0.532	1	-0.030
Cuneus L	0.445	0.445	0.001	0.602	1	0.024
Cuneus R	0.444	0.444	0.000	0.889	0.983941747572815	-0.007
Entorhinal area L	0.483	0.483	0.000	0.851	1	0.008
Entorhinal area R	0.536	0.536	0.000	0.883	0.986882352941177	-0.006
Frontal operculum L	0.412	0.412	0.002	0.340	1	-0.046
Frontal operculum R	0.366	0.368	0.001	0.473	1	-0.036

Frontal pole L	0.490	0.490	0.000	0.727	1	-0.016
Frontal pole R	0.461	0.462	0.001	0.560	1	0.027
Fusiform gyrus L	0.571	0.573	0.002	0.237	1	0.049
Fusiform gyrus R	0.614	0.615	0.000	0.549	1	0.023
Gyrus rectus L	0.506	0.508	0.002	0.292	1	-0.047
Gyrus rectus R	0.530	0.530	0.000	0.927	0.960709090909091	0.004
Hippocampus L	0.567	0.567	0.000	0.775	1	0.012
Hippocampus R	0.560	0.561	0.001	0.411	1	-0.034
Inferior occipital gyrus L	0.466	0.468	0.002	0.257	1	0.052
Inferior occipital gyrus R	0.528	0.528	0.000	0.876	0.99864	0.007
Inferior temporal gyrus L	0.553	0.553	0.000	0.797	1	-0.011
Inferior temporal gyrus R	0.584	0.584	0.000	0.646	1	0.019
Lateral orbital gyrus L	0.450	0.451	0.001	0.540	1	-0.029
Lateral orbital gyrus R	0.420	0.424	0.004	0.173	1	-0.065
Lingual gyrus L	0.515	0.519	0.004	0.119	1	0.068
Lingual gyrus R	0.537	0.537	0.000	0.610	1	0.022
Medial frontal cortex L	0.399	0.407	0.007	0.062	1	-0.091
Medial frontal cortex R	0.416	0.416	0.000	0.668	1	0.021
Medial orbital gyrus L	0.495	0.497	0.002	0.266	1	-0.050
Medial orbital gyrus R	0.484	0.485	0.001	0.553228	1	-0.027
Middle cingulate gyrus L	0.382	0.382	0.000	0.860	1	-0.009
Middle cingulate gyrus R	0.366	0.366	0.000	0.776	1	-0.014
Middle frontal gyrus L	0.489	0.489	0.000	0.788083	1	0.012
Middle frontal gyrus R	0.477	0.477	0.000	0.675	1	-0.019
Middle occipital gyrus L	0.446	0.446	0.000	0.912	0.990171428571428	-0.005
Middle occipital gyrus R	0.410	0.410	0.000	0.792	1	-0.013
Middle temporal gyrus L	0.512	0.512	0.000	0.926	0.97858407079646	-0.004
Middle temporal gyrus R	0.565	0.565	0.000	0.970	0.968477064220184	-0.002
Occipital fusiform gyrus L	0.495	0.501	0.006	0.060	1	0.084
Occipital fusiform gyrus R	0.583	0.583	0.000	0.623	1	0.020

Occipital pole L	0.368	0.369	0.001	0.517	1	0.032
Occipital pole R	0.387	0.387	0.000	0.787706	1	0.013
Opercular part of the inferior frontal gyrus L	0.323	0.335	0.012	0.027	1	-0.114
Opercular part of the inferior frontal gyrus R	0.338	0.349	0.011	0.033	1	-0.109
Orbital part of the inferior frontal gyrus L	0.311	0.312	0.001	0.478	1	-0.037
Orbital part of the inferior frontal gyrus R	0.288	0.293	0.005	0.152546	1	-0.076
Pallidum L	0.158	0.158	0.000	0.808	1	0.014
Pallidum R	0.135	0.135	0.000	0.689	1	-0.023
Parahippocampal gyrus L	0.559	0.563	0.004	0.100	1	0.068
Parahippocampal gyrus R	0.598	0.599	0.001	0.383	1	0.035
Parietal operculum L	0.357	0.357	0.000	0.747	1	-0.016
Parietal operculum R	0.340	0.341	0.001	0.575	1	-0.029
Planum polare L	0.517	0.517	0.001	0.562	1	0.025
Planum polare R	0.542	0.542	0.001	0.527	1	-0.027
Planum temporale L	0.413	0.413	0.000	0.861	1	0.008
Planum temporale R	0.448	0.448	0.000	0.658	1	-0.021
Postcentral gyrus L	0.424	0.427	0.003	0.213	1	-0.059
Postcentral gyrus R	0.427	0.428	0.001	0.496	1	0.032
Postcentral gyrus medial segment L	0.206	0.208	0.002	0.371	1	0.050
Postcentral gyrus medial segment R	0.260	0.262	0.002	0.388	1	-0.047
Posterior cingulate gyrus L	0.582	0.582	0.000	0.849	1	-0.008
Posterior cingulate gyrus R	0.540	0.541	0.000	0.641	1	-0.020
Posterior insula L	0.422	0.422	0.000	0.695	1	0.019
Posterior insula R	0.455	0.456	0.001	0.553356	1	0.028
Posterior orbital gyrus L	0.435	0.435	0.000	0.874	1	0.007
Posterior orbital gyrus R	0.452	0.453	0.001	0.414	1	-0.038
Precentral gyrus L	0.476	0.476	0.000	0.993	0.993	0.000
Precentral gyrus R	0.467	0.468	0.001	0.515	1	-0.030
Precentral gyrus medial segment L	0.350	0.350	0.000	0.960929	0.986900054054054	-0.002
Precentral gyrus medial segment R	0.375	0.375	0.000	0.961342	0.978508821428571	0.002

Precuneus L	0.507	0.507	0.000	0.722	1	0.016
Precuneus R	0.500	0.501	0.001	0.561	1	0.026
Putamen L	0.348	0.348	0.000	0.916	0.97592523364486	-0.005
Putamen R	0.375	0.376	0.000	0.673	1	-0.021
Subcallosal area L	0.544	0.546	0.002	0.280	1	-0.046
Subcallosal area R	0.558	0.558	0.000	0.714	1	-0.015
Superior frontal gyrus L	0.475	0.479	0.004	0.152898	1	-0.065
Superior frontal gyrus R	0.509	0.509	0.001	0.569	1	-0.025
Superior frontal gyrus medial segment L	0.440	0.444	0.003	0.212	1	-0.059
Superior frontal gyrus medial segment R	0.422	0.424	0.002	0.378	1	-0.042
Superior occipital gyrus L	0.369	0.369	0.000	0.881	0.99439603960396	-0.007
Superior occipital gyrus R	0.434	0.434	0.000	0.809	1	0.011
Superior parietal lobule L	0.442	0.443	0.001	0.534	1	0.029
Superior parietal lobule R	0.408	0.409	0.001	0.524	1	0.031
Superior temporal gyrus L	0.507	0.509	0.001	0.391	1	-0.038
Superior temporal gyrus R	0.485	0.485	0.000	0.852	1	-0.008
Supplementary motor cortex L	0.379	0.381	0.002	0.353	1	-0.046
Supplementary motor cortex R	0.396	0.397	0.001	0.579	1	-0.027
Supramarginal gyrus L	0.438	0.438	0.000	0.913	0.981905660377358	-0.005
Supramarginal gyrus R	0.407	0.408	0.001	0.485	1	0.034
Temporal pole L	0.491	0.491	0.000	0.644	1	-0.021
Temporal pole R	0.484	0.484	0.000	0.783	1	-0.012
Thalamus proper L	0.273	0.273	0.001	0.600	1	-0.028
Thalamus proper R	0.326	0.330	0.004	0.223	1	-0.063
Transverse temporal gyrus L	0.334	0.335	0.001	0.448	1	0.039
Transverse temporal gyrus R	0.437	0.438	0.000	0.780	1	-0.013
Triangular part of the inferior frontal gyrus L	0.384	0.387	0.003	0.249	1	-0.057
Triangular part of the inferior frontal gyrus R	0.356	0.360	0.004	0.185	1	-0.067

FDR: false discovery rate. L: left. PRS: polygenic risk score. R: right.

Table D.18: Associations between PRSwithoutAPOE Threshold 5 and 114 regions of interest in APOE ε4 non-carriers

Region of Interest	R Square (Model 1)	R Square (Model 2)	R Square Change	Sig. F Change (Model 2)	FDR Corrected value	Standardised beta of PRS
Accumbens area L	0.350	0.350	0.000	0.798	0.918909090909091	0.010
Accumbens area R	0.363	0.363	0.000	0.885	0.934166666666667	-0.006
Amygdala L	0.349	0.352	0.002	0.222603	1	-0.050
Amygdala R	0.400	0.402	0.002	0.256	0.94141935483871	-0.045
Angular gyrus L	0.369	0.370	0.001	0.496	0.8835	0.027
Angular gyrus R	0.378	0.380	0.002	0.248221	0.9432398	0.046
Anterior cingulate gyrus L	0.397	0.399	0.002	0.235	0.992222222222222	0.047
Anterior cingulate gyrus R	0.205	0.205	0.000	0.625650	0.963839189189189	-0.022
Anterior insula L	0.330	0.330	0.000	0.748	0.926869565217391	-0.013
Anterior insula R	0.363	0.364	0.001	0.489	0.913868852459016	-0.028
Anterior orbital gyrus L	0.399	0.400	0.001	0.477	0.9063	0.028
Anterior orbital gyrus R	0.346	0.348	0.003	0.199	1	0.053
Basal forebrain L	0.261	0.262	0.001	0.435	0.918333333333333	-0.034
Basal forebrain R	0.328	0.329	0.001	0.462	0.9405	-0.031
Calcarine cortex L	0.354	0.354	0.000	0.729	0.9234	-0.014
Calcarine cortex R	0.360	0.360	0.000	0.663	0.969	0.018
Caudate L	0.184	0.184	0.000	0.865	0.939142857142857	-0.008
Caudate R	0.180	0.182	0.001	0.417	0.896943396226415	-0.037
Central operculum L	0.352	0.355	0.003	0.186	1	0.054
Central operculum R	0.360	0.362	0.001	0.351	0.952714285714286	0.038
Cuneus L	0.379	0.381	0.002	0.214	1	0.050
Cuneus R	0.422	0.422	0.000	0.857	0.939403846153846	0.007
Entorhinal area L	0.351	0.351	0.000	0.726	0.9405	-0.014
Entorhinal area R	0.395	0.395	0.000	0.592	0.937333333333333	-0.021
Frontal operculum L	0.347	0.348	0.001	0.413	0.905423076923077	0.034
Frontal operculum R	0.320	0.320	0.000	0.918	0.942810810810811	0.004

Frontal pole L	0.399	0.414	0.015	0.001	0.114	0.125
Frontal pole R	0.382	0.385	0.003	0.132	1	0.060
Fusiform gyrus L	0.459	0.460	0.001	0.393	0.953234042553192	0.032
Fusiform gyrus R	0.458	0.460	0.001	0.312	0.912	0.038
Gyrus rectus L	0.390	0.392	0.003	0.181	1	0.053
Gyrus rectus R	0.391	0.391	0.000	0.851	0.941883495145631	-0.007
Hippocampus L	0.349	0.360	0.011	0.009	0.513	-0.107
Hippocampus R	0.402	0.408	0.006	0.044	0.716571428571429	-0.079
Inferior occipital gyrus L	0.371	0.371	0.000	0.978	0.978	-0.001
Inferior occipital gyrus R	0.418	0.424	0.006	0.041	0.779	0.079
Inferior temporal gyrus L	0.480	0.481	0.002	0.272	0.939636363636364	-0.040
Inferior temporal gyrus R	0.518	0.518	0.000	0.534	0.936553846153846	-0.022
Lateral orbital gyrus L	0.394	0.395	0.002	0.290	0.944571428571429	0.042
Lateral orbital gyrus R	0.325	0.326	0.001	0.347	0.98895	0.039
Lingual gyrus L	0.516	0.516	0.000	0.654	0.981	0.016
Lingual gyrus R	0.518	0.520	0.002	0.175	1	0.048
Medial frontal cortex L	0.346	0.348	0.001	0.404	0.92112	0.034
Medial frontal cortex R	0.354	0.356	0.002	0.295	0.934166666666667	0.043
Medial orbital gyrus L	0.470	0.473	0.003	0.116	1	0.058
Medial orbital gyrus R	0.407	0.409	0.002	0.205	1	0.049
Middle cingulate gyrus L	0.396	0.396	0.000	0.728	0.932494382022472	0.014
Middle cingulate gyrus R	0.336	0.337	0.001	0.551	0.897342857142857	0.025
Middle frontal gyrus L	0.467	0.469	0.002	0.263	0.9369375	0.041
Middle frontal gyrus R	0.468	0.468	0.000	0.784	0.931	0.010
Middle occipital gyrus L	0.295	0.295	0.000	0.655	0.96974025974026	0.019
Middle occipital gyrus R	0.327	0.329	0.002	0.247836	0.974251862068966	0.048
Middle temporal gyrus L	0.498	0.498	0.000	0.749	1	-0.011
Middle temporal gyrus R	0.509	0.511	0.002	0.163	0.918129032258065	0.050
Occipital fusiform gyrus L	0.460	0.461	0.001	0.379876	0.962352533333333	0.033
Occipital fusiform gyrus R	0.457	0.464	0.007	0.020	0.57	0.087

Occipital pole L	0.333	0.334	0.000	0.626114	0.95169328	0.020
Occipital pole R	0.367	0.372	0.005	0.080	0.912	0.070
Opercular part of the inferior frontal gyrus L	0.222	0.228	0.006	0.085	0.880909090909091	0.077
Opercular part of the inferior frontal gyrus R	0.236	0.243	0.007	0.057	0.722	0.084
Orbital part of the inferior frontal gyrus L	0.261	0.261	0.000	0.708	0.984292682926829	0.016
Orbital part of the inferior frontal gyrus R	0.255	0.255	0.000	0.872	0.937811320754717	-0.007
Pallidum L	0.183	0.183	0.000	0.711438	0.954163905882353	0.017
Pallidum R	0.160	0.160	0.000	0.904	0.936872727272727	0.006
Parahippocampal gyrus L	0.427	0.428	0.001	0.363	0.962372093023256	-0.035
Parahippocampal gyrus R	0.458	0.458	0.000	0.897	0.938146788990826	-0.005
Parietal operculum L	0.338	0.338	0.000	0.711003	0.976558337349398	0.015
Parietal operculum R	0.276	0.279	0.003	0.164	1	0.060
Planum polare L	0.401	0.403	0.003	0.183	1	-0.052
Planum polare R	0.442	0.443	0.000	0.674	0.972607594936709	-0.016
Planum temporale L	0.321	0.322	0.001	0.494856	0.895453714285714	-0.029
Planum temporale R	0.315	0.316	0.000	0.711462	0.943100790697674	0.016
Postcentral gyrus L	0.371	0.372	0.001	0.494766	0.909731032258064	0.027
Postcentral gyrus R	0.361	0.361	0.000	0.757	0.918063829787234	0.013
Postcentral gyrus medial segment L	0.208	0.208	0.000	0.823	0.928930693069307	0.010
Postcentral gyrus medial segment R	0.198	0.199	0.001	0.473	0.929689655172414	0.033
Posterior cingulate gyrus L	0.517	0.518	0.002	0.223329	0.979211769230769	-0.043
Posterior cingulate gyrus R	0.485	0.485	0.000	0.586	0.940901408450704	-0.020
Posterior insula L	0.383	0.384	0.000	0.711023	0.964959785714286	0.015
Posterior insula R	0.403	0.404	0.001	0.395	0.938125	0.033
Posterior orbital gyrus L	0.317	0.317	0.000	0.675	0.961875	0.018
Posterior orbital gyrus R	0.321	0.321	0.001	0.549	0.90704347826087	-0.025
Precentral gyrus L	0.446	0.446	0.001	0.470	0.94	0.027
Precentral gyrus R	0.415	0.417	0.002	0.242	0.985285714285714	0.045
Precentral gyrus medial segment L	0.258	0.258	0.000	0.794	0.923632653061225	0.011
Precentral gyrus medial segment R	0.304	0.305	0.000	0.746	0.93454945054945	0.014

Precuneus L	0.478	0.478	0.000	0.850	0.95	0.007
Precuneus R	0.491	0.491	0.000	0.941	0.949327433628319	0.003
Putamen L	0.227	0.229	0.001	0.398	0.925959183673469	-0.038
Putamen R	0.229	0.231	0.001	0.406	0.907529411764706	-0.037
Subcallosal area L	0.428	0.429	0.001	0.536	0.925818181818182	0.024
Subcallosal area R	0.370	0.371	0.001	0.474	0.915864406779661	0.029
Superior frontal gyrus L	0.446	0.447	0.001	0.542	0.922208955223881	-0.023
Superior frontal gyrus R	0.460	0.461	0.001	0.369	0.956045454545455	0.033
Superior frontal gyrus medial segment L	0.407	0.407	0.000	0.605	0.944794520547945	-0.020
Superior frontal gyrus medial segment R	0.406	0.406	0.000	0.808	0.92112	0.009
Superior occipital gyrus L	0.287	0.294	0.007	0.047	0.66975	0.085
Superior occipital gyrus R	0.268	0.270	0.002	0.296	0.912	0.045
Superior parietal lobule L	0.353	0.355	0.002	0.212	1	0.051
Superior parietal lobule R	0.374	0.374	0.000	0.785	0.922577319587629	0.011
Superior temporal gyrus L	0.373	0.374	0.001	0.349	0.970390243902439	0.038
Superior temporal gyrus R	0.348	0.349	0.002	0.304	0.912	0.042
Supplementary motor cortex L	0.356	0.357	0.000	0.770	0.924	-0.012
Supplementary motor cortex R	0.371	0.372	0.000	0.722	0.946068965517241	-0.014
Supramarginal gyrus L	0.287	0.294	0.007	0.039	0.8892	0.088
Supramarginal gyrus R	0.335	0.345	0.010	0.015	0.57	0.101
Temporal pole L	0.328	0.329	0.001	0.453	0.938945454545455	-0.031
Temporal pole R	0.358	0.358	0.000	0.684	0.962666666666667	-0.017
Thalamus proper L	0.200	0.202	0.002	0.279	0.935470588235294	0.049
Thalamus proper R	0.221	0.221	0.000	0.874	0.931177570093458	0.007
Transverse temporal gyrus L	0.237	0.238	0.001	0.380295	0.942470217391304	-0.039
Transverse temporal gyrus R	0.292	0.292	0.000	0.938	0.95475	-0.003
Triangular part of the inferior frontal gyrus L	0.274	0.275	0.001	0.543	0.910323529411765	0.026
Triangular part of the inferior frontal gyrus R	0.253	0.256	0.003	0.200	1	0.056

FDR: false discovery rate. L: left. PRS: polygenic risk score. R: right.

Table D.19: Associations between PRSwithoutAPOE Threshold 5 and 114 regions of interest in APOE ε4 carriers

Region of Interest	R Square (Model 1)	R Square (Model 2)	R Square Change	Sig. F Change (Model 2)	FDR Corrected value	Standardised beta of PRS
Accumbens area L	0.479	0.481	0.002	0.335	1	-0.044
Accumbens area R	0.444	0.446	0.001	0.450	1	-0.036
Amygdala L	0.496	0.496	0.000	0.728	1	-0.016
Amygdala R	0.544	0.544	0.000	0.952	1	-0.003
Angular gyrus L	0.465	0.465	0.000	0.655	1	-0.021
Angular gyrus R	0.479	0.479	0.000	0.941	1	0.003
Anterior cingulate gyrus L	0.445	0.448	0.003	0.206	1	-0.059
Anterior cingulate gyrus R	0.312	0.312	0.000	0.827	1	0.011
Anterior insula L	0.445	0.455	0.000	0.841	1	0.009
Anterior insula R	0.431	0.431	0.000	0.626	1	-0.023
Anterior orbital gyrus L	0.420	0.421	0.000	0.671	1	-0.020
Anterior orbital gyrus R	0.387	0.388	0.000	0.650	1	0.022
Basal forebrain L	0.375	0.375	0.000	0.926	1	0.005
Basal forebrain R	0.393	0.394	0.001	0.525	1	-0.031
Calcarine cortex L	0.417	0.417	0.000	0.835	1	0.010
Calcarine cortex R	0.424	0.424	0.003	0.207	1	-0.060
Caudate L	0.245	0.249	0.004	0.201	1	-0.070
Caudate R	0.238	0.244	0.005	0.154	1	-0.078
Central operculum L	0.432	0.432	0.000	0.831292	1	0.010
Central operculum R	0.425	0.425	0.000	0.720901	1	0.017
Cuneus L	0.445	0.445	0.001	0.586	1	0.026
Cuneus R	0.444	0.444	0.000	0.854	1	0.009
Entorhinal area L	0.483	0.483	0.000	0.928	1	0.004
Entorhinal area R	0.536	0.536	0.000	0.799	1	0.011
Frontal operculum L	0.412	0.412	0.000	0.986	1	-0.001
Frontal operculum R	0.366	0.367	0.000	0.783958	1	0.014

Frontal pole L	0.490	0.490	0.000	0.966	1	-0.002
Frontal pole R	0.461	0.463	0.002	0.370	1	0.042
Fusiform gyrus L	0.571	0.576	0.005	0.071	1	0.074
Fusiform gyrus R	0.614	0.616	0.002	0.271	1	0.043
Gyrus rectus L	0.506	0.507	0.000	0.649	1	-0.020
Gyrus rectus R	0.530	0.530	0.000	0.897	1	0.006
Hippocampus L	0.567	0.567	0.000	0.836	1	-0.009
Hippocampus R	0.560	0.561	0.001	0.364	1	-0.038
Inferior occipital gyrus L	0.466	0.468	0.002	0.341997	1	0.044
Inferior occipital gyrus R	0.528	0.528	0.000	0.968	1	-0.002
Inferior temporal gyrus L	0.553	0.553	0.000	0.956	1	-0.002
Inferior temporal gyrus R	0.584	0.584	0.000	0.616	1	0.020
Lateral orbital gyrus L	0.450	0.450	0.000	0.972	1	-0.002
Lateral orbital gyrus R	0.420	0.422	0.002	0.373	1	-0.043
Lingual gyrus L	0.515	0.518	0.003	0.192	1	0.057
Lingual gyrus R	0.537	0.537	0.000	0.747998	1	0.014
Medial frontal cortex L	0.399	0.400	0.001	0.474	1	-0.035
Medial frontal cortex R	0.416	0.418	0.002	0.285	1	0.051
Medial orbital gyrus L	0.495	0.496	0.000	0.603	1	-0.023
Medial orbital gyrus R	0.484	0.484	0.000	0.977152	1	-0.001
Middle cingulate gyrus L	0.382	0.382	0.000	0.805	1	0.012
Middle cingulate gyrus R	0.366	0.366	0.000	0.830882	1	-0.011
Middle frontal gyrus L	0.489	0.489	0.000	0.723	1	0.016
Middle frontal gyrus R	0.477	0.477	0.000	0.853	1	-0.008
Middle occipital gyrus L	0.446	0.447	0.000	0.783914	1	0.013
Middle occipital gyrus R	0.410	0.410	0.000	0.893	1	0.007
Middle temporal gyrus L	0.512	0.512	0.000	0.709	1	-0.016
Middle temporal gyrus R	0.565	0.565	0.000	0.844	1	-0.008
Occipital fusiform gyrus L	0.495	0.500	0.005	0.080	1	0.078
Occipital fusiform gyrus R	0.583	0.583	0.001	0.540	1	0.025

Occipital pole L	0.368	0.368	0.000	0.683	1	0.021
Occipital pole R	0.387	0.387	0.000	0.878	1	0.008
Opercular part of the inferior frontal gyrus L	0.323	0.334	0.011	0.031	1	-0.111
Opercular part of the inferior frontal gyrus R	0.338	0.344	0.006	0.119	1	-0.080
Orbital part of the inferior frontal gyrus L	0.311	0.311	0.000	0.796	1	-0.014
Orbital part of the inferior frontal gyrus R	0.288	0.290	0.002	0.425580	1	-0.042
Pallidum L	0.158	0.158	0.000	0.729	1	-0.020
Pallidum R	0.135	0.0137	0.002	0.425819	1	-0.047
Parahippocampal gyrus L	0.559	0.562	0.003	0.189	1	0.055
Parahippocampal gyrus R	0.598	0.599	0.001	0.328456	1	0.039
Parietal operculum L	0.357	0.358	0.001	0.433064	1	0.040
Parietal operculum R	0.340	0.340	0.000	0.977420	1	0.001
Planum polare L	0.517	0.517	0.000	0.755	1	0.014
Planum polare R	0.542	0.542	0.000	0.639	1	-0.020
Planum temporale L	0.413	0.413	0.000	0.846	1	0.009
Planum temporale R	0.448	0.449	0.001	0.518	1	-0.030
Postcentral gyrus L	0.424	0.432	0.007	0.057	1	-0.091
Postcentral gyrus R	0.427	0.427	0.000	0.852	1	-0.009
Postcentral gyrus medial segment L	0.206	0.207	0.001	0.663	1	0.024
Postcentral gyrus medial segment R	0.260	0.261	0.001	0.499	1	-0.037
Posterior cingulate gyrus L	0.582	0.582	0.000	0.678	1	-0.017
Posterior cingulate gyrus R	0.540	0.541	0.001	0.513	1	-0.028
Posterior insula L	0.422	0.424	0.002	0.278	1	0.052
Posterior insula R	0.455	0.459	0.003	0.188	1	0.061
Posterior orbital gyrus L	0.435	0.436	0.001	0.500	1	0.032
Posterior orbital gyrus R	0.452	0.452	0.000	0.710	1	-0.017
Precentral gyrus L	0.476	0.476	0.000	0.636	1	-0.022
Precentral gyrus R	0.467	0.468	0.001	0.541	1	-0.028
Precentral gyrus medial segment L	0.350	0.351	0.001	0.514	1	-0.033
Precentral gyrus medial segment R	0.375	0.375	0.000	0.901	1	-0.006

Precuneus L	0.507	0.507	0.000	0.747698	1	0.014
Precuneus R	0.500	0.500	0.000	0.721401	1	0.016
Putamen L	0.348	0.348	0.000	0.818	1	0.012
Putamen R	0.375	0.375	0.000	0.995	1	0.000
Subcallosal area L	0.544	0.544	0.000	0.980	1	0.001
Subcallosal area R	0.558	0.559	0.001	0.480	1	0.030
Superior frontal gyrus L	0.475	0.475	0.000	0.666	1	-0.020
Superior frontal gyrus R	0.509	0.509	0.000	0.998	0.998	0.000
Superior frontal gyrus medial segment L	0.440	0.444	0.004	0.161	1	-0.066
Superior frontal gyrus medial segment R	0.422	0.424	0.002	0.341660	1	-0.046
Superior occipital gyrus L	0.369	0.369	0.000	0.963	1	-0.002
Superior occipital gyrus R	0.434	0.434	0.000	0.992	1	0.000
Superior parietal lobule L	0.442	0.443	0.001	0.552	1	0.028
Superior parietal lobule R	0.408	0.408	0.000	0.732	1	0.017
Superior temporal gyrus L	0.507	0.512	0.005	0.090	1	-0.075
Superior temporal gyrus R	0.485	0.486	0.001	0.425	1	-0.036
Supplementary motor cortex L	0.379	0.384	0.005	0.125	1	-0.076
Supplementary motor cortex R	0.396	0.397	0.000	0.651	1	-0.022
Supramarginal gyrus L	0.438	0.438	0.000	0.967	1	-0.002
Supramarginal gyrus R	0.407	0.409	0.002	0.349	1	0.045
Temporal pole L	0.491	0.491	0.001	0.527	1	-0.028
Temporal pole R	0.484	0.484	0.000	0.763	1	-0.014
Thalamus proper L	0.273	0.274	0.002	0.433410	1	-0.042
Thalamus proper R	0.326	0.333	0.006	0.099	1	-0.085
Transverse temporal gyrus L	0.334	0.334	0.000	0.747	1	0.017
Transverse temporal gyrus R	0.437	0.437	0.000	0.865	1	-0.008
Triangular part of the inferior frontal gyrus L	0.384	0.387	0.003	0.276	1	-0.054
Triangular part of the inferior frontal gyrus R	0.356	0.359	0.002	0.328234	1	-0.049

FDR: false discovery rate. L: left. PRS: polygenic risk score. R: right.

Table D.20: Associations between PRSwithoutAPOE Threshold 10 and 114 regions of interest in APOE ε4 non-carriers

Region of Interest	R Square (Model 1)	R Square (Model 2)	R Square Change	Sig. F Change (Model 2)	FDR Corrected value	Standardised beta of PRS
Accumbens area L	0.350	0.350	0.000	0.601015	0.938571369863014	-0.022
Accumbens area R	0.363	0.363	0.001	0.539012	0.991086580645161	-0.026
Amygdala L	0.349	0.352	0.003	0.189	1	-0.056
Amygdala R	0.400	0.402	0.002	0.302	0.8607	-0.043
Angular gyrus L	0.369	0.372	0.003	0.155	1	0.060
Angular gyrus R	0.378	0.380	0.002	0.245	0.963103448275862	0.049
Anterior cingulate gyrus L	0.397	0.399	0.003	0.173770	1	0.056
Anterior cingulate gyrus R	0.205	0.205	0.000	0.681	0.892344827586207	0.019
Anterior insula L	0.330	0.331	0.001	0.391	0.89148	-0.037
Anterior insula R	0.363	0.365	0.002	0.261	0.9298125	-0.048
Anterior orbital gyrus L	0.399	0.400	0.001	0.462	0.9576	0.030
Anterior orbital gyrus R	0.346	0.347	0.002	0.285	0.9025	0.046
Basal forebrain L	0.261	0.264	0.003	0.174393	1	-0.062
Basal forebrain R	0.328	0.329	0.002	0.296	0.865230769230769	-0.045
Calcarine cortex L	0.354	0.355	0.001	0.336	0.870545454545455	-0.041
Calcarine cortex R	0.360	0.360	0.000	0.968	0.994162162162162	0.002
Caudate L	0.184	0.185	0.001	0.559	0.951134328358209	-0.028
Caudate R	0.180	0.182	0.001	0.416	0.912	-0.039
Central operculum L	0.352	0.354	0.002	0.295	0.885	0.045
Central operculum R	0.360	0.360	0.000	0.871	0.95475	0.007
Cuneus L	0.379	0.379	0.000	0.635	0.916329113924051	0.020
Cuneus R	0.422	0.423	0.001	0.547	0.989809523809524	-0.024
Entorhinal area L	0.351	0.351	0.000	0.600980	0.951551666666667	-0.022
Entorhinal area R	0.395	0.395	0.001	0.500	1	-0.028
Frontal operculum L	0.347	0.347	0.001	0.566	0.921771428571428	0.025
Frontal operculum R	0.320	0.321	0.000	0.610	0.9272	-0.022

Frontal pole L	0.399	0.411	0.013	0.003	0.342	0.120
Frontal pole R	0.382	0.387	0.005	0.064	0.810666666666667	0.077
Fusiform gyrus L	0.459	0.461	0.002	0.232	0.979555555555556	0.047
Fusiform gyrus R	0.458	0.461	0.002	0.204	0.969	0.050
Gyrus rectus L	0.390	0.391	0.001	0.378	0.89775	0.037
Gyrus rectus R	0.391	0.391	0.000	0.921	0.963247706422018	-0.004
Hippocampus L	0.349	0.359	0.010	0.011	0.418	-0.109
Hippocampus R	0.402	0.407	0.005	0.078	0.808363636363636	-0.072
Inferior occipital gyrus L	0.371	0.371	0.000	0.924	0.9576	0.004
Inferior occipital gyrus R	0.418	0.423	0.005	0.063	0.89775	0.075
Inferior temporal gyrus L	0.480	0.480	0.001	0.529	1	-0.024
Inferior temporal gyrus R	0.518	0.518	0.000	0.884	0.959771428571428	-0.005
Lateral orbital gyrus L	0.394	0.398	0.004	0.098	0.931	0.068
Lateral orbital gyrus R	0.325	0.325	0.000	0.859	0.960058823529412	-0.008
Lingual gyrus L	0.516	0.516	0.000	0.822	0.956204081632653	-0.008
Lingual gyrus R	0.518	0.520	0.003	0.142	1	0.054
Medial frontal cortex L	0.346	0.347	0.000	0.748	0.907148936170213	0.014
Medial frontal cortex R	0.354	0.355	0.001	0.563	0.930173913043478	0.025
Medial orbital gyrus L	0.470	0.473	0.003	0.124	1	0.059
Medial orbital gyrus R	0.407	0.408	0.001	0.327	0.86693023255814	0.040
Middle cingulate gyrus L	0.396	0.398	0.002	0.229	1	0.050
Middle cingulate gyrus R	0.336	0.339	0.003	0.197	1	0.056
Middle frontal gyrus L	0.467	0.468	0.001	0.445	0.939444444444445	0.030
Middle frontal gyrus R	0.468	0.468	0.000	0.911	0.961611111111111	-0.004
Middle occipital gyrus L	0.295	0.295	0.000	0.630	0.920769230769231	0.021
Middle occipital gyrus R	0.327	0.327	0.000	0.620	0.917922077922078	0.022
Middle temporal gyrus L	0.498	0.498	0.000	0.849	0.8664	0.007
Middle temporal gyrus R	0.509	0.513	0.004	0.076	0.977636363636364	0.066
Occipital fusiform gyrus L	0.460	0.460	0.000	0.609	0.938189189189189	0.020
Occipital fusiform gyrus R	0.457	0.463	0.006	0.036	0.8208	0.082

Occipital pole L	0.333	0.333	0.000	0.895	0.962547169811321	0.006
Occipital pole R	0.367	0.368	0.001	0.373	0.924391304347826	0.038
Opercular part of the inferior frontal gyrus L	0.222	0.224	0.002	0.280	0.912	0.051
Opercular part of the inferior frontal gyrus R	0.236	0.238	0.002	0.316	0.878634146341463	0.047
Orbital part of the inferior frontal gyrus L	0.261	0.261	0.000	0.679	0.900069767441861	0.019
Orbital part of the inferior frontal gyrus R	0.255	0.255	0.000	0.764	0.90725	-0.014
Pallidum L	0.183	0.183	0.000	0.742	0.909548387096774	0.016
Pallidum R	0.160	0.160	0.000	0.740	0.91695652173913	0.016
Parahippocampal gyrus L	0.427	0.427	0.000	0.619	0.9285	-0.020
Parahippocampal gyrus R	0.458	0.458	0.000	0.994647	1	0.000
Parietal operculum L	0.338	0.338	0.000	0.695	0.890224719101124	0.017
Parietal operculum R	0.276	0.277	0.001	0.415	0.927647058823529	0.037
Planum polare L	0.401	0.406	0.005	0.062	1	-0.077
Planum polare R	0.442	0.443	0.000	0.656	0.890285714285714	-0.018
Planum temporale L	0.321	0.328	0.007	0.042	0.798	-0.089
Planum temporale R	0.315	0.316	0.000	0.734	0.919516483516484	-0.015
Postcentral gyrus L	0.371	0.371	0.000	0.645	0.907777777777778	0.019
Postcentral gyrus R	0.361	0.363	0.002	0.289	0.890432432432432	0.045
Postcentral gyrus medial segment L	0.208	0.210	0.002	0.257	0.945096774193548	0.054
Postcentral gyrus medial segment R	0.198	0.203	0.005	0.123	1	0.073
Posterior cingulate gyrus L	0.517	0.517	0.000	0.723	0.9158	-0.013
Posterior cingulate gyrus R	0.485	0.485	0.000	0.759	0.9108	0.012
Posterior insula L	0.383	0.383	0.000	0.856	0.966178217821782	-0.008
Posterior insula R	0.403	0.403	0.000	0.640	0.912	0.019
Posterior orbital gyrus L	0.317	0.318	0.000	0.650	0.892771084337349	0.020
Posterior orbital gyrus R	0.321	0.321	0.000	0.815	0.957835051546392	-0.010
Precentral gyrus L	0.446	0.447	0.001	0.388	0.90269387755102	0.034
Precentral gyrus R	0.415	0.416	0.001	0.535	1	0.025
Precentral gyrus medial segment L	0.258	0.260	0.002	0.244	0.993428571428571	0.053
Precentral gyrus medial segment R	0.304	0.305	0.001	0.562	0.942176470588235	0.026

Precuneus L	0.478	0.479	0.001	0.423	0.909849056603774	0.031
Precuneus R	0.491	0.491	0.000	0.538618	1	0.023
Putamen L	0.227	0.228	0.001	0.555	0.958636363636364	-0.028
Putamen R	0.229	0.230	0.001	0.525	1	-0.030
Subcallosal area L	0.428	0.430	0.001	0.323	0.876714285714286	0.040
Subcallosal area R	0.370	0.372	0.002	0.252	0.9576	0.048
Superior frontal gyrus L	0.446	0.448	0.002	0.270904	0.935850181818182	-0.044
Superior frontal gyrus R	0.460	0.461	0.002	0.271357	0.909844058823529	0.043
Superior frontal gyrus medial segment L	0.407	0.408	0.001	0.551	0.98146875	-0.024
Superior frontal gyrus medial segment R	0.406	0.406	0.000	0.852	0.97128	0.008
Superior occipital gyrus L	0.287	0.290	0.003	0.202	1	0.057
Superior occipital gyrus R	0.268	0.269	0.000	0.648	0.900878048780488	0.021
Superior parietal lobule L	0.353	0.356	0.003	0.176	1	0.058
Superior parietal lobule R	0.374	0.374	0.000	0.905	0.964205607476635	0.005
Superior temporal gyrus L	0.373	0.373	0.000	0.686	0.888681818181818	0.017
Superior temporal gyrus R	0.348	0.350	0.002	0.210	0.9576	0.054
Supplementary motor cortex L	0.356	0.357	0.001	0.553	0.969876923076923	-0.025
Supplementary motor cortex R	0.371	0.371	0.000	0.863	0.955165048543689	0.007
Supramarginal gyrus L	0.287	0.297	0.010	0.015	0.4275	0.109
Supramarginal gyrus R	0.335	0.348	0.013	0.004	0.228	0.123
Temporal pole L	0.328	0.329	0.001	0.475	0.966964285714286	-0.031
Temporal pole R	0.358	0.358	0.000	0.995161	0.995161	0.000
Thalamus proper L	0.200	0.201	0.002	0.377	0.914425531914894	0.042
Thalamus proper R	0.221	0.221	0.000	0.665	0.891882352941176	0.020
Transverse temporal gyrus L	0.237	0.241	0.004	0.125	0.95	-0.071
Transverse temporal gyrus R	0.292	0.292	0.001	0.576	0.924845070422535	-0.025
Triangular part of the inferior frontal gyrus L	0.274	0.274	0.000	0.993	1	0.000
Triangular part of the inferior frontal gyrus R	0.253	0.254	0.001	0.364	0.922133333333333	0.041

FDR: false discovery rate. L: left. PRS: polygenic risk score. R: right.

Table D.21: Associations between PRSwithoutAPOE Threshold 10 and 114 regions of interest in APOE ε4 carriers

Region of Interest	R Square (Model 1)	R Square (Model 2)	R Square Change	Sig. F Change (Model 2)	FDR Corrected value	Standardised beta of PRS
Accumbens area L	0.479	0.484	0.004	0.128	1	-0.070
Accumbens area R	0.444	0.446	0.001	0.433	1	-0.037
Amygdala L	0.496	0.500	0.005	0.111	1	-0.072
Amygdala R	0.544	0.547	0.003	0.192	1	-0.056
Angular gyrus L	0.465	0.465	0.000	0.969	1	0.002
Angular gyrus R	0.479	0.479	0.001	0.522	1	0.029
Anterior cingulate gyrus L	0.445	0.448	0.003	0.190	1	-0.062
Anterior cingulate gyrus R	0.312	0.312	0.000	0.761	1	0.016
Anterior insula L	0.445	0.445	0.000	0.840	1	0.010
Anterior insula R	0.431	0.431	0.000	0.831	1	-0.010
Anterior orbital gyrus L	0.420	0.421	0.001	0.601	1	-0.025
Anterior orbital gyrus R	0.387	0.388	0.000	0.663	1	0.022
Basal forebrain L	0.375	0.375	0.000	0.715	1	0.018
Basal forebrain R	0.393	0.393	0.000	0.935780	1	-0.004
Calcarine cortex L	0.417	0.417	0.000	0.988	0.996743362831858	0.001
Calcarine cortex R	0.424	0.425	0.001	0.600	1	-0.025
Caudate L	0.245	0.247	0.002	0.344	1	-0.052
Caudate R	0.238	0.241	0.003	0.276	1	-0.060
Central operculum L	0.432	0.432	0.000	0.738	1	0.016
Central operculum R	0.425	0.427	0.003	0.267	1	0.053
Cuneus L	0.445	0.446	0.001	0.496925	1	0.032
Cuneus R	0.444	0.445	0.001	0.491	1	0.033
Entorhinal area L	0.483	0.486	0.003	0.197	1	-0.059
Entorhinal area R	0.536	0.538	0.002	0.254	1	-0.049
Frontal operculum L	0.412	0.412	0.000	0.649	1	0.022
Frontal operculum R	0.366	0.367	0.000	0.801	1	0.013

Frontal pole L	0.490	0.491	0.001	0.484	1	0.032
Frontal pole R	0.461	0.0465	0.003	0.182	1	0.062
Fusiform gyrus L	0.571	0.572	0.001	0.454842	1	0.031
Fusiform gyrus R	0.614	0.614	0.000	0.970	0.996216216216216	0.001
Gyrus rectus L	0.506	0.508	0.002	0.340	1	-0.043
Gyrus rectus R	0.530	0.530	0.000	0.860	1	0.008
Hippocampus L	0.567	0.572	0.005	0.085	1	-0.072
Hippocampus R	0.560	0.566	0.006	0.041	1	-0.086
Inferior occipital gyrus L	0.466	0.467	0.001	0.487	1	0.032
Inferior occipital gyrus R	0.528	0.528	0.000	0.606	1	0.023
Inferior temporal gyrus L	0.553	0.553	0.001	0.498	1	-0.029
Inferior temporal gyrus R	0.584	0.584	0.000	0.762	1	-0.012
Lateral orbital gyrus L	0.450	0.450	0.000	0.923	1	-0.005
Lateral orbital gyrus R	0.420	0.421	0.001	0.560	1	-0.028
Lingual gyrus L	0.515	0.516	0.001	0.454966	1	0.033
Lingual gyrus R	0.537	0.538	0.001	0.408	1	0.036
Medial frontal cortex L	0.399	0.403	0.004	0.172	1	-0.067
Medial frontal cortex R	0.416	0.417	0.001	0.494	1	0.033
Medial orbital gyrus L	0.495	0.496	0.001	0.520	1	-0.029
Medial orbital gyrus R	0.484	0.484	0.000	0.830	1	-0.010
Middle cingulate gyrus L	0.382	0.382	0.000	0.918	1	0.005
Middle cingulate gyrus R	0.366	0.367	0.000	0.647	1	0.023
Middle frontal gyrus L	0.489	0.490	0.001	0.508	1	0.030
Middle frontal gyrus R	0.477	0.477	0.000	0.829	1	0.010
Middle occipital gyrus L	0.446	0.446	0.000	0.796	1	0.012
Middle occipital gyrus R	0.410	0.410	0.000	0.700	1	0.019
Middle temporal gyrus L	0.512	0.513	0.001	0.424	1	-0.036
Middle temporal gyrus R	0.565	0.565	0.001	0.546	1	-0.025
Occipital fusiform gyrus L	0.495	0.497	0.002	0.304	1	0.046
Occipital fusiform gyrus R	0.583	0.583	0.000	0.926	1	0.004

Occipital pole L	0.368	0.368	0.000	0.794	1	-0.013
Occipital pole R	0.387	0.387	0.000	0.936229	0.997477626168224	0.004
Opercular part of the inferior frontal gyrus L	0.323	0.329	0.006	0.129	1	-0.079
Opercular part of the inferior frontal gyrus R	0.338	0.344	0.006	0.102	1	-0.084
Orbital part of the inferior frontal gyrus L	0.311	0.313	0.002	0.375	1	-0.047
Orbital part of the inferior frontal gyrus R	0.288	0.288	0.000	0.786	1	-0.015
Pallidum L	0.158	0.158	0.000	0.775	1	0.017
Pallidum R	0.135	0.135	0.000	0.807	1	0.014
Parahippocampal gyrus L	0.559	0.560	0.000	0.597	1	-0.022
Parahippocampal gyrus R	0.598	0.599	0.001	0.504	1	-0.027
Parietal operculum L	0.357	0.357	0.001	0.544675	1	0.031
Parietal operculum R	0.340	0.340	0.000	0.945	0.9975	0.004
Planum polare L	0.517	0.517	0.000	0.915	1	-0.005
Planum polare R	0.542	0.543	0.001	0.411	1	-0.035
Planum temporale L	0.413	0.414	0.001	0.489	1	0.034
Planum temporale R	0.448	0.448	0.000	0.956	0.999853211009174	0.003
Postcentral gyrus L	0.424	0.431	0.007	0.071	1	-0.087
Postcentral gyrus R	0.427	0.427	0.000	1.000	1	0.000
Postcentral gyrus medial segment L	0.206	0.207	0.001	0.544732	1	0.034
Postcentral gyrus medial segment R	0.260	0.260	0.000	0.823	1	-0.012
Posterior cingulate gyrus L	0.582	0.582	0.001	0.495	1	-0.028
Posterior cingulate gyrus R	0.540	0.540	0.000	0.894	1	-0.006
Posterior insula L	0.422	0.422	0.000	0.785	1	0.013
Posterior insula R	0.455	0.459	0.003	0.198	1	0.060
Posterior orbital gyrus L	0.435	0.435	0.000	0.898	1	0.006
Posterior orbital gyrus R	0.452	0.452	0.000	0.655	1	-0.021
Precentral gyrus L	0.476	0.476	0.000	0.704	1	-0.017
Precentral gyrus R	0.467	0.467	0.000	0.693	1	-0.018
Precentral gyrus medial segment L	0.350	0.350	0.000	0.886	1	-0.007
Precentral gyrus medial segment R	0.375	0.376	0.001	0.620	1	0.025

Precuneus L	0.507	0.509	0.002	0.353	1	0.041
Precuneus R	0.500	0.502	0.002	0.331	1	0.044
Putamen L	0.348	0.348	0.000	0.838	1	0.011
Putamen R	0.375	0.375	0.000	0.916	1	-0.005
Subcallosal area L	0.544	0.544	0.000	0.892	1	-0.006
Subcallosal area R	0.558	0.559	0.002	0.293	1	0.044
Superior frontal gyrus L	0.475	0.475	0.000	0.652	1	-0.021
Superior frontal gyrus R	0.509	0.509	0.000	0.625	1	0.022
Superior frontal gyrus medial segment L	0.440	0.442	0.001	0.425	1	-0.038
Superior frontal gyrus medial segment R	0.422	0.423	0.001	0.519	1	-0.031
Superior occipital gyrus L	0.369	0.371	0.001	0.420	1	-0.041
Superior occipital gyrus R	0.434	0.434	0.000	0.793	1	-0.013
Superior parietal lobule L	0.442	0.444	0.002	0.316	1	0.048
Superior parietal lobule R	0.408	0.408	0.000	0.645650	1	0.023
Superior temporal gyrus L	0.507	0.512	0.005	0.091	1	-0.075
Superior temporal gyrus R	0.485	0.485	0.000	0.746	1	-0.015
Supplementary motor cortex L	0.379	0.383	0.004	0.177	1	-0.068
Supplementary motor cortex R	0.396	0.396	0.000	0.773	1	-0.014
Supramarginal gyrus L	0.438	0.438	0.000	0.987	1	0.001
Supramarginal gyrus R	0.407	0.408	0.001	0.496724	1	0.033
Temporal pole L	0.491	0.494	0.004	0.158	1	-0.064
Temporal pole R	0.484	0.488	0.004	0.123	1	-0.070
Thalamus proper L	0.273	0.278	0.005	0.148	1	-0.078
Thalamus proper R	0.326	0.335	0.009	0.054	1	-0.100
Transverse temporal gyrus L	0.334	0.337	0.003	0.289	1	0.055
Transverse temporal gyrus R	0.437	0.438	0.000	0.723	1	0.017
Triangular part of the inferior frontal gyrus L	0.384	0.387	0.002	0.285	1	-0.053
Triangular part of the inferior frontal gyrus R	0.356	0.357	0.000	0.645647	1	-0.023

FDR: false discovery rate. L: left. PRS: polygenic risk score. R: right.

Table D.22: Associations between APOEonlyPRS Threshold 1 and 114 regions of interest in APOE ε4 non-carriers

Region of Interest	R Square (Model 1)	R Square (Model 2)	R Square Change	Sig. F Change (Model 2)	FDR Corrected value	Standardised beta of PRS
Accumbens area L	0.350	0.356	0.007	0.042	0.798	-0.083
Accumbens area R	0.363	0.365	0.003	0.197333	0.7029988125	-0.052
Amygdala L	0.349	0.352	0.003	0.185	0.703	-0.054
Amygdala R	0.400	0.404	0.004	0.120	0.651428571428571	-0.061
Angular gyrus L	0.369	0.370	0.001	0.353450	0.875941304347826	-0.037
Angular gyrus R	0.378	0.378	0.000	0.745	0.987558139534884	-0.013
Anterior cingulate gyrus L	0.397	0.398	0.001	0.399	0.928285714285714	-0.033
Anterior cingulate gyrus R	0.205	0.208	0.003	0.222255	0.723916285714286	-0.055
Anterior insula L	0.330	0.333	0.003	0.171	0.696214285714286	-0.057
Anterior insula R	0.363	0.368	0.004	0.094	0.765428571428571	-0.068
Anterior orbital gyrus L	0.399	0.403	0.004	0.097	0.691125	-0.065
Anterior orbital gyrus R	0.346	0.346	0.000	0.641	0.913425	-0.019
Basal forebrain L	0.261	0.266	0.005	0.108	0.648	-0.070
Basal forebrain R	0.328	0.333	0.005	0.084	0.798	-0.072
Calcarine cortex L	0.354	0.355	0.001	0.408	0.912	0.034
Calcarine cortex R	0.360	0.361	0.002	0.292	0.899675675675676	0.043
Caudate L	0.184	0.185	0.000	0.747	0.978827586206896	-0.015
Caudate R	0.180	0.180	0.000	0.880	0.993267326732673	0.007
Central operculum L	0.352	0.353	0.001	0.496	0.926950819672131	-0.028
Central operculum R	0.360	0.360	0.000	0.939	0.973145454545455	0.003
Cuneus L	0.379	0.379	0.000	0.721	0.9785	-0.014
Cuneus R	0.422	0.425	0.003	0.179	0.703655172413793	-0.052
Entorhinal area L	0.351	0.351	0.000	0.740	0.992470588235294	-0.014
Entorhinal area R	0.395	0.395	0.000	0.562	0.889833333333333	-0.023
Frontal operculum L	0.347	0.348	0.002	0.270	0.855	0.045
Frontal operculum R	0.320	0.322	0.002	0.314942	0.920599692307692	-0.042

Frontal pole L	0.399	0.399	0.000	0.586	0.902756756756757	-0.021
Frontal pole R	0.382	0.382	0.000	0.930	0.981666666666667	-0.003
Fusiform gyrus L	0.459	0.459	0.000	0.830	0.975463917525773	-0.008
Fusiform gyrus R	0.458	0.463	0.004	0.070	0.798	-0.068
Gyrus rectus L	0.390	0.391	0.002	0.315459	0.89905815	-0.040
Gyrus rectus R	0.391	0.392	0.001	0.548	0.905391304347826	-0.024
Hippocampus L	0.349	0.350	0.001	0.460	0.92	-0.030
Hippocampus R	0.402	0.405	0.002	0.196888	0.724039741935484	-0.051
Inferior occipital gyrus L	0.371	0.374	0.003	0.165	0.696666666666667	-0.056
Inferior occipital gyrus R	0.418	0.419	0.001	0.454	0.924214285714286	-0.029
Inferior temporal gyrus L	0.480	0.481	0.001	0.349	0.904227272727273	-0.034
Inferior temporal gyrus R	0.518	0.522	0.004	0.068	0.861333333333333	-0.064
Lateral orbital gyrus L	0.394	0.397	0.004	0.118	0.6726	-0.062
Lateral orbital gyrus R	0.325	0.326	0.001	0.378	0.916851063829787	-0.037
Lingual gyrus L	0.516	0.516	0.000	0.808	0.990451612903226	0.009
Lingual gyrus R	0.518	0.519	0.001	0.299	0.897	-0.037
Medial frontal cortex L	0.346	0.347	0.001	0.501	0.906571428571429	-0.028
Medial frontal cortex R	0.354	0.355	0.000	0.783	0.970239130434783	-0.011
Medial orbital gyrus L	0.470	0.471	0.001	0.392	0.931	-0.032
Medial orbital gyrus R	0.407	0.408	0.000	0.558	0.895943661971831	0.023
Middle cingulate gyrus L	0.396	0.400	0.004	0.096	0.7296	-0.065
Middle cingulate gyrus R	0.336	0.341	0.004	0.106	0.671333333333333	-0.067
Middle frontal gyrus L	0.467	0.472	0.005	0.060	0.977142857142857	-0.070
Middle frontal gyrus R	0.468	0.469	0.001	0.353371	0.895206533333333	-0.034
Middle occipital gyrus L	0.295	0.295	0.000	0.676	0.93980487804878	0.018
Middle occipital gyrus R	0.327	0.327	0.001	0.555	0.903857142857143	-0.025
Middle temporal gyrus L	0.498	0.498	0.000	0.933	0.92796	-0.003
Middle temporal gyrus R	0.509	0.510	0.001	0.407	0.975798165137615	-0.029
Occipital fusiform gyrus L	0.460	0.460	0.000	0.929	0.989775700934579	-0.003
Occipital fusiform gyrus R	0.457	0.458	0.001	0.440	0.928888888888889	-0.029

Occipital pole L	0.333	0.334	0.000	0.672	0.945777777777778	-0.018
Occipital pole R	0.367	0.367	0.000	0.775	0.981666666666667	-0.012
Opercular part of the inferior frontal gyrus L	0.222	0.228	0.005	0.090	0.789230769230769	0.076
Opercular part of the inferior frontal gyrus R	0.236	0.237	0.001	0.528678	0.913171090909091	-0.028
Orbital part of the inferior frontal gyrus L	0.261	0.261	0.000	0.776	0.972131868131868	-0.012
Orbital part of the inferior frontal gyrus R	0.255	0.255	0.000	0.836	0.962666666666667	-0.009
Pallidum L	0.183	0.191	0.008	0.041	0.9348	-0.093
Pallidum R	0.160	0.165	0.006	0.100	0.670588235294118	-0.076
Parahippocampal gyrus L	0.427	0.428	0.001	0.472	0.912	-0.028
Parahippocampal gyrus R	0.458	0.464	0.006	0.035	1	-0.078
Parietal operculum L	0.338	0.338	0.000	0.819	0.993255319148936	0.009
Parietal operculum R	0.276	0.276	0.001	0.570	0.89013698630137	0.025
Planum polare L	0.401	0.401	0.001	0.511	0.91021875	-0.026
Planum polare R	0.442	0.443	0.001	0.450	0.932727272727273	-0.029
Planum temporale L	0.321	0.324	0.004	0.139	0.68895652173913	-0.062
Planum temporale R	0.315	0.315	0.000	0.886	0.980621359223301	-0.006
Postcentral gyrus L	0.371	0.371	0.001	0.517	0.906738461538462	-0.026
Postcentral gyrus R	0.361	0.361	0.000	0.826	0.980875	-0.009
Postcentral gyrus medial segment L	0.208	0.208	0.000	0.628	0.929766233766234	-0.022
Postcentral gyrus medial segment R	0.198	0.198	0.000	0.973	0.981610619469027	0.002
Posterior cingulate gyrus L	0.517	0.517	0.001	0.485	0.9215	-0.025
Posterior cingulate gyrus R	0.485	0.485	0.000	0.632	0.923692307692308	-0.017
Posterior insula L	0.383	0.388	0.005	0.065	0.92625	-0.073
Posterior insula R	0.403	0.407	0.005	0.075	0.777272727272727	-0.070
Posterior orbital gyrus L	0.317	0.320	0.003	0.211	0.728909090909091	-0.052
Posterior orbital gyrus R	0.321	0.323	0.002	0.221973	0.744262411764706	-0.051
Precentral gyrus L	0.446	0.446	0.000	0.611	0.92872	-0.019
Precentral gyrus R	0.415	0.415	0.000	0.885	0.989117647058824	0.006
Precentral gyrus medial segment L	0.258	0.258	0.000	0.892	0.977769230769231	-0.006
Precentral gyrus medial segment R	0.304	0.305	0.001	0.434	0.933509433962264	-0.033

Precuneus L	0.478	0.478	0.000	0.909	0.986914285714286	0.004
Precuneus R	0.491	0.491	0.000	0.962	0.979178571428571	0.002
Putamen L	0.227	0.239	0.012	0.012	1	-0.112
Putamen R	0.229	0.238	0.008	0.036	1	-0.093
Subcallosal area L	0.428	0.428	0.000	0.756	0.979363636363636	0.012
Subcallosal area R	0.370	0.370	0.000	0.926	0.99588679245283	0.004
Superior frontal gyrus L	0.446	0.446	0.000	0.835	0.971326530612245	-0.008
Superior frontal gyrus R	0.460	0.460	0.001	0.497	0.913838709677419	-0.025
Superior frontal gyrus medial segment L	0.407	0.409	0.001	0.326	0.906439024390244	-0.038
Superior frontal gyrus medial segment R	0.406	0.406	0.000	0.639	0.922101265822785	-0.018
Superior occipital gyrus L	0.287	0.288	0.001	0.542	0.908647058823529	0.026
Superior occipital gyrus R	0.268	0.269	0.001	0.425	0.931730769230769	-0.035
Superior parietal lobule L	0.353	0.353	0.000	0.976	0.976	-0.001
Superior parietal lobule R	0.374	0.375	0.001	0.336	0.912	-0.039
Superior temporal gyrus L	0.373	0.373	0.000	0.820	0.984	-0.009
Superior temporal gyrus R	0.348	0.348	0.000	0.768	0.983730337078652	0.012
Supplementary motor cortex L	0.356	0.357	0.000	0.710	0.975180722891566	-0.015
Supplementary motor cortex R	0.371	0.371	0.000	0.848	0.96672	0.008
Supramarginal gyrus L	0.287	0.288	0.001	0.529227	0.900475791044776	-0.027
Supramarginal gyrus R	0.335	0.338	0.003	0.150667	0.68704152	-0.059
Temporal pole L	0.328	0.330	0.002	0.338	0.896093023255814	-0.040
Temporal pole R	0.358	0.361	0.003	0.151456	0.664076307692308	-0.058
Thalamus proper L	0.200	0.204	0.004	0.132	0.684	-0.068
Thalamus proper R	0.221	0.230	0.009	0.033	1	-0.095
Transverse temporal gyrus L	0.237	0.238	0.001	0.470	0.923793103448276	0.032
Transverse temporal gyrus R	0.292	0.292	0.000	0.940	0.965405405405405	0.003
Triangular part of the inferior frontal gyrus L	0.274	0.275	0.000	0.614	0.921	0.022
Triangular part of the inferior frontal gyrus R	0.253	0.257	0.004	0.143	0.67925	-0.064

FDR: false discovery rate. L: left. PRS: polygenic risk score. R: right.

Table D.23: Associations between APOEonlyPRS Threshold 1 and 114 regions of interest in APOE ε4 carriers

Region of Interest	R Square (Model 1)	R Square (Model 2)	R Square Change	Sig. F Change (Model 2)	FDR Corrected value	Standardised beta of PRS
Accumbens area L	0.479	0.488	0.009	0.031	0.7068	0.097
Accumbens area R	0.444	0.463	0.018	0.002	0.228	0.0142
Amygdala L	0.496	0.496	0.000	0.892	0.996941176470588	0.006
Amygdala R	0.544	0.544	0.000	0.770	0.9975	-0.012
Angular gyrus L	0.465	0.467	0.002	0.264	1	-0.051
Angular gyrus R	0.479	0.479	0.000	0.812	0.984765957446809	0.011
Anterior cingulate gyrus L	0.445	0.446	0.001	0.448	1	0.035
Anterior cingulate gyrus R	0.312	0.314	0.003	0.270	1	0.057
Anterior insula L	0.445	0.449	0.004	0.175	1	0.063
Anterior insula R	0.431	0.439	0.008	0.046	0.749142857142857	0.094
Anterior orbital gyrus L	0.420	0.421	0.000	0.624	0.974465753424658	-0.023
Anterior orbital gyrus R	0.387	0.393	0.006	0.096	0.841846153846154	-0.081
Basal forebrain L	0.375	0.377	0.002	0.361	1	0.045
Basal forebrain R	0.393	0.405	0.011	0.022	0.627	0.111
Calcarine cortex L	0.417	0.418	0.002	0.377	1	-0.042
Calcarine cortex R	0.424	0.430	0.006	0.094	0.893	-0.079
Caudate L	0.245	0.246	0.001	0.459431	1	0.040
Caudate R	0.238	0239	0.000	0.695	0.954578313253012	0.021
Central operculum L	0.432	0.432	0.000	0.903	0.999436893203884	0.006
Central operculum R	0.425	0.425	0.000	0.639845	0.9597675	-0.022
Cuneus L	0.445	0.448	0.003	0.223525	1	-0.057
Cuneus R	0.444	0.444	0.000	0.705	0.956785714285714	-0.018
Entorhinal area L	0.483	0.483	0.000	0.971	1	0.002
Entorhinal area R	0.536	0.537	0.001	0.475	0.966964285714286	0.030
Frontal operculum L	0.412	0.412	0.001	0.570	0.969850746268657	0.027
Frontal operculum R	0.366	0.368	0.002	0.355	1	0.046

Frontal pole L	0.490	0.491	0.001	0.384	1	-0.039
Frontal pole R	0.461	0.462	0.001	0.476	0.952	0.033
Fusiform gyrus L	0.571	0.571	0.000	0.881	1	0.006
Fusiform gyrus R	0.614	0.615	0.001	0.467	1	0.028
Gyrus rectus L	0.506	0.507	0.001	0.567	0.979363636363636	-0.025
Gyrus rectus R	0.530	0.531	0.000	0.588	0.9576	-0.023
Hippocampus L	0.567	0.567	0.000	0.724	0.959720930232558	-0.015
Hippocampus R	0.560	0.560	0.000	0.574	0.962294117647059	-0.023
Inferior occipital gyrus L	0.466	0.467	0.001	0.422	1	-0.037
Inferior occipital gyrus R	0.528	0.530	0.002	0.304	1	-0.044
Inferior temporal gyrus L	0.553	0.553	0.001	0.470287	0.992828111111111	0.030
Inferior temporal gyrus R	0.584	0.587	0.003	0.190	1	0.053
Lateral orbital gyrus L	0.450	0.450	0.000	0.944949	0.997446166666667	0.003
Lateral orbital gyrus R	0.420	0.422	0.001	0.432	1	-0.037
Lingual gyrus L	0.515	0.515	0.000	0.904412	0.981933028571429	-0.005
Lingual gyrus R	0.537	0.537	0.000	0.681	0.958444444444445	-0.018
Medial frontal cortex L	0.399	0.400	0.001	0.586	0.968173913043478	-0.026
Medial frontal cortex R	0.416	0.416	0.000	0.904404	0.991365923076923	-0.006
Medial orbital gyrus L	0.495	0.496	0.001	0.478	0.93951724137931	-0.032
Medial orbital gyrus R	0.484	0.485	0.001	0.469545	1	-0.032
Middle cingulate gyrus L	0.382	0.385	0.004	0.189	1	0.065
Middle cingulate gyrus R	0.366	0.368	0.001	0.458504	1	0.037
Middle frontal gyrus L	0.489	0.491	0.002	0.272	1	0.049
Middle frontal gyrus R	0.477	0.479	0.003	0.244	1	0.053
Middle occipital gyrus L	0.446	0.449	0.003	0.210	1	-0.058
Middle occipital gyrus R	0.410	0.414	0.005	0.142	0.952235294117647	-0.070
Middle temporal gyrus L	0.512	0.512	0.000	0.809	0.967575	-0.011
Middle temporal gyrus R	0.565	0.565	0.000	0.679	0.991677419354839	0.017
Occipital fusiform gyrus L	0.495	0.495	0.001	0.549	0.962861538461539	0.027
Occipital fusiform gyrus R	0.583	0.583	0.000	0.799	1	0.010

Occipital pole L	0.368	0.368	0.000	0.658847	0.962930230769231	-0.022
Occipital pole R	0.387	0.387	0.000	0.832	0.988	0.010
Opercular part of the inferior frontal gyrus L	0.323	0.326	0.003	0.303	1	0.053
Opercular part of the inferior frontal gyrus R	0.338	0.339	0.001	0.545	0.97078125	0.031
Orbital part of the inferior frontal gyrus L	0.311	0.311	0.001	0.647	0.957896103896104	-0.024
Orbital part of the inferior frontal gyrus R	0.288	0.289	0.001	0.635	0.978243243243243	-0.025
Pallidum L	0.158	0.0162	0.005	0.213	1	-0.071
Pallidum R	0.135	0.142	0.007	0.135	0.961875	-0.087
Parahippocampal gyrus L	0.559	0.559	0.000	0.975	1	0.001
Parahippocampal gyrus R	0.598	0.598	0.000	0.798	1	-0.010
Parietal operculum L	0.357	0.357	0.000	0.727	0.952620689655172	0.018
Parietal operculum R	0.340	0.347	0.007	0.087	0.901636363636364	0.087
Planum polare L	0.517	0.517	0.000	0.996	0.996	0.000
Planum polare R	0.542	0.542	0.000	0.823	0.9876	-0.009
Planum temporale L	0.413	0.141	0.001	0.459315	1	0.035
Planum temporale R	0.448	0.448	0.000	0.887	1	-0.007
Postcentral gyrus L	0.424	0.425	0.001	0.518	0.937333333333333	0.031
Postcentral gyrus R	0.427	0.428	0.000	0.803	1	-0.012
Postcentral gyrus medial segment L	0.206	0.213	0.007	0.112	0.912	-0.089
Postcentral gyrus medial segment R	0.260	0.260	0.001	0.639558	0.97212816	-0.025
Posterior cingulate gyrus L	0.582	0.582	0.000	0.659433	0.951586860759494	0.018
Posterior cingulate gyrus R	0.540	0.541	0.001	0.480	0.927457627118644	-0.030
Posterior insula L	0.422	0.429	0.008	0.053	0.75525	0.092
Posterior insula R	0.455	0.462	0.007	0.055	0.696666666666667	0.088
Posterior orbital gyrus L	0.435	0.435	0.000	0.848632	0.997361319587629	-0.009
Posterior orbital gyrus R	0.452	0.452	0.000	0.885	1	0.007
Precentral gyrus L	0.476	0.488	0.012	0.010	0.38	0.116
Precentral gyrus R	0.467	0.475	0.008	0.041	0.779	0.093
Precentral gyrus medial segment L	0.350	0.352	0.002	0.318	1	-0.050
Precentral gyrus medial segment R	0.375	0.377	0.002	0.383	1	-0.043

Precuneus L	0.507	0.507	0.000	0.849312	0.987975183673469	0.008
Precuneus R	0.500	0.501	0.001	0.490	0.915737704918033	-0.030
Putamen L	0.348	0.354	0.006	0.117	0.8892	0.079
Putamen R	0.375	0.383	0.007	0.068	0.7752	0.090
Subcallosal area L	0.544	0.545	0.000	0.614	0.972166666666667	0.021
Subcallosal area R	0.558	0.559	0.001	0.415	1	0.034
Superior frontal gyrus L	0.475	0.477	0.002	0.339	1	0.043
Superior frontal gyrus R	0.509	0.521	0.013	0.007	0.399	0.118
Superior frontal gyrus medial segment L	0.440	0.441	0.000	0.714	0.9576	0.017
Superior frontal gyrus medial segment R	0.422	0.425	0.003	0.236	1	0.056
Superior occipital gyrus L	0.369	0.369	0.000	0.983696	1	0.001
Superior occipital gyrus R	0.434	0.434	0.000	0.945071	0.988422880733945	0.003
Superior parietal lobule L	0.442	0.443	0.001	0.468584	1	-0.034
Superior parietal lobule R	0.408	0.409	0.001	0.481	0.9139	-0.034
Superior temporal gyrus L	0.507	0.508	0.000	0.605	0.971408450704225	-0.023
Superior temporal gyrus R	0.485	0.485	0.000	0.693	0.963439024390244	-0.018
Supplementary motor cortex L	0.379	0.379	0.000	0.808	1	0.012
Supplementary motor cortex R	0.396	0.398	0.002	0.398	1	0.041
Supramarginal gyrus L	0.438	0.439	0.001	0.458317	1	-0.035
Supramarginal gyrus R	0.407	0.408	0.001	0.504	0.926709677419355	0.032
Temporal pole L	0.491	0.491	0.001	0.474	0.982472727272727	0.032
Temporal pole R	0.484	0.486	0.002	0.308	1	0.046
Thalamus proper L	0.273	0.274	0.002	0.435	1	0.042
Thalamus proper R	0.326	0.330	0.004	0.224451	1	0.062
Transverse temporal gyrus L	0.334	0.334	0.000	0.928	0.998037735849057	-0.005
Transverse temporal gyrus R	0.437	0.437	0.000	0.930	0.990841121495327	-0.004
Triangular part of the inferior frontal gyrus L	0.384	0.385	0.001	0.469920	1	0.035
Triangular part of the inferior frontal gyrus R	0.356	0.356	0.000	0.983953	0.992660548672566	0.001

FDR: false discovery rate. L: left. PRS: polygenic risk score. R: right.

Table D.24: Associations between APOEonlyPRS Threshold 5 and 114 regions of interest in APOE ε4 non-carriers

Region of Interest	R Square (Model 1)	R Square (Model 2)	R Square Change	Sig. F Change (Model 2)	FDR Corrected value	Standardised beta of PRS
Accumbens area L	0.350	0.356	0.006	0.052	1	-0.079
Accumbens area R	0.363	0.365	0.002	0.226	0.805125	-0.049
Amygdala L	0.349	0.353	0.003	0.165	0.723461538461539	-0.057
Amygdala R	0.400	0.404	0.004	0.117	0.741	-0.061
Angular gyrus L	0.369	0.371	0.002	0.295	0.908918918918919	-0.042
Angular gyrus R	0.378	0.379	0.000	0.585	1	-0.022
Anterior cingulate gyrus L	0.397	0.398	0.001	0.472	0.978327272727273	-0.028
Anterior cingulate gyrus R	0.205	0.206	0.002	0.359	0.974428571428571	-0.041
Anterior insula L	0.330	0.334	0.004	0.119315	0.6800955	-0.064
Anterior insula R	0.363	0.368	0.004	0.099	0.7524	-0.066
Anterior orbital gyrus L	0.399	0.403	0.003	0.122	0.662285714285714	-0.060
Anterior orbital gyrus R	0.346	0.346	0.000	0.601	1	-0.021
Basal forebrain L	0.261	0.267	0.006	0.077	0.8778	-0.077
Basal forebrain R	0.328	0.333	0.005	0.070	0.886666666666667	-0.075
Calcarine cortex L	0.354	0.355	0.001	0.419	0.995125	0.033
Calcarine cortex R	0.360	0.361	0.002	0.307	0.897384615384615	0.041
Caudate L	0.184	0.185	0.000	0.663	0.969	-0.020
Caudate R	0.180	0.180	0.000	0.998	0.998	0.000
Central operculum L	0.352	0.353	0.001	0.521	0.973672131147541	-0.026
Central operculum R	0.360	0.360	0.000	0.931	0.973706422018349	0.003
Cuneus L	0.379	0.379	0.000	0.796	0.997186813186813	-0.010
Cuneus R	0.422	0.424	0.002	0.225	0.82741935483871	-0.047
Entorhinal area L	0.351	0.351	0.000	0.704	0.966939759036144	-0.015
Entorhinal area R	0.395	0.395	0.000	0.655	0.9825	-0.018
Frontal operculum L	0.347	0.348	0.002	0.289	0.915166666666667	0.043
Frontal operculum R	0.320	0.322	0.002	0.300	0.9	-0.043

Frontal pole L	0.399	0.399	0.000	0.682	0.97185	-0.016
Frontal pole R	0.382	0.382	0.000	0.859	1	-0.007
Fusiform gyrus L	0.459	0.459	0.000	0.865	1	-0.006
Fusiform gyrus R	0.458	0.462	0.004	0.093	0.815538461538462	-0.062
Gyrus rectus L	0.390	0.390	0.001	0.480	0.943448275862069	-0.028
Gyrus rectus R	0.391	0.391	0.000	0.594	1	-0.021
Hippocampus L	0.349	0.350	0.001	0.448	0.982153846153846	-0.031
Hippocampus R	0.402	0.404	0.002	0.222	0.8436	-0.048
Inferior occipital gyrus L	0.371	0.374	0.003	0.182	0.741	-0.053
Inferior occipital gyrus R	0.418	0.419	0.001	0.551	0.997047619047619	-0.023
Inferior temporal gyrus L	0.480	0.481	0.001	0.314	0.8949	-0.037
Inferior temporal gyrus R	0.518	0.521	0.004	0.078	0.808363636363636	-0.062
Lateral orbital gyrus L	0.394	0.397	0.003	0.169	0.713555555555556	-0.054
Lateral orbital gyrus R	0.325	0.326	0.001	0.370	0.980930232558139	-0.037
Lingual gyrus L	0.516	0.516	0.000	0.718949	0.964237482352941	0.013
Lingual gyrus R	0.518	0.518	0.001	0.389	1	-0.030
Medial frontal cortex L	0.346	0.347	0.000	0.653178	0.99283056	-0.018
Medial frontal cortex R	0.354	0.354	0.000	0.919	0.979121495327103	-0.004
Medial orbital gyrus L	0.470	0.471	0.001	0.390	0.988	-0.032
Medial orbital gyrus R	0.407	0.408	0.000	0.584	1	0.021
Middle cingulate gyrus L	0.396	0.400	0.004	0.118762	0.712572	-0.061
Middle cingulate gyrus R	0.336	0.340	0.003	0.158	0.72048	-0.058
Middle frontal gyrus L	0.467	0.472	0.004	0.066	0.9405	-0.068
Middle frontal gyrus R	0.468	0.468	0.001	0.471	0.994333333333333	-0.027
Middle occipital gyrus L	0.295	0.295	0.000	0.734	0.940179775280899	0.014
Middle occipital gyrus R	0.327	0.327	0.001	0.518	0.9842	-0.027
Middle temporal gyrus L	0.498	0.498	0.000	0.860	0.981512195121951	-0.006
Middle temporal gyrus R	0.509	0.510	0.001	0.353	1	-0.033
Occipital fusiform gyrus L	0.460	0.460	0.000	0.976	0.993428571428571	-0.001
Occipital fusiform gyrus R	0.457	0.458	0.001	0.474274	0.948548	-0.027

Occipital pole L	0.333	0.334	0.000	0.773	0.979133333333333	-0.012
Occipital pole R	0.367	0.367	0.000	0.955	0.989727272727273	-0.002
Opercular part of the inferior frontal gyrus L	0.222	0.227	0.005	0.097	0.789857142857143	0.074
Opercular part of the inferior frontal gyrus R	0.236	0.236	0.000	0.687	0.966888888888889	-0.018
Orbital part of the inferior frontal gyrus L	0.261	0.261	0.000	0.857	1	-0.008
Orbital part of the inferior frontal gyrus R	0.255	0.255	0.000	0.900	0.996116504854369	-0.005
Pallidum L	0.183	0.190	0.007	0.057	1	-0.087
Pallidum R	0.160	0.165	0.005	0.115	0.771176470588235	-0.073
Parahippocampal gyrus L	0.427	0.428	0.001	0.426	0.991102040816326	-0.030
Parahippocampal gyrus R	0.458	0.464	0.005	0.045	1	-0.074
Parietal operculum L	0.338	0.338	0.000	0.894	1	0.006
Parietal operculum R	0.276	0.276	0.000	0.666	0.96106329113924	-0.019
Planum polare L	0.401	0.401	0.001	0.427	0.97356	-0.031
Planum polare R	0.442	0.443	0.001	0.457	0.982981132075472	-0.028
Planum temporale L	0.321	0.324	0.004	0.142000	0.703826086956522	-0.061
Planum temporale R	0.315	0.315	0.000	0.975	1	0.001
Postcentral gyrus L	0.371	0.371	0.000	0.714	0.969	-0.015
Postcentral gyrus R	0.361	0.361	0.000	0.914817	0.993229885714286	-0.004
Postcentral gyrus medial segment L	0.208	0.208	0.000	0.616	1	-0.023
Postcentral gyrus medial segment R	0.198	0.198	0.000	0.689	0.957878048780488	0.018
Posterior cingulate gyrus L	0.517	0.517	0.000	0.656	0.971220779220779	-0.016
Posterior cingulate gyrus R	0.485	0.485	0.000	0.637	1	-0.017
Posterior insula L	0.383	0.389	0.005	0.060	0.977142857142857	-0.074
Posterior insula R	0.403	0.406	0.004	0.103	0.733875	-0.064
Posterior orbital gyrus L	0.317	0.320	0.002	0.229	0.791090909090909	-0.050
Posterior orbital gyrus R	0.321	0.323	0.002	0.275	0.922058823529412	-0.045
Precentral gyrus L	0.446	0.446	0.000	0.830	1	-0.008
Precentral gyrus R	0.415	0.415	0.000	0.893	1	0.005
Precentral gyrus medial segment L	0.258	0.258	0.000	0.988	0.996743362831858	-0.001
Precentral gyrus medial segment R	0.304	0.305	0.000	0.626974	1	-0.020

Precuneus L	0.478	0.478	0.000	0.814	0.997806451612903	0.009
Precuneus R	0.491	0.491	0.000	0.922	0.973222222222222	0.004
Putamen L	0.227	0.241	0.014	0.007	0.798	-0.119
Putamen R	0.229	0.240	0.011	0.018	0.684	-0.105
Subcallosal area L	0.428	0.429	0.000	0.607	1	0.020
Subcallosal area R	0.370	0.370	0.000	0.732	0.948272727272727	0.014
Superior frontal gyrus L	0.446	0.446	0.000	0.914917	0.983967339622641	-0.004
Superior frontal gyrus R	0.460	0.460	0.001	0.525	0.965322580645161	-0.024
Superior frontal gyrus medial segment L	0.407	0.408	0.001	0.428	0.956705882352941	-0.031
Superior frontal gyrus medial segment R	0.406	0.406	0.000	0.639	0.997890410958904	-0.018
Superior occipital gyrus L	0.287	0.289	0.001	0.396	0.981391304347826	0.036
Superior occipital gyrus R	0.268	0.269	0.000	0.724	0.948689655172414	-0.015
Superior parietal lobule L	0.353	0.353	0.000	0.885	1	0.006
Superior parietal lobule R	0.374	0.375	0.001	0.404	0.979914893617021	-0.033
Superior temporal gyrus L	0.373	0.373	0.000	0.812	1	-0.010
Superior temporal gyrus R	0.348	0.348	0.000	0.652658	1	0.018
Supplementary motor cortex L	0.356	0.356	0.000	0.897	1	-0.005
Supplementary motor cortex R	0.371	0.372	0.000	0.719374	0.953588790697674	0.014
Supramarginal gyrus L	0.287	0.288	0.001	0.474141	0.965215607142857	-0.031
Supramarginal gyrus R	0.335	0.338	0.003	0.186	0.731172413793103	-0.054
Temporal pole L	0.328	0.330	0.002	0.286	0.931542857142857	-0.044
Temporal pole R	0.358	0.361	0.003	0.140	0.725454545454545	-0.060
Thalamus proper L	0.200	0.206	0.006	0.081	0.7695	-0.079
Thalamus proper R	0.221	0.232	0.011	0.016	0.912	-0.107
Transverse temporal gyrus L	0.237	0.237	0.001	0.517	0.998949152542373	0.029
Transverse temporal gyrus R	0.292	0.292	0.000	0.912	0.999692307692308	0.005
Triangular part of the inferior frontal gyrus L	0.274	0.275	0.000	0.626812	1	0.021
Triangular part of the inferior frontal gyrus R	0.253	0.257	0.004	0.142481	0.67678475	-0.064

FDR: false discovery rate. L: left. PRS: polygenic risk score. R: right.

Table D.25: Associations between APOEonlyPRS Threshold 5 and 114 regions of interest in APOE ε4 carriers

Region of Interest	R Square (Model 1)	R Square (Model 2)	R Square Change	Sig. F Change (Model 2)	FDR Corrected value	Standardised beta of PRS
Accumbens area L	0.479	0.488	0.009	0.027	0.6156	0.099
Accumbens area R	0.444	0.462	0.018	0.002	0.228	0.141
Amygdala L	0.496	0.496	0.000	0.770	0.986292134831461	0.013
Amygdala R	0.544	0.544	0.000	0.816	0.959010309278351	-0.010
Angular gyrus L	0.465	0.467	0.002	0.277	1	-0.050
Angular gyrus R	0.479	0.479	0.000	0.815	0.9678125	0.011
Anterior cingulate gyrus L	0.445	0.446	0.001	0.385	1	0.040
Anterior cingulate gyrus R	0.312	0.315	0.004	0.225	1	0.063
Anterior insula L	0.445	0.449	0.004	0.156	0.988	0.066
Anterior insula R	0.431	0.439	0.008	0.042	0.5985	0.096
Anterior orbital gyrus L	0.420	0.421	0.000	0.690	0.995696202531645	-0.019
Anterior orbital gyrus R	0.387	0.393	0.006	0.090	0.789230769230769	-0.083
Basal forebrain L	0.375	0.377	0.002	0.308	1	0.050
Basal forebrain R	0.393	0.406	0.012	0.016	0.456	0.117
Calcarine cortex L	0.417	0.418	0.001	0.404	1	-0.040
Calcarine cortex R	0.424	0.429	0.005	0.115	0.874	-0.075
Caudate L	0.245	0.247	0.002	0.368	1	0.049
Caudate R	0.238	0.239	0.001	0.580849	1	0.030
Central operculum L	0.432	0.432	0.000	0.845860	0.9642804	0.009
Central operculum R	0.425	0.425	0.000	0.725	0.99578313253012	-0.017
Cuneus L	0.445	0.447	0.003	0.240	1	-0.055
Cuneus R	0.444	0.444	0.000	0.771	0.9766	-0.014
Entorhinal area L	0.483	0.483	0.000	0.846100	0.95500396039604	0.009
Entorhinal area R	0.536	0.537	0.001	0.421	0.999875	0.034
Frontal operculum L	0.412	0.412	0.001	0.525	0.965322580645161	0.030
Frontal operculum R	0.366	0.369	0.002	0.322	1	0.049

Frontal pole L	0.490	0.492	0.002	0.331	1	-0.043
Frontal pole R	0.461	0.462	0.001	0.567	0.994430769230769	0.026
Fusiform gyrus L	0.571	0.571	0.000	0.786	0.97395652173913	0.011
Fusiform gyrus R	0.614	0.615	0.001	0.449	0.96577358490566	0.029
Gyrus rectus L	0.506	0.507	0.000	0.618	0.9785	-0.022
Gyrus rectus R	0.530	0.531	0.001	0.581509	0.989433223880597	-0.024
Hippocampus L	0.567	0.567	0.000	0.789	0.967161290322581	-0.011
Hippocampus R	0.560	0.560	0.000	0.607	0.988542857142857	-0.021
Inferior occipital gyrus L	0.466	0.467	0.001	0.452	0.936872727272727	-0.034
Inferior occipital gyrus R	0.528	0.530	0.002	0.311	1	-0.043
Inferior temporal gyrus L	0.553	0.553	0.001	0.484	0.935186440677966	0.029
Inferior temporal gyrus R	0.584	0.587	0.003	0.177	1	0.054
Lateral orbital gyrus L	0.450	0.450	0.000	0.903	0.9804	0.006
Lateral orbital gyrus R	0.420	0.422	0.001	0.428	0.97584	-0.038
Lingual gyrus L	0.515	0.515	0.000	0.946	0.9804	-0.003
Lingual gyrus R	0.537	0.537	0.000	0.752	0.985379310344828	-0.013
Medial frontal cortex L	0.399	0.400	0.000	0.638	0.996328767123288	-0.023
Medial frontal cortex R	0.416	0.416	0.000	0.931	0.991906542056075	-0.004
Medial orbital gyrus L	0.495	0.496	0.001	0.529	0.957238095238095	-0.028
Medial orbital gyrus R	0.484	0.485	0.001	0.488	0.9272	-0.031
Middle cingulate gyrus L	0.382	0.386	0.004	0.178	1	0.066
Middle cingulate gyrus R	0.366	0.368	0.002	0.398	1	0.042
Middle frontal gyrus L	0.489	0.492	0.002	0.261	0.9918	0.050
Middle frontal gyrus R	0.477	0.480	0.003	0.214	1	0.056
Middle occipital gyrus L	0.446	0.449	0.003	0.236	1	-0.055
Middle occipital gyrus R	0.410	0.414	0.004	0.149	1	-0.069
Middle temporal gyrus L	0.512	0.512	0.000	0.833	1	-0.009
Middle temporal gyrus R	0.565	0.565	0.000	0.713551	0.969	0.015
Occipital fusiform gyrus L	0.495	0.496	0.001	0.434	0.951461538461539	0.035
Occipital fusiform gyrus R	0.583	0.583	0.000	0.713974	0.992598	0.015

Occipital pole L	0.368	0.368	0.000	0.744	0.986232558139535	-0.016
Occipital pole R	0.387	0.387	0.000	0.743	0.996494117647059	0.016
Opercular part of the inferior frontal gyrus L	0.323	0.327	0.003	0.253	0.994551724137931	0.059
Opercular part of the inferior frontal gyrus R	0.338	0.339	0.001	0.503	0.940032786885246	0.034
Orbital part of the inferior frontal gyrus L	0.311	0.311	0.000	0.676	1	-0.022
Orbital part of the inferior frontal gyrus R	0.288	0.289	0.001	0.612	0.982647887323944	-0.027
Pallidum L	0.158	0.162	0.004	0.245	0.9975	-0.067
Pallidum R	0.135	0.141	0.006	0.154	1	-0.083
Parahippocampal gyrus L	0.559	0.559	0.000	0.909	0.977603773584906	0.005
Parahippocampal gyrus R	0.598	0.598	0.000	0.794	0.962936170212766	-0.010
Parietal operculum L	0.357	0.357	0.000	0.672	1	0.021
Parietal operculum R	0.340	0.347	0.007	0.086	0.817	0.087
Planum polare L	0.517	0.517	0.000	0.870	0.962912621359223	0.007
Planum polare R	0.542	0.542	0.000	0.970	0.987321428571428	-0.002
Planum temporale L	0.413	0.415	0.001	0.418	1	0.039
Planum temporale R	0.448	0.448	0.000	0.936	0.988	-0.004
Postcentral gyrus L	0.424	0.425	0.001	0.586	0.968173913043478	0.026
Postcentral gyrus R	0.427	0.428	0.000	0.764	0.989727272727273	-0.014
Postcentral gyrus medial segment L	0.206	0.214	0.008	0.098	0.798	-0.092
Postcentral gyrus medial segment R	0.260	0.260	0.000	0.677	0.989461538461539	-0.022
Posterior cingulate gyrus L	0.582	0.582	0.000	0.665	1	0.017
Posterior cingulate gyrus R	0.540	0.541	0.001	0.451	0.952111111111111	-0.032
Posterior insula L	0.422	0.431	0.009	0.036	0.684	0.099
Posterior insula R	0.455	0.463	0.008	0.045	0.57	0.092
Posterior orbital gyrus L	0.435	0.435	0.000	0.981	0.989681415929204	-0.001
Posterior orbital gyrus R	0.452	0.452	0.000	0.799	0.9588	0.012
Precentral gyrus L	0.476	0.488	0.013	0.009	0.342	0.118
Precentral gyrus R	0.467	0.475	0.008	0.039	0.635142857142857	0.093
Precentral gyrus medial segment L	0.350	0.352	0.002	0.362	1	-0.046
Precentral gyrus medial segment R	0.375	0.377	0.001	0.432	0.965647058823529	-0.039

Precuneus L	0.507	0.507	0.000	0.869	0.971235294117647	0.007
Precuneus R	0.500	0.501	0.001	0.472	0.927724137931034	-0.032
Putamen L	0.348	0.355	0.007	0.077	0.798	0.089
Putamen R	0.375	0.384	0.009	0.048	0.5472	0.097
Subcallosal area L	0.544	0.545	0.000	0.581754	0.975293470588235	0.023
Subcallosal area R	0.558	0.559	0.001	0.402	1	0.035
Superior frontal gyrus L	0.475	0.477	0.002	0.337	1	0.043
Superior frontal gyrus R	0.509	0.521	0.012	0.008	0.456	0.115
Superior frontal gyrus medial segment L	0.440	0.441	0.000	0.642	0.989027027027027	0.022
Superior frontal gyrus medial segment R	0.422	0.426	0.003	0.206	1	0.060
Superior occipital gyrus L	0.369	0.369	0.000	0.871	0.95475	0.008
Superior occipital gyrus R	0.434	0.434	0.000	0.845252	0.973320484848485	0.009
Superior parietal lobule L	0.442	0.443	0.001	0.461	0.922	-0.034
Superior parietal lobule R	0.408	0.409	0.001	0.455	0.92625	-0.036
Superior temporal gyrus L	0.507	0.508	0.000	0.700	0.9975	-0.017
Superior temporal gyrus R	0.485	0.485	0.000	0.733	0.994785714285714	-0.015
Supplementary motor cortex L	0.379	0.379	0.000	0.782	0.979648351648352	0.014
Supplementary motor cortex R	0.396	0.398	0.001	0.406	1	0.040
Supramarginal gyrus L	0.438	0.439	0.001	0.408	1	-0.039
Supramarginal gyrus R	0.407	0.408	0.001	0.546	0.9725625	0.029
Temporal pole L	0.491	0.492	0.002	0.350	1	0.042
Temporal pole R	0.484	0.486	0.003	0.242	1	0.052
Thalamus proper L	0.273	0.275	0.002	0.378	1	0.047
Thalamus proper R	0.326	0.330	0.004	0.190	1	0.067
Transverse temporal gyrus L	0.334	0.334	0.000	0.961	0.986972972972973	-0.002
Transverse temporal gyrus R	0.437	0.437	0.000	0.943	0.986256880733945	0.003
Triangular part of the inferior frontal gyrus L	0.384	0.385	0.001	0.422	0.981795918367347	0.039
Triangular part of the inferior frontal gyrus R	0.356	0.356	0.000	0.992	0.992	0.000

FDR: false discovery rate. L: left. PRS: polygenic risk score. R: right.

Table D.26: Associations between APOEonlyPRS Threshold 10 and 114 regions of interest in APOE ε4 non-carriers

Region of Interest	R Square (Model 1)	R Square (Model 2)	R Square Change	Sig. F Change (Model 2)	FDR Corrected value	Standardised beta of PRS
Accumbens area L	0.350	0.353	0.004	0.136	0.7752	-0.060
Accumbens area R	0.363	0.364	0.002	0.296	0.912	-0.042
Amygdala L	0.349	0.352	0.002	0.230	1	-0.049
Amygdala R	0.400	0.404	0.004	0.101	0.885692307692308	-0.064
Angular gyrus L	0.369	0.371	0.002	0.251514	0.924922451612903	-0.046
Angular gyrus R	0.378	0.379	0.001	0.545	1	-0.024
Anterior cingulate gyrus L	0.397	0.398	0.001	0.451	0.988730769230769	-0.029
Anterior cingulate gyrus R	0.205	0.207	0.002	0.318	0.929538461538462	-0.045
Anterior insula L	0.330	0.334	0.004	0.109	0.887571428571429	-0.066
Anterior insula R	0.363	0.367	0.004	0.121	0.811411764705882	-0.062
Anterior orbital gyrus L	0.399	0.403	0.003	0.122	0.772666666666667	-0.060
Anterior orbital gyrus R	0.346	0.347	0.001	0.446	1	-0.031
Basal forebrain L	0.261	0.269	0.008	0.030	1	-0.094
Basal forebrain R	0.328	0.335	0.007	0.038	1	-0.085
Calcarine cortex L	0.354	0.354	0.000	0.977	0.994446428571429	0.001
Calcarine cortex R	0.360	0.360	0.000	0.605	1	0.021
Caudate L	0.184	0.185	0.000	0.706	1	-0.017
Caudate R	0.180	0.180	0.000	0.899	0.966849057	0.006
Central operculum L	0.352	0.353	0.000	0.895	0.971714285714286	-0.005
Central operculum R	0.360	0.361	0.000	0.697	1	0.016
Cuneus L	0.379	0.380	0.000	0.634	1	-0.019
Cuneus R	0.422	0.425	0.002	0.191	0.946695652173913	-0.050
Entorhinal area L	0.351	0.351	0.000	0.742777	1	-0.013
Entorhinal area R	0.395	0.395	0.000	0.593	1	-0.021
Frontal operculum L	0.347	0.349	0.002	0.236	0.996444444444444	0.048
Frontal operculum R	0.320	0.321	0.001	0.547	1	-0.025

Frontal pole L	0.399	0.399	0.000	0.886	0.971192307692308	-0.006
Frontal pole R	0.382	0.382	0.001	0.549	1	-0.024
Fusiform gyrus L	0.459	0.459	0.000	0.742751	1	-0.012
Fusiform gyrus R	0.458	0.461	0.003	0.143	0.741	-0.054
Gyrus rectus L	0.390	0.390	0.000	0.588	1	-0.021
Gyrus rectus R	0.391	0.392	0.001	0.560	1	-0.023
Hippocampus L	0.349	0.350	0.001	0.496	1	-0.028
Hippocampus R	0.402	0.404	0.002	0.259	0.894727272727273	-0.044
Inferior occipital gyrus L	0.371	0.375	0.004	0.118	0.84075	-0.062
Inferior occipital gyrus R	0.418	0.420	0.001	0.332	0.901142857142857	-0.037
Inferior temporal gyrus L	0.480	0.481	0.002	0.238	0.969	-0.043
Inferior temporal gyrus R	0.518	0.521	0.004	0.081	0.9234	-0.061
Lateral orbital gyrus L	0.394	0.395	0.001	0.443	1	-0.030
Lateral orbital gyrus R	0.325	0.326	0.001	0.449	1	-0.031
Lingual gyrus L	0.516	0.516	0.000	0.841	0.98839175257732	-0.007
Lingual gyrus R	0.518	0.518	0.001	0.412	1	-0.029
Medial frontal cortex L	0.346	0.346	0.000	0.928	0.97056880733945	-0.004
Medial frontal cortex R	0.354	0.354	0.000	0.880	0.983529411764706	-0.006
Medial orbital gyrus L	0.470	0.470	0.000	0.738	1	-0.012
Medial orbital gyrus R	0.407	0.407	0.000	0.632	1	0.019
Middle cingulate gyrus L	0.396	0.399	0.002	0.208	0.94848	-0.049
Middle cingulate gyrus R	0.336	0.340	0.004	0.114	0.8664	-0.065
Middle frontal gyrus L	0.467	0.470	0.003	0.139	0.754571428571429	-0.054
Middle frontal gyrus R	0.468	0.468	0.000	0.751825	0.996605232558139	-0.012
Middle occipital gyrus L	0.295	0.295	0.000	0.858	0.998081632653061	0.008
Middle occipital gyrus R	0.327	0.327	0.001	0.510	1	-0.027
Middle temporal gyrus L	0.498	0.498	0.000	0.980	1	-0.001
Middle temporal gyrus R	0.509	0.510	0.001	0.440	0.988672566371681	-0.027
Occipital fusiform gyrus L	0.460	0.460	0.000	0.835	1	0.008
Occipital fusiform gyrus R	0.457	0.457	0.000	0.754	0.988	-0.012

Occipital pole L	0.333	0.335	0.001	0.357	0.94646511627907	-0.038
Occipital pole R	0.367	0.367	0.000	0.837	0.9939375	-0.008
Opercular part of the inferior frontal gyrus L	0.222	0.229	0.007	0.059	0.960857143	0.084
Opercular part of the inferior frontal gyrus R	0.236	0.236	0.000	0.901	0.959943925	0.005
Orbital part of the inferior frontal gyrus L	0.261	0.261	0.000	0.621	1	0.021
Orbital part of the inferior frontal gyrus R	0.255	0.255	0.000	0.723005	1	0.015
Pallidum L	0.183	0.189	0.006	0.075769	1	-0.081
Pallidum R	0.160	0.163	0.003	0.203	0.96425	-0.059
Parahippocampal gyrus L	0.427	0.428	0.001	0.395	1	-0.032
Parahippocampal gyrus R	0.458	0.463	0.005	0.053	1	-0.072
Parietal operculum L	0.338	0.338	0.000	0.674	1	0.017
Parietal operculum R	0.276	0.276	0.000	0.870	1	-0.007
Planum polare L	0.401	0.401	0.000	0.819	0.993255319148936	-0.009
Planum polare R	0.442	0.443	0.001	0.525839	1	-0.024
Planum temporale L	0.321	0.322	0.002	0.328	0.912	-0.041
Planum temporale R	0.315	0.316	0.000	0.736	1	0.014
Postcentral gyrus L	0.371	0.371	0.001	0.568	1	-0.023
Postcentral gyrus R	0.361	0.361	0.000	0.872	0.99408	-0.006
Postcentral gyrus medial segment L	0.208	0.208	0.000	0.784	1	-0.012
Postcentral gyrus medial segment R	0.198	0.200	0.002	0.286	0.905666666666667	0.048
Posterior cingulate gyrus L	0.517	0.517	0.00	0.700	1	-0.013
Posterior cingulate gyrus R	0.485	0.486	0.001	0.323	0.92055	-0.036
Posterior insula L	0.383	0.388	0.005	0.083	0.860181818181818	-0.068
Posterior insula R	0.403	0.406	0.003	0.130	0.78	-0.059
Posterior orbital gyrus L	0.317	0.318	0.000	0.606	1	-0.021
Posterior orbital gyrus R	0.321	0.322	0.001	0.417	1	-0.034
Precentral gyrus L	0.446	0.446	0.000	0.905	0.955277778	-0.004
Precentral gyrus R	0.415	0.415	0.000	0.584	1	0.021
Precentral gyrus medial segment L	0.258	0.258	0.000	0.981	0.981	-0.001
Precentral gyrus medial segment R	0.304	0.305	0.000	0.795	0.995934065934066	-0.011

Precuneus L	0.478	0.478	0.000	0.793	1	0.010
Precuneus R	0.941	0.491	0.000	0.966	0.992108108108108	-0.002
Putamen L	0.227	0.238	0.011	0.016	0.912	-0.107
Putamen R	0.229	0.237	0.008	0.040	0.912	-0.091
Subcallosal area L	0.428	0.429	0.001	0.526432	1	0.024
Subcallosal area R	0.370	0.370	0.000	0.762	0.987136363636364	0.012
Superior frontal gyrus L	0.446	0.446	0.000	0.882	0.976194174757282	0.006
Superior frontal gyrus R	0.460	0.460	0.000	0.963	0.998018181818182	-0.002
Superior frontal gyrus medial segment L	0.407	0.408	0.000	0.562	1	-0.022
Superior frontal gyrus medial segment R	0.406	0.406	0.000	0.563	1	-0.022
Superior occipital gyrus L	0.287	0.289	0.001	0.399	1	0.036
Superior occipital gyrus R	0.268	0.268	0.000	0.876	0.988752475247525	-0.007
Superior parietal lobule L	0.353	0.353	0.000	0.808	0.990451612903226	-0.010
Superior parietal lobule R	0.374	0.376	0.002	0.311	0.933	-0.040
Superior temporal gyrus L	0.373	0.373	0.000	0.722961	1	0.014
Superior temporal gyrus R	0.348	0.348	0.000	0.653	1	0.018
Supplementary motor cortex L	0.356	0.357	0.000	0.751700	1	-0.013
Supplementary motor cortex R	0.371	0.371	0.000	0.803	0.995021739130435	0.010
Supramarginal gyrus L	0.287	0.287	0.000	0.609	1	-0.022
Supramarginal gyrus R	0.335	0.337	0.002	0.252040	0.8978925	-0.047
Temporal pole L	0.328	0.330	0.002	0.261	0.875117647058824	-0.046
Temporal pole R	0.358	0.362	0.004	0.100	0.95	-0.066
Thalamus proper L	0.200	0.206	0.006	0.076454	0.968417333	-0.080
Thalamus proper R	0.221	0.233	0.012	0.011	1	-0.113
Transverse temporal gyrus L	0.237	0.239	0.003	0.244	0.959172414	0.051
Transverse temporal gyrus R	0.292	0.292	0.000	0.742827	1	0.014
Triangular part of the inferior frontal gyrus L	0.274	0.277	0.002	0.248	0.9424	0.050
Triangular part of the inferior frontal gyrus R	0.253	0.255	0.002	0.273	0.8892	-0.048

FDR: false discovery rate. L: left. PRS: polygenic risk score. R: right.

Table D.27: Associations between APOEonlyPRS Threshold 10 and 114 regions of interest in APOE ε4 carriers

Region of Interest	R Square (Model 1)	R Square (Model 2)	R Square Change	Sig. F Change (Model 2)	FDR Corrected value	Standardised beta of PRS
Accumbens area L	0.479	0.488	0.009	0.026	0.423428571428571	0.099
Accumbens area R	0.444	0.463	0.019	0.002	0.228	0.142
Amygdala L	0.496	0.496	0.000	0.797151	0.998628725274725	0.011
Amygdala R	0.544	0.544	0.000	0.953593	1	-0.002
Angular gyrus L	0.465	0.467	0.002	0.352	0.978731707317073	-0.042
Angular gyrus R	0.479	0.479	0.000	0.712309	1	0.017
Anterior cingulate gyrus L	0.445	0.447	0.002	0.321	0.989027027027027	0.046
Anterior cingulate gyrus R	0.312	0.316	0.005	0.159	0.9063	0.073
Anterior insula L	0.445	0.450	0.005	0.129	0.865058823529412	0.070
Anterior insula R	0.431	0.442	0.011	0.018	0.342	0.111
Anterior orbital gyrus L	0.420	0.421	0.000	0.737	1	-0.016
Anterior orbital gyrus R	0.387	0.391	0.004	0.183	0.948272727272727	-0.065
Basal forebrain L	0.375	0.377	0.002	0.288	0.938057142857143	0.052
Basal forebrain R	0.393	0.407	0.014	0.011	0.3135	0.123
Calcarine cortex L	0.417	0.418	0.001	0.464	0.944571428571429	-0.035
Calcarine cortex R	0.424	0.428	0.004	0.178	0.966285714285714	-0.063
Caudate L	0.245	0.246	0.001	0.485	0.9215	0.038
Caudate R	0.238	0.238	0.000	0.741	1	0.018
Central operculum L	0.432	0.432	0.000	0.864	0.975207920792079	0.008
Central operculum R	0.425	0.425	0.000	0.721	1	-0.017
Cuneus L	0.445	0.447	0.002	0.263470	0.910169090909091	-0.052
Cuneus R	0.444	0.444	0.000	0.837	0.97365306122449	-0.010
Entorhinal area L	0.483	0.483	0.000	0.954043	0.997806440366972	0.003
Entorhinal area R	0.536	0.537	0.001	0.397	0.942875	0.036
Frontal operculum L	0.412	0.413	0.002	0.381	0.924127659574468	0.042
Frontal operculum R	0.366	0.369	0.002	0.302	0.956333333333333	0.051

Frontal pole L	0.490	0.491	0.001	0.501	0.921193548387097	-0.030
Frontal pole R	0.461	0.463	0.002	0.341	0.996769230769231	0.043
Fusiform gyrus L	0.571	0.571	0.000	0.767	0.993613636363636	0.012
Fusiform gyrus R	0.614	0.615	0.001	0.468	0.919862068965517	0.028
Gyrus rectus L	0.506	0.506	0.000	0.925	0.985514018691589	-0.004
Gyrus rectus R	0.530	0.530	0.000	0.806	0.9672	-0.010
Hippocampus L	0.567	0.567	0.000	0.819	0.9725625	-0.009
Hippocampus R	0.560	0.560	0.000	0.596	0.999176470588235	-0.022
Inferior occipital gyrus L	0.466	0.467	0.001	0.466	0.932	-0.033
Inferior occipital gyrus R	0.528	0.529	0.001	0.344	0.9804	-0.040
Inferior temporal gyrus L	0.553	0.553	0.001	0.480	0.927457627118644	0.029
Inferior temporal gyrus R	0.584	0.587	0.003	0.136	0.861333333333333	0.060
Lateral orbital gyrus L	0.450	0.450	0.000	0.795	1	0.012
Lateral orbital gyrus R	0.420	0.421	0.001	0.459	0.951381818181818	-0.035
Lingual gyrus L	0.515	0.515	0.000	0.747	1	-0.014
Lingual gyrus R	0.537	0.537	0.000	0.711848	1	-0.016
Medial frontal cortex L	0.399	0.399	0.000	0.760	1	-0.015
Medial frontal cortex R	0.416	0.416	0.000	0.761	1	0.014
Medial orbital gyrus L	0.495	0.495	0.000	0.644	1	-0.020
Medial orbital gyrus R	0.484	0.485	0.000	0.627	1	-0.022
Middle cingulate gyrus L	0.382	0.387	0.006	0.106	0.863142857142857	0.079
Middle cingulate gyrus R	0.366	0.370	0.004	0.203	0.92568	0.063
Middle frontal gyrus L	0.489	0.492	0.003	0.185	0.91695652173913	0.059
Middle frontal gyrus R	0.477	0.482	0.006	0.080	0.76	0.079
Middle occipital gyrus L	0.446	0.448	0.002	0.355338	0.9001896	-0.043
Middle occipital gyrus R	0.410	0.413	0.003	0.258	0.9804	-0.054
Middle temporal gyrus L	0.512	0.512	0.000	0.909	1	-0.005
Middle temporal gyrus R	0.565	0.565	0.000	0.594	1	0.022
Occipital fusiform gyrus L	0.495	0.496	0.002	0.355260	0.920446363636364	0.041
Occipital fusiform gyrus R	0.583	0.583	0.000	0.719	1	0.014

Occipital pole L	0.368	0.368	0.000	0.805	0.976276595744681	-0.012
Occipital pole R	0.387	0.388	0.000	0.667	1	0.021
Opercular part of the inferior frontal gyrus L	0.323	0.326	0.003	0.261	0.959806451612903	0.057
Opercular part of the inferior frontal gyrus R	0.338	0.339	0.001	0.611	1	0.026
Orbital part of the inferior frontal gyrus L	0.311	0.311	0.000	0.978	0.978	-0.001
Orbital part of the inferior frontal gyrus R	0.288	0.288	0.000	0.829	0.974288659793814	-0.011
Pallidum L	0.158	0.163	0.005	0.209	0.916384615384615	-0.072
Pallidum R	0.135	0.143	0.008	0.112630	0.855988	-0.092
Parahippocampal gyrus L	0.559	0.559	0.000	0.863	0.98382	-0.007
Parahippocampal gyrus R	0.598	0.598	0.000	0.786	1	-0.011
Parietal operculum L	0.357	0.358	0.001	0.446	0.959320754716981	0.038
Parietal operculum R	0.340	0.348	0.008	0.071	0.8094	0.091
Planum polare L	0.517	0.517	0.000	0.923	0.992660377358491	-0.004
Planum polare R	0.542	0.542	0.000	0.797277	0.987930195652174	-0.011
Planum temporale L	0.413	0.416	0.003	0.215	0.875357142857143	0.059
Planum temporale R	0.448	0.448	0.000	0.964	0.981214285714286	0.002
Postcentral gyrus L	0.424	0.426	0.001	0.425	0.95	0.038
Postcentral gyrus R	0.427	0.427	0.000	0.855	0.984545454545455	-0.009
Postcentral gyrus medial segment L	0.206	0.213	0.007	0.113117	0.805958625	-0.088
Postcentral gyrus medial segment R	0.260	0.260	0.000	0.799	0.97941935483871	-0.014
Posterior cingulate gyrus L	0.582	0.583	0.001	0.408	0.949224489795918	0.033
Posterior cingulate gyrus R	0.540	0.541	0.000	0.581	1	-0.023
Posterior insula L	0.422	0.431	0.009	0.035437	0.448868666666667	0.099
Posterior insula R	0.455	0.464	0.009	0.035239	0.50215575	0.096
Posterior orbital gyrus L	0.435	0.435	0.000	0.965	0.97353982300885	-0.002
Posterior orbital gyrus R	0.452	0.452	0.000	0.867	0.969	-0.008
Precentral gyrus L	0.476	0.490	0.014	0.005	0.19	0.126
Precentral gyrus R	0.467	0.478	0.011	0.015	0.342	0.110
Precentral gyrus medial segment L	0.350	0.351	0.002	0.415	0.9462	-0.041
Precentral gyrus medial segment R	0.375	0.376	0.001	0.507	0.917428571428571	-0.033

Precuneus L	0.507	0.508	0.000	0.616	1	0.022
Precuneus R	0.500	0.500	0.000	0.688	1	-0.018
Putamen L	0.348	0.353	0.005	0.142	0.852	0.074
Putamen R	0.375	0.382	0.007	0.072	0.746181818181818	0.088
Subcallosal area L	0.544	0.546	0.001	0.353704	0.960053714285714	0.039
Subcallosal area R	0.558	0.560	0.002	0.211	0.890888888888889	0.052
Superior frontal gyrus L	0.475	0.478	0.002	0.247	0.970965517241379	0.052
Superior frontal gyrus R	0.509	0.524	0.015	0.003	0.171	0.128
Superior frontal gyrus medial segment L	0.440	0.442	0.002	0.338	1	0.045
Superior frontal gyrus medial segment R	0.422	0.428	0.006	0.094	0.824307692307692	0.079
Superior occipital gyrus L	0.369	0.369	0.000	0.745	1	0.016
Superior occipital gyrus R	0.434	0.435	0.001	0.576	1	0.026
Superior parietal lobule L	0.442	0.443	0.000	0.762	0.99848275862069	-0.014
Superior parietal lobule R	0.408	0.408	0.000	0.913449	0.991744628571428	-0.005
Superior temporal gyrus L	0.507	0.508	0.000	0.676	1	-0.018
Superior temporal gyrus R	0.485	0.485	0.000	0.651	1	-0.020
Supplementary motor cortex L	0.379	0.380	0.001	0.533	0.94940625	0.031
Supplementary motor cortex R	0.396	0.398	0.002	0.354423	0.939633069767442	0.045
Supramarginal gyrus L	0.438	0.439	0.001	0.454	0.958444444444445	-0.035
Supramarginal gyrus R	0.407	0.408	0.001	0.498	0.930688524590164	0.032
Temporal pole L	0.491	0.493	0.002	0.279	0.935470588235294	0.048
Temporal pole R	0.484	0.487	0.003	0.193	0.91675	0.058
Thalamus proper L	0.273	0.275	0.002	0.363	0.899608695652174	0.048
Thalamus proper R	0.326	0.329	0.003	0.263363	0.9382306875	0.057
Transverse temporal gyrus L	0.334	0.334	0.000	0.959	0.993872727272727	0.003
Transverse temporal gyrus R	0.437	0.437	0.000	0.912707	1	0.005
Triangular part of the inferior frontal gyrus L	0.384	0.385	0.001	0.443	0.971192307692308	0.037
Triangular part of the inferior frontal gyrus R	0.356	0.356	0.000	0.961	0.986972972972973	0.002

FDR: false discovery rate. L: left. PRS: polygenic risk score. R: right.

Table D.28: Associations between PRSwithAPOE Threshold 1 and 114 regions of interest in CU participants

Region of Interest	R Square (Model 1)	R Square (Model 2)	R Square Change	Sig. F Change (Model 2)	FDR Corrected value	Standardised beta of PRS
Accumbens area L	0.346	0.347	0.001	0.582	0.753954545454545	-0.036
Accumbens area R	0.391	0.391	0.000	0.835557	0.907176171428571	0.013
Amygdala L	0.420	0.438	0.018	0.025	0.178125	-0.139
Amygdala R	0.477	0.497	0.020	0.013	0.18525	-0.146
Angular gyrus L	0.403	0.405	0.001	0.526	0.731268292682927	-0.040
Angular gyrus R	0.365	0.369	0.005	0.255	0.45421875	-0.074
Anterior cingulate gyrus L	0.447	0.449	0.002	0.445	0.658831168831169	-0.046
Anterior cingulate gyrus R	0.266	0.272	0.006	0.251	0.454190476190476	-0.080
Anterior insula L	0.407	0.408	0.000	0.783768	0.902520727272727	-0.017
Anterior insula R	0.408	0.408	0.000	0.713	0.8556	-0.023
Anterior orbital gyrus L	0.317	0.328	0.011	0.098	0.301945945945946	-0.112
Anterior orbital gyrus R	0.360	0.371	0.012	0.081046	0.288726375	-0.114
Basal forebrain L	0.294	0.307	0.013	0.081219	0.280574727272727	-0.119
Basal forebrain R	0.367	0.373	0.006	0.205	0.432777777777778	-0.082
Calcarine cortex L	0.384	0.395	0.011	0.087	0.283371428571429	-0.109
Calcarine cortex R	0.383	0.410	0.027	0.007	0.114	-0.0172
Caudate L	0.170	0.170	0.000	0.887	0.902839285714286	-0.011
Caudate R	0.169	0.169	0.000	0.796	0.898455445544554	-0.019
Central operculum L	0.447	0.448	0.001	0.597	0.7562	-0.032
Central operculum R	0.402	0.407	0.005	0.248	0.456	-0.073
Cuneus L	0.346	0.348	0.002	0.514408	0.72398162962963	-0.043
Cuneus R	0.424	0.427	0.003	0.381	0.594986301369863	-0.054
Entorhinal area L	0.408	0.415	0.007	0.172	0.400163265306122	-0.086
Entorhinal area R	0.466	0.471	0.006	0.191	0.410830188679245	-0.078
Frontal operculum L	0.437	0.437	0.000	0.784002	0.89376228	0.017
Frontal operculum R	0.287	0.306	0.019	0.034	0.204	-0.146

Frontal pole L	0.422	0.425	0.003	0.378	0.5985	0.055
Frontal pole R	0.413	0.415	0.001	0.543	0.745807228915663	0.038
Fusiform gyrus L	0.513	0.524	0.011	0.057	0.25992	-0.108
Fusiform gyrus R	0.471	0.486	0.015	0.032	0.202666666666667	-0.127
Gyrus rectus L	0.438	0.438	0.000	0.727	0.8633125	-0.021
Gyrus rectus R	0.467	0.470	0.003	0.335	0.57	-0.058
Hippocampus L	0.368	0.389	0.021	0.020	0.207272727272727	-0.150
Hippocampus R	0.380	0.426	0.046	0.000381263621789	0.043464052883946	-0.225
Inferior occipital gyrus L	0.363	0.364	0.001	0.606	0.750913043478261	-0.034
Inferior occipital gyrus R	0.500	0.508	0.008	0.103	0.29355	-0.094
Inferior temporal gyrus L	0.568	0.579	0.011	0.040	0.217142857142857	-0.110
Inferior temporal gyrus R	0.563	0.577	0.013	0.023699	0.207822	-0.122
Lateral orbital gyrus L	0.379	0.386	0.007	0.169	0.401375	-0.088
Lateral orbital gyrus R	0.384	0.398	0.013	0.058	0.254307692307692	-0.121
Lingual gyrus L	0.530	0.537	0.008	0.099	0.297	-0.092
Lingual gyrus R	0.515	0.524	0.009	0.073	0.308222222222222	-0.102
Medial frontal cortex L	0.430	0.430	0.000	0.806	0.900823529411765	0.015
Medial frontal cortex R	0.393	0.399	0.005	0.223	0.430881355932203	-0.078
Medial orbital gyrus L	0.451	0.461	0.009	0.097	0.307166666666667	-0.100
Medial orbital gyrus R	0.455	0.460	0.005	0.226	0.4294	-0.073
Middle cingulate gyrus L	0.453	0.454	0.001	0.621	0.761225806451613	-0.030
Middle cingulate gyrus R	0.352	0.367	0.015	0.050	0.247826086956522	-0.128
Middle frontal gyrus L	0.536	0.540	0.004	0.212	0.431571428571429	-0.069
Middle frontal gyrus R	0.496	0.501	0.005	0.210	0.435272727272727	-0.073
Middle occipital gyrus L	0.323	0.327	0.004	0.338	0.56664705882353	0.064
Middle occipital gyrus R	0.374	0.377	0.003	0.390	0.5928	-0.056
Middle temporal gyrus L	0.514	0.517	0.003	0.325	0.432	-0.056
Middle temporal gyrus R	0.524	0.528	0.004	0.216	0.561363636363636	-0.070
Occipital fusiform gyrus L	0.480	0.480	0.000	0.895	0.902920353982301	-0.008
Occipital fusiform gyrus R	0.474	0.476	0.002	0.437	0.6555	-0.046

Occipital pole L	0.360	0.362	0.001	0.553	0.741670588235294	0.039
Occipital pole R	0.333	0.335	0.002	0.514380	0.7329915	0.044
Opercular part of the inferior frontal gyrus L	0.306	0.307	0.000	0.838	0.892822429906542	-0.014
Opercular part of the inferior frontal gyrus R	0.308	0.311	0.003	0.371	0.59569014084507	-0.061
Orbital part of the inferior frontal gyrus L	0.405	0.421	0.017	0.031	0.207882352941176	-0.135
Orbital part of the inferior frontal gyrus R	0.282	0.288	0.006	0.238	0.444786885245902	-0.082
Pallidum L	0.203	0.271	0.015	0.078	0.306620689655172	-0.128
Pallidum R	0.166	0.176	0.011	0.149	0.361404255319149	-0.108
Parahippocampal gyrus L	0.506	0.523	0.016	0.019	0.2166	-0.134
Parahippocampal gyrus R	0.508	0.533	0.025	0.003	0.0855	-0.167
Parietal operculum L	0.354	0.356	0.002	0.510	0.735949367088608	0.043
Parietal operculum R	0.341	0.341	0.000	0.814	0.900932038834951	-0.016
Planum polare L	0.479	0.481	0.001	0.552	0.749142857142857	-0.035
Planum polare R	0.482	0.489	0.007	0.129	0.334227272727273	-0.089
Planum temporale L	0.407	0.411	0.003	0.351359	0.572213228571429	-0.059
Planum temporale R	0.360	0.360	0.000	0.886	0.909945945945946	-0.009
Postcentral gyrus L	0.372	0.376	0.004	0.307	0.538430769230769	-0.066
Postcentral gyrus R	0.351	0.360	0.009	0.127	0.336697674418605	-0.100
Postcentral gyrus medial segment L	0.131	0.151	0.020	0.053	0.25175	-0.147
Postcentral gyrus medial segment R	0.186	0.188	0.003	0.453	0.662076923076923	-0.055
Posterior cingulate gyrus L	0.476	0.483	0.007	0.130	0.329333333333333	-0.090
Posterior cingulate gyrus R	0.418	0.427	0.009	0.104	0.289170731707317	-0.101
Posterior insula L	0.396	0.396	0.000	0.954	0.954	0.004
Posterior insula R	0.435	0.435	0.000	0.846	0.884807339449541	-0.012
Posterior orbital gyrus L	0.382	0.416	0.035	0.002154	0.081852	-0.195
Posterior orbital gyrus R	0.388	0.423	0.035	0.001959	0.111663	-0.196
Precentral gyrus L	0.442	0.459	0.017	0.023922	0.194793428571429	-0.137
Precentral gyrus R	0.425	0.431	0.006	0.185	0.4218	-0.082
Precentral gyrus medial segment L	0.282	0.295	0.013	0.083	0.278294117647059	-0.120
Precentral gyrus medial segment R	0.324	0.336	0.013	0.079	0.3002	-0.118

Precuneus L	0.477	0.487	0.010	0.080	0.294193548387097	-0.103
Precuneus R	0.456	0.476	0.019	0.015	0.19	-0.146
Putamen L	0.287	0.309	0.022	0.024366	0.1851816	-0.154
Putamen R	0.300	0.313	0.013	0.075	0.305357142857143	-0.122
Subcallosal area L	0.513	0.514	0.001	0.573	0.750827586206896	-0.032
Subcallosal area R	0.492	0.498	0.005	0.188	0.420235294117647	-0.077
Superior frontal gyrus L	0.501	0.508	0.007	0.142	0.351913043478261	-0.085
Superior frontal gyrus R	0.523	0.523	0.000	0.842	0.888777777777778	-0.011
Superior frontal gyrus medial segment L	0.381	0.391	0.010	0.101	0.295230769230769	-0.105
Superior frontal gyrus medial segment R	0.395	0.397	0.001	0.560	0.742325581395349	-0.037
Superior occipital gyrus L	0.327	0.329	0.001	0.600	0.751648351648352	-0.035
Superior occipital gyrus R	0.305	0.306	0.001	0.584	0.748044943820225	-0.037
Superior parietal lobule L	0.402	0.403	0.001	0.670	0.812553191489362	-0.027
Superior parietal lobule R	0.417	0.445	0.027	0.005	0.114	-0.173
Superior temporal gyrus L	0.480	0.480	0.000	0.767	0.892224489795918	0.017
Superior temporal gyrus R	0.466	0.468	0.003	0.350650	0.579334782608696	-0.056
Supplementary motor cortex L	0.410	0.436	0.026	0.006	0.114	-0.169
Supplementary motor cortex R	0.428	0.430	0.003	0.382	0.588486486486486	-0.054
Supramarginal gyrus L	0.363	0.363	0.000	0.821	0.899942307692308	-0.015
Supramarginal gyrus R	0.429	0.429	0.000	0.874	0.905781818181818	-0.010
Temporal pole L	0.405	0.411	0.006	0.218	0.42848275862069	-0.078
Temporal pole R	0.409	0.415	0.006	0.189	0.414346153846154	-0.083
Thalamus proper L	0.293	0.312	0.019	0.036	0.2052	-0.143
Thalamus proper R	0.312	0.334	0.022	0.021	0.1995	-0.156
Transverse temporal gyrus L	0.310	0.311	0.000	0.731	0.859113402061856	0.023
Transverse temporal gyrus R	0.402	0.403	0.000	0.836376	0.899498716981132	0.013
Triangular part of the inferior frontal gyrus L	0.373	0.382	0.009	0.120	0.325714285714286	-0.100
Triangular part of the inferior frontal gyrus R	0.298	0.315	0.016	0.049	0.253909090909091	-0.134

FDR: false discovery rate. L: left. PRS: polygenic risk score. R: right.

Table D.29: Associations between PRSwithAPOE Threshold 1 and 114 regions of interest in MCI patients

Region of Interest	R Square (Model 1)	R Square (Model 2)	R Square Change	Sig. F Change (Model 2)	FDR Corrected value	Standardised beta of PRS
Accumbens area L	0.379	0.379	0.000	0.586	1	0.024
Accumbens area R	0.353	0.353	0.000	0.723308	1	0.016
Amygdala L	0.341	0.341	0.000	0.971	1	0.002
Amygdala R	0.408	0.409	0.001	0.362	1	-0.039
Angular gyrus L	0.375	0.376	0.000	0.575	1	-0.025
Angular gyrus R	0.405	0.405	0.000	0.779	1	-0.012
Anterior cingulate gyrus L	0.403	0.403	0.000	0.884	1	-0.006
Anterior cingulate gyrus R	0.229	0.229	0.000	0.986	1	0.001
Anterior insula L	0.315	0.318	0.003	0.1676515	1	0.064
Anterior insula R	0.328	0.329	0.001	0.488	1	0.032
Anterior orbital gyrus L	0.436	0.436	0.000	0.999	0.999	0.000
Anterior orbital gyrus R	0.373	0.374	0.001	0.348	1	-0.041
Basal forebrain L	0.255	0.255	0.000	0.909	1	0.005
Basal forebrain R	0.319	0.319	0.000	0.790	1	0.012
Calcarine cortex L	0.403	0.403	0.000	0.801	1	0.011
Calcarine cortex R	0.414	0.414	0.001	0.534284	1	-0.026
Caudate L	0.195	0.195	0.000	0.722943	1	0.018
Caudate R	0.201	0.201	0.000	0.814764	1	0.012
Central operculum L	0.391	0.402	0.010	0.010104	0.575928	0.111
Central operculum R	0.365	0.366	0.001	0.392	1	0.038
Cuneus L	0.411	0.412	0.001	0.482	1	-0.030
Cuneus R	0.429	0.432	0.003	0.143	1	-0.061
Entorhinal area L	0.335	0.336	0.002	0.314	1	0.046
Entorhinal area R	0.421	0.421	0.000	0.929	1	0.004
Frontal operculum L	0.362	0.366	0.003	0.152	1	0.063
Frontal operculum R	0.348	0.349	0.001	0.489	1	0.031

Frontal pole L	0.429	0.431	0.003	0.184994	1	0.056
Frontal pole R	0.426	0.429	0.003	0.124	1	0.065
Fusiform gyrus L	0.442	0.442	0.000	0.964	1	0.002
Fusiform gyrus R	0.500	0.500	0.000	0.859	1	-0.007
Gyrus rectus L	0.436	0.438	0.002	0.256	1	0.047
Gyrus rectus R	0.420	0.420	0.001	0.560	1	0.025
Hippocampus L	0.395	0.395	0.000	0.750	1	-0.014
Hippocampus R	0.422	0.426	0.004	0.094	1	-0.071
Inferior occipital gyrus L	0.379	0.381	0.002	0.235	1	-0.052
Inferior occipital gyrus R	0.446	0.447	0.001	0.508	1	-0.027
Inferior temporal gyrus L	0.459	0.459	0.000	0.791	1	0.011
Inferior temporal gyrus R	0.536	0.536	0.000	0.989	1	-0.001
Lateral orbital gyrus L	0.443	0.445	0.002	0.185128	1	0.055
Lateral orbital gyrus R	0.344	0.345	0.001	0.564	1	0.026
Lingual gyrus L	0.489	0.490	0.000	0.715	1	0.015
Lingual gyrus R	0.529	0.529	0.000	0.622	1	-0.019
Medial frontal cortex L	0.371	0.373	0.002	0.273	1	-0.048
Medial frontal cortex R	0.340	.340	0.000	0.842	1	0.009
Medial orbital gyrus L	0.451	0.451	0.000	0.758	1	0.013
Medial orbital gyrus R	0.420	0.420	0.000	0.722965	1	0.015
Middle cingulate gyrus L	0.355	0.355	0.000	0.870	1	0.007
Middle cingulate gyrus R	0.352	0.367	0.015	0.933	1	0.004
Middle frontal gyrus L	0.463	0.463	0.000	0.611	1	0.021
Middle frontal gyrus R	0.462	0.462	0.000	0.862	1	-0.007
Middle occipital gyrus L	0.335	0.336	0.001	0.477	1	-0.032
Middle occipital gyrus R	0.322	0.328	0.005	0.077133	1	-0.081
Middle temporal gyrus L	0.452	0.453	0.001	0.480	1	0.029
Middle temporal gyrus R	0.488	0.489	0.000	0.578	1	-0.022
Occipital fusiform gyrus L	0.463	0.463	0.000	0.751	1	0.013
Occipital fusiform gyrus R	0.520	0.521	0.001	0.481	1	-0.027

Occipital pole L	0.295	0.296	0.001	0.456	1	-0.035
Occipital pole R	0.375	0.375	0.000	0.624	1	-0.022
Opercular part of the inferior frontal gyrus L	0.281	0.292	0.011	0.016	0.608	0.113
Opercular part of the inferior frontal gyrus R	0.254	0.258	0.004	0.168	1	0.066
Orbital part of the inferior frontal gyrus L	0.285	0.293	0.008	0.034	0.969	0.099
Orbital part of the inferior frontal gyrus R	0.238	0.239	0.000	0.732	1	-0.017
Pallidum L	0.171	0.171	0.000	0.828	1	0.011
Pallidum R	0.138	0.138	0.000	0.938	1	-0.004
Parahippocampal gyrus L	0.433	0.437	0.004	0.089	1	0.071
Parahippocampal gyrus R	0.508	0.533	0.025	0.590	1	0.021
Parietal operculum L	0.334	0.335	0.001	0.533914	1	0.028
Parietal operculum R	0.279	0.279	0.000	0.709	1	0.018
Planum polare L	0.388	0.389	0.000	0.780	1	0.012
Planum polare R	0.429	0.429	0.000	0.977	1	-0.001
Planum temporale L	0.328	0.331	0.003	0.195	1	0.059
Planum temporale R	0.352	0.353	0.001	0.418	1	0.036
Postcentral gyrus L	0.369	0.369	0.000	0.908	1	0.005
Postcentral gyrus R	0.393	0.394	0.000	0.710	1	-0.016
Postcentral gyrus medial segment L	0.229	0.232	0.003	0.217	1	-0.060
Postcentral gyrus medial segment R	0.222	0.222	0.000	0.777	1	-0.014
Posterior cingulate gyrus L	0.560	0.562	0.002	0.166522	1	0.051
Posterior cingulate gyrus R	0.523	0.523	0.000	0.792	1	0.010
Posterior insula L	0.352	0.353	0.002	0.308	1	0.046
Posterior insula R	0.381	0.381	0.000	0.577	1	0.024
Posterior orbital gyrus L	0.351	0.358	0.007	0.045	1	0.090
Posterior orbital gyrus R	0.377	0.378	0.000	0.699	1	0.017
Precentral gyrus L	0.485	0.487	0.001	0.294	1	0.042
Precentral gyrus R	0.473	0.473	0.000	0.795	1	0.010
Precentral gyrus medial segment L	0.283	0.284	0.001	0.502	1	-0.032
Precentral gyrus medial segment R	0.314	0.317	0.002	0.270	1	-0.051

Precuneus L	0.463	0.463	0.000	0.983	1	-0.001
Precuneus R	0.489	0.489	0.000	0.904	1	-0.005
Putamen L	0.229	0.229	0.000	0.711	1	0.018
Putamen R	0.241	0.241	0.000	0.836	1	-0.010
Subcallosal area L	0.434	0.436	0.002	0.214	1	0.052
Subcallosal area R	0.380	0.390	0.010	0.010000	1	0.112
Superior frontal gyrus L	0.428	0.428	0.000	0.629	1	-0.020
Superior frontal gyrus R	0.465	0.466	0.001	0.397	1	0.034
Superior frontal gyrus medial segment L	0.414	0.415	0.001	0.498	1	0.029
Superior frontal gyrus medial segment R	0.384	0.386	0.002	0.218	1	0.054
Superior occipital gyrus L	0.338	0.339	0.000	0.762	1	-0.014
Superior occipital gyrus R	0.343	0.343	0.000	0.670	1	0.019
Superior parietal lobule L	0.368	0.368	0.000	0.960	1	0.002
Superior parietal lobule R	0.359	0.359	0.000	0.994	1	0.000
Superior temporal gyrus L	0.365	0.366	0.001	0.465	1	0.032
Superior temporal gyrus R	0.360	0.361	0.001	0.445	1	0.034
Supplementary motor cortex L	0.356	0.357	0.001	0.536	1	-0.028
Supplementary motor cortex R	0.347	0.347	0.000	0.625	1	-0.022
Supramarginal gyrus L	0.312	0.312	0.000	0.775	1	0.013
Supramarginal gyrus R	0.306	0.310	0.004	0.140	1	0.068
Temporal pole L	0.312	0.312	0.001	0.528	1	0.029
Temporal pole R	0.347	0.349	0.001	0.363444	1	-0.041
Thalamus proper L	0.213	0.217	0.004	0.141	1	0.073
Thalamus proper R	0.255	0.257	0.002	0.363310	1	0.044
Transverse temporal gyrus L	0.255	0.255	0.000	0.781	1	0.013
Transverse temporal gyrus R	0.307	0.307	0.000	0.815017	1	0.011
Triangular part of the inferior frontal gyrus L	0.340	0.345	0.005	0.076580	1	0.080
Triangular part of the inferior frontal gyrus R	0.285	0.286	0.001	0.441	1	0.036

FDR: false discovery rate. L: left. PRS: polygenic risk score. R: right.

Table D.30: Associations between PRSwithAPOE Threshold 1 and 114 regions of interest in AD dementia patients

Region of Interest	R Square (Model 1)	R Square (Model 2)	R Square Change	Sig. F Change (Model 2)	FDR Corrected value	Standardised beta of PRS
Accumbens area L	0.512	0.513	0.001	0.586	1	-0.041
Accumbens area R	0.497	0.799	0.002	0.523	1	0.049
Amygdala L	0.425	0.463	0.038	0.005	0.285	-0.226
Amygdala R	0.445	0.473	0.028	0.016	0.456	-0.193
Angular gyrus L	0.446	0.446	0.001	0.694	1	-0.032
Angular gyrus R	0.558	0.558	0.000	0.947	1	0.005
Anterior cingulate gyrus L	0.412	0.428	0.016	0.076	0.962666667	0.147
Anterior cingulate gyrus R	0.272	0.273	0.002	0.628	1	-0.045
Anterior insula L	0.505	0.509	0.004	0.347253	1	0.072
Anterior insula R	0.557	0.560	0.003	0.378	1	0.064
Anterior orbital gyrus L	0.499	0.502	0.003	0.398	1	-0.065
Anterior orbital gyrus R	0.495	0.495	0.000	0.867	1	0.013
Basal forebrain L	0.275	0.277	0.001	0.639	1	0.043
Basal forebrain R	0.376	0.379	0.003	0.499	1	0.058
Calcarine cortex L	0.390	0.390	0.000	0.830	1	0.018
Calcarine cortex R	0.439	0.439	0.000	0.799	1	0.021
Caudate L	0.362	0.367	0.005	0.343	1	-0.082
Caudate R	0.328	0.331	0.003	0.488	1	-0.062
Central operculum L	0.373	0.375	0.002	0.565	1	-0.049
Central operculum R	0.506	0.506	0.001	0.727	1	0.027
Cuneus L	0.491	0.494	0.003	0.381	1	-0.068
Cuneus R	0.473	0.473	0.000	0.959570	1	-0.004
Entorhinal area L	0.413	0.471	0.057	0.000629322254795	0.071742737	-0.277
Entorhinal area R	0.407	0.424	0.017	0.071	1	-0.150
Frontal operculum L	0.341	0.352	0.011	0.168	1	0.121
Frontal operculum R	0.405	0.431	0.026	0.024	0.5472	0.187

Frontal pole L	0.523	0.525	0.002	0.545	1	-0.045
Frontal pole R	0.496	0.497	0.001	0.708	1	0.029
Fusiform gyrus L	0.496	0.497	0.000	0.750	1	-0.025
Fusiform gyrus R	0.530	0.530	0.000	0.729672	1	-0.026
Gyrus rectus L	0.526	0.528	0.001	0.564	1	-0.043
Gyrus rectus R	0.541	0.544	0.003	0.363	1	0.067
Hippocampus L	0.471	0.499	0.029	0.012	0.456	-0.196
Hippocampus R	0.503	0.516	0.012	0.092	0.953454545	-0.128
Inferior occipital gyrus L	0.507	0.508	0.000	0.820	1	-0.017
Inferior occipital gyrus R	0.479	0.479	0.000	0.844	1	-0.015
Inferior temporal gyrus L	0.497	0.504	0.008	0.179	1	-0.103
Inferior temporal gyrus R	0.518	0.518	0.001	0.662	1	-0.033
Lateral orbital gyrus L	0.441	0.444	0.002	0.482	1	-0.057
Lateral orbital gyrus R	0.456	0.456	0.001	0.738	1	0.027
Lingual gyrus L	0.566	0.566	0.000	0.985037	1	-0.001
Lingual gyrus R	0.558	0.559	0.001	0.606	1	0.037
Medial frontal cortex L	0.353	0.353	0.001	0.725	1	-0.031
Medial frontal cortex R	0.414	0.423	0.009	0.192	1	0.108
Medial orbital gyrus L	0.594	0.594	0.000	0.757	1	-0.021
Medial orbital gyrus R	0.512	0.514	0.002	0.503	1	0.051
Middle cingulate gyrus L	0.433	0.434	0.001	0.648	1	0.037
Middle cingulate gyrus R	0.414	0.415	0.001	0.697	1	0.032
Middle frontal gyrus L	0.540	0.542	0.002	0.506	1	0.049
Middle frontal gyrus R	0.579	0.584	0.005	0.265	1	0.078
Middle occipital gyrus L	0.440	0.445	0.004	0.340	1	-0.077
Middle occipital gyrus R	0.433	0.438	0.006	0.277	1	-0.089
Middle temporal gyrus L	0.4884	0.492	0.008	0.174	1	-0.106
Middle temporal gyrus R	0.539	0.539	0.000	0.960223	1	-0.004
Occipital fusiform gyrus L	0.521	0.524	0.003	0.365	1	0.068
Occipital fusiform gyrus R	0.513	0.513	0.000	0.941	1	-0.006

Occipital pole L	0.429	0.431	0.002	0.574	1	-0.046
Occipital pole R	0.464	0.464	0.000	0.983560	1	0.002
Opercular part of the inferior frontal gyrus L	0.367	0.369	0.002	0.529	1	0.054
Opercular part of the inferior frontal gyrus R	0.403	0.410	0.007	0.248	1	0.097
Orbital part of the inferior frontal gyrus L	0.326	0.330	0.004	0.429	1	0.070
Orbital part of the inferior frontal gyrus R	0.306	0.307	0.001	0.730318	1	-0.031
Pallidum L	0.214	0.225	0.011	0.202	1	-0.122
Pallidum R	0.240	0.253	0.013	0.160	1	-0.133
Parahippocampal gyrus L	0.522	0.542	0.019	0.030	0.57	-0.161
Parahippocampal gyrus R	0.492	0.492	0.000	0.128	1	-0.112
Parietal operculum L	0.376	0.380	0.004	0.366	1	0.077
Parietal operculum R	0.358	0.360	0.002	0.552	1	0.052
Planum polare L	0.459	0.459	0.000	0.979	1	-0.002
Planum polare R	0.483	0.484	0.001	0.686	1	0.032
Planum temporale L	0.495	0.497	0.001	0.581	1	0.043
Planum temporale R	0.408	0.408	0.000	0.958620	1	-0.004
Postcentral gyrus L	0.553	0.554	0.000	0.817	1	0.017
Postcentral gyrus R	0.501	0.501	0.000	0.841	1	0.015
Postcentral gyrus medial segment L	0.371	0.371	0.000	0.993	1	-0.001
Postcentral gyrus medial segment R	0.330	0.330	0.000	0.803	1	-0.022
Posterior cingulate gyrus L	0.605	0.614	0.009	0.109	0.955846154	-0.109
Posterior cingulate gyrus R	0.597	0.602	0.005	0.213	1	-0.086
Posterior insula L	0.487	0.496	0.009	0.158	1	0.109
Posterior insula R	0.516	0.530	0.014	0.072	1	0.135
Posterior orbital gyrus L	0.434	0.435	0.001	0.678	1	-0.034
Posterior orbital gyrus R	0.418	0.421	0.002	0.490	1	0.057
Precentral gyrus L	0.507	0.513	0.006	0.224	1	0.092
Precentral gyrus R	0.463	0.469	0.006	0.251471	1	0.091
Precentral gyrus medial segment L	0.422	0.423	0.000	0.761	1	-0.025
Precentral gyrus medial segment R	0.406	0.406	0.000	0.829	1	0.018

Precuneus L	0.575	0.576	0.001	0.589	1	-0.038
Precuneus R	0.610	0.611	0.000	0.801	1	-0.017
Putamen L	0.429	0.429	0.000	0.994	0.994	-0.001
Putamen R	0.444	0.444	0.000	0.926	1	0.008
Subcallosal area L	0.571	0.573	0.004	0.325	1	0.070
Subcallosal area R	0.597	0.606	0.009	0.105	0.9975	0.111
Superior frontal gyrus L	0.565	0.565	0.000	0.897	1	-0.009
Superior frontal gyrus R	0.570	0.570	0.000	0.718	1	0.026
Superior frontal gyrus medial segment L	0.527	0.528	0.001	0.601	1	-0.039
Superior frontal gyrus medial segment R	0.504	0.509	0.006	0.251216	1	0.088
Superior occipital gyrus L	0.349	0.349	0.000	0.914	1	0.009
Superior occipital gyrus R	0.479	0.479	0.000	0.976	1	-0.003
Superior parietal lobule L	0.517	0.517	0.000	0.973	1	0.003
Superior parietal lobule R	0.486	0.486	0.000	0.984863	1	-0.001
Superior temporal gyrus L	0.489	0.489	0.000	0.990	1	-0.001
Superior temporal gyrus R	0.413	0.415	0.003	0.460	1	-0.061
Supplementary motor cortex L	0.427	0.428	0.001	0.703	1	0.031
Supplementary motor cortex R	0.434	0.442	0.007	0.222	1	0.099
Supramarginal gyrus L	0.459	0.462	0.003	0.432	1	0.063
Supramarginal gyrus R	0.451	0.456	0.004	0.346888	1	0.076
Temporal pole L	0.483	0.485	0.003	0.421	1	-0.063
Temporal pole R	0.433	0.433	0.000	0.965	1	-0.004
Thalamus proper L	0.199	0.213	0.015	0.148	1	-0.140
Thalamus proper R	0.264	0.272	0.008	0.278	1	-0.101
Transverse temporal gyrus L	0.332	0.338	0.005	0.334	1	0.086
Transverse temporal gyrus R	0.295	0.296	0.000	0.794	1	-0.024
Triangular part of the inferior frontal gyrus L	0.336	0.353	0.017	0.084	0.9576	0.152
Triangular part of the inferior frontal gyrus R	0.442	0.443	0.000	0.905	1	0.010

FDR: false discovery rate. L: left. PRS: polygenic risk score. R: right.

Table D.31: Associations between PRSwithAPOE Threshold 5 and 114 regions of interest in CU participants

Region of Interest	R Square (Model 1)	R Square (Model 2)	R Square Change	Sig. F Change (Model 2)	FDR Corrected value	Standardised beta of PRS
Accumbens area L	0.346	0.347	0.001	0.700	0.848936170212766	-0.025
Accumbens area R	0.391	0.391	0.000	0.765	0.8721	0.019
Amygdala L	0.420	0.439	0.018	0.021654	0.176325428571429	-0.142
Amygdala R	0.477	0.495	0.018	0.017	0.215333333333333	-0.140
Angular gyrus L	0.403	0.405	0.001	0.525923	0.731161243902439	-0.040
Angular gyrus R	0.364	0.369	0.005	0.273822	0.472965272727273	-0.071
Anterior cingulate gyrus L	0.447	0.449	0.001	0.526428	0.723045686746988	-0.039
Anterior cingulate gyrus R	0.266	0.271	0.005	0.302	0.484901408450704	-0.072
Anterior insula L	0.407	0.409	0.001	0.532	0.713505882352941	-0.039
Anterior insula R	0.408	0.409	0.002	0.507	0.731620253164557	-0.042
Anterior orbital gyrus L	0.317	0.326	0.009	0.152	0.385066666666667	-0.097
Anterior orbital gyrus R	0.360	0.369	0.010	0.118	0.344923076923077	-0.102
Basal forebrain L	0.294	0.307	0.013	0.081	0.2885625	-0.119
Basal forebrain R	0.367	0.373	0.006	0.227	0.424229508196721	-0.079
Calcarine cortex L	0.384	0.396	0.012	0.071	0.299777777777778	-0.115
Calcarine cortex R	0.383	0.409	0.026	0.008	0.1824	-0.168
Caudate L	0.170	0.170	0.000	0.999	0.999	0.000
Caudate R	0.169	0.169	0.000	0.898	0.947888888888889	-0.010
Central operculum L	0.447	0.448	0.001	0.508	0.7239	-0.040
Central operculum R	0.402	0.406	0.004	0.274070	0.466328059701492	-0.069
Cuneus L	0.346	0.348	0.002	0.530	0.719285714285714	-0.042
Cuneus R	0.424	0.427	0.002	0.403	0.61256	-0.052
Entorhinal area L	0.408	0.415	0.007	0.160	0.388085106382979	-0.088
Entorhinal area R	0.466	0.471	0.005	0.208710	0.432598909090909	-0.075
Frontal operculum L	0.437	0.437	0.000	0.746	0.876742268041237	-0.020
Frontal operculum R	0.287	0.310	0.023	0.019413	0.1844235	-0.160

Frontal pole L	0.422	0.427	0.004	0.264	0.47025	0.069
Frontal pole R	0.413	0.415	0.002	0.462	0.684	0.046
Fusiform gyrus L	0.513	0.523	0.009	0.077	0.283161290322581	-0.100
Fusiform gyrus R	0.471	0.483	0.011	0.058	0.300545454545455	-0.112
Gyrus rectus L	0.438	0.439	0.001	0.619	0.775450549450549	-0.030
Gyrus rectus R	0.467	0.470	0.004	0.298	0.485314285714286	-0.062
Hippocampus L	0.368	0.388	0.020	0.022154	0.1683704	-0.148
Hippocampus R	0.380	0.424	0.044	0.000541521531492	0.061733454590088	-0.219
Inferior occipital gyrus L	0.363	0.364	0.001	0.610	0.772666666666667	-0.033
Inferior occipital gyrus R	0.500	0.507	0.007	0.141	0.373813953488372	-0.085
Inferior temporal gyrus L	0.568	0.580	0.012	0.030	0.18	-0.116
Inferior temporal gyrus R	0.563	0.578	0.015	0.018576	0.2117664	-0.126
Lateral orbital gyrus L	0.379	0.384	0.006	0.217	0.42651724137931	-0.079
Lateral orbital gyrus R	0.384	0.396	0.012	0.072	0.293142857142857	-0.115
Lingual gyrus L	0.530	0.539	0.009	0.073	0.286965517241379	-0.100
Lingual gyrus R	0.515	0.524	0.009	0.075	0.285	0.213
Medial frontal cortex L	0.430	0.430	0.000	0.763	0.878606060606061	0.019
Medial frontal cortex R	0.393	0.399	0.006	0.218	0.421220338983051	-0.078
Medial orbital gyrus L	0.451	0.460	0.009	0.107	0.338833333333333	-0.097
Medial orbital gyrus R	0.455	0.459	0.004	0.245	0.443333333333333	-0.070
Middle cingulate gyrus L	0.453	0.454	0.000	0.733	0.8796	-0.021
Middle cingulate gyrus R	0.352	0.365	0.013	0.069480	0.304643076923077	-0.119
Middle frontal gyrus L	0.536	0.541	0.005	0.175	0.407142857142857	-0.075
Middle frontal gyrus R	0.496	0.501	0.005	0.187	0.418	-0.076
Middle occipital gyrus L	0.323	0.328	0.005	0.287	0.474173913043478	0.072
Middle occipital gyrus R	0.374	0.376	0.002	0.463	0.676692307692308	-0.048
Middle temporal gyrus L	0.514	0.518	0.004	0.236	0.4275	-0.067
Middle temporal gyrus R	0.524	0.528	0.005	0.210	0.433935483870968	-0.071
Occipital fusiform gyrus L	0.480	0.480	0.000	0.936	0.961297297297297	-0.005
Occipital fusiform gyrus R	0.474	0.475	0.001	0.558196	0.73142924137931	-0.035

Occipital pole L	0.360	0.362	0.002	0.511	0.719185185185185	0.043
Occipital pole R	0.333	0.335	0.002	0.456	0.684	0.050
Opercular part of the inferior frontal gyrus L	0.306	0.307	0.001	0.690	0.845806451612903	-0.027
Opercular part of the inferior frontal gyrus R	0.308	0.314	0.007	0.213	0.426	-0.084
Orbital part of the inferior frontal gyrus L	0.405	0.423	0.018	0.023419	0.157045058823529	-0.142
Orbital part of the inferior frontal gyrus R	0.282	0.289	0.007	0.200	0.430188679245283	-0.089
Pallidum L	0.203	0.214	0.011	0.126	0.3591	-0.111
Pallidum R	0.166	0.172	0.006	0.265	0.464769230769231	-0.083
Parahippocampal gyrus L	0.506	0.523	0.016	0.018948	0.196370181818182	-0.134
Parahippocampal gyrus R	0.508	0.533	0.025	0.004	0.114	-0.165
Parietal operculum L	0.354	0.355	0.001	0.609	0.780067415730337	0.034
Parietal operculum R	0.341	0.341	0.000	0.830	0.909807692307692	-0.014
Planum polare L	0.479	0.483	0.003	0.310	0.490833333333333	-0.060
Planum polare R	0.482	0.490	0.009	0.099	0.322457142857143	-0.097
Planum temporale L	0.407	0.413	0.005	0.222	0.4218	-0.077
Planum temporale R	0.360	0.361	0.001	0.687	0.851282608695652	-0.026
Postcentral gyrus L	0.372	0.376	0.004	0.314	0.490356164383562	0.076
Postcentral gyrus R	0.351	0.358	0.007	0.195	0.4275	-0.085
Postcentral gyrus medial segment L	0.131	0.149	0.018	0.066	0.327130434782609	-0.139
Postcentral gyrus medial segment R	0.186	0.186	0.000	0.783	0.875117647058824	-0.020
Posterior cingulate gyrus L	0.476	0.484	0.008	0.113	0.339	-0.094
Posterior cingulate gyrus R	0.418	0.430	0.012	0.067	0.31825	-0.114
Posterior insula L	0.396	0.396	0.000	0.874	0.931177570093458	-0.010
Posterior insula R	0.435	0.435	0.000	0.914	0.955926605504587	-0.007
Posterior orbital gyrus L	0.382	0.414	0.033	0.003	0.114	-0.189
Posterior orbital gyrus R	0.388	0.422	0.034	0.002	0.114	-0.193
Precentral gyrus L	0.442	0.460	0.017	0.022530	0.16052625	-0.138
Precentral gyrus R	0.425	0.431	0.006	0.177	0.40356	-0.083
Precentral gyrus medial segment L	0.282	0.291	0.010	0.138	0.374571428571429	-0.102
Precentral gyrus medial segment R	0.324	0.332	0.009	0.143	0.3705	-0.098

Precuneus L	0.477	0.485	0.008	0.110	0.338918918918919	-0.094
Precuneus R	0.456	0.478	0.022	0.010	0.162857142857143	-0.154
Putamen L	0.287	0.308	0.021	0.028	0.177333333333333	-0.151
Putamen R	0.300	0.313	0.013	0.082	0.283272727272727	-0.119
Subcallosal area L	0.513	0.514	0.001	0.557943	0.739598860465116	-0.033
Subcallosal area R	0.492	0.497	0.005	0.208647	0.440477	-0.073
Superior frontal gyrus L	0.501	0.507	0.006	0.159	0.39404347826087	-0.081
Superior frontal gyrus R	0.523	0.523	0.000	0.780	0.88039603960396	-0.016
Superior frontal gyrus medial segment L	0.381	0.391	0.010	0.097	0.325235294117647	-0.106
Superior frontal gyrus medial segment R	0.395	0.397	0.001	0.566	0.733227272727273	-0.037
Superior occipital gyrus L	0.327	0.328	0.000	0.794	0.878796116504854	-0.018
Superior occipital gyrus R	0.305	0.305	0.000	0.748	0.870122448979592	-0.022
Superior parietal lobule L	0.402	0.402	0.000	0.871	0.936735849056604	-0.010
Superior parietal lobule R	0.417	0.441	0.024	0.009	0.171	-0.162
Superior temporal gyrus L	0.480	0.480	0.000	0.735	0.8728125	0.020
Superior temporal gyrus R	0.466	0.469	0.004	0.284	0.476117647058823	-0.064
Supplementary motor cortex L	0.410	0.433	0.023	0.011	0.15675	-0.158
Supplementary motor cortex R	0.428	0.431	0.003	0.359	0.553054054054054	-0.057
Supramarginal gyrus L	0.363	0.363	0.000	0.917	0.950345454545455	-0.007
Supramarginal gyrus R	0.429	0.429	0.000	0.867	0.941314285714286	0.010
Temporal pole L	0.405	0.413	0.008	0.131	0.364243902439024	-0.095
Temporal pole R	0.409	0.416	0.007	0.164	0.3895	-0.087
Thalamus proper L	0.293	0.311	0.018	0.042	0.228	-0.139
Thalamus proper R	0.312	0.334	0.022	0.020	0.175384615384615	-0.157
Transverse temporal gyrus L	0.310	0.310	0.000	0.988	0.996743362831858	-0.001
Transverse temporal gyrus R	0.402	0.402	0.000	0.953	0.970017857142857	-0.004
Triangular part of the inferior frontal gyrus L	0.373	0.385	0.013	0.068570	0.3126792	-0.117
Triangular part of the inferior frontal gyrus R	0.298	0.318	0.019	0.033	0.1881	-0.145

FDR: false discovery rate. L: left. PRS: polygenic risk score. R: right.

Table D.32: Associations between PRSwithAPOE Threshold 5 and 114 regions of interest in MCI patients

Region of Interest	R Square (Model 1)	R Square (Model 2)	R Square Change	Sig. F Change (Model 2)	FDR Corrected value	Standardised beta of PRS
Accumbens area L	0.379	0.379	0.001	0.494	1	0.030
Accumbens area R	0.353	0.354	0.000	0.588	1	0.024
Amygdala L	0.341	0.341	0.000	0.896	1	-0.006
Amygdala R	0.408	0.409	0.002	0.308	1	-0.044
Angular gyrus L	0.375	0.376	0.000	0.655	0.9956	-0.020
Angular gyrus R	0.405	0.405	0.000	0.773	0.990134831460674	-0.012
Anterior cingulate gyrus L	0.403	0.403	0.000	0.942	1	0.003
Anterior cingulate gyrus R	0.229	0.229	0.000	0.712	0.977927710843373	0.018
Anterior insula L	0.315	0.320	0.004	0.108	1	0.074
Anterior insula R	0.328	0.329	0.001	0.408	1	0.038
Anterior orbital gyrus L	0.436	0.436	0.000	0.910	1	0.005
Anterior orbital gyrus R	0.373	0.374	0.001	0.394	1	-0.038
Basal forebrain L	0.255	0.256	0.000	0.851	1	0.009
Basal forebrain R	0.319	0.320	0.001	0.545	1	0.028
Calcarine cortex L	0.403	0.403	0.000	0.929	1	0.004
Calcarine cortex R	0.414	0.415	0.001	0.434	1	-0.033
Caudate L	0.195	0.195	0.001	0.596955	1	0.026
Caudate R	0.201	0.201	0.000	0.814	1	0.012
Central operculum L	0.391	0.403	0.012	0.006	0.342	0.119
Central operculum R	0.365	0.366	0.001	0.399	1	0.037
Cuneus L	0.411	0.411	0.000	0.576	1	-0.024
Cuneus R	0.429	0.431	0.002	0.209	0.99275	-0.053
Entorhinal area L	0.335	0.336	0.001	0.398	1	0.038
Entorhinal area R	0.421	0.421	0.000	0.908	1	0.005
Frontal operculum L	0.362	0.367	0.005	0.081	1	0.077
Frontal operculum R	0.348	0.349	0.001	0.452	1	0.034

Frontal pole L	0.428	0.431	0.003	0.140	0.84	0.062
Frontal pole R	0.426	0.429	0.004	0.119447	1	0.066
Fusiform gyrus L	0.442	0.442	0.000	0.751	0.984068965517241	0.013
Fusiform gyrus R	0.500	0.500	0.000	0.952	0.995669724770642	0.002
Gyrus rectus L	0.436	0.439	0.003	0.184	1	0.055
Gyrus rectus R	0.420	0.421	0.001	0.526	1	0.027
Hippocampus L	0.395	0.395	0.000	0.598	1	-0.023
Hippocampus R	0.422	0.427	0.005	0.065	1	-0.078
Inferior occipital gyrus L	0.379	0.381	0.002	0.236	1	-0.052
Inferior occipital gyrus R	0.446	0.447	0.001	0.503	1	-0.028
Inferior temporal gyrus L	0.568	0.580	0.012	0.807	1	0.010
Inferior temporal gyrus R	0.536	0.536	0.000	0.950673	1	0.002
Lateral orbital gyrus L	0.443	0.446	0.003	0.119314	1	0.065
Lateral orbital gyrus R	0.344	0.345	0.001	0.397	1	0.038
Lingual gyrus L	0.489	0.490	0.000	0.660	0.977142857142857	0.017
Lingual gyrus R	0.529	0.529	0.000	0.725	0.961046511627907	-0.013
Medial frontal cortex L	0.371	0.373	0.001	0.361	1	-0.040
Medial frontal cortex R	0.340	0.340	0.001	0.574	1	0.025
Medial orbital gyrus L	0.451	0.451	0.000	0.559	1	0.024
Medial orbital gyrus R	0.420	0.420	0.001	0.558	1	0.025
Middle cingulate gyrus L	0.355	0.355	0.000	0.925	1	0.004
Middle cingulate gyrus R	0.320	0.320	0.000	0.792	1	0.012
Middle frontal gyrus L	0.463	0.464	0.000	0.596684	1	0.022
Middle frontal gyrus R	0.462	0.462	0.000	0.931	1	-0.004
Middle occipital gyrus L	0.335	0.336	0.000	0.710	0.987073170731707	-0.017
Middle occipital gyrus R	0.322	0.326	0.004	0.133	0.947625	-0.069
Middle temporal gyrus L	0.452	0.452	0.001	0.533611	1	0.026
Middle temporal gyrus R	0.488	0.489	0.000	0.544	1	-0.024
Occipital fusiform gyrus L	0.463	0.463	0.000	0.666924	0.974735076923077	0.018
Occipital fusiform gyrus R	0.520	0.521	0.000	0.653460	1	-0.017

Occipital pole L	0.295	0.296	0.001	0.412	1	-0.038
Occipital pole R	0.375	0.375	0.000	0.708	0.996444444444444	-0.016
Opercular part of the inferior frontal gyrus L	0.281	0.293	0.012	0.011	0.418	0.119
Opercular part of the inferior frontal gyrus R	0.254	0.259	0.004	0.137	0.867666666666667	0.071
Orbital part of the inferior frontal gyrus L	0.285	0.294	0.009	0.023	0.6555	0.107
Orbital part of the inferior frontal gyrus R	0.238	0.238	0.000	0.869	1	-0.008
Pallidum L	0.171	0.171	0.000	0.644	1	0.023
Pallidum R	0.138	0.138	0.000	0.950553	1	0.003
Parahippocampal gyrus L	0.433	0.436	0.004	0.107	1	0.067
Parahippocampal gyrus R	0.492	0.492	0.000	0.599	1	0.021
Parietal operculum L	0.334	0.336	0.001	0.355	1	0.042
Parietal operculum R	0.279	0.280	0.001	0.534195	1	0.029
Planum polare L	0.388	0.389	0.000	0.686	0.97755	0.018
Planum polare R	0.429	0.429	0.000	0.924497	1	0.004
Planum temporale L	0.328	0.331	0.003	0.190	0.984545454545455	0.060
Planum temporale R	0.352	0.353	0.001	0.417	1	0.036
Postcentral gyrus L	0.369	0.369	0.000	0.928	1	-0.004
Postcentral gyrus R	0.393	0.394	0.000	0.659	0.9885	-0.019
Postcentral gyrus medial segment L	0.229	0.234	0.004	0.136	0.912	-0.073
Postcentral gyrus medial segment R	0.222	0.222	0.000	0.975	0.992410714285714	0.002
Posterior cingulate gyrus L	0.560	0.562	0.002	0.201	0.996260869565217	0.047
Posterior cingulate gyrus R	0.523	0.523	0.000	0.924136	1	0.004
Posterior insula L	0.352	0.354	0.003	0.185	1	0.059
Posterior insula R	0.381	0.382	0.001	0.419	1	0.035
Posterior orbital gyrus L	0.351	0.359	0.008	0.026	0.5928	0.099
Posterior orbital gyrus R	0.377	0.378	0.000	0.623	1	0.022
Precentral gyrus L	0.485	0.487	0.002	0.248	1	0.046
Precentral gyrus R	0.473	0.473	0.000	0.603	0.996260869565217	0.021
Precentral gyrus medial segment L	0.283	0.284	0.001	0.405	1	-0.039
Precentral gyrus medial segment R	0.314	0.316	0.002	0.315	1	-0.046

Precuneus L	0.463	0.463	0.000	0.958	0.992836363636364	0.002
Precuneus R	0.489	0.489	0.000	0.984	0.984	0.001
Putamen L	0.229	0.229	0.000	0.667341	0.962998405063291	0.021
Putamen R	0.241	0.241	0.000	0.871	1	-0.008
Subcallosal area L	0.434	0.438	0.004	0.095	1	0.070
Subcallosal area R	0.380	0.394	0.014	0.002	0.228	0.132
Superior frontal gyrus L	0.428	0.428	0.000	0.764	0.989727272727273	-0.013
Superior frontal gyrus R	0.465	0.467	0.001	0.305	1	0.042
Superior frontal gyrus medial segment L	0.414	0.415	0.001	0.420	1	0.034
Superior frontal gyrus medial segment R	0.384	0.385	0.002	0.280	1	0.047
Superior occipital gyrus L	0.338	0.338	0.000	0.972	0.99827027027027	-0.002
Superior occipital gyrus R	0.343	0.343	0.001	0.474	1	0.032
Superior parietal lobule L	0.368	0.368	0.000	0.983	0.991699115044248	-0.001
Superior parietal lobule R	0.359	0.359	0.000	0.873	1	-0.007
Superior temporal gyrus L	0.365	0.366	0.001	0.536	1	0.027
Superior temporal gyrus R	0.360	0.361	0.001	0.423	1	0.036
Supplementary motor cortex L	0.356	0.357	0.001	0.563	1	-0.026
Supplementary motor cortex R	0.347	0.347	0.000	0.652789	1	-0.020
Supramarginal gyrus L	0.312	0.312	0.000	0.724	0.971011764705882	0.016
Supramarginal gyrus R	0.306	0.310	0.004	0.128	0.9728	0.070
Temporal pole L	0.312	0.312	0.001	0.476	1	0.033
Temporal pole R	0.347	0.349	0.001	0.388	1	-0.039
Thalamus proper L	0.213	0.217	0.005	0.124	1	0.076
Thalamus proper R	0.255	0.256	0.001	0.455	1	0.036
Transverse temporal gyrus L	0.255	0.255	0.000	0.720	0.977142857142857	0.017
Transverse temporal gyrus R	0.307	0.307	0.000	0.611	0.995057142857143	0.024
Triangular part of the inferior frontal gyrus L	0.340	0.347	0.007	0.047	0.893	0.090
Triangular part of the inferior frontal gyrus R	0.285	0.286	0.002	0.352	1	0.044

FDR: false discovery rate. L: left. PRS: polygenic risk score. R: right.

Table D.33: Associations between PRSwithAPOE Threshold 5 and 114 regions of interest in AD dementia patients

Region of Interest	R Square (Model 1)	R Square (Model 2)	R Square Change	Sig. F Change (Model 2)	FDR Corrected value	Standardised beta of PRS
Accumbens area L	0.512	0.514	0.002	0.468	1	-0.055
Accumbens area R	0.497	0.499	0.001	0.567518	1	0.044
Amygdala L	0.425	0.468	0.043	0.003	0.171	-0.241
Amygdala R	0.445	0.474	0.028	0.015	0.342	-0.196
Angular gyrus L	0.446	0.447	0.001	0.658	1	-0.036
Angular gyrus R	0.558	0.558	0.000	0.803	1	0.018
Anterior cingulate gyrus L	0.412	0.426	0.014	0.095	0.984545454545455	0.139
Anterior cingulate gyrus R	0.272	0.273	0.001	0.753	1	-0.029
Anterior insula L	0.505	0.508	0.003	0.404802	1	0.064
Anterior insula R	0.557	0.560	0.003	0.367	1	0.065
Anterior orbital gyrus L	0.499	0.502	0.003	0.434	1	-0.060
Anterior orbital gyrus R	0.495	0.495	0.000	0.823	1	0.017
Basal forebrain L	0.275	0.277	0.001	0.677	1	0.039
Basal forebrain R	0.376	0.378	0.002	0.580	1	0.048
Calcarine cortex L	0.390	0.390	0.000	0.904	1	0.010
Calcarine cortex R	0.439	0.439	0.000	0.799	1	0.021
Caudate L	0.362	0.367	0.005	0.369	1	-0.078
Caudate R	0.328	0.330	0.002	0.573	1	-0.050
Central operculum L	0.373	0.3#3	0.000	0.816	1	-0.020
Central operculum R	0.506	0.509	0.003	0.405314	1	0.064
Cuneus L	0.491	0.494	0.003	0.429	1	-0.062
Cuneus R	0.473	0.473	0.000	0.961911	0.987908594594594	0.004
Entorhinal area L	0.413	0.473	0.059	0.000515937825294	0.058816912083516	-0.283
Entorhinal area R	0.407	0.423	0.016	0.077	0.975333333333333	-0.148
Frontal operculum L	0.341	0.355	0.014	0.120314	0.9143864	0.137
Frontal operculum R	0.405	0.438	0.033	0.011	0.3135	0.210

Frontal pole L	0.523	0.524	0.001	0.631509	1	-0.036
Frontal pole R	0.496	0.497	0.001	0.644	1	0.036
Fusiform gyrus L	0.496	0.496	0.000	0.956175	1	-0.004
Fusiform gyrus R	0.530	0.530	0.000	0.855864	1	-0.014
Gyrus rectus L	0.526	0.527	0.001	0.683	1	-0.031
Gyrus rectus R	0.541	0.544	0.003	0.376	1	0.065
Hippocampus L	0.471	0.503	0.032	0.008	0.304	-0.208
Hippocampus R	0.503	0.515	0.012	0.097	0.9215	-0.127
Inferior occipital gyrus L	0.507	0.507	0.000	0.854712	1	-0.014
Inferior occipital gyrus R	0.479	0.479	0.000	0.992	0.992	0.001
Inferior temporal gyrus L	0.459	0.459	0.000	0.217054	0.916450222222222	-0.095
Inferior temporal gyrus R	0.518	0.518	0.000	0.802	1	-0.019
Lateral orbital gyrus L	0.441	0.442	0.001	0.632430	1	-0.039
Lateral orbital gyrus R	0.456	0.456	0.000	0.769	1	0.024
Lingual gyrus L	0.566	0.566	0.000	0.906	1	0.008
Lingual gyrus R	0.558	0.559	0.002	0.510	1	0.048
Medial frontal cortex L	0.353	0.353	0.000	0.964	0.981214285714286	-0.004
Medial frontal cortex R	0.414	0.428	0.014	0.102	0.894461538461539	0.136
Medial orbital gyrus L	0.594	0.594	0.000	0.740	1	-0.023
Medial orbital gyrus R	0.512	0.514	0.002	0.492	1	0.052
Middle cingulate gyrus L	0.433	0.435	0.002	0.519	1	0.053
Middle cingulate gyrus R	0.414	0.417	0.003	0.452	0.990923076923077	0.063
Middle frontal gyrus L	0.540	0.542	0.003	0.418	1	0.060
Middle frontal gyrus R	0.579	0.585	0.006	0.215	0.9804	0.087
Middle occipital gyrus L	0.440	0.446	0.005	0.307	1	-0.083
Middle occipital gyrus R	0.433	0.436	0.004	0.381	1	-0.072
Middle temporal gyrus L	0.484	0.491	0.007	0.210	1	-0.098
Middle temporal gyrus R	0.539	0.539	0.000	0.890	0.9975	0.010
Occipital fusiform gyrus L	0.521	0.524	0.003	0.363	1	0.069
Occipital fusiform gyrus R	0.513	0.513	0.000	0.979	0.987663716814159	0.002

Occipital pole L	0.429	0.431	0.002	0.538	1	-0.051
Occipital pole R	0.464	0.464	0.000	0.893	1	0.011
Opercular part of the inferior frontal gyrus L	0.367	0.370	0.003	0.446	1	0.066
Opercular part of the inferior frontal gyrus R	0.403	0.413	0.011	0.152	0.962666666666667	0.120
Orbital part of the inferior frontal gyrus L	0.326	0.332	0.006	0.315	1	0.090
Orbital part of the inferior frontal gyrus R	0.306	0.307	0.001	0.735	1	-0.031
Pallidum L	0.214	0.225	0.012	0.193	1	-0.126
Pallidum R	0.240	0.254	0.014	0.145	1	-0.138
Parahippocampal gyrus L	0.522	0.542	0.020	0.029	0.551	-0.163
Parahippocampal gyrus R	0.539	0.547	0.009	0.146	0.979058823529412	-0.107
Parietal operculum L	0.376	0.384	0.008	0.216620	0.949795384615385	0.106
Parietal operculum R	0.358	0.361	0.003	0.447	1	0.066
Planum polare L	0.459	0.459	0.000	0.824	1	-0.018
Planum polare R	0.483	0.485	0.002	0.543	1	0.048
Planum temporale L	0.495	0.497	0.001	0.568426	1	0.044
Planum temporale R	0.408	0.408	0.000	0.930	1	-0.007
Postcentral gyrus L	0.553	0.553	0.000	0.866	1	0.012
Postcentral gyrus R	0.501	0.501	0.000	0.909	1	0.009
Postcentral gyrus medial segment L	0.371	0.371	0.000	0.954	1	0.005
Postcentral gyrus medial segment R	0.330	0.330	0.000	0.888	1	-0.013
Posterior cingulate gyrus L	0.605	0.612	0.006	0.174	0.944571428571429	-0.093
Posterior cingulate gyrus R	0.597	0.601	0.004	0.308641	1	-0.070
Posterior insula L	0.487	0.498	0.011	0.119673	0.974480142857143	0.121
Posterior insula R	0.516	0.532	0.016	0.054	0.879428571428571	0.145
Posterior orbital gyrus L	0.434	0.435	0.001	0.748	1	-0.026
Posterior orbital gyrus R	0.418	0.421	0.003	0.448	1	0.063
Precentral gyrus L	0.507	0.516	0.009	0.156519	0.8921583	0.108
Precentral gyrus R	0.463	0.469	0.007	0.240	0.943448275862069	0.094
Precentral gyrus medial segment L	0.422	0.422	0.000	0.856154	1	-0.015
Precentral gyrus medial segment R	0.406	0.406	0.000	0.847	1	0.016

Precuneus L	0.575	0.575	0.001	0.668	1	0.031
Precuneus R	0.610	0.610	0.000	0.956623	1	-0.004
Putamen L	0.429	0.429	0.000	0.925	1	0.008
Putamen R	0.444	0.444	0.000	0.844	1	0.016
Subcallosal area L	0.570	0.574	0.004	0.308937	1	0.073
Subcallosal area R	0.597	0.607	0.011	0.083	0.9462	0.120
Superior frontal gyrus L	0.565	0.565	0.00	0.880	1	0.011
Superior frontal gyrus R	0.570	0.571	0.002	0.498	1	0.049
Superior frontal gyrus medial segment L	0.527	0.529	0.002	0.512	1	-0.049
Superior frontal gyrus medial segment R	0.504	0.510	0.006	0.238	0.969	0.090
Superior occipital gyrus L	0.349	0.350	0.001	0.761	1	0.027
Superior occipital gyrus R	0.479	0.479	0.000	0.961718	0.996689563636364	0.004
Superior parietal lobule L	0.517	0.517	0.000	0.779	1	0.021
Superior parietal lobule R	0.486	0.487	0.000	0.814	1	0.018
Superior temporal gyrus L	0.489	0.489	0.000	0.940	1	-0.006
Superior temporal gyrus R	0.413	0.415	0.002	0.496	1	-0.057
Supplementary motor cortex L	0.427	0.428	0.001	0.712	1	0.031
Supplementary motor cortex R	0.434	0.442	0.008	0.204	1	0.104
Supramarginal gyrus L	0.459	0.463	0.004	0.389	1	0.069
Supramarginal gyrus R	0.451	0.458	0.006	0.257	0.9766	0.091
Temporal pole L	0.483	0.486	0.003	0.416	1	-0.064
Temporal pole R	0.433	0.433	0.000	0.956511	1	0.004
Thalamus proper L	0.199	0.213	0.014	0.156502	0.939012	-0.138
Thalamus proper R	0.264	0.270	0.006	0.339	1	-0.089
Transverse temporal gyrus L	0.332	0.336	0.004	0.406	1	0.074
Transverse temporal gyrus R	0.295	0.295	0.000	0.853959	1	-0.017
Triangular part of the inferior frontal gyrus L	0.336	0.356	0.020	0.061	0.86925	0.165
Triangular part of the inferior frontal gyrus R	0.355	0.350	0.001	0.719	1	0.029

FDR: false discovery rate. L: left. PRS: polygenic risk score. R: right.

Table D.34: Associations between PRSwithAPOE Threshold 10 and 114 regions of interest in CU participants

Region of Interest	R Square (Model 1)	R Square (Model 2)	R Square Change	Sig. F Change (Model 2)	FDR Corrected value	Standardised beta of PRS
Accumbens area L	0.346	0.346	0.000	0.837	0.900169811320755	-0.014
Accumbens area R	0.391	0.392	0.001	0.535	0.734819277108434	0.040
Amygdala L	0.420	0.445	0.025	0.008	0.101333333333333	-0.165
Amygdala R	0.477	0.498	0.021	0.010	0.114	-0.153
Angular gyrus L	0.403	0.404	0.001	0.652	0.807913043478261	-0.029
Angular gyrus R	0.364	0.369	0.005	0.250	0.518181818181818	-0.076
Anterior cingulate gyrus L	0.447	0.448	0.001	0.660	0.809032258064516	0.001
Anterior cingulate gyrus R	0.266	0.271	0.005	0.312	0.538909090909091	-0.071
Anterior insula L	0.407	0.410	0.003	0.364	0.576333333333333	-0.058
Anterior insula R	0.408	0.412	0.004	0.282	0.5358	-0.068
Anterior orbital gyrus L	0.317	0.322	0.005	0.275	0.53135593220339	-0.074
Anterior orbital gyrus R	0.360	0.367	0.008	0.164	0.445142857142857	-0.092
Basal forebrain L	0.294	0.307	0.014	0.071449	0.2715062	-0.124
Basal forebrain R	0.367	0.372	0.005	0.256	0.521142857142857	-0.074
Calcarine cortex L	0.384	0.399	0.014	0.049	0.242869565217391	-0.127
Calcarine cortex R	0.383	0.411	0.028	0.005795	0.08257875	-0.177
Caudate L	0.170	0.170	0.000	0.972	0.989357142857143	-0.003
Caudate R	0.169	0.169	0.000	0.954	0.979783783783784	-0.004
Central operculum L	0.447	0.449	0.002	0.456	0.658025316455696	-0.046
Central operculum R	0.402	0.408	0.006	0.198	0.45144	-0.082
Cuneus L	0.346	0.348	0.001	0.555	0.744352941176471	-0.039
Cuneus R	0.424	0.427	0.003	0.377	0.588739726027397	-0.055
Entorhinal area L	0.408	0.422	0.014	0.051	0.24225	-0.123
Entorhinal area R	0.466	0.476	0.010	0.080	0.294193548387097	-0.105
Frontal operculum L	0.437	0.438	0.001	0.595	0.788720930232558	-0.033
Frontal operculum R	0.287	0.324	0.037	0.003	0.114	-0.204

Frontal pole L	0.422	0.432	0.010	0.093	0.302914285714286	0.105
Frontal pole R	0.413	0.418	0.005	0.235	0.496111111111111	0.075
Fusiform gyrus L	0.513	0.523	0.010	0.070932	0.278836137931034	-0.103
Fusiform gyrus R	0.471	0.479	0.008	0.118	0.373666666666667	-0.093
Gyrus rectus L	0.438	0.440	0.002	0.419542	0.63770384	-0.050
Gyrus rectus R	0.467	0.470	0.004	0.295888	0.544052129032258	-0.063
Hippocampus L	0.368	0.397	0.029	0.005733	0.093366	-0.179
Hippocampus R	0.380	0.428	0.049	0.000261961809852	0.029863646323128	-0.233
Inferior occipital gyrus L	0.363	0.364	0.001	0.633	0.810808988764045	-0.031
Inferior occipital gyrus R	0.500	0.506	0.006	0.165	0.437441860465116	-0.081
Inferior temporal gyrus L	0.568	0.579	0.012	0.032	0.1824	-0.115
Inferior temporal gyrus R	0.563	0.576	0.013	0.028	0.187764705882353	-0.119
Lateral orbital gyrus L	0.379	0.382	0.003	0.381	0.586945945945946	-0.057
Lateral orbital gyrus R	0.384	0.401	0.017	0.031	0.186	-0.138
Lingual gyrus L	0.530	0.540	0.011	0.052	0.23712	-0.110
Lingual gyrus R	0.515	0.524	0.009	0.082	0.283272727272727	-0.100
Medial frontal cortex L	0.430	0.430	0.000	0.749	0.871285714285714	0.020
Medial frontal cortex R	0.393	0.397	0.003	0.351	0.571628571428571	-0.060
Medial orbital gyrus L	0.451	0.458	0.006	0.173382	0.429685826086957	-0.083
Medial orbital gyrus R	0.455	0.460	0.005	0.213	0.476117647058824	-0.076
Middle cingulate gyrus L	0.453	0.453	0.000	0.982	0.982	0.001
Middle cingulate gyrus R	0.352	0.360	0.007	0.169	0.437863636363636	-0.091
Middle frontal gyrus L	0.536	0.538	0.002	0.357	0.573211267605634	-0.052
Middle frontal gyrus R	0.496	0.499	0.003	0.301	0.53615625	-0.060
Middle occipital gyrus L	0.323	0.327	0.004	0.346	0.571652173913043	0.064
Middle occipital gyrus R	0.374	0.377	0.002	0.425	0.621153846153846	-0.052
Middle temporal gyrus L	0.514	0.520	0.007	0.130	0.537428571428571	-0.087
Middle temporal gyrus R	0.524	0.527	0.003	0.297	0.39	-0.059
Occipital fusiform gyrus L	0.480	0.480	0.000	0.800	0.902970297029703	-0.015
Occipital fusiform gyrus R	0.474	0.475	0.000	0.737	0.866164948453608	-0.020

Occipital pole L	0.360	0.362	0.002	0.481326	0.677421777777778	0.046
Occipital pole R	0.333	0.335	0.003	0.420056	0.630084	0.054
Opercular part of the inferior frontal gyrus L	0.306	0.307	0.001	0.640	0.810666666666667	-0.032
Opercular part of the inferior frontal gyrus R	0.308	0.320	0.012	0.086	0.288352941176471	-0.117
Orbital part of the inferior frontal gyrus L	0.405	0.427	0.022	0.013	0.134727272727273	-0.157
Orbital part of the inferior frontal gyrus R	0.282	0.290	0.008	0.178	0.431744680851064	-0.094
Pallidum L	0.203	0.214	0.011	0.126	0.388216216216216	-0.112
Pallidum R	0.166	0.170	0.005	0.342	0.573352941176471	-0.072
Parahippocampal gyrus L	0.506	0.530	0.024	0.004667	0.088673	-0.162
Parahippocampal gyrus R	0.508	0.540	0.032	0.000855326120037	0.048753588842109	-0.190
Parietal operculum L	0.354	0.354	0.000	0.817	0.904252427184466	0.015
Parietal operculum R	0.341	0.342	0.001	0.626	0.810954545454545	-0.033
Planum polare L	0.479	0.485	0.005	0.193	0.449020408163265	-0.077
Planum polare R	0.482	0.493	0.011	0.058579	0.256846384615385	-0.112
Planum temporale L	0.407	0.414	0.006	0.182	0.43225	-0.085
Planum temporale R	0.360	0.363	0.003	0.420267	0.622213480519481	-0.053
Postcentral gyrus L	0.372	0.374	0.002	0.486	0.675658536585366	-0.046
Postcentral gyrus R	0.351	0.352	0.001	0.613	0.803241379310345	-0.034
Postcentral gyrus medial segment L	0.131	0.138	0.007	0.258	0.516	-0.087
Postcentral gyrus medial segment R	0.186	0.187	0.001	0.661	0.801638297872341	0.033
Posterior cingulate gyrus L	0.476	0.482	0.006	0.163	0.453219512195122	-0.083
Posterior cingulate gyrus R	0.418	0.432	0.014	0.046	0.249714285714286	-0.125
Posterior insula L	0.396	0.396	0.000	0.726	0.862125	-0.022
Posterior insula R	0.435	0.435	0.000	0.827	0.906519230769231	-0.014
Posterior orbital gyrus L	0.382	0.411	0.030	0.004469	0.1273665	-0.182
Posterior orbital gyrus R	0.388	0.417	0.029	0.004648	0.1059744	-0.181
Precentral gyrus L	0.442	0.454	0.012	0.059872	0.252792888888889	-0.115
Precentral gyrus R	0.425	0.428	0.004	0.311	0.545446153846154	-0.063
Precentral gyrus medial segment L	0.282	0.284	0.002	0.480808	0.6851514	-0.049
Precentral gyrus medial segment R	0.324	0.328	0.004	0.325	0.552985074626866	-0.067

Precuneus L	0.477	0.482	0.005	0.223	0.488884615384615	-0.073
Precuneus R	0.456	0.474	0.017	0.021	0.1596	-0.139
Putamen L	0.287	0.313	0.025	0.015038	0.131871692307692	-0.168
Putamen R	0.300	0.315	0.015	0.060059	0.244525928571429	-0.129
Subcallosal area L	0.513	0.513	0.000	0.776	0.893575757575758	-0.016
Subcallosal area R	0.492	0.496	0.003	0.293	0.547573770491803	-0.062
Superior frontal gyrus L	0.501	0.505	0.004	0.263	0.516931034482759	-0.065
Superior frontal gyrus R	0.523	0.523	0.000	0.897	0.946833333333333	0.007
Superior frontal gyrus medial segment L	0.381	0.388	0.007	0.159	0.45315	-0.091
Superior frontal gyrus medial segment R	0.395	0.396	0.000	0.781	0.89034	-0.018
Superior occipital gyrus L	0.327	0.328	0.000	0.828	0.898971428571428	-0.015
Superior occipital gyrus R	0.305	0.305	0.001	0.700	0.84	-0.027
Superior parietal lobule L	0.402	0.402	0.000	0.912	0.953834862385321	0.007
Superior parietal lobule R	0.417	0.438	0.021	0.014779	0.1404005	-0.152
Superior temporal gyrus L	0.480	0.480	0.000	0.926	0.959672727272727	0.006
Superior temporal gyrus R	0.466	0.470	0.005	0.233	0.501169811320755	-0.072
Supplementary motor cortex L	0.410	0.427	0.017	0.029	0.183666666666667	-0.137
Supplementary motor cortex R	0.428	0.429	0.001	0.648	0.81178021978022	-0.029
Supramarginal gyrus L	0.363	0.363	0.000	0.858	0.914130841121495	0.012
Supramarginal gyrus R	0.429	0.429	0.000	0.973	0.981610619469027	0.002
Temporal pole L	0.405	0.416	0.011	0.081	0.2885625	-0.111
Temporal pole R	0.409	0.417	0.008	0.133	0.388769230769231	-0.095
Thalamus proper L	0.293	0.310	0.017	0.048	0.248727272727273	-0.136
Thalamus proper R	0.312	0.332	0.020	0.026	0.18525	-0.151
Transverse temporal gyrus L	0.310	0.311	0.000	0.813	0.908647058823529	-0.016
Transverse temporal gyrus R	0.402	0.404	0.001	0.552	0.749142857142857	-0.038
Triangular part of the inferior frontal gyrus L	0.373	0.380	0.007	0.173036	0.438357866666667	-0.089
Triangular part of the inferior frontal gyrus R	0.298	0.323	0.025	0.016	0.130285714285714	-0.165

FDR: false discovery rate. L: left. PRS: polygenic risk score. R: right.

Table D.35: Associations between PRSwithAPOE Threshold 10 and 114 regions of interest in MCI patients

Region of Interest	R Square (Model 1)	R Square (Model 2)	R Square Change	Sig. F Change (Model 2)	FDR Corrected value	Standardised beta of PRS
Accumbens area L	0.379	0.379	0.000	0.718	1	0.016
Accumbens area R	0.353	0.353	0.000	0.680	1	0.018
Amygdala L	0.341	0.341	0.000	0.942	1	-0.003
Amygdala R	0.408	0.409	0.001	0.355	1	-0.039
Angular gyrus L	0.375	0.376	0.000	0.816	1	-0.010
Angular gyrus R	0.405	0.405	0.000	0.727	1	-0.015
Anterior cingulate gyrus L	0.403	0.403	0.000	0.898	1	0.000
Anterior cingulate gyrus R	0.229	0.230	0.001	0.590	1	0.026
Anterior insula L	0.315	0.320	0.005	0.102	0.969	0.075
Anterior insula R	0.328	0.330	0.002	0.278	1	0.049
Anterior orbital gyrus L	0.436	0.436	0.000	0.989	1	-0.001
Anterior orbital gyrus R	0.373	0.374	0.001	0.368	1	-0.039
Basal forebrain L	0.255	0.255	0.000	0.967	1	0.002
Basal forebrain R	0.319	0.320	0.001	0.443	1	0.035
Calcarine cortex L	0.403	0.403	0.000	0.904	1	0.005
Calcarine cortex R	0.414	0.414	0.001	0.492	1	-0.029
Caudate L	0.195	0.195	0.001	0.593	1	0.027
Caudate R	0.201	0.201	0.000	0.769	1	0.015
Central operculum L	0.391	0.402	0.010	0.009	0.513	0.112
Central operculum R	0.365	0.366	0.001	0.403	1	0.037
Cuneus L	0.411	0.412	0.001	0.464162	1	-0.031
Cuneus R	0.429	0.432	0.003	0.150	0.9	-0.060
Entorhinal area L	0.335	0.336	0.001	0.464009	1	0.033
Entorhinal area R	0.421	0.421	0.000	0.974	1	0.001
Frontal operculum L	0.362	0.369	0.007	0.042841	0.813979	0.089
Frontal operculum R	0.348	0.350	0.002	0.322	1	0.044

Frontal pole L	0.428	0.432	0.003	0.133	0.947625	0.063
Frontal pole R	0.426	0.429	0.004	0.118	1	0.065
Fusiform gyrus L	0.442	0.442	0.000	0.806	1	0.010
Fusiform gyrus R	0.500	0.501	0.000	0.807	1	-0.010
Gyrus rectus L	0.436	0.438	0.002	0.198	0.981391304347826	0.054
Gyrus rectus R	0.420	0.420	0.000	0.608	1	0.022
Hippocampus L	0.395	0.395	0.000	0.750	1	-0.014
Hippocampus R	0.422	0.426	0.004	0.085	0.969	-0.072
Inferior occipital gyrus L	0.379	0.380	0.002	0.298	1	-0.045
Inferior occipital gyrus R	0.446	0.446	0.000	0.564	1	-0.024
Inferior temporal gyrus L	0.459	0.459	0.000	0.988	1	-0.001
Inferior temporal gyrus R	0.536	0.536	0.000	0.931062	1	-0.003
Lateral orbital gyrus L	0.443	0.447	0.004	0.099	1	0.068
Lateral orbital gyrus R	0.344	0.345	0.000	0.611	1	0.023
Lingual gyrus L	0.489	0.489	0.000	0.931211	1	0.003
Lingual gyrus R	0.529	0.529	0.000	0.894	1	-0.005
Medial frontal cortex L	0.371	0.373	0.002	0.284	1	-0.047
Medial frontal cortex R	0.340	0.340	0.000	0.659	1	0.020
Medial orbital gyrus L	0.451	0.451	0.001	0.515	1	0.027
Medial orbital gyrus R	0.420	0.420	0.000	0.694	1	0.017
Middle cingulate gyrus L	0.355	0.355	0.000	0.745	1	0.014
Middle cingulate gyrus R	0.320	0.320	0.000	0.729	1	0.016
Middle frontal gyrus L	0.463	0.463	0.000	0.626	1	0.020
Middle frontal gyrus R	0.462	0.462	0.000	0.940	1	-0.003
Middle occipital gyrus L	0.335	0.355	0.000	0.842	1	-0.009
Middle occipital gyrus R	0.322	0.326	0.004	0.120	0.977142857142857	-0.071
Middle temporal gyrus L	0.452	0.452	0.001	0.537	1	0.025
Middle temporal gyrus R	0.488	0.489	0.000	0.568	1	-0.023
Occipital fusiform gyrus L	0.463	0.463	0.000	0.703	1	0.015
Occipital fusiform gyrus R	0.520	0.521	0.000	0.582	1	-0.021

Occipital pole L	0.295	0.297	0.002	0.262	1	-0.052
Occipital pole R	0.375	0.376	0.001	0.495	1	-0.030
Opercular part of the inferior frontal gyrus L	0.281	0.293	0.012	0.011	0.418	0.118
Opercular part of the inferior frontal gyrus R	0.254	0.258	0.004	0.151	0.8607	0.069
Orbital part of the inferior frontal gyrus L	0.285	0.294	0.009	0.023	0.6555	0.106
Orbital part of the inferior frontal gyrus R	0.238	0.238	0.000	0.869	1	-0.008
Pallidum L	0.171	0.171	0.001	0.531	1	0.032
Pallidum R	0.138	0.138	0.000	0.787	1	0.014
Parahippocampal gyrus L	0.433	0.436	0.003	0.138	0.925411764705882	0.062
Parahippocampal gyrus R	0.492	0.492	0.000	0.709	1	0.015
Parietal operculum L	0.334	0.337	0.002	0.238	1	0.053
Parietal operculum R	0.279	0.279	0.001	0.555	1	0.028
Planum polare L	0.388	0.388	0.000	1.000	1	0.000
Planum polare R	0.4229	0.429	0.000	0.713	1	-0.015
Planum temporale L	0.328	0.331	0.003	0.195	1	0.059
Planum temporale R	0.352	0.353	0.001	0.484	1	0.031
Postcentral gyrus L	0.369	0.369	0.000	0.631	1	-0.021
Postcentral gyrus R	0.393	0.394	0.000	0.617	1	-0.022
Postcentral gyrus medial segment L	0.229	0.233	0.004	0.162	0.879428571428571	-0.068
Postcentral gyrus medial segment R	0.222	0.222	0.000	0.711	1	0.018
Posterior cingulate gyrus L	0.560	0.561	0.002	0.229	1	0.044
Posterior cingulate gyrus R	0.523	0.523	0.000	0.856	1	0.007
Posterior insula L	0.352	0.354	0.002	0.234	1	0.053
Posterior insula R	0.381	0.381	0.001	0.473	1	0.031
Posterior orbital gyrus L	0.351	0.358	0.007	0.042548	0.9700944	0.090
Posterior orbital gyrus R	0.377	0.377	0.000	0.810	1	0.010
Precentral gyrus L	0.485	0.487	0.002	0.277	1	0.043
Precentral gyrus R	0.473	0.473	0.001	0.465	1	0.029
Precentral gyrus medial segment L	0.283	0.285	0.002	0.340	1	-0.045
Precentral gyrus medial segment R	0.314	0.316	0.001	0.401	1	-0.039

Precuneus L	0.463	0.463	0.000	0.882	1	0.006
Precuneus R	0.489	0.489	0.000	0.996	1	0.000
Putamen L	0.229	0.230	0.001	0.546	1	0.029
Putamen R	0.241	0.241	0.000	0.913	1	0.005
Subcallosal area L	0.434	0439	0.005	0.067	0.95475	0.076
Subcallosal area R	0.380	0.399	0.019	0.000422421612259	0.048156063797526	0.153
Superior frontal gyrus L	0.428	0.428	0.000	0.937	1	-0.003
Superior frontal gyrus R	0.465	0.468	0.003	0.122	0.9272	0.063
Superior frontal gyrus medial segment L	0.414	0.415	0.001	0.411	1	0.035
Superior frontal gyrus medial segment R	0.384	0.385	0.002	0.318	1	0.043
Superior occipital gyrus L	0.338	0.339	0.000	0.827	1	-0.010
Superior occipital gyrus R	0.343	0.343	0.000	0.758	1	0.014
Superior parietal lobule L	0.368	0.368	0.000	0.954	1	-0.003
Superior parietal lobule R	0.359	0.359	0.000	0.644	1	-0.021
Superior temporal gyrus L	0.365	0.365	0.000	0.795	1	0.011
Superior temporal gyrus R	0.360	0.361	0.001	0.445	1	0.034
Supplementary motor cortex L	0.356	0.358	0.002	0.276	1	-0.048
Supplementary motor cortex R	0.347	0.347	0.000	0.647	1	-0.021
Supramarginal gyrus L	0.312	0.313	0.000	0.627	1	0.022
Supramarginal gyrus R	0.306	0.311	0.005	0.083	1	0.080
Temporal pole L	0.312	0.312	0.001	0.562	1	0.027
Temporal pole R	0.347	0.349	0.002	0.337	1	-0.043
Thalamus proper L	0.213	0.217	0.004	0.141	0.893	0.072
Thalamus proper R	0.255	0.256	0.001	0.550	1	0.029
Transverse temporal gyrus L	0.255	0.255	0.000	0.724	1	0.017
Transverse temporal gyrus R	0.307	0.307	0.000	0.752	1	0.015
Triangular part of the inferior frontal gyrus L	0.340	0.346	0.006	0.058	0.944571428571429	0.085
Triangular part of the inferior frontal gyrus R	0.285	0.287	0.002	0.309	1	0.048

FDR: false discovery rate. L: left. PRS: polygenic risk score. R: right.

Table D.36: Associations between PRSwithAPOE Threshold 10 and 114 regions of interest in AD dementia patients

Region of Interest	R Square (Model 1)	R Square (Model 2)	R Square Change	Sig. F Change (Model 2)	FDR Corrected value	Standardised beta of PRS
Accumbens area L	0.512	0.516	0.004	0.326	1	-0.074
Accumbens area R	0.497	0.498	0.000	0.904	1	0.009
Amygdala L	0.425	0.460	0.036	0.007	0.399	-0.217
Amygdala R	0.445	0.466	0.021	0.037	0.703	-0.166
Angular gyrus L	0.446	0.446	0.000	0.882	1	0.012
Angular gyrus R	0.558	0.560	0.002	0.424	1	0.057
Anterior cingulate gyrus L	0.412	0.423	0.012	0.129	1	0.012
Anterior cingulate gyrus R	0.272	0.272	0.000	0.945	1	-0.006
Anterior insula L	0.505	0.509	0.004	0.352	1	0.071
Anterior insula R	0.557	0.560	0.004	0.339	1	0.069
Anterior orbital gyrus L	0.499	0.502	0.003	0.402	1	-0.064
Anterior orbital gyrus R	0.495	0.496	0.001	0.641	1	0.036
Basal forebrain L	0.275	0.277	0.001	0.662	1	0.040
Basal forebrain R	0.376	0.377	0.001	0.688	1	0.034
Calcarine cortex L	0.390	0.390	0.000	0.950	1	-0.005
Calcarine cortex R	0.439	0.440	0.001	0.710	1	0.030
Caudate L	0.362	0.371	0.009	0.204	1	-0.109
Caudate R	0.328	0.334	0.006	0.314	1	-0.089
Central operculum L	0.373	0.373	0.000	0.876	1	-0.013
Central operculum R	0.506	0.511	0.005	0.296	1	0.079
Cuneus L	0.491	0.494	0.003	0.429	1	-0.061
Cuneus R	0.473	0.473	0.000	0.926	1	0.007
Entorhinal area L	0.413	0.460	0.046	0.002	0.228	-0.248
Entorhinal area R	0.407	0.417	0.010	0.157	1	-0.117
Frontal operculum L	0.341	0.357	0.016	0.092	1	0.147
Frontal operculum R	0.405	0.437	0.032	0.012	0.456	0.206

Frontal pole L	0.523	0.523	0.000	0.967	1	-0.003
Frontal pole R	0.496	0.498	0.001	0.614	1	0.039
Fusiform gyrus L	0.496	0.496	0.000	0.890	1	0.011
Fusiform gyrus R	0.530	0.530	0.000	0.941	1	-0.005
Gyrus rectus L	0.526	0.527	0.000	0.798	1	-0.019
Gyrus rectus R	0.541	0.544	0.003	0.377	1	0.065
Hippocampus L	0.471	0.499	0.029	0.012	0.342	-0.195
Hippocampus R	0.503	0.514	0.011	0.114	1	-0.120
Inferior occipital gyrus L	0.507	0.507	0.000	0.899	1	0.010
Inferior occipital gyrus R	0.479	0.479	0.000	0.818	1	0.018
Inferior temporal gyrus L	0.497	0.501	0.004	0.317	1	-0.077
Inferior temporal gyrus R	0.518	0.518	0.000	0.895	1	-0.010
Lateral orbital gyrus L	0.441	0.442	0.001	0.718	1	-0.029
Lateral orbital gyrus R	0.456	0.456	0.000	0.775	1	0.023
Lingual gyrus L	0.566	0.566	0.000	0.888	1	0.010
Lingual gyrus R	0.558	0.561	0.003	0.370	1	0.064
Medial frontal cortex L	0.353	0.353	0.000	0.963	1	-0.004
Medial frontal cortex R	0.414	0.425	0.011	0.147	1	0.119
Medial orbital gyrus L	0.594	0.595	0.001	0.598	1	-0.036
Medial orbital gyrus R	0.512	0.513	0.001	0.606	1	0.039
Middle cingulate gyrus L	0.433	0.436	0.003	0.437	1	0.063
Middle cingulate gyrus R	0.414	0.420	0.006	0.281	1	0..089
Middle frontal gyrus L	0.540	0.543	0.004	0.345	1	0.069
Middle frontal gyrus R	0.579	0.587	0.007	0.161	1	0.098
Middle occipital gyrus L	0.440	0.442	0.002	0.546	1	-0.049
Middle occipital gyrus R	0.433	0.434	0.001	0.645	1	-0.037
Middle temporal gyrus L	0.484	0.486	0.003	0.449	1	-0.059
Middle temporal gyrus R	0.539	0.539	0.001	0.678	1	0.030
Occipital fusiform gyrus L	0.521	0.525	0.005	0.290	1	0.079
Occipital fusiform gyrus R	0.513	0.513	0.000	0.913	1	-0.008

Occipital pole L	0.429	0.431	0.002	0.578	1	-0.045
Occipital pole R	0.464	0.464	0.000	0.816	1	0.018
Opercular part of the inferior frontal gyrus L	0.367	0.372	0.005	0.358	1	0.079
Opercular part of the inferior frontal gyrus R	0.403	0.411	0.008	0.225	1	0.101
Orbital part of the inferior frontal gyrus L	0.326	0.329	0.003	0.479	1	0.063
Orbital part of the inferior frontal gyrus R	0.306	0.307	0.001	0.665	1	-0.039
Pallidum L	0.214	0.224	0.010	0.223	1	-0.116
Pallidum R	0.240	0.252	0.013	0.168	1	-0.129
Parahippocampal gyrus L	0.522	0.541	0.019	0.034	0.7752	-0.157
Parahippocampal gyrus R	0.539	0.544	0.005	0.270	1	-0.081
Parietal operculum L	0.376	0.388	0.013	0.125	1	0.130
Parietal operculum R	0.358	0.361	0.003	0.459	1	0.064
Planum polare L	0.459	0.459	0.000	0.750	1	-0.025
Planum polare R	0.483	0.485	0.002	0.465	1	0.057
Planum temporale L	0.495	0.498	0.003	0.428	1	0.061
Planum temporale R	0.408	0.408	0.000	0.952	1	-0.005
Postcentral gyrus L	0.553	0.553	0.000	0.953	1	0.004
Postcentral gyrus R	0.501	0.501	0.000	0.951	1	-0.005
Postcentral gyrus medial segment L	0.371	0.371	0.000	0.887	1	0.012
Postcentral gyrus medial segment R	0.330	0.330	0.000	0.834	1	-0.018
Posterior cingulate gyrus L	0.605	0.609	0.003	0.322	1	-0.067
Posterior cingulate gyrus R	0.597	0.598	0.001	0.535	1	-0.042
Posterior insula L	0.487	0.497	0.010	0.128	1	0.117
Posterior insula R	0.516	0.533	0.017	0.045	0.732857142857143	0.149
Posterior orbital gyrus L	0.434	0.435	0.001	0.676	1	-0.034
Posterior orbital gyrus R	0.418	0.420	0.001	0.600	1	0.043
Precentral gyrus L	0.507	0.515	0.008	0.170	0.969	0.104
Precentral gyrus R	0.463	0.467	0.004	0.363	1	0.072
Precentral gyrus medial segment L	0.422	0.423	0.000	0.804	1	-0.020
Precentral gyrus medial segment R	0.406	0.406	0.000	0.795	1	0.022

Precuneus L	0.575	0.575	0.000	0.925	1	-0.007
Precuneus R	0.610	0.611	0.001	0.673	1	0.028
Putamen L	0.429	0.429	0.000	0.999	0.999	0.000
Putamen R	0.444	0.444	0.000	0.991	0.999769911504425	0.001
Subcallosal area L	0.570	0.572	0.002	0.427	1	0.056
Subcallosal area R	0.597	0.605	0.008	0.131	1	0.103
Superior frontal gyrus L	0.565	0.565	0.000	0.858	1	-0.013
Superior frontal gyrus R	0.570	0.570	0.001	0.666	1	0.031
Superior frontal gyrus medial segment L	0.527	0.528	0.001	0.584	1	-0.041
Superior frontal gyrus medial segment R	0.504	0.507	0.003	0.390	1	0.065
Superior occipital gyrus L	0.349	0.349	0.000	0.967	0.993135135135135	0.004
Superior occipital gyrus R	0.479	0.479	0.000	0.933	1	0.007
Superior parietal lobule L	0.517	0.518	0.001	0.629	1	0.036
Superior parietal lobule R	0.486	0.488	0.002	0.494	1	0.053
Superior temporal gyrus L	0.489	0.489	0.001	0.716	1	0.028
Superior temporal gyrus R	0.413	0.413	0.001	0.704	1	-0.031
Supplementary motor cortex L	0.427	0.428	0.000	0.813	1	0.019
Supplementary motor cortex R	0.434	0.439	0.005	0.318	1	0.081
Supramarginal gyrus L	0.459	0.465	0.006	0.280	1	0.086
Supramarginal gyrus R	0.451	0.460	0.009	0.181	0.982571428571429	0.106
Temporal pole L	0.483	0.485	0.003	0.457	1	-0.058
Temporal pole R	0.433	0.433	0.000	0.902	1	0.010
Thalamus proper L	0.199	0.214	0.016	0.136	1	-0.143
Thalamus proper R	0.264	0.271	0.007	0.303	1	-0.095
Transverse temporal gyrus L	0.332	0.334	0.002	0.581	1	0.049
Transverse temporal gyrus R	0.295	0.295	0.000	0.986	1	-0.002
Triangular part of the inferior frontal gyrus L	0.336	0.351	0.015	0.111	1	0.139
Triangular part of the inferior frontal gyrus R	0.442	0.443	0.001	0.698	1	0.031

FDR: false discovery rate. L: left. PRS: polygenic risk score. R: right.

Table D.37: Associations between PRSwithoutAPOE Threshold 1 and 114 regions of interest in CU participants

Region of Interest	R Square (Model 1)	R Square (Model 2)	R Square Change	Sig. F Change (Model 2)	FDR Corrected value	Standardised beta of PRS
Accumbens area L	0.346	0.347	0.001	0.581	1	0.038
Accumbens area R	0.391	0.391	0.000	0.803	1	0.016
Amygdala L	0.420	0.421	0.000	0.711	1	0.024
Amygdala R	0.477	0.478	0.001	0.679546	1	-0.025
Angular gyrus L	0.403	0.405	0.002	0.458	1	0.048
Angular gyrus R	0.364	0.374	0.010	0.100	1	0.110
Anterior cingulate gyrus L	0.447	0.451	0.004	0.285	1	0.067
Anterior cingulate gyrus R	0.266	0.267	0.000	0.760	1	-0.022
Anterior insula L	0.407	0.413	0.005	0.226	1	0.078
Anterior insula R	0.408	0.411	0.003	0.370	1	0.058
Anterior orbital gyrus L	0.317	0.317	0.000	0.988871	1	0.001
Anterior orbital gyrus R	0.360	0.369	0.009	0.126	1	0.103
Basal forebrain L	0.294	0.300	0.006	0.228291	1	-0.085
Basal forebrain R	0.367	0.370	0.003	0.397	1	-0.057
Calcarine cortex L	0.384	0.385	0.001	0.682	1	0.027
Calcarine cortex R	0.383	0.383	0.000	0.989321	1	0.001
Caudate L	0.170	0.170	0.000	0.850	1	0.015
Caudate R	0.169	0.169	0.000	0.940	1	0.006
Central operculum L	0.447	0.449	0.002	0.439	1	0.048
Central operculum R	0.402	0.410	0.008	0.144043	1	0.095
Cuneus L	0.346	0.346	0.000	0.895	1	0.009
Cuneus R	0.424	0.425	0.000	0.743	1	-0.021
Entorhinal area L	0.408	0.411	0.003	0.404	1	0.054
Entorhinal area R	0.466	0.466	0.000	0.994	1	0.000
Frontal operculum L	0.437	0.440	0.003	0.375	1	0.056
Frontal operculum R	0.287	0.287	0.000	0.871	1	-0.012

Frontal pole L	0.422	0.425	0.003	0.344	1	0.061
Frontal pole R	0.413	0.418	0.005	0.239	1	0.076
Fusiform gyrus L	0.513	0.521	0.007	0.114	1	0.092
Fusiform gyrus R	0.471	0.480	0.009	0.093	1	0.102
Gyrus rectus L	0.438	0.439	0.001	0.571	1	0.036
Gyrus rectus R	0.467	0.467	0.001	0.675	1	0.026
Hippocampus L	0.368	0.370	0.002	0.509	1	0.044
Hippocampus R	0.380	0.381	0.001	0.615	1	-0.033
Inferior occipital gyrus L	0.363	0.369	0.006	0.234	1	0.080
Inferior occipital gyrus R	0.500	0.501	0.000	0.689	1	0.024
Inferior temporal gyrus L	0.568	0.568	0.000	0.970	1	0.002
Inferior temporal gyrus R	0.563	0.563	0.000	0.701369	1	0.021
Lateral orbital gyrus L	0.379	0.387	0.008	0.143503	1	0.097
Lateral orbital gyrus R	0.384	0.385	0.001	0.667	1	0.028
Lingual gyrus L	0.530	0.537	0.008	0.098	1	0.095
Lingual gyrus R	0.515	0.518	0.003	0.291	1	0.062
Medial frontal cortex L	0.430	0.431	0.001	0.635	1	0.030
Medial frontal cortex R	0.393	0.393	0.000	0.907	1	-0.008
Medial orbital gyrus L	0.451	0.456	0.004	0.259537	1	0.070
Medial orbital gyrus R	0.455	0.459	0.004	0.264	1	0.069
Middle cingulate gyrus L	0.453	0.455	0.002	0.410	1	0.051
Middle cingulate gyrus R	0.352	0.353	0.001	0.572	1	-0.038
Middle frontal gyrus L	0.536	0.536	0.001	0.636	1	0.027
Middle frontal gyrus R	0.496	0.496	0.000	0.853	1	0.011
Middle occipital gyrus L	0.323	0.324	0.001	0.710	1	0.026
Middle occipital gyrus R	0.374	0.375	0.000	0.839	1	0.014
Middle temporal gyrus L	0.514	0.514	0.000	0.911	1	0.007
Middle temporal gyrus R	0.524	0.536	0.012	0.041	1	0.118
Occipital fusiform gyrus L	0.480	0.496	0.016	0.025	1	0.136
Occipital fusiform gyrus R	0.474	0.482	0.008	0.118	1	0.095

Occipital pole L	0.360	0.365	0.005	0.263	1	0.075
Occipital pole R	0.333	0.334	0.001	0.562928	1	0.040
Opercular part of the inferior frontal gyrus L	0.306	0.306	0.000	0.985	1	-0.001
Opercular part of the inferior frontal gyrus R	0.308	0.310	0.002	0.504	1	0.047
Orbital part of the inferior frontal gyrus L	0.405	0.408	0.004	0.319	1	0.065
Orbital part of the inferior frontal gyrus R	0.282	0.284	0.002	0.543476	1	0.043
Pallidum L	0.203	0.203	0.000	0.810	1	0.018
Pallidum R	0.166	0.166	0.000	0.958	1	0.004
Parahippocampal gyrus L	0.506	0.510	0.004	0.236	1	0.070
Parahippocampal gyrus R	0.508	0.512	0.004	0.227534	1	0.071
Parietal operculum L	0.354	0..357	0.003	0.403	1	-0.057
Parietal operculum R	0.341	0.342	0.001	0.567831	1	-0.039
Planum polare L	0.479	0.480	0.001	0.680030	1	0.025
Planum polare R	0.482	0.484	0.003	0.352	1	0.056
Planum temporale L	0.407	0.409	0.001	0.531	1	0.041
Planum temporale R	0.360	0.361	0.001	0.543493	1	0.094
Postcentral gyrus L	0.372	0.372	0.000	0.904	1	0.008
Postcentral gyrus R	0.351	0.361	0.010	0.112	1	0.107
Postcentral gyrus medial segment L	0.131	0.132	0.000	0.804	1	0.020
Postcentral gyrus medial segment R	0.186	0.187	0.001	0.625	1	0.037
Posterior cingulate gyrus L	0.476	0.477	0.001	0.556	1	-0.036
Posterior cingulate gyrus R	0.418	0.418	0.000	0.887	1	-0.009
Posterior insula L	0.396	0.399	0.004	0.326	1	0.064
Posterior insula R	0.435	0.441	0.006	0.177	1	0.085
Posterior orbital gyrus L	0.382	0.383	0.002	0.518	1	0.043
Posterior orbital gyrus R	0.388	0.388	0.000	0.764	1	-0.020
Precentral gyrus L	0.442	0.448	0.006	0.203	1	-0.080
Precentral gyrus R	0.425	0.425	0.000	0.832	1	0.014
Precentral gyrus medial segment L	0.282	0.282	0.000	0.817	1	-0.017
Precentral gyrus medial segment R	0.324	0.324	0.000	0.903	1	-0.008

Precuneus L	0.477	0.478	0.001	0.568186	1	-0.035
Precuneus R	0.456	0.458	0.002	0.480	1	-0.044
Putamen L	0.287	0.289	0.001	0.558	1	0.042
Putamen R	0.300	0.302	0.003	0.425	1	0.056
Subcallosal area L	0.513	0.517	0.004	0.233	1	0.070
Subcallosal area R	0.492	0.494	0.002	0.454	1	0.045
Superior frontal gyrus L	0.501	0.509	0.007	0.125	1	-0.091
Superior frontal gyrus R	0.523	0.524	0.001	0.562909	1	-0.034
Superior frontal gyrus medial segment L	0.381	0.381	0.001	0.700618	1	-0.025
Superior frontal gyrus medial segment R	0.395	0.396	0.000	0.844	1	-0.013
Superior occipital gyrus L	0.327	0.328	0.001	0.633	1	-0.033
Superior occipital gyrus R	0.305	0.308	0.003	0.372	1	-0.063
Superior parietal lobule L	0.402	0.402	0.000	0.966	1	-0.003
Superior parietal lobule R	0.417	0.422	0.004	0.260385	1	-0.072
Superior temporal gyrus L	0.480	0.480	0.000	0.999	0.999	0.000
Superior temporal gyrus R	0.466	0.466	0.000	0.773	1	0.018
Supplementary motor cortex L	0.410	0.419	0.009	0.107	1	-0.104
Supplementary motor cortex R	0.428	0.428	0.000	0.984	1	0.001
Supramarginal gyrus L	0.363	0.371	0.008	0.158	1	0.095
Supramarginal gyrus R	0.429	0.437	0.008	0.141	1	0.093
Temporal pole L	0.405	0.406	0.001	0.631	1	-0.031
Temporal pole R	0.409	0.409	0.000	0.726	1	-0.023
Thalamus proper L	0.293	0.295	0.002	0.519	1	0.046
Thalamus proper R	0.312	0.313	0.002	0.547	1	-0.042
Transverse temporal gyrus L	0.310	0.312	0.002	0.510	1	-0.046
Transverse temporal gyrus R	0.402	0.403	0.000	0.849	1	-0.012
Triangular part of the inferior frontal gyrus L	0.373	0.373	0.000	0.938	1	-0.005
Triangular part of the inferior frontal gyrus R	0.298	0.299	0.001	0.673	1	-0.030

FDR: false discovery rate. L: left. PRS: polygenic risk score. R: right.

Table D.38: Associations between PRSwithoutAPOE Threshold 1 and 114 regions of interest in MCI patients

Region of Interest	R Square (Model 1)	R Square (Model 2)	R Square Change	Sig. F Change (Model 2)	FDR Corrected value	Standardised beta of PRS
Accumbens area L	0.379	0.379	0.001	0.539	1	-0.025
Accumbens area R	0.353	0.354	0.001	0.391	1	-0.036
Amygdala L	0.341	0.342	0.001	0.357	1	-0.039
Amygdala R	0.408	0.409	0.002	0.290	1	-0.042
Angular gyrus L	0.375	0.376	0.001	0.439	1	-0.032
Angular gyrus R	0.405	0.405	0.000	0.899	1	0.005
Anterior cingulate gyrus L	0.403	0.403	0.000	0.800	1	0.010
Anterior cingulate gyrus R	0.229	0.230	0.001	0.570	1	-0.026
Anterior insula L	0.315	0.315	0.000	0.742	1	-0.014
Anterior insula R	0.328	0.332	0.003	0.159	1	-0.060
Anterior orbital gyrus L	0.436	0.436	0.000	0.746	1	0.013
Anterior orbital gyrus R	0.373	0.373	0.000	0.604	1	0.021
Basal forebrain L	0.255	0.256	0.000	0.652	1	-0.020
Basal forebrain R	0.319	0.322	0.003	0.169275	1	-0.059
Calcarine cortex L	0.403	0.403	0.000	0.902	1	-0.005
Calcarine cortex R	0.414	0.414	0.000	0.828	1	-0.009
Caudate L	0.195	0.197	0.002	0.277	1	-0.050
Caudate R	0.201	0.207	0.005	0.100	1	-0.076
Central operculum L	0.391	0.392	0.001	0.425	1	0.032
Central operculum R	0.365	0.365	0.000	0.832	1	0.009
Cuneus L	0.411	0.412	0.001	0.443	1	0.030
Cuneus R	0.429	0.429	0.000	0.889	1	-0.005
Entorhinal area L	0.335	0.335	0.000	0.907	1	0.005
Entorhinal area R	0.421	0.422	0.001	0.378	1	-0.035
Frontal operculum L	0.362	0.363	0.000	0.773	1	0.012
Frontal operculum R	0.348	0.349	0.001	0.471	1	-0.030

Frontal pole L	0.428	0.432	0.004	0.106304	1	0.063
Frontal pole R	0.0426	0.429	0.003	0.155	1	0.056
Fusiform gyrus L	0.442	0.442	0.000	0.657	1	0.017
Fusiform gyrus R	0.500	0.500	0.000	0.947	1	-0.002
Gyrus rectus L	0.436	0.438	0.002	0.221	1	0.047
Gyrus rectus R	0.420	0.420	0.000	0.920	1	0.004
Hippocampus L	0.395	0.401	0.006	0.040	1	-0.082
Hippocampus R	0.422	0.429	0.007	0.030	1	-0.085
Inferior occipital gyrus L	0.379	0.379	0.000	0.944	1	-0.003
Inferior occipital gyrus R	0.446	0.448	0.002	0.272	1	0.042
Inferior temporal gyrus L	0.459	0.462	0.003	0.131	1	-0.057
Inferior temporal gyrus R	0.536	0.537	0.000	0.550	1	-0.021
Lateral orbital gyrus L	0.443	0.443	0.000	0.993	0.993	0.000
Lateral orbital gyrus R	0.344	0.344	0.000	0.714	1	-0.015
Lingual gyrus L	0.489	0.489	0.000	0.875	1	0.006
Lingual gyrus R	0.529	0.531	0.002	0.168765	1	0.049
Medial frontal cortex L	0.371	0.371	0.000	0.836	1	-0.008
Medial frontal cortex R	0.340	0.342	0.002	0.271	1	0.046
Medial orbital gyrus L	0.451	0.451	0.000	0.895	1	-0.005
Medial orbital gyrus R	0.420	0.420	0.001	0.531	1	0.025
Middle cingulate gyrus L	0.355	0.355	0.000	0.861	1	0.007
Middle cingulate gyrus R	0.320	0.320	0.000	0.591	1	0.023
Middle frontal gyrus L	0.463	0.466	0.003	0.128	1	0.058
Middle frontal gyrus R	0.462	0.462	0.000	0.985	1	0.001
Middle occipital gyrus L	0.335	0.335	0.000	0.983	1	0.001
Middle occipital gyrus R	0.322	0.322	0.000	0.921	1	-0.004
Middle temporal gyrus L	0.452	0.452	0.000	0.649	1	-0.017
Middle temporal gyrus R	0.488	0.489	0.001	0.462	1	-0.027
Occipital fusiform gyrus L	0.463	0.463	0.000	0.616	1	0.019
Occipital fusiform gyrus R	0.520	0.521	0.001	0.324	1	0.035

Occipital pole L	0.295	0.295	0.000	0.931815	1	-0.004
Occipital pole R	0.375	0.376	0.001	0.414	1	0.033
Opercular part of the inferior frontal gyrus L	0.281	0.282	0.000	0.620	1	0.022
Opercular part of the inferior frontal gyrus R	0.254	0.255	0.000	0.756	1	0.014
Orbital part of the inferior frontal gyrus L	0.285	0.285	0.000	0.932380	1	-0.004
Orbital part of the inferior frontal gyrus R	0.238	0.241	0.003	0.237	1	-0.053
Pallidum L	0.171	0.171	0.000	0.978	1	0.001
Pallidum R	0.138	0.138	0.000	0.716	1	-0.017
Parahippocampal gyrus L	0.433	0.433	0.001	0.519	1	0.190
Parahippocampal gyrus R	0.492	0.492	0.000	0.788	1	0.010
Parietal operculum L	0.334	0.335	0.001	0.495	1	0.029
Parietal operculum R	0.279	0.279	0.000	0.698	1	-0.017
Planum polare L	0.388	0.389	0.001	0.428	1	-0.032
Planum polare R	0.429	0.433	0.004	0.097	1	-0.065
Planum temporale L	0.328	0.329	0.000	0.626	1	-0.021
Planum temporale R	0.352	0.352	0.000	0.874	1	-0.007
Postcentral gyrus L	0.369	0.369	0.000	0.963	1	-0.002
Postcentral gyrus R	0.393	0.393	0.000	0.794	1	-0.011
Postcentral gyrus medial segment L	0.229	0.230	0.000	0.647	1	0.021
Postcentral gyrus medial segment R	0.222	0.222	0.000	0.766	1	-0.014
Posterior cingulate gyrus L	0.560	0.560	0.000	0.882	1	-0.005
Posterior cingulate gyrus R	0.523	0.523	0.000	0.926	1	0.003
Posterior insula L	0.352	0.352	0.000	0.820	1	0.009
Posterior insula R	0.381	0.381	0.000	0.755	1	0.013
Posterior orbital gyrus L	0.351	0.351	0.000	0.823	1	0.009
Posterior orbital gyrus R	0.377	0.380	0.002	0.231	1	-0.049
Precentral gyrus L	0.485	0.488	0.003	0.148	1	0.054
Precentral gyrus R	0.473	0.476	0.000	0.937	1	0.003
Precentral gyrus medial segment L	0.283	0.283	0.000	0.918	1	0.004
Precentral gyrus medial segment R	0.314	0.315	0.000	0.787	1	-0.012

Precuneus L	0.463	0.463	0.000	0.803	1	0.009
Precuneus R	0.489	0.489	0.000	0.969	1	0.001
Putamen L	0.229	0.231	0.002	0.264	1	-0.051
Putamen R	0.241	0.248	0.007	0.055	1	-0.086
Subcallosal area L	0.434	0.435	0.001	0.440	1	-0.030
Subcallosal area R	0.380	0.380	0.000	0.894	1	0.005
Superior frontal gyrus L	0.428	0.430	0.003	0.161	1	-0.055
Superior frontal gyrus R	0.465	0.465	0.000	0.981	1	0.001
Superior frontal gyrus medial segment L	0.414	0.416	0.001	0.316	1	-0.040
Superior frontal gyrus medial segment R	0.384	0.384	0.000	0.988	0.996743362831858	-0.001
Superior occipital gyrus L	0.338	0.340	0.002	0.276	1	0.046
Superior occipital gyrus R	0.343	0.347	0.004	0.110	1	0.067
Superior parietal lobule L	0.368	0.372	0.003	0.139	1	0.061
Superior parietal lobule R	0.359	0.361	0.002	0.241	1	0.048
Superior temporal gyrus L	0.365	0.365	0.000	0.897	1	-0.005
Superior temporal gyrus R	0.360	0.361	0.001	0.398	1	0.035
Supplementary motor cortex L	0.356	0.357	0.001	0.490	1	-0.029
Supplementary motor cortex R	0.347	0.350	0.003	0.210	1	-0.052
Supramarginal gyrus L	0.312	0.313	0.001	0.494	1	0.029
Supramarginal gyrus R	0.306	0.311	0.005	0.106402	1	0.069
Temporal pole L	0.312	0.312	0.001	0.469	1	-0.031
Temporal pole R	0.347	0.349	0.001	0.342	1	-0.040
Thalamus proper L	0.213	0.213	0.000	0.784	1	0.013
Thalamus proper R	0.255	0.255	0.000	0.797	1	0.011
Transverse temporal gyrus L	0.255	0.255	0.000	0.644	1	-0.021
Transverse temporal gyrus R	0.307	0.310	0.003	0.217	1	-0.053
Triangular part of the inferior frontal gyrus L	0.340	0.341	0.001	0.535	1	0.026
Triangular part of the inferior frontal gyrus R	0.285	0.285	0.001	0.579	1	0.024

FDR: false discovery rate. L: left. PRS: polygenic risk score. R: right.

Table D.39: Associations between PRSwithoutAPOE Threshold 1 and 114 regions of interest in AD dementia patients

Region of Interest	R Square (Model 1)	R Square (Model 2)	R Square Change	Sig. F Change (Model 2)	FDR Corrected value	Standardised beta of PRS
Accumbens area L	0.512	0.521	0.010	0.135	0.81	-0.110
Accumbens area R	0.497	0.503	0.005	0.277	0.809692307692308	0.004
Amygdala L	0.425	0.426	0.002	0.579	0.835518987341772	-0.044
Amygdala R	0.445	0.445	0.000	0.965	0.991081081081081	0.003
Angular gyrus L	0.446	0.446	0.000	0.876	0.979058823529412	-0.012
Angular gyrus R	0.558	0.559	0.002	0.532	0.842333333333333	-0.044
Anterior cingulate gyrus L	0.412	0.426	0.014	0.099	0.705375	-0.133
Anterior cingulate gyrus R	0.272	0.296	0.024	0.051	0.5814	-0.174
Anterior insula L	0.505	0.510	0.005	0.308	0.816558139534884	-0.076
Anterior insula R	0.557	0.558	0.001	0.536	0.837041095890411	-0.044
Anterior orbital gyrus L	0.499	0.509	0.009	0.145	0.787142857142857	-0.109
Anterior orbital gyrus R	0.495	0.508	0.013	0.090	0.732857142857143	-0.127
Basal forebrain L	0.275	0.285	0.010	0.216809	0.7723820625	-0.111
Basal forebrain R	0.379	0.412	0.036	0.009	1	-0.214
Calcarine cortex L	0.390	0.397	0.007	0.244	0.732	0.096
Calcarine cortex R	0.439	0.441	0.002	0.487	0.816441176470588	0.055
Caudate L	0.362	0.373	0.011	0.157	0.74575	-0.119
Caudate R	0.328	0.338	0.010	0.191	0.806444444444445	-0.113
Central operculum L	0.373	0.392	0.018	0.066	0.627	-0.153
Central operculum R	0.506	0.512	0.007	0.217246	0.750486181818182	-0.091
Cuneus L	0.491	0.495	0.005	0.312	0.808363636363636	0.076
Cuneus R	0.473	0.475	0.002	0.546	0.841135135135135	0.046
Entorhinal area L	0.413	0.421	0.008	0.220	0.737647058823529	-0.099
Entorhinal area R	0.407	0.407	0.000	0.982	0.990690265486726	0.002
Frontal operculum L	0.341	0.346	0.006	0.328324	0.7797695	-0.084
Frontal operculum R	0.405	0.406	0.000	0.857	0.967306930693069	-0.015

Frontal pole L	0.523	0.524	0.001	0.623	0.866121951219512	-0.036
Frontal pole R	0.496	0.501	0.004	0.328228	0.796127489361702	-0.073
Fusiform gyrus L	0.496	0.496	0.000	0.778	0.943531914893617	-0.021
Fusiform gyrus R	0.530	0.530	0.001	0.719	0.931431818181818	-0.026
Gyrus rectus L	0.526	0.540	0.014	0.069	0.605076923076923	-0.131
Gyrus rectus R	0.541	0.557	0.016	0.045	0.64125	-0.142
Hippocampus L	0.471	0.473	0.003	0.449	0.79978125	-0.058
Hippocampus R	0.503	0.504	0.000	0.834	0.980164948453608	0.016
Inferior occipital gyrus L	0.507	0.507	0.000	0.846	0.96444	0.014
Inferior occipital gyrus R	0.479	0.479	0.000	0.744	0.9424	0.025
Inferior temporal gyrus L	0.497	0.504	0.007	0.198	0.806142857142857	-0.096
Inferior temporal gyrus R	0.518	0.520	0.003	0.425	0.781451612903226	-0.059
Lateral orbital gyrus L	0.441	0.455	0.013	0.097	0.7372	-0.130
Lateral orbital gyrus R	0.456	0.479	0.023	0.026	0.5928	-0.172
Lingual gyrus L	0.566	0.570	0.004	0.325	0.805434782608696	0.068
Lingual gyrus R	0.558	0.561	0.003	0.386	0.800072727272727	0.061
Medial frontal cortex L	0.353	0.382	0.029	0.023	0.874	-0.192
Medial frontal cortex R	0.414	0.419	0.004	0.353	0.789058823529412	-0.075
Medial orbital gyrus L	0.594	0.608	0.014	0.044	0.716571428571429	-0.135
Medial orbital gyrus R	0.512	0.529	0.017	0.046	0.582666666666667	-0.146
Middle cingulate gyrus L	0.433	0.434	0.001	0.687	0.932357142857143	-0.032
Middle cingulate gyrus R	0.414	0.420	0.005	0.318	0.8056	-0.081
Middle frontal gyrus L	0.540	0.547	0.007	0.188	0.824307692307692	-0.094
Middle frontal gyrus R	0.579	0.579	0.000	0.840	0.977142857142857	-0.014
Middle occipital gyrus L	0.440	0.451	0.010	0.151	0.748434782608696	-0.113
Middle occipital gyrus R	0.433	0.436	0.003	0.439	0.794380952380952	-0.062
Middle temporal gyrus L	0.484	0.491	0.007	0.215	0.981666666666667	-0.094
Middle temporal gyrus R	0.539	0.539	0.000	0.930	0.790645161290323	0.006
Occipital fusiform gyrus L	0.521	0.522	0.002	0.531	0.852591549295775	0.046
Occipital fusiform gyrus R	0.513	0.513	0.000	0.887	0.972288461538462	-0.010

Occipital pole L	0.429	0.430	0.001	0.696	0.933458823529412	0.031
Occipital pole R	0.464	0.465	0.001	0.704	0.933209302325581	0.029
Opercular part of the inferior frontal gyrus L	0.367	0.376	0.009	0.202	0.794068965517241	-0.107
Opercular part of the inferior frontal gyrus R	0.403	0.414	0.011	0.142	0.8094	-0.119
Orbital part of the inferior frontal gyrus L	0.326	0.331	0.005	0.361	0.791423076923077	-0.079
Orbital part of the inferior frontal gyrus R	0.306	0.334	0.028	0.031	0.589	-0.188
Pallidum L	0.214	0.221	0.007	0.307	0.833285714285714	-0.096
Pallidum R	0.240	0.254	0.014	0.149	0.772090909090909	-0.133
Parahippocampal gyrus L	0.522	0.522	0.000	0.954	0.988690909090909	-0.004
Parahippocampal gyrus R	0.539	0.542	0.003	0.405	0.796034482758621	0.060
Parietal operculum L	0.376	0.380	0.005	0.347	0.79116	-0.078
Parietal operculum R	0.358	0.358	0.000	0.936	0.978935779816514	0.007
Planum polare L	0.459	0.467	0.008	0.186	0.84816	-0.102
Planum polare R	0.483	0.485	0.002	0.556	0.834	-0.045
Planum temporale L	0.495	0.495	0.000	0.902	0.970075471698113	0.009
Planum temporale R	0.408	0.408	0.000	0.912	0.971663551401869	-0.009
Postcentral gyrus L	0.553	0.555	0.001	0.560	0.829090909090909	-0.041
Postcentral gyrus R	0.501	0506	0.005	0.293	0.83505	0.078
Postcentral gyrus medial segment L	0.371	0.379	0.008	0.232	0.734666666666667	0.100
Postcentral gyrus medial segment R	0.330	0.332	0.003	0.498	0.811028571428571	-0.059
Posterior cingulate gyrus L	0.605	0.614	0.009	0.107	0.677666666666667	-0.107
Posterior cingulate gyrus R	0.597	0.599	0.003	0.400	0.8	-0.056
Posterior insula L	0.487	0.487	0.001	0.727	0.931213483146067	-0.026
Posterior insula R	0.516	0.517	0.001	0.590	0.84075	0.040
Posterior orbital gyrus L	0.434	0.442	0.007	0.231	0.7524	-0.095
Posterior orbital gyrus R	0.418	0.422	0.004	0.392	0.798	-0.069
Precentral gyrus L	0.507	0.508	0.001	0.676	0.928481927710843	-0.031
Precentral gyrus R	0.463	0.463	0.000	0.803	0.9535625	0.019
Precentral gyrus medial segment L	0.422	0.422	0.000	0.891	0.967371428571429	-0.011
Precentral gyrus medial segment R	0.406	0.406	0.000	0.783	0.9396	0.022

Precuneus L	0.575	0.575	0.000	0.775	0.95	-0.020
Precuneus R	0.610	0.613	0.002	0.407	0.786406779661017	0.055
Putamen L	0.429	0.432	0.003	0.415	0.7885	-0.065
Putamen R	0.444	0.447	0.003	0.421	0.786786885245902	-0.063
Subcallosal area L	0.570	0.594	0.024	0.011	0.627	-0.175
Subcallosal area R	0.597	0.614	0.017	0.025	0.7125	-0.149
Superior frontal gyrus L	0.565	0.570	0.005	0.235	0.724054054054054	-0.083
Superior frontal gyrus R	0.570	0.573	0.003	0.371	0.798	-0.062
Superior frontal gyrus medial segment L	0.527	0.538	0.011	0.103	0.690705882352941	-0.118
Superior frontal gyrus medial segment R	0.504	0.504	0.000	0.752	0.942065934065934	-0.024
Superior occipital gyrus L	0.349	0.349	0.000	0.845	0.973030303030303	0.017
Superior occipital gyrus R	0.479	0.480	0.002	0.549	0.83448	0.046
Superior parietal lobule L	0.517	0.517	0.000	0.977	0.994446428571429	0.002
Superior parietal lobule R	0.486	0.487	0.000	0.754	0.934304347826087	0.024
Superior temporal gyrus L	0.489	0.491	0.003	0.452	0.792738461538462	-0.057
Superior temporal gyrus R	0.413	0.415	0.002	0.488	0.806260869565217	-0.056
Supplementary motor cortex L	0.427	0.428	0.001	0.619	0.871185185185185	-0.040
Supplementary motor cortex R	0.434	0.435	0.001	0.717	0.93951724137931	-0.029
Supramarginal gyrus L	0.459	0.465	0.005	0.299	0.831365853658537	0.081
Supramarginal gyrus R	0.451	0.451	0.000	0.885	0.979514563106796	-0.011
Temporal pole L	0.483	0.498	0.016	0.062	0.642545454545455	-0.141
Temporal pole R	0.433	0.433	0.000	0.983	0.983	0.002
Thalamus proper L	0.199	0.202	0.004	0.465	0.803181818181818	-0.069
Thalamus proper R	0.264	0.269	0.005	0.385	0.812777777777778	-0.079
Transverse temporal gyrus L	0.332	0.338	0.005	0.338	0.786367346938776	0.083
Transverse temporal gyrus R	0.295	0.297	0.002	0.576	0.841846153846154	0.050
Triangular part of the inferior frontal gyrus L	0.336	0.339	0.003	0.470	0.799701492537313	-0.062
Triangular part of the inferior frontal gyrus R	0.442	0.450	0.008	0.212	0.8056	-0.098

FDR: false discovery rate. L: left. PRS: polygenic risk score. R: right.

Table D.40: Associations between PRSwithoutAPOE Threshold 5 and 114 regions of interest in CU participants

Region of Interest	R Square (Model 1)	R Square (Model 2)	R Square Change	Sig. F Change (Model 2)	FDR Corrected value	Standardised beta of PRS
Accumbens area L	0.346	0.347	0.001	0.652	1	0.031
Accumbens area R	0.391	0.391	0.000	0.746354	1	0.021
Amygdala L	0.420	0.420	0.000	0.929	0.989775700934579	0.006
Amygdala R	0.477	0.477	0.000	0.837	1	-0.012
Angular gyrus L	0.403	0.404	0.001	0.576	1	0.036
Angular gyrus R	0.364	0.373	0.009	0.124	1	0.102
Anterior cingulate gyrus L	0.447	0.449	0.002	0.450	1	0.047
Anterior cingulate gyrus R	0.266	0.267	0.001	0.619	1	-0.036
Anterior insula L	0.407	0.407	0.000	0.994	0.994	-0.001
Anterior insula R	0.408	0.408	0.000	0.812	1	-0.015
Anterior orbital gyrus L	0.317	0.318	0.001	0.657	1	0.031
Anterior orbital gyrus R	0.360	0.370	0.011	0.098	1	0.111
Basal forebrain L	0.294	0.300	0.006	0.235	1	-0.084
Basal forebrain R	0.367	0.368	0.001	0.538683	1	-0.041
Calcarine cortex L	0.384	0.384	0.000	0.891	1	-0.009
Calcarine cortex R	0.383	0.383	0.000	0.759	1	-0.020
Caudate L	0.170	0.170	0.000	0.970	1	0.003
Caudate R	0.169	0.169	0.000	0.992	1	0.001
Central operculum L	0.447	0.448	0.001	0.559484	1	0.036
Central operculum R	0.402	0.409	0.007	0.175	1	0.088
Cuneus L	0.346	0.347	0.000	0.801	1	-0.017
Cuneus R	0.424	0.425	0.001	0.624	1	-0.031
Entorhinal area L	0.408	0.410	0.002	0.440	1	0.050
Entorhinal area R	0.466	0.466	0.000	0.926	0.99588679245283	0.006
Frontal operculum L	0.437	0.438	0.001	0.622	1	-0.031
Frontal operculum R	0.287	0.290	0.003	0.419	1	-0.057

Frontal pole L	0.422	0.429	0.007	0.163	1	0.089
Frontal pole R	0.413	0.420	0.007	0.161	1	0.090
Fusiform gyrus L	0.513	0.518	0.004	0.240	1	0.069
Fusiform gyrus R	0.471	0.479	0.008	0.114	1	0.096
Gyrus rectus L	0.438	0.438	0.000	0.802	1	-0.016
Gyrus rectus R	0.467	0.467	0.000	0.746132	1	-0.020
Hippocampus L	0.368	0.368	0.000	0.898	1	0.009
Hippocampus R	0.380	0.382	0.002	0.428	1	-0.052
Inferior occipital gyrus L	0.363	0.364	0.001	0.666	1	0.029
Inferior occipital gyrus R	0.500	0.501	0.001	0.600	1	0.031
Inferior temporal gyrus L	0.568	0.568	0.000	0.873	1	-0.009
Inferior temporal gyrus R	0.563	0.563	0.000	0.975	1	0.002
Lateral orbital gyrus L	0.379	0.384	0.005	0.232	1	0.079
Lateral orbital gyrus R	0.384	0.385	0.000	0.758	1	0.020
Lingual gyrus L	0.530	0.532	0.002	0.352	1	0.053
Lingual gyrus R	0.515	0.516	0.001	0.555	1	0.034
Medial frontal cortex L	0.430	0.430	0.000	0.792	1	0.017
Medial frontal cortex R	0.393	0.395	0.002	0.504	1	-0.044
Medial orbital gyrus L	0.451	0.454	0.002	0.396	1	0.053
Medial orbital gyrus R	0.455	0.459	0.004	0.280	1	0.067
Middle cingulate gyrus L	0.453	0.455	0.002	0.416	1	0.050
Middle cingulate gyrus R	0.352	0.354	0.002	0.461	1	-0.050
Middle frontal gyrus L	0.536	0.536	0.000	0.852	1	0.011
Middle frontal gyrus R	0.496	0.496	0.000	0.720	1	-0.021
Middle occipital gyrus L	0.323	0.324	0.000	0.753	1	0.022
Middle occipital gyrus R	0.374	0.374	0.000	0.924537	1	0.006
Middle temporal gyrus L	0.514	0.514	0.001	0.670	1	-0.025
Middle temporal gyrus R	0.524	0.531	0.008	0.101	1	0.095
Occipital fusiform gyrus L	0.480	0.493	0.013	0.041	1	0.123
Occipital fusiform gyrus R	0.474	0.483	0.009	0.092	1	0.102

Occipital pole L	0.360	0.363	0.002	0.430	1	0.053
Occipital pole R	0.333	0.335	0.002	0.462	1	0.050
Opercular part of the inferior frontal gyrus L	0.306	0.307	0.001	0.685	1	-0.028
Opercular part of the inferior frontal gyrus R	0.308	0.308	0.000	0.882	1	-0.010
Orbital part of the inferior frontal gyrus L	0.405	0.405	0.000	0.972	1	-0.002
Orbital part of the inferior frontal gyrus R	0.282	0.282	0.000	0.782	1	0.020
Pallidum L	0.203	0.204	0.002	0.535	1	0.046
Pallidum R	0.166	0.169	0.003	0.453	1	0.057
Parahippocampal gyrus L	0.506	0.508	0.001	0.509	1	0.039
Parahippocampal gyrus R	0.508	0.508	0.000	0.767	1	0.017
Parietal operculum L	0.354	0.356	0.002	0.518	1	-0.044
Parietal operculum R	0.341	0.341	0.000	0.917	1	0.007
Planum polare L	0.479	0.481	0.001	0.539049	1	-0.037
Planum polare R	0.482	0.482	0.000	0.925466	1	0.006
Planum temporale L	0.407	0.408	0.000	0.816	1	0.015
Planum temporale R	0.360	0.360	0.000	0.900	1	0.008
Postcentral gyrus L	0.372	0.373	0.000	0.724	1	-0.023
Postcentral gyrus R	0.351	0.358	0.007	0.187500	1	0.089
Postcentral gyrus medial segment L	0.131	0.132	0.001	0.633268	1	-0.037
Postcentral gyrus medial segment R	0.186	0.188	0.003	0.475	1	0.054
Posterior cingulate gyrus L	0.476	0.479	0.003	0.321	1	-0.060
Posterior cingulate gyrus R	0.418	0.422	0.004	0.286	1	-0.068
Posterior insula L	0.396	0.396	0.000	0.892	1	0.009
Posterior insula R	0.435	0.438	0.003	0.325760	1	0.062
Posterior orbital gyrus L	0.382	0.382	0.000	0.726	1	0.023
Posterior orbital gyrus R	0.388	0.388	0.000	0.743	1	-0.022
Precentral gyrus L	0.442	0.450	0.008	0.121	1	-0.097
Precentral gyrus R	0.425	0.425	0.000	0.973	1	-0.002
Precentral gyrus medial segment L	0.282	0.282	0.000	0.864	1	-0.012
Precentral gyrus medial segment R	0.324	0.324	0.001	0.692	1	-0.027

Precuneus L	0.477	0.478	0.001	0.632934	1	-0.029
Precuneus R	0.456	0.462	0.005	0.205	1	-0.078
Putamen L	0.287	0.287	0.000	0.913	1	0.008
Putamen R	0.300	0.301	0.001	0.567	1	0.040
Subcallosal area L	0.513	0.515	0.002	0.445	1	0.045
Subcallosal area R	0.492	0.494	0.001	0.497	1	0.041
Superior frontal gyrus L	0.501	0.507	0.005	0.188000	1	-0.078
Superior frontal gyrus R	0.523	0.524	0.000	0.680	1	-0.024
Superior frontal gyrus medial segment L	0.381	0.382	0.001	0.571	1	-0.037
Superior frontal gyrus medial segment R	0.395	0.396	0.000	0.851	1	-0.012
Superior occipital gyrus L	0.327	0.328	0.001	0.693	1	-0.027
Superior occipital gyrus R	0.305	0.308	0.004	0.358	1	-0.064
Superior parietal lobule L	0.402	0.403	0.001	0.688	1	0.026
Superior parietal lobule R	0.417	0.424	0.006	0.191	1	-0.083
Superior temporal gyrus L	0.480	0.480	0.000	0.827	1	0.013
Superior temporal gyrus R	0.466	0.466	0.000	0.980	0.9975	0.002
Supplementary motor cortex L	0.410	0.421	0.011	0.079	1	-0.113
Supplementary motor cortex R	0.428	0.428	0.000	0.808	1	-0.015
Supramarginal gyrus L	0.363	0.374	0.011	0.089	1	0.113
Supramarginal gyrus R	0.429	0.443	0.014	0.045	1	0.126
Temporal pole L	0.405	0.409	0.003	0.326644	1	-0.063
Temporal pole R	0.409	0.410	0.001	0.620	1	-0.032
Thalamus proper L	0.293	0.294	0.001	0.706	1	0.027
Thalamus proper R	0.312	0.314	0.003	0.439	1	-0.054
Transverse temporal gyrus L	0.310	0.316	0.005	0.257	1	-0.079
Transverse temporal gyrus R	0.402	0.404	0.002	0.465	1	-0.047
Triangular part of the inferior frontal gyrus L	0.373	0.374	0.001	0.558785	1	-0.039
Triangular part of the inferior frontal gyrus R	0.298	0.302	0.003	0.375	1	-0.062

FDR: false discovery rate. L: left. PRS: polygenic risk score. R: right.

Table D.41: Associations between PRSwithoutAPOE Threshold 5 and 114 regions of interest in MCI patients

Region of Interest	R Square (Model 1)	R Square (Model 2)	R Square Change	Sig. F Change (Model 2)	FDR Corrected value	Standardised beta of PRS
Accumbens area L	0.379	0.379	0.000	0.879	0.963519230769231	0.006
Accumbens area R	0.353	0.353	0.000	0.902	0.970075471698113	-0.005
Amygdala L	0.341	0.342	0.001	0.364361	1	-0.038
Amygdala R	0.408	0.409	0.002	0.315	1	-0.040
Angular gyrus L	0.375	0.376	0.000	0.931	0.973706422018349	-0.004
Angular gyrus R	0.405	0.405	0.000	0.970	0.987321428571428	-0.002
Anterior cingulate gyrus L	0.403	0.404	0.000	0.569	1	0.023
Anterior cingulate gyrus R	0.229	0.230	0.001	0.551	1	0.027
Anterior insula L	0.315	0.316	0.001	0.494	1	0.029
Anterior insula R	0.328	0.330	0.001	0.386	1	-0.037
Anterior orbital gyrus L	0.436	0.437	0.001	0.499	1	0.026
Anterior orbital gyrus R	0.373	0.374	0.001	0.373	1	0.037
Basal forebrain L	0.255	0.256	0.000	0.825	0.9405	0.010
Basal forebrain R	0.319	0.319	0.000	0.761	0.985840909090909	-0.013
Calcarine cortex L	0.403	0.403	0.000	0.646004	0.969006	-0.018
Calcarine cortex R	0.414	0.415	0.001	0.439	1	-0.031
Caudate L	0.195	0.195	0.000	0.718	0.998195121951219	-0.017
Caudate R	0.201	0.205	0.004	0.188	1	-0.061
Central operculum L	0.391	0.393	0.001	0.363502	1	0.037
Central operculum R	0.365	0.365	0.000	0.935	0.969	0.100
Cuneus L	0.411	0.413	0.002	0.289	1	0.042
Cuneus R	0.429	0.429	0.001	0.527488	1	0.025
Entorhinal area L	0.335	0.335	0.000	0.999	0.999	0.000
Entorhinal area R	0.421	0.421	0.000	0.613202	1	-0.020
Frontal operculum L	0.362	0.365	0.003	0.191	1	0.054
Frontal operculum R	0.348	0.348	0.000	0.847	0.946647058823529	-0.008

Frontal pole L	0.428	0.435	0.007	0.029	1	0.085
Frontal pole R	0.426	0.429	0.003	0.128	1	0.060
Fusiform gyrus L	0.442	0.445	0.003	0.125	1	0.059
Fusiform gyrus R	0.500	0.501	0.001	0.410	1	0.030
Gyrus rectus L	0.436	0.440	0.004	0.102	1	0.063
Gyrus rectus R	0.420	0.420	0.000	0.943	0.968486486486486	0.003
Hippocampus L	0.395	0.401	0.006	0.046	1	-0.080
Hippocampus R	0.422	0.429	0.007	0.027	1	-0.087
Inferior occipital gyrus L	0.379	0.379	0.000	0.804	0.95475	0.010
Inferior occipital gyrus R	0.446	0.448	0.002	0.200	1	0.049
Inferior temporal gyrus L	0.459	0.460	0.001	0.526833	1	-0.024
Inferior temporal gyrus R	0.536	0.536	0.000	0.843	0.951504950495049	-0.007
Lateral orbital gyrus L	0.443	0.443	0.001	0.500	1	0.026
Lateral orbital gyrus R	0.344	0.345	0.001	0.534	1	0.026
Lingual gyrus L	0.489	0.490	0.000	0.667	0.950475	0.016
Lingual gyrus R	0.529	0.530	0.002	0.239	1	0.042
Medial frontal cortex L	0.371	0.372	0.000	0.643	0.97736	0.019
Medial frontal cortex R	0.340	0.345	0.005	0.079	1	0.074
Medial orbital gyrus L	0.451	0.452	0.001	0.353	1	0.036
Medial orbital gyrus R	0.420	0.421	0.001	0.316	1	0.040
Middle cingulate gyrus L	0.355	0.355	0.000	0.992	1	0.000
Middle cingulate gyrus R	0.320	0.321	0.001	0.381	1	0.037
Middle frontal gyrus L	0.463	0.467	0.003	0.112	1	0.060
Middle frontal gyrus R	0.462	0.462	0.000	0.822	0.946545454545455	0.009
Middle occipital gyrus L	0.335	0.337	0.002	0.322	1	0.042
Middle occipital gyrus R	0.322	0.324	0.002	0.281	1	0.046
Middle temporal gyrus L	0.452	0.452	0.000	0.788204	1	-0.010
Middle temporal gyrus R	0.488	0.489	0.000	0.613161	0.966185548387097	-0.019
Occipital fusiform gyrus L	0.463	0.464	0.001	0.358	1	0.035
Occipital fusiform gyrus R	0.520	0.523	0.003	0.136	1	0.053

Occipital pole L	0.295	0.295	0.000	0.850	0.940776699029126	-0.008
Occipital pole R	0.375	0.376	0.001	0.441	1	0.032
Opercular part of the inferior frontal gyrus L	0.281	0.282	0.001	0.493	1	0.030
Opercular part of the inferior frontal gyrus R	0.254	0.255	0.001	0.446	1	0.034
Orbital part of the inferior frontal gyrus L	0.285	0.285	0.001	0.533	1	0.027
Orbital part of the inferior frontal gyrus R	0.238	0.239	0.000	0.730	0.979058823529412	-0.016
Pallidum L	0.171	0.171	0.000	0.770	0.964615384615385	0.014
Pallidum R	0.138	0.138	0.000	0.731	0.969	-0.017
Parahippocampal gyrus L	0.433	0.433	0.000	0.596	1	0.021
Parahippocampal gyrus R	0.492	0.492	0.000	0.653	0.954384615384615	0.017
Parietal operculum L	0.334	0.338	0.004	0.150	1	0.061
Parietal operculum R	0.279	0.280	0.001	0.435645	1	0.034
Planum polare L	0.388	0.389	0.000	0.589	1	-0.022
Planum polare R	0.429	0.431	0.002	0.226	1	-0.047
Planum temporale L	0.328	0.329	0.000	0.632	0.986958904109589	-0.020
Planum temporale R	0.352	0.352	0.000	0.904	0.963140186915888	-0.005
Postcentral gyrus L	0.369	0.369	0.001	0.508	1	-0.027
Postcentral gyrus R	0.393	0.394	0.000	0.646277	0.956825688311688	-0.019
Postcentral gyrus medial segment L	0.229	0.230	0.000	0.788264	0.955979744680851	0.012
Postcentral gyrus medial segment R	0.222	0.222	0.001	0.611	1	0.023
Posterior cingulate gyrus L	0.560	0.560	0.000	0.752	0.985379310344828	-0.011
Posterior cingulate gyrus R	0.523	0.523	0.000	0.810	0.942244897959184	-0.009
Posterior insula L	0.352	0.354	0.003	0.202	1	0.053
Posterior insula R	0.381	0.383	0.002	0.208	1	0.051
Posterior orbital gyrus L	0.351	0.353	0.002	0.308	1	0.043
Posterior orbital gyrus R	0.377	0.379	0.001	0.377	1	-0.036
Precentral gyrus L	0.485	0.487	0.002	0.185	1	0.049
Precentral gyrus R	0.473	0.474	0.001	0.402	1	0.032
Precentral gyrus medial segment L	0.283	0.283	0.000	0.883	0.958685714285714	-0.006
Precentral gyrus medial segment R	0.314	0.315	0.000	0.777	0.962804347826087	0.012

Precuneus L	0.463	0.463	0.000	0.612	1	0.019
Precuneus R	0.489	0.489	0.000	0.631	0.999083333333333	0.018
Putamen L	0.229	0.230	0.001	0.574	1	-0.026
Putamen R	0.241	0.244	0.003	0.206	1	-0.057
Subcallosal area L	0.434	0.435	0.000	0.563	1	0.023
Subcallosal area R	0.380	0.382	0.002	0.274	1	0.045
Superior frontal gyrus L	0.428	0.428	0.000	0.769	0.974066666666667	-0.012
Superior frontal gyrus R	0.465	0.466	0.001	0.364024	1	0.034
Superior frontal gyrus medial segment L	0.414	0.415	0.000	0.637	0.981324324324324	-0.019
Superior frontal gyrus medial segment R	0.384	0.384	0.000	0.674	0.948592592592593	-0.017
Superior occipital gyrus L	0.338	0.343	0.005	0.090	1	0.071
Superior occipital gyrus R	0.343	0.347	0.005	0.098	1	0.070
Superior parietal lobule L	0.368	0.371	0.002	0.215	1	0.051
Superior parietal lobule R	0.359	0.359	0.000	0.628	1	0.020
Superior temporal gyrus L	0.365	0.365	0.000	0.768	0.983730337078652	-0.012
Superior temporal gyrus R	0.360	0.360	0.000	0.654	0.943746835443038	0.019
Supplementary motor cortex L	0.356	0.356	0.000	0.720	0.988915662650602	-0.015
Supplementary motor cortex R	0.347	0.348	0.001	0.435654	1	-0.033
Supramarginal gyrus L	0.312	0.314	0.002	0.304	1	0.044
Supramarginal gyrus R	0.306	0.312	0.006	0.065	1	0.079
Temporal pole L	0.312	0.312	0.000	0.926	0.977444444444445	-0.004
Temporal pole R	0.347	0.348	0.001	0.581	1	-0.023
Thalamus proper L	0.213	0.213	0.000	0.729	0.989357142857143	0.016
Thalamus proper R	0.255	0.255	0.000	0.797	0.9564	-0.012
Transverse temporal gyrus L	0.255	0.255	0.000	0.807	0.948432989690722	-0.011
Transverse temporal gyrus R	0.307	0.307	0.000	0.624	1	-0.021
Triangular part of the inferior frontal gyrus L	0.340	0.342	0.002	0.314	1	0.042
Triangular part of the inferior frontal gyrus R	0.285	0.287	0.003	0.233	1	0.052

FDR: false discovery rate. L: left. PRS: polygenic risk score. R: right.

Table D.42: Associations between PRSwithoutAPOE Threshold 5 and 114 regions of interest in AD dementia patients

Region of Interest	R Square (Model 1)	R Square (Model 2)	R Square Change	Sig. F Change (Model 2)	FDR Corrected value	Standardised beta of PRS
Accumbens area L	0.512	0.534	0.022	0.023	0.874	-0.166
Accumbens area R	0.497	0.505	0.008	0.188	0.7144	-0.098
Amygdala L	0.425	0.439	0.015	0.087	0.762923076923077	-0.136
Amygdala R	0.445	0.446	0.001	0.676	0.975493670886076	-0.033
Angular gyrus L	0.446	0.448	0.003	0.471	1	-0.057
Angular gyrus R	0.558	0.558	0.000	0.933606	1	0.006
Anterior cingulate gyrus L	0.412	0.436	0.024	0.029	0.6612	-0.174
Anterior cingulate gyrus R	0.272	0.289	0.017	0.105	0.748125	-0.145
Anterior insula L	0.505	0.515	0.010	0.133905	0.63604875	-0.111
Anterior insula R	0.557	0.560	0.003	0.376	1	-0.062
Anterior orbital gyrus L	0.499	0.509	0.010	0.127	0.658090909090909	-0.113
Anterior orbital gyrus R	0.495	0.504	0.009	0.160	0.675555555555556	-0.105
Basal forebrain L	0.275	0.291	0.016	0.116	0.6612	-0.140
Basal forebrain R	0.376	0.422	0.046	0.003	0.342	-0.241
Calcarine cortex L	0.390	0.392	0.001	0.613	1	0.042
Calcarine cortex R	0.439	0.441	0.002	0.527	0.984885245901639	0.050
Caudate L	0.362	0.374	0.011	0.153	0.69768	-0.120
Caudate R	0.328	0.336	0.007	0.260	0.871764705882353	-0.097
Central operculum L	0.373	0.376	0.003	0.498	1	-0.057
Central operculum R	0.506	0.506	0.000	0.839	1	0.015
Cuneus L	0.491	0.494	0.003	0.391	1	0.064
Cuneus R	0.473	0.475	0.002	0.541	0.994741935483871	0.047
Entorhinal area L	0.413	0.431	0.017	0.066	0.684	-0.147
Entorhinal area R	0.407	0.407	0.000	0.872	1	-0.013
Frontal operculum L	0.341	0.342	0.001	0.623	0.986416666666667	-0.042
Frontal operculum R	0.405	0.412	0.006	0.277	0.877166666666667	0.088

Frontal pole L	0.523	0.524	0.001	0.617	0.990676056338028	-0.036
Frontal pole R	0.496	0.498	0.002	0.512138	1	-0.049
Fusiform gyrus L	0.496	0.496	0.000	0.816	1	0.017
Fusiform gyrus R	0.530	0.530	0.000	0.892630	1	0.010
Gyrus rectus L	0.526	0.537	0.010	0.118	0.640571428571429	-0.113
Gyrus rectus R	0.541	0.556	0.015	0.052	0.5928	-0.137
Hippocampus L	0.471	0.482	0.011	0.114	0.684	-0.120
Hippocampus R	0.503	0.503	0.000	0.944	0.978327272727273	0.005
Inferior occipital gyrus L	0.507	0.507	0.000	0.943	0.986256880733945	0.005
Inferior occipital gyrus R	0.479	0.481	0.002	0.523	1	0.049
Inferior temporal gyrus L	0.497	0.504	0.008	0.189	0.695032258064516	-0.098
Inferior temporal gyrus R	0.518	0.518	0.000	0.833	1	-0.015
Lateral orbital gyrus L	0.441	0.445	0.004	0.355	1	-0.073
Lateral orbital gyrus R	0.456	0.476	0.020	0.039	0.635142857142857	-0.159
Lingual gyrus L	0.566	0.569	0.003	0.396	1	0.059
Lingual gyrus R	0.558	0.562	0.005	0.268	0.872914285714286	0.078
Medial frontal cortex L	0.353	0.364	0.011	0.157	0.688384615384615	-0.120
Medial frontal cortex R	0.414	0.414	0.000	0.959	0.984918918918919	0.004
Medial orbital gyrus L	0.594	0.609	0.015	0.038	0.722	-0.138
Medial orbital gyrus R	0.512	0.524	0.012	0.090	0.732857142857143	-0.124
Middle cingulate gyrus L	0.433	0.433	0.000	0.903	0.999436893203884	-0.010
Middle cingulate gyrus R	0.414	0.416	0.001	0.631	0.985397260273973	-0.039
Middle frontal gyrus L	0.540	0.547	0.007	0.183	0.719379310344827	-0.095
Middle frontal gyrus R	0.579	0.580	0.001	0.599	1	-0.036
Middle occipital gyrus L	0.440	0.454	0.013	0.101	0.7676	-0.129
Middle occipital gyrus R	0.433	0.433	0.000	0.888	1	-0.011
Middle temporal gyrus L	0.484	0.494	0.010	0.133894	0.96615	-0.113
Middle temporal gyrus R	0.539	0.539	0.001	0.678	0.66364852173913	0.030
Occipital fusiform gyrus L	0.521	0.522	0.001	0.596	1	0.039
Occipital fusiform gyrus R	0.513	0.513	0.000	0.873442	1	0.012

Occipital pole L	0.429	0.429	0.000	0.825	1	0.018
Occipital pole R	0.464	0.466	0.002	0.513	1	0.050
Opercular part of the inferior frontal gyrus L	0.367	0.371	0.004	0.399	1	-0.071
Opercular part of the inferior frontal gyrus R	0.403	0.403	0.000	0.939	0.991166666666667	0.006
Orbital part of the inferior frontal gyrus L	0.326	0.326	0.000	0.934028	1	-0.007
Orbital part of the inferior frontal gyrus R	0.306	0.329	0.023	0.049	0.620666666666667	-0.172
Pallidum L	0.214	0.227	0.013	0.168	0.684	-0.128
Pallidum R	0.240	0.256	0.017	0.113	0.715666666666667	-0.145
Parahippocampal gyrus L	0.522	0.524	0.002	0.526	0.9994	-0.046
Parahippocampal gyrus R	0.539	0.541	0.003	0.414	1	0.058
Parietal operculum L	0.376	0.376	0.000	0.804	1	-0.021
Parietal operculum R	0.358	0.359	0.001	0.751	0.972886363636364	0.027
Planum polare L	0.459	0.473	0.015	0.079	0.7505	-0.035
Planum polare R	0.483	0.483	0.000	0.962	0.979178571428571	-0.004
Planum temporale L	0.495	0.495	0.000	0.988	0.996743362831858	0.001
Planum temporale R	0.408	0.408	0.000	0.785	1	-0.022
Postcentral gyrus L	0.553	0.555	0.002	0.481	1	-0.050
Postcentral gyrus R	0.501	0.501	0.000	0.934244	0.99536276635514	0.006
Postcentral gyrus medial segment L	0.371	0.374	0.003	0.447	1	0.063
Postcentral gyrus medial segment R	0.330	0.333	0.003	0.454	1	-0.065
Posterior cingulate gyrus L	0.605	0.608	0.003	0.328	0.984	-0.065
Posterior cingulate gyrus R	0.597	0.598	0.001	0.675	0.986538461538462	-0.028
Posterior insula L	0.487	0.487	0.000	0.873398	1	0.012
Posterior insula R	0.516	0.518	0.002	0.475	1	0.052
Posterior orbital gyrus L	0.434	0.437	0.003	0.438	1	-0.061
Posterior orbital gyrus R	0.418	0.420	0.001	0.616206	1	-0.040
Precentral gyrus L	0.507	0.508	0.001	0.683	0.961259259259259	-0.030
Precentral gyrus R	0.463	0.463	0.000	0.991	0.991	0.001
Precentral gyrus medial segment L	0.422	0.423	0.001	0.664	0.996	-0.035
Precentral gyrus medial segment R	0.406	0.406	0.000	0.866	1	-0.014

Precuneus L	0.575	0.575	0.000	0.887	1	-0.010
Precuneus R	0.610	0.613	0.003	0.346	1	0.062
Putamen L	0.429	0.430	0.001	0.616236	1	-0.040
Putamen R	0.444	0.445	0.001	0.707	0.971060240963855	-0.030
Subcallosal area L	0.570	0.588	0.018	0.026	0.741	-0.153
Subcallosal area R	0.597	0.606	0.009	0.108	0.724235294117647	-0.107
Superior frontal gyrus L	0.565	0.565	0.000	0.742	0.972275862068965	-0.023
Superior frontal gyrus R	0.570	0.570	0.000	0.893140	0.998215294117647	-0.009
Superior frontal gyrus medial segment L	0.527	0.550	0.023	0.017	0.969	-0.171
Superior frontal gyrus medial segment R	0.504	0.504	0.001	0.653	0.99256	-0.033
Superior occipital gyrus L	0.349	0.350	0.001	0.686	0.953707317073171	0.034
Superior occipital gyrus R	0.479	0.482	0.003	0.385	1	0.066
Superior parietal lobule L	0.517	0.519	0.002	0.512028	1	0.048
Superior parietal lobule R	0.486	0.493	0.007	0.222	0.766909090909091	0.092
Superior temporal gyrus L	0.489	0.496	0.007	0.219	0.7801875	-0.092
Superior temporal gyrus R	0.413	0.416	0.003	0.444	1	-0.062
Supplementary motor cortex L	0.427	0.432	0.005	0.306	0.942810810810811	-0.081
Supplementary motor cortex R	0.434	0.435	0.001	0.665	0.984545454545455	-0.034
Supramarginal gyrus L	0.459	0.462	0.002	0.511619	1	0.051
Supramarginal gyrus R	0.451	0.153	0.002	0.548	0.991619047619048	0.047
Temporal pole L	0.483	0.501	0.018	0.043	0.61275	-0.152
Temporal pole R	0.433	0.433	0.000	0.930	1	0.007
Thalamus proper L	0.199	0.201	0.002	0.559	0.99571875	-0.055
Thalamus proper R	0.264	0.266	0.001	0.632	0.973621621621622	-0.043
Transverse temporal gyrus L	0.332	0.333	0.001	0.714	0.969	0.032
Transverse temporal gyrus R	0.295	0.296	0.001	0.721358	0.967468376470588	0.032
Triangular part of the inferior frontal gyrus L	0.336	0.338	0.002	0.566	0.992676923076923	-0.049
Triangular part of the inferior frontal gyrus R	0.442	0.443	0.001	0.721412	0.956290325581395	-0.028

FDR: false discovery rate. L: left. PRS: polygenic risk score. R: right.

Table D.43: Associations between PRSwithoutAPOE Threshold 10 and 114 regions of interest in CU participants

Region of Interest	R Square (Model 1)	R Square (Model 2)	R Square Change	Sig. F Change (Model 2)	FDR Corrected value	Standardised beta of PRS
Accumbens area L	0.346	0.346	0.000	0.884	1	-0.010
Accumbens area R	0.391	0.391	0.000	0.918	1	0.007
Amygdala L	0.420	0.426	0.005	0.217	1	-0.080
Amygdala R	0.477	0.479	0.001	0.501	1	-0.041
Angular gyrus L	0.403	0.406	0.003	0.378627	1	0.058
Angular gyrus R	0.364	0.369	0.005	0.247	1	0.078
Anterior cingulate gyrus L	0.447	0.449	0.001	0.561	1	0.037
Anterior cingulate gyrus R	0.266	0.266	0.000	0.915803	1	-0.008
Anterior insula L	0.407	0.410	0.003	0.348	1	-0.061
Anterior insula R	0.408	0.414	0.006	0.189	1	-0.086
Anterior orbital gyrus L	0.317	0.317	0.000	0.870	1	0.012
Anterior orbital gyrus R	0.360	0.366	0.007	0.190	1	0.089
Basal forebrain L	0.294	0.301	0.008	0.177	1	-0.096
Basal forebrain R	0.367	0.367	0.001	0.699	1	-0.026
Calcarine cortex L	0.384	0.388	0.004	0.298	1	-0.069
Calcarine cortex R	0.383	0.386	0.003	0.347	1	-0.063
Caudate L	0.170	0.174	0.004	0.392	1	-0.066
Caudate R	0.169	0.171	0.002	0.542	1	-0.047
Central operculum L	0.447	0.447	0.000	0.935	1	-0.005
Central operculum R	0.402	0.403	0.001	0.636	0.979783783783784	0.031
Cuneus L	0.346	0.347	0.000	0.796	0.986347826086956	-0.018
Cuneus R	0.424	0.425	0.001	0.582629	1	-0.035
Entorhinal area L	0.408	0.410	0.002	0.456	1	-0.049
Entorhinal area R	0.466	0.468	0.003	0.378923	1	-0.055
Frontal operculum L	0.437	0.436	0.002	0.474	1	-0.046
Frontal operculum R	0.287	0.306	0.019	0.034	1	-0.151

Frontal pole L	0.422	0.433	0.010	0.087	1	0.110
Frontal pole R	0.413	0.423	0.010	0.099	1	0.107
Fusiform gyrus L	0.513	0.514	0.001	0.608	0.949479452054795	0.030
Fusiform gyrus R	0.471	0.481	0.010	0.085072	1	0.106
Gyrus rectus L	0.438	0.442	0.005	0.251	1	-0.073
Gyrus rectus R	0.467	0.467	0.000	0.712929	0.979203686746988	-0.023
Hippocampus L	0.368	0.373	0.004	0.284	1	-0.072
Hippocampus R	0.380	0.385	0.005	0.260	1	-0.075
Inferior occipital gyrus L	0.363	0.363	0.000	0.959	1	-0.004
Inferior occipital gyrus R	0.500	0.500	0.000	0.954	1	-0.003
Inferior temporal gyrus L	0.568	0.569	0.001	0.482	1	-0.039
Inferior temporal gyrus R	0.563	0.563	0.000	0.829066	0.9948792	-0.012
Lateral orbital gyrus L	0.379	0.384	0.006	0.225	1	0.081
Lateral orbital gyrus R	0.384	0.387	0.003	0.406	1	-0.055
Lingual gyrus L	0.530	0.530	0.000	0.948	1	-0.004
Lingual gyrus R	0.515	0.515	0.000	0.904	1	0.007
Medial frontal cortex L	0.430	0.430	0.000	0.949	1	0.004
Medial frontal cortex R	0.393	0.394	0.001	0.594	0.995823529411765	-0.035
Medial orbital gyrus L	0.451	0.452	0.000	0.735	0.963103448275862	0.021
Medial orbital gyrus R	0.455	0.456	0.001	0.605660	0.972468169014085	0.032
Middle cingulate gyrus L	0.453	0.456	0.002	0.399	1	0.053
Middle cingulate gyrus R	0.352	0.352	0.000	0.790	0.98967032967033	-0.018
Middle frontal gyrus L	0.536	0.536	0.000	0.706	0.99362962962963	0.022
Middle frontal gyrus R	0.496	0.497	0.001	0.596	0.984695652173913	-0.032
Middle occipital gyrus L	0.323	0.324	0.001	0.726	0.973694117647059	0.024
Middle occipital gyrus R	0.374	0.375	0.001	0.712848	0.991032585365854	-0.025
Middle temporal gyrus L	0.514	0.521	0.007	0.117	1	-0.093
Middle temporal gyrus R	0.524	0.526	0.002	0.419	1	0.047
Occipital fusiform gyrus L	0.480	0.483	0.003	0.296	1	0.064
Occipital fusiform gyrus R	0.474	0.481	0.007	0.150181	1	0.088

Occipital pole L	0.360	0.363	0.003	0.421	0.999875	0.055
Occipital pole R	0.333	0.333	0.001	0.700	0.9975	0.027
Opercular part of the inferior frontal gyrus L	0.306	0.307	0.001	0.669	0.977769230769231	-0.030
Opercular part of the inferior frontal gyrus R	0.308	0.313	0.005	0.268	1	-0.078
Orbital part of the inferior frontal gyrus L	0.405	0.408	0.004	0.309	1	-0.067
Orbital part of the inferior frontal gyrus R	0.282	0.282	0.000	0.944	1	-0.005
Pallidum L	0.203	0.203	0.001	0.734	0.972976744186046	0.026
Pallidum R	0.166	0.171	0.005	0.318	1	0.078
Parahippocampal gyrus L	0.506	0.507	0.001	0.533	1	-0.037
Parahippocampal gyrus R	0.508	0.509	0.001	0.604	0.983657142857143	-0.031
Parietal operculum L	0.354	0.356	0.002	0.428	0.995755102040816	-0.054
Parietal operculum R	0.341	0.341	0.000	0.828819	1	-0.015
Planum polare L	0.479	0.485	0.006	0.169	1	-0.084
Planum polare R	0.482	0.482	0.000	0.966	1	-0.003
Planum temporale L	0.407	0.407	0.000	0.995	0.995	0.000
Planum temporale R	0.360	0.363	0.003	0.352	1	-0.063
Postcentral gyrus L	0.372	0.373	0.000	0.804	0.985548387096774	0.017
Postcentral gyrus R	0.351	0.369	0.018	0.031	1	0.147
Postcentral gyrus medial segment L	0.131	0.133	0.001	0.605678	0.958990166666667	0.041
Postcentral gyrus medial segment R	0.186	0.200	0.015	0.084985	1	0.132
Posterior cingulate gyrus L	0.476	0.476	0.001	0.648	0.972	-0.028
Posterior cingulate gyrus R	0.418	0.420	0.002	0.504	1	-0.043
Posterior insula L	0.396	0.399	0.003	0.391	1	-0.057
Posterior insula R	0.435	0.436	0.001	0.545	1	0.039
Posterior orbital gyrus L	0.382	0.383	0.001	0.590	1	-0.036
Posterior orbital gyrus R	0.388	0.388	0.000	0.970	1	0.003
Precentral gyrus L	0.442	0.446	0.004	0.292	1	-0.067
Precentral gyrus R	0.425	0.425	0.000	0.916147	1	-0.007
Precentral gyrus medial segment L	0.282	0.285	0.003	0.373	1	0.064
Precentral gyrus medial segment R	0.324	0.324	0.000	0.992	1	0.001

Precuneus L	0.477	0.478	0.001	0.563	1	0.036
Precuneus R	0.456	0.457	0.000	0.763	0.966466666666667	-0.019
Putamen L	0.287	0.290	0.003	0.383	1	-0.063
Putamen R	0.300	0.301	0.001	0.653	0.966779220779221	-0.032
Subcallosal area L	0.513	0.515	0.002	0.472	1	0.043
Subcallosal area R	0.492	0.494	0.001	0.514	1	0.040
Superior frontal gyrus L	0.501	0.506	0.004	0.234	1	-0.071
Superior frontal gyrus R	0.523	0.523	0.000	0.981	1	-0.001
Superior frontal gyrus medial segment L	0.381	0.381	0.001	0.715	0.970357142857143	-0.024
Superior frontal gyrus medial segment R	0.395	0.395	0.000	0.973	1	-0.002
Superior occipital gyrus L	0.327	0.329	0.001	0.551	1	-0.042
Superior occipital gyrus R	0.305	0.313	0.009	0.155	1	-0.101
Superior parietal lobule L	0.402	0.405	0.003	0.361	1	0.060
Superior parietal lobule R	0.417	0.421	0.003	0.349	1	-0.061
Superior temporal gyrus L	0.480	0.480	0.000	0.747	0.967704545454545	-0.020
Superior temporal gyrus R	0.466	0.467	0.001	0.582571	1	-0.034
Supplementary motor cortex L	0.410	0.413	0.004	0.324	1	-0.064
Supplementary motor cortex R	0.428	0.429	0.002	0.500	1	0.043
Supramarginal gyrus L	0.363	0.371	0.008	0.149978	1	0.097
Supramarginal gyrus R	0.429	0.439	0.010	0.091	1	0.108
Temporal pole L	0.405	0.415	0.010	0.096	1	-0.109
Temporal pole R	0.409	0.410	0.001	0.538	1	-0.040
Thalamus proper L	0.293	0.294	0.000	0.751	0.961955056179775	-0.023
Thalamus proper R	0.312	0.313	0.001	0.637	0.96824	-0.033
Transverse temporal gyrus L	0.310	0.320	0.009	0.138	1	-0.104
Transverse temporal gyrus R	0.402	0.409	0.006	0.192	1	-0.086
Triangular part of the inferior frontal gyrus L	0.373	0.373	0.000	0.993	1	0.001
Triangular part of the inferior frontal gyrus R	0.298	0.305	0.007	0.213	1	-0.089

FDR: false discovery rate. L: left. PRS: polygenic risk score. R: right.

Table D.44: Associations between PRSwithoutAPOE Threshold 10 and 114 regions of interest in MCI patients

Region of Interest	R Square (Model 1)	R Square (Model 2)	R Square Change	Sig. F Change (Model 2)	FDR Corrected value	Standardised beta of PRS
Accumbens area L	0.379	0.379	0.001	0.495	1	-0.029
Accumbens area R	0.353	0.353	0.000	0.755	1	-0.014
Amygdala L	0.341	0.342	0.002	0.333	1	-0.043
Amygdala R	0.408	0.411	0.003	0.166	1	-0.058
Angular gyrus L	0.375	0.376	0.000	0.614	1	0.022
Angular gyrus R	0.405	0.405	0.000	0.867	0.959592233009709	0.007
Anterior cingulate gyrus L	0.403	0.403	0.000	0.820	1	0.010
Anterior cingulate gyrus R	0.229	0.231	0.002	0.339	1	0.046
Anterior insula L	0.315	0.316	0.001	0.473	1	0.032
Anterior insula R	0.328	0.328	0.000	0.831	1	-0.009
Anterior orbital gyrus L	0.436	0.436	0.001	0.512	1	0.027
Anterior orbital gyrus R	0.373	0.374	0.001	0.368	0.953454545454545	0.039
Basal forebrain L	0.255	0.256	0.000	0.851	0.989938775510204	-0.009
Basal forebrain R	0.319	0.319	0.000	0.864652	0.975943841584158	-0.008
Calcarine cortex L	0.403	0.403	0.000	0.760	1	-0.013
Calcarine cortex R	0.414	0.414	0.000	0.865400	0.967211764705882	-0.007
Caudate L	0.195	0.195	0.000	0.940	0.965405405405405	-0.004
Caudate R	0.201	0.202	0.001	0.553	1	-0.029
Central operculum L	0.391	0.392	0.001	0.413	1	0.035
Central operculum R	0.365	0.365	0.000	0.794455	1	0.011
Cuneus L	0.411	0.412	0.001	0.438	1	0.032
Cuneus R	0.429	0.429	0.000	0.785	1	0.011
Entorhinal area L	0.335	0.355	0.000	0.817	1	-0.010
Entorhinal area R	0.421	0.422	0.002	0.311	1	-0.042
Frontal operculum L	0.362	0.367	0.004	0.099	1	0.071
Frontal operculum R	0.348	0.348	0.000	0.605351	1	0.023

Frontal pole L	0.428	0.434	0.005	0.057	1	0.078
Frontal pole R	0.426	0.430	0.005	0.072	1	0.074
Fusiform gyrus L	0.442	0.444	0.003	0.169	1	0.056
Fusiform gyrus R	0.500	0.500	0.000	0.858564	0.988649454545455	0.007
Gyrus rectus L	0.436	0.438	0.002	0.224	1	0.050
Gyrus rectus R	0.420	0.420	0.000	0.924	0.966385321100917	-0.004
Hippocampus L	0.395	0.399	0.004	0.090	1	-0.071
Hippocampus R	0.422	0.428	0.006	0.045	1	-0.083
Inferior occipital gyrus L	0.379	0.379	0.000	0.735	0.9975	0.014
Inferior occipital gyrus R	0.446	0.449	0.003	0.114682	1	0.064
Inferior temporal gyrus L	0.459	0.460	0.001	0.538	1	-0.025
Inferior temporal gyrus R	0.536	0.537	0.000	0.713	1	-0.014
Lateral orbital gyrus L	0.443	0.444	0.001	0.312	1	0.041
Lateral orbital gyrus R	0.344	0.345	0.001	0.522	1	0.028
Lingual gyrus L	0.489	0.489	0.000	0.993	0.993	0.000
Lingual gyrus R	0.529	0.533	0.004	0.074	1	0.066
Medial frontal cortex L	0.371	0.371	0.000	0.922	0.982317757009346	-0.004
Medial frontal cortex R	0.340	0.342	0.002	0.255	1	0.050
Medial orbital gyrus L	0.451	0.452	0.001	0.306	1	0.041
Medial orbital gyrus R	0.420	0.421	0.001	0.437	1	0.032
Middle cingulate gyrus L	0.355	0.355	0.000	0.648	1	0.020
Middle cingulate gyrus R	0.320	0.322	0.002	0.272	1	0.049
Middle frontal gyrus L	0.463	0.465	0.002	0.247	1	0.046
Middle frontal gyrus R	0.462	0.462	0.000	0.953	0.970017857142857	0.002
Middle occipital gyrus L	0.335	0.336	0.001	0.517	1	0.029
Middle occipital gyrus R	0.322	0.323	0.001	0.576	1	0.025
Middle temporal gyrus L	0.452	0.452	0.000	0.833	0.97967952	0.008
Middle temporal gyrus R	0.488	0.489	0.000	0.859368	0.9996	-0.007
Occipital fusiform gyrus L	0.463	0.463	0.000	0.695	1	0.016
Occipital fusiform gyrus R	0.520	0.521	0.001	0.366	0.970325581395349	0.034

Occipital pole L	0.295	0.297	0.002	0.286	1	-0.049
Occipital pole R	0.375	0.375	0.000	0.965	0.97353982300885	-0.002
Opercular part of the inferior frontal gyrus L	0.281	0.282	0.001	0.468	1	0.033
Opercular part of the inferior frontal gyrus R	0.254	0.255	0.001	0.487	1	0.033
Orbital part of the inferior frontal gyrus L	0.285	0.287	0.003	0.217	1	0.057
Orbital part of the inferior frontal gyrus R	0.238	0.238	0.000	0.888	0.964114285714286	0.007
Pallidum L	0.171	0.171	0.001	0.605142	1	0.026
Pallidum R	0.138	0.138	0.000	0.910	0.978679245283019	0.006
Parahippocampal gyrus L	0.433	0.433	0.000	0.660925	0.9913875	0.018
Parahippocampal gyrus R	0.492	0.492	0.000	0.850	0.998969072164948	-0.007
Parietal operculum L	0.334	0.337	0.003	0.213	1	0.055
Parietal operculum R	0.279	0.279	0.000	0.671	0.980692307692308	0.020
Planum polare L	0.388	0.390	0.001	0.346	0.962048780487805	-0.040
Planum polare R	0.429	0.432	0.003	0.124	1	-0.063
Planum temporale L	0.328	0.331	0.002	0.237	1	-0.053
Planum temporale R	0.352	0.352	0.000	0.923	0.974277777777778	0.004
Postcentral gyrus L	0.369	0.371	0.002	0.232	1	-0.051
Postcentral gyrus R	0.393	0.394	0.000	0.726	0.997156626506024	-0.015
Postcentral gyrus medial segment L	0.229	0.230	0.001	0.599	1	0.025
Postcentral gyrus medial segment R	0.222	0.224	0.002	0.328	1	0.047
Posterior cingulate gyrus L	0.560	0.560	0.000	0.619	1	-0.018
Posterior cingulate gyrus R	0.523	0.523	0.000	0.711	1	0.014
Posterior insula L	0.352	0.353	0.001	0.353	0.958142857142857	0.041
Posterior insula R	0.381	0.382	0.002	0.298	1	0.044
Posterior orbital gyrus L	0.351	0.355	0.003	0.150	1	0.063
Posterior orbital gyrus R	0.377	0.378	0.000	0.660531	1	-0.019
Precentral gyrus L	0.485	0.487	0.002	0.246	1	0.045
Precentral gyrus R	0.473	0.473	0.001	0.453	1	0.030
Precentral gyrus medial segment L	0.283	0.283	0.000	0.869	0.952557692307692	0.008
Precentral gyrus medial segment R	0.314	0.315	0.000	0.625	1	0.022

Precuneus L	0.463	0.463	0.000	0.584	1	0.022
Precuneus R	0.489	0.489	0.000	0.836	0.99275	0.008
Putamen L	0.229	0.229	0.000	0.721	1	0.017
Putamen R	0.241	0.241	0.000	0.813	1	-0.011
Subcallosal area L	0.434	0.435	0.001	0.471	1	0.029
Subcallosal area R	0.380	0.385	0.004	0.091	1	0.072
Superior frontal gyrus L	0.428	0.428	0.000	0.626	1	-0.020
Superior frontal gyrus R	0.465	0.469	0.003	0.114939	1	0.062
Superior frontal gyrus medial segment L	0.414	0.415	0.000	0.643	1	-0.019
Superior frontal gyrus medial segment R	0.384	0.384	0.000	0.593	1	-0.023
Superior occipital gyrus L	0.338	0.341	0.002	0.265	1	0.049
Superior occipital gyrus R	0.343	0.344	0.002	0.304	1	0.045
Superior parietal lobule L	0.368	0.370	0.002	0.332	1	0.042
Superior parietal lobule R	0.359	0.359	0.000	0.659	1	-0.019
Superior temporal gyrus L	0.365	0.367	0.001	0.345	0.98325	-0.041
Superior temporal gyrus R	0.360	0.362	0.002	0.263	1	0.049
Supplementary motor cortex L	0.356	0.359	0.003	0.185	1	-0.058
Supplementary motor cortex R	0.347	0.348	0.001	0.535	1	-0.027
Supramarginal gyrus L	0.312	0.314	0.002	0.340	0.993846153846154	0.043
Supramarginal gyrus R	0.306	0.311	0.005	0.087	1	0.077
Temporal pole L	0.312	0.312	0.000	0.794453	1	-0.012
Temporal pole R	0.347	0.349	0.002	0.324	1	-0.043
Thalamus proper L	0.213	0.213	0.000	0.803	1	0.012
Thalamus proper R	0.255	0.255	0.000	0.667	0.987506493506494	-0.020
Transverse temporal gyrus L	0.255	0.255	0.000	0.926	0.959672727272727	0.004
Transverse temporal gyrus R	0.307	0.307	0.000	0.615	1	-0.023
Triangular part of the inferior frontal gyrus L	0.340	0.341	0.001	0.557	1	0.026
Triangular part of the inferior frontal gyrus R	0.285	0.289	0.004	0.121	1	0.071

FDR: false discovery rate. L: left. PRS: polygenic risk score. R: right.

Table D.45: Associations between PRSwithoutAPOE Threshold 10 and 114 regions of interest in AD dementia patients

Region of Interest	R Square (Model 1)	R Square (Model 2)	R Square Change	Sig. F Change (Model 2)	FDR Corrected value	Standardised beta of PRS
Accumbens area L	0.512	0.526	0.014	0.066	1	-0.133
Accumbens area R	0.497	0.505	0.008	0.184	0.912	-0.098
Amygdala L	0.425	0.428	0.004	0.389	0.96404347826087	-0.068
Amygdala R	0.445	0.446	0.001	0.652	0.978	0.035
Angular gyrus L	0.446	0.448	0.002	0.540	1	0.047
Angular gyrus R	0.558	0.570	0.012	0.074978	1	0.122
Anterior cingulate gyrus L	0.412	0.423	0.012	0.131	1	-0.120
Anterior cingulate gyrus R	0.272	0.274	0.002	0.604	0.969802816901408	-0.046
Anterior insula L	0.505	0.507	0.001	0.564	0.974181818181818	-0.042
Anterior insula R	0.557	0.557	0.000	0.865	0.976336633663366	-0.012
Anterior orbital gyrus L	0.499	0.503	0.004	0.355	0.941162790697674	-0.068
Anterior orbital gyrus R	0.495	0.496	0.002	0.556	1	-0.043
Basal forebrain L	0.275	0.277	0.001	0.659	0.975662337662338	-0.039
Basal forebrain R	0.376	0.398	0.021	0.047	1	-0.162
Calcarine cortex L	0.390	0.392	0.002	0.590	0.974782608695652	0.044
Calcarine cortex R	0.439	0.445	0.006	0.271113	1	0.086
Caudate L	0.362	0.377	0.015	0.105448	1	-0.134
Caudate R	0.328	0.343	0.015	0.109	1	-0.136
Central operculum L	0.373	0.374	0.001	0.702	0.975951219512195	0.032
Central operculum R	0.506	0.515	0.009	0.145	0.918333333333333	0.106
Cuneus L	0.491	0.492	0.001	0.612	0.969	0.038
Cuneus R	0.473	0.477	0.004	0.341	0.97185	0.072
Entorhinal area L	0.413	0.416	0.003	0.484	1	-0.056
Entorhinal area R	0.407	0.410	0.003	0.476	1	0.057
Frontal operculum L	0.341	0.341	0.000	0.916	0.97592523364486	-0.009
Frontal operculum R	0.405	0.411	0.006	0.293	1	0.084

Frontal pole L	0.523	0.524	0.001	0.682	0.97185	0.029
Frontal pole R	0.496	0.496	0.000	0.979	0.987663716814159	0.002
Fusiform gyrus L	0.496	0.501	0.005	0.302	1	0.076
Fusiform gyrus R	0.530	0.531	0.002	0.515	1	0.046
Gyrus rectus L	0.526	0.529	0.002	0.477	1	-0.051
Gyrus rectus R	0.541	0..543	0.003	0.397	0.962936170212766	-0.060
Hippocampus L	0.471	0.475	0.005	0.320	0.985945945945946	-0.075
Hippocampus R	0.503	0.504	0.000	0.846	0.96444	0.014
Inferior occipital gyrus L	0.507	0.512	0.005	0.286	1	0.078
Inferior occipital gyrus R	0.479	0.489	0.010	0.134	1	0.112
Inferior temporal gyrus L	0.497	0.497	0.000	0.889	0.983941747572815	-0.010
Inferior temporal gyrus R	0.518	0.519	0.001	0.558321	1	0.042
Lateral orbital gyrus L	0.441	0.441	0.000	0.839009	0.97599006122449	-0.016
Lateral orbital gyrus R	0.456	0.471	0.015	0.070	1	-0.138
Lingual gyrus L	0.566	0.569	0.003	0.353	0.958142857142857	0.064
Lingual gyrus R	0.558	0.565	0.008	0.156	0.936	0.098
Medial frontal cortex L	0.353	0.360	0.007	0.262	1	-0.094
Medial frontal cortex R	0.414	0.414	0.000	0.907	0.984742857142857	0.009
Medial orbital gyrus L	0.594	0.602	0.008	0.138	0.98325	-0.098
Medial orbital gyrus R	0.512	0.515	0.003	0.374	0.947466666666667	-0.064
Middle cingulate gyrus L	0.433	0.435	0.002	0.555	1	0.046
Middle cingulate gyrus R	0.414	0.419	0.004	0.349	0.970390243902439	0.074
Middle frontal gyrus L	0.540	0.541	0.001	0.583	0.977382352941176	-0.039
Middle frontal gyrus R	0.579	0.580	0.000	0.763	0.999793103448276	0.020
Middle occipital gyrus L	0.440	0.440	0.000	0.989	0.989	0.001
Middle occipital gyrus R	0.433	0.438	0.005	0.306	0.996685714285714	0.080
Middle temporal gyrus L	0.484	0.484	0.000	0.943	1	-0.005
Middle temporal gyrus R	0.539	0.543	0.005	0.288	0.977290909090909	0.075
Occipital fusiform gyrus L	0.521	0.524	0.003	0.370	0.958636363636364	0.064
Occipital fusiform gyrus R	0.513	0.513	0.000	0.768	0.994909090909091	0.021

Occipital pole L	0.429	0.430	0.001	0.748	1	0.025
Occipital pole R	0.464	0.470	0.006	0.271247	1	0.084
Opercular part of the inferior frontal gyrus L	0.367	0.367	0.000	0.776	0.993977528089888	-0.024
Opercular part of the inferior frontal gyrus R	0.403	0.405	0.002	0.559232	0.980806892307692	-0.047
Orbital part of the inferior frontal gyrus L	0.326	0.328	0.002	0.558873	0.99549253125	-0.050
Orbital part of the inferior frontal gyrus R	0.306	0.323	0.017	0.092	1	-0.145
Pallidum L	0.214	0.214	0.000	0.975	0.992410714285714	-0.003
Pallidum R	0.240	0.240	0.000	0.900	0.986538461538462	-0.011
Parahippocampal gyrus L	0.522	0.523	0.000	0.780	0.988	-0.020
Parahippocampal gyrus R	0.539	0.547	0.008	0.160492	0.871242285714286	0.099
Parietal operculum L	0.376	0.377	0.001	0.638	0.982864864864865	0.039
Parietal operculum R	0.358	0.361	0.003	0.482	1	0.059
Planum polare L	0.459	0.463	0.005	0.313	0.991166666666667	-0.077
Planum polare R	0.483	0.487	0.004	0.340	0.993846153846154	0.071
Planum temporale L	0.495	0.495	0.000	0.935	0.986944444444445	0.006
Planum temporale R	0.408	0.409	0.001	0.669	0.965392405063291	0.034
Postcentral gyrus L	0.553	0.555	0.001	0.572	0.973253731343284	-0.039
Postcentral gyrus R	0.501	0.501	0.000	0.838882	0.985902556701031	0.015
Postcentral gyrus medial segment L	0.371	0.377	0.006	0.280	1	0.089
Postcentral gyrus medial segment R	0.330	0.335	0.005	0.338	1	-0.081
Posterior cingulate gyrus L	0.605	0.605	0.000	0.843	0.970727272727273	-0.013
Posterior cingulate gyrus R	0.597	0.597	0.000	0.721	0.990289156626506	0.024
Posterior insula L	0.487	0.487	0.000	0.791	0.990923076923077	0.020
Posterior insula R	0.516	0.522	0.006	0.241	1	0.085
Posterior orbital gyrus L	0.434	0.435	0.001	0.701	0.986592592592593	-0.030
Posterior orbital gyrus R	0.418	0.419	0.000	0.807	0.989225806451613	-0.019
Precentral gyrus L	0.507	0.507	0.000	0.808	0.979914893617021	-0.018
Precentral gyrus R	0.463	0.463	0.000	0.818	0.971375	-0.018
Precentral gyrus medial segment L	0.422	0.422	0.000	0.870	0.972352941176471	0.013
Precentral gyrus medial segment R	0.406	0.407	0.001	0.666	0.973384615384615	0.035

Precuneus L	0.575	0.576	0.001	0.534	1	0.042
Precuneus R	0.610	0.624	0.014	0.044	1	0.130
Putamen L	0.429	0.429	0.000	0.911	0.979754716981132	-0.009
Putamen R	0.444	0.445	0.001	0.727	0.986642857142857	-0.027
Subcallosal area L	0.570	0.580	0.010	0.104797	1	-0.110
Subcallosal area R	0.597	0.599	0.002	0.462	1	-0.048
Superior frontal gyrus L	0.565	0.567	0.002	0.496	1	-0.047
Superior frontal gyrus R	0.570	0.570	0.001	0.629	0.98227397260274	-0.033
Superior frontal gyrus medial segment L	0.527	0.536	0.009	0.143	0.958941176470588	-0.104
Superior frontal gyrus medial segment R	0.504	0.505	0.001	0.602	0.9804	-0.038
Superior occipital gyrus L	0.349	0.350	0.000	0.794	0.983869565217391	-0.022
Superior occipital gyrus R	0.479	0.488	0.009	0.159585	0.9096345	0.105
Superior parietal lobule L	0.517	0.522	0.005	0.295	1	0.076
Superior parietal lobule R	0.486	0.511	0.025	0.017	1	0.175
Superior temporal gyrus L	0.489	0.489	0.000	0.945	0.97054054054054	-0.005
Superior temporal gyrus R	0.413	0.415	0.003	0.466	1	0.058
Supplementary motor cortex L	0.427	0.429	0.002	0.550	1	-0.047
Supplementary motor cortex R	0.434	0.437	0.003	0.460	1	-0.058
Supramarginal gyrus L	0.459	0.472	0.013	0.102	1	0.124
Supramarginal gyrus R	0.451	0.467	0.015	0.074562	1	0.136
Temporal pole L	0.483	0.488	0.006	0.252	1	-0.086
Temporal pole R	0.433	0.435	0.002	0.544	1	0.048
Thalamus proper L	0.199	0.200	0.001	0.647	0.98344	-0.043
Thalamus proper R	0.264	0.265	0.000	0.816	0.9792	-0.021
Transverse temporal gyrus L	0.332	0.332	0.000	0.941	0.984165137614679	0.006
Transverse temporal gyrus R	0.295	0.307	0.011	0.175	0.906818181818182	0.118
Triangular part of the inferior frontal gyrus L	0.336	0.351	0.015	0.112	0.982153846153846	-0.134
Triangular part of the inferior frontal gyrus R	0.442	0.443	0.000	0.760	1	-0.024

FDR: false discovery rate. L: left. PRS: polygenic risk score. R: right.

Table D.46: Associations between APOEonlyPRS Threshold 1 and 114 regions of interest in CU participants

Region of Interest	R Square (Model 1)	R Square (Model 2)	R Square Change	Sig. F Change (Model 2)	FDR Corrected value	Standardised beta of PRS
Accumbens area L	0.346	0.349	0.003	0.402	0.552144578313253	-0.055
Accumbens area R	0.391	0.391	0.000	0.970	0.97858407079646	0.002
Amygdala L	0.420	0.439	0.019	0.020024	0.142671	-0.142
Amygdala R	0.477	0.493	0.016	0.025125	0.1432125	-0.130
Angular gyrus L	0.403	0.407	0.004	0.286	0.472521739130435	-0.067
Angular gyrus R	0.364	0.375	0.011	0.089	0.25365	-0.109
Anterior cingulate gyrus L	0.447	0.451	0.004	0.297	0.483685714285714	-0.063
Anterior cingulate gyrus R	0.266	0.271	0.005	0.299	0.480084507042254	-0.072
Anterior insula L	0.407	0.409	0.002	0.517	0.64767032967033	-0.040
Anterior insula R	0.408	0.409	0.002	0.516	0.6536	-0.040
Anterior orbital gyrus L	0.317	0.328	0.011	0.109	0.264382978723404	-0.107
Anterior orbital gyrus R	0.360	0.379	0.019	0.024981	0.149886	-0.144
Basal forebrain L	0.294	0.301	0.008	0.179	0.377888888888889	-0.091
Basal forebrain R	0.367	0.370	0.003	0.346	0.519	-0.061
Calcarine cortex L	0.384	0.397	0.013	0.065	0.211714285714286	-0.117
Calcarine cortex R	0.383	0.408	0.025	0.009167	0.13062975	-0.164
Caudate L	0.170	0.171	0.001	0.721	0.805823529411765	-0.026
Caudate R	0.169	0.170	0.001	0.671	0.76494	-0.031
Central operculum L	0.447	0.449	0.002	0.435	0.576627906976744	-0.047
Central operculum R	0.402	0.412	0.010	0.103	0.266863636363636	-0.102
Cuneus L	0.346	0.349	0.002	0.433	0.580729411764706	-0.051
Cuneus R	0.424	0.426	0.002	0.422	0.572714285714286	-0.049
Entorhinal area L	0.408	0.417	0.009	0.119	0.282625	-0.097
Entorhinal area R	0.466	0.470	0.004	0.253	0.45065625	-0.068
Frontal operculum L	0.437	0.437	0.000	0.987	0.987	0.001
Frontal operculum R	0.287	0.305	0.018	0.043	0.188538461538462	-0.138

Frontal pole L	0.422	0.423	0.001	0.571	0.707543478260869	0.035
Frontal pole R	0.413	0.414	0.000	0.735	0.813495145631068	0.021
Fusiform gyrus L	0.513	0.531	0.017	0.015	0.1425	-0.136
Fusiform gyrus R	0.471	0.495	0.023	0.006690	0.152532	-0.158
Gyrus rectus L	0.438	0.439	0.001	0.576	0.706064516129032	-0.034
Gyrus rectus R	0.467	0.471	0.005	0.232	0.42658064516129	-0.071
Hippocampus L	0.368	0.395	0.027	0.008	0.130285714285714	-0.169
Hippocampus R	0.380	0.425	0.045	0.000470162697876	0.053598547557864	-0.219
Inferior occipital gyrus L	0.363	0.366	0.003	0.364754	0.526353873417722	-0.059
Inferior occipital gyrus R	0.500	0.508	0.008	0.099	0.26246511627907	-0.094
Inferior temporal gyrus L	0.568	0.578	0.010	0.048	0.188689655172414	-0.105
Inferior temporal gyrus R	0.563	0.578	0.015	0.018710	0.152352857142857	-0.125
Lateral orbital gyrus L	0.379	0.391	0.012	0.070	0.215675675675676	-0.115
Lateral orbital gyrus R	0.384	0.399	0.015	0.047086	0.191707285714286	-0.126
Lingual gyrus L	0.530	0.544	0.015	0.023178	0.155428941176471	-0.125
Lingual gyrus R	0.515	0.531	0.017	0.017	0.149076923076923	-0.133
Medial frontal cortex L	0.430	0.430	0.000	0.924	0.948972972972973	0.006
Medial frontal cortex R	0.393	0.399	0.006	0.219	0.4161	-0.077
Medial orbital gyrus L	0.451	0.466	0.014	0.039	0.17784	-0.123
Medial orbital gyrus R	0.455	0.463	0.008	0.129184	0.29453952	-0.090
Middle cingulate gyrus L	0.453	0.455	0.002	0.465	0.602386363636364	-0.044
Middle cingulate gyrus R	0.352	0.365	0.013	0.067	0.212166666666667	-0.119
Middle frontal gyrus L	0.536	0.542	0.006	0.152	0.326943396226415	-0.079
Middle frontal gyrus R	0.496	0.502	0.005	0.183	0.379309090909091	-0.076
Middle occipital gyrus L	0.323	0.327	0.003	0.363	0.530538461538462	-0.011
Middle occipital gyrus R	0.374	0.378	0.003	0.354	0.524103896103896	-0.059
Middle temporal gyrus L	0.514	0.517	0.003	0.300	0.1862	-0.058
Middle temporal gyrus R	0.524	0.535	0.011	0.049	0.475	-0.109
Occipital fusiform gyrus L	0.480	0.482	0.003	0.365450	0.52076625	-0.053
Occipital fusiform gyrus R	0.474	0.479	0.005	0.204	0.394169491525424	-0.074

Occipital pole L	0.360	0.361	0.000	0.882	0.914072727272727	0.010
Occipital pole R	0.333	0.334	0.001	0.664	0.772408163265306	0.029
Opercular part of the inferior frontal gyrus L	0.306	0.306	0.000	0.871	0.910954128440367	-0.011
Opercular part of the inferior frontal gyrus R	0.308	0.315	0.007	0.196	0.385241379310345	-0.087
Orbital part of the inferior frontal gyrus L	0.405	0.429	0.024	0.009243	0.117078	-0.161
Orbital part of the inferior frontal gyrus R	0.282	0.290	0.008	0.184	0.374571428571429	-0.091
Pallidum L	0.203	0.220	0.018	0.055	0.1959375	-0.138
Pallidum R	0.166	0.178	0.012	0.129426	0.289305176470588	-0.112
Parahippocampal gyrus L	0.506	0.528	0.022	0.006929	0.131651	-0.152
Parahippocampal gyrus R	0.508	0.541	0.033	0.000703372594884	0.040092237908388	-0.189
Parietal operculum L	0.354	0.358	0.004	0.317	0.495041095890411	0.065
Parietal operculum R	0.341	0.341	0.000	0.858	0.905666666666667	0.012
Planum polare L	0.479	0.481	0.002	0.482	0.617393258426966	-0.041
Planum polare R	0.482	0.491	0.010	0.079	0.230923076923077	-0.102
Planum temporale L	0.407	0.412	0.004	0.274023	0.473312454545455	-0.068
Planum temporale R	0.360	0.360	0.000	0.767	0.84075	-0.019
Postcentral gyrus L	0.372	0.377	0.004	0.285	0.477794117647059	-0.069
Postcentral gyrus R	0.351	0.370	0.019	0.028	0.145090909090909	-0.143
Postcentral gyrus medial segment L	0.131	0.157	0.026	0.026	0.141142857142857	-0.167
Postcentral gyrus medial segment R	0.186	0.191	0.006	0.280	0.476417910447761	-0.079
Posterior cingulate gyrus L	0.476	0.481	0.006	0.186	0.372	-0.077
Posterior cingulate gyrus R	0.418	0.428	0.010	0.095	0.264146341463415	-0.103
Posterior insula L	0.396	0.396	0.000	0.801	0.853401869158879	-0.016
Posterior insula R	0.435	0.436	0.001	0.589	0.71431914893617	-0.033
Posterior orbital gyrus L	0.382	0.422	0.040	0.000912309718823	0.034667769315274	-0.208
Posterior orbital gyrus R	0.388	0.419	0.031	0.004	0.114	-0.182
Precentral gyrus L	0.442	0.454	0.012	0.059	0.203818181818182	-0.114
Precentral gyrus R	0.425	0.432	0.007	0.149	0.326653846153846	-0.088
Precentral gyrus medial segment L	0.282	0.297	0.015	0.060	0.201176470588235	-0.129
Precentral gyrus medial segment R	0.324	0.339	0.015	0.052	0.191225806451613	-0.129

Precuneus L	0.477	0.486	0.009	0.096	0.260571428571429	-0.097
Precuneus R	0.456	0.474	0.018	0.019667	0.1494692	-0.138
Putamen L	0.287	0.315	0.027	0.011	0.1254	-0.172
Putamen R	0.300	0.318	0.019	0.036	0.171	-0.141
Subcallosal area L	0.513	0.516	0.003	0.342	0.51984	-0.054
Subcallosal area R	0.492	0.501	0.008	0.105	0.266	-0.093
Superior frontal gyrus L	0.501	0.504	0.003	0.340	0.523783783783784	-0.055
Superior frontal gyrus R	0.523	0.523	0.000	0.965	0.982232142857143	0.002
Superior frontal gyrus medial segment L	0.381	0.390	0.010	0.107	0.265173913043478	-0.102
Superior frontal gyrus medial segment R	0.395	0.396	0.001	0.609	0.715731958762887	-0.032
Superior occipital gyrus L	0.327	0.328	0.001	0.670	0.771515151515152	-0.028
Superior occipital gyrus R	0.305	0.305	0.000	0.780	0.838867924528302	-0.019
Superior parietal lobule L	0.402	0.403	0.001	0.592	0.7104	-0.034
Superior parietal lobule R	0.417	0.439	0.021	0.014	0.145090909090909	-0.151
Superior temporal gyrus L	0.480	0.480	0.000	0.769	0.834914285714286	0.017
Superior temporal gyrus R	0.466	0.470	0.005	0.233	0.421619047619048	-0.070
Supplementary motor cortex L	0.410	0.428	0.018	0.023695	0.150068333333333	-0.140
Supplementary motor cortex R	0.428	0.431	0.003	0.367	0.516518518518518	-0.055
Supramarginal gyrus L	0.363	0.366	0.003	0.378	0.525512195121951	-0.057
Supramarginal gyrus R	0.429	0.430	0.001	0.596	0.70775	-0.032
Temporal pole L	0.405	0.409	0.004	0.273799	0.480201323076923	-0.068
Temporal pole R	0.409	0.414	0.005	0.227	0.424229508196721	-0.075
Thalamus proper L	0.293	0.314	0.020	0.030	0.148695652173913	-0.147
Thalamus proper R	0.312	0.328	0.016	0.046995	0.198423333333333	-0.133
Transverse temporal gyrus L	0.310	0.313	0.002	0.458	0.600137931034483	0.050
Transverse temporal gyrus R	0.402	0.403	0.001	0.704	0.794613861386139	0.024
Triangular part of the inferior frontal gyrus L	0.373	0.382	0.009	0.128886	0.299857224489796	-0.097
Triangular part of the inferior frontal gyrus R	0.298	0.312	0.014	0.075	0.225	-0.121

FDR: false discovery rate. L: left. PRS: polygenic risk score. R: right.

Table D.47: Associations between APOEonlyPRS Threshold 1 and 114 regions of interest in MCI patients

Region of Interest	R Square (Model 1)	R Square (Model 2)	R Square Change	Sig. F Change (Model 2)	FDR Corrected value	Standardised beta of PRS
Accumbens area L	0.379	0.379	0.001	0.488	1	0.030
Accumbens area R	0.353	0.354	0.001	0.525	1	0.028
Amygdala L	0.341	0.341	0.000	0.747	1	0.014
Amygdala R	0.477	0.493	0.016	0.455	1	-0.032
Angular gyrus L	0.375	0.376	0.000	0.791	1	-0.012
Angular gyrus R	0.405	0.405	0.000	0.726	1	-0.015
Anterior cingulate gyrus L	0.403	0.403	0.000	0.845	1	-0.008
Anterior cingulate gyrus R	0.229	0.229	0.000	0.880	1	0.007
Anterior insula L	0.315	0.319	0.004	0.141758	1	0.067
Anterior insula R	0.328	0.330	0.002	0.298	1	0.047
Anterior orbital gyrus L	0.436	0.436	0.000	0.989	0.99775221238938	-0.001
Anterior orbital gyrus R	0.373	0.375	0.002	0.257	1	-0.049
Basal forebrain L	0.255	0.256	0.000	0.806	1	0.012
Basal forebrain R	0.319	0.320	0.001	0.490	1	0.031
Calcarine cortex L	0.403	0.403	0.000	0.581	1	0.024
Calcarine cortex R	0.414	0.414	0.000	0.704	1	-0.016
Caudate L	0.195	0.196	0.001	0.451	1	0.037
Caudate R	0.201	0.202	0.001	0.449	1	0.037
Central operculum L	0.391	0.400	0.009	0.016	0.912	0.104
Central operculum R	0.365	0.366	0.001	0.369	1	0.039
Cuneus L	0.411	0.412	0.001	0.393	1	-0.036
Cuneus R	0.429	0.432	0.003	0.154	1	-0.059
Entorhinal area L	0.335	0.336	0.002	0.314	1	0.045
Entorhinal area R	0.421	0.421	0.000	0.798	1	0.011
Frontal operculum L	0.362	0.365	0.003	0.175	1	0.060
Frontal operculum R	0.348	0.350	0.002	0.297	1	0.046

Frontal pole L	0.428	0.429	0.001	0.418	1	0.034
Frontal pole R	0.426	0.427	0.002	0.289	1	0.044
Fusiform gyrus L	0.442	0.442	0.000	0.938	0.999364485981308	-0.003
Fusiform gyrus R	0.500	0.500	0.000	0.828851	1	-0.008
Gyrus rectus L	0.436	0.437	0.001	0.497	1	0.028
Gyrus rectus R	0.420	0.420	0.000	0.643	1	0.019
Hippocampus L	0.395	0.395	0.000	0.715	1	0.016
Hippocampus R	0.422	0.424	0.002	0.264	1	-0.047
Inferior occipital gyrus L	0.379	0.381	0.002	0.261	1	-0.049
Inferior occipital gyrus R	0.446	0.448	0.002	0.276	1	-0.045
Inferior temporal gyrus L	0.459	0.460	0.001	0.513	1	0.027
Inferior temporal gyrus R	0.536	0.536	0.000	0.959	0.984918918918919	0.002
Lateral orbital gyrus L	0.443	0.445	0.002	0.190	1	0.054
Lateral orbital gyrus R	0.355	0.345	0.001	0.506	1	0.030
Lingual gyrus L	0.489	0.490	0.000	0.649	1	0.018
Lingual gyrus R	0.529	0.530	0.001	0.434166	1	-0.030
Medial frontal cortex L	0.371	0.373	0.002	0.255	1	-0.050
Medial frontal cortex R	0.340	0.340	0.000	0.890	0.994705882352941	-0.006
Medial orbital gyrus L	0.451	0.451	0.000	0.728	1	0.014
Medial orbital gyrus R	0.420	0.420	0.000	0.829496	1	0.009
Middle cingulate gyrus L	0.355	0.355	0.000	0.949	0.992532110091743	0.003
Middle cingulate gyrus R	0.320	0.320	0.000	0.950	0.984545454545455	-0.003
Middle frontal gyrus L	0.463	0.463	0.000	0.882	1	0.006
Middle frontal gyrus R	0.462	0.462	0.000	0.885882	0.999906415841584	-0.006
Middle occipital gyrus L	0.335	0.336	0.001	0.433966	1	-0.035
Middle occipital gyrus R	0.322	0.329	0.006	0.052	0.988	-0.088
Middle temporal gyrus L	0.452	0.453	0.001	0.409	1	0.034
Middle temporal gyrus R	0.488	0.489	0.000	0.727	1	0.147
Occipital fusiform gyrus L	0.463	0.463	0.000	0.860	1	0.007
Occipital fusiform gyrus R	0.520	0.522	0.001	0.304	1	-0.039

Occipital pole L	0.295	0.295	0.000	0.606	1	-0.024
Occipital pole R	0.375	0.376	0.001	0.491	1	-0.030
Opercular part of the inferior frontal gyrus L	0.281	0.292	0.010	0.017	0.646	0.112
Opercular part of the inferior frontal gyrus R	0.254	0.258	0.004	0.158	1	0.067
Orbital part of the inferior frontal gyrus L	0.285	0.293	0.008	0.031	0.8835	0.100
Orbital part of the inferior frontal gyrus R	0.238	0.238	0.000	0.947	0.999611111111111	-0.003
Pallidum L	0.171	0.171	0.000	0.862	1	0.009
Pallidum R	0.138	0.138	0.000	0.999	0.999	0.000
Parahippocampal gyrus L	0.433	0.436	0.004	0.104	1	0.067
Parahippocampal gyrus R	0.492	0.492	0.000	0.646	1	0.018
Parietal operculum L	0.334	0.335	0.000	0.611	1	0.023
Parietal operculum R	0.279	0.279	0.000	0.661	1	0.021
Planum polare L	0.388	0.389	0.001	0.549313	1	0.026
Planum polare R	0.429	0.429	0.000	0.621	1	0.021
Planum temporale L	0.328	0.332	0.004	0.147	1	0.065
Planum temporale R	0.352	0.353	0.001	0.346	1	0.042
Postcentral gyrus L	0.369	0.369	0.000	0.885658	1	0.006
Postcentral gyrus R	0.393	0.393	0.000	0.730	1	-0.015
Postcentral gyrus medial segment L	0.229	0.234	0.005	0.115	1	-0.076
Postcentral gyrus medial segment R	0.222	0.222	0.000	0.717	1	-0.018
Posterior cingulate gyrus L	0.560	0.562	0.002	0.137	1	0.054
Posterior cingulate gyrus R	0.523	0.523	0.000	0.812	1	0.009
Posterior insula L	0.352	0.353	0.001	0.347	1	0.042
Posterior insula R	0.381	0.381	0.000	0.723	1	0.015
Posterior orbital gyrus L	0.351	0.358	0.006	0.047	1	0.088
Posterior orbital gyrus R	0.377	0.378	0.001	0.452	1	0.033
Precentral gyrus L	0.485	0.486	0.000	0.548	1	0.024
Precentral gyrus R	0.473	0.473	0.000	0.832	1	0.009
Precentral gyrus medial segment L	0.283	0.284	0.001	0.405	1	-0.039
Precentral gyrus medial segment R	0.314	0.317	0.002	0.239	1	-0.054

Precuneus L	0.463	0.463	0.000	0.937	1	-0.003
Precuneus R	0.489	0.489	0.000	0.903	0.999436893203884	-0.005
Putamen L	0.229	0.230	0.001	0.505	1	0.032
Putamen R	0.241	0.241	0.000	0.785	1	0.013
Subcallosal area L	0.434	0.437	0.003	0.142149	1	0.061
Subcallosal area R	0.380	0.391	0.011	0.009	1	0.114
Superior frontal gyrus L	0.428	0.428	0.000	0.931	1	-0.004
Superior frontal gyrus R	0.465	0.466	0.001	0.401	1	0.034
Superior frontal gyrus medial segment L	0.414	0.416	0.001	0.332	1	0.041
Superior frontal gyrus medial segment R	0.384	0.386	0.002	0.208	1	0.054
Superior occipital gyrus L	0.338	0.339	0.000	0.586	1	-0.024
Superior occipital gyrus R	0.343	0.343	0.000	0.963	0.980196428571429	-0.002
Superior parietal lobule L	0.368	0.369	0.000	0.707	1	-0.016
Superior parietal lobule R	0.359	0.359	0.000	0.749	1	-0.014
Superior temporal gyrus L	0.365	0.366	0.001	0.467	1	0.032
Superior temporal gyrus R	0.360	0.361	0.001	0.549208	1	0.026
Supplementary motor cortex L	0.356	0.357	0.001	0.534	1	-0.028
Supplementary motor cortex R	0.347	0.347	0.000	0.783	1	-0.012
Supramarginal gyrus L	0.312	0.312	0.000	0.929	1	0.004
Supramarginal gyrus R	0.306	0.308	0.002	0.300	1	0.048
Temporal pole L	0.312	0.313	0.001	0.402	1	0.038
Temporal pole R	0.347	0.348	0.001	0.478	1	-0.032
Thalamus proper L	0.213	0.217	0.004	0.148	1	0.071
Thalamus proper R	0.255	0.257	0.002	0.359	1	0.044
Transverse temporal gyrus L	0.255	0.255	0.000	0.653	1	0.021
Transverse temporal gyrus R	0.307	0.308	0.001	0.567	1	0.026
Triangular part of the inferior frontal gyrus L	0.34	0.344	0.004	0.111	1	0.071
Triangular part of the inferior frontal gyrus R	0.285	0.285	0.001	0.563	1	0.027

FDR: false discovery rate. L: left. PRS: polygenic risk score. R: right.

Table D.48: Associations between APOEonlyPRS Threshold 1 and 114 regions of interest in AD dementia patients

Region of Interest	R Square (Model 1)	R Square (Model 2)	R Square Change	Sig. F Change (Model 2)	FDR Corrected value	Standardised beta of PRS
Accumbens area L	0.512	0.512	0.000	0.812	1	-0.018
Accumbens area R	0.497	0.502	0.004	0.317	0.821318181818182	0.077
Amygdala L	0.425	0.462	0.038	0.005	0.285	-0.227
Amygdala R	0.445	0.475	0.030	0.012	0.342	-0.201
Angular gyrus L	0.446	0.447	0.001	0.647	1	-0.037
Angular gyrus R	0.558	0.558	0.000	0.837	1	0.015
Anterior cingulate gyrus L	0.412	0.440	0.029	0.017	0.323	0.197
Anterior cingulate gyrus R	0.272	0.272	0.000	0.981	1	0.002
Anterior insula L	0.505	0.513	0.007	0.191	0.87096	0.100
Anterior insula R	0.557	0.562	0.006	0.229	0.842129032258064	0.087
Anterior orbital gyrus L	0.499	0.500	0.001	0.603	1	-0.040
Anterior orbital gyrus R	0.495	0.497	0.002	0.500	1	0.052
Basal forebrain L	0.275	0.280	0.004	0.405	0.982340425531915	0.077
Basal forebrain R	0.376	0.388	0.012	0.138068	0.749512	0.128
Calcarine cortex L	0.390	0.390	0.000	0.989	1	-0.001
Calcarine cortex R	0.439	0.439	0.000	0.980	1	-0.002
Caudate L	0.362	0.365	0.002	0.516	1	-0.057
Caudate R	0.328	0.329	0.001	0.699	1	-0.035
Central operculum L	0.373	0.373	0.000	0.923	0.992660377358491	-0.008
Central operculum R	0.506	0.508	0.002	0.469	1	0.056
Cuneus L	0.491	0.497	0.006	0.236	0.84075	-0.092
Cuneus R	0.473	0.473	0.000	0.759	1	-0.024
Entorhinal area L	0.413	0.467	0.054	0.00097581239454	0.11124261297756	-0.270
Entorhinal area R	0.407	0.426	0.019	0.056	0.6384	-0.160
Frontal operculum L	0.341	0.358	0.017	0.081841	0.666419571428571	0.154
Frontal operculum R	0.405	0.438	0.033	0.011	0.418	0.011

Frontal pole L	0.523	0.524	0.001	0.579	1	-0.042
Frontal pole R	0.496	0.499	0.002	0.498	1	0.053
Fusiform gyrus L	0.496	0.496	0.000	0.764	1	-0.023
Fusiform gyrus R	0.530	0.530	0.000	0.778	1	-0.021
Gyrus rectus L	0.526	0.527	0.000	0.880	1	-0.011
Gyrus rectus R	0.541	0.550	0.010	0.119	0.714	0.115
Hippocampus L	0.471	0.498	0.027	0.014	0.3192	-0.193
Hippocampus R	0.503	0.518	0.015	0.063	0.5985	-0.142
Inferior occipital gyrus L	0.507	0.508	0.001	0.718	1	-0.028
Inferior occipital gyrus R	0.479	0.479	0.001	0.724	1	-0.028
Inferior temporal gyrus L	0.497	0.501	0.005	0.295	0.84075	-0.081
Inferior temporal gyrus R	0.518	0.518	0.000	0.792	1	-0.020
Lateral orbital gyrus L	0.441	0.442	0.001	0.747	1	-0.026
Lateral orbital gyrus R	0.456	0.460	0.004	0.354	0.877304347826087	0.075
Lingual gyrus L	0.566	0.566	0.000	0.809	1	-0.017
Lingual gyrus R	0.558	0.558	0.000	0.849	1	0.014
Medial frontal cortex L	0.353	0.353	0.000	0.872	1	0.014
Medial frontal cortex R	0.414	0.429	0.014	0.094	0.630352941176471	0.139
Medial orbital gyrus L	0.594	0.594	0.000	0.784	1	0.019
Medial orbital gyrus R	0.512	0.519	0.007	0.200	0.844444444444445	0.098
Middle cingulate gyrus L	0.433	0.434	0.001	0.608	1	0.042
Middle cingulate gyrus R	0.414	0.417	0.003	0.475	1	0.060
Middle frontal gyrus L	0.540	0.545	0.005	0.274	0.867666666666667	0.081
Middle frontal gyrus R	0.579	0.585	0.006	0.214	0.841241379310345	0.088
Middle occipital gyrus L	0.440	0.443	0.003	0.457	1	-0.061
Middle occipital gyrus R	0.433	0.438	0.005	0.308	0.836	-0.084
Middle temporal gyrus L	0.484	0.489	0.005	0.276	1	-0.085
Middle temporal gyrus R	0.539	0.539	0.000	0.918	0.850378378378378	-0.008
Occipital fusiform gyrus L	0.521	0.523	0.003	0.437	1	0.059
Occipital fusiform gyrus R	0.513	0.513	0.000	0.919	1	-0.008

Occipital pole L	0.429	0.432	0.002	0.494	1	-0.056
Occipital pole R	0.464	0.464	0.000	0.836	1	-0.017
Opercular part of the inferior frontal gyrus L	0.367	0.373	0.006	0.281	0.843	0.094
Opercular part of the inferior frontal gyrus R	0.403	0.419	0.016	0.081969	0.6229644	0.146
Orbital part of the inferior frontal gyrus L	0.326	0.333	0.006	0.298	0.828585365853658	0.093
Orbital part of the inferior frontal gyrus R	0.306	0.306	0.000	0.908	1	0.010
Pallidum L	0.214	0.222	0.009	0.264	0.859885714285714	-0.108
Pallidum R	0.240	0.249	0.009	0.243	0.839454545454545	-0.111
Parahippocampal gyrus L	0.522	0.544	0.022	0.021002	0.342032571428571	-0.172
Parahippocampal gyrus R	0.539	0.553	0.014	0.058	0.601090909090909	-0.140
Parietal operculum L	0.376	0.384	0.009	0.204	0.830571428571429	0.109
Parietal operculum R	0.358	0.361	0.002	0.507	1	0.058
Planum polare L	0.459	0.459	0.000	0.787	1	0.022
Planum polare R	0.483	0.484	0.001	0.598	1	0.041
Planum temporale L	0.495	0.497	0.001	0.575	1	0.044
Planum temporale R	0.408	0.408	0.000	0.956	0.999853211009174	-0.005
Postcentral gyrus L	0.553	0.554	0.001	0.637	1	0.034
Postcentral gyrus R	0.501	0.501	0.000	0.993	0.993	-0.001
Postcentral gyrus medial segment L	0.371	0.371	0.000	0.768	1	-0.026
Postcentral gyrus medial segment R	0.330	0.330	0.000	0.916	1	-0.010
Posterior cingulate gyrus L	0.605	0.611	0.006	0.195	0.855	-0.089
Posterior cingulate gyrus R	0.597	0601	0.004	0.287	0.838923076923077	-0.074
Posterior insula L	0.487	0.499	0.012	0.105	0.665	0.126
Posterior insula R	0.516	0.529	0.013	0.075	0.657692307692308	0.134
Posterior orbital gyrus L	0.434	0.434	0.000	0.931	0.982722222222222	-0.007
Posterior orbital gyrus R	0.418	0.423	0.005	0.329	0.833466666666667	0.081
Precentral gyrus L	0507	0.516	0.009	0.137809	0.7855113	0.113
Precentral gyrus R	0.463	0.470	0.007	0.224	0.8512	0.097
Precentral gyrus medial segment L	0.422	0.423	0.000	0.776	1	-0.024
Precentral gyrus medial segment R	0.406	0.406	0.000	0.896	1	0.011

Precuneus L	0.575	0.576	0.001	0.613	1	-0.036
Precuneus R	0.610	0.611	0.001	0.658	1	-0.030
Putamen L	0.429	0.429	0.000	0.796	1	0.021
Putamen R	0.444	0.445	0.001	0.712	1	0.030
Subcallosal area L	0.570	0.580	0.011	0.092	0.6555	0.120
Subcallosal area R	0.597	0.615	0.018	0.021360	0.30438	0.158
Superior frontal gyrus L	0.565	0.565	0.000	0.832	1	0.015
Superior frontal gyrus R	0.570	0.571	0.001	0.565	1	0.041
Superior frontal gyrus medial segment L	0.527	0.527	0.000	0.894	1	-0.010
Superior frontal gyrus medial segment R	0.504	0.511	0.008	0.188	0.893	0.101
Superior occipital gyrus L	0.349	0.349	0.000	0.920	0.998857142857143	0.009
Superior occipital gyrus R	0.479	0.479	0.000	0.773	1	-0.023
Superior parietal lobule L	0.517	0.517	0.000	0.991	0.999769911504425	-0.001
Superior parietal lobule R	0.486	0.487	0.000	0.806	1	-0.019
Superior temporal gyrus L	0.489	0.489	0.000	0.900	1	0.010
Superior temporal gyrus R	0.413	0.415	0.002	0.513	1	-0.055
Supplementary motor cortex L	0.427	0.429	0.002	0.555	1	0.049
Supplementary motor cortex R	0.434	0.443	0.009	0.178	0.882260869565217	0.110
Supramarginal gyrus L	0.459	0.461	0.002	0.553	1	0.048
Supramarginal gyrus R	0.451	0.458	0.006	0.252	0.844941176470588	0.093
Temporal pole L	0.483	0.483	0.001	0.687	1	-0.032
Temporal pole R	0.433	0.433	0.000	0.930	0.990841121495327	-0.007
Thalamus proper L	0.199	0.212	0.014	0.161	0.834272727272727	-0.137
Thalamus proper R	0.264	0.271	0.007	0.311	0.824511627906977	-0.095
Transverse temporal gyrus L	0.332	0.336	0.003	0.441	1	0.069
Transverse temporal gyrus R	0.295	0.296	0.001	0.663	1	-0.040
Triangular part of the inferior frontal gyrus L	0.336	0.358	0.022	0.049	0.620666666666667	0.174
Triangular part of the inferior frontal gyrus R	0.442	0.443	0.001	0.681	1	0.034

FDR: false discovery rate. L: left. PRS: polygenic risk score. R: right.

Table D.49: Associations between APOEonlyPRS Threshold 5 and 114 regions of interest in CU participants

Region of Interest	R Square (Model 1)	R Square (Model 2)	R Square Change	Sig. F Change (Model 2)	FDR Corrected value	Standardised beta of PRS
Accumbens area L	0.346	.348	0.002	0.474	0.628325581395349	-0.047
Accumbens area R	0.391	0.391	0.000	0.915	0.93972972972973	0.007
Amygdala L	0.420	0.438	0.017	0.027118	0.19321575	-0.135
Amygdala R	0.477	0.491	0.014	0.035	0.19	-0.122
Angular gyrus L	0.403	0.407	0.004	0.322	0.547880597014925	-0.062
Angular gyrus R	0.364	0.376	0.012	0.084	0.2736	-0.111
Anterior cingulate gyrus L	0.447	0.451	0.003	0.328	0.549882352941176	-0.059
Anterior cingulate gyrus R	0.266	0.270	0.004	0.351	0.563577464788732	-0.065
Anterior insula L	0.407	0.409	0.001	0.550	0.689010989010989	-0.037
Anterior insula R	0.408	0.409	0.001	0.599	0.734258064516129	-0.033
Anterior orbital gyrus L	0.317	0.327	0.010	0.122	0.316090909090909	-0.103
Anterior orbital gyrus R	0.360	0.378	0.019	0.027226	0.182574352941176	-0.142
Basal forebrain L	0.294	0.300	0.006	0.230	0.452068965517241	-0.082
Basal forebrain R	0.367	0.370	0.003	0.402	0.595168831168831	-0.054
Calcarine cortex L	0.384	0.398	0.013	0.060	0.228	-0.119
Calcarine cortex R	0.383	0.408	0.026	0.008563	0.162697	-0.165
Caudate L	0.170	0.170	0.000	0.819479	0.889720057142857	-0.017
Caudate R	0.169	0.170	0.001	0.712	0.803643564356436	-0.027
Central operculum L	0.447	0.449	0.002	0.424	0.6042	-0.048
Central operculum R	0.402	0.412	0.010	0.097	0.291	-0.103
Cuneus L	0.346	0.348	0.002	0.482	0.631586206896552	-0.046
Cuneus R	0.424	0.426	0.002	0.488	0.632181818181818	-0.043
Entorhinal area L	0.408	0.416	0.008	0.145	0.324117647058824	-0.090
Entorhinal area R	0.466	0.468	0.003	0.371	0.579369863013699	-0.053
Frontal operculum L	0.437	0.437	0.000	0.967	0.967	-0.003
Frontal operculum R	0.287	0.303	0.016	0.054851	0.223321928571429	-0.130

Frontal pole L	0.422	0.424	0.002	0.463	0.635927710843374	0.045
Frontal pole R	0.413	0.414	0.000	0.763	0.852764705882353	0.019
Fusiform gyrus L	0.513	0.529	0.016	0.021018	0.199671	-0.129
Fusiform gyrus R	0.471	0.491	0.020	0.012	0.152	-0.147
Gyrus rectus L	0.438	0.438	0.001	0.688782	0.801236204081633	-0.024
Gyrus rectus R	0.467	0.471	0.004	0.263	0.48358064516129	-0.066
Hippocampus L	0.368	0.393	0.025	0.011	0.15675	-0.163
Hippocampus R	0.380	0.420	0.040	0.001019	0.116166	-0.206
Inferior occipital gyrus L	0.363	0.365	0.002	0.452	0.636148148148148	-0.049
Inferior occipital gyrus R	0.500	0.507	0.007	0.126	0.312260869565217	-0.087
Inferior temporal gyrus L	0.568	0.577	0.010	0.054741	0.231128666666667	-0.102
Inferior temporal gyrus R	0.563	0.576	0.013	0.028	0.177333333333333	-0.116
Lateral orbital gyrus L	0.379	0.389	0.010	0.099976	0.2849316	-0.105
Lateral orbital gyrus R	0.384	0.397	0.013	0.066	0.242709677419355	-0.116
Lingual gyrus L	0.530	0.544	0.014	0.026	0.1976	-0.123
Lingual gyrus R	0.515	0.530	0.015	0.021369	0.187389692307692	-0.129
Medial frontal cortex L	0.430	0.430	0.000	0.819075	0.897832211538462	0.014
Medial frontal cortex R	0.393	0.398	0.005	0.243	0.469525423728814	-0.074
Medial orbital gyrus L	0.451	0.465	0.013	0.046731	0.21309336	-0.119
Medial orbital gyrus R	0.455	0.462	0.007	0.134	0.31825	-0.089
Middle cingulate gyrus L	0.453	0.455	0.001	0.518	0.656133333333333	-0.039
Middle cingulate gyrus R	0.352	0.364	0.012	0.082	0.274941176470588	-0.113
Middle frontal gyrus L	0.536	0.541	0.005	0.171	0.367811320754717	-0.075
Middle frontal gyrus R	0.496	0.501	0.005	0.210	0.435272727272727	-0.072
Middle occipital gyrus L	0.323	0.3277	0.003	0.358	0.566833333333333	0.061
Middle occipital gyrus R	0.374	0.378	0.003	0.339	0.552085714285714	-0.061
Middle temporal gyrus L	0.514	0.517	0.003	0.298	0.206857384615385	-0.059
Middle temporal gyrus R	0.524	0.535	0.011	0.047178	0.522646153846154	-0.110
Occipital fusiform gyrus L	0.480	0.482	0.002	0.410	0.599230769230769	-0.048
Occipital fusiform gyrus R	0.474	0.479	0.005	0.227	0.454	-0.071

Occipital pole L	0.360	0.361	0.000	0.799	0.884330097087379	0.016
Occipital pole R	0.333	0.334	0.001	0.557	0.690195652173913	0.039
Opercular part of the inferior frontal gyrus L	0.306	0.306	0.000	0.857	0.913065420560748	-0.012
Opercular part of the inferior frontal gyrus R	0.308	0.313	0.005	0.255	0.47655737704918	-0.076
Orbital part of the inferior frontal gyrus L	0.405	0.429	0.024	0.009369	0.152580857142857	-0.161
Orbital part of the inferior frontal gyrus R	0.282	0.290	0.007	0.194	0.409555555555556	-0.089
Pallidum L	0.203	0.218	0.016	0.070	0.249375	-0.130
Pallidum R	0.166	0.177	0.011	0.137	0.318734693877551	-0.109
Parahippocampal gyrus L	0.506	0.527	0.021	0.008156	0.1859568	-0.149
Parahippocampal gyrus R	0.508	0.537	0.029	0.002	0.076	-0.177
Parietal operculum L	0.354	0.357	0.003	0.382	0.58064	0.057
Parietal operculum R	0.341	0.341	0.000	0.925	0.941517857142857	0.006
Planum polare L	0.479	0.481	0.002	0.490	0.627640449438202	-0.040
Planum polare R	0.482	0.490	0.008	0.105	0.285	-0.094
Planum temporale L	0.407	0.412	0.005	0.249	0.4731	-0.072
Planum temporale R	0.360	0.360	0.000	0.838	0.901245283018868	-0.013
Postcentral gyrus L	0.372	0.375	0.003	0.385	0.5775	-0.056
Postcentral gyrus R	0.351	0.369	0.018	0.032	0.192	-0.139
Postcentral gyrus medial segment L	0.131	0.154	0.023	0.036	0.186545454545455	-0.157
Postcentral gyrus medial segment R	0.186	0.189	0.004	0.378	0.582324324324324	-0.064
Posterior cingulate gyrus L	0.476	0.480	0.005	0.223	0.453964285714286	-0.071
Posterior cingulate gyrus R	0.418	0.428	0.009	0.101	0.280829268292683	-0.101
Posterior insula L	0.396	0.396	0.000	0.892	0.924436363636364	-0.009
Posterior insula R	0.435	0.435	0.001	0.695	0.80030303030303	-0.024
Posterior orbital gyrus L	0.382	0.419	0.038	0.001336	0.076152	-0.201
Posterior orbital gyrus R	0.388	0.416	0.028	0.006	0.171	-0.172
Precentral gyrus L	0.442	0.453	0.011	0.072	0.248727272727273	-0.108
Precentral gyrus R	0.425	0.432	0.007	0.150	0.328846153846154	-0.088
Precentral gyrus medial segment L	0.282	0.294	0.013	0.089	0.274216216216216	-0.116
Precentral gyrus medial segment R	0.324	0.335	0.011	0.099801	0.291726	-0.109

Precuneus L	0.477	0.485	0.008	0.123	0.3116	-0.090
Precuneus R	0.456	0.473	0.017	0.024	0.195428571428571	-0.133
Putamen L	0.287	0.312	0.025	0.016	0.1824	-0.163
Putamen R	0.300	0.317	0.017	0.043	0.20425	-0.136
Subcallosal area L	0.513	0.515	0.002	0.412	0.59453164556962	-0.046
Subcallosal area R	0.492	0.499	0.007	0.133	0.322595744680851	-0.086
Superior frontal gyrus L	0.501	0.503	0.002	0.459	0.638121951219512	-0.042
Superior frontal gyrus R	0.523	0.523	0.000	0.890	0.930825688073394	0.008
Superior frontal gyrus medial segment L	0.381	0.389	0.008	0.143	0.32604	-0.093
Superior frontal gyrus medial segment R	0.395	0.396	0.001	0.688621	0.809307154639175	-0.025
Superior occipital gyrus L	0.327	0.328	0.000	0.872	0.920444444444445	-0.011
Superior occipital gyrus R	0.305	0.305	0.000	0.957	0.965469026548673	0.004
Superior parietal lobule L	0.408	0.403	0.001	0.684	0.81225	-0.025
Superior parietal lobule R	0.417	0.437	0.019	0.020	0.207272727272727	-0.143
Superior temporal gyrus L	0.480	0.480	0.001	0.605	0.733723404255319	0.030
Superior temporal gyrus R	0.466	0.469	0.004	0.281065	0.50859380952381	-0.064
Supplementary motor cortex L	0.410	0.425	0.015	0.039	0.193304347826087	-0.128
Supplementary motor cortex R	0.428	0.430	0.002	0.464	0.629714285714286	-0.045
Supramarginal gyrus L	0.363	0.367	0.004	0.338	0.558434782608696	-0.062
Supramarginal gyrus R	0.429	0.430	0.001	0.631	0.7572	-0.029
Temporal pole L	0.405	0.409	0.004	0.317	0.547545454545455	-0.062
Temporal pole R	0.409	0.413	0.004	0.281327	0.50111371875	-0.067
Thalamus proper L	0.293	0.313	0.019	0.033	0.1881	-0.144
Thalamus proper R	0.312	0.327	0.015	0.055229	0.217107103448276	-0.128
Transverse temporal gyrus L	0.310	0.313	0.002	0.467	0.626329411764706	0.049
Transverse temporal gyrus R	0.402	0.403	0.001	0.703	0.80142	0.024
Triangular part of the inferior frontal gyrus L	0.373	0.382	0.009	0.120	0.318139534883721	-0.099
Triangular part of the inferior frontal gyrus R	0.298	0.311	0.012	0.087	0.2755	-0.115

FDR: false discovery rate. L: left. PRS: polygenic risk score. R: right.

Table D.50: Associations between APOEonlyPRS Threshold 5 and 114 regions of interest in MCI patients

Region of Interest	R Square (Model 1)	R Square (Model 2)	R Square Change	Sig. F Change (Model 2)	FDR Corrected value	Standardised beta of PRS
Accumbens area L	0.379	0.379	0.001	0.489835	1	0.030
Accumbens area R	0.353	0.354	0.001	0.529	1	0.028
Amygdala L	0.341	0.341	0.000	0.739	1	0.015
Amygdala R	0.408	0.409	0.001	0.431	1	-0.033
Angular gyrus L	0.375	0.376	0.000	0.706	1	-0.016
Angular gyrus R	0.405	0.405	0.000	0.646	1	-0.020
Anterior cingulate gyrus L	0.403	0.403	0.000	0.935	1	-0.003
Anterior cingulate gyrus R	0.229	0.229	0.000	0.787	1	0.013
Anterior insula L	0.315	0.318	0.003	0.171	1	0.063
Anterior insula R	0.328	0.330	0.002	0.319650	1	0.045
Anterior orbital gyrus L	0.436	0.436	0.000	0.983	0.991699115044248	0.001
Anterior orbital gyrus R	0.373	0.375	0.002	0.221	1	-0.054
Basal forebrain L	0.255	0.255	0.000	0.882646	1	0.007
Basal forebrain R	0.319	0.320	0.001	0.507	1	0.030
Calcarine cortex L	0.403	0.403	0.001	0.528	1	0.027
Calcarine cortex R	0.414	0.414	0.000	0.779	1	-0.012
Caudate L	0.195	0.196	0.001	0.511	1	0.033
Caudate R	0.201	0.202	0.001	0.503	1	0.033
Central operculum L	0.391	0.400	0.009	0.016038	0.914166	0.103
Central operculum R	0.365	0.367	0.001	0.355	1	0.041
Cuneus L	0.411	0.412	0.001	0.407	1	-0.035
Cuneus R	0.429	0.431	0.003	0.174	1	-0.057
Entorhinal area L	0.335	0.336	0.002	0.319565	1	0.045
Entorhinal area R	0.421	0.421	0.000	0.796	1	0.011
Frontal operculum L	0.362	0.365	0.003	0.183	1	0.059
Frontal operculum R	0.348	0.350	0.002	0.334	1	0.043

Frontal pole L	0.428	0.429	0.001	0.505	1	0.028
Frontal pole R	0.426	0.427	0.001	0.362	1	0.038
Fusiform gyrus L	0.442	0.442	0.000	0.894	1	-0.005
Fusiform gyrus R	0.500	0.501	0.000	0.797498	0.988204043478261	-0.010
Gyrus rectus L	0.436	0.437	0.001	0.469	1	0.030
Gyrus rectus R	0.420	0.420	0.000	0.671774	1	0.018
Hippocampus L	0.368	0.393	0.025	0.713	1	0.016
Hippocampus R	0.422	0.424	0.002	0.257	1	-0.048
Inferior occipital gyrus L	0.379	0.381	0.002	0.241844	1	-0.051
Inferior occipital gyrus R	0.446	0.448	0.002	0.275	1	-0.045
Inferior temporal gyrus L	0.459	0.460	0.000	0.619	1	0.020
Inferior temporal gyrus R	0.536	0.536	0.000	0.992	0.992	0.000
Lateral orbital gyrus L	0.443	0.445	0.002	0.184	1	0.055
Lateral orbital gyrus R	0.344	0.345	0.001	0.566	1	0.026
Lingual gyrus L	0.489	0.490	0.000	0.636	1	0.019
Lingual gyrus R	0.529	0.529	0.001	0.489820	1	-0.026
Medial frontal cortex L	0.371	0.373	0.002	0.265	1	-0.049
Medial frontal cortex R	0.340	0.340	0.000	0.939	1	-0.003
Medial orbital gyrus L	0.451	0.451	0.000	0.756	1	0.013
Medial orbital gyrus R	0.420	0.420	0.000	0.840	1	0.008
Middle cingulate gyrus L	0.355	0.355	0.000	0.947	0.999611111111111	0.003
Middle cingulate gyrus R	0.320	0.320	0.000	0.970647	0.996880702702703	-0.002
Middle frontal gyrus L	0.463	0.463	0.000	0.949397	0.983920527272727	0.003
Middle frontal gyrus R	0.462	0.462	0.000	0.931	1	-0.003
Middle occipital gyrus L	0.335	0.336	0.001	0.423	1	-0.036
Middle occipital gyrus R	0.322	0.329	0.007	0.048	0.912	-0.090
Middle temporal gyrus L	0.452	0.453	0.001	0.424	1	0.033
Middle temporal gyrus R	0.488	0.489	0.000	0.667913	1	-0.017
Occipital fusiform gyrus L	0.463	0.463	0.000	0.785	1	0.011
Occipital fusiform gyrus R	0.520	0.521	0.001	0.336	1	-0.037

Occipital pole L	0.295	0.295	0.000	0.667199	1	-0.020
Occipital pole R	0.375	0.376	0.000	0.583	1	-0.024
Opercular part of the inferior frontal gyrus L	0.281	0.292	0.010	0.016366	0.621908	0.112
Opercular part of the inferior frontal gyrus R	0.254	0.258	0.004	0.156	1	0.068
Orbital part of the inferior frontal gyrus L	0.285	0.293	0.009	0.028	0.798	0.102
Orbital part of the inferior frontal gyrus R	0.238	0.238	0.000	0.923	1	-0.005
Pallidum L	0.171	0.171	0.000	0.797008	0.998449582417583	0.013
Pallidum R	0.138	0.138	0.000	0.918	1	0.005
Parahippocampal gyrus L	0.433	0.436	0.003	0.119	1	0.065
Parahippocampal gyrus R	0.492	0.492	0.000	0.702	1	0.015
Parietal operculum L	0.334	0.335	0.000	0.644	1	0.021
Parietal operculum R	0.279	0.279	0.000	0.618	1	0.023
Planum polare L	0.388	0.389	0.001	0.548	1	0.026
Planum polare R	0.429	0.429	0.000	0.627	1	0.020
Planum temporale L	0.328	0.332	0.004	0.142	1	0.067
Planum temporale R	0.352	0.354	0.002	0.311	1	0.045
Postcentral gyrus L	0.369	0.369	0.000	0.932	1	0.004
Postcentral gyrus R	0.351	0.369	0.018	0.668455	1	-0.018
Postcentral gyrus medial segment L	0.229	0.236	0.006	0.077	1	-0.086
Postcentral gyrus medial segment R	0.222	0.222	0.000	0.771	1	-0.014
Posterior cingulate gyrus L	0.560	0.562	0.002	0.137	1	0.054
Posterior cingulate gyrus R	0.523	0.523	0.000	0.883229	1	0.006
Posterior insula L	0.352	0.353	0.001	0.370	1	0.040
Posterior insula R	0.381	0.381	0.000	0.726	1	0.015
Posterior orbital gyrus L	0.351	0.358	0.007	0.041	0.9348	0.091
Posterior orbital gyrus R	0.377	0.379	0.001	0.400	1	0.037
Precentral gyrus L	0.485	0.486	0.001	0.526	1	0.025
Precentral gyrus R	0.473	0.473	0.000	0.875	1	0.006
Precentral gyrus medial segment L	0.283	0.285	0.001	0.375	1	-0.042
Precentral gyrus medial segment R	0.314	0.317	0.002	0.242361	1	-0.053

Precuneus L	0.463	0.463	0.000	0.886	1	-0.006
Precuneus R	0.489	0.489	0.000	0.845	1	-0.008
Putamen L	0.229	0.230	0.001	0.559	1	0.028
Putamen R	0.241	0.241	0.000	0.889	1	0.007
Subcallosal area L	0.434	0.438	0.003	0.124	1	0.064
Subcallosal area R	0.380	0.392	0.012	0.006	0.684	0.119
Superior frontal gyrus L	0.428	0.428	0.000	0.819	1	-0.010
Superior frontal gyrus R	0.465	0.466	0.001	0.474	1	0.029
Superior frontal gyrus medial segment L	0.414	0.416	0.002	0.294	1	0.044
Superior frontal gyrus medial segment R	0.384	0.386	0.002	0.212	1	0.054
Superior occipital gyrus L	0.338	0.339	0.000	0.593	1	-0.024
Superior occipital gyrus R	0.343	0.343	0.000	0.970764	0.988099071428571	0.002
Superior parietal lobule L	0.368	0.369	0.000	0.714	1	-0.016
Superior parietal lobule R	0.359	0.359	0.000	0.694	1	-0.017
Superior temporal gyrus L	0.365	0.366	0.001	0.531	1	0.028
Superior temporal gyrus R	0.360	0.361	0.001	0.538	1	0.027
Supplementary motor cortex L	0.356	0.357	0.001	0.530	1	-0.028
Supplementary motor cortex R	0.347	0.347	0.000	0.758	1	-0.014
Supramarginal gyrus L	0.312	0.312	0.000	0.949129	0.992667027522936	-0.003
Supramarginal gyrus R	0.306	0.308	0.002	0.330	1	0.045
Temporal pole L	0.312	0.313	0.001	0.382	1	0.040
Temporal pole R	0.347	0.348	0.001	0.484	1	-0.031
Thalamus proper L	0.213	0.217	0.004	0.160	1	0.069
Thalamus proper R	0.255	0.256	0.001	0.405	1	0.040
Transverse temporal gyrus L	0.255	0.255	0.000	0.671557	1	0.020
Transverse temporal gyrus R	0.307	0.308	0.001	0.537	1	0.028
Triangular part of the inferior frontal gyrus L	0.340	0.344	0.004	0.111	1	0.071
Triangular part of the inferior frontal gyrus R	0.285	0.285	0.000	0.626	1	0.023

FDR: false discovery rate. L: left. PRS: polygenic risk score. R: right.

Table D.51: Associations between APOEonlyPRS Threshold 5 and 114 regions of interest in AD dementia patients

Region of Interest	R Square (Model 1)	R Square (Model 2)	R Square Change	Sig. F Change (Model 2)	FDR Corrected value	Standardised beta of PRS
Accumbens area L	0.512	0.512	0.000	0.865	1	-0.013
Accumbens area R	0.497	0.502	0.005	0.308	0.8778	0.079
Amygdala L	0.425	0.462	0.037	0.006	0.342	-0.226
Amygdala R	0.445	0.475	0.030	0.012	0.342	-0.201
Angular gyrus L	0.446	0.447	0.001	0.655	1	-0.036
Angular gyrus R	0.558	0.558	0.000	0.848	1	0.014
Anterior cingulate gyrus L	0.412	0.441	0.029	0.016	0.304	0.200
Anterior cingulate gyrus R	0.272	0.272	0.000	0.940	1	0.007
Anterior insula L	0.505	0.513	0.007	0.189	0.798	0.101
Anterior insula R	0.557	0.563	0.006	0.208769	0.7933222	0.091
Anterior orbital gyrus L	0.499	0.500	0.001	0.673	1	-0.033
Anterior orbital gyrus R	0.495	0.497	0.002	0.506	1	0.052
Basal forebrain L	0.275	0.280	0.005	0.395	0.958085106382979	0.079
Basal forebrain R	0.376	0.389	0.012	0.130	0.705714285714286	0.130
Calcarine cortex L	0.390	0.390	0.000	0.927	1	-0.008
Calcarine cortex R	0.439	0.439	0.000	0.946	0.989394495412844	-0.006
Caudate L	0.362	0.364	0.001	0.619	1	-0.043
Caudate R	0.328	0.329	0.000	0.809	1	-0.022
Central operculum L	0.373	0.373	0.000	0.993	1	-0.001
Central operculum R	0.506	0.509	0.003	0.397	0.942875	0.065
Cuneus L	0.491	0.497	0.006	0.233	0.781235294117647	-0.093
Cuneus R	0.473	0.473	0.000	0.763	1	-0.024
Entorhinal area L	0.413	0.465	0.052	0.001	0.114	-0.266
Entorhinal area R	0.407	0.426	0.019	0.057	0.6498	-0.159
Frontal operculum L	0.341	0.360	0.019	0.066300	0.5814	0.162
Frontal operculum R	0.405	0.439	0.034	0.010	0.38	0.215

Frontal pole L	0.523	0.524	0.001	0.598	1	-0.040
Frontal pole R	0.496	0.498	0.002	0.502	1	0.052
Fusiform gyrus L	0.496	0.496	0.000	0.866	1	-0.013
Fusiform gyrus R	0.530	0.530	0.000	0.796	1	-0.019
Gyrus rectus L	0.526	0.526	0.000	0.939	1	-0.006
Gyrus rectus R	0.541	0.550	0.010	0.122	0.6954	0.114
Hippocampus L	0.471	0.498	0.028	0.013	0.2964	-0.195
Hippocampus R	0.503	0.519	0.015	0.061	0.5795	-0.144
Inferior occipital gyrus L	0.507	0.508	0.001	0.703	1	-0.029
Inferior occipital gyrus R	0.479	0.479	0.001	0.735	1	-0.026
Inferior temporal gyrus L	0.497	0.500	0.004	0.343	0.888681818181818	-0.073
Inferior temporal gyrus R	0.518	0.518	0.000	0.795	1	-0.020
Lateral orbital gyrus L	0.441	0.441	0.000	0.785	1	-0.022
Lateral orbital gyrus R	0.456	0.460	0.004	0.366	0.90704347826087	0.073
Lingual gyrus L	0.566	0.566	0.000	0.803	1	-0.018
Lingual gyrus R	0.558	0.558	0.000	0.857	1	0.013
Medial frontal cortex L	0.353	0.353	0.000	0.815	1	0.021
Medial frontal cortex R	0.414	0.429	0.015	0.086	0.576705882352941	0.143
Medial orbital gyrus L	0.594	0.594	0.000	0.730	1	0.024
Medial orbital gyrus R	0.512	0.519	0.007	0.191	0.777642857142857	0.100
Middle cingulate gyrus L	0.433	0.435	0.002	0.564	1	0.048
Middle cingulate gyrus R	0.414	0.418	0.004	0.402	0.935265306122449	0.070
Middle frontal gyrus L	0.540	0.546	0.006	0.220	0.78375	0.091
Middle frontal gyrus R	0.579	0.586	0.007	0.173	0.82175	0.096
Middle occipital gyrus L	0.440	0.443	0.003	0.441	0.966807692307692	-0.063
Middle occipital gyrus R	0.433	0.438	0.005	0.315	0.855	-0.083
Middle temporal gyrus L	0.484	0.489	0.005	0.276	1	-0.085
Middle temporal gyrus R	0.539	0.539	0.000	0.912	0.806769230769231	-0.008
Occipital fusiform gyrus L	0.521	0.523	0.003	0.427	0.954470588235294	0.060
Occipital fusiform gyrus R	0.513	0.513	0.000	0.922	1	-0.008

Occipital pole L	0.429	0.432	0.003	0.471	0.994333333333333	-0.059
Occipital pole R	0.464	0.464	0.000	0.825	1	-0.018
Opercular part of the inferior frontal gyrus L	0.367	0.375	0.008	0.226	0.780727272727273	0.105
Opercular part of the inferior frontal gyrus R	0.403	0.420	0.017	0.072	0.5472	0.151
Orbital part of the inferior frontal gyrus L	0.326	0.334	0.008	0.255	0.785675675675676	0.102
Orbital part of the inferior frontal gyrus R	0.306	0.306	0.000	0.913	1	0.010
Pallidum L	0.214	0.222	0.008	0.275	0.825	-0.106
Pallidum R	0.240	0.249	0.009	0.235	0.765428571428571	-0.113
Parahippocampal gyrus L	0.522	0.543	0.020	0.026	0.3705	-0.167
Parahippocampal gyrus R	0.539	0.553	0.014	0.059	0.611454545454545	-0.139
Parietal operculum L	0.376	0.385	0.010	0.179	0.784846153846154	0.116
Parietal operculum R	0.358	0.361	0.003	0.459	0.987283018867925	0.065
Planum polare L	0.459	0.459	0.001	0.737	1	0.027
Planum polare R	0.483	0.485	0.002	0.538	1	0.048
Planum temporale L	0.495	0.497	0.002	0.546	1	0.047
Planum temporale R	0.408	0.408	0.000	0.893	1	-0.011
Postcentral gyrus L	0.553	0.554	0.001	0.641	1	0.034
Postcentral gyrus R	0.501	0.501	0.000	1.000	1	0.000
Postcentral gyrus medial segment L	0.371	0.371	0.000	0.818	1	-0.020
Postcentral gyrus medial segment R	0.330	0.330	0.000	0.945	0.9975	-0.006
Posterior cingulate gyrus L	0.605	0.611	0.005	0.208540	0.819777931034483	-0.086
Posterior cingulate gyrus R	0.597	0.601	0.004	0.316	0.837767441860465	-0.070
Posterior insula L	0.487	0.500	0.014	0.082	0.58425	0.136
Posterior insula R	0.516	0.530	0.014	0.066313	0.539977285714286	0.139
Posterior orbital gyrus L	0.434	0.434	0.000	0.965	0.991081081081081	-0.004
Posterior orbital gyrus R	0.418	0.423	0.005	0.346	0.876533333333333	0.078
Precentral gyrus L	0.507	0.519	0.012	0.100	0.6	0.126
Precentral gyrus R	0.463	0.470	0.007	0.209163	0.769180064516129	0.100
Precentral gyrus medial segment L	0.422	0.422	0.000	0.871	1	-0.014
Precentral gyrus medial segment R	0.406	0.406	0.000	0.849	1	0.016

Precuneus L	0.575	0.576	0.001	0.626	1	-0.035
Precuneus R	0.610	0.611	0.001	0.670	1	-0.029
Putamen L	0.429	0.430	0.001	0.699	1	0.032
Putamen R	0.444	0.445	0.001	0.639	1	0.038
Subcallosal area L	0.570	0.580	0.010	0.095	0.601666666666667	0.119
Subcallosal area R	0.597	0.614	0.017	0.025	0.407142857142857	0.154
Superior frontal gyrus L	0.565	0.565	0.000	0.745	1	0.023
Superior frontal gyrus R	0.570	0.571	0.002	0.504	1	0.048
Superior frontal gyrus medial segment L	0.527	0.527	0.000	0.904	1	-0.009
Superior frontal gyrus medial segment R	0.504	0.511	0.008	0.175	0.798	0.104
Superior occipital gyrus L	0.349	0.349	0.000	0.844	1	0.017
Superior occipital gyrus R	0.479	0.479	0.000	0.806	1	-0.019
Superior parietal lobule L	0.517	0.517	0.000	0.997	1	0.000
Superior parietal lobule R	0.486	0.487	0.000	0.854	1	-0.014
Superior temporal gyrus L	0.489	0.489	0.000	0.852	1	0.015
Superior temporal gyrus R	0.413	0.415	0.002	0.522	0.9918	-0.054
Supplementary motor cortex L	0.427	0.429	0.002	0.511	1	0.054
Supplementary motor cortex R	0.434	0.444	0.009	0.166	0.822782608695652	0.113
Supramarginal gyrus L	0.459	0.461	0.002	0.518	1	0.052
Supramarginal gyrus R	0.451	0.458	0.006	0.248	0.785333333333333	0.093
Temporal pole L	0.483	0.483	0.001	0.722	1	-0.028
Temporal pole R	0.433	0.433	0.000	0.956	0.990763636363636	-0.005
Thalamus proper L	0.199	0.212	0.014	0.159	0.823909090909091	-0.137
Thalamus proper R	0.264	0.271	0.007	0.312	0.867512195121951	-0.095
Transverse temporal gyrus L	0.332	0.336	0.004	0.417	0.95076	0.073
Transverse temporal gyrus R	0.295	0.296	0.001	0.742	1	-0.030
Triangular part of the inferior frontal gyrus L	0.336	0.360	0.024	0.040	0.506666666666667	0.182
Triangular part of the inferior frontal gyrus R	0.442	0.443	0.001	0.656	1	0.036

FDR: false discovery rate. L: left. PRS: polygenic risk score. R: right.

Table D.52: Associations between APOEonlyPRS Threshold 10 and 114 regions of interest in CU participants

Region of Interest	R Square (Model 1)	R Square (Model 2)	R Square Change	Sig. F Change (Model 2)	FDR Corrected value	Standardised beta of PRS
Accumbens area L	0.346	0.347	0.001	0.718	0.826787878787879	-0.024
Accumbens area R	0.391	0.391	0.001	0.667	0.7920625	0.027
Amygdala L	0.420	0.436	0.016	0.035	0.221666666666667	-0.130
Amygdala R	0.477	0.493	0.016	0.023669	0.2698266	-0.132
Angular gyrus L	0.403	0.406	0.003	0.393	0.62225	-0.054
Angular gyrus R	0.364	0.377	0.013	0.065	0.264642857142857	-0.119
Anterior cingulate gyrus L	0.447	0.450	0.002	0.410	0.6232	-0.050
Anterior cingulate gyrus R	0.266	0.270	0.003	0.394	0.615287671232877	-0.059
Anterior insula L	0.407	0.408	0.001	0.604	0.773662921348315	-0.033
Anterior insula R	0.408	0.408	0.000	0.725	0.8265	-0.022
Anterior orbital gyrus L	0.317	0.322	0.005	0.263439	0.5460372	-0.075
Anterior orbital gyrus R	0.360	0.378	0.018	0.030	0.228	-0.141
Basal forebrain L	0.294	0.300	0.006	0.239	0.534235294117647	-0.080
Basal forebrain R	0.367	0.369	0.003	0.416914	0.617249298701299	-0.053
Calcarine cortex L	0.384	0.398	0.014	0.052	0.247	-0.123
Calcarine cortex R	0.383	0.407	0.024	0.011	0.3135	-0.162
Caudate L	0.170	0.170	0.000	0.982	0.999535714285714	0.002
Caudate R	0.169	0.169	0.000	0.912	0.962666666666667	-0.008
Central operculum L	0.447	0.448	0.001	0.575	0.753448275862069	-0.034
Central operculum R	0.402	0.409	0.007	0.163	0.432139534883721	-0.088
Cuneus L	0.346	0.349	0.003	0.372	0.605828571428571	-0.059
Cuneus R	0.424	0.427	0.003	0.349	0.576608695652174	-0.058
Entorhinal area L	0.408	0.414	0.006	0.189	0.468391304347826	-0.082
Entorhinal area R	0.466	0.469	0.003	0.331	0.554911764705882	-0.058
Frontal operculum L	0.437	0.437	0.000	0.985	0.993716814159292	-0.001
Frontal operculum R	0.287	0.298	0.011	0.110	0.368823529411765	-0.109

Frontal pole L	0.422	0.426	0.003	0.321	0.554454545454545	0.061
Frontal pole R	0.413	0.414	0.001	0.693	0.806142857142857	0.025
Fusiform gyrus L	0.513	0.528	0.014	0.027174	0.258153	-0.125
Fusiform gyrus R	0.471	0.487	0.016	0.027278	0.239207076923077	-0.130
Gyrus rectus L	0.438	0.438	0.000	0.995	0.995	0.000
Gyrus rectus R	0.467	0.470	0.004	0.293	0.547573770491803	-0.062
Hippocampus L	0.368	0.391	0.023	0.014	0.228	-0.157
Hippocampus R	0.380	0.421	0.041	0.000764492060287	0.087152094872718	-0.212
Inferior occipital gyrus L	0.363	0.366	0.003	0.398	0.613135135135135	-0.055
Inferior occipital gyrus R	0.500	0.507	0.007	0.134	0.412864864864865	-0.086
Inferior temporal gyrus L	0.568	0.576	0.008	0.073	0.2774	-0.096
Inferior temporal gyrus R	0.563	0.574	0.011	0.045169	0.234057545454545	-0.107
Lateral orbital gyrus L	0.379	0.384	0.005	0.254	0.546339622641509	-0.073
Lateral orbital gyrus R	0.384	0.392	0.007	0.162	0.439714285714286	-0.089
Lingual gyrus L	0.530	0.546	0.017	0.015	0.21375	-0.135
Lingual gyrus R	0.515	0.527	0.012	0.041	0.246	-0.115
Medial frontal cortex L	0.430	0.431	0.001	0.638	0.790565217391304	0.029
Medial frontal cortex R	0.393	0.398	0.004	0.272	0.544	-0.070
Medial orbital gyrus L	0.451	0.458	0.007	0.155624	0.454900923076923	-0.085
Medial orbital gyrus R	0.455	0.460	0.005	0.199440	0.47367	-0.077
Middle cingulate gyrus L	0.453	0.454	0.001	0.580	0.751363636363636	-0.033
Middle cingulate gyrus R	0.352	0.360	0.008	0.156995	0.44743575	-0.093
Middle frontal gyrus L	0.536	0.540	0.004	0.241	0.528346153846154	-0.065
Middle frontal gyrus R	0.496	0.499	0.003	0.312	0.5472	-0.058
Middle occipital gyrus L	0.323	0.325	0.002	0.519	0.712843373493976	0.043
Middle occipital gyrus R	0.374	0.379	0.004	0.289	0.558406779661017	-0.068
Middle temporal gyrus L	0.514	0.516	0.002	0.416729	0.432681818181818	-0.046
Middle temporal gyrus R	0.524	0.529	0.006	0.167	0.6250935	-0.077
Occipital fusiform gyrus L	0.480	0.482	0.002	0.435	0.627721518987342	-0.046
Occipital fusiform gyrus R	0.474	0.476	0.002	0.459	0.654075	-0.044

Occipital pole L	0.360	0.361	0.000	0.899	0.966849056603774	-0.008
Occipital pole R	0.333	0.334	0.001	0.557	0.747035294117647	0.039
Opercular part of the inferior frontal gyrus L	0.306	0.307	0.000	0.779	0.870647058823529	-0.019
Opercular part of the inferior frontal gyrus R	0.308	0.312	0.004	0.330	0.561492537313433	-0.066
Orbital part of the inferior frontal gyrus L	0.405	0.417	0.013	0.062	0.261777777777778	-0.117
Orbital part of the inferior frontal gyrus R	0.282	0.285	0.003	0.387	0.621380281690141	-0.060
Pallidum L	0.203	0.221	0.018	0.053	0.24168	-0.140
Pallidum R	0.166	0.179	0.014	0.102	0.363375	-0.121
Parahippocampal gyrus L	0.506	0.527	0.021	0.008	0.304	-0.150
Parahippocampal gyrus R	0.508	0.538	0.030	0.001	0.057	-0.182
Parietal operculum L	0.354	0.359	0.005	0.263087	0.555405888888889	0.073
Parietal operculum R	0.341	0.341	0.000	0.960	0.994909090909091	-0.003
Planum polare L	0.479	0.481	0.001	0.568	0.752930232558139	-0.034
Planum polare R	0.482	0.491	0.009	0.085	0.31258064516129	-0.100
Planum temporale L	0.407	0.413	0.005	0.231	0.52668	-0.075
Planum temporale R	0.360	0.360	0.000	0.973	0.999297297297297	0.002
Postcentral gyrus L	0.372	0.375	0.002	0.425	0.621153846153846	-0.051
Postcentral gyrus R	0.351	0.367	0.016	0.043	0.2451	-0.132
Postcentral gyrus medial segment L	0.131	0.148	0.017	0.071	0.279103448275862	-0.136
Postcentral gyrus medial segment R	0.186	0.187	0.001	0.663	0.7956	-0.032
Posterior cingulate gyrus L	0.476	0.481	0.005	0.195	0.472978723404255	-0.076
Posterior cingulate gyrus R	0.418	0.430	0.012	0.060	0.263076923076923	-0.116
Posterior insula L	0.396	0.396	0.000	0.907	0.966336448598131	-0.007
Posterior insula R	0.435	0.436	0.001	0.675	0.793298969072165	-0.026
Posterior orbital gyrus L	0.382	0.404	0.023	0.013	0.247	-0.158
Posterior orbital gyrus R	0.388	0.406	0.018	0.027351	0.222715285714286	-0.140
Precentral gyrus L	0.442	0.451	0.008	0.114	0.371314285714286	-0.096
Precentral gyrus R	0.425	0.430	0.006	0.199469	0.464070734693878	-0.079
Precentral gyrus medial segment L	0.282	0.290	0.008	0.169	0.428133333333333	-0.095
Precentral gyrus medial segment R	0.324	0.332	0.008	0.157316	0.437415219512195	-0.094

Precuneus L	0.477	0.485	0.007	0.126	0.399	-0.090
Precuneus R	0.456	0.474	0.018	0.021	0.266	-0.138
Putamen L	0.287	0.314	0.027	0.012	0.2736	-0.172
Putamen R	0.300	0.319	0.019	0.032	0.228	-0.145
Subcallosal area L	0.513	0.514	0.001	0.646	0.783446808510638	-0.026
Subcallosal area R	0.492	0.496	0.004	0.282	0.554275862068965	-0.062
Superior frontal gyrus L	0.501	0.502	0.000	0.737	0.831861386138614	-0.019
Superior frontal gyrus R	0.523	0.524	0.001	0.634396	0.794737846153846	0.027
Superior frontal gyrus medial segment L	0.381	0.385	0.005	0.268	0.545571428571429	-0.071
Superior frontal gyrus medial segment R	0.395	0.395	0.000	0.897	0.973885714285714	-0.008
Superior occipital gyrus L	0.327	0.328	0.000	0.826	0.905423076923077	-0.015
Superior occipital gyrus R	0.305	0.305	0.000	0.924	0.966385321100917	0.006
Superior parietal lobule L	0.402	0.403	0.001	0.633847	0.802872866666667	-0.030
Superior parietal lobule R	0.417	0.435	0.018	0.024470	0.253598181818182	-0.139
Superior temporal gyrus L	0.480	0.481	0.001	0.551	0.747785714285714	0.035
Superior temporal gyrus R	0.466	0.469	0.004	0.290	0.551	-0.063
Supplementary motor cortex L	0.410	0.424	0.014	0.044533	0.241750571428571	-0.125
Supplementary motor cortex R	0.428	0.432	0.004	0.298	0.547935483870968	-0.064
Supramarginal gyrus L	0.363	0.365	0.002	0.499	0.702296296296296	-0.044
Supramarginal gyrus R	0.429	0.430	0.001	0.643	0.788193548387097	-0.029
Temporal pole L	0.405	0.407	0.002	0.505	0.702073170731707	-0.042
Temporal pole R	0.409	0.413	0.004	0.301	0.544666666666667	-0.065
Thalamus proper L	0.293	0.10	0.016	0.051	0.252782608695652	-0.133
Thalamus proper R	0.312	0.331	0.019	0.034	0.228	-0.142
Transverse temporal gyrus L	0.310	0.315	0.004	0.310	0.5521875	0.069
Transverse temporal gyrus R	0.402	0.403	0.000	0.799	0.884330097087379	0.016
Triangular part of the inferior frontal gyrus L	0.373	0.381	0.008	0.145	0.435	-0.094
Triangular part of the inferior frontal gyrus R	0.298	0.309	0.011	0.109	0.376545454545455	-0.109

FDR: false discovery rate. L: left. PRS: polygenic risk score. R: right.

Table D.53: Associations between APOEonlyPRS Threshold 10 and 114 regions of interest in MCI patients

Region of Interest	R Square (Model 1)	R Square (Model 2)	R Square Change	Sig. F Change (Model 2)	FDR Corrected value	Standardised beta of PRS
Accumbens area L	0.379	0.380	0.001	0.428	1	0.034
Accumbens area R	0.353	0.354	0.001	0.513747	1	0.029
Amygdala L	0.341	0.341	0.000	0.736	1	0.015
Amygdala R	0.408	0.408	0.001	0.512	1	-0.028
Angular gyrus L	0.375	0.376	0.001	0.534	1	-0.027
Angular gyrus R	0.405	0.405	0.000	0.697	1	-0.017
Anterior cingulate gyrus L	0.403	0.403	0.000	0.949	1	-0.003
Anterior cingulate gyrus R	0.229	0.229	0.000	0.720	1	0.017
Anterior insula L	0.315	0.318	0.003	0.205358	1	0.058
Anterior insula R	0.328	0.330	0.002	0.274	1	0.049
Anterior orbital gyrus L	0.436	0.436	0.000	0.881	1	-0.006
Anterior orbital gyrus R	0.373	0.375	0.002	0.221	1	-0.053
Basal forebrain L	0.255	0.255	0.000	0.956	1	0.003
Basal forebrain R	0.319	0.320	0.001	0.459	1	0.034
Calcarine cortex L	0.403	0.403	0.000	0.803	0.973851063829787	0.011
Calcarine cortex R	0.414	0.414	0.000	0.593	0.979739130434783	-0.022
Caudate L	0.195	0.195	0.001	0.608	0.976225352112676	0.025
Caudate R	0.201	0.202	0.001	0.581745	1	0.027
Central operculum L	0.391	0.402	0.010	0.010	0.38	0.110
Central operculum R	0.365	0.367	0.001	0.342	1	0.042
Cuneus L	0.411	0.412	0.001	0.364	1	-0.038
Cuneus R	0.429	0.431	0.003	0.184	1	-0.055
Entorhinal area L	0.335	0.336	0.001	0.406	1	0.037
Entorhinal area R	0.421	0.421	0.000	0.801	0.981870967741936	0.011
Frontal operculum L	0.362	0.366	0.004	0.123	1	0.067
Frontal operculum R	0.348	0.350	0.002	0.308	1	0.045

Frontal pole L	0.428	0.429	0.001	0.371	1	0.037
Frontal pole R	0.426	0.427	0.001	0.372	1	0.037
Fusiform gyrus L	0.442	0.442	0.000	0.757	1	-0.013
Fusiform gyrus R	0.500	0.501	0.000	0.660	1	-0.017
Gyrus rectus L	0.436	0.437	0.001	0.424	1	0.033
Gyrus rectus R	0.420	0.420	0.000	0.583	1	0.023
Hippocampus L	0.395	0.395	0.000	0.762	1	0.013
Hippocampus R	0.422	0.424	0.002	0.253	1	-0.048
Inferior occipital gyrus L	0.379	0.381	0.003	0.204732	1	-0.055
Inferior occipital gyrus R	0.446	0.448	0.002	0.225418	1	-0.050
Inferior temporal gyrus L	0.459	0.459	0.000	0.777	1	0.011
Inferior temporal gyrus R	0.536	0.536	0.000	0.988	0.996743362831858	-0.001
Lateral orbital gyrus L	0.443	0.446	0.003	0.162	1	0.057
Lateral orbital gyrus R	0.344	0.344	0.000	0.819	0.9828	0.010
Lingual gyrus L	0.489	0.489	0.000	0.927	1	0.004
Lingual gyrus R	0.529	0.530	0.001	0.284	1	-0.040
Medial frontal cortex L	0.371	0.373	0.001	0.356	1	-0.040
Medial frontal cortex R	0.340	0.340	0.000	0.938	1	0.003
Medial orbital gyrus L	0.451	0.451	0.000	0.648	1	0.019
Medial orbital gyrus R	0.420	0.420	0.000	0.782477	0.991137533333333	0.012
Middle cingulate gyrus L	0.355	0.355	0.000	0.795	0.985108695652174	0.011
Middle cingulate gyrus R	0.320	0.320	0.000	0.947	1	-0.003
Middle frontal gyrus L	0.463	0.463	0.000	0.871	1	0.007
Middle frontal gyrus R	0.462	0.462	0.000	0.773	1	0.012
Middle occipital gyrus L	0.335	0.336	0.001	0.527	1	-0.028
Middle occipital gyrus R	0.322	0.328	0.005	0.079	1	-0.079
Middle temporal gyrus L	0.452	0.452	0.001	0.528	1	0.026
Middle temporal gyrus R	0.488	0.489	0.000	0.582491	1	-0.022
Occipital fusiform gyrus L	0.463	0.463	0.000	0.696	1	0.016
Occipital fusiform gyrus R	0.520	0.522	0.001	0.302	1	-0.039

Occipital pole L	0.295	0.295	0.001	0.565	1	-0.027
Occipital pole R	0.375	0.376	0.001	0.498	1	-0.029
Opercular part of the inferior frontal gyrus L	0.281	0.294	0.013	0.009	0.513	0.122
Opercular part of the inferior frontal gyrus R	0.254	0.258	0.004	0.148	1	0.069
Orbital part of the inferior frontal gyrus L	0.285	0.294	0.010	0.021	0.5985	0.107
Orbital part of the inferior frontal gyrus R	0.238	0.238	0.000	0.985	1	-0.001
Pallidum L	0.171	0.171	0.000	0.837	0.9939375	0.010
Pallidum R	0.138	0.138	0.000	0.937	1	0.004
Parahippocampal gyrus L	0.433	0.435	0.002	0.225464	1	0.050
Parahippocampal gyrus R	0.492	0.492	0.000	0.783	0.980901098901099	0.011
Parietal operculum L	0.334	0.335	0.001	0.545	1	0.027
Parietal operculum R	0.279	0.280	0.001	0.478	1	0.033
Planum polare L	0.388	0.389	0.000	0.606	0.986914285714286	0.022
Planum polare R	0.429	0.429	0.000	0.670945	1	0.018
Planum temporale L	0.328	0.334	0.006	0.063	1	0.083
Planum temporale R	0.352	0.354	0.002	0.275	1	0.048
Postcentral gyrus L	0.369	0.369	0.000	0.990	0.99	-0.001
Postcentral gyrus R	0.393	0.394	0.001	0.564	1	-0.025
Postcentral gyrus medial segment L	0.229	0.236	0.007	0.061	1	-0.090
Postcentral gyrus medial segment R	0.222	0.222	0.000	0.925	1	-0.005
Posterior cingulate gyrus L	0.560	0.563	0.003	0.092941	0.963206727272727	0.061
Posterior cingulate gyrus R	0.523	0.523	0.000	0.973	0.999297297297297	0.001
Posterior insula L	0.352	0.353	0.001	0.369	1	0.040
Posterior insula R	0.381	0.381	0.000	0.663	1	0.019
Posterior orbital gyrus L	0.351	0.357	0.006	0.058	1	0.084
Posterior orbital gyrus R	0.377	0.378	0.000	0.646	1	0.020
Precentral gyrus L	0.485	0.486	0.001	0.470	1	0.028
Precentral gyrus R	0.473	0.473	0.001	0.519	1	0.026
Precentral gyrus medial segment L	0.283	0.285	0.002	0.328	1	-0.045
Precentral gyrus medial segment R	0.314	0.316	0.002	0.286	1	-0.049

Precuneus L	0.463	0.463	0.000	0.961	0.995945454545454	-0.002
Precuneus R	0.489	0.489	0.000	0.909	1	-0.004
Putamen L	0.229	0.230	0.001	0.542	1	0.029
Putamen R	0.241	0.241	0.000	0.781	1	0.013
Subcallosal area L	0.434	0.438	0.004	0.092726	1	0.069
Subcallosal area R	0.380	0.393	0.013	0.004	0.456	0.123
Superior frontal gyrus L	0.428	0.428	0.000	0.958	1	-0.002
Superior frontal gyrus R	0.465	0.467	0.001	0.305	1	0.041
Superior frontal gyrus medial segment L	0.414	0.416	0.002	0.237	1	0.050
Superior frontal gyrus medial segment R	0.384	0.386	0.003	0.200	1	0.055
Superior occipital gyrus L	0.338	0.339	0.000	0.671029	0.993471506493506	-0.019
Superior occipital gyrus R	0.343	0.343	0.000	0.847	0.985285714285714	0.009
Superior parietal lobule L	0.368	0.368	0.000	0.722	1	-0.016
Superior parietal lobule R	0.359	0.359	0.000	0.761	1	-0.013
Superior temporal gyrus L	0.365	0.366	0.001	0.484	1	0.031
Superior temporal gyrus R	0.360	0.360	0.000	0.592	0.992470588235294	0.024
Supplementary motor cortex L	0.356	0.357	0.000	0.588	1	-0.024
Supplementary motor cortex R	0.347	0.347	0.000	0.782022	1	-0.012
Supramarginal gyrus L	0.312	0.312	0.000	0.841	0.98839175257732	-0.009
Supramarginal gyrus R	0.306	0.308	0.002	0.317	1	0.046
Temporal pole L	0.312	0.312	0.001	0.474	1	0.033
Temporal pole R	0.347	0.348	0.001	0.455	1	-0.033
Thalamus proper L	0.213	0.216	0.003	0.199	1	0.063
Thalamus proper R	0.255	0.256	0.001	0.489	1	0.033
Transverse temporal gyrus L	0.255	0.255	0.001	0.581802	1	0.026
Transverse temporal gyrus R	0.307	0.308	0.001	0.437	1	0.036
Triangular part of the inferior frontal gyrus L	0.340	0.345	0.005	0.078	1	0.078
Triangular part of the inferior frontal gyrus R	0.285	0.286	0.001	0.513803	1	0.030

FDR: false discovery rate. L: left. PRS: polygenic risk score. R: right.

Table D.54: Associations between APOEonlyPRS Threshold 10 and 114 regions of interest in AD dementia patients

Region of Interest	R Square (Model 1)	R Square (Model 2)	R Square Change	Sig. F Change (Model 2)	FDR Corrected value	Standardised beta of PRS
Accumbens area L	0.512	0.512	0.000	0.738	1	-0.025
Accumbens area R	0.497	0.501	0.004	0.371	0.899872340425532	0.069
Amygdala L	0.425	0.460	0.035	0.008	0.456	-0.216
Amygdala R	0.445	0.471	0.026	0.020	0.456	-0.185
Angular gyrus L	0.446	0.446	0.001	0.707	1	-0.030
Angular gyrus R	0.58	0.558	0.000	0.839	1	0.015
Anterior cingulate gyrus L	0.412	0.438	0.026	0.024	0.456	0.186
Anterior cingulate gyrus R	0.272	0.272	0.000	0.957	0.982864864864865	0.005
Anterior insula L	0.505	0.514	0.008	0.164	0.812869565217391	0.106
Anterior insula R	0.557	0.564	0.007	0.167	0.76152	0.100
Anterior orbital gyrus L	0.499	0.501	0.002	0.504	0.990620689655172	-0.051
Anterior orbital gyrus R	0.495	0.497	0.002	0.466	0.983777777777778	0.056
Basal forebrain L	0.275	0.278	0.002	0.544	1	0.056
Basal forebrain R	0.376	0.386	0.009	0.193	0.785785714285714	0.111
Calcarine cortex L	0.390	0.390	0.000	0.927	0.987644859813084	-0.008
Calcarine cortex R	0.439	0.439	0.000	0.933	0.984833333333333	0.007
Caudate L	0.362	0.365	0.003	0.478	0.973071428571428	-0.062
Caudate R	0.328	0.329	0.001	0.669	1	-0.038
Central operculum L	0.373	0.373	0.000	0.841	1	-0.017
Central operculum R	0.506	0.507	0.002	0.545	0.986190476190476	0.046
Cuneus L	0.491	0.496	0.005	0.274	0.867666666666667	-0.085
Cuneus R	0.473	0.473	0.000	0.818	1	-0.018
Entorhinal area L	0.413	0.460	0.047	0.002	0.228	-0.251
Entorhinal area R	0.407	0.422	0.015	0.086	0.754153846153846	-0.143
Frontal operculum L	0.341	0.361	0.021	0.056	0.6384	0.167
Frontal operculum R	0.405	0.435	0.030	0.016	0.608	0.200

Frontal pole L	0.523	0.525	0.001	0.556	0.990375	-0.044
Frontal pole R	0.496	0.498	0.001	0.566	0.992676923076923	0.044
Fusiform gyrus L	0.496	0.496	0.000	0.796	1	-0.020
Fusiform gyrus R	0.530	0.530	0.000	0.813	1	-0.018
Gyrus rectus L	0.526	0.526	0.000	0.953	0.987654545454545	-0.004
Gyrus rectus R	0.541	0.550	0.009	0.136	0.738285714285714	0.109
Hippocampus L	0.471	0.496	0.025	0.018	0.513	-0.185
Hippocampus R	0.503	0.516	0.013	0.087	0.708428571428571	-0.130
Inferior occipital gyrus L	0.507	0.508	0.001	0.646	1	-0.035
Inferior occipital gyrus R	0.479	0.480	0.001	0.650	1	-0.036
Inferior temporal gyrus L	0.497	0.501	0.005	0.293	0.83505	-0.081
Inferior temporal gyrus R	0.518	0.518	0.000	0.803	1	-0.019
Lateral orbital gyrus L	0.441	0.442	0.001	0.716	1	-0.030
Lateral orbital gyrus R	0.456	0.460	0.005	0.330	0.874883720930233	0.078
Lingual gyrus L	0.566	0.566	0.000	0.785	1	-0.020
Lingual gyrus R	0.558	0.558	0.001	0.691	1	0.029
Medial frontal cortex L	0.353	0.353	0.000	0.880	1	0.013
Medial frontal cortex R	0.414	0.429	0.015	0.091	0.648375	0.140
Medial orbital gyrus L	0.594	0.594	0.000	0.923	0.992660377358491	0.007
Medial orbital gyrus R	0.512	0.517	0.006	0.248	0.8835	0.088
Middle cingulate gyrus L	0.433	0.435	0.002	0.525	0.981147540983607	0.052
Middle cingulate gyrus R	0.414	0.419	0.004	0.354261	0.8974612	0.077
Middle frontal gyrus L	0.540	0.545	0.005	0.261810	0.877833529411765	0.083
Middle frontal gyrus R	0.579	0.586	0.007	0.181	0.764222222222222	0.094
Middle occipital gyrus L	0.440	0.444	0.003	0.410	0.9348	-0.067
Middle occipital gyrus R	0.433	0.438	0.006	0.287	0.838923076923077	-0.087
Middle temporal gyrus L	0.484	0.489	0.005	0.280	1	-0.084
Middle temporal gyrus R	0.539	0.539	0.000	0.914	0.84	-0.008
Occipital fusiform gyrus L	0.521	0.523	0.002	0.443	0.990235294117647	0.058
Occipital fusiform gyrus R	0.513	0.513	0.000	0.866	1	-0.013

Occipital pole L	0.429	0.432	0.003	0.467	0.967963636363636	-0.060
Occipital pole R	0.464	0.464	0.000	0.812	1	-0.019
Opercular part of the inferior frontal gyrus L	0.367	0.375	0.008	0.222	0.8436	0.105
Opercular part of the inferior frontal gyrus R	0.403	0.419	0.016	0.080	0.76	0.146
Orbital part of the inferior frontal gyrus L	0326	0.333	0.007	0.279	0.859621621621622	0.096
Orbital part of the inferior frontal gyrus R	0.306	0.306	0.000	0.848	1	0.017
Pallidum L	0.214	0.222	0.009	0.261936	0.853162971428571	-0.108
Pallidum R	0.240	0.250	0.010	0.217	0.853034482758621	-0.116
Parahippocampal gyrus L	0.522	0.540	0.018	0.038	0.5415	-0.155
Parahippocampal gyrus R	0.539	0.549	0.010	0.118	0.708	-0.115
Parietal operculum L	0.376	0.386	0.011	0.159	0.823909090909091	0.120
Parietal operculum R	0.358	0.361	0.003	0.455	0.9975	0.065
Planum polare L	0.459	0.459	0.001	0.697	1	0.031
Planum polare R	0.483	0.484	0.001	0.582	0.990268656716418	0.043
Planum temporale L	0.495	0.498	0.003	0.400	0.930612244897959	0.065
Planum temporale R	0.408	0.408	0.000	0.877	1	-0.013
Postcentral gyrus L	0.553	0.555	0.001	0.571	0.986272727272727	0.041
Postcentral gyrus R	0.501	0.501	0.000	0.976	0.984637168141593	0.002
Postcentral gyrus medial segment L	0.371	0.371	0.000	0.794	1	-0.022
Postcentral gyrus medial segment R	0.330	0.330	0.000	0.934	0.976844036697248	-0.007
Posterior cingulate gyrus L	0.605	0.610	0.004	0.259	0.894727272727273	-0.077
Posterior cingulate gyrus R	0.597	0.600	0.003	0.321	0.871285714285714	-0.068
Posterior insula L	0.487	0.500	0.013	0.090	0.684	0.131
Posterior insula R	0.516	0.530	0.014	0.072	0.746181818181818	0.135
Posterior orbital gyrus L	0.434	0.434	0.000	0.973	0.990375	-0.003
Posterior orbital gyrus R	0.418	0.423	0.004	0.370	0.91695652173913	0.074
Precentral gyrus L	0.507	0.518	0.011	0.108	0.724235294117647	0.122
Precentral gyrus R	0.463	0.469	0.006	0.242	0.889935483870968	0.093
Precentral gyrus medial segment L	0.422	0.423	0.000	0.754	1	-0.026
Precentral gyrus medial segment R	0.406	0.406	0.000	0.857	1	0.015

Precuneus L	0.575	0.575	0.001	0.694	1	-0.028
Precuneus R	0.610	0.611	0.001	0.678	1	-0.028
Putamen L	0.429	0.429	0.000	0.843	1	0.016
Putamen R	0.444	0.444	0.001	0.745	1	0.026
Subcallosal area L	0.570	0.579	0.009	0.115	0.728333333333333	0.112
Subcallosal area R	0.597	0.612	0.015	0.040	0.506666666666667	0.141
Superior frontal gyrus L	0.565	0.565	0.000	0.830	1	0.015
Superior frontal gyrus R	0.570	0.572	0.002	0.463	0.99588679245283	0.052
Superior frontal gyrus medial segment L	0.527	0.527	0.000	0.899	0.995009708737864	0.009
Superior frontal gyrus medial segment R	0.504	0.512	0.008	0.173	0.758538461538462	0.104
Superior occipital gyrus L	0.349	0.350	0.000	0.832	1	0.019
Superior occipital gyrus R	0.479	0.479	0.000	0.898	1	-0.010
Superior parietal lobule L	0.517	0.517	0.000	0.883	0.996653465346535	0.011
Superior parietal lobule R	0.486	0.486	0.000	0.989	0.989	0.001
Superior temporal gyrus L	0.489	0.489	0.000	0.769	1	0.023
Superior temporal gyrus R	0.413	0.415	0.002	0.495	0.99	-0.057
Supplementary motor cortex L	0.427	0.429	0.002	0.510	0.969	0.054
Supplementary motor cortex R	0.434	0.446	0.012	0.125	0.7125	0.125
Supramarginal gyrus L	0.459	0.462	0.002	0.505	0.975762711864407	0.053
Supramarginal gyrus R	0.451	0.456	0.005	0.306	0.850829268292683	0.082
Temporal pole L	0.483	0.483	0.000	0.743	1	-0.026
Temporal pole R	0.433	0.433	0.000	0.922	1	0.008
Thalamus proper L	0.199	0.212	0.013	0.166	0.7885	-0.134
Thalamus proper R	0.264	0.270	0.006	0.353551	0.9160185	-0.086
Transverse temporal gyrus L	0.332	0.337	0.004	0.397	0.942875	0.075
Transverse temporal gyrus R	0.295	0.296	0.001	0.722	1	-0.033
Triangular part of the inferior frontal gyrus L	0.336	0.364	0.028	0.028	0.456	0.192
Triangular part of the inferior frontal gyrus R	0.442	0.443	0.001	0.681	1	0.033

FDR: false discovery rate. L: left. PRS: polygenic risk score. R: right.

Table D.55: Associations between PRSwithAPOE Threshold 1 and 114 regions of interest in amyloid negative participants

Region of Interest	R Square (Model 1)	R Square (Model 2)	R Square Change	Sig. F Change (Model 2)	FDR Corrected value	Standardised beta of PRS
Accumbens area L	0.390	0.391	0.000	0.693	1	0.02
Accumbens area R	0.433	0.433	0.000	0.790	1	0.013
Amygdala L	0.444	0.445	0.001	0.517	0.950612903225806	-0.031
Amygdala R	0.461	0.463	0.002	0.358	1	-0.044
Angular gyrus L	0.428	0.428	0.000	0.931	1	0.004
Angular gyrus R	0.370	0.371	0.000	0.765	1	-0.015
Anterior cingulate gyrus L	0.444	0.446	0.002	0.350	1	0.045
Anterior cingulate gyrus R	0.269	0.271	0.002	0.360	1	0.051
Anterior insula L	0.347	0.348	0.002	0.441	1	0.041
Anterior insula R	0.345	0.347	0.002	0.424	1	0.042
Anterior orbital gyrus L	0.384	0.385	0.001	0.489	1	-0.035
Anterior orbital gyrus R	0.323	0.325	0.001	0.507	0.979627118644068	0.036
Basal forebrain L	0.348	0.351	0.002	0.338	1	0.050
Basal forebrain R	0.382	0.382	0.000	0.982	0.982	0.001
Calcarine cortex L	0.388	0.390	0.002	0.428	1	-0.040
Calcarine cortex R	0.368	0.371	0.003	0.302	1	-0.053
Caudate L	0.189	0.189	0.000	0.891	1	-0.008
Caudate R	0.183	0.183	0.000	0.723183	1	-0.021
Central operculum L	0.351	0.355	0.004	0.211	1	0.065
Central operculum R	0.322	0.324	0.001	0.527	0.93871875	0.034
Cuneus L	0.337	0.338	0.001	0.623	0.972904109589041	0.026
Cuneus R	0.377	0.381	0.004	0.193	1	-0.067
Entorhinal area L	0.374	0.375	0.001	0.461	0.991584905660377	0.038
Entorhinal area R	0.422	0.422	0.000	0.758	1	0.015
Frontal operculum L	0.298	0.310	0.012	0.043	1	0.110
Frontal operculum R	0.309	0.310	0.001	0.500	0.982758620689655	0.037

Frontal pole L	0.369	0.369	0.000	0.950	0.984545454545455	0.003
Frontal pole R	0.398	0.403	0.004	0.183	1	0.067
Fusiform gyrus L	0.471	0.475	0.003	0.220	1	-0.058
Fusiform gyrus R	0.495	0.496	0.001	0.436	1	-0.036
Gyrus rectus L	0.392	0.397	0.005	0.176	1	0.069
Gyrus rectus R	0.412	0.415	0.003	0.292338	1	0.053
Hippocampus L	0.430	0.432	0.002	0.413	1	-0.040
Hippocampus R	0.490	0.495	0.004	0.150	1	-0.067
Inferior occipital gyrus L	0.379	0.379	0.000	0.703	1	-0.020
Inferior occipital gyrus R	0.432	0.433	0.000	0.722685	1	-0.017
Inferior temporal gyrus L	0.495	0.495	0.001	0.535	0.938307692307692	-0.029
Inferior temporal gyrus R	0.533	0.535	0.002	0.319	1	-0.044
Lateral orbital gyrus L	0.391	0.397	0.006	0.120	1	0.079
Lateral orbital gyrus R	0.308	0.311	0.003	0.291501	1	0.057
Lingual gyrus L	0.500	0.500	0.000	0.737	1	-0.016
Lingual gyrus R	0.537	0.539	0.002	0.284	1	-0.047
Medial frontal cortex L	0.376	0.376	0.000	0.804	0.996260869565217	0.013
Medial frontal cortex R	0.354	0.355	0.001	0.540	0.932727272727273	0.032
Medial orbital gyrus L	0.469	0.469	0.000	0.669	1	0.020
Medial orbital gyrus R	0.385	0.388	0.004	0.226	1	0.062
Middle cingulate gyrus L	0.400	0.403	0.004	0.219	1	0.062
Middle cingulate gyrus R	0.382	0.384	0.003	0.312	1	0.052
Middle frontal gyrus L	0.441	0.441	0.000	0.772	1	0.014
Middle frontal gyrus R	0.403	0.403	0.000	0.924	1	0.005
Middle occipital gyrus L	0.385	0.386	0.000	0.836	1	0.011
Middle occipital gyrus R	0.347	0.347	0.000	0.854	1	0.010
Middle temporal gyrus L	0.521	0.523	0.001	0.386	1	0.039
Middle temporal gyrus R	0.503	0.504	0.001	0.409	1	0.038
Occipital fusiform gyrus L	0.464	0.468	0.004	0.157	1	-0.076
Occipital fusiform gyrus R	0.501	0.501	0.000	0.802	1	-0.012

Occipital pole L	0.323	0.333	0.009	0.068	1	-0.098
Occipital pole R	0.336	0.336	0.000	0.900	1	0.007
Opercular part of the inferior frontal gyrus L	0.188	0.200	0.012	0.059	1	0.111
Opercular part of the inferior frontal gyrus R	0.277	0.284	0.007	0.116	1	0.087
Orbital part of the inferior frontal gyrus L	0.289	0.293	0.003	0.289	1	0.058
Orbital part of the inferior frontal gyrus R	0.188	0.195	0.007	0.145	1	0.085
Pallidum L	0.187	0.188	0.001	0.602	0.994608695652174	-0.031
Pallidum R	0.157	0.158	0.001	0.586	0.982411764705882	-0.033
Parahippocampal gyrus L	0.483	0.483	0.000	0.829	1	0.010
Parahippocampal gyrus R	0.491	0.492	0.000	0.692	1	-0.018
Parietal operculum L	0.355	0.356	0.001	0.615	0.987464788732394	0.026
Parietal operculum R	0.268	0.267	0.000	0.881	1	0.008
Planum polare L	0.385	0.385	0.000	0.838	0.995125	-0.010
Planum polare R	0.424	0.426	0.001	0.447	0.999176470588235	-0.038
Planum temporale L	0.346	0.348	0.001	0.490	0.9975	0.036
Planum temporale R	0.375	0.376	0.001	0.479	1	0.036
Postcentral gyrus L	0.390	0.391	0.000	0.751	1	0.016
Postcentral gyrus R	0.349	0.349	0.000	0.954	0.971035714285714	0.003
Postcentral gyrus medial segment L	0.213	0.213	0.000	0.939	0.991166666666667	-0.004
Postcentral gyrus medial segment R	0.196	0.196	0.001	0.616	0.975333333333333	-0.029
Posterior cingulate gyrus L	0.517	0.519	0.001	0.387	1	0.039
Posterior cingulate gyrus R	0.477	0.478	0.001	0.442	1	0.036
Posterior insula L	0.388	0.389	0.001	0.494	0.988	-0.035
Posterior insula R	0.408	0.408	0.000	0.935	0.996168224299065	0.004
Posterior orbital gyrus L	0.423	0.425	0.002	0.335	1	0.048
Posterior orbital gyrus R	0.377	0.377	0.000	0.879	1	-0.008
Precentral gyrus L	0.476	0.480	0.003	0.200	1	0.060
Precentral gyrus R	0.445	0.447	0.002	0.328	1	0.047
Precentral gyrus medial segment L	0.306	0.306	0.000	0.969	0.977575221238938	0.002
Precentral gyrus medial segment R	0.361	0.363	0.002	0.355	1	-0.048

Precuneus L	0.453	0.454	0.002	0.373	1	-0.043
Precuneus R	0.496	0.496	0.000	0.800	1	-0.012
Putamen L	0.293	0.297	0.004	0.249	1	-0.063
Putamen R	0.298	0.299	0.002	0.417	1	-0.044
Subcallosal area L	0.470	0.476	0.007	0.079	1	0.083
Subcallosal area R	0.411	0.418	0.008	0.073	1	0.089
Superior frontal gyrus L	0.441	0.442	0.001	0.613	0.998314285714286	0.025
Superior frontal gyrus R	0.462	0.463	0.000	0.685	1	0.019
Superior frontal gyrus medial segment L	0.420	0.420	0.000	0.860	1	0.009
Superior frontal gyrus medial segment R	0.392	0.392	0.000	0.908	1	0.006
Superior occipital gyrus L	0.253	0.253	0.000	0.952	0.97772972972973	0.003
Superior occipital gyrus R	0.256	0.257	0.001	0.668	1	0.024
Superior parietal lobule L	0.379	0.380	0.001	0.449	0.984346153846154	0.039
Superior parietal lobule R	0.395	0.397	0.002	0.331	1	-0.049
Superior temporal gyrus L	0.358	0.362	0.004	0.204	1	0.066
Superior temporal gyrus R	0.383	0.383	0.000	0.801	1	0.013
Supplementary motor cortex L	0.393	0.393	0.000	0.926	1	-0.005
Supplementary motor cortex R	0.372	0.373	0.001	0.521	0.942761904761905	-0.033
Supramarginal gyrus L	0.302	0.305	0.003	0.295	1	0.057
Supramarginal gyrus R	0.362	0.363	0.000	0.666	1	0.022
Temporal pole L	0.356	0.356	0.000	0.946	0.989394495412844	-0.004
Temporal pole R	0.375	0.376	0.002	0.414	1	-0.042
Thalamus proper L	0.272	0.274	0.001	0.515	0.962459016393443	0.036
Thalamus proper R	0.304	0.304	0.000	0.820	1	-0.012
Transverse temporal gyrus L	0.216	0.222	0.006	0.169	1	0.079
Transverse temporal gyrus R	0.308	0.309	0.001	0.556	0.946029850746269	0.032
Triangular part of the inferior frontal gyrus L	0.263	0.264	0.001	0.513	0.9747	0.037
Triangular part of the inferior frontal gyrus R	0.256	0.260	0.004	0.269	1	0.062

FDR: false discovery rate. L: left. PRS: polygenic risk score. R: right.

Table D.56: Associations between PRSwithAPOE Threshold 1 and 114 regions of interest in amyloid positive participants

Region of Interest	R Square (Model 1)	R Square (Model 2)	R Square Change	Sig. F Change (Model 2)	FDR Corrected value	Standardised beta of PRS
Accumbens area L	0.398	0.400	0.002	0.272	0.544	-0.043
Accumbens area R	0.374	0.374	0.000	0.772	0.888969696969697	-0.012
Amygdala L	0.383	0.400	0.017	0.000472838207668	0.0107807111348304	-0.137
Amygdala R	0.444	0.465	0.021	0.000037671893269	0.002147297916333	-0.153
Angular gyrus L	0.391	0.394	0.004	0.094	0.345677419354839	-0.065
Angular gyrus R	0.430	0.433	0.003	0.130	0.39	-0.057
Anterior cingulate gyrus L	0.388	0.388	0.000	0.780	0.8892	-0.011
Anterior cingulate gyrus R	0.224	0.230	0.006	0.073	0.33288	-0.079
Anterior insula L	0.401	0.401	0.000	0.820	0.907572815533981	0.009
Anterior insula R	0.415	0.415	0.000	0.923	0.947945945945946	-0.004
Anterior orbital gyrus L	0.413	0.416	0.003	0.166	0.420533333333333	-0.053
Anterior orbital gyrus R	0.390	0.396	0.007	0.028	0.245538461538462	-0.086
Basal forebrain L	0.261	0.264	0.003	0.164	0.424909090909091	-0.060
Basal forebrain R	0.347	0.349	0.001	0.389	0.59927027027027	-0.035
Calcarine cortex L	0.361	0.361	0.001	0.507	0.688071428571429	-0.027
Calcarine cortex R	0.385	0.389	0.004	0.083	0.350444444444444	-0.068
Caudate L	0.223	0.224	0.001	0.358	0.583028571428571	-0.041
Caudate R	0.212	0.214	0.002	0.347	0.599363636363636	-0.042
Central operculum L	0.384	0.386	0.002	0.290	0.551	0.042
Central operculum R	0.399	0.399	0.000	0.744	0.87439175257732	-0.013
Cuneus L	0.441	0.446	0.005	0.040	0.285	-0.077
Cuneus R	0.446	0.451	0.005	0.042	0.281647058823529	-0.076
Entorhinal area L	0.397	0.409	0.012	0.002617	0.049723	-0.117
Entorhinal area R	0.452	0.463	0.011	0.002789	0.0454208571428571	-0.110
Frontal operculum L	0.392	0.392	0.000	0.792	0.893940594059406	0.010
Frontal operculum R	0.320	0.320	0.000	0.877	0.917229357798165	-0.006

Frontal pole L	0.469	0.470	0.001	0.421	0.615307692307692	0.029
Frontal pole R	0.431	0.432	0.001	0.353	0.591794117647059	0.035
Fusiform gyrus L	0.510	0.513	0.003	0.104	0.3705	-0.057
Fusiform gyrus R	0.538	0.542	0.004	0.044741	0.283359666666667	-0.068
Gyrus rectus L	0.451	0.452	0.001	0.457	0.651225	-0.028
Gyrus rectus R	0.464	0.465	0.000	0.554	0.70961797752809	0.022
Hippocampus L	0.422	0.443	0.021	0.000042616776615	0.00161943751137	-0.155
Hippocampus R	0.442	0.469	0.027	0.000002591982173	0.000295485967722	-0.174
Inferior occipital gyrus L	0.424	0.428	0.004	0.092900	0.365193103448276	-0.064
Inferior occipital gyrus R	0.479	0.485	0.006	0.022	0.2508	-0.083
Inferior temporal gyrus L	0.493	0.499	0.005	0.029615	0.241150714285714	-0.077
Inferior temporal gyrus R	0.540	0.544	0.004	0.046	0.2622	-0.068
Lateral orbital gyrus L	0.433	0.434	0.001	0.367	0.581083333333333	-0.034
Lateral orbital gyrus R	0.408	0.409	0.001	0.452	0.652253164556962	-0.029
Lingual gyrus L	0.506	0.506	0.000	0.739	0.8775625	-0.012
Lingual gyrus R	0.517	0.518	0.001	0.301	0.553451612903226	-0.036
Medial frontal cortex L	0.348	0.352	0.003	0.122	0.375891891891892	-0.062
Medial frontal cortex R	0.371	0.371	0.000	0.857992	0.922746113207547	-0.007
Medial orbital gyrus L	0.483	0.484	0.001	0.277571	0.545570586206897	-0.039
Medial orbital gyrus R	0.468	0.468	0.000	0.718	0.8616	-0.013
Middle cingulate gyrus L	0.397	0.398	0.001	0.293	0.547573770491803	-0.041
Middle cingulate gyrus R	0.332	0.337	0.005	0.080	0.350769230769231	-0.072
Middle frontal gyrus L	0.498	0.498	0.000	0.627	0.7942	-0.017
Middle frontal gyrus R	0.504	0.505	0.001	0.355	0.586521739130435	-0.033
Middle occipital gyrus L	0.360	0.365	0.005	0.056487	0.26831325	-0.076
Middle occipital gyrus R	0.354	0.372	0.018	0.000370955730528	0.010572238320048	-0.142
Middle temporal gyrus L	0.480	0.484	0.004	0.053	0.228	-0.070
Middle temporal gyrus R	0.520	0.526	0.006	0.018	0.274636363636364	-0.082
Occipital fusiform gyrus L	0.470	0.471	0.000	0.632	0.791736263736264	0.017
Occipital fusiform gyrus R	0.517	0.520	0.003	0.093197	0.3541486	-0.058

Occipital pole L	0.328	0.328	0.000	0.994	0.994	0.000
Occipital pole R	0.396	0.397	0.001	0.361	0.579633802816901	-0.036
Opercular part of the inferior frontal gyrus L	0.302	0.303	0.001	0.413166	0.619749	0.034
Opercular part of the inferior frontal gyrus R	0.270	0.270	0.000	0.757	0.880591836734694	0.013
Orbital part of the inferior frontal gyrus L	0.275	0.275	0.000	0.697	0.845297872340426	-0.017
Orbital part of the inferior frontal gyrus R	0.310	0.316	0.006	0.056280	0.278953043478261	-0.079
Pallidum L	0.120	0.123	0.003	0.221	0.475358490566038	-0.058
Pallidum R	0.103	0.108	0.004	0.144	0.390857142857143	-0.069
Parahippocampal gyrus L	0.477	0.483	0.006	0.024	0.228	-0.082
Parahippocampal gyrus R	0.514	0.521	0.007	0.012	0.171	-0.087
Parietal operculum L	0.314	0.315	0.000	0.679	0.841369565217391	0.017
Parietal operculum R	0.294	0.294	0.000	0.843	0.924057692307692	0.008
Planum polare L	0.457	0.458	0.001	0.395	0.6004	-0.031
Planum polare R	0.466	0.467	0.001	0.278163	0.537467491525424	-0.040
Planum temporale L	0.354	0.354	0.000	0.892	0.924436363636364	-0.005
Planum temporale R	0.329	0.329	0.000	0.845	0.917428571428571	-0.008
Postcentral gyrus L	0.394	0.395	0.001	0.489	0.679829268292683	-0.027
Postcentral gyrus R	0.411	0.415	0.003	0.113	0.368057142857143	-0.061
Postcentral gyrus medial segment L	0.186	0.193	0.007	0.044812	0.268872	-0.091
Postcentral gyrus medial segment R	0.245	0.248	0.004	0.140	0.399	-0.064
Posterior cingulate gyrus L	0.546	0.550	0.004	0.051	0.276857142857143	-0.066
Posterior cingulate gyrus R	0.511	0.517	0.006	0.023	0.238363636363636	-0.079
Posterior insula L	0.395	0.397	0.002	0.259	0.52725	0.044
Posterior insula R	0.423	0.423	0.000	0.803	0.897470588235294	0.009
Posterior orbital gyrus L	0.348	0.349	0.001	0.479	0.674148148148148	-0.029
Posterior orbital gyrus R	0.394	0.397	0.002	0.190	0.45125	-0.051
Precentral gyrus L	0.457	0.457	0.000	0.858234	0.91438014953271	-0.007
Precentral gyrus R	0.448	0.449	0.001	0.499	0.685373493975904	-0.025
Precentral gyrus medial segment L	0.286	0.290	0.004	0.133	0.388769230769231	-0.063
Precentral gyrus medial segment R	0.315	0.318	0.002	0.206433	0.461438470588235	-0.052

Precuneus L	0.499	0.501	0.002	0.206391	0.47057148	-0.045
Precuneus R	0.482	0.485	0.003	0.091	0.3705	-0.061
Putamen L	0.280	0.281	0.001	0.537	0.703655172413793	-0.026
Putamen R	0.285	0.287	0.002	0.257	0.532690909090909	-0.048
Subcallosal area L	0.478	0.478	0.000	0.984	0.99270796460177	-0.001
Subcallosal area R	0.473	0.474	0.001	0.320	0.561230769230769	0.036
Superior frontal gyrus L	0.468	0.471	0.003	0.112	0.375529411764706	-0.058
Superior frontal gyrus R	0.499	0.499	0.000	0.695	0.851935483870968	0.014
Superior frontal gyrus medial segment L	0.421	0.423	0.002	0.169	0.418826086956522	-0.052
Superior frontal gyrus medial segment R	0.397	0.398	0.001	0.304	0.550095238095238	0.040
Superior occipital gyrus L	0.353	0.355	0.002	0.216	0.473538461538462	-0.050
Superior occipital gyrus R	0.366	0.369	0.003	0.170	0.412340425531915	-0.055
Superior parietal lobule L	0.392	0.394	0.003	0.143	0.397609756097561	-0.057
Superior parietal lobule R	0.377	0.379	0.002	0.205	0.476938775510204	-0.050
Superior temporal gyrus L	0.442	0.443	0.001	0.375	0.585616438356164	-0.033
Superior temporal gyrus R	0.387	0.388	0.001	0.315	0.56109375	-0.039
Supplementary motor cortex L	0.341	0.344	0.003	0.160	0.424186046511628	-0.057
Supplementary motor cortex R	0.378	0.378	0.000	0.945	0.961875	0.003
Supramarginal gyrus L	0.377	0.377	0.001	0.508	0.681317647058823	-0.026
Supramarginal gyrus R	0.340	0.340	0.001	0.511	0.677372093023256	0.027
Temporal pole L	0.409	0.412	0.003	0.119	0.376833333333333	-0.060
Temporal pole R	0.405	0.412	0.006	0.030286	0.2301736	-0.084
Thalamus proper L	0.221	0.224	0.002	0.240	0.506666666666667	-0.052
Thalamus proper R	0.239	0.243	0.004	0.105	0.362727272727273	-0.071
Transverse temporal gyrus L	0.299	0.299	0.000	0.865	0.913055555555556	0.007
Transverse temporal gyrus R	0.332	0.333	0.001	0.413482	0.612168155844156	-0.033
Triangular part of the inferior frontal gyrus L	0.349	0.349	0.001	0.548	0.709909090909091	0.024
Triangular part of the inferior frontal gyrus R	0.324	0.325	0.001	0.352	0.598925373134328	-0.038

FDR: false discovery rate. L: left. PRS: polygenic risk score. R: right.

Table D.57: Associations between PRSwithAPOE Threshold 5 and 114 regions of interest in amyloid negative participants

Region of Interest	R Square (Model 1)	R Square (Model 2)	R Square Change	Sig. F Change (Model 2)	FDR Corrected value	Standardised beta of PRS
Accumbens area L	0.390	0.391	0.001	0.638	1	0.024
Accumbens area R	0.433	0.434	0.000	0.654	0.99408	0.022
Amygdala L	0.444	0.446	0.002	0.294	1	-0.051
Amygdala R	0.461	0.464	0.003	0.265	1	-0.053
Angular gyrus L	0.428	0.428	0.000	0.960	1	0.002
Angular gyrus R	0.370	0.370	0.000	0.910	1	-0.006
Anterior cingulate gyrus L	0.444	0.446	0.002	0.409080	1	0.040
Anterior cingulate gyrus R	0.269	0.272	0.003	0.336	1	0.054
Anterior insula L	0.347	0.347	0.000	0.825	1	0.012
Anterior insula R	0.345	0.345	0.001	0.661	0.9915	0.023
Anterior orbital gyrus L	0.384	0.386	0.001	0.448	1	-0.039
Anterior orbital gyrus R	0.323	0.324	0.001	0.634	1	0.025
Basal forebrain L	0.348	0.350	0.001	0.463	1	0.039
Basal forebrain R	0.382	0.382	0.000	0.963	1	0.002
Calcarine cortex L	0.388	0.391	0.003	0.303	1	-0.052
Calcarine cortex R	0.368	0.373	0.004	0.196	1	-0.067
Caudate L	0.189	0.189	0.000	0.957411	1	-0.003
Caudate R	0.183	0.183	0.000	0.828	1	-0.013
Central operculum L	0.351	0.355	0.004	0.229	1	0.063
Central operculum R	0.322	0.323	0.001	0.543	1	0.033
Cuneus L	0.337	0.338	0.001	0.652	1	0.024
Cuneus R	0.377	0.382	0.005	0.162	1	-0.072
Entorhinal area L	0.374	0.375	0.001	0.619	1	0.026
Entorhinal area R	0.422	0.422	0.000	0.833	1	0.010
Frontal operculum L	0.298	0.305	0.006	0.139	1	0.081
Frontal operculum R	0.309	0.309	0.001	0.662	0.980103896103896	0.024

Frontal pole L	0.369	0.369	0.000	0.883	1	0.008
Frontal pole R	0.398	0.402	0.004	0.194743	1	0.065
Fusiform gyrus L	0.471	0.474	0.003	0.231	1	-0.057
Fusiform gyrus R	0.495	0.496	0.001	0.413601	1	-0.038
Gyrus rectus L	0.392	0.395	0.003	0.257	1	0.058
Gyrus rectus R	0.412	0.415	0.003	0.287	1	0.053
Hippocampus L	0.430	0.433	0.003	0.263	1	-0.055
Hippocampus R	0.490	0.496	0.006	0.098	1	-0.077
Inferior occipital gyrus L	0.379	0.379	0.000	0.706	0.981512195121951	-0.019
Inferior occipital gyrus R	0.432	0.432	0.000	0.779355	0.998274943820225	-0.014
Inferior temporal gyrus L	0.495	0.496	0.001	0.495	1	-0.032
Inferior temporal gyrus R	0.533	0.535	0.002	0.315	1	-0.045
Lateral orbital gyrus L	0.391	0.396	0.005	0.151	1	0.073
Lateral orbital gyrus R	0.308	0.310	0.002	0.374	1	0.048
Lingual gyrus L	0.500	0.500	0.001	0.532	1	-0.029
Lingual gyrus R	0.537	0.541	0.004	0.164	1	-0.062
Medial frontal cortex L	0.376	0.376	0.000	0.745	0.999176470588235	0.017
Medial frontal cortex R	0.354	0.356	0.002	0.399114	1	0.044
Medial orbital gyrus L	0.469	0.469	0.000	0.700	0.9975	0.018
Medial orbital gyrus R	0.385	0.388	0.003	0.244	1	0.059
Middle cingulate gyrus L	0.400	0.401	0.002	0.399454	1	0.043
Middle cingulate gyrus R	0.382	0.384	0.002	0.341	1	0.049
Middle frontal gyrus L	0.441	0.441	0.000	0.917	1	0.005
Middle frontal gyrus R	0.403	0.403	0.000	0.962	1	-0.002
Middle occipital gyrus L	0.385	0.386	0.001	0.637	1	0.024
Middle occipital gyrus R	0.347	0.348	0.001	0.589256	1	0.028
Middle temporal gyrus L	0.521	0.522	0.001	0.438	1	0.035
Middle temporal gyrus R	0.503	0.504	0.002	0.338	1	0.044
Occipital fusiform gyrus L	0.464	0.468	0.004	0.155	1	-0.068
Occipital fusiform gyrus R	0.501	0.501	0.000	0.863	1	-0.008

Occipital pole L	0.323	0.333	0.009	0.066	1	-0.098
Occipital pole R	0.336	0.336	0.000	0.774	1	0.015
Opercular part of the inferior frontal gyrus L	0.188	0.196	0.008	0.118	1	0.092
Opercular part of the inferior frontal gyrus R	0.277	0.282	0.005	0.194907	1	0.072
Orbital part of the inferior frontal gyrus L	0.289	0.291	0.003	0.278	1	0.059
Orbital part of the inferior frontal gyrus R	0.188	0.194	0.006	0.176	1	0.079
Pallidum L	0.187	0.187	0.000	0.967	1	-0.002
Pallidum R	0.157	0.157	0.000	0.968	1	-0.002
Parahippocampal gyrus L	0.483	0.483	0.000	0.952	1	-0.003
Parahippocampal gyrus R	0.491	0.492	0.000	0.685	1	-0.019
Parietal operculum L	0.355	0.355	0.001	0.644	1	0.024
Parietal operculum R	0.267	0.267	0.000	0.771	1	0.016
Planum polare L	0.385	0.385	0.001	0.588828	1	-0.028
Planum polare R	0.424	0.426	0.002	0.352	1	-0.046
Planum temporale L	0.346	0.347	0.001	0.588548	1	0.028
Planum temporale R	0.375	0.376	0.001	0.499	0.998	0.035
Postcentral gyrus L	0.390	0.390	0.000	0.980	1	0.001
Postcentral gyrus R	0.349	0.349	0.000	0.987	0.995734513274336	0.001
Postcentral gyrus medial segment L	0.213	0.213	0.000	0.843	1	-0.011
Postcentral gyrus medial segment R	0.196	0.196	0.000	0.887	1	-0.008
Posterior cingulate gyrus L	0.517	0.518	0.001	0.497	1	0.031
Posterior cingulate gyrus R	0.477	0.477	0.000	0.740	1	0.016
Posterior insula L	0.388	0.390	0.002	0.404	1	-0.043
Posterior insula R	0.408	0.408	0.000	0.986	1	0.001
Posterior orbital gyrus L	0.423	0.425	0.002	0.386	1	0.043
Posterior orbital gyrus R	0.377	0.377	0.000	0.724	0.994409638554217	-0.018
Precentral gyrus L	0.476	0.478	0.002	0.297	1	0.049
Precentral gyrus R	0.445	0.447	0.002	0.365	1	0.044
Precentral gyrus medial segment L	0.306	0.306	0.000	0.957328	1	0.003
Precentral gyrus medial segment R	0.361	0.362	0.001	0.466	1	-0.038

Precuneus L	0.453	0.454	0.002	0.390	1	-0.041
Precuneus R	0.496	0.496	0.000	0.778576	1	-0.013
Putamen L	0.293	0.297	0.004	0.241	1	-0.064
Putamen R	0.298	0.299	0.001	0.488	1	-0.038
Subcallosal area L	0.470	0.477	0.007	0.069	1	0.086
Subcallosal area R	0.411	0.420	0.010	0.041	1	0.102
Superior frontal gyrus L	0.441	0.442	0.001	0.627	1	0.024
Superior frontal gyrus R	0.462	0.463	0.000	0.703	0.989407407407407	0.018
Superior frontal gyrus medial segment L	0.420	0.420	0.000	0.956	1	-0.003
Superior frontal gyrus medial segment R	0.392	0.392	0.000	0.885	1	-0.007
Superior occipital gyrus L	0.253	0.254	0.000	0.691	0.997139240506329	0.022
Superior occipital gyrus R	0.256	0.257	0.001	0.597	1	0.030
Superior parietal lobule L	0.379	0.380	0.001	0.464	1	0.038
Superior parietal lobule R	0.395	0.397	0.002	0.413880	1	-0.041
Superior temporal gyrus L	0.358	0.362	0.004	0.234	1	0.062
Superior temporal gyrus R	0.383	0.383	0.000	0.909	1	0.006
Supplementary motor cortex L	0.393	0.393	0.000	0.990	0.99	0.001
Supplementary motor cortex R	0.372	0.373	0.001	0.482	1	-0.036
Supramarginal gyrus L	0.302	0.305	0.003	0.291	1	0.057
Supramarginal gyrus R	0.362	0.364	0.002	0.408584	1	0.043
Temporal pole L	0.356	0.356	0.000	0.842	1	-0.010
Temporal pole R	0.375	0.376	0.002	0.418	1	-0.042
Thalamus proper L	0.272	0.273	0.001	0.650	1	0.025
Thalamus proper R	0.304	0.305	0.001	0.520	1	-0.035
Transverse temporal gyrus L	0.216	0.220	0.004	0.280	1	0.062
Transverse temporal gyrus R	0.308	0.309	0.001	0.651	1	0.025
Triangular part of the inferior frontal gyrus L	0.263	0.264	0.001	0.562	1	0.032
Triangular part of the inferior frontal gyrus R	0.256	0.259	0.003	0.288	1	0.060

FDR: false discovery rate. L: left. PRS: polygenic risk score. R: right.

Table D.58: Associations between PRSwithAPOE Threshold 5 and 114 regions of interest in amyloid positive participants

Region of Interest	R Square (Model 1)	R Square (Model 2)	R Square Change	Sig. F Change (Model 2)	FDR Corrected value	Standardised beta of PRS
Accumbens area L	0.398	0.400	0.002	0.260	0.538909090909091	-0.044
Accumbens area R	0.374	0.374	0.000	0.764	0.862336633663366	-0.012
Amygdala L	0.383	0.401	0.018	0.000259596982423	0.0073985139990555	-0.143
Amygdala R	0.444	0.466	0.021	0.000028248424746	0.001073440140348	-0.155
Angular gyrus L	0.391	0.394	0.004	0.105	0.443333333333333	-0.063
Angular gyrus R	0.430	0.433	0.003	0.142	0.476117647058823	-0.056
Anterior cingulate gyrus L	0.388	0.388	0.000	0.901	0.951055555555556	-0.005
Anterior cingulate gyrus R	0.224	0.228	0.004	0.141	0.487090909090909	-0.065
Anterior insula L	0.401	0.401	0.000	0.658295	0.798357765957447	0.017
Anterior insula R	0.415	0.415	0.000	0.939	0.955767857142857	0.003
Anterior orbital gyrus L	0.413	0.415	0.002	0.256	0.540444444444445	-0.044
Anterior orbital gyrus R	0.390	0.395	0.005	0.059	0.395647058823529	-0.074
Basal forebrain L	0.261	0.264	0.003	0.183	0.52155	-0.057
Basal forebrain R	0.347	0.348	0.001	0.476	0.6783	-0.029
Calcarine cortex L	0.361	0.362	0.001	0.426	0.665260273972603	-0.032
Calcarine cortex R	0.385	0.389	0.004	0.080	0.414545454545455	-0.069
Caudate L	0.223	0.224	0.001	0.416910	0.669404788732394	-0.036
Caudate R	0.212	0.214	0.002	0.352	0.608	-0.041
Central operculum L	0.384	0.386	0.002	0.192	0.533853658536585	0.051
Central operculum R	0.399	0.399	0.000	0.929	0.962781818181818	-0.003
Cuneus L	0.441	0.445	0.004	0.066	0.3762	-0.069
Cuneus R	0.446	0.450	0.004	0.083	0.411391304347826	-0.065
Entorhinal area L	0.397	0.410	0.013	0.002	0.038	-0.122
Entorhinal area R	0.452	0.463	0.010	0.003	0.0488571428571429	-0.109
Frontal operculum L	0.392	0.392	0.001	0.507087	0.704974609756097	0.026
Frontal operculum R	0.320	0.320	0.000	0.959	0.967486725663717	0.002

Frontal pole L	0.469	0.471	0.001	0.268	0.536	0.040
Frontal pole R	0.431	0.432	0.002	0.255	0.548490566037736	0.043
Fusiform gyrus L	0.510	0.512	0.002	0.202	0.53553488372093	-0.045
Fusiform gyrus R	0.538	0.541	0.003	0.094	0.42864	-0.057
Gyrus rectus L	0.451	0.451	0.000	0.683	0.802701030927835	-0.015
Gyrus rectus R	0.464	0.465	0.001	0.507300	0.696773493975904	0.024
Hippocampus L	0.422	0.445	0.023	0.000016484627976	0.000939623794632	-0.163
Hippocampus R	0.442	0.470	0.028	0.000001467153272	0.000167255473008	-0.178
Inferior occipital gyrus L	0.424	0.428	0.003	0.102	0.447230769230769	-0.062
Inferior occipital gyrus R	0.479	0.484	0.005	0.034	0.276857142857143	-0.077
Inferior temporal gyrus L	0.493	0.499	0.005	0.027239	0.282295090909091	-0.079
Inferior temporal gyrus R	0.540	0.543	0.004	0.060	0.38	-0.064
Lateral orbital gyrus L	0.433	0.434	0.000	0.581	0.744202247191011	-0.021
Lateral orbital gyrus R	0.408	0.409	0.000	0.679	0.8063125	-0.016
Lingual gyrus L	0.506	0.506	0.000	0.894	0.961471698113208	-0.005
Lingual gyrus R	0.517	0.517	0.001	0.461	0.682519480519481	-0.026
Medial frontal cortex L	0.348	0.351	0.002	0.2187940	0.51963575	-0.050
Medial frontal cortex R	0.371	0.371	0.000	0.856	0.938307692307692	0.007
Medial orbital gyrus L	0.483	0.484	0.001	0.399455	0.659969130434783	-0.030
Medial orbital gyrus R	0.468	0.468	0.000	0.903	0.944422018348624	-0.004
Middle cingulate gyrus L	0.397	0.397	0.001	0.447	0.6705	-0.030
Middle cingulate gyrus R	0.332	0.335	0.003	0.179	0.523230769230769	-0.055
Middle frontal gyrus L	0.498	0.498	0.000	0.718	0.835224489795918	-0.013
Middle frontal gyrus R	0.504	0.505	0.001	0.465	0.679615384615385	-0.026
Middle occipital gyrus L	0.360	0.364	0.004	0.079	0.428857142857143	-0.070
Middle occipital gyrus R	0.354	0.370	0.016	0.000714956424545	0.016301006479626	-0.136
Middle temporal gyrus L	0.480	0.485	0.005	0.041	0.228	-0.074
Middle temporal gyrus R	0.520	0.526	0.006	0.018	0.292125	-0.082
Occipital fusiform gyrus L	0.470	0.471	0.000	0.570	0.738409090909091	0.021
Occipital fusiform gyrus R	0.517	0.519	0.002	0.159	0.5035	-0.049

Occipital pole L	0.328	0.328	0.000	0.974	0.974	-0.001
Occipital pole R	0.396	0.397	0.001	0.417112	0.660427333333333	-0.032
Opercular part of the inferior frontal gyrus L	0.302	0.304	0.002	0.303	0.566262295081967	0.043
Opercular part of the inferior frontal gyrus R	0.270	0.270	0.000	0.638	0.790565217391304	0.020
Orbital part of the inferior frontal gyrus L	0.275	0.275	0.000	0.760	0.8664	-0.013
Orbital part of the inferior frontal gyrus R	0.310	0.315	0.004	0.088	0.418	-0.071
Pallidum L	0.120	0.123	0.003	0.212	0.537066666666667	-0.059
Pallidum R	0.103	0.108	0.005	0.122	0.4636	-0.073
Parahippocampal gyrus L	0.477	0.483	0.006	0.021	0.2394	-0.084
Parahippocampal gyrus R	0.514	0.521	0.007	0.010	0.1425	-0.090
Parietal operculum L	0.314	0.315	0.001	0.436	0.671675675675676	0.032
Parietal operculum R	0.294	0.295	0.000	0.658231	0.806863806451613	0.019
Planum polare L	0.457	0.458	0.001	0.398720	0.668442352941176	-0.031
Planum polare R	0.466	0.467	0.001	0.384	0.653373134328358	-0.032
Planum temporale L	0.354	0.354	0.000	0.823	0.910893203883495	-0.009
Planum temporale R	0.329	0.329	0.000	0.751	0.864787878787879	-0.013
Postcentral gyrus L	0.394	0.395	0.001	0.439	0.66728	-0.030
Postcentral gyrus R	0.411	0.414	0.003	0.125	0.459677419354839	-0.059
Postcentral gyrus medial segment L	0.186	0.193	0.008	0.040	0.304	-0.093
Postcentral gyrus medial segment R	0.245	0.247	0.002	0.267	0.543535714285714	-0.048
Posterior cingulate gyrus L	0.546	0.550	0.003	0.065	0.39	-0.062
Posterior cingulate gyrus R	0.511	0.517	0.005	0.027359	0.2599105	-0.077
Posterior insula L	0.395	0.398	0.003	0.167	0.514540540540541	0.054
Posterior insula R	0.423	0.423	0.000	0.559	0.73248275862069	0.022
Posterior orbital gyrus L	0.348	0.348	0.000	0.601	0.761266666666667	-0.021
Posterior orbital gyrus R	0.394	0.396	0.002	0.246	0.539307692307692	-0.045
Precentral gyrus L	0.457	0.457	0.000	0.932	0.957189189189189	0.003
Precentral gyrus R	0.448	0.448	0.000	0.678	0.8136	-0.015
Precentral gyrus medial segment L	0.286	0.290	0.003	0.145	0.472285714285714	-0.062
Precentral gyrus medial segment R	0.315	0.318	0.002	0.237	0.529764705882353	-0.049

Precuneus L	0.499	0.500	0.001	0.274	0.538551724137931	-0.039
Precuneus R	0.482	0.484	0.003	0.127	0.4524375	-0.055
Putamen L	0.280	0.281	0.001	0.529	0.717928571428571	-0.027
Putamen R	0.285	0.287	0.002	0.235	0.5358	-0.050
Subcallosal area L	0.478	0.478	0.000	0.790	0.882941176470588	0.010
Subcallosal area R	0.473	0.475	0.002	0.196	0.532	0.047
Superior frontal gyrus L	0.468	0.470	0.002	0.213	0.527869565217391	-0.046
Superior frontal gyrus R	0.499	0.499	0.000	0.532	0.713505882352941	0.022
Superior frontal gyrus medial segment L	0.421	0.423	0.002	0.218221	0.529302	-0.047
Superior frontal gyrus medial segment R	0.397	0.398	0.002	0.287	0.5453	0.041
Superior occipital gyrus L	0.353	0.354	0.001	0.349	0.612092307692308	-0.038
Superior occipital gyrus R	0.366	0.367	0.001	0.315	0.579193548387097	-0.040
Superior parietal lobule L	0.392	0.394	0.002	0.220	0.511836734693878	-0.048
Superior parietal lobule R	0.377	0.379	0.002	0.209	0.5415	-0.050
Superior temporal gyrus L	0.442	0.443	0.001	0.331	0.598952380952381	-0.036
Superior temporal gyrus R	0.387	0.388	0.001	0.344	0.61275	-0.037
Supplementary motor cortex L	0.341	0.344	0.003	0.173	0.519	-0.055
Supplementary motor cortex R	0.378	0.379	0.000	0.896	0.954616822429906	0.005
Supramarginal gyrus L	0.377	0.377	0.000	0.612	0.766681318681319	-0.020
Supramarginal gyrus R	0.340	0.341	0.001	0.466	0.672455696202532	0.030
Temporal pole L	0.409	0.412	0.003	0.109	0.443785714285714	-0.062
Temporal pole R	0.405	0.411	0.006	0.033	0.289384615384615	-0.082
Thalamus proper L	0.221	0.223	0.002	0.277	0.535220338983051	-0.048
Thalamus proper R	0.239	0.243	0.004	0.112	0.440275862068966	-0.069
Transverse temporal gyrus L	0.299	0.299	0.000	0.857	0.930457142857143	0.008
Transverse temporal gyrus R	0.332	0.333	0.001	0.541	0.717139534883721	-0.025
Triangular part of the inferior frontal gyrus L	0.349	0.350	0.001	0.416343	0.678044314285714	0.033
Triangular part of the inferior frontal gyrus R	0.324	0.324	0.001	0.481	0.676962962962963	-0.029

FDR: false discovery rate. L: left. PRS: polygenic risk score. R: right.

Table D.59: Associations between PRSwithAPOE Threshold 10 and 114 regions of interest in amyloid negative participants

Region of Interest	R Square (Model 1)	R Square (Model 2)	R Square Change	Sig. F Change (Model 2)	FDR Corrected value	Standardised beta of PRS
Accumbens area L	0.390	0.390	0.000	0.893	1	0.007
Accumbens area R	0.433	0.433	0.000	0.766	1	0.015
Amygdala L	0.444	0.451	0.007	0.074	1	-0.088
Amygdala R	0.461	0.466	0.006	0.108	1	-0.077
Angular gyrus L	0.428	0.428	0.000	0.924	1	0.005
Angular gyrus R	0.370	0.371	0.001	0.653456	1	-0.023
Anterior cingulate gyrus L	0.444	0.446	0.001	0.430081	1	0.039
Anterior cingulate gyrus R	0.269	0.271	0.002	0.382	1	0.049
Anterior insula L	0.347	0.347	0.000	0.720	1	-0.019
Anterior insula R	0.345	0.345	0.000	0.981	0.998517857142857	0.001
Anterior orbital gyrus L	0.384	0.387	0.003	0.309	1	-0.053
Anterior orbital gyrus R	0.323	0.323	0.000	0.973355	0.999661891891892	0.002
Basal forebrain L	0.348	0.348	0.000	0.836	1	-0.011
Basal forebrain R	0.382	0.383	0.001	0.520	1	-0.033
Calcarine cortex L	0.388	0.395	0.006	0.112	1	-0.082
Calcarine cortex R	0.368	0.376	0.008	0.082088	1	-0.091
Caudate L	0.189	0.189	0.000	0.765	1	-0.018
Caudate R	0.183	0.183	0.000	0.876133	1	-0.009
Central operculum L	0.351	0.353	0.003	0.324	1	0.052
Central operculum R	0.322	0.323	0.000	0.891	1	0.007
Cuneus L	0.337	0.338	0.000	0.762	1	-0.016
Cuneus R	0.377	0.387	0.010	0.046	1	-0.104
Entorhinal area L	0.374	0.374	0.000	0.691	1	-0.021
Entorhinal area R	0.422	0.422	0.000	0.793	1	-0.013
Frontal operculum L	0.298	0.303	0.005	0.186	1	0.073
Frontal operculum R	0.309	0.309	0.000	0.753	1	0.017

Frontal pole L	0.369	0.369	0.000	0.961	1	-0.003
Frontal pole R	0.398	0.401	0.003	0.271	1	0.056
Fusiform gyrus L	0.471	0.475	0.004	0.178	1	-0.064
Fusiform gyrus R	0.495	0.497	0.002	0.359	1	-0.043
Gyrus rectus L	0.392	0.392	0.000	0.745	1	0.017
Gyrus rectus R	0.412	0.413	0.001	0.532	1	0.032
Hippocampus L	0.430	0.436	0.006	0.122	1	-0.077
Hippocampus R	0.490	0.496	0.006	0.081596	1	-0.082
Inferior occipital gyrus L	0.379	0.380	0.001	0.580	1	-0.029
Inferior occipital gyrus R	0.432	0.433	0.001	0.613	1	-0.025
Inferior temporal gyrus L	0.945	0.497	0.002	0.329	1	-0.046
Inferior temporal gyrus R	0.533	0.535	0.002	0.323	1	-0.044
Lateral orbital gyrus L	0.391	0.395	0.004	0.194	1	0.067
Lateral orbital gyrus R	0.308	0.308	0.000	0.886	1	0.008
Lingual gyrus L	0.500	0.503	0.003	0.200	1	-0.060
Lingual gyrus R	0.537	0.541	0.004	0.132	1	-0.067
Medial frontal cortex L	0.376	0.376	0.000	0.763	1	-0.016
Medial frontal cortex R	0.354	0.355	0.001	0.615	1	0.027
Medial orbital gyrus L	0.469	0.469	0.000	0.990	0.998761061946903	0.001
Medial orbital gyrus R	0.385	0.385	0.000	0.670	1	0.022
Middle cingulate gyrus L	0.400	0.401	0.001	0.445	1	0.039
Middle cingulate gyrus R	0.382	0.384	0.002	0.363	1	0.047
Middle frontal gyrus L	0.441	0.441	0.000	0.919	1	0.005
Middle frontal gyrus R	0.403	0.403	0.000	0.791	1	-0.013
Middle occipital gyrus L	0.385	0.386	0.000	0.805	1	0.013
Middle occipital gyrus R	0.347	0.347	0.000	0.944	1	0.004
Middle temporal gyrus L	0.521	.522	0.001	0.530	1	0.029
Middle temporal gyrus R	0.503	0.505	0.002	0.312	1	0.047
Occipital fusiform gyrus L	0.464	0.467	0.003	0.232	1	-0.058
Occipital fusiform gyrus R	0.501	0.501	0.000	0.921	1	0.005

Occipital pole L	0.323	0.338	0.015	0.021	1	-0.125
Occipital pole R	0.336	0.336	0.000	0.997	0.997	0.000
Opercular part of the inferior frontal gyrus L	0.188	0.196	0.008	0.113	1	0.094
Opercular part of the inferior frontal gyrus R	0.277	0.282	0.004	0.227	1	0.068
Orbital part of the inferior frontal gyrus L	0.289	0.291	0.002	0.413	1	0.045
Orbital part of the inferior frontal gyrus R	0.188	0.189	0.002	0.491	1	0.041
Pallidum L	0.187	0.187	0.000	0.935	1	0.005
Pallidum R	0.157	0.158	0.000	0.757	1	0.019
Parahippocampal gyrus L	0.483	0.485	0.001	0.435	1	-0.037
Parahippocampal gyrus R	0.491	0.493	0.001	0.430657	1	-0.037
Parietal operculum L	0.355	0.355	0.001	0.647	1	0.024
Parietal operculum R	0.267	0.267	0.000	0.971	1	0.002
Planum polare L	0.385	0.388	0.003	0.241	1	-0.060
Planum polare R	0.424	0.429	0.004	0.166	1	-0.069
Planum temporale L	0.346	0.347	0.000	0.779	1	0.015
Planum temporale R	0.375	0.375	0.000	0.801	1	0.013
Postcentral gyrus L	0.390	0.390	0.000	0.831	1	-0.011
Postcentral gyrus R	0.349	0.349	0.000	0.798	1	0.014
Postcentral gyrus medial segment L	0.213	0.213	0.001	0.608	1	0.030
Postcentral gyrus medial segment R	0.196	0.197	0.001	0.534	1	0.037
Posterior cingulate gyrus L	0.517	0.518	0.000	0.621	1	0.023
Posterior cingulate gyrus R	0.477	0.477	0.000	0.898	1	0.006
Posterior insula L	0.388	0.391	0.003	0.285	1	-0.055
Posterior insula R	0.408	0.408	0.000	0.661	1	-0.022
Posterior orbital gyrus L	0.423	0.423	0.000	0.768	1	0.015
Posterior orbital gyrus R	0.377	0.379	0.002	0.355	1	-0.048
Precentral gyrus L	0.476	0.477	0.001	0.499	1	0.032
Precentral gyrus R	0.445	0.446	0.001	0.431214	1	0.039
Precentral gyrus medial segment L	0.306	0.307	0.001	0.509	1	0.036
Precentral gyrus medial segment R	0.361	0.361	0.000	0.847	1	-0.010

Precuneus L	0.453	0.454	0.001	0.513	1	-0.032
Precuneus R	0.496	0.496	0.000	0.922	1	-0.005
Putamen L	0.293	0.298	0.005	0.197	1	-0.071
Putamen R	0.298	0.300	0.002	0.394	1	-0.047
Subcallosal area L	0.470	0.475	0.005	0.110	1	0.076
Subcallosal area R	0.411	0.418	0.007	0.087	1	0.086
Superior frontal gyrus L	0.441	0.441	0.000	0.653472	1	0.022
Superior frontal gyrus R	0.462	0.463	0.001	0.573	1	0.027
Superior frontal gyrus medial segment L	0.420	0.421	0.000	0.685	1	-0.020
Superior frontal gyrus medial segment R	0.392	0.393	0.001	0.611	1	-0.026
Superior occipital gyrus L	0.253	0.253	0.000	0.880	1	-0.009
Superior occipital gyrus R	0.256	0.257	0.000	0.787	1	-0.015
Superior parietal lobule L	0.379	0.379	0.001	0.607	1	0.027
Superior parietal lobule R	0.395	0.398	0.003	0.283	1	-0.055
Superior temporal gyrus L	0.358	0.360	0.002	0.402	1	0.044
Superior temporal gyrus R	0.383	0.383	0.000	0.972602	1	-0.002
Supplementary motor cortex L	0.393	0.393	0.000	0.875577	1	-0.008
Supplementary motor cortex R	0.372	0.372	0.000	0.726	1	-0.018
Supramarginal gyrus L	0.302	0.309	0.007	0.124	1	0.084
Supramarginal gyrus R	0.362	0.365	0.002	0.344	1	0.050
Temporal pole L	0.356	0.357	0.001	0.543	1	-0.032
Temporal pole R	0.375	0.377	0.003	0.284	1	-0.056
Thalamus proper L	0.272	0.272	0.000	0.908	1	-0.006
Thalamus proper R	0.304	0.306	0.002	0.420	1	-0.044
Transverse temporal gyrus L	0.216	0.217	0.002	0.484	1	0.041
Transverse temporal gyrus R	0.308	0.308	0.000	0.817	1	-0.013
Triangular part of the inferior frontal gyrus L	0.263	0.264	0.001	0.605	1	0.029
Triangular part of the inferior frontal gyrus R	0.256	0.257	0.001	0.579	1	0.032

FDR: false discovery rate. L: left. PRS: polygenic risk score. R: right.

Table D.60: Associations between PRSwithAPOE Threshold 10 and 114 regions of interest in amyloid positive participants

Region of Interest	R Square (Model 1)	R Square (Model 2)	R Square Change	Sig. F Change (Model 2)	FDR Corrected value	Standardised beta of PRS
Accumbens area L	0.398	0.400	0.002	0.210	0.63	-0.049
Accumbens area R	0.374	0.374	0.000	0.674	0.835173913043478	-0.017
Amygdala L	0.383	0.399	0.016	0.000681427503963	0.0194206838629455	-0.134
Amygdala R	0.444	0.463	0.019	0.000090073131599	0.003422779000762	-0.146
Angular gyrus L	0.391	0.393	0.002	0.247	0.639954545454545	-0.045
Angular gyrus R	0.430	0.432	0.002	0.250	0.633333333333333	-0.044
Anterior cingulate gyrus L	0.388	0.388	0.000	0.876	0.94211320754717	-0.006
Anterior cingulate gyrus R	0.224	0.226	0.002	0.256	0.620936170212766	-0.050
Anterior insula L	0.401	0.401	0.000	0.545	0.767037037037037	0.024
Anterior insula R	0.415	0.415	0.000	0.825	0.931188118811881	0.009
Anterior orbital gyrus L	0.413	0.414	0.001	0.356	0.634125	-0.036
Anterior orbital gyrus R	0.390	0.393	0.003	0.129	0.544666666666667	-0.060
Basal forebrain L	0.261	0.263	0.002	0.283	0.632588235294118	-0.046
Basal forebrain R	0.347	0.348	0.000	0.791	0.90174	-0.011
Calcarine cortex L	0.361	0.361	0.001	0.463762	0.70491824	-0.030
Calcarine cortex R	0.385	0.388	0.003	0.142	0.5396	-0.058
Caudate L	0.223	0.224	0.001	0.426	0.665260273972603	-0.035
Caudate R	0.212	0.214	0.002	0.308	0.627	-0.046
Central operculum L	0.384	0.386	0.002	0.201	0.619297297297297	0.050
Central operculum R	0.399	0.399	0.000	0.936	0.961297297297297	0.003
Cuneus L	0.441	0.444	0.003	0.104	0.538909090909091	-0.061
Cuneus R	0.446	0.0449	0.003	0.120	0.57	-0.058
Entorhinal area L	0.397	0.409	0.012	0.002678	0.0610584	-0.117
Entorhinal area R	0.452	0.463	0.010	0.003458	0.056316	-0.109
Frontal operculum L	0.392	0.393	0.001	0.392	0.6384	0.034
Frontal operculum R	0.320	0.320	0.000	0.927	0.9785	-0.004

Frontal pole L	0.469	0.473	0.004	0.077	0.462	0.065
Frontal pole R	0.431	0.433	0.003	0.134	0.545571428571429	0.057
Fusiform gyrus L	0.510	0.512	0.001	0.253	0.627	-0.040
Fusiform gyrus R	0.538	0.541	0.003	0.098	0.532	-0.057
Gyrus rectus L	0.451	0.451	0.000	0.834	0.923067961165048	-0.008
Gyrus rectus R	0.464	0.465	0.001	0.447	0.688621621621622	0.028
Hippocampus L	0.422	0.445	0.023	0.000022393761377	0.001276444398489	-0.161
Hippocampus R	0.442	0.471	0.029	0.000001092852195	0.00012458515023	-0.181
Inferior occipital gyrus L	0.424	0.427	0.002	0.170	0.553714285714286	-0.052
Inferior occipital gyrus R	0.479	0.483	0.004	0.073	0.462333333333333	-0.065
Inferior temporal gyrus L	0.493	0.498	0.005	0.038	0.361	-0.074
Inferior temporal gyrus R	0.540	0.543	0.004	0.064	0.521142857142857	-0.063
Lateral orbital gyrus L	0.433	0.434	0.000	0.854	0.936115384615385	-0.007
Lateral orbital gyrus R	0.408	0.409	0.000	0.595	0.788720930232558	-0.021
Lingual gyrus L	0.506	0.506	0.000	0.828	0.925411764705882	-0.008
Lingual gyrus R	0.517	0.517	0.000	0.741	0.8892	-0.012
Medial frontal cortex L	0.348	0.351	0.002	0.239	0.633627906976744	-0.048
Medial frontal cortex R	0.371	0.371	0.000	0.778	0.895878787878788	0.011
Medial orbital gyrus L	0.483	0.484	0.000	0.537	0.765225	-0.022
Medial orbital gyrus R	0.468	0.468	0.000	0.935	0.969	-0.003
Middle cingulate gyrus L	0.397	0.397	0.000	0.720	0.873191489361702	-0.014
Middle cingulate gyrus R	0.332	0.333	0.001	0.418	0.671154929577465	-0.033
Middle frontal gyrus L	0.498	0.498	0.000	0.967	0.975557522123894	-0.001
Middle frontal gyrus R	0.504	0.504	0.000	0.767	0.901422680412371	-0.011
Middle occipital gyrus L	0.360	0.362	0.003	0.160	0.536470588235294	-0.057
Middle occipital gyrus R	0.354	0.367	0.013	0.002896	0.055024	-0.120
Middle temporal gyrus L	0.480	0.484	0.004	0.071	0.331636363636364	-0.066
Middle temporal gyrus R	0.520	0.525	0.005	0.032	0.476117647058823	-0.075
Occipital fusiform gyrus L	0.470	0.471	0.000	0.604	0.791448275862069	0.019
Occipital fusiform gyrus R	0.517	0.519	0.002	0.150	0.534375	-0.050

Occipital pole L	0.328	0.328	0.000	0.985	0.985	0.001
Occipital pole R	0.396	0.397	0.001	0.463884	0.695826	-0.029
Opercular part of the inferior frontal gyrus L	0.302	0.303	0.001	0.421	0.666583333333333	0.034
Opercular part of the inferior frontal gyrus R	0.270	0.270	0.000	0.901	0.959943925233645	0.005
Orbital part of the inferior frontal gyrus L	0.275	0.275	0.000	0.657	0.841550561797753	-0.019
Orbital part of the inferior frontal gyrus R	0.310	0.314	0.003	0.149	0.547935483870968	-0.060
Pallidum L	0.120	0.122	0.002	0.277	0.63156	-0.051
Pallidum R	0.103	0.107	0.004	0.181	0.573166666666667	-0.064
Parahippocampal gyrus L	0.477	0.483	0.006	0.020	0.253333333333333	-0.084
Parahippocampal gyrus R	0.514	0.521	0.007	0.008	0.114	-0.092
Parietal operculum L	0.314	0.316	0.001	0.341	0.617047619047619	0.040
Parietal operculum R	0.294	0.295	0.000	0.679	0.832322580645161	0.018
Planum polare L	0.457	0.458	0.001	0.335	0.626065573770492	-0.036
Planum polare R	0.466	0.467	0.001	0.291037	0.626004113207547	-0.039
Planum temporale L	0.354	0.354	0.000	0.934	0.976844036697248	-0.003
Planum temporale R	0.329	0.330	0.000	0.666	0.83432967032967	-0.018
Postcentral gyrus L	0.394	0.395	0.001	0.383585	0.643068970588235	-0.034
Postcentral gyrus R	0.411	0.414	0.003	0.153	0.528545454545455	-0.055
Postcentral gyrus medial segment L	0.186	0.192	0.007	0.057	0.499846153846154	-0.086
Postcentral gyrus medial segment R	0.245	0.246	0.001	0.384289	0.634912260869565	-0.038
Posterior cingulate gyrus L	0.546	0.549	0.002	0.125	0.57	-0.052
Posterior cingulate gyrus R	0.511	0.515	0.004	0.065	0.494	-0.065
Posterior insula L	0.395	0.397	0.002	0.218	0.637230769230769	0.048
Posterior insula R	0.423	0.423	0.001	0.486	0.710307692307692	0.027
Posterior orbital gyrus L	0.348	0.349	0.000	0.559	0.767783132530121	-0.024
Posterior orbital gyrus R	0.394	0.396	0.002	0.228	0.618857142857143	-0.047
Precentral gyrus L	0.457	0.458	0.000	0.750	0.890625	0.012
Precentral gyrus R	0.448	0.448	0.000	0.769	0.894551020408163	-0.011
Precentral gyrus medial segment L	0.286	0.290	0.004	0.137	0.538551724137931	-0.063
Precentral gyrus medial segment R	0.315	0.317	0.001	0.329	0.635694915254237	-0.041

Precuneus L	0.499	0.499	0.001	0.494	0.712860759493671	-0.024
Precuneus R	0.482	0.483	0.002	0.224	0.6384	-0.044
Putamen L	0.280	0.281	0.001	0.568	0.770857142857143	-0.024
Putamen R	0.285	0.287	0.002	0.302	0.625963636363636	-0.044
Subcallosal area L	0.478	0.478	0.000	0.574	0.769835294117647	0.020
Subcallosal area R	0.473	0.477	0.004	0.070	0.49875	0.066
Superior frontal gyrus L	0.468	0.469	0.001	0.266	0.63175	-0.041
Superior frontal gyrus R	0.499	0.500	0.001	0.290879	0.637696269230769	0.038
Superior frontal gyrus medial segment L	0.421	0.422	0.001	0.380	0.646567164179105	-0.034
Superior frontal gyrus medial segment R	0.397	0.399	0.002	0.226	0.628390243902439	0.047
Superior occipital gyrus L	0.353	0.354	0.002	0.301	0.635444444444444	-0.042
Superior occipital gyrus R	0.366	0.367	0.001	0.332	0.6308	-0.039
Superior parietal lobule L	0.392	0.393	0.001	0.374	0.646	-0.035
Superior parietal lobule R	0.377	0.379	0.001	0.313	0.615206896551724	-0.040
Superior temporal gyrus L	0.442	0.443	0.001	0.309	0.618	-0.038
Superior temporal gyrus R	0.387	0.388	0.001	0.339	0.623322580645161	-0.038
Supplementary motor cortex L	0.341	0.345	0.004	0.117	0.579913043478261	-0.064
Supplementary motor cortex R	0.378	0.378	0.000	0.957	0.974089285714286	0.002
Supramarginal gyrus L	0.377	0.377	0.000	0.660	0.836	-0.018
Supramarginal gyrus R	0.340	0.341	0.001	0.363	0.636646153846154	0.037
Temporal pole L	0.409	0.412	0.003	0.126	0.552461538461539	-0.059
Temporal pole R	0.405	0.412	0.006	0.031	0.3534	-0.084
Thalamus proper L	0.221	0.223	0.002	0.276	0.642122448979592	-0.048
Thalamus proper R	0.239	0.244	0.005	0.082	0.4674	-0.076
Transverse temporal gyrus L	0.299	0.299	0.000	0.859	0.932628571428571	0.008
Transverse temporal gyrus R	0.332	0.333	0.000	0.622	0.805772727272727	-0.020
Triangular part of the inferior frontal gyrus L	0.349	0.349	0.001	0.468	0.692883116883117	0.030
Triangular part of the inferior frontal gyrus R	0.324	0.324	0.001	0.553	0.768804878048781	-0.025

FDR: false discovery rate. L: left. PRS: polygenic risk score. R: right.

Table D.61: Associations between PRSwithoutAPOE Threshold 1 and 114 regions of interest in amyloid negative participants

Region of Interest	R Square (Model 1)	R Square (Model 2)	R Square Change	Sig. F Change (Model 2)	FDR Corrected value	Standardised beta of PRS
Accumbens area L	0.390	0.391	0.001	0.627441	1	0.025
Accumbens area R	0.433	0.433	0.000	0.845	1	-0.010
Amygdala L	0.444	0.445	0.002	0.408698	1	-0.041
Amygdala R	0.461	0.468	0.007	0.075	1	-0.087
Angular gyrus L	0.428	0.428	0.000	0.700	0.973170731707317	-0.019
Angular gyrus R	0.370	0.373	0.003	0.318	1	0.053
Anterior cingulate gyrus L	0.444	0.445	0.000	0.664	1	0.022
Anterior cingulate gyrus R	0.269	0.0273	0.004	0.234867	1	-0.067
Anterior insula L	0.347	0.347	0.001	0.660	1	0.024
Anterior insula R	0.345	0.346	0.001	0.597	1	0.028
Anterior orbital gyrus L	0.384	0.385	0.001	0.508193	1	-0.034
Anterior orbital gyrus R	0.323	0.325	0.002	0.455	1	0.041
Basal forebrain L	0.348	0.349	0.000	0.672	0.982153846153846	-0.023
Basal forebrain R	0.382	0.385	0.004	0.231	1	-0.063
Calcarine cortex L	0.388	0.389	0.001	0.630375	1	0.025
Calcarine cortex R	0.368	0.368	0.000	0.920	0.998857142857143	-0.005
Caudate L	0.189	0.190	0.001	0.617	1	0.030
Caudate R	0.183	0.183	0.000	0.889	1	0.008
Central operculum L	0.351	0.353	0.002	0.409047	1	0.044
Central operculum R	0.322	0.326	0.003	0.260	1	0.062
Cuneus L	0.337	0.337	0.000	0.945	0.9975	0.004
Cuneus R	0.377	0.379	0.002	0.406	1	-0.044
Entorhinal area L	0.374	0.374	0.000	0.740	0.980930232558139	0.017
Entorhinal area R	0.422	0.423	0.001	0.592	1	-0.027
Frontal operculum L	0.298	0.300	0.001	0.511	1	0.037
Frontal operculum R	0.309	0.311	0.002	0.389	1	-0.048

Frontal pole L	0.369	0.369	0.000	0.758	0.960133333333333	0.016
Frontal pole R	0.398	0.399	0.001	0.628	1	-0.025
Fusiform gyrus L	0.471	0.471	0.000	0.938	0.999364485981308	-0.004
Fusiform gyrus R	0.495	0.495	0.000	0.892	1	-0.006
Gyrus rectus L	0.392	0.397	0.005	0.158	1	0.073
Gyrus rectus R	0.412	0.413	0.001	0.633	1	0.024
Hippocampus L	0.430	0.438	0.008	0.058	1	-0.095
Hippocampus R	0.490	0.498	0.008	0.045	1	-0.095
Inferior occipital gyrus L	0.379	0.380	0.000	0.668369	0.989533324675325	0.022
Inferior occipital gyrus R	0.432	0.432	0.000	0.780	0.956129032258065	0.014
Inferior temporal gyrus L	0.495	0.498	0.004	0.169	1	-0.065
Inferior temporal gyrus R	0.533	0.536	0.002	0.264	1	-0.051
Lateral orbital gyrus L	0.391	0.391	0.000	0.884	1	0.008
Lateral orbital gyrus R	0.308	0.310	0.002	0.436	1	-0.043
Lingual gyrus L	0.500	0.501	0.002	0.331	1	0.046
Lingual gyrus R	0.537	0.537	0.000	0.616	1	0.023
Medial frontal cortex L	0.376	0.376	0.000	0.815	0.988404255319149	-0.012
Medial frontal cortex R	0.354	0.354	0.000	0.755	0.967078651685393	-0.017
Medial orbital gyrus L	0.469	0.471	0.002	0.329	1	0.047
Medial orbital gyrus R	0.385	0.385	0.000	0.675	0.974050632911392	0.022
Middle cingulate gyrus L	0.400	0.400	0.001	0.581	1	0.028
Middle cingulate gyrus R	0.382	0.384	0.003	0.307	1	-0.053
Middle frontal gyrus L	0.441	0.443	0.003	0.276	1	0.054
Middle frontal gyrus R	0.403	0.403	0.000	0.751	0.972886363636364	0.016
Middle occipital gyrus L	0.385	0.387	0.002	0.419	1	-0.042
Middle occipital gyrus R	0.347	0.349	0.002	0.418213	1	-0.043
Middle temporal gyrus L	0.521	0.521	0.000	0.897	1	-0.006
Middle temporal gyrus R	0.503	0.504	0.001	0.395	0.992796116504854	0.040
Occipital fusiform gyrus L	0.464	0.464	0.000	0.691	0.984675	0.019
Occipital fusiform gyrus R	0.501	0.503	0.001	0.400	1	0.039

Occipital pole L	0.323	0.324	0.001	0.598	1	-0.029
Occipital pole R	0.336	0.337	0.001	0.508391	1	0.036
Opercular part of the inferior frontal gyrus L	0.188	0.188	0.000	0.749	0.981448275862069	0.019
Opercular part of the inferior frontal gyrus R	0.277	0.277	0.000	0.910	0.9975	0.006
Orbital part of the inferior frontal gyrus L	0.289	0.290	0.000	0.778	0.96404347826087	0.016
Orbital part of the inferior frontal gyrus R	0.188	0.188	0.000	0.973	0.990375	0.002
Pallidum L	0.187	0.187	0.000	0.893	1	-0.008
Pallidum R	0.157	0.158	0.001	0.631	1	-0.029
Parahippocampal gyrus L	0.483	0.483	0.000	0.999	0.999	0.000
Parahippocampal gyrus R	0.491	0.491	0.000	0.953	0.996715596330275	0.003
Parietal operculum L	0.355	0.355	0.000	0.668264	1	-0.023
Parietal operculum R	0.267	0.267	0.001	0.662	1	-0.025
Planum polare L	0.385	0.387	0.003	0.303	1	-0.054
Planum polare R	0.424	0.425	0.001	0.587	1	-0.027
Planum temporale L	0.346	0.347	0.001	0.582	1	0.030
Planum temporale R	0.375	0.375	0.000	0.922	0.991584905660377	-0.005
Postcentral gyrus L	0.390	0.391	0.001	0.626607	1	-0.025
Postcentral gyrus R	0.349	0.350	0.001	0.619	1	0.027
Postcentral gyrus medial segment L	0.213	0.214	0.001	0.544	1	0.036
Postcentral gyrus medial segment R	0.196	0.199	0.004	0.273	1	-0.065
Posterior cingulate gyrus L	0.517	0.519	0.001	0.451	1	-0.035
Posterior cingulate gyrus R	0.477	0.477	0.000	0.859	1	0.009
Posterior insula L	0.388	0.389	0.001	0.568	1	0.030
Posterior insula R	0.408	0.409	0.001	0.507	1	0.034
Posterior orbital gyrus L	0.423	0.423	0.000	0.958	0.992836363636364	-0.003
Posterior orbital gyrus R	0.377	0.381	0.005	0.167	1	-0.072
Precentral gyrus L	0.476	0.477	0.000	0.641	1	-0.022
Precentral gyrus R	0.445	0.445	0.000	0.977	0.985646017699115	-0.001
Precentral gyrus medial segment L	0.306	0.306	0.000	0.817	0.9804	-0.013
Precentral gyrus medial segment R	0.361	0.362	0.001	0.601	1	-0.028

Precuneus L	0.453	0.454	0.001	0.528	1	-0.031
Precuneus R	0.496	0.498	0.001	0.397	1	-0.040
Putamen L	0.293	0.293	0.000	0.896	1	-0.007
Putamen R	0.298	0.298	0.000	0.728	0.988	-0.019
Subcallosal area L	0.470	0.471	0.001	0.439	1	0.037
Subcallosal area R	0.411	0.412	0.001	0.521	1	0.033
Superior frontal gyrus L	0.441	0.446	0.005	0.124	1	-0.076
Superior frontal gyrus R	0.462	0.463	0.001	0.629592	1	-0.023
Superior frontal gyrus medial segment L	0.420	0.422	0.002	0.418139	1	-0.041
Superior frontal gyrus medial segment R	0.392	0.393	0.000	0.705	0.968313253012048	-0.020
Superior occipital gyrus L	0.253	0.254	0.001	0.595	1	-0.030
Superior occipital gyrus R	0.256	0.260	0.003	0.287	1	-0.061
Superior parietal lobule L	0.379	0.379	0.001	0.654	1	-0.023
Superior parietal lobule R	0.395	0.396	0.001	0.651	1	-0.023
Superior temporal gyrus L	0.358	0.358	0.000	0.760	0.952087912087912	0.016
Superior temporal gyrus R	0.383	0.383	0.000	0.692	0.973925925925926	-0.021
Supplementary motor cortex L	0.393	0.398	0.006	0.134	1	-0.077
Supplementary motor cortex R	0.372	0.376	0.004	0.234792	1	-0.062
Supramarginal gyrus L	0.302	0.304	0.002	0.384	1	0.048
Supramarginal gyrus R	0.362	0.364	0.002	0.359	1	0.049
Temporal pole L	0.356	0.359	0.003	0.301	1	-0.055
Temporal pole R	0.375	0.378	0.004	0.230	1	-0.063
Thalamus proper L	0.272	0.287	0.015	0.023	1	0.128
Thalamus proper R	0.304	0.308	0.004	0.221	1	0.068
Transverse temporal gyrus L	0.216	0.217	0.001	0.498	1	-0.040
Transverse temporal gyrus R	0.308	0.310	0.002	0.444	1	-0.042
Triangular part of the inferior frontal gyrus L	0.263	0.264	0.000	0.734	0.984423529411765	-0.019
Triangular part of the inferior frontal gyrus R	0.256	0.0256	0.000	0.968	0.994162162162162	0.002

FDR: false discovery rate. L: left. PRS: polygenic risk score. R: right.

Table D.62: Associations between PRSwithoutAPOE Threshold 1 and 114 regions of interest in amyloid positive participants

Region of Interest	R Square (Model 1)	R Square (Model 2)	R Square Change	Sig. F Change (Model 2)	FDR Corrected value	Standardised beta of PRS
Accumbens area L	0.398	0.400	0.003	0.171	0.928285714285714	-0.052
Accumbens area R	0.374	0.376	0.002	0.229	1	-0.046
Amygdala L	0.383	0.384	0.000	0.691	1	-0.015
Amygdala R	0.444	0.444	0.000	0.963	0.989027027027027	-0.002
Angular gyrus L	0.391	0.391	0.000	0.790	1	0.010
Angular gyrus R	0.430	0.431	0.000	0.888	1	-0.005
Anterior cingulate gyrus L	0.388	0.388	0.000	0.872	1	0.006
Anterior cingulate gyrus R	0.224	0.225	0.001	0.406	1	-0.036
Anterior insula L	0.401	0.401	0.000	0.692	1	-0.015
Anterior insula R	0.415	0.418	0.003	0.142	0.952235294117647	-0.055
Anterior orbital gyrus L	0.413	0.413	0.000	0.691	1	0.015
Anterior orbital gyrus R	0.390	0.390	0.000	0.698	1	0.015
Basal forebrain L	0.261	0.264	0.002	0.221	1	-0.051
Basal forebrain R	0.347	0.352	0.004	0.089152	0.923938909090909	-0.067
Calcarine cortex L	0.361	0.361	0.001	0.515	1	0.025
Calcarine cortex R	0.385	0.385	0.000	0.843	1	0.008
Caudate L	0.223	0.230	0.007	0.045	1	-0.086
Caudate R	0.212	0.222	0.010	0.016	1	-0.104
Central operculum L	0.384	0.384	0.000	0.793	1	0.010
Central operculum R	0.399	0.399	0.000	0.901	1	-0.005
Cuneus L	0.441	0.445	0.004	0.073	1	0.065
Cuneus R	0.446	0.446	0.000	0.832	1	0.008
Entorhinal area L	0.397	0.397	0.000	0.808	1	-0.009
Entorhinal area R	0.452	0.453	0.000	0.757	1	-0.011
Frontal operculum L	0.392	0.392	0.000	0.991	0.999769911504425	0.000
Frontal operculum R	0.320	0.320	0.000	0.809549	1	0.010

Frontal pole L	0.469	0.474	0.004	0.055	1	0.068
Frontal pole R	0.431	0.436	0.005	0.046	1	0.073
Fusiform gyrus L	0.510	0.512	0.002	0.190	0.984545454545455	0.045
Fusiform gyrus R	0.538	0.539	0.000	0.497	1	0.022
Gyrus rectus L	0.451	0.451	0.000	0.904	1	-0.004
Gyrus rectus R	0.464	0.464	0.000	0.776	1	-0.010
Hippocampus L	0.422	0.423	0.002	0.272	1	-0.041
Hippocampus R	0.442	0.444	0.002	0.210	1	-0.046
Inferior occipital gyrus L	0.424	0.425	0.001	0.528	1	0.023
Inferior occipital gyrus R	0.479	0.481	0.002	0.161	0.9177	0.049
Inferior temporal gyrus L	0.493	0.494	0.001	0.500	1	-0.023
Inferior temporal gyrus R	0.540	0.540	0.000	0.966	0.98325	0.001
Lateral orbital gyrus L	0.433	0.433	0.000	0.909324	1	-0.004
Lateral orbital gyrus R	0.408	0.408	0.000	0.780	1	-0.010
Lingual gyrus L	0.506	0.507	0.001	0.249	1	0.039
Lingual gyrus R	0.517	0.519	0.002	0.137	0.976125	0.050
Medial frontal cortex L	0.348	0.349	0.000	0.616	1	-0.020
Medial frontal cortex R	0.371	0.372	0.002	0.260	0.988	0.043
Medial orbital gyrus L	0.483	0.483	0.000	0.630	1	-0.017
Medial orbital gyrus R	0.468	0.468	0.000	0.994	0.994	0.000
Middle cingulate gyrus L	0.397	0.397	0.000	0.768	1	-0.011
Middle cingulate gyrus R	0.332	0.332	0.000	0.632	1	0.019
Middle frontal gyrus L	0.498	0.198	0.001	0.452	1	0.026
Middle frontal gyrus R	0.504	0.504	0.000	0.935	1	-0.003
Middle occipital gyrus L	0.360	0.360	0.000	0.778	1	0.011
Middle occipital gyrus R	0.354	0.354	0.000	0.880499	1	0.006
Middle temporal gyrus L	0.480	0.480	0.000	0.684	1	-0.014
Middle temporal gyrus R	0.520	0.520	0.000	0.931	1	-0.003
Occipital fusiform gyrus L	0.470	0.474	0.003	0.090	0.855	0.060
Occipital fusiform gyrus R	0.517	0.518	0.001	0.292	0.951085714285714	0.036

Occipital pole L	0.328	0.332	0.004	0.093	0.815538461538462	0.067
Occipital pole R	0.396	0.397	0.001	0.344	1	0.036
Opercular part of the inferior frontal gyrus L	0.302	0.303	0.000	0.635	1	-0.019
Opercular part of the inferior frontal gyrus R	0.270	0.270	0.000	0.810183	1	-0.010
Orbital part of the inferior frontal gyrus L	0.275	0.275	0.000	0.700	1	-0.016
Orbital part of the inferior frontal gyrus R	0.310	0.316	0.006	0.054493	1	-0.078
Pallidum L	0.120	0.120	0.000	0.856	1	-0.008
Pallidum R	0.103	0.104	0.001	0.545	1	-0.028
Parahippocampal gyrus L	0.477	0.477	0.001	0.470	1	0.025
Parahippocampal gyrus R	0.514	0.515	0.001	0.420	1	0.027
Parietal operculum L	0.314	0.314	0.000	0.781	1	0.011
Parietal operculum R	0.294	0.294	0.000	0.947105	0.990550183486238	0.003
Planum polare L	0.457	0.457	0.000	0.696	1	0.014
Planum polare R	0.466	0.466	0.000	0.525	1	-0.023
Planum temporale L	0.354	0.355	0.002	0.298	0.943666666666667	-0.041
Planum temporale R	0.329	0.329	0.000	0.752	1	0.013
Postcentral gyrus L	0.394	0.394	0.000	0.688	1	0.015
Postcentral gyrus R	0.411	0.412	0.001	0.441	1	0.029
Postcentral gyrus medial segment L	0.186	0.186	0.000	0.640	1	0.021
Postcentral gyrus medial segment R	0.245	0.245	0.000	0.946755	0.9993525	0.003
Posterior cingulate gyrus L	0.546	0.547	0.001	0.290	0.972352941176471	-0.035
Posterior cingulate gyrus R	0.511	0.512	0.001	0.478	1	-0.024
Posterior insula L	0.395	0.395	0.000	0.899	1	0.005
Posterior insula R	0.423	0.423	0.000	0.535	1	0.023
Posterior orbital gyrus L	0.348	0.348	0.000	0.909473	1	0.004
Posterior orbital gyrus R	0.394	0.395	0.000	0.576	1	-0.021
Precentral gyrus L	0.457	0.458	0.000	0.706	1	0.013
Precentral gyrus R	0.448	0.448	0.000	0.950	0.984545454545455	-0.002
Precentral gyrus medial segment L	0.286	0.286	0.000	0.937	0.998299065420561	-0.003
Precentral gyrus medial segment R	0.315	0.315	0.000	0.924	1	0.004

Precuneus L	0.499	0.499	0.000	0.717	1	0.012
Precuneus R	0.482	0.482	0.001	0.460	1	0.026
Putamen L	0.280	0.282	0.002	0.273	0.9725625	-0.045
Putamen R	0.285	0.289	0.004	0.118	0.960857142857143	-0.064
Subcallosal area L	0.478	0.480	0.002	0.149	0.943666666666667	-0.051
Subcallosal area R	0.473	0.474	0.001	0.409	1	-0.029
Superior frontal gyrus L	0.468	0.472	0.004	0.085	1	-0.061
Superior frontal gyrus R	0.499	0.499	0.000	0.817	1	-0.008
Superior frontal gyrus medial segment L	0.421	0.423	0.002	0.255	1	-0.042
Superior frontal gyrus medial segment R	0.397	0.397	0.000	0.647	1	0.017
Superior occipital gyrus L	0.353	0.356	0.003	0.130	0.988	0.059
Superior occipital gyrus R	0.366	0.370	0.004	0.088945	1	0.066
Superior parietal lobule L	0.392	0.393	0.002	0.230	1	0.045
Superior parietal lobule R	0.377	0.378	0.001	0.418	1	0.031
Superior temporal gyrus L	0.442	0.442	0.000	0.661	1	-0.016
Superior temporal gyrus R	0.387	0.389	0.002	0.279	0.963818181818182	0.041
Supplementary motor cortex L	0.341	0.342	0.000	0.579	1	-0.022
Supplementary motor cortex R	0.378	0.379	0.000	0.879683	1	-0.006
Supramarginal gyrus L	0.377	0.378	0.002	0.259	1	0.043
Supramarginal gyrus R	0.340	0.345	0.005	0.071	1	0.071
Temporal pole L	0.409	0.409	0.000	0.553	1	-0.022
Temporal pole R	0.405	0.405	0.000	0.891	1	-0.005
Thalamus proper L	0.221	0.225	0.004	0.155	0.93	-0.061
Thalamus proper R	0.239	0.245	0.006	0.053550	1	-0.082
Transverse temporal gyrus L	0.299	0.299	0.000	0.879697	1	0.006
Transverse temporal gyrus R	0.332	0.332	0.000	0.840	1	0.008
Triangular part of the inferior frontal gyrus L	0.349	0.349	0.000	0.801	1	-0.010
Triangular part of the inferior frontal gyrus R	0.324	0.324	0.000	0.586	1	-0.022

FDR: false discovery rate. L: left. PRS: polygenic risk score. R: right.

Table D.63: Associations between PRSwithoutAPOE Threshold 5 and 114 regions of interest in amyloid negative participants

Region of Interest	R Square (Model 1)	R Square (Model 2)	R Square Change	Sig. F Change (Model 2)	FDR Corrected value	Standardised beta of PRS
Accumbens area L	0.390	0.390	0.000	0.746	1	0.017
Accumbens area R	0.433	0.433	0.000	0.994	1	0.000
Amygdala L	0.444	0.449	0.006	0.118	1	-0.077
Amygdala R	0.461	0.471	0.010	0.029	1	-0.106
Angular gyrus L	0.428	0.428	0.000	0.987	1	0.001
Angular gyrus R	0.370	0.376	0.006	0.137	1	0.078
Anterior cingulate gyrus L	0.444	0.444	0.000	0.949	1	0.003
Anterior cingulate gyrus R	0.269	0.273	0.004	0.247	1	-0.066
Anterior insula L	0.347	0.348	0.001	0.558	1	-0.031
Anterior insula R	0.345	0.346	0.001	0.595	1	-0.029
Anterior orbital gyrus L	0.384	0.385	0.000	0.742082	1	-0.017
Anterior orbital gyrus R	0.323	0.325	0.002	0.460	1	0.040
Basal forebrain L	0.348	0.350	0.002	0.382	1	-0.047
Basal forebrain R	0.382	0.386	0.004	0.213	1	-0.065
Calcarine cortex L	0.388	0.389	0.000	0.879	1	-0.008
Calcarine cortex R	0.368	0.369	0.001	0.571	1	-0.030
Caudate L	0.189	0.190	0.001	0.601	1	0.031
Caudate R	0.183	0.183	0.001	0.681	1	0.025
Central operculum L	0.351	0.353	0.002	0.373	1	0.048
Central operculum R	0.322	0.327	0.004	0.210	1	0.068
Cuneus L	0.337	0.337	0.000	0.995	0.995	0.000
Cuneus R	0.377	0.379	0.002	0.330	1	-0.051
Entorhinal area L	0.374	0.374	0.000	0.856	1	-0.010
Entorhinal area R	0.422	0.423	0.001	0.478	1	-0.036
Frontal operculum L	0.298	0.299	0.000	0.792163	1	-0.015
Frontal operculum R	0.309	0.313	0.004	0.258	1	-0.062

Frontal pole L	0.369	0.370	0.001	0.546	1	0.032
Frontal pole R	0.398	0.398	0.000	0.939	1	-0.004
Fusiform gyrus L	0.471	0.471	0.000	0.903	1	0.006
Fusiform gyrus R	0.495	0.495	0.000	0.970	1	-0.002
Gyrus rectus L	0.392	0.393	0.001	0.536	1	0.032
Gyrus rectus R	0.412	0.413	0.000	0.755	1	0.016
Hippocampus L	0.430	0.444	0.014	0.012397	0.706629	-0.124
Hippocampus R	0.490	0.503	0.013	0.012029	1	-0.118
Inferior occipital gyrus L	0.379	0.379	0.000	0.710	1	0.019
Inferior occipital gyrus R	0.432	0.434	0.001	0.434	1	0.039
Inferior temporal gyrus L	0.495	0.496	0.002	0.341	1	-0.045
Inferior temporal gyrus R	0.533	0.534	0.001	0.458	1	-0.034
Lateral orbital gyrus L	0.391	0.391	0.000	0.968295	1	0.002
Lateral orbital gyrus R	0.308	0.310	0.002	0.464306	1	-0.040
Lingual gyrus L	0.500	0.500	0.001	0.532	1	0.029
Lingual gyrus R	0.537	0.537	0.000	0.954	1	0.003
Medial frontal cortex L	0.376	0.376	0.000	0.873	1	-0.008
Medial frontal cortex R	0.354	0.354	0.000	0.953	1	-0.003
Medial orbital gyrus L	0.469	0.471	0.002	0.307	1	0.049
Medial orbital gyrus R	0.385	0.386	0.001	0.513	1	0.034
Middle cingulate gyrus L	0.400	0.400	0.000	0.835	1	-0.011
Middle cingulate gyrus R	0.382	0.386	0.005	0.167	1	-0.072
Middle frontal gyrus L	0.441	0.443	0.002	0.371	1	0.044
Middle frontal gyrus R	0.403	0.403	0.000	0.984	1	-0.001
Middle occipital gyrus L	0.385	0.386	0.000	0.844	1	0.010
Middle occipital gyrus R	0.347	0.348	0.001	0.652	1	0.024
Middle temporal gyrus L	0.521	0.521	0.000	0.931	1	0.004
Middle temporal gyrus R	0.503	0.507	0.004	0.143	1	0.068
Occipital fusiform gyrus L	0.464	0.464	0.001	0.556	1	0.029
Occipital fusiform gyrus R	0.501	0.505	0.004	0.182	1	0.063

Occipital pole L	0.323	0.325	0.001	0.484	1	-0.038
Occipital pole R	0.336	0.338	0.002	0.410	1	0.045
Opercular part of the inferior frontal gyrus L	0.188	0.188	0.000	0.908	1	-0.007
Opercular part of the inferior frontal gyrus R	0.277	0.278	0.000	0.704	1	-0.021
Orbital part of the inferior frontal gyrus L	0.289	0.290	0.000	0.792067	1	0.015
Orbital part of the inferior frontal gyrus R	0.188	0.188	0.000	0.960	1	0.003
Pallidum L	0.187	0.189	0.002	0.413	1	0.049
Pallidum R	0.157	0.158	0.001	0.633	1	0.029
Parahippocampal gyrus L	0.483	0.484	0.001	0.607	1	-0.025
Parahippocampal gyrus R	0.491	0.491	0.000	0.955	1	-0.003
Parietal operculum L	0.355	0.355	0.000	0.841	1	-0.011
Parietal operculum R	0.267	0.267	0.000	0.818	1	0.013
Planum polare L	0.385	0.391	0.006	0.121	1	-0.081
Planum polare R	0.424	0.426	0.002	0.339	1	-0.048
Planum temporale L	0.346	0.347	0.000	0.699	1	0.021
Planum temporale R	0.375	0.375	0.000	0.742468	1	-0.017
Postcentral gyrus L	0.390	0.394	0.004	0.224	1	-0.063
Postcentral gyrus R	0.349	0.349	0.000	0.875	1	0.008
Postcentral gyrus medial segment L	0.213	0.213	0.000	0.840	1	0.012
Postcentral gyrus medial segment R	0.196	0.197	0.002	0.477	1	-0.042
Posterior cingulate gyrus L	0.517	0.520	0.002	0.311	1	-0.047
Posterior cingulate gyrus R	0.477	0.478	0.001	0.464386	1	-0.035
Posterior insula L	0.388	0.388	0.000	0.795	1	0.013
Posterior insula R	0.408	0.408	0.001	0.593	1	0.027
Posterior orbital gyrus L	0.423	0.423	0.000	0.881	1	0.008
Posterior orbital gyrus R	0.377	0.382	0.006	0.138	1	-0.078
Precentral gyrus L	0.476	0.477	0.001	0.455	1	-0.036
Precentral gyrus R	0.445	0.445	0.000	0.900	1	-0.006
Precentral gyrus medial segment L	0.306	0.306	0.000	0.855	1	-0.010
Precentral gyrus medial segment R	0.361	0.361	0.000	0.763	1	-0.016

Precuneus L	0.453	0.453	0.000	0.703	1	-0.019
Precuneus R	0.496	0.497	0.001	0.469	1	-0.034
Putamen L	0.293	0.293	0.000	0.917	1	-0.006
Putamen R	0.298	0.298	0.000	0.956	1	-0.003
Subcallosal area L	0.470	0.471	0.001	0.411	1	0.040
Subcallosal area R	0.411	0.412	0.002	0.392	1	0.044
Superior frontal gyrus L	0.441	0.443	0.002	0.386	1	-0.043
Superior frontal gyrus R	0.462	0.462	0.000	0.927	1	0.004
Superior frontal gyrus medial segment L	0.420	0.424	0.003	0.236	1	-0.060
Superior frontal gyrus medial segment R	0.392	0.393	0.001	0.495	1	-0.035
Superior occipital gyrus L	0.253	0.253	0.000	0.897	1	-0.007
Superior occipital gyrus R	0.256	0.261	0.005	0.209	1	-0.072
Superior parietal lobule L	0.379	0.379	0.000	0.967850	1	-0.002
Superior parietal lobule R	0.395	0.395	0.000	0.899	1	-0.007
Superior temporal gyrus L	0.358	0.359	0.001	0.579	1	0.029
Superior temporal gyrus R	0.383	0.383	0.001	0.618	1	-0.026
Supplementary motor cortex L	0.393	0.396	0.003	0.234	1	-0.061
Supplementary motor cortex R	0.372	0.374	0.002	0.390	1	-0.045
Supramarginal gyrus L	0.302	0.307	0.004	0.221	1	0.068
Supramarginal gyrus R	0.362	0.371	0.009	0.068	1	0.096
Temporal pole L	0.356	0.358	0.002	0.418	1	-0.043
Temporal pole R	0.375	0.376	0.002	0.383	1	-0.046
Thalamus proper L	0.272	0.280	0.007	0.122	1	0.087
Thalamus proper R	0.304	0.305	0.001	0.664	1	0.024
Transverse temporal gyrus L	0.216	0.219	0.003	0.305	1	-0.060
Transverse temporal gyrus R	0.308	0.312	0.004	0.232	1	-0.066
Triangular part of the inferior frontal gyrus L	0.263	0.264	0.000	0.734	1	-0.019
Triangular part of the inferior frontal gyrus R	0.256	0.256	0.000	0.943	1	0.004

FDR: false discovery rate. L: left. PRS: polygenic risk score. R: right.

Table D.64: Associations between PRSwithoutAPOE Threshold 5 and 114 regions of interest in amyloid positive participants

Region of Interest	R Square (Model 1)	R Square (Model 2)	R Square Change	Sig. F Change (Model 2)	FDR Corrected value	Standardised beta of PRS
Accumbens area L	0.398	0.399	0.000	0.320	1	-0.038
Accumbens area R	0.374	0.375	0.001	0.402	1	-0.032
Amygdala L	0.383	0.384	0.001	0.520	0.92625	-0.025
Amygdala R	0.444	0.444	0.000	0.997	0.997	0.000
Angular gyrus L	0.391	0.391	0.000	0.830	1	0.008
Angular gyrus R	0.430	0.430	0.000	0.936	0.997233644859813	-0.003
Anterior cingulate gyrus L	0.388	0.388	0.000	0.836	0.982515463917526	0.008
Anterior cingulate gyrus R	0.224	0.224	0.000	0.851	0.979939393939394	0.008
Anterior insula L	0.401	0.401	0.000	0.606221	0.933908027027027	0.020
Anterior insula R	0.415	0.416	0.001	0.443	1	-0.029
Anterior orbital gyrus L	0.413	0.414	0.001	0.490	0.915737704918033	0.026
Anterior orbital gyrus R	0.390	0.391	0.001	0.306	1	0.039
Basal forebrain L	0.261	0.262	0.000	0.615	0.910519480519481	-0.021
Basal forebrain R	0.347	0.348	0.001	0.459	0.987283018867925	-0.029
Calcarine cortex L	0.361	0.361	0.000	0.918	1	0.004
Calcarine cortex R	0.385	0.385	0.000	0.908	1	-0.004
Caudate L	0.223	0.226	0.004	0.153	0.918	-0.062
Caudate R	0.212	0.220	0.008	0.032	1	-0.093
Central operculum L	0.384	0385	0.001	0.335	1	0.037
Central operculum R	0.399	0.399	0.000	0.790	0.98967032967033	0.010
Cuneus L	0.441	0.445	0.004	0.087	0.9918	0.063
Cuneus R	0.446	0.447	0.001	0.303	1	0.038
Entorhinal area L	0.397	0.397	0.000	0.729	0.989357142857143	-0.013
Entorhinal area R	0.452	0.452	0.000	0.953525	0.997264678899082	0.002
Frontal operculum L	0.392	0.394	0.002	0.198504	1	0.049
Frontal operculum R	0.320	0.322	0.002	0.250	1	0.046

Frontal pole L	0.469	0.478	0.009	0.006	0.684	0.097
Frontal pole R	0.431	0.438	0.007	0.017	0.969	0.088
Fusiform gyrus L	0.510	0.515	0.005	0.038	0.8664	0.071
Fusiform gyrus R	0.538	0.540	0.002	0.129	0.9804	0.050
Gyrus rectus L	0.451	0.452	0.001	0.450	1	0.027
Gyrus rectus R	0.464	0.464	0.000	0.745	0.987558139534884	-0.012
Hippocampus L	0.422	0.425	0.003	0.157	0.8949	-0.053
Hippocampus R	0.442	0.444	0.002	0.191	1	-0.048
Inferior occipital gyrus L	0.424	0.425	0.000	0.594	0.967371428571429	0.020
Inferior occipital gyrus R	0.479	0.482	0.003	0.114	0.999692307692308	0.056
Inferior temporal gyrus L	0.493	0.494	0.000	0.612	0.918	-0.018
Inferior temporal gyrus R	0.540	0.540	0.000	0.834	0.990375	0.007
Lateral orbital gyrus L	0.433	0.434	0.001	0.441	1	0.028
Lateral orbital gyrus R	0.408	0.409	0.001	0.452	0.990923076923077	0.028
Lingual gyrus L	0.506	0.507	0.002	0.236	1	0.041
Lingual gyrus R	0.517	0.519	0.002	0.146	0.924666666666667	0.049
Medial frontal cortex L	0.348	0.349	0.000	0.723	0.993036144578313	0.014
Medial frontal cortex R	0.371	0.375	0.005	0.068	0.861333333333333	0.071
Medial orbital gyrus L	0.483	0.483	0.000	0.646	0.944153846153846	0.016
Medial orbital gyrus R	0.468	0.468	0.000	0.556	0.946029850746269	0.021
Middle cingulate gyrus L	0.397	0.397	0.000	0.605800	0.946043835616438	0.020
Middle cingulate gyrus R	0.332	0.334	0.002	0.223	1	0.049
Middle frontal gyrus L	0.498	0.498	0.001	0.407	1	0.029
Middle frontal gyrus R	0.504	0.504	0.000	0.924	1	0.003
Middle occipital gyrus L	0.360	0.360	0.000	0.717	0.99680487804878	0.014
Middle occipital gyrus R	0.354	0.354	0.000	0.597	0.95856338028169	0.021
Middle temporal gyrus L	0.480	0.481	0.001	0.363	0.99066	-0.032
Middle temporal gyrus R	0.520	0.520	0.000	0.869	1	-0.006
Occipital fusiform gyrus L	0.470	0.474	0.004	0.067	0.95475	0.065
Occipital fusiform gyrus R	0.517	0.52	0.002	0.136	0.969	0.051

Occipital pole L	0.328	0.331	0.003	0.142	0.952235294117647	0.059
Occipital pole R	0.396	0.397	0.001	0.302	1	0.039
Opercular part of the inferior frontal gyrus L	0.302	0.302	0.000	0.850	0.988775510204082	0.008
Opercular part of the inferior frontal gyrus R	0.270	0.271	0.001	0.461	0.973222222222222	0.031
Orbital part of the inferior frontal gyrus L	0.275	0.275	0.000	0.954360	0.989064	0.002
Orbital part of the inferior frontal gyrus R	0.310	0.312	0.001	0.354	1	-0.038
Pallidum L	0.12	0.121	0.001	0.550	0.95	-0.027
Pallidum R	0.103	0.105	0.002	0.324	1	-0.046
Parahippocampal gyrus L	0.477	0.477	0.000	0.705	0.992222222222222	0.013
Parahippocampal gyrus R	0.514	0.514	0.000	0.568	0.952235294117647	0.019
Parietal operculum L	0.314	0.316	0.002	0.237	1	0.048
Parietal operculum R	0.294	0.297	0.003	0.199129	0.986987217391304	0.053
Planum polare L	0.457	0.457	0.000	0.735	0.985764705882353	0.012
Planum polare R	0.466	0.466	0.000	0.946	0.998555555555556	-0.002
Planum temporale L	0.354	0.355	0.001	0.352	1	-0.037
Planum temporale R	0.329	0.329	0.000	0.831	1	0.009
Postcentral gyrus L	0.394	0.394	0.000	0.919	1	-0.004
Postcentral gyrus R	0.411	0.411	0.000	0.779	0.997820224719101	0.011
Postcentral gyrus medial segment L	0.186	0.486	0.000	0.996	1	0.000
Postcentral gyrus medial segment R	0.245	0.246	0.001	0.403	1	0.036
Posterior cingulate gyrus L	0.546	0.547	0.001	0.416	1	-0.027
Posterior cingulate gyrus R	0.511	0.512	0.001	0.485	0.9215	-0.024
Posterior insula L	0.395	0.397	0.002	0.277	1	0.041
Posterior insula R	0.423	0.426	0.003	0.102629	0.9749755	0.061
Posterior orbital gyrus L	0.348	0.349	0.001	0.476	0.952	0.028
Posterior orbital gyrus R	0.394	0.394	0.000	0.987	1	0.001
Precentral gyrus L	0.457	0.458	0.000	0.548	0.961107692307692	0.022
Precentral gyrus R	0.448	0.449	0.001	0.449	1	0.028
Precentral gyrus medial segment L	0.286	0.286	0.000	0.753	0.986689655172414	-0.013
Precentral gyrus medial segment R	0.315	0.315	0.000	0.872	0.984237623762376	0.007

Precuneus L	0.499	0.499	0.000	0.591	0.976434782608696	0.019
Precuneus R	0.482	0.482	0.001	0.434	1	0.028
Putamen L	0.280	0.281	0.001	0.426	1	-0.033
Putamen R	0.285	0.287	0.002	0.285	1	-0.044
Subcallosal area L	0.478	0.478	0.000	0.832	0.9984	-0.007
Subcallosal area R	0.473	0.473	0.000	0.689	0.981825	0.014
Superior frontal gyrus L	0.468	0.468	0.000	0.605	0.957916666666667	-0.018
Superior frontal gyrus R	0.499	0.499	0.001	0.481	0.929389830508475	0.024
Superior frontal gyrus medial segment L	0.421	0.422	0.001	0.477	0.937551724137931	-0.026
Superior frontal gyrus medial segment R	0.397	0.397	0.000	0.787	0.996866666666667	0.010
Superior occipital gyrus L	0.353	0.358	0.006	0.051	0.830571428571429	0.077
Superior occipital gyrus R	0.366	0.372	0.006	0.036	1	0.082
Superior parietal lobule L	0.392	0.395	0.003	0.127	1	0.058
Superior parietal lobule R	0.377	0.378	0.000	0.608	0.92416	0.020
Superior temporal gyrus L	0.442	0.443	0.001	0.417	1	-0.030
Superior temporal gyrus R	0.387	0.388	0.001	0.470	0.956785714285714	0.028
Supplementary motor cortex L	0.341	0.342	0.001	0.465	0.963818181818182	-0.029
Supplementary motor cortex R	0.378	0.378	0.000	0.983	1	-0.001
Supramarginal gyrus L	0.377	0.379	0.002	0.220	1	0.047
Supramarginal gyrus R	0.340	0.346	0.006	0.049	0.931	0.078
Temporal pole L	0.409	0.409	0.001	0.501	0.906571428571429	-0.025
Temporal pole R	0.405	0.405	0.000	0.932	1	-0.003
Thalamus proper L	0.221	0.223	0.001	0.379	1	-0.038
Thalamus proper R	0.239	0.243	0.005	0.102506	1	-0.070
Transverse temporal gyrus L	0.299	0.299	0.000	0.807	0.999978260869565	0.010
Transverse temporal gyrus R	0.332	0.333	0.001	0.499	0.917516129032258	0.027
Triangular part of the inferior frontal gyrus L	0.349	0.349	0.000	0.777	1	0.011
Triangular part of the inferior frontal gyrus R	0.324	0.324	0.000	0.685	0.988481012658228	0.016

FDR: false discovery rate. L: left. PRS: polygenic risk score. R: right.

Table D.65: Associations between PRSwithoutAPOE Threshold 10 and 114 regions of interest in amyloid negative participants

Region of Interest	R Square (Model 1)	R Square (Model 2)	R Square Change	Sig. F Change (Model 2)	FDR Corrected value	Standardised beta of PRS
Accumbens area L	0.390	0.392	0.002	0.359	0.852625	-0.050
Accumbens area R	0.433	0.431	0.001	0.609	0.977830985915493	-0.027
Amygdala L	0.444	0.459	0.015	0.010	0.285	-0.134
Amygdala R	0.461	0.474	0.013	0.014	0.3192	-0.125
Angular gyrus L	0.428	0.428	0.000	0.774	0.9804	-0.015
Angular gyrus R	0.370	0.372	0.001	0.462	0.993735849056604	0.041
Anterior cingulate gyrus L	0.444	0.445	0.001	0.628	0.967459459459459	-0.025
Anterior cingulate gyrus R	0.269	0.272	0.003	0.328	0.849818181818182	-0.058
Anterior insula L	0.347	0.353	0.007	0.116	0.8265	-0.088
Anterior insula R	0.345	0.349	0.004	0.220	0.864827586206896	-0.069
Anterior orbital gyrus L	0.384	0.388	0.004	0.225	0.82741935483871	-0.066
Anterior orbital gyrus R	0.323	0.324	0.000	0.781	0.967760869565217	-0.016
Basal forebrain L	0.348	0.368	0.020	0.005521	0.314697	-0.155
Basal forebrain R	0.382	0.393	0.012	0.031	0.44175	-0.118
Calcarine cortex L	0.388	0.391	0.003	0.279	0.837	-0.059
Calcarine cortex R	0.368	0.371	0.003	0.311	0.824511627906977	-0.056
Caudate L	0.189	0.190	0.001	0.530	1	-0.039
Caudate R	0.183	0.183	0.000	0.949	1	-0.004
Central operculum L	0.351	0.351	0.000	0.981	1	-0.001
Central operculum R	0.322	0.322	0.000	0.925	1	-0.005
Cuneus L	0.337	0.340	0.003	0.308	0.836	-0.058
Cuneus R	0.377	0.384	0.007	0.103	0.903230769230769	-0.089
Entorhinal area L	0.374	0.378	0.004	0.196570	0.861883846153846	-0.071
Entorhinal area R	0.422	0.425	0.003	0.250	0.77027027027027	-0.061
Frontal operculum L	0.298	0.300	0.002	0.420	0.9576	-0.047
Frontal operculum R	0.309	0.315	0.006	0.155	0.93	-0.082

Frontal pole L	0.369	0.369	0.000	0.710	0.941162790697674	-0.021
Frontal pole R	0.398	0.399	0.001	0.648	0.98496	-0.025
Fusiform gyrus L	0.471	0.471	0.000	0.995	0.995	0.000
Fusiform gyrus R	0.495	0.495	0.000	0.889	1	0.007
Gyrus rectus L	0.392	0.396	0.004	0.196508	0.89607648	-0.070
Gyrus rectus R	0.412	0.413	0.001	0.538	0.97352380952381	-0.033
Hippocampus L	0.430	0.452	0.022	0.002	0.228	-0.161
Hippocampus R	0.490	0.501	0.011	0.023	0.437	-0.113
Inferior occipital gyrus L	0.379	0.379	0.000	0.815	0.988404255319149	-0.013
Inferior occipital gyrus R	0.432	0.432	0.000	0.934	1	0.004
Inferior temporal gyrus L	0.495	0.497	0.003	0.242	0.766333333333333	-0.058
Inferior temporal gyrus R	0.533	0.534	0.001	0.569	0.982818181818182	-0.027
Lateral orbital gyrus L	0.391	0.391	0.000	0.775	0.970879120879121	-0.016
Lateral orbital gyrus R	0.308	0.316	0.008	0.091	0.8645	-0.098
Lingual gyrus L	0.500	0.500	0.000	0.711	0.931655172413793	-0.018
Lingual gyrus R	0.537	0.537	0.000	0.891	1	0.006
Medial frontal cortex L	0.376	0.382	0.006	0.126	0.798	-0.084
Medial frontal cortex R	0.354	0.355	0.001	0.533	0.996098360655738	-0.035
Medial orbital gyrus L	0.469	0.469	0.000	0.674	0.96045	-0.021
Medial orbital gyrus R	0.385	0.386	0.001	0.471	0.976254545454545	-0.039
Middle cingulate gyrus L	0.400	0.400	0.000	0.736	0.953454545454545	-0.018
Middle cingulate gyrus R	0.382	0.385	0.004	0.223	0.8474	-0.067
Middle frontal gyrus L	0.441	0.441	0.001	0.581	0.988567164179104	0.029
Middle frontal gyrus R	0.403	0.404	0.001	0.529	1	-0.034
Middle occipital gyrus L	0.385	0.386	0.001	0.535	0.983709677419355	-0.034
Middle occipital gyrus R	0.347	0.349	0.002	0.437	0.976823529411765	-0.044
Middle temporal gyrus L	0.521	0.521	0.000	0.938	0.875110636363636	-0.004
Middle temporal gyrus R	0.503	0.506	0.004	0.168881	1	0.067
Occipital fusiform gyrus L	0.464	0.464	0.001	0.623	0.972904109589041	0.025
Occipital fusiform gyrus R	0.501	0.505	0.004	0.167989	0.911940285714286	0.068

Occipital pole L	0.323	0.330	0.007	0.109	0.887571428571429	-0.092
Occipital pole R	0.336	0.336	0.000	0.907	1	-0.007
Opercular part of the inferior frontal gyrus L	0.188	0.189	0.001	0.586	0.982411764705882	-0.034
Opercular part of the inferior frontal gyrus R	0.277	0.278	0.001	0.655	0.96974025974026	-0.026
Orbital part of the inferior frontal gyrus L	0.289	0.290	0.000	0.690	0.959268292682927	-0.023
Orbital part of the inferior frontal gyrus R	0.188	0.189	0.002	0.497	0.994	-0.043
Pallidum L	0.187	0.189	0.002	0.401	0.932938775510204	0.053
Pallidum R	0.157	0.161	0.004	0.284	0.830153846153846	0.068
Parahippocampal gyrus L	0.483	0.486	0.003	0.235	0.811818181818182	-0.059
Parahippocampal gyrus R	0.491	0.492	0.001	0.622	0.984833333333333	-0.025
Parietal operculum L	0.355	0.355	0.000	0.753	0.964516853932584	-0.018
Parietal operculum R	0.267	0.267	0.000	0.838	0.995125	-0.012
Planum polare L	0.385	0.404	0.019	0.005636	0.214168	-0.150
Planum polare R	0.424	0.428	0.004	0.198	0.836	-0.068
Planum temporale L	0.346	0.347	0.000	0.688	0.968296296296296	-0.023
Planum temporale R	0.375	0.376	0.001	0.452	0.990923076923077	-0.041
Postcentral gyrus L	0.390	0.395	0.004	0.185	0.87875	-0.072
Postcentral gyrus R	0.349	0.350	0.001	0.660	0.952405063291139	0.025
Postcentral gyrus medial segment L	0.213	0.219	0.006	0.169009	0.837696782608696	0.085
Postcentral gyrus medial segment R	0.196	0.197	0.001	0.564052	1	0.036
Posterior cingulate gyrus L	0.517	0.520	0.001	0.303	0.86355	-0.050
Posterior cingulate gyrus R	0.477	0.477	0.000	0.699	0.937482352941176	-0.019
Posterior insula L	0.388	0.390	0.002	0.357	0.865914893617021	-0.050
Posterior insula R	0.408	0.408	0.000	0.694768	0.954259662650602	-0.021
Posterior orbital gyrus L	0.423	0.426	0.003	0.231	0.8229375	-0.063
Posterior orbital gyrus R	0.377	0.389	0.013	0.024	0.390857142857143	-0.124
Precentral gyrus L	0.476	0.478	0.002	0.346	0.857478260869565	-0.047
Precentral gyrus R	0.445	0.446	0.001	0.491	0.999535714285714	-0.036
Precentral gyrus medial segment L	0.306	0.309	0.003	0.305	0.848048780487805	0.059
Precentral gyrus medial segment R	0.361	0.361	0.001	0.656	0.958769230769231	0.025

Precuneus L	0.453	0.453	0.000	0.888	1	0.007
Precuneus R	0.496	0.496	0.000	0.955	1	0.003
Putamen L	0.293	0.294	0.001	0.564072	0.989295507692308	-0.034
Putamen R	0.298	0.298	0.001	0.650	0.975	-0.026
Subcallosal area L	0.470	0.470	0.000	0.939	1	-0.004
Subcallosal area R	0.411	0.411	0.000	0.993	1	0.000
Superior frontal gyrus L	0.441	0.445	0.004	0.161	0.9177	-0.073
Superior frontal gyrus R	0.462	0.463	0.000	0.807	0.989225806451613	-0.012
Superior frontal gyrus medial segment L	0.420	0.426	0.006	0.125	0.838235294117647	-0.081
Superior frontal gyrus medial segment R	0.392	0.396	0.004	0.219	0.891642857142857	-0.067
Superior occipital gyrus L	0.253	0.255	0.002	0.470	0.992222222222222	-0.043
Superior occipital gyrus R	0.256	0.267	0.010	0.064	0.7296	-0.111
Superior parietal lobule L	0.379	0.379	0.000	0.957	1	0.003
Superior parietal lobule R	0.395	0.396	0.001	0.500	0.982758620689655	-0.037
Superior temporal gyrus L	0.358	0.358	0.000	0.846	0.994268041237113	-0.011
Superior temporal gyrus R	0.383	0.383	0.000	0.833	0.9996	-0.012
Supplementary motor cortex L	0.393	0.396	0.003	0.237	0.794647058823529	-0.064
Supplementary motor cortex R	0.372	0.372	0.000	0.986	1	-0.001
Supramarginal gyrus L	0.302	0.306	0.004	0.241	0.784971428571429	0.068
Supramarginal gyrus R	0.362	0.369	0.007	0.112	0.8512	0.088
Temporal pole L	0.356	0.358	0.002	0.339	0.8588	-0.053
Temporal pole R	0.375	0.375	0.001	0.587	0.969826086956522	-0.030
Thalamus proper L	0.272	0.272	0.000	0.980	1	-0.001
Thalamus proper R	0.304	0.304	0.000	0.953	1	-0.003
Transverse temporal gyrus L	0.216	0.225	0.010	0.082	0.849818181818182	-0.107
Transverse temporal gyrus R	0.308	0.319	0.011	0.052	0.658666666666667	-0.112
Triangular part of the inferior frontal gyrus L	0.263	0.264	0.001	0.602	0.9804	-0.031
Triangular part of the inferior frontal gyrus R	0.256	0.256	0.000	0.694942	0.943135571428571	-0.024

FDR: false discovery rate. L: left. PRS: polygenic risk score. R: right.

Table D.66: Associations between PRSwithoutAPOE Threshold 10 and 114 regions of interest in amyloid positive participants

Region of Interest	R Square (Model 1)	R Square (Model 2)	R Square Change	Sig. F Change (Model 2)	FDR Corrected value	Standardised beta of PRS
Accumbens area L	0.398	0.400	0.002	0.187	0.969	-0.051
Accumbens area R	0.374	0.375	0.001	0.339	0.822255319148936	-0.038
Amygdala L	0.360	0.360	0.001	0.332	0.822782608695652	-0.038
Amygdala R	0.444	0.445	0.000	0.573173	0.827110405063291	-0.021
Angular gyrus L	0.391	0.392	0.002	0.254	0.934064516129032	0.045
Angular gyrus R	0.430	0.432	0.001	0.358	0.770037735849057	0.035
Anterior cingulate gyrus L	0.388	0.388	0.000	0.685	0.918705882352941	0.016
Anterior cingulate gyrus R	0.224	0.226	0.002	0.345	0.80265306122449	0.042
Anterior insula L	0.401	0.401	0.001	0.494	0.804514285714286	0.027
Anterior insula R	0.415	0.415	0.000	0.709	0.908157303370786	-0.014
Anterior orbital gyrus L	0.413	0.415	0.002	0.225	0.95	0.047
Anterior orbital gyrus R	0.390	0.393	0.003	0.115	0.771176470588235	0.062
Basal forebrain L	0.261	0.261	0.000	0.694185	0.920198720930233	0.017
Basal forebrain R	0.347	0.347	0.000	0.914	0.982981132075472	0.004
Calcarine cortex L	0.361	0.361	0.000	0.962	0.979178571428571	0.002
Calcarine cortex R	0.385	0.385	0.000	0.631848	0.889267555555555	0.019
Caudate L	0.223	0.224	0.002	0.311	0.824511627906977	-0.045
Caudate R	0.212	0.217	0.005	0.087	0.762923076923077	-0.076
Central operculum L	0.384	0.386	0.002	0.220	0.964615384615385	0.048
Central operculum R	0.399	0.401	0.002	0.268	0.925818181818182	0.043
Cuneus L	0.441	0.445	0.004	0.086	0.817	0.064
Cuneus R	0.446	0.448	0.002	0.210	0.9576	0.047
Entorhinal area L	0.397	0.398	0.001	0.461803	0.785754358208955	-0.029
Entorhinal area R	0.452	0.453	0.001	0.418	0.7942	-0.030
Frontal operculum L	0.392	0.395	0.004	0.104	0.7904	0.063
Frontal operculum R	0.320	0.321	0.001	0.530	0.816486486486487	0.026

Frontal pole L	0.469	0.484	0.015	0.000316516665049	0.036082899815586	0.131
Frontal pole R	0.431	0.444	0.013	0.001	0.057	0.121
Fusiform gyrus L	0.510	0.513	0.003	0.101	0.822428571428571	0.057
Fusiform gyrus R	0.538	0.539	0.001	0.401	0.802	0.029
Gyrus rectus L	0.451	0.452	0.001	0.282	0.893	0.040
Gyrus rectus R	0.464	0.464	0.000	0.739	0.92578021978022	0.012
Hippocampus L	0.422	0.426	0.004	0.069	0.98325	-0.069
Hippocampus R	0.442	0.447	0.004	0.059	0.960857142857143	-0.071
Inferior occipital gyrus L	0.424	0.425	0.001	0.433315	0.796740483870968	0.030
Inferior occipital gyrus R	0.479	0.485	0.006	0.025	0.7125	0.081
Inferior temporal gyrus L	0.493	0.494	0.000	0.703	0.910704545454545	-0.014
Inferior temporal gyrus R	0.540	0.540	0.000	0.992	0.992	0.000
Lateral orbital gyrus L	0.433	0.436	0.003	0.146	0.924666666666667	0.055
Lateral orbital gyrus R	0.408	0.409	0.000	0.637	0.874915662650602	0.018
Lingual gyrus L	0.506	0.506	0.000	0.511	0.798	0.023
Lingual gyrus R	0.517	0.521	0.004	0.052	0.988	0.068
Medial frontal cortex L	0.348	0.349	0.000	0.863	0.993757575757576	0.007
Medial frontal cortex R	0.371	0.373	0.003	0.174	0.944571428571429	0.054
Medial orbital gyrus L	0.483	0.484	0.001	0.287	0.88427027027027	0.038
Medial orbital gyrus R	0.468	0.469	0.001	0.279	0.908742857142857	0.040
Middle cingulate gyrus L	0.397	0.398	0.002	0.249	0.9462	0.045
Middle cingulate gyrus R	0.332	0.339	0.007	0.028	0.6384	0.090
Middle frontal gyrus L	0.498	0.499	0.001	0.343	0.814625	0.034
Middle frontal gyrus R	0.504	0.505	0.000	0.546	0.82992	0.021
Middle occipital gyrus L	0.360	0.361	0.001	0.402	0.790137931034483	0.034
Middle occipital gyrus R	0.354	0.356	0.002	0.294	0.882	0.042
Middle temporal gyrus L	0.480	0.481	0.001	0.445	0.9861	-0.028
Middle temporal gyrus R	0.520	0.520	0.000	0.865	0.780461538461538	-0.006
Occipital fusiform gyrus L	0.470	0.472	0.001	0.320	0.829090909090909	0.036
Occipital fusiform gyrus R	0.517	0.518	0.001	0.350	0.798	0.033

Occipital pole L	0.328	0.330	0.002	0.262	0.933375	0.046
Occipital pole R	0.396	0.397	0.001	0.375	0.777272727272727	0.035
Opercular part of the inferior frontal gyrus L	0.302	0.302	0.000	0.900	0.986538461538462	0.005
Opercular part of the inferior frontal gyrus R	0.270	0.270	0.000	0.768	0.931404255319149	-0.013
Orbital part of the inferior frontal gyrus L	0.275	0.275	0.000	0.990	0.998761061946903	0.001
Orbital part of the inferior frontal gyrus R	0.310	0.310	0.000	0.855	0.994591836734694	-0.008
Pallidum L	0.120	0.120	0.000	0.929979	0.963796418181818	0.004
Pallidum R	0.103	0.103	0.000	0.915	0.974859813084112	-0.005
Parahippocampal gyrus L	0.477	0.477	0.000	0.898	0.993902912621359	-0.005
Parahippocampal gyrus R	0.514	0.514	0.000	0.773	0.9179375	-0.010
Parietal operculum L	0.314	0.316	0.001	0.356	0.780461538461539	0.038
Parietal operculum R	0.294	0.296	0.002	0.297	0.84645	0.044
Planum polare L	0.457	0.457	0.000	0.743	0.920673913043478	0.012
Planum polare R	0.466	0.466	0.000	0.929738	0.972386532110092	-0.003
Planum temporale L	0.354	0.356	0.002	0.188	0.931826086956522	-0.053
Planum temporale R	0.329	0.329	0.000	0.884	0.997782178217822	0.006
Postcentral gyrus L	0.394	0.394	0.000	0.753	0.923032258064516	-0.012
Postcentral gyrus R	0.411	0.412	0.001	0.503	0.796416666666667	0.026
Postcentral gyrus medial segment L	0.186	0.186	0.000	0.827	0.971938144329897	0.010
Postcentral gyrus medial segment R	0.245	0.246	0.001	0.409	0.790271186440678	0.036
Posterior cingulate gyrus L	0.546	0.546	0.000	0.671	0.910642857142857	-0.014
Posterior cingulate gyrus R	0.511	0.511	0.000	0.912	0.990171428571428	0.004
Posterior insula L	0.395	0.396	0.001	0.498	0.799605633802817	0.026
Posterior insula R	0.423	0.427	0.004	0.075	0.95	0.068
Posterior orbital gyrus L	0.348	0.349	0.001	0.328	0.830933333333333	0.040
Posterior orbital gyrus R	0.394	0.395	0.001	0.439	0.794380952380952	0.030
Precentral gyrus L	0.457	0.458	0.001	0.461569	0.797255545454545	0.027
Precentral gyrus R	0.448	0.449	0.000	0.558	0.815538461538462	0.022
Precentral gyrus medial segment L	0.286	0.286	0.000	0.946	0.971567567567567	0.003
Precentral gyrus medial segment R	0.315	0.316	0.000	0.726	0.9196	0.015

Precuneus L	0.499	0.500	0.001	0.302	0.839707317073171	0.037
Precuneus R	0.482	0.483	0.001	0.361	0.762111111111111	0.033
Putamen L	0.2280	0.280	0.000	0.894	0.999176470588235	-0.006
Putamen R	0.285	0.285	0.001	0.552	0.817246753246753	-0.025
Subcallosal area L	0.478	0.478	0.000	0.632398	0.879187463414634	0..017
Subcallosal area R	0.473	0.476	0.003	0.105	0.748125	0.059
Superior frontal gyrus L	0.468	0.468	0.000	0.573433	0.817142025	-0.021
Superior frontal gyrus R	0.499	0.501	0.002	0.154	0.924	0.051
Superior frontal gyrus medial segment L	0.421	0.421	0.000	0.916	0.966888888888889	-0.004
Superior frontal gyrus medial segment R	0.397	0.397	0.000	0.550	0.825	0.023
Superior occipital gyrus L	0.353	0.354	0.001	0.354	0.791294117647059	0.037
Superior occipital gyrus R	0.366	0.370	0.004	0.082	0.849818181818182	0.069
Superior parietal lobule L	0.392	0.396	0.004	0.078	0.8892	0.069
Superior parietal lobule R	0.377	0.378	0.001	0.432766	0.808775803278688	0.031
Superior temporal gyrus L	0.442	0.444	0.001	0.275	0.922058823529412	-0.041
Superior temporal gyrus R	0.387	0.388	0.001	0.387	0.787821428571429	0.034
Supplementary motor cortex L	0.341	0.343	0.002	0.295	0.862307692307692	-0.043
Supplementary motor cortex R	0.378	0.379	0.000	0.769	0.9228	-0.012
Supramarginal gyrus L	0.377	0.379	0.002	0.189	0.89775	0.052
Supramarginal gyrus R	0.340	0.347	0.007	0.024	0.912	0.092
Temporal pole L	0.409	0.411	0.002	0.233	0.948642857142857	-0.046
Temporal pole R	0.405	0.407	0.001	0.309	0.838714285714286	-0.039
Thalamus proper L	0.221	0.222	0.001	0.474	0.783130434782609	-0.032
Thalamus proper R	0.239	0.242	0.003	0.158	0.9006	-0.062
Transverse temporal gyrus L	0.299	0.300	0.001	0.442	0.7873125	0.032
Transverse temporal gyrus R	0.332	0.334	0.002	0.240	0.943448275862069	0.048
Triangular part of the inferior frontal gyrus L	0.349	0.349	0.000	0.694431	0.909944068965517	-0.016
Triangular part of the inferior frontal gyrus R	0.324	0.324	0.001	0.463	0.776205882352941	0.030

FDR: false discovery rate. L: left. PRS: polygenic risk score. R: right.

Table D.67: Associations between APOEonlyPRS Threshold 1 and 114 regions of interest in amyloid negative participants

Region of Interest	R Square (Model 1)	R Square (Model 2)	R Square Change	Sig. F Change (Model 2)	FDR Corrected value	Standardised beta of PRS
Accumbens area L	0.390	0.390	0.000	0.965	0.982232142857143	-0.002
Accumbens area R	0.433	0.433	0.000	0.861	0.9348	0.009
Amygdala L	0.444	0.444	0.001	0.630	1	-0.024
Amygdala R	0.461	0.461	0.000	0.745	0.976206896551724	-0.016
Angular gyrus L	0.428	0.428	0.000	0.939	0.991166666666667	0.004
Angular gyrus R	0.370	0.372	0.002	0.435	1	-0.041
Anterior cingulate gyrus L	0.444	0.445	0.001	0.458	1	0.037
Anterior cingulate gyrus R	0.269	0.274	0.005	0.179	1	0.076
Anterior insula L	0.347	0.347	0.000	0.675	0.974050632911392	0.022
Anterior insula R	0.345	0.345	0.001	0.654	0.981	0.024
Anterior orbital gyrus L	0.384	0.385	0.000	0.705	0.980121951219512	-0.020
Anterior orbital gyrus R	0.323	0.324	0.000	0.671	0.980692307692308	0.023
Basal forebrain L	0.348	0.350	0.002	0.345	1	0.050
Basal forebrain R	0.382	0.382	0.000	0.694	0.98895	0.020
Calcarine cortex L	0.388	0.391	0.003	0.277	1	-0.056
Calcarine cortex R	0.368	0.372	0.003	0.272	1	-0.058
Caudate L	0.189	0.190	0.001	0.616183	1	-0.030
Caudate R	0.183	0.184	0.001	0.562	1	-0.035
Central operculum L	0.351	0.353	0.002	0.354	1	0.049
Central operculum R	0.322	0.323	0.000	0.859	0.941596153846154	0.010
Cuneus L	0.337	0.338	0.000	0.729	0.966348837209302	0.019
Cuneus R	0.377	0.380	0.003	0.242	1	-0.061
Entorhinal area L	0.374	0.375	0.001	0.555	1	0.031
Entorhinal area R	0.422	0.423	0.001	0.600	1	0.026
Frontal operculum L	0.298	0.307	0.009	0.076658	1	0.098
Frontal operculum R	0.309	0.312	0.003	0.308	1	0.056

Frontal pole L	0.369	0.369	0.000	0.986	0.986	-0.001
Frontal pole R	0.398	0.405	0.006	0.104	1	0.083
Fusiform gyrus L	0.471	0.476	0.004	0.155	1	-0.068
Fusiform gyrus R	0.495	0.496	0.001	0.397	1	-0.040
Gyrus rectus L	0.392	0.394	0.001	0.446272	1	0.039
Gyrus rectus R	0.412	0.414	0.001	0.436	1	0.039
Hippocampus L	0.430	0.430	0.000	0.790	0.938125	-0.013
Hippocampus R	0.490	0.492	0.002	0.339728	1	-0.045
Inferior occipital gyrus L	0.379	0.380	0.001	0.521	1	-0.033
Inferior occipital gyrus R	0.432	0.433	0.001	0.635	1	-0.024
Inferior temporal gyrus L	0.495	0.495	0.000	0.818	0.93252	-0.011
Inferior temporal gyrus R	0.533	0.534	0.001	0.530	1	-0.028
Lateral orbital gyrus L	0.391	0.397	0.007	0.101	1	0.084
Lateral orbital gyrus R	0.308	0.314	0.006	0.146	1	0.080
Lingual gyrus L	0.500	0.501	0.002	0.375	1	-0.041
Lingual gyrus R	0.537	0.541	0.004	0.135	1	-0.067
Medial frontal cortex L	0.376	0.376	0.000	0.816	0.939636363636364	0.012
Medial frontal cortex R	0.354	0.355	0.001	0.499	1	0.036
Medial orbital gyrus L	0.469	0.469	0.000	0.949	0.974648648648649	-0.003
Medial orbital gyrus R	0.385	0.388	0.003	0.270	1	0.057
Middle cingulate gyrus L	0.400	0.402	0.002	0.339834	1	0.049
Middle cingulate gyrus R	0.382	0.386	0.005	0.177	1	0.070
Middle frontal gyrus L	0.441	0.441	0.000	0.838	0.936588235294118	-0.010
Middle frontal gyrus R	0.403	0.403	0.000	0.919	0.979121495327103	-0.005
Middle occipital gyrus L	0.385	0.386	0.001	0.638914	0.984272918918919	0.024
Middle occipital gyrus R	0.347	0.348	0.001	0.628	1	0.026
Middle temporal gyrus L	0.521	0.523	0.002	0.380	0.990467532467533	0.040
Middle temporal gyrus R	0.503	0.503	0.000	0.669	1	0.020
Occipital fusiform gyrus L	0.464	0.470	0.007	0.076550	1	-0.085
Occipital fusiform gyrus R	0.501	0.502	0.001	0.558	1	-0.027

Occipital pole L	0.323	0.332	0.008	0.083	1	-0.094
Occipital pole R	0.336	0.336	0.000	0.785270	0.942324	-0.015
Opercular part of the inferior frontal gyrus L	0.188	0.200	0.011	0.062	1	0.111
Opercular part of the inferior frontal gyrus R	0.277	0.285	0.008	0.094	1	0.094
Orbital part of the inferior frontal gyrus L	0.289	0.292	0.002	0.372	1	0.050
Orbital part of the inferior frontal gyrus R	0.188	0.195	0.007	0.139	1	0.088
Pallidum L	0.187	0.188	0.001	0.542	1	-0.036
Pallidum R	0.157	0.158	0.001	0.643	0.97736	-0.028
Parahippocampal gyrus L	0.483	0.483	0.000	0.837	0.944732673267327	0.010
Parahippocampal gyrus R	0.491	0.492	0.001	0.619	1	-0.023
Parietal operculum L	0.355	0.356	0.001	0.506	1	0.035
Parietal operculum R	0.267	0.267	0.000	0.765	0.969	0.017
Planum polare L	0.385	0.385	0.000	0.967	0.975557522123894	0.002
Planum polare R	0.424	0.425	0.001	0.497	1	-0.034
Planum temporale L	0.346	0.347	0.000	0.720	0.965647058823529	0.019
Planum temporale R	0.375	0.376	0.001	0.445	1	0.040
Postcentral gyrus L	0.390	0.391	0.001	0.616437	1	0.026
Postcentral gyrus R	0.349	0.349	0.000	0.808	0.939918367346939	-0.013
Postcentral gyrus medial segment L	0.213	0.214	0.001	0.553	1	-0.035
Postcentral gyrus medial segment R	0.196	0.196	0.000	0.784533	0.951454914893617	-0.016
Posterior cingulate gyrus L	0.517	0.520	0.002	0.259	1	0.052
Posterior cingulate gyrus R	0.477	0.478	0.001	0.599	1	0.025
Posterior insula L	0.388	0.391	0.003	0.260454	1	-0.058
Posterior insula R	0.408	0.408	0.000	0.757	0.969640449438202	-0.016
Posterior orbital gyrus L	0.423	0.425	0.002	0.322	1	0.050
Posterior orbital gyrus R	0.377	0.377	0.000	0.704	0.990814814814815	0.020
Precentral gyrus L	0.476	0.481	0.005	0.143	1	0.070
Precentral gyrus R	0.445	0.447	0.002	0.327	1	0.048
Precentral gyrus medial segment L	0.306	0.306	0.000	0.942	0.985211009174312	-0.004
Precentral gyrus medial segment R	0.361	0.364	0.003	0.287	1	-0.056

Precuneus L	0.453	0.454	0.001	0.424	1	-0.039
Precuneus R	0.496	0.496	0.000	0.946	0.9804	-0.003
Putamen L	0.293	0.298	0.005	0.201	1	-0.071
Putamen R	0.298	0.299	0.002	0.438	1	-0.043
Subcallosal area L	0.470	0.474	0.004	0.166	1	0.066
Subcallosal area R	0.411	0.415	0.005	0.167	1	0.070
Superior frontal gyrus L	0.441	0.444	0.003	0.280	1	0.053
Superior frontal gyrus R	0.462	0.463	0.001	0.510	1	0.032
Superior frontal gyrus medial segment L	0.420	0.421	0.000	0.718450	0.975039285714286	0.018
Superior frontal gyrus medial segment R	0.392	0.392	0.000	0.856	0.947417475728155	0.009
Superior occipital gyrus L	0.253	0.253	0.000	0.779137	0.965452369565217	0.016
Superior occipital gyrus R	0.256	0.258	0.002	0.445973	1	0.043
Superior parietal lobule L	0.379	0.381	0.002	0.336	1	0.050
Superior parietal lobule R	0.395	0.396	0.001	0.456	1	-0.038
Superior temporal gyrus L	0.358	0.361	0.003	0.260462	1	0.060
Superior temporal gyrus R	0.383	0.383	0.000	0.747	0.967704545454545	0.017
Supplementary motor cortex L	0.393	0.393	0.000	0.779321	0.955296709677419	0.014
Supplementary motor cortex R	0.372	0.372	0.000	0.717806	0.98590221686747	-0.019
Supramarginal gyrus L	0.302	0.304	0.001	0.495	1	0.038
Supramarginal gyrus R	0.362	0.362	0.000	0.882	0.948566037735849	0.008
Temporal pole L	0.356	0.356	0.000	0.802	0.942556701030928	0.013
Temporal pole R	0.375	0.375	0.001	0.638808	0.997590575342466	-0.025
Thalamus proper L	0.272	0.273	0.000	0.776	0.972131868131868	-0.016
Thalamus proper R	0.304	0.306	0.002	0.418	1	-0.045
Transverse temporal gyrus L	0.216	0.225	0.009	0.096	1	0.097
Transverse temporal gyrus R	0.308	0.310	0.002	0.411	1	0.045
Triangular part of the inferior frontal gyrus L	0.263	0.265	0.002	0.403	1	0.047
Triangular part of the inferior frontal gyrus R	0.256	0.260	0.004	0.247	1	0.066

FDR: false discovery rate. L: left. PRS: polygenic risk score. R: right.

Table D.68: Associations between APOEonlyPRS Threshold 1 and 114 regions of interest in amyloid positive participants

Region of Interest	R Square (Model 1)	R Square (Model 2)	R Square Change	Sig. F Change (Model 2)	FDR Corrected value	Standardised beta of PRS
Accumbens area L	0.398	0.399	0.001	0.463	0.68548051948052	-0.029
Accumbens area R	0.374	0.374	0.000	0.889	0.913027027027027	0.006
Amygdala L	0.383	0.399	0.016	0.000733126509912	0.0167152844259936	-0.132
Amygdala R	0.444	0.466	0.022	0.00002535428647	0.00144519432879	-0.156
Angular gyrus L	0.391	0.395	0.004	0.082	0.301548387096774	-0.068
Angular gyrus R	0.430	0.433	0.003	0.146925	0.408523170731707	-0.055
Anterior cingulate gyrus L	0.388	0.388	0.000	0.848	0.903476635514019	-0.008
Anterior cingulate gyrus R	0.224	0.228	0.004	0.116	0.348	-0.069
Anterior insula L	0.401	0.401	0.000	0.650	0.842045454545455	0.018
Anterior insula R	0.415	0.415	0.000	0.698	0.864913043478261	0.015
Anterior orbital gyrus L	0.413	0.416	0.003	0.148888	0.394726325581395	-0.055
Anterior orbital gyrus R	0.390	0.397	0.007	0.019217	0.1825615	-0.091
Basal forebrain L	0.261	0.263	0.002	0.327	0.601258064516129	-0.042
Basal forebrain R	0.347	0.348	0.000	0.773	0.890121212121212	-0.012
Calcarine cortex L	0.361	0.361	0.001	0.541	0.752121951219512	-0.025
Calcarine cortex R	0.385	0.389	0.004	0.088	0.3135	-0.067
Caudate L	0.223	0.223	0.000	0.729	0.8748	-0.015
Caudate R	0.212	0.212	0.000	0.791	0.884058823529412	-0.012
Central operculum L	0.384	0.386	0.002	0.270	0.559636363636364	0.043
Central operculum R	0.399	0.399	0.000	0.877	0.917229357798165	-0.006
Cuneus L	0.441	0.448	0.007	0.014	0.1596	-0.091
Cuneus R	0.446	0.451	0.005	0.037	0.234333333333333	-0.078
Entorhinal area L	0.397	0.409	0.012	0.002939	0.0478637142857143	-0.115
Entorhinal area R	0.452	0.463	0.011	0.002661	0.050559	-0.111
Frontal operculum L	0.392	0.392	0.000	0.721	0.883806451612903	0.014
Frontal operculum R	0.320	0.320	0.000	0.990	0.99	0.000

Frontal pole L	0.469	0.469	0.000	0.799	0.875826923076923	0.009
Frontal pole R	0.431	0.431	0.000	0.648	0.849103448275862	0.017
Fusiform gyrus L	0.510	0.514	0.004	0.056	0.277565217391304	-0.067
Fusiform gyrus R	0.538	0.542	0.005	0.028	0.1995	-0.075
Gyrus rectus L	0.451	0.452	0.001	0.431700	0.683525	-0.029
Gyrus rectus R	0.464	0.465	0.001	0.497	0.717189873417721	0.025
Hippocampus L	0.422	0.440	0.018	0.000147192598373	0.0041949890536305	-0.144
Hippocampus R	0.442	0.467	0.024	0.000008321614941	0.000948664103274	-0.165
Inferior occipital gyrus L	0.424	0.428	0.004	0.073380	0.278844	-0.068
Inferior occipital gyrus R	0.479	0.488	0.009	0.006	0.076	-0.100
Inferior temporal gyrus L	0.493	0.498	0.004	0.050	0.259090909090909	-0.070
Inferior temporal gyrus R	0.540	0.544	0.004	0.040	0.24	-0.070
Lateral orbital gyrus L	0.433	0.435	0.001	0.356	0.634125	-0.035
Lateral orbital gyrus R	0.408	0.409	0.001	0.489	0.714692307692308	-0.027
Lingual gyrus L	0.506	0.506	0.000	0.640	0.848372093023256	-0.016
Lingual gyrus R	0.517	0.519	0.002	0.148998	0.386040272727273	-0.050
Medial frontal cortex L	0.348	0.352	0.003	0.147130	0.399352857142857	-0.059
Medial frontal cortex R	0.371	0.371	0.000	0.679	0.860066666666667	-0.016
Medial orbital gyrus L	0.483	0.484	0.001	0.373	0.654184615384615	-0.032
Medial orbital gyrus R	0.468	0.468	0.000	0.813070	0.882761714285714	-0.009
Middle cingulate gyrus L	0.397	0.398	0.001	0.325	0.607377049180328	-0.038
Middle cingulate gyrus R	0.332	0.337	0.005	0.069	0.291333333333333	-0.074
Middle frontal gyrus L	0.498	0.498	0.000	0.549	0.754048192771084	-0.021
Middle frontal gyrus R	0.504	0.505	0.001	0.393	0.678818181818182	-0.030
Middle occipital gyrus L	0.360	0.365	0.006	0.046	0.249714285714286	-0.080
Middle occipital gyrus R	0.354	0.375	0.021	0.000117732027101	0.004473817029838	-0.154
Middle temporal gyrus L	0.480	0.484	0.004	0.065	0.170815846153846	-0.066
Middle temporal gyrus R	0.520	0.526	0.006	0.019479	0.2964	-0.081
Occipital fusiform gyrus L	0.470	0.470	0.000	0.909	0.925232142857143	0.004
Occipital fusiform gyrus R	0.517	0.521	0.004	0.045	0.2565	-0.070

Occipital pole L	0.328	0.328	0.000	0.813366	0.874752113207547	-0.010
Occipital pole R	0.396	0.398	0.002	0.257	0.542555555555556	-0.044
Opercular part of the inferior frontal gyrus L	0.302	0.304	0.002	0.291	0.562271186440678	0.044
Opercular part of the inferior frontal gyrus R	0.270	0.270	0.000	0.659	0.844112359550562	0.019
Orbital part of the inferior frontal gyrus L	0.275	0.275	0.000	0.728	0.882893617021277	-0.015
Orbital part of the inferior frontal gyrus R	0.310	0.314	0.003	0.134	0.391692307692308	-0.062
Pallidum L	0.120	0.123	0.003	0.207	0.462705882352941	-0.059
Pallidum R	0.103	0.107	0.004	0.175	0.424468085106383	-0.064
Parahippocampal gyrus L	0.477	0.484	0.007	0.015	0.155454545454545	-0.088
Parahippocampal gyrus R	0.514	0.523	0.009	0.004	0.057	-0.099
Parietal operculum L	0.314	0.315	0.000	0.611	0.829214285714286	0.021
Parietal operculum R	0.294	0.294	0.000	0.737	0.866164948453608	0.014
Planum polare L	0.457	0.458	0.001	0.419310	0.682876285714286	-0.030
Planum polare R	0.466	0.467	0.001	0.420	0.674366197183099	-0.030
Planum temporale L	0.354	0.354	0.000	0.792	0.876582524271845	0.011
Planum temporale R	0.329	0.329	0.000	0.851	0.898277777777778	-0.008
Postcentral gyrus L	0.394	0.395	0.001	0.460	0.6992	-0.029
Postcentral gyrus R	0.411	0.416	0.004	0.071884	0.292670571428571	-0.069
Postcentral gyrus medial segment L	0.186	0.195	0.009	0.023	0.187285714285714	-0.103
Postcentral gyrus medial segment R	0.245	0.249	0.004	0.109585	0.356934	-0.070
Posterior cingulate gyrus L	0.546	0.549	0.003	0.100	0.345454545454545	-0.055
Posterior cingulate gyrus R	0.511	0.516	0.005	0.036	0.241411764705882	-0.073
Posterior insula L	0.395	0.397	0.002	0.211	0.462576923076923	0.049
Posterior insula R	0.423	0.423	0.000	0.879	0.910963636363636	0.006
Posterior orbital gyrus L	0.348	0.349	0.001	0.461	0.6915	-0.030
Posterior orbital gyrus R	0.394	0.396	0.002	0.249	0.535584905660377	-0.045
Precentral gyrus L	0.457	0.458	0.000	0.780	0.8892	-0.010
Precentral gyrus R	0.448	0.449	0.001	0.521	0.733259259259259	-0.024
Precentral gyrus medial segment L	0.286	0.290	0.004	0.110203	0.348976166666667	-0.068
Precentral gyrus medial segment R	0.315	0.318	0.003	0.165	0.418	-0.058

Precuneus L	0.499	0.501	0.002	0.186	0.432734693877551	-0.047
Precuneus R	0.482	0.486	0.004	0.063	0.29925	-0.067
Putamen L	0.280	0.281	0.000	0.731	0.8680625	-0.015
Putamen R	0.285	0.286	0.001	0.436	0.671675675675676	-0.033
Subcallosal area L	0.478	0.478	0.000	0.696	0.871912087912088	0.014
Subcallosal area R	0.473	0.475	0.002	0.168	0.416347826086957	0.050
Superior frontal gyrus L	0.468	0.469	0.001	0.274	0.557785714285714	-0.040
Superior frontal gyrus R	0.499	0.499	0.000	0.639	0.857011764705882	0.017
Superior frontal gyrus medial segment L	0.421	0.422	0.002	0.279	0.558	-0.041
Superior frontal gyrus medial segment R	0.397	0.398	0.001	0.309	0.5871	0.040
Superior occipital gyrus L	0.353	0.356	0.004	0.113	0.348162162162162	-0.064
Superior occipital gyrus R	0.366	0.371	0.005	0.066	0.289384615384615	-0.073
Superior parietal lobule L	0.392	0.396	0.004	0.072963	0.286820068965517	-0.070
Superior parietal lobule R	0.377	0.381	0.004	0.106	0.355411764705882	-0.064
Superior temporal gyrus L	0.442	0.443	0.001	0.419191	0.692576434782609	-0.030
Superior temporal gyrus R	0.387	0.389	0.002	0.194	0.44232	-0.051
Supplementary motor cortex L	0.341	0.344	0.003	0.180	0.4275	-0.054
Supplementary motor cortex R	0.378	0.378	0.000	0.938	0.946300884955752	0.003
Supramarginal gyrus L	0.377	0.378	0.001	0.335	0.606190476190476	-0.038
Supramarginal gyrus R	0.340	0.340	0.000	0.750	0.872448979591837	0.013
Temporal pole L	0.409	0.412	0.003	0.146053	0.41625105	-0.056
Temporal pole R	0.405	0.412	0.006	0.027	0.2052	-0.085
Thalamus proper L	0.221	0.222	0.001	0.432321	0.675131424657534	-0.035
Thalamus proper R	0.239	0.241	0.002	0.282	0.554275862068965	-0.047
Transverse temporal gyrus L	0.299	0.299	0.000	0.784	0.884910891089109	0.011
Transverse temporal gyrus R	0.332	0.333	0.001	0.418664	0.701877882352941	-0.033
Triangular part of the inferior frontal gyrus L	0.349	0.349	0.001	0.519	0.739575	0.026
Triangular part of the inferior frontal gyrus R	0.324	0.325	0.001	0.405	0.68910447761194	-0.034

FDR: false discovery rate. L: left. PRS: polygenic risk score. R: right.

Table D.69: Associations between APOEonlyPRS Threshold 5 and 114 regions of interest in amyloid negative participants

Region of Interest	R Square (Model 1)	R Square (Model 2)	R Square Change	Sig. F Change (Model 2)	FDR Corrected value	Standardised beta of PRS
Accumbens area L	0.390	0.390	0.000	0.958551	0.984457783783784	0.003
Accumbens area R	0.433	0.434	0.000	0.701	0.940164705882353	0.019
Amygdala L	0.444	0.445	0.001	0.610	0.965833333333333	-0.025
Amygdala R	0.461	0.461	0.000	0.766	0.938967741935484	-0.014
Angular gyrus L	0.428	0.428	0.000	0.977	0.985646017699115	0.001
Angular gyrus R	0.370	0.372	0.002	0.412	0.958530612244898	-0.043
Anterior cingulate gyrus L	0.444	0.446	0.002	0.397	0.983869565217391	0.042
Anterior cingulate gyrus R	0.269	0.276	0.007	0.119	1	0.088
Anterior insula L	0.347	0.347	0.000	0.671	0.956175	0.023
Anterior insula R	0.345	0.346	0.001	0.551	1	0.032
Anterior orbital gyrus L	0.384	0.385	0.000	0.728	0.932494382022472	-0.018
Anterior orbital gyrus R	0.323	0.324	0.000	0.757	0.94832967032967	0.017
Basal forebrain L	0.348	0.351	0.003	0.304956	1	0.055
Basal forebrain R	0.382	0.382	0.001	0.593	0.979739130434783	0.028
Calcarine cortex L	0.388	0.392	0.004	0.217	1	-0.064
Calcarine cortex R	0.368	0.372	0.004	0.220	1	-0.064
Caudate L	0.189	0.190	0.001	0.617594	0.93874288	-0.030
Caudate R	0.183	0.184	0.001	0.557	1	-0.035
Central operculum L	0.351	0.353	0.003	0.330	1	0.052
Central operculum R	0.322	0.323	0.000	0.847	0.946647058823529	0.011
Cuneus L	0.337	0.338	0.000	0.760	0.941739130434783	0.016
Cuneus R	0.377	0.380	0.003	0.292	1	-0.055
Entorhinal area L	0.374	0.375	0.001	0.552	1	0.031
Entorhinal area R	0.422	0.423	0.001	0.519	1	0.032
Frontal operculum L	0.298	0.307	0.008	0.089	1	0.094
Frontal operculum R	0.309	0.312	0.003	0.279	1	0.059

Frontal pole L	0.369	0.369	0.000	0.958771	0.975891910714286	0.003
Frontal pole R	0.398	0.405	0.006	0.111	1	0.082
Fusiform gyrus L	0.471	0.475	0.004	0.191	1	-0.063
Fusiform gyrus R	0.495	0.496	0.001	0.492	1	-0.032
Gyrus rectus L	0.392	0.394	0.002	0.388	1	0.045
Gyrus rectus R	0.412	0.414	0.002	0.382	1	0.044
Hippocampus L	0.430	0.430	0.000	0.778	0.9336	-0.014
Hippocampus R	0.490	0.492	0.002	0.371	1	-0.042
Inferior occipital gyrus L	0.379	0.380	0.001	0.571	0.986272727272727	-0.030
Inferior occipital gyrus R	0.432	0.433	0.000	0.723	0.936613636363636	-0.018
Inferior temporal gyrus L	0.495	0.495	0.000	0.819	0.93366	-0.011
Inferior temporal gyrus R	0.533	0.534	0.001	0.533	1	-0.028
Lateral orbital gyrus L	0.391	0.398	0.007	0.090	1	0.087
Lateral orbital gyrus R	0.308	0.314	0.006	0.155	1	0.078
Lingual gyrus L	0.500	0.502	0.002	0.305268	1	-0.048
Lingual gyrus R	0.537	0.542	0.005	0.105	1	-0.073
Medial frontal cortex L	0.376	0.376	0.000	0.710	0.941162790697674	0.019
Medial frontal cortex R	0.354	0.356	0.002	0.393	0.9956	0.045
Medial orbital gyrus L	0.469	0.469	0.000	0.889	0.9652	-0.007
Medial orbital gyrus R	0.385	0.387	0.003	0.299	1	0.054
Middle cingulate gyrus L	0.400	0.402	0.003	0.307	1	0.052
Middle cingulate gyrus R	0.382	0.388	0.006	0.109	1	0.083
Middle frontal gyrus L	0.441	0.441	0.000	0.866	0.958485436893204	-0.008
Middle frontal gyrus R	0.403	0.403	0.000	0.941	0.993277777777778	0.004
Middle occipital gyrus L	0.385	0.386	0.001	0.634	0.938649350649351	0.025
Middle occipital gyrus R	0.347	0.348	0.001	0.656	0.946632911392405	0.024
Middle temporal gyrus L	0.521	0.523	0.001	0.390	0.941133333333333	0.039
Middle temporal gyrus R	0.503	0.503	0.000	0.743	1	0.015
Occipital fusiform gyrus L	0.464	0.471	0.007	0.074	1	-0.086
Occipital fusiform gyrus R	0.501	0.502	0.001	0.512	1	-0.031

Occipital pole L	0.323	0.331	0.007	0.102	1	-0.089
Occipital pole R	0.336	0.336	0.000	0.832	0.939089108910891	-0.011
Opercular part of the inferior frontal gyrus L	0.188	0.199	0.011	0.071	1	0.107
Opercular part of the inferior frontal gyrus R	0.277	0.287	0.010	0.067	1	0.102
Orbital part of the inferior frontal gyrus L	0.289	0.292	0.003	0.343	1	0.053
Orbital part of the inferior frontal gyrus R	0.188	0.196	0.008	0.126	1	0.091
Pallidum L	0.187	0.188	0.001	0.583	0.991970149253731	-0.033
Pallidum R	0.157	0.158	0.001	0.690	0.947710843373494	-0.024
Parahippocampal gyrus L	0.483	0.483	0.000	0.890	0.957169811320755	0.007
Parahippocampal gyrus R	0.491	0.492	0.000	0.687	0.95509756097561	-0.019
Parietal operculum L	0.355	0.356	0.001	0.534	1	0.033
Parietal operculum R	0.267	0.267	0.000	0.711	0.931655172413793	0.021
Planum polare L	0.385	0.385	0.000	0.930	0.990841121495327	0.005
Planum polare R	0.424	0.425	0.001	0.569	0.997938461538461	-0.029
Planum temporale L	0.346	0.347	0.000	0.675	0.95	0.022
Planum temporale R	0.375	0.377	0.003	0.309	1	0.053
Postcentral gyrus L	0.390	0.391	0.001	0.556	1	0.030
Postcentral gyrus R	0.349	0.349	0.000	0.805	0.9559375	-0.013
Postcentral gyrus medial segment L	0.213	0.214	0.001	0.561	0.99928125	-0.034
Postcentral gyrus medial segment R	0.196	0.196	0.000	0.993	0.993	-0.001
Posterior cingulate gyrus L	0.517	0.521	0.003	0.196	1	0.059
Posterior cingulate gyrus R	0.477	0.478	0.001	0.592	0.992470588235294	0.026
Posterior insula L	0.388	0.391	0.003	0.302	1	-0.053
Posterior insula R	0.408	0.408	0.000	0.870	0.953653846153846	-0.008
Posterior orbital gyrus L	0.423	0.425	0.002	0.369	1	0.045
Posterior orbital gyrus R	0.377	0.377	0.001	0.646	0.944153846153846	0.024
Precentral gyrus L	0.476	0.481	0.005	0.130	1	0.072
Precentral gyrus R	0.445	0.447	0.002	0.367	1	0.044
Precentral gyrus medial segment L	0.306	0.306	0.000	0.944	0.987302752293578	0.004
Precentral gyrus medial segment R	0.361	0.363	0.002	0.406	0.96425	-0.044

Precuneus L	0.453	0.454	0.001	0.448334	0.964341056603774	-0.037
Precuneus R	0.496	0.496	0.000	0.953	0.987654545454545	-0.003
Putamen L	0.293	0.298	0.005	0.187	1	-0.073
Putamen R	0.298	0.299	0.002	0.421	0.95988	-0.045
Subcallosal area L	0.470	0.475	0.005	0.131	0.9956	0.073
Subcallosal area R	0.411	0.417	0.006	0.112	1	0.080
Superior frontal gyrus L	0.441	0.444	0.003	0.242	1	0.058
Superior frontal gyrus R	0.462	0.464	0.001	0.447694	0.981483	0.037
Superior frontal gyrus medial segment L	0.420	0.421	0.001	0.599	0.975514285714286	0.026
Superior frontal gyrus medial segment R	0.392	0.392	0.000	0.814722	0.947737836734694	0.012
Superior occipital gyrus L	0.253	0.254	0.001	0.617532	0.951333081081081	0.029
Superior occipital gyrus R	0.256	0.259	0.003	0.319	1	0.057
Superior parietal lobule L	0.379	0.381	0.003	0.297	1	0.054
Superior parietal lobule R	0.395	0.397	0.0022	0.432	0.965647058823529	-0.040
Superior temporal gyrus L	0.358	0.361	0.003	0.251	1	0.061
Superior temporal gyrus R	0.383	0.384	0.001	0.602	0.966591549295775	0.027
Supplementary motor cortex L	0.393	0.393	0.001	0.616	0.961972602739726	0.026
Supplementary motor cortex R	0.372	0.372	0.000	0.771	0.935042553191489	-0.015
Supramarginal gyrus L	0.302	0.304	0.001	0.513	1	0.036
Supramarginal gyrus R	0.362	0.362	0.000	0.807	0.948432989690722	0.013
Temporal pole L	0.356	0.356	0.000	0.815302	0.938832606060606	0.012
Temporal pole R	0.375	0.375	0.001	0.627	0.9405	-0.025
Thalamus proper L	0.272	0.273	0.000	0.696	0.944571428571429	-0.022
Thalamus proper R	0.304	0.307	0.003	0.334	1	-0.053
Transverse temporal gyrus L	0.216	0.225	0.009	0.099	1	0.096
Transverse temporal gyrus R	0.308	0.310	0.002	0.372	1	0.049
Triangular part of the inferior frontal gyrus L	0.263	0.265	0.002	0.402	0.975063829787234	0.048
Triangular part of the inferior frontal gyrus R	0.256	0.260	0.004	0.237	1	0.067

FDR: false discovery rate. L: left. PRS: polygenic risk score. R: right.

Table D.70: Associations between APOEonlyPRS Threshold 5 and 114 regions of interest in amyloid positive participants

Region of Interest	R Square (Model 1)	R Square (Model 2)	R Square Change	Sig. F Change (Model 2)	FDR Corrected value	Standardised beta of PRS
Accumbens area L	0.398	0.399	0.001	0.478	0.72656	-0.028
Accumbens area R	0.374	0.374	0.000	0.954	0.962442477876106	0.002
Amygdala L	0.383	0.398	0.015	0.000933869988176	0.0212922357304128	-0.130
Amygdala R	0.444	0.466	0.022	0.00002478797785	0.00141291473745	-0.156
Angular gyrus L	0.391	0.395	0.004	0.078	0.2964	-0.069
Angular gyrus R	0.430	0.434	0.003	0.120798	0.382527	-0.059
Anterior cingulate gyrus L	0.388	0.388	0.000	0.882	0.914072727272727	-0.006
Anterior cingulate gyrus R	0.224	0.228	0.004	0.129	0.377076923076923	-0.067
Anterior insula L	0.401	0.401	0.000	0.706081	0.904418359550562	0.015
Anterior insula R	0.415	0.415	0.000	0.736	0.902193548387097	0.013
Anterior orbital gyrus L	0.413	0.415	0.002	0.172817	0.469074714285714	-0.052
Anterior orbital gyrus R	0.390	0.397	0.007	0.019	0.166615384615385	-0.092
Basal forebrain L	0.261	0.263	0.002	0.291	0.562271186440678	-0.046
Basal forebrain R	0.347	0.348	0.000	0.739044	0.8868528	-0.013
Calcarine cortex L	0.361	0.361	0.000	0.583	0.800746987951807	-0.022
Calcarine cortex R	0.385	0.388	0.004	0.105	0.362727272727273	-0.064
Caudate L	0.223	0.223	0.000	0.765	0.899072164948454	-0.013
Caudate R	0.212	0.212	0.000	0.811	0.897611650485437	-0.011
Central operculum L	0.384	0.386	0.002	0.275	0.559821428571429	0.043
Central operculum R	0.399	0.399	0.000	0.914	0.938702702702703	-0.004
Cuneus L	0.441	0.448	0.007	0.018	0.171	-0.089
Cuneus R	0.446	0.451	0.005	0.042853	0.271402333333333	-0.075
Entorhinal area L	0.397	0.408	0.011	0.003528	0.057456	-0.113
Entorhinal area R	0.452	0.463	0.011	0.002844	0.054036	-0.110
Frontal operculum L	0.392	0.392	0.000	0.705637	0.914120659090909	0.015
Frontal operculum R	0.320	0.320	0.000	0.963	0.963	-0.002

Frontal pole L	0.469	0.469	0.000	0.847	0.910924528301887	0.007
Frontal pole R	0.431	0.431	0.000	0.738607	0.895757425531915	0.013
Fusiform gyrus L	0.510	0.514	0.004	0.060	0.297391304347826	-0.066
Fusiform gyrus R	0.538	0.543	0.005	0.026	0.1976	-0.076
Gyrus rectus L	0.451	0.451	0.001	0.488	0.722493506493507	-0.026
Gyrus rectus R	0.464	0.465	0.000	0.540	0.7695	0.022
Hippocampus L	0.422	0.440	0.018	0.000174092528873	0.0049616370728805	-0.142
Hippocampus R	0.442	0.466	0.024	0.000008815998196	0.001005023794344	-0.165
Inferior occipital gyrus L	0.424	0.428	0.004	0.072	0.304	-0.068
Inferior occipital gyrus R	0.479	0.488	0.009	0.006	0.076	-0.099
Inferior temporal gyrus L	0.493	0.498	0.005	0.045	0.244285714285714	-0.071
Inferior temporal gyrus R	0.540	0.544	0.004	0.043443	0.260658	-0.069
Lateral orbital gyrus L	0.433	0.434	0.001	0.397	0.696276923076923	-0.032
Lateral orbital gyrus R	0.408	0.409	0.001	0.483	0.7245	-0.027
Lingual gyrus L	0.506	0.506	0.000	0.721	0.903230769230769	-0.013
Lingual gyrus R	0.517	0.519	0.002	0.198	0.45144	-0.045
Medial frontal cortex L	0.348	0.351	0.003	0.163	0.453219512195122	-0.056
Medial frontal cortex R	0.371	0.371	0.000	0.666	0.882837209302326	-0.017
Medial orbital gyrus L	0.483	0.484	0.001	0.403	0.696090909090909	-0.030
Medial orbital gyrus R	0.468	0.468	0.000	0.809	0.904176470588235	-0.009
Middle cingulate gyrus L	0.397	0.398	0.001	0.335	0.606190476190476	-0.038
Middle cingulate gyrus R	0.332	0.337	0.005	0.073	0.297214285714286	-0.073
Middle frontal gyrus L	0.498	0.498	0.000	0.548	0.761853658536585	-0.021
Middle frontal gyrus R	0.504	0.505	0.001	0.413	0.702716417910448	-0.029
Middle occipital gyrus L	0.360	0.365	0.006	0.044	0.2508	-0.081
Middle occipital gyrus R	0.354	0.375	0.021	0.000120875910294	0.004593284591172	-0.154
Middle temporal gyrus L	0.480	0.484	0.004	0.063	0.181270363636364	-0.067
Middle temporal gyrus R	0.520	0.526	0.006	0.017491	0.28728	-0.082
Occipital fusiform gyrus L	0.470	0.471	0.000	0.808	0.912	0.009
Occipital fusiform gyrus R	0.517	0.521	0.004	0.058	0.300545454545455	-0.066

Occipital pole L	0.328	0.28	0.000	0.872	0.912	-0.007
Occipital pole R	0.396	0.397	0.001	0.330	0.606774193548387	-0.038
Opercular part of the inferior frontal gyrus L	0.302	0.304	0.002	0.260	0.559245283018868	0.047
Opercular part of the inferior frontal gyrus R	0.270	0.270	0.000	0.637	0.854329411764706	0.020
Orbital part of the inferior frontal gyrus L	0.275	0.275	0.000	0.760	0.9025	-0.013
Orbital part of the inferior frontal gyrus R	0.310	0.314	0.004	0.122	0.366	-0.064
Pallidum L	0.120	0.123	0.003	0.244	0.534923076923077	-0.055
Pallidum R	0.103	0.107	0.003	0.194	0.45134693877551	-0.062
Parahippocampal gyrus L	0.477	0.483	0.007	0.016590	0.189126	-0.087
Parahippocampal gyrus R	0.514	0.523	0.009	0.003692	0.052611	-0.101
Parietal operculum L	0.314	0.315	0.000	0.621	0.842785714285714	0.021
Parietal operculum R	0.294	0.294	0.000	0.725	0.898369565217391	0.015
Planum polare L	0.457	0.458	0.001	0.414	0.694058823529412	-0.030
Planum polare R	0.466	0.466	0.001	0.436	0.690333333333333	-0.029
Planum temporale L	0.354	0.354	0.000	0.819	0.8892	0.009
Planum temporale R	0.329	0.329	0.000	0.805	0.9177	-0.010
Postcentral gyrus L	0.394	0.395	0.001	0.446	0.687081081081081	-0.030
Postcentral gyrus R	0.411	0.416	0.004	0.071	0.311307692307692	-0.069
Postcentral gyrus medial segment L	0.186	0.195	0.010	0.021	0.171	-0.104
Postcentral gyrus medial segment R	0.245	0.249	0.004	0.121255	0.373596486486487	-0.067
Posterior cingulate gyrus L	0.546	0.549	0.003	0.099	0.3526875	-0.056
Posterior cingulate gyrus R	0.511	0.516	0.005	0.032685	0.232880625	-0.075
Posterior insula L	0.395	0.397	0.002	0.205	0.458235294117647	0.049
Posterior insula R	0.423	0.423	0.000	0.861	0.908833333333333	0.007
Posterior orbital gyrus L	0.348	0.349	0.001	0.541	0.761407407407407	-0.025
Posterior orbital gyrus R	0.394	0.396	0.002	0.266852	0.553111418181818	-0.043
Precentral gyrus L	0.457	0.457	0.000	0.853	0.908803738317757	-0.007
Precentral gyrus R	0.448	0.449	0.000	0.524	0.756151898734177	-0.024
Precentral gyrus medial segment L	0.286	0.290	0.004	0.119	0.3876	-0.066
Precentral gyrus medial segment R	0.315	0.318	0.003	0.184	0.456	-0.055

Precuneus L	0.499	0.501	0.002	0.190	0.45125	-0.046
Precuneus R	0.482	0.486	0.004	0.062	0.2945	-0.067
Putamen L	0.280	0.281	0.000	0.775	0.901530612244898	-0.012
Putamen R	0.285	0.286	0.001	0.419	0.692260869565217	-0.034
Subcallosal area L	0.478	0.478	0.000	0.679	0.889724137931035	0.015
Subcallosal area R	0.473	0.475	0.002	0.173417	0.459756697674419	0.050
Superior frontal gyrus L	0.468	0.469	0.001	0.266800	0.563244444444444	-0.041
Superior frontal gyrus R	0.499	0.499	0.000	0.707	0.895533333333333	0.013
Superior frontal gyrus medial segment L	0.421	0.422	0.001	0.297	0.5643	-0.040
Superior frontal gyrus medial segment R	0.397	0.398	0.001	0.298	0.556918032786885	0.041
Superior occipital gyrus L	0.353	0.356	0.003	0.133	0.37905	-0.061
Superior occipital gyrus R	0.366	0.370	0.004	0.090	0.330967741935484	-0.068
Superior parietal lobule L	0.392	0.396	0.004	0.076	0.298758620689655	-0.069
Superior parietal lobule R	0.377	0.381	0.003	0.113	0.378882352941177	-0.063
Superior temporal gyrus L	0.442	0.443	0.001	0.433	0.695239436619718	-0.029
Superior temporal gyrus R	0.387	0.389	0.002	0.187	0.453574468085106	-0.052
Supplementary motor cortex L	0.341	0.344	0.003	0.183	0.4636	-0.054
Supplementary motor cortex R	0.378	0.379	0.000	0.920	0.936428571428571	0.004
Supramarginal gyrus L	0.377	0.378	0.002	0.283	0.556241379310345	-0.043
Supramarginal gyrus R	0.340	0.340	0.000	0.794	0.91430303030303	0.011
Temporal pole L	0.409	0.411	0.002	0.174	0.450818181818182	-0.052
Temporal pole R	0.405	0.411	0.006	0.033148	0.222286588235294	-0.082
Thalamus proper L	0.221	0.222	0.001	0.422	0.687257142857143	-0.035
Thalamus proper R	0.239	0.241	0.002	0.277	0.554	-0.048
Transverse temporal gyrus L	0.299	0.299	0.000	0.817	0.895557692307692	0.010
Transverse temporal gyrus R	0.332	0.333	0.001	0.443	0.691808219178082	-0.031
Triangular part of the inferior frontal gyrus L	0.349	0.349	0.001	0.497	0.726384615384615	0.027
Triangular part of the inferior frontal gyrus R	0.324	0.325	0.001	0.371	0.66084375	-0.037

FDR: false discovery rate. L: left. PRS: polygenic risk score. R: right.

Table D.71: Associations between APOEonlyPRS Threshold 10 and 114 regions of interest in amyloid negative participants

Region of Interest	R Square (Model 1)	R Square (Model 2)	R Square Change	Sig. F Change (Model 2)	FDR Corrected value	Standardised beta of PRS
Accumbens area L	0.390	0.391	0.000	0.657	0.891642857142857	0.023
Accumbens area R	0.433	0.434	0.001	0.593	0.938916666666667	0.026
Amygdala L	0.444	0.444	0.000	0.713	0.8556	-0.018
Amygdala R	0.461	0.461	0.000	0.702	0.860516129032258	-0.018
Angular gyrus L	0.428	0.428	0.000	0.878	0.918275229357798	0.008
Angular gyrus R	0.370	0.372	0.001	0.474	0.982472727272727	-0.037
Anterior cingulate gyrus L	0.444	0.447	0.003	0.243	0.791485714285714	0.057
Anterior cingulate gyrus R	0.269	0.278	0.009	0.080	0.912	0.098
Anterior insula L	0.347	0.348	0.001	0.565532	0.934357217391304	0.030
Anterior insula R	0.345	0.347	0.002	0.395	0.938125	0.045
Anterior orbital gyrus L	0.384	0.384	0.000	0.908	0.941018181818182	-0.006
Anterior orbital gyrus R	0.323	0.324	0.000	0.696	0.862434782608696	0.021
Basal forebrain L	0.348	0.352	0.004	0.219	0.805354838709677	0.065
Basal forebrain R	0.382	0.383	0.001	0.549	0.934119402985075	0.031
Calcarine cortex L	0.388	0.396	0.007	0.083	0.860181818181818	-0.089
Calcarine cortex R	0.368	0.375	0.007	0.104414	0.7935464	-0.085
Caudate L	0.189	0.189	0.001	0.652	0.906439024390244	-0.027
Caudate R	0.183	0.183	0.001	0.647594	0.92282145	-0.027
Central operculum L	0.351	0.356	0.005	0.149	0.738521739130435	0.076
Central operculum R	0.322	0.323	0.001	0.604	0.91808	0.028
Cuneus L	0.337	0.337	0.000	0.947	0.963910714285714	0.004
Cuneus R	0.377	0.381	0.005	0.180	0.789230769230769	-0.069
Entorhinal area L	0.374	0.375	0.001	0.551	0.923735294117647	0.031
Entorhinal area R	0.422	0.423	0.001	0.541	0.978952380952381	0.031
Frontal operculum L	0.298	0.312	0.014	0.027641	1	0.121
Frontal operculum R	0.309	0.315	0.006	0.136066	0.738644	0.081

Frontal pole L	0.369	0.369	0.001	0.646	0.93220253164557	0.024
Frontal pole R	0.398	0.405	0.007	0.091	0.8645	0.086
Fusiform gyrus L	0.471	0.474	0.003	0.262	0.786	-0.053
Fusiform gyrus R	0.495	0.496	0.001	0.547	0.959353846153846	-0.028
Gyrus rectus L	0.392	0.395	0.003	0.283	0.827230769230769	0.055
Gyrus rectus R	0.412	0.414	0.002	0.343	0.931	0.048
Hippocampus L	0.430	0.430	0.000	0.938	0.963351351351351	-0.004
Hippocampus R	0.490	0.492	0.002	0.380	0.941739130434783	-0.041
Inferior occipital gyrus L	0.379	0.381	0.002	0.422411	0.926054884615385	-0.042
Inferior occipital gyrus R	0.432	0.433	0.000	0.712	0.863489361702128	-0.018
Inferior temporal gyrus L	0.495	0.495	0.000	0.819	0.8892	-0.011
Inferior temporal gyrus R	0.533	0.534	0.001	0.579	0.929661971830986	-0.025
Lateral orbital gyrus L	0.391	0.402	0.012	0.028218	1	0.112
Lateral orbital gyrus R	0.308	0.314	0.006	0.151	0.71725	0.078
Lingual gyrus L	0.500	0.504	0.005	0.129	0.774	-0.070
Lingual gyrus R	0.537	0.545	0.008	0.043	0.700285714285714	-0.090
Medial frontal cortex L	0.376	0.377	0.001	0.484	0.935186440677966	0.036
Medial frontal cortex R	0.354	0.356	0.002	0.364	0.922133333333333	0.048
Medial orbital gyrus L	0.469	0.469	0.000	0.666	0.853078651685393	0.021
Medial orbital gyrus R	0.385	0.388	0.004	0.232	0.801454545454546	0.061
Middle cingulate gyrus L	0.400	0.403	0.004	0.222	0.790875	0.062
Middle cingulate gyrus R	0.382	0.389	0.007	0.097	0.850615384615385	0.085
Middle frontal gyrus L	0.441	0.441	0.000	0.801198	0.878236269230769	0.012
Middle frontal gyrus R	0.403	0.404	0.000	0.660331	0.8856204	0.022
Middle occipital gyrus L	0.385	0.386	0.001	0.522	0.959806451612903	0.033
Middle occipital gyrus R	0.347	0.348	0.001	0.548	0.946545454545455	0.032
Middle temporal gyrus L	0.521	0.522	0.001	0.402	0.844866666666667	0.038
Middle temporal gyrus R	0.503	0.503	0.000	0.667	0.935265306122449	0.020
Occipital fusiform gyrus L	0.464	0.469	0.005	0.118	0.747333333333333	-0.075
Occipital fusiform gyrus R	0.501	0.501	0.000	0.731	0.859113402061856	-0.016

Occipital pole L	0.323	0.336	0.012	0.033336	0.950076	-0.114
Occipital pole R	0.336	0.336	0.000	0.755	0.869393939393939	-0.017
Opercular part of the inferior frontal gyrus L	0.188	0.204	0.016	0.026804	1	0.130
Opercular part of the inferior frontal gyrus R	0.277	0.290	0.013	0.037	0.703	0.116
Orbital part of the inferior frontal gyrus L	0.289	0.297	0.007	0.113	0.757764705882353	0.087
Orbital part of the inferior frontal gyrus R	0.188	0.196	0.008	0.108	0.7695	0.095
Pallidum L	0.187	0.189	0.002	0.496	0.9424	-0.040
Pallidum R	0.157	0.158	0.001	0.660567	0.875635325581395	-0.026
Parahippocampal gyrus L	0.483	0.483	0.000	0.959	0.967486725663717	0.002
Parahippocampal gyrus R	0.491	0.492	0.000	0.662	0.857590909090909	-0.020
Parietal operculum L	0.355	0.357	0.002	0.346	0.917302325581395	0.050
Parietal operculum R	0.267	0.267	0.001	0.635	0.94012987012987	0.027
Planum polare L	0.385	0.385	0.001	0.647910	0.911873333333333	0.024
Planum polare R	0.424	0.425	0.001	0.636	0.929538461538462	-0.024
Planum temporale L	0.346	0.348	0.002	0.393	0.953234042553192	0.045
Planum temporale R	0.375	0.378	0.003	0.251	0.794833333333333	0.060
Postcentral gyrus L	0.390	0.391	0.000	0.693	0.868153846153846	0.020
Postcentral gyrus R	0.349	0.350	0.001	0.625	0.9375	-0.026
Postcentral gyrus medial segment L	0.213	0.213	0.001	0.655	0.899638554216867	-0.026
Postcentral gyrus medial segment R	0.196	0.197	0.001	0.566404	0.922429371428571	0.034
Posterior cingulate gyrus L	0.517	0.521	0.003	0.186352	0.758718857142857	0.060
Posterior cingulate gyrus R	0.477	0.477	0.000	0.757	0.86298	0.015
Posterior insula L	0.388	0.389	0.001	0.476	0.952	-0.037
Posterior insula R	0.408	0.408	0.000	0.985	0.985	-0.001
Posterior orbital gyrus L	0.423	0.428	0.005	0.135957	0.7749549	0.074
Posterior orbital gyrus R	0.377	0.377	0.001	0.544	0.969	0.031
Precentral gyrus L	0.476	0.482	0.006	0.103772	0.845000571428571	0.077
Precentral gyrus R	0.445	0.448	0.003	0.253	0.779513513513514	0.056
Precentral gyrus medial segment L	0.306	0.306	0.000	0.839	0.89388785046729	0.011
Precentral gyrus medial segment R	0.361	0.361	0.001	0.660856	0.86594924137931	-0.023

Precuneus L	0.453	0.454	0.001	0.508	0.949377049180328	-0.032
Precuneus R	0.496	0.496	0.000	0.875	0.923611111111111	-0.007
Putamen L	0.293	0.298	0.005	0.194	0.762620689655172	-0.072
Putamen R	0.298	0.299	0.002	0.455	0.978679245283019	-0.041
Subcallosal area L	0.470	0.477	0.007	0.063	0.798	0.089
Subcallosal area R	0.411	0.420	0.009	0.048	0.684	0.099
Superior frontal gyrus L	0.441	0.445	0.004	0.172	0.78432	0.067
Superior frontal gyrus R	0.462	0.466	0.003	0.210	0.798	0.060
Superior frontal gyrus medial segment L	0.420	0.422	0.001	0.475	0.966964285714286	0.036
Superior frontal gyrus medial segment R	0.395	0.392	0.000	0.747	0.868959183673469	0.016
Superior occipital gyrus L	0.253	0.254	0.000	0.719	0.8538125	0.020
Superior occipital gyrus R	0.256	0.258	0.002	0.465	0.981666666666667	0.041
Superior parietal lobule L	0.379	0.381	0.002	0.351	0.909409090909091	0.048
Superior parietal lobule R	0.395	0.397	0.002	0.404	0.92112	-0.043
Superior temporal gyrus L	0.358	0.362	0.005	0.185579	0.783555777777778	0.070
Superior temporal gyrus R	0.383	0.384	0.001	0.600	0.936986301369863	0.027
Supplementary motor cortex L	0.393	0.393	0.001	0.601	0.925864864864865	0.027
Supplementary motor cortex R	0.372	0.372	0.000	0.821	0.882962264150943	-0.012
Supramarginal gyrus L	0.302	0.304	0.002	0.421935	0.943148823529412	0.044
Supramarginal gyrus R	0.362	0.362	0.000	0.795	0.888529411764706	0.014
Temporal pole L	0.356	0.356	0.000	0.786	0.887168316831683	0.014
Temporal pole R	0.375	0.376	0.001	0.483	0.949344827586207	-0.036
Thalamus proper L	0.272	0.273	0.000	0.800726	0.886240427184466	-0.014
Thalamus proper R	0.304	0.307	0.003	0.308	0.856390243902439	-0.056
Transverse temporal gyrus L	0.216	0.230	0.014	0.033447	0.7625916	0.123
Transverse temporal gyrus R	0.308	0.311	0.003	0.307	0.87495	0.056
Triangular part of the inferior frontal gyrus L	0.263	0.267	0.004	0.234	0.784588235294118	0.067
Triangular part of the inferior frontal gyrus R	0.256	0.263	0.007	0.142	0.735818181818182	0.083

FDR: false discovery rate. L: left. PRS: polygenic risk score. R: right.

Table D.72: Associations between APOEonlyPRS Threshold 10 and 114 regions of interest in amyloid positive participants

Region of Interest	R Square (Model 1)	R Square (Model 2)	R Square Change	Sig. F Change (Model 2)	FDR Corrected value	Standardised beta of PRS
Accumbens area L	0.398	0.399	0.001	0.504043	0.776498675675676	-0.026
Accumbens area R	0.374	0.374	0.000	0.871	0.919388888888889	0.006
Amygdala L	0.383	0.397	0.014	0.001	0.0228	-0.126
Amygdala R	0.444	0.464	0.019	0.000066277022741	0.003777790296237	-0.148
Angular gyrus L	0.391	0.395	0.004	0.071	0.32376	-0.070
Angular gyrus R	0.430	0.434	0.003	0.115	0.422903225806452	-0.060
Anterior cingulate gyrus L	0.388	0.388	0.000	0.791	0.884058823529412	-0.010
Anterior cingulate gyrus R	0.224	0.228	0.004	0.142	0.462514285714286	-0.065
Anterior insula L	0.401	0.401	0.000	0.758	0.890845360824742	0.012
Anterior insula R	0.415	0.415	0.000	0.662	0.838533333333333	0.017
Anterior orbital gyrus L	0.413	0.416	0.003	0.137728	0.475787636363636	-0.057
Anterior orbital gyrus R	0.390	0.397	0.007	0.022853	0.200403230769231	-0.089
Basal forebrain L	0.261	0.264	0.003	0.195	0.494	-0.056
Basal forebrain R	0.347	0.348	0.000	0.771	0.870237623762376	-0.012
Calcarine cortex L	0.361	0.361	0.000	0.576	0.800780487804878	-0.022
Calcarine cortex R	0.385	0.388	0.003	0.138284	0.463658117647059	-0.058
Caudate L	0.223	0.223	0.000	0.710	0.870322580645161	-0.016
Caudate R	0.212	0.212	0.000	0.738	0.895021276595745	-0.015
Central operculum L	0.384	0.386	0.002	0.294	0.588	0.041
Central operculum R	0.399	0.399	0.000	0.881	0.921412844036697	-0.006
Cuneus L	0.441	0.448	0.007	0.020837	0.215947090909091	-0.086
Cuneus R	0.446	0.450	0.004	0.060	0.310909090909091	-0.070
Entorhinal area L	0.397	0.408	0.011	0.003585	0.068115	-0.113
Entorhinal area R	0.452	0.462	0.010	0.003951	0.0643448571428571	-0.107
Frontal operculum L	0.392	0.392	0.000	0.739	0.8868	0.013
Frontal operculum R	0.320	0.320	0.000	0.936	0.952714285714286	-0.002

Frontal pole L	0.469	0.469	0.000	0.770	0.8778	0.011
Frontal pole R	0.431	0.431	0.000	0.747	0.8870625	0.012
Fusiform gyrus L	0.510	0.515	0.004	0.048	0.288	-0.069
Fusiform gyrus R	0.538	0.543	0.005	0.031	0.2356	-0.073
Gyrus rectus L	0.451	0.451	0.000	0.607	0.814094117647059	-0.019
Gyrus rectus R	0.464	0.465	0.001	0.453	0.71725	0.028
Hippocampus L	0.422	0.439	0.017	0.000209902674354	0.005982226219089	-0.140
Hippocampus R	0.442	0.465	0.023	0.000015609235453	0.001779452841642	-0.160
Inferior occipital gyrus L	0.424	0.429	0.004	0.070	0.3325	-0.069
Inferior occipital gyrus R	0.479	0.489	0.010	0.003961	0.05644425	-0.104
Inferior temporal gyrus L	0.493	0.498	0.005	0.041	0.274941176470588	-0.073
Inferior temporal gyrus R	0.540	0.543	0.004	0.055666	0.3172962	-0.065
Lateral orbital gyrus L	0.433	0.434	0.001	0.420640	0.705190588235294	-0.030
Lateral orbital gyrus R	0.408	0.409	0.001	0.488	0.762082191780822	-0.027
Lingual gyrus L	0.506	0.506	0.000	0.608	0.805953488372093	-0.018
Lingual gyrus R	0.517	0.518	0.001	0.247	0.531283018867925	-0.040
Medial frontal cortex L	0.348	0.351	0.002	0.193	0.511674418604651	-0.053
Medial frontal cortex R	0.371	0.371	0.000	0.805	0.890970873786408	-0.010
Medial orbital gyrus L	0.483	0.484	0.001	0.420533	0.71553376119403	-0.029
Medial orbital gyrus R	0.468	0.468	0.000	0.811	0.888980769230769	-0.009
Middle cingulate gyrus L	0.397	0.398	0.001	0.416	0.718545454545454	-0.032
Middle cingulate gyrus R	0.332	0.336	0.004	0.101	0.397034482758621	-0.067
Middle frontal gyrus L	0.498	0.498	0.000	0.560	0.788148148148148	-0.021
Middle frontal gyrus R	0.504	0.505	0.000	0.588	0.807614457831325	-0.019
Middle occipital gyrus L	0.360	0.365	0.006	0.046	0.291333333333333	-0.080
Middle occipital gyrus R	0.354	0.374	0.020	0.000177286320585	0.00673688018223	-0.150
Middle temporal gyrus L	0.480	0.483	0.003	0.085	0.190502142857143	-0.062
Middle temporal gyrus R	0.520	0.525	0.005	0.023395	0.372692307692308	-0.079
Occipital fusiform gyrus L	0.470	0.471	0.000	0.703	0.871108695652174	0.014
Occipital fusiform gyrus R	0.517	0.521	0.004	0.068	0.33704347826087	-0.063

Occipital pole L	0.328	0.328	0.000	0.860	0.916261682242991	-0.007
Occipital pole R	0.396	0.397	0.001	0.361	0.663774193548387	-0.036
Opercular part of the inferior frontal gyrus L	0.302	0.304	0.002	0.309	0.597050847457627	0.043
Opercular part of the inferior frontal gyrus R	0.270	0.270	0.000	0.612	0.801931034482759	0.022
Orbital part of the inferior frontal gyrus L	0.275	0.275	0.000	0.940	0.948318584070796	-0.003
Orbital part of the inferior frontal gyrus R	0.310	0.313	0.002	0.204	0.4845	-0.053
Pallidum L	0.120	0.123	0.003	0.224	0.51072	-0.057
Pallidum R	0.103	0.107	0.004	0.180	0.513	-0.064
Parahippocampal gyrus L	0.477	0.484	0.007	0.012	0.1368	-0.091
Parahippocampal gyrus R	0.514	0.522	0.009	0.005	0.0633333333333333	-0.098
Parietal operculum L	0.314	0.315	0.001	0.504061	0.76617272	0.028
Parietal operculum R	0.294	0.295	0.000	0.623	0.807068181818182	0.021
Planum polare L	0.457	0.458	0.001	0.359	0.670918032786885	-0.034
Planum polare R	0.466	0.467	0.001	0.368	0.665904761904762	-0.033
Planum temporale L	0.354	0.354	0.000	0.655	0.838988764044944	0.018
Planum temporale R	0.329	0.329	0.000	0.908	0.941018181818182	-0.005
Postcentral gyrus L	0.394	0.395	0.000	0.598	0.811571428571429	-0.021
Postcentral gyrus R	0.411	0.415	0.003	0.106	0.4028	-0.062
Postcentral gyrus medial segment L	0.186	0.195	0.010	0.021687	0.2060265	-0.104
Postcentral gyrus medial segment R	0.245	0.248	0.004	0.146125	0.450222972972973	-0.063
Posterior cingulate gyrus L	0.546	0.548	0.002	0.157	0.471	-0.048
Posterior cingulate gyrus R	0.511	0.516	0.005	0.035	0.249375	-0.074
Posterior insula L	0.395	0.397	0.002	0.251	0.529888888888889	0.045
Posterior insula R	0.423	0.423	0.000	0.824	0.894628571428571	0.008
Posterior orbital gyrus L	0.348	0.349	0.001	0.532	0.777538461538462	-0.025
Posterior orbital gyrus R	0.394	0.397	0.002	0.202	0.489957446808511	-0.050
Precentral gyrus L	0.457	0.457	0.000	0.976	0.976	-0.001
Precentral gyrus R	0.448	0.448	0.000	0.765	0.889897959183673	-0.011
Precentral gyrus medial segment L	0.286	0.290	0.004	0.117	0.4168125	-0.066
Precentral gyrus medial segment R	0.315	0.318	0.003	0.182	0.506048780487805	-0.055

Precuneus L	0.499	0.500	0.001	0.279	0.567964285714286	-0.038
Precuneus R	0.482	0.485	0.003	0.099	0.403071428571429	-0.059
Putamen L	0.280	0.281	0.000	0.701	0.878175824175824	-0.016
Putamen R	0.285	0.286	0.001	0.422	0.697217391304348	-0.034
Subcallosal area L	0.478	0.478	0.000	0.549	0.782325	0.022
Subcallosal area R	0.473	0.476	0.002	0.145576	0.460990666666667	0.053
Superior frontal gyrus L	0.468	0.469	0.001	0.336	0.6384	-0.035
Superior frontal gyrus R	0.499	0.499	0.000	0.546	0.787898734177215	0.021
Superior frontal gyrus medial segment L	0.421	0.422	0.001	0.451	0.724140845070423	-0.029
Superior frontal gyrus medial segment R	0.397	0.398	0.002	0.259	0.536836363636364	0.044
Superior occipital gyrus L	0.353	0.355	0.002	0.191	0.518428571428571	-0.053
Superior occipital gyrus R	0.366	0.368	0.002	0.194	0.502636363636364	-0.052
Superior parietal lobule L	0.392	0.395	0.004	0.098	0.413777777777778	-0.065
Superior parietal lobule R	0.377	0.379	0.002	0.197	0.488217391304348	-0.051
Superior temporal gyrus L	0.442	0.443	0.001	0.506	0.759	-0.025
Superior temporal gyrus R	0.387	0.390	0.003	0.163	0.476461538461538	-0.055
Supplementary motor cortex L	0.341	0.344	0.002	0.234	0.513	-0.048
Supplementary motor cortex R	0.378	0.378	0.000	0.926	0.951027027027027	0.004
Supramarginal gyrus L	0.377	0.378	0.001	0.300	0.589655172413793	-0.041
Supramarginal gyrus R	0.340	0.340	0.000	0.768	0.884363636363636	0.012
Temporal pole L	0.409	0.411	0.002	0.219	0.509510204081633	-0.047
Temporal pole R	0.405	0.410	0.005	0.056457	0.306480857142857	-0.074
Thalamus proper L	0.221	0.223	0.001	0.400	0.701538461538462	-0.037
Thalamus proper R	0.239	0.243	0.002	0.231	0.516352941176471	-0.052
Transverse temporal gyrus L	0.299	0.299	0.000	0.836	0.899094339622641	0.009
Transverse temporal gyrus R	0.332	0.333	0.001	0.512	0.758025974025974	-0.027
Triangular part of the inferior frontal gyrus L	0.349	0.350	0.001	0.429	0.698657142857143	0.032
Triangular part of the inferior frontal gyrus R	0.324	0.325	0.001	0.391	0.69646875	-0.035

FDR: false discovery rate. L: left. PRS: polygenic risk score. R: right.

APPENDIX E1 (Chapter 5: Experiment Two Part A)

Table E1.1: Associations between PRSs and cross-sectional CSF Aβ42 status in the whole group when CSF p-tau181 status was not controlled for

PRS & Threshold	Chi-square	df	*p*	Nagelkerke R^2	Wald	df	*p*	OR	95% CI	Nagelkerke R^2 Model 1
PRSwithAPOE										
Threshold 1	176.411	16	<0.001	0.389	53.163	1	0.000000000000307	2.567	1.993-3.308	0.256
Threshold 5	174.969	16	<0.001	0.386	52.198	1	0.0000000000005017	2.550	1.978-3.288	0.256
Threshold 10	168.462	16	<0.001	0.374	48.758	1	0.0000000000028955	2.441	1.900-3.135	0.256
PRSwithoutAPOE										
Threshold 1	109.903	16	<0.001	0.258	0.807	1	0.369	1.091	0.903-1.318	0.256
Threshold 5	109.747	16	<0.001	0.257	0.650	1	0.420	1.084	0.891-1.318	0.256
Threshold 10	109.984	16	<0.001	0.258	0.886	1	0.347	1.105	0.898-1.359	0.256
APOEonlyPRS										
Threshold 1	176.835	16	<0.001	0.390	53.127	1	0.00000000000031273	2.579	1.999-3.328	0.256
Threshold 5	177.310	16	<0.001	0.391	53.212	1	0.00000000000029938	2.606	2.015-3.370	0.256
Threshold 10	173.077	16	<0.001	0.383	50.894	1	0.00000000000097476	2.501	1.944-3.217	0.256

APOE: apolipoprotein E. CI: confidence interval. df: degrees of freedom. OR: odds ratio. PRS: polygenic risk score.

Table E1.2: Associations between PRSs and cross-sectional CSF Aβ42 status in the whole group when CSF p-tau181 status was controlled for

PRS & Threshold	Chi-square	df	*p*	Nagelkerke R^2	Wald	df	*p*	OR	95% CI	Nagelkerke R^2 Model 1
PRSwithAPOE										
Threshold 1	207.758	17	<0.001	0.445	46.186	1	0.000000000010753	2.459	1.897-3.187	0.341
Threshold 5	204.922	17	<0.001	0.440	44.313	1	0.000000000027988	2.411	1.861-3.124	0.341
Threshold 10	199.591	17	<0.001	0.431	41.242	1	0.00000000013452	2.313	1.790-2.987	0.341
PRSwithoutAPOE										
Threshold 1	152.002	17	<0.001	0.343	1.024	1	0.312	1.107	0.909-1.349	0.341
Threshold 5	151.329	17	<0.001	0.341	0.355	1	0.551	1.064	0.868-1.303	0.341
Threshold 10	151.610	17	<0.001	0.342	0.635	1	0.426	1.091	0.881-1.351	0.341
APOEonlyPRS										
Threshold 1	207.456	17	<0.001	0.445	45.778	1	0.000000000013243	2.459	1.895-3.191	0.341
Threshold 5	207.568	17	<0.001	0.445	45.689	1	0.000000000013862	2.477	1.904-3.223	0.341
Threshold 10	203.268	17	<0.001	0.437	43.137	1	0.00000000005105	2.367	1.831-3.062	0.341

APOE: apolipoprotein E. CI: confidence interval. df: degrees of freedom. OR: odds ratio. PRS: polygenic risk score.

Table E1.3: Associations between PRSs and cross-sectional CSF Aβ42 status in APOE ε4 carriers when CSF p-tau181 status was not controlled for

PRS & Threshold	Chi-square	df	*p*	Nagelkerke R^2	Wald	df	*p*	OR	95% CI	Nagelkerke R^2 Model 1
PRSwithAPOE										
Threshold 1	50.299	16	<0.001	0.371	9.351	1	0.002	2.888	1.464-5.700	0.292
Threshold 5	50.459	16	<0.001	0.372	9.649	1	0.002	2.815	1.465-5.410	0.292
Threshold 10	50.106	16	<0.001	0.370	9.550	1	0.002	2.737	1.445-5.184	0.292
PRSwithoutAPOE										
Threshold 1	44.973	16	<0.001	0.336	5.780	1	0.016	1.821	1.117-2.969	0.292
Threshold 5	43.674	16	<0.001	0.327	4.589	1	0.032	1.761	1.049-2.954	0.292
Threshold 10	42.554	16	<0.001	0.320	3.732	1	0.053	1.608	0.993-2.603	0.292
APOEonlyPRS										
Threshold 1	45.909	16	<0.001	0.342	6.279	1	0.012	2.290	1.198-4.380	0.292
Threshold 5	45.297	16	<0.001	0.338	5.812	1	0.016	2.212	1.160-4.217	0.292
Threshold 10	44.388	16	<0.001	0.332	5.197	1	0.023	2.061	1.107-3.838	0.292

APOE: apolipoprotein E. CI: confidence interval. df: degrees of freedom. OR: odds ratio. PRS: polygenic risk score.

Table E1.4: Associations between PRSs and cross-sectional CSF Aβ42 status in APOE ε4 non-carriers when CSF p-tau181 status was not controlled for

PRS & Threshold	Chi-square	df	*p*	Nagelkerke R^2	Wald	df	*p*	OR	95% CI	Nagelkerke R^2 Model 1
PRSwithAPOE										
Threshold 1	64.588	16	<0.001	0.258	0.967	1	0.325	0.777	0.470-1.285	0.255
Threshold 5	64.426	16	<0.001	0.372	0.806	1	0.369	0.802	0.495-1.299	0.255
Threshold 10	64.501	16	<0.001	0.258	0.880	1	0.348	0.806	0.514-1.265	0.255
PRSwithoutAPOE										
Threshold 1	63.808	16	<0.001	0.255	0.187	1	0.665	0.946	0.738-1.214	0.255
Threshold 5	63.638	16	<0.001	0.255	0.018	1	0.894	0.983	0.767-1.261	0.255
Threshold 10	63.747	16	<0.001	0.255	0.127	1	0.722	1.051	0.799-1.382	0.255
APOEonlyPRS										
Threshold 1	64.243	16	<0.001	0.257	0.622	1	0.430	0.806	0.472-1.377	0.255
Threshold 5	64.147	16	<0.001	0.257	0.526	1	0.468	0.819	0.477-1.406	0.255
Threshold 10	64.615	16	<0.001	0.258	0.993	1	0.319	0.767	0.455-1.292	0.255

APOE: apolipoprotein E. CI: confidence interval. df: degrees of freedom. OR: odds ratio. PRS: polygenic risk score.

Table E1.5: Associations between PRSs and cross-sectional CSF Aβ42 status in APOE ε4 carriers when CSF p-tau181 status was controlled for

PRS & Threshold	Chi-square	df	*p*	Nagelkerke R^2	Wald	df	*p*	OR	95% CI	Nagelkerke R^2 Model 1
PRSwithAPOE										
Threshold 1	55.208	17	<0.001	0.403	10.006	1	0.002	3.128	1.543-6.341	0.319
Threshold 5	54.855	17	<0.001	0.401	10.010	1	0.002	2.947	1.509-5.757	0.319
Threshold 10	54.321	17	<0.001	0.397	9.800	1	0.002	2.845	1.478-5.476	0.319
PRSwithoutAPOE										
Threshold 1	49.217	17	<0.001	0.364	5.958	1	0.015	1.878	1.132-3.115	0.319
Threshold 5	47.296	17	<0.001	0.352	4.228	1	0.040	1.746	1.026-2.970	0.319
Threshold 10	46.037	17	<0.001	0.343	3.259	1	0.071	1.576	0.962-2.584	0.319
APOEonlyPRS										
Threshold 1	50.405	17	<0.001	0.372	6.645	1	0.010	2.411	1.235-4.706	0.319
Threshold 5	49.761	17	<0.001	0.368	6.163	1	0.013	2.328	1.195-4.535	0.319
Threshold 10	48.642	17	<0.001	0.360	5.420	1	0.020	2.132	1.127-4.034	0.319

APOE: apolipoprotein E. CI: confidence interval. df: degrees of freedom. OR: odds ratio. PRS: polygenic risk score.

Table E1.6: Associations between PRSs and cross-sectional CSF Aβ42 status in APOE ε4 non-carriers when CSF p-tau181 status was controlled for

PRS & Threshold	Chi-square	df	*p*	Nagelkerke R^2	Wald	df	*p*	OR	95% CI	Nagelkerke R^2 Model 1
PRSwithAPOE										
Threshold 1	85.152	17	<0.001	0.330	1.037	1	0.308	0.762	0.452-1.285	0.326
Threshold 5	85.211	17	<0.001	0.330	1.096	1	0.295	0.764	0.462-1.264	0.326
Threshold 10	85.153	17	<0.001	0.330	1.037	1	0.308	0.786	0.495-1.249	0.326
PRSwithoutAPOE										
Threshold 1	84.273	17	<0.001	0.327	0.160	1	0.689	0.949	0.736-1.224	0.326
Threshold 5	84.192	17	<0.001	0.326	0.080	1	0.778	0.964	0.746-1.245	0.326
Threshold 10	84.184	17	<0.001	0.326	0.072	1	0.789	1.039	0.787-1.372	0.326
APOEonlyPRS										
Threshold 1	84.788	17	<0.001	0.328	0.675	1	0.411	0.792	0.454-1.382	0.326
Threshold 5	84.719	17	<0.001	0.328	0.606	1	0.436	0.800	0.456-1.403	0.326
Threshold 10	85.325	17	<0.001	0.330	1.210	1	0.271	0.739	0.432-1.266	0.326

APOE: apolipoprotein E. CI: confidence interval. df: degrees of freedom. OR: odds ratio. PRS: polygenic risk score.

Table E1.7: Associations between PRSs and cross-sectional CSF Aβ42 status in MCI patients when CSF p-tau181 status was not controlled for

PRS & Threshold	Chi-square	df	*p*	Nagelkerke R^2	Wald	df	*p*	OR	95% CI	Nagelkerke R^2 Model 1
PRSwithAPOE										
Threshold 1	98.443	16	<0.001	0.377	38.390	1	0.00000000057928	3.050	2.143-4.340	0.189
Threshold 5	99.708	16	<0.001	0.381	38.863	1	0.00000000045464	3.176	2.209-4.568	0.189
Threshold 10	93.025	16	<0.001	0.359	36.220	1	0.0000000017625	2.962	2.080-4.219	0.189
PRSwithoutAPOE										
Threshold 1	48.373	16	<0.001	0.201	3.069	1	0.080	1.257	0.973-1.625	0.189
Threshold 5	47.570	16	<0.001	0.197	2.281	1	0.131	1.225	0.941-1.595	0.189
Threshold 10	46.559	16	<0.001	0.194	1.294	1	0.255	1.178	0.889-1.561	0.189
APOEonlyPRS										
Threshold 1	95.633	16	<0.001	0.368	36.780	1	0.0000000013227	2.956	2.083-4.197	0.189
Threshold 5	96.066	16	<0.001	0.369	36.813	1	0.0000000013	2.995	2.101-4.269	0.189
Threshold 10	93.180	16	<0.001	0.360	35.698	1	0.0000000023045	2.835	2.014-3.990	0.189

APOE: apolipoprotein E. CI: confidence interval. df: degrees of freedom. OR: odds ratio. PRS: polygenic risk score.

Table E1.8: Associations between PRSs and cross-sectional CSF Aβ42 status in CU participants when CSF p-tau181 status was not controlled for

PRS & Threshold	Chi-square	df	*p*	Nagelkerke R^2	Wald	df	*p*	OR	95% CI	Nagelkerke R^2 Model 1
PRSwithAPOE										
Threshold 1	15.901	16	0.460	0.173	3.221	1	0.073	1.628	0.956-2.770	0.138
Threshold 5	15.054	16	0.521	0.165	2.438	1	0.118	1.500	0.902-2.495	0.138
Threshold 10	15.113	16	0.516	0.165	2.497	1	0.114	1.503	0.907-2.490	0.138
PRSwithoutAPOE										
Threshold 1	12.913	16	0.679	0.142	0.369	1	0.543	0.887	0.602-1.306	0.138
Threshold 5	12.694	16	0.695	0.140	0.153	1	0.696	0.926	0.631-1.360	0.138
Threshold 10	12.565	16	0.704	0.139	0.024	1	0.877	0.968	0.647-1.451	0.138
APOEonlyPRS										
Threshold 1	16.854	16	0.395	0.183	4.038	1	0.044	1.723	1.013-2.930	0.138
Threshold 5	17.056	16	0.382	0.185	4.214	1	0.040	1.755	1.026-3.001	0.138
Threshold 10	16.952	16	0.389	0.184	4.131	1	0.042	1.753	1.020-3.011	0.138

APOE: apolipoprotein E. CI: confidence interval. df: degrees of freedom. OR: odds ratio. PRS: polygenic risk score.

Table E1.9: Associations between PRSs and cross-sectional CSF Aβ42 status in AD dementia patients when CSF p-tau181 status was not controlled for

PRS & Threshold	Chi-square	df	*p*	Nagelkerke R^2	Wald	df	*p*	OR	95% CI	Nagelkerke R^2 Model 1
PRSwithAPOE										
Threshold 1	51.015	16	<0.001	1.000	0.012	1	0.912	4.572E+249	0.000-not available	0.349
Threshold 5	51.015	16	<0.001	1.000	0.000	1	0.992	2.084E+87	0.000-not available	0.349
Threshold 10	51.015	16	<0.001	1.000	0.017	1	0.897	2.659E+293	0.000-not available	0.349
PRSwithoutAPOE										
Threshold 1	23.571	16	0.099	0.524	5.153	1	0.023	6.898	1.302-36.544	0.349
Threshold 5	21.258	16	0.169	0.478	4.206	1	0.040	4.825	1.072-21.710	0.349
Threshold 10	18.133	16	0.316	0.141	2.455	1	0.117	2.568	0.789-8.352	0.349
APOEonlyPRS										
Threshold 1	28.830	16	0.025	0.626	3.046	1	0.081	157.377	0.537-46142.913	0.349
Threshold 5	29.749	16	0.019	0.643	3.219	1	0.073	253.283	0.600-107008.695	0.349
Threshold 10	32.679	16	0.008	0.697	1.082	1	0.298	2104999.023	0.000-1.721E+18	0.349

APOE: apolipoprotein E. CI: confidence interval. df: degrees of freedom. OR: odds ratio. PRS: polygenic risk score.

Table E1.10: Associations between PRSs and cross-sectional CSF Aβ42 status in MCI patients when CSF p-tau181 status was controlled for

PRS & Threshold	Chi-square	df	*p*	Nagelkerke R^2	Wald	df	*p*	OR	95% CI	Nagelkerke R^2 Model 1
PRSwithAPOE										
Threshold 1	121.956	17	<0.001	0.450	33.546	1	0.0000000069589	2.933	2.038-4.220	0.304
Threshold 5	121.347	17	<0.001	0.448	33.185	1	0.000000008378	2.981	2.056-4.322	0.304
Threshold 10	115.784	17	<0.001	0.431	30.727	1	0.000000029695	2.796	1.944-4.023	0.304
PRSwithoutAPOE										
Threshold 1	79.857	17	<0.001	0.315	2.934	1	0.087	1.268	0.966-1.663	0.304
Threshold 5	78.121	17	<0.001	0.309	1.253	1	0.263	1.172	0.888-1.547	0.304
Threshold 10	77.483	17	<0.001	0.307	0.622	1	0.430	1.126	0.838-1.512	0.304
APOEonlyPRS										
Threshold 1	118.643	17	<0.001	0.440	31.660	1	0.000000018362	2.794	1.953-3.995	0.304
Threshold 5	118.612	17	<0.001	0.440	31.482	1	0.000000020127	2.813	1.960-4.038	0.304
Threshold 10	115.876	17	<0.001	0.431	30.287	1	0.000000037266	2.671	1.883-3.791	0.304

APOE: apolipoprotein E. CI: confidence interval. df: degrees of freedom. OR: odds ratio. PRS: polygenic risk score.

Table E1.11: Associations between PRSs and cross-sectional CSF Aβ42 status in CU participants when CSCF p-tau181 status was controlled for

PRS & Threshold	Chi-square	df	*p*	Nagelkerke R^2	Wald	df	*p*	OR	95% CI	Nagelkerke R^2 Model 1
PRSwithAPOE										
Threshold 1	16.730	17	0.473	0.182	3.126	1	0.077	1.621	0.949-2.767	0.148
Threshold 5	15.906	17	0.531	0.173	2.356	1	0.125	1.494	0.895-2.494	0.148
Threshold 10	15.980	17	0.525	0.174	2.429	1	0.119	1.496	0.901-2.482	0.148
PRSwithoutAPOE										
Threshold 1	13.798	17	0.681	0.152	0.309	1	0.578	0.896	0.608-1.320	0.148
Threshold 5	13.616	17	0.694	0.150	0.129	1	0.719	0.932	0.634-1.369	0.148
Threshold 10	13.490	17	0.703	0.148	0.004	1	0.952	0.988	0.658-1.482	0.148
APOEonlyPRS										
Threshold 1	17.596	17	0.415	0.190	3.883	1	0.049	1.709	1.003-2.913	0.148
Threshold 5	17.775	17	0.403	0.192	4.038	1	0.044	1.739	1.014-2.984	0.148
Threshold 10	17.549	17	0.418	0.190	3.846	1	0.050	1.723	1.000-2.968	0.148

APOE: apolipoprotein E. CI: confidence interval. df: degrees of freedom. OR: odds ratio. PRS: polygenic risk score.

Table E1.12: Associations between PRSs and cross-sectional CSF Aβ42 status in AD dementia patients when CSF p-tau181 status was controlled for

PRS & Threshold	Chi-square	df	*p*	Nagelkerke R^2	Wald	df	*p*	OR	95% CI	Nagelkerke R^2 Model 1
PRSwithAPOE										
Threshold 1	51.015	17	<0.001	1.000	0.002	1	0.967	5.655E+54	0.000-not available	0.401
Threshold 5	51.015	17	<0.001	1.000	0.001	1	0.969	1.102E+46	0.000-not available	0.401
Threshold 10	51.015	17	<0.001	1.000	0.002	1	0.963	1.804E+63	0.000-not available	0.401
PRSwithoutAPOE										
Threshold 1	28.985	17	0.035	0.629	4.578	1	0.032	13.085	1.241-137.944	0.401
Threshold 5	25.159	17	0.091	0.555	4.704	1	0.030	5.470	1.178-25.404	0.401
Threshold 10	21.237	17	0.216	0.478	3.003	1	0.083	2.695	0.878-8.272	0.401
APOEonlyPRS										
Threshold 1	30.130	17	0.025	0.650	3.189	1	0.074	108.126	0.633-18465.278	0.401
Threshold 5	30.681	17	0.022	0.660	3.225	1	0.073	137.383	0.637-29610.649	0.401
Threshold 10	34.190	17	0.008	0.724	1.197	1	0.274	32567.448	0.000-3.966E+12	0.401

APOE: apolipoprotein E. CI: confidence interval. df: degrees of freedom. OR: odds ratio. PRS: polygenic risk score.

Table E1.13: Associations between PRSs and cross-sectional CSF p-tau181 status in the whole group when CSF Aβ42 status was not controlled for

PRS & Threshold	Chi-square	df	*p*	Nagelkerke R^2	Wald	df	*p*	OR	95% CI	Nagelkerke R^2 Model 1
PRSwithAPOE										
Threshold 1	91.222	16	<0.001	0.220	13.382	1	0.000254054306593	1.437	1.183-1.745	0.190
Threshold 5	94.018	16	<0.001	0.226	16.010	1	0.000062017805674	1.492	1.227-1.814	0.190
Threshold 10	92.401	16	<0.001	0.223	14.488	1	0.000141043200499	1.476	1.208-1.803	0.190
PRSwithoutAPOE										
Threshold 1	78.055	16	<0.001	0.191	0.399	1	0.528	0.940	0.776-1.139	0.190
Threshold 5	77.925	16	<0.001	0.191	0.270	1	0.603	1.053	0.867-1.279	0.190
Threshold 10	77.876	16	<0.001	0.190	0.221	1	0.638	1.050	0.856-1.288	0.190
APOEonlyPRS										
Threshold 1	93.828	16	<0.001	0.226	15.809	1	0.000070064027593	1.481	1.220-1.798	0.190
Threshold 5	94.315	16	<0.001	0.227	16.261	1	0.000055199027228	1.491	1.228-1.811	0.190
Threshold 10	93.853	16	<0.001	0.226	15.812	1	0.000069975440667	1.485	1.222-1.805	0.190

APOE: apolipoprotein E. CI: confidence interval. df: degrees of freedom. OR: odds ratio. PRS: polygenic risk score.

Table E1.14: Associations between PRSs and cross-sectional CSF p-tau181 status in the whole group when CSF Aβ42 status was controlled for

PRS & Threshold	Chi-square	df	*p*	Nagelkerke R^2	Wald	df	*p*	OR	95% CI	Nagelkerke R^2 Model 1
PRSwithAPOE										
Threshold 1	125.818	17	<0.001	0.294	2.170	1	0.141	1.168	0.950-1.437	0.290
Threshold 5	127.201	17	<0.001	0.297	3.541	1	0.060	1.221	0.992-1.502	0.290
Threshold 10	126.719	17	<0.001	0.296	3.065	1	0.080	1.209	0.978-1.496	0.290
PRSwithoutAPOE										
Threshold 1	124.505	17	<0.001	0.291	0.857	1	0.355	0.909	0.743-1.112	0.290
Threshold 5	123.727	17	<0.001	0.290	0.083	1	0.774	1.031	0.840-1.265	0.290
Threshold 10	123.668	17	<0.001	0.290	0.024	1	0.877	1.017	0.820-1.261	0.290
APOEonlyPRS										
Threshold 1	127.021	17	<0.001	0.297	3.356	1	0.067	1.212	0.987-1.488	0.290
Threshold 5	127.279	17	<0.001	0.297	3.611	1	0.057	1.221	0.994-1.501	0.290
Threshold 10	127.230	17	<0.001	0.297	3.562	1	0.059	1.220	0.992-1.500	0.290

APOE: apolipoprotein E. CI: confidence interval. df: degrees of freedom. OR: odds ratio. PRS: polygenic risk score.

Table E1.15: Associations between PRSs and cross-sectional CSF p-tau181 status in MCI patients when CSF Aβ42 status was not controlled for

PRS & Threshold	Chi-square	df	*p*	Nagelkerke R^2	Wald	df	*p*	OR	95% CI	Nagelkerke R^2 Model 1
PRSwithAPOE										
Threshold 1	41.796	16	<0.001	0.181	7.704	1	0.006	1.449	1.115-1.883	0.150
Threshold 5	44.289	16	<0.001	0.191	10.066	1	0.002	1.537	1.178-2.004	0.150
Threshold 10	42.761	16	<0.001	0.185	8.599	1	0.003	1.505	1.145-1.977	0.150
PRSwithoutAPOE										
Threshold 1	34.018	16	0.005	0.150	0.008	1	0.927	1.012	0.783-1.309	0.150
Threshold 5	35.538	16	0.003	0.156	1.522	1	0.217	1.179	0.908-1.531	0.150
Threshold 10	34.761	16	0.004	0.153	0.748	1	0.387	1.133	0.853-1.506	0.150
APOEonlyPRS										
Threshold 1	42.555	16	<0.001	0.184	8.396	1	0.004	1.466	1.132-1.900	0.150
Threshold 5	43.060	16	<0.001	0.187	8.864	1	0.003	1.483	1.144-1.923	0.150
Threshold 10	42.934	16	<0.001	0.186	8.713	1	0.003	1.480	1.141-1.920	0.150

APOE: apolipoprotein E. CI: confidence interval. df: degrees of freedom. OR: odds ratio. PRS: polygenic risk score.

Table E1.16: Associations between PRSs and cross-sectional CSF p-tau181 status in CU participants when CSF Aβ42 status was not controlled for

PRS & Threshold	Chi-square	df	*p*	Nagelkerke R^2	Wald	df	*p*	OR	95% CI	Nagelkerke R^2 Model 1
PRSwithAPOE										
Threshold 1	22.205	16	0.137	0.287	0.554	1	0.457	1.297	0.654-2.575	0.281
Threshold 5	22.008	16	0.143	0.285	0.351	1	0.554	1.226	0.625-2.407	0.281
Threshold 10	21.876	16	0.147	0.283	0.216	1	0.642	1.174	0.596-2.313	0.281
PRSwithoutAPOE										
Threshold 1	22.034	16	0.142	0.285	0.371	1	0.543	0.848	0.499-1.442	0.281
Threshold 5	21.909	16	0.146	0.284	0.246	1	0.620	0.879	0.529-1.462	0.281
Threshold 10	22.642	16	0.124	0.292	0.967	1	0.325	0.758	0.436-1.317	0.281
APOEonlyPRS										
Threshold 1	22.604	16	0.125	0.292	0.979	1	0.322	1.406	0.716-2.763	0.281
Threshold 5	22.813	16	0.119	0.294	1.198	1	0.274	1.459	0.742-2.868	0.281
Threshold 10	23.637	16	0.098	0.304	2.051	1	0.152	1.631	0.835-3.188	0.281

APOE: apolipoprotein E. CI: confidence interval. df: degrees of freedom. OR: odds ratio. PRS: polygenic risk score.

Table E1.17: Associations between PRSs and cross-sectional CSF p-tau181 status in AD dementia patients when CSF Aβ42 status was not controlled for

PRS & Threshold	Chi-square	df	*p*	Nagelkerke R^2	Wald	df	*p*	OR	95% CI	Nagelkerke R^2 Model 1
PRSwithAPOE										
Threshold 1	26.097	16	0.053	0.321	3.263	1	0.071	1.545	0.964-2.478	0.284
Threshold 5	26.696	16	0.045	0.328	3.802	1	0.051	1.621	0.997-2.635	0.284
Threshold 10	26.721	16	0.045	0.328	3.790	1	0.052	1.638	0.997-2.691	0.284
PRSwithoutAPOE										
Threshold 1	24.206	16	0.085	0.301	1.458	1	0.227	0.675	0.357-1.277	0.284
Threshold 5	23.655	16	0.097	0.295	0.926	1	0.336	0.727	0.379-1.393	0.284
Threshold 10	22.760	16	0.120	0.285	0.050	1	0.823	0.938	0.538-1.637	0.284
APOEonlyPRS										
Threshold 1	27.882	16	0.033	0.341	4.792	1	0.029	1.758	1.061-2.913	0.284
Threshold 5	28.081	16	0.031	0.343	4.947	1	0.026	1.789	1.072-2.987	0.284
Threshold 10	26.811	16	0.044	0.329	3.835	1	0.050	1.655	1.000-2.742	0.284

APOE: apolipoprotein E. CI: confidence interval. df: degrees of freedom. OR: odds ratio. PRS: polygenic risk score.

Table E1.18: Associations between PRSs and cross-sectional CSF p-tau181 status in CU participants when CSF Aβ42 status was controlled for

PRS & Threshold	Chi-square	df	*p*	Nagelkerke R^2	Wald	df	*p*	OR	95% CI	Nagelkerke R^2 Model 1
PRSwithAPOE										
Threshold 1	23.485	17	0.134	0.302	0.201	1	0.654	1.174	0.583-2.362	0.300
Threshold 5	23.388	17	0.137	0.301	0.104	1	0.747	1.119	0.564-2.220	0.300
Threshold 10	23.324	17	0.139	0.300	0.039	1	0.843	1.072	0.539-2.134	0.300
PRSwithoutAPOE										
Threshold 1	23.658	17	0.129	0.304	0.372	1	0.542	0.843	0.488-1.459	0.300
Threshold 5	23.550	17	0.132	0.303	0.265	1	0.607	0.870	0.512-1.478	0.300
Threshold 10	24.375	17	0.110	0.312	1.076	1	0.300	0.737	0.414-1.312	0.300
APOEonlyPRS										
Threshold 1	23.711	17	0.128	0.305	0.434	1	0.510	1.263	0.630-2.534	0.300
Threshold 5	23.852	17	0.124	0.306	0.578	1	0.447	1.311	0.652-2.634	0.300
Threshold 10	24.477	17	0.107	0.314	1.211	1	0.271	1.476	0.738-2.955	0.300

APOE: apolipoprotein E. CI: confidence interval. df: degrees of freedom. OR: odds ratio. PRS: polygenic risk score.

Table E1.19: Associations between PRSs and cross-sectional CSF p-tau181 status in MCI patients when CSF Aβ42 status was controlled for

PRS & Threshold	Chi-square	df	*p*	Nagelkerke R^2	Wald	df	*p*	OR	95% CI	Nagelkerke R^2 Model 1
PRSwithAPOE										
Threshold 1	67.655	17	<0.001	0.282	0.572	1	0.450	1.117	0.839-1.487	0.279
Threshold 5	68.524	17	<0.001	0.285	1.439	1	0.230	1.193	0.894-1.591	0.279
Threshold 10	68.243	17	<0.001	0.284	1.159	1	0.282	1.176	0.875-1.581	0.279
PRSwithoutAPOE										
Threshold 1	67.328	17	<0.001	0.280	0.243	1	0.622	0.934	0.713-1.224	0.279
Threshold 5	67.612	17	<0.001	0.281	0.526	1	0.468	1.107	0.841-1.456	0.279
Threshold 10	67.295	17	<0.001	0.280	0.210	1	0.647	1.072	0.797-1.441	0.279
APOEonlyPRS										
Threshold 1	68.098	17	<0.001	0.283	1.013	1	0.314	1.155	0.873-1.527	0.279
Threshold 5	68.309	17	<0.001	0.284	1.223	1	0.269	1.171	0.885-1.550	0.279
Threshold 10	68.337	17	<0.001	0.284	1.249	1	0.264	1.173	0.886-1.553	0.279

APOE: apolipoprotein E. CI: confidence interval. df: degrees of freedom. OR: odds ratio. PRS: polygenic risk score.

Table E1.20: Associations between PRSs and cross-sectional CSF p-tau181 status in AD dementia patients when CSF Aβ42 status was controlled for

PRS & Threshold	Chi-square	df	*p*	Nagelkerke R^2	Wald	df	*p*	OR	95% CI	Nagelkerke R^2 Model 1
PRSwithAPOE										
Threshold 1	27.930	17	0.046	0.341	1.722	1	0.189	1.396	0.848-2.299	0.322
Threshold 5	28.325	17	0.041	0.345	2.097	1	0.148	1.462	0.874-2.443	0.322
Threshold 10	28.420	17	0.040	0.346	2.177	1	0.140	1.482	0.879-2.498	0.322
PRSwithoutAPOE										
Threshold 1	29.421	17	0.031	0.357	3.061	1	0.080	0.537	0.268-1.078	0.322
Threshold 5	28.325	17	0.041	0.345	2.082	1	0.149	0.602	0.302-1.200	0.322
Threshold 10	26.408	17	0.067	0.325	0.224	1	0.636	0.870	0.488-1.551	0.322
APOEonlyPRS										
Threshold 1	29.545	17	0.030	0.358	3.201	1	0.074	1.614	0.955-2.725	0.322
Threshold 5	29.722	17	0.028	0.360	3.355	1	0.067	1.644	0.966-2.799	0.322
Threshold 10	28.594	17	0.038	0.348	2.318	1	0.128	1.505	0.889-2.547	0.322

APOE: apolipoprotein E. CI: confidence interval. df: degrees of freedom. OR: odds ratio. PRS: polygenic risk score.

Table E1.21: Associations between PRSs and cross-sectional CSF p-tau181 status in APOE ε4 non-carriers when CSF Aβ42 status was not controlled for

PRS & Threshold	Chi-square	df	*p*	Nagelkerke R^2	Wald	df	*p*	OR	95% CI	Nagelkerke R^2 Model 1
PRSwithAPOE										
Threshold 1	36.380	16	0.003	0.166	0.232	1	0.630	1.138	0.673-1.925	0.165
Threshold 5	36.851	16	0.002	0.168	0.696	1	0.404	1.242	0.747-2.066	0.165
Threshold 10	36.888	16	0.002	0.169	0.735	1	0.391	1.229	0.767-1.969	0.165
PRSwithoutAPOE										
Threshold 1	36.175	16	0.003	0.166	0.027	1	0.869	1.023	0.780-1.343	0.165
Threshold 5	36.681	16	0.002	0.168	0.533	1	0.465	1.105	0.845-1.444	0.165
Threshold 10	36.851	16	0.002	0.168	0.700	1	0.403	1.133	0.846-1.518	0.165
APOEonlyPRS										
Threshold 1	36.278	16	0.003	0.166	0.130	1	0.719	1.108	0.633-1.941	0.165
Threshold 5	36.326	16	0.003	0.166	0.178	1	0.674	1.130	0.640-1.997	0.165
Threshold 10	36.555	16	0.002	0.167	0.405	1	0.524	1.197	0.688-2.082	0.165

APOE: apolipoprotein E. CI: confidence interval. df: degrees of freedom. OR: odds ratio. PRS: polygenic risk score.

Table E1.22: Associations between PRSs and cross-sectional CSF p-tau181 status in APOE ε4 carriers when CSF Aβ42 status was not controlled for

PRS & Threshold	Chi-square	df	*p*	Nagelkerke R^2	Wald	df	*p*	OR	95% CI	Nagelkerke R^2 Model 1
PRSwithAPOE										
Threshold 1	31.397	16	0.012	0.181	0.600	1	0.438	0.866	0.601-1.247	0.178
Threshold 5	30.853	16	0.014	0.178	0.059	1	0.809	0.956	0.667-1.371	0.178
Threshold 10	30.934	16	0.014	0.179	0.140	1	0.709	0.934	0.651-1.338	0.178
PRSwithoutAPOE										
Threshold 1	32.951	16	0.008	0.190	2.118	1	0.146	0.798	0.588-1.082	0.178
Threshold 5	30.865	16	0.014	0.179	0.070	1	0.791	0.959	0.702-1.309	0.178
Threshold 10	30.852	16	0.014	0.178	0.058	1	0.810	0.963	0.710-1.307	0.178
APOEonlyPRS										
Threshold 1	30.818	16	0.014	0.178	0.024	1	0.876	0.972	0.679-1.391	0.178
Threshold 5	30.799	16	0.014	0.178	0.005	1	0.943	0.987	0.690-1.412	0.178
Threshold 10	30.846	16	0.014	0.178	0.052	1	0.819	0.959	0.672-1.369	0.178

APOE: apolipoprotein E. CI: confidence interval. df: degrees of freedom. OR: odds ratio. PRS: polygenic risk score.

Table E1.23: Associations between PRSs and cross-sectional CSF p-tau181 status in APOE ε4 non-carriers when CSF Aβ42 status was controlled for

PRS & Threshold	Chi-square	df	*p*	Nagelkerke R^2	Wald	df	*p*	OR	95% CI	Nagelkerke R^2 Model 1
PRSwithAPOE										
Threshold 1	57.929	17	<0.001	0.256	0.560	1	0.454	1.231	0.715-2.119	0.254
Threshold 5	58.563	17	<0.001	0.259	1.180	1	0.277	1.338	0.791-2.261	0.254
Threshold 10	58.627	17	<0.001	0.259	1.245	1	0.265	1.324	0.808-2.170	0.254
PRSwithoutAPOE										
Threshold 1	57.410	17	<0.001	0.254	0.047	1	0.829	1.032	0.776-1.372	0.254
Threshold 5	57.887	17	<0.001	0.256	0.522	1	0.470	1.109	0.838-1.468	0.254
Threshold 10	57.860	17	<0.001	0.256	0.494	1	0.482	1.117	0.821-1.520	0.254
APOEonlyPRS										
Threshold 1	57.721	17	<0.001	0.255	0.355	1	0.551	1.191	0.670-2.117	0.254
Threshold 5	57.798	17	<0.001	0.256	0.431	1	0.511	1.216	0.678-2.183	0.254
Threshold 10	58.239	17	<0.001	0.257	0.865	1	0.352	1.311	0.741-2.321	0.254

APOE: apolipoprotein E. CI: confidence interval. df: degrees of freedom. OR: odds ratio. PRS: polygenic risk score.

Table E1.24: Associations between PRSs and cross-sectional CSF p-tau181 status in APOE ε4 carriers when CSF Aβ42 status was controlled for

PRS & Threshold	Chi-square	df	*p*	Nagelkerke R^2	Wald	df	*p*	OR	95% CI	Nagelkerke R^2 Model 1
PRSwithAPOE										
Threshold 1	37.808	17	0.003	0.215	1.640	1	0.200	0.782	0.536-1.140	0.207
Threshold 5	36.736	17	0.004	0.210	0.582	1	0.445	0.865	0.596-1.256	0.207
Threshold 10	36.965	17	0.003	0.211	0.808	1	0.369	0.842	0.579-1.225	0.207
PRSwithoutAPOE										
Threshold 1	39.439	17	0.002	0.224	3.195	1	0.074	0.752	0.549-1.028	0.207
Threshold 5	36.471	17	0.004	0.208	0.318	1	0.573	0.913	0.665-1.254	0.207
Threshold 10	36.411	17	0.004	0.208	0.259	1	0.611	0.922	0.675-1.260	0.207
APOEonlyPRS										
Threshold 1	36.457	17	0.004	0.208	0.305	1	0.581	0.902	0.626-1.300	0.207
Threshold 5	36.354	17	0.004	0.208	0.203	1	0.652	0.920	0.639-1.324	0.207
Threshold 10	36.499	17	0.004	0.208	0.347	1	0.556	0.897	0.625-1.288	0.207

APOE: apolipoprotein E. CI: confidence interval. df: degrees of freedom. OR: odds ratio. PRS: polygenic risk score.

Table E1.25: Associations between PRSs and cross-sectional CSF biomarker status of both Aβ42 and p-tau181 in the whole group

PRS & Threshold	Chi-square	df	*p*	Nagelkerke R^2	Wald	df	*p*	OR	95% CI	Nagelkerke R^2 Model 1
PRSwithAPOE										
Threshold 1	183.381	16	<0.001	0.554	36.124	1	0.0000000018512	3.020	2.106-4.330	0.440
Threshold 5	185.368	16	<0.001	0.559	37.237	1	0.0000000010463	3.111	2.161-4.479	0.440
Threshold 10	180.150	16	<0.001	0.547	34.535	1	0.0000000041875	2.963	2.062-4.256	0.440
PRSwithoutAPOE										
Threshold 1	136.633	16	<0.001	0.440	0.049	1	0.825	1.030	0.794-1.337	0.440
Threshold 5	137.273	16	<0.001	0.441	0.685	1	0.408	1.122	0.854-1.475	0.440
Threshold 10	137.451	16	<0.001	0.442	0.861	1	0.354	1.151	0.855-1.548	0.440
APOEonlyPRS										
Threshold 1	187.522	16	<0.001	0.563	38.518	1	0.00000000054241	3.214	2.223-4.646	0.440
Threshold 5	188.052	16	<0.001	0.565	38.628	1	0.00000000051275	3.254	2.243-4.721	0.440
Threshold 10	186.338	16	<0.001	0.561	37.729	1	0.00000000081276	3.158	2.188-4.558	0.440

APOE: apolipoprotein E. CI: confidence interval. df: degrees of freedom. OR: odds ratio. PRS: polygenic risk score.

Table E1.26: Associations between PRSs and cross-sectional CSF biomarker status of both Aβ42 and p-tau181 in APOE ε4 non-carriers

PRS & Threshold	Chi-square	df	*p*	Nagelkerke R^2	Wald	df	*p*	OR	95% CI	Nagelkerke R^2 Model 1
PRSwithAPOE										
Threshold 1	62.626	16	<0.001	0.378	0.054	1	0.816	0.917	0.444-1.896	0.378
Threshold 5	65.572	16	<0.001	0.378	0.000	1	0.982	0.992	0.492-2.001	0.378
Threshold 10	62.675	16	<0.001	0.378	0.103	1	0.748	0.898	0.464-1.735	0.378
PRSwithoutAPOE										
Threshold 1	62.655	16	<0.001	0.378	0.083	1	0.773	0.944	0.640-1.393	0.378
Threshold 5	62.614	16	<0.001	0.378	0.042	1	0.838	1.041	0.706-1.537	0.378
Threshold 10	62.845	16	<0.001	0.379	0.272	1	0.602	1.121	0.730-1.722	0.378
APOEonlyPRS										
Threshold 1	62.574	16	<0.001	0.378	0.002	1	0.963	0.981	0.444-2.169	0.378
Threshold 5	62.573	16	<0.001	0.378	0.001	1	0.979	0.989	0.443-2.209	0.378
Threshold 10	62.630	16	<0.001	0.378	0.058	1	0.809	0.909	0.418-1.975	0.378

APOE: apolipoprotein E. CI: confidence interval. df: degrees of freedom. OR: odds ratio. PRS: polygenic risk score.

Table E1.27: Associations between PRSs and cross-sectional CSF biomarker status of both Aβ42 and p-tau181 in APOE ε4 carriers

PRS & Threshold	Chi-square	df	*p*	Nagelkerke R^2	Wald	df	*p*	OR	95% CI	Nagelkerke R^2 Model 1
PRSwithAPOE										
Threshold 1	57.977	16	<0.001	0.582	1.131	1	0.288	1.575	0.682-3.635	0.572
Threshold 5	58.202	16	<0.001	0.584	1.343	1	0.247	1.614	0.718-3.629	0.572
Threshold 10	58.542	16	<0.001	0.587	1.643	1	0.200	1.696	0.756-3.802	0.572
PRSwithoutAPOE										
Threshold 1	57.120	16	<0.001	0.575	0.355	1	0.551	1.209	0.648-2.256	0.572
Threshold 5	57.243	16	<0.001	0.576	0.474	1	0.491	1.263	0.650-2.452	0.572
Threshold 10	57.845	16	<0.001	0.581	1.034	1	0.309	1.413	0.726-2.753	0.572
APOEonlyPRS										
Threshold 1	57.720	16	<0.001	0.580	0.898	1	0.343	1.532	0.634-3.703	0.572
Threshold 5	57.613	16	<0.001	0.579	0.803	1	0.370	1.489	0.623-3.558	0.572
Threshold 10	58.030	16	<0.001	0.583	1.174	1	0.279	1.622	0.676-3.891	0.572

APOE: apolipoprotein E. CI: confidence interval. df: degrees of freedom. OR: odds ratio. PRS: polygenic risk score.

Table E1.28: Associations between PRSs and cross-sectional CSF biomarker status of both Aβ42 and p-tau181 in MCI patients

PRS & Threshold	Chi-square	df	*p*	Nagelkerke R^2	Wald	df	*p*	OR	95% CI	Nagelkerke R^2 Model 1
PRSwithAPOE										
Threshold 1	83.839	16	<0.001	0.473	26.501	1	0.0000002634	3.442	2.150-5.510	0.295
Threshold 5	87.649	16	<0.001	0.490	28.084	1	0.00000011616	3.812	2.324-6.252	0.295
Threshold 10	82.771	16	<0.001	0.469	25.857	1	0.00000036757	3.575	2.188-5.843	0.295
PRSwithoutAPOE										
Threshold 1	49.056	16	<0.001	0.302	1.202	1	0.273	1.206	0.863-1.686	0.295
Threshold 5	50.854	16	<0.001	0.311	2.925	1	0.087	1.365	0.956-1.950	0.295
Threshold 10	50.092	16	<0.001	0.307	2.194	1	0.139	1.350	0.908-2.009	0.295
APOEonlyPRS										
Threshold 1	84.634	16	<0.001	0.477	26.531	1	0.00000025935	3.589	2.207-5.835	0.295
Threshold 5	85.260	16	<0.001	0.480	26.557	1	0.00000025582	3.678	2.241-6.036	0.295
Threshold 10	83.549	16	<0.001	0.472	25.690	1	0.00000040088	3.468	2.144-5.610	0.295

APOE: apolipoprotein E. CI: confidence interval. df: degrees of freedom. OR: odds ratio. PRS: polygenic risk score.

Table E1.29: Associations between PRSs and cross-sectional CSF biomarker status of both Aβ42 and p-tau181 in CU participants

PRS & Threshold	Chi-square	df	*p*	Nagelkerke R^2	Wald	df	*p*	OR	95% CI	Nagelkerke R^2 Model 1
PRSwithAPOE										
Threshold 1	20.216	16	0.211	0.457	2.860	1	0.091	3.646	0.814-16.327	0.386
Threshold 5	19.408	16	0.248	0.441	2.301	1	0.129	2.954	0.729-11.974	0.386
Threshold 10	18.516	16	0.295	0.423	1.648	1	0.199	2.449	0.624-9.618	0.386
PRSwithoutAPOE										
Threshold 1	19.066	16	0.265	0.434	1.970	1	0.160	0.390	0.105-1.453	0.386
Threshold 5	17.497	16	0.354	0.403	0.778	1	0.378	0.625	0.220-1.777	0.386
Threshold 10	18.290	16	0.307	0.419	1.454	1	0.228	0.492	0.155-1.558	0.386
APOEonlyPRS										
Threshold 1	21.908	16	0.146	0.490	3.900	1	0.048	4.698	1.012-21.818	0.386
Threshold 5	22.145	16	0.139	0.494	4.075	1	0.044	4.837	1.047-22.353	0.386
Threshold 10	23.566	16	0.099	0.521	4.703	1	0.030	6.668	1.200-37.044	0.386

APOE: apolipoprotein E. CI: confidence interval. df: degrees of freedom. OR: odds ratio. PRS: polygenic risk score.

Table E1.30: Associations between PRSs and cross-sectional CSF biomarker status of both Aβ42 and p-tau181 in AD dementia patients

PRS & Threshold	Chi-square	df	*p*	Nagelkerke R^2	Wald	df	*p*	OR	95% CI	Nagelkerke R^2 Model 1
PRSwithAPOE										
Threshold 1	36.740	16	0.002	1.000	0.000	1	0.991	4.609E+28	0.000-not available	0.530
Threshold 5	36.740	16	0.002	1.000	0.000	1	0.994	7.483E+28	0.000-not available	0.530
Threshold 10	36.739	16	0.002	1.000	0.000	1	0.986	7.042E+39	0.000-not available	0.530
PRSwithoutAPOE										
Threshold 1	17.466	16	0.356	0.536	0.223	1	0.637	1.787	0.161-19.876	0.530
Threshold 5	17.315	16	0.365	0.532	0.097	1	0.756	0.660	0.048-9.093	0.530
Threshold 10	17.437	16	0.358	0.536	0.209	1	0.648	0.556	0.045-6.892	0.530
APOEonlyPRS										
Threshold 1	36.740	16	0.002	1.000	0.000	1	0.998	5.204E+27	0.000-not available	0.530
Threshold 5	36.740	16	0.002	1.000	0.000	1	0.998	2.294E+29	0.000-not available	0.530
Threshold 10	36.740	16	0.002	1.000	0.000	1	0.995	3.727E+26	0.000-not available	0.530

APOE: apolipoprotein E. CI: confidence interval. df: degrees of freedom. OR: odds ratio. PRS: polygenic risk score.

APPENDIX E2 (Chapter 5: Experiment Two Part B)

Table E2.1: Associations between PRSs and cross-sectional cognitive composite scores in the whole group

	PRSwithAPOE					PRSwithoutAPOE					APOEonlyPRS				
PRS Threshold (T)	R Square (Model 1)	R Square (Model 2)	R Square Change	Sig. F Change (Model 2)	Standardised beta of PRS	R Square (Model 1)	R Square (Model 2)	R Square Change	Sig. F Change (Model 2)	Standardised beta of PRS	R Square (Model 1)	R Square (Model 2)	R Square Change	Sig. F Change (Model 2)	Standardised beta of PRS
MEMORY															
T1	0.566	0.571	0.005	0.003*	-0.080	0.566	0.566	0.000	0.843	-0.005	0.566	0.572	0.005	0.003*	-0.080
T5	0.566	0.571	0.005	0.003*	-0.080	0.566	0.566	0.000	0.933	-0.002	0.566	0.572	0.006	0.002***	-0.081
T10	0.566	0.571	0.005	0.006**	-0.074	0.566	0.566	0.000	0.915	-0.003	0.566	0.571	0.005	0.006**	-0.074
EXECUTIVE FUNCTION															
T1	0.498	0.499	0.000	0.505	-0.019	0.498	0.500	0.002	0.133	0.041	0.498	0.499	0.001	0.295	-0.030
T5	0.498	0.499	0.000	0.581	-0.016	0.498	0.500	0.001	0.169	0.038	0.498	0.499	0.001	0.299	-0.030
T10	0.498	0.498	0.000	0.926	0.003	0.498	0.500	0.002	0.088	0.048	0.498	0.499	0.001	0.356	-0.027
LANGUAGE															
T1	0.472	0.472	0.000	0.719	-0.011	0.472	0.472	0.000	0.692	0.011	0.472	0.472	0.000	0.614	-0.015
T5	0.472	0.472	0.000	0.760	-0.009	0.472	0.472	0.000	0.790	0.007	0.472	0.472	0.000	0.676	-0.012
T10	0.472	0.472	0.000	0.738	-0.010	0.472	0.472	0.000	0.980	-0.001	0.472	0.472	0.000	0.682	-0.012
VISUOSPATIAL															
T1	0.242	0.247	0.005	0.029	-0.078	0.242	0.242	0.001	0.388	-0.029	0.242	0.245	0.004	0.060	-0.067
T5	0.242	0.245	0.004	0.064	-0.066	0.242	0.242	0.000	0.713	-0.012	0.242	0.245	0.003	0.077	-0.063
T10	0.242	0.243	0.002	0.210	-0.045	0.242	0.242	0.001	0.471	0.025	0.242	0.245	0.003	0.089	-0.060

APOE: apolipoprotein E. PRS: polygenic risk score.

Asterisks indicate associations that withstood corrective measures (false discovery rate) at the 0.05 level: *0.012; **0.024; ***0.008.

Table E2.2: Associations between PRSs and cross-sectional cognitive composite scores in APOE ε4 carriers

	PRSwithAPOE					PRSwithoutAPOE					APOEonlyPRS				
PRS Threshold (T)	R Square (Model 1)	R Square (Model 2)	R Square Change	Sig. F Change (Model 2)	Standardised beta of PRS	R Square (Model 1)	R Square (Model 2)	R Square Change	Sig. F Change (Model 2)	Standardised beta of PRS	R Square (Model 1)	R Square (Model 2)	R Square Change	Sig. F Change (Model 2)	Standardised beta of PRS
MEMORY															
T1	0.598	0.601	0.003	0.159	-0.056	0.598	0.599	0.001	0.323	-0.039	0.598	0.599	0.001	0.385	-0.034
T5	0.598	0.600	0.003	0.169	-0.055	0.598	0.598	0.001	0.497	-0.027	0.598	0.599	0.001	0.406	-0.033
T10	0.598	0.599	0.001	0.398	-0.034	0.598	0.598	0.000	0.680	-0.017	0.598	0.598	0.000	0.601	-0.021
EXECUTIVE FUNCTION															
T1	0.504	0.507	0.003	0.201	-0.057	0.504	0.504	0.000	0.829	0.010	0.504	0.506	0.002	0.238	-0.052
T5	0.504	0.506	0.002	0.255	-0.051	0.504	0.504	0.000	0.604	0.023	0.504	0.506	0.002	0.234	-0.052
T10	0.504	0.504	0.000	0.728	-0.016	0.504	0.506	0.002	0.318	0.044	0.504	0.506	0.002	0.297	-0.045
LANGUAGE															
T1	0.546	0.547	0.001	0.373	-0.038	0.546	0.547	0.000	0.585	-0.023	0.546	0.547	0.001	0.541	-0.026
T5	0.546	0.547	0.001	0.369	-0.038	0.546	0.547	0.001	0.493	-0.029	0.546	0.546	0.000	0.613	-0.021
T10	0.546	0.547	0.001	0.495	-0.029	0.546	0.546	0.000	0.620	-0.021	0.546	0.546	0.000	0.615	-0.021
VISUOSPATIAL															
T1	0.317	0.333	0.016	0.010*	-0.135	0.317	0.320	0.002	0.349	-0.048	0.317	0.329	0.012	0.028	-0.113
T5	0.317	0.329	0.012	0.027	-0.116	0.317	0.317	0.000	0.922	0.005	0.317	0.329	0.011	0.031	-0.110
T10	0.317	0.322	0.005	0.169	-0.072	0.317	0.321	0.003	0.252	0.060	0.317	0.329	0.012	0.026	-0.114

APOE: apolipoprotein E. PRS: polygenic risk score.

*Association withstood corrective measures (false discovery rate) at the 0.05 level: 0.040.

Table E2.3: Associations between PRSs and cross-sectional cognitive composite scores in APOE ε4 non-carriers

	PRSwithAPOE					PRSwithoutAPOE					APOEonlyPRS				
PRS Threshold (T)	R Square (Model 1)	R Square (Model 2)	R Square Change	Sig. F Change (Model 2)	Standardised beta of PRS	R Square (Model 1)	R Square (Model 2)	R Square Change	Sig. F Change (Model 2)	Standardised beta of PRS	R Square (Model 1)	R Square (Model 2)	R Square Change	Sig. F Change (Model 2)	Standardised beta of PRS
MEMORY															
T1	0.501	0.501	0.000	0.751	0.011	0.501	0.501	0.001	0.514	0.023	0.501	0.501	0.000	0.714	-0.013
T5	0.501	0.501	0.000	0.909	0.004	0.501	0.501	0.000	0.671	0.015	0.501	0.501	0.000	0.608	-0.018
T10	0.501	0.501	0.000	0.842	-0.007	0.501	0.501	0.000	0.950	0.002	0.501	0.501	0.000	0.734	-0.012
EXECUTIVE FUNCTION															
T1	0.482	0.483	0.002	0.253	0.041	0.482	0.485	0.003	0.127	0.055	0.482	0.482	0.000	0.761	0.011
T5	0.482	0.483	0.002	0.268	0.040	0.482	0.483	0.002	0.258	0.041	0.482	0.482	0.000	0.753	0.011
T10	0.482	0.484	0.003	0.149	0.053	0.482	0.483	0.002	0.244	0.044	0.482	0.482	0.000	0.627	0.017
LANGUAGE															
T1	0.401	0.401	0.000	0.703	0.015	0.401	0.401	0.001	0.501	0.026	0.401	0.401	0.000	0.921	-0.004
T5	0.401	0.401	0.000	0.638	0.018	0.401	0.401	0.001	0.532	0.024	0.401	0.401	0.000	0.983	0.001
T10	0.401	0.401	0.000	0.761	0.012	0.401	0.401	0.000	0.707	0.015	0.401	0.401	0.000	0.949	0.002
VISUOSPATIAL															
T1	0.200	0.201	0.001	0.491	-0.031	0.200	0.200	0.000	0.946	-0.003	0.200	0.200	0.001	0.527	-0.028
T5	0.200	0.200	0.000	0.631	-0.022	0.200	0.200	0.000	0.676	-0.019	0.200	0.200	0.000	0.656	-0.020
T10	0.200	0.200	0.000	0.828	-0.010	0.200	0.200	0.000	0.972	-0.002	0.200	0.200	0.000	0.966	-0.002

APOE: apolipoprotein E. PRS: polygenic risk score.

Table E2.4: Associations between PRSs and cross-sectional cognitive composite scores in AD dementia patients

	PRSwithAPOE					PRSwithoutAPOE					APOEonlyPRS				
PRS Threshold (T)	R Square (Model 1)	R Square (Model 2)	R Square Change	Sig. F Change (Model 2)	Standardised beta of PRS	R Square (Model 1)	R Square (Model 2)	R Square Change	Sig. F Change (Model 2)	Standardised beta of PRS	R Square (Model 1)	R Square (Model 2)	R Square Change	Sig. F Change (Model 2)	Standardised beta of PRS
MEMORY															
T1	0.423	0.425	0.002	0.544	-0.049	0.423	0.441	0.017	0.063	-0.147	0.423	0.424	0.000	0.898	-0.010
T5	0.423	0.425	0.001	0.608	-0.042	0.423	0.435	0.011	0.134	-0.117	0.423	0.424	0.000	0.862	-0.014
T10	0.423	0.423	0.000	0.980	-0.002	0.423	0.425	0.001	0.591	-0.041	0.423	0.423	0.000	0.978	-0.002
EXECUTIVE FUNCTION															
T1	0.405	0.429	0.024	0.029	0.178	0.405	0.406	0.000	0.828	-0.017	0.405	0.434	0.028	0.018	0.194
T5	0.405	0.433	0.027	0.020	0.191	0.405	0.406	0.000	0.885	0.012	0.405	0.433	0.028	0.019	0.192
T10	0.405	0.441	0.035	0.008*	0.215	0.405	0.408	0.002	0.493	0.053	0.405	0.430	0.024	0.029	0.179
LANGUAGE															
T1	0.425	0.433	0.008	0.207	0.102	0.425	0.428	0.004	0.391	-0.068	0.425	0.437	0.012	0.120	0.126
T5	0.425	0.433	0.009	0.189	0.106	0.425	0.427	0.002	0.486	-0.055	0.425	0.436	0.011	0.128	0.123
T10	0.425	0.436	0.011	0.131	0.121	0.425	0.425	0.000	0.945	0.005	0.425	0.435	0.011	0.143	0.119
VISUOSPATIAL															
T1	0.331	0.333	0.002	0.591	-0.047	0.331	0.331	0.000	0.857	-0.015	0.331	0.333	0.002	0.571	-0.050
T5	0.331	0.331	0.000	0.781	-0.024	0.331	0.332	0.001	0.634	0.040	0.331	0.332	0.002	0.593	-0.047
T10	0.331	0.331	0.000	0.955	0.005	0.331	0.338	0.008	0.249	0.095	0.331	0.333	0.002	0.520	-0.056

APOE: apolipoprotein E. PRS: polygenic risk score.

*Association withstood corrective measures (false discovery rate) at the 0.05 level: 0.032.

Table E2.5: Associations between PRSs and cross-sectional cognitive composite scores in CU participants

	PRSwithAPOE					PRSwithoutAPOE					APOEonlyPRS				
PRS Threshold (T)	R Square (Model 1)	R Square (Model 2)	R Square Change	Sig. F Change (Model 2)	Standardised beta of PRS	R Square (Model 1)	R Square (Model 2)	R Square Change	Sig. F Change (Model 2)	Standardised beta of PRS	R Square (Model 1)	R Square (Model 2)	R Square Change	Sig. F Change (Model 2)	Standardised beta of PRS
MEMORY															
T1	0.217	0.219	0.002	0.530	-0.045	0.217	0.218	0.001	0.596	0.039	0.217	0.220	0.003	0.401	-0.059
T5	0.217	0.219	0.001	0.576	-0.040	0.217	0.219	0.002	0.562	0.043	0.217	0.221	0.004	0.364	-0.064
T10	0.217	0.219	0.002	0.511	-0.047	0.217	0.220	0.003	0.397	0.063	0.217	0.222	0.005	0.312	-0.072
EXECUTIVE FUNCTION															
T1	0.178	0.178	0.000	0.854	0-.013	0.178	0.181	0.004	0.399	0.063	0.178	0.179	0.001	0.595	-0.039
T5	0.178	0.178	0.000	0.934	-0.006	0.178	0.179	0.001	0.597	0.040	0.178	0.179	0.001	0.641	-0.034
T10	0.178	0.178	0.000	0.845	0.014	0.178	0.179	0.001	0.624	0.037	0.178	0.179	0.001	0.673	-0.031
LANGUAGE															
T1	0.230	0.240	0.009	0.155	0.100	0.230	0.233	0.002	0.489	-0.050	0.230	0.244	0.013	0.091	0.118
T5	0.230	0.239	0.009	0.171	0.097	0.230	0.233	0.002	0.500	-0.049	0.230	0.244	0.014	0.085	0.121
T10	0.230	0.237	0.007	0.234	0.085	0.230	0.233	0.002	0.479	-0.052	0.230	0.241	0.011	0.123	0.108
VISUOSPATIAL															
T1	0.144	0.149	0.005	0.316	-0.075	0.144	0.147	0.003	0.438	-0.059	0.144	0.146	0.002	0.527	-0.047
T5	0.144	0.150	0.006	0.266	-0.083	0.144	0.152	0.007	0.229	-0.092	0.144	0.145	0.001	0.631	-0.036
T10	0.144	0.150	0.006	0.285	-0.080	0.144	0.146	0.001	0.598	-0.041	0.144	0.146	0.001	0.595	-0.039

APOE: apolipoprotein E. PRS: polygenic risk score.

Table E2.6: Associations between PRSs and cross-sectional cognitive composite scores in MCI patients

	PRSwithAPOE					PRSwithoutAPOE					APOEonlyPRS				
PRS Threshold (T)	R Square (Model 1)	R Square (Model 2)	R Square Change	Sig. F Change (Model 2)	Standardised beta of PRS	R Square (Model 1)	R Square (Model 2)	R Square Change	Sig. F Change (Model 2)	Standardised beta of PRS	R Square (Model 1)	R Square (Model 2)	R Square Change	Sig. F Change (Model 2)	Standardised beta of PRS
MEMORY															
T1	0.362	0.363	0.001	0.529	-0.028	0.362	0.362	0.000	0.929	0.004	0.362	0.363	0.001	0.461	-0.032
T5	0.362	0.363	0.001	0.524	-0.028	0.362	0.362	0.000	0.831	0.009	0.362	0.363	0.001	0.450	-0.033
T10	0.362	0.362	0.000	0.711	-0.016	0.362	0.363	0.001	0.407	0.036	0.362	0.363	0.001	0.503	-0.029
EXECUTIVE FUNCTION															
T1	0.353	0.354	0.001	0.558	-0.026	0.353	0.359	0.006	0.059	0.078	0.335	0.355	0.002	0.263	-0.049
T5	0.353	0.354	0.001	0.557	-0.026	0.353	0.358	0.005	0.097	0.069	0.353	0.355	0.002	0.246	-0.051
T10	0.353	0.353	0.000	0.817	-0.010	0.353	0.360	0.007	0.046	0.087	0.353	0.355	0.002	0.269	-0.048
LANGUAGE															
T1	0.281	0.282	0.001	0.592	-0.025	0.281	0.286	0.005	0.097	0.072	0.281	0.284	0.002	0.257	-0.053
T5	0.281	0.282	0.000	0.644	-0.022	0.281	0.285	0.003	0.185	0.058	0.281	0.283	0.002	0.309	-0.047
T10	0.281	0.282	0.001	0.576	-0.026	0.281	0.284	0.002	0.275	0.050	0.281	0.283	0.002	0.320	-0.046
VISUOSPATIAL															
T1	0.136	0.139	0.003	0.230	-0.062	0.136	0.136	0.000	0.829	-0.010	0.136	0.139	0.003	0.255	-0.058
T5	0.136	0.139	0.002	0.294	-0.054	0.136	0.136	0.000	0.899	-0.006	0.136	0.139	0.003	0.258	-0.058
T10	0.136	0.137	0.001	0.483	0.036	0.136	0.136	0.000	0.777	0.014	0.136	0.138	0.002	0.310	-0.052

APOE: apolipoprotein E. PRS: polygenic risk score.

Table E2.7: Associations between PRSs and cross-sectional cognitive composite scores in AD dementia ε4 non-carriers

	PRSwithAPOE					PRSwithoutAPOE					APOEonlyPRS				
PRS Threshold (T)	R Square (Model 1)	R Square (Model 2)	R Square Change	Sig. F Change (Model 2)	Standardised beta of PRS	R Square (Model 1)	R Square (Model 2)	R Square Change	Sig. F Change (Model 2)	Standardised beta of PRS	R Square (Model 1)	R Square (Model 2)	R Square Change	Sig. F Change (Model 2)	Standardised beta of PRS
MEMORY															
T1	0.625	0.627	0.002	0.729	0.048	0.625	0.625	0.000	0.889	0.028	0.625	0.628	0.002	0.703	0.054
T5	0.625	0.625	0.002	0.702	0.053	0.625	0.625	0.000	0.960	0.008	0.625	0.630	0.004	0.609	0.073
T10	0.625	0.632	0.007	0.521	0.091	0.625	0.625	0.001	0.818	0.040	0.625	0.638	0.013	0.370	0.129
EXECUTIVE FUNCTION															
T1	0.568	0.604	0.037	0.158	0.207	0.568	0.618	0.050	0.095	0.342	0.568	0.585	0.017	0.339	0.143
T5	0.568	0.616	0.048	0.102	0.236	0.568	0.630	0.062	0.062	0.322	0.568	0.589	0.021	0.289	0.160
T10	0.568	0.614	0.046	0.112	0.237	0.568	0.614	0.046	0.113	0.290	0.568	0.585	0.017	0.335	0.149
LANGUAGE															
T1	0.655	0.660	0.005	0.558	0.078	0.655	0.666	0.011	0.395	0.159	0.655	0.658	0.003	0.676	0.056
T5	0.655	0.663	0.008	0.474	0.094	0.655	0.668	0.013	0.361	0.145	0.655	0.661	0.006	0.526	0.086
T10	0.655	0.668	0.013	0.354	0.125	0.655	0.668	0.013	0.353	0.154	0.655	0.666	0.011	0.397	0.117
VISUOSPATIAL															
T1	0.359	0.361	0.002	0.802	0.046	0.359	0.366	0.007	0.625	0.126	0.359	0.359	0.000	0.957	-0.010
T5	0.359	0.369	0.010	0.544	0.109	0.359	0.404	0.045	0.200	0.274	0.359	0.359	0.000	0.949	0.012
T10	0.359	0.385	0.026	0.331	0.179	0.359	0.437	0.078	0.088	0.378	0.359	0.359	0.000	0.969	-0.007

APOE: apolipoprotein E. PRS: polygenic risk score.

Table E2.8: Associations between PRSs and cross-sectional cognitive composite scores in AD dementia ε4 carriers

	PRSwithAPOE					PRSwithoutAPOE					APOEonlyPRS				
PRS Threshold (T)	R Square (Model 1)	R Square (Model 2)	R Square Change	Sig. F Change (Model 2)	Standardised beta of PRS	R Square (Model 1)	R Square (Model 2)	R Square Change	Sig. F Change (Model 2)	Standardised beta of PRS	R Square (Model 1)	R Square (Model 2)	R Square Change	Sig. F Change (Model 2)	Standardised beta of PRS
MEMORY															
T1	0.448	0.450	0.003	0.558	-0.060	0.448	0.469	0.021	0.089	-0.164	0.448	0.448	0.000	0.989	-0.001
T5	0.448	0.449	0.001	0.666	-0.044	0.448	0.458	0.010	0.250	-0.116	0.448	0.448	0.000	0.915	-0.011
T10	0.448	0.448	0.001	0.767	0.030	0.448	0.448	0.000	0.926	-0.009	0.448	0.448	0.000	0.942	-0.007
EXECUTIVE FUNCTION															
T1	0.514	0.525	0.011	0.191	-0.126	0.514	0.532	0.019	0.089	-0.154	0.514	0.517	0.003	0.490	-0.066
T5	0.514	0.522	0.009	0.251	-0.110	0.514	0.523	0.009	0.231	-0.113	0.514	0.517	0.004	0.456	-0.071
T10	0.514	0.515	0.001	0.664	-0.041	0.514	0.514	0.000	0.911	-0.010	0.514	0.517	0.004	0.452	-0.071
LANGUAGE															
T1	0.423	0.426	0.003	0.559	-0.062	0.423	0.438	0.015	0.164	-0.138	0.423	0.423	0.000	0.928	-0.009
T5	0.423	0.425	0.001	0.674	-0.044	0.423	0.430	0.007	0.335	-0.099	0.423	0.424	0.000	0.816	-0.024
T10	0.423	0.423	0.000	0.994	-0.001	0.423	0.423	0.000	0.924	0.009	0.423	0.425	0.001	0.681	-0.042
VISUOSPATIAL															
T1	0.512	0.555	0.044	0.008*	-0.250	0.512	0.517	0.005	0.360	-0.084	0.512	0.545	0.033	0.022	-0.216
T5	0.512	0.554	0.042	0.010**	-0.246	0.512	0.517	0.006	0.343	-0.090	0.512	0.545	0.033	0.022	-0.216
T10	0.512	0.549	0.037	0.015	-0.226	0.512	0.513	0.001	0.675	-0.037	0.512	0.548	0.036	0.016	-0.222

APOE: apolipoprotein E. PRS: polygenic risk score.

Asterisks indicate associations that withstood corrective measures (false discovery rate) at the 0.05 level: *0.032; **0.040.

Table E2.9: Associations between PRSs and cross-sectional cognitive composite scores in MCI ε4 non-carriers

	PRSwithAPOE					PRSwithoutAPOE					APOEonlyPRS				
PRS Threshold (T)	R Square (Model 1)	R Square (Model 2)	R Square Change	Sig. F Change (Model 2)	Standardised beta of PRS	R Square (Model 1)	R Square (Model 2)	R Square Change	Sig. F Change (Model 2)	Standardised beta of PRS	R Square (Model 1)	R Square (Model 2)	R Square Change	Sig. F Change (Model 2)	Standardised beta of PRS
MEMORY															
T1	0.341	0.342	0.001	0.551	-0.034	0.341	0.341	0.000	0.974	0.002	0.341	0.344	0.003	0.297	-0.059
T5	0.341	0.343	0.001	0.476	-0.040	0.341	0.341	0.000	0.871	0.009	0.341	0.344	0.003	0.275	-0.061
T10	0.341	0.343	0.002	0.464	-0.042	0.341	0.342	0.001	0.631	0.028	0.341	0.346	0.005	0.171	-0.076
EXECUTIVE FUNCTION															
T1	0.399	0.399	0.000	0.702	0.021	0.399	0.403	0.004	0.216	0.064	0.399	0.399	0.001	0.652	-0.024
T5	0.399	0.399	0.000	0.702	0.021	0.399	0.402	0.003	0.307	0.053	0.399	0.399	0.000	0.664	-0.023
T10	0.399	0.400	0.001	0.478	0.039	0.399	0.405	0.006	0.124	0.085	0.399	0.399	0.001	0.629	-0.026
LANGUAGE															
T1	0.246	0.250	0.004	0.254	-0.069	0.246	0.251	0.005	0.218	0.072	0.246	0.261	0.015	0.034	-0.127
T5	0.246	0.248	0.002	0.397	-0.051	0.246	0.251	0.005	0.229	0.070	0.246	0.259	0.013	0.043	-0.121
T10	0.246	0.249	0.003	0.338	-0.059	0.246	0.250	0.004	0.287	0.066	0.246	0.259	0.013	0.042	-0.12
VISUOSPATIAL															
T1	0.147	0.150	0.003	0.392	-0.055	0.147	0.147	0.000	0.714	-0.023	0.147	0.149	0.002	0.800	-0.043
T5	0.147	0.148	0.001	0.651	-0.029	0.147	0.148	0.001	0.667	-0.027	0.147	0.148	0.001	0.540	-0.039
T10	0.147	0.148	0.001	0.653	-0.029	0.147	0.148	0.001	0.620	-0.033	0.147	0.147	0.000	0.891	-0.009

APOE: apolipoprotein E. PRS: polygenic risk score.

Table E2.10: Associations between PRSs and cross-sectional cognitive composite scores in MCI ε4 carriers

	PRSwithAPOE					PRSwithoutAPOE					APOEonlyPRS				
PRS Threshold (T)	R Square (Model 1)	R Square (Model 2)	R Square Change	Sig. F Change (Model 2)	Standardised beta of PRS	R Square (Model 1)	R Square (Model 2)	R Square Change	Sig. F Change (Model 2)	Standardised beta of PRS	R Square (Model 1)	R Square (Model 2)	R Square Change	Sig. F Change (Model 2)	Standardised beta of PRS
MEMORY															
T1	0.465	0.465	0.000	0.778	-0.018	0.465	0.465	0.000	0.996	0.000	0.465	0.465	0.000	0.889	-0.009
T5	0.465	0.465	0.000	0.826	-0.014	0.465	0.465	0.000	0.886	-0.009	0.465	0.465	0.000	0.921	-0.006
T10	0.465	0.465	0.000	0.787	0.017	0.465	0.466	0.001	0.575	0.037	0.465	0.465	0.000	0.928	0.006
EXECUTIVE FUNCTION															
T1	0.350	0.350	0.000	0.934	-0.006	0.350	0.359	0.009	0.149	0.100	0.350	0.351	0.001	0.635	-0.034
T5	0.350	0.350	0.000	0.885	-0.010	0.350	0.357	0.007	0.195	0.091	0.350	0.351	0.001	0.582	-0.039
T10	0.350	0.350	0.000	0.843	0.014	0.350	0.357	0.007	0.197	0.093	0.350	0.351	0.001	0.654	-0.032
LANGUAGE															
T1	0.436	0.436	0.000	0.986	-0.001	0.436	0.439	0.004	0.322	0.064	0.436	0.436	0.000	0.725	-0.023
T5	0.436	0.436	0.000	0.938	-0.005	0.436	0.437	0.002	0.497	0.045	0.436	0.436	0.000	0.872	-0.011
T10	0.436	0.436	0.000	0.950	0.004	0.436	0.437	0.002	0.509	0.045	0.436	0.436	0.000	0.907	-0.008
VISUOSPATIAL															
T1	0.203	0.210	0.007	0.259	-0.089	0.203	0.203	0.000	0.926	-0.007	0.203	0.210	0.006	0.277	-0.085
T5	0.203	0.210	0.007	0.267	-0.088	0.203	0.204	0.001	0.729	0.027	0.203	0.210	0.007	0.267	-0.087
T10	0.203	0.204	0.001	0.709	-0.030	0.203	0.210	0.007	0.265	0.089	0.203	0.210	0.007	0.262	-0.088

APOE: apolipoprotein E. PRS: polygenic risk score.

Table E2.11: Associations between PRSs and cross-sectional cognitive composite scores in amyloid positive participants

	PRSwithAPOE					PRSwithoutAPOE					APOEonlyPRS				
PRS Threshold (T)	R Square (Model 1)	R Square (Model 2)	R Square Change	Sig. F Change (Model 2)	Standardised beta of PRS	R Square (Model 1)	R Square (Model 2)	R Square Change	Sig. F Change (Model 2)	Standardised beta of PRS	R Square (Model 1)	R Square (Model 2)	R Square Change	Sig. F Change (Model 2)	Standardised beta of PRS
MEMORY															
T1	0.572	0.580	0.007	0.005*	-0.091	0.572	0.572	0.000	0.997	0.000	0.572	0.579	0.007	0.005*	-0.091
T5	0.572	0.580	0.008	0.004**	-0.093	0.572	0.572	0.000	0.945	-0.002	0.572	0.580	0.008	0.005*	-0.092
T10	0.572	0.578	0.006	0.010***	-0.084	0.572	0.572	0.000	0.986	-0.001	0.572	0.578	0.006	0.010***	-0.083
EXECUTIVE FUNCTION															
T1	0.491	0.491	0.000	0.525	-0.023	0.491	0.492	0.001	0.250	0.040	0.491	0.492	0.001	0.384	-0.031
T5	0.491	0.491	0.000	0.577	-0.020	0.491	0.493	0.001	0.250	0.040	0.491	0.492	0.001	0.369	-0.032
T10	0.491	0.491	0.000	0.973	0.001	0.491	0.494	0.003	0.126	0.054	0.491	0.492	0.001	0.418	-0.029
LANGUAGE															
T1	0.503	0.503	0.000	0.511	-0.023	0.503	0.503	0.000	0.970	0.001	0.503	0.503	0.000	0.538	-0.022
T5	0.503	0.503	0.000	0.545	-0.021	0.503	0.503	0.000	0.874	-0.005	0.503	0.503	0.000	0.569	-0.020
T10	0.503	0.503	0.000	0.744	-0.012	0.503	0.503	0.000	0.685	0.014	0.503	0.503	0.000	0.559	-0.021
VISUOSPATIAL															
T1	0.248	0.251	0.003	0.173	-0.059	0.248	0.248	0.000	0.711	-0.016	0.248	0.250	0.003	0.215	-0.053
T5	0.248	0.249	0.001	0.356	-0.040	0.248	0.248	0.001	0.471	0.031	0.248	0.250	0.002	0.245	-0.050
T10	0.248	0.248	0.000	0.615	-0.022	0.248	0.251	0.003	0.178	0.058	0.248	0.250	0.002	0.258	-0.049

APOE: apolipoprotein E. PRS: polygenic risk score.

Asterisks indicate associations that withstood corrective measures (false discovery rate) at the 0.05 level: *0.020; **0.016; ***0.040.

Table E2.12: Associations between PRSs and cross-sectional cognitive composite scores in amyloid negative participants

	PRSwithAPOE					PRSwithoutAPOE					APOEonlyPRS				
PRS Threshold (T)	R Square (Model 1)	R Square (Model 2)	R Square Change	Sig. F Change (Model 2)	Standardised beta of PRS	R Square (Model 1)	R Square (Model 2)	R Square Change	Sig. F Change (Model 2)	Standardised beta of PRS	R Square (Model 1)	R Square (Model 2)	R Square Change	Sig. F Change (Model 2)	Standardised beta of PRS
MEMORY															
T1	0.334	0.336	0.002	0.424	-0.042	0.334	0.336	0.001	0.524	-0.034	0.334	0.336	0.002	0.451	-0.040
T5	0.334	0.336	0.001	0.531	-0.033	0.334	0.335	0.000	0.869	-0.009	0.334	0.336	0.002	0.417	-0.044
T10	0.334	0.336	0.001	0.457	-0.040	0.334	0.335	0.000	0.865	-0.010	0.334	0.336	0.002	0.407	-0.044
EXECUTIVE FUNCTION															
T1	0.340	0.340	0.000	0.916	-0.006	0.340	0.342	0.002	0.398	0.045	0.340	0.341	0.000	0.671	-0.023
T5	0.340	0.340	0.000	0.959	0.003	0.340	0.341	0.001	0.510	0.035	0.340	0.340	0.000	0.740	-0.018
T10	0.340	0.340	0.000	0.906	0.006	0.340	0.341	0.001	0.570	0.032	0.340	0.340	0.000	0.774	-0.015
LANGUAGE															
T1	0.274	0.274	0.000	0.718	0.020	0.274	0.274	0.000	0.720	0.020	0.274	0.274	0.000	0.936	0.004
T5	0.274	0.274	0.000	0.685	0.022	0.274	0.275	0.001	0.636	0.027	0.274	0.274	0.000	0.864	0.010
T10	0.274	0.274	0.000	0.936	-0.005	0.274	0.275	0.001	0.659	-0.026	0.274	0.274	0.000	0.888	0.008
VISUOSPATIAL															
T1	0.184	0.196	0.012	0.060	-0.110	0.184	0.187	0.003	0.339	-0.057	0.184	0.191	0.007	0.138	-0.088
T5	0.184	0.499	0.015	0.034	-0.123	0.184	0.195	0.011	0.068	-0.109	0.184	0.191	0.007	0.157	-0.084
T10	0.184	0.493	0.009	0.103	-0.096	0.184	0.187	0.003	0.364	-0.057	0.184	0.189	0.005	0.212	-0.074

APOE: apolipoprotein E. PRS: polygenic risk score.

Table E2.13: Associations between PRSs and cross-sectional cognitive composite scores in amyloid negative ε4 carriers

	PRSwithAPOE					PRSwithoutAPOE					APOEonlyPRS				
PRS Threshold (T)	R Square (Model 1)	R Square (Model 2)	R Square Change	Sig. F Change (Model 2)	Standardised beta of PRS	R Square (Model 1)	R Square (Model 2)	R Square Change	Sig. F Change (Model 2)	Standardised beta of PRS	R Square (Model 1)	R Square (Model 2)	R Square Change	Sig. F Change (Model 2)	Standardised beta of PRS
MEMORY															
T1	0.547	0.549	0.002	0.713	-0.056	0.547	0.557	0.010	0.426	-0.137	0.547	0.547	0.000	0.947	0.009
T5	0.547	0.547	0.000	0.914	-0.017	0.547	0.550	0.003	0.668	-0.075	0.547	0.548	0.001	0.760	0.043
T10	0.547	0.547	0.001	0.815	-0.037	0.547	0.555	0.008	0.475	-0.128	0.547	0.552	0.005	0.571	0.081
EXECUTIVE FUNCTION															
T1	0.569	0.592	0.023	0.215	0.182	0.569	0.569	0.000	0.995	0.001	0.569	0.606	0.037	0.110	0.215
T5	0.569	0.598	0.029	0.161	0.207	0.569	0.572	0.003	0.678	0.070	0.569	0.610	0.041	0.092	0.226
T10	0.569	0.581	0.012	0.370	0.139	0.569	0.569	0.000	0.975	0.006	0.569	0.593	0.024	0.200	0.177
LANGUAGE															
T1	0.570	0.605	0.035	0.121	-0.225	0.570	0.614	0.044	0.079	-0.289	0.570	0.584	0.013	0.345	-0.129
T5	0.570	0.602	0.032	0.140	-0.218	0.570	0.610	0.040	0.095	-0.277	0.570	0.578	0.007	0.481	-0.096
T10	0.570	0.606	0.035	0.118	-0.239	0.570	0.601	0.031	0.147	-0.250	0.570	0.574	0.004	0.624	-0.068
VISUOSPATIAL															
T1	0.575	0.629	0.053	0.050	-0.279	0.575	0.604	0.028	0.160	-0.232	0.575	0.611	0.036	0.111	-0.213
T5	0.575	0.621	0.046	0.071	-0.262	0.575	0.592	0.016	0.291	-0.177	0.575	0.613	0.038	0.101	-0.219
T10	0.575	0.610	0.035	0.116	-0.239	0.575	0.580	0.005	0.569	-0.099	0.575	0.626	0.051	0.057	-0.256

APOE: apolipoprotein E. PRS: polygenic risk score.

Table E2.14: Associations between PRSs and cross-sectional cognitive composite scores in amyloid negative ε4 non-carriers

	PRSwithAPOE					PRSwithoutAPOE					APOEonlyPRS				
PRS Threshold (T)	R Square (Model 1)	R Square (Model 2)	R Square Change	Sig. F Change (Model 2)	Standardised beta of PRS	R Square (Model 1)	R Square (Model 2)	R Square Change	Sig. F Change (Model 2)	Standardised beta of PRS	R Square (Model 1)	R Square (Model 2)	R Square Change	Sig. F Change (Model 2)	Standardised beta of PRS
MEMORY															
T1	0.324	0.324	0.000	0.891	-0.008	0.324	0.325	0.001	0.574	-0.034	0.324	0.324	0.000	0.920	-0.006
T5	0.324	0.324	0.000	0.998	0.000	0.324	0.324	0.000	0.929	-0.005	0.324	0.324	0.000	0.785	-0.017
T10	0.324	0.324	0.000	0.882	-0.009	0.324	0.324	0.000	0.985	-0.001	0.324	0.324	0.001	0.601	-0.031
EXECUTIVE FUNCTION															
T1	0.323	0.323	0.000	0.840	0.012	0.323	0.326	0.003	0.310	0.061	0.323	0.323	0.001	0.640	-0.028
T5	0.323	0.323	0.000	0.785	0.016	0.323	0.324	0.002	0.467	0.044	0.323	0.323	0.001	0.696	-0.024
T10	0.323	0.323	0.001	0.653	0.027	0.323	0.324	0.002	0.488	0.043	0.323	0.323	0.000	0.843	-0.012
LANGUAGE															
T1	0.244	0.245	0.001	0.619	0.031	0.244	0.245	0.001	0.673	0.027	0.244	0.244	0.000	0.949	0.004
T5	0.244	0.245	0.001	0.598	0.033	0.244	0.245	0.001	0.560	0.037	0.244	0.244	0.000	0.920	0.006
T10	0.244	0.244	0.000	0.916	-0.007	0.244	0.244	0.000	0.757	-0.021	0.244	0.244	0.000	0.873	-0.010
VISUOSPATIAL															
T1	0.163	0.173	0.010	0.125	-0.101	0.163	0.163	0.000	0.804	-0.017	0.163	0.171	0.008	0.169	-0.093
T5	0.163	0.178	0.015	0.056	0.143	0.163	0.172	0.009	0.148	-0.096	0.163	0.169	0.006	0.218	-0.083
T10	0.163	0.170	0.007	0.187	-0.087	0.163	0.166	0.003	0.436	-0.054	0.163	0.166	0.002	0.439	-0.052

APOE: apolipoprotein E. PRS: polygenic risk score.

Table E2.15: Associations between PRSs and cross-sectional cognitive composite scores in amyloid positive ε4 carriers

	PRSwithAPOE					PRSwithoutAPOE					APOEonlyPRS				
PRS Threshold (T)	R Square (Model 1)	R Square (Model 2)	R Square Change	Sig. F Change (Model 2)	Standardised beta of PRS	R Square (Model 1)	R Square (Model 2)	R Square Change	Sig. F Change (Model 2)	Standardised beta of PRS	R Square (Model 1)	R Square (Model 2)	R Square Change	Sig. F Change (Model 2)	Standardised beta of PRS
MEMORY															
T1	0.581	0.584	0.003	0.163	-0.062	0.581	0.582	0.001	0.357	-0.040	0.581	0.582	0.001	0.372	-0.039
T5	0.581	0.584	0.003	0.174	-0.060	0.581	0.581	0.000	0.620	-0.022	0.581	0.582	0.001	0.369	-0.039
T10	0.581	0.582	0.001	0.453	-0.033	0.581	0.581	0.000	0.911	-0.005	0.581	0.582	0.001	0.523	-0.028
EXECUTIVE FUNCTION															
T1	0.490	0.495	0.005	0.115	-0.077	0.490	0.490	0.000	0.903	0.006	0.490	0.495	0.005	0.141	-0.071
T5	0.490	0.495	0.005	0.140	-0.072	0.490	0.490	0.000	0.681	0.020	0.490	0.495	0.005	0.134	-0.072
T10	0.490	0.491	0.001	0.535	-0.030	0.490	0.492	0.002	0.322	0.048	0.490	0.494	0.004	0.187	-0.064
LANGUAGE															
T1	0.536	0.537	0.001	0.393	-0.040	0.536	0.536	0.000	0.704	-0.018	0.536	0.537	0.001	0.529	-0.029
T5	0.536	0.537	0.001	0.390	-0.040	0.536	0.536	0.001	0.607	-0.024	0.536	0.536	0.001	0.567	-0.026
T10	0.536	0.536	0.001	0.578	-0.026	0.536	0.536	0.000	0.849	-0.009	0.536	0.537	0.001	0.508	-0.031
VISUOSPATIAL															
T1	0.319	0.335	0.016	0.018	-0.133	0.319	0.320	0.001	0.595	-0.030	0.319	0.331	0.012	0.039	-0.115
T5	0.319	0.330	0.011	0.045	-0.112	0.319	0.319	0.000	0.688	0.023	0.319	0.330	0.011	0.047	-0.110
T10	0.319	0.323	0.005	0.202	-0.072	0.319	0.324	0.005	0.192	0.074	0.319	0.331	0.012	0.040	-0.114

APOE: apolipoprotein E. PRS: polygenic risk score.

Table E2.16: Associations between PRSs and cross-sectional cognitive composite scores in amyloid positive ε4 non-carriers

	PRSwithAPOE					PRSwithoutAPOE					APOEonlyPRS				
PRS Threshold (T)	R Square (Model 1)	R Square (Model 2)	R Square Change	Sig. F Change (Model 2)	Standardised beta of PRS	R Square (Model 1)	R Square (Model 2)	R Square Change	Sig. F Change (Model 2)	Standardised beta of PRS	R Square (Model 1)	R Square (Model 2)	R Square Change	Sig. F Change (Model 2)	Standardised beta of PRS
MEMORY															
T1	0.568	0.568	0.000	0.676	0.021	0.568	0.572	0.004	0.180	0.065	0.568	0.568	0.000	0.725	-0.017
T5	0.568	0.568	0.000	0.853	0.009	0.568	0.569	0.001	0.506	0.032	0.568	0.568	0.000	0.689	-0.019
T10	0.568	0.568	0.000	0.960	-0.003	0.568	0.568	0.000	0.768	0.015	0.568	0.568	0.000	0.984	-0.001
EXECUTIVE FUNCTION															
T1	0.528	0.531	0.003	0.277	0.056	0.528	0.532	0.004	0.226	0.061	0.528	0.529	0.001	0.629	0.024
T5	0.528	0.531	0.003	0.303	0.052	0.528	0.530	0.002	0.363	0.046	0.528	0.529	0.000	0.675	0.021
T10	0.528	0.531	0.003	0.267	0.058	0.528	0.530	0.001	0.452	0.040	0.528	0.529	0.000	0.652	0.023
LANGUAGE															
T1	0.486	0.486	0.000	0.870	0.009	0.486	0.486	0.001	0.654	0.024	0.486	0.486	0.000	0.958	-0.003
T5	0.486	0.486	0.000	0.764	0.016	0.486	0.486	0.000	0.770	0.016	0.486	0.486	0.000	0.993	0.000
T10	0.486	0.487	0.001	0.514	0.035	0.486	0.488	0.002	0.342	0.053	0.486	0.486	0.000	0.851	0.010
VISUOSPATIAL															
T1	0.235	0.235	0.000	0.853	0.012	0.235	0.235	0.000	0.894	0.009	0.235	0.235	0.000	0.994	0.000
T5	0.235	0.236	0.002	0.504	0.043	0.235	0.236	0.002	0.490	0.045	0.235	0.235	0.000	0.944	0.005
T10	0.235	0.236	0.001	0.580	0.037	0.235	0.235	0.001	0.659	0.030	0.235	0.235	0.000	0.751	0.020

APOE: apolipoprotein E. PRS: polygenic risk score.

APPENDIX F1 (Chapter 6: Experiment Three Part A)

Table F1.1: Associations between PRSs and longitudinal change in CSF Aβ42 measurement in the whole group when CSF p-tau181 status was not controlled for

PRS & Threshold	Chi-square	df	*p*	Nagelkerke R^2	Wald	df	*p*	OR	95% CI	Nagelkerke R^2 Model 1
PRSwithAPOE										
Threshold 1	20.345	16	0.205	0.151	0.783	1	0.376	1.165	0.830-1.636	0.145
Threshold 5	21.008	16	0.178	0.155	1.432	1	0.231	1.232	0.876-1.732	0.145
Threshold 10	21.239	16	0.170	0.157	1.657	1	0.198	1.256	0.888-1.778	0.145
PRSwithoutAPOE										
Threshold 1	23.353	16	0.105	0.172	3.599	1	0.058	0.705	0.491-1.012	0.145
Threshold 5	20.018	16	0.219	0.149	0.459	1	0.498	0.888	0.631-1.251	0.145
Threshold 10	19.609	16	0.238	0.146	0.053	1	0.818	1.043	0.730-1.491	0.145
APOEonlyPRS										
Threshold 1	21.648	16	0.155	0.160	2.041	1	0.153	1.286	0.911-1.816	0.145
Threshold 5	21.735	16	0.152	0.161	2.124	1	0.145	1.294	0.915-1.831	0.145
Threshold 10	20.683	16	0.191	0.153	1.110	1	0.292	1.204	0.853-1.700	0.145

APOE: apolipoprotein E. CI: confidence interval. df: degrees of freedom. OR: odds ratio. PRS: polygenic risk score.

Table F1.2: Associations between PRSs and longitudinal change in CSF Aβ42 measurement in the whole group when CSF p-tau181 status was controlled for

PRS & Threshold	Chi-square	df	*p*	Nagelkerke R^2	Wald	df	*p*	OR	95% CI	Nagelkerke R^2 Model 1
PRSwithAPOE										
Threshold 1	22.884	17	0.153	0.168	0.277	1	0.599	1.099	0.774-1.560	0.167
Threshold 5	23.281	17	0.140	0.171	0.669	1	0.413	1.159	0.814-1.650	0.167
Threshold 10	23.478	17	0.134	0.173	0.864	1	0.353	1.185	0.828-1.696	0.167
PRSwithoutAPOE										
Threshold 1	26.965	17	0.059	0.196	4.098	1	0.043	0.684	0.474-0.988	0.167
Threshold 5	23.380	17	0.137	0.172	0.767	1	0.381	0.856	0.605-1.212	0.167
Threshold 10	22.617	17	0.162	0.167	0.010	1	0.920	1.019	0.711-1.459	0.167
APOEonlyPRS										
Threshold 1	23.869	17	0.123	0.175	1.245	1	0.265	1.224	0.858-1.744	0.167
Threshold 5	23.927	17	0.121	0.176	1.300	1	0.254	1.230	0.861-1.758	0.167
Threshold 10	23.177	17	0.144	0.170	0.566	1	0.452	1.146	0.804-1.633	0.167

APOE: apolipoprotein E. CI: confidence interval. df: degrees of freedom. OR: odds ratio. PRS: polygenic risk score.

Table F1.3: Associations between PRSs and longitudinal change in CSF Aβ42 measurement in APOE ε4 carriers when CSF p-tau181 status was not controlled for

PRS & Threshold	Chi-square	df	*p*	Nagelkerke R^2	Wald	df	*p*	OR	95% CI	Nagelkerke R^2 Model 1
PRSwithAPOE										
Threshold 1	22.825	16	0.118	0.360	3.747	1	0.053	2.436	0.989-5.999	0.303
Threshold 5	24.988	16	0.070	0.388	5.488	1	0.019	3.092	1.203-7.951	0.303
Threshold 10	26.114	16	0.052	0.403	6.281	1	0.012	3.615	1.323-9.876	0.303
PRSwithoutAPOE										
Threshold 1	19.161	16	0.260	0.309	0.403	1	0.525	0.814	0.431-1.538	0.303
Threshold 5	18.803	16	0.279	0.304	0.051	1	0.822	1.074	0.577-1.997	0.303
Threshold 10	19.817	16	0.229	0.318	1.029	1	0.310	1.421	0.721-2.803	0.303
APOEonlyPRS										
Threshold 1	23.867	16	0.092	0.374	4.649	1	0.031	2.612	1.091-6.253	0.303
Threshold 5	23.885	16	0.092	0.374	4.682	1	0.030	2.622	1.095-6.279	0.303
Threshold 10	22.209	16	0.137	0.351	3.202	1	0.074	2.238	0.926-5.409	0.303

APOE: apolipoprotein E. CI: confidence interval. df: degrees of freedom. OR: odds ratio. PRS: polygenic risk score.

Table F1.4: Associations between PRSs and longitudinal change in CSF Aβ42 measurement in APOE ε4 non-carriers when CSF p-tau181 status was not controlled for

PRS & Threshold	Chi-square	df	*p*	Nagelkerke R^2	Wald	df	*p*	OR	95% CI	Nagelkerke R^2 Model 1
PRSwithAPOE										
Threshold 1	21.657	16	0.155	0.268	0.798	1	0.372	1.499	0.617-3.641	0.259
Threshold 5	22.232	16	0.136	0.274	1.351	1	0.245	1.685	0.699-4.065	0.259
Threshold 10	22.924	16	0.116	0.282	1.998	1	0.158	1.853	0.788-4.356	0.259
PRSwithoutAPOE										
Threshold 1	22.302	16	0.134	0.275	1.404	1	0.236	0.736	0.444-1.222	0.259
Threshold 5	20.877	16	0.183	0.259	0.024	1	0.876	0.963	0.600-1.545	0.259
Threshold 10	21.234	16	0.170	0.263	0.381	1	0.537	1.174	0.706-1.951	0.259
APOEonlyPRS										
Threshold 1	22.991	16	0.114	0.283	2.086	1	0.149	1.963	0.786-4.904	0.259
Threshold 5	22.535	16	0.127	0.278	1.654	1	0.198	1.833	0.728-4.613	0.259
Threshold 10	21.849	16	0.148	0.270	0.990	1	0.320	1.605	0.632-4.077	0.259

APOE: apolipoprotein E. CI: confidence interval. df: degrees of freedom. OR: odds ratio. PRS: polygenic risk score.

Table F1.5: Associations between PRSs and longitudinal change in CSF Aβ42 measurement in APOE ε4 carriers when CSF p-tau181 status was controlled for

PRS & Threshold	Chi-square	df	*p*	Nagelkerke R^2	Wald	df	*p*	OR	95% CI	Nagelkerke R^2 Model 1
PRSwithAPOE										
Threshold 1	24.143	17	0.116	0.377	3.582	1	0.058	2.398	0.969-5.934	0.325
Threshold 5	25.891	17	0.076	0.400	4.985	1	0.026	2.948	1.141-7.615	0.325
Threshold 10	27.085	17	0.057	0.415	5.843	1	0.016	3.457	1.264-9.450	0.325
PRSwithoutAPOE										
Threshold 1	20.646	17	0.243	0.330	0.372	1	0.542	0.819	0.431-1.556	0.325
Threshold 5	20.280	17	0.260	0.325	0.009	1	0.925	1.031	0.550-1.931	0.325
Threshold 10	21.260	17	0.215	0.338	0.958	1	0.328	1.411	0.708-2.812	0.325
APOEonlyPRS										
Threshold 1	25.196	17	0.090	0.391	4.492	1	0.034	2.610	1.075-6.339	0.325
Threshold 5	25.154	17	0.091	0.391	4.480	1	0.034	2.602	1.073-6.307	0.325
Threshold 10	23.669	17	0.129	0.371	3.162	1	0.075	2.245	0.921-5.476	0.325

APOE: apolipoprotein E. CI: confidence interval. df: degrees of freedom. OR: odds ratio. PRS: polygenic risk score.

Table F1.6: Associations between PRSs and longitudinal change in CSF Aβ42 measurement in APOE ε4 non-carriers when CSF p-tau181 status was controlled for

PRS & Threshold	Chi-square	df	*p*	Nagelkerke R^2	Wald	df	*p*	OR	95% CI	Nagelkerke R^2 Model 1
PRSwithAPOE										
Threshold 1	24.208	17	0.114	0.296	0.821	1	0.365	1.520	0.614-3.761	0.287
Threshold 5	24.681	17	0.102	0.301	1.280	1	0.258	1.676	0.685-4.103	0.287
Threshold 10	25.392	17	0.086	0.308	1.948	1	0.163	1.868	0.777-4.490	0.287
PRSwithoutAPOE										
Threshold 1	25.343	17	0.087	0.308	1.871	1	0.171	0.694	0.411-1.171	0.287
Threshold 5	23.526	17	0.133	0.288	0.146	1	0.703	0.910	0.560-1.477	0.287
Threshold 10	23.596	17	0.131	0.289	0.216	1	0.642	1.129	0.676-1.886	0.287
APOEonlyPRS										
Threshold 1	25.905	17	0.076	0.314	2.443	1	0.118	2.126	0.826-5.472	0.287
Threshold 5	25.401	17	0.086	0.309	1.971	1	0.160	1.977	0.763-5.119	0.287
Threshold 10	24.767	17	0.100	0.302	1.363	1	0.243	1.787	0.674-4.739	0.287

APOE: apolipoprotein E. CI: confidence interval. df: degrees of freedom. OR: odds ratio. PRS: polygenic risk score.

Table F1.7: Associations between PRSs and longitudinal change in CSF Aβ42 measurement in CU participants when CSF p-tau181 status was not controlled for

PRS & Threshold	Chi-square	df	*p*	Nagelkerke R^2	Wald	df	*p*	OR	95% CI	Nagelkerke R^2 Model 1
PRSwithAPOE										
Threshold 1	23.760	16	0.095	0.620	3.484	1	0.062	26.715	0.849-841.046	0.429
Threshold 5	23.678	16	0.097	0.618	3.600	1	0.058	22.134	0.903-542.696	0.429
Threshold 10	23.417	16	0.103	0.613	3.303	1	0.069	23.453	0.781-704-467	0.429
PRSwithoutAPOE										
Threshold 1	15.157	16	0.513	0.437	0.346	1	0.556	0.653	0.158-2.696	0.429
Threshold 5	14.804	16	0.539	0.429	0.000	1	0.998	0.999	0.287-3.481	0.429
Threshold 10	14.897	16	0.532	0.431	0.093	1	0.760	0.820	0.229-2.940	0.429
APOEonlyPRS										
Threshold 1	25.471	16	0.062	0.651	3.563	1	0.059	35.991	0.872-1486.279	0.429
Threshold 5	24.448	16	0.080	0.633	3.404	1	0.065	26.966	0.814-892.932	0.429
Threshold 10	26.684	16	0.045	0.673	3.943	1	0.047	73.733	1.057-5142.963	0.429

APOE: apolipoprotein E. CI: confidence interval. df: degrees of freedom. OR: odds ratio. PRS: polygenic risk score.

Table F1.8: Associations between PRSs and longitudinal change in CSF Aβ42 measurement in MCI patients when CSF p-tau181 status was not controlled for

PRS & Threshold	Chi-square	df	*p*	Nagelkerke R^2	Wald	df	*p*	OR	95% CI	Nagelkerke R^2 Model 1
PRSwithAPOE										
Threshold 1	26.783	16	0.044	0.294	0.397	1	0.529	0.857	0.530-1.385	0.290
Threshold 5	26.632	16	0.046	0.293	0.247	1	0.619	0.884	0.542-1.439	0.290
Threshold 10	26.760	16	0.044	0.294	0.374	1	0.541	0.853	0.513-1.419	0.290
PRSwithoutAPOE										
Threshold 1	28.712	16	0.026	0.313	2.185	1	0.139	0.668	0.391-1.141	0.290
Threshold 5	26.834	16	0.043	0.295	0.445	1	0.505	0.841	0.507-1.398	0.290
Threshold 10	26.413	16	0.048	0.290	0.028	1	0.866	1.047	0.611-1.796	0.290
APOEonlyPRS										
Threshold 1	26.434	16	0.048	0.291	0.049	1	0.825	0.948	0.589-1.525	0.290
Threshold 5	26.399	16	0.049	0.290	0.014	1	0.906	0.972	0.601-1.569	0.290
Threshold 10	26.835	16	0.043	0.295	0.451	1	0.502	0.850	0.529-1.366	0.290

APOE: apolipoprotein E. CI: confidence interval. df: degrees of freedom. OR: odds ratio. PRS: polygenic risk score.

Table F1.9: Associations between PRSs and longitudinal change in CSF Aβ42 measurement in CU participants when CSF p-tau181 status was controlled for

PRS & Threshold	Chi-square	df	*p*	Nagelkerke R^2	Wald	df	*p*	OR	95% CI	Nagelkerke R^2 Model 1
PRSwithAPOE										
Threshold 1	24.181	17	0.115	0.628	3.796	1	0.051	20.645	0.982-433.974	0.444
Threshold 5	24.307	17	0.111	0.630	4.067	1	0.044	19.577	1.087-352.529	0.444
Threshold 10	24.036	17	0.118	0.625	3.689	1	0.055	20.400	0.940-442.734	0.444
PRSwithoutAPOE										
Threshold 1	15.711	17	0.544	0.450	0.253	1	0.615	0.689	0.162-2.936	0.444
Threshold 5	15.479	17	0.561	0.445	0.024	1	0.876	1.110	0.298-4.142	0.444
Threshold 10	15.458	17	0.563	0.444	0.004	1	0.950	0.957	0.245-3.739	0.444
APOEonlyPRS										
Threshold 1	25.771	17	0.079	0.657	3.779	1	0.052	27.025	0.973-750.305	0.444
Threshold 5	25.013	17	0.094	0.643	3.911	1	0.048	23.596	1.029-541.193	0.444
Threshold 10	27.134	17	0.056	0.681	3.995	1	0.046	55.052	1.081-2804.252	0.444

APOE: apolipoprotein E. CI: confidence interval. df: degrees of freedom. OR: odds ratio. PRS: polygenic risk score.

Table F1.10: Associations between PRSs and longitudinal change in CSF Aβ42 measurement in MCI patients when CSF p-tau181 status was controlled for

PRS & Threshold	Chi-square	df	*p*	Nagelkerke R^2	Wald	df	*p*	OR	95% CI	Nagelkerke R^2 Model 1
PRSwithAPOE										
Threshold 1	27.374	17	0.053	0.300	0.609	1	0.435	0.822	0.502-1.345	0.294
Threshold 5	27.202	17	0.055	0.298	0.439	1	0.508	0.844	0.510-1.395	0.294
Threshold 10	27.314	17	0.054	0.299	0.550	1	0.458	0.822	0.490-1.380	0.294
PRSwithoutAPOE										
Threshold 1	29.427	17	0.031	0.319	2.477	1	0.115	0.646	0.374-1.113	0.294
Threshold 5	27.415	17	0.052	0.300	0.643	1	0.423	0.809	0.482-1.358	0.294
Threshold 10	26.783	17	0.061	0.294	0.020	1	0.888	1.039	0.606-1.783	0.294
APOEonlyPRS										
Threshold 1	26.886	17	0.060	0.295	0.122	1	0.726	0.917	0.563-1.492	0.294
Threshold 5	26.823	17	0.061	0.294	0.059	1	0.807	0.941	0.576-1.537	0.294
Threshold 10	27.395	17	0.053	0.300	0.632	1	0.426	0.822	0.506-1.333	0.294

APOE: apolipoprotein E. CI: confidence interval. df: degrees of freedom. OR: odds ratio. PRS: polygenic risk score.

Table F1.11: Associations between PRSs and longitudinal change in CSF Aβ42 measurement in CU ε4 non-carriers when CSF p-tau181 status was not controlled for

PRS & Threshold	Chi-square	df	*p*	Nagelkerke R^2	Wald	df	*p*	OR	95% CI	Nagelkerke R^2 Model 1
PRSwithAPOE										
Threshold 1	38.496	15	<0.001	1.000	0.000	1	0.992	6.531E+57	0.000-not available	0.581
Threshold 5	38.496	15	<0.001	1.000	0.000	1	0.990	2.541E+64	0.000-not available	0.581
Threshold 10	38.496	15	<0.001	1.000	0.000	1	0.984	2.365E+80	0.000-not available	0.581
PRSwithoutAPOE										
Threshold 1	16.209	15	0.368	0.583	0.074	1	0.786	0.787	0.140-4.430	0.581
Threshold 5	16.545	15	0.347	0.592	0.393	1	0.531	1.764	0.299-10.420	0.581
Threshold 10	16.137	15	0.373	0.581	0.003	1	0.956	1.056	0.151-7.401	0.581
APOEonlyPRS										
Threshold 1	38.496	15	<0.001	1.000	0.000	1	0.994	5.493E+55	0.000-not available	0.581
Threshold 5	38.496	15	<0.001	1.000	0.000	1	0.991	1.081E+95	0.000-not available	0.581
Threshold 10	38.496	15	<0.001	1.000	0.000	1	0.997	1.454E+56	0.000-not available	0.581

APOE: apolipoprotein E. CI: confidence interval. df: degrees of freedom. OR: odds ratio. PRS: polygenic risk score.

Table F1.12: Associations between PRSs and longitudinal change in CSF Aβ42 measurement in MCI ε4 non-carriers when CSF p-tau181 status was not controlled for

PRS & Threshold	Chi-square	df	*p*	Nagelkerke R^2	Wald	df	*p*	OR	95% CI	Nagelkerke R^2 Model 1
PRSwithAPOE										
Threshold 1	24.731	16	0.075	0.446	0.301	1	0.584	1.571	0.313-7.888	0.442
Threshold 5	25.759	16	0.058	0.461	1.263	1	0.261	2.681	0.480-14.975	0.442
Threshold 10	25.471	16	0.062	0.457	0.996	1	0.318	2.081	0.494-8.771	0.442
PRSwithoutAPOE										
Threshold 1	26.324	16	0.050	0.469	1.730	1	0.788	0.571	0.248-1.316	0.442
Threshold 5	24.427	16	0.081	0.442	0.000	1	0.997	0.999	0.470-2.120	0.442
Threshold 10	24.987	16	0.070	0.450	0.559	1	0.454	1.344	0.619-2.919	0.442
APOEonlyPRS										
Threshold 1	26.250	16	0.047	0.472	1.942	1	0.163	3.401	0.608-19.016	0.442
Threshold 5	26.320	16	0.050	0.469	1.778	1	0.182	3.210	0.578-17.826	0.442
Threshold 10	24.647	16	0.076	0.445	0.219	1	0.640	1.443	0.310-6.710	0.442

APOE: apolipoprotein E. CI: confidence interval. df: degrees of freedom. OR: odds ratio. PRS: polygenic risk score.

Table F1.13: Associations between PRSs and longitudinal change in CSF Aβ42 measurement in MCI ε4 carriers when CSF p-tau181 status was not controlled for

PRS & Threshold	Chi-square	df	*p*	Nagelkerke R^2	Wald	df	*p*	OR	95% CI	Nagelkerke R^2 Model 1
PRSwithAPOE										
Threshold 1	24.598	15	0.056	0.545	1.531	1	0.216	2.744	0.555-13.573	0.517
Threshold 5	25.317	15	0.046	0.557	2.170	1	0.141	3.403	0.667-17.356	0.517
Threshold 10	24.750	15	0.053	0.548	1.662	1	0.197	2.977	0.567-15.630	0.517
PRSwithoutAPOE										
Threshold 1	22.951	15	0.085	0.517	0.001	1	0.976	0.986	0.388-2.501	0.517
Threshold 5	23.178	15	0.080	0.521	0.227	1	0.634	1.236	0.517-2.951	0.517
Threshold 10	23.608	15	0.072	0.528	0.638	1	0.424	1.498	0.556-4.039	0.517
APOEonlyPRS										
Threshold 1	24.072	15	0.064	0.536	1.080	1	0.299	1.991	0.543-7.299	0.517
Threshold 5	24.200	15	0.062	0.539	1.205	1	0.272	2.083	0.562-7.724	0.517
Threshold 10	23.521	15	0.074	0.527	0.564	1	0.453	1.640	0.451-5.960	0.517

APOE: apolipoprotein E. CI: confidence interval. df: degrees of freedom. OR: odds ratio. PRS: polygenic risk score.

Table F1.14: Associations between PRSs and longitudinal change in CSF Aβ42 measurement in CU ε4 non-carriers when CSF p-tau181 status was controlled for

PRS & Threshold	Chi-square	df	*p*	Nagelkerke R^2	Wald	df	*p*	OR	95% CI	Nagelkerke R^2 Model 1
PRSwithAPOE										
Threshold 1	38.496	16	0.001	1.000	0.000	1	0.991	1.290E+54	0.000-not available	0.582
Threshold 5	38.496	16	0.001	1.000	0.000	1	0.988	2.843E+64	0.000-not available	0.582
Threshold 10	38.496	16	0.001	1.000	0.000	1	0.991	3.173E+69	0.000-not available	0.582
PRSwithoutAPOE										
Threshold 1	16.244	16	0.436	0.584	0.072	1	0.788	0.791	0.142-4.392	0.582
Threshold 5	16.551	16	0.415	0.592	0.363	1	0.547	1.742	0.287-10.587	0.582
Threshold 10	16.172	16	0.441	0.582	0.000	1	0.983	1.021	0.141-7.414	0.582
APOEonlyPRS										
Threshold 1	38.496	16	0.001	1.000	0.000	1	0.995	4.775E+77	0.000-not available	0.582
Threshold 5	38.496	16	0.001	1.000	0.000	1	0.992	9.074E+84	0.000-not available	0.582
Threshold 10	38.496	16	0.001	1.000	0.000	1	0.997	1.177E+48	0.000-not available	0.582

APOE: apolipoprotein E. CI: confidence interval. df: degrees of freedom. OR: odds ratio. PRS: polygenic risk score.

Table F1.15: Associations between PRSs and longitudinal change in CSF Aβ42 measurement in MCI ε4 non-carriers when CSF p-tau181 status was controlled for

PRS & Threshold	Chi-square	df	*p*	Nagelkerke R^2	Wald	df	*p*	OR	95% CI	Nagelkerke R^2 Model 1
PRSwithAPOE										
Threshold 1	27.195	17	0.055	0.482	0.035	1	0.852	1.175	0.217-6.359	0.481
Threshold 5	27.810	17	0.047	0.490	0.633	1	0.426	2.063	0.347-12.285	0.481
Threshold 10	27.850	17	0.047	0.491	0.670	1	0.413	1.875	0.416-8.454	0.481
PRSwithoutAPOE										
Threshold 1	29.672	17	0.029	0.516	2.199	1	0.138	0.519	0.218-1.235	0.481
Threshold 5	27.189	17	0.055	0.482	0.029	1	0.865	0.935	0.430-2.032	0.481
Threshold 10	27.553	17	0.050	0.487	0.391	1	0.532	1.288	0.583-2.847	0.481
APOEonlyPRS										
Threshold 1	28.640	17	0.038	0.502	1.400	1	0.237	2.911	0.496-17.087	0.481
Threshold 5	28.455	17	0.040	0.499	1.235	1	0.266	2.732	0.464-16.076	0.481
Threshold 10	27.294	17	0.054	0.483	0.134	1	0.715	1.352	0.268-6.813	0.481

APOE: apolipoprotein E. CI: confidence interval. df: degrees of freedom. OR: odds ratio. PRS: polygenic risk score.

Table F1.16: Associations between PRSs and longitudinal change in CSF Aβ42 measurement in MCI ε4 carriers when CSF p-tau181 status was controlled for

PRS & Threshold	Chi-square	df	*p*	Nagelkerke R^2	Wald	df	*p*	OR	95% CI	Nagelkerke R^2 Model 1
PRSwithAPOE										
Threshold 1	25.177	16	0.067	0.555	1.796	1	0.180	3.129	0.590-16.587	0.522
Threshold 5	26.277	16	0.050	0.573	2.753	1	0.097	4.350	0.766-24.709	0.522
Threshold 10	25.510	16	0.061	0.561	2.081	1	0.149	3.671	0.627-21.478	0.522
PRSwithoutAPOE										
Threshold 1	23.206	16	0.108	0.522	0.001	1	0.976	1.014	0.397-2.589	0.522
Threshold 5	23.597	16	0.099	0.528	0.389	1	0.533	1.330	0.543-3.262	0.522
Threshold 10	23.920	16	0.091	0.534	0.694	1	0.405	1.523	0.566-4.098	0.522
APOEonlyPRS										
Threshold 1	24.505	16	0.079	0.544	1.240	1	0.266	2.132	0.562-8.087	0.522
Threshold 5	24.652	16	0.076	0.546	1.381	1	0.240	2.243	0.583-8.629	0.522
Threshold 10	23.915	16	0.091	0.534	0.696	1	0.404	1.764	0.465-6.691	0.522

APOE: apolipoprotein E. CI: confidence interval. df: degrees of freedom. OR: odds ratio. PRS: polygenic risk score.

Table F1.17: Associations between PRSs and longitudinal change in CSF p-tau181 measurement in APOE ε4 non-carriers when CSF Aβ42 status was not controlled for

PRS & Threshold	Chi-square	df	*p*	Nagelkerke R^2	Wald	df	*p*	OR	95% CI	Nagelkerke R^2 Model 1
PRSwithAPOE										
Threshold 1	26.141	16	0.052	0.321	7.598	1	0.006	0.242	0.088-0.664	0.224
Threshold 5	26.391	16	0.049	0.324	7.803	1	0.005	0.249	0.094-0.660	0.224
Threshold 10	22.090	16	0.140	0.277	4.333	1	0.037	0.394	0.164-0.947	0.224
PRSwithoutAPOE										
Threshold 1	17.486	16	0.355	0.224	0.025	1	0.876	1.040	0.639-1.691	0.224
Threshold 5	17.488	16	0.355	0.224	0.026	1	0.871	1.040	0.647-1.672	0.224
Threshold 10	18.123	16	0.317	0.232	0.657	1	0.418	1.240	0.737-2.085	0.224
APOEonlyPRS										
Threshold 1	28.939	16	0.024	0.351	9.573	1	0.002	0.185	0.064-0.539	0.224
Threshold 5	29.113	16	0.023	0.353	9.728	1	0.002	0.180	0.061-0.528	0.224
Threshold 10	25.746	16	0.058	0.317	7.300	1	0.007	0.235	0.082-0.672	0.224

APOE: apolipoprotein E. CI: confidence interval. df: degrees of freedom. OR: odds ratio. PRS: polygenic risk score.

Table F1.18: Associations between PRSs and longitudinal change in CSF p-tau181 measurement in APOE ε4 carriers when CSF Aβ42 status was not controlled for

PRS & Threshold	Chi-square	df	*p*	Nagelkerke R^2	Wald	df	*p*	OR	95% CI	Nagelkerke R^2 Model 1
PRSwithAPOE										
Threshold 1	21.969	16	0.144	0.378	0.204	1	0.651	1.244	0.482-3.208	0.375
Threshold 5	21.766	16	0.151	0.375	0.001	1	0.975	1.015	0.397-2.595	0.375
Threshold 10	21.771	16	0.151	0.375	0.006	1	0.938	1.038	0.407-2.649	0.375
PRSwithoutAPOE										
Threshold 1	21.765	16	0.151	0.375	0.000	1	0.985	0.993	0.484-2.039	0.375
Threshold 5	22.812	16	0.119	0.390	1.026	1	0.311	0.668	0.306-1.459	0.375
Threshold 10	21.939	16	0.145	0.377	0.172	1	0.678	0.843	0.375-1.892	0.375
APOEonlyPRS										
Threshold 1	21.949	16	0.145	0.377	0.184	1	0.668	1.218	0.495-2.996	0.375
Threshold 5	21.831	16	0.149	0.376	0.067	1	0.796	1.126	0.456-2.784	0.375
Threshold 10	21.784	16	0.150	0.375	0.019	1	0.890	1.067	0.423-2.692	0.375

APOE: apolipoprotein E. CI: confidence interval. df: degrees of freedom. OR: odds ratio. PRS: polygenic risk score.

Table F1.19: Associations between PRSs and longitudinal change in CSF p-tau181 measurement in APOE ε4 non-carriers when CSF Aβ42 status was controlled for

PRS & Threshold	Chi-square	df	*p*	Nagelkerke R^2	Wald	df	*p*	OR	95% CI	Nagelkerke R^2 Model 1
PRSwithAPOE										
Threshold 1	26.348	17	0.068	0.323	7.723	1	0.005	0.234	0.084-0.652	0.224
Threshold 5	26.463	17	0.066	0.325	7.838	1	0.005	0.246	0.092-0.657	0.224
Threshold 10	22.090	17	0.181	0.277	4.332	1	0.037	0.394	0.164-0.947	0.224
PRSwithoutAPOE										
Threshold 1	17.487	17	0.422	0.224	0.022	1	0.881	1.038	0.635-1.698	0.224
Threshold 5	17.490	17	0.422	0.224	0.026	1	0.873	1.040	0.647-1.671	0.224
Threshold 10	18.128	17	0.381	0.232	0.659	1	0.417	1.240	0.737-2.086	0.224
APOEonlyPRS										
Threshold 1	29.030	17	0.034	0.352	9.598	1	0.002	0.183	0.062-0.535	0.224
Threshold 5	29.170	17	0.033	0.353	9.755	1	0.002	0.178	0.060-0.526	0.224
Threshold 10	25.749	17	0.079	0.317	7.300	1	0.007	0.235	0.082-0.672	0.224

APOE: apolipoprotein E. CI: confidence interval. df: degrees of freedom. OR: odds ratio. PRS: polygenic risk score.

Table F1.20: Associations between PRSs and longitudinal change in CSF p-tau181 measurement in APOE ε4 carriers when CSF Aβ42 status was controlled for

PRS & Threshold	Chi-square	df	*p*	Nagelkerke R^2	Wald	df	*p*	OR	95% CI	Nagelkerke R^2 Model 1
PRSwithAPOE										
Threshold 1	22.443	17	0.168	0.385	0.131	1	0.717	1.194	0.457-3.118	0.383
Threshold 5	22.314	17	0.173	0.383	0.002	1	0.967	0.980	0.377-2.545	0.383
Threshold 10	22.314	17	0.173	0.383	0.001	1	0.971	1.017	0.393-2.629	0.383
PRSwithoutAPOE										
Threshold 1	22.320	17	0.173	0.383	0.007	1	0.932	0.969	0.468-2.006	0.383
Threshold 5	23.423	17	0.136	0.399	1.084	1	0.298	0.654	0.294-1.455	0.383
Threshold 10	22.502	17	0.166	0.386	0.188	1	0.665	0.834	0.366-1.900	0.383
APOEonlyPRS										
Threshold 1	22.442	17	0.168	0.385	0.130	1	0.718	1.183	0.475-2.943	0.383
Threshold 5	22.349	17	0.172	0.383	0.037	1	0.848	1.094	0.437-2.737	0.383
Threshold 10	22.325	17	0.173	0.383	0.013	1	0.910	1.056	0.411-2.713	0.383

APOE: apolipoprotein E. CI: confidence interval. df: degrees of freedom. OR: odds ratio. PRS: polygenic risk score.

Table F1.21: Associations between PRSs and longitudinal change in CSF p-tau181 measurement in MCI ε4 non-carriers when CSF Aβ42 status was not controlled for

PRS & Threshold	Chi-square	df	*p*	Nagelkerke R^2	Wald	df	*p*	OR	95% CI	Nagelkerke R^2 Model 1
PRSwithAPOE										
Threshold 1	23.382	16	0.104	0.431	4.468	1	0.035	0.165	0.031-0.877	0.347
Threshold 5	23.120	16	0.111	0.427	4.325	1	0.038	0.174	0.034-0.904	0.347
Threshold 10	21.110	16	0.174	0.396	2.755	1	0.097	0.310	0.078-1.236	0.347
PRSwithoutAPOE										
Threshold 1	18.031	16	0.322	0.347	0.004	1	0.948	1.022	0.527-1.981	0.347
Threshold 5	18.042	16	0.321	0.347	0.015	1	0.902	0.958	0.480-1.909	0.347
Threshold 10	18.371	16	0.303	0.352	0.343	1	0.558	1.227	0.618-2.436	0.347
APOEonlyPRS										
Threshold 1	25.039	16	0.069	0.456	5.417	1	0.020	0.122	0.021-0.718	0.347
Threshold 5	25.384	16	0.063	0.461	5.515	1	0.019	0.103	0.015-0.687	0.347
Threshold 10	23.248	16	0.107	0.429	4.276	1	0.039	0.166	0.030-0.911	0.347

APOE: apolipoprotein E. CI: confidence interval. df: degrees of freedom. OR: odds ratio. PRS: polygenic risk score.

Table F1.22: Associations between PRSs and longitudinal change in CSF p-tau181 measurement in CU ε4 non-carriers when CSF Aβ42 status was not controlled for

PRS & Threshold	Chi-square	df	*p*	Nagelkerke R^2	Wald	df	*p*	OR	95% CI	Nagelkerke R^2 Model 1
PRSwithAPOE										
Threshold 1	37.363	15	0.001	1.000	0.004	1	0.950	0.000	0.000-not available	0.592
Threshold 5	37.363	15	0.001	1.000	0.004	1	0.948	0.000	0.000-not available	0.592
Threshold 10	37.363	15	0.001	1.000	0.002	1	0.968	0.000	0.000-not available	0.592
PRSwithoutAPOE										
Threshold 1	16.252	15	0.365	0.592	0.000	1	0.987	1.015	0.166-6.213	0.592
Threshold 5	17.097	15	0.313	0.615	0.750	1	0.387	2.120	0.387-11.611	0.592
APOEonlyPRS										
Threshold 1	37.363	15	0.001	1.000	0.000	1	0.996	0.000	0.000-not available	0.592
Threshold 10	19.478	15	0.193	0.675	0.374	1	0.541	0.000	0.000-1.219E+13	0.592

APOE: apolipoprotein E. CI: confidence interval. df: degrees of freedom. OR: odds ratio. PRS: polygenic risk score.

PRSwithoutAPOE Threshold 10 and APOEonlyPRS Threshold 5 not available.

Table F1.23: Associations between PRSs and longitudinal change in CSF p-tau181 measurement in MCI ε4 carriers when CSF Aβ42 status was not controlled for

PRS & Threshold	Chi-square	df	*p*	Nagelkerke R^2	Wald	df	*p*	OR	95% CI	Nagelkerke R^2 Model 1
PRSwithAPOE										
Threshold 1	14.774	15	0.468	0.418	1.212	1	0.271	2.725	0.457-16.233	0.386
Threshold 5	13.789	15	0.542	0.394	0.312	1	0.576	1.601	0.307-8.338	0.386
Threshold 10	13.472	15	0.566	0.386	0.000	1	0.990	0.989	0.175-5.590	0.386
PRSwithoutAPOE										
Threshold 1	13.552	15	0.560	0.388	0.080	1	0.778	1.186	0.363-3.874	0.386
Threshold 5	14.011	15	0.525	0.400	0.521	1	0.471	0.638	0.189-2.160	0.386
Threshold 10	17.327	15	0.300	0.478	2.410	1	0.121	0.158	0.015-1.623	0.386
APOEonlyPRS										
Threshold 1	14.488	15	0.489	0.411	0.962	1	0.327	2.258	0.443-11.493	0.386
Threshold 5	14.198	15	0.511	0.404	0.696	1	0.404	1.998	0.393-10.161	0.386
Threshold 10	14.121	15	0.516	0.402	0.632	1	0.427	1.960	0.373-10.303	0.386

APOE: apolipoprotein E. CI: confidence interval. df: degrees of freedom. OR: odds ratio. PRS: polygenic risk score.

Table F1.24: Associations between PRSs and longitudinal change in CSF p-tau181 measurement in MCI ε4 non-carriers when CSF Aβ42 status was controlled for

PRS & Threshold	Chi-square	df	*p*	Nagelkerke R^2	Wald	df	*p*	OR	95% CI	Nagelkerke R^2 Model 1
PRSwithAPOE										
Threshold 1	23.605	17	0.131	0.435	3.871	1	0.049	0.180	0.033-0.993	0.363
Threshold 5	23.656	17	0.129	0.435	3.964	1	0.046	0.187	0.036-0.974	0.363
Threshold 10	22.188	17	0.178	0.413	2.815	1	0.093	0.302	0.075-1.223	0.363
PRSwithoutAPOE										
Threshold 1	19.036	17	0.326	0.363	0.027	1	0.870	1.057	0.543-2.058	0.363
Threshold 5	19.035	17	0.327	0.363	0.025	1	0.874	0.945	0.474-1.887	0.363
Threshold 10	19.248	17	0.314	0.367	0.239	1	0.625	1.187	0.598-2.356	0.363
APOEonlyPRS										
Threshold 1	25.357	17	0.087	0.461	4.961	1	0.026	0.132	0.022-0.784	0.363
Threshold 5	25.760	17	0.079	0.467	5.084	1	0.024	0.110	0.016-0.750	0.363
Threshold 10	24.153	17	0.115	0.443	4.176	1	0.041	0.168	0.030-0.929	0.363

APOE: apolipoprotein E. CI: confidence interval. df: degrees of freedom. OR: odds ratio. PRS: polygenic risk score.

Table F1.25: Associations between PRSs and longitudinal change in CSF p-tau181 measurement in CU ε4 non-carriers when CSF Aβ42 status was controlled for

PRS & Threshold	Chi-square	df	*p*	Nagelkerke R^2	Wald	df	*p*	OR	95% CI	Nagelkerke R^2 Model 1
PRSwithAPOE										
Threshold 1	37.363	16	0.002	1.000	0.000	1	0.999	0.000	0.000-not available	1.000
Threshold 5	37.363	16	0.002	1.000	0.000	1	0.999	0.000	0.000-not available	1.000
Threshold 10	37.363	16	0.002	1.000	0.000	1	0.999	0.000	0.000-not available	1.000
PRSwithoutAPOE										
Threshold 1	37.363	16	0.002	1.000	0.000	1	0.999	0.000	0.000-not available	1.000
Threshold 5	37.363	16	0.002	1.000	0.000	1	0.998	0.000	0.000-not available	1.000
Threshold 10	37.363	16	0.002	1.000	0.000	1	0.999	0.000	0.000-not available	1.000
APOEonlyPRS										
Threshold 1	37.363	16	0.002	1.000	.000	1	1.000	716.731	0.000-not available	1.000
Threshold 5	37.363	16	0.002	1.000	.000	1	1.000	1496.020	0.000-not available	1.000
Threshold 10	37.363	16	0.002	1.000	000	1	1.000	3476.490	0.000-not available	1.000

APOE: apolipoprotein E. CI: confidence interval. df: degrees of freedom. OR: odds ratio. PRS: polygenic risk score.

Table F1.26: Associations between PRSs and longitudinal change in CSF p-tau181 measurement in MCI ε4 carriers when CSF Aβ42 status was controlled for

PRS & Threshold	Chi-square	df	*p*	Nagelkerke R^2	Wald	df	*p*	OR	95% CI	Nagelkerke R^2 Model 1
PRSwithAPOE										
Threshold 1	20.515	16	0.198	0.549	0.745	1	0.388	3.474	0.205-58.788	0.532
Threshold 5	19.754	16	0.232	0.532	0.008	1	0.927	0.881	0.058-13.305	0.532
Threshold 10	20.523	16	0.198	0.549	0.709	1	0.400	0.288	0.016-5.216	0.532
PRSwithoutAPOE										
Threshold 1	20.091	16	0.216	0.539	0.337	1	0.562	1.638	0.309-8.677	0.532
Threshold 5	20.310	16	0.207	0.544	0.527	1	0.468	0.576	0.130-2.552	0.532
Threshold 10	22.769	16	0.120	0.595	1.598	1	0.206	0.137	0.006-2.987	0.532
APOEonlyPRS										
Threshold 1	19.952	16	0.222	0.536	0.200	1	0.655	1.752	0.150-20.490	0.532
Threshold 5	19.837	16	0.228	0.534	0.090	1	0.764	1.457	0.125-17.007	0.532
Threshold 10	19.813	16	0.229	0.533	0.067	1	0.796	1.372	0.125-15.006	0.532

APOE: apolipoprotein E. CI: confidence interval. df: degrees of freedom. OR: odds ratio. PRS: polygenic risk score.

Table F1.27: Associations between PRSs and longitudinal change in CSF p-tau181 measurement in the whole group when CSF Aβ42 status was not controlled for

PRS & Threshold	Chi-square	df	*p*	Nagelkerke R^2	Wald	df	*p*	OR	95% CI	Nagelkerke R^2 Model 1
PRSwithAPOE										
Threshold 1	11.446	16	0.781	0.090	0.006	1	0.940	0.986	0.692-1.406	0.090
Threshold 5	11.552	16	0.774	0.091	0.111	1	0.739	0.942	0.661-1.341	0.090
Threshold 10	11.442	16	0.781	0.090	0.001	1	0.976	0.995	0.694-1.425	0.090
PRSwithoutAPOE										
Threshold 1	12.183	16	0.731	0.096	0.735	1	0.391	1.164	0.823-1.647	0.090
Threshold 5	11.458	16	0.780	0.090	0.018	1	0.895	1.024	0.721-1.455	0.090
Threshold 10	12.225	16	0.728	0.096	0.779	1	0.377	1.185	0.813-1.725	0.090
APOEonlyPRS										
Threshold 1	11.605	16	0.771	0.091	0.164	1	0.685	0.929	0.651-1.327	0.090
Threshold 5	11.674	16	0.766	0.092	0.234	1	0.629	0.916	0.640-1.309	0.090
Threshold 10	11.482	16	0.779	0.090	0.042	1	0.838	0.963	0.671-1.382	0.090

APOE: apolipoprotein E. CI: confidence interval. df: degrees of freedom. OR: odds ratio. PRS: polygenic risk score.

Table F1.28: Associations between PRSs and longitudinal change in CSF p-tau181 measurement in the whole group when CSF Aβ42 status was controlled for

PRS & Threshold	Chi-square	df	*p*	Nagelkerke R^2	Wald	df	*p*	OR	95% CI	Nagelkerke R^2 Model 1
PRSwithAPOE										
Threshold 1	13.945	17	0.671	0.109	0.576	1	0.448	0.856	0.574-1.278	0.105
Threshold 5	14.396	17	0.639	0.112	1.021	1	0.312	0.815	0.547-1.213	0.105
Threshold 10	13.734	17	0.686	0.108	0.366	1	0.545	0.885	0.596-1.314	0.105
PRSwithoutAPOE										
Threshold 1	13.807	17	0.681	0.108	0.438	1	0.508	1.126	0.792-1.602	0.105
Threshold 5	13.366	17	0.711	0.105	0.000	1	0.998	1.000	0.701-1.426	0.105
Threshold 10	14.006	17	0.667	0.110	0.637	1	0.425	1.166	0.799-1.703	0.105
APOEonlyPRS										
Threshold 1	14.535	17	0.629	0.114	1.159	1	0.282	0.803	0.538-1.198	0.105
Threshold 5	14.733	17	0.615	0.115	1.353	1	0.245	0.788	0.527-1.177	0.105
Threshold 10	14.022	17	0.666	0.110	0.653	1	0.419	0.848	0.569-1.264	0.105

APOE: apolipoprotein E. CI: confidence interval. df: degrees of freedom. OR: odds ratio. PRS: polygenic risk score.

Table F1.29: Associations between PRSs and longitudinal change in CSF p-tau181 measurement in CU participants when CSF Aβ42 status was not controlled for

PRS & Threshold	Chi-square	df	*p*	Nagelkerke R^2	Wald	df	*p*	OR	95% CI	Nagelkerke R^2 Model 1
PRSwithAPOE										
Threshold 1	12.177	16	0.732	0.378	1.033	1	0.309	0.493	0.126-1.926	0.350
Threshold 5	12.286	16	0.724	0.381	1.147	1	0.284	0.502	0.142-1.773	0.350
Threshold 10	12.552	16	0.705	0.388	1.405	1	0.236	0.477	0.141-1.621	0.350
PRSwithoutAPOE										
Threshold 1	11.126	16	0.802	0.350	0.009	1	0.923	1.062	0.311-3.623	0.350
Threshold 5	11.546	16	0.775	0.361	0.428	1	0.513	1.409	0.505-3.933	0.350
Threshold 10	11.159	16	0.800	0.351	0.042	1	0.837	0.881	0.263-2.951	0.350
APOEonlyPRS										
Threshold 1	12.512	16	0.708	0.387	1.324	1	0.250	0.449	0.115-1.757	0.350
Threshold 5	12.551	16	0.705	0.388	1.367	1	0.242	0.442	0.113-1.736	0.350
Threshold 10	12.125	16	0.735	0.377	0.983	1	0.321	0.496	0.124-1.984	0.350

APOE: apolipoprotein E. CI: confidence interval. df: degrees of freedom. OR: odds ratio. PRS: polygenic risk score.

Table F1.30: Associations between PRSs and longitudinal change in CSF p-tau181 measurement in MCI patients when CSF Aβ42 status was not controlled for

PRS & Threshold	Chi-square	df	*p*	Nagelkerke R^2	Wald	df	*p*	OR	95% CI	Nagelkerke R^2 Model 1
PRSwithAPOE										
Threshold 1	14.295	16	0.577	0.174	0.804	1	0.370	1.260	0.760-2.091	0.165
Threshold 5	13.782	16	0.615	0.168	0.301	1	0.583	1.154	0.691-1.927	0.165
Threshold 10	13.580	16	0.630	0.166	0.101	1	0.750	1.089	0.643-1.856	0.165
PRSwithoutAPOE										
Threshold 1	14.577	16	0.556	0.177	1.080	1	0.299	1.279	0.804-2.033	0.165
Threshold 5	13.481	16	0.637	0.165	0.003	1	0.960	0.987	0.606-1.608	0.165
Threshold 10	13.489	16	0.637	0.165	0.011	1	0.915	0.972	0.577-1.637	0.165
APOEonlyPRS										
Threshold 1	13.790	16	0.614	0.168	0.310	1	0.578	1.156	0.694-1.924	0.165
Threshold 5	13.705	16	0.621	0.167	0.225	1	0.635	1.133	0.677-1.895	0.165
Threshold 10	13.812	16	0.613	0.169	0.331	1	0.565	1.162	0.697-1.938	0.165

APOE: apolipoprotein E. CI: confidence interval. df: degrees of freedom. OR: odds ratio. PRS: polygenic risk score.

Table F1.31: Associations between PRSs and longitudinal change in CSF p-tau181 measurement in CU participants when CSF Aβ42 status was controlled for

PRS & Threshold	Chi-square	df	*p*	Nagelkerke R^2	Wald	df	*p*	OR	95% CI	Nagelkerke R^2 Model 1
PRSwithAPOE										
Threshold 1	23.108	17	0.146	0.631	2.933	1	0.087	0.155	0.018-1.309	0.549
Threshold 5	22.694	17	0.159	0.622	2.755	1	0.097	0.211	0.033-1.326	0.549
Threshold 10	22.860	17	0.154	0.626	2.882	1	0.090	0.211	0.035-1.272	0.549
PRSwithoutAPOE										
Threshold 1	20.867	17	0.232	0.584	1.195	1	0.274	0.278	0.028-2.761	0.549
Threshold 5	19.268	17	0.313	0.550	0.044	1	0.833	0.870	0.238-3.177	0.549
Threshold 10	20.365	17	0.256	0.574	0.900	1	0.343	0.392	0.057-2.709	0.549
APOEonlyPRS										
Threshold 1	22.433	17	0.169	0.617	2.531	1	0.112	0.206	0.030-1.442	0.549
Threshold 5	22.422	17	0.169	0.617	2.585	1	0.108	0.208	0.031-1.410	0.549
Threshold 10	21.539	17	0.203	0.599	2.012	1	0.156	0.252	0.038-1.692	0.549

APOE: apolipoprotein E. CI: confidence interval. df: degrees of freedom. OR: odds ratio. PRS: polygenic risk score.

Table F1.32: Associations between PRSs and longitudinal change in CSF p-tau181 measurement in MCI patients when CSF Aβ42 status was controlled for

PRS & Threshold	Chi-square	df	*p*	Nagelkerke R^2	Wald	df	*p*	OR	95% CI	Nagelkerke R^2 Model 1
PRSwithAPOE										
Threshold 1	14.567	17	0.627	0.177	1.067	1	0.302	1.355	0.761-2.410	0.165
Threshold 5	13.879	17	0.676	0.169	0.398	1	0.528	1.203	0.678-2.136	0.165
Threshold 10	13.609	17	0.695	0.166	0.130	1	0.719	1.111	0.626-1.972	0.165
PRSwithoutAPOE										
Threshold 1	14.621	17	0.623	0.178	1.125	1	0.289	1.289	0.806-2.063	0.165
Threshold 5	13.481	17	0.703	0.165	0.002	1	0.962	0.988	0.605-1.614	0.165
Threshold 10	13.490	17	0.703	0.165	0.011	1	0.916	0.972	0.577-1.638	0.165
APOEonlyPRS										
Threshold 1	13.886	17	0.675	0.169	0.404	1	0.525	1.203	0.681-2.123	0.165
Threshold 5	13.776	17	0.683	0.168	0.296	1	0.587	1.173	0.660-2.082	0.165
Threshold 10	13.893	17	0.675	0.169	0.411	1	0.522	1.200	0.687-2.096	0.165

APOE: apolipoprotein E. CI: confidence interval. df: degrees of freedom. OR: odds ratio. PRS: polygenic risk score.

Table F1.33: Associations between PRSs and differential scores of longitudinal change in CSF Aβ42 measurements in the whole group when CSF p-tau181 status was not controlled for

PRS & Threshold	R Square (Model 1)	R Square (Model 2)	R Square Change	Sig. F Change (Model 2)	Standardised beta of PRS
PRSwithAPOE					
Threshold 1	0.054	0.061	0.007	0.292	-0.094
Threshold 5	0.054	0.062	0.008	0.262	-0.101
Threshold 10	0.054	0.062	0.008	0.260	-0.101
PRSwithoutAPOE					
Threshold 1	0.054	0.071	0.017	0.097	0.138
Threshold 5	0.054	0.065	0.011	0.182	0.112
Threshold 10	0.054	0.060	0.006	0.306	0.086
APOEonlyPRS					
Threshold 1	0.054	0.067	0.013	0.141	-0.130
Threshold 5	0.054	0.068	0.014	0.130	-0.134
Threshold 10	0.054	0.066	0.012	0.162	-0.124

APOE: apolipoprotein E. PRS: polygenic risk score.

Table F1.34: Associations between PRSs and differential scores of longitudinal change in CSF Aβ42 measurements in the whole group when CSF p-tau181 status was controlled for

PRS & Threshold	R Square (Model 1)	R Square (Model 2)	R Square Change	Sig. F Change (Model 2)	Standardised beta of PRS
PRSwithAPOE					
Threshold 1	0.070	0.073	0.003	0.465	-0.067
Threshold 5	0.070	0.073	0.004	0.439	-0.071
Threshold 10	0.070	0.073	0.004	0.423	-0.073
PRSwithoutAPOE					
Threshold 1	0.070	0.089	0.019	0.072	0.150
Threshold 5	0.070	0.084	0.014	0.123	0.130
Threshold 10	0.070	0.077	0.008	0.253	0.096
APOEonlyPRS					
Threshold 1	0.070	0.078	0.008	0.238	-0.106
Threshold 5	0.070	0.079	0.009	0.223	-0.110
Threshold 10	0.070	0.077	0.008	0.259	-0.101

APOE: apolipoprotein E. PRS: polygenic risk score.

Table F1.35: Associations between PRSs and differential scores of longitudinal change in CSF Aβ42 measurements in APOE ε4 non-carriers when CSF p-tau181 status was not controlled for

PRS & Threshold	R Square (Model 1)	R Square (Model 2)	R Square Change	Sig. F Change (Model 2)	Standardised beta of PRS
PRSwithAPOE					
Threshold 1	0.122	0.123	0.002	0.690	0.044
Threshold 5	0.122	0.123	0.001	0.740	0.037
Threshold 10	0.122	0.122	0.000	0.885	0.016
PRSwithoutAPOE					
Threshold 1	0.122	0.146	0.024	0.135	0.170
Threshold 5	0.122	0.132	0.011	0.323	0.110
Threshold 10	0.122	0.130	0.008	0.393	0.097
APOEonlyPRS					
Threshold 1	0.122	0.122	0.000	0.905	-0.013
Threshold 5	0.122	0.122	0.000	0.944	-0.008
Threshold 10	0.122	0.122	0.000	0.915	-0.012

APOE: apolipoprotein E. PRS: polygenic risk score.

Table F1.36: Associations between PRSs and differential scores of longitudinal change in CSF Aβ42 measurements in APOE ε4 carriers when CSF p-tau181 status was not controlled for

PRS & Threshold	R Square (Model 1)	R Square (Model 2)	R Square Change	Sig. F Change (Model 2)	Standardised beta of PRS
PRSwithAPOE					
Threshold 1	0.121	0.134	0.013	0.353	-0.170
Threshold 5	0.121	0.140	0.019	0.262	-0.203
Threshold 10	0.121	0.148	0.027	0.183	-0.238
PRSwithoutAPOE					
Threshold 1	0.121	0.133	0.012	0.371	0.134
Threshold 5	0.121	0.130	0.009	0.453	0.107
Threshold 10	0.121	0.121	0.000	0.993	-0.001
APOEonlyPRS					
Threshold 1	0.121	0.146	0.025	0.201	-0.218
Threshold 5	0.121	0.148	0.027	0.187	-0.225
Threshold 10	0.121	0.144	0.023	0.224	-0.213

APOE: apolipoprotein E. PRS: polygenic risk score.

Table F1.37: Associations between PRSs and differential scores of longitudinal change in CSF Aβ42 measurements in APOE ε4 non-carriers when CSF p-tau181 status was controlled for

PRS & Threshold	R Square (Model 1)	R Square (Model 2)	R Square Change	Sig. F Change (Model 2)	Standardised beta of PRS
PRSwithAPOE					
Threshold 1	0.124	0.126	0.002	0.675	0.047
Threshold 5	0.124	0.126	0.002	0.709	0.042
Threshold 10	0.124	0.125	0.000	0.854	0.021
PRSwithoutAPOE					
Threshold 1	0.124	0.150	0.026	0.124	0.176
Threshold 5	0.124	0.137	0.012	0.290	0.119
Threshold 10	0.124	0.133	0.009	0.369	0.103
APOEonlyPRS					
Threshold 1	0.124	0.125	0.000	0.906	-0.013
Threshold 5	0.124	0.125	0.000	0.944	-0.008
Threshold 10	0.124	0.125	0.000	0.905	-0.014

APOE: apolipoprotein E. PRS: polygenic risk score.

Table F1.38: Associations between PRSs and differential scores of longitudinal change in CSF Aβ42 measurements in APOE ε4 carriers when CSF p-tau181 status was controlled for

PRS & Threshold	R Square (Model 1)	R Square (Model 2)	R Square Change	Sig. F Change (Model 2)	Standardised beta of PRS
PRSwithAPOE					
Threshold 1	0.137	0.148	0.011	0.388	-0.158
Threshold 5	0.137	0.152	0.016	0.312	-0.184
Threshold 10	0.137	0.160	0.024	0.215	-0.223
PRSwithoutAPOE					
Threshold 1	0.137	0.149	0.012	0.370	0.135
Threshold 5	0.137	0.148	0.011	0.400	0.120
Threshold 10	0.137	0.137	0.000	0.966	0.006
APOEonlyPRS					
Threshold 1	0.137	0.159	0.022	0.230	-0.205
Threshold 5	0.137	0.160	0.023	0.217	-0.212
Threshold 10	0.137	0.158	0.021	0.241	-0.205

APOE: apolipoprotein E. PRS: polygenic risk score.

Table F1.39: Associations between PRSs and differential scores of longitudinal change in CSF Aβ42 measurements in CU participants when CSF p-tau181 status was not controlled for

PRS & Threshold	R Square (Model 1)	R Square (Model 2)	R Square Change	Sig. F Change (Model 2)	Standardised beta of PRS
PRSwithAPOE					
Threshold 1	0.211	0.220	0.009	0.627	-0.118
Threshold 5	0.211	0.215	0.003	0.759	-0.075
Threshold 10	0.211	0.217	0.006	0.690	-0.094
PRSwithoutAPOE					
Threshold 1	0.211	0.238	0.027	0.386	0.254
Threshold 5	0.211	0.248	0.037	0.309	0.263
Threshold 10	0.211	0.242	0.031	0.353	0.246
APOEonlyPRS					
Threshold 1	0.211	0.225	0.014	0.535	-0.160
Threshold 5	0.211	0.224	0.012	0.559	-0.152
Threshold 10	0.211	0.223	0.012	0.565	-0.150

APOE: apolipoprotein E. PRS: polygenic risk score.

Table F1.40: Associations between PRSs and differential scores of longitudinal change in CSF Aβ42 measurements in MCI patients when CSF p-tau181 status was not controlled for

PRS & Threshold	R Square (Model 1)	R Square (Model 2)	R Square Change	Sig. F Change (Model 2)	Standardised beta of PRS
PRSwithAPOE					
Threshold 1	0.131	0.133	0.003	0.599	-0.060
Threshold 5	0.131	0.136	0.005	0.456	-0.087
Threshold 10	0.131	0.136	0.005	0.478	-0.083
PRSwithoutAPOE					
Threshold 1	0.131	0.134	0.003	0.579	0.059
Threshold 5	0.131	0.131	0.000	0.919	-0.011
Threshold 10	0.131	0.131	0.000	0.845	-0.022
APOEonlyPRS					
Threshold 1	0.131	0.136	0.005	0.468	-0.083
Threshold 5	0.131	0.138	0.007	0.390	-0.099
Threshold 10	0.131	0.135	0.004	0.496	-0.077

APOE: apolipoprotein E. PRS: polygenic risk score.

Table F1.41: Associations between PRSs and differential scores of longitudinal change in CSF Aβ42 measurements in CU participants when CSF p-tau181 status was controlled for

PRS & Threshold	R Square (Model 1)	R Square (Model 2)	R Square Change	Sig. F Change (Model 2)	Standardised beta of PRS
PRSwithAPOE					
Threshold 1	0.218	0.226	0.008	0.647	-0.113
Threshold 5	0.218	0.221	0.003	0.775	-0.071
Threshold 10	0.218	0.223	0.005	0.717	-0.088
PRSwithoutAPOE					
Threshold 1	0.218	0.249	0.031	0.359	0.276
Threshold 5	0.218	0.260	0.042	0.286	0.284
Threshold 10	0.218	0.257	0.039	0.305	0.283
APOEonlyPRS					
Threshold 1	0.218	0.232	0.014	0.542	-0.160
Threshold 5	0.218	0.230	0.012	0.570	-0.151
Threshold 10	0.218	0.228	0.011	0.594	-0.142

APOE: apolipoprotein E. PRS: polygenic risk score.

Table F1.42: Associations between PRSs and differential scores of longitudinal change in CSF Aβ42 measurements in MCI patients when CSF p-tau181 status was controlled for

PRS & Threshold	R Square (Model 1)	R Square (Model 2)	R Square Change	Sig. F Change (Model 2)	Standardised beta of PRS
PRSwithAPOE					
Threshold 1	0.144	0.145	0.001	0.741	-0.039
Threshold 5	0.144	0.147	0.003	0.600	-0.062
Threshold 10	0.144	0.147	0.003	0.596	-0.062
PRSwithoutAPOE					
Threshold 1	0.144	0.150	0.006	0.420	0.088
Threshold 5	0.144	0.144	0.000	0.830	0.024
Threshold 10	0.144	0.144	0.000	0.946	-0.008
APOEonlyPRS					
Threshold 1	0.144	0.147	0.003	0.562	-0.066
Threshold 5	0.144	0.149	0.005	0.475	-0.083
Threshold 10	0.144	0.147	0.003	0.582	-0.063

APOE: apolipoprotein E. PRS: polygenic risk score.

Table F1.43: Associations between PRSs and differential scores of longitudinal change in CSF Aβ42 measurements in CU ε4 non-carriers when CSF p-tau181 status was not controlled for

PRS & Threshold	R Square (Model 1)	R Square (Model 2)	R Square Change	Sig. F Change (Model 2)	Standardised beta of PRS
PRSwithAPOE					
Threshold 1	0.369	0.377	0.007	0.699	0.109
Threshold 5	0.369	0.388	0.019	0.532	0.179
Threshold 10	0.369	0.389	0.020	0.529	0.188
PRSwithoutAPOE					
Threshold 1	0.369	0.417	0.048	0.321	0.302
Threshold 5	0.369	0.412	0.043	0.349	0.276
Threshold 10	0.369	0.405	0.036	0.390	0.265
APOEonlyPRS					
Threshold 1	0.369	0.371	0.002	0.854	0.052
Threshold 5	0.369	0.375	0.006	0.736	0.096
Threshold 10	0.369	0.381	0.012	0.628	0.145

APOE: apolipoprotein E. PRS: polygenic risk score.

Table F1.44: Associations between PRSs and differential scores of longitudinal change in CSF Aβ42 measurements in MCI ε4 non-carriers when CSF p-tau181 status was not controlled for

PRS & Threshold	R Square (Model 1)	R Square (Model 2)	R Square Change	Sig. F Change (Model 2)	Standardised beta of PRS
PRSwithAPOE					
Threshold 1	0.259	0.260	0.001	0.785	-0.042
Threshold 5	0.259	0.274	0.015	0.346	-0.147
Threshold 10	0.259	0.277	0.018	0.301	-0.157
PRSwithoutAPOE					
Threshold 1	0.259	0.273	0.015	0.349	0.141
Threshold 5	0.259	0.260	0.001	0.813	-0.035
Threshold 10	0.259	0.261	0.002	0.729	-0.051
APOEonlyPRS					
Threshold 1	0.259	0.270	0.011	0.417	-0.125
Threshold 5	0.259	0.273	0.014	0.361	-0.144
Threshold 10	0.259	0.270	0.011	0.420	-0.124

APOE: apolipoprotein E. PRS: polygenic risk score.

Table F1.45: Associations between PRSs and differential scores of longitudinal change in CSF Aβ42 measurements in MCI ε4 carriers when CSF p-tau181 status was not controlled for

PRS & Threshold	R Square (Model 1)	R Square (Model 2)	R Square Change	Sig. F Change (Model 2)	Standardised beta of PRS
PRSwithAPOE					
Threshold 1	0.355	0.393	0.037	0.182	-0.353
Threshold 5	0.355	0.412	0.057	0.094	-0.425
Threshold 10	0.355	0.380	0.025	0.274	-0.285
PRSwithoutAPOE					
Threshold 1	0.355	0.358	0.003	0.728	-0.062
Threshold 5	0.355	0.366	0.010	0.481	-0.119
Threshold 10	0.355	0.360	0.004	0.652	-0.080
APOEonlyPRS					
Threshold 1	0.355	0.376	0.020	0.324	-0.225
Threshold 5	0.355	0.382	0.027	0.256	-0.259
Threshold 10	0.355	0.378	0.022	0.299	-0.244

APOE: apolipoprotein E. PRS: polygenic risk score.

Table F1.46: Associations between PRSs and differential scores of longitudinal change in CSF Aβ42 measurements in CU ε4 non-carriers when CSF p-tau181 status was controlled for

PRS & Threshold	R Square (Model 1)	R Square (Model 2)	R Square Change	Sig. F Change (Model 2)	Standardised beta of PRS
PRSwithAPOE					
Threshold 1	0.371	0.377	0.006	0.739	0.106
Threshold 5	0.371	0.388	0.018	0.565	0.179
Threshold 10	0.371	0.389	0.018	0.561	0.188
PRSwithoutAPOE					
Threshold 1	0.371	0.419	0.048	0.340	0.303
Threshold 5	0.371	0.416	0.045	0.353	0.288
Threshold 10	0.371	0.408	0.037	0.401	0.270
APOEonlyPRS					
Threshold 1	0.371	0.371	0.001	0.909	0.038
Threshold 5	0.371	0.375	0.004	0.779	0.091
Threshold 10	0.371	0.381	0.010	0.663	0.141

APOE: apolipoprotein E. PRS: polygenic risk score.

Table F1.47: Associations between PRSs and differential scores of longitudinal change in CSF Aβ42 measurements in MCI ε4 non-carriers when CSF p-tau181 status was controlled for

PRS & Threshold	R Square (Model 1)	R Square (Model 2)	R Square Change	Sig. F Change (Model 2)	Standardised beta of PRS
PRSwithAPOE					
Threshold 1	0.268	0.268	0.000	0.903	-0.019
Threshold 5	0.268	0.278	0.011	0.432	-0.127
Threshold 10	0.268	0.283	0.015	0.349	-0.145
PRSwithoutAPOE					
Threshold 1	0.268	0.289	0.021	0.267	0.171
Threshold 5	0.268	0.268	0.000	0.936	-0.012
Threshold 10	0.268	0.269	0.001	0.794	-0.039
APOEonlyPRS					
Threshold 1	0.268	0.277	0.009	0.461	-0.115
Threshold 5	0.268	0.280	0.012	0.400	-0.135
Threshold 10	0.268	0.278	0.011	0.431	-0.122

APOE: apolipoprotein E. PRS: polygenic risk score.

Table F1.48: Associations between PRSs and differential scores of longitudinal change in CSF Aβ42 measurements in MCI ε4 carriers when CSF p-tau181 status was controlled for

PRS & Threshold	R Square (Model 1)	R Square (Model 2)	R Square Change	Sig. F Change (Model 2)	Standardised beta of PRS
PRSwithAPOE					
Threshold 1	0.367	0.398	0.031	0.220	-0.331
Threshold 5	0.367	0.415	0.048	0.128	-0.402
Threshold 10	0.367	0.386	0.019	0.340	-0.256
PRSwithoutAPOE					
Threshold 1	0.367	0.368	0.001	0.810	-0.044
Threshold 5	0.367	0.373	0.006	0.605	-0.091
Threshold 10	0.367	0.370	0.003	0.719	-0.065
APOEonlyPRS					
Threshold 1	0.367	0.385	0.018	0.362	-0.211
Threshold 5	0.367	0.390	0.023	0.292	-0.244
Threshold 10	0.367	0.386	0.019	0.342	-0.227

APOE: apolipoprotein E. PRS: polygenic risk score.

Table F1.49: Associations between PRSs and differential scores of longitudinal change in CSF p-tau181 measurements in CU participants when CSF Aβ42 status was not controlled for

PRS & Threshold	R Square (Model 1)	R Square (Model 2)	R Square Change	Sig. F Change (Model 2)	Standardised beta of PRS
PRSwithAPOE					
Threshold 1	0.303	0.455	0.152	0.021	-0.495
Threshold 5	0.303	0.442	0.140	0.028	-0.476
Threshold 10	0.303	0.479	0.176	0.012	-0.520
PRSwithoutAPOE					
Threshold 1	0.303	0.309	0.006	0.666	-0.120
Threshold 5	0.303	0.304	0.001	0.865	-0.042
Threshold 10	0.303	0.313	0.010	0.569	-0.143
APOEonlyPRS					
Threshold 1	0.303	0.469	0.166	0.016	-0.550
Threshold 5	0.303	0.465	0.162	0.017	-0.549
Threshold 10	0.303	0.468	0.165	0.016	-0.554

APOE: apolipoprotein E. PRS: polygenic risk score.

Table F1.50: Associations between PRSs and differential scores of longitudinal change in CSF p-tau181 measurements in MCI patients when CSF Aβ42 status was not controlled for

PRS & Threshold	R Square (Model 1)	R Square (Model 2)	R Square Change	Sig. F Change (Model 2)	Standardised beta of PRS
PRSwithAPOE					
Threshold 1	0.065	0.087	0.023	0.134	0.178
Threshold 5	0.065	0.084	0.020	0.165	0.167
Threshold 10	0.065	0.090	0.025	0.115	0.189
PRSwithoutAPOE					
Threshold 1	0.065	0.108	0.043	0.038	0.228
Threshold 5	0.065	0.080	0.016	0.212	0.139
Threshold 10	0.065	0.088	0.023	0.132	0.172
APOEonlyPRS					
Threshold 1	0.065	0.074	0.010	0.334	0.114
Threshold 5	0.065	0.073	0.009	0.356	0.110
Threshold 10	0.065	0.074	0.010	0.330	0.115

APOE: apolipoprotein E. PRS: polygenic risk score.

Table F1.51: Associations between PRSs and differential scores of longitudinal change in CSF p-tau181 measurements in CU participants when CSF Aβ42 status was controlled for

PRS & Threshold	R Square (Model 1)	R Square (Model 2)	R Square Change	Sig. F Change (Model 2)	Standardised beta of PRS
PRSwithAPOE					
Threshold 1	0.381	0.621	0.240	0.002	-0.648
Threshold 5	0.381	0.594	0.213	0.003	-0.608
Threshold 10	0.381	0.619	0.238	0.002	-0.617
PRSwithoutAPOE					
Threshold 1	0.381	0.435	0.054	0.171	-0.404
Threshold 5	0.381	0.404	0.023	0.379	-0.225
Threshold 10	0.381	0.424	0.043	0.224	-0.307
APOEonlyPRS					
Threshold 1	0.381	0.595	0.214	0.003	-0.634
Threshold 5	0.381	0.589	0.208	0.004	-0.631
Threshold 10	0.381	0.582	0.201	0.005	-0.617

APOE: apolipoprotein E. PRS: polygenic risk score.

Table F1.52: Associations between PRSs and differential scores of longitudinal change in CSF p-tau181 measurements in MCI patients when CSF Aβ42 status was controlled for

PRS & Threshold	R Square (Model 1)	R Square (Model 2)	R Square Change	Sig. F Change (Model 2)	Standardised beta of PRS
PRSwithAPOE					
Threshold 1	0.072	0.088	0.016	0.210	0.167
Threshold 5	0.072	0.085	0.013	0.256	0.152
Threshold 10	0.072	0.090	0.019	0.175	0.177
PRSwithoutAPOE					
Threshold 1	0.072	0.111	0.039	0.050	0.219
Threshold 5	0.072	0.086	0.014	0.238	0.132
Threshold 10	0.074	0.094	0.022	0.139	0.169
APOEonlyPRS					
Threshold 1	0.072	0.076	0.005	0.498	0.088
Threshold 5	0.072	0.076	0.004	0.529	0.083
Threshold 10	0.072	0.077	0.005	0.481	0.090

APOE: apolipoprotein E. PRS: polygenic risk score.

Table F1.53: Associations between PRSs and differential scores of longitudinal change in CSF p-tau181 measurements in CU ε4 non-carriers when CSF Aβ42 status was not controlled for

PRS & Threshold	R Square (Model 1)	R Square (Model 2)	R Square Change	Sig. F Change (Model 2)	Standardised beta of PRS
PRSwithAPOE					
Threshold 1	0.461	0.590	0.129	0.064	-0.451
Threshold 5	0.461	0.583	0.123	0.072	-0.450
Threshold 10	0.461	0.629	0.168	0.030	-0.549
PRSwithoutAPOE					
Threshold 1	0.461	0.465	0.004	0.762	-0.087
Threshold 5	0.461	0.463	0.002	0.810	-0.067
Threshold 10	0.461	0.474	0.013	0.580	-0.159
APOEonlyPRS					
Threshold 1	0.461	0.596	0.135	0.057	-0.468
Threshold 5	0.461	0.579	0.118	0.078	-0.438
Threshold 10	0.461	0.548	0.087	0.137	-0.395

APOE: apolipoprotein E. PRS: polygenic risk score.

Table F1.54: Associations between PRSs and differential scores of longitudinal change in CSF p-tau181 measurements in MCI ε4 non-carriers when CSF Aβ42 status was not controlled for

PRS & Threshold	R Square (Model 1)	R Square (Model 2)	R Square Change	Sig. F Change (Model 2)	Standardised beta of PRS
PRSwithAPOE					
Threshold 1	0.100	0.117	0.017	0.367	-0.153
Threshold 5	0.100	0.105	0.005	0.635	-0.082
Threshold 10	0.100	0.101	0.001	0.851	-0.032
PRSwithoutAPOE					
Threshold 1	0.100	0.102	0.001	0.789	0.044
Threshold 5	0.100	0.107	0.006	0.581	0.089
Threshold 10	0.100	0.126	0.025	0.265	0.181
APOEonlyPRS					
Threshold 1	0.100	0.122	0.021	0.310	-0.172
Threshold 5	0.100	0.118	0.018	0.350	-0.163
Threshold 10	0.100	0.110	0.010	0.489	-0.117

APOE: apolipoprotein E. PRS: polygenic risk score.

Table F1.55: Associations between PRSs and differential scores of longitudinal change in CSF p-tau181 measurements in MCI ε4 carriers when CSF Aβ42 status was not controlled for

PRS & Threshold	R Square (Model 1)	R Square (Model 2)	R Square Change	Sig. F Change (Model 2)	Standardised beta of PRS
PRSwithAPOE					
Threshold 1	0.338	0.338	0.000	0.938	-0.021
Threshold 5	0.338	0.338	0.001	0.841	-0.053
Threshold 10	0.338	0.340	0.003	0.729	0.092
PRSwithoutAPOE					
Threshold 1	0.338	0.376	0.038	0.179	0.240
Threshold 5	0.338	0.348	0.010	0.496	0.116
Threshold 10	0.338	0.363	0.025	0.275	0.194
APOEonlyPRS					
Threshold 1	0.338	0.346	0.009	0.523	-0.148
Threshold 5	0.338	0.348	0.011	0.477	-0.166
Threshold 10	0.338	0.350	0.012	0.450	0.181

APOE: apolipoprotein E. PRS: polygenic risk score.

Table F1.56: Associations between PRSs and differential scores of longitudinal change in CSF p-tau181 measurements in CU ε4 non-carriers when CSF Aβ42 status was controlled for

PRS & Threshold	R Square (Model 1)	R Square (Model 2)	R Square Change	Sig. F Change (Model 2)	Standardised beta of PRS
PRSwithAPOE					
Threshold 1	0.549	0.711	0.162	0.024	-0.510
Threshold 5	0.549	0.725	0.176	0.017	-0.551
Threshold 10	0.549	0.738	0.189	0.012	-0.585
PRSwithoutAPOE					
Threshold 1	0.549	0.647	0.098	0.092	-0.553
Threshold 5	0.549	0.643	0.094	0.100	-0.531
Threshold 10	0.549	0.624	0.075	0.147	-0.427
APOEonlyPRS					
Threshold 1	0.549	0.663	0.114	0.067	-0.432
Threshold 5	0.549	0.651	0.102	0.085	-0.409
Threshold 10	0.549	0.627	0.079	0.137	-0.375

APOE: apolipoprotein E. PRS: polygenic risk score.

Table F1.57: Associations between PRSs and differential scores of longitudinal change in CSF p-tau181 measurements in MCI ε4 non-carriers when CSF Aβ42 status was controlled for

PRS & Threshold	R Square (Model 1)	R Square (Model 2)	R Square Change	Sig. F Change (Model 2)	Standardised beta of PRS
PRSwithAPOE					
Threshold 1	0.102	0.118	0.016	0.388	-0.149
Threshold 5	0.102	0.106	0.004	0.651	-0.079
Threshold 10	0.102	0.103	0.001	0.844	-0.033
PRSwithoutAPOE					
Threshold 1	0.102	0.104	0.002	0.777	0.048
Threshold 5	0.102	0.108	0.006	0.597	0.086
Threshold 10	0.102	0.126	0.024	0.279	0.178
APOEonlyPRS					
Threshold 1	0.102	0.122	0.020	0.327	-0.169
Threshold 5	0.102	0.119	0.017	0.367	-0.160
Threshold 10	0.102	0.112	0.010	0.494	-0.117

APOE: apolipoprotein E. PRS: polygenic risk score.

Table F1.58: Associations between PRSs and differential scores of longitudinal change in CSF p-tau181 measurements in MCI ε4 carriers when CSF Aβ42 status was controlled for

PRS & Threshold	R Square (Model 1)	R Square (Model 2)	R Square Change	Sig. F Change (Model 2)	Standardised beta of PRS
PRSwithAPOE					
Threshold 1	0.340	0.340	0.000	0.886	-0.040
Threshold 5	0.340	0.341	0.002	0.785	-0.075
Threshold 10	0.340	0.341	0.002	0.793	0.074
PRSwithoutAPOE					
Threshold 1	0.340	0.376	0.036	0.197	0.237
Threshold 5	0.340	0.349	0.009	0.525	0.111
Threshold 10	0.340	0.363	0.023	0.303	0.192
APOEonlyPRS					
Threshold 1	0.340	0.350	0.010	0.497	-0.161
Threshold 5	0.340	0.352	0.013	0.453	-0.179
Threshold 10	0.340	0.353	0.013	0.436	-0.190

APOE: apolipoprotein E. PRS: polygenic risk score.

Table F1.59: Associations between PRSs and differential scores of longitudinal change in CSF p-tau181 measurements in the whole group when CSF Aβ42 status was not controlled for

PRS & Threshold	R Square (Model 1)	R Square (Model 2)	R Square Change	Sig. F Change (Model 2)	Standardised beta of PRS
PRSwithAPOE					
Threshold 1	0.079	0.091	0.012	0.148	0.128
Threshold 5	0.079	0.089	0.010	0.197	0.115
Threshold 10	0.079	0.094	0.015	0.112	0.141
PRSwithoutAPOE					
Threshold 1	0.079	0.090	0.012	0.159	0.116
Threshold 5	0.079	0.081	0.003	0.500	0.056
Threshold 10	0.079	0.092	0.014	0.128	0.126
APOEonlyPRS					
Threshold 1	0.079	0.086	0.007	0.282	0.094
Threshold 5	0.079	0.085	0.006	0.296	0.091
Threshold 10	0.079	0.086	0.007	0.271	0.096

APOE: apolipoprotein E. PRS: polygenic risk score.

Table F1.60: Associations between PRSs and differential scores of longitudinal change in CSF p-tau181 measurements in the whole group when CSF Aβ42 status was controlled for

PRS & Threshold	R Square (Model 1)	R Square (Model 2)	R Square Change	Sig. F Change (Model 2)	Standardised beta of PRS
PRSwithAPOE					
Threshold 1	0.089	0.094	0.005	0.335	0.095
Threshold 5	0.089	0.093	0.004	0.419	0.079
Threshold 10	0.089	0.097	0.008	0.241	0.113
PRSwithoutAPOE					
Threshold 1	0.089	0.098	0.009	0.216	0.103
Threshold 5	0.089	0.091	0.002	0.562	0.048
Threshold 10	0.089	0.101	0.012	0.147	0.120
APOEonlyPRS					
Threshold 1	0.089	0.091	0.002	0.566	0.055
Threshold 5	0.089	0.091	0.002	0.590	0.052
Threshold 10	0.089	0.091	0.002	0.527	0.060

APOE: apolipoprotein E. PRS: polygenic risk score.

Table F1.61: Associations between PRSs and differential scores of longitudinal change in CSF p-tau181 measurements in APOE ε4 non-carriers when CSF Aβ42 status was not controlled for

PRS & Threshold	R Square (Model 1)	R Square (Model 2)	R Square Change	Sig. F Change (Model 2)	Standardised beta of PRS
PRSwithAPOE					
Threshold 1	0.047	0.071	0.024	0.153	-0.164
Threshold 5	0.047	0.063	0.015	0.255	-0.131
Threshold 10	0.047	0.052	0.005	0.513	-0.076
PRSwithoutAPOE					
Threshold 1	0.047	0.047	0.000	0.991	0.001
Threshold 5	0.047	0.048	0.001	0.816	0.027
Threshold 10	0.047	0.062	0.014	0.267	0.132
APOEonlyPRS					
Threshold 1	0.047	0.077	0.030	0.109	-0.187
Threshold 5	0.047	0.075	0.027	0.126	-0.180
Threshold 10	0.047	0.062	0.015	0.258	-0.133

APOE: apolipoprotein E. PRS: polygenic risk score.

Table F1.62: Associations between PRSs and differential scores of longitudinal change in CSF p-tau181 measurements in APOE ε4 carriers when CSF Aβ42 status was not controlled for

PRS & Threshold	R Square (Model 1)	R Square (Model 2)	R Square Change	Sig. F Change (Model 2)	Standardised beta of PRS
PRSwithAPOE					
Threshold 1	0.247	0.265	0.018	0.239	0.198
Threshold 5	0.247	0.260	0.013	0.320	0.166
Threshold 10	0.247	0.278	0.031	0.125	0.253
PRSwithoutAPOE					
Threshold 1	0.247	0.252	0.004	0.570	0.079
Threshold 5	0.247	0.247	0.000	0.958	-0.007
Threshold 10	0.247	0.259	0.011	0.354	0.119
APOEonlyPRS					
Threshold 1	0.247	0.259	0.011	0.351	0.147
Threshold 5	0.247	0.257	0.010	0.383	0.138
Threshold 10	0.247	0.254	0.007	0.479	0.115

APOE: apolipoprotein E. PRS: polygenic risk score.

Table F1.63: Associations between PRSs and differential scores of longitudinal change in CSF p-tau181 measurements in APOE ε4 non-carriers when CSF Aβ42 status was controlled for

PRS & Threshold	R Square (Model 1)	R Square (Model 2)	R Square Change	Sig. F Change (Model 2)	Standardised beta of PRS
PRSwithAPOE					
Threshold 1	0.047	0.072	0.024	0.153	-0.166
Threshold 5	0.047	0.063	0.015	0.257	-0.131
Threshold 10	0.047	0.052	0.005	0.516	-0.076
PRSwithoutAPOE					
Threshold 1	0.047	0.047	0.000	0.993	0.001
Threshold 5	0.047	0.048	0.001	0.817	0.027
Threshold 10	0.047	0.062	0.014	0.270	0.132
APOEonlyPRS					
Threshold 1	0.047	0.077	0.030	0.111	-0.188
Threshold 5	0.047	0.075	0.027	0.128	-0.180
Threshold 10	0.047	0.062	0.015	0.261	-0.133

APOE: apolipoprotein E. PRS: polygenic risk score.

Table F1.64: Associations between PRSs and differential scores of longitudinal change in CSF p-tau181 measurements in APOE ε4 carriers when CSF Aβ42 status was controlled for

PRS & Threshold	R Square (Model 1)	R Square (Model 2)	R Square Change	Sig. F Change (Model 2)	Standardised beta of PRS
PRSwithAPOE					
Threshold 1	0.252	0.269	0.017	0.265	-0.190
Threshold 5	0.252	0.264	0.012	0.348	0.159
Threshold 10	0.252	0.281	0.029	0.141	0.245
PRSwithoutAPOE					
Threshold 1	0.252	0.255	0.003	0.618	0.070
Threshold 5	0.252	0.252	0.000	0.920	-0.013
Threshold 10	0.252	0.262	0.010	0.398	0.110
APOEonlyPRS					
Threshold 1	0.252	0.263	0.011	0.373	0.142
Threshold 5	0.252	0.261	0.009	0.405	0.133
Threshold 10	0.252	0.259	0.007	0.479	0.479

APOE: apolipoprotein E. PRS: polygenic risk score.

APPENDIX F2 (Chapter 6: Experiment Three Part B)

Table F2.1: Associations between PRSs and longitudinal cognitive decline in the whole group

PRS & Threshold	Chi-square	df	*p*	Nagelkerke R^2	Wald	df	*p*	OR	95% CI	Nagelkerke R^2 Model 1
PRSwithAPOE										
Threshold 1	69.546	17	<0.001	0.174	0.768	1	0.381	1.098	0.890-1.355	0.172
Threshold 5	69.401	17	<0.001	0.173	0.623	1	0.430	1.088	0.883-1.339	0.172
Threshold 10	69.008	17	<0.001	0.172	0.231	1	0.631	1.053	0.854-1.297	0.172
PRSwithoutAPOE										
Threshold 1	69.486	17	<0.001	0.173	0.706	1	0.401	0.921	0.760-1.116	0.172
Threshold 5	69.031	17	<0.001	0.172	0.254	1	0.614	0.951	0.783-1.155	0.172
Threshold 10	68.886	17	<0.001	0.172	0.109	1	0.741	0.966	0.789-1.184	0.172
APOEonlyPRS										
Threshold 1	70.423	17	<0.001	0.176	1.640	1	0.200	1.148	0.929-1.417	0.172
Threshold 5	70.194	17	<0.001	0.175	1.413	1	0.235	1.136	0.921-1.401	0.172
Threshold 10	69.577	17	<0.001	0.174	0.798	1	0.372	1.100	0.892-1.357	0.172

APOE: apolipoprotein E. CI: confidence interval. df: degrees of freedom. OR: odds ratio. PRS: polygenic risk score.

Table F2.2: Associations between PRSs and longitudinal cognitive decline in APOE ε4 non-carriers

PRS & Threshold	Chi-square	df	*p*	Nagelkerke R^2	Wald	df	*p*	OR	95% CI	Nagelkerke R^2 Model 1
PRSwithAPOE										
Threshold 1	29.546	17	0.030	0.124	1.348	1	0.246	1.309	0.831-2.060	0.118
Threshold 5	28.828	17	0.036	0.121	0.638	1	0.424	1.192	0.774-1.836	0.118
Threshold 10	28.242	17	0.043	0.119	0.055	1	0.815	1.049	0.703-1.566	0.118
PRSwithoutAPOE										
Threshold 1	28.321	17	0.041	0.119	0.133	1	0.715	0.956	0.751-1.217	0.118
Threshold 5	28.205	17	0.043	0.118	0.018	1	0.892	0.983	0.770-1.256	0.118
Threshold 10	28.230	17	0.042	0.119	0.042	1	0.837	0.973	0.750-1.263	0.118
APOEonlyPRS										
Threshold 1	31.265	17	0.019	0.131	3.030	1	0.082	1.553	0.946-2.551	0.118
Threshold 5	30.655	17	0.022	0.128	2.435	1	0.119	1.481	0.904-2.427	0.118
Threshold 10	29.143	17	0.033	0.122	0.949	1	0.330	1.265	0.788-2.032	0.118

APOE: apolipoprotein E. CI: confidence interval. df: degrees of freedom. OR: odds ratio. PRS: polygenic risk score.

Table F2.3: Associations between PRSs and longitudinal cognitive decline in APOE ε4 carriers

PRS & Threshold	Chi-square	df	*p*	Nagelkerke R^2	Wald	df	*p*	OR	95% CI	Nagelkerke R^2 Model 1
PRSwithAPOE										
Threshold 1	44.625	17	<0.001	.280	1.529	1	0.216	0.767	0.503-1.168	0.271
Threshold 5	44.244	17	<0.001	.277	1.158	1	0.282	0.797	0.528-1.204	0.271
Threshold 10	44.415	17	<0.001	.278	1.322	1	0.250	0.786	0.521-1.185	0.271
PRSwithoutAPOE										
Threshold 1	43.193	17	<0.001	0.272	0.122	1	0.727	0.939	0.658-1.339	0.271
Threshold 5	43.167	17	<0.001	0.271	0.096	1	0.757	0.946	0.664-1.347	0.271
Threshold 10	43.080	17	<0.001	0.271	0.009	1	0.926	0.984	0.696-1.390	0.271
APOEonlyPRS										
Threshold 1	44.487	17	<0.001	0.279	1.394	1	0.238	0.772	0.503-1.186	0.271
Threshold 5	44.484	17	<0.001	0.279	1.391	1	0.238	0.774	0.506-1.185	0.271
Threshold 10	44.489	17	<0.001	0.279	1.397	1	0.237	0.776	0.510-1.182	0.271

APOE: apolipoprotein E. CI: confidence interval. df: degrees of freedom. OR: odds ratio. PRS: polygenic risk score.

Table F2.4: Associations between PRSs and longitudinal cognitive decline in CU participants

PRS & Threshold	Chi-square	df	*p*	Nagelkerke R^2	Wald	df	*p*	OR	95% CI	Nagelkerke R^2 Model 1
PRSwithAPOE										
Threshold 1	14.702	17	0.617	0.126	0.228	1	0.633	1.120	0.703-1.784	0.124
Threshold 5	14.482	17	0.633	0.124	0.008	1	0.930	1.021	0.648-1.608	0.124
Threshold 10	14.608	17	0.624	0.125	0.133	1	0.715	0.920	0.589-1.437	0.124
PRSwithoutAPOE										
Threshold 1	15.270	17	0.576	0.131	0.785	1	0.376	0.853	0.599-1.213	0.124
Threshold 5	15.349	17	0.570	0.131	0.872	1	0.351	0.849	0.602-1.197	0.124
Threshold 10	14.914	17	0.507	0.128	0.440	1	0.507	0.888	0.625-1.262	0.124
APOEonlyPRS										
Threshold 1	15.527	17	0.558	0.133	1.051	1	0.305	1.264	0.808-1.978	0.124
Threshold 5	15.114	17	0.587	0.129	0.640	1	0.424	1.201	0.767-1.882	0.124
Threshold 10	14.571	17	0.626	0.125	0.097	1	0.755	1.074	0.685-1.683	0.124

APOE: apolipoprotein E. CI: confidence interval. df: degrees of freedom. OR: odds ratio. PRS: polygenic risk score.

Table F2.5: Associations between PRSs and longitudinal cognitive decline in MCI patients

PRS & Threshold	Chi-square	df	*p*	Nagelkerke R^2	Wald	df	*p*	OR	95% CI	Nagelkerke R^2 Model 1
PRSwithAPOE										
Threshold 1	29.964	17	0.059	0.122	0.008	1	0.929	0.988	0.749-1.302	0.122
Threshold 5	26.964	17	0.059	0.122	0.009	1	0.926	1.013	0.768-1.336	0.122
Threshold 10	26.957	17	0.059	0.122	0.001	1	0.969	1.006	0.759-1.332	0.122
PRSwithoutAPOE										
Threshold 1	28.649	17	0.038	0.129	1.678	1	0.195	0.838	0.641-1.095	0.122
Threshold 5	27.201	17	0.055	0.123	0.245	1	0.621	0.934	0.712-1.225	0.122
Threshold 10	27.106	17	0.057	0.122	0.150	1	0.699	0.945	0.710-1.258	0.122
APOEonlyPRS										
Threshold 1	27.055	17	0.057	0.122	0.099	1	0.753	1.046	0.792-1.381	0.122
Threshold 5	27.073	17	0.057	0.122	0.117	1	0.732	1.050	0.796-1.385	0.122
Threshold 10	27.056	17	0.057	0.122	0.100	1	0.752	1.045	0.794-1.377	0.122

APOE: apolipoprotein E. CI: confidence interval. df: degrees of freedom. OR: odds ratio. PRS: polygenic risk score.

Table F2.6: Associations between PRSs and longitudinal cognitive decline in AD dementia patients

PRS & Threshold	Chi-square	df	*p*	Nagelkerke R^2	Wald	df	*p*	OR	95% CI	Nagelkerke R^2 Model 1
PRSwithAPOE										
Threshold 1	29.297	17	0.042	0.603	0.435	1	0.510	0.668	0.202-2.215	0.596
Threshold 5	28.363	17	0.041	0.604	0.491	1	0.484	0.651	0.196-2.160	0.596
Threshold 10	28.814	17	0.036	0.612	0.874	1	0.350	0.574	0.179-1.839	0.596
PRSwithoutAPOE										
Threshold 1	30.405	17	0.024	0.638	1.882	1	0.170	4.957	0.504-48.794	0.596
Threshold 5	28.495	17	0.039	0.607	0.596	1	0.440	1.951	0.358-10.642	0.596
Threshold 10	28.006	17	0.045	0.598	0.156	1	0.693	1.359	0.297-6.209	0.596
APOEonlyPRS										
Threshold 1	29.005	17	0.034	0.615	1.049	1	0.306	0.513	0.143-1.841	0.596
Threshold 5	28.904	17	0.035	0.613	0.965	1	0.326	0.530	0.150-1.880	0.596
Threshold 10	29.218	17	0.033	0.619	1.194	1	0.275	0.477	0.127-1.798	0.596

APOE: apolipoprotein E. CI: confidence interval. df: degrees of freedom. OR: odds ratio. PRS: polygenic risk score.

Table F2.7: Associations between PRSs and longitudinal cognitive decline in CU ε4 non-carriers

PRS & Threshold	Chi-square	df	*p*	Nagelkerke R^2	Wald	df	*p*	OR	95% CI	Nagelkerke R^2 Model 1
PRSwithAPOE										
Threshold 1	12.630	17	0.761	0.144	0.194	1	0.660	1.193	0.544-2.612	0.142
Threshold 5	12.451	17	0.772	0.142	0.014	1	0.907	0.957	0.460-1.992	0.142
Threshold 10	12.971	17	0.738	0.148	0.526	1	0.468	0.775	0.389-1.544	0.142
PRSwithoutAPOE										
Threshold 1	12.450	17	0.772	0.142	0.013	1	0.910	1.024	0.675-1.553	0.142
Threshold 5	12.483	17	0.770	0.143	0.045	1	0.831	0.957	0.639-1.433	0.142
Threshold 10	12.636	17	0.760	0.144	0.199	1	0.655	0.906	0.586-1.399	0.142
APOEonlyPRS										
Threshold 1	12.902	17	0.743	0.147	0.465	1	0.495	1.344	0.574-3.145	0.142
Threshold 5	12.622	17	0.761	0.144	0.185	1	0.667	1.210	0.507-2.889	0.142
Threshold 10	12.561	17	0.765	0.144	0.123	1	0.725	0.860	0.370-1.998	0.142

APOE: apolipoprotein E. CI: confidence interval. df: degrees of freedom. OR: odds ratio. PRS: polygenic risk score.

Table F2.8: Associations between PRSs and longitudinal cognitive decline in MCI ε4 non-carriers

PRS & Threshold	Chi-square	df	*p*	Nagelkerke R^2	Wald	df	*p*	OR	95% CI	Nagelkerke R^2 Model 1
PRSwithAPOE										
Threshold 1	19.575	17	0.297	0.145	1.316	1	0.251	1.502	0.750-3.008	0.135
Threshold 5	19.690	17	0.290	0.145	1.426	1	0.232	1.508	0.768-2.958	0.135
Threshold 10	18.972	17	0.330	0.140	0.723	1	0.395	1.307	0.705-2.420	0.135
PRSwithoutAPOE										
Threshold 1	18.548	17	0.355	0.138	0.304	1	0.581	0.909	0.648-1.276	0.135
Threshold 5	18.262	17	0.373	0.135	0.019	1	0.891	1.025	0.717-1.467	0.135
Threshold 10	18.267	17	0.372	0.136	0.024	1	0.877	1.031	0.702-1.513	0.135
APOEonlyPRS										
Threshold 1	21.224	17	0.216	0.156	2.911	1	0.088	1.879	0.910-3.877	0.135
Threshold 5	20.864	17	0.232	0.154	2.568	1	0.109	1.793	0.878-3.662	0.135
Threshold 10	20.425	17	0.253	0.151	2.136	1	0.144	1.680	0.838-3.370	0.135

APOE: apolipoprotein E. CI: confidence interval. df: degrees of freedom. OR: odds ratio. PRS: polygenic risk score.

Table F2.9: Associations between PRSs and longitudinal cognitive decline in MCI ε4 carriers

PRS & Threshold	Chi-square	df	*p*	Nagelkerke R^2	Wald	df	*p*	OR	95% CI	Nagelkerke R^2 Model 1
PRSwithAPOE										
Threshold 1	24.454	17	0.108	0.264	1.206	1	0.272	0.722	0.403-1.292	0.252
Threshold 5	23.933	17	0.121	0.259	0.704	1	0.401	0.782	0.440-1.389	0.252
Threshold 10	23.890	17	0.122	0.259	0.661	1	0.416	0.787	0.442-1.402	0.252
PRSwithoutAPOE										
Threshold 1	23.841	17	0.124	0.258	0.618	1	0.432	0.824	0.508-1.335	0.252
Threshold 5	23.400	17	0.137	0.254	0.181	1	0.670	0.902	0.561-1.450	0.252
Threshold 10	23.412	17	0.136	0.254	0.193	1	0.660	0.896	0.548-1.463	0.252
APOEonlyPRS										
Threshold 1	24.266	17	0.112	0.262	1.026	1	0.311	0.733	0.403-1.336	0.252
Threshold 5	24.052	17	0.118	0.260	0.819	1	0.365	0.760	0.420-1.376	0.252
Threshold 10	23.955	17	0.121	0.259	0.727	1	0.394	0.777	0.434-1.389	0.252

APOE: apolipoprotein E. CI: confidence interval. df: degrees of freedom. OR: odds ratio. PRS: polygenic risk score.

Table F2.10: Associations between PRSs and longitudinal cognitive decline in AD ε4 carriers

PRS & Threshold	Chi-square	df	*p*	Nagelkerke R^2	Wald	df	*p*	OR	95% CI	Nagelkerke R^2 Model 1
PRSwithAPOE										
Threshold 1	42.121	17	<0.001	1.000	0.000	1	0.998	289115.288	0.000-not available	1.000
Threshold 5	42.121	17	<0.001	1.000	0.000	1	0.999	0.000	0.000-not available	1.000
Threshold 10	42.121	17	<0.001	1.000	0.000	1	0.991	0.000	0.000-not available	1.000
PRSwithoutAPOE										
Threshold 1	42.121	17	<0.001	1.000	0.000	1	0.999	2.748E+20	0.000-not available	1.000
Threshold 5	42.121	17	<0.001	1.000	0.000	1	0.997	3.085E+24	0.000-not available	1.000
Threshold 10	42.121	17	<0.001	1.000	0.000	1	0.992	1.671E48	0.000-not available	1.000
APOEonlyPRS										
Threshold 1	42.121	17	<0.001	1.000	0.000	1	0.988	0.000	0.000-not available	1.000
Threshold 5	42.121	17	<0.001	1.000	0.000	1	0.988	0.000	0.000-not available	1.000

APOE: apolipoprotein E. CI: confidence interval. df: degrees of freedom. OR: odds ratio. PRS: polygenic risk score.

APOEonlyPRS Threshold 10 not available.

Table F2.11: Associations between PRSs and longitudinal cognitive decline in amyloid negative participants

PRS & Threshold	Chi-square	df	*p*	Nagelkerke R^2	Wald	df	*p*	OR	95% CI	Nagelkerke R^2 Model 1
PRSwithAPOE										
Threshold 1	5.112	16	0.995	0.035	0.333	1	0.564	1.134	0.739-1.740	0.033
Threshold 5	5.117	16	0.995	0.035	0.338	1	0.561	1.134	0.743-1.730	0.033
Threshold 10	4.810	16	0.997	0.033	0.029	1	0.865	1.037	0.684-1.572	0.033
PRSwithoutAPOE										
Threshold 1	4.847	16	0.996	0.034	0.066	1	0.797	1.039	0.779-1.385	0.033
Threshold 5	5.413	16	0.993	0.037	0.629	1	0.428	1.130	0.835-1.531	0.033
Threshold 10	5.114	16	0.995	0.035	0.332	1	0.565	1.099	0.797-1.514	0.033
APOEonlyPRS										
Threshold 1	5.214	16	0.995	0.036	0.436	1	0.509	1.156	0.751-1.779	0.033
Threshold 5	5.089	16	0.995	0.035	0.310	1	0.577	1.129	0.738-1.727	0.033
Threshold 10	5.499	16	0.996	0.035	0.220	1	0.639	1.105	0.727-1.681	0.033

APOE: apolipoprotein E. CI: confidence interval. df: degrees of freedom. OR: odds ratio. PRS: polygenic risk score.

Table F2.12: Associations between PRSs and longitudinal cognitive decline in amyloid positive participants

PRS & Threshold	Chi-square	df	*p*	Nagelkerke R^2	Wald	df	*p*	OR	95% CI	Nagelkerke R^2 Model 1
PRSwithAPOE										
Threshold 1	35.138	16	0.004	0.149	0.428	1	0.513	1.087	0.847-1.395	0.148
Threshold 5	35.017	16	0.004	0.149	0.308	1	0.579	1.073	0.837-1.374	0.148
Threshold 10	34.911	16	0.004	0.148	0.202	1	0.653	1.059	0.825-1.359	0.148
PRSwithoutAPOE										
Threshold 1	36.122	16	0.003	0.153	1.402	1	0.236	0.850	0.649-1.113	0.148
Threshold 5	36.101	16	0.003	0.153	1.386	1	0.239	0.854	0.656-1.111	0.148
Threshold 10	35.275	16	0.004	0.150	0.564	1	0.453	0.901	0.686-1.183	0.148
APOEonlyPRS										
Threshold 1	35.737	16	0.003	0.152	1.023	1	0.312	1.138	0.886-1.462	0.148
Threshold 5	35.658	16	0.003	0.151	0.945	1	0.331	1.132	0.882-1.453	0.148
Threshold 10	35.205	16	0.004	0.150	0.495	1	0.482	1.094	0.851-1.406	0.148

APOE: apolipoprotein E. CI: confidence interval. df: degrees of freedom. OR: odds ratio. PRS: polygenic risk score.

Table F2.13: Associations between PRSs and longitudinal cognitive decline in amyloid negative ε4 non-carriers

PRS & Threshold	Chi-square	df	*p*	Nagelkerke R^2	Wald	df	*p*	OR	95% CI	Nagelkerke R^2 Model 1
PRSwithAPOE										
Threshold 1	12.599	16	0.702	0.104	0.955	1	0.328	1.402	0.712-2.759	0.096
Threshold 5	12.399	16	0.716	0.102	0.755	1	0.385	1.331	0.698-2.539	0.096
Threshold 10	11.787	16	0.758	0.098	0.144	1	0.705	1.122	0.619-2.032	0.096
PRSwithoutAPOE										
Threshold 1	12.391	16	0.717	0.102	0.747	1	0.388	1.154	0.834-1.597	0.096
Threshold 5	12.494	16	0.709	0.102	0.844	1	0.358	1.174	0.834-1.653	0.096
Threshold 10	12.064	16	0.740	0.100	0.418	1	0.518	1.130	0.780-1.639	0.096
APOEonlyPRS										
Threshold 1	12.368	16	0.718	0.102	0.723	1	0.395	1.390	0.651-2.969	0.096
Threshold 5	12.320	16	0.722	0.102	0.676	1	0.411	1.370	0.647-2.899	0.096
Threshold 10	11.878	16	0.752	0.098	0.235	1	0.628	1.197	0.578-2.478	0.096

APOE: apolipoprotein E. CI: confidence interval. df: degrees of freedom. OR: odds ratio. PRS: polygenic risk score.

Table F2.14: Associations between PRSs and longitudinal cognitive decline in amyloid negative ε4 carriers

PRS & Threshold	Chi-square	df	*p*	Nagelkerke R^2	Wald	df	*p*	OR	95% CI	Nagelkerke R^2 Model 1
PRSwithAPOE										
Threshold 1	45.829	16	<0.001	1.000	0.000	1	0.993	4.684E+35	0.000-not available	1.000
Threshold 5	45.829	16	<0.001	1.000	0.000	1	0.990	1.226E+40	0.000-not available	1.000
Threshold 10	45.829	16	<0.001	1.000	0.000	1	0.995	0.000	0.000-not available	1.000
PRSwithoutAPOE										
Threshold 1	45.829	16	<0.001	1.000	0.000	1	0.998	0.000	0.000-not available	1.000
Threshold 5	45.829	16	<0.001	1.000	0.000	1	0.998	0.000	0.000-not available	1.000
Threshold 10	45.829	16	<0.001	1.000	0.000	1	0.997	0.000	0.000-not available	1.000
APOEonlyPRS										
Threshold 1	45.829	16	<0.001	1.000	0.000	1	0.996	8.827E+36	0.000-not available	1.000
Threshold 5	45.829	16	<0.001	1.000	0.000	1	0.997	8.497E+40	0.000-not available	1.000
Threshold 10	45.829	16	<0.001	1.000	0.000	1	0.996	1.675E+20	0.000-not available	1.000

APOE: apolipoprotein E. CI: confidence interval. df: degrees of freedom. OR: odds ratio. PRS: polygenic risk score.

Table F2.15: Associations between PRSs and longitudinal cognitive decline in amyloid positive ε4 non-carriers

PRS & Threshold	Chi-square	df	*p*	Nagelkerke R^2	Wald	df	*p*	OR	95% CI	Nagelkerke R^2 Model 1
PRSwithAPOE										
Threshold 1	17.122	16	0.378	0.151	0.823	1	0.364	1.367	0.696-2.683	0.144
Threshold 5	16.535	16	0.416	0.146	0.246	1	0.620	1.176	0.620-2.233	0.144
Threshold 10	16.300	16	0.432	0.144	0.012	1	0.911	1.034	0.573-1.865	0.144
PRSwithoutAPOE										
Threshold 1	17.949	16	0.327	0.157	1.640	1	0.200	0.765	0.508-1.153	0.144
Threshold 5	17.414	16	0.359	0.153	1.118	1	0.290	0.811	0.549-1.196	0.144
Threshold 10	17.002	16	0.385	0.150	0.708	1	0.400	0.835	0.548-1.271	0.144
APOEonlyPRS										
Threshold 1	19.445	16	0.246	0.170	3.038	1	0.081	1.919	0.922-3.994	0.144
Threshold 5	18.722	16	0.283	0.164	2.355	1	0.125	1.787	0.851-3.753	0.144
Threshold 10	17.324	16	0.365	0.152	1.018	1	0.313	1.425	0.716-2.833	0.144

APOE: apolipoprotein E. CI: confidence interval. df: degrees of freedom. OR: odds ratio. PRS: polygenic risk score.

Table F2.16: Associations between PRSs and longitudinal cognitive decline in amyloid positive ε4 carriers

PRS & Threshold	Chi-square	df	*p*	Nagelkerke R^2	Wald	df	*p*	OR	95% CI	Nagelkerke R^2 Model 1
PRSwithAPOE										
Threshold 1	33.715	16	0.006	0.267	0.552	1	0.457	0.845	0.541-1.318	0.263
Threshold 5	33.492	16	0.006	0.266	0.332	1	0.564	0.878	0.564-1.367	0.263
Threshold 10	33.399	16	0.007	0.265	0.240	1	0.624	0.895	0.573-1.396	0.263
PRSwithoutAPOE										
Threshold 1	33.239	16	0.007	0.264	0.081	1	0.776	1.059	0.713-1.574	0.263
Threshold 5	33.159	16	0.007	0.263	0.001	1	0.977	1.006	0.679-1.490	0.263
Threshold 10	33.175	16	0.007	0.264	0.017	1	0.897	1.027	0.691-1.526	0.263
APOEonlyPRS										
Threshold 1	33.935	16	0.006	0.269	0.768	1	0.381	0.816	0.517-1.286	0.263
Threshold 5	33.847	16	0.006	0.268	0.683	1	0.409	0.826	0.526-1.299	0.263
Threshold 10	33.884	16	0.006	0.269	0.719	1	0.396	0.823	0.524-1.291	0.263

APOE: apolipoprotein E. CI: confidence interval. df: degrees of freedom. OR: odds ratio. PRS: polygenic risk score.

Table F2.17: Associations between PRSs and longitudinal cognitive decline in tau negative participants

PRS & Threshold	Chi-square	df	*p*	Nagelkerke R^2	Wald	df	*p*	OR	95% CI	Nagelkerke R^2 Model 1
PRSwithAPOE										
Threshold 1	26.480	16	0.048	0.127	0.931	1	0.335	1.159	0.859-1.565	0.123
Threshold 5	26.094	16	0.053	0.125	0.543	1	0.461	1.119	0.829-1.510	0.123
Threshold 10	25.698	16	0.058	0.124	0.145	1	0.703	1.060	0.785-1.432	0.123
PRSwithoutAPOE										
Threshold 1	25.845	16	0.056	0.124	0.291	1	0.590	0.931	0.719-1.206	0.123
Threshold 5	25.870	16	0.056	0.124	0.316	1	0.574	0.926	0.710-1.209	0.123
Threshold 10	26.043	16	0.053	0.125	0.488	1	0.485	0.905	0.685-1.197	0.123
APOEonlyPRS										
Threshold 1	26.991	16	0.042	0.130	1.444	1	0.229	1.203	0.890-1.626	0.123
Threshold 5	26.924	16	0.042	0.129	1.377	1	0.241	1.197	0.886-1.618	0.123
Threshold 10	26.561	16	0.047	0.128	1.011	1	0.315	1.166	0.864-1.574	0.123

APOE: apolipoprotein E. CI: confidence interval. df: degrees of freedom. OR: odds ratio. PRS: polygenic risk score.

Table F2.18: Associations between PRSs and longitudinal cognitive decline in tau positive participants

PRS & Threshold	Chi-square	df	*p*	Nagelkerke R^2	Wald	df	*p*	OR	95% CI	Nagelkerke R^2 Model 1
PRSwithAPOE										
Threshold 1	23.937	16	0.091	0.218	0.534	1	0.465	1.164	0.775-1.747	0.214
Threshold 5	24.307	16	0.083	0.221	0.893	1	0.345	1.219	0.809-1.837	0.214
Threshold 10	24.763	16	0.074	0.225	1.335	1	0.248	1.280	0.842-1.947	0.214
PRSwithoutAPOE										
Threshold 1	23.485	16	0.101	0.215	0.088	1	0.767	1.063	0.709-1.596	0.214
Threshold 5	24.713	16	0.075	0.225	1.293	1	0.256	1.272	0.840-1.927	0.214
Threshold 10	26.117	16	0.052	0.236	2.601	1	0.107	1.431	0.926-2.212	0.214
APOEonlyPRS										
Threshold 1	23.978	16	0.090	0.219	0.574	1	0.449	1.170	0.780-1.756	0.214
Threshold 5	23.844	16	0.093	0.218	0.443	1	0.506	1.147	0.765-1.721	0.214
Threshold 10	23.732	16	0.096	0.217	0.333	1	0.564	1.128	0.749-1.697	0.214

APOE: apolipoprotein E. CI: confidence interval. df: degrees of freedom. OR: odds ratio. PRS: polygenic risk score.

Table F2.19: Associations between PRSs and longitudinal cognitive decline in tau positive ε4 non-carriers

PRS & Threshold	Chi-square	df	*p*	Nagelkerke R^2	Wald	df	*p*	OR	95% CI	Nagelkerke R^2 Model 1
PRSwithAPOE										
Threshold 1	19.112	16	0.263	0.327	3.900	1	0.048	3.668	1.010-13.327	0.260
Threshold 5	19.095	16	0.264	0.326	3.870	1	0.049	3.592	1.005-12.845	0.260
Threshold 10	20.114	16	0.215	0.341	4.722	1	0.030	3.536	1.132-11.047	0.260
PRSwithoutAPOE										
Threshold 1	14.954	16	0.528	0.263	0.192	1	0.661	0.872	0.472-1.611	0.260
Threshold 5	14.781	16	0.541	0.260	0.021	1	0.885	1.046	0.564-1.941	0.260
Threshold 10	16.332	16	0.430	0.284	1.496	1	0.221	1.503	0.782-2.888	0.260
APOEonlyPRS										
Threshold 1	22.141	16	0.139	0.370	6.311	1	0.012	6.305	1.499-26.520	0.260
Threshold 5	20.759	16	0.188	0.351	5.325	1	0.021	5.322	1.286-22.021	0.260
Threshold 10	20.094	16	0.216	0.341	4.792	1	0.029	4.808	1.179-19.615	0.260

APOE: apolipoprotein E. CI: confidence interval. df: degrees of freedom. OR: odds ratio. PRS: polygenic risk score.

Table F2.20: Associations between PRSs and longitudinal cognitive decline in tau positive ε4 carriers

PRS & Threshold	Chi-square	df	*p*	Nagelkerke R^2	Wald	df	*p*	OR	95% CI	Nagelkerke R^2 Model 1
PRSwithAPOE										
Threshold 1	15.771	16	0.469	0.289	0.029	1	0.866	0.941	0.468-1.895	0.289
Threshold 5	15.750	16	0.471	0.289	0.008	1	0.931	1.031	0.517-2.057	0.289
Threshold 10	15.742	16	0.471	0.289	0.000	1	0.996	0.998	0.492-2.024	0.289
PRSwithoutAPOE										
Threshold 1	17.648	16	0.345	0.319	1.804	1	0.179	1.557	0.816-2.970	0.289
Threshold 5	18.562	16	0.292	0.334	2.588	1	0.108	1.782	0.881-3.604	0.289
Threshold 10	16.970	16	0.388	0.309	1.177	1	0.278	1.460	1.737-2.892	0.289
APOEonlyPRS										
Threshold 1	16.105	16	0.446	0.295	0.359	1	0.549	0.801	0.388-1.654	0.289
Threshold 5	16.087	16	0.447	0.294	0.341	1	0.559	0.809	0.396-1.649	0.289
Threshold 10	16.210	16	0.438	0.296	0.463	1	0.496	0.780	0.382-1.595	0.289

APOE: apolipoprotein E. CI: confidence interval. df: degrees of freedom. OR: odds ratio. PRS: polygenic risk score.

Table F2.21: Associations between PRSs and longitudinal cognitive decline in tau negative ε4 non-carriers

PRS & Threshold	Chi-square	df	*p*	Nagelkerke R^2	Wald	df	*p*	OR	95% CI	Nagelkerke R^2 Model 1
PRSwithAPOE										
Threshold 1	19.026	16	0.267	0.131	0.201	1	0.654	1.153	0.619-2.147	0.130
Threshold 5	18.828	16	0.278	0.130	0.004	1	0.951	1.019	0.564-1.839	0.130
Threshold 10	18.981	16	0.270	0.131	0.156	1	0.693	0.893	0.510-1.564	0.130
PRSwithoutAPOE										
Threshold 1	18.836	16	0.277	0.130	0.012	1	0.914	1.017	0.750-1.378	0.130
Threshold 5	18.828	16	0.278	0.130	0.003	1	0.954	1.009	0.737-1.382	0.130
Threshold 10	18.894	16	0.274	0.131	0.069	1	0.793	0.956	0.680-1.342	0.130
APOEonlyPRS										
Threshold 1	19.242	16	0.256	0.133	0.417	1	0.518	1.260	0.625-2.542	0.130
Threshold 5	19.206	16	0.258	0.133	0.381	1	0.537	1.247	0.619-2.513	0.130
Threshold 10	18.856	16	0.276	0.130	0.031	1	0.860	1.062	0.542-2.081	0.130

APOE: apolipoprotein E. CI: confidence interval. df: degrees of freedom. OR: odds ratio. PRS: polygenic risk score.

Table F2.22: Associations between PRSs and longitudinal cognitive decline in tau negative ε4 carriers

PRS & Threshold	Chi-square	df	*p*	Nagelkerke R^2	Wald	df	*p*	OR	95% CI	Nagelkerke R^2 Model 1
PRSwithAPOE										
Threshold 1	15.883	16	0.461	0.243	0.027	1	0.869	0.944	0.474-1.879	0.243
Threshold 5	15.866	16	0.462	0.243	0.010	1	0.920	0.966	0.492-1.897	0.243
Threshold 10	15.903	16	0.460	0.243	0.047	1	0.828	0.930	0.481-1.797	0.243
PRSwithoutAPOE										
Threshold 1	15.976	16	0.455	0.244	0.120	1	0.729	0.901	0.500-1.625	0.243
Threshold 5	15.885	16	0.461	0.243	0.029	1	0.866	0.951	0.530-1.706	0.243
Threshold 10	15.867	16	0.462	0.243	0.011	1	0.916	1.030	0.594-1.786	0.243
APOEonlyPRS										
Threshold 1	15.886	16	0.461	0.243	0.030	1	0.863	0.941	0.473-1.872	0.243
Threshold 5	15.918	16	0.459	0.243	0.062	1	0.804	0.917	0.462-1.818	0.243
Threshold 10	15.941	16	0.457	0.244	0.084	1	0.771	0.902	0.451-1.806	0.243

APOE: apolipoprotein E. CI: confidence interval. df: degrees of freedom. OR: odds ratio. PRS: polygenic risk score.